VOLUME 28 / NUMBER 11
JUNE 8, 1990
ACC. NOS. N90-18361 TO N90-19189

STAR
AN ABSTRACT JOURNAL

Scientific and Technical Aerospace Reports

PRODUCED BY THE
SCIENTIFIC AND TECHNICAL
INFORMATION
DIVISION

NASA

NATIONAL AERONAUTICS AND SPACE ADMINISTRATION

WHAT YOU CAN DO FOR *STAR*

All users of this abstract service are urged to forward reports to be considered for announcement in *STAR*. This will aid NASA in its efforts to provide the fullest possible coverage of all scientific and technical publications that might support aeronautics and space research and development. If you have prepared relevant reports (other than those that you will transmit to NASA, DOD, or DOE through the usual contract- or grant-reporting channels), please send them for consideration to the NASA Scientific and Technical Information Facility, P.O. Box 8757, BWI Airport, MD 21240.

Reprints of journal articles, book chapters, and conference papers are also welcome. These will be considered for announcement in *STAR's* companion journal, *International Aerospace Abstracts*.

You may specify a particular source to be included in a report announcement if you wish; otherwise the report will be placed on public sale at the National Technical Information Service. Copyrighted publications will be announced but not distributed or sold.

PURCHASE OF *STAR*

The semimonthly issues are available to registered users on annual subscription from the NASA Scientific and Technical Information Facility, ATTN: Registration Services, P.O. Box 8757, BWI Airport, MD 21240. *STAR* is publicly available on annual subscription from the Superintendent of Documents, U.S. Government Printing Office, Washington, DC 20402.

PUBLISHED BY:

UNITED STATES GOVERNMENT
NATIONAL AERONAUTICS AND SPACE ADMINISTRATION
SCIENTIFIC AND TECHNICAL INFORMATION DIVISION
Scientific and Technical Aerospace Reports, Volume 28, is prepared by the NASA Scientific and Technical Information Facility operated for the National Aeronautics and Space Administration by RMS Associates.

The Administrator of the National Aeronautics and Space Administration has determined that the publication of this periodical is necessary in the transaction of the public business required by law of this agency. Use of funds for printing this periodical has been approved by the Director of the Office of Management and Budget through March 22, 1991.

US ISSN 0036-8741

Scientific and Technical Aerospace Reports (STAR) is issued twice a month and contains abstracts and indexes of meeting papers, conference proceedings, and unlimited distribution reports that have been added to the NASA Scientific and Technical Information Database during the preceding period. These citations may also be accessed online via NASA/RECON or via AIAA's Aerospace Database (File 108) through Dialog Information Services, Inc.

STAR subject coverage includes all aerospace-related areas that will help NASA achieve its mission. Material is gathered from all over the world and includes significant input from many countries under exchange and access agreements.

Consult the indexes at the back of this volume to help zero in on what you are looking for. These include:

Subject Index
Personal Author Index
Corporate Source Index
Contract Number Index
Report/Accession Number Index

STAR's companion abstract journal *International Aerospace Abstracts* should be used if you are looking for references to periodicals, books, and published meeting papers or conference proceedings.

Questions and comments should be addressed to:

NASA Scientific and Technical Information Facility
User Services
P.O. Box 8757
BWI Airport, MD 21240
301-621-0150

VOLUME 28 NUMBER 11 / JUNE 8, 1990

TABLE OF CONTENTS

AERONAUTICS

Includes aeronautics (general); aerodynamics; air transportation and safety; aircraft communications and navigation; aircraft design, testing and performance; aircraft instrumentation; aircraft propulsion and power; aircraft stability and control; and research and support facilities (air).

For related information see also *Astronautics.*

01 AERONAUTICS (GENERAL) **N.A.**

02 AERODYNAMICS **1451**

Includes aerodynamics of bodies, combinations, wings, rotors, and control surfaces; and internal flow in ducts and turbomachinery.

For related information see also *34 Fluid Mechanics and Heat Transfer.*

03 AIR TRANSPORTATION AND SAFETY **1453**

Includes passenger and cargo air transport operations; and aircraft accidents.

For related information see also *16 Space Transportation* and *85 Urban Technology and Transportation.*

04 AIRCRAFT COMMUNICATIONS AND NAVIGATION **1454**

Includes digital and voice communication with aircraft; air navigation systems (satellite and ground based); and air traffic control.

For related information see also *17 Space Communications, Spacecraft Communications, Command and Tracking* and *32 Communications and Radar.*

05 AIRCRAFT DESIGN, TESTING AND PERFORMANCE **1455**

Includes aircraft simulation technology.

For related information see also *18 Spacecraft Design, Testing and Performance* and *39 Structural Mechanics.* For land transportation vehicles see *85 Urban Technology and Transportation.*

06 AIRCRAFT INSTRUMENTATION **1457**

Includes cockpit and cabin display devices; and flight instruments.

For related information see also *19 Spacecraft Instrumentation* and *35 Instrumentation and Photography.*

07 AIRCRAFT PROPULSION AND POWER **1457**

Includes prime propulsion systems and systems components, e.g., gas turbine engines and compressors; and onboard auxiliary power plants for aircraft.

For related information see also *20 Spacecraft Propulsion and Power, 28 Propellants and Fuels,* and *44 Energy Production and Conversion.*

08 AIRCRAFT STABILITY AND CONTROL **1464**

Includes aircraft handling qualities; piloting; flight controls; and autopilots.

For related information see also *05 Aircraft Design, Testing and Performance.*

09 RESEARCH AND SUPPORT FACILITIES (AIR) **1465**

Includes airports, hangars and runways; aircraft repair and overhaul facilities; wind tunnels; shock tubes; and aircraft engine test stands.

For related information see also *14 Ground Support Systems and Facilities (Space).*

ASTRONAUTICS

Includes astronautics (general); astrodynamics; ground support systems and facilities (space); launch vehicles and space vehicles; space transportation; space communications, spacecraft communications, command and tracking; spacecraft design, testing and performance; spacecraft instrumentation; and spacecraft propulsion and power.

For related information see also *Aeronautics.*

12 ASTRONAUTICS (GENERAL) **1465**

For extraterrestrial exploration see *91 Lunar and Planetary Exploration.*

13 ASTRODYNAMICS **1465**

Includes powered and free-flight trajectories; and orbital and launching dynamics.

14 GROUND SUPPORT SYSTEMS AND FACILITIES (SPACE) **1466**

Includes launch complexes, research and production facilities; ground support equipment, e.g., mobile transporters; and simulators.

For related information see also *09 Research and Support Facilities (Air).*

15 LAUNCH VEHICLES AND SPACE VEHICLES **1466**

Includes boosters; operating problems of launch/space vehicle systems; and reusable vehicles.

For related information see also *20 Spacecraft Propulsion and Power.*

16 SPACE TRANSPORTATION **1466**

Includes passenger and cargo space transportation, e.g., shuttle operations; and space rescue techniques.

For related information see also *03 Air Transportation and Safety* and *18 Spacecraft Design, Testing and Performance.* For space suits see *54 Man/System Technology and Life Support.*

17 SPACE COMMUNICATIONS, SPACECRAFT COMMUNICATIONS, COMMAND AND TRACKING **1467**

Includes telemetry; space communications networks; astronavigation and guidance; and radio blackout.

For related information see also *04 Aircraft Communications and Navigation* and *32 Communications and Radar.*

18 SPACECRAFT DESIGN, TESTING AND PERFORMANCE 1467

Includes satellites; space platforms; space stations; spacecraft systems and components such as thermal and environmental controls; and attitude controls.

For life support systems see *54 Man/System Technology and Life Support.* For related information see also *05 Aircraft Design, Testing and Performance, 39 Structural Mechanics,* and *16 Space Transportation.*

19 SPACECRAFT INSTRUMENTATION 1470

For related information see also *06 Aircraft Instrumentation* and *35 Instrumentation and Photography.*

20 SPACECRAFT PROPULSION AND POWER 1470

Includes main propulsion systems and components, e.g. rocket engines; and spacecraft auxiliary power sources.

For related information see also *07 Aircraft Propulsion and Power, 28 Propellants and Fuels, 44 Energy Production and Conversion,* and *15 Launch Vehicles and Space Vehicles.*

CHEMISTRY AND MATERIALS

Includes chemistry and materials (general); composite materials; inorganic and physical chemistry; metallic materials; nonmetallic materials; propellants and fuels; and materials processing.

23 CHEMISTRY AND MATERIALS (GENERAL) 1476

24 COMPOSITE MATERIALS 1476

Includes physical, chemical, and mechanical properties of laminates and other composite materials.

For ceramic materials see *27 Nonmetallic Materials.*

25 INORGANIC AND PHYSICAL CHEMISTRY 1482

Includes chemical analysis, e.g., chromatography; combustion theory; electrochemistry; and photochemistry.

For related information see also *77 Thermodynamics and Statistical Physics.*

26 METALLIC MATERIALS 1486

Includes physical, chemical, and mechanical properties of metals, e.g., corrosion; and metallurgy.

27 NONMETALLIC MATERIALS 1488

Includes physical, chemical, and mechanical properties of plastics, elastomers, lubricants, polymers, textiles, adhesives, and ceramic materials.

For composite materials see *24 Composite Materials.*

28 PROPELLANTS AND FUELS 1494

Includes rocket propellants, igniters and oxidizers; their storage and handling procedures; and aircraft fuels.

For related information see also *07 Aircraft Propulsion and Power, 20 Spacecraft Propulsion and Power,* and *44 Energy Production and Conversion.*

29 MATERIALS PROCESSING 1495

Includes space-based development of products and processes for commercial application.

For biological materials see *55 Space Biology.*

ENGINEERING

Includes engineering (general); communications and radar; electronics and electrical engineering; fluid mechanics and heat transfer; instrumentation and photography; lasers and masers; mechanical engineering; quality assurance and reliability; and structural mechanics.

For related information see also *Physics.*

31 ENGINEERING (GENERAL) 1496

Includes vacuum technology; control engineering; display engineering; cryogenics; and fire prevention.

32 COMMUNICATIONS AND RADAR 1496

Includes radar; land and global communications; communications theory; and optical communications.

For related information see also *04 Aircraft Communications and Navigation* and *17 Space Communications, Spacecraft Communications, Command and Tracking.* For search and rescue see *03 Air Transportation and Safety,* and *16 Space Transportation.*

33 ELECTRONICS AND ELECTRICAL ENGINEERING 1500

Includes test equipment and maintainability; components, e.g., tunnel diodes and transistors; microminiaturization; and integrated circuitry.

For related information see also *60 Computer Operations and Hardware* and *76 Solid-State Physics.*

34 FLUID MECHANICS AND HEAT TRANSFER 1505

Includes boundary layers; hydrodynamics; fluidics; mass transfer and ablation cooling.

For related information see also *02 Aerodynamics* and *77 Thermodynamics and Statistical Physics.*

35 INSTRUMENTATION AND PHOTOGRAPHY 1510

Includes remote sensors; measuring instruments and gauges; detectors; cameras and photographic supplies; and holography.

For aerial photography see *43 Earth Resources and Remote Sensing.* For related information see also *06 Aircraft Instrumentation* and *19 Spacecraft Instrumentation.*

36 LASERS AND MASERS 1513

Includes parametric amplifiers.

For related information see also *76 Solid-State Physics.*

37 MECHANICAL ENGINEERING 1516

Includes auxiliary systems (nonpower); machine elements and processes; and mechanical equipment.

38 QUALITY ASSURANCE AND RELIABILITY 1518

Includes product sampling procedures and techniques; and quality control.

39 STRUCTURAL MECHANICS 1518

Includes structural element design and weight analysis; fatigue; and thermal stress.

For applications see *05 Aircraft Design, Testing and Performance* and *18 Spacecraft Design, Testing and Performance.*

GEOSCIENCES

Includes geosciences (general); earth resources and remote sensing; energy production and conversion; environment pollution; geophysics; meteorology and climatology; and oceanography.

For related information see also *Space Sciences.*

42 GEOSCIENCES (GENERAL) N.A.

43 EARTH RESOURCES AND REMOTE SENSING 1520

Includes remote sensing of earth resources by aircraft and spacecraft; photogrammetry; and aerial photography.

For instrumentation see *35 Instrumentation and Photography.*

44 ENERGY PRODUCTION AND CONVERSION 1527

Includes specific energy conversion systems, e.g., fuel cells; global sources of energy; geophysical conversion; and windpower.

For related information see also *07 Aircraft Propulsion and Power, 20 Spacecraft Propulsion and Power,* and *28 Propellants and Fuels.*

45 ENVIRONMENT POLLUTION 1531

Includes atmospheric, noise, thermal, and water pollution.

46 GEOPHYSICS 1533

Includes aeronomy; upper and lower atmosphere studies; ionospheric and magnetospheric physics; and geomagnetism.

For space radiation see *93 Space Radiation.*

47 METEOROLOGY AND CLIMATOLOGY 1535

Includes weather forecasting and modification.

48 OCEANOGRAPHY 1537

Includes biological, dynamic, and physical oceanography; and marine resources.

For related information see also *43 Earth Resources and Remote Sensing.*

LIFE SCIENCES

Includes life sciences (general); aerospace medicine; behavioral sciences; man/system technology and life support; and space biology.

51 LIFE SCIENCES (GENERAL) 1538

52 AEROSPACE MEDICINE 1538

Includes physiological factors; biological effects of radiation; and effects of weightlessness on man and animals.

53 BEHAVIORAL SCIENCES 1541

Includes psychological factors; individual and group behavior; crew training and evaluation; and psychiatric research.

54 MAN/SYSTEM TECHNOLOGY AND LIFE SUPPORT 1541

Includes human engineering; biotechnology; and space suits and protective clothing.

For related information see also *16 Space Transportation.*

55 SPACE BIOLOGY N.A.

Includes exobiology; planetary biology; and extraterrestrial life.

MATHEMATICAL AND COMPUTER SCIENCES

Includes mathematical and computer sciences (general); computer operations and hardware; computer programming and software; computer systems; cybernetics; numerical analysis; statistics and probability; systems analysis; and theoretical mathematics.

59 MATHEMATICAL AND COMPUTER SCIENCES (GENERAL) N.A.

60 COMPUTER OPERATIONS AND HARDWARE 1542

Includes hardware for computer graphics, firmware, and data processing.

For components see *33 Electronics and Electrical Engineering.*

61 COMPUTER PROGRAMMING AND SOFTWARE 1543

Includes computer programs, routines, algorithms, and specific applications, e.g., CAD/CAM.

62 COMPUTER SYSTEMS 1547

Includes computer networks and special application computer systems.

63 CYBERNETICS 1548

Includes feedback and control theory, artificial intelligence, robotics and expert systems.

For related information see also *54 Man/System Technology and Life Support.*

64 NUMERICAL ANALYSIS 1550

Includes iteration, difference equations, and numerical approximation.

65 STATISTICS AND PROBABILITY 1554

Includes data sampling and smoothing; Monte Carlo method; and stochastic processes.

66 SYSTEMS ANALYSIS 1555

Includes mathematical modeling; network analysis; and operations research.

67 THEORETICAL MATHEMATICS N.A.

Includes topology and number theory.

PHYSICS

Includes physics (general); acoustics; atomic and molecular physics; nuclear and high-energy physics; optics; plasma physics; solid-state physics; and thermodynamics and statistical physics.

For related information see also *Engineering.*

70 PHYSICS (GENERAL) 1555

For precision time and time interval (PTTI) see *35 Instrumentation and Photography;* for geophysics, astrophysics or solar physics see *46 Geophysics, 90 Astrophysics,* or *92 Solar Physics.*

71 ACOUSTICS 1562
Includes sound generation, transmission, and attenuation.
For noise pollution see *45 Environment Pollution.*

72 ATOMIC AND MOLECULAR PHYSICS 1562
Includes atomic structure, electron properties, and molecular spectra.

73 NUCLEAR AND HIGH-ENERGY PHYSICS 1565
Includes elementary and nuclear particles; and reactor theory.
For space radiation see *93 Space Radiation.*

74 OPTICS 1566
Includes light phenomena and optical devices.
For lasers see *36 Lasers and Masers.*

75 PLASMA PHYSICS 1567
Includes magnetohydrodynamics and plasma fusion.
For ionospheric plasmas see *46 Geophysics.* For space plasmas see *90 Astrophysics.*

76 SOLID-STATE PHYSICS 1569
Includes superconductivity.
For related information see also *33 Electronics and Electrical Engineering* and *36 Lasers and Masers.*

77 THERMODYNAMICS AND STATISTICAL PHYSICS 1573
Includes quantum mechanics; theoretical physics; and Bose and Fermi statistics.
For related information see also *25 Inorganic and Physical Chemistry* and *34 Fluid Mechanics and Heat Transfer.*

SOCIAL SCIENCES

Includes social sciences (general); administration and management; documentation and information science; economics and cost analysis; law, political science, and space policy; and urban technology and transportation.

80 SOCIAL SCIENCES (GENERAL) N.A.
Includes educational matters.

81 ADMINISTRATION AND MANAGEMENT 1574
Includes management planning and research.

82 DOCUMENTATION AND INFORMATION SCIENCE 1574
Includes information management; information storage and retrieval technology; technical writing; graphic arts; and micrography.
For computer documentation see *61 Computer Programming and Software.*

83 ECONOMICS AND COST ANALYSIS N.A.
Includes cost effectiveness studies.

84 LAW, POLITICAL SCIENCE AND SPACE POLICY N.A.
Includes NASA appropriation hearings; aviation law; space law and policy; international law; international cooperation; and patent policy.

85 URBAN TECHNOLOGY AND TRANSPORTATION 1575
Includes applications of space technology to urban problems; technology transfer; technology assessment; and surface and mass transportation.
For related information see *03 Air Transportation and Safety, 16 Space Transportation,* and *44 Energy Production and Conversion.*

SPACE SCIENCES

Includes space sciences (general); astronomy; astrophysics; lunar and planetary exploration; solar physics; and space radiation.
For related information see also *Geosciences.*

88 SPACE SCIENCES (GENERAL) N.A.

89 ASTRONOMY 1577
Includes radio, gamma-ray, and infrared astronomy; and astrometry.

90 ASTROPHYSICS 1590
Includes cosmology; celestial mechanics; space plasmas; and interstellar and interplanetary gases and dust.
For related information see also *75 Plasma Physics.*

91 LUNAR AND PLANETARY EXPLORATION 1593
Includes planetology; and manned and unmanned flights.
For spacecraft design or space stations see *18 Spacecraft Design, Testing and Performance.*

92 SOLAR PHYSICS 1594
Includes solar activity, solar flares, solar radiation and sunspots.
For related information see *93 Space Radiation.*

93 SPACE RADIATION 1594
Includes cosmic radiation; and inner and outer earth's radiation belts.
For biological effects of radiation see *52 Aerospace Medicine.* For theory see *73 Nuclear and High-Energy Physics.*

GENERAL

Includes aeronautical, astronautical, and space science related histories, biographies, and pertinent reports too broad for categorization; histories or broad overviews of NASA programs.

99 GENERAL 1595

Note: N.A. means that no abstracts were assigned to this category for this issue.

SUBJECT INDEX I-1
PERSONAL AUTHOR INDEX I-55
CORPORATE SOURCE INDEX I-63
CONTRACT NUMBER INDEX I-75
REPORT/ACCESSION NUMBER INDEX .. I-77
APPENDIX—ABOUT STAR A-1

TYPICAL CITATION AND ABSTRACT

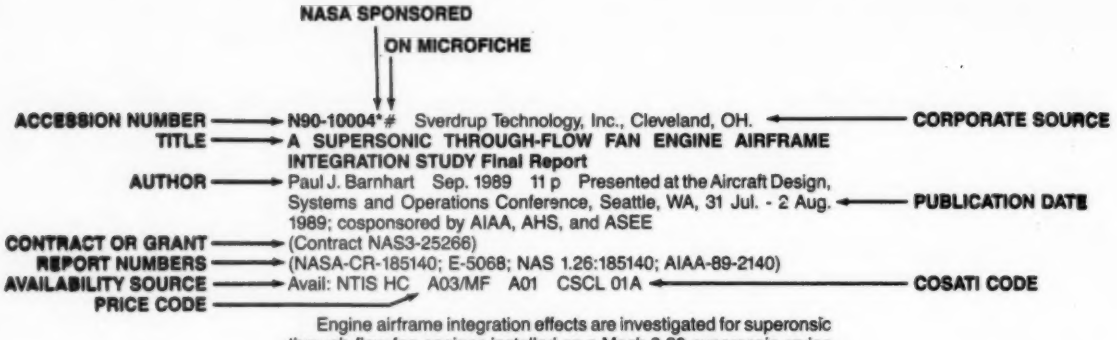
NASA SPONSORED
ON MICROFICHE
ACCESSION NUMBER
N90-10004*# Sverdrup Technology, Inc., Cleveland, OH.
CORPORATE SOURCE
TITLE
A SUPERSONIC THROUGH-FLOW FAN ENGINE AIRFRAME INTEGRATION STUDY Final Report
AUTHOR
Paul J. Barnhart Sep. 1989 11 p Presented at the Aircraft Design, Systems and Operations Conference, Seattle, WA, 31 Jul. - 2 Aug. 1989; cosponsored by AIAA, AHS, and ASEE
PUBLICATION DATE
CONTRACT OR GRANT
(Contract NAS3-25266)
REPORT NUMBERS
(NASA-CR-185140; E-5068; NAS 1.26:185140; AIAA-89-2140)
AVAILABILITY SOURCE
Avail: NTIS HC A03/MF A01 CSCL 01A
COSATI CODE
PRICE CODE

Engine airframe integration effects are investigated for superonsic through-flow fan engines installed on a Mach 3.20 supersonic cruise vehicle. Six different supersonic through-flow fan engine installations covering the effects of engine size, nacelle contour, nacelle placement, and approximate bypass plume effects are presented. The different supersonic through-flow fan installations are compared with a conventional turbine bypass engine configuration on the same basic airframe. The supersonic through-flow fan engine integrations are shown to be comparable to the turbine bypass engine configuration on the basis of installed nacelle wave drag. The supersonic through-flow fan engine airframe integrated vehicles have superior aerodynamic performance on the basis of maximum lift-to-drag ratio than the turbine bypass engine installation over the entire operating Mach number range from 1.10 to 3.20. When approximate bypass plume modeling is included, the supersonic through-flow fan engine configuration shows even larger improvements over the turbine bypass engine configuration. Author

VOLUME 28 NUMBER 11 / JUNE 8, 1990

Scientific and Technical Aerospace Reports

A Semimonthly Publication of the National Aeronautics and Space Administration

01 AERONAUTICS (GENERAL)

No abstracts in this category.

02 AERODYNAMICS

Includes aerodynamics of bodies, combinations, wings, rotors, and control surfaces; and internal flow in ducts and turbomachinery.

For related information see also *34 Fluid Mechanics and Heat Transfer.*

N90-18361# Bihrle Applied Research, Inc., Jericho, NY.
STATIC AND ROTATIONAL AERODYNAMIC DATA FROM 0 DEG TO 90 DEG ANGLE OF ATTACK FOR A SERIES OF BASIC AND ALTERED FOREBODY SHAPES Final Report, Sep. 1986 - Feb. 1989
W. Bihrle, Jr., B. Barnhart, and E. Dickes Sep. 1989 368 p
(Contract F33615-86-C-3624)
(AD-A216582; BAR-89-2; WRDC-TR-89-3090) Avail: NTIS HC A16/MF A02 CSCL 01/1

This report contains static and rotational aerodynamic data from 0 to 90 degrees angle of attack for a series of basic and altered forebody shapes. GRA

N90-18362# Midwest Research Inst., Golden, CO. Solar Energy Research Inst.
AERODYNAMIC TESTING OF A ROTATING WIND TURBINE BLADE
C. P. Butterfield and E. N. Nelsen Jan. 1990 8 p Presented at the American Solar Energy Society Annual Meeting, Denver, CO, 19-23 Jun. 1989
(Contract DE-AC02-83CH-10093)
(DE90-000312; SERI/TP-257-3490; CONF-890610-7) Avail: NTIS HC A02/MF A01

Aerodynamic, load, flow-visualization, and inflow measurements were taken on a downwind horizontal-axis wind turbine (HAWT). A video camera mounted on the rotor recorded video images of tufts attached to the low-pressure side of the blade. Strain gages, mounted every 10 pct of the blade's span, provided load and pressure measurements. Pressure taps at 32 chordwise positions recorded pressure distributions. Wind inflow was measured via a vertical-plane array of anemometers located 10 m upwind. The objectives of the test were to address whether airfoil pressure distributions measured on a rotating blade differed from those measured in the wind tunnel, if radial flow near or in the boundary layer of the airfoil affected pressure distributions, if dynamic stall could result in increased dynamic loads, and if the location of the separation boundary measured on the rotating blade agreed with that measured in two-dimensional flow in the wind tunnel. DOE

N90-18363*# Institute for Computer Applications in Science and Engineering, Hampton, VA.
THE INVISCID STABILITY OF SUPERSONIC FLOW PAST A SHARP CONE Final Report
Peter W. Duck and Stephen J. Shaw Feb. 1990 61 p Submitted for publication
(Contract NAS1-18605)
(NASA-CR-181996; NAS 1.26:181996; ICASE-90-14) Avail: NTIS HC A04/MF A01 CSCL 01A

The laminar boundary layer which forms on a sharp cone in a supersonic freestream, where lateral curvature plays a key role in the physics of the problem is considered. This flow is then analyzed from the point of view of linear, temporal, inviscid stability. The basic, non-axisymmetric disturbance equations are derived for general flows of this class, and a so called triply generalized inflexion condition is found for the existence of subsonic neutral modes of instability. This condition is analogous to the well-known generalized inflexion condition found in planar flows, although in the present case the condition depends on both axial and aximuthal wavenumbers. Extensive numerical results are presented for the stability problem at a freestream Mach number of 3.8, for a range of streamwise locations. These results reveal that a new mode of instability may occur, peculiar to flows of this type involving curvature. Additionally, asymptotic analyses valid close to the tip of the cone, far downstream of the cone are presented, and these give a partial (asymptotic) description of this additional mode of instability. Author

N90-18364* McDonnell Aircraft Co., Houston, TX. Engineering Technology Div.
RESEARCH ON A TWO-DIMENSIONAL INLET FOR A SUPERSONIC V/STOL PROPULSION SYSTEM. APPENDIX A Final Report, Sep. 1979 - Jun. 1984
J. L. Mark, M. A. McGarry, and P. V. Reagan Jun. 1984 880 p
(Contract NAS3-22158)
(NASA-CR-174945; NAS 1.26:174945) Avail: NTIS HC A99/MF E06 CSCL 01A

The inlet system performance requirements associated with supersonic V/STOL aircraft place extreme demands on the inlet designer. The present effort makes maximum use of flow improvement techniques, proven for high subsonic maneuvering flight and adapts them to the critical static and low speed/high angle-of-attack flight regime of the supersonic V/STOL aircraft. A description of the aerodynamic design, model characteristics, data analysis, discussion, and conclusions concerning the most promising inlet design approaches are contained. The appendix contains the reduced wind tunnel data plots and pressure distribution. Author

N90-18365# Institut Franco-Allemand de Recherches, Saint-Louis (France).
PREDICTION OF ROTOR BLADE-VORTEX INTERACTION NOISE FROM 2-D AERODYNAMIC CALCULATIONS AND MEASUREMENTS
J. Haertig and M. Caplot (Office National d'Etudes et de Recherches Aerospatiales, Paris, France) 3 Nov. 1988 23 p Presented at 14th European Rotorcraft Forum, Milan, Italy, 20-23 Sep. 1988 Previously announced in IAA as A89-29280 Sponsored by Direction des Recherches, Etudes et Techniques, Paris, France
(ISL-CO-243/88; ETN-90-96247) Avail: NTIS HC A03/MF A01

The problem of blade-vortex interaction is studied numerically and experimentally. Aerodynamic analysis is based on the computation of the velocity potential in a two dimensional,

incompressible, inviscid and unsteady flow. It gives the instantaneous velocity field around a lifting Joukowski airfoil under the action of an incident vortex; pressure, lift and drag coefficients are deduced. Theoretical results are compared with measurements in a water tunnel where the vortex is generated by an oscillating airfoil upstream of the airfoil under study. A laser anemometer is used to measure the instantaneous vorticity field behind the first airfoil and a balance measures the forces acting on the receiving airfoil. Good agreement is found between measured and calculated lift coefficients. The aerodynamic analysis provides the inputs of an acoustic code. Two dimensional data are transformed to study the case of a parallel blade-vortex interaction of a helicopter rotor. The acoustic method is described and preliminary results are presented, showing some limitations of the technique. ESA

N90-18366# Institut Franco-Allemand de Recherches, Saint-Louis (France).

SUPERSONIC WIND TUNNEL INVESTIGATION OF A TUBULAR PROJECTILE

C. Berner and M. Giraud 1989 10 p Presented at the 11th International Symposium on Ballistics, Brussels, Belgium, 9-11 May 1989

(ISL-CO-306/89; ETN-90-96252) Avail: NTIS HC A02/MF A01

An experimental investigation of a tubular projectile was performed in a supersonic wind tunnel in order to complete results obtained in the aeroballistic range facility. Experiments were conducted in a blow down type supersonic wind tunnel at Mach numbers 2.06, 3.02, and 4.38 and for angles of attack between -7-5 deg. Circular models and a model with an equivalent squared cross-section equipped with glass side walls were used for flow visualization and to obtain pressure distributions on the internal and external surfaces. Results show some interesting features of the choked and started flow regimes, namely the internal shock pattern originating from the leading edge. Comparison made between the free-flight and wind tunnel results shows good qualitative agreement. ESA

N90-18367# Aix-Marseilles Univ. (France). Inst. de Mecanique de la Turbulence.

AERODYNAMICS OF UNSTEADY SYSTEMS. NUMERICAL STUDY OF POTENTIAL FLOW/BOUNDARY LAYER COUPLING [AERODYNAMIQUE INSTATIONNAIRE: ETUDE NUMERIQUE DU COUPLAGE ECOULEMENT POTENTIEL/COUCHE LIMITE: RAPPORT D'AVANCEMENT DES TRAVAUX]

C. Beguier, P. Fraunie, A. Maatouch, and D. Foussekis Jun. 1989 87 p In FRENCH

(Contract DRET-82-272)

(ETN-90-96257) Avail: NTIS HC A05/MF A01

Software is developed for the two-dimensional calculation of the unsteady flow around a moving wing. The software allows the analysis of potential flow/boundary layer coupling, occurring under different cyclic movements such as helicopter rotors. The determination of the instantaneous pressure and flow velocity distribution on a moving wing are obtained. The results of the experiments carried out on a flat plate are given. The proposed coupling solution method seems to be to date the most suitable to describe the unsteady aerodynamic field around a moving wing. ESA

N90-18368# Technische Univ., Delft (Netherlands).

COMPUTATIONAL AERODYNAMICS OF ORDERED VORTEX FLOWS Ph.D. Thesis

H. W. M. Hoeijmakers 1989 199 p Sponsored in part by Directorate of Material of the Royal Netherlands Air Force

(ETN-90-96272) Avail: NTIS HC A09/MF A02

The physical aspects, the mathematical modeling, the development and application of computational methods for the simulation of vortical flows are described. The high Reynolds number vortex flows considered are assumed to be steady, subcritical and such that the structure of the flow is well ordered and consists of thin shear layers and slender vortex cores embedded in otherwise irrotational flow. The applications considered are vortex wakes and the flow about 3-D (slender) configurations with the flow separating from known separation lines, mostly the sharp leading edges. The computing times required for the two quasi 2-D flow methods are quite modest. The ones for the 3-D flow method become quite substantial for the cases with the finer panel schemes, although remain modest compared to those required for Euler or Navier-Stokes based methods. ESA

N90-18369# Bristol Univ. (England). Dept. of Aerospace Engineering.

OPTIMUM SPANWISE CAMBER FOR MINIMUM INDUCED DRAG

Martin V. Lowson Nov. 1989 18 p

(BU-403; ETN-90-96286) Avail: NTIS HC A03/MF A01

Linear theory is used to develop optimum circulation distributions and their associated minimum induced drag for wakes from lifting surfaces with arbitrary spanwise camber. The work is largely computational, and results for cases previously investigated analytically are generally in good agreement. Some previously published results are found to be in error, and a new solution for the induced drag of a wing with dihedral is given. New results are computed for polynomial and superelliptic camber lines which may be of practical interest. An empirical correlation is demonstrated between the induced drag factor and the inverse arc length for a variety of optimum cases. Conclusions are given which suggest that the most effective form of camber for a given maximum displacement is the end plate, but elliptic and superelliptic shapes are slightly more effective in terms of minimum length of wing for a given displacement. ESA

N90-18370# Deutsche Forschungsanstalt fuer Luft- und Raumfahrt, Goettingen (Germany, F.R.). Hauptabt. Windkanale.

HALF MODEL TESTS ON AN ONERA CALIBRATION MODEL IN THE TRANSONIC WIND TUNNEL GOETTINGEN, FEDERAL REPUBLIC OF GERMANY

Wolfgang Lorenz-Meyer May 1989 44 p In GERMAN; ENGLISH summary Report will also be announced as translation (ESA-TT-1195)

(DLR-Mitt-89-20; ISSN-0176-7739; ETN-90-96275; ESA-TT-1195)

Avail: NTIS HC A03/MF A01; DLR, Wissenschaftliches Berichtswesen, Postfach 90 60 58, 5000 Cologne 90, Fed. Republic of Germany, 18.50 deutsche marks

Force and pressure distribution measurements in three wing sections are performed in the 1 m by 1 m transonic wind tunnel of the DLR using an ONERA calibration model. The model is mounted on the scale without a splitter-plate but with a 5 mm thick boundary layer trap. The results are compared to complete model tests carried out at ONERA and DLR. Standard wind tunnel correction is shown not to be sufficient for correcting half-model data. Flow visualization is obtained using oil-flow techniques. ESA

N90-18427# Vrije Univ., Brussels (Belgium). Dept. of Fluid Mechanics.

MEASUREMENT OF VELOCITY PROFILES AND REYNOLDS STRESSES ON AN OSCILLATING AIRFOIL

J. DeRuyck, B. Hazarika, and C. Hirsch *In* AGARD, Unsteady Aerodynamic Phenomena in Turbomachines Feb. 1990 15 p

(For primary document see N90-18405 11-07)

(Contract DAJA45-85-C-0039)

Copyright Avail: NTIS HC A14/MF A02; Non-NATO Nationals requests available only from AGARD/Scientific Publications Executive

03 AIR TRANSPORTATION AND SAFETY

Includes passenger and cargo air transport operations; and aircraft accidents.

For related information see also *16 Space Transportation* and *85 Urban Technology and Transportation.*

N90-18371*# Environmental Research Inst. of Michigan, Ann Arbor.
SYNTHETIC APERTURE RADAR IMAGERY OF AIRPORTS AND SURROUNDING AREAS: ARCHIVED SAR DATA Final Report, 31 Aug. 1987 - 30 Nov. 1989
Robert G. Onstott and Denise J. Gineris Washington NASA Feb. 1990 214 p
(Contract NAS1-18465)
(NASA-CR-4275; NAS 1.26:4275; DOT/FAA/DS-89/14) Avail: NTIS HC A10/MF A02 CSCL 17I

The statistical description of ground clutter at an airport and in the surrounding area is addressed. These data are being utilized in a program to detect microbursts. Synthetic aperture radar (SAR) data were acquired from the ERIM SAR data archive and were examined for utility to this program. Eight digital scattering coefficient images were created of five airports. These data are described along with the results of the clutter study. These scenes were imaged at 9.38 GHz and HH- and VV-polarizations and contained airport grounds and facilities, industrial, residential, fields, forest, and water. Incidence angles ranged from 12 to 72 deg. Even at the smallest incidence angles, the distributed targets such as forest, fields, water, and residential rarely had mean scattering coefficients greater than -10 dB. Eighty-seven percent of the image had scattering coefficients less than -17.5 dB. About 1 percent of the scattering coefficients exceeded 0 dB, with about 0.1 percent above 10 dB. Sources which produced the largest cross sections were largely confined to the airport grounds and areas highly industrialized. The largest cross sections were produced by observing large buildings surrounded by smooth surfaces.
Author

N90-18372*# Environmental Research Inst. of Michigan, Ann Arbor.
SYNTHETIC APERTURE RADAR IMAGERY OF AIRPORTS AND SURROUNDING AREAS: PHILADELPHIA AIRPORT Final Report, 31 Aug. 1987 - 30 Nov. 1989
Robert G. Onstott and Denise J. Gineris Mar. 1990 108 p
(Contract NAS1-18465)
(NASA-CR-4280; NAS 1.26:4280; DOT/FAA/DS-89/15) Avail: NTIS HC A06/MF A01 CSCL 01C

The statistical description of ground clutter at an airport and in the surrounding area is addressed. These data are being utilized in a program to detect microbursts. Synthetic Aperture Radar (SAR) data were collected at the Philadelphia Airport. These data and the results of the clutter study are described. This 13 km x 10 km scene was imaged at 9.38 GHz and HH-polarization and contained airport grounds and facilities (6 percent), industrial (14 percent), residential (14 percent), fields (10 percent), forest (8 percent), and water (33 percent). Incidence angles ranged from 40 to 84 deg. Even at the smallest incidence angles, the distributed targets such as forest, fields, water, and residential rarely had mean scattering coefficients greater than -10 dB. Eighty-seven percent of the image had scattering coefficients less than -17.5 dB. About 1 percent of the scattering coefficients exceeded 0 dB, with about 0.1 percent above 10 dB. Sources which produced the largest cross sections were largely confined to the airport grounds and areas highly industrialized. The largest cross sections were produced by observing broadside large buildings surrounded by smooth surfaces.
Author

N90-18373# Federal Aviation Administration, Washington, DC.
NATIONAL AIRSPACE SYSTEM PLAN: FACILITIES, EQUIPMENT, ASSOCIATED DEVELOPMENT AND OTHER CAPITAL NEEDS Annual Report
Sep. 1989 380 p
(AD-A215882) Avail: NTIS HC A17/MF A02 CSCL 17/7

The National Airspace System (NAS) is the busiest and most complex in the world. It is a mixture of equipment, techniques, and skills that has evolved over 50 years. Without question, it is the world's safest and most efficient, yet, at the outset of this plan, its expansion capability was limited and adaptability to changing requirements was difficult. Aviation activity is forecast to increase substantially over the next two decades. Continuing growth in the number of aircraft operations, number of aircraft, enplanements, diversity of operations, DOD operations and sophistication of aircraft will place unprecedented demands on the NAS. Meeting this challenge requires improved and expanded services, additional facilities and equipment, improved work force productivity, and the orderly replacement of aging equipment. In December, 1981, the Federal Aviation Administration (FAA) chartered a comprehensive NAS Plan for modernizing and improving air traffic control and airway facilities services through the year 2000. This is the seventh annual update of the NAS Plan. The Plan addresses the compelling problems of how best to improve safety and efficiency, accommodate spiraling demands for aviation services, deal with the problems of aging or obsolete facilities, recognize the users desires for minimal restrictions on the use of the airspace, allow for a reduced Federal role, and create a foundation for continued evolution which exploits newer technologies and developments.
GRA

N90-18374# Federal Aviation Administration, Washington, DC. Office of Aviation Medicine.
THE EFFECTS OF WEARING PASSENGER PROTECTIVE BREATHING EQUIPMENT ON EVACUATION TIMES THROUGH TYPE 3 AND TYPE 4 EMERGENCY AIRCRAFT EXITS IN CLEAR AIR AND SMOKE. PHASE 1: EVACUATIONS IN CLEAR AIR. PHASE 2: EVACUATIONS IN SMOKE Final Report
Garnet A. McLean, E. Arnold Higgins, Peggy J. Lyne, and James H. B. Vant (Oxford Univ., England) Nov. 1989 33 p Sponsored by FAA, Washington, DC
(AD-A216798; DOT/FAA/AM-89/12-Phase-1/2) Avail: NTIS HC A03/MF A01 CSCL 01/5

The effects of Passenger Protective Breathing Equipment (PPBE) on the time required for simulated emergency evacuations through Type 3 and Type 4 overwing aircraft exits were studied in two quasi-independent experiments, one in clear air and another in smoke. Two different types of PPBE, the Dupont PELS and the Sabre Industries Sabre, were used in both experiments. Eight groups of 20 subjects participated in each experiment; each group of subjects evacuated with/without PPBE. The order of PPBE presentation condition was counterbalanced to allow analysis of evacuation experience, i.e., learning. The results obtained supported the conclusion that exit hatch opening size was the most important factor in determining the time required to evacuate through these exits, followed next by the effects of smoke, and finally by the wearing of PPBE. It was further concluded that because the PPBE effects were isolated to the time required to cross the exit hatch opening, the effects of PPBE were actually dependent on exit hatch opening size. The effects of smoke were seen to result from the necessity of using tactile information to control egress in the impoverished visual environment afforded subjects. These results were discussed in relation to passenger ergonomics and aircraft design.
GRA

N90-18375# Dayton Univ., OH. Structural Integrity Div.
STUDY OF BIRD INGESTIONS INTO SMALL INLET AREA, AIRCRAFT TURBINE ENGINES (MAY 1987 TO APRIL 1988) Interim Report
Joseph P. Martino and Donald A. Skinn Atlantic City, NJ FAA Dec. 1989 70 p
(Contract DTFA03-88-C-00024)
(DOT/FAA/CT-89/17; UDR-TR-89-03) Avail: NTIS HC A04/MF A01

The Federal Aviation Administration Technical Center initiated a study to determine the numbers, sizes, and types of birds which are being ingested into small inlet area turbofan and turbine engines and to determine what damage, if any, results. Bird ingestion data

are being collected for the ALF502, TFE731, and TPE331 engines. The first of 2 years of data collection is analyzed. Author

N90-18376# Centre d'Essais Aeronautique Toulouse (France). Lab. Essais d'Impacts sur Structures.
BIRD IMPACT TESTS ON A KEVLAR 49 STRUCTURE. MONOLITHIC PLATES. OBLIQUE-ANGLED IMPACT Partial Test Report No. 2 [ESSAIS D'IMPACTS D'OISEAUX SUR STRUCTURE KEVLAR 49. PLAQUES MONOLITHES-TIRS OBLIQUES. PROCES-VERBAL S3-4273 PARTIEL NO. 2]
6 Jul. 1988 51 p In FRENCH
(Rept-S3-4273; CEAT-NT-10/S/83; ETN-90-96258) Avail: NTIS HC A04/MF A01

The results of experiments concerning the impacts of 4 pound birds on flat rectangular and square monolithic Kevlar 49 plates are reported. Projectile trajectories and different angles of attack are investigated. It is observed that the painted coating used for protecting Kevlar 49 surfaces improves the sliding of the birds over the surface after the impact. The results show that the impact energy perpendicular to the surface is lower in the oblique-angled shot than in the normal shot and remains lower than the piercing energy. ESA

N90-18377# Deutsche Forschungsanstalt fuer Luft- und Raumfahrt, Oberpfaffenhofen (Germany, F.R.). Abt. Wolkenphysik.
THE SIGNALS OF AN ICE WARNING DEVICE IN DEPENDENCE ON TOTAL WATER CONTENT AND NORMALIZED ICING DEGREE
Hans-Eberhard Hoffmann, Johann Demmel, and Joachim Schuster Jun. 1989 59 p In GERMAN; ENGLISH summary
(DLR-FB-89-52; ISSN-0171-1342; ETN-90-96279) Avail: NTIS HC A04/MF A01; DLR, Wissenschaftliches Berichtswesen, Postfach 90 60 58, 5000 Cologne 90, Fed. Republic of Germany, 22.50 deutsche marks

The performance of an icing warning device, type 871, is described. The device worked well over the course of 70 hours of all icing flights. The ice accretion on a metal rod with the same diameter as the ice warning device was photographed over the course of special flights. Even at temperatures of above -4.5 C, only a part of the water of the impinging undercooled cloud particles adhered as ice on the sensor rod. The sensitivity of the output signal of ice accretion velocity as a measure of short term total water content became lower when the inhomogenity of the clouds increased. ESA

04 AIRCRAFT COMMUNICATIONS AND NAVIGATION

Includes digital and voice communication with aircraft; air navigation systems (satellite and ground based); and air traffic control.

For related information see also *17 Space Communications, Spacecraft Communications, Command and Tracking* and *Communications and Radar.*

N90-18378*# National Aeronautics and Space Administration. Langley Research Center, Hampton, VA.
DELIVERY PERFORMANCE OF CONVENTIONAL AIRCRAFT BY TERMINAL-AREA, TIME-BASED AIR TRAFFIC CONTROL: A REAL-TIME SIMULATION EVALUATION
Leonard Credeur, Jacob A. Houck, William R. Capron, and Gary W. Lohr (Embry-Riddle Aeronautical Univ., Daytona Beach, FL.) Washington Apr. 1990 66 p
(NASA-TP-2978; L-16615; NAS 1.60:2978) Avail: NTIS HC A04/MF A01 CSCL 17G

A description and results are presented of a study to measure the performance and reaction of airline flight crews, in a full workload DC-9 cockpit, flying in a real-time simulation of an air traffic control (ATC) concept called Traffic Intelligence for the Management of Efficient Runway-scheduling (TIMER). Experimental objectives were to verify earlier fast-time TIMER time-delivery precision results and obtain data for the validation or refinement of existing computer models of pilot/airborne performance. Experimental data indicated a runway threshold, interarrival-time-error standard deviation in the range of 10.4 to 14.1 seconds. Other real-time system performance parameters measured include approach speeds, response time to controller turn instructions, bank angles employed, and ATC controller message delivery-time errors. Author

N90-18379*# National Aeronautics and Space Administration. Pasadena Office, CA.
EFFICIENT DETECTION AND SIGNAL PARAMETER ESTIMATION WITH APPLICATION TO HIGH DYNAMIC GPS RECEIVER Patent Application
Rajendra Kumar, inventor (to NASA) (Jet Propulsion Lab., California Inst. of Tech., Pasadena.) 31 Oct. 1989 45 p
(Contract NAS7-918)
(NASA-Case-NPO-17820-1-CU; US-Patent-Appl-SN-429734; NAS 1.71:NPO-17820-1-CU) Avail: NTIS HC A03/MF A01 CSCL 17G

In a system for deriving position, velocity, and acceleration information from a received signal emitted from an object to be tracked wherein the signal comprises a carrier signal phase modulated by unknown binary data and experiencing very high Doppler and Doppler rate, this invention provides combined estimation/detection apparatus for simultaneously detecting data bits and obtaining estimates of signal parameters such as carrier phase and frequency related to receiver dynamics in a sequential manner. There is a first stage for obtaining estimates of the signal parameters related to phase and frequency in the vicinity of possible data transitions on the basis of measurements obtained within a current data bit. A second stage uses the estimates from the first stage to decide whether or not a data transition has actually occurred. There is a third stage for removing data modulation from the received signal when a data transition has occurred and a fourth stage for using the received signal with data modulation removed therefrom to update global parameters which are dependent only upon receiver dynamics and independent of data modulation. Finally, there is a fifth stage for using the global parameters to determine the position, velocity, and acceleration of the object. NASA

N90-18380# Federal Aviation Administration, Atlantic City, NJ.
DALLAS/FORT WORTH SIMULATION. VOLUME 2: APPENDIXES D, E, AND F
Lloyd Hitchcock, Lee E. Paul, Ephraim Shocket, and Richard D. Algeo Nov. 1989 289 p
(AD-A216613; DOT/FAA/CT-TN89/28-Vol-2) Avail: NTIS HC A13/MF A02 CSCL 01/5

A series of dynamic, real time, air traffic control simulations of selected aspects of the D/FW Metroplex Air Traffic System Plan were conducted. Using D/FW controllers as subjects, the simulations provided an opportunity to evaluate proposed changes in area flow patterns and traffic management and to experience simultaneous approaches to the four parallel runway configuration under consideration for D/FW. The results of these simulations demonstrated that, even when faced with up to twice their normal traffic load, the controllers could maintain a smooth and safe flow of traffic using the new configurations proposed for the D/FW area. The D/FW Evaluation Team declared that the parallel arrival routes, separate altitudes for high performance turboprops, increased departure routes, and stratified sectors all proved to be valuable controller tools. In addition, simulation of the four simultaneous parallel approaches led to the Evaluation Team to enthusiastically endorse the concept of four simultaneous approaches to the D/FW airport and to affirm that in each and every case the concept proved to be safe even though frequently challenged by the unlikely conditions of 30 degree blunders without communications. GRA

N90-18381# Defence Research Establishment, Ottawa (Ontario).
AN ERROR SENSITIVITY MODEL FOR DOPPLER POSITIONING USING TRANSIT SATELLITES
J. Christopher McMillan Aug. 1989 142 p
(AD-A216724; DREO-1015) Avail: NTIS HC A07/MF A01 CSCL 17/7

The Transit satellite positioning system is a commonly used navigation aid included in the Marine Integrated Navigation System (MINS-B II) and Primary Land Arctic Navigation System (PLANS). MINS and PLANS are both Kalman filter based multi-sensor optimally integrated navigation systems and as such require detailed stochastic and deterministic error models for all of their sensors (to form the Kalman filter measurement error sensitivity matrices). This paper provides a detailed geometric derivation of the deterministic error model relating the position error of a Transit satellite Doppler position fix (or similarly a SARSAT fix) to the error in the velocity and height that is fed into the Transit receiver (or assumed for the SARSAT transponder). This error model is presented in the form of explicit functions of variables which are normally provided by a Transit receiver with each position fix, namely the satellite maximum elevation angle, the satellite direction of travel and the receiver latitude. For generality the satellite orbital parameters are left in the expressions. GRA

N90-18382# Massachusetts Inst. of Tech., Cambridge. Dept. of Electrical Engineering and Computer Science.
VISUAL NAVIGATION: CONSTRUCTING AND UTILIZING SIMPLE MAPS OF AN INDOOR ENVIRONMENT M.S. Thesis
Karen Beth Sarachik Mar. 1989 94 p
(Contracts N00014-86-K-0685; N00014-85-K-0124)
(AD-A216761; AI-TR-1113) Avail: NTIS HC A05/MF A01 CSCL 17/7

Much work with mobile robots has been done in the past using both vision and sonar to build maps, or, given a map, to successfully plan and execute trajectories to a goal. The most successful examples of robot navigation occurred in carefully engineered environments where the robot was able to accurately predict what its sensory input should be at any point, and correct for drift by comparing actual input to the projected input. In unstructured environments however, the problem became much harder, and the obvious approaches failed to produce good results. The problem is further complicated by the fact that most interesting environments are not static, but rather are changing continually. In this thesis I have attempted to attack the problem from a different angle altogether, using the way people navigate through buildings as insight and inspiration. The goal is to navigate through an office environment using only visual information gathered from four cameras, whose initial detailed configuration is not known, placed onboard a mobile robot. The method is insensitive to physical changes within the room it is inspecting, such as moving objects. GRA

N90-18383# Test Group (6585th), Holloman AFB, NM.
THE FOURTEENTH BIENNIAL GUIDANCE TEST SYMPOSIUM, VOLUME 1
30 Oct. 1989 495 p Symposium held in Holloman AFB, NM, 3-5 Oct. 1989
(AD-A216925; MSD-TR-89-21-Vol-1) Avail: NTIS HC A21/MF A03 CSCL 17/7

This symposium was directed toward the exchange of information, simulation of new ideas, and discussion of current techniques associated with the development and evaluation of inertial guidance and navigation systems. The papers presented included such topics as new test and calibration techniques for accelerometers and ring laser gyros, advances in flight reference systems, new test equipment, and new software developments. GRA

N90-18384# Technische Univ., Delft (Netherlands). Faculty of Geodesy.
PRACTICAL APPLICATIONS OF LORAN-C FOR LAND MOBILE USE OR THE POSSIBILITY TO USE LORAN-C AS A VEHICLE-LOCATION OR VEHICLE-NAVIGATION SYSTEM Thesis
P. G. Quik Aug. 1989 113 p
(ETN-90-96265) Avail: NTIS HC A06/MF A01

A theoretical description of the Loran-C (Long Range Navigation) system is presented with a comparison between the different systems for vehicle-location systems. Landbased vehicles are studied. Different propagation models are described and the most effective model is calculated. During mobile testing use was made of the most simplified model, a position, time and range invariant model. Measurements to find out the influence of sky wave were taken. It is proposed that an enlargement of the present transmitter network as well as the extension of the system with a dead-reckoning sensor will result in a higher accuracy and will minimize the effect of propagation errors and cycle-slips. ESA

05 AIRCRAFT DESIGN, TESTING AND PERFORMANCE

Includes aircraft simulation technology.

For related information see also *18 Spacecraft Design, Testing and Performance* and *39 Structural Mechanics*.For land transportation vehicles see *85 Urban Technology and Transportation*.

N90-18385*# National Aeronautics and Space Administration. Langley Research Center, Hampton, VA.
FUSELAGE DESIGN FOR A SPECIFIED MACH-SLICED AREA DISTRIBUTION
Raymond L. Barger and Mary S. Adams Washington Feb. 1990 88 p
(NASA-TP-2975; L-16651; NAS 1.60:2975) Avail: NTIS HC A05/MF A01 CSCL 01C

A procedure for designing a fuselage having a prescribed effective area distribution computed from -90 deg Mach slices is described. This type of calculation is an essential tool in designing a complete configuration with an effective area distribution that corresponds to a desired sonic boom signature shape. Sample calculations are given for M=2 and M=3 designs. The examples include fuselages constrained to have circular cross sections and fuselages having cross sections of arbitrary shape. It is found that, for a prescribed effective area distribution having sharp variations, the iterative procedure converges to a smoothed approximation to the prescribed distribution. For a smooth prescribed area distribution, the solution is not unique. Author

N90-18386# Air Force Inst. of Tech., Wright-Patterson AFB, OH. School of Engineering.
VISUAL SERVOING FOR AUTONOMOUS AIRCRAFT REFUELING M.S. Thesis
Richard P. Shipman 14 Dec. 1989 92 p
(AD-A216042; AFIT/GE/ENG/89D-48) Avail: NTIS HC A05/MF A01 CSCL 23/3

The design and development of autonomous robotic systems for autonomous aircraft refueling is a major interest to the Air Force. The approach being undertaken is the integration of vision and robot technologies allowing visual information, regarding identification and location of an aerial refueling receptacle on an aircraft, to be fed back to a robot controller which develops trajectory information needed for compliant robot motion. The purpose was to modify, develop, and evaluate existing visual processing algorithms to allow the AFIT PUMA-560 to visually acquire and track a half-scale mock-up UARRSI aerial refueling receptacle, and place a simulated refueling nozzle in the close proximity of the receptacle's slipway. This was accomplished by developing visual object recognition and robot serving algorithms which: analyzed images, recognizes and determined the position of the receptacle, and calculated proper PUMA joint angles for

end-effector placement. Based on this approach, a static look-and-move robotic visual serving system (RVSS) was demonstrated which: identified, located, and served the PUMA's end-effector to the close proximity of the refueling receptacle. The RVSS provides the visual recognition and serving necessary so that when combined with a compliant motion controller completes the insertion task, thereby completely demonstrating the AFIT concept for robot refueling. In addition, the initial architecture for a dynamic look-and-move RVSS was developed based on parallel processing. GRA

N90-18387# Arnold Engineering Development Center, Arnold Air Force Station, TN.
THE EFFECTS OF WIND TUNNEL DATA UNCERTAINTY ON AIRCRAFT POINT PERFORMANCE PREDICTIONS Final Report, Oct. 1988 - Sep. 1989
J. D. Cloyd Dec. 1989 51 p Submitted for publication
(AD-A216091; AEDC-TR-89-14) Avail: NTIS HC A04/MF A01 CSCL 01/1

A study was conducted to determine the effects of uncertainties in wind tunnel test data on the point performance predictions for a typical fighter at medium altitude and subsonic velocity. The equations of motion of selected parameters were formulated in terms of the aerodynamic coefficients and thrust model. A computer code was written to calculate the performance parameters from the aerodynamic and thrust model inputs. An aerodynamic model closely approaching a typical fighter flying at 30,000 ft mean sea level was developed from wind tunnel, flight test, and flight manual data. The effects of the uncertainties in the aerodynamic coefficients on the performance parameters were determined by varying the aerodynamic coefficients input to the computer code. GRA

N90-18388# Bihrle Applied Research, Inc., Jericho, NY.
INFLUENCE OF FOREBODY GEOMETRY ON AERODYNAMIC CHARACTERISTICS AND A DESIGN GUIDE FOR DEFINING DEPARTURE/SPIN RESISTANT FOREBODY CONFIGURATIONS Final Report, Sep. 1986 - Feb. 1989
W. Bihrle, Jr., B. Barnhart, and E. Dickes Sep. 1989 295 p
(Contract F33615-86-C-3624)
(AD-A216714; BAR-89-3; WRDC-TR-89-3079) Avail: NTIS HC A13/MF A02 CSCL 01/1

The loss of airplanes and occupants attributable to departures from controlled flight and ensuing spins has been a problem since the earliest days of aviation. These losses have plagued both the military and general aviation communities. The phenomena responsible for such losses take on added significance because, in the past ten years, high angle-of-attack capability in the post-stall region has been shown to significantly enhance the air combat maneuvering effectiveness of fighter airplanes and, therefore, this is not a region to be avoided, but rather exploited, if possible. Fortunately, the aerodynamic characteristics that produce departures and spins have been identified within the past few years through rotary balance tests, which identify an airplane's aerodynamic characteristics in a steady rotational flow environment. It was demonstrated in the Phase 1 that the high angle-of-attack aerodynamic characteristics are very configuration dependent and that forebody geometry can have a significant influence on these characteristics. In the extreme case, an aircraft's undesirable aerodynamics can be completely attributable to the forebody. In this instance, autorotative yawing and rolling moments, as well as increasing nose-up pitching moments with increasing rotation rate, are realized. GRA

N90-18389# Army Aviation Research and Development Command, Moffett Field, CA. Aeroflight Dynamics Directorate.
TIME AND FREQUENCY-DOMAIN IDENTIFICATION AND VERIFICATION OF BO-105 DYNAMIC MODELS
Juergen Kaletka, Wolfgang V. Gruenhagen (Deutsche Forschungs- und Versuchsanstalt fuer Luft- und Raumfahrt, Brunswick, Germany, F.R.), Mark B. Tischler, and Jay W. Fletcher 15 Sep. 1989 26 p Presented at the 15th European Rotorcraft Forum, Amsterdam, Netherlands, 12-15 Sep. 1989
(AD-A216828) Avail: NTIS HC A03/MF A01 CSCL 01/3

Mathematical models for the dynamics of the DLR BO 105 helicopter are extracted from flight test data using two different approaches: frequency-domain and time-domain identification. Both approaches are reviewed. Results from an extensive data consistency analysis are given. Identifications for 6 degrees of freedom (DOF) rigid body models are presented and compared in detail. The extracted models compare favorably and their prediction capability is demonstrated in verification results. Approaches to extend the 6 DOF models are addressed and first results are presented. System identification is broadly defined as the deduction of system characteristics from measured data. It provides the only possibility to extract both non-parametric (e.g., frequency responses) and parametric (e.g., state space matrices) aircraft models from flight test data and therefore gives a reliable characterization of the dynamics of the actually existing aircraft. Main applications of system identification are seen in areas where higher accuracies of the mathematical models are required: Simulation validation, control system design (in particular model-following control system design for in-flight simulation), and handling qualities. GRA

N90-18390*# Ohio State Univ., Columbus. ElectroScience Lab.
A USER'S MANUAL FOR THE METHOD OF MOMENTS AIRCRAFT MODELING CODE (AMC) Final Report
M. E. Peters and E. H. Newman Sep. 1989 193 p
(Grant NsG-1498)
(NASA-CR-186371; NAS 1.26:186371; FR-716199-14) Avail: NTIS HC A09/MF A01 CSCL 01C

This report serves as a user's manual for the Aircraft Modeling Code or AMC. AMC is a user-oriented computer code, based on the method of moments (MM), for the analysis of the radiation and/or scattering from geometries consisting of a main body or fuselage shape with attached wings and fins. The shape of the main body is described by defining its cross section at several stations along its length. Wings, fins, rotor blades, and radiating monopoles can then be attached to the main body. Although AMC was specifically designed for aircraft or helicopter shapes, it can also be applied to missiles, ships, submarines, jet inlets, automobiles, spacecraft, etc. The problem geometry and run control parameters are specified via a two character command language input format. The input command language is described and several examples which illustrate typical code inputs and outputs are also included. Author

N90-18391# Institut Franco-Allemand de Recherches, Saint-Louis (France).
STUDY OF THE BLADE/VORTICE INTERACTION ON A ONE-BLADE ROTOR DURING FORWARD FLIGHT (INCOMPRESSIBLE, NON VISCOUS FLUID) [ETUDE DE L'INTERACTION PALE/TOURBILLON SUR UN ROTOR MONOPALE EN VOL D'AVANCEMENT (FLUIDE NON VISQUEUX ET INCOMPRESSIBLE)]
M. Schaffar and J. Haertig 19 Aug. 1988 54 p In FRENCH Original contains color illustrations
(ISL-R-115/88; ETN-90-96237) Avail: NTIS HC A04/MF A01

The applications of two and three dimensional numercical methods to the profile/vortice are reviewed. An application of the vortical network method to a rotor, during steady and forward flight, is presented. It is shown that the simultaneous use of the vortical network method and the conformal transformation can be applied to a thick rotor case, and the pressure coefficients can be calculated and used in acoustical analysis. The influence of the height, the vortice intensity and the angle between the blade and the vortice are studied. ESA

N90-18392# Institut Franco-Allemand de Recherches, Saint-Louis (France).
POSSIBLE PILOTING TECHNIQUES AT HYPERSONIC SPEEDS [LENKMOEGLICHKEITEN IM HYPERSCHALL]
K. W. Naumann 20 Jun. 1988 75 p In GERMAN
(ISL-CO-216/88; ETN-90-96244) Avail: NTIS HC A04/MF A01

The laws determining gas flow at hypersonic speeds are reviewed. Different piloting techniques presently known and considered promising for use in hypersonic flight are outlined. A detailed explanation of piloting techniques using lateral jets, or a combined control using flaps and jets, is presented. The general direction in which piloting research is heading is described. The improvements needed in each of the different piloting techniques presented are outlined. ESA

06 AIRCRAFT INSTRUMENTATION

Includes cockpit and cabin display devices; and flight instruments.

For related information see also *19 Spacecraft Instrumentation* and *35 Instrumentation and Photography.*

N90-18393*# National Aeronautics and Space Administration. Langley Research Center, Hampton, VA.
A SIMULATION EVALUATION OF THE ENGINE MONITORING AND CONTROL SYSTEM DISPLAY
Terence S. Abbott Washington Feb. 1990 39 p Original contains color illustrations
(NASA-TP-2960; L-16637; NAS 1.60:2960) Avail: NTIS HC A03/MF A01; 6 functional color pages CSCL 01D

The Engine Monitoring and Control System (E-MACS) display is a new concept for an engine instrument display, the purpose of which is to provide an enhanced means for a pilot to control and monitor aircraft engine performance. It provides graphically-presented information about performance capabilities, current performance, and engine component or subsystem operational conditions relative to nominal conditions. The concept was evaluated by sixteen pilot-subjects against a traditional, state-of-the-art electronic engine display format. The results of this evaluation showed a substantial pilot preference for the E-MACS display relative to the traditional display. The results of the failure detection portion of the evaluation showed a 100 percent detection rate for the E-MACS display relative to a 57 percent rate for the traditional display. From these results, it is concluded that by providing this type of information in the cockpit, a reduction in pilot workload and an enhanced ability for detecting degraded or off-nominal conditions is probable, thus leading to an increase in operational safety. Author

N90-18394*# National Aeronautics and Space Administration. Langley Research Center, Hampton, VA.
THREE INPUT CONCEPTS FOR FLIGHT CREW INTERACTION WITH INFORMATION PRESENTED ON A LARGE-SCREEN ELECTRONIC COCKPIT DISPLAY
Denise R. Jones Washington Apr. 1990 26 p
(NASA-TM-4173; L-16642; NAS 1.15:4173) Avail: NTIS HC A03/MF A01 CSCL 01D

A piloted simulation study was conducted comparing three different input methods for interfacing to a large-screen, multiwindow, whole-flight-deck display for management of transport aircraft systems. The thumball concept utilized a miniature trackball embedded in a conventional side-arm controller. The touch screen concept provided data entry through a capacitive touch screen. The voice concept utilized a speech recognition system with input through a head-worn microphone. No single input concept emerged as the most desirable method of interacting with the display. Subjective results, however, indicate that the voice concept was the most preferred method of data entry and had the most potential for future applications. The objective results indicate that, overall, the touch screen concept was the most effective input method. There was also significant differences between the time required to perform specific tasks and the input concept employed, with each concept providing better performance relative to a specific task. These results suggest that a system combining all three input concepts might provide the most effective method of interaction. Author

N90-18395*# National Aeronautics and Space Administration. Hugh L. Dryden Flight Research Facility, Edwards, CA.
WIND-TUNNEL INVESTIGATION OF A FLUSH AIRDATA SYSTEM AT MACH NUMBERS FROM 0.7 TO 1.4
Terry J. Larson, Timothy R. Moes, and Paul M. Siemers, III (National Aeronautics and Space Administration. Langley Research Center, Hampton, VA.) Apr. 1990 35 p
(NASA-TM-101697; H-1544; NAS 1.15:101697) Avail: NTIS HC A03/MF A01 CSCL 01D

Flush pressure orifices installed on the nose section of a 1/7-scale model of the F-14 airplane were evaluated for use as a flush airdata system (FADS). Wing-tunnel tests were conducted in the 11- by 11-ft Unitary Wind Tunnel at NASA Ames Research Center. A full-scale FADS of the same configuration was previously tested using an F-14 aircraft at the Dryden Flight Research Facility of NASA Ames Research Center (Ames-Dryden). These tests, which were published, are part of a NASA program to assess accuracies of FADS for use on aircraft. The test program also provides data to validate algorithms for the shuttle entry airdata system developed at the NASA Langley Research Center. The wind-tunnel test Mach numbers were 0.73, 0.90, 1.05, 1.20, and 1.39. Angles of attack were varied in 2 deg increments from -4 deg to 20 deg. Sideslip angles were varied in 4 deg increments from -8 deg to 8 deg. Airdata parameters were evaluated for determination of free-stream values of stagnation pressure, static pressure, angle of attack, angle of sideslip, and Mach number. These parameters are, in most cases, the same as the parameters investigated in the flight test program. The basic FADS wind-tunnel data are presented in tabular form. A discussion of the more accurate parameters is included. Author

07 AIRCRAFT PROPULSION AND POWER

Includes prime propulsion systems and systems components, e.g., gas turbine engines and compressors; and onboard auxilliary power plants for aircraft.

For related information see also *20 Spacecraft Propulsion and Power, 28 Propellants and Fuels,* and *44 Energy Production and Conversion.*

N90-18396# Advisory Group for Aerospace Research and Development, Neuilly-Sur-Seine (France). Structures and Materials.
AGARD/SMP REVIEW: DAMAGE TOLERANCE FOR ENGINE STRUCTURES. 2: DEFECTS AND QUANTITATIVE MATERIALS BEHAVIOUR
Aug. 1989 105 p In ENGLISH and FRENCH Meeting held in Mierlo, Netherlands, 2-7 Oct. 1988
(AGARD-R-769; ISBN-92-835-0518-2) Avail: NTIS HC A06/MF A01; Non-NATO Nationals requests available only from AGARD/Scientific Publications Executive

Most current military and all civil engines are operated under safe life procedures for their critical components. Experience has shown that this philosophy presented two drawbacks: the move towards designs allowing higher operational stresses, and the use of advanced high strength alloys make it likely that a disc burst could happen (followed by a rapid crack growth) well before the statistically-based safe life was achieved; and it is potentially wasteful of expensive components, since it was estimated that over 80 percent of engine discs have ten or more low cycle fatigue lives remaining when discarded under safe life rules. Damage tolerance being an alternative life philosophy, it was therefore decided to conduct a series of four workshops addressing the areas critical to damage tolerance design of engine parts. For individual titles, see N90-18397 through N90-18404.

N90-18397# Rolls-Royce Ltd., Derby (England). Dept. of Materials and Mechanics Technology.
DEFECTS: THEIR BEHAVIOUR AND RELATED DESIGN ASSUMPTIONS c26
R. H. Jeal *In* AGARD, AGARD/SMP Review: Damage Tolerance

for Engine Structures. 2: Defects and Quantitative Materials Behaviour Aug. 1989 7 p (For primary document see N90-18396 11-07)
Avail: NTIS HC A06/MF A01; Non-NATO Nationals requests available only from AGARD/Scientific Publications Executive

The design engineers traditional view of materials was enshrined in the assumptions he makes - namely, all materials are homogeneous elastic isotropic media free from defects. The metallurgical and manufacturing engineers job was to produce materials that met those assumptions as nearly as possible and design criteria were set to keep operating conditions within the limits of behavior described by those assumptions. Where the assumptions broke down, usually because of the presence of manufacturing aberrations or lack of understanding of operating conditions, the method of manufacture or component design was changed to make the assumption valid again. If the component could not be designed within the criteria of the current material then a new material was developed with a higher yield stress or better creep properties so the operating conditions again fell inside the assumed envelopes. As the designers of engines sought for greater efficiency and lower weight the stresses and temperature imposed on components gradually rose. Under these more arduous conditions the basic design assumptions started breakdown on three counts: defect free material cannot be produced in spite of cleaner, better control manufacturing routes; materials are not continuous isotropic media but do have a microstructure and directionally that changes their behavior; and materials are not elastic, they exhibit plasticity, fatigue and creep effects which are critical in determining their behavior. How far materials deviate from the traditional assumptions of their nature and behavior and the changes required in design, analysis and manufacture practices to maintain safe efficient engines with the required integrity, are discussed. Author

N90-18398# Societe Nationale d'Etude et de Construction de Moteurs d'Aviation, Evry Cedex (France). Lab. Materiaux et Procedes.
THE DAMAGE TOLERANCE OF DISC MATERIALS: METALLURGICAL FACTORS; RELATIONSHIP WITH PROCESSING PARAMETERS **c26**
E. J. Bachelet *In* AGARD, AGARD/SMP Review: Damage Tolerance for Engine Structures. 2: Defects and Quantitative Materials Behaviour Aug. 1989 20 p (For primary document see N90-18396 11-07)
Avail: NTIS HC A06/MF A01; Non-NATO Nationals requests available only from AGARD/Scientific Publications Executive

Until recently, the development of discs material were conducted within the framework of design and aging methods which essentially took into account the resistance to burst, fatigue crack initiation and creep, of these parts. Based on these criteria, alloy design and processing options, aiming at increased stresses or temperatures in operation, were often accompanied, for metallurgical reasons which shall be reviewed, by a decrease in the intrinsic damage tolerance of discs materials. In the early eighties such an evolution was the origin of difficulties which prompted basic research to understand and improve the damage tolerance of these materials, and more recently to develop more adapted materials. In parrallel, evolutions in regulations put explicit damands to insure an adequate damage tolerance of the newer engines, ENSIP for instance. The metallurgical factors which effect the damage tolerance of discs materials belonging to the classes of alloys presently used, Titanium-base and Nickel-base are reviewed. The main challenges facing the materials designers are presented. Author

N90-18399# Rolls-Royce Ltd., Derby (England).
REVIEW OF COMPONENT DEFECTS, THEIR RELATIONSHIP TO MANUFACTURING PROCESS, AND THEIR EFFECT ON MATERIALS BEHAVIOUR (FOR CRITICAL ROTATING PARTS) **c26**
A. C. Pickard *In* AGARD, AGARD/SMP Review: Damage Tolerance for Engine Structures. 2: Defects and Quantitative Materials Behaviour Aug. 1989 15 p (For primary document see N90-18396 11-07)
Avail: NTIS HC A06/MF A01; Non-NATO Nationals requests available only from AGARD/Scientific Publications Executive

All engineering materials contain defects. These may range from microstructural inhomogeneities through to gross abnormalities which are independent of the underlying microstructure. The key to understanding the importance of these defects is the determination of their effect on full scale component behavior. In general, the most dangerous defects are those which, when subjected to cyclic loading conditions, behave as propagating cracks, with little or no crack nucleation life. Danger is a relative concept here, however; for instance, where the density of such defects is high, and the size uniform, tests on specimens and components may automatically take into account the presence of the worst defect. If the equivalent initial crack size is small, use of the material will result in a component with a viable life. When the presence of a defect is an infrequent occurrence, however, it is unlikely that specimen and component tests will cover the behavior of the defect. In these circumstances, it is necessary to assess the risk of failure from defects and to ensure that this is acceptably low for in-servive components. Author

N90-18400# Turbomeca S.A. - Brevets Szydlowski, Bizanos (France).
DEFECTS IN MONOBLOCK CAST TURBINE WHEELS [LES DEFAUTS DANS LES ROUES DE TURBINE COULEES MONOBLOC] **c26**
D. Fournier *In* AGARD, AGARD/SMP Review: Damage Tolerance for Engine Structures. 2: Defects and Quantitative Materials Behaviour Aug. 1989 11 p In FRENCH (For primary document see N90-18396 11-07)
Avail: NTIS HC A06/MF A01; Non-NATO Nationals requests available only from AGARD/Scientific Publications Executive

Results of a study of cast alloy turbine wheels (blisks) are presented. The alloy used in the experiments was the nickel-based superalloy MAR M 004. The metallurgical structure, microstructure, and mechanical properties of the alloy are briefly described. Approximately 5000 specimens were evaluated using various destructive and non-destructive techniques. Data showing the nature and frequency of defects are presented and discussed. Factors affecting the propagation of semi-elliptical cracks are also addressed. Transl. by M.G.

N90-18401# La Sapienza Univ., Rome (Italy). Dipartimento Aerospaziale.
CRACK PROPAGATION FROM ARTIFICIAL DEFECTS IN TYPICAL ENGINE DISK MATERIALS; INTERPRETATION OF EXPERIMENTAL RESULTS BY MEANS OF 3D J INTEGRAL **c39**
Aldo Frediani and Roberto Galatolo (Pisa Univ., Italy) *In* AGARD, AGARD/SMP Review: Damage Tolerance for Engine Structures. 2: Defects and Quantitative Materials Behaviour Aug. 1989 10 p (For primary document see N90-18396 11-07)
Avail: NTIS HC A06/MF A01; Non-NATO Nationals requests available only from AGARD/Scientific Publications Executive

The results are shown for crack propagation tests performed on corner cracked specimens built in Powder Metals, AP1 and AF115, at high temperatures and different values of the stress ratio R. Analysis of the final crack shapes shows that discrepancies exist between the crack shapes expected on the basis of the behavior of the stress intensity factor and actual crackshapes; similar conclusions are obtained in other significant examples. The three-dimensional J-Integral (or GJ) is, then, introduced; the GJ values are computed along the crack fronts of circular shaped cracks and the actual cracks. It transpires that the values of GJ are virtually constant along the fronts of the actual cracks. Finally, future possibilities or application are outlined. Author

N90-18402# Pratt and Whitney Aircraft of Canada Ltd., Longueuil (Quebec).
REVIEW OF MODELLING METHODS TO TAKE ACCOUNT OF MATERIAL STRUCTURE AND DEFECTS
R. N. Tadros and K. Rezai *In* AGARD, AGARD/SMP Review:

Damage Tolerance for Engine Structures. 2: Defects and Quantitative Materials Behaviour Aug. 1989 15 p (For primary document see N90-18396 11-07)
Avail: NTIS HC A06/MF A01; Non-NATO Nationals requests available only from AGARD/Scientific Publications Executive

Among the many requirements for the design of gas turbine engine components, understanding the behavior of these components and the alloys used to make them is fundamental in order to ensure structural integrity and safe operation of the engines. The conventional Safe Life Approach is discussed together with an overview of crack growth modeling used at Pratt and Whitney Canada. The intention is not to compare the two approaches, but rather to highlight their applications and required improvement for the design and production of next generation gas turbine engines. Author

N90-18403# Utah Univ., Salt Lake City. Dept. of Mechanical Engineering.
FUTURE TECHNOLOGY REQUIREMENTS (RELATED TO DEFECTS AND QUANTITATIVE MATERIAL BEHAVIOR TO AID IN IMPLEMENTATION OF DAMAGE TOLERANCE FOR DESIGN OF ENGINE STRUCTURES)
David W. Hoeppner *In* AGARD, AGARD/SMP Review: Damage Tolerance for Engine Structures. 2: Defects and Quantitative Materials Behaviour Aug. 1989 11 p (For primary document see N90-18396 11-07)
Avail: NTIS HC A06/MF A01; Non-NATO Nationals requests available only from AGARD/Scientific Publications Executive

Issues are presented that are viewed as critical to an increased rate if implementation of damage tolerance concepts to the design of critical engine components. Areas emphasized are defect definition, inspection, modeling of discontinuities, evaluation of subcritical crack propagation behavior, development of material properties data banks, increasing the understanding of microstructural influences on material behavior, methods of comparing materials and various processing methods for modifying defect tolerance, and development of lifting methods that will enable designers, operators, and maintenance personnel to understand and incorporate all the concepts necessary to assure integrity of critical engine components. Various conclusions, including suggestions for expanding knowledge, are presented. Author

N90-18404# Centre d'Essais Aeronautique Toulouse (France). Groupe Materiaux et Technologies.
THE NEED FOR A COMMON APPROACH WITHIN AGARD [LE BESOIN D'ACTIONS CONCERTEES AU SEIN DE L'AGARD]
Th. Pardessus *In* AGARD, AGARD/SMP Review: Damage Tolerance for Engine Structures. 2: Defects and Quantitative Materials Behaviour Aug. 1989 5 p In FRENCH (For primary document see N90-18396 11-07)
Avail: NTIS HC A06/MF A01; Non-NATO Nationals requests available only from AGARD/Scientific Publications Executive

The need for agreement within AGARD on what constitutes a fully integrated material specification for damage tolerance is addressed. Suggestions are made regarding a test procedure that would help define more precisely defect sizes and populations. Test methods, the role of materials behavior modeling, component life, and the notion of usable strength are discussed. Transl. by M.G.

N90-18405# Advisory Group for Aerospace Research and Development, Neuilly-Sur-Seine (France). Propulsion and Energetics Panel.
UNSTEADY AERODYNAMIC PHENOMENA IN TURBOMACHINES
Feb. 1990 325 p In ENGLISH and FRENCH Meeting held in Luxembourg, 28-30 Aug. 1989
(AGARD-CP-468; ISBN-92-835-0543-3) Copyright Avail: NTIS HC A14/MF A02; Non-NATO Nationals requests available only from AGARD/Scientific Publications Executive

The Specialists' Meeting was arranged in the following sessions: Flutter or oscillating cascades; wakes or complete stage; transonic and supersonic unsteady phenomena; and experimental studies and instrumentation problems. While around isolated airfoils many results on unsteady aerodynamic phenomena are available; reliable experimental data for unsteady turbomachinery flows were still missing. Therefore a forum was offered to experts to discuss the degree of advancements in this field. It was found that computational fluid dynamics with large numerical codes will be more and more developed and offer a useful tool for designers to improve their products. The experimental work for code verification is lagging somewhat behind. For individual titles, see N90-18406 through N90-18429.

N90-18406# Motoren- und Turbinen-Union Muenchen G.m.b.H. (Germany, F.R.).
A COMPARISON OF FLUTTER CALCULATIONS BASED ON EIGENVALUE AND ENERGY METHOD
A. Klose and K. Heinig *In* AGARD, Unsteady Aerodynamic Phenomena in Turbomachines Feb. 1990 9 p (For primary document see N90-18405 11-07)
Copyright Avail: NTIS HC A14/MF A02; Non-NATO Nationals requests available only from AGARD/Scientific Publications Executive

The effect of unsteady aerodynamic loads on the natural modes and frequencies of unshrouded blades of axial flow turbomachinery is investigated. It is shown that significant shifts in eigenfrequencies and aerodynamic coupling between different modes do no occur for blades with a large mass ratio. Even for compressor and turbine bladings of recent design, it is generally possible to neglect the effect of unsteady aerodynamic forces on the vibration characteristics. Therefore, the energy method is applicable for the theoretical flutter investigation of these machines. However, for future light-weight designs, e.g., hollow fan blades or blades made of fiber-reinforced plastics, the effects of unsteady airloads on the vibration characteristics will be larger. In these cases, the eigenvalue method will have to be employed for flutter prediction as well as for the calculation of eigen frequencies and natural modes. Author

N90-18407# Technische Hochschule, Aachen (Germany, F.R.). Inst. fuer Strahlantriebe und Turboarbeitsmaschinen.
NUMERICAL INVESTIGATION OF UNSTEADY FLOW IN OSCILLATING TURBINE AND COMPRESSOR CASCADES
H. P. Kau and H. E. Gallus *In* AGARD, Unsteady Aerodynamic Phenomena in Turbomachines Feb. 1990 11 p (For primary document see N90-18405 11-07)
Copyright Avail: NTIS HC A14/MF A02; Non-NATO Nationals requests available only from AGARD/Scientific Publications Executive

A method of computing the unsteady two dimensional, inviscid subsonic flow through an oscillating compressor and turbine cascades is presented. The nonlinear Euler equations in conservative law form are solved taking into account the time dependent geometry. For interior points MacCormack's explicit predictor-corrector scheme is used. Boundary conditions are formulated by characteristics methods. A comparison of computational results and experimental data is given. A study is performed showing the influence of important aerodynamic and geometric parameters on the time-dependent forces and moments. Author

N90-18408# Office National d'Etudes et de Recherches Aerospatiales, Paris (France).
UNSTEADY VISCOUS CALCULATION METHOD FOR CASCADES WITH LEADING EDGE INDUCED SEPARATION
M. Gazaix, P. Girodroux-Lavigne, and J. C. LeBalleur *In* AGARD, Unsteady Aerodynamic Phenomena in Turbomachines Feb. 1990 13 p In FRENCH; ENGLISH summary Sponsored by SNECMA, France (For primary document see N90-18405 11-07)
Copyright Avail: NTIS HC A14/MF A02; Non-NATO Nationals requests available only from AGARD/Scientific Publications Executive

The recent progress in viscous-inviscid interaction methods

for computation of unsteady separated flows over airfoils, in forced oscillations, as well as, in the buffet regime, makes it possible to develop a numerical method for computations of unsteady flows over airfoils and cascades where the flow separation or stall is induced by sharp leading-edges. The aptitude of the method to describe the leading-edge separation in unsteady flow gives some hope for the prediction of subsonic flutter in cascades. The method solves unsteady thin-layer integral viscous equations, in defect-formulation, including two transport equations for turbulence. The equations are closed by turbulent mean velocity profiles which are modeled and discretized along the normal. The viscous method is strongly coupled time-consistently, by the so-called semi-implicit numerical technique, with a pseudo-inviscid solver based on potential small perturbation approximations. The numerical technique is able to enforce the separation at a sharp leading-edge. A viscous calculation method for airfoils is first shown to predict the leading-edge separation over a sharp flat plate at incidence, and over isolated compressor blades. Steady and unsteady computations are presented, and compared with experimental results. A numerical method for internal flows, including conditions of periodicity in space for steady flows, and in space-time for unsteady flows, is secondly obtained to compute separated flows in a cascade configuration. Steady and preliminary unsteady results are shown. Author

N90-18409# Stuttgart Univ. (Germany, F.R.). Inst. fuer Aerodynamik und Gasdynamik.

CALCULATION OF THE UNSTEADY TWO-DIMENSIONAL, INVISCID, COMPRESSIBLE FLOW AROUND A STRONGLY CAMBERED OSCILLATING SINGLE BLADE

K. M. Foerster *In* AGARD, Unsteady Aerodynamic Phenomena in Turbomachines Feb. 1990 8 p (For primary document see N90-18405 11-07)

Copyright Avail: NTIS HC A14/MF A02; Non-NATO Nationals requests available only from AGARD/Scientific Publications Executive

Some numerical experiments done with a computational method which was developed recently are described. Its main features are an extension of the computational domain to infinity and a moving grid fixed to the body in question. The first part describes this method in some detail. The second part presents some results about the aerodynamic characteristics of an oscillating blade with respect to the reduced frequency, to the free stream Mach number and to the oscillation amplitude, including an investigation of the higher harmonics introduced by the nonlinearity of the problem. Author

N90-18410# Ecole Polytechnique Federale de Lausanne (Switzerland).

AERODYNAMIC SUPERPOSITION PRINCIPLE IN VIBRATING TURBINE CASCADES

A. Boelcs, T. H. Fransson, and D. Schlaefli *In* AGARD, Unsteady Aerodynamic Phenomena in Turbomachines Feb. 1990 20 p Sponsored by Asea Brown Boveri, Swiss Federal Inst. of Tech. and the Swiss Commission for Scientific Research (For primary document see N90-18405 11-07)

Copyright Avail: NTIS HC A14/MF A02; Non-NATO Nationals requests available only from AGARD/Scientific Publications Executive

In unsteady aerodynamics the superposition principle states that the unsteady aerodynamic perturbatins generated in a vibrating cascade are the same as the sum of the perturbations generated by vibrating single blades. This principle was subjected to controversy in the past; today it was verified experimentally for torsional vibration modes in linear compressor cascades in subsonic and incompressible flow. Experiments on turbine cascades performed in an annular nonrotating test facility in order to validate the above mentioned superposition principle are described. Using an annular test facility eliminated the problems with lateral boundaries encountered in linear cascades: the annular cascade flow is truly periodic both for steady and unsteady flow. In the following, experiments are presented: that performed with three different cascades, vibrating in a translational mode, simulating a bending vibration; that cover supersonic, transonic, and subsonic flow; and that cover the entire interblade phase angle range possible with 20 blades. The blade sections of the cascades are typical for the last stages of gas- and steam-turbines. The results obtained show that, within the limitations of experimental accuracy, the superposition principle is valid, i.e., from experiments with single vibrating blades the same conclusions can be drawn as from experiments with the whole cascade vibrating at constant amplitudes and interblade phase angles. Author

N90-18411# Pennsylvania State Univ., University Park. Applied Research Lab.

DESIGN GUIDANCE TO MINIMIZE UNSTEADY FORCES IN TURBOMACHINES

R. E. Henderson and J. H. Horlock (Open Univ., Milton, England) *In* AGARD, Unsteady Aerodynamic Phenomena in Turbomachines Feb. 1990 12 p (For primary document see N90-18405 11-07)

Copyright Avail: NTIS HC A14/MF A02; Non-NATO Nationals requests available only from AGARD/Scientific Publications Executive

A method is discussed for the development of design charts which provide guidance in the selection of a stage design loading coefficient and flow coefficient which minimizes the generation of unsteady forces in a blade row due to its interaction with the wakes of an unstream blade row. Two configurations are discussed, the forces on a rotor operating in the wakes of an inlet stator or guide vane and the forces on a stator downstream of a rotor. An example demonstrating the generation of a design chart for the first configuration is presented. Author

N90-18412# Societe Nationale d'Etude et de Construction de Moteurs d'Aviation, Moissy-Cramayel (France).

AERODYNAMIC STUDY ON FORCED VIBRATIONS ON STATOR ROWS OF AXIAL COMPRESSORS

H. Joubert and V. Ronchetti *In* AGARD, Unsteady Aerodynamic Phenomena in Turbomachines Feb. 1990 11 p In FRENCH; ENGLISH summary (For primary document see N90-18405 11-07)

Copyright Avail: NTIS HC A14/MF A02; Non-NATO Nationals requests available only from AGARD/Scientific Publications Executive

Stator vane rows of axial compressors are dependent on fluctuations induced by the wakes of the previous upstream blades row. The unsteady flow resulting from this rotor-stator interaction creates aerodynamic exitations which may initiate vibrating fatique stress in the vanes and disable the engine. In order to take into account these phenomena, a numerical model based on two dimensional Euler equations was studied. The upstream condition fluctuations come from correlations established from wake experimental testing. The unsteady pressures calculated from the model are afterwards introduced in a mechanical model which estimate the dynamic stress inside the vane-structure. The variation of aerodynamic values such as pressure loss in the blade and geometric one such as rotor-stator spacing or fluctuation of the number of the vanes or stator were studied; therefore, as soon as the aeromechanic design charts of the compressor are designed, some sizing choice could be made to minimize the stress on the blade assembly. Author

N90-18413# Motoren- und Turbinen-Union Muenchen G.m.b.H. (Germany, F.R.).

UNSTEADY BLADE LOADS DUE TO WAKE INFLUENCE

S. Servaty and H. E. Gallus (Technische Hochschule, Aachen, Germany, F.R.) in AGARD, Unsteady Aerodynamic Phenomena in Turbomachines Feb. 1990 12 p (For primary document see N90-18405 11-07)

Copyright Avail: NTIS HC A14/MF A02; Non-NATO Nationals requests available only from AGARD/Scientific Publications Executive

An algorithm for calculating unsteady blade forces and moments due to incoming wakes is presented. The mathematical model describes the unsteady two-dimensional flow through compressor

and turbine cascades. Only inviscid transport of the wake is considered. The nonlinear Euler equations in conservative law form are solved by a combined method. MacCormack's explicit predictor-corrector scheme is used at interior points. Time-dependent boundary conditions are formulated by means of a characteristics method. Fundamental studies and several test cases are presented to check the algorithm. Comparisons with experimental results are discussed as well. Author

N90-18414# Schlumberger Cambridge Research (England).
UNSTEADY AERODYNAMIC PHENOMENA IN A SIMULATED WAKE AND SHOCK WAVE PASSING EXPERIMENT
A. B. Johnson, M. J. Rigby, and M. L. G. Oldfield (Oxford Univ., England) *In* AGARD, Unsteady Aerodynamic Phenomena in Turbomachines Feb. 1990 13 p (For primary document see N90-18405 11-07)
(Contract F33615-84-C-2475)
Copyright Avail: NTIS HC A14/MF A02; Non-NATO Nationals requests available only from AGARD/Scientific Publications Executive

The propagation of nozzle guide vane trailing edge shock waves and wakes through a turbine rotor passage, using experimental data from a transient cascade tunnel with a rotating bar shock and wake generator are studied. Both unsteady and mean blade surface pressure measurements, together with Schlieren flow visualization were used to unravel the complex sequence of refraction, reflection, and re-reflection of the moving NGV shock waves, together with the effects they have on both the unsteady and time averaged blade surface pressure. The effects of the wakes are similarly described. As well as contributing to the fundamental understanding of the inherently unsteady turbine aerodynamics, the phenomena is shown which must be predicted by any successful unsteady computational fluid dynamic prediction of the flow. Author

N90-18415*# United Technologies Research Center, East Hartford, CT. Computational and Theoretical Fluid Dynamics.
GUST RESPONSE ANALYSIS FOR CASCADES OPERATING IN NONUNIFORM MEAN FLOWS
Kenneth C. Hall and Joseph M. Verdon *In* AGARD, Unsteady Aerodynamic Phenomena in Turbomachines Feb. 1990 13 p (For primary document see N90-18405 11-07)
(Contract NAS3-25425)
Copyright Avail: NTIS HC A14/MF A02; Non-NATO Nationals requests available only from AGARD/Scientific Publications Executive CSCL 21E

The linearized unsteady aerodynamic response of a cascade of airfoils subjected to entropic, vortical, and acoustic gusts is analyzed. Field equations for the first-order unsteady perturbation flow are obtained by linearizing the full time-dependent mass, momentum, and energy conservation equations about a nonlinear, isentropic, and irrotational mean or steady flow. A splitting technique is then used to decompose the unsteady velocity field into irrotational and rotational parts leading to field equations for the unsteady entropy, rotational velocity, and irrotational velocity fluctuations that are coupled only sequentially. The entropic and rotational velocity fluctuations can be described in terms of the mean-flow drift and stream functions which can be computed numerically. The irrotational unsteady velocity is described by an inhomogeneous linearized potential equation which contains a source term that depends on the rotational velocity field. This equation is solved via a finite difference technique. Results are presented to indicate the status of the numerical solution procedure and to demonstrate the impact of blade geometry and mean blade loading on the aerodynamic response of cascades to vortical gust excitations. The analysis described leads to very efficient predictions of cascade unsteady aerodynamic phenomena making it useful for turbomachinery aeroelastic and aeroacoustic design applications. Author

N90-18416*# National Aeronautics and Space Administration. Marshall Space Flight Center, Huntsville, AL.
NUMERICAL PREDICTION OF AXIAL TURBINE STAGE AERODYNAMICS
H. V. McConnaughey and L. W. Griffin *In* AGARD, Unsteady Aerodynamic Phenomena in Turbomachines Feb. 1990 15 p (For primary document see N90-18405 11-07)
Copyright Avail: NTIS HC A14/MF A02; Non-NATO Nationals requests available only from AGARD/Scientific Publications Executive CSCL 21E

A preliminary assessment is made of two NASA-developed unsteady turbine stage computer codes. The methodology and previous partial validation of the codes are briefly outlined. Application of these codes to a Space Shuttle main engine turbine for two sets of operating conditions is then described. Steady and unsteady, two and three-dimensional results are presented, compared, and discussed. These results include time-mean and instantaneous airfoil pressure distributions and pressure fluctuations, streamlines on the airfoil surfaces and endwalls, and relative total pressure contours at different axial locations in the rotor passage. Although not available at the time of this writing, experimental data for one of the operating conditions simulated is forthcoming and will be used to assess the accuracy of the unsteady, as well as, the steady predictions presented. Issues related to code usage and resource requirements of the two codes are also discussed. Author

N90-18417# Office National d'Etudes et de Recherches Aerospatiales, Paris (France).
NUMERICAL SIMULATION OF THREE-DIMENSIONAL UNSTEADY FLOWS IN TURBOMACHINES
Antoine Fourmaux, Gilles Billonnet, Alain LeMeur, and Alain Lesain *In* AGARD, Unsteady Aerodynamic Phenomena in Turbomachines Feb. 1990 12 p In FRENCH; ENGLISH summary (For primary document see N90-18405 11-07)
Copyright Avail: NTIS HC A14/MF A02; Non-NATO Nationals requests available only from AGARD/Scientific Publications Executive

For the aerodynamic study of turbomachinery, the numerical flow-simulation takes a larger and larger place. These viscous and compressible fluid flows are three-dimensional and unsteady; so they are governed by the full Navier-Stokes equations. Nevertheless, the use of numerical methods to solve these equations is limited at the present time, and only applications of the Euler methods are presented. After a short description of the physical phenomena and of the numerical method used, the conditions on the calculation domain boundaries are described. The simplifying assumptions which allow the complete stage computation, are emphasized. The examples presented concern unsteady flow simulations in a turbine stage and in a supersonic nozzle. Author

N90-18418# Rolls-Royce Ltd., Derby (England).
DEVELOPMENT OF A MASS AVERAGING TEMPERATURE PROBE
S. C. Cook and R. L. Elder (Cranfield Inst. of Tech., Bedford, England) *In* AGARD, Unsteady Aerodynamic Phenomena in Turbomachines Feb. 1990 14 p Sponsored by Ministry of Defence, England (For primary document see N90-18405 11-07)
Copyright Avail: NTIS HC A14/MF A02; Non-NATO Nationals requests available only from AGARD/Scientific Publications Executive

In research and development testing of axial flow fan and compressor rigs, the overall performance can normally be determined to a satisfactory accuracy using conventional methods. It is known, however, that conventional slow response instrumentation does not respond correctly to the highly unsteady flows encountered between blade rows in high speed turbomachines. Consequently measurements made in these areas, in an attempt to split the loss of the machine, typically lead to gross errors in stage, or blade element, performance assessments. A slow response temperature sensor, the Reverse-Kiel probe, was

created by employing a judicious shield design in an attempt to allow the probe to indicate the correct mass-weighted temperature of such unsteady turbomachinery flows. The mass-weighted Reverse-Kiel temperature probe was developed using some simple arguments supported by flow visualization and computational modeling. The predicted best probe designs were evaluated and confirmed on the purposed blade-wake rig. The optimum probe was built as a standard rig probe and now is undergoing preliminary test studies. Author

N90-18419# Massachusetts Inst. of Tech., Cambridge. Gas Turbine Lab.

BLADE ROW INTERACTION EFFECTS ON COMPRESSOR MEASUREMENTS

A. H. Epstein, M. B. Giles, T. Shang, and A. K. Sehra (Textron Lycoming, Stratford, CT.) *In* AGARD, Unsteady Aerodynamic Phenomena in Turbomachines Feb. 1990 11 p (For primary document see N90-18405 11-07)

Copyright Avail: NTIS HC A14/MF A02; Non-NATO Nationals requests available only from AGARD/Scientific Publications Executive

The influence of a downstream stator row on the measurement of compressor rotor performance was examined using a computational fluid dynamic code backed by laser anemometry data on a transonic fan stage. The upstream potential influence of the stator causes unsteady circulation about the rotor blades which is a function of the rotor circumferential position. This, in turn, results in a nonuniform circumferential pattern of time averaged temperature and pressure in the stationary frame. An analytical theory relating the temperature and pressure variations to circulation perturbation is presented and shown to give good agreement with the numerical calculations. The results of a parametric study show that the magnitude of this effect is a strong function of rotor-stator blade row spacing and relative blade counts. The effects range from negligible for large spacings typical of high bypass ratio fans to several percent of the stage pressure and temperature rise for closely spaced blade rows typical of high compressors. Because the temperature and pressure perturbations are in spatial phase, the net effect on measured rotor efficiency is negligible so long as the pressure and temperature measurements are made in the same location relative to the stators. If they are not, errors of + or - 1.5 percent can result. The effects of axial position and stator loading are shown to be relatively small. Author

N90-18420# Catania Univ. (Italy). Istituto di Macchine.

HIGH-RESOLUTION EULER COMPUTATIONS OF UNSTEADY TRANSONIC FLOWS IN CASCADES

F. Bassi, C. Osnaghi, and M. Savini (Consiglio Nazionale delle Ricerche, Peschiera Borromeo, Italy) *In* AGARD, Unsteady Aerodynamic Phenomena in Turbomachines Feb. 1990 12 p (For primary document see N90-18405 11-07)

Copyright Avail: NTIS HC A14/MF A02; Non-NATO Nationals requests available only from AGARD/Scientific Publications Executive

A two-dimensional finite volume total variation diminishing (TVD) Euler solver, suited to handle time-dependent transonic flow fields in turbomachinery components, is presented and used together with a method of characteristics (using a shock fitting technique) and with an explicit central difference finite volume code in order to investigate unsteady flow fields. Special care is given to the accurate treatment of boundary conditions, both of solid-wall and far-field type. The method is used to compute two unsteady flow problems which have features of transonic internal flows of practical importance in the analysis of turbomachinery components. The problems are the unsteady flow in a transonic nozzle with oscillating back pressure and the transonic flow in a rotor blade row with translating disturbances at the inflow boundary simulating the wakes shed by a preceding stator blade row. In the first problem the influence of oscillation frequency upon the flow field is investigated with the three methods so as to obtain some indications of the relative accuracies of the schemes and a better understanding of the physical phenomena occurring. Author

N90-18421# Wien Univ. (Austria). Inst. for Stroemungslehre und Waermeuebertragung.

ASYMPTOTIC ANALYSIS OF TRANSONIC FLOW THROUGH OSCILLATING CASCADES

Franz Koller and Alfred Kluwick *In* AGARD, Unsteady Aerodynamic Phenomena in Turbomachines Feb. 1990 10 p (For primary document see N90-18405 11-07)

Copyright Avail: NTIS HC A14/MF A02; Non-NATO Nationals requests available only from AGARD/Scientific Publications Executive

The plane flow of a perfect gas through an oscillating cascade at a Mach number close to one is analyzed using matched asymptotic expansions. In the case of steady flow the field quantities in the regions between airfoils are governed by the equations for one-dimensional flow in a first approximation if thickness, camber, and angle of incidence of the blades are small. Moreover, for a particular range of these parameters the velocity disturbances satisfy linear equations ahead of and behind the cascade. The same property is shown to hold in the case of unsteady flow provided the reduced frequency and the amplitudes of the oscillations are small compared to unity. Furthermore, the effects of the sizes of the various parameters on the flow field are discussed. Surface pressures are calculated for cascades of flat plate and double circular arc airfoils. Author

N90-18422# Technische Hochschule, Aachen (Germany, F.R.). Inst. fuer Strahlantriebe und Turboarbeitsmaschinen.

EXPERIMENTS ON THE UNSTEADY FLOW IN A SUPERSONIC COMPRESSOR STAGE

W. Elmendorf, G. K. Kauke, and K. D. Broichhausen (Motoren- und Turbinen-Union Muenchen G.m.b.H., Germany, F.R.) *In* AGARD, Unsteady Aerodynamic Phenomena in Turbomachines Feb. 1990 13 p (For primary document see N90-18405 11-07)

Copyright Avail: NTIS HC A14/MF A02; Non-NATO Nationals requests available only from AGARD/Scientific Publications Executive

The intensity of unsteadiness in compressors strongly depends on the flow velocity and the overall pressure ratio. Thus investigations of the unsteady effects in the case of supersonic flow are of great importance with regard to performance and reliability. For that purpose the unsteady flow in a supersonic compressor stage was studied in a series of experiments. A review on the specially developed measuring techniques including flow visualization and the design of miniaturized semiconductor probes is given. The main feature of unsteady supersonic flow in the compressor are discussed by means of characteristic experimental results. Author

N90-18423# Cambridge Univ. (England). Dept. of Engineering.

MODELLING UNSTEADY TRANSITION AND ITS EFFECTS ON PROFILE LOSS

H. P. Hodson *In* AGARD, Unsteady Aerodynamic Phenomena in Turbomachines Feb. 1990 15 p (For primary document see N90-18405 11-07)

Copyright Avail: NTIS HC A14/MF A02; Non-NATO Nationals requests available only from AGARD/Scientific Publications Executive

The effects of wake interactions on the transition processes of turbomachinery blade boundary layers are considered. A simple model of unsteady transition is proposed which is then used to identify a relationship between a new reduced frequency parameter and the profile loss of a blade row which is subjected to unsteady inflow. The value of this parameter is also used to identify the nature of the boundary layer development on the blade surface. The influence of other parameters on the transition process is also discussed. The model is then extended to deal with the more general case. The validity of the model is demonstrated by a comparison with a correlation of the effects of wake-generated unsteadiness on profile loss which was originally proposed by Speidel. The effects of unsteady inflow on four idealized turbine blades are considered. Author

N90-18424# Ecole Polytechnique Federale de Lausanne (Switzerland).
TIME-DEPENDENT MEASUREMENTS ON VIBRATING ANNULAR TURBINE CASCADES UNDER VARIOUS STEADY STATE CONDITIONS c39
A. Boelcs, T. H. Fransson, and D. Schlaefli *In* AGARD, Unsteady Aerodynamic Phenomena in Turbomachines Feb. 1990 14 p (For primary document see N90-18405 11-07)
Copyright Avail: NTIS HC A14/MF A02; Non-NATO Nationals requests available only from AGARD/Scientific Publications Executive

Two-dimensional sections of three turbine blades were investigated experimentally in a non-rotating annular cascade facility with respect to its steady-state and unsteady aerodynamic characteristics. The sections are representative for the near tip sections of the blades where the nominal flow conditions are subsonic at the inlet and near sonic or supersonic at the outlet. Emphasis was put on the time dependent aerodynamic coupling effects between the neighbor blades. Unsteady experimental data were obtained with the blades vibrating both in the traveling wave mode as well as with single blade excitation. Decomposition of the experimental data, obtained in the traveling wave mode, into local (along the blade surfaces) and integrated unsteady aerodynamic influence coefficients indicates that the largest aerodynamic excitation comes from the suction surface leading edge region and, in some cases, from the pressure surface trailing edge region for all three cascades. The unsteady aerodynamic influence coefficients indicate that for sub- and supersonic outlet flow velocities, all three blade-geometries are self-damped (i.e., a single vibrating blade has a damping influence on itself), but an instability may arise because of the aerodynamic coupling effects between, essentially, the reference blade and its immediate suction side neighbor and, to a lesser extent, its pressure side neighbor. For transonic outlet flow velocities however, a clear destabilizing effect of the (for this flow regime) almost normal shock on the blade itself appears, constituting an excitation mechanism leading eventually to single blade flutter. Author

N90-18425# Technische Hochschule, Aachen (Germany, F.R.). Inst. fuer Strahlantriebe und Turboarbeitsmaschinen.
EXPERIMENTAL INVESTIGATION OF THE INFLUENCE OF ROTOR WAKES ON THE DEVELOPMENT OF THE PROFILE BOUNDARY LAYER AND THE PERFORMANCE OF AN ANNULAR COMPRESSOR CASCADE
H. D. Schulz and H. E. Gallus *In* AGARD, Unsteady Aerodynamic Phenomena in Turbomachines Feb. 1990 15 p (For primary document see N90-18405 11-07)
Copyright Avail: NTIS HC A14/MF A02; Non-NATO Nationals requests available only from AGARD/Scientific Publications Executive

The development of the profile boundary layers, particularly the loci of transition and separation, largely depend on the turbulence level of the free-stream and the wake flow effects. For comparison, a detailed survey of the profile boundary layers in an annular compressor cascade was carried out first at a steady, uniform incoming flow and secondly with a rotor upstream. The rotor incorporates cylindrical spokes causing periodic wakes and thus a higher overall turbulence level of the flow. Its impact on the profile boundary layer history and the performance of the compressor cascade will be discussed. Author

N90-18426# Oxford Univ. (England). Dept. of Engineering Science.
METHODS FOR MAKING UNSTEADY AERODYNAMIC PRESSURE MEASUREMENTS IN A ROTATING TURBINE STAGE
R. W. Ainsworth, J. L. Allen, and A. J. Dietz *In* AGARD, Unsteady Aerodynamic Phenomena in Turbomachines Feb. 1990 14 p (For primary document see N90-18405 11-07)
Copyright Avail: NTIS HC A14/MF A02; Non-NATO Nationals requests available only from AGARD/Scientific Publications Executive

A new method for obtaining detailed unsteady pressure measurements in a rotating turbine stage is described. The technique is based on the use of miniature semiconductor pressure sensors attached directly to the surface where the measurement is required, permitting simultaneously a high surface density of instrumentation together with a high frequency response. In reviewing typical semiconductor behavior, attention is drawn to some of the traditional constraints encountered with these devices. In describing the development of the technology employed here, the methods used to circumvent these traditional constraints are outlined. Author

N90-18427# Vrije Univ., Brussels (Belgium). Dept. of Fluid Mechanics.
MEASUREMENT OF VELOCITY PROFILES AND REYNOLDS STRESSES ON AN OSCILLATING AIRFOIL c02
J. DeRuyck, B. Hazarika, and C. Hirsch *In* AGARD, Unsteady Aerodynamic Phenomena in Turbomachines Feb. 1990 15 p (For primary document see N90-18405 11-07)
(Contract DAJA45-85-C-0039)
Copyright Avail: NTIS HC A14/MF A02; Non-NATO Nationals requests available only from AGARD/Scientific Publications Executive

The flow around a sinusoidally oscillating NACA 0012 airfoil in the presence of the leading edge separation bubble and with leading edge stall, including laminar-turbulent transition is described. The airfoil oscillates about an axis at 25 percent chord from the leading edge, with a nominal reduced frequency of 0.3 and Reynolds number of 300,000. The experiments are made at 4 to 14 deg, 5 to 15 deg, 6 to 16 deg, and 8 to 18 deg angle of attack, covering flow conditions from no stall to full leading edge stall. It is found that the most probable cause of leading edge stall is due to the leading edge separation bubble burst and it occurs as soon as the static stall limit is exceeded. The leading edge stall is not due to the rapid upstream movement of the trailing edge separation. The velocity vectors and the Reynolds stress tensors are measured using a slanted rotating single sensor hot-wire. The complete suction side boundary layer profile and the near wake is surveyed at 5 to 15 deg oscillation where no interaction is observed between the leading edge and the trailing edge flows, and at 8 to 18 deg in full stall conditions. Author

N90-18428# Wright Research Development Center, Wright-Patterson AFB, OH. Turbine Engine Div.
COMPRESSOR PERFORMANCE TESTS IN THE COMPRESSOR RESEARCH FACILITY
F. R. Ostdiek, W. W. Copenhaver, and D. C. Rabe *In* AGARD, Unsteady Aerodynamic Phenomena in Turbomachines Feb. 1990 16 p (For primary document see N90-18405 11-07)
Copyright Avail: NTIS HC A14/MF A02; Non-NATO Nationals requests available only from AGARD/Scientific Publications Executive

An advanced compressor test facility, the Compressor Research Facility (CRF) was established. The CRF is designed for exploration of steady-state and transient behavior of full-scale, multistage gas turbine engine fans, and compressors. Since construction and check-out of the facility, the CRF test team has completed its first five years of testing with a variety of test articles. Customers besides the Air Force have included other Government agencies and industry. Turbine engine technology is changing rapidly with new mission demands on the engine resulting in new aerodynamic, stability, and performance demands on each of its components. The role of the CRF in meeting the challenges inherent in such a rapidly changing field is described. The facility characteristics are described along with a description of the changes, modifications, and enhancements made to the facility in its short history. Several examples of tests performed in the CRF (both steady-state and transient) are used to demonstrate the impact of the CRF results on engine development. Finally, the plans for further facility modifications and enhancement are given. This affords a preview of the impact which this and other test facilities will have on turbine engine technology. Author

N90-18429# Virginia Polytechnic Inst. and State Univ., Blacksburg. Dept. of Mechanical Engineering.
STALL AND RECOVERY IN MULTISTAGE AXIAL FLOW COMPRESSORS
Walter F. OBrien and Keith M. Boyer (Wright Research Development Center, Wright-Patterson AFB, OH.) *In* AGARD, Unsteady Aerodynamic Phenomena in Turbomachines Feb. 1990 11 p Sponsored by AFOSR, Washington, DC (For primary document see N90-18405 11-07)
Copyright Avail: NTIS HC A14/MF A02; Non-NATO Nationals requests available only from AGARD/Scientific Publications Executive

At low flows relative to the design point, multistage axial flow compressors may enter a globally-stable operational state involving rotating stall within the blade passages. For continued operation in a turbine engine, recovery of the compressor to normal operation is required. Operation in rotating stall is generally characterized by recovery hysteresis; that is, to produce recovery, compressor flow must be allowed to increase substantially beyond the initial flow level observed with rotating stall. In turbine engine applications, it is desirable to reduce compressor recovery hysteresis to a minimum. Stage flow behavior and stage matching at low flows are shown to have a major influence on recovery behavior. Conclusions are supported through the use of an analytical model recently validated with experimental data from tests of a multistage compressor in the Compressor Research Facility at Wright-Patterson Air Force Base. Author

N90-18430# Army Aviation Engineering Flight Activity, Edwards AFB, CA.
PRELIMINARY AIRWORTHINESS EVALUATION OF THE WOODWARD HYDROMECHANICAL UNIT INSTALLED ON T700-GE-700 ENGINES IN THE UH-60A HELICOPTER Final Report, 14 May - 14 Jun. 1989
Joseph L. Piotrowski, Christopher J. Young, Thomas P. Walsh, and Julie Sandman Aug. 1989 56 p Sponsored by Army Aviation Systems Command, Saint Louis, MO
(AD-A216751; AEFA-89-14) Avail: NTIS HC A04/MF A01 CSCL 01/3

The U.S. Army Aviation Engineering Flight Activity conducted a Preliminary Airworthiness Evaluation of the Woodward Hydromechanical Unit (HMU) installed on T700-GE-700 engines in the UH-60A helicopter from 14 May 1989 to 14 June 1989. The evaluation was conducted at Edwards AFB, California (elevation 2302 feet) and Coyote Flat, California (elevation 9980 feet) on aircraft S/N 88-26015. The evaluation consisted of eleven flights for a total of 15.5 productive flight hours. Performance of the Woodward HMU and the Hamilton Standard HMU, presently used on T700-GE-700 engines, was similar. The poor engine/rotor transient droop characteristics, as noted in previous testing, remain a shortcoming regardless of the HMU installed. Operation of T700-GE-700 engines with Woodard HMUs installed is satisfactory. GRA

08 AIRCRAFT STABILITY AND CONTROL

Includes aircraft handling qualities; piloting; flight controls; and autopilots.

For related information see also *05 Aircraft Design, Testing and Performance.*

N90-18431# Air Force Inst. of Tech., Wright-Patterson AFB, OH. School of Engineering.
DISCRETE PROPORTIONAL PLUS INTEGRAL (PI) MULTIVARIABLE CONTROL LAWS FOR THE CONTROL RECONFIGURABLE COMBAT AIRCRAFT (CRCA) M.S. Thesis
Jamie L. Foelker Dec. 1989 158 p
(AD-A215664; AFIT/GE/ENG/89-12) Avail: NTIS HC A08/MF A01 CSCL 01/3

Multivariable control laws developed by Dr. Brian Porter of the University of Salford, England are used to successfully perform maneuvering tracking tasks with the NASA/Grumman Control Reconfigurable Combat Aircraft (CRCA). Porter's method is used to design discrete Proportional plus Integral (PI) control laws. Output and selected state rate feedback are used. The results in three no failure flight conditions show robust tracking control of the CRCA for five selected maneuvers. Single failures are introduced to test the ability of the fixed-gain designs to successfully control the aircraft and perform the maneuvers. The time responses show that discrete PI control law can make the CRCA successfully perform all five maneuvers for two of the three control surface failures investigated in two of the three point designs. The step response PI control law results in stable control for only one of three failure situations. GRA

N90-18432# Advisory Group for Aerospace Research and Development, Neuilly-Sur-Seine (France). Guidance and Control Panel.
THE IMPLICATIONS OF USING INTEGRATED SOFTWARE SUPPORT ENVIRONMENT FOR DESIGN OF GUIDANCE AND CONTROL SYSTEMS SOFTWARE
Edwin B. Stear, ed. and John T. Shepherd, ed. (GEC-Marconi Ltd., Borehamwood, England) 1990 192 p
(AGARD-AR-229; ISBN-92-835-0538-7) Copyright Avail: NTIS HC A09/MF A01; Non-NATO Nationals requests available only from AGARD/Scientific Publications Executive

The deliberations and conclusions of Working Group 8 of the Guidance and Control Panel of AGARD are summarized, which are: (1) to develop and consider a set of requirements for a high level language software support environment from a guidance and control systems viewpoint; (2) to evaluate the characteristics and capabilities offered by advanced language support environments, either existing or in the course of development, with respect to the requirements defined in 1; and (3) if necessary, to determine the modifications which would have to be contemplated to meet fully the needs expressed in 1. The Working Group attempted to consider all software design and development technologies which existed or were known to be under development at the time. Author

N90-18433# Thermacore, Inc., Lancaster, PA.
FLEXIBLE HEAT PIPE COLD PLATE Final Report, 2 Feb. - 30 Nov. 1988
Nelson J. Gernert 13 Jan. 1989 71 p
(Contract N62269-88-C-0210)
(AD-A216053; S3912A; NADC-89067-60) Avail: NTIS HC A04/MF A01 CSCL 01/4

The Naval Air Development Center is taking action to improve the reliability of aircraft flight control hydraulic actuators. Feedback and loop closure electronics are being mounted on the actuator, thereby eliminating numbers of electrical conductors between the actuator and the flight control computer. Methods for the electronics are required to help assure reliability. The Thermacore effort documented in this report investigated the feasibility of using heat pipe technology to thermally protect the flight critical actuator electronics. The cooling method investigated used a flexible heat pipe cold plate that interfaced with the integrally connected flexible hose to a nearby heat sink. The flexible section accommodates relative motion between the actuator and the heat sink. The successful Phase 1 work program first established the design requirements; evaluated cold plate to actuator integration techniques; conducted analysis to select the best heat pipe material/working fluid system; and concluded with the design, fabrication and testing of a flexible heat pipe cold plate assembly that integrates with the SMART aileron actuator being developed by H.R. Textron. The cold plate transferred over 60 watts. This power exceeded the 44.5 watt requirement. GRA

N90-18434*# National Aeronautics and Space Administration. Langley Research Center, Hampton, VA.
APPLICATION OF VARIABLE-GAIN OUTPUT FEEDBACK FOR HIGH-ALPHA CONTROL
Aaron J. Ostroff Feb. 1990 11 p Previously announced in

IAA as A89-52659
(NASA-TM-102603; NAS 1.15:102603) Avail: NTIS HC A03/MF A01 CSCL 01C

A variable-gain, optimal, discrete, output feedback design approach that is applied to a nonlinear flight regime is described. The flight regime covers a wide angle-of-attack range that includes stall and post stall. The paper includes brief descriptions of the variable-gain formulation, the discrete-control structure and flight equations used to apply the design approach, and the high performance airplane model used in the application. Both linear and nonlinear analysis are shown for a longitudinal four-model design case with angles of attack of 5, 15, 35, and 60 deg. Linear and nonlinear simulations are compared for a single-point longitudinal design at 60 deg angle of attack. Nonlinear simulations for the four-model, multi-mode, variable-gain design include a longitudinal pitch-up and pitch-down maneuver and high angle-of-attack regulation during a lateral maneuver. Author

N90-18435# Construcciones Aeronauticas S.A., Madrid (Spain). Div. de Fabricacion Materiales Compuestos.
DESIGN OF A NEW CONTROL SYSTEM FOR HOVERCRAFTS
A. Martin-Carrillo 19 Jan. 1989 73 p
(ETN-90-96230) Avail: NTIS HC A04/MF A01

A system for a control device which will improve the directional control performances of hovercrafts, making them almost as maneuverable as automobiles, was designed. The system is presented in terms of conceptual, preliminary and detailed design. Easier handling, closer turns and shorter braking by the control system were addressed to increase potential missions of the craft such as use over roads or small rivers. Low maintenance requirements and non-interference with soil surface were taken into account. Inspection and testing procedures, operational deployment and distribution, maintenance and costs are reported. Graphics of the system are included. ESA

09 RESEARCH AND SUPPORT FACILITIES (AIR)

Includes airports, hangars and runways; aircraft repair and overhaul facilities; wind tunnels; shock tubes; and aircraft engine test stands.

For related information see also *14 Ground Support Systems and Facilities (Space).*

N90-18436# European Space Agency, Paris (France).
THE DFVLR 3-m X 3-m LOW SPEED WIND TUNNEL (NWG) IN GOETTINGEN Status Report, 1988
Werner Baumert (Deutsche Forschungs- und Versuchsanstalt fuer Luft- und Raumfahrt, Goettingen, Germany, F.R.) Dec. 1989 78 p Transl. into ENGLISH of Der 3-m x 3-m-Niedergeschwindigkeits-Windkanal (NWG) der DFVLR in Goettingen (Stand 1988) (Goettingen, Fed. Republic of Germany, DFVLR), May 1988 p 1-67 Original language document was announced as N89-26021
(ESA-TT-1156; DFVLR-Mitt-89-05; ETN-90-96219) Avail: NTIS HC A05/MF A01; original German version available from DFVLR, VB-PL-DO, Postfach 90 60 58, 5000 Cologne 90, Fed. Republic of Germany, 36 DM

Significant auxiliary facilities available to users of the DFVLR low speed wind tunnel in Goettingen (Germany, F.R.) (NWG) are presented. The NWG is a continously working wind tunnel where investigations from industry and research institutes are carried out. Measurements are also carried out on model buildings and building components, and on unusual aspects relating to the sports scene (skiing). Model vehicles form a large proportion of the work. The open jet test section has a 3 m by 3 m cross-section with a length of 6 m. The maximum wind speed is 65 m/s giving a maximum Reynolds number of Re=1.3 10 to the sixth power on a length of 0.3 m. ESA

12 ASTRONAUTICS (GENERAL)

For extraterrestrial exploration see *91 Lunar and Planetary Exploration.*

N90-18437# Deutsche Forschungsanstalt fuer Luft- und Raumfahrt, Cologne (Germany, F.R.).
SPACE ORIENTATION AND ORBITAL TECHNOLOGY [ORIENTIERUNGSRAHMEN ORBITALTECHNOLOGIEN]
May 1989 106 p In GERMAN
(ISBN-3-89100-015-4; ETN-90-96282) Avail: NTIS HC A06/MF A01

The results of research conducted by study groups, industry, high school students and the DLR are presented. The research presented is in the fields of automation and robotics, communication technologies, materials science and human factor engineering. Diagrams of various antennas, capsules, spacesuits, and lunar vehicles are shown. The problems specific to various areas of space research are described. Possible answers to these problems are presented. ESA

N90-18438# Deutsche Forschungsanstalt fuer Luft- und Raumfahrt, Cologne (Germany, F.R.).
LONG TERM PLANNING FOR SPACE FLIGHT ACTIVITIES WITHIN THE DFVLR [LANGFRISTPERSPEKTIVE FUER DIE RAUMFAHRTAKTIVITAETEN DER DFVLR]
Hartmut Sax 7 Jun. 1988 18 p In GERMAN Presented at Senatssitzung, Cologne, Fed. Republic of Germany, 22 Jun. 1988
(DFVLR-IB-303-88/2; ETN-90-96283) Avail: NTIS HC A03/MF A01

The general goals for future research in space flight technologies are outlined. Research programs in aerothermodynamics and material and structural design are described. Research in data management and automation technology is reviewed. Earth station programs, human factor engineering, and low gravity conditions are discussed. The role of international cooperation in achieving these research goals is stressed. ESA

13 ASTRODYNAMICS

Includes powered and free-flight trajectories; and orbital and launching dynamics.

N90-18439# Instituto de Pesquisas Espaciais, Sao Jose dos Campos (Brazil).
DATA COLLECTION AND LOCATION PLATFORMS EXPERIMENTAL NETWORK: DESCRIPTION OF AN ORBIT ROUTINE [REDE EXPERIMENTAL DE PLATAFORMA DE COLETA DE DADOS E LOCALIZACAO - DESCRICAO DA ROTINA ORBIT]
Luiz Carlos GadelhadeSouza Feb. 1989 25 p In PORTUGUESE; ENGLISH summary Presented at the 4th Brazilian Colloquium on Orbital Dynamics, Rio de Janeiro, Brazil, 21-24 Nov. 1988
(INPE-4798-NTE/287) Avail: NTIS HC A03/MF A01

The function of the ORBIT routine is to determine the position and attitude of the satellite in its orbit, besides calculating some necessary parameters to simulate a Data Collection and Location Platforms Experimental network. Also determined is the impact on orbital geometry (dispersion in orbital elements) due to errors in position, velocity, and pitch angle at the injection point of the satellite. Author

N90-18440# Instituto de Pesquisas Espaciais, Sao Jose dos Campos (Brazil).
ORBIT DETERMINATION OF ARTIFICIAL EARTH SATELLITES THROUGH ESTMATION TECHNIQUES COMBINED WITH STATE SMOOTHING TECHNIQUES Ph.D. Thesis
Helio KoitiKuga Nov. 1989 261 p In PORTUGUESE; ENGLISH summary
(INPE-4959-TDL/388) Avail: NTIS HC A12/MF A02

Filtering and smoothing techniques applied to orbit determination of earth satellites are presented. A Kalman filter is

implemented in the UD factorization form along with an adaptive procedure for estimating the dynamic noise level, which prevents the divergence of estimates due to inaccurate modeling of the orbital motion. The smoother used is a numerically efficient version of the Rauch-Tung-Strievel smoother as proposed by Bierman in 1983. This smoother, developed in the UD form, has proven to be economical, compact and competitive for computer implementation. Digital simulations were performed for 2 situations of orbit determination: shorts arcs with favorable tracking geometry; long arcs with existing tracking stations. Tests containing many levels of modeling degradation were carried out. The adaptive UD filter deals with these modeling nuisances and does not allow the divergence phenomenon to occur. The UD smoother is used to improve the accuracy of the estimates and of the covariances. The results show that in general the UD smoother enhances the accuracy, therefore being a useful tool to reproduce accurately the trajectory of the orbital motion. Author

N90-18441# Instituto de Pesquisas Espaciais, Sao Jose dos Campos (Brazil).
EVALUATION OF INFLUENCES OF ERRORS INVOLVED IN ORBIT PROPAGATION OF ARTIFICIAL SATELLITES Ph.D. Thesis
Kondapalli RamaRao Nov. 1989 262 p In PORTUGUESE; ENGLISH summary
(INPE-4962-TDL/391) Avail: NTIS HC A12/MF A02

The ephemerides of low-altitude artificial satellites generated by orbit propagation procedures of special perturbation methods are, in general, subject to various types of errors. The predominant among them are the errors due to the truncation of disturbing force models, as in the case of terrestrial gravitational force; the errors in force model parameters, as in the case of atmospheric drag force; and the errors in the numerical integration. Treating these principal errors, this work develops a stochastic procedure to evaluate the order of magnitude of the accumulated global error in propagating low-altitude circular and quase-circular orbits. In the case of numerical integration errors, the proposed procedure models the errors through the distribution of zero mean random variables belonging to stochastic sequences, which consider the influence of both local truncation and round-off errors. In the case of truncation of the geopotential function, the lunear estimation methods are combined with spectral representation of terrestrial gravitation, and the statistical estimates of uncertainties in orbital elements are deduced in terms of their covariances. In the theory developed for the case of atmospheric drag force, the drag parameters are considered to be stochastic quantities in order to have statistical estimates to uncertainties in orbital elements in terms of their covariances. The three theories developed are at first tested separately in various types of problems, comparing the estimated errors with the true errors in all the cases, and then are combined and successfully applied to a satellite with the orbital and structural configuration similar to that of the first Brazilian satellite. Author

N90-18442# Instituto de Pesquisas Espaciais, Sao Jose dos Campos (Brazil).
AUTONOMOUS ORBIT DETERMINATION USING GPS Ph.D. Thesis
Ricardo NegreirosdePaiva Jun. 1989 319 p In PORTUGUESE; ENGLISH summary
(INPE-4815-TDL/361) Avail: NTIS HC A14/MF A02

State estimation procedures for satellite onboard orbit determination are developed and presented. In face of restrictions imposed by the on-board computer, simple analytical models for the satellite dynamics are used in conjunction with a Kalman filter for real time processing of Global Positioning System (GPS) observations. The satellite motion is either represented by polynomial expressions that approximate the behavior in time of the orbital elements or by a harmonic oscillator that has an analytical solution thus avoiding a numerical integration. The GPS observations are then sequentially processed to identify the coefficients of the polynomials (dynamic model) and evaluate the orbit or to determine directly the satellite position and velocity independent of ground support. With the proposed procedures the use of a more complex satellite dynamical model is avoided and the numerical integration, needed in standard orbit estimation, to propagate the orbit and the state error covariance matrix. The results of the numerical tests conducted under simulated conditions in a digital computer indicate that the proposed procedures are candidates for use in autonomous systems for real time orbit determination. Author

14 GROUND SUPPORT SYSTEMS AND FACILITIES (SPACE)

Includes launch complexes, research and production facilities; ground support equipment, e.g., mobile transporters; and simulators.

For related information see also *09 Research and Support Facilities (Air).*

N90-18443# Jet Propulsion Lab., California Inst. of Tech., Pasadena.
SIMULATION OF THE DYNAMIC ENVIRONMENT FOR MISSILE COMPONENT TESTING: DEMONSTRATION Final Report, 17 Dec. 1984 - 31 May 1989
Kurng Y. Chang 15 Sep. 1989 74 p
(Contracts ARO-MIPR-118-86; ARO-MIPR-141-87; ARO-MIPR-125-85)
(AD-A216979; JPL-D-6041; ARO-21113.2-EG) Avail: NTIS HC A04/MF A01 CSCL 12/4

The problems in defining a realistic test requirement for missile and space vehicle components can be classified into two categories: (1) definition of the test environment representing the expected service condition, and (2) simulation of the desired environment in the test laboratory. Recently, a new three-dimensional (3-D) test facility was completed at the U.S. Army Harry Diamond Laboratory (HDL) to simulate triaxial vibration input to a test specimen. The vibration test system is designed to support multi-axial vibration tests over the frequency range of 5 to 2000 Hertz. The availability of this 3-D test system motivates the development of new methodologies addressing environmental definition and simulation. GRA

15 LAUNCH VEHICLES AND SPACE VEHICLES

Includes boosters; operating problems of launch/space vehicle systems; and reusable vehicles.

For related information see also *20 Spacecraft Propulsion and Power.*

No abstracts in this category.

16 SPACE TRANSPORTATION

Includes passenger and cargo space transportation, e.g., shuttle operations; and space rescue techniques.

For related information see also *03 Air Transportation and Safety* and *18 Spacecraft Design, Testing and Performance.* For space suits see *54 Man/System Technology and Life Support.*

N90-18485*# National Aeronautics and Space Administration. Lyndon B. Johnson Space Center, Houston, TX.
SPACE SHUTTLE RCS OXIDIZER LEAK REPAIR FOR STS-26
R. A. Delventhal and N. M. Faget *In* Johns Hopkins Univ., The 1989 JANNAF Propulsion Meeting, Volume 1 May 1989 p 489-495 (For primary document see N90-18462 11-20)
Avail: NTIS HC A25/MF A04 CSCL 22B

17 SPACE COMM., SPACECRAFT COMM., COMMAND & TRACKING

Includes telemetry; space communications networks; astronavigation and guidance; and radio blackout.

For related information see also *04 Aircraft Communications and Navigation* and *32 Communications and Radar.*

N90-18444*# Jet Propulsion Lab., California Inst. of Tech., Pasadena.
SHARP: A MULTI-MISSION ARTIFICIAL INTELLIGENCE SYSTEM FOR SPACECRAFT TELEMETRY MONITORING AND DIAGNOSIS
Denise L. Lawson and Mark L. James 1 May 1989 26 p Previously announced in IAA as A90-18038
(Contract NAS7-918)
(NASA-CR-186285; JPL-Publ-89-23; NAS 1.26:186285) Avail: NTIS HC A03/MF A01 CSCL 09F

The Spacecraft Health Automated Reasoning Prototype (SHARP) is a system designed to demonstrate automated health and status analysis for multi-mission spacecraft and ground data systems operations. Telecommunications link analysis of the Voyager 2 spacecraft is the initial focus for the SHARP system demonstration which will occur during Voyager's encounter with the planet Neptune in August, 1989, in parallel with real time Voyager operations. The SHARP system combines conventional computer science methodologies with artificial intelligence techniques to produce an effective method for detecting and analyzing potential spacecraft and ground systems problems. The system performs real time analysis of spacecraft and other related telemetry, and is also capable of examining data in historical context. A brief introduction is given to the spacecraft and ground systems monitoring process at the Jet Propulsion Laboratory. The current method of operation for monitoring the Voyager Telecommunications subsystem is described, and the difficulties associated with the existing technology are highlighted. The approach taken in the SHARP system to overcome the current limitations is also described, as well as both the conventional and artificial intelligence solutions developed in SHARP. Author

N90-18445# European Space Agency, Paris (France).
NAVIGATION EXPERIMENT NAVEX DATA STORAGE AND PROCESSING
Jens Hammesfahr (Deutsche Forschungs- und Versuchsanstalt fuer Luft- und Raumfahrt, Oberpfaffenhofen, Germany, F.R.) Dec. 1989 48 p Transl. into ENGLISH of Navigation experiment NAVE Messdatenspeicherung und -aufbereitung (Oberpfaffenhofen, Fed. Republic of Germany), Sep. 1989 p 1-45 Original language document was announced as N90-11727
(ESA-TT-1175; DFVLR-Mitt-89-09; ETN-90-96222) Avail: NTIS HC A03/MF A01; original German version available from DFVLR, VB-PL-DO, Postfach 90 60 58, 5000 Cologne 90, Fed. Republic of Germany, 19 DM

The formats of the data stored during NAVEX (navigation experiment) are given. Any disturbances in the instruments or from the measuring technique which led to erroneous data are dealt with. Distribution is made between the raw data and preprocessed data. Raw data from flight station, ground stations and radar, and preprocessed data from these and orbital data of the Space Shuttle, refractive index from atmospheric data, data from clock calibration, are included. The names of all associated files in the DFVLR central computer are listed. All obvious data errors from the data evaluation are mentioned. ESA

N90-18446# European Space Agency, Paris (France).
NAVIGATION EXPERIMENT NAVEX: THE SELF-TEST DELAY TIMES IN THE D1 SPACELAB MISSION
Jens Hammesfahr and Anita Zimmermann (Deutsche Forschungs- und Versuchsanstalt fuer Luft- und Raumfahrt, Oberpfaffenhofen, Germany, F.R.) Dec. 1989 48 p Transl. into ENGLISH of Navigation experiment NAVEX die Selbsttestlaufzeiten Waehrend der D1-mission (Oberpfaffenhofen, Fed. Republic of Germany), Oct. 1989 p 1-41 Original language document was announced as N90-11728
(ESA-TT-1176; DFVLR-Mitt-89-10; ETN-90-96223) Avail: NTIS HC A03/MF A01; original German version available from DFVLR, VB-PL-DO, Postfach 90 60 58, 5000 Cologne 90, Fed. Republic of Germany, 18 DM

The self-test delay times of the NAVEX (navigation experiment) stations, provided to gain information on delay times of radio signals during mission progress, are shown and their variations with temperature are determined. These delay times are correlated with the equipment delay times for the timing signals. Delay times for all passes of the Spacelab with radio contact to the ground stations are investigated. A final assessment is included showing that the self-test delay times show a significant dependence of the delay times on temperature for the flight and receiving stations. The analysis of the self-test measurement is discussed with recommendations for improvements. ESA

N90-18447# European Space Agency, Paris (France). Standards Approval Boards for Space Data Communications.
PACKET TELEMETRY STANDARD
Jan. 1988 76 p
(ESA-PSS-04-106-Issue-1; ISSN-0379-4059; ETN-90-96304)
Copyright Avail: NTIS HC A05/MF A01

A standard which aims at establishing uniform requirements for the implementation of spacecraft packet telemetry systems by ESA is presented. Requirements for packet telemetry protocols and techniques to be used on board ESA spacecraft and at the ESA ground network facilities are defined. Telemetry formats which are generated by the spacecraft in order to execute its role in both the end-to-end transport of space mission data sets from source application processes located on the ground, and the immediate transfer of these data sets through space data-acquisition networks are described. Data structures for a source packet, telemetry packet, and a transfer frame are specified. ESA

18 SPACECRAFT DESIGN, TESTING AND PERFORMANCE

Includes satellites; space platforms; space stations; spacecraft systems and components such as thermal and environmental controls; and attitude controls.

For life support systems see *54 Man/System Technology and Life Support.* For related information see also *05 Aircraft Design, Testing and Performance, 39 Structural Mechanics,* and *16 Space Transportation.*

N90-18448# Instituto de Pesquisas Espaciais, Sao Jose dos Campos (Brazil).
ANALYTICAL FORMULATION FOR THE INTERACTION PROBLEM OF DYNAMIC REENTRY, AND EFFECTS DUE TO FLEXIBILITY AND VIBRATION IN AN AEROSPACE VEHICLE M.S. Thesis [FORMULACAO ANALITICA PARA O PROBLEMA DA INTERACAO DA DINAMICA DE REENTRADA COM EFEITOS DE FLEXIBILIDADE E VIBRACAO EM VEICULOS AEROESPACIALS]
Leonardo deOliveFerreira Nov. 1989 231 p In PORTUGUESE; ENGLISH summary
(INPE-4963-TDL/392) Avail: NTIS HC A11/MF A02

The interaction between reentry dynamics and effects due to structural flexibility and vibrations in aerospace vehicles is studied. An attempt is made to establish a fairly general, comprehensive analytical formulation of the problem. In the sequence, the formulation is applied to a particular vehicle, along with a search for the conditions for an analytical solution. Author

N90-18449# Instituto de Pesquisas Espaciais, Sao Jose dos Campos (Brazil).
ATTITUDE ESTIMATION PROCEDURE FOR SPIN STABILIZED SATELLITES M.S. Thesis [PROCEDIMENTO DE ESTIMACAO DE ATITUDE PARA SATELITES ESTABILIZADOS POR ROTACAO]

Ulisses Thadeu VieiraGuedes Aug. 1989 110 p In PORTUGUESE; ENGLISH summary
(INPE-4866-TDL/377) Avail: NTIS HC A06/MF A01

An attitude estimation procedure is proposed for spin stabilized satellites which considers disturbing torques of magnetic nature. It is assumed that the sensor's data were previously selected and compressed. The resulting observations are submitted to the proposed procedure. Then the magnetics coefficients (residual magnetic moment and Eddy coefficient) are estimated and the satellite's attitude is refined through a extended Kalman filter. A better trust is warranted by employing this estimated and refined values at the attitude prediction. Author

N90-18450# Instituto de Pesquisas Espaciais, Sao Jose dos Campos (Brazil).
OPTIMIZATION OF SENSORS AND ACTUATORS POSITIONING AIMED AT OBTAINING REDUCED MODELS FOR THE SYNTHESIS OF OPTIMAL CONTROL REGULATORS OF FLEXIBLE STRUCTURES Ph.D. Thesis [OTIMIZACAO DO POSICIONAMENTO DE SENSO RES E ATUADORES VISANDO A OBTENCAO DE MODELOS REDUZIDOS PARA A SINTESE DE REGULADORES OTIMOS EM CONTROLE DE ESTRUTURAS FLEXIVEIS]
Paulo Tadeu deMelloLourencao Dec. 1988 138 p In PORTUGUESE; ENGLISH summary
(INPE-4760-TDL/348) Avail: NTIS HC A07/MF A01

Two approaches are presented which are proposed to obtain reduced order models for the active control of flexible structures, specifically considering the problem of positioning actuators and sensors. The first method consists in truncating the original model to the dominant modes only, the actuators and sensors placed according to a criterion that minimizes the spillover (interaction between controller and nondominant modes). In the second approach, the matrices of the reduced order model and the positions of actuators and sensors are determined to minimize the difference between the outputs of the original and reduced models. Based on these reduced models, two optimal controllers are synthesized assuming direct output feedback. These controllers are finally validated against the original model and their performances are compared: the closed-loop eigenvalues and eigenvectors, and limit values of a quadratic performance index. Author

N90-18451# Air Force Inst. of Tech., Wright-Patterson AFB, OH. School of Engineering.
USING THE METHOD OF MATCHED ASYMPTOTIC EXPANSIONS, ANALYTICALLY INVESTIGATE THE THREE-DIMENSIONAL, ATMOSPHERE ENTRY PROBLEM M.S. Thesis
Tadeusz J. Masternak Dec. 1989 180 p
(AD-A216287; AFIT/GA/ENY/89D-4) Avail: NTIS HC A09/MF A01 CSCL 22/3

Although numerical techniques exist to obtain solutions to highly nonlinear and highly coupled systems, the trends and subtleties of the solution are frequently lost in the volume and form of tabular and graphical data in covering a wide range of initial conditions. An analytical investigation is presented of the 3-D equations of motion for lifting entry into a planetary atmosphere. The equations of motion for lifting entry into a planetary atmosphere are derived. A non-rotating, spherical planet is assumed, as is a non-rotating, strictly exponential atmospheric model. The derived equations of motion are transformed to a variable set relating the classical orbital elements to the vehicle's altitude. Solutions to the resulting five nonlinear, coupled, first order, ordinary differential equations are obtained by using the Method of Matched Asymptotic Expansions and a computerized symbolic manipulator, which performs the detailed algebraic computations. By using the planetary scale height-mean equatorial radius product as a small parameter, both zero and first order expansions to the equations of motion are obtained. GRA

N90-18452# Air Force Systems Command, Wright-Patterson AFB, OH. Foreign Technology Div.
A DIFFERENCE SCHEME WITH AUTOCONTROL ARTIFICIAL VISCOSITY TO PREDICT ABLATED NOSETIP SHAPE
Maozhag Yang 29 Sep. 1989 14 p Transl. into ENGLISH from Yuhang Xuebao (Peoples Rep. of China), no. 3, 1988 p 55-60
(AD-A216625) Avail: NTIS HC A03/MF A01 CSCL 16/2

The trio-layer explicit difference scheme which is an added artificial viscosity item is found by using filteration in the computation of ablated nosetip shape. The scheme is of first order accuracy in regions where shape change is wavy and second order accuracy in regions where its smooth. Numerical experiments show that the scheme developed is effective. GRA

N90-18453*# National Aeronautics and Space Administration. Langley Research Center, Hampton, VA.
SUPPORT TRUSSES FOR LARGE PRECISION SEGMENTED REFLECTORS: PRELIMINARY DESIGN AND ANALYSIS
Timothy J. Collins and W. B. Fichter Mar. 1989 24 p
(NASA-TM-101560; NAS 1.15:101560) Avail: NTIS HC A03/MF A01 CSCL 22B

Precision Segmented Reflector (PSR) technology is currently being developed for a range of future applications such as the Large Deployable Reflector. The structures activities at NASA-Langley are outlined in support of the PSR program. Design concepts are explored for erectable and deployable support structures which are envisioned to be the backbone of these precision reflectors. Important functional requirements for the support trusses related to stiffness, mass, and surface accuracy are reviewed. Proposed geometries for these structures and factors motivating the erectable and deployable designs are discussed. Analytical results related to stiffness, dynamic behavior, and surface accuracy are presented and considered in light of the functional requirements. Results are included for both a 4-meter-diameter prototype support truss which is currently being designed as the Test Bed for the PSR technology development program, and for two 20-meter support structures. Author

N90-18454*# Lockheed Missiles and Space Co., Sunnyvale, CA.
PROCESS DEVELOPMENT AND FABRICATION OF SPACE STATION TYPE ALUMINUM-CLAD GRAPHITE EPOXY STRUTS
L. R. Ring Jan. 1990 37 p
(Contract NAS1-18229)
(NASA-CR-181873; NAS 1.26:181873; LMSC/F186352) Avail: NTIS HC A03/MF A01 CSCL 22B

The manufacture of aluminum-clad graphite epoxy struts, designed for application to the Space Station truss structure, is described. The strut requirements are identified, and the strut material selection rationale is discussed. The manufacturing procedure is described, and shop documents describing the details are included. Dry graphite fiber, Pitch-75, is pulled between two concentric aluminum tubes. Epoxy resin is then injected and cured. After reduction of the aluminum wall thickness by chemical milling the end fittings are bonded on the tubes. A discussion of the characteristics of the manufactured struts, i.e., geometry, weight, and any anomalies of the individual struts is included. Author

N90-18455# European Space Agency, Paris (France).
SPACECRAFT THERMAL CONTROL DESIGN DATA, VOLUME 1
Nov. 1989 613 p Prepared in cooperation with ESA/ESTEC, Noordwijk, Netherlands and Univ. Politecnica de Madrid, Spain
(ESA-PSS-03-108-Issue-1-Vol-1; ISSN-0379-4059; ETN-90-96211) Copyright Avail: NTIS HC A99/MF A04

A handbook in several volumes was prepared with the aim of assisting the thermal control design engineer by presenting a single document containing all the information relevant to spacecraft thermal control design. It is intended to issue revisions and additions as they become available so that the handbook will remain up to date with state of the art information and development in the

field. View factors, holes, grooves and cavities, spacecraft surface temperature, conductive heat transfer and structural materials are detailed. ESA

N90-18456# European Space Agency, Paris (France).
SPACECRAFT THERMAL CONTROL DESIGN DATA, VOLUME 2
Nov. 1989 630 p Prepared in cooperation with ESA/ESTEC, Noordwijk, Netherlands and Univ. Politecnica de Madrid, Spain
(ESA-PSS-03-108-Issue-1-Vol-2; ISSN-0379-4059; ETN-90-96212)
Copyright Avail: NTIS HC A99/MF A04

A handbook in several volumes was prepared with the aim of assisting the thermal control design engineer by presenting a single document containing all the information relevant to spacecraft thermal control design. It is intended to issue revision and additions as they become available so that the handbook will remain up to date with state of the art information and developments in the field. Thermal control surfaces and insulations are detailed. ESA

N90-18457# European Space Agency, Paris (France).
SPACECRAFT THERMAL CONTROL DESIGN DATA, VOLUME 3
Nov. 1989 539 p Prepared in cooperation with ESA/ESTEC, Noordwijk, Netherlands and Univ. Politecnica de Madrid, Spain
(ESA-PSS-03-108-Issue-1-Vol-3; ISSN-0379-4059; ETN-90-96213)
Copyright Avail: NTIS HC A23/MF A03

A handbook in several volumes was prepared with the aim of assisting the thermal control design engineer by presenting a single document containing all the information relevant to spacecraft thermal control design. It is intended to issue revision and additions as they become available so that the handbook will remain up to date with state of the art information and developments in the field. Heat pipes, radiators, phase-change capacitors, electrical heating and louvers are detailed. ESA

N90-18458# European Space Agency, Paris (France).
SPACECRAFT THERMAL CONTROL DESIGN DATA, VOLUME 4
Nov. 1989 559 p Prepared in cooperation with ESA/ESTEC, Noordwijk, Netherlands and Univ. Politecnica de Madrid, Spain
(ESA-PSS-03-108-Issue-1-Vol-4; ISSN-0379-4059; ETN-90-96214)
Copyright Avail: NTIS HC A24/MF A03

A handbook in several volumes was prepared with the aim of assisting the thermal control design engineer by presenting a single document containing all the information relevant to spacecraft thermal control design. It is intended to issue revisions and additions as they become available so that the handbook will remain up to date with state of the art information and developments in the field. Fluid loops are detailed. ESA

N90-18459# European Space Agency. European Space Research and Technology Center, ESTEC, Noordwijk (Netherlands). Structures and Mechanisms Div.
COMPOSITES DESIGN HANDBOOK FOR SPACE STRUCTURE APPLICATIONS
Apr. 1989 271 p Revised
(ESA-PSS-03-1101-Issue-1-Rev-1; ETN-90-96297) Copyright
Avail: NTIS HC A12/MF A02

The handbook is divided into several sections and detailed subsections which are fully described in a table of contents. The main section titles relate to: material properties and applications, calculation methods of laminates, general design aspects, load transfer and design of joints, design of structures, integrity control, verification guidelines and manufacturing aspects. Issue status and control sheets are included as a reference to new and revised pages. A glossary of terms is presented to ensure precision of meaning and consistency of usage in relation to composites. All references are detailed. ESA

N90-18460# European Space Agency. European Space Research and Technology Center, ESTEC, Noordwijk (Netherlands). Product Assurance and Safety Dept.
SYSTEM SAFETY REQUIREMENTS FOR ESA SPACE SYSTEMS AND ASSOCIATED EQUIPMENT
Sep. 1988 68 p
(ESA-PSS-01-40-Issue-2; ISSN-0379-4059; ETN-90-96301)
Copyright Avail: NTIS HC A04/MF A01

A specification defining the system safety requirements which implement the ESA safety policy and which are applicable to ESA space systems and associated equipment is presented. Safety program requirements are detailed under the following headings: general, safety organization and management, safety personnel access and authority, system safety program plan, safety program tasks, project technical safety specification, and safety assurance. Technical system safety requirements are detailed under the following headings: general system design, manned system safety, launcher systems, payload safety, and ground equipment and facilities. ESA

N90-18461# European Space Agency. European Space Research and Technology Center, ESTEC, Noordwijk (Netherlands). Product Assurance and Safety Dept.
THE DETERMINATION OF OFFGASSING PRODUCTS FROM MATERIALS AND ASSEMBLED ARTICLES TO BE USED IN A MANNED SPACE VEHICLE CREW COMPARTMENT
Feb. 1989 18 p
(ESA-PSS-01-729-Issue-1; ISSN-0379-4059; ETN-90-96303)
Copyright Avail: NTIS HC A03/MF A01

A specification describing a test to provide data for aid in the evaluation of the suitability of assembled articles and materials for use in a space vehicle crew compartment is presented. The data obtained concern the nature and quantity of organic and inorganic volatile contaminants evolved when the articles and materials are subjected to the crew compartment environment. Preparatory conditions, test performance, acceptance limits and quality assurance are covered. ESA

N90-18482*# National Aeronautics and Space Administration. Lyndon B. Johnson Space Center, Houston, TX.
SPACE STATION TECHNOLOGY SUMMARY
R. Iacabucci, S. Evans, G. Briley, R. A. Delventhal, and E. Braunscheidel (National Aeronautics and Space Administration. Lewis Research Center, Cleveland, OH.) *In* Johns Hopkins Univ., The 1989 JANNAF Propulsion Meeting, Volume 1 May 1989 p 457-470 (For primary document see N90-18462 11-20)
Avail: NTIS HC A25/MF A04 CSCL 22B

N90-18486*# National Aeronautics and Space Administration. Lyndon B. Johnson Space Center, Houston, TX.
ZERO-GRAVITY VORTEX VENT AND PVT GAGING SYSTEM
M. G. Downey and J. T. Trevathan *In* Johns Hopkins Univ., The 1989 JANNAF Propulsion Meeting, Volume 1 May 1989 p 497-500 (For primary document see N90-18462 11-20)
Avail: NTIS HC A25/MF A04 CSCL 22B

N90-18487*# Martin Marietta Space Systems, Inc., Denver, CO.
ORBITAL FLUID RESUPPLY ASSESSMENT
Ralph N. Eberhardt *In* Johns Hopkins Univ., The 1989 JANNAF Propulsion Meeting, Volume 1 May 1989 p 501-511 (For primary document see N90-18462 11-20)
(Contracts NAS9-17585; NAS9-17854)
Avail: NTIS HC A25/MF A04 CSCL 22B

N90-18488*# National Aeronautics and Space Administration. Lyndon B. Johnson Space Center, Houston, TX.
SUPERFLUID HELIUM ORBITAL RESUPPLY COUPLING
M. O. Ryder, D. H. Morash (Moog, Inc., East Aurora, NY.), and R. J. Schoenberg *In* Johns Hopkins Univ., The 1989 JANNAF Propulsion Meeting, Volume 1 May 1989 p 529-539 (For primary document see N90-18462 11-20)

(Contract NAS9-17872)
Avail: NTIS HC A25/MF A04 CSCL 22B

19 SPACECRAFT INSTRUMENTATION

For related information see also *06 Aircraft Instrumentation* and *35 Instrumentation and Photography.*

No abstracts in this category.

20 SPACECRAFT PROPULSION AND POWER

Includes main propulsion systems and components, e.g., rocket engines; and spacecraft auxiliary power sources.

For related information see also *07 Aircraft Propulsion and Power, 28 Propellants and Fuels, 44 Energy Production and Conversion,* and *15 Launch Vehicles and Space Vehicles.*

N90-18462# Johns Hopkins Univ., Laurel, MD. Chemical Propulsion Information Agency.
THE 1989 JANNAF PROPULSION MEETING, VOLUME 1
Debra S. Eggleston, ed. and Karen L. Strange, ed. May 1989 579 p Meeting held in Cleveland, OH, 23-25 May 1989
(Contract N00039-89-C-5301)
(CPIA-Publ-515-Vol-1) Avail: NTIS HC A25/MF A04

Specific subjects discussed include space shuttle solid rocket motor, motor insulation, bipropellant engines, space propulsion, orbital propellant feed systems, and electric propulsion. For individual titles, see N90-18463 through N90-18489.

N90-18463*# National Aeronautics and Space Administration. Marshall Space Flight Center, Huntsville, AL.
TRANSIENT PRESSURE TEST ARTICLE TEST PROGRAM
Charles M. Vibbart *In* Johns Hopkins Univ., The 1989 JANNAF Propulsion Meeting, Volume 1 May 1989 p 35-43 Previously announced in IAA as A89-54690 (For primary document see N90-18462 11-20)
Avail: NTIS HC A25/MF A04 CSCL 21H

The Transient Pressure Test Article (TPTA) test program is being conducted at a new test facility located in the East Test Area at the National Aeronautics and Space Administration's (NASA's) Marshall Space Flight Center (MSFC) in Huntsville, Alabama. This facility, along with the special test equipment (STE) required for facility support, was constructed specifically to test and verify the sealing capability of the Redesigned Solid Rocket Motor (RSRM) field, igniter, and nozzle joints. The test article consists of full scale RSRM hardware loaded with inert propellant and assembled in a short stack configuration. The TPTA is pressurized by igniting a propellant cartridge capable of inducing a pressure rise rate which stimulates the ignition transient that occurs during launch. Dynamic loads are applied during the pressure cycle to simulate external tank attach (ETA) strut loads present on the ETA ring. Sealing ability of the redesigned joints is evaluated under joint movement conditions produced by these combined loads since joint sealing ability depends on seal resilience velocity being greater than gap opening velocity. Also, maximum flight dynamic loads are applied to the test article which is either pressurized to 600 psia using gaseous nitrogen (GN2) or applied to the test article as the pressure decays inside the test article on the down cycle after the ignition transient cycle. This new test facility is examined with respect to its capabilities. In addition, both the topic of test effectiveness versus space vehicle flight performance and new aerospace test techniques, as well as a comparison between the old SRM design and the RSRM are presented. Author

N90-18464*# National Aeronautics and Space Administration. Marshall Space Flight Center, Huntsville, AL.
TEST DATA OF FLOW FIELD OF SHUTTLE SRM NOZZLE JOINT WITH BOND DEFECTS, USING UNHEATED AIR
Leroy M. Hair, James V. McAnally (Huntsville Sciences Corp., AL.), and John E. Hengel *In* Johns Hopkins Univ., The 1989 JANNAF Propulsion Meeting, Volume 1 May 1989 p 45-55 (For primary document see N90-18462 11-20)
(Contracts NAS8-36300; NAS8-37505)
Avail: NTIS HC A25/MF A04 CSCL 21H

The nozzle-to-case joint on the Shuttle SRM (as redesigned after the Challenger accident) features an adhesive sealant filling and bonding the joint, with a wiper O-ring to prevent the adhesive from reaching and disabling the closure O-ring. Flawless implementation of that joint design would ensure that hot, corrosive propellant combustion gases never reach the closure O-ring. However, understanding the flow field related to bonding defects is prudent. A comprehensive test program was conducted to quantify such flow fields and associated heating environments. A two-dimensional, full-scale model represented 65 inches of the nozzle joint, using unheated air as the test medium, in a blowdown mode. Geometry variations modeled RSRM assembly tolerances, and two types of bonding defects: pullaways and blowholes. A range of the magnitude of each type defect was tested. Also a range of operational parameters was tested, representative of the RSRM flow environment, including duplication of RSRM Mach and Reynolds numbers. Extensive instrumentation was provided to quantify pressures, heat rates, and velocities. The resulting data established that larger geometric defects cause larger pressure and larger heating, at the closure O-ring region. Velocity trends were not so straight-forward. Variations in assembly tolerances did not generally affect flow fields or heating. Operational parameters affected flow fields and heating as might be expected, increasing density or velocity increased heating. Complete details of this test effort are presented. Author

N90-18465*# National Aeronautics and Space Administration. Marshall Space Flight Center, Huntsville, AL.
COLD FLOW DETERMINATION OF THE INTERNAL FLOW ENVIRONMENT AROUND THE SUBMERGED TVC NOZZLE FOR THE SPACE SHUTTLE SRM
R. H. Whitesides, A. Ghosh, S. L. Jenkins (Spectra Research Systems, Inc., Huntsville, AL.), and D. L. Bacchus *In* Johns Hopkins Univ., The 1989 JANNAF Propulsion Meeting, Volume 1 May 1989 p 57-69 (For primary document see N90-18462 11-20)
(Contract NAS8-36300)
Avail: NTIS HC A25/MF A04 CSCL 21H

A series of subscale cold flow tests was performed to quantify the gas flow characteristics at the aft end of the Space Shuttle Solid Rocket Motor. This information was used to support the analyses of the redesigned nozzle/case joint. A portion of the thermal loads at the joint are due to the circumferential velocities and pressure gradients caused primarily by the gimbaling of the submerged nose TVC nozzle. When the nozzle centerline is vectored with respect to the motor centerline, asymmetries are set up in the flow field under the submerged nozzle and immediately adjacent to the nozzle/case joint. Specific program objectives included: determination of the effects of nozzle gimbal angle and propellant geometry on the circumferential flow field; measurement of the static pressure and gas velocities in the vicinity of the nozzle/case joint; use of scaling laws to apply the subscale cold flow data to the full scale SRM; and generation of data for use in validation of 3-D computational fluid dynamic, CFD, models of the SRM flow field. These tests were conducted in the NASA Marshall Space Flight Center Airflow Facility with a 7.5 percent scale model of the aft segment of the SRM. Static and dynamic pressures were measured in the model to quantify the flow field. Oil flow data was also acquired to obtain qualitative visual descriptions of the flow field. Nozzle gimbal angles of 0, 3.5, and 7 deg were used with propellant grain configurations corresponding to motor burn times of 0, 9, 19, and 114 seconds. This experimental program was successful in generating velocity and pressure gradient data

for the flow field around the submerged nose nozzle of the Space Shuttle SRM at various burn times and gimbal angles. The nature of the flow field adjacent to the nozzle/case joint was determined with oil droplet streaks, and the velocity and pressure gradients were quantified with pitot probes and wall static pressure measurements. The data was applied to the full scale SRM thru a scaling analysis and the results compared well with the 3-D computational fluid dynamics computer model. Author

N90-18466*# Jet Propulsion Lab., California Inst. of Tech., Pasadena.
TECHNIQUE FOR EVALUATING THE EROSIVE PROPERTIES OF ABLATIVE INTERNAL INSULATION MATERIALS
J. C. McComb and J. M. Hitner *In* Johns Hopkins Univ., The 1989 JANNAF Propulsion Meeting, Volume 1 May 1989 p 83-90 (For primary document see N90-18462 11-20)
Avail: NTIS HC A25/MF A04 CSCL 21H

A technique for determining the average erosion rate versus Mach number of candidate internal insulation materials was developed for flight motor applications in 12 inch I.D. test firing hardware. The method involved the precision mounting of a mechanical measuring tool within a conical test cartridge fabricated from either a single insulation material or two non-identical materials each of which constituted one half of the test cartridge cone. Comparison of the internal radii measured at nine longitudinal locations and between eight to thirty two azimuths, depending on the regularity of the erosion pattern before and after test firing, permitted calculation of the average erosion rate and Mach number. Systematic criteria were established for identifying erosion anomalies such as the formation of localized ridges and for excluding such anomalies from the calculations. The method is discussed and results presented for several asbestos-free materials developed in-house for the internal motor case insulation in solid propellant rocket motors. Author

N90-18467*# Pratt and Whitney Aircraft, West Palm Beach, FL.
EFFECT OF CORRELATION ON MULTI-ENGINE ROCKET PROPULSION SYSTEMS
J. R. Baker and J. E. Breneman *In* Johns Hopkins Univ., The 1989 JANNAF Propulsion Meeting, Volume 1 May 1989 p 113-120 (For primary document see N90-18462 11-20)
(Contract NAS8-36868)
Avail: NTIS HC A25/MF A04 CSCL 21H

A matter of great concern in the design and operation of multi-engine rocket propulsion systems is the effect of the premature shutdown of one engine on the vehicle. This probability that a premature shutdown will cause a vehicle loss is termed correlation. Based on airbreathing experiences as well as rocket engine data the best estimate of this correlation is made and then applied to the overall multi-engine reliability problem to demonstrate its potential effect. At this point, follow-on analyses are pointed out that illustrate how any potential failures that may cause a correlatable event can be eliminated; thus bringing this correlation to almost 0. Author

N90-18468*# National Aeronautics and Space Administration. Marshall Space Flight Center, Huntsville, AL.
EFFECT OF PROPELLANT FLOWRATE AND PURITY ON CARBON DEPOSITION IN LO2/METHANE GAS GENERATORS
J. A. Bossard, W. M. Burkhardt, K. Y. Niiya (Aerojet TechSystems Co., Sacramento, CA.), and F. Braam *In* Johns Hopkins Univ., The 1989 JANNAF Propulsion Meeting, Volume 1 May 1989 p 131-144 (For primary document see N90-18462 11-20)
Avail: NTIS HC A25/MF A04 CSCL 21H

The generation and deposition of carbon was studied in the Carbon Deposition Program using subscale hardware with LO2/Liquid Natural Gas (LNG) and LO2/Methane propellants at low mixture ratios. The purpose of the testing was to evaluate the effect of methane purity and full scale injection density on carbon deposition. The LO2/LNG gas generator/preburner testing was performed at mixture ratios between 0.24 and 0.58 and chamber pressures from 5.8 to 9.4 MPa (840 to 1370 psia). A total of seven 200 second duration tests were performed. The LNG testing occurred at low injection densities, similar to the previous LO2/RP-1, LO2/propane, and LO2/methane testing performed on the carbon deposition program. The current LO2/methane test series occurred at an injection density factor of approximately 10 times higher than the previous testing. The high injection density LO2/methane testing was performed at mixture ratios between from 0.23 to 0.81 and chamber pressures from 6.4 to 15.2 MPa (925 to 2210 psia). A total of nine high injection density tests were performed. The testing performed demonstrated that low purity methane (LNG) did not produce any detectable change in carbon deposition when compared to pure methane. In addition, the C* performance and the combustion gas temperatures measured were similar to those obtained for pure methane. Similar results were obtained testing pure methane at higher propellant injection densities with coarse injector elements. Author

N90-18469*# National Aeronautics and Space Administration. Marshall Space Flight Center, Huntsville, AL.
EXPERIMENTAL FLOW MODELS FOR SSME FLOWFIELD CHARACTERIZATION
L. C. Abel (Micro Craft, Inc., Tullahoma, TN.) and P. E. Ramsey *In* Johns Hopkins Univ., The 1989 JANNAF Propulsion Meeting, Volume 1 May 1989 p 145-154 (For primary document see N90-18462 11-20)
(Contracts NAS8-37505; NAS2-12037)
Avail: NTIS HC A25/MF A04 CSCL 21H

Full scale flow models with extensive instrumentation were designed and manufactured to provide data necessary for flow field characterization in rocket engines of the Space Shuttle Main Engine (SSME) type. These models include accurate flow path geometries from the pre-burner outlet through the throat of the main combustion chamber. The turbines are simulated with static models designed to provide the correct pressure drop and swirl for specific power levels. The correct turbopump-hot gas manifold interfaces were designed into the flow models to permit parametric/integration studies for new turbine designs. These experimental flow models provide a vehicle for understanding the fluid dynamics associated with specific engine issues and also fill the more general need for establishing a more detailed fluid dynamic base to support development and verification of advanced math models. Author

N90-18470*# National Aeronautics and Space Administration. Lewis Research Center, Cleveland, OH.
PROBABILITY OF FAILURE AND RISK ASSESSMENT OF PROPULSION STRUCTURAL COMPONENTS c39
Michael C. Shiao (Sverdrup Technology, Inc., Cleveland, OH.) and Christos C. Chamis *In* Johns Hopkins Univ., The 1989 JANNAF Propulsion Meeting, Volume 1 May 1989 p 135-162 (For primary document see N90-18462 11-20)
Avail: NTIS HC A25/MF A04 CSCL 20K

Due to increasing need to account for the uncertainties in material properties, loading conditions, or geometries, a methodology was developed to determine structural reliability and the assess the risk associated with it. The methodology consists of a probabilistic structural analysis by a probabilistic finite element computer code Nonlinear Evaluation of Stochastic Structures Under Stress (NESSUS) and a generic probabilistic material properties model. The methodology is versatile and is equally applicable to high and cryogenic temperature structures. Results obtained demonstrate that the whole issue of structural reliability and risk can be formally evaluated using the methodology developed which is inclusive of uncertainties in material properties, structural parameters and loading conditions. The methodology is described in some detail with illustrative examples. Author

N90-18471*# National Aeronautics and Space Administration. Lewis Research Center, Cleveland, OH.
THE PATHFINDER CHEMICAL TRANSFER PROPULSION PROGRAM
Ned P. Hannum, Frank D. Berkopec, and Robert L. Zurawski (National Aeronautics and Space Administration, Washington, DC.) *In* Johns Hopkins Univ., The 1989 JANNAF Propulsion

Meeting, Volume 1 May 1989 p 191-197 Previously announced as N89-24409 (For primary document see N90-18462 11-20)
Avail: NTIS HC A25/MF A04 CSCL 21H

Pathfinder is a research and technology initiative by the National Aeronautics and Space Administration (NASA) intended to strengthen the technology base of the United States civil space program in preparation for future space exploration missions. Pathfinder begins in FY-89. One of the four major thrusts is the Chemical Transfer Propulsion program which will provide the propulsion technology for high performance, liquid oxygen/liquid hydrogen expander cycle engines which are expected to be operated and maintained in space. These advanced engines will enhance or enable a variety of future space exploration missions. The goals and objectives, management, technical plan, and technology transfer for the Chemical Transfer Propulsion element of Pathfinder are described. Author

N90-18472*# National Aeronautics and Space Administration. Lewis Research Center, Cleveland, OH.
ADVANCED APS IMPACTS ON VEHICLE PAYLOADS
Steven J. Schneider and Brian D. Reed *In* Johns Hopkins Univ., The 1989 JANNAF Propulsion Meeting, Volume 1 May 1989 p 209-218 Previously announced as N89-25254 (For primary document see N90-18462 11-20)
Avail: NTIS HC A25/MF A04 CSCL 21H

Advanced auxiliary propulsion system (APS) technology has the potential to both, increase the payload capability of earth-to-orbit (ETO) vehicles by reducing APS propellant mass, and simplify ground operations and logistics by reducing the number of fluids on the vehicle and eliminating toxic, corrosive propellants. The impact of integrated cryogenic APS on vehicle payloads is addressed. In this system, launch propulsion system residuals are scavenged from integral launch propulsion tanks for use in the APS. Sufficient propellant is preloaded into the APS to return to earth with margin and noncomplete scavenging assumed. No propellant conditioning is required by the APS, but ambient heat soak is accommodated. High temperature rocket materials enable the use of the unconditioned hydrogen/oxygen in the APS and are estimated to give APS rockets specific impulse of up to about 444 sec. The payload benefits are quantified and compared with an uprated monomethyl hydrazine/nitrogen tetroxide system in a conservative fashion, by assuming a 25.5 percent weight growth for the hydrogen/oxygen system and a 0 percent weight growth for the uprated system. The combination and scavenging and high performance gives payload impacts which are highly mission specific. A payload benefit of 861 kg (1898 lbm) was estimated for a Space Station Freedom rendezvous mission and 2099 kg (4626 lbm) for a sortie mission, with payload impacts varying with the amount of launch propulsion residual propellants. Missions without liquid propellant scavenging were estimated to have payload penalties, however, operational benefits were still possible.
Author

N90-18473*# National Aeronautics and Space Administration. Lyndon B. Johnson Space Center, Houston, TX.
A PERSPECTIVE ON THE USE OF STORABLE PROPELLANTS FOR FUTURE SPACE VEHICLE PROPULSION
William C. Boyd and Warren L. Brasher *In* Johns Hopkins Univ., The 1989 JANNAF Propulsion Meeting, Volume 1 May 1989 p 219-228 (For primary document see N90-18462 11-20)
Avail: NTIS HC A25/MF A04 CSCL 21H

Propulsion system configurations for future NASA and DOD space initiatives are driven by the continually emerging new mission requirements. These initiatives cover an extremely wide range of mission scenarios, from unmanned planetary programs, to manned lunar and planetary programs, to earth-oriented (Mission to Planet Earth) programs, and they are in addition to existing and future requirements for near-earth missions such as to geosynchronous earth orbit (GEO). Increasing space transportation costs, and anticipated high costs associated with space-basing of future vehicles, necessitate consideration of cost-effective and easily maintainable configurations which maximize the use of existing technologies and assets, and use budgetary resources effectively. System design considerations associated with the use of storable propellants to fill these needs are presented. Comparisons in areas such as complexity, performance, flexibility, maintainability, and technology status are made for earth and space storable propellants, including nitrogen tetroxide/monomethylhydrazine and LOX/monomethylhydrazine. Author

N90-18474*# National Aeronautics and Space Administration. Lewis Research Center, Cleveland, OH.
ELECTRIC PROPULSION OPTIONS FOR 10 kW CLASS EARTH-SPACE MISSIONS
M. J. Patterson and Francis M. Curran *In* Johns Hopkins Univ., The 1989 JANNAF Propulsion Meeting, Volume 1 May 1989 p 239-265 Previously announced as N89-26906 (For primary document see N90-18462 11-20)
Avail: NTIS HC A25/MF A04 CSCL 21H

Five and 10 kW ion and arcjet propulsion system options for a near-term space demonstration experiment were evaluated. Analyses were conducted to determine first-order propulsion system performance and system component mass estimates. Overall mission performance of the electric propulsion systems was quantified in terms of the maximum thrusting time, total impulse, and velocity increment capability available when integrated onto a generic spacecraft under fixed mission model assumptions. Maximum available thrusting times for the ion-propelled spacecraft options, launched on a DELTA 2 6920 vehicle, range from approximately 8,600 hours for a 4-engine 10 kW system to more than 29,600 hours for a single-engine 5 kW system. Maximum total impulse values and maximum delta-v's range from 1.2x10 (exp 7) to 2.1x10 (exp 7) N-s, and 3550 to 6200 m/s, respectively. Maximum available thrusting times for the arcjet propelled spacecraft launched on the DELTA 2 6920 vehicle range from approximately 528 hours for the 6-engine 10 kW hydrazine system to 2328 hours for the single-engine 5 kW system. Maximum total impulse values and maximum delta-v's range from 2.2x10 (exp 6) to 3.6x10 (exp 6) N-s, and approximately 662 to 1072 m/s, respectively. Author

N90-18475*# National Aeronautics and Space Administration. Lewis Research Center, Cleveland, OH.
PERFORMANCE OF LARGE AREA XENON ION THRUSTERS FOR ORBIT TRANSFER MISSIONS
Vincent K. Rawlin *In* Johns Hopkins Univ., The 1989 JANNAF Propulsion Meeting, Volume 1 May 1989 p 267-276 (For primary document see N90-18462 11-20)
Avail: NTIS HC A25/MF A04 CSCL 21H

Studies have indicated that xenon ion propulsion systems can enable the use of smaller earth-launch vehicles for satellite placement which results in significant cost savings. These analyses have assumed the availability of advanced, high power ion thrusters-operating at about 10 kW or higher. A program was initiated to explore the viability of operating 50 cm diameter ion thrusters at this power level. Operation with several discharge chamber and ion extraction grid set combinations was demonstrated and data were obtained at power levels to 16 kW. Fifty cm diameter thrusters using state of the art 30 cm diameter grids or advanced technology 50 cm diameter grids allow discharge power and beam current densities commensurate with long life at power levels up to 10 kW. In addition, 50 cm diameter thrusters are shown to have potential for growth in thrust and power levels beyond 10 kW. Author

N90-18476*# National Aeronautics and Space Administration. Lewis Research Center, Cleveland, OH.
TEST FACILITY AND PRELIMINARY PERFORMANCE OF A 100 kW CLASS MPD THRUSTER
J. S. Sovey, M. A. Mantenieks, Thomas W. Haag, P. Raitano, and J. E. Parkes (Sverdrup Technology, Inc., Cleveland, OH.) *In* Johns Hopkins Univ., The 1989 JANNAF Propulsion Meeting, Volume 1 May 1989 p 325-338 Previously announced as N89-23520 (For primary document see N90-18462 11-20)
Avail: NTIS HC A25/MF A04 CSCL 21H

A 260 kW magnetoplasmadynamic (MPD) thruster test facility was assembled and used to characterize thrusters at power levels up to 130 kW using argon and helium propellants. Sensitivities of discharge characteristics to arc current, mass flow rate, and applied magnetic field were investigated. A thermal efficiency correlation developed by others for low power MPD thrusters defined parametric guidelines to minimize electrode losses in MPD thrusters. Argon and helium results suggest that a parameter defined as the product of arc voltage and the square root of the mass flow rate must exceed 0.7 V/kg(sup 1/2)/sec(sup 1/2) in order to obtain thermal efficiencies in excess of 60 percent.
Author

N90-18477*# National Aeronautics and Space Administration. Lewis Research Center, Cleveland, OH.
ARCJET CATHODE PHENOMENA
Francis M. Curran, Thomas W. Haag, and John F. Raquet (Air Force Academy, CO.) *In* Johns Hopkins Univ., The 1989 JANNAF Propulsion Meeting, Volume 1 May 1989 p 349-366 Previously announced as N89-27121 (For primary document see N90-18462 11-20)
Avail: NTIS HC A25/MF A04 CSCL 21H

Cathode tips made from a number of different materials were tested in a modular arcjet thruster in order to examine cathode phenomena. Periodic disassembly and examination, along with the data collected during testing, indicated that all of the tungsten-based materials behaved similarly despite the fact that in one of these samples the percentage of thorium oxide was doubled and another was 25 percent rhenium. The mass loss rate from a 2 percent thoriated rhenium cathode was found to be an order of magnitude greater than that observed using 2 percent thoriated tungsten. Detailed analysis of one of these cathode tips showed that the molten crater contained pure tungsten to a depth of about 150 microns. Problems with thermal stress cracking were encountered in the testing of a hafnium carbide tip. Post test analysis showed that the active area of the tip had chemically reacted with the propellant. A 100 hour continuous test was run at about 1 kW. Post test analysis revealed no dendrite formation, such as observed in a 30 kW arcjet lifetest, near the cathode crater. The cathodes from both this test and a previously run 1000 hour cycled test displayed nearly identical arc craters. Data and calculations indicate that the mass losses observed in testing can be explained by evaporation.
Author

N90-18478*# National Aeronautics and Space Administration. Lewis Research Center, Cleveland, OH.
ARCJET NOZZLE DESIGN IMPACTS
Francis M. Curran, Amy J. Sovie (Ohio Univ., Athens.), and Thomas W. Haag *In* Johns Hopkins Univ., The 1989 JANNAF Propulsion Meeting, Volume 1 May 1989 p 367-380 Previously announced as N89-23522 (For primary document see N90-18462 11-20)
Avail: NTIS HC A25/MF A04 CSCL 21H

The effect of nozzle configuration on the operating characteristics of a low power dc arcjet thruster was determined. A conical nozzle with a 30 deg converging angle, a 20 deg diverging angle, and an area ratio of 225 served as the baseline case. Variations on the geometry included bell-shaped contours both up and downstream, and a downstream trumpet-shaped contour. The nozzles were operated over a range of specific power near that anticipated for on-orbit operation. Mass flow rate, thrust, current, and voltage were monitored to provide accurate comparisons between nozzles. The upstream contour was found to have minimal effect on arcjet operation. It was determined that the contour of the divergent section of the nozzle, that serves as the anode, was very important in determining the location of arc attachment, and thus had a significant impact on arcjet performance. The conical nozzle was judged to have the optimal current/voltage characteristics and produced the best performance of the nozzles tested.
Author

N90-18479*# Jet Propulsion Lab., California Inst. of Tech., Pasadena.
MISSION OPTIONS FOR AN ELECTRIC PROPULSION DEMONSTRATION FLIGHT TEST
Charles Garner *In* Johns Hopkins Univ., The 1989 JANNAF Propulsion Meeting, Volume 1 May 1989 p 413-420 (For primary document see N90-18462 11-20)
Avail: NTIS HC A25/MF A04 CSCL 21H

Several mission options are discussed for an electric propulsion space test which provides operational and performance data for ion and arcjet propulsion systems and testing of APSA arrays and a super power system. The results of these top-level studies are considered preliminary. Ion propulsion system design and architecture for the purposes of performing orbit raising missions for payloads in the range of 2400 to 2700 kg are described. Focus was placed on a design which can be characterized by simplicity, reliability, and performance. Systems of this design are suitable for an electric propulsion precursor flight which would provide proof of principle data necessary for more ambitious and complex missions.
Author

N90-18480*# Jet Propulsion Lab., California Inst. of Tech., Pasadena.
ELECTRIC PROPULSION FOR MANNED MARS EXPLORATION
Bryan Palaszewski *In* Johns Hopkins Univ., The 1989 JANNAF Propulsion Meeting, Volume 1 May 1989 p 421-435 (For primary document see N90-18462 11-20)
Avail: NTIS HC A25/MF A04 CSCL 21H

Advanced high-power electric propulsion systems can significantly enhance piloted Mars missions. An increase in the science payload delivered to Mars and the reduction of the total Earth-departure mass are the major system-level benefits of electric propulsion. Other potential benefits are the return of the cargo vehicle to Earth orbit and the availability of high power in Mars orbit for high-power science and communications. Parametric analyses for sizing the cargo mission vehicle for Mars exploration missions are presented. The nuclear-electric propulsion system thruster size, power level, mass, propellant type and payload mass capability are considered in these system-level trade studies. Descriptions of the propulsion system selection issues for both ion and MPD thruster technologies are also discussed. On a manned Mars mission, the total launch mass for an unmanned cargo vehicle in low earth orbit (LEO) can be reduced by up to 50 percent over the baseline oxygen/hydrogen propulsion system. Because the cargo vehicle is sent to Mars prior to the manned mission, the trip time for the vehicle is not a critical factor. By taking advantage of the high specific impulse (I sub sp) of an ion or a Magneto-Plasma-Dynamic (MPD) thruster system, the total LEO mass is reduced from 590,000 kg for the oxygen/hydrogen propulsion system to 309,000 kg for the MPD system and 295,000 kg for the ion system. Many factors must be analyzed in the design of a electric propulsion Mars cargo vehicle. The propellant selection, the number of thrusters, the power level and the specific impulse are among the most important of the parameters. To fully address the electric propulsion system design, trade studies for the differing ion and MPD propulsion system configurations (thruster power levels, number of thrusters, propellants and power systems) must be conducted.
Author

N90-18481*# Jet Propulsion Lab., California Inst. of Tech., Pasadena.
FEASIBILITY DEMONSTRATION OF A 445N HIGH-PERFORMANCE ROCKET ENGINE
Marshall A. Appel, Leonard Schoenman, Jerrold E. Franklin, and P. Tina Lansaw (Aerojet TechSystems Co., Sacramento, CA.) *In* Johns Hopkins Univ., The 1989 JANNAF Propulsion Meeting, Volume 1 May 1989 p 445-455 (For primary document see N90-18462 11-20)
Avail: NTIS HC A25/MF A04 CSCL 21H

A program to demonstrate the feasibility of a high-performance 445 Newton (100 lb(sub f)) NTO/NMH rocket engine is presented. An existing high-performance injector was coupled with three different thrust chambers to acquire test data for the program. A

stainless-steel sea-level chamber was used for test stand checkout, calibration and initial injector performance determinations. Two high-temperature iridium lined rhenium thrust chambers were used to determine altitude performance and durability. The first chamber was tested for a total duration of 3381 s and the second was tested for a total duration of 15,000 s with no measurable degradation. Extrapolation of epsilon = 44:1 experimental data to the recommended epsilon = 467:1 expansion nozzle, using the JANNAF methodology, showed that a performance of 3138 to 3167 N-s/kg (320 to 323 lb(sub f-s)/lb(sub m) could be achieved with the present design. Recommendations are presented which would allow a redesigned engine to achieve the 3195 N-s/kg (326 lb(sub f-s)/lb(sub m)) program goal. Author

N90-18482*# National Aeronautics and Space Administration. Lyndon B. Johnson Space Center, Houston, TX.
SPACE STATION TECHNOLOGY SUMMARY **c18**
R. Iacabucci, S. Evans, G. Briley, R. A. Delventhal, and E. Braunscheidel (National Aeronautics and Space Administration. Lewis Research Center, Cleveland, OH.) *In* Johns Hopkins Univ., The 1989 JANNAF Propulsion Meeting, Volume 1 May 1989 p 457-470 (For primary document see N90-18462 11-20)
Avail: NTIS HC A25/MF A04 CSCL 22B

The completion of the Space Station Propulsion Advanced Technology Programs established an in-depth data base for the baseline gaseous oxygen/gaseous hydrogen thruster, the waste gas resistojet, and the associated system operations. These efforts included testing of a full end-to-end system at National Aeronautics and Space Administration (NASA)-Marshall Space Flight Center (MSFC) in which oxygen and hydrogen were generated from water by electrolysis at 6.89 MPa (1,000 psia), stored and fired through the prototype thruster. Recent end-to-end system tests which generate the oxygen/hydrogen propellants by electrolysis of water at 20.67 MPa (3,000 psia) were completed on the Integrated Propulsion Test Article (IPTA) at NASA-Johnson Space Center (JSC). Resistojet testing has included 10,000 hours of life testing, plume characterization, and electromagnetic interference (EMI) testing. Extensive 25-lbf thruster testing was performed defining operating performance characteristics across the required mixture ratio and thrust level ranges. Life testing has accumulated 27 hours of operation on the prototype thruster. A total of seven injectors and five thrust chambers were fabricated to the same basic design. Five injectors and three thrust chambers designed to incorporate improved life, performance, and producibility characteristics are ready for testing. Five resistojets were fabricated and tested, with modifications made to improve producibility. The lessons learned in the area of producibility for both the O2/H2 thrusters and for the resistojet have resolved critical fabrication issues. The test results indicate that all major technology issues for long life and reliability for space station application were resolved. Author

N90-18483*# Ball Aerospace Systems Div., Boulder, CO.
RF MODAL QUANTITY GAGING **c35**
K. VanLeuven *In* Johns Hopkins Univ., The 1989 JANNAF Propulsion Meeting, Volume 1 May 1989 p 471-478 (For primary document see N90-18462 11-20)
(Contract NAS9-17378)
Avail: NTIS HC A25/MF A04 CSCL 14B

The primary objective is to provide a concept of a radio frequency (RF) modal resonance technique which is being investigated as a method for gaging the quantities of subcritical cryogenic propellants in metallic tanks. Of special interest are the potential applications of the technique to microgravity propellant gaging situations. The results of concept testing using cryogenic oxygen, hydrogen, and nitrogen, as well as paraffin simulations of microgravity fluid orientations, are reported. These test results were positive and showed that the gaging concept was viable. Author

N90-18484*# National Aeronautics and Space Administration. Lyndon B. Johnson Space Center, Houston, TX.
ELECTRONICALLY VARIABLE PRESSURE REGULATOR (EVPR) **c35**
R. H. Reinicke, R. O. Nelson (Eaton Corp., El Segundo, CA.), and E. Hurlbert *In* Johns Hopkins Univ., The 1989 JANNAF Propulsion Meeting, Volume 1 May 1989 p 479-488 (For primary document see N90-18462 11-20)
(Contract NAS9-17907)
Avail: NTIS HC A25/MF A04 CSCL 14B

A new programmable electronically variable pressure regulator (EVPR) concept accurately controls the local outlet or remote system pressure. It uses an integral pulse width modulated rare earth permanent magnet motor operating in response to redundant pressure transducer feedback signals. The EVPR is a simple single stage device that does not use dynamic seals or pilot valving. Conversion of partial revolution motor torque to poppet lifting force is accomplished by pure flexure action to avoid using bearings. The flexure drive (called the ROTAX) has a variable lead to minimize motor weight and power consumption. Breadboard tests were completed successfully on two critical design elements of the EVPR: the ROTAX and the motor. The ROTAX cable system was tested for 250,000 cycles without failure. The breadboard motor met the basic design requirements including the design torque and power consumption. Prototype parts were fabricated, and testing of the prototype EVPR has started. It is PC computer controlled to facilitate programming, data acquisition and analysis. A lightweight dedicated microprocessor is planned for the flightweight EVPR. Author

N90-18485*# National Aeronautics and Space Administration. Lyndon B. Johnson Space Center, Houston, TX.
SPACE SHUTTLE RCS OXIDIZER LEAK REPAIR FOR STS-26 **c16**
R. A. Delventhal and N. M. Faget *In* Johns Hopkins Univ., The 1989 JANNAF Propulsion Meeting, Volume 1 May 1989 p 489-495 (For primary document see N90-18462 11-20)
Avail: NTIS HC A25/MF A04 CSCL 22B

Following propellant loading of the Space Shuttle's reaction control system (RCS) for mission STS 26, an oxidizer leak was detected in the left orbital maneuvering system (OMS) pod, where the RCS is located. Subsequent investigation determined that the leak was isolated at a mechanical Dynatube fitting near the RCS nitrogen tetroxide tank. An intense effort was initiated to design, fabricate, and qualify a sealing device to stop the oxidizer leak externally so that the Space Shuttle launch could proceed. It was discovered that sealing devices called clamshells were widely used throughout the petrochemical and power generation industries to stop leaks developed in large diameter pipes which carry steam or other hazardous fluids. These clamshells are available in different diameters and strengths and are placed around the pipe at the location of the leak. A sealing compound is then injected under high pressure into the clamshell to stop the leak. This technology was scaled down and applied to the problem of stopping the leak on the Orbiter, which was on a half-inch diameter line in a nearly inaccessible location. Many obstacles had to be overcome such as determining that the sealing material would be compatible with the nitrogen tetroxide and ensuring that the clamshell would actually fit around the Dynatube fitting without interfering with other lines which were in close proximity. The effort at the NASA Johnson Space Center included materials compatibility testing of several sealants, design of a clamshell to fit in the confined compartment, and manufacture and qualification of the flight hardware. A clamshell was successfully placed around the Dynatube fitting on the Orbiter and the oxidizer leak was terminated. Then it was decided to apply this technology further and design clamshells for other mechanical fittings onboard the Orbiter and develop sealing compounds which will be compatible with fuels such as monomethyl hydrazine (MMH). The potential exists for using this type of sealing device in numerous other applications throughout the aerospace industry. Author

N90-18486*# National Aeronautics and Space Administration. Lyndon B. Johnson Space Center, Houston, TX.
ZERO-GRAVITY VORTEX VENT AND PVT GAGING SYSTEM **c18**
M. G. Downey and J. T. Trevathan *In* Johns Hopkins Univ., The 1989 JANNAF Propulsion Meeting, Volume 1 May 1989 p 497-500 (For primary document see N90-18462 11-20)
Avail: NTIS HC A25/MF A04 CSCL 22B

Space Station and satellite reservicing will require the ability to vent gas on orbit from liquid supply or storage tanks and to gage liquid quantity under microgravity conditions. In zero gravity, (zero-g) the vortex vent is capable of venting gas from a tank of liquid containing gas randomly distributed as bubbles. The concept uses a spinning impeller to create centrifugal force inside a vortex tube within a tank. This creates a gas pocket and forces the liquid through a venturi and back into the tank. Gas is then vented from the gas pocket through a liquid detector and then out through an exhaust port. If the liquid detector senses liquid in the vent line, the fluid is directed to the low-pressure port on the venturi and is returned to the tank. The advantages of this system is that it has no rotating seals and is compatible with most corrosive and cryogenic fluids. A prototype was designed and built at the NASA Johnson Space Center and flown on the KC-135 zero-g aircraft. During these test flights, where microgravity conditions are obtained for up to 30 sec, the prototype demonstrated that less than 0.10 percent of the volume of fluid vented was liquid when the tank was half full of liquid. The pressure volume temperature (PVT) gaging system is used in conjunction with the vortex vent to calculate the amount of liquid remaining in a tank under microgravity conditions. The PVT gaging system is used in conjunction with the vortex vent to gage liquid quantity in zero or low gravity. The system consists of a gas compressor, accumulator, and temperature and pressure instrumentation. To measure the liquid in a tank a small amount of gas is vented from the tank to the compressor and compressed into the accumulator. Pressure and temperature in the tank and accumulator are measured before and after the gas transfer occurs. Knowing the total volume of the tank, the volume of the accumulator, the volume of the intermediate lines, and initial and final pressures and temperatures, the mass of the gas leaving the tank is equated to the mass of the gas entering the accumulator. The volume of liquid remaining in the tank is calculated using the ideal gas law. Author

N90-18487*# Martin Marietta Space Systems, Inc., Denver, CO.
ORBITAL FLUID RESUPPLY ASSESSMENT **c18**
Ralph N. Eberhardt *In* Johns Hopkins Univ., The 1989 JANNAF Propulsion Meeting, Volume 1 May 1989 p 501-511 (For primary document see N90-18462 11-20)
(Contracts NAS9-17585; NAS9-17854)
Avail: NTIS HC A25/MF A04 CSCL 22B

Orbital fluid resupply can significantly increase the cost-effectiveness and operational flexibility of spacecraft, satellites, and orbiting platforms and observatories. Reusable tankers are currently being designed for transporting fluids to space. A number of options exist for transporting the fluids and propellant to the space-based user systems. The fluids can be transported to space either in the Shuttle cargo bay or using expendable launch vehicles (ELVs). Resupply can thus be accomplished either from the Shuttle bay, or the tanker can be removed from the Shuttle bay or launched on an ELV and attached to a carrier such as the Orbital Maneuvering Vehicle (OMV) or Orbital Transfer Vehicle (OTV) for transport to the user to be serviced. A third option involves locating the tanker at the space station or an unmanned platform as a quasi-permanent servicing facility or depot which returns to the ground for recycling once its tanks are depleted. Current modular tanker designs for monopropellants, bipropellants, and water for space station propulsion are discussed. Superfluid helium tankers are addressed, including trade-offs in tanker sizes, shapes to fit the range of ELVs currently available, and boil-off losses associated with longer-term (greater than 6-month) space-basing. It is concluded that the mixed fleet approach to on-orbit consumables resupply offers significant advantages to the overall logistics requirements. Author

N90-18488*# National Aeronautics and Space Administration. Lyndon B. Johnson Space Center, Houston, TX.
SUPERFLUID HELIUM ORBITAL RESUPPLY COUPLING **c18**
M. O. Ryder, D. H. Morash (Moog, Inc., East Aurora, NY.), and R. J. Schoenberg *In* Johns Hopkins Univ., The 1989 JANNAF Propulsion Meeting, Volume 1 May 1989 p 529-539 (For primary document see N90-18462 11-20)
(Contract NAS9-17872)
Avail: NTIS HC A25/MF A04 CSCL 22B

The resupply of superfluid helium to satellites and other space-based experiment packages can increase the useful longevity of these devices far beyond their present life expectancies which are many times determined by the supply of helium coolant. The transfer of superfluid helium to spacecraft in space will require a reusable coupling that functions at 1.8 Kelvin with little heat leak and low pressure drop. Moog has designed the Helium Resupply Coupling to meet these operational requirements. Initially, the coupling manual mode operation will be demonstrated on orbit by an EVA crew member during the Space Shuttle borne Superfluid Helium On-Orbit Transfer (SHOOT) experiment. The ultimate application will use robotic (automatic) coupling operation to which the present design readily adapts. The utilization of Moog's exclusive Rotary Shut-Off (RSO) technology in the development of the Superfluid Helium Resupply Coupling is described. The coupling not only performs the function of a flow control valve and disconnect but also provides adequate safety features for a shuttle launched man-rated payload. In addition, the coupling incorporates the necessary features to provide the high thermal isolation of the internal flow path from the external environment. Author

N90-18489*# National Aeronautics and Space Administration. Lyndon B. Johnson Space Center, Houston, TX.
SMALL DISPLACEMENT, LONG LIFE ON-ORBIT COMPRESSOR DESIGN AND FABRICATION **c31**
C. R. Gerlach, E. C. Schroeder, D. D. Deffenbaugh (Southwest Research Inst., San Antonio, TX.), and J. P. Masetta *In* Johns Hopkins Univ., The 1989 JANNAF Propulsion Meeting, Volume 1 May 1989 p 541-550 (For primary document see N90-18462 11-20)
(Contract NAS9-18051)
Avail: NTIS HC A25/MF A04 CSCL 13B

The focus is the generation of technology and fabrication of prototype hardware applicable to seven Space Station compressor system applications. The compressors are of the single acting reciprocating piston type and, in general, may be termed miniature in size compared with normal commercially available equipment. The initial technology development is focused on improved valve designs, and the control of pulsations and heating effects in order to increase compressor efficiency and reduce cycle temperatures, thus permitting significantly increased stage pressure ratios. The initial test compressor was successfully operated at pressure ratios of up to 50:1, and this significant extension of allowable pressure ratio will result in a reduction of the number of required stages and, hence, total hardware thereby reducing system weight and volume. These experiments have also identified the need to employ low shaft speeds, on the order of 250 to 500 rpm, to enhance heat transfer and increase life. The prototype compressor currently being designed, is to be driven by a low-speed brushless dc motor sealed in a case common to the compressor drive mechanism case. The compressor and motor case will communicate with stage suction pressure so that any minor gas leakage past the piston rings will be returned to the suction. Emphasis in this prototype design is being placed on simplicity, durability, commonality of components, and high efficiency. Author

N90-18490# Instituto de Pesquisas Espaciais, Sao Jose dos Campos (Brazil).
VIABILITY STUDY OF IONIC MICROTHRUSTER TESTS ON MECB SATELLITE [ESTUDO DA VIABILIDADE DE TESTES DE UM MICROPROPULSOR IONICO EM SATELITES DA MECB]
Gilberto Marrega Sandonato, Antonio Montes Filho, Gerson Otto

Ludwig, Jose Leonardo Ferreira, and Julio Guimaraes Ferreira Nov. 1989 58 p In PORTUGUESE; ENGLISH summary
(INPE-4973-RPE/605) Avail: NTIS HC A04/MF A01

A technical evaluation of a electron bombardment ion thruster, using inert gases, to be tested in one of the satellites under development by the Brazilian Complete Space Program (MECB) is made. This thruster is intended to be used in the attitude control or orbit transfer of small geostationary satellites. Author

N90-18491# Air Force Office of Scientific Research, Bolling AFB, Washington, DC.
AFOSR/ONR (AIR FORCE OFFICE OF SCIENTIFIC RESEARCH/OFFICE OF NAVAL RESEARCH) CONTRACTORS' MEETING ON COMBUSTION ROCKET PROPULSION DIAGNOSTICS OF REACTING FLOW Technical Report, Jun. 1988 - Jun. 1989
J. M. Tishkoff, M. A. Birkan, G. S. Roy, and S. G. Lekoudis 19 Jun. 1989 370 p Meeting held in Ann Arbor, MI, 19-23 Jun. 1989
(Contract F49620-86-K-0022)
(AD-A216094; AFOSR-89-1711TR) Avail: NTIS HC A16/MF A02 CSCL 20/4

Abstracts are given for research on airbreathing combustion, rocket propulsion, and diagnostic of reacting flow supported by the Air Force Office of Scientific Research and the Office of Naval Research. GRA

N90-18492# Georgia Inst. of Tech., Atlanta. School of Aerospace Engineering.
COMBUSTION INSTABILITY IN SOLID PROPELLANT ROCKETS Final Report, Oct. 1985 - Mar. 1989
Edward W. Price and Gary A. Flandro 21 Mar. 1989 291 p
(Contract F49620-86-C-0005)
(AD-A216740; AFOSR-89-0460TR) Avail: NTIS HC A13/MF A02 CSCL 21/8

This report constitutes the principal of a book on combustion stability in solid propellant rockets. The present report contains nine chapters that are each substantially complete except for some editorial, bibliographical and art work in some chapters. Chapters 1 thru 9 include: Introduction to Combustion Instability; Combustion Chamber Processes; Guidance in Missile System and Motor Design; Fundamentals of Propellant Combustion; Analytical Modeling of Combustor Flow; Modeling of Combustion Dynamics; Bulk Mode Oscillations and L asterisk Instability; and Combustor Stability Analysis. GRA

23 CHEMISTRY AND MATERIALS (GENERAL)

N90-18493# Dartmouth Coll., Hanover, NH. Dept. of Chemistry.
PERFLUORINATED LIGANDS IN ORGANOMETALLIC CHEMISTRY Final Report, 1 Jan. 1986 - 31 Aug. 1989
Russell P. Hughes 12 Dec. 1989 12 p
(Grant AF-AFOSR-0075-86; AF Proj. 2303)
(AD-A216415; AFOSR-89-1819TR) Avail: NTIS HC A02/MF A01 CSCL 07/3

New coordination modes for octafluoro cyclooctatetraene (OFCOT) bound to rhodium, cobalt, nickel, palladium, platinum and manganese were discovered. All complexes show good air and thermal stability compared to hydrocarbon analogues. Photochemical rearrangements of cobalt and rhodium OFCOT complexes, and unprecedented transannular ring closure chemistry were discovered. Comparison of the bonding properties of OFCOT with those of its hydrocarbon analogue was achieved using crystallographic and NMR studies. The first examples of a new family of (trialkyl(tricarbonyl)) organometallic compounds, stabilized by tridentate perfluorinated ligands. Dinuclear rhodium complexes of OFCOT undergo a selective C-F bond activation reaction. Electrochemical reduction of OFCOT bound to cobalt yields the first example of a fluorinated organometallic radical anion. Metal substitution on the OFCOT ring was achieved, and vicinal defluorination of OFCOT gives a series of compounds containing the previously unknown mu-hexafluorocyclooctatrieneyne ligand. Stereospecific cleavage of a fluorinated C-C bond sigma-bond in perfluoro cyclopropene by platinum and iridium complexes was achieved. GRA

24 COMPOSITE MATERIALS

Includes physical, chemical, and mechanical properties of laminates and other composite materials.
For ceramic materials see *27 Nonmetallic Materials.*

N90-18494# European Office of Aerospace Research and Development, FPO New York, NY.
THIRD EUROPEAN CONFERENCE ON COMPOSITE MATERIALS
Chester J. Dymek, Jr. and James G. R. Hansen 1989 19 p Conference held in Bordeaux, France, 20-23 Mar. 1989
(EOARD-LR-89-050) Avail: NTIS HC A03/MF A01

The Third European Conference on Composite Materials was held in Bordeaux, France from 20 to 23 March 1989. In terms of research reported, there was nearly equal representation from academia on the one hand and industry and government labs on the other. The subjects of the technical presentations were about equally divided among polymer, ceramic and metal matrix composites. Areas receiving the greatest emphasis were SiC and carbon-containing composites, fiber structure and coatings, thermosets and thermoplastics, and laminate mechanics. For individual titles, see N90-18495 through N90-18503.

N90-18495# Technochemie G.m.b.H., Dossenheim (Germany, F.R.). Verfahrenstechnik.
MODIFIED BISMALEIMIDES FOR CARBON FIBRE COMPOSITES Abstract Only
P. Konig, H. Stenzenberger, M. Herzog, and W. Romer *In* European Office of Aerospace Research and Development, Third European Conference on Composite Materials 1989 1 p
(For primary document see N90-18494 11-24)
Avail: NTIS HC A03/MF A01

Polybismaleimides are a class of thermosetting resins which, due to high cross-link density and aromatic backbone structure, show excellent temperature stability and outstanding hot wet performance. On account of the brittleness of the bismaleimide resins, they have to be modified to achieve tough networks. This work describes chemical concepts to improve the fracture toughness of bismaleimide resins, such as addition of reactive elastomers, Michael addition chain extension, copolymerization with allyl terminated comonomers, copolymerization with propenyl terminated comonomers, and modification with thermoplastics. Depending on the modification method, fracture toughness improvements of up to twentyfold compared with unmodified bismaleimides can be attained. Author

N90-18496# Kenrich Petrochemicals, Inc., Bayonne, NJ.
ENHANCED BONDING OF FIBER REINFORCEMENTS TO THERMOSET RESINS Abstract Only
G. Sugerman, S. M. Gabayson, W. E. Chitwood (General Dynamics Corp., San Diego, CA.), and S. J. Monte *In* European Office of Aerospace Research and Development, Third European Conference on Composite Materials 1989 1 p Previously announced in IAA as A89-29986 (For primary document see N90-18494 11-24)
Avail: NTIS HC A03/MF A01

Improved bonding of fiberglass, Kevlar and carbon fiber to a variety of thermoset resins was achieved via the addition of minor amounts of organotitanate and/or organozirconate coupling agents. Peel strength, fiber pullout and chemical resistance data is provided to demonstrate significant improvements in bonding between these fibers and epoxy, polyurethane, polyester and vinyl ester resins. Author

N90-18497# Ecole Polytechnique Federale de Lausanne (Switzerland). Lab. de Polymeres.
INTERLAMINAR FRACTURE TESTING OF CARBON FIBRE/PEEK COMPOSITES VALIDITY AND APPLICATIONS Abstract Only
P. Davies, W. Cantwell, H. Richard, C. Moulin, and H. H. Kausch *In* European Office of Aerospace Research and Development, Third European Conference on Composite Materials 1989 1 p (For primary document see N90-18494 11-24)
Avail: NTIS HC A03/MF A01

The application of interlaminar fracture testing to carbon fiber reinforced PEEK (poly-ether-ether-ketone) composites is examined. An experimental study of over 100 specimens is reported, in which the influence of specimen thickness, stiffness, width and defect type have been systematically varied. A significant effect of specimen stiffness was revealed in certain cases, which must be taken into account if useful results are to be obtained. Following the optimization of the specimen, the influences of fiber type (AS4 or IM6) and rate of cooling after molding (50 C/min. down to 0.3 C/min.) were studied. Author

N90-18498# Aerospatiale Aquitaine, Saint-Medard en Jalles (France).
STATE OF THE ART AND FUTURE PROSPECTS FOR HIGH TEMPERATURE COMPOSITES Abstract Only
J. F. Jamet *In* European Office of Aerospace Research and Development, Third European Conference on Composite Materials 1989 2 p (For primary document see N90-18494 11-24)
Avail: NTIS HC A03/MF A01

Interest in the carbon and ceramic composites field is the result of their new potentialities. These composites meet the requirements of thermostability, reliability and specific performances mainly imposed by the new projects of aeronautical and space systems. Toughness, damage stress levels, and thermochemical resistance of these new materials are now determinative for further developments and uses. After an analysis of the microstructural rupture of these composites and of the evolution of models describing this rupture, this paper develops briefly the main aspects of carbon composites protection and ceramic composites manufacturing in order to emphasize: (1) the rules governing the relations between microstructure and rupture; and (2) the consequences upon architecture, processing and using methods. Author

N90-18499# Swedish Inst. for Silicate Research, Gotheborg.
SILICON CARBO-NITRIDE CERAMIC MATRIX COMPOSITES BY POLYMER PYROLYSIS Abstract Only
R. Lundberg and P. Goursat (Limoges Univ., France) *In* European Office of Aerospace Research and Development, Third European Conference on Composite Materials 1989 1 p (For primary document see N90-18494 11-24)
Avail: NTIS HC A03/MF A01

Polymer pyrolysis as a route to fiber-reinforced Si-N-C materials was identified and demonstrated. The synthesis and pyrolysis of polysilazane precursors were optimized with respect to ceramic yield and minimum bloating during pyrolysis. Solution infiltration of stacked Nicalon SiC fiber weaves was performed. Repeated impregnations/pyrolyses yielded fairly strong composites exhibiting non-brittle fracture behavior, especially when a polymer free from low molecular weight oligomers was used and the fibers given a carbon coating. Author

N90-18500# Societe Europeenne de Propulsion, Saint-Medard-en-Jalles (France).
CERAMIC MATRIX COMPOSITES, NEW HIGH PERFORMANCE MATERIALS [COMPOSITES A MATRICE CERAMIQUE, NOUVEAUX MATERIAUX A TRES HAUTES PERFORMANCES]
J. C. Cavalier, A. Lacombe, and J. M. Rouges *In* European Office of Aerospace Research and Development, Third European Conference on Composite Materials 1989 3 p In FRENCH; ENGLISH summary (For primary document see N90-18494 11-24)
Avail: NTIS HC A03/MF A01

Composite materials with refractory reinforcements (carbon or ceramic) associated with a ceramic matrix were developed. These thermostructural composite SiC/SiC and C/SiC materials combine a good resistance to oxidation and to chemical aggression with a high mechanical behavior at high temperature and an exceptional toughness compared to the classical ceramics. New applications were found for these new composites in the fields of engines and for very high temperature structures. Very large industrial installations were implemented since 1986 in order to meet the production requirements yielded by these new applications under development. Author

N90-18501# Lyon-1 Univ., Villeurbanne (France). Lab. de Physico-Chimie Minerale.
CONTINUOUS PREPARATION OF A THIN REFRACTORY CARBIDE DEPOSIT ON THE SURFACE OF CARBON FIBERS: CHARACTERIZATION OF THE C/SiC FIBER Abstract Only [ELABORATION EN CONTINU D'UN DEPOT MINCE DE CARBURE REFRACTAIRE EN SURFACE DES FIBRES DE CARBONE: CARACTERISATION DE LA FIBRE C/SiC]
H. Vincent, C. Vincent, J. L. Ponthenier, H. Mourichoux, and J. Bouix *In* European Office of Aerospace Research and Development, Third European Conference on Composite Materials 1989 1 p In FRENCH; ENGLISH summary (For primary document see N90-18494 11-24)
Avail: NTIS HC A03/MF A01

Reactive chemical vapor deposition (RCVD) was used for the coating of the single filaments of a PAN-based carbon yarn by SiC. A continuous process was developed. It consists of reacting a mixture of SiCl4-H2 with the fiber, at 1000 C, under atmospheric pressure. With the aid of thermodynamic calculations and experimentation, the conditions of RCVD (gas composition, temperature, reaction time) are optimized to create a coating without degrading the fiber. It is shown that a SiC-B coating, 0.05 micron thick, modified slightly in characteristics, is sufficient to reduce the rate of combustion of the fibers by a factor close to 100. Author

N90-18502# Cambridge Univ. (England). Dept. of Materials Science and Metallurgy.
SPUTTER DEPOSITION OF DIFFUSION BARRIER COATINGS ON SiC MONOFILAMENTS FOR USE IN TI-BASED COMPOSITES Abstract Only
R. Kieschke, R. Somekh, and T. W. Clyne *In* European Office of Aerospace Research and Development, Third European Conference on Composite Materials 1989 1 p (For primary document see N90-18494 11-24)
Avail: NTIS HC A03/MF A01

Procedures are described for the formation of thin layers on monofilaments by sputter deposition, with the aim of controlling high temperature degradation by interfacial chemical reaction. Factors affecting material selection and coating structure are briefly considered. Advantages are identified in having a relatively high fiber temperature during deposition, in encouraging stored compressive stresses, and in generating a duplex coating structure, comprising an inner layer of metal and an outer layer of oxide. Author

N90-18503# British Aerospace Public Ltd. Co., Kingston-upon-Thames (England). Military Aircraft Div.
MEASURING STRAIN IN CARBON FIBRE COMPOSITE LAMINATES USING THE RAMAN OPTOMECHANICAL STRAIN GAUGE Abstract Only
F. Underwood, D. Sharpe, and D. Batchelder (London Univ., England) *In* European Office of Aerospace Research and Development, Third European Conference on Composite Materials 1989 1 p (For primary document see N90-18494 11-24)
Avail: NTIS HC A03/MF A01

Polydiacetylene fibers were placed within a carbon fiber composite laminate in the ply direction during the lay-up procedure. Laser light was guided to the polydiacetylene (polyDCH) by means of fiber optics. After curing, the laminates were tested in four-point bending and the internal ply strains measured. The results show

that strains could be measured at any specific point within the laminate. Results were consistent and the technique proved to be repeatable. Author

N90-18504*# National Aeronautics and Space Administration. Lewis Research Center, Cleveland, OH.
ANALYSIS OF WHISKER-TOUGHENED CERAMIC COMPONENTS: A DESIGN ENGINEER'S VIEWPOINT
Stephen F. Duffy, Jane M. Manderscheid, and Joseph L. Palko (Cleveland State Univ., OH.) Dec. 1989 10 p Original contains color illustrations
(NASA-TM-102333; E-5042; NAS 1.15:102333) Avail: NTIS HC A02/MF A01; 1 functional color page CSCL 11D

The use of ceramics components in gas turbines, cutting tools, and heat exchangers has been limited by the relatively low flaw tolerance of monolithic ceramics. The development of whisker toughened ceramic composites offers the potential for considerable improvement in fracture toughness as well as strength. However, the variability of strength is still too high for the application of deterministic design approaches. Several phenomenological reliability theories proposed for this material system are reviewed and the development is reported of a public domain computer algorithm. This algorithm, when coupled with a general purpose finite element program, predicts the fast fracture reliability of a structural component under multiaxial loading conditions. Author

N90-18505# Utah Univ., Salt Lake City. Mechanics of Composites Lab.
COMPRESSIVE STRENGTH OF CARBON/EPOXY LAMINATED UNDER MULTIAXIAL STRESS
S. R. Swanson and G. E. Colvin, Jr. Sep. 1989 25 p Prepared in cooperation with Lawrence Livermore National Lab., CA
(Contract W-7405-eng-48)
(DE90-005552; UCRL-21235) Avail: NTIS HC A03/MF A01

The strength was determined of carbon/epoxy laminates under conditions of multiaxial compressive stress. It was found that the compressive strength of the critical plies in a laminate depends on the total layup of the laminate, and thus compressive strength is an apparent or in-situ property. Variations in apparent strength by a factor of 2 were found over the range of laminates investigated. Biaxial compression loadings showed lower than expected failure by buckling under external pressure. The multiaxial compression apparatus was redesigned to eliminate specimen end brooming under conditions of high axial load. DOE

N90-18506# Pennsylvania State Univ., University Park. Composites Manufacturing Technology Center.
THREADED JOINT DESIGN FOR COMPOSITES
H. T. Hahn and M. N. Kallas Jun. 1989 22 p Prepared in cooperation with Lawrence Livermore Lab., CA
(Contract W-7405-eng-48)
(DE90-005553; UCRL-21236) Avail: NTIS HC A03/MF A01

The design of a composite threaded joint is summarized. Only partial results are provided on the design of a threaded joint. Composite joining is one of the major obstacles preventing composites from side usage. The difficulties in joining composite structures arise from factors associated with the anisotropic nature of these materials which are strong and stiff in the fiber direction and very weak in the transverse direction. One well known type of joints is the threaded joint which is used extensively in metallic structures. Among the common thread types is the buttress thread which has advantages when loading is in one direction only. The flank of the thread which almost takes all the thrust is referred to as the pressure flank. It is nearly perpendicular to the thread axis so that the radial component of the thrust is almost zero. Therefore, this form of thread is particularly applicable where tubular members are screwed together as in the case of breech mechanisms of large guns and airplane propeller hubs. A buttress type thread is used in a composite laminate. The following sections will define the problem and describe the finite element model proposed to solve the problem. Some preliminary results are also included. DOE

N90-18507# California Univ., Santa Barbara.
THE PROCESSING AND MECHANICAL PROPERTIES OF HIGH TEMPERATURE/HIGH PERFORMANCE COMPOSITES. BOOK 2, SECTION 2: STRENGTH AND FRACTURE RESISTANCE Annual Report No. 3, 15 Sep. 1988 - 14 Sep. 1989
A. G. Evans and R. Mehrabian 15 Oct. 1989 392 p
(Contract N00014-86-K-0753)
(AD-A216142) Avail: NTIS HC A17/MF A03 CSCL 20/11

The third annual report of the University Research Initiative project at UCSB on high-temperature, high-performance composites consists of sections compiled in a total of six books. The first section in Book 1 is concerned with the properties and structure of bimaterial interfaces and the related problem of coating decohesion and cracking. The second section describes research on the strengths and fracture resistance of brittle matrix composites manufactured with fibers, whiskers and ductile phases. This information is presented in Books 2 and 3. The third section addresses the flow and creep strength of reinforced systems, with emphasis on effects of aspect ratio and the incidence of damage, and is offered in Book 4. The fourth section, Books 5 and 6, describes work on processing of intermetallic and ceramic matrices and composites, as well as numerical modeling of the melt-spinning process. GRA

N90-18508# California Univ., Santa Barbara.
THE PROCESSING AND MECHANICAL PROPERTIES OF HIGH TEMPERATURE/HIGH PERFORMANCE COMPOSITES. BOOK 3, SECTION 2: STRENGTH AND FRACTURE RESISTANCE, PART Annual Report No. 3, 15 Sep. 1988 - 14 Sep. 1989
A. G. Evans and R. Mehrabian 15 Oct. 1989 442 p
(Contract N00014-86-K-0753)
(AD-A216143) Avail: NTIS HC A19/MF A03 CSCL 11/4

The third annual report of the University Research Initiative project at UCSB on High-Temperature, High-Performance Composites consists of sections compiled in a total of six books. The first section in Book 1 is concerned with the properties and structure of bimaterial interfaces and the related problem of coating decohesion and cracking. The second section describes research on the strengths and fracture resistance of brittle matrix composites manufactured with fibers, whiskers and ductile phases. This information is presented in Books 2 and 3. The third section addresses the flow and creep strength of reinforced systems, with emphasis on effects of aspect ratio and the incidence of damage, and is offered in Book 4. The fourth section, Books 5 and 6, describes work on processing of intermetallic and ceramic matrices and composites, as well as numerical modelling of the melt-spinning process. This is Book 3, Section 2 of the series. Contents of this section pertain to: Strength and fracture resistance - Ductile reinforcement; and Matrix toughening. GRA

N90-18509# Soreq Research Establishment, Israel Atomic Energy Commission, Yavneh.
SPALLATION AND DYNAMIC FRACTURE AS AN EFFECT OF LASER INDUCED SHOCK WAVES IN CARBON BASED COMPOSITE MATERIALS Final Technical Report
S. Eliezer and I. Gilath Oct. 1989 47 p
(Contract DAJA45-87-C-0032)
(AD-A216540; R/D-5528-MS-01) Avail: NTIS HC A03/MF A01 CSCL 19/10

A high irradiance single beam short pulsed Nd:glass laser was used to generate shock waves in carbon-carbon and carbon epoxy composites. Dynamic brittle fracture at hypervelocity impact conditions was observed as a result of reflected shock waves as tensile waves from the back surface of samples. Successive stages of damage from incipient spallation to complete sample perforation were obtained by increasing gradually the laser energy. The thermomechanical damage on the front surface as a result of laser interaction with the target material, and the mechanical damage at the back surface as a result of shock wave reflection were characterized by optical and scanning electron microscopy. The failure properties of the carbon composites were related to the processing of densification and graphitization mode, while the failure properties for carbon epoxy composites were related to

impact direction versus fiber direction. A comparison was made between spall properties of carbon epoxy composites with aluminum and iron. A new experimental method was developed to calculate the attenuation of laser generated shock waves. This technique enables also the evaluation of the laser induced spall pressure in different materials. GRA

N90-18510# Pennsylvania State Univ., University Park. Composites Manufacturing Technology Center.
DAMAGE ASSESSMENT IN COMPOSITES BY ACOUSTO-ULTRASONIC TECHNIQUE Final Report
J. Lee and H. T. Hahn Dec. 1989 4 p
(Contract N00014-87-0143)
(AD-A216590) Avail: NTIS HC A01/MF A01 CSCL 20/1

The main objective of the research was to develop and refine the acousto-ultrasonic technique to assess damage in composite materials. Specifically, this research was directed toward three goals: (1) to improve the acousto-ultrasonic technique by focusing on the understanding of the relationship between material properties and wave propagation, (2) to establish operational methods for research and industrial applications, and (3) to improve material characterization and damage assessment using the refined technique. Both analytical and experimental approaches were employed to optimize the acousto-ultrasonic technique. The following topics were investigated in the study: Calibration of acoustic emission system and preamplifier; Characteristics of the output wave from transducer; Acousto-ultrasonic wave propagation in composite laminates; Evolution of acousto-ultrasonic wave envelope in composite laminates; Propagation of different waveforms; Assessment of impact damage; Assessment of ply cracks; and Assessment of cut fibers. GRA

N90-18511# APTEK, Inc., San Jose, CA.
THEORY AND VERIFICATION OF THE FIBER COMPOSITE DAMAGE MODEL IMPLEMENTED IN DYNA3D Technical Report, 11 Jan. - 1 Jun. 1989
Yvonne D. Murray 1 Dec. 1989 77 p
(Contract DNA001-88-C-0040)
(AD-A216600; A-89-4R; DNA-TR-89-132) Avail: NTIS HC A05/MF A01 CSCL 11/4

A laminated shell formulation and damage model for fiber composite materials are implemented in DYNA3D, a 3-D finite element code to analyze the large deflection and materially nonlinear response of structures and solids. The damage model consists of an interactive failure criterion and a post-failure degradation rule. The failure criterion identifies 3 modes of failure: matrix cracking, matrix compression failure, and fiber breakage. When a failure criterion is met, some of all of the lamina's elastic constants are set to zero. The failure and model and post-failure degradation rule are compared with experimental results available from the literature to establish the validity of the damage model. Comparisons between the failure criteria and experimental results indicate that the Chang fiber breakage criterion is in agreement with biaxial stress test data if reasonable assumptions are made regarding matrix cracking prior to fiber breakage. However, the matrix failure criteria do not adequately model matrix strength under combined loading conditions. A modified form of the Tsai-Wu criterion is in better agreement with the test data and is recommended for implementation into DYNA3D. A flexible post-failure degradation rule is also recommended: modifications to the current implementation are suggested which allow the user to specify the degradation behavior for each mode of failure. GRA

N90-18512# George Washington Univ., Washington, DC. Dept. of Chemistry.
SPECTROSCOPIC EVIDENCE FOR CARBON-CARBON BONDING IN CARBIDE LAYERS ON METALS Interim Technical Report
F. L. Hutson, David E. Ramaker, and B. E. Koel (Colorado Univ., Boulder.) Dec. 1989 20 p
(Contract N00014-89-J-1103)
(AD-A216726; TR-49) Avail: NTIS HC A03/MF A01 CSCL 07/4

We examine previously reported ultraviolet photoelectron, C K electron energy loss, and C KVV Auger spectroscopic data from carbidic layers formed at temperatures between 500 to 650K on Ni(100), Ru(001), and other metals. These data indicate that significant amounts of carbon-carbon bonding, such as that from C2, C3, etc. fragments, exists on the surface in addition to the carbon-metal bonding with the substrate. The carbidic layers can be made from either CO or C2H2 exposure to the metal substrate. Quantitative interpretation of the Auger data indicate that the carbon-carbon to carbon-metal bonding ratio lies between 0.3 and 0.5. Observed changes in the spectra obtained from different surfaces or at different coverages are accounted for by variations in this ratio. GRA

N90-18513# David Taylor Research Center, Bethesda, MD. Dept. of Ship Materials Engineering
INSTRUMENTED IMPACT TESTING OF FABRIC-REINFORCED COMPOSITE MATERIALS Research and Development Report
T. D. Juska, R. M. Crane, and T. Mixon May 1989 43 p
Sponsored by Naval Oceanographic Office
(AD-A216764; DTRC/SME-89-20) Avail: NTIS HC A03/MF A01 CSCL 11/4

Instrumented impact and ultrasonic inspection were used to assess the impact damage resistance of six fabric-reinforced laminates. Polyester and vinylester resins reinforced with woven roving, biaxial reinforcement, and glass/Kevlar hybrid were evaluated. Biaxial fabric reinforced resins had the best impact resistance. This determination is based on the ability of these materials to survive impact with the lowest friction of impact energy resulting in damage. In addition laminates with biaxial reinforcement had comparable damage areas to the other materials. GRA

N90-18514# Air Force Systems Command, Wright-Patterson AFB, OH. Foreign Technology Div.
INSPECTION OF CARBON/EPOXY AND ALUMINUM HONEYCOMB PARABOLOIDAL COMPONENTS BY HNDT
Huang Guanhua and Wei Ensheng 21 Sep. 1989 10 p Transl. into ENGLISH from Nondestructive Testing (China), v. 10, no. 3, Mar. 1988 p 69-71 LIMITED REPRODUCIBILITY: Availability: Document partially illegible
(AD-A216796; FTD-ID(RS)T-0718-89) Avail: NTIS HC A02/MF A01 CSCL 11/4

Examples are discussed of the use of the double exposure method to inspect carbon/epoxy skin and aluminum honeycomb core paraboidal components. Laser holographic technology can detect separation style and closely attached style glue-loss defects, but its sensitivity in detecting the closely attached style defects is lower than its sensitivity in detecting the separation style defects. Laser holographic technology has the capacity of detecting confused areas within the honeycomb core, but the results are not so good as with direct x ray observation. GRA

N90-18515# Army Armament Research, Development and Engineering Center, Watervliet, NY.
CALCULATIONS OF BRAIDING PARAMETERS Final Report
Philip C. Wheeler Nov. 1989 22 p Sponsored by Army Armament Research, Development and Engineering Center, Picatinny Arsenal, NJ
(AD-A216836; ARCCB-TR-89032) Avail: NTIS HC A03/MF A01 CSCL 13/9

The New England Butt 144 carrier braiding machine is designed to braid (knit) fibrous material into cylindrical, but not necessarily symmetric, shapes over a mandrel form. The braiding machine is capable of applying 144 continuous strands of material simultaneously onto a mandrel as well as 72 longitudinal strands to give lateral strength to the component. As the 144 strands of fiber are being applied to the mandrel, each fiber is coated with a specific amount of resin from a resin applicator. The resin applicator is an added piece of hardware to the braiding machine and was fabricated by U.S. Composites Corporation. Coating of the fibers with wet resin occurs just prior to the fibers being applied to the

mandrel. During the braiding operation, the braiding machine remains stationary while a mandrel form is traversed horizontally in and out of the center of the braider's braid ring to apply layers of composite material to the mandrel's surface. This report addresses some of the braiding parameters such as braider speed, mandrel traverse rate, fiber flow rates, and resin flow rates onto a mandrel during the braiding process. GRA

N90-18516# Massachusetts Inst. of Tech., Cambridge. Materials Processing Center.
LABORATORY FOR THE PROCESSING AND EVALUATION OF INORGANIC MATRIX COMPOSITES Annual Technical Report
James A. Cornie Jun. 1989 192 p
(Contract N00014-85-K-0645)
(AD-A216881) Avail: NTIS HC A09/MF A01 CSCL 11/4

The research program at MIT on the fundamentals of processing of inorganic matrix composites focuses on developing a basic understanding of solidification processing of metal matrix composites and the behavior and modification of interfaces. This understanding is applied to the development of processes for the manufacture of evaluation specimens which are used, in turn, to determine the microstructure/processing/materials properties relationships. Technical areas discussed include: Kinetics of Fiber Preform Infiltration; Infiltration of Fibrous Preforms by a Pure Metal; Intrinsic Toughness of Interfaces Between SiC Coatings and Substrates of Si or C Fiber; Interfaces with Controlled Toughness as Mechanical Fuses to Isolate Fibers from Damage; A High Resolution Transmission Electron Microscopy Study of the SiC Coated Graphite Fiber/Aluminum Composite; Wetting of Ceramic Particulates with Liquid Aluminum Alloys; Wettability of SiC Particulates with Zn and Zn-Al Alloys; Interface Chemistry of Inorganic Composite Materials; Preparation of Boron-Containing Ceramic Materials by Pyrolysis of the decaboran (14) derived BiOH12-Ph2POPPh(x) polymer; Non-Polymeric Binders for Ceramic Powders: Utilization of Neutral and Ionic Species Derived from Decaborane (14); and Phosphorus Containing Derivatives of Dacaborane (14) as Precursors to Boron Containing Materials. GRA

N90-18517# Naval Ocean Systems Center, San Diego, CA. Structural Mechanical Analysis and Design Branch.
DEVELOPMENT OF A PROGRESSIVE FAILURE MODEL FOR STRENGTH OF LAMINATED COMPOSITE STRUCTURE Interim Report
P. Y. Tang Nov. 1989 18 p Sponsored by ONR, Arlington, VA
(AD-A216966; NOSC/TD-1687) Avail: NTIS HC A03/MF A01 CSCL 11/4

This report briefly describes the background information and current work plan for a multiyear effort to develop a progressive failure model for predicting strength of laminated composite structure under static loads and fractured in the in-plane failure modes. It also highlights the intermediate results obtained in FY89. GRA

N90-18518# Argonne National Lab., IL. Materials and Components Technology Div.
MECHANICAL PROPERTIES AND MICROSTRUCTURE OF Si3N4-WHISKER-REINFORCED Si3N4 MATRIX COMPOSITE
C.-Y. Chu and J. P. Singh 1990 22 p Presented at the 14th Annual Conference on Composites and Advanced Ceramics, Cocoa Beach, FL, 14-17 Jan. 1990
(Contract W-31-109-eng-38)
(DE90-005651; CONF-900160-1) Avail: NTIS HC A03/MF A01

Room-temperature elastic modulus, hardness, flexural strength and fracture toughness of Si3 N4 whisker-reinforced Si3 N4 matrix composite with up to 35 vol. percent of whisker were measured and correlated with microstructures. Both SEM and TEM were used for structural characterization. The toughness of the composite was observed to increase from 6.5 MPa(radical)m to 8.8 MPa(radical)m with addition of 5 vol. percent Si3 N4 whisker. This represents a 1.4-fold increase in toughness. Correspondingly, the strength increased from 673 to 802 MPa. The toughness and strength behavior of the composites is believed to be controlled by the whisker strengthening and matrix grain size. DOE

N90-18519# Los Alamos National Lab., NM.
APPLICATION OF ARTIFICIAL INTELLIGENCE CONTROL TO THE VAPOR-LIQUID-SOLID SILICON CARBIDE WHISKER PROCESS
Peter D. Shalek and W. J. Parkinson 1989 13 p Presented at the Materials Research Society Fall Meeting, Boston, MA, 27 Nov. - 2 Dec. 1989
(Contract W-7405-eng-36)
(DE90-007835; LA-UR-90-33; CONF-891119-93) Avail: NTIS HC A03/MF A01

Silicon carbide whiskers have excellent mechanical and chemical properties, making them very desirable as a reinforcement for structural ceramic and other composite materials. Los Alamos has developed a laboratory-scale batch process for producing very high quality SiC whiskers by the vapor-liquid-solid (VLS) method which is an active candidate for technology transfer involving significant scale-up. The process, however, involves quite complex chemical/physical and parametric relationships and has not as yet lent itself successfully to modeling. An expert computer system was therefore developed to facilitate the transfer of this technology to industry. Optimum conditions were determined by relating the many process parameters to product results to establish a set of rules for running the process. These are incorporated in a two-phase expert system designed to guide inexperienced users. In Phase 1: an expert consultant program provides the user with information that enables him to set up the run. This information is incorporated into the rule base that makes up Phase 2: the control system. At present, the operator functions as the controller by responding to the decisions of the expert system; automation can be added later. DOE

N90-18520# Aalborg Portland (Denmark). Cement and Concrete Lab.
COMPACT REINFORCED COMPOSITE BASIC PRINCIPLES
Hans Henrik Bache May 1987 93 p
(CBL-41; ISBN-87-89132-02-5; ISSN-0902-8277; ETN-90-96208)
Avail: NTIS HC A09/MF A01; Aalborg Portland, 44 Roerdalsvej, P.O. Box 156, DK-9100 Aalborg, Denmark, 118 Dannish crowns

A strategy based on fracture mechanics for the development of a compact reinforced composite is presented. The main principles are: to enable brittle matrix materials to strain harden by reinforcing them with a high concentration of fine, strong and stiff fibers which increases the tensile stresses and tensile strains at which the matrix material cracks; to increase still further the ultimate tensile strains of the matrix materials when these deform together with the reinforcing bars by effective fixation to the bars; to achieve a high degree of global and local ductility by means that ensure a small brittleness number. Bending tests presented showed that the load capacity in bending was 5 to 10 times that of traditional, good reinforced concrete and almost the same as for structural steel, the formalized ultimate bending stress (normalized bending moment: M/1/6 b (h to the power of 2)) being slightly more than 160 MPa. The matrix material remained uncracked under tensile loading right up to the yield limit of the reinforcing steel (tensile strains about 3 mm/m), whereas ordinary reinforced concrete cracks at tensile strains of only 3 to 5 percent of the yield limit of the reinforcing steel. ESA

N90-18521# European Space Agency, Paris (France).
DAMAGE IN A PERFORATED GRAPHITE-EPOXY COMPOSITE PLATE UNDER MONOTONIC AND CYCLIC BIAXIAL LOADING
G. Inizan (Office National d'Etudes et de Recherches Aerospatiales, Paris, France) Dec. 1989 233 p Transl. into ENGLISH of Endommagement d'une Plaque Composite Trouee, en Carbone-Epoxy, sous Chargement Biaxial Monotone et Cyclique (Paris, France, ONERA), 1987 p 1-205 Original language document was announced as N88-26708
(ESA-TT-1117; ONERA-NT-1987-5; ETN-90-96215) Avail: NTIS HC A11/MF A02

Damage propagation in a graphite-epoxy T300-5208 composite plate, under monotonic and cyclic biaxial loadings is studied. The biaxial state of stress is induced by a plane loading in two perpendicular directions. A hole in the center localized the damage initiation. The main technique of damage investigation under monotonic and cyclic loadings is penetrant-enhanced x ray radiography. The results obtained from a two-dimensional finite element calculation of damage propagation are compared with the experimental results. This calculation predicts, for each monotonic biaxial loading, the damage initiation load and its localization, the damage propagation in each ply of the laminate, and finally the failure load. A convergence study shows that it is stable. A comparison between calculation and experiment is presented for the tensile curves and for the damage geometry. The tests under cyclic biaxial loading give reproducible stable damage propagation, depending on the applied load and the biaxial coefficient. ESA

N90-18522# Office National d'Etudes et de Recherches Aerospatiales, Paris (France). Direction des Materiaux.
STRUCTURAL STUDY OF THERMO-HARDENABLE MATRICES. DEFORMATION PROCESSES OF COMPOSITE MATRICES AS A FUNCTION OF THEIR MOLECULAR STRUCTURE [ETUDE STRUCTURALE DES MATRICES THERMODURCISSABLES: PROCESSUS DE DEFORMATION DES MATRICES DE COMPOSITES EN RELATION AVEC LEUR STRUCTURE MOLECULAIRE]
B. Bloch and P. Sigety Dec. 1988 24 p In FRENCH
(Contract DRET-87-34-001)
(ONERA-RT-10/3521-M; ETN-90-96292) Avail: NTIS HC A03/MF A01

The results of the structural study on model resins, with non-reinforced well known structures, and standard materials are reported. The fabrication procedures of the resins and composite materials are described. Measurements of K sub IC factor and strain relaxation on composite materials are carried out. The preliminary results show that the observed strain relaxation can be interpreted by a proposed thermodynamic model. The analysis of the structural hardening factor of composite materials is considered. ESA

N90-18523# Office National d'Etudes et de Recherches Aerospatiales, Paris (France). Direction des Materiaux.
COMPARISON BETWEEN THE DAMAGE MODES OF THERMO-HARDENABLE AND THERMO-PLASTIC COMPOSITE MATRICES [COMPARAISON DES MODES D'ENDOMMAGEMENT ELEMENTAIRES DES COMPOSITES A MATRICES THERMO-DURCISSABLE ET THERMOPLASTIQUE]
J. P. Favre, P. Sigety, and C. Cottenot Apr. 1989 107 p In FRENCH
(Contract DRET-88-34-001)
(ONERA-RT-47/7086-M; ETN-90-96294) Avail: NTIS HC A06/MF A01

The mechanical characteristics of thermo-hardenable and thermoplastic composite materials are investigated. The work is focused on the materials' damage modes. The expected mechanical performances of non-reinforced resins and composite materials are reviewed. The techniques applied in the micro-mechanical analysis of matrix deformations are summarized. The investigation leads to the conclusion that, as a first step, the mechanical test must be chosen and, as a second step, the feasibility of the possible analytical methods must be studied. ESA

N90-18524# Lawrence Livermore National Lab., CA. Mechanical Engineering Dept.
PRELIMINARY EVALUATION OF THE STRENGTH OF PIN-JOINTS IN LAMINATED COMPOSITE MATERIALS
Scott E. Groves Mar. 1989 5 p
(Contract W-7405-eng-48)
(DE90-006353; UCID-21947) Avail: NTIS HC A01/MF A01

The objective is to determine the base line bearing strength of a pinned joint in a laminated composite structure. The bearing strength is defined as the load in the pin divided by the bearing area which is the product of the pin diameter and the plate thickness. The bearing strength of composite materials is not very well characterized, and it is hoped that some understanding will be shed on the matter. In typical metals the bearing strength is usually twice the ultimate tensile strength. However, in composites, local anisotropies and flaws will result in the formation of high interlaminar normal stresses which cause delaminations to occur locally and thus prevents a laminated composite from ever reproducing the comparable bearing strengths found in metals. Nevertheless, composites can be designed to sustain significant bearing loads. To substantiate this claim, a series of simple tests were performed on laminated coupons. Results indicate that it is possible to achieve a very conservative bearing strength of 75 ksi in a quasi-isotropic laminated composite structure. Furthermore, it is believed that by minimizing the formation of the delaminations, bearing strengths on the order of the comparable quasi-isotropic tensile strength can be achieved. Thus the bearing strength is directly related to the unidirectional strength of the composite, and therefore systems with a higher fiber strength should yield a higher bearing strength. DOE

N90-18525# Sandia National Labs., Albuquerque, NM. Advanced Systems Div.
A STATISTICAL EVALUATION OF THE VARIATION IN LAMINATED COMPOSITE PROPERTIES RESULTING FROM PLY MISALIGNMENT
C. Martin Hinckley Feb. 1990 49 p
(Contract DE-AC04-76DR-00789)
(DE90-006371; SAND-90-8205) Avail: NTIS HC A03/MF A01

A Monte Carlo simulation of ply angle deviations has been used to evaluate the distribution in properties for symmetric laminates formed from P75/930 graphite epoxy unidirectional tape. In applications where consistency of particular properties is critical, this evaluation has shown that important distinctions may be made even when laminates have essentially identical properties based on nominal ply angles. A laminate formed of 0, 60 and minus 60 degree plies can provide a more consistent product than one formed of 0, 90, and plus or minus 45 degree plies for the specific application requiring dimensional stability considered here. This type of analysis provides a sound basis for predicting the variation in laminate properties resulting from ply angle deviations that are likely to occur in manufacturing processes. DOE

N90-18526# Construcciones Aeronauticas S.A., Madrid (Spain). Subdireccion de Investigacion y Desarrollo de Tecnologia y Materiales.
CALCULATION OF MECHANICAL PROPERTIES VARIATIONS DEPENDING ON MATRIX PARAMETERS IN A COMPOSITE, AS A FUNCTION OF THE TEST TEMPERATURE [CALCULO DE LA VARIACION DE PROPIEDADES MECANICAS DEPENDIENTES DE LA MATRIZ EN UN COMPOSITE EN FUNCION DE LA TEMPERATURA DE ENSAYO]
J. Sanchez and A. Lavia 10 Jan. 1989 24 p In SPANISH Revised
(DT-311/88; ETN-90-96229) Avail: NTIS HC A03/MF A01

The validity of theoretical estimation of the ratio of hot-wet composite properties to dry-room temperature properties is studied. The temperature parameter is the square root of a function of the glass transition temperature. The experimental results were obtained using six types of matrix in carbon fiber composites. A good correlation between theoretical and experimental results is obtained. ESA

N90-18527# Construcciones Aeronauticas S.A., Madrid (Spain). Div. de Fabricacion Materiales Compuestos.
IMPACT OF COMPOSITES IN THE AEROSPACE INDUSTRY [IMPACTO DE LOS COMPOSITES EN LA INDUSTRIA AEROESPACIAL]
A. Martin-Carrillo 17 Apr. 1989 16 p In SPANISH
(ETN-90-96231) Avail: NTIS HC A03/MF A01

The utilization of composites is described, including carbon glass, boron or Kevlar fibers in epoxy or phenolic matrices. The

substitution of metals by composites in the American helicopter ACAP illustrates the weight saving, technological improvements, changes in manufacturing procedures and impact on the overall economic result introduced by composites utilization. ESA

N90-18528# Construcciones Aeronauticas S.A., Madrid (Spain). Div. de Fabricacion.
THE MANUFACTURING PROCEDURES FOR COMPOSITE MATERIALS, AUTOMATION, AND ROBOTIZATION [LOS PROCESOS DE FABRICACION DE LOS MATERIALES COMPUESTOS, SU AUTOMATIZACON Y ROBOTIZACION]
P. Munoz-Esquer May 1989 60 p In SPANISH
(ETN-90-96232) Avail: NTIS HC A04/MF A01

The state of the art in the utilization of composites in the aerospace industry is described. The operations discussed include curing, preimpregnation, cutting, pick-up, lay-up, hor-forming, debulking, trimming, drilling, riveting and finishing. Applications to the Airbus program illustrate the analysis. The automation systems studied by the CASA aerospace industry are examined. ESA

25 INORGANIC AND PHYSICAL CHEMISTRY

Includes chemical analysis, e.g., chromatography; combustion theory; electrochemistry; and photochemistry.

For related information see also *77 Thermodynamics and Statistical Physics.*.

N90-18529# Brookhaven National Lab., Upton, NY. Chemistry Dept.
THE EFFECT OF ELECTRIC FIELD ON ATTACHMENT OF ELECTRONS TO SOLUTES IN LIQUID ARGON
Richard A. Holroyd 1989 6 p
(Contract DE-AC02-76CH-00016)
(DE90-003969; BNL-43129) Avail: NTIS HC A02/MF A01

The use of liquid argon and xenon in detectors like time projection chambers (TPC) requires long electron drift times. This necessarily means that adventitious impurities must be reduced to very low levels. But because some impurities like oxygen may remain, it is important to understand how they affect the charge collection. In particular the effectiveness of many solutes is field dependent in liquid argon and xenon. The results of a recent study of the effect of oxygen on the attenuation length of electrons in argon are reanalyzed to illustrate this effect. It is also shown that the addition of non-attaching solutes like methane will also change the effectiveness of impurities in capturing electrons. DOE

N90-18530# Iowa Univ., Iowa City. Dept. of Mechanical Engineering.
WICK-TYPE LIQUID-METAL COMBUSTION Annual Report, 15 Oct. 1988 - 14 Oct. 1989
L. D. Chen, H. Y. Lyu, and K. Y. Hsu Oct. 1989 68 p
(Contract N00014-89-J-1188)
(AD-A216019) Avail: NTIS HC A04/MF A01 CSCL 21/4

An experimental and theoretical investigation was conducted to study the wick combustion of Lithium and Sulfur hexafluoride. A single-line laser induced fluorescence thermometry with Li2 as fluorescence species was developed. The calibration experiments yielded promising results; refinements, however, are needed before the technique can be applied to combustion flame measurements. Wick combustion of ethanol and hexane in air as well as Li and SF6 was conducted in a vacuum chamber at atmospheric and sub-atmospheric pressures. The ethanol and hexane wick diffusion flames showed flame oscillations, similar to flame flickers in buoyant jet diffusion flames. The oscillation frequency was estimated in the range 5 to 8 Hz at the pressures examined. The flame stand-off distance was estimated in the range 5 to 8 Hz at the pressures examined. The flame stand-off distance was found to increase when the system pressure was decreased. The wick combustion of Li and SF6 resulted in a bright pinkish flame. The luminous zone appeared quite close to the wick surface at the condition examined. Near the complete consumption of lithium, the wick was burned out due to loss of liquid lithium as a heat sink. On the analysis, a conserved scalar approach was employed to model the wick flame. A single equation was obtained to describe the interface condition of the wick combustion. Numerical solutions were obtained for laminar wick diffusion flames. The prediction yields similarity profiles for both ethanol air and LiSF6 wick diffusion flames although non-similar governing equations were retained in the formulation. GRA

N90-18531# International Business Machines Corp., San Jose, CA. Research Div.
TEMPERATURE DEPENDENCE OF PHOTON-GATED PERSISTENT SPECTRAL HOLE-BURNING FOR THE MESO-TETRA-P-TOLYL Zn-TETRABENZOPORPHYRIN/CHLOROFORM SYSTEM IN POLY(METHYLMETHACRYLATE)
W. P. Ambrose and W. E. Moerner 6 Nov. 1989 27 p Submitted for publication
(Contract N00014-84-C-0708)
(AD-A216086; TR-23) Avail: NTIS HC A03/MF A01 CSCL 07/5

Persistent spectral hole burning was utilized as both a tool for studying relaxation processes in amorphous solids and as a means for possibly achieving high density frequency-domain optical storage. Persistent spectral holes are formed in inhomogeneously broadened absorption lines when a photoinduced change occurs in the subset of absorbers that are in resonance with a narrowband laser beam. If the photoreacted centers do not absorb at the original wavelength, a dip in absorption or spectral hole is formed that may be detected by subsequent measurement of the absorption line. One- and two color persistent spectral hole burning properties of the electron donor-acceptor system meso tetra p-tolyl Zn tetrabenzo porphyrin/chloroform in poly(methylmethacrylate) are examined versus temperature from 1.5 to 90 K. The efficiency for photo-gated (two color) hole burning is independent of temperature, while the one-color hole burning efficiency decreases as the temperature is raised from 1.5 K. Raising the temperature improves the gating ratio (ratio of two- to one-color hole burning efficiencies) from 100 at 1.5 K to 10,000 at 90 K. The loin-power, short-burn-time hole width is also measured from 1.5 K to 90 K and is found to have a T(2.17 + or - 0.07) power law behavior. GRA

N90-18532# Aerospace Corp., El Segundo, CA. Chemistry and Physics Lab.
INTERFACIAL CHEMISTRY OF MoS2 FILMS ON SI Annual Technical Report
P. A. Bertrand 10 Nov. 1989 31 p
(Contract F04701-88-C-0089)
(AD-A216527; ATR-89(4752)-3) Avail: NTIS HC A03/MF A01 CSCL 07/4

The adhesion of thin films to their substrates is an important factor in their use in electronics, corrosion prevention, and lubrication. In particular, adhesion may be the critical parameter that determines the wear life of solid lubricant films; it has been suggested that films fail when they are pushed out of the wear track. Systems with chemical bonds across the interface will have enhanced adhesion over systems in which only van der Waals interactions are operative. Covalent materials, such as the important engineering ceramics SiC and Si3N4 and the solid lubricant MoS2, have strong directional bonds. If the same kind of bonds could be formed between such materials, a strongly adhesive lubricant-substrate system should result. The interface between rf-sputter-deposited MoS2 films and single-crystal Si was studied by observing thin (greater than 100 A) films with electron energy loss spectroscopy, Auger electron spectroscopy, and x ray photoelectron spectroscopy. The interface is not atomically smooth; it is a broad and chemically complex region. The surface of the native oxide (SiO2) is sulfated by the plasma. The initial MoS2 in films deposited at 220 C is chemically the same as crystalline MoS2; that is, there is no chemical bonding between the film and the substrate. There is evidence that the initial MoS2 in films

deposited at 70 C is chemically bonded to the crystal, perhaps through Mo-S-O or Mo-O linkages. GRA

N90-18533# State Univ. of New York, Buffalo.
FUNDAMENTAL STUDIES OF SURFACE PROCESSES AND TRACE ANALYSIS USING SOLID ELECTRODES Final Report, 1 Nov. 1986 - 31 Jul. 1988
Stanley Bruckenstein 1 Nov. 1989 10 p
(Grant AF-AFOSR-0037-87; AF Proj. 2303)
(AD-A216538; AFOSR-89-1779TR) Avail: NTIS HC A02/MF A01 CSCL 07/4

Physical electrochemical and electroanalytical studies were undertaken on silver, gold, and platinum electrodes. Underpotential deposition (UPD) studies were undertaken on polycrystalline silver electrodes. Using the electrochemical quartz crystal microbalance, it was shown that Pb(II) species are adsorbed at silver when the Pb(II) exists as an anion in solution. The anionic Pb(II) adsorbate is ultimately reduced to a underpotential Pb(0) with concomitant anion (ligand) expulsion from the electrode surface. Adsorption of sulfide ion (UPD without faradaic charge transfer) also occurs at silver from alkaline sulfide solutions. Three distinct UPD states were identified. The coulostatic formation of UPD Hg(0) at a gold electrode was studied in sulfuric acid using the EQCM. It was found that a monolayer of Hg(0) is formed along with an overlayer of mercury (I) bisulfate. The formation of silver sulfide during the electrooxidation of thioacetamide was established. A theoretical analysis of cathodic stripping peaks based on a hemispherical model with progressive nucleation was performed. The results were used in interpreting induction times associated with the formation of cathodic stripping peaks at silver electrodes. The uncompensated ohmic potential drop at microelectrodes under steady state diffusion conditions was shown to be susceptible to a theoretical analysis. GRA

N90-18534# Princeton Univ., NJ. Dept. of Chemical Engineering.
SURFACE INTERMEDIATES IN THIN FILM DEPOSITION ON SILICON Final Report, 15 Nov. 1985 - 14 Nov. 1988
Jay B. Benziger 28 Aug. 1989 16 p
(Grant AF-AFOSR-0050-86; AF Proj. 2303)
(AD-A216662; AFOSR-89-1754TR) Avail: NTIS HC A03/MF A01 CSCL 20/5

This project examined the fundamental processes of surface reactions using infrared spectroscopy. The novelty was the development of a dynamic infrared spectroscopic technique capable of following reaction dynamics on well defined single crystal surfaces. The dynamic infrared technique was applied to two experiments. The first experiment was used to follow single shot experiments: the technique was used to follow thermally induced reactions using temperature programmed reflection absorption infrared spectroscopy (TPRAIS). The second experiment is to follow dynamics of repetitive processes combining modulated molecular beams with reflection infrared. This was demonstrated for simple adsorption desorption of CO on Pt; difficulties in achieving proper conditions for film growth have precluded the application to film deposition, but this problem is still being pursued. GRA

N90-18535# Flow Research, Inc., Kent, WA.
NUMERICAL SIMULATIONS OF COHERENT STRUCTURES IN A JET FLAME WITH A NONCIRCULAR CROSS SECTION Final Report, 1 Jun. 1988 - 30 Sep. 1989
S. Menon, P. A. McMurtry, and W. H. Jou Dec. 1989 15 p
(Contract N00014-88-C-0588)
(AD-A216710; FLOW-RR-494) Avail: NTIS HC A03/MF A01 CSCL 21/2

The presence of coherent structures in turbulent shear flows and their importance in enhancing mixing and entrainment of chemical species has been established in recent years through extensive experimental and numerical studies. When non-premixed combustion is considered, the combustion processes could be enhanced by enhancing the fuel-air mixing and entrainment processes associated with these large coherent structures. In recent experimental studies, the entrainment characteristics of jets with different cross sections were studied, and it was determined that an elliptical jet with a certain cross-sectional shape was more efficient in entraining fluid than a circular jet with the same jet area. This increase was attributed to the complex self-induction process and the subsequent three-dimensional deformation of the elliptical vortex ring during its propagation. To understand the complex flow features associated with elliptical jets with and without heat release, a numerical study was undertaken. A new three-dimensional hybrid Navier-Stokes code was developed using spectral techniques and compact schemes to study the spatial evolution of elliptical jets. The simulation code is now ready for carrying out a detailed study of the effect of jet geometry on the mixing and combustion processes. GRA

N90-18536# George Washington Univ., Washington, DC. Dept. of Chemistry.
LOWER LIMITS ON THE ABSOLUTE DISSOCIATIVE ELECTRON ATTACHMENT CROSS SECTION FROM O2 CONDENSED ON RARE-GAS FILMS Interim Technical Report
H. Sambe, David E. Ramaker, M. Deschenes, and L. Sanche Dec. 1989 4 p Submitted for publication
(Contract N00014-89-J-1103)
(AD-A216727; TR-53) Avail: NTIS HC A01/MF A01 CSCL 07/4

The approach for experimentally obtaining a lower limit on the absolute cross section for production of O(-) by dissociative electron attachment from O2 condensed on a Kr film is summarized here. Comparison of this result with the dissociative attachment cross section for gas phase O2 reveals a factor of 17 enhancement on the surface. It is semiquantitatively shown that a decreased autoionization rate, arising from the electronic polarization of the neighboring Kr atoms, can account for most of this large enhancement. GRA

N90-18537# George Washington Univ., Washington, DC. Dept. of Chemistry.
EXTRACTING CHEMICAL INFORMATION FORM AUGER LINE SHAPES Interim Technical Report
David E. Ramaker Dec. 1989 23 p
(Contract N00014-89-J-1103)
(AD-A216729; TR-51) Avail: NTIS HC A03/MF A01 CSCL 07/4

We have developed a generally applicable semi-empirical approach for quantitatively interpreting Auger line shapes. Detailed information on hybridization, electron delocalization and correlation, screening effects, bonding, and covalency can be obtained from the line shape. Methods for extracting the Auger line shape from the experimental data are briefly described. We summarize our recent results from the C KVV Auger line shapes of five different gas phase hydrocarbons (methane, ethane, cyclohexane, benzene, and ethylene), three solids (polyethylene, diamond, and graphite), and a molecularly chemisorbed system (ethylene/Ni). The normal KVV component accounts for only about half of the total experimental KVV intensity for the hydrocarbon gases; much larger fractions for the three solids. The remaining part of the experimental line shape can be attributed to satellites resulting from resonant excitation or dynamic screening processes. The normal KVV component line shapes are seen to reflect delocalized holes, however correlation effects are very evident. Although these screening and correlation effects complicate the interpretation of the line shapes, they indeed cause the chemical effects seen in the experimental line shapes. GRA

N90-18538# Stanford Univ., CA. Dept. of Aeronautics and Astronautics.
AN INVESTIGATION OF FLOW STRUCTURE, MIXING AND CHEMICAL REACTION IN COMBUSTING TURBULENT FLOWS Final Technical Report, 1 Sep. 1984 - 30 Jun. 1989
Brian J. Cantwell and Craig T. Bowman 23 Oct. 1989 33 p
(Grant AF-AFOSR-0373-84; AF Proj. 2308)
(AD-A216739; AFOSR-89-1679TR) Avail: NTIS HC A03/MF A01 CSCL 21/1

An experimental investigation of the relationship between flow

structure and flame structure in a low-speed, co-flowing, non-premixed, methane-air jet diffusion flame has been completed. The purpose of the research was to examine the spatial structure of the unsteady reaction process as it relates to the unsteady velocity field and to use topological methods in the interpretation of flame dynamics. A small, acoustically produced, perturbation in the fuel jet velocity was used to phaselock the basic flickering instability of the flame thus creating a very periodic and controllable flow, suitable for conditional sampling. Various diagnostic techniques were used in the research including single-component laser anemometry, direct and schlieren photography, Mie scattering from seed particles introduced into the flow, planar, laser-induced fluorescence the OH radical and particle tracking for measuring instantaneous planar velocity field data. Velocity fields have been measured as a function of the phase of the flickering cycle over the first 20 diameters of the flame. GRA

N90-18539# Colorado State Univ., Fort Collins. Dept. of Chemistry.

DETERMINATION OF THE MINIMUM ENERGY CONFORMATION OF ALKYL SUBSTITUTED PYRAZINES

Hoong-Sun Im, E. R. Bernstein, J. I. Seeman, H. V. Secor, and J. Payne (Philip Morris Research Center, Richmond, VA.) 15 Dec. 1989 33 p Submitted for publication

(Contract N00014-79-C-0647)

(AD-A216974; TR-67) Avail: NTIS HC A03/MF A01 CSCL 07/4

Supersonic jet laser spectroscopy has been utilized to identify the minimum energy conformers of substituted aromatic molecules in the gas phase. These determinations have been performed based on the observation that each conformer produces its own origin transition for the excitation. Thus the counting of origin transition in the mass resolved excitation spectrum reveals the number of conformers present for a given system. Conformational preferences for methyl, ethyl, isopropyl and n-propyl substituted pyrazines are determined by mass resolved excitation spectroscopy for the supersonic jet cooled molecules and MOPAC 5.0 semiempirical conformational calculations. The results of these studies suggest that the behavior of the alkyl substituted pyrazines is very different from that of alkyl substituted benzenes. This difference is caused by substantial hydrogen bonding between the alpha-hydrogens of the alkyl substituent and the adjacent lone pair nonbonding electrons on the ring nitrogen atom. One of these hydrogen atoms becomes nearly planar (ca. approx 10 according to the MOPAC 5.0 calculations) with the aromatic ring. GRA

N90-18540# Arizona Univ., Tucson. Optical Sciences Center.

FLUORESCENCE AND ELASTIC SCATTERING FROM LASER DYE-FILLED CAPILLARIES M.S. Thesis

Edward M. Sekerak 23 Aug. 1989 72 p

(AD-A217026) Avail: NTIS HC A04/MF A01 CSCL 07/4

Capillary Zone Electrophoresis (CZE) is a newly developing field of analysis whereby laser excitation causes biological materials in a hollow core capillary to fluoresce. The fluorescence is then studied to identify constituent elements and/or characterize specific properties in the core materials under investigation. We investigated the elastic scattering and fluorescence from laser dye solutions inside 5000, 1100, and 96.5 micron inner-diameter hollow-core capillaries. Incident 4416 laser illumination of Coumarin 7 dye dissolved in ethanol caused fluorescence from approximately 4600 to 6000. This was studied over an angular range from 0 deg to 360 deg. A light scattering nephelometer coupled with a spectrometer gave intensity measurements as functions of wavelength (at fixed detection angles) and angle (at fixed wavelengths), while the illumination source, dye-filled capillary, and detector remained stationary. We saw capillary size and detection-angle dependence of the fluorescence and elastic scattering. Results show that angular variations of the elastic scattering and emitted fluorescence can be used to determine an optimum detection angle from the capillary with respect to the incident illumination direction. GRA

N90-18541# Sandia National Labs., Albuquerque, NM. Fluid and Thermal Sciences Dept.

MICROCONVECTIVE HEATING OF GRANULAR EXPLOSIVES BY A SEMICONDUCTOR BRIDGE

M. J. Martinez and M. R. Baer Dec. 1989 53 p

(Contract DE-AC04-76DP-00789)

(DE90-005710; SAND-89-2033) Avail: NTIS HC A04/MF A01

The ignition of reactive powders by a semiconductor bridge (SCB) is analyzed by applying a multiphase flow model based upon the theory of mixtures. The hot plasma produced by the SCB permeates the cold granular explosive, deposits its latent heat upon fusing to the grains, thereby heating the explosive granular surfaces to energy states required for self-sustained reaction. This mechanism is predicted to heat the granular explosive in a region local to the SCB to temperatures well above those required for thermal ignition. The analysis demonstates that this mechanism explains the prompt ignition of explosives using SCB's as opposed to the conductively controlled heating of conventional bridgewires. DOE

N90-18542# Argonne National Lab., IL. Analytical Chemistry Lab.

EVALUATION OF A COMMERCIAL GAS CHROMATOGRAPHY/MATRIX ISOLATION-INFRARED SPECTROMETER FOR QUANTITATIVE ANALYSIS OF PRIORITY POLLUTANTS

John F. Schneider, Ken R. Schneider, and Stephanie E. Spiro Oct. 1989 35 p

(Contract W-31-109-eng-38)

(DE90-006033; ANL/ACL-89/2) Avail: NTIS HC A03/MF A01

Gas chromatography/matrix isolation-infrared spectrometry (GC/MI-IR) is being applied to many analyses normally done by gas chromatography/mass spectrometry. Qualitatively, the infrared spectra of matrix-isolated compounds contain much information about their structure. The information obtained from the infrared spectrum is complementary to the information obtained from mass spectrometry. The technique of GC/MI-IR should also be useful as a quantitative detector. In this study, the utility of a commercial GC/MI-IR for quantitative trace organic analysis was evaluated. Results indicate that the reproducibility of the commercial instrument is only suitable for semiquantitative analysis. The precision of the commercial instrument might be improved by redesign of its open-split interface. DOE

N90-18543# European Space Agency, Paris (France).

THEORETICAL INVESTIGATION OF THE STABILIZATION OF A DIFFUSION FLAME ABOVE A RECIRCULATION REGION

Matthias Konczalla (Deutsche Forschungs- und Versuchsanstalt fuer Luft- und Raumfahrt, Lampoldshausen, West Germany) Dec. 1989 137 p Transl. into ENGLISH of Theoretische Untersuchung zur Stabilisierung einer Diffusionsflame ueber einem Rezirkulationsgebeit (Lampoldshausen, Fed. Republic of Germany), Jan. 1989 p 1-120 Original language document was announced as N89-26075

(ESA-TT-1149; DFVLR-FB-89-02; ETN-90-96216) Avail: NTIS HC A07/MF A01; original German version available from DFVLR, VB-PL-DO, Postfach 90 60 58, 5000 Cologne 90, Fed. Republic of Germany, 44 DM

A flame stabilized by a flame holder is the result of the interaction between transport processes and an exothermic chemical reaction. The stabilization of a diffusion flame above a reverse flow region downstream of a backward-facing step is investigated. The special features of this flow are taken into acount. A strongly nonlinear Arrhenius expression is introduced into the conversation equations to describe the reaction. The activation energy of the reaction is used as the major parameter in a singular perturbation formulation. Ignition points are defined in terms of a particular singularity on the dividing streamline. Downstream from the ignition point a flame is observed. Using Linan's premixed diffusion flame analysis, an equation for the flame front is derived. The flame only penetrates the mixing zone above the recirculation zone for entry velocities up to a certain value. ESA

N90-18544# Construcciones Aeronauticas S.A., Madrid (Spain). Subdireccion de Investigacion y Desarrollo de Tecnnologia y Materiales.

RHEOLOGICAL TESTS OF RIGIDITE 5245 USING THE CONE-PLATE AND PARALLEL PLATES METHOD

J. Sanchez 10 Jan. 1989 6 p

(DT-310/88; ETN-90-96228) Avail: NTIS HC A02/MF A01

Comparative rheological tests using parallel plates and cone and plate viscosimeters were performed on neat resin Rigidite 5245C. The equipment used was the RDS-7700 (rheometrics dynamic spectrometer). Parameters are given. Conclusions indicate similar results obtained from both methods. The parallel plates method is considered more advisable for operative purposes, since the use of disposable plates allows continuation of the test beyond the gel point without taking special care for the equipment cleaning or maintenance. ESA

N90-18545# West Virginia Univ., Morgantown. Dept. of Physics.

HIGH TEMPERATURE INTERACTION OF SO2 WITH OXIDE SORBENTS Final Report

M. S. Seehra and G. R. Thevar Jun. 1989 53 p

(Contract DE-AC21-86MC-23259)

(DE90-000435; DOE/MC-23259/2781) Avail: NTIS HC A04/MF A01

A thorough investigation was made of the kinetics of the interaction of SO2 gas with CaO particles at temperatures between 25 and 1000 C. The goal was to develop the new technique of FTIR (Fourier Transform Infra Red) spectroscopy for studies of the SO2-CaO interaction so as to determine not only the kinetics but also the nature of the chemical products of the reaction for temperatures to 1000 C. Further, the goal was to determine the effect of oxygen on the kinetics and products of the reaction. In addition, techniques of ESR (Electron Spin Resonance) spectroscopy and TGA (Thermogravimetric Analysis) were to be employed to support these studies. It was hoped that results of these studies would clear many of the inconsistencies reported in literature on the sulfation of CaO. Results of these studies as well as results on the interaction of SO2 with calcined CaCO3 and MgCO3 (calcined at 700 C), for temperatures up to 700 C, are given. DOE

N90-18546# Rutgers - The State Univ., Piscataway, NJ. Physics Lab.

STRUCTURE AND REACTIVITY OF MODEL THIN FILM CATALYSTS Annual Performance Report, 16 Jan. 1989 - 15 Jan. 1990

Theodore E. Madey 31 Aug. 1989 8 p

(Contract DE-FG05-89ER-13985)

(DE90-007365; DOE/ER-13985/1) Avail: NTIS HC A02/MF A01

The purpose of this project is to characterize the structure and reactivity of model bimetallic catalysts, e.g., ultrathin films of Pt deposited on single crystal surface of tungsten. Studies during this reporting period (January 15, 1989 to the present) have involved a comparison between the atomically smooth W(110) surface and the atomically rough W(111) surface using several ultrahigh vacuum surface science methods (low energy electron diffraction, LEED, Auger electron spectroscopy, AES, and thermal desorption spectroscopy, TDS). In addition, we have used scanning tunneling microscopy (STM) to provide a microscopic view of Pt induced surface structures with Angstrom level resolution. On W(110), a single Pt monolayer is stable upon heating to greater than 1800 K. It grows in a layer-by-layer mode at 300 K, but Pt coverages in excess of one monolayer will cluster into three-dimensional bulk Pt crystallites upon annealing to (approx gt) 800 K. When W(111) is covered by (approx gt) 1 times 10(15) Pt atoms/sq cm and heated in the range 800 to 1600 K, the surface undergoes a massive restructuring to form microscopic facets. At 1200 K, the average facet dimensions are approx. 100 Angstrom, and the dominant facet orientations is W(211). The faceting appears to be driven by a Pt-enhanced anisotropy in the surface free energy. DOE

N90-18547# Institut Franco-Allemand de Recherches, Saint-Louis (France).

EXPERIMENTAL AND THEORETICAL RESEARCH ON THE INJECTION OF IGNITION GASES INTO A BED OF INERT POWDER [EXPERIMENTELLE UND THEORETISCHE UNTERSUCHUNG DES EINSTROEMVORGANGS IN EIN INERTPULVERBETT]

H. Mach and H. J. Schittke 24 Nov. 1988 35 p In GERMAN Presented at 14th Symposium Innenballistische Leitungssteigerung von Rohrwaffen, Swisttal-Heimerzheim, Fed. Republic of Germany, 8-10 Nov. 1988

(ISL-CO-251/88; ETN-90-96251) Avail: NTIS HC A03/MF A01

The temperature of ignition gases from an igniter are measured in order to develop a simulation program. The temperature is measured using spectroscopy. A laser interferometer is used to measure the speed of gas flow. A DYSMAS/E simulation code is used to process the data. The penetration of the ignition gases into a bed of inert nonflammable cellulose nitrate beads 4 mm in diameter with graphite coatings, is studied. Comparisons between experimental and theoretical results show close agreement. ESA

N90-18548# Deutsche Forschungsanstalt fuer Luft- und Raumfahrt, Stuttgart (Germany, F.R.). Inst. fuer Technische Thermodynamik.

ON THE DYNAMICS OF THE COMBUSTION PROCESS OF HYDROGEN-AIR AND HYDROGEN-METHANE-AIR MIXTURES Ph.D. Thesis - Tech. Univ. Munich

Helmut Eichert Jul. 1989 118 p In GERMAN; ENGLISH summary Report will also be announced as translation (ESA-TT-1198)

(DLR-FB-89-39; ISSN-0171-1342; ETN-90-96276; ESA-TT-1198)

Avail: NTIS HC A06/MF A01; DLR, Wissenschaftliches Berichtswesen, Postfach 90 60 58, 5000 Cologne 90, Fed. Republic of Germany, 35 DM

The dynamics of the combustion process of hydrogen-air and hydrogen-methane-air mixtures in long tubes, the boundary conditions for the deflagration-to-detonation transition and the associated pressure signals are investigated experimentally and numerically. To influence this combustion process and, in particular, to narrow the range of possible detonations of hydrogen-air mixtures, different inhibitors are considered. For numerical modeling, the one dimensional random-choice-method is used and further developed. The numerical calculations are compared to the experimental results. The potential and the limitations of this numerical method are shown. ESA

N90-18549# Beleidscommie Remote Sensing, Delft (Netherlands).

INVESTIGATION OF MULTIPLE SCATTERING IN AQUEOUS SUSPENSIONS OF NON-ABSORBING POLYSTRENE MICROSPHERES USING SPECTROPHOTOMETRY

G. B. J. Dubelaar, J. Krijgsman, and M. Donze (Technische Hogeschool, Delft, Netherlands) Oct. 1989 62 p Prepared in cooperation with Organisatie voor Toegepast NatuurwətenschappelijkOnderzoek, Rijswijk (Netherlands), and Keruling van Electrotechnische Materialen N. V., Arnhem (Netherlands)

(BCRS-89-09; ETN-90-96316) Avail: NTIS HC A04/MF A01

The establishment of the maximum accuracy in concentration estimates that can be obtained from spectral reflection measurements using natural light (passive remote sensing in the optical window) is investigated. Only laboratory and shipboard conditions are considered, so atmospheric correction is excluded. The results can be used to obtain a priori estimates about what might be attainable using air or spaceborne instruments, as, vice versa, to abort projects comprising unattainable goals. Techniques for quantification of sources or error are attempted. Accuracy of distinction made between physical interactions of light and matter is particularly addressed: absorption, scattering, multiple scattering, anomalous scattering, and fluorescence. Experimental difficulties are discussed. ESA

26 METALLIC MATERIALS

Includes physical, chemical, and mechanical properties of metals, e.g., corrosion; and metallurgy.

N90-18550# Westinghouse Savannah River Co., Aiken, SC.
FAILURE PROBABILITY ESTIMATE OF TYPE 304 STAINLESS STEEL PIPING
W. L. Daugherty, N. G. Awadalla, R. L. Sindelar, H. S. Mehta, and S. Ranganath (General Electric Co., San Jose, CA.) 1989 7 p Presented at the 2nd DOE Natural Phenomena Hazards Mitigation Conference, Knoxville, TN, 3-5 Oct. 1989 Submitted for publication
(Contracts DE-AC09-89SR-18035; DE-AC09-76SR-00001)
(DE90-003896; DP-MS-89-83-Rev-1; CONF-8910192-8-Rev-1)
Avail: NTIS HC A02/MF A01

The primary source of in-service degradation of the SRS production reactor process water piping is intergranular stress corrosion cracking (IGSCC). IGSCC has occurred in a limited number of weld heat affected zones, areas known to be susceptible to IGSCC. A model was developed to combine crack growth rates, crack size distributions, in-service examination reliability estimates and other considerations to estimate the pipe large-break frequency. This frequency estimates the probability that an IGSCC crack will initiate, escape detection by ultrasonic (UT) examination, and grow to instability prior to extending through-wall and being detected by the sensitive leak detection system. These four factors estimate the occurrence of several conditions that must coexist in order for a crack to lead to a large break of the process piping. When evaluated for the SRS production reactors, they produce an extremely low break frequency. The objective is to present the assumptions, methodology, results and conclusion of a probabilistic evaluation for the direct failure of the primary coolant piping resulting from normal operation and seismic loads. This evaluation was performed to support the ongoing PRA effort and to complement deterministic analyses addressing the credibility of a double-ended guillotine break. DOE

N90-18551# Argonne National Lab., IL. Materials Components and Technology Div.
RESPONSE OF UNIRRADIATED AND NEUTRON-IRRADIATED VANADIUM ALLOYS TO CHARPY-IMPACT LOADING
B. A. Loomis and D. L. Smith 23 Oct. 1989 11 p Presented at the 4th International Conference on Fusion Reactor Materials, Kyoto, Japan, 4-8 Dec. 1989 Submitted for publication
(Contract W-31-109-eng-38)
(DE90-004878; CONF-891204-14) Avail: NTIS HC A03/MF A01

The ductile-brittle transition temperature (DBTT) was determined by Charpy-impact impact tests for dehydrogenated (less than 30 appm H) and hydrogenated (400 to 1200 appm H) V-7.2Cr-14.5Ti, V-9.9Cr-9.2Ti, V-13.5Cr-5.2Ti, V-17.7Ti, V-9.2Cr-4.9Ti, V-9.0Cr-3.2Fe-1.2Zr, V-3.1Ti-0.5Si, V-4.1Cr-4.3Ti, V-4.6Ti, and V-2.5Ti-1.0Si alloys. The DBTT was also determined for the V-13.5Cr-5.2Ti, V-9.2Cr-4.9Ti, V-7.2Cr-14.5Ti, and V-17.7Ti alloys after neutron irradiation at 420 and 600 C to 41 to 44 atom displacements per atom. The DBTTs determined for these vanadium alloys show that a vanadium alloy containing Cr and/or Ti and Si alloying additions to be used as a structural material in a fusion reactor should contain 3 to 11 wt percent total alloying addition for maximum resistance to hydrogen and/or irradiation induced embrittlement. DOE

N90-18552# Battelle Columbus Labs., OH.
LOW TEMPERATURE SPECIFIC HEAT AND MAGNETIC SUSCEPTIBILITY OF NbTi AND NbTiMn ALLOYS
E. W. Collings, R. D. Smith, J. C. Ho, and C. Y. Wu (Wichita State Univ., KS.) 1989 9 p Presented at the International Cryogenic Materials Conference, Los Angeles, CA, 24-28 Jul. 1989
(Contract DE-AC02-86ER-40296)
(DE90-005390; CONF-890701-25) Avail: NTIS HC A02/MF A01

The results are reported of a low temperature specific heat and magnetic susceptibility studies of a series of annealed-and-quenched binary NbTi alloys in the concentration range 41 approx. 53 wt. percent Nb, which includes most compositions of technical interest. Also discussed is the influence of Mn on the calorimetrically measured properties of NbTi. Three series of alloys are considered: (1) a set of binary control alloys; (2) alloys with Mn content fixed at approx. 0.5 wt. percent and with Nb concentration between about 41 and 53 wt. percent; (3) alloys with an almost fixed Ti content (approx. 46 wt. percent) and with Mn concentration between 0 and (approx. 5 wt. percent). In alloys such as Ti-52Nb it is demonstrated that the addition of several percent of Mn causes a decrease in the electronic specific heat coefficient and a concomitant decrease in (Tc). In that regard the effect of Mn on (Tc) (d(Tc)/dc = - 0.22 K/at. percent) is comparable to that of Cr, Mo, or Re (for which d(Tc)/dc = - 0.2 K/at. percent). It is concluded that Mn is a strong stabilizer of the bcc phase in Ti-base alloys and that Mn in bcc NbTi acts like any other nonmagnetic transition-element and influences (Tc) through its influence on the band density of states. DOE

N90-18553# Johns Hopkins Univ., Baltimore, MD. Dept. of Materials Science and Engineering.
A FUNDAMENTAL UNDERSTANDING OF THE EFFECT OF ALLOYING ELEMENTS ON THE CORROSION RESISTANCE OF RAPIDLY SOLIDIFIED Mg ALLOYS Final Report, 30 Sep. 1988 - 31 Oct. 1989
J. Kruger, G. L. Makar, and K. Sieradzki 17 Nov. 1989 67 p
(Grant AF-AFOSR-0339-88; AF Proj. 2306)
(AD-A216767; AFOSR-89-1671TR) Avail: NTIS HC A04/MF A01 CSCL 11/6

This report consists of four publications, two resulting from a previous contract F496620-86-C-0014, P00002. The titles are: Environment-assisted cracking of rapidly solidified Mg-Al alloys; Structure of the Passive films on cast and rapidly solidified Mg alloys; The effect of alloying elements on the corrosion resistance of rapidly solidified magnesium alloys; and Corrosion studies of rapidly solidified magnesium alloys. GRA

N90-18554# Naval Postgraduate School, Monterey, CA. Dept. of Mechanical Engineering.
PROCESSING AND ELEVATED TEMPERATURE DUCTILITY OF ALUMINUM ALLOY 7475 M.S. Thesis
John Ratkovich Jun. 1989 59 p
(AD-A216840) Avail: NTIS HC A04/MF A01 CSCL 11/6

This research has initiated investigation of Aluminum alloy 7475 Aluminum-Zinc-Magnesium-Copper in regard to the effects of thermomechanical process (TMP) variables on superplasticity. These effects are evaluated by pct. elongation at temperatures ranging from 300 to 450 C and strain rates of .0067 to .000067/s and microstructural analysis. In comparison to results in the literature, superplastic ductility for lower temperature, higher rate superplasticity may be enhanced. GRA

N90-18555# Allied-Signal Corp., Morristown, NJ.
IMPROVED AMORPHOUS METAL MATERIALS FOR MAGNETIC PULSE COMPRESSION
Aug. 1989 62 p Prepared for Sandia National Labs., Albuquerque, NM
(Contract DE-AC04-76DP-00789)
(DE90-005723; SAND-89-7095) Avail: NTIS HC A04/MF A01

This program was undertaken by Allied-Signal Inc., under contract from Sandia National Laboratories to examine methods to improve the performance of ferromagnetic amorphous metal alloys for magnetic pulse compression applications. The alloy studied was METGLAS (trademark) alloy 2605CO, an alloy with maximum saturation induction used in magnetic pulse compression projects. In order to reduce losses under rapid pulse magnetization, the limits of casting thinner ribbons, both in air and in vacuum, were explored as well as methods of reducing thickness after casting. The magnetic properties of these ribbons were characterized as a function of thickness. The voltage hold off and the effects of conformal insulative coatings on magnetic properties were studied in an attempt to develop an annealable insulation

capable of withstanding 100 volt pulses. Finally, recommendations were made based on this work for scaling up to larger quantities of thin ribbon. DOE

N90-18556# Lehigh Univ., Bethlehem, PA. Dept. of Mechanical Engineering and Mechanics.
CORROSION FATIGUE OF IRON-CHROMIUM-NICKEL ALLOYS: FRACTURE MECHANICS AND CHEMISTRY Progress Report, 1 Jan. - 31 Dec. 1989
Robert P. Wei 26 Jan. 1990 13 p
(Contract DE-FG02-88ER-45354)
(DE90-006318; DOE/ER-45354/T2) Avail: NTIS HC A03/MF A01

A multi-disciplinary research program is undertaken to address certain fundamental issues relating to corrosion fatigue crack growth in structurally important alloys in aqueous environments. The principal goal is to develop and expand the scientific understanding of the processes that control corrosion fatigue crack growth, particularly for ferrous alloys in terms of the controlling mechanical and chemical/electrochemical processes and their interactions with the microstructure. DOE

N90-18557# Michigan State Univ., East Lansing. Dept. of Metallurgy, Mechanics, and Materials Science.
SOFTENING MECHANISMS AND MICROSTRUCTURAL INSTABILITIES DURING HIGH TEMPERATURE, LOW CYCLE FATIGUE OF Ni, Ni3Al, AND THEIR METAL MATRIX COMPOSITES Progress Report, 1 Jun. 1989 - 31 May 1990
D. S. Grummon and G. Gottstein Jan. 1989 5 p
(Contract DE-FG02-85ER-45205)
(DE90-006487; DOE/ER-45205/5) Avail: NTIS HC A01/MF A01

The program in the previous year has focused on the interaction of crack growth and dynamic recrystallization during high temperature low cycle fatigue (HTLCF) of nickel, the static and dynamic recrystallization behavior of boron doped Ni3Al, computer simulation of microstructure evolution during HTLCF, and the processing of Al2O3/Ni3Al(B) continuous fiber composites. The program was subdivided into 4 projects, which are summarized below. DOE

N90-18558# National Inst. of Standards and Technology, Gaithersburg, MD. Materials Science and Engineering Lab.
THE MECHANISM, MEASUREMENT, AND INFLUENCE OF PROPERTIES ON THE GALLING OF METALS Final Report
L. K. Ives, M. B. Peterson, and E. P. Whitenton Dec. 1989 93 p Prepared for ORNL, TN
(Contracts DE-AI05-83OR-21322; DE-AC05-84OR-21400)
(DE90-006533; ORNL/Sub-83-21322/01; NISTIR-89-4064) Avail: NTIS HC A06/MF A01

This report presents the results of an extensive investigation of the process of galling. The work was motivated by the need to develop a better understanding of the process of galling as it affects various fossil energy related systems, and by the need to find solutions to the problem of galling in these systems. Three areas were emphasized: (1) the elucidation of the mechanism of galling, (2) the quantitative characterization and measurement of the amount of damage associated with galling, and (3) the determination of relationship between galling and materials properties. On the basis of a review of the literature and experiments on a variety of different metals it was concluded that the primary event in the process of galling is that of prow or wedge formation. A method based on surface topography was developed to measure quantitatively the amount and character of galling. By studying a range of pure metals and selected experimental alloys it was demonstrated that among the most important properties influencing galling are crystal structure and stacking fault energy. Hardness and strength do not in general correlate with galling severity, but it was shown that hardening steels by heat treatment is an effective means of reducing the damage due to galling. Carburizing and nitriding were also shown to diminish significantly the damage due to galling. DOE

N90-18559*# United Technologies Research Center, East Hartford, CT.
IDENTIFICATION OF A CAST IRON ALLOY CONTAINING NONSTRATEGIC ELEMENTS Final Report
C. V. Cooper, D. L. Anton, F. D. Lemkey, H. Nowotny, R. S. Bailey, L. H. Favrow, J. G. Smeggil, and D. B. Snow Jun. 1989 79 p
(Contracts DEN3-282; DE-AI01-77CS-51040)
(NASA-CR-185174; DOE/NASA/0282-1; NAS 1.26:185174; R89-917447-32) Avail: NTIS HC A05/MF A01 CSCL 11F

A program was performed to address the mechanical and environmental needs of Stirling engine heater head and regenerator housing components, while reducing the dependence on strategic materials. An alloy was developed which contained no strategic elemental additions per se. The base is iron with additions of manganese, molybdenum, carbon, silicon, niobium, and ferro-chromium. Such an alloy should be producible on a large scale at very low cost. The resulting alloy, designated as NASAUT 4G-Al, contained 15 Mn, 15 Cr, 2 Mo, 1.5 C, 1.0 Si, 1.0 Nb (in weight percent) with a balance of Fe. This alloy was optimized for chemistry, based upon tensile strength, creep-rupture strength, fracture behavior, and fatigue resistance up to 800 C. Alloys were also tested for environmental compatibility. The microstructure and mechanic properties (including hardness) were assessed in the as-cast condition and following several heat treatments, including one designed to simulate a required braze cycle. The alloy was fabricated and characterized in the form of both equiaxed and columnar-grained castings. The columnar grains were produced by directional solidification, and the properties were characterized in both the longitudinal and transverse orientations. The NASAUT 4G-Al alloy was found to be good in cyclic-oxidation resistance and excellent in both hydrogen and hot-corrosion resistance, especially in comparison to the baseline XF-818 alloy. The mechanical properties of yield strength, stress-rupture life, high-cycle-fatigue resistance, and low-cycle-fatigue resistance were good to excellent in comparison to the current alloy for this application, HS-31 (X-40), with precise results depending in a complex manner on grain orientation and temperature. If required, the ductility could be improved by lowering the carbon content.
Author

N90-18560# European Space Agency, Paris (France).
SIGNIFICANCE OF OXIDE SKINS ON POWDER FOR THE QUALITY OF PM Al MATERIALS
Hugo Schlich Dec. 1989 150 p Transl. into ENGLISH of Bedeutung der Oxidschichten auf Pulver fuer die Qualitaet von PM Al-Werkstoffen (Cologne, Fed. Republic of Germany), Apr. 1989 p 1-143 Original language document was announced as N90-11873
(ESA-TT-1178; DFVLR-FB-89-11; ETN-90-96224) Avail: NTIS HC A08/MF A01; original German version available from DFVLR, VB-PL-DO, Postfach 90 60 58, 5000 Cologne 90, Fed. Republic of Germany, 52 DM

The surface layers (oxides/hydroxides and adsorbates) of atomized PM (powder metallurgy) Al alloy powders were conditioned by degassing. Quadrupole mass spectrometer measurements were performed in order to optimize the degassing treatment. The composition and compound state of the surface layers were characterized by Auger and x ray electron spectroscopy before and after degassing. In a degassed and consolidated powder less internal defects caused by oxide/hydroxide skins are found. This is due to desorption of adsorbates and dehydration of hydroxides by degassing, and to the consolidation in vacuum.
ESA

N90-18561# Technische Univ., Delft (Netherlands).
SINTERING OF A MODEL NICKEL/ALUMINA CATALYST Ph.D. Thesis
Lucretia Agnes Correia 1989 168 p Sponsored by Netherlands Foundation for Chemical Research and Netherlands Organization for the Advancement of Pure Research
(ETN-90-96270) Avail: NTIS HC A08/MF A01

A thesis on the sinter mechanism of supported metal dispersions

and the influence of additives on this part of the process is presented. The physical principle by which the catalytic activity of a metal/oxide catalyst decreases is coarsening of the metal dispersion, one of the causes of which may be sintering of the support. Sintering of nickel/alumina catalysts is summarized. Preparation and sinter experiments of four model systems are described. Analysis is carried out with x ray photoelectron spectroscopy, combined with ion etching, to obtain depth profiles, using thin layer composites aged for 100 hours in hydrogen at 973K. The kinetics of the sintering of a supported particle dispersion are discussed. Results of the experimental studies are compared with theoretical predictions. ESA

N90-18562# Idaho National Engineering Lab., Idaho Falls.
HELIUM PERMEABILITY THROUGH AUSTENITIC STAINLESS STEEL
R. A. Anderl and P. K. Nagata Sep. 1989 24 p
(Contract DE-AC07-76ID-01570)
(DE90-007046; EGG-MS-8714) Avail: NTIS HC A03/MF A01

The by-product canister for the Special Isotope Separation Project will be austenitic stainless steel. The by-product produces, among other things, helium gas from alpha particle decay. To determine whether the helium gas pressure will increase with time, the permeability of helium through austenitic stainless steel was calculated using data from the literature. It was found that stainless steel is essentially impermeable to helium at 523 K (250 C), the predicted maximum canister storage temperature. Therefore, based on the estimated helium production rate and the canister volume, the helium gas pressure will increase with time up to about 0.9 atm at the end of the canister's 50-year life. DOE

N90-18563# Oak Ridge National Lab., TN. Alloying Behavior and Design Group.
DEFORMATION AND FRACTURE OF ORDERED INTERMETALLIC COMPOUNDS Foreign Trip Report
M. H. Yoo 14 Feb. 1990 13 p
(Contract DE-AC05-84OR-21400)
(DE90-007422; ORNL/FTR-3529) Avail: NTIS HC A03/MF A01

The research at Tohoku University was primarily on mechanistic interpretation of the available mechanical properties of ordered intermetallic alloys. This included initiation mechanisms of the active slip and twinning, anomalous yield and flow behavior, and electron microscopic analyses of dislocation substructures. The assignee presented invited papers on deformation and fracture behavior of ordered intermetallic compounds at technical society meetings, and participated in topical symposia and workshops. The assignee became better acquainted with the Japanese strategy on base technology development for advanced structural materials. DOE

N90-18564# Sandia National Labs., Albuquerque, NM.
TIME-RESOLVED MEASUREMENTS OF SOLIDIFICATION AND UNDERCOOLING IN METALS AND ALLOYS
Harry A. Atwater, Jeffrey A. West, Patrick M. Smith, M. J. Aziz, J. Y. Tsao, Paul S. Peercy, and Michael O. Thompson (Cornell Univ., Ithaca, NY.) 1989 7 p Presented at the Materials Research Society Fall Meeting, Boston, MA, 27 Nov. - 2 Dec. 1989
(Contract DE-AC04-76DP-00789)
(DE90-007074; SAND-90-0152C; CONF-891119-98) Avail: NTIS HC A02/MF A01

Nanosecond-resolution measurements were made of the lateral electrical resistivity of thin metal films on insulating substrates. Comparison of transient resistivity measurements with optical reflectivity measurements and heat-flow calculations permits the determination of the position and velocity of a planar crystal/melt in interface, and an estimate of undercooling during pulsed laser melting of metals. Detailed results are reported for rapid solidification of Ni, including the observation of hypercooling of liquid Ni. DOE

N90-18397# Rolls-Royce Ltd., Derby (England). Dept. of Materials and Mechanics Technology.
DEFECTS: THEIR BEHAVIOUR AND RELATED DESIGN ASSUMPTIONS
R. H. Jeal *In* AGARD, AGARD/SMP Review: Damage Tolerance for Engine Structures. 2: Defects and Quantitative Materials Behaviour Aug. 1989 7 p (For primary document see N90-18396 11-07)
Avail: NTIS HC A06/MF A01; Non-NATO Nationals requests available only from AGARD/Scientific Publications Executive

N90-18398# Societe Nationale d'Etude et de Construction de Moteurs d'Aviation, Evry Cedex (France). Lab. Materiaux et Procedes.
THE DAMAGE TOLERANCE OF DISC MATERIALS: METALLURGICAL FACTORS; RELATIONSHIP WITH PROCESSING PARAMETERS
E. J. Bachelet *In* AGARD, AGARD/SMP Review: Damage Tolerance for Engine Structures. 2: Defects and Quantitative Materials Behaviour Aug. 1989 20 p (For primary document see N90-18396 11-07)
Avail: NTIS HC A06/MF A01; Non-NATO Nationals requests available only from AGARD/Scientific Publications Executive

N90-18399# Rolls-Royce Ltd., Derby (England).
REVIEW OF COMPONENT DEFECTS, THEIR RELATIONSHIP TO MANUFACTURING PROCESS, AND THEIR EFFECT ON MATERIALS BEHAVIOUR (FOR CRITICAL ROTATING PARTS)
A. C. Pickard *In* AGARD, AGARD/SMP Review: Damage Tolerance for Engine Structures. 2: Defects and Quantitative Materials Behaviour Aug. 1989 15 p (For primary document see N90-18396 11-07)
Avail: NTIS HC A06/MF A01; Non-NATO Nationals requests available only from AGARD/Scientific Publications Executive

N90-18400# Turbomeca S.A. - Brevets Szydlowski, Bizanos (France).
DEFECTS IN MONOBLOCK CAST TURBINE WHEELS [LES DEFAUTS DANS LES ROUES DE TURBINE COULEES MONOBLOC]
D. Fournier *In* AGARD, AGARD/SMP Review: Damage Tolerance for Engine Structures. 2: Defects and Quantitative Materials Behaviour Aug. 1989 11 p In FRENCH (For primary document see N90-18396 11-07)
Avail: NTIS HC A06/MF A01; Non-NATO Nationals requests available only from AGARD/Scientific Publications Executive

27 NONMETALLIC MATERIALS

Includes physical, chemical, and mechanical properties of plastics, elastomers, lubricants, polymers, textiles, adhesives, and ceramic materials.

For composite materials see *24 Composite Materials*.

N90-18565# Sandia National Labs., Albuquerque, NM.
COMPOSITE FOR SMOOTHING THE SURFACE OF CERAMIC SUBSTRATES
Michi Maeda and Eiji Nishida 1988 7 p Transl. into ENGLISH of Japanese Patent No. 63-74985 (5 Apr. 1988) 4 p Prepared in cooperation with Nihon Univ., Tokyo (Japan)
(Contract DE-AC04-76DP-00789)
(DE90-004005; ALS/TR-89-02) Avail: NTIS HC A02/MF A01

The present invention relates to a composite for smoothing the surface of ceramic substrates, in particular, to a composite for the formation of a SiO2 film, in which the main constituents are copolymers of tetra-alkoxysilane and trialkoxysilane and/or dialkoxysilane. The composite of the present invention can be utilized to good advantage for smoothing the surfaces of ceramic substrates used for integrated circuit modules. DOE

N90-18566# Lehigh Univ., Bethlehem, PA. Dept. of Chemistry.
PERFORATED MONOLAYERS Progress Report, 1 Jul. 1987 - 31 Dec. 1989

S. L. Regen Dec. 1989 10 p
(Contract DE-FG02-85ER-13403)
(DE90-005469; DOE/ER-13403/2) Avail: NTIS HC A02/MF A01

The goals of this DOE-sponsored program are to create novel organic thin films that possess well defined and adjustable molecular pores; i.e., perforated monolayers, and to use such film for fabricating composite membranes that have unique permeation characteristics. The specific strategy that has been adopted involves: (1) the synthesis of surfactant molecules bearing internal pores, i.e., porous surfactants, (2) the assembly of such molecules at an air-water interface, and (3) the stabilization of the resulting assembly via polymerization, before or after transfer to a macroporous support. Research that has been carried out to date has demonstrated the feasibility of using suitably designed calix(n)arene molecules as a basis for constructing perforated monolayers. Specifically, a broad range of calix(n)arenes were mercurated with mercury trifluoracetate, and used to form polymerized and porous monolayers at the air-water interface. In related studies, p-tert- butylcalix(6)arene was shown to produce stable monolayers at the air-water interface; removal of the p-tert-butyl groups afford a unique vesicle forming surfactact, calix(n)arene. DOE

N90-18567# University of Southern California, Los Angeles. Dept. of Chemical Engineering.
MODEL FILLED POLYMERS 3. RHEOLOGICAL BEHAVIOR OF POLYSTYRENE CONTAINING CROSSLINKED POLYSTYRENE BEADS Technical Report, No. 3, 1 May 1988 - 30 Nov. 1989
M. Park, K. Gandhi, L. Sun, J. J. Aklonis, and R. Salovey 30 Nov. 1989 32 p Submitted for publication
(Contract N00014-88-K-0302)
(AD-A215867) Avail: NTIS HC A03/MF A01 CSCL 11/4

The steady shear viscosity and dynamic moduli, at 180 and 200 C, of polystyrene composites, containing crosslinked monodisperse polystyrene beads varying in diameter from 0.2 to 0.8 microns, are independent of bead size and crosslink density, but increase with the volume fraction of beads. Steady shear viscosities exhibit power law regions up to 40 percent concentration of beads, but no yield stress. Storage and loss moduli are initially linear with frequency, on double logarithmic plots, with limiting slopes of 1.3 and 0.9, respectively. Uncrosslinked beads and beads crosslinked with 0.1 percent divinylbenzene are destroyed by thermomechanical dispersion in the melt. GRA

N90-18568# State Univ. of New York, Buffalo. Dept. of Chemistry.
NONLINEAR OPTICAL PROCESSES IN ONE-DIMENSIONAL POLYMERS
Xiao-Shen Li, Duo L. Lin, and Thomas F. George Dec. 1989 19 p Submitted for publication
(Contract N00014-90-J-1193)
(AD-A216103; UBUFFALO/DC/89/TR-3) Avail: NTIS HC A02/MF A01 CSCL 07/6

New phenomena are observed theoretically in nonlinear optical responses of polydiacetylene toluene sulfonate (PTS) irradiated by a strong laser beam. Within a two-level model of PTS, the transient behavior of the induced susceptibility is investigated. Optical nutation is found, and the optical Stark blue shift and bleaching are also found in qualitative agreement with experiments. In the steady state, a new type of optical tristability mediated by phonons is found. A possible mechanism responsible for this tristability is discussed. GRA

N90-18569# Cincinnati Univ., OH. Dept. of Materials Science and Engineering.
POLYMERIZATION OF NITRO COMPOUNDS ON SILVER SURFACES DURING SURFACE-ENHANCED RAMAN SCATTERING
W. H. Tsai, F. J. Boerio, S. J. Clarson, and Giorgio Montaudo (Catania Univ., Italy) 1 Dec. 1989 36 p Submitted for publication Sponsored in part by NSF
(Contract N00014-89-J-1590)
(AD-A216116; TR-3) Avail: NTIS HC A03/MF A01 CSCL 07/6

Surface enhanced Raman scattering was observed from thin films formed by 1,4- and 1,3- dinitrobenzene spin coated onto silver island films from dilute solutions. During laser irradiation of 1,4-DNB films on silver substrates at relatively high laser powers, new bands appeared near 1152, 1350, 1412, and 1460/cm and bands near 1118, 1358, and 1372/cm decreased in intensity. A band near 1598/cm shifted to near 1605/ cm. The bands near 1152 and 1412/ cm were assigned to stretching modes of Phi-N and -N=N- bonds of azo compounds, respectively, indicating that polymerization of 1,4-DNB had occurred. The extent of polymerization was greatest when the surface coverage of adsorbed 1,4-DNB was greatest and when the SERS experiments were carried out in a nitrogen atmosphere, indicating that reducing conditions were required for the polymerization. No polymerization was observed for 1,3-DNB under similar circumstances. The difference was attributed to orientation of the adsorbed species. Thus, it was concluded that 1,4-DNB was adsorbed with a horizontal configuration in which the aromatic rings were parallel to the substrate surface and both nitro groups were in contact with the surface while 1,3-DNB was adsorbed with a vertical configuration in which the rings were perpendicular to the surface and only one nitro group was in contact with the surface. GRA

N90-18570# Columbia Univ., New York, NY. Dept. of Chemistry.
DYNAMICS AND STABILIZATION OF MATERIALS POSSESSING HIGH ENERGY CONTENT Final Report, 1987 - 1989
Nicholas J. Turro 13 Nov. 1989 15 p
(Grant AF-AFOSR-0043-88; AF Proj. 2303)
(AD-A216320; AFOSR-89-1818TR) Avail: NTIS HC A02/MF A01 CSCL 11/6

The accomplished research has involved the construction of new instrumentation for the investigation of transient high energy materials, the exploration of how the chemistry of transient high energy materials is modified by adsorption on the surfaces at interfaces, and the exploration of how the chemistry and dynamics of high energy density materials respond to systematic variations in structure, and experimental variables such as pressure, magnetic fields and temperature. Particular emphasis was given to reactions in microheterogeneous environments and interfaces provided by micelles, polymers and porous solids. Since the initiation of this grant, a time resolved electron spin resonance spectrometer and a time resolved NMR spectrometer capable of measuring CIDNP spectra on a routine basis have been constructed. GRA

N90-18571# State Univ. of New York, Buffalo. Dept. of Chemistry.
STRONGLY COUPLED ONE-DIMENSIONAL SYSTEM AND THE POLYMER
Xin Sun, Chang-Qin Wu, Rouli Fu (Academia Sinica, Shanghai, China), Duo L. Lin, and Thomas F. George Nov. 1989 11 p Submitted for publication
(Contracts N00014-86-K-0043; F49620-86-C-0009; NSFC-863-715-22; NSF CHE-86-20274)
(AD-A216330; UBUFFALO/DC/89/TR-118) Avail: NTIS HC A02/MF A01 CSCL 07/6

What is the effect of the electron interaction on the lattice instability of 1-D systems with strong electron correlation is a controversial problem. One side believes the electron interaction enhances the instability; but the other side declares the instability is reduced by the electron interaction. The origin of this controversy is analyzed, and it was found that the range of the electron interaction plays a decisive role. When the range is long, the electron interaction enhances the lattices instability, whereas, if the range is short, the electron interaction reduces the instability. Based on this conclusion, the dispute about the effect of the electron interaction on the dimerization of the conducting polymers is clarified. GRA

N90-18572# Utah Univ., Salt Lake City. Coll. of Engineering.
CHARACTERIZATION OF BIOPOLYMER SURFACES USING SCANNING MICROSCOPIES Final Progress Report, for period ending Sep. 1989
J. D. Andrade, J. N. Lin, L. Feng, and W. Bascom 15 Nov. 1989 37 p
(Contract N00014-88-K-0415)
(AD-A216572) Avail: NTIS HC A03/MF A01 CSCL 07/6

The objective of this contract was to establish the feasibility of studying proteins on surfaces by scanning tunneling microscopy (STM) and atomic force microscopy (ATM). Amino acids and proteins deposited on highly oriented pyrolytic graphite (HOPG) were viewed by STM. A preliminary experiment was conducted in the laboratory of Dr. Paul Hansma, University of California, Santa Barbara, which demonstrated the observation of immunoglobulin (IgG) on quartz and mica surfaces. An underwater real time observation of IgG adsorption on mica suggests that the process is not homogeneous. We now have a functioning AFM in our lab - (thanks to the generosity and assistance of Paul Hansma and coworkers) - and protein imaging studies are in progress. GRA

N90-18573# Texas A&M Univ., College Station. Dept. of Chemistry.
ELECTROCHEMICAL INVESTIGATIONS OF ELECTRONICALLY CONDUCTIVE POLYMERS. PART 4: BY CONTROLLING THE SUPERMOLECULAR STRUCTURE, CHARGE TRANSPORT RATES CAN BE ENHANCED
Leon S. VanDyke and Charles R. Martin 2 Jan. 1990 36 p Submitted for publication
(Contract N00014-82-K-0612)
(AD-A216603; TR-43) Avail: NTIS HC A03/MF A01 CSCL 20/3

It was shown that electrically conductive polymers with fibrillar supermolecular structures can be prepared by synthesizing the polymer within the pores of a microporous membrane. Charge transport rates are compared in fibrillar polypyrrole with the corresponding rates in ordinary polypyrrole films; charge transport rates in the fibrillar versions were found to be significantly higher. GRA

N90-18574# Massachusetts Univ., Amherst. Dept. of Chemistry.
METAL COORDINATION POLYMERS AS POTENTIAL HIGH-ENERGY LITHOGRAPHIC RESISTS
Ronald D. Archer, Valentino J. Tramontano, Ven O. Ochaya, Paul V. West, and William Cumming 15 May 1989 11 p Submitted for publication
(Contract N00014-86-K-0345)
(AD-A216668; TR-16) Avail: NTIS HC A03/MF A01 CSCL 17/6

A number of linear coordination polymers were developed which have interesting properties. One type of study has centered on polymers which would provide sensitive lithographic resists based on the fact that the photoelectric effect interacts with nuclei approximately to the fourth power of the atomic number. A number of uranyl carboxylate polymers were prepared which are very sensitive to gamma and electron beam radiation with G sub s values higher than any currently available resist material (Archer, Hardiman and Lee, 1987). This work was extended to cobalt and chromium coordination polymers as well. Coordination polymers of other metals are also under development. GRA

N90-18575# Massachusetts Univ., Amherst. Dept. of Chemistry.
THE IMPROVED ADHESION OF ORGANIC POLYMERS TO SILICA AND TO ALUMINUM METAL WITH ZIRCONIUM SCHIFF-BASE BLOCK COPOLYMER COATINGS
Ronald D. Archer and Bing Wang 15 May 1989 11 p Submitted for publication
(Contract N00014-86-K-0345)
(AD-A216669; TR-17) Avail: NTIS HC A03/MF A01 CSCL 07/6

The thermally stable Schiff-base coordination polymer polyN, N', N", N"' tetrasalicylident 3,3' diaminobenzidine zirconium (IV) exhibits strong interactions with aluminum (apparently with OH groups of analogous zirconium Schiff-base oligomers, block copolymers were made which have large polyester blocks which make the polymers compatible with polyesters and polyacrylates. Peel tests prove that silica and aluminum surfaces pretreated with the zirconium/lactone block polymers provide improved adhesion with polyacrylates. XPS measurements indicate that the zirconium copolymers remain intact when the polyacrylates are peeled from the surfaces. Stearyl chloride condensed with the zirconium Schiff-base oligomer amine and groups provides hydrocarbon chains for compatibility with polyolefins. Peel tests again provide proof of enhanced adhesion to both silica and aluminum. GRA

N90-18576# Clarkson Univ., Potsdam, NY.
COLLOID AND INTERFACE CHEMISTRY ASPECTS OF CERAMICS Final Technical Report, 1 Aug. 1985 - 31 Aug. 1989
Egon Matijevic 29 Nov. 1989 21 p
(Contract F49620-85-C-0142)
(AD-A216715; AFOSR-89-1672TR) Avail: NTIS HC A03/MF A01 CSCL 11/2

This comprehensive, long term, interdisciplinary program has a dual purpose: (1) To generate new or better defined dispersed solids as starting materials for controlled microstructures, with special emphasis on electrooptic ceramics, as well as composites that meet armor and antiarmor requirements; (2) To develop a better understanding of interfacial processes responsible for different properties of high performance ceramics. With respect to (1), several powders of simple and mixed composition were prepared including zirconium, cerium, yttrium, gadolinium, europium, samarium, and terbium compounds. Furthermore, particles of internally mixed composition of Y(III)/Ce(III) and Zr(IV)/Y(III) basic carbonates and oxides in varying molar ratios have been synthesized. Finally, particles of different cores coated with other compounds were obtained, such as oxides of chromium, iron, and titanium covered with alumina, or of iron oxide coated with zirconia or yttria. The powders so obtained were of narrow size distribution with particles of different morphologies, including spheres. These materials were characterized in terms of their various properties (porosity, optical, magnetic, electrokinetic, etc.). With respect to (2), the studies involved solid/solute and solid/solid interactions. The adsorption of chelating agents on iron oxides was used to affect the surface potential and dissolution of the finely dispersed solids. GRA

N90-18577# Notre Dame Univ., IN.
METALLABORANES AS PRECURSORS TO METALLIC GLASSES Final Report, 1 Jul. 1986 - 30 Sep. 1989
Thomas P. Fehlner 9 Dec. 1989 13 p
(Contract DAAL03-86-K-0136)
(AD-A216946; ARO-23547.2-CH) Avail: NTIS HC A02/MF A01 CSCL 20/12

Metal organic chemical vapor deposition (MOCVD) is a well established, practical technique for forming simple as well as complex solid state films. Metal rich metallaboranes constitute practical, low temperature precursors for the vapor deposition of pure, amorphous alloy thin films. This was demonstrated for the compositions Fe4B and Fe3B. Further, the same approach permits the deposition of refractory borides, e.g., MnB4, under mild conditions. Reaction observed during deposition suggests a route to ternary films of precise composition. The results also suggest that main group transition element clusters in general constitute sources of solid state materials with composition fixed by the precursor. GRA

N90-18578# Rhode Island Univ., Kingston. Dept. of Mechanical Engineering.
THERMAL ANALYSIS OF POLYMER COMPOSITES Final Report, 1 Sep. 1986 - 31 Dec. 1989
John Florio, Jr., Jack B. Henderson, and Frederick L. Test 31 Dec. 1989 20 p

(Contract DAAL03-86-G-0072)
(AD-A216947; ARO-23801.5-MS-F) Avail: NTIS HC A03/MF A01 CSCL 11/4

An experimental and analytical study is made of the high temperature behavior of two different phenol-formaldehyde resins with fiberglass reinforcing. The analytical model is general but it is supported by the specific experimental results. The analysis assumes thermal equilibrium is not present and the experimental results support this. In order to support the model the following experimental programs were conducted: (1) Dilatometer experiments to determine expansion characteristics up to 2000 C, (2) Permeability measurements at various stages of decomposition, (3) Internal heat transfer coefficient measurements at various stages of decomposition, and (4) Internal pressure and temperature measurements to verify analytical results. GRA

N90-18579# Texas Univ., Arlington. Dept. of Biology.
ELECTRONIC AND IONIC TRANSPORT IN POLYMERS Final Report, 15 Sep. 1986 - 30 Sep. 1989
Martin Pomerantz, John R. Reynolds, Krishnan Rajeshwar, Dennis S. Marynick, and Timothy D. Shaffer 29 Dec. 1989 11 p
(Contract N00014-86-K-0769)
(AD-A217028) Avail: NTIS HC A03/MF A01 CSCL 20/12

We have prepared and studied a variety of electroactive polymers including self-doped conducting polypyrroles, high molecular weight poly(3-alkylthiophenes), new polymers containing both various aryl groups along the main chain and solublizing substituents, electroactive polymers containing main chain transition metal complexes, fluoropolymers for high permittivity materials, liquid crystalline polymers and polymers containing PN linkages in the main chain. We have also prepared films and/or fibers of these materials both pure and as blends and molecular composites (using polyelectrolytes). We have used spectroscopy, electrochemistry and microgravimetry to study ion transport and redox switching in these systems and have developed in situ techniques to monitor and quantify this ion transport. We have used theoretical calculations (PRDDO and ab initio) to study HOMOLUMO gaps, spin densities, structures and conformations in monomers and oligomers and have used these methods and Extended Huekel calculations to estimate band gaps and to help understand substituent effects in these polymers. GRA

N90-18580# Texas Univ., Austin. Dept. of Chemical Engineering.
CONTROL OF PHASE STRUCTURE IN POLYMER BLENDS
Donald R. Paul 1988 11 p Presented at the 6th Annual IUCCP Symposium on Functional Polymers, College Station, TX, 22-24 Mar. 1988
(Contract DAAL03-88-K-0004; NSF DMR-86-03131)
(AD-A217034; ARO-25229.7-CH) Avail: NTIS HC A03/MF A01 CSCL 07/6

Polymer blending is presently in a state of rapid scientific and commercial development. Another related physical approach is polymer-polymer composites in the form of fibers, film, and sheet materials often made via co-extrusion technology. Polymer blends can be divided into two major classes based on their thermodynamic phase behavior. Miscible blends are homogeneous to the polymer segmental level and a major factor is the energetics of segmental interaction. The first section outlines some of the incentives for polymer blending and gives examples of the types of problems that can be solved by this route. In every case, the property relationships for blends depend critically on control of phase structure. Therefore, subsequent sections will deal with some of the important scientific issues in this area. The first of these is the selection or design of components when a homogeneous or miscible mixture is needed. The second involves phase separated systems where improved interfacial adhesion and morphological control are required, i.e., the concept of (compatibilization). Copolymerization into random, block, or graft structures is shown to be a powerful way of dealing with these problems. GRA

N90-18581# UHT Corp., Dobbs Ferry, NY.
HYDROGENATED AMORPHOUS SILICON FILMS PREPARED BY GLOW DISCHARGE OF DISILANE Final Subcontract Report, 16 Dec. 1987 - 28 Feb. 1989
H. J. Weismann Jan. 1990 46 p Prepared for Midwest Research Inst., Golden, CO
(Contract DE-AC02-83CH-10093)
(DE90-000309; SERI/STR-211-3620) Avail: NTIS HC A03/MF A01

This report describes the results of an investigation of the properties of hydrogenated amorphous silicon films and the efficiency of amorphous silicon solar cells deposited from disilane at rates of 1.5 nanometers/second or greater. The study was divided into two parts, investigation of basic materials properties of hydrogenated amorphous silicon thin films and the fabrication of glass-P-I-N-metal solar cells. The thin film materials properties investigated included the dark conductivity, photoconductivity, dihydride/monohydride concentration ratio, activation energy, and mobility-lifetime product. Hydrogenated amorphous silicon solar cells were fabricated with an intrinsic layer which was deposited at 1.5 nanometers/second. The absolute and reverse bias quantum yields were measured and solar cell efficiencies of 5 percent were achieved. Attempts to increase the efficiency by reverse bias annealing are also reported. DOE

N90-18582# Astrosystems International, Inc., Newark, DE. AstroPower Div.
RESEARCH RELATING TO CRYSTALLINE SILICON-FILM ON A FOREIGN SUBSTRATE
Robert B. Hall, Frances A. Domian, Bryan W. Feyock, David H. Ford, Christopher L. Kendall, James A. Rand, Mary Lou Rock, Todd R. Ruffins, and Allen M. Barnett Dec. 1989 29 p Prepared for Sandia National Labs., Albuquerque, NM
(Contract DE-AC04-76DP-00789)
(DE90-005720; SAND-89-7033) Avail: NTIS HC A03/MF A01

The Silicon-Film process is based on thin, optically confined polycrystalline silicon on a foreign substrate. The primary feature of this approach is that the high efficiency and stability of silicon can be preserved while using an inexpensive growth process. Solar cell efficiencies in excess of 19 percent are expected as a consequence of employing thin (20 to 40 micron) active silicon layers and optical confinement. The potential of this process to be cost-effective has been assessed, and a solar cell cost of $1.26/watt for the initial product and $0.74/watt for the advanced process is indicated. The maturity of the approach recently was demonstrated by the attainment of a 78 sq cm commercial size solar cell, with an 8.5 percent conversion efficiency. The Silicon-Film process on a laboratory-scale 1.0 sq cm solar cell achieved a conversion efficiency of 15.7 percent. DOE

N90-18583# Sandia National Labs., Albuquerque, NM.
MICROSTRUCTURAL VARIATIONS IN ALUMINUM OXIDE COATINGS DEPOSITED USING A DUAL BEAM ION SYSTEM
J. K. G. Panitz, C. R. Hills, and D. R. Tallant 1989 21 p Presented at the 36th American Vacuum Society National Vacuum Symposium, Boston, MA, 23-27 Oct. 1989
(Contract DE-AC04-76DP-00789)
(DE90-006040; SAND-89-2569C; CONF-891093-23) Avail: NTIS HC A03/MF A01

Aluminum oxide coatings were sputter deposited using a dual ion beam system with a mixture of argon plus 10 percent oxygen as the working gas. Ambient substrate temperatures and substrate temperatures of 360 C were maintained. The coatings were deposited at deposition rates between 7 and 10 nm/min, with and without concurrent ion bombardment from the second ion gun. Substantial variations in the microstructure and the amount of entrained gas in the coatings were observed. The coatings contain a mixture of varying amounts of gamma-Al2O3 and amorphous aluminum oxide. Relatively large, 0.5 microns islands of gamma-Al2O3 crystallites surrounded by an amorphous matrix were observed in coatings deposited onto heated substrates with ion bombardment from the second ion gun during deposition. Coatings bombarded with a second ion beam during deposition

contain more argon as determined by energy dispersive x ray analysis. The Raman spectra exhibited by the coatings suggest a variation in chemical reactivity and/or porosity which depends on the deposition conditions. DOE

N90-18584# California Univ., Berkeley. Lawrence Berkeley Lab. Materials and Chemical Sciences Div.
ELECTROCHEMICAL INVESTIGATIONS OF NOVEL SOLID REDOX POLYMERIZATION ELECTRODES
Meilin Liu, Steven J. Visco, and Lutgard C. DeJonghe (California Univ., Berkeley.) Oct. 1989 12 p Presented at the Electrochemical Society Fall Meeting, Hollywood, FL, 15-20 Oct. 1989 Submitted for publication
(Contract DE-AC03-76SF-00098)
(DE90-006087; LBL-27963; CONF-8910107-9) Avail: NTIS HC A03/MF A01

Electrochemical investigations of a group of novel solid redox polymerization electrodes, recently discovered in our laboratory, indicate that these materials are excellent candidates for all-solid-state, thin-film, energy-storage systems. Some of the advantages offered by the batteries based on these solid cathodes include high energy density and rate capability, extensive utilization of cathode capacity, ease of fabrication, low cost, and superior reliability and safety. In addition, these materials are reversible to lithium and sodium (as well as many alkaline earth and transition metals), allowing for a much greater choice of anode materials in stark contrast to cells based on analogous intercalation compounds. Further, and in particular, a great advantage of redox polymerization electrodes is the ability to alter the physical, chemical, and electrochemical properties of these materials in a very predictable manner through manipulation of various functional groups, electron-withdrawing heteroatoms, and the molecular architecture. DOE

N90-18585# Rensselaer Polytechnic Inst., Troy, NY.
MICROCOMPUTER ENHANCED OPTICAL INVESTIGATION OF SPREADING AND EVAPORATIVE PROCESSES IN ULTRA THIN FILMS Progress Report, 1 Jul. 1989 - 31 Jan. 1990
P. C. Wayner, Jr., M. Sujanani, and A. H. Liu Jan. 1990 11 p
(Contract DE-FG02-89ER-14045)
(DE90-006323; DOE/ER-14045/1) Avail: NTIS HC A03/MF A01

The general objective is to determine the heat transfer characteristics of evaporating ultra-thin films. The immediate objective is to develop a microscopic image-processing system (IPS), a complementary heat transfer cell and related analytical techniques. The IPS is used to measure the thickness profile of the evaporating liquid film and has two general parts: an image analyzing interferometer (IAI) and an image analyzing ellipsometer (IAE). An image processing system was designed, assembled and used in conjunction with an interferometer (IAI) to measure the thickness profile of a thin curved liquid film. Isothermal, non-isothermal and transient data were obtained. A preliminary design of an image analyzing ellipsometer (IAE) was completed. Two of the main objectives of the optical design are simplicity in use and high resolution. DOE

N90-18586# Oak Ridge National Lab., TN.
COMPARISON OF TENSION, COMPRESSION, AND FLEXURE CREEP FOR ALUMINA AND SILICON NITRIDE CERAMICS
M. K. Ferber 1989 24 p Presented at the 14th Annual Conference on Composites and Advanced Ceramics, Cocoa Beach, FL, 14-17 Jan. 1990
(Contract DE-AC05-84OR-21400)
(DE90-006154; CONF-900160-2) Avail: NTIS HC A03/MF A01

The stress sensitivity of the creep rate of commercially available Al2O3 and Si3 N4 ceramics was measured at elevated temperatures using tension, compression, and flexure specimens. Pronounced differences in creep deformation behavior measured in compression and tension were observed for both ceramics. Fractographic studies suggested that these differences were attributed to the effects of creep cavitation which occurred under tensile loading. Data generated from the flexure creep testing were found to be in fair agreement with results predicted from existing creep deformation models. DOE

N90-18587# North Carolina State Univ., Raleigh. Dept. of Materials Science and Engineering.
FUNDAMENTAL ASPECTS OF EROSION AND IMPACT DAMAGE
1990 93 p
(Contract DE-FG05-84ER-45118)
(DE90-006640; DOE/ER-45115/6) Avail: NTIS HC A05/MF A01

The research conducted during the current program year has resulted in a number of significant advances. One important area deals with the effect of erodent properties on impact damage and erosion resistance of ceramics. However, the effects were poorly understood and very few systematic investigations were available. Based on the work carried out in the current program, new theoretical models have been developed, which include erodent properties. In particular, it now appears that fragmentation of the erodent has a major effect on performance. Fracture toughness emerges as one of the key material properties. Various features of solid-particle erosion can be explained from this new approach. A second major area deals with fracture toughness in advanced ceramics, with particular emphasis on crack growth-resistance (R-curve) effects. R-curve behavior, wherein toughness decreases for small crack sizes, is inherent to virtually all modern ceramic materials. It has important implications for performance in areas like erosion or grinding damage, where crack-size scales are necessarily small. New techniques have been developed in the current program to measure toughness properties as a function of crack-size scale. DOE

N90-18588# Joint Inst. for Nuclear Research, Dubna (USSR). Lab. of Nuclear Problems.
MICROWAVE RADIATION ABSORPTION BY Ho(Y)-Ba-Cu-O SUPERCONDUCTING CERAMICS
Ya. Vavryshchuk, M. K. Aliev, S. P. Volosyanyj, T. M. Muminov, B. A. Olimov, and I. Kholbev 1988 4 p In RUSSIAN; ENGLISH summary
(DE90-610665; JINR-R-14-88-477) Avail: NTIS (US Sales Only) HC A01/MF A01

The derivative delta R/delta H=f(HT) of microwave power absorption for superconducting ceramics as a function of temperature and magnetic field was investigated. A new narrow peak is discovered at T-T(sub c). It is shown that maxima f(H,T) divide the phase space (H,T) into three regions having the features of the Meissner, mixed and normal phases, respectively. It is pointed to a possibility of interpreting these states as similar states of Josephson's transitions. DOE

N90-18589# Aalborg Portland (Denmark). Cement and Concrete Lab.
HIGH-STRENGTH CONCRETE DEVELOPMENT THROUGH 25 YEARS
Hans Henrik Bache 1987 31 p Presented at Dansk Betondag, 13 Nov. 1987
(CBL-Reprint-17; ETN-90-96207) Avail: NTIS HC A03/MF A01

The development of stronger concrete to make structures with greater carrying capacity (or with small cross-sectional dimensions or greater spans) is described. Development of high strength concrete was aimed primarily at its use in reinforced concrete, where the reinforcement resists the tensile stresses and the concrete resists the compressive stresses and transmits forces to and from the reinforcement. Research and development in this field, concentrating on creating materials with high compressive strength, and requirements made in ductility to exploit the high strength in reinforced concrete, is presented. A note added in proof relating to experiments confirming presented experience and expectations is included. ESA

N90-18590# Technische Univ., Delft (Netherlands).
HYDROGENATED AMORPHOUS AND MICROCRYSTALLINE SILICON DEPOSITED FROM SILANE-HYDROGEN MIXTURES Ph.D. Thesis
Ronald Cornelis vanOort 1989 128 p Sponsored by Netherlands Organization for the Advancement of Pure Research
(ETN-90-96267) Avail: NTIS HC A07/MF A01

A thesis giving a description of the influence of the RF power and the dilution of silane gas with hydrogen on the electrical, optical, and structural properties of amorphous silicon is presented. A description of the above mentioned process parameters on the growth process of amorphous and microcrystalline silicon is included. The amorphous silicon film preparation is described and experimentally determined growth rate-RF power dependence is compared to the predicted one. The structure of amorphous silicon films is studied by infrared spectroscopy. ESA

N90-18591# MRC Bearings-SKF Aerospace, Jamestown, NY.
THE JOINT EFFECT OF SURFACE MICROTOPOGRAPHY AND NEAR-SURFACE STRUCTURE ON MICROCONTACT CONDITIONS
John I. McCool 1989 7 p
(Contract DE-AC02-87CE-90001)
(DE90-006494; DOE/CE-90001/7) Avail: NTIS HC A02/MF A01

Pin-on-disk tests are now complete on all 27 ceramic Phase 1 specimens. The relationship between measured pin wear and both mean asperity flash temperature and mean real contact stress is examined for the subset of tests that was run at high sliding speed. Fracture indentation tests were completed at the University of Michigan on a second set of 9 ceramic specimens. The last set of nine specimens for indentation testing have been delivered to the University of Michigan. A total of 45 hardened M50 high alloy steel disks have been coated with WC, TiC and TiN and comprehensive surface roughness measurements have been made. A number of 3/8 in. diameter balls have been similarly coated. These balls will serve as the pin element in pin-on-disk tests to be performed at ORNL. Nonlinear curve fits were made to a series of correction factors that account for the presence of a coating in computing the load and area of spherical asperities. The fitted functions have been incorporated into a simulation model for analyzing the behavior of coated asperities. Example calculations are given for a steel substrate with the coating modulus spanning the range from 1/10 to 10 times the substrate modulus. DOE

N90-18592# Oak Ridge National Lab., TN. Metals and Ceramics Div.
THE DESIGN OF ADVANCED CERAMIC COMPOSITES
Paul F. Becher 1990 11 p Presented at the International Forum on Fine Ceramics 1990, Nagoya Japan, 12-16 Mar. 1990
(Contract DE-AC05-84OR-21400)
(DE90-006613; CONF-900393-1) Avail: NTIS HC A03/MF A01

Ceramics with improved fracture resisfance are achieved by incorporation of brittle reinforcing phases and phases which exhibit a stress-induced martensitic transformation and by tailoring the matrix microstructure. The optimization of the toughening effects due to each mechanism must rely on knowledge of microstructural and compositional factors. Recent advances in toughening models are used as a basis for designing these systems. DOE

N90-18593# Oak Ridge National Lab., TN.
SYNTHESIS OF HIGH-PURITY SINTERABLE SILICON NITRIDE POWDER
G. M. Crosbie, R. L. Predmesky, and J. M. Nicholson (Ford Motor Co., Dearborn, MI.) 1989 7 p Presented at the Annual Automotive Technology Development Contractors Coordination Meeting, Dearborn, MI, 23-26 Oct. 1989
(Contract DE-AC05-84OR-21400)
(DE90-007050; CONF-8910248-6) Avail: NTIS HC A02/MF A01

A process is under development for the synthesis of silicon nitride powders to meet the special needs for vehicular applications, as part of the Ceramic Technology for Advanced Heat Engines (CTAHE) program. The process study is directed toward a modification of the low temperature reaction of SiCl4 with liquid NH3 which is characterized by absence of organics (a source of carbon contamination) and by pressurization (for improved by-product extraction efficiency). This year, the first vapor-chloride-liquid ammonia runs were made with the prepilot equipment. Equi-axed microstructures were obtained which were similar to those of the 1986 lab demonstration phase product. By use of a revised saturator-mixer design, the vapor inlet stayed clear through multiple runs. Through improvements to the agitator seal and infrared handling, the intermediate product of the vapor reaction with liquid ammonia was shown to be the same imide as obtained by Billy, et al. (1975). Thermal decomposition led to a nitride without the Si2N2O phase previously seen. A pressureless sintered density of 88 percent of theoretical was obtained. DOE

N90-18594# Carborundum Co., Niagara Falls, NY.
MICROSTRUCTURAL CHARACTERIZATION OF SILICON NITRIDE CERAMICS PROCESSED BY PRESSURELESS SINTERING, OVERPRESSURE SINTERING, AND SINTER/HIP
K. R. Selkregg, K. L. More (Oak Ridge National Lab., TN.), S. G. Seshadri, and C. H. McMurtry 1990 17 p Presented at the 14th Annual Conference on Composites and Advanced Ceramics, Cocoa Beach, FL, 14-17 Jan. 1990
(Contract DE-AC05-84OR-21400)
(DE90-007126; CONF-900160-3) Avail: NTIS HC A03/MF A01

Silicon nitride ceramics of the same nominal silicon composition have been sintered under different conditions including atmospheric sintering, overpressure sintering, reaction bonded (nitrided pressureless sinter) and sinter/HIP cycles. The sintered ceramics, which exhibited dramatic differences in fracture toughness, have been characterized by x ray diffraction, scanning electron microscopy, analytical transmission electron microscopy, and image analysis techniques. Fracture toughness data have been correlated to the microstructural and chemical analysis of the grain boundary phases. The microstructure was the strongest influencing factor on the observed fracture toughness difference. DOE

N90-18595# Oak Ridge National Lab., TN. Chemistry Div.
HEAT CAPACITIES OF SOLID POLYMERS (THE ADVANCED THERMAL ANALYSIS SYSTEM, ATHAS)
Bernhard Wunderlich 1990 18 p Presented at the 3rd Minerals, Metals, and Materials Society World Symposium on Lead-zinc (Pb-Zn) and Related Metals, Anaheim, CA, 18-21 Feb. 1990 Prepared in cooperation with Tennessee Univ., Knoxville, TN
(Contract DE-AC05-84OR-21400; NSF DMR-88-18412)
(DE90-007130; CONF-900268-1) Avail: NTIS HC A03/MF A01

The thermal properties of solid, linear macromolecules are accessible through heat capacity measurements from about 10 K to the glass transition. By measuring and collecting data on over 150 polymers, a data bank was established and used as a base for detailed correlation with an approximate frequency spectrum for the polymers. Besides assessment of the entropy at zero Kelvin of disordered polymers, this heat capacity knowledge has helped in the elucidation of partial phase transitions and conformationally disordered crystal phases. A link has also been established to measurements of mobility through solid state nuclear magnetic resonance. Most recently heat capacity measurements have been linked to full dynamic simulations of crystal segments of 1900 chain atoms. Questions of disorder and anharmonicity can thus be analyzed. The work is summarized as the Advanced Thermal Analysis System, ATHAS. DOE

N90-18596# Rutgers - The State Univ., New Brunswick, NJ. Dept. of Ceramics.
MULTICOMPONENT GLASS SURFACES STRUCTURE AND ADSORPTION Progress Report, 1 Jan. - 31 Dec. 1989
Stephen H. Garofalini 1989 3 p
(Contract DE-FG05-88ER-45368)
(DE90-007179; DOE/ER-45368/2) Avail: NTIS HC A01/MF A01

In this research program, we are determining the surface structure of multicomponent silicate glasses and the effect of that

structure on adsorption behavior using both computational techniques (molecular dynamics simulations) and experimental surface analysis. DOE

N90-18597# MSE, Inc., Butte, MT.
COHESIVE CERAMIC FABRICATION Quarterly Technical Progress Report, 1 Jun. - 31 Aug. 1989
1989 24 p
(Contract DE-AC07-88ID-12735)
(DE90-007333; DOE/ID-12735/T5) Avail: NTIS HC A03/MF A01

The project is separated into three tasks. The first task is a design and modeling effort to be carried out by MSE, Inc. The initial undertaking of Task 1 is the design of an advanced ceramic MHD electrode. The second task, subcontracted to Applied Technology Laboratories (ATL), is directed at characterizing the mechanical properties of monolithic and bonded ceramics produced with the cohesive ceramic fabrication (CCF) process. The third task, subcontracted to Ceramic Binder Systems, Inc. (CBSi), is to fabricate the components designed in Task 1 and to fabricate a model planar solid oxide fuel cell. These tasks are discussed separately in this report. Areas of technical progress included in this first quarterly report are: assessing design specifications for a hot ceramic MHD electrode; reviewing components suited for CCF process design demonstration; transferring the CCF process technology from CBSi to MSE and ATL personnel; reviewing test methods suited to characterizing mechanical properties of CCF process ceramics; and fabricating individual components for a planar solid oxide fuel cell. DOE

N90-18598# Sandia National Labs., Albuquerque, NM.
MORPHOLOGICAL CONSEQUENCES OF CATALYTIC HYDROGENATION OF POLYMERS IN THE BULK
Laura R. Gilliom, Dale W. Schaefer, and James E. Mark 1989 13 p Presented at the Materials Research Society Fall Meeting, Boston, MA, 27 Nov. - 2 Dec. 1989
(Contract DE-AC04-76DP-00789)
(DE90-007276; SAND-89-1712C; CONF-891119-97) Avail: NTIS HC A03/MF A01

When suitable catalysts are molecularly dispersed in polymers, the polymers can be modified without added solvent. Studies are described on the morphology of samples of trans-1,4-polybutadiene and syn-1,2-polybutadiene which were partially deuterated in the bulk. The development of a peak in the SANS data for the 1,2-polybutadiene suggests the formation of small domains upon deuteration. Possible explanations for this observation, including chemical and physical heterogeneity, are evaluated. Results of SAXS and thermal measurements are also considered. DOE

28 PROPELLANTS AND FUELS

Includes rocket propellants, igniters, and oxidizers; their storage and handling procedures; and aircraft fuels.

For related information see also *07 Aircraft Propulsion and Power, 20 Spacecraft Propulsion and Power,* and *44 Energy Production and Conversion.*

N90-18599# Fraunhofer-Inst. fuer Chemische Technologie, Berghausen (Germany, F.R.).
INVESTIGATION OF THE PHASE STABILIZING EFFECT OF 4 PERCENT POTASSIUM FLUORIDE ON AMMONIUM NITRATE Final Report
Walter Engel 6 Nov. 1989 95 p
(Contract DAJA45-89-M-0078; DA Proj. 1L1-61102-BH-57)
(AD-A215313) Avail: NTIS HC A05/MF A01 CSCL 07/1

Ammonium nitrate is an interesting oxidizer in the field of propellants and explosives. The drawbacks of the substance are caused by its polymorphic properties. It crystallizes at ambient pressure in 5 modifications. Some phase transitions take place at temperatures which occur under normal storage conditions. These transitions are connected with volume changes that influence severely the properties of products containing ammonium nitrate. Samples of ammonium nitrate containing 4 weight percent potassium fluoride were investigated during cycling the material between -70 and 80 C. The incorporation of 4 percent KF into the ammonium nitrate lattice extends the stability range of phase 3 to deeper temperatures. The results differ in dry and humid samples. In dry samples phase 3 changes directly into phase 5 on cooling at temperatures between -10 and -65 C. The transitions are not complete. Phase 4 is excluded. In the humid samples the transition into phase 5 is complete occurring at higher temperatures between 5 and -10 C. Besides, phase 4 cannot be excluded reliably. The differences can be explained by a retarded nucleation of phase 5 in the dry samples. On heating the transition 5/4 occurs in all samples at temperatures slightly above 0 C followed by the transition 4/3 at 30 to 35 C. Due to the extended stability range of phase 3 a direct transition 5/3 is observed in the dry samples. GRA

N90-18600# Union Carbide Corp., South Charleston, WV. Solvent and Coatings Materials Div.
OPTIMUM CATALYTIC PROCESS FOR ALCOHOL FUELS FROM SYNGAS Quarterly Report No. 10, Apr. - Jun. 1989
B. Duane Dombek 28 Jul. 1989 37 p
(Contract DE-AC22-86PC-90013)
(DE90-005290; DOE/PC-90013/T10) Avail: NTIS HC A03/MF A01

The objectives are to discover and evaluate the catalytic properties of novel homogeneous, heterogeneous, or combination catalytic systems for the production of alcohol fuel extenders from syngas, to evaluate analytically and on the bench scale novel reactor concepts for use in converting syngas to liquid fuel products, and to develop on the bench scale the best combination of chemistry, reactor, and total process configuration to achieve the minimum product cost for conversion of syngas to liquid fuel products. Work continues on optimization of higher alcohol catalysts consisting of transition metals supported on metal oxides having the spinel structure. The results of the second-level experiments performed this quarter are optimistic and predict that a catalyst of this type capable of an alcohol yield of 12 lb/cu ft/hr at greater than 90 percent alcohol selectivity is currently feasible. Reaction Engineering programs for the past quarter have been largely in support of the Phase 2 Reaction Engineering Laboratory. The mechanical construction of the continuous slurry reaction system is 98 percent complete and installation of electrical and control wiring is commencing. Conceptual studies of the effects of residence-time distribution on product yields and distribution in sequential reactions were continued. DOE

N90-18601# Utah Univ., Salt Lake City. Dept. of Fuels Engineering.
PRODUCTION OF HIGH DENSITY AVIATION FUELS VIA NOVEL ZEOLITE CATALYST ROUTES Final Report, Dec. 1985 - May 1987
Francis V. Hanson 23 Oct. 1989 484 p
(Contract F33615-85-C-2567; AF Proj. 3048)
(AD-A216444; WRDC-TR-89-2097) Avail: NTIS HC A21/MF A03 CSCL 21/4

The production of high density aviation fuels from reliable, domestic fossil fuel sources is of considerable importance to the USAF. The production of high density aviation fuels can be achieved by a number of alternative process sequences, for example, shape selective cracking of normal paraffins from an appropriate boiling range fraction of a napthenic crude; saturation of an aromatic FCC cycle stock of the appropriate boiling range; saturation of an appropriate boiling range fraction from a hydrocracker recycle stream when the feed to the hydrotreater is aromatic in nature; synthesis of the appropriate boiling range aromatic species from oxygenates over cyrstalline aluminosilicates followed by hydrogenation of the aromatic species; and direct synthesis of the aromatic hydrocarbons from hydrogen and carbon monoxide over crystalline aluminosilicate-supported metal catalysis followed by hydrogenation of the aromatic species. A research program is summarized which was aimed at developing catalyst and processing

concepts for the production of high density aviation turbine fuels via novel zeolite catalyst routes. GRA

N90-18602# Los Alamos National Lab., NM.
A PROGRAM OF FUNDAMENTAL RESEARCH ON EXPLOSIVES AT LOS ALAMOS
Thomas Rivera 1990 10 p Presented at the 1990 National Symposium of the Society of Mexican-American Engineers and Scientists, Albuquerque, NM, 28-31 Mar. 1990
(Contract W-7405-eng-36)
(DE90-006509; LA-UR-90-255; CONF-900394-1) Avail: NTIS HC A02/MF A01

The Fundamental Research on Explosives (FRE) program was initiated as a five-year program beginning in FY 1982. It was established as a Laboratory-wide coordinated theoretical and experimental effort to gain a fundamental understanding of detonation behavior using state-of-the-art techniques not previously applied to explosives. During the five years a variety of significant scientific achievements was made in both theory and experiment by developing new methods and techniques to study equation-of-state (EOS), shock initiation, and detonation phenomena. The FRE program comprised scientific experimental and theoretical investigations into the chemical and mechanical processes leading to and subsequently sustaining detonation of the simple liquid prototypical explosive, nitric oxide (NO). The goals of the FRE program were to understand the energetics and chemistry of initiation and detonation in liquid NO and to compare experimental results with existing theory. The knowledge gained and the techniques developed have led not only to advances in explosives science but in the theoretical and experimental sciences in general. This report is a brief overview of the FRE achievements during the 5 year program. DOE

N90-18603# Oak Ridge National Lab., TN.
ALTERNATIVE FUELS R/D NEEDS: PROGRAM DIRECTIONS
R. L. Graves 1989 11 p Presented at the Annual Automotive Technology Development Contractors Coordination Meeting, Dearborn, MI, 23-26 Oct. 1989 Submitted for publication
(Contract DE-AC05-84OR-21400)
(DE90-007053; CONF-8910248-5) Avail: NTIS HC A03/MF A01

The findings are described of a review of alternative fuel utilization research and development needs, as well as activities planned to meet those needs in the Department of Energy Alternative Fuels Utilization Program (AFUP). The technology status review was accomplished through numerous visits to auto and engine manufacturers, through workshops with engine and fuel industries, and visits to universities and laboratories. Research projects planned in AFUP will address diesel fuel chemistry effects on emissions, ignition and combustion of methanol for heavy duty engines, and methanol engine wear and lubrication in the Federal Methanol Fleet vehicles. DOE

N90-18604# Union Carbide Corp., South Charleston, WV. Solvents and Coatings Materials Div.
OPTIMUM CATALYTIC PROCESS FOR ALCOHOL FUELS FROM SYNGAS Quarterly Technical Progress Report No. 11, Jul. - Sep. 1989
31 Oct. 1989 36 p
(Contract DE-AC22-86PC-90013)
(DE90-007188; DOE/PC-90013/T11) Avail: NTIS HC A03/MF A01

The contract work is composed of three tasks. Task 1, the preparation of a Project Work Plan, has been completed. Task 2 comprises the chemical investigation of novel and existing catalysts for the production of fuel alcohols from syngas, either directly or through a step-wise process. Task 3 consists of engineering activities which will support the chemical investigations and develop economic evaluations and process conceptualization. Tasks 2 and 3 will proceed for the entire duration of the program. In current work under Task 2, the effort has been mainly on heterogeneous catalysts. Novel systems which may exhibit superior behavior are being investigated. Task 3 work has involved engineering support for the chemical investigations. Economic evaluations of a base case process for conversion of syngas to fuel alcohols were also pursued. Task 3 work has also involved experiments with selected catalytic systems. Further work in Task 3 will include the evaluation of slurry-catalyzed processes for the production of fuel alcohols or their derivatives. DOE

N90-18605# Institut Franco-Allemand de Recherches, Saint-Louis (France).
ANALYSIS OF PROPULSIVE POWDER COMBUSTION PRODUCTS AND THEIR CORROSIVE EFFECTS [SCHWADENZUSAMMENSETZUNG UND EROSIONSWIRKUNG VON TREIBLADUNGSPULVERN]
H. H. Licht 21 Nov. 1988 14 p In GERMAN Presented at 14th Symposium Innenballistiche Leistungssteigerung von Rohrwaffen, Swisttal-Heimerzheim, Fed. Republic of Germany, 8-10 Nov. 1988
(ISL-CO-248/88; ETN-90-96249) Avail: NTIS HC A03/MF A01

The erosive effects of classic colloidal propulsive powders are compared to those of nitramine based powders. The erosive power is determined by tests using a ballistic bomb equipped with an erosion vent on which the combustion gases are fixed. An empirical formula, taking into account the average molecular mass of the combustion products, various thermal ratios and the temperature of the flames, allows predictions to be made of the erosive power of the powders. The nitramine based powders prove to have less erosive power than theoretically predicted. The temperature of the flames is shown to be very important in determining the erosive power. ESA

N90-18606# Swedish Defence Research Establishment, Stockholm. Dept. of Weapons Technology.
MICROCALOMETRIC STUDIES OF GUN PROPELLANT KKR 8
Jan Hansson Oct. 1989 23 p In SWEDISH; ENGLISH summary
(FOA-C-20770-2.1; ISSN-0347-3694; ETN-90-96305) Avail: NTIS HC A03/MF A01

Microcalorimetric measurements on particularly bad lots of Swedish gun propellants at 40 and 80 C are described. All lots were discarded as they did not pass the 65 C redgassing test. One of the lots is reported as self-igniting on one occasion. Results are given in tabular and graph form. ESA

29 MATERIALS PROCESSING

Includes space-based development of products and processes for commercial applications.

For biological materials see *55 Space Biology*.

N90-18607# Pacific Northwest Lab., Richland, WA.
CONDENSATION FLUID DYNAMICS AND HEAT TRANSFER ON ROTATING SPHERICAL SURFACES IN A MICROGRAVITATIONAL FIELD
Keith A. Pauley, Andrew C. Klein (Oregon State Univ., Corvallis.), and Brent J. Webb Jan. 1990 4 p Presented at the 7th Symposium on Space Nuclear Power Systems, Albuquerque, NM, 7-11 Jan. 1990
(Contract DE-AC06-76RL-01830)
(DE90-005540; PNL-SA-17331; CONF-900109-18) Avail: NTIS HC A01/MF A01

A heat injection system is an integral part of any space mission. The successful operation of the spacecraft and other secondary equipment is related to the effectiveness and survivability of the thermal management system. The heat rejection system should have a small launch volume and weight in relation to the entire mission payload. This has not previously been the case. An advanced thermal management system was developed for space power applications which is both effective and light weight. The Bubble Membrane Radiator (BMR) is a space-based heat rejection system which uses direct radiation to space and operating fluid condensation as the primary heat transfer mechanisms. This heat exchanger rotates about a central axis in order to induce a small

artificial gravity. The working fluid enters the radiator via feed lines incorporated in the axis of rotation and is then sprayed.
DOE

31 ENGINEERING (GENERAL)

Includes vacuum technology; control engineering; display engineering; cryogenics; and fire prevention.

N90-18608# Lawrence Livermore National Lab., CA.
EVALUATING A GLASS SURFACE PRODUCED BY DUCTILE GRINDING
K. L. Blaedel and P. J. Davis 24 Apr. 1989 12 p Presented at the American Society for Precision Engineering Spring Conference, Tucson, AZ, 25-27 Apr. 1989
(Contract W-7405-eng-48)
(DE90-006782; UCRL-100755; CONF-8904259-2) Avail: NTIS HC A03/MF A01

Ductile grinding results in very smooth, specular surfaces, in many ways similar to polished surfaces. Our hypothesis is that the subsurface is also similar to that produced by polishing. To test this hypothesis, a set of surfaces of glass (BK7) was fabricated by ductile grinding, another set by polishing and then the sets were compared. Three techniques are used to evaluate the glass surfaces: rate of etch, indentation and laser damage threshold. Although all the evaluations are not yet complete, these three techniques indicate little difference between the subsurfaces. No cracks (on the order of a micron or more) were detected of the kind that usually accompanies conventional bound abrasive grinding. DOE

N90-18609# European Space Agency, Paris (France).
MATERIALS AND STRUCTURES FOR 2000 AND BEYOND: AN ATTEMPTED FORECAST BY THE MATERIALS AND STRUCTURES DEPARTMENT OF THE DLR
Carl-Jochen Winter, Martin Mailaender (Deutsche Forschungs- und Versuchsanstalt fuer Luft- und Raumfahrt, Stuttgart, Germany, F.R.), Heinrich Bergmann, Hans Foersching, Wolfgang Bunk, Gerhard Grueninger, and Berndt Feuerbacher Dec. 1989 83 p Transl. into ENGLISH of Werkstoffe und Bauweisen fuer 2000 und danach Ein Versuch des DLR-Forschungsbereichs Werkstoffe und Bauweisen (Stuttgart, Fed. Republic of Germany, DFVLR), Feb. 1989 p 1-82 Original language document was announced as N89-25358
(ESA-TT-1154; DFVLR-Mitt-89-02; ETN-90-96218) Avail: NTIS HC A05/MF A01; original German version available from DFVLR, VB-PL-DO, Postfach 90 60 58, 5000 Cologne 90, Fed. Republic of Germany, 20.50 DM

The following forecasts were attempted on 21 to 22 Oct. 1988: to estimate what challenges the next 15 years might bring, and what would be the consequences for the direction and methodology of work, and for the organization of the institutes and of the research department. Building on the basis of the current position and of the discussions, the views of the five institutes, namely those for aeroelasticity, advanced design and manufacturing technology, space simulation, structural mechanics and materials research, on the future, are presented. A summary drawn up, and derived action guidelines, are given. ESA

N90-18610# Energy Concepts Co., Annapolis, MD.
INTERMITTENT SOLAR AMMONIA ABSORPTION CYCLE (ISAAC) REFRIGERATION FOR LESSER DEVELOPED COUNTRIES Final Report, 23 Apr. 1987 - 22 Oct. 1989
Donald C. Erickson 6 Feb. 1990 4 p
(Contract DE-FG01-87CE-15325)
(DE90-006700; DOE/CE-15325/T4) Avail: NTIS HC A01/MF A01

The Intermittent Solar Ammonia Absorption Cycle (ISAAC) refrigerator is a solar thermal technology which provides low cost, efficient, reliable ice-making to areas without ready access to electricity. An ISAAC refrigeration system consists of a compound parabolic solar collector, two pressure vessels, a condenser, a cold box or refrigerated space, and simple connective piping -- no moving parts or electrical components. Most parts are simple construction or plumbing grade materials, locally available in many remote areas. This technology has numerous potential benefits in lesser developed countries both by providing a cheap, reliable source of ice, and, since manufacture requires only semi-skilled labor, a source of employment to the local economy. Applications include vaccine storage for health care clinics; fish, meat, and dairy product storage; and personal consumption. Importantly, this technology increases the quality of life for people in lesser developed countries without depleting fossil fuel resources or increasing the release of greenhouse gases such as CO2 and chlorofluorocarbons. DOE

N90-18489*# National Aeronautics and Space Administration. Lyndon B. Johnson Space Center, Houston, TX.
SMALL DISPLACEMENT, LONG LIFE ON-ORBIT COMPRESSOR DESIGN AND FABRICATION
C. R. Gerlach, E. C. Schroeder, D. D. Deffenbaugh (Southwest Research Inst., San Antonio, TX.), and J. P. Masetta *In* Johns Hopkins Univ., The 1989 JANNAF Propulsion Meeting, Volume 1 May 1989 p 541-550 (For primary document see N90-18462 11-20)
(Contract NAS9-18051)
Avail: NTIS HC A25/MF A04 CSCL 13B

32 COMMUNICATIONS AND RADAR

Includes radar; land and global communications; communications theory; and optical communications.

For related information see also *04 Aircraft Communications and Navigation* and *17 Space Communications, Spacecraft Communications, Command and Tracking.* For search and rescue see *03 Air Transportation and Safety,* and *16 Space Transportation.*

N90-18611# Air Force Occupational Measurement Center, Randolph AFB, TX.
AIRBORNE RADAR SYSTEMS SPECIALIST, AFSC 118X2 Occupational Survey Report
Aug. 1989 48 p
(AD-A215450) Avail: NTIS HC A03/MF A01 CSCL 05/9

The results are presented of an occupational survey of the Airborne Radar Systems Specialty completed by the Occupational Analysis Division, USAF Occupational Measurement Center, in June 1989. This survey was requested by HQ TAC/DOY at Langley AFB VA, for evaluating the current AFSC 118X2 training program since this specialty was separated from AFSC A328X2 (now AFSC 445X4) and designated the 118X2 specialty (effective 31 October 1984). GRA

N90-18612# Institute for Telecommunication Sciences, Boulder, CO.
MILLIMETER-WAVE PROPAGATION IN THE MESOSPHERE
George A. Hufford and Hans J. Liebe Sep. 1989 60 p Sponsored by DOD, Fort Meade, MD
(PB90-119868; NTIA-89-249) Avail: NTIS HC A04/MF A01 CSCL 20N

At heights between 30 and 100 km above the Earth, the oxygen absorption lines near 60 GHz together with the geomagnetic field cause the atmosphere to become an anisotropic medium. Reasons why this is so, and how to compute the consequent effects, are discussed. A computer program (ZEEMAN) is described, which allows the user to display in either graphical or tabular form many aspects of how radio waves propagate through the medium. GRA

N90-18613# Mission Research Corp., Santa Barbara, CA.
ACIRF USER'S GUIDE: THEORY AND EXAMPLES Technical Report, 1 Oct. 1987 - 15 Dec. 1988
Roger A. Dana 1 Dec. 1989 82 p

(Contract DNA001-87-C-0169)
(AD-A216436; MRC-R-1198; DNA-TR-88-175) Avail: NTIS HC A05/MF A01 CSCL 20/14

Design and evaluation of radio frequency systems that must operate through ionospheric disturbances resulting from high altitude nuclear detonations requires an accurate channel model. This model must include the effects of high gain antennas that may be used to receive the signals. Such a model can then be used to construct realizations of the received signal for use in digital simulations of trans-ionospheric links or for use in hardware channel simulators. The FORTRAN channel model ACIRF (Antenna Channel Impulse Response Function) generates random realizations of the impulse response function at the outputs of multiple antennas. This user's guide describes the FORTRAN program ACIRF (version 2.0) that generates realizations of channel impulse response functions at the outputs of multiple antennas with arbitrary beamwidths, pointing angles, and relatives positions. This channel model is valid under strong scattering conditions when Rayleigh fading statistics apply. Both frozen-in and turbulent models for the temporal fluctuations are included in this version of ACIRF. The theory of the channel model is described and several examples are given. GRA

N90-18614# Naval Ocean Systems Center, San Diego, CA.
TRENDS IN VLF/LF (VERY LOW FREQUENCY/LOW FREQUENCY) MODEM PERFORMANCE TESTING
Paul A. Singer 1989 3 p Repr. from MILCOM 89, v. 1, Oct. 1989 Submitted for publication
(AD-A216576) Avail: NTIS HC A01/MF A01 CSCL 25/2

Very Low Frequency (VLF)/Low Frequency (LF) communications represent the backbone of the U.S. Navy's communications from command authorities to submarine forces. The paper covers the historical development of digital VLF/LF modem testing. The paper discusses the introduction of test equipment in the following four major functional areas: (1) transmit simulation, (2) channel simulation, (3) noise and interference generation, and (4) reception characterization. The paper will demonstrate two major trends: (1) the use of general purpose hardware and off-line software replacing special purpose hardware; and (2) Gaussian noise, atmospheric laboratory test environments being replaced by tailored simulated electromagnetic interference (EMI) and atmospheric noise. GRA

N90-18615# Naval Postgraduate School, Monterey, CA.
AN ADAPTIVE ARQ (AUTOMATIC REPEAT REQUEST) STRATEGY FOR PACKET SWITCHING DATA COMMUNICATION NETWORKS M.S. Thesis
Kurtis J. Guth Jun. 1989 74 p
(AD-A216597) Avail: NTIS HC A04/MF A01 CSCL 17/2

Automatic Repeat Request (ARQ) techniques are often used by a packet switching data communication network to provide an error-free communications link between stations. The ARQ technique ensures consistent data quality under varying link conditions. Unfortunately, the information throughput is link dependent and as the noise or interference on the link increases, the throughput decreases. In an effort to improve the throughput on a short range, RF, packet switching data communications network, an adaptive ARQ strategy applied to Stop-and-Wait (SW) protocols was developed. To provide a system designer with flexibility, different adaptive strategies for different system and link conditions were developed. Examples of information transfer between two stations using the adaptive SW protocol are presented. A simulation to compute the throughput efficiency of several adaptive SW protocols was performed. A comparison of the throughput efficiencies of the simulated adaptive SW protocol with the non-adaptive SW protocol showed good gains could be achieved using the adaptive strategy when the networks are subject to high channel bit error rates. GRA

N90-18616# Air Force Systems Command, Wright-Patterson AFB, OH. Foreign Technology Div.
APPLICATIONS OF ACOUSTO-OPTICAL CORRELATION DEVICES IN RADAR SIGNAL PROCESSING
Jieping Xu and Kuanxin Yu 29 Sep. 1989 17 p Transl. into ENGLISH of Applied Acoustics (Peoples Rep. of China), v. 5, no. 1, Jan. 1986 p 1-5
(AD-A216624; FTD-ID(RS)T-0712-89) Avail: NTIS HC A03/MF A01 CSCL 17/9

The actual efficiency of acousto-optical correlation devices in radar signal processing was investigated experimentally. As far as centimeter wave band (3GHz) single carrier frequency square pulse radar signals and unmodulated random wave interference is concerned, if measured different pulse widths, different signal-to-noise ratios and, for these periods of time, the height of correlation peaks as well as the size of the correlation gain when there were different pulse widths. When the pulse width was 2.5 micro s, the correlation gain was 30dB. When the pulse width was 0.5 micro s, the correlation gain was 23dB. As far as the correlation peaks of acousto-optical correlation device outputs are concerned, they were all several score mV or higher. It was not necessary to go through any amplification. Rather, it was possible to make use of an oscillascope to directly carry out observations and measurements. GRA

N90-18617# Naval Ocean Systems Center, San Diego, CA.
EFFECTS OF STRONG SCATTERING ON TRANSIONOSPHERIC PROPAGATION Final Report, Oct. 1987 - Sep. 1988
Richard A. Sprague Sep. 1989 36 p
(AD-A216708; NOSC/TR-1312) Avail: NTIS HC A03/MF A01 CSCL 20/14

This report presents preliminary results of an effort to model the effects of ionospheric electron density irregularities on transionospheric propagation. The focus of the report is on propagation at HF and low VHF, where strong multiple scattering is often encountered. A strong scattering model is therefore used to predict the effects on such parameters as the phase autocorrelation function, the spectrum of intensity fluctuations, and the fluctuation in angle of arrival. Requirements for improvements in the model and directions for later work are discussed. GRA

N90-18618# Defence Research Establishment, Ottawa (Ontario). Space-Based Radar Project Office.
SPACE-BASED RADAR SIMULATION LABORATORY
S. Y. Maskell Sep. 1989 23 p
(AD-A216722; DREO-TN-89-24) Avail: NTIS HC A03/MF A01 CSCL 17/9

The Defense Research Establishment Ottawa is developing a Space-Based Radar Simulation Laboratory. Initially, this Laboratory will consist of two simulators, an SBR System Simulator and an Integrated Surveillance and Interception Response System Simulator. This Technical Note describes both simulators and the expected capability of the Space-Based Radar Simulation Laboratory. Details on the development approach and on laboratory hardware are provided. A high level overview of the use operations for the two simulators is also given. GRA

N90-18619# Defence Research Establishment, Ottawa (Ontario).
RATE COMPATIBLE PUNCTURED CODES, THEIR USE IN MILITARY SATELLITE COMMUNICATION SYSTEMS
Lyle C. Wagner Aug. 1989 31 p
(AD-A216723; DREO-TN-89-19) Avail: NTIS HC A03/MF A01 CSCL 12/9

The problem of interfacing older military terminal equipments, which work exclusively from an internal timing source, into a communication system that requires all terminals to synchronize to the network clock is addressed in this paper. These data communication systems would typically operate with a fixed symbol transmission rate and employ end-to-end convolutional coding for channel errors. A scheme is proposed which would allow a clock discrepancy of up to + or - 4 percent between the terminal clock and the network clock. The method proposed is to add control bits to the information stream between terminals. The control bits would allow the effective information rate to be either increased or decreased by + or - 4 percent. The overall symbol rate of the

communication link is held constant by selecting a higher rate convolutional code from the set of rate compatible punctured codes (RCPCs). This paper describes the methodology used to select an optimal RCPC and presents some examples. The probability of error for a selected code is compared with that of a convolutional code for an application typical of a satellite communication system. The conclusion is that the increase in signal to noise required to sustain the same probability of error is minimal. GRA

N90-18620# Air Force Human Resources Lab., Brooks AFB, TX. Operations Training Div.
SIMULATION OF SYNTHETIC APERTURE RADAR 3: EVALUATION OF PROTOTYPE DIGITAL FEATURE ANALYSIS DATA Interim Report, Oct. 1987 - Jan. 1989
Peter M. Crane and Herbert H. Bell Dec. 1989 19 p
(AD-A216750; AFHRL-TR-89-4) Avail: NTIS HC A03/MF A01 CSCL 12/6

This experiment evaluated the suitability of the Defense Mapping Agency (DMA) prototype Level 3c Digital Feature Analysis Data (DFAD) for the simulation of Synthetic Aperture Radar (SAR). The suitability of Prototype Level 3c DFAD was evaluated by comparing simulations generated from samples of Level 3c and from samples of DFAD previously demonstrated to be adequate for SAR simulation; these products, however, were unsuitable for production in the quantities required to meet Air Force needs. B-1B Offensive Systems Officers performed a navigation update task using simulated and actual SAR images. Crosshair placement accuracy, operator confidence in the placement, and ratings of acceptability for use in a Weapon System Trainer were recorded using both simulated and actual SAR images. The results indicated that SAR simulation can be supported as well by Level 3c DFAD as by the other products. GRA

N90-18621# Naval Research Lab., Washington, DC. Target Characteristics Branch.
ANGLE ESTIMATION IN THE PRESENCE OF MAINBEAM INTERFERENCE
Feng-Ling C. Lin and Frank F. Kretschmer, Jr. 28 Dec. 1989 26 p Sponsored by Naval Sea Systems Command, Washington, DC
(AD-A216832; NRL-9234) Avail: NTIS HC A03/MF A01 CSCL 12/3

Angle of arrival of a desired signal in a mainbeam interference environment can be estimated by incorporating adaptive array processing. Adapted sum and difference beams that suppress the undesired noise sources are used to determine the monopulse error curve. The resultant distorted error curve across the mainbeam tracking angle region is used directly for angle estimation. The Cramer-Rao bound on the angle estimation error is derived with generalized assumptions on the signal characteristics. A Monte Carlo simulation is performed for the estimation procedure described, and the angle estimation error is then compared with the Cramer-Rao bound. It is shown that good performance in angle measurement can be achieved with sufficient signal-to-noise ratio and angular separation between the target and the interference sources. GRA

N90-18622# Illinois Univ., Urbana.
RECONFIGURABLE ANTENNAS, MONOLITHIC MICROWAVE INTEGRATED CIRCUITS WITH FEEDING NETWORKS FOR MICROSTRIP ANTENNAS Interim Technical Report, Sep. 1986 - Sep. 1987
Y. T. Lo, S. L. Chuang, and P. Aoyagi Aug. 1989 164 p
(Contract F19628-85-K-0052; AF Proj. 2305)
(AD-A216916; RADC-TR-89-123) Avail: NTIS HC A08/MF A01 CSCL 09/1

Six viable interfacing techniques between the microstrip integrated circuits and the microstrip antennas through the feeding networks are discussed with the comments on their advantages and disadvantages. The microstrip antenna fed by a slot line is investigated both theoretically and experimentally. This configuration is an attractive element for use in active integrated arrays. This new hybrid technology attempts to incorporate active devices such as amplifier and phase shifters with printed microstrip antennas into a single monolithic package. The boundary value problem for the antenna is analyzed in terms of the integral equations for the equivalent electric currents on the patch and magnetic currents representing the slot line. The integral equations are discretized by Galerkin's method and solved on the computer. GRA

N90-18623*# Jet Propulsion Lab., California Inst. of Tech., Pasadena.
RADIO INTERFERENCE IN THE NEAR-EARTH ENVIRONMENT
W. C. Erickson 1 Sep. 1988 28 p
(NASA-CR-180479; JPL-Publ-88-30; NAS 1.26:180479) Avail: NTIS HC A03/MF A01 CSCL 20N

Natural and man-made radio frequency interference (RFI) are potentially serious obstacles to the successful operation of an array of spacecraft used for low frequency (1 to 30 MHz) radio interferometry in the near-earth environment. Several satellites and planetary probes have carried radio astronomy experiments, and the moderate data base that they provide are examined to help understand the near-earth RFI environment. The general conclusion is that the region of space within 100 earth-radii of the earth is a hostile environment for any radio astronomy experiment. If a low frequency array in earth orbit is to yield useful astronomical results, severe interference problems must be anticipated and overcome. A number of recommendations are made to further examine the feasibility of such an array. Author

N90-18624# Los Alamos National Lab., NM.
QUICK, RELIABLE ESTIMATES OF HIGH-POWER MICROWAVE FLUENCES: THE SNEAKY-2 PROGRAM
T. W. Tunnell (EG and G Energy Measurements, Inc., Los Alamos, NM.) and R. Roussel-Dupre Jan. 1990 38 p
(Contract W-7405-eng-36)
(DE90-006347; LA-11680-MS) Avail: NTIS HC A03/MF A01

The propagation of high-power microwave pulses through the atmosphere is often modeled with time-dependent fluid or kinetic codes that require a fine mesh of range and time points. The computational time to run these codes precludes their use to determine the optimum pulse characteristics and propagation paths for delivery of a desired fluence to a specified target. In this work, a universal, parameterized scaling law for microwave-induced air breakdown is integrated into the SNEAKY model to produce a new microwave propagation code, SNEAKY-2. It estimates microwave fluences to within 1 percent to 13 percent agreement with the more elaborate time-dependent fluid codes while running a hundred to several thousand times faster. The purpose of this report is to document the SNEAKY-2 code, complete with benchmarking and specifications of the inherent limitations. DOE

N90-18625# Los Alamos National Lab., NM.
BEAR ELECTROSTATIC ANALYZER: FLIGHT RESULTS
Hugh R. Anderson, Douglas W. Potter, David L. Morse, Joseph R. Olson, J. Lorraine Johnson (Science Applications International Corp., Bellevue, WA.), and Morris Pongratz 3 Jan. 1990 8 p Presented at the Spacecraft Charging Technology Conference, Monterey, CA, 31 Oct. - 3 Nov. 1989 Submitted for publication
(Contracts W-7405-eng-36; LANL-9-X58-7568P-1)
(DE90-006511; LA-UR-90-296; CONF-8910358-1) Avail NTIS HC A02/MF A01

The Electrostatic Analyzer (ESA) measured the intensity of charged particles returning to the BEAR payload during flight on 13 July 1989. These particles form part or all of the current that returns to the payload to neutralize the charge ejected with the beam. By measuring the return flux with high time resolution, we can study the physics of charging processes. When the neutralizer was off, the payload emitted 10 mA negative and charged to several hundred volts with a maximum of approximately 800 V. With the neutralizer on (normal configuration), the payload emitted approximately 1 mA negative and received electrons with energies up to a few hundred volts in some attitudes. This suggests charging to a few hundred volts. The charging rate of the payload is

consistent with the rocket body capacitance with respect to a vacuum. DOE

N90-18626# Sandia National Labs., Albuquerque, NM.
SCATTERING FROM AN ARBITRARY CYLINDER IN THE PRESENCE OF A PLANAR MEDIA INTERFACE USING THE BYMOMENT METHOD
Robert Lee and Andreas C. Cangellaris Nov. 1989 43 p Prepared in cooperation with Arizona Univ., Tucson
(Contract DE-AC04-76DP-00789)
(DE90-006465; SAND-89-7153) Avail: NTIS HC A03/MF A01

We apply the bymoment method to the problem of electromagnetic scattering from a cylinder in the presence of two semi-infinite half-spaces. The finite-element method is used to generate the solution over the region occupied by the cylinder, using a grid which is truncated at a small distance from the scatterer by a surface that conforms to the cross-section of the cylinder. We then couple the properties of the region exterior to the finite-element mesh to the interior solution by using Green's theorem in conjunction with a set of linearly independent functions which satisfy the boundary conditions along the interface and at infinity. Numerical results are obtained and compared to those in the literature. DOE

N90-18627# Lawrence Livermore National Lab., CA.
THE EXTENDED EQUIVALENT SOURCE TECHNIQUE WITH UNDERDETERMINED SOURCES
R. M. Bevensee 12 Jan. 1989 3 p Presented at the IEEE Antennas Propagation Society International Symposium, San Jose, CA, 26-30 Jun. 1989
(Contract W-7405-eng-48)
(DE90-006989; UCRL-100232; CONF-890660-10) Avail: NTIS HC A01/MF A01

The Extended Equivalent Source Technique (EEST) is a method of computing electromagnetic scattered fields from discrete equivalent sources which lie some distance away from a surface where a boundary condition is enforced. Possible sources include electric and/or magnetic multipoles and current filaments. Kennaugh extended a spherical multiple solution to nonspherical geometries via a matrix equation. Generally the number K of unknown complex source amplitudes is taken equal to the number I of known complex boundary conditions. However, one can inquire whether there is any advantage to utilizing more unknown sources than there are boundary conditions and solving their amplitudes by a renormalization, maximum likelihood, or maximum entropy procedure. Here we consider a Gibbs' maximum entropy method appropriate for complex data processing if I greater than K/2. DOE

N90-18628# Nationaal Inst. voor Kernfysica en Hoge Energiefysica, Amsterdam (Netherlands).
INSTABILITY INVESTIGATION FOR STORAGE MODE. MICROWAVE INSTABILITY (SINGLE-BUNCH INSTABILITY)
Y. Y. Wu May 1989 16 p
(NIKHEF-K/AmPS/89/05; ETN-90-96261) Avail: NTIS HC A03/MF A01

Simulation results for bunched beam instabilities in storage rings are presented. Useful information for choosing the RF parameters of the Amsterdam Pulse Stretcher (AmPS) is derived. For storing a beam of 200 mA in an energy region 300 to 900 MeV, it seems very difficult to have only one RF cavity system in AmPS. In the low energy region of 300 to 500 MeV, in order to avoid too low a threshold, a high RF frequency has to be chosen (f=2856 MHz). In the high-energu region of 600 to 900 MeV, in order to avoid too high an overvoltage, a low frequency has to be chosen (f=476 MHz or even lower). Bunch lengthening may help to store more current in the region of 500 to 600 MeV for f(RF)=476 MHz. Another remedy to cure single-bunch instability is to reduce the ring impedance to less than 10 ohms. This seems more difficult than to change the RF parameters. ESA

N90-18629# Deutsche Forschungsanstalt fuer Luft- und Raumfahrt, Oberpfaffenhofen (Germany, F.R.). Abt. Hochfrequenzphysik.
ON THE RANGE RESOLUTION OF POINT TARGETS WITH FMCW RADAR SYSTEMS
Reinhard Hammel Aug. 1989 75 p In GERMAN; ENGLISH summary
(DLR-FB-89-47; ISSN-0171-1342; ETN-90-96277) Avail: NTIS HC A04/MF A01; DLR, Wissenschaftliches Berichtswesen, Postfach 90 60 58, 5000 Cologne 90, Fed. Republic of Germany, 24 deutsche marks

The range information with Frequency Modulated Continuous Wave (FMCW) radar systems is discrete within multiples of the modulation frequency. There is a correspondance between the spectral lines and discrete distance values. Even though the classical spectral theory defines the resolution to be 1.2 it is shown that with a FMCW-radar a resolution of only 2.1 is attainable because of harmonic interferences. The prerequisite of the equipment in order to achieve this resolution is a limitation of the relative fluctuation of the slope of the transmitting frequency variation. Without any control circuit for the transmitting frequency slope, this condition can be satisfied with a programmable wave-form device if a dynamic correction of the transmitting frequency slope was determined before. It is shown that by a variation of the modulation frequency and the modulation-bandwidth simultaneously, the envelope of the pseudo-Doppler spectrum can be sampled at much more discrete, but not any longer equidistant points, resulting in an improved resolution of 1.5. ESA

N90-18630# Deutsche Forschungsanstalt fuer Luft- und Raumfahrt, Oberpfaffenhofen (Germany, F.R.). Abt. Wolkenphysik.
DOPPLER SPECTRA FROM INCOHERENT BACKSCATTER: PRINCIPLES AND EXAMPLES FOR APPLICATION FOR POLDIRAD
Werner Meyer and Thomas Jank Aug. 1989 49 p In GERMAN; ENGLISH summary Report will also be announced as translation (ESA-TT-1197)
(DLR-FB-89-48; ISSN-0171-1342; ETN-90-96278; ESA-TT-1197) Avail: NTIS HC A03/MF A01; DLR, Wissenschaftliches Berichtswesen, Postfach 60 90 58, 5000 Cologne 90, Fed. Republic of Germany, 16.50 deutsche marks

The principles of Doppler spectra analysis of incoherent backscatter are summarized. Using simulations of spectra, how accurately one can determine mean velocity and spectral width is analyzed. Turbulence parameters are calculated and drop size spectra are derived from vertical radar scans as an example of applications of the technique. ESA

N90-18631# Messerschmitt-Boelkow-Blohm G.m.b.H., Ottobrunn (Germany, F.R.). Kommunikationssysteme und Antriebe.
TELEMETRY AND TELECOMMAND OMNIDIRECTIONAL ANTENNA IN THE SHORT WAVE BAND [TELEMETRIE- UND TELEKOMMANDORUNDSTRAHLANTENNE IM KU-BAND]
Guenter Braun, WuLu Chang, and Detlef Leistner Apr. 1989 90 p In GERMAN
(Contract BMFT-FZ-01-YH-86-112)
(ETN-90-96285) Avail: NTIS HC A05/MF A01

Breadboard models of two different telemetry and telecommand omnidirection antennas in the short wave band were developed, built and tested. The related critical technologies and procedures were examined and documented with a view to future developments. A simultion program was developed based on the geometrical theory of diffraction to predict the perturbations of the radiation pattern due to electrically objects in the neighborhood of the antenna. ESA

N90-18632# Nationaal Inst. voor Kernfysica en Hoge Energiefysica, Amsterdam (Netherlands).
INJECTION PARAMETERS AND BEAM OSCILLATIONS DURING EXTRACTION
R. Maas Aug. 1989 25 p

(NIKHEF-K/AmPS/89-07; ETN-90-96326) Avail: NTIS HC A03/MF A01

The dynamics of the combustion process of hydrogen-air and hydrogen-methane-air mixtures in long tubes, the boundary conditions for the deflagration-to-detonation transition, and the associated pressure signals are investigated experimentally and numerically. To influence this combustion process and, in particular, to narrow the range of possible detonations of hydrogen-air-mixtures, different inhibitors are considered. For numerical modeling, the one dimensional random-choice-method is used and further developed. The numerical calculations are compared to the experimental results. The potential and the limitations of this numerical method are shown. ESA

N90-18633# European Space Agency, Paris (France).
MULTITARGET TRACKING BY SINGLE SENSOR: ANALYSIS OF THE MAIN APPROACHES DEVELOPED IN THIS AREA
Jean Dezert (Office National d'Etudes et de Recherches Aerospatiales, Paris, France) Jan. 1990 194 p Transl. into ENGLISH of Poursuite Multi-Cibles Mono-Senseur: Analyse des Principales Approches Developpees dans le Domaine (Paris, France, ONERA), 1988 Original language document was announced as N89-28702
(ESA-TT-1171; ONERA-NT-1988-10; ETN-90-96332) Avail: NTIS HC A09/MF A01

The increasing sophistication of surveillance systems now makes it possible to consider real time multitarget tracking by single and/or multisensor systems. An analysis, based on a review of published papers, of the main multitarget tracking methods using a single sensor system is presented. Two basic approaches are proposed, the Bayes decision rule approach and the maximum likelihood approach. At present, the methods using the Bayes decision rule supercede those based on maximum likelihood theory and special attention is therefore given to them in this analysis. ESA

33 ELECTRONICS AND ELECTRICAL ENGINEERING

Includes test equipment and maintainability; components, e.g., tunnel diodes and transistors; microminiaturization; and integrated circuitry.

For related information see also *60 Computer Operations and Hardware* and *76 Solid-State Physics*.

N90-18634*# National Aeronautics and Space Administration. Lewis Research Center, Cleveland, OH.
PERFORMANCE AND MODELING OF SUPERCONDUCTING RING RESONATORS AT MILLIMETER-WAVE FREQUENCIES
K. B. Bhasin, C. M. Chorey, J. D. Warner, R. R. Romanofsky, V. O. Heinen, K. S. Kong, H. Y. Lee, and T. Itoh (Texas Univ., Austin.) 1990 9 p Prepared for presentation at the 1990 IEEE MIT-S International Microwave Symposium, Dallas, TX, 8-10 May 1990
(NASA-TM-102526; E-5334; NAS 1.15:102526) Avail: NTIS HC A02/MF A01 CSCL 09A

Microstrip ring resonators operating at 35 GHz were fabricated from laser ablated YBCO thin films deposited on lanthanum aluminate substrates. They were measured over a range of temperatures and their performance compared to identical resonators made of evaporated gold. Below 60 Kelvin the superconducting strip performed better than the gold, reaching an unloaded Q approximately 1.5 times that of gold at 25 K. A shift in the resonant frequency follows the form predicted by the London equations. The Phenomenological Loss Equivalence Method is applied to the ring resonator and the theoretically calculated Q values are compared to the experimental results. Author

N90-18635# Central Research Inst. of Electric Power Industry, Tokyo (Japan). Energy and Environment Lab.
BACK SWING PHENOMENON OF SYNCHRONOUS GENERATOR. STUDY ON ac-dc POWER SYSTEM SIMULATOR TESTS
Hiroto Taniguchi, Yuichi Hirata, Yoshitake Kosasa, Minoru Asada, Kenichi Suzuki, Teruhisa Kumano, and Seiichi Takaso Sep. 1988 63 p In JAPANESE; ENGLISH summary
(DE89-782321; CRIE-T-87080) Avail: NTIS (US Sales Only) HC A04/MF A01

After a fault occurs in power system, the electromagnetic torque of synchronous generator has unidirectional components and alternating components which oscillate with rated frequency and its double frequency. These alternating components make the generator swing angle move to backward for a short while after fault and the acceleration starts after this. This phenomenon is called back swing and is not considered in general simulation program for power system stability study. Therefore the effects of this phenomenon should be cleared. To grasp the fundamental aspects and to clear the effects of various factors to the phenomenon, the following results are summarized and discussed: (1) testing at ac-dc power system simulator, (2) theoretical and qualitative analysis of the test results, and (3) simulation of the test by EMTP. DOE

N90-18636# Central Research Inst. of Electric Power Industry, Tokyo (Japan). Energy and Environment Lab.
OPTIMAL PLANNING METHOD OF UNDERGROUND DISTRIBUTION SYSTEM, PART 2. APPLICATION TO VARIOUS TYPES OF SYSTEM CONFIGURATIONS
Atsushi Fukutome and Tsukasa Yoshimitsu Sep. 1988 40 p In JAPANESE; ENGLISH summary
(DE89-782323; CRIE-T-87090) Avail: NTIS (US Sales Only) HC A03/MF A01

A general purpose and practical method was developed that can be applied to various system configurations in order to contribute to rational selection of areas and timing for construction of underground distribution systems and optimal design of such systems. Its feature is the applicability to almost all system configurations in Japan. Computational conditions, such as road maps, distribution of demands, and candidate locations of equipment installation, can be graphically input using the CRT screen. Conditions to particular area can also be entered. Systems based on designer's concept other than basic system configuration model can also be input. Computational conditions are modified in interactive manner to give more rational solutions. Minimum cost solutions can be obtained for conditions not specified using the network optimization technique. With this method applied to model areas, the cost and material requirements for various system configurations were analyzed. With one circuit and T-branch system applied to low voltage system, cost reduction is possible as compared with conventional multi-circuit branch system. DOE

N90-18637# Air Force Inst. of Tech., Wright-Patterson AFB, OH. School of Engineering.
TECHNOLOGY DEVELOPMENT AND CIRCUIT DESIGN FOR A PARALLEL LASER PROGRAMMABLE FLOATING POINT APPLICATION SPECIFIC PROCESSOR M.S. Thesis
Michael W. Scriber Dec. 1989 123 p
(AD-A215870; AFIT/GCE/ENG/89D-6) Avail: NTIS HC A06/MF A01 CSCL 12/7

The laser programmable floating point application specific processor (LPASP) is a new approach at rapid development of custom VLSI chips. The LPASP is a generic application specific processor that can be programmed to perform a specific function. The effort of this thesis is to develop and test the double precision floating point adder and the laser programmable read-only memory (LPROM) that are macrocells within the LPASP. In addition, the applicability of an LPASP parallel processing system is analyzed. The double precision floating point adder is an adder/subtractor macrocell designed to comply with the IEEE double precision floating point standard. An 84-pin chip of the adder was fabricated using 2 micron feature sizes. The fastest processing time was

measured at 120 nanoseconds over 23 worst case test vectors. The adder uses the optimized carry multiplexed (OCM) adder that was developed at AFIT. The OCM adder is a new adder architecture that uses four parallel carry paths to attain a performance time on the order of (cubed root of M) with a gate count on the order of O(n). The redundant logic associated with the parallel propagation banks is eliminated in the OCM adder so that the largest bit-slice of the adder contains only eight 2-to-1 multiplexer gates. A 57-bit adder was fabricated using 2 micron feature sizes. The processing time for the adder is 31 nsec. GRA

N90-18638# Army Communications-Electronics Command, Fort Monmouth, NJ.
PROCEEDINGS OF THE 38TH INTERNATIONAL WIRE AND CABLE SYMPOSIUM
Nov. 1989 734 p Symposium held in Atlanta, GA, 14-16 Nov. 1989
(AD-A216023) Avail: NTIS HC A99/MF A04 CSCL 09/1

Session topics include: (1) How and when will fiber optics expand into the subscriber loop telephone networks; (2) Copper cable design/applications; (3) Fiber optic cable installation and field test methods; (4) Cable materials; (5) Subscriber networks; (6) Military applications; (7) Fiber optic splices and connectors; (8) Fire, smoke and toxicity technology; (9) Building cabling and wiring distribution design; (10) Fiber optic cable design; (11) Testing of cable, components and materials; (12) Processing and testing of fibers cables. GRA

N90-18639# Minnesota Univ., Minneapolis. Dept. of Chemical Engineering and Materials Science.
CELL PERFORMANCE OF ULTRA-THIN POLYMER CATHODE SYSTEMS. PART 1: ANION INTERCALATING POLYMER CATHODE Technical Report, Jul. 1988 - Oct. 1989
Katsuhiko Naoi, Boone B. Owens, and William H. Smyrl 1 Nov. 1989 20 p Submitted for publication
(Contract N00014-88-K-0360)
(AD-A216037; TR-20-ONR-Pt-1) Avail: NTIS HC A02/MF A01 CSCL 09/1

Theoretical energy and power density values for thin film Li/liquid electrolyte/polymer cell systems were calculated by designing a specific cell model for both a prismatic cell with only the basic cell element (no hardware) and a bipolar-design cell with some practical hardware. The cell performance is compared for three different cathode polymer materials, viz., polyaniline, polypyrrole, and polyvinylferrocene. The energy and power densities are estimated as a function of cathode thickness, active cell area, and initial concentration of electrolyte for very thin cathode films (cathode thickness). For the practical cell, the authors used a bipolar design, for which the energy and the power were calculated also as a function of the number of bipolar units (X). GRA

N90-18640# International Business Machines Corp., San Jose, CA. Research Div.
PERSISTANT SPECTRAL HOLE-BURNING: PHOTON-GATING AND FUNDAMENTAL STATISTICAL LIMITS
W. E. Moerner 3 Nov. 1989 17 p Submitted for publication
(Contract N00014-84-C-0708)
(AD-A216084; TR-22) Avail: NTIS HC A02/MF A01 CSCL 09/5

Fundamental limits on frequency-domain optical storage using persistent spectral hole burning follow from both the expected configuration of the storage system and from physical effects such as the photophysics of the light the material, photon quantum (shot) noise, and statistical fluctuations in additive random quantities. When frequency-domain reading and writing in focused spots is considered, the large class of single-photon materials can be shown to have serious limitations from a signal-to-noise point of view. This has stimulated interest in photon grated material which effectively have a threshold in the writing process, controlled by a second light beam of a different color. Fundamental statistical limits on persistent spectral hole burning can also be illustrated using recent measurements of statistical fine structure in solids. Other recent experiments in which the absorption spectrum of a single absorbing molecule in a solid was measured represent an extreme limit on persistent spectral hole burning effects. GRA

N90-18641# Pittsburgh Univ., PA. Dept. of Computer Science.
PARALLEL MEMORY ADDRESSING USING COINCIDENT OPTICAL PULSES Final Report, 15 Jul. 1988 - 14 Jul. 1989
Donald M. Chiarulli, Rami G. Melhem, and Steven P. Levitan 15 Sep. 1989 86 p
(Grant AF-AFOSR-0198-88)
(AD-A216302; AFOSR-89-1702TR) Avail: NTIS HC A05/MF A01 CSCL 09/5

A preliminary investigation was made of the applicability of coincident optical pulse techniques to hybrid electronic-optical computing systems. The results of the investigation are focused in two areas. First, it was determined that the technological constraints for pulse generation, detection, and synchronization do not substantially restrict the applicability of the technique. This conclusion was based on the results of pulse coincidence experiments. Second, the application of the technique is not restricted to memory addressing structures as had been originally proposed. It was demonstrated that coincident pulse methods can be applied to general multiprocessor interconnections. In this context they can be used to provide the functionality and performance of fully interconnected systems while using low cost and low complexity optical structures. GRA

N90-18642# Aerospace Corp., El Segundo, CA. Electronics Research Lab.
DETERMINING THE EFFECTS OF MICROWAVE POWER AND C-FIELD SETTING ON THE FREQUENCY OF A CESIUM ATOMIC FREQUENCY STANDARD
Sarunas K. Karuza, Walter A. Johnson, and Frank J. Volt 31 Dec. 1989 27 p
(Contract F04701-88-C-0089)
(AD-A216599; TR-0089(4470-03)-1; SSD-TR-89-91) Avail: NTIS HC A03/MF A01 CSCL 20/5

In experiments at the United States National Institute of Standards and Technology, Andrea De Marchi showed that there exist optimum values of the C-field setting in a commercial dual-beam cesium frequency standard that make the output frequency insensitive to variations in microwave power. Moreover, and most important, De Marchi demonstrated that the long-term stability of the clock is improved if the C-field is set at one of these optimum settings. To see if these results can be obtained with a clock having a different modulation scheme, the authors, using a completely automated measuring system, performed a similar study on another manufacturer's commercial cesium standard; this standard employed single-beam tube optics and a modulation scheme different from that used by the clocks studied by De Marchi. Our results, similar to those of De Marchi, show that optimum C-field settings exist for the standard we investigated. GRA

N90-18643# Missouri Univ., Rolla. Dept. of Ceramic Engineering.
RELIABILITY STUDIES OF CERAMIC CAPACITORS Final Report, 1 Mar. 1982 - 31 Aug. 1987
H. U. Anderson Dec. 1989 142 p
(Contract N00014-82-K-0294)
(AD-A216763) Avail: NTIS HC A07/MF A01 CSCL 09/1

This report covers a contract which studied low voltage degradation, the thermally stimulated polarization/depolarization current (TSPC/DC) spectra of Barium Titanate, and the dielectric and electrical properties of BaTiO3 composites (polymer and air), processing of BaTiO3 dielectrics, and the synthesis of relaxor dielectrics from both organometallic and mixed oxide precursors. The measurements were electrical conductivity, dielectric properties, and current-time voltage behavior as a function of chemical composition, temperature, and humidity. GRA

N90-18644# Wilson Greatbatch Ltd., Clarence, NY.
FEASIBILITY OF A SUPER HIGH ENERGY DENSITY BATTERY OF THE Li/BrF3 ELECTROCHEMICAL SYSTEM
Michael F. Pyszczek, Steven J. Ebel, and Christine A. Frysz 1989 15 p
(AD-A216794; WGL-MLR-89-30) Avail: NTIS HC A03/MF A01 CSCL 07/1

To date, design and construction of a material handling and measurement system along with the apparatus required for waste material disposal has been completed. Preliminary corrosion screening of potential case materials is currently underway. A review of the literature, has led to the use of Monel (trademark) 400 as the material of construction for the handling and measurement system. The inherent stability of this material with bromine trifluoride in its liquid state is crucial to ensure that contamination does not occur during storage and handling. For applications which require a flexible or transparent material, items fabricated from perfluoroalkyoxy polymers (Teflon (trademark) PFA) were utilized. One such application encountered was in the design of the graduated tank which allows visual inspection of the material prior to dispensing. Containers used for compatibility/corrosion testing were also constructed of PFA. GRA

N90-18645# Massachusetts Inst. of Tech., Lexington. Lincoln Lab.
OUTPUT PERFORMANCE OF IDEALIZED MICROWAVE POWER AMPLIFIERS
Lawrence J. Kushner Oct. 1989 9 p Submitted for publication
(Contract F19628-90-C-0002)
(AD-A216797; JA-6281; ESD-TR-89-291) Avail: NTIS HC A02/MF A01 CSCL 09/1

Output power, efficiency, power dissipation and optimum load resistance expressions for idealized microwave class A and class B power amplifiers are derived based on a waveform analysis. The effects of device transconductance variation with bias and circuit harmonic termination are examined. GRA

N90-18646# Naval Research Lab., Washington, DC. Underwater Sound Reference Detachment.
A TEST METHOD FOR MEASURING CORONA INCEPTION VOLTAGE FOR TRANSDUCER AUTOTRANSFORMERS Final Report, FY87 - FY88
Dean L. Diebel and A. C. Tims 15 Nov. 1989 38 p Sponsored by Naval Sea Systems Command, Washington, DC
(AD-A216818; NRL-MR-6559) Avail: NTIS HC A03/MF A01 CSCL 20/3

An autotransformer corona inception test circuit was developed and a prototype was constructed and demonstrated. Circuit diagrams and component values are presented. Ancillary equipment for the test is identified and recommended, test procedures and precautions are presented, and measured corona inception voltage data as well as pictorial data represented for autotransformers of different manufacture and type. Included is a computer program which is used to model and calculate values of test circuit filter components. GRA

N90-18647# Rome Air Development Center, Griffiss AFB, NY.
RELIABILITY ASSESSMENT USING FINITE ELEMENT TECHNIQUES Report, Jan. - Jul. 1988
Gretchen A. Bivens Nov. 1989 70 p
(AF Proj. 2338)
(AD-A216907; RADC-TR-89-281) Avail: NTIS HC A04/MF A01 CSCL 09/1

Finite element analysis (FEA) is a computer simulation technique that is used to predict the thermal and mechanical response of a structure. FEA was used to predict the response in various electronic assemblies. This particular study was concerned with the reliability of surface mounted microwire boards. A FEA of this assembly was simulated and the results used to estimating its useful life. A detailed account is given of the factors to be considered when performing a FEA and the procedure used to transfer the results to a reliability figure-of-merit. GRA

N90-18648# San Diego State Univ., CA.
SIGNAL PROCESSING DEVICE TO CONTROL MICROWAVE OUTPUT Final Report
J. G. Pinto Aug. 1989 11 p
(Contract N66001-85-D-0203)
(AD-A216931; NOSC/TR-1633) Avail: NTIS HC A02/MF A01 CSCL 06/12

The development of an electronic device to control the operation of a commercial microwave oven is discussed. This device when installed in conjunction with the existing circuitry of SHARP MICROWAVE OVEN (model R-9524) is capable of automatically advancing through a sequence of thawing recipes programmed and stored in the memory bank of the oven. The device therefore eliminates or minimizes human operator action needed in previous prototype version of a blood thawing device. GRA

N90-18649# Sandia National Labs., Albuquerque, NM. Discrete Semiconductors Div.
CHARACTERIZATION AND DEVELOPMENT REPORT FOR THE SA3274-1 AND SA3274-2 TRANSIENT VOLTAGE SUPPRESSORS
J. B. Vinson, D. K. Holck, and A. M. Gurule Sep. 1989 53 p
(Contract DE-AC04-76DP-00789)
(DE90-005712; SAND-89-2267) Avail: NTIS HC A04/MF A01

The SA3274-1 and SA3274-2 are bi-directional transient voltage suppressors that have a nominal breakdown voltage of 12 Volts and 22 Volts, respectively. These devices are packaged in an axial-leaded cylindrical glass package. These devices were manufactured by and procured from Microsemi Corporation in Santa Ana, California. They were tested by the Design Agency in accordance with PS319848. DOE

N90-18650# Sandia National Labs., Albuquerque, NM. Exploratory Batteries Div.
LITHIUM AMBIENT-TEMPERATURE BATTERY RELIABILITY Final Report
Calvin D. Jaeger and Edward V. Thomas Dec. 1989 27 p
(Contract DE-AC04-76DP-00789)
(DE90-005758; SAND-87-2119) Avail: NTIS HC A03/MF A01

A program to develop nondestructive testing techniques to enable prediction of the reliability of primary lithium cells has been underway since FY 1981. Various candidate techniques, such as microcalorimetry and complex impedance analysis were considered and tried. Statistical analysis of available data from this program indicates that several measurements derived from complex impedance analysis directly relate to the capacity condition of the cell. These measurements could form the basis for predicting cell performance and therefore cell reliability for a particular application. DOE

N90-18651# Lawrence Livermore National Lab., CA.
A NEW BROADBAND PULSED HIGH VOLTAGE MONITOR
W. R. Cravey, R. A. Anderson, P. Wheeler, D. Kraybill, N. E. Molau, and D. Wojtowicz 27 Sep. 1989 6 p Presented at the 7th IEEE Pulsed Power Conference, Monterey, CA, 12-14 Jun. 1989 Submitted for publication
(Contract W-7405-eng-48)
(DE90-006264; UCRL-100364; CONF-890665-54) Avail: NTIS HC A02/MF A01

Experimental results of a new GHz-bandwidth diagnostic for measuring pulsed high voltage are presented. The probe is a small helical coil that self-magnetically insulates to prevent turn-to-turn flashover. A small external B-dot sensor measures I-dot, the time rate of change of current in the probe. The voltage to be measured is equal to L times I-dot. The experimental apparatus used to measure a 1 MV, 60 ns pulse with a rise time of 1.5 ns generated by LLNL's 2 MV accelerator is described. Excellent agreement is obtained when comparing the output of the new probe with a conventional resistive divider technique. The major difference in the temporal shape of the waveforms was determined to be caused by the bandwidth limitation of the resistive divider probe. DOE

N90-18652# Allied-Signal Aerospace Co., Kansas City, MO. Technical Communications Div.

ION CHROMATOGRAPHY IN THE MANUFACTURE OF MULTILAYER CIRCUIT BOARDS

Robert E. Smith Jan. 1990 16 p Presented at the Ion Chromatography in the Semiconductor, Electronics, and Plating Industries, San Jose, CA, 16 Jan. 1990 Submitted for publication

(Contract DE-AC04-76DP-00613)

(DE90-005560; KCP-613-4247; CONF-900159-1) Avail: NTIS HC A03/MF A01

Ion chromatography (IC) has proven useful in analyzing chemical solutions used in the manufacture of multilayer circuit boards. Unlike other chemical quantification techniques, IC provides results on ions not expected in the production solutions. Thus, solution contamination and break-down products can be monitored in every phase of the circuit board manufacturing. During the first phase, epoxy laminates experience an etchback, first in chromic acid, which can be analyzed for trace chloride and sulfate, then in ammonium bifluoride/HCl, which can be analyzed for fluoride and chloride. Following a wet-blasting to roughen up the surface, 20 microinches of copper are deposited using an electroless bath. Again, IC is applicable for monitoring formate, tartarate, and sulfate levels. Next, an acid copper bath is used to electroplate the through holes with 0.001 inches of ductile copper. This bath is analyzed for trace chloride. Photoimaging is then performed, and the organic solvents used can be assayed for trace ionic chloride. Finally, a fluoroboric acid-based tin-lead bath is used to deposit a solderable alloy. This bath is analyzed for fluoroborate, tin, and lead. In addition, mobile phase ion chromatography (MPIC) is used to monitor the nonionic organic brighteners in the baths. DOE

N90-18653# Rochester Inst. of Tech., NY. Dept. of Microelectronic Engineering.

RESEARCH PROJECT IN MICROELECTRONIC ENGINEERING AND IMAGING SCIENCE Final Report, Oct. 1988 - 30 Nov. 1989

Lynn Fuller 1989 6 p

(Contract DE-FG01-88DP-20153)

(DE90-006907; DOE/DP-20153/T1) Avail: NTIS HC A02/MF A01

The objective of this work is the development of improved processes in microelectronics manufacturing, and in particular microlithography. The approach includes the setting up an electron beam lithography system and initiating research efforts in microlithography, microlithographic materials evaluation and process development. The results will be the capability for research in lithography, electron beam maskmaking, submicron electron beam imaging, electron beam resist material evaluation and direct write on wafer. A video tape course on the principles of clean rooms and contamination control will be produced and used for orientation of new personnel to the proper use of the clean room facility. DOE

N90-18654# Technische Univ., Delft (Netherlands).

INTEGRATED SILICON FLIP-FLOP SENSORS Ph.D. Thesis

Weijian Lian 1989 129 p Sponsored by Netherlands Foundation for Technical Science

(ETN-90-96271) Avail: NTIS HC A07/MF A01

A thesis on a class of silicon sensors (input transducers) called flip-flop sensors is presented. An understanding of the operating principles of the flip-flop sensor with a subsequent development of analytical expressions to describe its characteristics is given. The implementation of the flip-flop sensor in a standard IC (integrated circuit) process was investigated and sensor characteristics were measured through experiments. Application of the sensors in sensor arrays is described. A design of a sense amplifier is introduced and several methods in which the array can be operated are analyzed. ESA

N90-18655# Idaho National Engineering Lab., Idaho Falls.

A BATTERY DATA BASE FOR ELECTRIC VEHICLE APPLICATIONS

A. F. Burke, J. E. Hardin, and D. M. Kiser 1989 7 p Presented at the 4th Annual Battery Conference on Applications and Advances, Long Beach, CA, 17-19 Jan. 1989

(Contract DE-AC07-76ID-01570)

(DE90-007085; EGG-M-89410; CONF-890160-2) Avail: NTIS HC A02/MF A01

Work is progressing on the development of a battery data base for electric vehicle applications. This data base is intended to provide the electric vehicle community access to the large volume of battery data taken at the Idaho National Engineering Laboratory (INEL), Argonne National Laboratory, and Sandia National Laboratory on a desk-top PC. The initial version of the data base will be distributed on a single floppy disk. The data base will include the physical characteristics of the various batteries tested as well as summary tables showing the test results for each cycle of the battery test programs. Second-by-second data from constant power discharges, peak power tests, and variable power SFUDS cycle tests will also be included in the data base. The data base is being prepared using dBASE IV. The user selects the battery and data desired through a series of screen displayed menus. The design of the data base and menus are complete and INEL battery summary table and data files are being read into the data base. Nearly 100 MB of data have been prepared for eventual inclusion into the data base. DOE

N90-18656# Pacific Northwest Lab., Richland, WA.

COST AND ENERGY CONSUMPTION ESTIMATES FOR THE ALUMINUM-AIR BATTERY ANODE FUEL CYCLE

Jan. 1990 68 p

(Contract DE-AC06-76RL-01830)

(DE90-005810; PNL-7230) Avail: NTIS HC A04/MF A01

At the request of DOE's Office of Energy Storage and Distribution (OESD), Pacific Northwest Laboratory (PNL) conducted a study to generate estimates of the energy use and costs associated with the aluminum anode fuel cycle of the aluminum-air (Al-air) battery. The results of this analysis indicate that the cost and energy consumption characteristics of the mechanically rechargeable Al-air battery system are not as attractive as some other electrically rechargeable electric vehicle battery systems being developed by OESD. However, there are distinct advantages to mechanically rechargeable batteries, which may make the Al-air battery (or other mechanically rechargeable batteries) attractive for other uses, such as stand-alone applications. Fuel cells, such as the proton exchange membrane (PEM), and advanced secondary batteries may be better suited to electric vehicle applications. DOE

N90-18657# Lawrence Livermore National Lab., CA.

PERFORMANCE OF A 500 WATT Nd:GGG ZIGZAG SLAB OSCILLATOR

L. Zapata, K. Manes, D. Christie, J. Davin, J. Blink, J. Penland, R. Demaret, and G. Dallum 12 Jan. 1990 17 p Presented at the SPIE Optics, Electro-optics and Laser Applications in Science and Engineering Conference and Exhibition, Los Angeles, CA, 14-19 Jan. 1990 Submitted for publication

(Contracts W-7405-eng-48; MIPR-W31-RPD-63-A072)

(DE90-006263; UCRL-102275; CONF-900140-4) Avail: NTIS HC A03/MF A01

Realization of practical multi-kilowatt Nd:garnet lasers will require the scale-up of crystal dimensions as well as more powerful pumping sources. A high average power zigzag slab crystal amplifier testing facility has been established at LLNL which employs two 100 kW(sub e) vortex stabilized arc lamps, cooled reflectors and a cooled, spectrally filtered, crystal slab mounting fixture. The operational characteristics of the first crystal laser to be tested in this setup, a Nd:GGG zigzag oscillator, are presented. A Nd:GGG crystal of dimensions 18 x 7 x 0.5 cu cm, doped at 2 x 10(exp 20)/cu cm Nd(3+) atomic density, was pumped by up to 40 kW of filtered argon line emission. A small-signal single pass gain (losses excluded) of 1.09 was measured with a probe laser when the dc input to the lamps was 43 kW(sub e). The power supply was then modified to operate in a pulsed mode and provided one to three milliseconds pulses at 120 Hz. An average optical output

power of 490 watts was obtained at a lamp input power of 93 kW(sub e) in an unoptimized resonator. The laser output power declined after a few tens of seconds since the slab tips were not properly cooled. A birdhouse specular lamp reflector and a contoured diffuse reflector were tested; in both cases the pump illuminated crystal surface was smaller than the total crystal face area. Fluorescence imaging of the zigzag amplifier's output aperture registered a smoother, more uniform pumping profile when the diffuse reflector was used. Uniformity of pumping results in decreased resonator loss and yields higher laser output power. Thermo-optic distortions observed in these preliminary tests are analyzed with the aid of computer simulations of the thermal fields, stresses, and surface displacements of the crystal slab. DOE

N90-18658# Sandia National Labs., Albuquerque, NM. Scientific Computing and Applied Mathematics Div.

DANCIR (DEVICE AND CIRCUIT SIMULATOR): A THREE DIMENSIONAL STEADY-STATE SEMICONDUCTOR DEVICE SIMULATOR

J. C. Meza and J. F. Grear Jan. 1990 28 p
(Contract DE-AC04-76DP-00789)
(DE90-006370; SAND-89-8266) Avail: NTIS HC A03/MF A01

This report discusses a program called DANCIR that was developed to model semiconductor devices. DANCIR, which stands for Device and Circuit Simulator, enables the user to compute the steady-state solution to the drift-diffusion equations for a single semiconductor device. The drift-diffusion equations that describe carrier motion in a semiconductor device can be used to compute operating characteristics for a semiconductor device. This allows the engineer to design different devices and predict the behavior of these devices without resorting to the time-consuming process of building many prototypes. DOE

N90-18659# Sandia National Labs., Albuquerque, NM.

COATING POSSIBILITIES FOR MAGNETIC SWITCHES

D. J. Sharp, H. C. Harjes, G. A. Mann, and F. A. Morgan 1990 9 p Presented at the International Workshop on Magnetic Pulse Compression, Lake Tahoe, CA, 12-14 Feb. 1990
(Contract DE-AC04-76DP-00789)
(DE90-006536; SAND-90-0277C; CONF-900280-1) Avail: NTIS HC A02/MF A01

High average power magnetic pulse compression systems are now being considered for use in several applications such as the High Power Radiation Source (HiPoRS) project. Such systems will require high reliability magnetic switches (saturable inductors) that are very efficient and have long lifetimes. One of the weakest components in magnetic switches is their interlaminar insulation. Considerations related to dielectric breakdown, thermal management of compact designs, and economical approaches for achieving these needs must be addressed. Various dielectric insulation and coating materials have been applied to Metglas foil in an attempt to solve the complex technical and practical problems associated with large magnetic switch structures. This work reports various needs, studies, results, and proposals in selecting and evaluating continuous coating approaches for magnetic foil. Techniques such as electrophoretic polymer deposition and surface chemical oxidation are discussed. We also propose continuous photofabrication processes for applying dielectric ribs or spacers to the foil which permit circulation of dielectric liquids for cooling during repetitive operation. DOE

N90-18660# Nationaal Inst. voor Kernfysica en Hoge Energiefysica, Amsterdam (Netherlands).

LINEAR VARIABLE DIFFERENTIAL TRANSFORMER (LVDT) WITH CONDITIONER FOR THE CONTROL OF STEPPING MOTOR DRIVERS (PART OF THE SLIDING-FOIL FOLLOWER SYSTEM OF THE EMIN SPECTROMETERS) [LVDT MET CONDITIONER VOOR AANSTURING VAN STAPPENMOTORDRIVERS/ ONDERDEEL VAN HET SLIDING-FOIL VOLGSYSTEEM VAN DE EMIN SPECTROMETERS]

J. T. vanEs and J. vanTrigt 1 Nov. 1989 10 p In DUTCH
(DIGEL-1989-9; ETN-90-96263) Avail: NTIS HC A02/MF A01

A Linear Variable Differential Transformer (LVDT) was developed to control a stepping motor which drives the sliding foil of Emin spectrometers. The LVDT gives a signal proportional to the follower error. This signal is converted in the conditioner into a frequency proportional to the follower error. The result is that the stepping motor turns continuously in order to reduce the error to zero. The LVDT has no wearing parts, is not sensitive to pollution and can resist a rather high radiation dose. ESA

N90-18661# Nationaal Inst. voor Kernfysica en Hoge Energiefysica, Amsterdam (Netherlands). Afdeling DIGEL.

LOW WEIGHT VARIABLE GRV POWER SUPPLY AS PART OF THE INJECTOR ELECTRONICS TO BE DEVELOPED FOR THE ELECTRON ACCELERATOR MEA [LICHT GEWICHT REGELABARE 6KV VOEDING. ONDERDEEL VAN DE NIEUW TE ONTWIKKELEN INJECTOR ELECTRONICA VOOR DE ELEKTRONEN VERSNELLER MEA]

Ronald vanderPutten 1989 21 p In DUTCH
(DIGEL-1989-6; ETN-90-96266) Avail: NTIS HC A03/MF A01

A power supply variable between 1 and 6 kV was developed for the injector electronics of MEA. A power resonant converter working at 50 kHz was selected. Electrolytic capacitors were not used because they cannot withstand vacuum and high pressure. The power supply is resistant to vacuum and a pressure of 8 at. It has a low weight and a small volume, and a high efficiency. ESA

N90-18662# Deutsche Forschungsanstalt fuer Luft- und Raumfahrt, Brunswick (Germany, F.R.). Abt. Messtechnik und Sensoren.

DEVELOPMENT AND TEST OF POWER AMPLIFIERS FOR THE DRIVING OF LOW-VOLTAGE PIEZO-ACTUATORS IN MULTISTABLE INTERFEROMETERS

Hans Naumann and Walter Schmidt Jun. 1989 42 p In GERMAN; ENGLISH summary Report will also be announced as translation (ESA-TT-1196)
(DLR-Mitt-89-19; ISSN-0176-7739; ETN-90-96274; ESA-TT-1196)
Avail: NTIS HC A03/MF A01; DLR, Wissenschaftliches Berichtswesen, Postfach 90 60 58, 5000 Cologne 90, Fed. Republic of Germany, 17.50 deutsche marks

A power amplifier for capacitive loads such as low voltage piezoelectric translators is described. Several features of the amplifier are discussed: the offset regulator, fader, electric-wave filter and hysteresis compensation. These are required in certain applications of multistable interferometers. ESA

N90-18663# Nationaal Inst. voor Kernfysica en Hoge Energiefysica, Amsterdam (Netherlands).

TOROID MONITOR [TOROIDEMONITOR]

J. T. vanEs and J. C. Boes 15 Jun. 1989 17 p In DUTCH
(DIGEL-1989-8; ETN-90-96327) Avail: NTIS HC A03/MF A01

A toroid monitor was developed for the measurement of the bundle pulsed current of the electron accelerator MEA. The monitor is a broadband current-to-voltage. The current transformer, which is in a high radiation environment, is connected to the converter electronics by a transmission line of at least 20 m. For low frequencies the current transformer is apparently shortcircuited, providing a high inductance-to-resistance ratio and avoiding the use of a large transformer core. For high frequencies the transmission line is connected to its characteristic impedance. The transformer has a zero line corrector and an output circuit capable of driving 50 ohm lines. ESA

34 FLUID MECHANICS AND HEAT TRANSFER

Includes boundary layers; hydrodynamics; fluidics; mass transfer; and ablation cooling.

For related information see also *02 Aerodynamics* and *77 Thermodynamics and Statistical Physics.*

N90-18664*# California Univ., Berkeley.
SEMIDISCRETE GALERKIN MODELLING OF COMPRESSIBLE VISCOUS FLOW PAST A CIRCULAR CONE AT INCIDENCE Ph.D. Thesis
Andrew James Meade, Jr. 30 Oct. 1989 81 p
(Grant NAG2-483)
(NASA-CR-186323; NAS 1.26:186323) Avail: NTIS HC A05/MF A01 CSCL 20D

A numerical study of the laminar and compressible boundary layer, about a circular cone in a supersonic free stream, is presented. It is thought that if accurate and efficient numerical schemes can be produced to solve the boundary layer equations, they can be joined to numerical codes that solve the inviscid outer flow. The combination of these numerical codes is competitive with the accurate, but computationally expensive, Navier-Stokes schemes. The primary goal is to develop a finite element method for the calculation of 3-D compressible laminar boundary layer about a yawed cone. The proposed method can, in principle, be extended to apply to the 3-D boundary layer of pointed bodies of arbitrary cross section. The 3-D boundary layer equations governing supersonic free stream flow about a cone are examined. The 3-D partial differential equations are reduced to 2-D integral equations by applying the Howarth, Mangler, Crocco transformations, a linear relation between viscosity, and a Blasius-type of similarity variable. This is equivalent to a Dorodnitsyn-type formulation. The reduced equations are independent of density and curvature effects, and resemble the weak form of the 2-D incompressible boundary layer equations in Cartesian coordinates. In addition the coordinate normal to the wall has been stretched, which reduces the gradients across the layer and provides high resolution near the surface. Utilizing the parabolic nature of the boundary layer equations, a finite element method is applied to the Dorodnitsyn formulation. The formulation is presented in a Petrov-Galerkin finite element form and discretized across the layer using linear interpolation functions. The finite element discretization yields a system of ordinary differential equations in the circumferential direction. The circumferential derivatives are solved by an implicit and noniterative finite difference marching scheme. Solutions are presented for a 15 deg half angle cone at angles of attack of 5 and 10 deg. The numerical solutions assume a laminar boundary layer with free stream Mach number of 7. Results include circumferential distribution of skin friction and surface heat transfer, and cross flow velocity distributions across the layer. Author

N90-18665*# National Aeronautics and Space Administration. Lewis Research Center, Cleveland, OH.
INVESTIGATION OF METHODS TO PRODUCE A UNIFORM CLOUD OF FUEL PARTICLES IN A FLAME TUBE
Clifford E. Siegert, Frederic G. Pla, Robert Rubinstein (Sverdrup Technology, Inc., Cleveland, OH.), Thomas F. Niezgoda, Robert J. Burns, and Jerome A. Johnson Feb. 1990 25 p
(NASA-TM-102376; E-5110; NAS 1.15:102376) Avail: NTIS HC A03/MF A01 CSCL 20D

The combustion of a uniform, quiescent cloud of 30-micron fuel particles in a flame tube was proposed as a space-based, low-gravity experiment. The subject is the normal- and low-gravity testing of several methods to produce such a cloud, including telescoping propeller fans, air pumps, axial and quadrature acoustical speakers, and combinations of these devices. When operated in steady state, none of the methods produced an acceptably uniform cloud (+ or - 5 percent of the mean concentration), and voids in the cloud were clearly visible. In some cases, severe particle agglomeration was observed; however, these clusters could be broken apart by a short acoustic burst from an axially in-line speaker. Analyses and experiments reported elsewhere suggest that transient, acoustic mixing methods can enhance cloud uniformity while minimizing particle agglomeration. Author

N90-18666# Heat Pump Technology Center of Japan, Tokyo.
INVESTIGATION REPORT OF THE INVESTIGATION COMMISSION FOR INTERCHANGE OF HEAT PUMP TECHNOLOGY IN EUROPE
Naritake Kawasaki Oct. 1988 143 p
(DE89-782293; HPTC-07) Avail: NTIS (US Sales Only) HC A07/MF A01

This investigation was made in June 1988 as a part of independent researches of the Heat Pump Technology Development Center to help develop and promote heat pump technology in Japan. Investigation themes were heat supplying systems utilizing heat pumps as a city infrastructure, and application of sea water, lake water, city sewage and geothermal as new heat sources to use heat pumps in clod districts. The commission visited 22 places in Sweden, Norway, Iceland, Switzerland, Australia and France. The Center has interchanges with member countries of international joint researches on IEA improved model heat pump system enforcement agreement, and those related with heat pumps in these countries cooperated in the selection of investigation objects. In addition to the visits, a technical interchange conference was held in Norway so that members of the commission might have further interchanges with the specialists on the spot and might be able to exchange information in the future. DOE

N90-18667*# National Aeronautics and Space Administration. Lewis Research Center, Cleveland, OH.
A SIMPLE ALGEBRAIC GRID ADAPTATION SCHEME WITH APPLICATIONS TO TWO- AND THREE-DIMENSIONAL FLOW PROBLEMS
Andrew T. Hsu (Sverdrup Technology, Inc., Cleveland, OH.) and John K. Lytle 1989 10 p Presented at the 9th Computational Fluid Dynamics Conference, Buffalo, NY, 14-16 Jun. 1989; sponsored by AIAA Previously announced in IAA as A89-41827
(Contract NAS3-25266)
(NASA-TM-102446; E-5229; NAS 1.15:102446) Avail: NTIS HC A02/MF A01 CSCL 20D

An algebraic adaptive grid scheme based on the concept of arc equidistribution is presented. The scheme locally adjusts the grid density based on gradients of selected flow variables from either finite difference or finite volume calculations. A user-prescribed grid stretching can be specified such that control of the grid spacing can be maintained in areas of known flowfield behavior. For example, the grid can be clustered near a wall for boundary layer resolution and made coarse near the outer boundary of an external flow. A grid smoothing technique is incorporated into the adaptive grid routine, which is found to be more robust and efficient than the weight function filtering technique employed by other researchers. Since the present algebraic scheme requires no iteration or solution of differential equations, the computer time needed for grid adaptation is trivial, making the scheme useful for three-dimensional flow problems. Applications to two- and three-dimensional flow problems show that a considerable improvement in flowfield resolution can be achieved by using the proposed adaptive grid scheme. Although the scheme was developed with steady flow in mind, it is a good candidate for unsteady flow computations because of its efficiency. Author

N90-18668# Air Force Inst. of Tech., Wright-Patterson AFB, OH. School of Engineering.
MULTICELLULAR NATURAL CONVECTION IN A NARROW VERTICAL SLOT M.S. Thesis
David C. Jarman Dec. 1989 153 p
(AD-A216411; AFIT/GAE/ENY/89D-16) Avail: NTIS HC A08/MF A01 CSCL 20/4

The influence was investigated of Prandtl number on steady, or unsteady, flow behavior in a narrow vertical slot. The focus is to examine the effects of Prandtl number on natural convective flows, and the formation of single and multiple cells, over a range

of Prandtl numbers from Pr = 0 to Pr = infinity. Both numerical as well as analytical approaches are undertaken in studying these phenomena. By assuming a large Rayleigh number and small gap, the two-dimensional Navier-Stokes equations are reduced to the simpler boundary layer form. Boundary layer equations are then derived for both the low and high Prandtl number regimes, including the limiting conditions of Pr approaches limit of 0 and Pr approaches limit of infinity. Furthermore, the equations obtained for the low Prandtl number regime also hold any finite Prandtl number in the range 0 less than Pr less than or = 1.0. Numerical solutions to these equations are obtained by using a stable, second order, fully implicit, time accurate, Gauss-Siedel iterative procedure. In addition to numerical solutions, steady state analytical solutions are derived using perturbative methods. GRA

N90-18669# Naval Postgraduate School, Monterey, CA.
STUDY OF VORTEX ARRAYS INDUCED ARTIFICIALLY AND FROM CENTRIFUGAL INSTABILITIES M.S. Thesis
Michael F. Tuzzolo Jun. 1989 95 p
(AD-A216499) Avail: NTIS HC A05/MF A01 CSCL 20/4

Experimental results are presented which describe the development and structure of vortex pairs and vortex arrays which are embedded in turbulent boundary layers, and vortex arrays developing as a result of centrifugal instabilities in a curved channel. Streamwise vortex pairs embedded in a turbulent boundary layer on a flat plate are induced artificially using vortex generators. Mean velocity surveys, total pressure surveys, and wall heat transfer distributions show that Stanton numbers are augmented when vortex pairs have a common downwash. With common upwash, the Stanton number perturbation from vortex pairs is much less. Vortex arrays induced from centrifugal instabilities were studied in a 40:1 aspect ratio channel with mild curvature. Mean velocity and total pressure surveys for Dean numbers from 50 to 150 illustrate some structural characteristics of vortex pairs. GRA

N90-18670# Naval Postgraduate School, Monterey, CA.
AUTOMATION AND EXTENSION OF LDV (LASER-DOPPLER VELOCIMETRY) MEASUREMENTS OF OFF-DESIGN FLOW IN A SUBSONIC CASCADE WIND TUNNEL M.S. Thesis
Kenneth D. Murray Jun. 1989 147 p
(AD-A216627) Avail: NTIS HC A07/MF A01 CSCL 20/4

A two component Laser Doppler velocimetry system was successfully automated to speed the data acquisition and reduction process for flow measurements in a subsonic linear cascade wind tunnel. A three-axis traverse table was installed for computer controlled positioning of the LDV probe volume and a modification was made to permit measurements close to test blade surfaces. Commercial software was used for control and acquisition of the LDV data. Software was generated in-house to record tunnel conditions and to reduce and present the survey data. Detailed measurements were made of the flow through a controlled diffusion compressor cascade at an inlet flow angle of 48 degrees (8 degrees above design) to extend a database for viscous code validation. Test conditions were held nominally at M=0.25 and Rec=720000. The flow was shown to remain attached at the blade trailing edge but the measurements also indicated the presence of a less stable flow field in the blade passage when compared with previous observations at lower inlet flow angles. GRA

N90-18671# Washington Univ., Seattle. Dept. of Aeronautics and Astronautics.
TURBULENCE STRUCTURE OF MIXING SWIRLING FLOWS Final Technical Report, 1 Oct. 1985 - 30 Sep. 1989
Fredrick B. Gessner 10 Dec. 1989 18 p
(Grant AF-AFOSR-0273-85; AF Proj. 2307)
(AD-A216628; AFOSR-89-1877TR) Avail: NTIS HC A03/MF A01 CSCL 20/4

A swirling inner flow which develops along a constant-diameter centerbody in the presence of an unconfined, axially-directed outer flow was investigated. The data which were acquired include local mean velocity and static pressure profiles at six streamwise locations for different prescribed mass flow rate ratios. Local wall shear stress measurements were made at these six streamwise locations in order to investigate local law-of-the-wall behavior in the vicinity of the centerbody. Reynolds stress measurements were also made in order to quantify the local turbulence structure. The scope of these measurements and the physical characteristics of the flow which were deduced from the data are described. The implications of the results from a turbulence modeling point of view is also discussed. GRA

N90-18672# Massachusetts Inst. of Tech., Cambridge. Dept. of Aeronautics and Astronautics.
ACTIVE STABILIZATION OF AEROMECHANICAL SYSTEMS Final Report, Sep. 1987 - Oct. 1989
J. Dugundji, A. H. Epstein, E. M. Greitzer, G. R. Guenette, and L. Valavani Dec. 1989 136 p
(Grant AF-AFOSR-0398-87; AF Proj. 2307)
(AD-A216629; AFOSR-89-1878TR) Avail: NTIS HC A07/MF A01 CSCL 20/4

Three separate sections are included. The first is a brief review of the work done on active control of rotating stall. The second is on the existence of precursor travelling waves in compressor annuli and on some of the signal processing techniques used to examine such waves. The third section describes first-of-a-kind experiments in which tailored system structural properties were used to suppress compression system aerodynamic instability (surge). GRA

N90-18673# Texas A&M Univ., College Station. Dept. of Mechanical Engineering.
ANALYTICAL AND EXPERIMENTAL INVESTIGATION OF MINIATURE HEAT PIPES, PHASE 2 Final Report, Mar. - Dec. 1988
G. P. Peterson, B. R. Babin, and D. Wu 24 Jun. 1989 70 p
(Contract F33615-86-C-2723)
(AD-A216945; WRDC-TR-89-2067) Avail: NTIS HC A04/MF A01 CSCL 13/1

A combined experimental and analytical investigation was conducted in order to identify and better understand the phenomena which govern the performance limitations and operating characteristics of micro heat pipes (heat pipes so small that the mean curvature of the vapor-liquid interface is comparable in magnitude to the reciprocal of the hydraulic radius of the flow channel). A steady state model was developed in which the effects of the extremely small characteristic dimensions on the conventional steady state heat pipe modeling techniques were examined. To further understand the behavior of these types of devices, a transient analytical model was developed, which could be used to predict steady state and transient behavior during start-up or variations in the evaporator thermal load. In the experimental portion of the investigation, two micro heat pipes, one copper and one silver, in cross-sectional area and in length, were evaluated experimentally to determine the accuracy of both the steady state and transient model and to provide verification of the micro heat pipe concept. Tests were conducted in a vacuum environment to eliminate conduction and convection losses. GRA

N90-18674# Stanford Univ., CA. Dept. of Aeronautics and Astronautics.
IMPROVED COMPUTATIONAL FLUID DYNAMICS FOR CONTINUUM HYPERSONIC FLOW Final Report, 1 Sep. 1986 - 31 Dec. 1989
Dean R. Chapman and Robert W. MacCormack Jan. 1990 19 p
(Contract DAAL03-86-K-0139)
(AD-A216981; ARO-24461.12-EG) Avail: NTIS HC A03/MF A01 CSCL 20/4

Two separate objectives were stated at the beginning of this research project: (1) to develop new numerical algorithms for the efficient and accurate solution of the continuum equations of viscous motion for high-temperature, chemically non-equilibrium, radiating hypersonic flow; and (2) to develop a new non-linear stress strain tensor for continuum equations of motion at high altitudes that is more accurate than the Navier-Stokes equations. The bottom line of this final report is that, relative to each of

these two objectives, much more has been accomplished than anticipated. For example, in regard to (1), a complete code was developed for computing hard-body flow-field radiation from Navier-Stokes equations taking into account thermodynamic, chemical, and ionization nonequilibrium; and in regard to (2), hypersonic solutions to the Burnett equations were obtained for the first time, and shown to provide both the non-linear stress-strain tensor and heat flux vector needed to yield computations at high altitudes that are much more accurate than the Navier-Stokes equations. This latter development reverses a commonly accepted opinion of thirty years that the Burnett equations can not be used for such purposes. GRA

N90-18675*# North Carolina State Univ., Raleigh. Dept. of Mechanical and Aerospace Engineering.

DEVELOPMENT OF A DEFECT STREAM FUNCTION, LAW OF THE WALL/WAKE METHOD FOR COMPRESSIBLE TURBULENT BOUNDARY LAYERS Ph.D. Thesis

Richard A. Wahls Washington NASA Mar. 1990 125 p
(Contract NCC1-117)
(NASA-CR-4286; NAS 1.26:4286) Avail: NTIS HC A06/MF A01 CSCL 20D

The method presented is designed to improve the accuracy and computational efficiency of existing numerical methods for the solution of flows with compressible turbulent boundary layers. A compressible defect stream function formulation of the governing equations assuming an arbitrary turbulence model is derived. This formulation is advantageous because it has a constrained zero-order approximation with respect to the wall shear stress and the tangential momentum equation has a first integral. Previous problems with this type of formulation near the wall are eliminated by using empirically based analytic expressions to define the flow near the wall. The van Driest law of the wall for velocity and the modified Crocco temperature-velocity relationship are used. The associated compressible law of the wake is determined and it extends the valid range of the analytical expressions beyond the logarithmic region of the boundary layer. The need for an inner-region eddy viscosity model is completely avoided. The near-wall analytic expressions are patched to numerically computed outer region solutions at a point determined during the computation. A new boundary condition on the normal derivative of the tangential velocity at the surface is presented; this condition replaces the no-slip condition and enables numerical integration to the surface with a relatively coarse grid using only an outer region turbulence model. The method was evaluated for incompressible and compressible equilibrium flows and was implemented into an existing Navier-Stokes code using the assumption of local equilibrium flow with respect to the patching. The method has proven to be accurate and efficient. Author

N90-18676# GTE Sylvania, Inc., Towanda, PA. Chemical and Metallurgical Div.

LOW COST FILTER DEVELOPMENT AND CONTROL OF PERMEABILITY IN HIGH TEMPERATURE, HIGH PRESSURE CERAMIC FILTER ELEMENTS Final Report

R. A. Long and J. L. Ferri Jun. 1989 48 p
(Contract DE-AC21-86MC-23250)
(DE90-000403; DOE/MC-23250/2750) Avail: NTIS HC A04/MF A01

For over a decade GTE Chemical and Metallurgical Division has been manufacturing cordierite ceramic crossflow heat exchangers. The heat exchanger application calls for a ceramic body that can withstand thermal shock, has good compressive strength and is capable of being formed into a impermeable membrane. With this experience base, it was a logical technology extension to pursue the engineering of this type of structure into a ceramic crossflow filter. The majority of this effort involved improving the permeability of the ceramic membrane to an adequate level for use in the hot gas particle removal from coal derived gas streams. When the permeability is achieved then the area of interest could shift to improvements of strength. As in most engineering situations, creating porosity was known to decrease strength and some trade off was probably going to be required. In addition to incorporating permeability into the existing extrusion and lay up technology, a secondary task was developed to investigate the possibility of creating the crossflow shape by means of some type of casting technique. The casting technique was of interest because it held promise of lower manufacturing costs and elimination of the interlayer bonds used in the other process. DOE

N90-18677# Lawrence Livermore National Lab., CA.

ANALYTIC SOLUTIONS FOR THE DECAY OF TURBULENT SWIRLING FLOW IN A CYLINDER

Lawrence D. Cloutman 12 Dec. 1989 22 p
(Contract W-7405-eng-48)
(DE90-005744; UCID-21862) Avail: NTIS HC A03/MF A01

A simple analytic model of the decay of turbulent swirling flow in constant volume combustion bombs and engine cylinders has been developed. The model is based on a simplified version of the Navier-Stokes equation with a specified eddy viscosity. The analytic solutions are compared to experimental results. The model provides adequate parametric fits to the data along with some insight into the processes affecting the swirling in-cylinder flows. DOE

N90-18678# Laboratorio de Computacao Cientifica, Rio de Janeiro (Brazil).

STRONG SOURCE HEAT TRANSFER SIMULATIONS BASED ON A GALERKIN/GRADIENT LEAST SQUARES METHOD

Leopoldo P. Franca and Eduardo G. DutradoCarmo May 1989 17 p
(DE90-608613; LNCC-011/89) Avail: NTIS (US Sales Only) HC A03/MF A01

Heat conduction problems with temperature-dependent strong sources are modeled by an equation with a laplacian term, a linear term and a given source distribution term. When the linear-temperature-dependent source term is much larger than the laplacian term, we have a singular perturbation problem. In this case, boundary layers are formed to satisfy the Dirichlet boundary conditions. Although this is an elliptic equation, the standard Galerkin method solution is contaminated by spurious oscillations in the neighborhood of the boundary layers. Herein we employ a Galerkin/Gradient-least-squares method which eliminates all pathological phenomena of the Galerkin method. The method is constructed by adding to the Galerkin method a mesh-dependent term obtained by the least-squares form of the gradient of the Euler-Lagrange equation. Error estimates, numerical simulations in one-and multi-dimensions are given that attest the good stability and accuracy properties of the method. DOE

N90-18679# Institut Franco-Allemand de Recherches, Saint-Louis (France).

STUDY OF THE DYNAMICAL BEHAVIOR OF COPPER IN A SHOCK WAVE Ph.D. Thesis - Inst. National Polytechnique de Lorraine [ETUDE DU COMPORTEMENT DYNAMIQUE DU CUIVRE SOUMIS A UNE ONDE DE CHOC]

Sophie Dujardin 31 Dec. 1988 216 p In FRENCH
(Contract DRET-87-070)
(ISL-R-123/88; ETN-90-96240) Avail: NTIS HC A10/MF A01

A method to test the dynamical behavior of systems under shock waves is proposed. The aim of the project is to show the shock pressure effect. A critical analysis of dynamical behavior laws of the metallic materials is supplied. Theoretical basis and experimental requirements of the proposed method are given. Computer aided design is applied. Experimental tests on copper are performed. A behavior law, as a function of shock hardening, strain rate effect and strain effect, is obtained and discussed. ESA

N90-18680# Institut Franco-Allemand de Recherches, Saint-Louis (France).

MEASUREMENT OF GAS INTENSITY AT HIGH DYNAMIC PRESSURES

F. Seiler, A. George, and G. Mathieu 6 Mar. 1989 16 p

Presented at the 3rd International Symposium on High Dynamic Pressures, La Grande Motte, France, 5-9 Jun. 1989
(ISL-CO-204/89; ETN-90-96242) Avail: NTIS HC A03/MF A01

For density detection, the laser-Doppler-velocimeter, commonly used for flow velocity measurements was chosen. With this device it is possible to determine the temporal variation of the refractive index distribution caused by density changes in the gas volume crossed by a laser beam. A Michelson interferometer with different legs is used for light processing. Taking into account the relation between the gas density and the refractive index, the gas density distribution versus time is obtained. This measuring technique for gas density determination seems not to be affected by high gas pressures and high pressure gradients. ESA

N90-18681# Institut Franco-Allemand de Recherches, Saint-Louis (France).
DIRECT SIMULATION MONTE CARLO OF SHOCK REFLEXION ON A WEDGE WITH BOUNDARY LAYER
F. Seiler, H. Oertel, and B. Schmidt (Karlsruhe Univ., Germany, F.R.) 21 Nov. 1988 21 p Presented at the 16th International Symposium on Rarefield Gas Dynamics, Pasadena, CA, 10-16 Jul. 1988
(ISL-CO-245/88; ETN-90-96248) Avail: NTIS HC A03/MF A01

A numerical investigation of pseudo-steady oblique shock wave reflexion by a wedge at low densities is presented. The real gas flow is simulated at the molecular level by a large number of model particles following their positions in phase space. A two dimensional computational model is used to generate the shock reflexion. Calculations are carried out for a shock Mach number 3 and a monatic gas. Simulation results give information about the time dependent regular and Mach reflexion flow field development, beginning at the wedge leading edge and switching into a quasi-stationary shock reflexion arrangement. ESA

N90-18682# Institut de Mecanique des Fluides de Marseille (France).
EXPERIMENTAL INVESTIGATIONS OF THE UNSTEADY BOUNDARY LAYER ON AN OSCILLATING FLAT PLATE. OPTIMIZATION AND VALIDATION OF A CODE, FOR CALCULATING THE POTENTIAL FLOW/BOUNDARY LAYER COUPLING OF A FLAT PLATE AND OF AN OSCILLATING PROFILE Interim Report [ETUDE EXPERIMENTALE DE LA COUCHE LIMITE INSTATIONNAIRE SUR UNE PLAQUE PLANE OSCILLANTE. OPTIMISATION ET VALIDATION D'UN CODE DE CALCUL DE COUPLAGE ECOULEMENT POTENTIEL/COUCHE LIMITE AUTOUR D'UNE PLAQUE PLANE ET D'UN PROFIL OSCILLANT]
D. Favier, C. Maresca, J. Belleudy, M. AliPacha, C. Barbi, A. Agnes, S. Gagliano, G. Molinard, and D. Poupinet Jul. 1989 34 p In FRENCH
(Contract DRET-87-272)
(ETN-90-96254) Avail: NTIS HC A03/MF A01

In the scope of the project for the development of an onboard laser anemometer, the feasibility of onboard measurements, the materials and software for data acquisition are analyzed. The experimental results of the unsteady boundary layer on an oscillating flat plate, performed by means of an optical fiber laser anemometer, are given. The tests carried out on the oscillating profile are summarized. The selected tests for the validation of the code to be applied on the potential flow/boundary layer coupling calculations are presented. Theoretical and experimental calculations are compared. ESA

N90-18683# Ecole Normale Superieure, Paris (France). Groupe de Physique des Solides.
CONCEPTS AND EXPERIMENTS ON SPACE-TIME CHAOS Status Report [A PROPOS DU CHAOS SPATIO-TEMPOREL, CONCEPTS ET EXPERIENCES: RAPPORT DE MISE AU POINT]
Arnaud Chiffaudel 1988 65 p In FRENCH
(Contract IEP-87/22)
(ETN-90-96255) Avail: NTIS HC A04/MF A01

The space-time behavior of hydrodynamic turbulent flow is investigated. The theoretical background equations for spatial description of chaos are given. The nonlinear systems under investigation are analyzed. Several nonlinear regimes observed are described and their contribution to the understanding of the turbulence flow transition are underlined. The similarities and particularities of those systems allow the main space-time chaos characteristics to be described. An accurate analysis of the theoretical equations application limits must be carried out to allow a better fitting to the experimental results. ESA

N90-18684# Technische Univ., Delft (Netherlands).
A STUDY ON DEFORMATION AND BREAK-UP OF DISPERSED PARTICLES IN ELONGATIONAL FLOW Ph.D. Thesis
Christine vanderReijden-Stolk 1989 166 p
(ETN-90-96268) Avail: NTIS HC A08/MF A01

In a study to predict the morphology of dispersions of molten polymers by means of process and material parameters, the behavior of one droplet during deformation and breakup caused by a flow was studied. A four-roller apparatus was built to realize a steady elongational flow. The time-dependency of the deformation was studied by measuring the relaxation of the deformation in the four-roller apparatus. General deformation theories are described. The fluids and molten polymers used, and the deformation experiments carried out are described. The breakup of single droplets and the formation of dispersions in real blenders are examined. ESA

N90-18685# Office National d'Etudes et de Recherches Aerospatiales, Paris (France).
SPECTRAL MULTI-DOMAIN APPROXIMATION OF THE NAVIER-STOKES EQUATIONS IN CURVED COMPLEX GEOMETRIES Ph.D. Thesis - Paris Univ. 6
Brigitte Metivet 1987 182 p In FRENCH; ENGLISH summary
(ONERA-NT-1987-2; ISSN-0078-3781; ETN-90-96288) Copyright Avail: NTIS HC A09/MF A01

A spectral method for solving the Navier-Stokes equations for incompressible viscous fluids is proposed. Cases involving nonperiodic boundary conditions and complex three dimensional geometries are considered. The two following subjects are theoretically and numerically analyzed: discretization, where a finite difference time and collocation space scheme is used, and discrete velocity and pressure spaces fulfilling the inf-sup condition are chosen; the handling of the geometry, where the solution domain is divided into subdomains which can be mapped onto a cube and the patching method is related to Schwarz algorithm. ESA

N90-18686# Office National d'Etudes et de Recherches Aerospatiales, Paris (France).
NUMERICAL SIMULATION OF THE INCOMPRESSIBLE INHOMOGENEOUS TURBULENCE IN A PLANE CHANNEL FLOW Ph.D. Thesis - Inst. National Polytechnique de Toulouse [SIMULATION NUMERIQUE DE LA TURBULENCE INHOMOGENE INCOMPRESSIBLE DANS UN ECOULEMENT DE CANAL PLAN]
Veronique Deschamps 1988 236 p Partly in FRENCH and ENGLISH
(ONERA-NT-1988-5; ISSN-0078-3781; ETN-90-96289) Avail: NTIS HC A11/MF A02

The physical problem is modeled by Navier-Stokes equations for an incompressible fluid with periodic boundary conditions in homogeneous directions and no slip conditions in the inhomogeneous direction. The flow rate, energy predictions and energy equations depend strongly on the imposed mean pressure gradient. In a numerical method, derivatives are discretized by a fourth order finite difference scheme in space and a second order one in time; the incompressibility condition is achieved by a global technique. Substational gains in computational time are obtained. A detailed analysis of the simulations, first validated by experiments, is completed by energy balances for each Reynolds stress component. Use of direct simulation in statistical modeling, especially second order modeling, is discussed. Results obtained by large eddy simulation with subgrid models are shown. ESA

N90-18687# Office National d'Etudes et de Recherches Aerospatiales, Paris (France). Direction Scientifique de la Resistance des Structures.
TRANSIENT RESPONSES OF COUPLED SYSTEMS Final Report [REPONSES TRANSITOIRES DE SYSTEMES COUPLES]
H. Berger and R. Ohayon Feb. 1989 42 p In FRENCH
(Contract DRET-87-34-001)
(ONERA-RT-13/3596-RY-070-R; ETN-90-96293) Avail: NTIS HC A03/MF A01

The transient response of fluid-structure coupled systems, submitted to weak shock waves, is investigated. Plane or spherical waves are considered. The analysis is performed by applying structural element and fluid finite element methods, and the infinite field two-fold asymptotic development. The time integration algorithm allows a modular organization of the calculations. The procedure leads to reasonable calculation times, when compared to those obtained by direct methods, such as the Kirchoff lag potential. ESA

N90-18688# Office National d'Etudes et de Recherches Aerospatiales, Paris (France). Direction de l'Aerodynamique.
INTERACTION BETWEEN OBLIQUE-ANGLED INCIDENT SHOCK WAVE AND TURBULENT BOUNDARY LAYER ON A HEATED WALL. EXPERIMENTAL RESULTS [INTERACTION ONDE DE CHOC OBLIQUE/COUCHE LIMITE TURBULENTE SUR PAROI CHAUFFEE. RESULTATS EXPERIMENTAUX]
M. Stalter and J. Delery Mar. 1989 107 p In FRENCH
(Contract DRET-87-34-001)
(ONERA-RT-84/7078-AY; ETN-90-96295) Avail: NTIS HC A06/MF A01

The interaction resulting from the reflection of an incident oblique-angled shock wave on a turbulent boundary layer, developed on a heated wall, is investigated. The experiments are carried out in a 2-D plane device, with a Mach number equal to 2.4. Two different incident shock wave intensities are considered. The interactions are examined under adiabatic conditions and for a wall heating ratio of T sub p/T sub f=2. The observations were performed by means of temperature and pressure sounding techniques and laser anemometry. ESA

N90-18689# Office National d'Etudes et de Recherches Aerospatiales, Paris (France). Direction de l'Aerodynamique.
NUMERICAL SIMULATION OF THE VORTEX BREAKDOWN Final Report [SIMULATION NUMERIQUE DE L'ECLATEMENT TOURBILLONNAIRE]
P. Mege and T. H. Le Jun. 1989 37 p In FRENCH
(Contract DRET-88-34-001)
(ONERA-RSF-4/4368-AY-004A; ETN-90-96296) Avail: NTIS HC A03/MF A01

The results of the numerical calculations of the rupture of an isolated vortex are presented. The chosen method applies Navier-Stokes equations on velocity and pressure field formulations. Concerning boundary values, periodicity conditions in transversal directions and input/output conditions in the axial direction are considered. The discretization is carried out by means of space and time calculations, involving respectively 4th and 2nd orders. ESA

N90-18690# Oak Ridge National Lab., TN. Mathematical Sciences Section.
MODELING CONVECTIVE MARANGONI FLOWS WITH VOID MOVEMENT IN THE PRESENCE OF SOLID-LIQUID PHASE CHANGE
John B. Drake Jan. 1990 34 p
(Contract DE-AC05-84OR-21400)
(DE90-006474; ORNL-6516) Avail: NTIS HC A03/MF A01

This report describes a numerical method for solving heat conduction and fluid flow problems that involve phase changes. The complications arising from materials with different liquid and solid densities are discussed, and approximations are developed for Marangoni stress, curvature dependent pressure jumps and void movement. Applications to both 0-g and 1-g environments are discussed. The fluid flow algorithm is a variant of the projection method for incompressible liquids. A control volume method of discretization along with an appropriate formulation of the conservation laws for mass and momentum yield a weak form which applies throughout the computational region. In this form no fronts between liquid and solid or between liquid and void are explicitly tracked, though the position of the fronts is readily determined from the solution field variables. The discrete equations use an implicit Crank-Nicolson method. The non-linear implicit equations are solved using a Newton method with an Approximate Factorization method for the iterative solution of the Jacobian system. DOE

N90-18691# University of Southern California, Los Angeles. Dept. of Mechanical Engineering.
FLUIDIZATION MECHANISMS IN SLURRY FLOW
Charles S. Campbell 1989 59 p Prepared for Pittsburgh Energy Technology Center, PA
(Contract DE-FG22-86PC-90957)
(DE90-006497; DOE/PC-90957/T8) Avail: NTIS HC A04/MF A01

There are two mechanisms by which heavy settling particles may be suspended in a horizontal slurry flow: (1) by particle-particle interactions (e.g., Bagnold dispersive stresses), and (2) by particle-fluid interactions (e.g., entrainment of the particles by turbulent eddies). The purpose of this investigation is to determine to what extent each fluidization mechanism is active and the effect of the fluidization mechanism on the global properties of the slurry. The technique employs the understanding that the particles entrained in the turbulence of the fluid will appear as an increased hydrostatic head across the channel. This may be directly measured and can be related to the fraction of the mass of particles that are supported by fluid-particle forces. The rest must therefore be supported by particle-particle forces. DOE

N90-18692# Edgerton, Germeshausen and Grier, Inc., Idaho Falls, ID. Energy and Systems Technology.
DRYOUT STABILITY AND INCEPTION AT LOW FLOWRATES
R. B. Duffey and E. D. Hughes Nov. 1989 32 p
(Contract DE-AC07-76ID-01570)
(DE90-006955; EGG-EAST-8491) Avail: NTIS HC A03/MF A01

A theoretical model for the heat flux required to maintain a stable hot patch on a heated surface cooled by a falling liquid film is developed. The dryout patch may be initially formed by hydrodynamic processes within the liquid film, but a higher heat flux is required to maintain the patch at an equilibrium size, neither growing or shrinking. The theoretical model is based on an analytical solution of the 2-D heat equation with boundary conditions supplied by heat transfer coefficient correlations appropriate to the fluid conditions at the hot dry patch and at the wet region from the patch. The analytical results show that the heat flux required to maintain a dry patch is a function of only these correlations. This functional dependency has also been observed for the physically similar processes associated with quenching of an initially hot surface by a falling (or rising) liquid film. Using physically reasonable correlation forms for the dry patch and wet region heat transfer correlations, the heat flux is expressed as a function of the liquid film Reynolds number. The experimental data were obtained for liquid films falling on the outside of heated rods with heated lengths from 0.50 to 3.66 m and heated diameters from 7.5 to 52.0 mm. The liquid film Reynolds number for the experimental data ranges from about 100 to about 10,000 and the heat flux ranges from about 1 to about 300 kW/sq m. DOE

N90-18693# Oak Ridge National Lab., TN. Efficiency and Renewables Research Section.
TRANSFER OF HEAT PUMP TECHNOLOGY Foreign Trip Report
Martin A. Broders 23 Feb. 1990 12 p
(Contract DE-AC05-84OR-21400)
(DE90-007373; ORNL/FTR-3524) Avail: NTIS HC A03/MF A01

The traveler participated in the activities of the first meeting of the IEA Heat Pump Center National Team Working Group. The meeting provided a forum for National Team representatives from seven participating countries to share information about their respective National Team organization, activities and priorities; and the status of heat pumps in their countries. Particular attention was given to discussion of topics and content of future IEA-HPC Newsletters, analysis studies and workshops. In-depth, follow-up discussions of U.S. National Team activities with both the IEA-HPC and IEA-CADDET were held with staff personnel at the operating agent Netherlands Agency for Energy and the Environment (NOVEM) headquarters in Sittard, The Netherlands. DOE

N90-18694# Institut Franco-Allemand de Recherches, Saint-Louis (France).
MEASUREMENT OF GAS LEAKS BETWEEN A PROJECTILE AND THE WALLS OF A TUBE IN A BALLISTIC COMPRESSOR [MESSUNG DES GASSCHLUPFS IN EINEM BALLISTISCHEN KOMPRESSOR]
H. Mach 30 Nov. 1988 23 p In GERMAN Presented at 14th Symposium Innenballistische Leistungssteigerung von Rohrwaffen, Swisttal-Heimerzheim, Fed. Republic of Germany, 8-10 Nov. 1988
(ISL-CO-250/88; ETN-90-96250) Avail: NTIS HC A03/MF A01

Parameters affecting gas leaks between the projectile and the tube walls are investigated. A piston type ballistic compressor is used in order to recreate the temperature and pressure conditions of a real weapon 20 mm in caliber. Experiments are carried out using N2, H2 and a mixture of He and H2 gases. To measure the amount of gas leaking between the projectile and the tube walls, the gas volume behind the projectile is measured using interferometric methods. Different gas pressures, length of projectile and type of gas are used in the course of the experimentation. The results show that a circular groove around the outside of the projectile minimizes gas leaks. ESA

N90-18695# Institut de Mecanique des Fluides de Marseille (France). Equipe Mecanique des Fluides Numerique.
NUMERICAL INVESTIGATIONS OF HEAT TRANSFER AND FLOW RATES IN ROTATING CAVITIES. SIMULATION OF THE MOVEMENT GENERATED BY WALL TEMPERATURE GRADIENTS, BY SOURCE-SINK MASS FLOWS OR BY THE DIFFERENTIAL ROTATION OF THE WALLS, UNDER THE INFLUENCE OR CORIOLIS AND CENTRIFUGAL FORCES Final Report, Sep. 1987- Sep. 1988 [ETUDE NUMERIQUE DES TRANSFERTS THERMIQUES ET DES REGIMES D'ECOULEMENTS DANS LES CAVITES EN ROTATION. SIMULATION DES MOUVEMENTS GENERES PAR LES GRADIENTS DE TEMPERATURE PARIETAUX, PAR LES FLUX DE MASSE SOURCE-PUITS OU PAR UNE ROTATION DIFFERENTIELLE]
A. Randriamampianina, A. Chaouche, P. Bontoux, G. P. Extremet, E. Segura, L. Outters, J. P. Fontaine, C. Long, C. Vaughan, and B. Roux et al 15 Feb. 1989 181 p In FRENCH
(Contract DRET-87-34-083-00-470-75-01)
(ETN-90-96253) Avail: NTIS HC A09/MF A01

The aim of the study is the simulation of a rotor-stator cavity model, reflecting real situations occurring in turbomachinery. The investigations performed on rotating disks systems are reviewed. The mathematical models and different numerical resolution methods are summarized. The results obtained in the case of rotating cavities, assuming the uniform rotation of the walls, are reported. The rotor-stator configurations, analyzed in the case of the differential rotation of the walls, are described. With regard to thermal effects, the density variation effects must be taken into account. ESA

N90-18696# European Space Agency, Paris (France).
STUDY ON THE THERMODYNAMICAL AND MECHANICAL CONDITIONS FOR THE GENERATION OF HIGH OPERATING PRESSURES WITH LIQUEFIED GASES FOR LOW AND VERY LOW FLOW RATES Ph.D. Thesis - Univ. of Stuttgart
Willi Nieratschker Dec. 1989 182 p Transl. into ENGLISH of Untersuchung der physikalischen und mechanischen Voraussetzungen zur Erzeugung hoher Betriebsdruecke mit Fluessiggasen fuer kleine und kleinste Foerdermengen, Dec. 1988 146 p Original language document was announced as N89-25429
(ESA-TT-1148; DFVLR-FB-88-54; ETN-90-96329) Avail: NTIS HC A09/MF A01; original German version available from DFVLR, Postfach 90 60 58, 5000 Cologne 90, Fed. Republic of Germany, 51 DM

An investigation of the thermodynamical and mechanical conditions for extending the flow rate range in the direction of low flow rates with regard to the delivery of liquefied gases at high operating pressures is presented. For low flow rates, the especially critical cavitation problem connected with the pumping of liquefied gases becomes more acute, since with decreasing volume the ratio of heat losses to the hydraulic power becomes ever more unfavorable. A first prototype is designed, produced and investigated to evaluate design-related heat loss and piston seal problems. An approach to the solution is indicated for both problem areas with the application of a new and patented pump principle, and through investigation of a second prototype modified in several respects. By reducing the pump mass when designing the second pump prototype, the nonstationary cooling phase is greatly shortened, so that intermittent pump operation becomes possible when the pump is housed external to the storage tank. ESA

N90-18697# European Space Agency, Paris (France).
CONTRIBUTION TO THE STUDY OF THREE-DIMENSIONAL SEPARATION IN TURBULENT INCOMPRESSIBLE FLOW
Bruno Chanetz (Office National d'Etudes et de Recherches Aerospatiales, Paris, France) Jan. 1990 171 p Transl. into ENGLISH of Contribution a l'Etude du Decollement Tridimensionnel en Ecoulement Turbulent Incompressible (Paris, France, ONERA), 1988 Original language document was announced as N89-29723
(ESA-TT-1169; ONERA-NT-1988-6; ETN-90-96331) Avail: NTIS HC A08/MF A01

An ellipsoid cylinder of revolution model consisting of half an ellipsoid with a cylindrical extension is considered. Pressure measurements at the wall made it possible to obtain a precise description of wall flow for a wide range of velocities (from 10 to 90 m/s) and angles of attack (from 0 to 40 deg). Oil-streak patterns were used for visualization of separation and transition lines. A discussion on the topology of flow patterns based on the experimental data and the work of Legendre is given. An oblate ellipsoid cylinder model whose front section is half an oblate ellipsoid and whose rear section is a cylindrical extension is considered. The surrounding flow for fixed velocity (50 m/s) and angle of attack (30 deg), was investigated with a 5-hole pressure probe and a three-direction laser Doppler velocimeter. Detailed information about the mean and turbulent values of the external field on the upper surface in the region where vortex structures originate and develop is derived. Pressure, velocity and vorticity fields reveal the vortex structure. The analysis based on mean values is completed by a detailed examination of results on turbulent flow. ESA

35 INSTRUMENTATION AND PHOTOGRAPHY

Includes remote sensors; measuring instruments and gages; detectors; cameras and photographic supplies; and holography.

For aerial photography see *43 Earth Resources and Remote Sensing*. For related information see also *06 Aircraft Instrumentation*, and *19 Spacecraft Instrumentation*.

N90-18698# Central Research Inst. of Electric Power Industry, Tokyo (Japan). Energy and Environment Lab.
MEASUREMENT OF SPECTRAL EMISSIVITY BY FOURIER TRANSFORM INFRARED SPECTROMETER

Yukio Nakano and Minoru Miyakawa Sep. 1988 25 p In JAPANESE; ENGLISH summary
(DE89-782319; CRIE-T-87109) Avail: NTIS (US Sales Only) HC A03/MF A01

An experimental model of a spectral emissivity measurement apparatus was made using Fourier Transform Infrared Spectrometer (FT-IR) and a blackbody radiator to measure the power radiated from infrared radiators. FT-IR is a kind of an interference type spectrometer. By guiding the light to be measured to the interferometer, the spectrum is obtained from interference fringes by Fourier transform. The blackbody radiator is a sham apparatus of an imaginary closed space (blackbody) in thermal equilibrium state. The object of the apparatus is infrared radiators of more than about 40 C, so the infrared rays radiated from the radiators of comparatively low temperature such as heaters may be applied and it is made to measure the spectral emissivity collectively in the range of more than about 2 m wavelength. Applying this apparatus, 70 to 90 percent of the whole power radiated from the sample was measured. The apparatus makes it possible to calculate correct spectral emissivity by confirming the linearity of the apparatus response to the incident power and at the same time measuring at two different temperatures. DOE

N90-18699# Instituto de Pesquisas Espaciais, Sao Jose dos Campos (Brazil).
BEAM COLLECTOR AND OUTPUT WINDOW FOR A 35 GHz 100 kW GYROTRON
J. J. Barroso Nov. 1989 24 p
(INPE-4958-RPE/603) Avail: NTIS HC A03/MF A01

Practical considerations for the beam collector and output window design of a 35 GHz, 100 kW gyrotron are presented. A ballistic model for the electron flow in the collector region is developed with the subsequent determination of a large collecting area to withstand the power deposited by the impinging electron beam. The cooling system was devised in order that the collector cool-down time be compatible with the pulsed regime of one shot per minute. Thermophysical properties of dielectric windows relevant to powerful gyrotrons are also reported. Author

N90-18700# Instituto de Pesquisas Espaciais, Sao Jose dos Campos (Brazil).
CONSTRUCTION AND CALIBRATION OF A GAS PRESSURE METER WITH HIGH TEMPORAL RESOLUTION [CONSTRUCAO E CALIBRACAO DE UM MEDIDOR DE PRESSAO DE GAS COM ALTA RESOLUCAO TEMPORAL]
J. O. Rossi, C. Santos, and M. Ueda Nov. 1989 32 p In PORTUGUESE; ENGLISH summary
(INPE-4953-RPE/602) Avail: NTIS HC A03/MF A01

The construction and calibration of a gas pressure meter with a time resolution better than 20 microsec are described. The meter consists basically of a sensor of the Fast Ionization Gage (FIG) type and an adequate electronic circuit. A 6AU6A pentode vacuum tube without the glass envelope is used as the sensor head. Author

N90-18701# Instituto de Pesquisas Espaciais, Sao Jose dos Campos (Brazil).
MULTIPARAMETER SCATTEROMETER FOR REMOTE SENSING (RADSER). PROJECT SCATTER: STATE-OF-THE-ART AND FUTURE APPLICATIONS [RADAR DIFUSOMETRO DE SENSORIAMENTO REMOTO (RADSER) - PROJETO SCATTER-ESTADO DA ARTE E APLICACOES FUTURAS]
Joao VianeiSoares, Hermann Johann HeinrichKux, Luiz Flavio Rodrigues, Flavio Magina, Jose Luiz Sarmento, Leopoldo MessengerParada, Luciano Sacilotti, and Joao BoscoPereirados-Reis Aug. 1989 9 p In PORTUGUESE; ENGLISH summary Presented at the 5th Brazilian Symposium on Remote Sensing, Natal, Brazil, 11-15 Oct. 1988
(INPE-4871-PRE/1482) Avail: NTIS HC A02/MF A01

The Brazilian Space Research (INPE), decided to build a multiparameter Scatterometer (C and X bands, H and V polarization) in order to acquire technology in the field of Microwave Remote Sensing, since there is a great tendency for utilizing microwave data in the next decade (for example, ERS-1, JERS-1, RADARSAT and the SARs of the Eos program). The main applications envisaged of such instrument are: (1) estimation of soil moisture; (2) crop classification and identification of phenological status; (3) sea surface wind speed; and (4) wave pattern of the sea. The general characteristics are described and the applications envisaged are pointed out in a more detailed manner. Author

N90-18702# California Univ., Berkeley. Lawrence Berkeley Lab. Dept. of Electronics Engineering.
HIGH SPEED IMAGING WITH A TAPPED SOLID STATE SENSOR
Bojan T. Turko and Mauro Fardo Oct. 1989 6 p Presented at the IEEE Nuclear Science Symposium, San Francisco, CA, 22-26 Jan. 1990
(Contract DE-AC03-76SF-00098)
(DE90-006116; LBL-27048; CONF-900143-17) Avail: NTIS HC A02/MF A01

A high speed camera with a solid state diode array sensor is described. 500 frames/second rates are achieved by dividing the 256 times 256 pixel array into eight sections. The detected photocharge is tapped in parallel from each section into independent signal processing channels. The circuits for video signal extraction and processing are described and data on measured signal-to-noise ratio, sensitivity and crosstalk are presented. Image artifacts are also discussed and the effectiveness of the sensor fast clear procedure for their elimination shown. DOE

N90-18703# Institut Franco-Allemand de Recherches, Saint-Louis (France).
DEVELOPMENT AND POLARIZATION OF FERROELECTRIC POLYMER GAUGES, FOR DYNAMICAL ACCELERATION EXPERIMENTS, AS THOSE IN BALLISTICS SHOCKS [REALISATION ET POLARISATION DE JAUGES EN POLYMERE FERROELECTRIQUE POUR ESSAIS DE MESURES D'ACCELERATIONS EN DYNAMIQUE DANS LE CAS, PAR EXEMPLE, DE CHOCS BALISTIQUES]
F. Bauer, K. Harnischmacher, and J. Riha 24 Aug. 1988 20 p In FRENCH
(Contract ETCA/CTME/RM-20221/85)
(ISL-R-119/88; ETN-90-96239) Avail: NTIS HC A03/MF A01

Studies concerning the development and polarization of ferroelectric polymer gages for acceleration measurements are summarized. The acceleration intensities may reach 300,000 g. Polyvinylidene fluoride films of 40 microns, of polarized active surface between 1 and 25 sq mm, are obtained. The gages piezoelectric coefficient is about 48 pC/N. The accelerometer's design is given and the electrical and mechanical parameters are calculated. The accelerometer's behavior in a Hopkinson system is analyzed and the results are given. ESA

N90-18704# Institut Franco-Allemand de Recherches, Saint-Louis (France).
PROBLEMS OF THE MICRO-HOLOGRAPHIC IMAGE ANALYSIS [LES PROBLEMES DE L'EXPLOITATION DES IMAGES EN MICROHOLOGRAPHIE]
H. Royer 4 Jan. 1989 23 p In FRENCH Presented at the 2nd Colloguium Franco-Allemand sur les Applications de l'Holographie, Saint-Louis, France, 24-25 Nov. 1988
(ISL-CO-201/89; ETN-90-96241) Avail: NTIS HC A03/MF A01

A method for the analysis of holographic images is proposed. The problems involving the analysis of reconstructed images are reviewed: the time needed for the analysis, the distinction between small particles and speckle grains, image resolution and pattern recognition. The improvements obtained by the automatization of the analysis as well as the limitations concerning granulometry and velocimetry, are discussed. Scattering methods in granulometry and Fourier transform application in velocimetry are suggested. ESA

N90-18705# Institut Franco-Allemand de Recherches, Saint-Louis (France).
PIEZOELECTRIC POLYMER PVDF SHOCK GAUGE: STATE OF THE RESEARCH ART
F. Bauer, R. A. Graham, L. M. Lee, G. Samara, K. Hirnischmacher, and J. Riha 12 Apr. 1989 25 p Presented at the 39th Aeroballistic Range Association, Alberquerque, NM, 10-14 Oct. 1988
(ISL-CO-207/89; ETN-90-96243) Avail: NTIS HC A03/MF A01

Ferroelectric properties of PVDF (polyvinylidene fluoride) polymers are presented. The polarization process of these organic materials influences the piezoelectric properties and their behavior under dynamic compression and shock loading. Using pressure wave propagation the polarization distribution obtained by the process is measured. The polarization homogeneity is observed to be very good over the whole thickness of the samples. The standard poled PVDF gage is presented: preparation, polarization, process. The electrical response of PVDF shock gages was studied under shock loading. The observed response shows good fidelity until 30 GPa. Shock calibration data of standardized gauges are examined in the case of impact loading. The frequency, temperature and hydrostatic pressure dependencies of the dielectric properties, molecular relaxations and phase transition in PVDF are reported. The dynamic melting temperature of PVDF shows a large increase with pressure which suggests explanation of why it is possible to use these polymers as shock wave gages at relatively high shock pressure. A characteristic example of PVDF shock pressure measurement is shown. ESA

N90-18706# Brookhaven National Lab., Upton, NY.
STATE OF THE ART IN SEMICONDUCTOR DETECTORS
P. Rehak and E. Gatti (Politecnico di Milano, Italy) 1989 19 p Presented at the 4th Pisa Meeting on Advanced Detectors: Frontier Detectors From Frontier Physics, La Biodola, Italy, 21-26 May 1989 Submitted for publication Sponsored in part by Instituto Nazionale di Fisica Nucleare and CNR
(Contract DE-AC02-76CH-00016)
(DE90-005567; BNL-43538; CONF-8905194-7) Avail: NTIS HC A03/MF A01

The state of the art in semiconductor detectors for elementary particle physics and x ray astronomy is briefly reviewed. Semiconductor detectors are divided into two groups, classical semiconductor diode detectors and semiconductor memory detectors. Principles of signal formation for both groups of detectors are described and their performance is compared. New developments of silicon detectors are reported. DOE

N90-18707# Lawrence Livermore National Lab., CA.
COMPUTATIONAL AND VISIBLE LIGHT EXPERIMENTS FOR X RAY LASER HOLOGRAPHY
James M. Brase, Thomas J. Yorkey, and Donald C. Peters 1989 9 p Presented at the Conference on X ray Microimaging for the Life Sciences, Berkeley, CA, 24-26 May 1989
(Contract W-7405-eng-48)
(DE90-006774; UCRL-101572; CONF-8905192-3) Avail: NTIS HC A02/MF A01

Due to the fact that most biological objects of interest are embedded in a complex three-dimensional, it is difficult to estimate the usefulness of x ray images of complex objects using usual measures of resolution such as Rayleigh criteria. We are approaching this problem for the design and characterization of x ray holography systems by developing computational tools for the simulation of x ray hologram formation and for their computational reconstruction. These efforts are closely coupled with a scaled visible light experimental program which validates both the simulations and the reconstruction techniques. The use of simulations allows us not only to establish resolution limits for complex objects but also to vary the parameter space in a controlled manner to optimize imaging system designs. DOE

N90-18708# Sandia National Labs., Albuquerque, NM. Div. of Explosives Applications.
EXCESS TRANSIT TIME AS A FUNCTION OF BURST CURRENT IN AN EXPLODING BRIDGEWIRE DETONATOR
Paul W. Cooper, Rodney N. Owenby, and Jerome H. Stofleth 1990 10 p Presented at the 14th Symposium on Explosives and Pyrotechnics, Burlingame, 13-15 Feb. 1990
(Contract DE-AC04-76DP-00789)
(DE90-007168; SAND-89-2327C; CONF-900254-1) Avail: NTIS HC A03/MF A01

Transit time, the time from bridgewire burst until breakout of detonation from the output pellet of an exploding bridgewire detonator, was measured as a function of burst current. From this data, in conjunction with known equations for run distance versus pressure, unreacted explosive Hugoniots, and detonation properties of the initial pressing pellet, the run distance in the initial pressing explosive pellet and shock pressure from the exploding bridgewire were determined, both as a function of burst current. DOE

N90-18709# Institut Franco-Allemand de Recherches, Saint-Louis (France).
VELOCITY MEASUREMENT USING INTERFEROMETRY [INTERFEROMETRISCHE GESCHWINDIGKEITSMESSUNGEN]
G. Smeets 11 Aug. 1988 33 p In GERMAN Presented at Kolloquium Mechanik und Stroemungsmechanik, Essen, Fed. Republic of Germany, 26 May 1988
(ISL-CO-221/88; ETN-90-96245) Avail: NTIS HC A03/MF A01

Doppler velocity measuring techniques using a Michelson spectrometer, to analyze wave length variation in a beam of light after diffusion, are described. An electric signal directly proportional to variations in wave length is obtained. This signal is used to determine the speed of the diffusing object. Applications of this technique to mechanics and fluid mechanics are described. The way in which Doppler imaging can be used to analyze the instantaneous speeds of flow around a flat or luminous surface is described. ESA

N90-18710# Erno Raumfahrttechnik G.m.b.H. Bremen (Germany, F.R.). Ressort Neue Programme und Technologie.
REFURBISHMENT AND MODIFICATION OF THE METRIC CAMERA (RMK) FOR REFLIGHT ON EOM-1 SPACELAB MISSION Final Report, 12 Dec. 1987
Tuncer Miski Jan. 1988 30 p In GERMAN; ENGLISH summary Presented at the DFVLR-RF-TN1 Conference, Porz-Wahn, Fed. Republic of Germany, Jan. 1988 Prepared in cooperation with MBB GmbH, Bremen, Fed. Republic of Germany
(Contract BMFT-01-QS-104)
(ETN-90-96284) Avail: NTIS HC A03/MF A01

The steps involved in rebuilding and modifying the metric camera for reflight on the Spacelab Earth Observation Mission (EOM) are described. Diagrams of the camera storage racks and control keyboard are presented. Photographs of the camera itself are presented. The steps involved in research and development of the camera improvements are presented in diagrammatic form. The results of audible noise and vibration tests are presented. The modifications carried out on the camera are described. ESA

N90-18711# European Space Agency, Paris (France).
SYNCHRONIZATION OF THE GROUND STATION ATOMIC CLOCKS USING THREE WEIGHTED TRANSPORTABLE CESIUM TIME STANDARDS IN THE NAVEX NAVIGATION EXPERIMENT
Herbert Schild (Deutsche Forschungs- und Versuchsanstalt fuer Luft- und Raumfahrt, Oberpfaffenhofen, Germany, F.R.) Jan. 1990 43 p Transl. into ENGLISH of Synchronisierung der Bodenstationscaesiumnormale mittels Uhrentransport unter Benutzung von drei gewichteten Caesiumuhren beim Navigationsexperiment NAVEX (Oberpfaffenhofen, Fed. Republic of Germany, DFVLR), Jul. 1989 34 p Original language document was announced as N89-25448
(ESA-TT-1153; DFVLR-Mitt-89-01; ETN-90-96330) Avail: NTIS HC A03/MF A01; original German version available from

DFVLR, Postfach 90 60 58, 5000 Cologne 90, Fed. Republic of Germany, 15.50 DM

In the Navex experiment performed during the D1 Spacelab mission, time signals were transmitted from on board the Spacelab to three ground stations. Each of these stations was equipped with a cesium time standard, which were required to be synchronized because of various experimental objectives. This synchronization was accomplished by means of two-way clock transfers, for which three traveling cesium standards with different weighting were used for averaging reasons. It is shown how the weighting factors were derived from the rates of the traveling clocks at rest and from their rates while traveling, using the UTC(PTB) (coordinated universal time as output by Physikalisch-Technische Bundesanstalt) as reference time scale. ESA

N90-18483*# Ball Aerospace Systems Div., Boulder, CO.
RF MODAL QUANTITY GAGING
K. VanLeuven *In* Johns Hopkins Univ., The 1989 JANNAF Propulsion Meeting, Volume 1 May 1989 p 471-478 (For primary document see N90-18462 11-20)
(Contract NAS9-17378)
Avail: NTIS HC A25/MF A04 CSCL 14B

N90-18484*# National Aeronautics and Space Administration. Lyndon B. Johnson Space Center, Houston, TX.
ELECTRONICALLY VARIABLE PRESSURE REGULATOR (EVPR)
R. H. Reinicke, R. O. Nelson (Eaton Corp., El Segundo, CA.), and E. Hurlbert *In* Johns Hopkins Univ., The 1989 JANNAF Propulsion Meeting, Volume 1 May 1989 p 479-488 (For primary document see N90-18462 11-20)
(Contract NAS9-17907)
Avail: NTIS HC A25/MF A04 CSCL 14B

N90-19161# Consejo Superior de Investigaciones Cientificas, Madrid (Spain). Instituto de Optica.
PERFORMANCE PARAMETER CHARACTERISATION OF VARIOUS TYPES OF IR SINGLE ELEMENT DETECTORS
P. Corredera, J. Campos, A. Pons, and A. Corrons *In* ESA, Infrared Spectroscopy in Astronomy Sep. 1989 p 545-548 (For primary document see N90-19084 11-89)
Copyright Avail: NTIS HC A23/MF A04; ESA Publications Div., ESTEC, Noordwijk, Netherlands, 80 Dutch guilders

N90-19162# Laboratorium voor Ruimteonderzoek, Utrecht (Netherlands).
THE ISO SHORT WAVELENGTH SPECTROMETER
Th. deGraauw, D. A. Beintema, A. J. Boonstra, W. Luinge, G. Ploeger, J. Spakman, P. R. Wesselius, K. Wildeman, J. Wijnbergen, and S. W. Drapatz (Max-Planck-Inst. fuer Extraterrestrische Physik, Garching, Germany, F.R.) et al *In* ESA, Infrared Spectroscopy in Astronomy Sep. 1989 p 549-551 (For primary document see N90-19084 11-89)
Copyright Avail: NTIS HC A23/MF A04; ESA Publications Div., ESTEC, Noordwijk, Netherlands, 80 Dutch guilders

N90-19164# Max-Planck-Inst. fuer Astronomie, Heidelberg (Germany, F.R.).
SPECTROPHOTOMETRY OF DUST WITH ISOPHOT
D. Lemke, W. Kraetschmer, R. J. Tuffs, E. Kreysa, and A. Leger (Paris VII Univ., France) *In* ESA, Infrared Spectroscopy in Astronomy Sep. 1989 p 559-561 Sponsored by DFVLR, Porz, Fed. Republic of Germany (For primary document see N90-19084 11-89)
Copyright Avail: NTIS HC A23/MF A04; ESA Publications Div., ESTEC, Noordwijk, Netherlands, 80 Dutch guilders

N90-19165# Royal Observatory, Edinburgh (Scotland).
AN ADVANCED COOLED GRATING SPECTROMETER FOR UKIRT-CGS4
C. M. Mountain, R. Wade, D. J. Robertson, and T. J. Lee *In* ESA, Infrared Spectroscopy in Astronomy Sep. 1989 p 563-566 Sponsored by the United Kingdom Science and Engineering Research Council (For primary document see N90-19084 11-89)
Copyright Avail: NTIS HC A23/MF A04; ESA Publications Div., ESTEC, Noordwijk, Netherlands, 80 Dutch guilders

N90-19167# Imperial Coll. of Science and Technology, London (England).
ISOPHOT-S, A LOW RESOLUTION 2.5 TO 12 MICRONS SPECTROMETER FOR ISO
M. Wells, S. Chakaveh, R. D. Joseph, A. V. Pattni, M. J. Selby, D. Lemke, P. Lutzow-Wentzky, P. Vaughn, and F. Garzon (Universidad de la Laguna, Spain) *In* ESA, Infrared Spectroscopy in Astronomy Sep. 1989 p 571-573 (For primary document see N90-19084 11-89)
Copyright Avail: NTIS HC A23/MF A04; ESA Publications Div., ESTEC, Noordwijk, Netherlands, 80 Dutch guilders

36 LASERS AND MASERS

Includes parametric amplifiers.
For related information see also *76 Solid-State Physics.*

N90-18712# Los Alamos National Lab., NM.
INEX (INTEGRATED NUMERICAL EXPERIMENT) SIMULATIONS OF THE BOEING FEL SYSTEM
Robert L. Tokar, Alexander H. Lumpkin, Lloyd M. Young, Brian D. McVey, Lester E. Thode, C. D. Chan, Steven C. Bender, A. D. Yeremian, D. H. Dowell, and A. R. Lowrey (Boeing Aerospace Co., Seattle, WA.) 1989 29 p Presented at the 11th International Free Electron Laser Conference, Naples, FL, 28 Aug. - 1 Sep. 1989 Sponsored by Army Strategic Defense Command
(Contract W-7405-eng-36)
(DE90-004846; LA-UR-89-4165; CONF-8908134-20) Avail: NTIS HC A03/MF A01

The INEX (integrated numerical experiment) numerical model is applied to the 0.6 muons FEL oscillator at Boeing Aerospace and Electronics Company. This system consists of a 110 MeV L-band RF linac, a beam transport line from the accelerator to the entrance of the wiggler, the 5.0 meter THUNDER variable taper wiggler, and a near concentric two mirror optical oscillator. Many aspects of the model for the electron beam accelerator and transport line agree with experimental measurements. Predictions for lasing performance are compared with data obtained in May and June 1989 using a mild tapered wiggler. Good agreement was obtained with the achieved extraction efficiency, while 1D pulse simulations reproduce the observed sideband instability. DOE

N90-18713# Sandia National Labs., Albuquerque, NM.
PULSED LASER-INDUCED MELTING OF INTERMEDIATE Cu-Zn PHASES
David M. Follstaedt, Paul S. Peercy, and John H. Perepezko (Wisconsin Univ., Madison.) 1989 6 p Presented at the Materials Research Society Fall Meeting, Boston, MA, 27 Nov. - 2 Dec. 1989
(Contracts DE-AC04-76DP-00789; N00014-86-K-0753)
(DE90-005404; SAND-89-1558C; CONF-891119-60) Avail: NTIS HC A02/MF A01

It was discovered that the beta and gamma brasses of Cu-Zn exhibit clearly resolved increases in reflectance upon melting with a 30 ns ruby laser, which allow their melt durations to be readily measured. This system thus offers potential for obtaining quantitative information about the solidification kinetics of metals. It was also found that a heteroepitaxial layer of beta (prime) brass is formed on the surface of (ordered) gamma brass with 63 wt percent Zn following pulsed laser induced melting. The beta (prime) layer is interpreted to mean that the metastable beta phase (bcc) formed on the liquid-solid interface as the gamma substrate attempted to regrow, and that beta ordered to beta (prime) (B2) during cooling. The beta formation implies that undercoolings greater than 16 K were attained during the attempted regrowth of the gamma phase. DOE

N90-18714# Berkeley Research Associates, Inc., CA.
THEORY FOR HIGH GAIN, HIGH POWER FREE ELECTRON LASERS
William B. Colson 1990 91 p Prepared in cooperation with Lawrence Livermore National Lab., CA
(Contract W-7405-eng-48)
(DE90-005546; UCRL-21280; BRA-89-347R) Avail: NTIS HC A05/MF A01

The understanding of the effects of beam quality has improved both experimentally and theoretically. There have been three publications and a few talks at LLNL to serve as interim reports. The research included the derivation of better high efficiency equations for describing the free electron laser (FEL) in the strongly saturated regime. The equations retain much of the simplicity of the old theory, but are accurate for high energy extraction. DOE

N90-18715# Berkeley Research Associates, Inc., CA.
RESEARCH ON FREE ELECTRON LASERS Final Report
William B. Colson 1989 135 p
(Contract N00014-87-C-0490)
(AD-A215865; BRA-89-349R) Avail: NTIS HC A07/MF A01 CSCL 09/3

The research includes the derivation of better high-efficiency equations for describing the free electron lasers (FEL) in the strongly saturated regime. The equations retain much of the simplicity of the old theory, but are accurate for high energy extraction. The dimensionless parameters of the equations are used to describe the LANL and LLNL FEL experiments. In a publication, the importance of the dimensionless current density j is emphasized for describing many diverse FEL physical effects. The effects of waveguides on the FEL radiation interaction are derived and presented. The ELF FEL amplifier used a wave guide and is used as an example. It was found during the study that the gain spectrum of high-gain amplifiers like ELF can have sharp spikes. The spikes are not related to the use of a waveguide, but are an important result of this contract. A review paper invited by SPIE discusses some the techniques used to simulate FELs of many different kinds. GRA

N90-18716# International Business Machines Corp., San Jose, CA. Research Div.
ULTRASENSITIVE LASER SPECTROSCOPY IN SOLIDS: SINGLE-MOLECULE DETECTION
W. E. Moerner, W. P. Ambrose, and L. Kador (Bayreuth Univ., Germany, F.R.) 25 Oct. 1989 13 p Submitted for publication
(Contract N00014-84-C-0708)
(AD-A216085; TR-21) Avail: NTIS HC A02/MF A01 CSCL 20/5

In spite of detection intensity constraints necessary to avoid power broadening, the optical absorption spectrum of single molecules of pentacene in p-terphenyl crystals can be measured by using laser FM spectroscopy combined with Stark and/or ultrasonic double modulation (to remove residual amplitude modulation) and recording spectra far out in the wings of the inhomogeneous line to reduce the number of molecules in resonance to one. GRA

N90-18717# California Inst. of Tech., Pasadena.
ULTRAFAST CHEMICAL DYNAMICS OF REACTIONS IN BEAMS Final Report, 1 Nov. 1986 - 31 Oct. 1989
Ahmed H. Zewail 31 Oct. 1989 17 p
(Grant AF-AFOSR-0071-87; AF Proj. 2303)
(AD-A216319; AFOSR-89-1817TR) Avail: NTIS HC A02/MF A01 CSCL 07/5

The purpose of this research was to initiate the field of femtochemistry by interfacing state-of-the-art femtosecond laser systems to a beam system. This plan allows the study, for the first time, the ultrafast dynamics of chemical bond breakage in reactions under collisionless conditions (beams). The success of these experiments, which view the process directly in real time, created a wealth of information on the nature of the transition state and the resultant internal states distribution. A summary of the achievements together with the list publications is presented. GRA

N90-18718# Air Force Inst. of Tech., Wright-Patterson AFB, OH. School of Engineering.
A NUMERICAL SOLUTION TO THE BOLTZMANN EQUATION FOR USE IN CALCULATING PUMPING RATES IN A CO2 DISCHARGE LASER M.S. Thesis
David Alan Honey Dec. 1989 131 p
(AD-A216376; AFIT/GEP/ENP/89D-5) Avail: NTIS HC A07/MF A01 CSCL 09/3

The collisional Boltzmann equation was solved numerically to obtain excitation rates for use in a CO2 laser design program. The program was written in Microsoft QuickBasic for use on the IBM Personal Computer or equivalent. Program validation involved comparisons of computed transport coefficients with experimental data and previous theoretical work. Four different numerical algorithms were evaluated in terms of accuracy and efficiency. L-U decomposition was identified as the preferred approach. The calculated transport coefficients were found to agree with empirical data within one to five percent. The program was integrated into a CO2 laser design program. Studies were then performed to evaluate the effects on predicted laser output power and energy density as parameters affecting electron kinetics were changed. Plotting routines were written for both programs. GRA

N90-18719# California Univ., Berkeley. Lawrence Berkeley Lab. Accelerator and Fusion Research Div.
VUV (VACUUM ULTRAVIOLOT) LASER DIAGNOSTICS OF H(-) ION SOURCES
A. T. Young, G. C. Stutzin, K. N. Leung, and W. B. Kunkel Nov. 1989 9 p Presented at the 5th International Symposium on the Production and Neutralization of Negative Ions and Beams, Upton, NY, 30 Oct. - 3 Nov. 1989
(Contracts DE-AC03-76SF-00098; W-7405-eng-36)
(DE90-006072; LBL-28111; CONF-891055-6) Avail: NTIS HC A02/MF A01

Vacuum ultraviolet laser absorption spectroscopy was employed to measure the populations and temperatures of ground electronic state H-atoms and vibrationally excited H2 molecules in a volume H(-) ion source. Measurements of both species were made under a variety of discharge conditions. Vibrational levels to v(double prime)=8 were measured, with the vibrational population distribution well described by a temperature of 4150 K. DOE

N90-18720# California Univ., Berkeley. Lawrence Berkeley Lab. Accelerator and Fusion Research Div.
RESONATOR MODES IN HIGH GAIN FREE ELECTRON LASERS
Ming Xie, David A. G. Deacon, and John M. J. Madey (Duke Univ., Durham, NC.) Oct. 1989 13 p Presented at the 11th International Free Electron Laser Conference, Naples, FL, 28 Aug. - 1 Sep. 1989
(Contracts DE-AC03-76SF-00098; F49620-84-C-0012; N00014-85-K-0535; DALL03-86-0122)
(DE90-006098; LBL-27893; CONF-8908134-24; ESG-80) Avail: NTIS HC A03/MF A01

When the gain in a free electron laser is high enough to produce optical guiding, the resonator mode distorts and loses its forward-backward symmetry. We show that the resonator mode in a high gain FEL can be easily constructed using the mode expansion technique taken separately in the interaction and the free-space regions. We propose design strategies to achieve maximal gain and optimal mode quality, and discuss the stability of the optimized mode. DOE

N90-18721# Oak Ridge National Lab., TN. Applied Technology Div.
SOLID-STATE FLUORESCENCE ABOVE 1000 C: APPLICATION TO HIGH-TEMPERATURE LASER THERMOGRAPHY
S. W. Allison, M. R. Cates, G. J. Pogatshnik, and A. R. Bugos (Tennessee Univ., Knoxville.) Jan. 1990 9 p Prepared for

LANL, NM
(Contract DE-AC05-84OR-21400)
(DE90-006422; ORNL/ATD-21) Avail: NTIS HC A03/MF A01

Rare-earth-doped phosphors that exhibit intense fluorescence well above 1000 C are discussed. This is a rare characteristic for solid-state materials. One immediate application for them is thermometry. For example, surface temperatures of rotating components, systems in hostile or restricted environments, and systems in environments with very high temperature backgrounds are measurable with phosphor thermographic methods. The subject phosphors, Y2O3:Eu, LuPO4:Eu, YPO4:Eu, and LuPO4:Dy, provide the capability to extend these methods to very high temperatures. The use of pulsed ultraviolet laser activation of these phosphors leads to numerous practical application possibilities. The phosphor characteristics and various fluorescent decay times vs temperature are shown, and of their high-temperature applications are discussed. DOE

N90-18722# Los Alamos National Lab., NM.
ABSORPTION EXPERIMENTS ON ELECTRON-BEAM PUMPED RARE GASES
A. W. McCown, E. A. Rose, B. J. Krohn, D. E. Hanson, and S. J. Czuchlewski 1989 9 p Presented at the International Conference on Lasers 1989, New Orleans, LA, 3-8 Dec. 1989 Submitted for publication
(Contract W-7405-eng-36)
(DE90-006504; LA-UR-90-200; CONF-891261-6) Avail: NTIS HC A02/MF A01

Absorption experiments have been performed on electron-beam pumped rare gases (argon and krypton) as a function of pump power using the frequency-doubled output of a tunable dye laser at 248.4 nm and 257.3 nm. Energy deposition into the gas was varied by attenuating the electron beam with one or two stainless steel screens and by filling the gas chamber with different rare gas densities. The results from two energy deposition diagnostics were compared, and found to agree within 20 percent. Kinetics code calculations agreed with experimental results when absorption cross sections in the code were lowered. DOE

N90-18723# Los Alamos National Lab., NM.
CLOUD HOLE-BORING WITH INFRARED LASERS: THEORY AND EXPERIMENT
E. J. Caramana, R. L. Morse, G. P. Quigley, J. R. Stephens, R. B. Webster, and G. W. York 1989 6 p Presented at the International Conference on Lasers 1989, New Orleans, LA, 3-8 Dec. 1989 Submitted for publication
(Contract W-7405-eng-36)
(DE90-006519; LA-UR-90-166; CONF-891261-4) Avail: NTIS HC A02/MF A01

Results of experimental attempts to produce an optically clear channel in a water cloud by evaporating the cloud droplets with a CO2 laser are presented. Using scattered light it is possible to visualize the clear channel produced. Measurements of the fraction of power transmitted through the channel at visible wavelengths give insight into the clearing mechanisms. The present data suggest that the water droplets explode in the process of clearing. A theoretical explanation of why this should occur is presented and predictions of the onset of droplet explosions are made. The ability to clear an optical channel in a cloud has applications ranging from defense to ground based meteorological observation. The interior of many natural clouds cannot be probed by conventional optical means due to the large optical depths often encountered. By evaporating the liquid water in a cloud, it is possible to temporarily create an optically clear channel. The results are presented of laboratory experiments performed with the objectives of determining the conditions under which a high power pulsed CO2 laser can produce an optically clear channel and the physical mechanisms responsible for the cleaning and closure of such a channel are identified. In the present experiments, it appears that the droplets first explode resulting in an initial increase in turbidity. The smaller droplets formed by the explosion then evaporate leaving a partially cleared channel. This channel remains clear for a time period on the order of a second, finally closing by advection due to turbulence in the cloud. These findings are consistent with previous work using shorter and longer pulse lengths. DOE

N90-18724# Institut Franco-Allemand de Recherches, Saint-Louis (France).
CINEHOLOGRAPHY: A RELATION BETWEEN THE COHERENCE LENGTH OF THE LASER AND THE OBJECT VELOCITY
F. Albe and H. Fagot 5 Oct. 1988 11 p Presented at Optics-ECOOSA 88 Congress, Birmingham, England, 22-25 Mar. 1988
(ISL-CO-234/88; ETN-90-96246) Avail: NTIS HC A03/MF A01

Cineholograms are recorded nowadays with a YAG or ruby laser. The coherence length of the laser puts a limit on the scene volume. To increase this volume, the use flashpumped dye lasers with a greater coherence length is envisaged. But this will imply that the velocity of the holographed object will have to be decreased. A relation between the maximum velocity of the object and the coherence length of the laser is described. The new generation of pulsed lasers is concluded to allow increase of the volume of scenes to be holographed, with however a disadvantage to the velocity of the holographed objects. ESA

N90-18725# Los Alamos National Lab., NM.
ELECTRON BEAM AND HIGH-SPEED OPTICAL DIAGNOSTICS FOR THE LOS ALAMOS HIBAF (HIGH BRIGHTNESS ACCELERATOR FEL) FACILITY
A. H. Lumpkin, W. D. Cornelius, W. E. Stein, R. B. Feldman, K. L. Meier, and Lloyd M. Young 1989 18 p Presented at the 11th International Free Electron Laser Conference, Naples, FL, 28 Aug. - 1 Sep. 1989 Sponsored by Army Strategic Defense Command
(Contract W-7405-eng-36)
(DE90-007828; LA-UR-90-98; CONF-8908134-27) Avail: NTIS HC A03/MF A01

Characterization of the electron beam's properties will be a major task after the upgrade of the Los Alamos Free-Electron Laser (FEL) Facility with a photoelectric injector (PEI) and increased acceleration capability to 40 MeV. Adjustments to the previous diagnostics package that address the lower beam emittance, higher energy, and wakefield source reduction issues will be discussed. DOE

N90-18726# Los Alamos National Lab., NM. Chemical and Laser Sciences Div.
DEVELOPMENT OF KrF LASERS FOR FUSION
Joseph F. Figueira 1989 5 p Presented at the 12th International Conference on Lasers and Applications, New Orleans, LA, 3-8 Dec. 1989
(Contract W-7405-eng-36)
(DE90-007830; LA-UR-90-72; CONF-891261-7) Avail: NTIS HC A01/MF A01

Short-pulse, high-intensity excimer lasers are being developed for a variety of atomic physics and inertial confinement fusion (INF) applications. In this paper, we will discuss the status of KrF laser technology and its application to INF. Current progress worldwide will be described with emphasis on the Los Alamos program. DOE

N90-18727# Lawrence Livermore National Lab., CA.
FAST ALGORITHMS FOR CALCULATING LASER WAVEFRONT PHASE COMPENSATION GIVEN NOISY MEASUREMENTS OF PHASE GRADIENT
Don Gavel Sep. 1989 50 p
(Contracts W-7405-eng-48; MIPR-W31-RPD-7-D4041)
(DE90-006357; UCID-21814) Avail: NTIS HC A03/MF A01

Laser light propagating through atmosphere will become distorted as a result of the changing index of refraction along the light path. Wavefront distortions can be actively compensated using adaptive optic systems, which sense the wavefront aberations and compensate by changing the shape of a reflecting surface. Corrections must be done rapidly in order to keep up with the variations in the atmosphere. Numerically, the calculation of the

correcting surface is a least-squares fit problem. However, since a typical adaptive optic system has a large number of actuators and sensors, the ordinary solution methods, such as Gaussian elimination, are infeasible for real time application. Instead, advantage must be taken of the structure and sparseness of the equations in order to speed up the calculation. The algorithm proposed requires only O(nq) calculation steps and uses only O(n) memory storage, where n is the total number of actuators and q is the influence width of a single actuator. The derivation of the proposed algorithm, proofs of convergence, and results of several test runs are presented. The algorithm was incorporated into Y division's ORACLE simulation code where it is used to calculate the phase conjugate surfaces necessary to precompensate a high powered laser beam for atmospheric propagation. DOE

N90-18728# Lawrence Livermore National Lab., CA.
PROPERTIES AND PERFORMANCE OF THE LiCaAlF6:Cr(3+) LASER MATERIAL
Stephen A. Payne, L. L. Chase, L. J. Atherton, J. A. Caird, W. L. Kway, M. D. Shinn, R. S. Hughes, and L. K. Smith Jan. 1990 10 p Presented at the SPIE Optics, Electro-optics and Laser Applications in Science and Engineering Conference and Exhibition, Los Angeles, CA, 14-19 Jan. 1990
(Contract W-7405-eng-48)
(DE90-007242; UCRL-101720; CONF-900140-8) Avail: NTIS HC A03/MF A01

The laser properties of the LiCaAlF6:Cr(3+) (Cr:LiCAF) material are reviewed. The impact of the absorption and emission spectra on the laser performance is discussed. Laser pumping and flashlamp pumping experiments have shown that Cr:LiCAF has potential for high efficiency, although the presence of scattering losses remains a significant problem. The gradient freeze growth technique was found to generate lower-loss material compared to Czochralski growth. The thermal lensing of Cr:LiCAF was measured to be small and is in rough agreement with the magnitude expected on the basis of the intrinsic thermo-optical properties. DOE

N90-18729# Lawrence Livermore National Lab., CA. High Temperature Physics Div.
THE DYNAMICS OF ELECTRONS IN VERY INTENSE LASERS
J. N. Bardsley and B. M. Penetrante 27 Nov. 1989 14 p Presented at the Aspects of Electron-Molecule Scattering and Photoionization, New Haven, CT, 22-25 Jul. 1989
(Contract W-7405-eng-48)
(DE90-007246; UCRL-102651; CONF-8907183-1) Avail: NTIS HC A03/MF A01

The dynamics of relativistic plasmas created by intense short pulsed lasers is illustrated using analytic solutions for unconstrained electrons and numerical simulations of space charge effects. These models provide a basis for the analysis of laser induced nuclear reactions, recombination lasers and wakefield accelerators. DOE

N90-18730# Lawrence Livermore National Lab., CA.
A SIMPLE MODEL FOR AMPLIFIED SPONTANEOUS EMISSION IN DYES
John C. Garrison, Chung K. Hong, and Howard Nathel Jan. 1990 9 p
(Contract W-7405-eng-48)
(DE90-007249; UCID-21950) Avail: NTIS HC A03/MF A01

Amplified spontaneous emission in dyes is modelled by replacing the actual molecular spectrum by an effective four level atom which includes the levels involved in pumping and stimulated emission. Propagation of the signal and pump waves is described in the slowly varying envelope approximation. It is shown that the saturation intensity of the signal depends on the pump intensity, and reciprocally that the pump saturation intensity depends on the signal intensity. DOE

N90-18731# Institut Franco-Allemand de Recherches, Saint-Louis (France).
EFFECTS PRODUCED BY PULSED CO2 LASERS [WIRKUNG VON GEPULSTEN CO2-LASERN]
M. Hugenschmidt 18 Jul. 1988 34 p In GERMAN Original contains color illustrations
(ISL-R-112/88; ETN-90-96234) Avail: NTIS HC A03/MF A01

The different physical processes involved in the interaction between the beam of a pulsed CO2 laser and a target are studied. Variations in beam intensity over time and the transfer of energy from the beam to the material making up the target are given special attention. This research attempts to optimize the thermal and mechanical energy transfer. It is shown that this goal can be reached for absorbant as well as reflective target materials by using repeated laser pulses with power peaks of one megawatt and average power outputs of several kilowatts. ESA

N90-18732# Institut Franco-Allemand de Recherches, Saint-Louis (France).
RESEARCH ON SLIDING SPARK PREIONIZATION IN A TEA CO2 LASER [UNTERSUCHUNG EINER GLEITFUNKENSTRECKE ZUR VORIONISATION AN EINEM TEA-CO2-LASER]
W. Bott and Th. Ross 4 Aug. 1988 35 p In GERMAN
(ISL-R-113/88; ETN-90-96235) Avail: NTIS HC A03/MF A01

A Pyrex tube 12 mm in diameter in which 25 copper electrodes are glued every 2 mm is used to obtain a discharge space 50 cm in length. The radiation intensity of this ultraviolet source is carried by fiber optics to a spectrograph. The effect of varying power circuits on the intensity of emission is studied. It is shown that the tension under charge, the condensor capacity and the inductance and attenuation effects of the circuit all play important roles. They must be taken into account in attempting to optimize the ultraviolet emission in view of using it as a preionization source for TEA (Transversely Excited Atmospheric) lasers. ESA

N90-18733# Institut Franco-Allemand de Recherches, Saint-Louis (France).
STUDY OF DISCHARGE MECHANISMS AND THE STABILITY OF TRANSVERSE ELECTRIC DISCHARGES IN THE GAS MIXTURES Thesis - Karlsruhe Univ. [UNTERSUCHUNG DES ENTLADUNGSVERHALTENS UND DER STABILITAET TRANSVERSALER ELEKTRISCHER HOCHDRUCKENTLADUNGEN IN CO2-LASER-GASGEMISCHEN]
R. Schmitt 5 Aug. 1988 60 p In GERMAN
(ISL-R-114/88; ETN-90-96236) Avail: NTIS HC A04/MF A01

Optimization of laser discharge values are obtained by determining the stability of the different components of the gas mixture. From these measurements the amount of electric transfer can be calculated and the impedance of the discharge evaluated. Without any optimization work on the laser cavity, power of over 11 joules was obtained by this method. ESA

37 MECHANICAL ENGINEERING

Includes auxiliary systems (nonpower); machine elements and processes; and mechanical equipment.

N90-18734# National Inst. of Standards and Technology, Gaithersburg, MD. National Engineering Lab.
ROBOT CRANE TECHNOLOGY PROGRAM Final Report
Nicholas G. Dagalakis, James S. Albus, Kenneth R. Goodwin, James D. Lee, Tsung-Ming Tsai, Hoosh Abrishamian, Roger Bostelman, and Charles Yancey Jul. 1989 65 p
(ARPA Order 6380)
(PB90-111667; NIST/TN-1267) Avail: NTIS HC A04/MF A01; SOD HC $3.25 as 003-003-02953-0 CSCL 13I

The effort to develop kinematically constrained, dynamically stabilizd, robot cranes capable of lifting, moving and positioning heavy loads over large volumes, capable of supporting fabrication tools and the inspection of large size and difficult to reach structures, is described. The approach taken was to build on previous work at the NIST Robot Systems Division which has analyzed and measured the stiffness of a small model six cable suspension system. The system is a modified Stewart plaform.

Under DARPA Sponsorship, the work was extended to measure and optimize the stiffness of full size models, actively damped oscillations in a small scale six cable suspension flatform, and constructed an intermediate size six cable suspension platform for an industrial robot. Author

N90-18735# Massachusetts Univ., Amherst. Automation and Robotics Lab.
ON THE KINEMATIC BEHAVIOR OF ROBOTS WHILE EXECUTING GENERAL ROBOT LEVEL COMMANDS
Bartholomew O. Nnaji and Mehran Kamran May 1989 16 p Presented at the World Conference on Robotics, Gaithersburg, MD, 7-11 May 1989
(Grant NSF DMC-86-10417)
(PB90-120965; NSF/ENG-89050) Avail: NTIS HC A03/MF A01 CSCL 13I

As manufacturing becomes more automated, the need for automatic programming of robots increases. One of the most important steps in the realization of automatic robot programming is the ability of the robot planner to generate robot independent commands which are executable by any type of manipulator. Principles necessary to transform these general robot level commands into joint servo motion commands for all generic robot kinematic structures, are developed. GRA

N90-18736# Instituto de Pesquisas Espaciais, Sao Jose dos Campos (Brazil).
PRELIMINARY DESIGN OF A POINTER FOR MOVEMENT OF A SOLAR SIMULATOR M.S. Thesis [PROJETO PRELIMINAR DE UM POSICIONADOR PARA MOVIMENTACAO DE UM SIMULADOR SOLAR]
Alcy Rodolfo dosSantosCarrara Jun. 1989 177 p In PORTUGUESE; ENGLISH summary
(INPE-4864-TDL/375) Avail: NTIS HC A09/MF A01

The purpose is to perform the preliminary design of a mechanical manipulator (a robot) to accurately move and point a sun simulator for use in satellite AOCS tests. This equipment is to be installed in Brazilian Institute for Space Research (INPE's) existing facilities. In the first part, types and tests requirements are analyzed and robot configuration and geometry are determined according to the test facilities. In the second part the kinematic and kinetic models are obtained and simulated through the Denavit-Hartenberg's homogeneous transformations. Recursive Newton-Euler dynamic formulation computer program are codified in FORTRAN IV. Taking into account the achieved results of these model simulations the actuators and control system can be designed for the manipulator in the next phase of the project. Author

N90-18737# Instituto de Pesquisas Espaciais, Sao Jose dos Campos (Brazil).
AN APPROACH CENTERED IN PRODUCTION RULES FOR A PARTITION OF ENVIRONMENT AND PLANNING IN A VISUAL NAVIGATION SYSTEM (SNV) M.S. Thesis - 12 Dec. 1988 [UMA ABORDAGEM CENTRADA EM REGRAS DE PRODUCAO PARA A DIVISAO DE AMBIENTES E PLANEJAMENTO NO SISTEMA DE NAVEGACAO VISUAL (SNV)]
Carlos Antonio MarquesNogueira Jun. 1989 89 p In PORTUGUESE; ENGLISH summary
(INPE-4813-TDL/360) Avail: NTIS HC A05/MF A01

A proposal is presented for the planning of the navigation of an intelligent mobile robot in structured environments. For this purpose a mixed approach based is used on objects (obstacles) and empty spaces. The representation of knowledge about the environment is hierarchical while abstraction levels are used in the problem solution. Geometric concepts which permit the partition of any environment into convex polygonal regions are developed. The path between any two points is determined according to a monotonic procedure. Author

N90-18738# MRC Bearings-SKF Aerospace, Jamestown, NY.
LIFE OF CONCENTRATED CONTACTS IN THE MIXED EHD AND BOUNDARY FILM REGIMES Final Report
John I. McCool Aug. 1989 155 p
(Contract N00140-83-C-7149)
(AD-A216673; NAPC-PE-204C) Avail: NTIS HC A08/MF A01 CSCL 20/11

This analytical and experimental program investigates the influence of surface finish, material and lubricant on rolling contact bearings operating in the low or marginal lubricant film regime. The investigation includes failure analysis of field failures encountered with helicopter mast support and planetary gear transmission bearings, computer analysis of the above two bearing applications using SKF computer programs SHABERTH and PLANETSYS and testing of specimens made of M50 and 9310 steel using a geared roller tester at NAPC. GRA

N90-18739# Oak Ridge National Lab., TN. Engineering Technology Div.
EFFECTS OF OBLIQUE IMPACT ON HYPERVELOCITY SHIELD PERFORMANCE
E. D. Brewer, W. R. Hendrich, D. G. Thomas, and J. E. Smith Jan. 1990 45 p Prepared for Air Force Weapons Lab., Kirtland AFB, NM
(Contract DE-AC05-84OR-21400)
(DE90-006936; ORNL/TM-11390) Avail: NTIS HC A03/MF A01

As part of the Advanced Shield Phenomenology Program, conducted from 1987 to 1989, a study of the effects of oblique impact on hypervelocity shield damage was performed. The specific threat used was an aluminum cylinder with a mass of 1.75 grams and a length to diameter ratio of one. Incidence angles of 30, 60, and 90 degrees were studied. The same layered shield assembly was tested at the different incidence angles. Testing was performed at the Arnold Engineering Development Center, Arnold Air Force Base, Tullahoma, Tennessee. Hydrocode analysis of the interaction of the projectile with the front plate was performed for each of the different incidence angles. DOE

N90-18740*# National Aeronautics and Space Administration. Lewis Research Center, Cleveland, OH.
FASTENER DESIGN MANUAL
Richard T. Barrett Mar. 1990 99 p
(NASA-RP-1228; E-4911; NAS 1.61:1228) Avail: NTIS HC A05/MF A01 CSCL 13K

This manual was written for design engineers to enable them to choose appropriate fasteners for their designs. Subject matter includes fastener material selection, platings, lubricants, corrosion, locking methods, washers, inserts, thread types and classes, fatigue loading, and fastener torque. A section on design criteria covers the derivation of torque formulas, loads on a fastener group, combining simultaneous shear and tension loads, pullout load for tapped holes, grip length, head styles, and fastener strengths. The second half of this manual presents general guidelines and selection criteria for rivets and lockbolts. Author

N90-18741# Oak Ridge National Lab., TN.
FEDERAL METHANOL FLEET UPDATE
R. N. McGill 1989 22 p Presented at the Annual Automotive Technology Development Contractors Coordination Meeting, Dearborn, MI, 23-26 Oct. 1989 Submitted for publication
(Contract DE-AC05-84OR-21400)
(DE90-006851; CONF-8910248-4) Avail: NTIS HC A03/MF A01

The Federal Methanol Fleet Project, managed by Oak Ridge National Laboratory for the Department of Energy, has operated methanol-fueled vehicles since 1985 in routine government fleet operations. Presently, 20 methanol vehicles of four different types are operating at three different sites alongside 14 gasoline cars in similar assignments. Over one million miles have been accumulated on fleet vehicles so far, and driver acceptance has been generally good for the methanol vehicles. Equipment varies between vehicle type, especially with regard to their systems for cold starting, and those with minimal cold-start systems have not performed as well in winter weather. Also, climate varies considerably between the three sites, and this is reflected in the comparison of cold weather

performance. Accumulation of metals in the lubricating oil is at a greater rate in the methanol vehicles, and data are presented which demonstrate the dependence of these phenomena on ambient temperature. Generally, metals accumulate in the oil of the methanol vehicles at a much greater rate in colder months. DOE

38 QUALITY ASSURANCE AND RELIABILITY

Includes product sampling procedures and techniques; and quality control.

N90-18742# European Space Agency, Paris (France).
KNOWLEDGE-BASED FAULT DETECTION AND ANALYSIS FOR ROBOTS: FIRST RESULTS FOR THE ROTEX ROBOTS
Hans-Juergen Hotop and Claus-Dieter Strube (Deutsche Forschungs- und Versuchsanstalt fuer Luft- und Raumfahrt, Brunswick, Germany, F.R.) Dec. 1989 64 p Transl. into ENGLISH of Wissensbasierte Fehlererkennung und -diagnose fuer Roboter - Erste Ergebnisse fuer den ROTEX-Roboter (Brunswick, Fed. Republic of Germany, DFVLR), 1989 p 1-47 Original language document was announced as N89-26622
(ESA-TT-1150; DFVLR-FB-89-03; ETN-90-96217) Avail: NTIS HC A04/MF A01; original German version available from DFVLR, VB-PL-DO, Postfach 90 60 58, 5000 Cologne 90, Fed. Republic of Germany, 18.50 DM

The concept of self-monitoring by robots in space is presented for the health and fault management (HFM) system of a robot in the German D2 Spacelab mission. Starting with the description of the robot experiment (ROTEX), the subsystems developed by using conventional techniques and methods of artificial intelligence are explained. The hardware and software (TI Explorer/KEE) is described and the implementation of the expert system is discussed in detail, using voltage monitoring as an example. Future aims to be achieved are described. ESA

39 STRUCTURAL MECHANICS

Includes structural element design and weight analysis; fatigue; and thermal stress.

For applications see *05 Aircraft Design, Testing and Performance* and *18 Spacecraft Design, Testing and Performance*.

N90-18743*# Boeing Helicopter Co., Philadelphia, PA.
CALCULATION OF FLIGHT VIBRATION LEVELS OF THE AH-1G HELICOPTER AND CORRELATION WITH EXISTING FLIGHT VIBRATION MEASUREMENTS Final Report
R. A. DiTaranto and V. Sankewitsch Nov. 1989 110 p
(Contract NAS1-17497)
(NASA-CR-181923; NAS 1.26:181923) Avail: NTIS HC A06/MF A01 CSCL 20K

Boeing Helicopters, together with other U.S. Helicopter manufacturers, participated in a finite element applications program to give the United States a superior capability to utilize finite element analysis models in support of helicopter airframe design. The program was sponsored by the NASA Langley Research Center. Under this program, an activity was sponsored to evaluate existing analysis methods applicable to calculate coupled rotor-airframe vibrations. The helicopter used in this evaluation was the AH-1G helicopter. The results of the Boeing Helicopters efforts are summarized. The planned analytical procedure is reviewed. Changes to the planned procedure are discussed, and results of the correlation study are presented. Author

N90-18744*# Texas A&M Univ., College Station. Dept. of Mechanical Engineering.
PAYLOAD VIBRATION ISOLATION IN A MICROGRAVITY ENVIRONMENT Final Report, 1 Jun. 1988 - 31 Dec. 1989
Richard M. Alexander 15 Jan. 1990 67 p
(Contract NAS9-17972)
(NASA-CR-186191; NAS 1.26:186191) Avail: NTIS HC A04/MF A01 CSCL 20K

Many in-space research experiments require the microgravity environment attainable near the center of mass of the Space Station. Disturbances to the structure surrounding an experiment may lead to vibration levels that will degrade the microgravity environment and undermine the experiment's validity. In-flight disturbances will include vibration transmission from nearby equipment and excitation from crew activity. Isolation of these vibration-sensitive experiments is required. Analytical and experimental work accomplished to develop a payload (experiment) isolation system for use in space is described. The isolation scheme allows the payload to float freely within a prescribed boundary while being kept centered with forces generated by small jets of air. The vibration criterion was a maximum payload acceleration of 10 micro-g's (9.81x10(exp -5)m/s(exp 2), independent of frequency. An experimental setup, composed of a cart supported by air bearings on a flat granite slab, was designed and constructed to simulate the microgravity environment in the horizontal plane. Experimental results demonstrate that the air jet control system can effectively manage payload oscillatory response. An analytical model was developed and verified by comparing predicted and measured payload response. The mathematical model, which includes payload dynamics, control logic, and air jet forces, is used to investigate payload response to disturbances likely to be present in the Space Station. Author

N90-18745*# National Aeronautics and Space Administration. Lewis Research Center, Cleveland, OH.
A GLOBAL APPROACH FOR THE IDENTIFICATION OF STRUCTURAL CONNECTION PROPERTIES
Charles Lawrence and Arthur A. Huckelbridge (Case Western Reserve Univ., Cleveland, OH.) Feb. 1990 16 p
(NASA-TM-102502; E-5303; NAS 1.15:102502) Avail: NTIS HC A03/MF A01 CSCL 20K

A general procedure is developed for identifying properties of structural joints. The procedure, which uses experimental response data, is considered general because it is applicable to any size or type of structural system. The present procedure, which identifies characteristics such as damping and stiffness, accommodates both linear and nonlinear joint properties and may process test data measured at arbitrary stations on the structural system. The method identifies joint characteristics by performing a global fit between predicted and measured data. It overcomes limitations of previous methods in that it can better deal with parameter-dependent constraints (e.g., gaps). The method is demonstrated with a simplified model of a bladed disk assembly having friction damping and mistuning. Author

N90-18746*# National Aeronautics and Space Administration. Langley Research Center, Hampton, VA.
FATIGUE CRACK INITIATION AND SMALL CRACK GROWTH IN SEVERAL AIRFRAME ALLOYS
M. H. Swain, J. C. Newman, Jr., E. P. Phillips, and R. A. Everett, Jr. (Army Aerostructures Directorate, Hampton, VA.) Jan. 1990 8 p
(NASA-TM-102598; NAS 1.15:102598; AVSCOM-TM-90-B-001)
Avail: NTIS HC A02/MF A01 CSCL 20K

The growth of naturally-initiated small cracks under a variety of constant amplitude and variable amplitude load sequences is examined for several airframe materials: the conventional aluminum alloys, 2024-T3 and 7075-T6, the aluminum-lithium alloy, 2090-T8E41, and 4340 steel. Loading conditions investigated include constant amplitude loading at R = 0.5, 0, -1 and -2 and the variable amplitude sequences FALSTAFF, Mini-TWIST and FELIX/28. Crack growth was measured at the root of semicircular edge notches using acetate replicas. Crack growth rates are compared on a stress intensity factor basis, to those for large cracks to evaluate the extent of the small crack effect in each alloy. In addition, the various alloys are compared on a crack initiation and crack growth morphology basis. Author

N90-18747# California Inst. of Tech., Pasadena. Div. of Engineering and Applied Science.
KINETIC RELATIONS AND THE PROPAGATION OF PHASE BOUNDARIES IN SOLIDS
Rohan Abeyaratne and James K. Knowles Sep. 1989 65 p Prepared in cooperation with Massachusetts Inst. of Tech.
(Contract N00014-87-K-0117)
(AD-A215881; TR-10) Avail: NTIS HC A04/MF A01 CSCL 11/7

The dynamics of phase transformations in elastic bars are investigated. The specific issue studied is the compatibility of the field equations and jump conditions of the one-dimensional theory of such bars with two additional constitutive requirements: the first of these is a kinetic relation controlling the rate at which the phase transition takes place; the second is a nucleation criterion for the initiation of the phase transition. A special elastic material with a piecewise-linear, non-monotonic stress-strain relation is considered, and the Riemann problem for this material is analyzed. For a large class of initial data, it is found that the kinetic relation and the nucleation criterion together will single out a unique solution to this problem from among the infinitely many solutions that satisfy the entropy jump condition at all strain discontinuities. GRA

N90-18748# Virginia Polytechnic Inst. and State Univ., Blacksburg. Dept. of Mathematics.
ENERGY DECAY AND BOUNDARY CONTROL FOR DISTRIBUTED PARAMETER SYSTEMS WITH VISCOELASTIC DAMPING Final Technical Report, 1 Jun. 1986 - 31 May 1989
Kenneth B. Hannsgen and Robert L. Wheeler 24 Jul. 1989 18 p
(Grant AF-AFOSR-0085-86; AF Proj. 2304)
(AD-A216468; AFOSR-89-1895TR) Avail: NTIS HC A02/MF A01 CSCL 20/11

Several aspects of active and passive stabilization of materials and structures are considered, together with related dynamic problems with potential applications to stabilization. Results are described for determination of the interacting effects of viscoelastic and feedback dissipation in the damping of oscillations in certain rods and beams. Loss of stability or of well-posedness due to feedback delays is described. Additional results concern analysis of energy decay in elastic beams and an investigation of the Signorini problem for motion of an elastic body that abuts a rigid obstacle. Numerical and analytic studies are described for Bingham fluids as well as for several problems involving two-fluid flows. Finally, work on control problems for the Navier-Stokes equations is summarized. GRA

N90-18749# Naval Postgraduate School, Monterey, CA. Dept. of Mathematics.
THE PROPAGATION OF TIME HARMONIC RAYLEIGH-LAMB WAVES IN A BIMATERIAL PLATE Technical Report, Oct. 1988 - Sep. 1989
Clyde Scandrett and Naresh Vasudevan 7 Nov. 1989 31 p
(AD-A216834; NPS53-90-001) Avail: NTIS HC A03/MF A01 CSCL 20/11

The present study involves two semi-infinite homogeneous, isotropic, linearly elastic plates perfectly bonded end to end. The plates have dissimilar material properties (e.g., copper and aluminum). Incident on the interface are both the lowest symmetric and the lowest antisymmetric Rayleigh-Lamb eigenmodes. The resulting transmitted and reflected fields contain contributions from all of the real, imaginary and complex plate modes which are active at the given excitation frequency. A study of the distribution of energy among the various reflected and transmitted Rayleigh eigenmodes over a range of frequencies is undertaken for a number of material combinations of the bimaterial plate. GRA

N90-18750# Army Materials Technology Lab., Watertown, MA. Ceramics Research Branch.
BIAXIAL STRENGTH AND STRESS RUPTURE OF HOT-PRESSED SILICON NITRIDE Final Report
George D. Quinn and Gunter Wirth (Institut fuer Werkstoff-Forschung, Cologne, Germany, F.R.) Nov. 1989 19 p Sponsored by Army Lab. Command, Adelphi, MD
(DA Proj. 1L1-61205-AH-84)
(AD-A216950; MTL-TR-89-101) Avail: NTIS HC A03/MF A01 CSCL 20/11

Static fatigue failure of structural ceramics can be caused by a variety of phenomena including stress corrosion, slow crack growth, surface pit formation, and creep fracture. Hot-pressed silicon nitride (HPSN) with magnesia sintering has been extensively studied due to its extremely consistent behavior. Slow crack growth from preexisting flaws, or creep fracture, can control static fatigue in HPSN. An extensive data base of flexural stress rupture experiments has culminated in a fracture mechanism map. The vast majority of static fatigue experiments for engineering ceramics have been in a uniaxial stress state, indeed, usually in four-point flexure. Two studies have compared uniaxial and biaxial slow crack growth for alumina, glass, and a glass ceramic, and a vitreous-bonded abrasive. Testing done was only at room temperature, and with short duration, dynamic fatigue experiments. These studies were encouraging, however, showing that the multiaxial stress state had no effect upon crack growth parameters determined by strength test methods. This study reports high temperature and long duration equibiaxial stress rupture experiments for HPSN. HPSN was chosen because of its high static fatigue reproducibility. It was also possible to examine more than one failure mechanism. Biaxial testing was performed in both the slow crack growth and creep fracture regimes. GRA

N90-18751*# National Aeronautics and Space Administration. Langley Research Center, Hampton, VA.
DEVELOPMENT OF AN EXPERIMENTAL SPACE STATION MODEL FOR STRUCTURAL DYNAMICS RESEARCH
Paul E. McGowan, Harold E. Edighoffer (AS&M, Inc., Hampton, VA.), and John W. Wallace Jan. 1990 19 p Presented at the 60th Shock and Vibration Symposium, Virginia Beach, VA, 14-16 Nov. 1989
(NASA-TM-102601; NAS 1.15:102601) Avail: NTIS HC A03/MF A01 CSCL 20K

Design, analysis, and testing of an experimental space station scale model is presented. The model contains hardware components with dynamic characteristics similar to those expected for other large space structures. Validation of analysis models is achieved through correlation with dynamic tests of hardware components and representative assembly configurations. A component mode synthesis analysis method is examined through comparisons with results from fully mated system models. Selection of input requirements for accurate component synthesis analysis predictions are assessed. Author

N90-18752*# National Aeronautics and Space Administration. Langley Research Center, Hampton, VA.
STRUCTURES AND MATERIALS TECHNOLOGY FOR HYPERSONIC AEROSPACECRAFT
Harvey G. McComb, Jr. (Analytical Services and Materials, Inc., Hampton, VA.), Harold N. Murrow, and Michael F. Card Jan. 1990 46 p
(NASA-TM-102583; NAS 1.15:102583) Avail: NTIS HC A03/MF A01 CSCL 20K

Major considerations in structural design of a transatmospheric aerospacecraft are discussed. The general direction of progress in structures and materials technology is indicated, and technical areas in structures and materials where further research and development is necessary are indicated. Various structural concepts under study and materials which appear to be most applicable are discussed. Structural design criteria are discussed with particular attention to the factor-of-safety approach and the probabilistic approach. Structural certification requirements for the aerospacecraft are discussed. The kinds of analyses and tests which would be required to certify the structural integrity, safety, and durability of the aerospacecraft are discussed, and the type of test facility needed to perform structural certification tests is identified. Author

N90-18753# California Univ., Berkeley. Lawrence Berkeley Lab. Materials and Chemical Sciences Div.
CREEP IN SHEAR OF EXPERIMENTAL SOLDER JOINTS
D. Tribula and J. W. Morris, Jr. Sep. 1989 29 p Presented at the Winter Annual Meeting of the ASME, San Francisco, CA, 10-15 Dec. 1989 Prepared in cooperation with California Univ., Berkeley
(Contract DE-AC03-76SF-00098)
(DE90-007062; LBL-27775; CONF-891208-29) Avail: NTIS HC A03/MF A01

Thermal fatigue failures of solder joints in electronic devices are a great concern in the electronics industry. Since the fatigue load is often in shear the details of thermal fatigue failure in shear are of particular interest. Recent work indicates that similar failure mechanisms operate in both thermal fatigue in shear and unidirectional creep in shear. Additionally, since the operative temperatures during thermal fatigue represent high solder homologous temperatures, creep deformation is certainly involved. These factors and the relative ease of conducting creep experiments encourage the study of solder joints under shear creep conditions. Steady state shear creep rate vs shear stress data are presented for several solder compositions, including the binary eutectic alloy and Pb-Sn alloyed with small amounts of Bi, Cd, In, and Sb, in a joint configuration. These data indicate that conventional creep mechanisms operate in the temperature and shear strain rate ranges studied. Extensive microstructural information is also reported. The microstructural evolution under creep conditions indicates that the instability of the as-cast binary Pb-Sn eutectic microstructure initiates creep failure. Changes of the as-solidified microstructure with the third element addition are reported as are the microstructural responses of each of these alloys to creep deformation. The efficacy of postponing the microstructural instability with the addition of small amounts of ternary elements is discussed. DOE

N90-18754# Southampton Univ. (England). Inst. of Sound and Vibration Research.
SYSTEM PROPERTIES FROM FREQUENCY RESPONSE FUNCTIONS, PART 1
H. G. Lee and B. J. Dobson Oct. 1988 52 p
(ISVR-TR-166-Pt-1; ETN-90-96262) Avail: NTIS HC A04/MF A01

Two system identification methods which can be used to obtain the system properties from the experimental frequency response function are presented. System identification is the process of determining physical properties in the equation of motion of a system directly from test data. The first method gives approximately the same system properties as those from Guyan static condensation of the analytical model when applying appropriate fixing frequencies. Both methods are proposed for the identification of the errors in the modeling of elements in a system. ESA

N90-18755# Southampton Univ. (England). Inst. of Sound and Vibration Research.
A STUDY OF THE VIBRATIONAL TRANSMISSION THROUGH FLANGED JOINTS
R. S. Ming, G. J. Stimpson, and N. Lalor Jul. 1988 42 p
(ISVR-TR-181; ETN-90-96264) Avail: NTIS HC A03/MF A01

An investigation into the vibrational behavior of plate structures coupled by flanged joints, including the effects of gasket materials is presented. Formulas for calculating coupling loss factors through flanged joints with or without gaskets are derived and information for minimizing vibration transmission presented. A series of experiments was carried out to measure the coupling between two plates connected by different thicknesses of flanged joint and incorporating a range of gasket materials. The general agreement of predicted coupling factors with measured values was found to be quite good. ESA

N90-18401# La Sapienza Univ., Rome (Italy). Dipartimento Aerospaziale.
CRACK PROPAGATION FROM ARTIFICIAL DEFECTS IN TYPICAL ENGINE DISK MATERIALS; INTERPRETATION OF EXPERIMENTAL RESULTS BY MEANS OF 3D J INTEGRAL
Aldo Frediani and Roberto Galatolo (Pisa Univ., Italy) *In* AGARD, AGARD/SMP Review: Damage Tolerance for Engine Structures. 2: Defects and Quantitative Materials Behaviour Aug. 1989 10 p (For primary document see N90-18396 11-07)
Avail: NTIS HC A06/MF A01; Non-NATO Nationals requests available only from AGARD/Scientific Publications Executive

N90-18424# Ecole Polytechnique Federale de Lausanne (Switzerland).
TIME-DEPENDENT MEASUREMENTS ON VIBRATING ANNULAR TURBINE CASCADES UNDER VARIOUS STEADY STATE CONDITIONS
A. Boelcs, T. H. Fransson, and D. Schlaefli *In* AGARD, Unsteady Aerodynamic Phenomena in Turbomachines Feb. 1990 14 p (For primary document see N90-18405 11-07)
Copyright Avail: NTIS HC A14/MF A02; Non-NATO Nationals requests available only from AGARD/Scientific Publications Executive

N90-18470*# National Aeronautics and Space Administration. Lewis Research Center, Cleveland, OH.
PROBABILITY OF FAILURE AND RISK ASSESSMENT OF PROPULSION STRUCTURAL COMPONENTS
Michael C. Shiao (Sverdrup Technology, Inc., Cleveland, OH.) and Christos C. Chamis *In* Johns Hopkins Univ., The 1989 JANNAF Propulsion Meeting, Volume 1 May 1989 p 135-162 (For primary document see N90-18462 11-20)
Avail: NTIS HC A25/MF A04 CSCL 20K

42 GEOSCIENCES (GENERAL)

No abstracts in this category.

43 EARTH RESOURCES AND REMOTE SENSING

Includes remote sensing of earth resources by aircraft and spacecraft; photogrammetry; and aerial photography.

For instrumentation see *35 Instrumentation and Photography.*

N90-18756# Instituto de Pesquisas Espaciais, Sao Jose dos Campos (Brazil).
FRACTURE ANALYSIS THROUGH PHOTOGRAPHIC IMAGERY OF LOW SPATIAL RESOLUTION: A CONTRIBUTION TO THE STUDY OF TECTONIC EVOLUATION OF THE ARARIPE PLATEAU REGION [ANALISE DE FRATURAS ATRAVES DE IMAGENS FOTOGRAFICAS DE BAIXA RESOLUCAO ESPACIAL: UMA CONTRIBUICAO AOY OF TECTONIC EVOLUTION OF THE ARARIPE PLATEAU REGION]
Edison Crepani May 1989 17 p In PORTUGUESE; ENGLISH summary Presented at the 5th Brazilian Symposium on Remote Sensing, Natal, Brazil, 11-15 Oct. 1988
(INPE-4876-PRE/1487) Avail: NTIS HC A03/MF A01

Based on existing geological data, the analysis of the TM, MSS, and RBV images of LANDSAT and the mosaics of SLAR imagery to the application of morphostructural analysis and statistic treatment of the fractures, this work shows the active participation of the ancient lines of weakness of the basement, with the directions of N45E, N45W and EW in the tectonic configuration of the Araripe Basin. During Mesozoic time, the behavior of such

lines of weakness was essentially characterized by vertical movements in a gravitational tectonics which caused the formation of the Araripe Basin, divided into two subbasins: the West Subbasin, which forms a sequence of structural terraces as stairs from west to east according to the direction of N45W, and the East Subbasin, which forms a basin of rift type with alternative structural highs and lows according to the direction of N45E, in a broad low according to the direction EW between the Patos and Cariris Velhos lineaments. The N45E lines of weakness, which control the structural highs and lows in the East Subbasin of Araripe, show the continuity up to the Rio do Peixe Basin and this continuity seems to connect these two basins. These lines of weakness extending to the northeast up to the Potiguar Basin emphasize the hypothesis of the existence of an aborted branch of triple junction with the center between Areia Branca and Macau. This aborted branch may connect the Araripe, Rio do Peixe and Potiguar basins. Author

N90-18757# Instituto de Pesquisas Espaciais, Sao Jose dos Campos (Brazil).
GEOMETRIC CORRECTION MODELS FOR HRV-SPOT IMAGES M.S. Thesis [MODELOS DE CORRECAO GEOMETRICA PARA IMAGENS HRV - SPOT]
Antonio Jose FerreiraMachadoeSilva Oct. 1989 235 p In PORTUGUESE; ENGLISH summary
(INPE-5001-TDL/395) Avail: NTIS HC A11/MF A02

Geometric correction is a very important tool of remote sensing applications. Therefore, it must include tasks which compose the preprocessing of the images. There are several mathematical models for the geometric correction itself, and also for its refinement. Here, some geometric correction methods are presented, analyzed and compared, and the relation between computational costs and precision is studied. Some geometric evaluation standards are discussed, as they are the instrument to confirm the quality of the adopted models. Author

N90-18758# Instituto de Pesquisas Espaciais, Sao Jose dos Campos (Brazil).
ORBITAL REMOTE SENSING IN THE DECADE OF THE NINETIES: NEW APPROACHES AND CHALLENGES IN GEOLOGY [SENSORIAMENTO REMOTO ORBITAL NA DECADA DE NOVENTA: NOVAS ABORDAGENS E DESAFIOS EM GEOLOGIA]
Raimundo AlmeidaFilho Jun. 1989 8 p In PORTUGUESE; ENGLISH summary Presented at the 5th Brazilian Symposium on Remote Sensing, Natal, Brazil, 11-15 Oct. 1988
(INPE-4838-PRE/1467) Avail: NTIS HC A02/MF A01

Besides following-up on the LANDSAT and SPOT Programs, a new generation of remote sensing systems will be available in the 90's. The ERS-1, RADARSAT, JERS-1, and Eos-SAR systems will provide, for the first time, a systematical and global based collection of orbital radar images. Because the good penetration capability of the L-band radar systems through the vegetation cover, JERS-1 and Eos-SAR systems are believed to be a very powerful tool to study the Amazonia. Other very important Eos instrument for geological purposes is the Spectrometer HIRIS, which will be able to obtain up to 194 multispectral simultaneous images in the spectral range from 400 to 2.500 nm. It will make possible the direct identification of many miners on the earth surface, based on their spectral diagnostic features. At the same time that these new instruments open new opportunities they bring about new challenges to the remote sensing community. If these data are to be used efficiently, new approaches involving both digital imagery processing and interpretation techniques will be required. Author

N90-18759# Instituto de Pesquisas Espaciais, Sao Jose dos Campos (Brazil).
TVI: A MATHEMATICAL MODEL FOR GLOBAL ESTIMATION OF BRAZILIAN CERRADO PHYTOMASS [TVI: UM MODELO NUMERICO PARA ESTIMATIVA GLOBAL DA FITOMASSA DOS CERRADOS BRASILEIROS]
Joao Roberto dosSantos Jun. 1989 8 p In PORTUGUESE; ENGLISH summary Presented at the 5th Brazilian Symposium on Remote Sensing, Natal, Brazil, 11-15 Oct. 1988
(INPE-4836-PRE/1465) Avail: NTIS HC A02/MF A01

The main objective is to discuss the Transformed Vegetation Index (TVI) potentialities to estimate the cerrado phytomass. The ground and remote sensing data (thematic mapper/LANDSAT-5) were gathered on three selected areas: Roncador Ecological Reserve (IBGE), Experimental Station of Brasilia University (UNB), and CPAC/EMBRAPA Station, located at the Federal District region. The regression analysis, with linear and exponential models, were used to analyze the relationship between TVI and cerrado phytomass. From the results it can be gathered: the function which presents the best fitting of ground data and TVI; the percentage variation explained by this vegetation index in the phytomass estimated by the regression. The research methodology was developed for the local level. In the future, this methodology will be adapted to estimate and monitor the Brazilian Cerrado phytomass. Author

N90-18760# Instituto de Pesquisas Espaciais, Sao Jose dos Campos (Brazil).
RELATIONSHIPS BETWEEN THE AERIAL BIOMASS FROM GROUND LAYERS OF CERRADO AND ITS SPECTRAL REFLECTANCE [RELACOES ENTRE A BIOMASSA AEREA DO ESTRATO RASTEIRO DO CERRADO E SUA REFLECTANCIA ESPECTRAL]
Dalton deMorissonValeriano and Marisa Dantas BitencourtPereira (Sao Paulo Univ., Brazil) May 1989 9 p In PORTUGUESE; ENGLISH summary Presented at the 5th Brazilian Symposium on Remote Sensing, Natal, Brazil, 11-15 Oct. 1988 Sponsored in part by CPAC/EMBRAPA
(INPE-4848-PRE/1477) Avail: NTIS HC A02/MF A01

In 47 samples of 1 sq m of the gound layer of typical and sparse cerrado vegetation the following parameters were measured: fresh and dry total biomass (FTB, DTB), fresh and dry green biomass (FGB, DGB), water content of the total and of the green biomass (TWC, GWC), the proportion of green biomass (PGB), and the spectral reflectance (rho lambda) at every 25 nm from 400 to 700 nm and at every 100 nm from 750 to 1050 nm. The analysis of the correlations between these parameters showed that: total biomass presents negative correlation with rho lambda in nearly all the analyzed spectral bands, with a maximum in 650 nm for FTB (r= -0.59) and in 1050 nm for DTB (r= -0.24 and -.18 for FGB and DGB, respectively); the water conyent and the proportion of green biomass present negative correlations with the rho lambda in the blue bands, with a maximum at 400 nm (4= -0.46, -0.41 and -0.35 for TWC, GWC and PGB, respectively), absence of correlation in the green-red spectral bands and positive correlations in the near infrared, with maximum at 1050 nm (r= -0.51, 0.34 and 0.51 for TWT, GWC and PGB, respectively). Such results suggest the need of different spectral bands combinations for the calculation of vegetation index appropriated to the estimation of each of the vegetation parameters investigated. Author

N90-18761# Instituto de Pesquisas Espaciais, Sao Jose dos Campos (Brazil).
LAND SUITABILITY MAPS AND APPROPRIATE LAND USE: AN APPROACH USING SGI AND SATELLITE IMAGERY [MAPA DE APTIDAO AGRICOLA DAS TERRAS E USO ADEQUADO DAS TERRAS: UMA ABORDAGEM USANDO SGI E IMAGENS DE SATELITE]
Getulio VargasdeAssuncao, Antonio Roberto Formaggio, and Diogenes SalasAlves Jun. 1989 7 p In PORTUGUESE; ENGLISH summary Presented at the 5th Brazilian Symposium on Remote Sensing, Natal, Brazil, 11-15 Oct. 1988
(INPE-4827-PRE/1458) Avail: NTIS HC A02/MF A01

The objective is to present a developing methodology that uses Geographic Information Systems (GIS): (1) to aid the making of land suitability maps through the use of topographic maps and data/maps of soil surveys; and (2) to verify the actual land use in each obtained land suitability class with the purpose of detecting agricultural areas with inadequate land use. TM/LANDSAT imagery, topographic maps and soil survey data of the study area 22 deg

00 min to 22 deg 15 min S and 47 deg 15 min to 47 deg 30 min W and the GIS developed at INPE are used. The methodology consists of the digitization and superposition of those data using the GIS/INPE and obtaining as a result, the land suitability map of the study area. This map will be combined with a land use map obtained with the TM/LANDSAT imagery with the objective of verifying the appropriate use of the suitability classes obtained. Preliminary results will be presented. Author

N90-18762# Instituto de Pesquisas Espaciais, Sao Jose dos Campos (Brazil).

THERMAL REMOTE SENSING IN THE DIFFERENTIATION OF SOYBEAN CROPS (GLYCINE MAX (L.) MERRILL) SUBMITTED TO WATER DEFICIT [SENSORIAMENTO REMOTO TERMAL NA DIFERENCIACAO DE CULTIVARES DE SOJA (GLYCINE MAX (L.) MERRILL) SUBMETIDAS AO DEFICIT HIDRICO]

Jose Carlos Neves Epiphanio, Mario ValerioFilho, and Icaro Vitorello Aug. 1989 11 p IN PORTUGUESE; ENGLISH summary Presented at the 3rd Brazilian Symposium on Remote Sensing, Rio de Janeiro, Brazil, 28-30 Nov. 1984 Prepared in cooperation with Centro de Pesquisas Agropecuaria dos Cerrados, Planaltina (Brazil)

(INPE-4900-PRE/1501) Avail: NTIS HC A03/MF A01

Remote sensing applications in the thermal infrared band (8 to 14 micrometers) have great potential in studies of urban thermal inertia, and water deficit in crops. The shortage or excess of water produces anomalous vegetal metabolism, the water deficit being directly responsible for opening and closing the stomas and consequently raising the foliage temperature, due to the shuting down of energy consumption associated to the halting of water evaporation. The objective is the evaluation of thermal behavior among several soybean cultivars submitted to water deficit. The experiment consisted of irrigated and non-irrigated plots and in each case three plots for each soybean cultivar. Canopy temperature determinations were done with a thermal infrared radiometer (PRT-5) and simultaneously, air temperature were also obtained. The results demonstrated no thermal behavior differentiation among irrigated soybean cultivars. However, in the non-irrigated plots, the soybean cultivars presented different thermal behavior, facilitating their separation into distinct groups according to their mechanism of water loss control. The results show that the potential of thermal infrared remote sensing in studies related to the development and selection of cultivars resistant to dry spells. Author

N90-18763# Instituto de Pesquisas Espaciais, Sao Jose dos Campos (Brazil).

EVALUATION OF TWO METHODS FOR ACQUISITION OF TRAINING STATISTICS FOR DIGITAL ANALYSIS OF AREAS PREPARED FOR PLOWING [AVALIACAO DE DOIS METODOS DE AQUISICAO DE ESTATISTICAS DE TREINAMENTO PARA A ANALISE DIGITAL DE AREAS DE SOLO PREPARADO PARA PLANTIO]

Getulio VargasdeAssuncao, Antonio Roberto Formaggio, and Mauricio Alves Moreira Aug. 1989 12 p In PORTUGUESE; ENGLISH summary Presented at the 3rd Brazilian Symposium on Remote Sensing, Rio de Janeiro, Brazil, 28-30 Nov. 1984

(INPE-4901-PRE/1502) Avail: NTIS HC A03/MF A01

Two methods to obtain training statistics (mean vector and covariance matrix) of digital analysis of areas featuring plowed land areas in Latosolic B (Terr Roxa) are studied. A study area of approximately 400 sq km localized in the Regional Agricultural Division of Ribeirao Preto, at the northeastern part of Sao Paulo State was selected. The applied methodology consisted of a digital analysis in which two approaches for the training statistics acquisition were utilized. In the first one, training areas were obtained on known land lots which were representatives of interest targets (supervised method), to be input to a maximum likelihood classifier (MAXVER). In the second approach an unsupervised classifier (K-means) was utilized to group pixels with homogeneous spectral signatures. After the grouping an identification of the land cover types which corresponded to the obtained spectral classes (information classes) was accomplished. Based on the results of the grouping, training areas with pure pixels (pixels without influence from the border of the land lot) were acquired to be utilized in the MAXVER. The evaluation of the performance of the two methods was made through the application of the t - test (alpha = 0.05) to the factors of correct classification (CC) and commission error (EI) obtained from the 8 randomly scene segments of the study area with different densities of plowed land. Author

N90-18764# Instituto de Pesquisas Espaciais, Sao Jose dos Campos (Brazil).

MONITORING OF REFORESTED AREAS THROUGH DIGITAL ANALYSIS OF TM DATA [MONITORAMENTO DE AREAS REFLORESTADAS ATRAVES DE ANALISE DIGITAL DE DADOS TM]

David Chung Liang Lee, Pedro Hernandez Filho, and Yosio Edemir Shimabukuro Sep. 1989 8 p In PORTUGUESE; ENGLISH summary Presented at the 5th Brazilian Symposium on Remote Sensing, Natal, Brazil, 11-15 Oct. 1988

(INPE-4930-PRE/1420) Avail: NTIS HC A02/MF A01

The objective is to develop and evaluate a method of computer processing of the LANDSAT-TM digital data to monitor the detectable changes of the reforestation areas during the years 1986 and 1987. The study area includes the Campininha pine experimental station of Forestry Institute of Sao Paulo State and the Santa Terezinha eucalyptus plantation of the Champion Celullose and Paper Company. The LANDSAT-TM CCTs were processed with the IMAGE-100 interactive multispectral analyzer by means of themes intersection function and multidate classification. The results showed the changes of the areas of Pinus spp and Eucalyptus spp and also the clear cuttings of the plantation forest. Author

N90-18765# Instituto de Pesquisas Espaciais, Sao Jose dos Campos (Brazil).

EVALUATION OF SELECTION TECHNIQUES FOR MULTISPECTRAL BANDS EMPLOYED IN THE DISCRIMINATION OF CARBONATIC ROCKS M.S. Thesis [AVALIACAO DE TECNICAS DE SELECAO DE BANDAS MULTIESPECTRAIS VISANDO A DISCRIMINACAO DE ROCHAS CARBONATICAS]

Wougran SoaresGalvao Jul. 1989 309 p In PORTUGUESE; ENGLISH summary

(INPE-4850-TDL/365) Avail: NTIS HC A14/MF A02

This work focused on the evaluation of different digital image processing techniques in the selection of TM-LANDSAT data for lithological discrimination. As a test-site was choosen carbonatic sequences of the Estancia Group, part of the Sergipana folded belt occurring in the northern of the Bahia State (morro do Cambaio). Three selection criteria were used to select the best subsets of three and four bands using as input six TM original bands (TM 1, 2, 3, 4, 5 and 7) and six ratios (TM 3/1, 5/2, 5/4, 7/1, 7/2 and 7/4): (1) ranking on the value of the product of three eigenvalues associated with the variance - covariance matrix for any given band triplet; (2) ratio of the sum of the standard deviation of three bands comprising the triplet correlation coefficients - Optimum Index Factor; and (3) maximization of the average distance among the JM distance for all pairs of the thematic classes. All the investigation was based on the visual analysis of the enhancements products (color composites of original bands, band-ratios and principal component transformation). Author

N90-18766# Instituto de Pesquisas Espaciais, Sao Jose dos Campos (Brazil).

REMOTE SENSING APPLIED TO THE MONITORING OF MINERAL EXTRACTION IN THE PROXIMITY OF URBAN AREAS: PROS AND CONS

Dalton deMorissonValeriano Jun. 1989 13 p In PORTUGUESE; ENGLISH summary Presented at the National Meeting on Remote Sensing Applied to Municipal Planning, Campos do Jordao-SP, 22-23 Oct. 1987

(INPE-4867-PRE/1478) Avail: NTIS HC A03/MF A01

Within the economic activities that are directly related to the

exploration of natural resources, quarrying is one of those that are able to cause great environmental disturbances. The lowering of the life quality standard that generally follows environmental degradation justifies the need of a relatively high frequency monitoring of mineral extraction activity when it takes place in urban fringes. Due to its inherent periodicity, spaceborne remote sensing is potentially a fundamental tool to the execution of such monitoring. Nevertheless, due to the operational peculiarities of the activities and the the variability of materials envolved in the mineral extraction, the application of remote sensing to its monitoring requires methodological attentions that are specific to each type of quarrying. These methodological aspects are discussed through the analysis of a case study: the coal mining in Southeastern Santa Catarina State. Author

N90-18767# Instituto de Pesquisas Espaciais, Sao Jose dos Campos (Brazil).

RADIOMETRIC STUDY OF WHEAT AND BEAN CROPS IN THREE TYPES OF LATOSSOLO [ESTUDOS RADIOMETRICOS DAS CULTURAS DE TRIGO E DE FEIJAO EM TRES TIPOS DE LATOSSOLOS]

Antonio Roberto Formaggio and Jose Carlos NevesEpiphanio May 1989 9 p In PORTUGESE; ENGLISH summary Presented at the 5th Brazilian Symposium on Remote Sensing, Natal, Brazil, 11-15 Oct. 1988

(INPE-4843-PRE/1472) Avail: NTIS HC A02/MF A01

A more detailed knowledge about the crops and soils spectral behavior is needed when developing the potential of the multispectral measurement acquired by aerospace sensors with the purpose of monitoring, mapping, and inventoring agricultural resources. In this work, 46 spectral curves (400 to 1050 nm) were obtained for wheat and bean, in the NW region of Sao Paulo State, where three important types of Brazilian oxisols occur: Latossolo Roxo, Latossolo Vermelho Escuro and Latossolo Bermelho Amarelo. The spectral measurement included a wide range of cultural conditions during the bean and wheat biological cycles. Some cultural indices were also obtained, as percent soil cover, leaf area index, and phytomass. The results lead to some indications: there were good simple linear correlations between spectral variables (TM simulated bands RTM1, 2, 3, 4, and vegetation indices: simple ratio, normalized difference ratio and transformed vegetation index) and agronomic variables (LAI, phytomass, and percent soil cover) for bean. On the other hand, there were good correlations between LAI and RTM4, simple ratio and normalized difference ratio, as well as between percent soil cover and RTM4, using simple linear model, for wheat. Author

N90-18768# Instituto de Pesquisas Espaciais, Sao Jose dos Campos (Brazil).

RELATIONSHIPS BETWEEN SPECTRAL PARAMETERS AND AGRONOMICS OF WHEAT AND BEAM CROPS

Antonio Roberto Formaggio and Jose Carlos NevesEpiphanio Jan. 1989 80 p In PORTUGUESE; ENGLISH summary Project DINAGR, performed at the Convention INPE/EMBRAPA (CNPDA), Jaguariuna-SP

(INPE-4791-RPE/584) Avail: NTIS HC A05/MF A01

Data of 18 cultural parameters of wheat and bean were collected. Wheat and bean were grown over three types of oxisols in the NW region of Sao Paulo State. Spectral data (TM/LANDSAT and 400 to 1100 nm field spectroscopy) were collected too and three types of vegetation indexes were obtained: IR/red simple ratio (RS), normalized difference (ND) and transformed vegetation index (TVI). Graphic and simple linear correlation analyses were made between spectral and agronomic variables. Spectral parameters correlated very interestingly with agronomic variables during wheat and bean cycles phonological variations. TM3, TM4, and TM5 were the singular bands which contained more information about crop canopy; these three bands answered very well to phonological variations during the crop cycles. TM4 correlated better with agronomic variables which indicate foliage conditions (ex.: vegetal covering, number of green leaf/plant and LAI). TM5 band correlated better with agronomic variables which indicate crop mass (phytomass and weight of dry material, for example). Field spectroscopy was considered an excellent way for studying and modeling agronomic/spectral variables. For field spectroscopy there was smaller correlation for what than for bean. Spectral/agronomic correlations for vegetation indexes weren't better than for singular TM bands, probably due to the uniform conditions in the moment of the data collection. Author

N90-18769# Instituto de Pesquisas Espaciais, Sao Jose dos Campos (Brazil).

MULTISTAGE FOREST VOLUME ESTIMATION USING A SAMPLING SYSTEM WITH PROBABILITY VARIABLES

Pedro HernandezFilho, David Chung Liang Lee, Yosio Edemir Shimabukuro, Oswaldo RoquedeAssis, and Jose SimeaodeMedeiros Aug. 1989 15 p In PORTUGUESE; ENGLISH summary Presented at the 3rd Brazilian Symposium on Remote Sensing, Rio de Janeiro-RJ, 28-30 Nov. 1984

(INPE-4897-PRE/1498) Avail: NTIS HC A03/MF A01

A multistage sampling technique was evaluated with probability proportional to size, of forest volume inventory using remote sensing data. LANDSAT photographic imagery channel 5 and 7, from May 1981, was used in the first stage for visual classification of reforested areas. The classes were defined based on genus and age of forest plantation. A grid (1.0 x 1.0 cm) was fixed on the image, at the scale of 1:250,000. The Primary Sampling Units (PSUs) were selected based on the Probability Proportional to Size (PPS) ratio. CIR aerial photographs were obtained in July, 1983, at the scale of 1:20,000 in each PSU's selected. In the second stage a grid (2.5 x 2.5 cm) was fixed on the aerial photographs. The Second Sampling Units (SSU's) were selected based on the PPS. A grid (0.5 x 0.5 cm) was fixed for each SSU selected. The Tertiary Sampling Units (TSUs) were selected based on the PPS. In the third stage (ground level), the timber volume was expanded for the Mato Grosso do Sul state through a statistical procedure taking into account all the three stages. Author

N90-18770# Instituto de Pesquisas Espaciais, Sao Jose dos Campos (Brazil).

REMOTE SENSING APPLIED TO VEGETATION AS SUBSIDIZED IN MUNICIPAL PLANNING

Dalton deMorissonValeriano, Joao Roberto dosSantos, Pedro HernandezFilho, and Vitor CelsodeCarvalho Aug. 1989 16 p In PORTUGUESE; ENGLISH summary Presented at the National Meeting on Remote Sensing Applied to Municipal Planning, Campo do Jordao-SP, 22-23 Oct. 1987

(INPE-4908-PRE/1509) Avail: NTIS HC A03/MF A01

The rational exploration of the natural resources of a municipality must be one of the objectives of its administration. New technologies offer means and alternatives that make possible the full utilization of the natural resources within the limits of the carrying capacity of the environment. Remote sensing of the vegetation is one of these available means. The assessment of the vegetation cover though mapping and inventories provides basic information for the establishment of polities and strategies for the development. The monitoring of the vegetation, which is made through periodic updating of its assessment, allows the evaluation of the results of politics, besides the fact that it depicts trends in the pattern of resources exploration. The applicability of the remote sensing of the vegetation to the municipal planning through the analysis of its foundations and methodological pecularities is discussed. Case studies of the Brazilian vegetation are presented in order to picture the state of art of the subject in Brazil. Author

N90-18771# Instituto de Pesquisas Espaciais, Sao Jose dos Campos (Brazil).

INTERRELATIONSHIP OF SPATIAL AND RADIOMETRIC RESOLUTION IN THE THERMAL INFRARED BAND M.S. Thesis [A INTER-RELACAO DAS RESOLUCOES ESPACIAL E RADIOMETRICA NA FAIXA DO INFRAVERMELHO TERMAL]

Antonio Frederico Bastos Aug. 1989 123 p In PORTUGUESE; ENGLISH summary

(INPE-4860-TDL/371) Avail: NTIS HC A06/MF A01

The geometric and radiometric resolutions of a thermal imaging system was determined and its relationship was established. The

geometric resolution was determined through the MTF of the system which was obtained from experiments where artificial targets were imaged. Emissivity or temperature differences were explored. The targets used in the experiments allowed that the impulsive function and step function to be simulated as input functions to the system. The radiometric resolution was obtained from laboratory experiments where a noise equivalent temperature difference (NETD) was determined. The quality of the minimum detectable temperature difference (MDTD) was evaluated. The results obtained were analyzed as well as some observed discrepancies. By analyzing the resolution relationship, a new parameter NETD* was proposed to describe it. It is considered that a methodology was established for the thermal imaging systems characterization. A study of the possibilities of the NETD* was suggested. Author

N90-18772# Instituto de Pesquisas Espaciais, Sao Jose dos Campos (Brazil).

EVALUATION OF TM/LANDSAT AND HRV/SPOT DATA IN REFORESTED AREAS [AVALIACAO DE DADOS TM/LANDSAT E HRV/SPOT EM AREAS REFLORESTADAS]

Pedro Hernandez Filho, David Chung Liang Lee, Facundo Salomon RecaldeRamos, and Sergio Alberto deOliveiraAlmeida Jun. 1988 96 p In PORTUGUESE; ENGLISH summary

(INPE-4575-RPE/567) Avail: NTIS HC A05/MF A01

The objective is to evaluate the TM/LANDSAT and HRV/SPOT data. The study area, Mogi Guacu-Sao Paulo State, is located at 44 degrees 00 minutes to 47 degrees 15 minutes W and 22 degrees 5 minutes to 22 degrees 15 minutes S. This area includes pine and eucalyptus plantations, with different ages and density canopy. Based on visual and digital analysis of TM/LANDSAT and HRV/SPOT data, the Pinus-1, Pinus-2, and Euca classes were defined. The interpretation and mapping accuracy of the classes were estimated. The combination bands were selected by JM distance algorithm. Author

N90-18773# Instituto de Pesquisas Espaciais, Sao Jose dos Campos (Brazil).

DEVELOPMENT OF THE AGRICULTURAL INFORMATION SYSTEM. CHARACTERISTICS AND RESULTS OF THE DISTRITO FEDERAL MODEL [DESENVOLVIMENTO DO SISTEMA DE INFORMACOES AGROPECUARIAS. CARACTERISTICAS E RESULTA DOS DO MODELO NO DISTRITO FEDERAL]

Alvaro GonzalezVillalobos, Mauricio AlvesMoreira, Gil Silva (Instituto Brasiliero de Geografia e Estatistica, Rio de Janeiro.), and Antonio Jose deSouzaBiffi Sep. 1989 17 p In PORTUGUESE; ENGLISH summary Presented at the 5th Brazilian Symposium on Remote Sensing, Natal, Brazil, 11-15 Oct. 1988

(INPE-4940-PRE/1430) Avail: NTIS HC A03/MF A01

The Agricultural Information System (AIS) is the national program to produce current agricultural data corresponding to the summer crops, based on the application of probabilistic area survey sample methods and the use of satellite images. The program was initiated in 1986 and is now already implemented in the states of Parana, Santa Catarina and Distrito Federal. It will be applied also to the states of Sao Paulo, Mato Grosso do Sul, Rio Grande do Sul and Minas Gerais, so that, from 1991, the AIS will cover Brazil's most important agricultural region. The model is based, on each state, in the design and selection of a one-stage, systematic and self-weighted sample of segments, stratified by land-use. These segments are used annually to collect ground data. During the field work, a questionnaire is applied for each agricultural establishment partially or totally included in the sampled segments. Also, all fields and establishments are located, delineated, and measured on aerial photographs covering the sampled segments. The construction of the sampling frame, formed by a large number of subdivisions of the strata, is accomplished by using satellite images (TM/LANDSAT-5), 1985 Census data, topographic maps, aerial photographs, and an INTERGRAPH computer graphic system. Closed and weighted multiple frame estimators (based on list frames of special establishment), are used in order to produce AIS annual agricultural estimates. The basic characteristics of the model and its application to the Distrito Federal, for the first time, during December 1987, are presented. Author

N90-18774# Instituto de Pesquisas Espaciais, Sao Jose dos Campos (Brazil).

SPECTRAL RESPONSE OF WHEAT AND ITS RELATIONSHIP WITH AGRONOMICAL PRAMETERS [RESPOSTA ESPECTRAL DO TRIGO E SUA RELACAO COM PARAMETROS AGRONOMICOS]

Bernardo F. T. Rudorff and Getulio TeixeiraBatista Sep. 1989 67 p In PORTUGUESE; ENGLISH summary Sponsored in part by Bank of Brazil

(INPE-4950-RPE/599) Avail: NTIS HC A04/MF A01

The spectral behavior of three varieties of wheat (Anahuac, IAC-24, and BH-1146) was analyzed using field radiometry throughout the 1988 growing season, in the region of Assis, SP. The field radiometric data were obtained in the visible and near infrared portion of the electromagnetic spectrum of 30 sampled fields distributed in commercially planted fields of four farms. The radiometric data were transformed into vegetation indices which are expected to represent crop growing conditions and development. These indices were related to agronomic variables (grain yield, green phytomass, dry phytomass, canopy height) obtained in ten measurement campaigns carried out weekly beginning at initial stages of growing (approximately 30 days after planting) until harvesting. The main objective was to verify the potential of spectral data to estimate grain yield of wheat growing in tropical region. It was observed that the vegetation index obtained at the beginning of the flowering stages was quite well related to the final grain yield and correlation coefficients of 0.82 to 0.93 were obtained. The radiometric data were analyzed multitemporally also, where the vegetation indices were integrated throughout the growing cycle and related to the final yield. Another analysis, included the incorporation of spectral data into an yield estimation model called the agrometeorological-spectral model. This model was developed to provide an assessment of the growing conditions of a crop through meteorological and spectral variables. Results obtained clearly indicated that the reflected energy at certain stages of the crop development and at certain wavelength bands are well related to the final grain yield. Therefore, spectral data, transformed into vegetation indices have great potential to be used in yield predicting models. Author

N90-18775# Instituto de Pesquisas Espaciais, Sao Jose dos Campos (Brazil).

PERSPECTIVE REVISION OF SYSTEMATIC MAPPING THROUGH ORBITAL IMAGERY [PERSPECTIVAS DE ATUALIZACAO DO MAPEAMENTO SISTEMATICO ATRAVES DE IMAGENS ORBITAIS]

Julio Cesar LimadAlge and Nilson Alves Pereira Jun. 1989 7 p In PORTUGUESE; ENGLISH summary Presented at the 5th Brazilian Symposium on Remote Sensing, Natal, Brazil, 11-15 Oct. 1988

(INPE-4817-PRE/1453) Avail: NTIS HC A02/MF A01

The existing unmapped areas and the lack of revision of topographic maps are the basic problems regarding the systematic mapping in Brazil. An efficient national mapping program is required to solve these problems, including the use of TM-LANDSAT and HRV-SPOT images as an alternative for the revision of systematic mapping. Tests point out the viability of map revision at scales of 1:250,000 and 1:100,000, with some restrictions related to the spatial resolution of the images. A map revision proposal is presented which is supported by the Geographic Information System under development at INPE. Author

N90-18776# Instituto de Pesquisas Espaciais, Sao Jose dos Campos (Brazil).
PHYSIOGNOMY OF VEGETATION COVER IN THE PNPM IDENTIFIED THROUGH THE TM/LANDSAT SENSOR: A MULTITEMPORAL ANALYSIS [A FISIONOMIA DA COBERTURA VEGETAL DO PNPM IDENTIFICADA ATRAVES DO SENSOR TM/LANDSAT: UMA ANALISE MULTITEMPORAL]
Flavio Jorge Ponzoni and Pedro HernandezFilho Jun. 1989 7 p In PORTUGUESE; ENGLISH summary Presented at the 5th Brazilian Symposium on Remote Sensing, Natal, Brazil, 11-15 Oct. 1988
(INPE-4834-PRE/1464) Avail: NTIS HC A02/MF A01

Thematic mapper satellite images and 35 mm aerial photographs were utilized in the physiognomic survey of the Pantanal Matogrossense National Park vegetation cover. Two dates were considered (dry and wet season) in order to evaluate the water level influence in the vegetation physiognomies identified. Visual interpretation and digital processing were considered. Through the first, two vegetation maps (both seasons) were done and the second allowed a quantitative study of the water level variations. Author

N90-18777# Instituto de Pesquisas Espaciais, Sao Jose dos Campos (Brazil).
PROJECT FLOVAL: CORRECTION OF RELIEF EFFECTS IN EUCALYPTUS REFORESTRATION Final Report [RELATORIO FINAL DO PROJETO FLOVAL - CORRECAO DOS EFEITOS DO RELEVO EM REFLORESTAMENTO DE EUCALIPTUS]
Luiz Alberto VieiraDias, Flavio Jorge Ponzoni, Eni AlvimdeOliveira, David Lee, and Mauricio MarquesFernandes Jun. 1989 18 p In PORTUGUESE; ENGLISH summary
(INPE-4814-RPE/590) Avail: NTIS HC A03/MF A01

If the targets are in a plane horizontal region then targets with the same characteristics will produce the same spectral response. However if the targets are located on mountainous terrain, the same targets may produce different spectral response, due to the terrain slope. The PROJECT FLOVAL objective was concerned with the development of a methodology for the mapping of reforestation areas on mountainous regions, using LANDSAT Thematic Mapper data and Digital Elevation Models (DEM). To correct the relief effect on satellite images a cartographic map of the region must first be obtained, next a DEM of the region under study is prepared, and an illumination model for radiance correction choosen. With the slope information from the DEM and the illumination model, each pixel (picture element) is then radiometric corrected. Author

N90-18778# Instituto de Pesquisas Espaciais, Sao Jose dos Campos (Brazil).
CLASSIFICATION OF HIGH RESOLUTION IMAGERY USING TEXTURE ATTRIBUTES M.S. Thesis [CLASSIFICACAO DE IMAGENS DE ALTA RESOLUCAO USANDO ATRIBUTOS DE TEXTURA]
Valeria Maria BarrosdeAndrade 1989 97 p In PORTUGUESE; ENGLISH summary
(INPE-4888-TDL/379) Avail: NTIS HC A05/MF A01

Most classifiers commonly used in image analysis rely solely on spectral characteristics to differentiate classes. These classifiers were originally developed to be used with LANDSAT-MSS data. With the news sensors at different spatial resolutions it is necessary to revise the image classification methods. Studies about spatial resolution effects on classification shows that classification accuracy is influenced by two factors: the mixed pixels and scene noise. The presence of scene noise provides one more image characteristic, the texture. The classification accuracy is evaluated as a function of spatial resolution is made. It is verified that confusion error rates decrease with smaller resolutions. However, for small resolution image, it can be observed, due to the increasing rate of mixed pixels, an increasing rate of non-classified pixels. In the second part, some texture measures (or features) are proposed. They are extracted from small image windows. By extraction of the textural feature at each pixel, texture bands are created. The twenty proposed texture bands are visually and statistically analyzed from an image of Sao Jose dos Campos urban area. From this analysis, two texture bands are selected and used to classify this image. A better classification accuracy is verified, in the sense that a decreasing confusion error rate without a significant increasing rate of non-classified pixels is observed. Author

N90-18779# Naval Research Lab., Washington, DC. Tactical Electronic Warfare Div.
EARTH MODEL SELECTION FOR COMPUTER SIMULATIONS Final Report
J. J. Pich and S. S. Leroy 15 Dec. 1989 52 p Sponsored by Naval Air Systems Command, Washington, DC
(AD-A216843; NRL-9227) Avail: NTIS HC A04/MF A01 CSCL 08/5

Many scientific problems require the use of appropriate Earth models. This report presents a method of selecting from a variety of these models on the basis of range and and bearing errors and CPU timing considerations that are incurred by each. The report begins by examining two types of Flat models and determines the better of the two. The reference for the determinations of all errors is the DoD standard Earth model representation, the World Geodetic System (WGS-84) reference ellipsoid. The report shows that for short distances a Midpoint Flat Earth model is adequate at low latitudes. However, for longer ranges, better Earth models must be employed. The model proceeds to compare five spherical Earth models (different radii based on different assumptions). A model referred to as the Spherical Approximation is shown to be a superior representation that allows for an increase in the permissible distance coverage under various constraining error budgets. For an error budget of 1000 m, the representation can be used to compute distances up to 250 nmi in the midlatitudinal region of 40 N to 70 N. For distances beyond 250 nmi, only a WGS-84 reference ellipsoid representation is adequate for the 1000 m error budget. GRA

N90-18780# Naval Research Lab., Washington, DC. Space Systems Technology Dept.
AN EVALUATION OF AN AIRBORNE LASER PROFILING SYSTEM FOR HIGH PRECISION TERRAIN MAPPING
J. L. Shuhy, B. W. McCoy (Bendix Field Engineering Corp., Columbia, MD.), E. A. Uliana, and L. W. Choy 22 Nov. 1989 67 p
(AD-A217025; NRL-MR-6581) Avail: NTIS HC A04/MF A01 CSCL 08/2

This report presents the results of an evaluation of the capabilities of an airborne laser profile system to obtain ground truth data for the evaluation of the range tracking capability of high resolution radar altimeters. Quantitative evaluations were made of man-made objects such as seats/steps at a football stadium and various buildings. Qualitative evaluations were made with natural terrain such as trees, lakes, land elevations, and power lines along a trackline over Florida. GRA

N90-18781# Deutsche Forschungsanstalt fuer Luft- und Raumfahrt, Cologne (Germany, F.R.).
[ACTIVITIES REPORT IN DLR RESEARCH FIELD COMMUNICATION ENGINEERING AND RECONNAISSANCE] Annual Report, 1989 [FORSCHUNGSBEREICH NACHRICHTENTECHNIK UND ERKUNDUNG. WISSENSCHAFTLICHER BERICHT: STAND 1989]
Joachim Holtz 1989 138 p In GERMAN Original contains color illustrations
(ISSN-0173-0118; ETN-90-96281) Avail: NTIS HC A07/MF A01

The Institute of High Frequency Engineering carried out research in the fields of radar remote sensing and reconnaissance, satellite assisted position finding and navigation, and satellite communication. The Institute of Optoelectronics developed optical sensors for space applications, radiation models, and laser methods for remote sensing, ranging and communication; and made environmental surveys using remote sensing, and planetary fields

of atmospheric dynamics, meteorological environmental research, meteorological remote sensing, cloud physics, and meteorological flight measuring systems. The Institute of Communication Engineering carried out research in the fields of channel modeling and simulation, coding and modulation, and assignment and error securing. ESA

N90-18782# European Space Agency, Paris (France).
ERS-1 EUROPEAN REMOTE SENSING SATELLITE: A NEW TOOL FOR GLOBAL ENVIRONMENTAL MONITORING IN THE 1990'S
Evert Attema, Gianna Calabresi, Maurizio Fea, Richard Francis, and Duc Guyenne, ed. Nov. 1989 40 p Original contains color illustrations
(ESA-BR-36; ISBN-92-9092-019-X; ETN-90-96298) Copyright Avail: NTIS HC A03/MF A01; ESA Publications Div., ESTEC, Noordwijk, Netherlands, 10 US dollars or 20 Dutch guilders

The First European Remote Sensing Satellite (ERS-1) is described in brochure format. Advanced microwave or radar techniques, used previously in the short Seasat mission, which enable global measurements and imaging to take place independently of clouds and sunlight conditions are described. The measurement of parameters previously not covered by satellites, including those of sea state, sea surface winds, ocean circulation and sea/ice levels, and all-weather imaging of ocean, ice and land, are covered. A ground segment overview, satellite control and operations, and data acquisition and fast processing are included. The ERS-1 has been designed to satisfy operational requirements for data products within a short timeframe. The significant contributions to the scientific study of the environment are discussed. ESA

N90-18783# Beleidscommie Remote Sensing, Delft (Netherlands).
ON THE APPLICABILITY OF CAESAR FOR THE REMOTE SENSING OF BOTTOM DEPTH AND BOTTOM COMPOSITION OF SHALLOW WATERS: A MODEL STUDY Final Report
G. Marees and D. Spitzer Jul. 1989 37 p
(BCRS-89-13; NIOZ-1988-10; ETN-90-96317) Avail: NTIS HC A03/MF A01

Characteristic spectral signatures of various seawater and seabottom composition types are chosen as input parameters of a two-flow radiative transfer model. From this model waterleaving irradiance spectra are calculated for several types of seawater, bottom composition, and varying bottom depths. The resulting signals for the spectral bands of the aircraft remote sensing scanner Caesar are computed in order to deduce appropriate algorithms for remote determination of bottom depth and bottom composition. The deduced Caesar bottom algorithms are found to be more accurate than similar algorithms earlier found for LANDSAT Thematic Mapper. In case of clear water in combination with a sandy bottom composition. Caesar can detect the bottom features down to depths of 24 to 31 m. ESA

N90-18784# Beleidscommie Remote Sensing, Delft (Netherlands).
INTRODUCTION OF AERIAL PHOTOGRAPHY IN AGRICULTURAL RESEARCH [INTRODUCTIE VAN LUCHTFOTOGRAFIE IN HET LANDBOUWKUNDIG ONDERZOEK]
J. G. P. W. Clevers (State Agricultural Univ., Wageningen, Netherlands) Oct. 1989 58 p In DUTCH
(BCRS-89-14; ETN-90-96318) Avail: NTIS HC A04/MF A01

The operational use of aerial photography for agricultural applications was investigated. The method used for Multispectral Aerial Photography (MAP) is explained. The determination of IR reflection percentages using MAP allows the mapping of the soil heterogeneity. The more accurate estimate of vegetation properties by MAP provides improved statistical analysis of the test fields. The MAP opens possibilities for the agricultural practice, namely the mapping of individual parcels with a view to the optimization of the cultivation techniques. ESA

N90-18785# Beleidscommie Remote Sensing, Delft (Netherlands).
EROSION MONITORING USING REMOTE SENSING, PART 2
J. R. Moll, ed. (Delft Hydraulics Lab., DeVoorst, Netherlands), R. L. M. Nieuwkamer, Joyce Martha Widjaya, Lanny Martawati, Heni Rengganis, and S. Fadillah Sep. 1989 61 p Prepared in cooperation with Pusat Litbang Pengairan, Bandung (Indonesia)
(BCRS-89-15; Q-764; ETN-90-96319) Avail: NTIS HC A04/MF A01

Results of the second phase of a research project aimed at developing a method to monitor erosion based on remote sensing imagery are given. The approach focuses on the measurement of the output from erosion processes, that is, concentrations of suspended sediments in reservoirs. Citarum river basin (west Java) was investigated. LANDSAT and SPOT radiance values were related to in situ measured concentrations of suspended sediment and chlorophyll-a, after application of atmospheric correction procedures. Computations with the mathematical model SERES-1 (sedimentation in reservoirs) supplemented in situ data. Results indicate that good quality quantitative classifications of concentrations can be made for individual images, but that development of an automatic classification requires further research. ESA

N90-18786# Beleidscommie Remote Sensing, Delft (Netherlands).
IMPROVEMENT OF CLASSIFICATION RESULTS FROM SATELLITE IMAGERY TO UPDATE AND DIFFERENTIATE LAND USE CLASSES ON TOPOGRAPHIC MAPS
Oct. 1989 89 p Prepared in cooperation with NLR, Emmeloord, Netherlands and DHV Raadgevend Ingenieursbureau B.V., Amersfoort, Netherlands
(BCRS-89-17; NLR-TR-88155-U; DHV-JWvdB-8902; ETN-90-96320) Avail: NTIS HC A05/MF A01

The extent to which digitized information from a topographic map was of use to improve classification results and to what extent land use change could be mapped was investigated. Information from a LANDSAT Thematic Mapper (1986 situation) and land use information from a 1:50,000 scale topographic map (1980 situation) of the area digitized on a drum scanner was combined and interpreted using additional knowledge about the classification result and the topographic map and landscape and landscape dynamics. The accuracy attained and the simplicity and feasibility of the method suggest that the use of remote sensing can be stimulated for practical applications. ESA

N90-18787# Beleidscommie Remote Sensing, Delft (Netherlands).
SPOT FOR LANDSCAPE: DEVELOPMENT OF A METHOD FOR THE USE OF SPOT PICTURES FOR THE UPDATING OF THE DATA BASE SCALE OF THE LANDSCAPE [SPOT VOOR LANDSCHAP METHODE ONTWIKKELING VOOR HET GEBRUIK VAN SPOT-BEELDEN VOOR DE BIJSTELLING VAN HET GEGEVENSBESTAND SCHAAL VAN HET LANDSCHAP]
G. H. P. Dirkx, A. A. deVeer, H. A. M. Thunnissen, and F. B. vanderLaan (National Aerospace Lab., Amsterdam, Netherlands) Oct. 1989 38 p In DUTCH
(BCRS-89-18; ETN-90-96321) Avail: NTIS HC A03/MF A01

The use of SPOT images for landscape studies was analyzed, with emphasis on the visual aspect and the updating of a part of the data base. The visual-manual method and a method which classifies SPOT images digitally were applied. It is found that the resolution of the SPOT images is not sufficient for the pattern recognition of the thin, interrupted lines of vegetation in the Dutch landscape, although these images provide substantially more detail than those of the LANDSAT-TM satellite. ESA

N90-18788# Beleidscommie Remote Sensing, Delft (Netherlands).
REMOTE SENSING AND RUN-OFF MODELLING IN THE LAKE VICTORIA BASIN, KENYA Final Report
J. P. vanderLinden (Delft Hydraulics Lab., Netherlands), J. W. Wesseling, and P. Wit Oct. 1989 36 p Prepared in cooperation

with DHV Raadgevend Ingenieursbureau B.V., Amersfoort, Netherlands
(BCRS-89-19; ETN-90-96322) Avail: NTIS HC A03/MF A01

The use of remote sensing in rainfall runoff modeling is investigated with emphasis on the development of a method for determination of hydrological parameters using satellite imagery to ameliorate results of hydrological modeling for areas where hardly anything is measured. Interpretation of the selected imagery resulted in a land cover map, a vegetation index image (biomass), and a thermal image using LANDSAT-TM thermal canal. The hydrological response model used, the Sacramento generalized streamflow simulation system, is a conceptual lumped parameter model in which model parameters have physical meaning. With more groundtruth data available when the satellite image is taken, and necessary hydrological information of a larger number of subcatchments available covering the period of the imaging, a better use of remote sensing data, especially in the infrared zone is forecast. ESA

N90-18789# Beleidscommie Remote Sensing, Delft (Netherlands).
RESULTS OF AGRISAR-86 FOR THE FLEVOPOLDER (NETHERLANDS) TEST AREA Final Report
J. S. Groot and P. Hoogeboom (Physics and Electronics Lab. TNO, The Hague, Netherlands) Oct. 1989 32 p
(BCRS-89-21; ETN-90-96323) Avail: NTIS HC A03/MF A01

Results of the Dutch contribution to the European Agrisar 1986 campaign, relating to radar remote sensing of agricultural areas are presented. Objectives of the research were: analysis of the potential of multitemporal synthetic aperture radar (SAR) images taken from the same test sites during the crop growing period for crop identification and monitoring of growth; and cross-calibration of SAR data taken from the same test sites at different measurement times. ESA

N90-18790# Beleidscommie Remote Sensing, Delft (Netherlands).
REMOTE SENSING FOR THE CLASSIFICATION AND QUANTIFICATION OF VEGETATION IN SPRING STAGING AREAS OF BRENT GEESE ON THE FRISIAN ISLANDS (NETHERLANDS) Final Report [REMOTE SENSING VOOR DE CLASSIFICATIE EN KWANTIFICATIE VAN DE VEGETATIE OP GANZENPLEISTERPLAATSEN IN HET WADDENGEBIED]
R. J. Bijlsma Oct. 1989 62 p In DUTCH
(BCRS-89-27; RIN-89/5; ETN-90-96324) Avail: NTIS HC A04/MF A01

The vegetation development during Spring staging of Brent geese was monitored for the main staging habitats in the Dutch Wadden Sea (Netherlands). Digital image processing techniques were used for the evaluation of the color IR photographs. A relative calibration procedure was developed, based on the assumption of the existence of pixel regions with bare soil and on the similarity of the reflectance values of bare soil in green, red and IR. For reliable detailed calibration the use of reference panels with known reflectance properties is obligatory. Eight vegetation types were classified. The arctan (IR/red) vegetation index proved to be valuable for graphical interpretation and simple implementation. For an optimal use of remote sensing of vegetation in grazing studies, information on the relation between spectral properties and aerial biomass, and preferable also food quality, must be available. ESA

N90-18791# Beleidscommie Remote Sensing, Delft (Netherlands).
LANDSAT THEMATIC MAPPER FOR HYDROGEOLOGICAL MAPPING IN EGYPT Final Report
Nov. 1989 65 p
(BCRS-89-28; ETN-90-96325) Avail: NTIS HC A04/MF A01

The management of water in the eastern Nile delta between Port Said and Suez, and in the Nile Valley between Beni Suef and Minya, (Egypt) is addressed. Aims are to show the value of satellite remote sensing for production of hydrogeological maps and for groundwater management, to introduce new techniques in regional groundwater investigations to the Research Institute for Ground Water (RIGW), and to develop and produce professional satellite base maps for the areas of study. Results and discussions with the participating Egyptian institutes are given. Recommendations include multitemporal observations for particular regions of interest. ESA

44 ENERGY PRODUCTION AND CONVERSION

Includes specific energy conversion systems, e.g., fuel cells; global sources of energy; geophysical conversion; and windpower.

For related information see also *07 Aircraft Propulsion and Power, 20 Spacecraft Propulsion and Power,* and *28 Propellants and Fuels.*

N90-18792# Midwest Research Inst., Golden, CO.
PROGRESS IN THIN FILM SOLAR PHOTOVOLTAIC TECHNOLOGIES
H. S. Ullal and K. Zweibel Dec. 1989 12 p Presented at the 9th Miami International Congress on Energy and Environment, Miami Beach, FL, 11-13 Dec. 1989
(Contract DE-AC02-83CH-10093)
(DE89-009513; SERI/TP-211-3604; CONF-891210-1) Avail: NTIS HC A03/MF A01

This paper focuses on the rapid recent advances made by thin film solar cell technologies, namely, amorphous silicon, copper indium diselenide, and cadmium telluride. It also indicates the several advantages of thin films. Various consumer products and power applications using thin film solar cells are also discussed. The increasing interest among the utilities for PV system applications is also elucidated. DOE

N90-18793# Institute of Energy Economics of Japan.
ANALYSIS OF COMPETITION AMONG THE KINDS OF ENERGY AT THE ERA OF COMPLEXED ENERGY: GENERAL REVIEW
31 Dec. 1989 125 p In JAPANESE
(DE89-910215; IEE-SR-205) Avail: NTIS (US Sales Only) HC A06/MF A01

Present situation of competition among kinds of energy was analyzed, and energy industries and national policy for energy at the era of complexed energy. Possibilities of progress were reviewed and explained under the guiding principle of fair competition among the kinds of energy. Energy industries were classified into petroleum, town gas, and electricity. It was explained that decisive factors of competition among them were not only purchasing price but characteristics of application equipment. Problems involved in them were discussed. Competitive feature in the fields of industry and public welfare was explained in detail with review of future features. National policy for energy was discussed from the view points of holding of security, cost reduction, and adaptation to demands. Explanations of the present situation in Europe and America are mentioned. DOE

N90-18794# Institute of Energy Economics of Japan.
ANALYSIS OF INTER-ENERGY COMPETITION IN THE AGE OF COMPLEX ENERGIES
31 Dec. 1989 185 p In JAPANESE
(DE89-910216; IEE-SR-206) Avail: NTIS (US Sales Only) HC A09/MF A01

This is a survey report of the Japan Energy Economics Research Institute. Section 1 describes the energy industry in time of complex energies (History of changes and competition of energy sources. Formation of the energy market. Energy tax). Section 2 describes the present situation and the prospect of the competition among the energies (Present images of competition between industrial sector, civil household sector, transportation sector and the energy conversion sector. Development of the energy utilization system (cogeneration, regional air conditioning, waste heat recovery system, individual air conditioning system. Strategic meaning of

the expansion of inter-energy competition market). Section 3 describes the arrangement of the fair competition conditions and the energy policy (Energy policy effect and cost. Energy industrial regulation and its abatement. Competitive energy market and fair competing conditions). DOE

N90-18795# Heat Pump Technology Center of Japan, Tokyo.
STIRLING ENGINE TECHNOLOGIES IN JAPAN
Dec. 1988 313 p Presented at the International Symposium on the Stirling Engine and Its Application To Heat Pump Systems, Tokyo (Japan), 1-2 Dec. 1986 Prepared in cooperation with Agency of Industrial Science and Technology, Tokyo (Japan)
(DE89-782296; ETDE/JP-mf-9782296; CONF-8612178) Avail: NTIS (US Sales Only) HC A14/MF A02

Research and Development of Stirling Engine for Wide Use, one of the big national projects for energy conservation, also known as the Moonlight Project, was established to do applied research of Stirling engines for heat pump and small capacity electric generator applications. This project started at 1982 is scheduled to end in 1988. It is expected to bring 3 kW and 30 kW kinematic Stirling engines into general use to encourage the utilization of non-petroleum alternative fuels. Fundamental studies of engine components were conducted by three national research institutes, and the outline of the performance tests and analyses of four basic engines for an interim assessment at 1984 and their principal results obtained by 1985, an experimental analysis and numerical modeling of Stirling combustors, and a study on the grate combustion of wood residue fuels were reported in this proceeding. Four private companies have been respectively developing Stirling engines and their application, under the management and the promotion by NEDO (New Energy and Industrial Technology Development Organization). Most of the final goals for engines and systems, such as NO sub x emissions less than 150 ppm, has been achieving satisfactorily. Further improvement of these basic engines are currently being under taken toward achieving several final goals including less weight, more compactness, longer life and so on. DOE

N90-18796# Texas A&M Univ., College Station. Dept. of Chemical Engineering.
OXYGEN ELECTRODE IN MOLTEN CARBONATE FUEL CELLS Quarterly Report No. 9, 1 Aug. - 31 Oct. 1989
Bhasker B. Dave, Supramaniam Srinivasan, Ralph E. White, and A. John Appleby 1989 21 p
(Contract DE-FG22-87PC-79931)
(DE90-005377; DOE/PC-79931/T5) Avail: NTIS HC A03/MF A01

The oxygen reduction reaction on a gold electrode in lithium carbonate melt was investigated to determine the influence of partial pressure of carbon dioxide and temperature on electrode kinetic and oxygen solubility by using cyclic voltammetry and impedance analysis techniques. During this quarter, the impedance data were analyzed by a Complex Nonlinear Least Square (CNLS) parameter estimation program to determine the kinetic and the mass transfer related parameters such as charge transfer resistance, double layer capacitance solution resistance, and Warburg coefficient. The estimated parameters were used to obtain the CO2 reaction orders and apparent activation energies for the exchange current density and the mass transfer parameter (D(sub O)(sup 1/2)C(sub O)*). DOE

N90-18797# Pacific Northwest Lab., Richland, WA.
ENERGY MARKETS IN THE 1990'S AND BEYOND: A COMPARISON OF ENERGY INTENSITY IN THE UNITED STATES AND JAPAN
S. C. McDonald Oct. 1989 12 p Presented at the 11th Annual North American Conference of the International Association for Energy Economics, Los Angeles, CA, 16-18 Oct. 1989
(Contract DE-AC06-76RL-01830)
(DE90-005535; PNL-SA-17325; CONF-8910162-6) Avail: NTIS HC A03/MF A01

A comparative analysis is provided of energy intensity in the U.S. and Japan. According to aggregate International Energy Agency (IEA) data, the U.S. has one of the most energy-intensive economies while Japan has one of the least. Energy-intensity measures are constructed and examined which that are more detailed than aggregate measures used by the IEA to see if they can better explain these differences. The year chosen for this analysis is 1985. The issue of energy intensity may become particularly critical if scientific findings on global climate change and greenhouse emissions lead to negotiations on restricting carbon emissions. The burning of fossil fuels is the most important anthropogenic source of carbon emissions. As shown by this analysis, developing a consistent and fair set of goals for each country for carbon emissions, which are interlocked with energy intensity, may be a difficult task. DOE

N90-18798# Instituto de Pesquisas Espaciais, Sao Jose dos Campos (Brazil).
OPTIMIZATION OF THE REFERENCE PARAMETERS IN THE ACCOMPANYING SOLAR PANEL DYNAMICS [OTIMIZACAO DE PARAMETROS REFERENTES AO COMPORTAMENTO DINAMICO DE PAINEIS SO LARES]
Cassia deAssisFleury, Jose Augusto PenteadoAranha, and Atair RiosNeto Feb. 1989 7 p In PORTUGUESE; ENGLISH summary Presented at the 7th SBA Brazilian Conference on Automation, Sao Jose dos Campos, Brazil, 15-19 Aug. 1988
(INPE-4795-PRE/1449) Avail: NTIS HC A02/MF A01

A procedure is presented for mass minimization of solar panels used in artificial satellite, considering mechanical strength and first mode vibration frequency constraints. These constraints are used in order to avoid undesirable effects of the solar panels dynamics on the attitude and orbit control system. The solar panel is modelled as an imperfect cantilevered beam discretized by the finite element method. For a given panel, the optimization problem is the achievement of the minimal cross-section area along the beam to maintain an imposed frequency, considering geometric and strength constraints. A gradient projection method is used for numerical solution in a digital computer. This procedure is applied to a medium size satellite solar panel. Numerical results are presented and discussed. Author

N90-18799# Wilson Greatbatch Ltd., Clarence, NY.
FEASIBILITY OF A SUPER HIGH ENERGY DENSITY BATTERY OF THE Li/BrF3 ELECTROCHEMICAL SYSTEM Progress Report, 15 Oct. - 15 Dec. 1989
Michael F. Pyszczek, Steven J. Ebel, and Christine A. Frysz 15 Dec. 1989 20 p
(Contract N00014-89-C-0232)
(AD-A216575; WGL-MLR-89-41) Avail: NTIS HC A03/MF A01 CSCL 07/1

The feasibility of developing a lithium/bromine trifluoride battery is being studied. Critical to this product development is materials selection. Consequently, efforts have been directed toward identifying candidate porous electrode separators, glasses for insulated electrical feed-throughs and metals for lid, case and current collector fabrication. Samples were evaluated via electrochemical testing techniques and one month storage in Teflon vials. Vial test results for metal samples did not vary significantly from those reported in technical report 0001AA. Of the separator samples tested, Raychem proves to be most promising. Further study is required regarding glass selection. Electrochemical testing is still in progress. GRA

N90-18800# Spire Corp., Bedford, MA.
RADIATION-HARD HIGH-EFFICIENCY InP SPACE SOLAR CELL DEVELOPMENT Quarterly Progress Report, 12 Aug. - 11 Nov. 1989
Dec. 1989 33 p
(Contract N00014-89-C-2148)
(AD-A216857; SPIRE-QR-10120-02) Avail: NTIS HC A03/MF A01 CSCL 10/2

This quarter was marked by two serious problems which have delayed fabrication and delivery of the cells. The first of these problems, the failure of the front contact metallization, was solved in early November. The second problem, the abnormally low

open-circuit voltages and fill factors, was not solved as of the end of the quarter, although promising indications have been seen in the interval between the end of the reporting period and this writing. Despite these problems, we were able to continue work on the emitter structures; advanced thin emitters have been grown without any post-growth thinning step and have demonstrated improved quantum efficiency. Development of the processing sequence has continued as well; details of the back contact formation process have been elucidated in order to give maximum flexibility for the processing of thin cells. GRA

N90-18801# Luz International Ltd., Los Angeles, CA.
PHASE-CHANGE THERMAL ENERGY STORAGE Final Subcontract Report
Nov. 1989 147 p Symposium held in Helendale, CA, 19-20 Oct. 1988 Prepared in cooperation with Midwest Research Inst., Golden, CO and CBY Associates, Inc. Washington, DC
(Contract DE-AC02-83CH-10093)
(DE89-009426; SERI/STR-250-3516; CONF-8810464-Summ)
Avail: NTIS HC A07/MF A01

The goal of this program is to advance the engineering and scientific understanding of solar thermal technology and to establish the technology base from which private industry can develop solar thermal power production options for introduction into the competitive energy market. Solar thermal technology concentrates the solar flux using tracking mirrors or lenses onto a receiver where the solar energy is absorbed as heat and converted into electricity or incorporated into products as process heat. The two primary solar thermal technologies, central receivers and distributed receivers, employ various point and line-focus optics to concentrate sunlight. Current central receiver systems use fields of heliostats (two-axes tracking mirrors) to focus the sun's radiant energy onto a single, tower-mounted receiver. Point focus concentrators up to 17 meters in diameter track the sun in two axes and use parabolic dish mirrors or Fresnel lenses to focus radiant energy onto a receiver. Troughs and bowls are line-focus tracking reflectors that concentrate sunlight onto receiver tubes along their focal lines. Concentrating collector modules can be used alone or in a multimodule system. The concentrated radiant energy absorbed by the solar thermal receiver is transported to the conversion process by a circulating working fluid. Receiver temperatures range from 100 C in low-temperature troughs to over 1500 C in dish and central receiver systems. DOE

N90-18802# Midwest Research Inst., Golden, CO. Solar Energy Research Inst.
RESOURCE ASSESSMENT PROJECT: USER NEEDS SURVEY RESULTS
R. L. Hulstrom Nov. 1989 26 p
(Contract DE-AC02-83CH-10093)
(DE89-009502; SERI/PR-215-2981) Avail: NTIS HC A03/MF A01

This document presents the results of an extensive survey conducted by the Solar Energy Research Institute's (SERI) Resource Assessment and Instrumentation Branch. This survey addressed the needs for solar radiation data, models, algorithms, forecasts, and instrumentation, according to the various solar energy conversion technologies (photovoltaics, solar thermal, passive heating/cooling/daylighting, active solar heating/cooling (ASHC), and biomass). The survey was actually conducted during fiscal years 1984 and 1985 as input to the establishment of a formal Department of Energy (DOE) Resource Assessment Program. The survey included only solar radiation, as opposed to wind and other renewable resources. SERI is responsible for the solar radiation portion of the DOE Resource Assessment Program. The survey was conducted by sending a questionnaire to 135 individuals at DOE, the Department of Agriculture, industry, and various national laboratories, universities, and utilities, to represent a cross section of the previously named solar energy conversion technologies. The results of the survey were analyzed and summarized. The exact needs for solar radiation data, models, algorithms, forecasts, and instrumentation will surely change with time. Therefore, the SERI Resource Assessment and Instrumentation Branch will update the list continually. DOE

N90-18803# Delaware Univ., Newark. Inst. of Energy Conversion.
CHEMICAL VAPOR DEPOSITION AND PHOTOCHEMICAL VAPOR DEPOSITION OF AMORPHOUS SILICON PHOTOVOLTAIC DEVICES
B. N. Baron, R. E. Rocheleau, and S. S. Hegedus Nov. 1989 88 p Prepared for Midwest Research Inst., Golden, CO
(Contract DE-AC02-83CH-10093)
(DE89-009510; SERI/STR-211-3601) Avail: NTIS HC A05/MF A01

The objectives of this research were to study, develop and assess chemical and photochemical vapor deposition as alternate deposition methods for the fabrication of amorphous silicon thin-film photovoltaic solar cells to meet the performance and cost goals of the National Photovoltaics Program. DOE

N90-18804# Indal Technologies, Inc., Mississauga (Ontario).
VERTICAL AXIS WIND TURBINE TURBULENT RESPONSE MODEL. PART 2: RESPONSE OF SANDIA NATIONAL LABORATORIES' 34-METER VAWT WITH AEROELASTIC EFFECTS
Jan. 1990 151 p Prepared for Sandia National Labs., Albuquerque, NM
(Contract DE-AC04-76DP-00789)
(DE90-005721; SAND-89-7042-Pt-2) Avail: NTIS HC A08/MF A01

The dynamic response of Sandia National Laboratories' 34-m Darrieus rotor wind turbine at Bushland, Texas, is presented. The formulation used a double-multiple streamtube aerodynamic model with a turbulent airflow and included the effects of linear aeroelastic forces. The structural analysis used established procedures with the program MSC/NASTRAN. The effects of aeroelastic forces on the damping of natural modes agree well with previous results at operating rotor speeds, but show some discrepancies at very high rotor speeds. A number of alternative expressions for the spectrum of turbulent wind were investigated. The model loading represented by each does not differ significantly; a more significant difference is caused by imposing a full lateral coherence of the turbulent flow. Spectra of the predicted stresses at various locations show that without aeroelastic forces, very severe resonance is likely to occur at certain natural frequencies. Inclusion of aeroelastic effects greatly attenuates this stochastic response, especially in modes involving in-plane blade bending. DOE

N90-18805# Washington and Lee Univ., Lexington, VA.
MEASUREMENTS OF SURFACE PRESSURES ON AN OPERATING VERTICAL-AXIS WIND TURBINE
Robert E. Akins Nov. 1989 84 p Prepared for Sandia National Labs., Albuquerque, NM
(Contract DE-AC04-76DP-00789)
(DE90-005722; SAND-89-7051) Avail: NTIS HC A05/MF A01

This report describes measurements of surface pressures on a vertical-axis wind turbine using pressure transducers mounted at the equator of one blade of the rotor. These pressure transducers were monitored as a function of relative rotor position and incident wind speed to obtain the distribution of surface pressure. The measured pressure distributions are substantially different from wind-tunnel results. The surface pressures were integrated to obtain tangential and normal force coefficients as a function of rotor position relative to the incident wind. These measured force coefficients are compared with wind-tunnel results for tip-speed ratios from 2.20 to 4.60. At low tip-speed ratios there is evidence of dynamic stall for the upwind portion of the rotation. DOE

N90-18806# Sandia National Labs., Albuquerque, NM.
ADVANCED BATTERY DEVELOPMENT
1989 31 p
(Contract DE-AC04-76DP-00789)
(DE90-006073; SAND-89-1489) Avail: NTIS HC A03/MF A01

In order to promote national security by ensuring that the

United States has an adequate supply of safe, assured, affordable, and environmentally acceptable energy, the Storage Batteries Division at Sandia National Laboratories (SNL), Albuquerque, is responsible for engineering development of advanced rechargeable batteries for energy applications. This effort is conducted within the Exploratory Battery Technology Development and Testing (ETD) Lead center, whose activities are coordinated by staff within the Storage Batteries Division. The ETD Project, directed by SNL, is supported by the U.S. Department of Energy, Office of Energy Systems Research, Energy Storage and Distribution Division (DOE/OESD). SNL is also responsible for technical management of the Electric Vehicle Advanced Battery Systems (EV-ABS) Development Project, which is supported by the U.S. Department of Energy's Office of Transportation Systems (OTS). The ETD Project is operated in conjunction with the Technology Base Research (TBR) Project, which is under the direction of Lawrence Berkeley Laboratory. Together these two projects seek to establish the scientific feasibility of advanced electrochemical energy storage systems, and conduct the initial engineering development on systems suitable for mobile and stationary commercial applications. DOE

N90-18807# New Energy Development Organization, Tokyo (Japan).
STUDY ON THE MEASURES TO PROMOTE THE USE OF PHOTOVOLTAIC POWER GENERATING SYSTEM OVERSEAS
Mar. 1989 167 p In JAPANESE and ENGLISH
(DE90-742056; NEDOJ-P-8821) Avail: NTIS (US Sales Only) HC A08/MF A01

In order to understand the state of the utilizing photovoltaic power generating system, the present situation to promote its development, the actual status of the assistance for developing countries by each country or by each international organization, research was done for USA, principal western countries, UN and EC. First, development conditions of the solar cell utilizing technique were classified by each country at the standpoint of developing and promoting systems. Second, the projects and policies in each country or international organization were arranged to promote research, development and introduction. Next, the present situation of the photovoltaic power generation projects by civilian parties and the problems to assist the projects by each country were arranged. While, the present sutuation of the photovoltaic power generation projects assisted by the governments and international organizations were classified by each country and each international organizations. Finally, in view of importance in the photovoltaic power generation project, it was concluded that not only developed country governments and international organizations but also private enterprises in developed countries were required to expand the understanding about the photovoltaic power generation system. DOE

N90-18808*# International Fuel Cells Corp., South Windsor, CT.
INTEGRATED REGENERATIVE FUEL CELL EXPERIMENTAL EVALUATION Final Report, 11 Jan. 1988 - 30 Jun. 1989
Ronald E. Martin 1990 65 p
(Contract NAS3-22234)
(NASA-CR-185183; NAS 1.26:185183; FCR-10555A) Avail: NTIS HC A04/MF A01 CSCL 10B

An experimental test program was conducted to investigate the performance characteristics of an integrated regenerative fuel cell (IRFC) concept. The IRFC consists of a separate fuel cell unit and electrolysis cell unit in the same structure, with internal storage of fuel cell product water and external storage of electrolysis cell produced hydrogen and oxygen. The fuel cell unit incorporates an enhanced Orbiter-type cell capable of improved performance at reduced weight. The electrolysis cell features a NiCo2O4 catalyst oxygen evolution eletrode with a porous Teflon cover to retard electrolyte loss. Six complete IRFC assemblies were assembled and performance tested at an operating temperature of 200 F (93.3 C) and reactant pressures up to 170 psia (117.2 n/cu cm) on IRFC No. 4. Anomalous pressure charge/discharge characteristics were encountered during performance evaluation. A reversible fuel cell incorporating a proprietary bi-functional oxygen electrode operated satisfactory at 200 F (93.3 C) at reactant pressures up to 50 psia (41.4 n/cu cm) as a regenerative fuel cell for one cycle, before developing an electrical short in the fuel cell mode. Electrolysis cell 300-hour endurance tests demonstrated the electrolyte retention capability of the electrode Teflon cover and the performance stability of the bi-functional oxygen electrode at high potential. Author

N90-18809# Midwest Research Inst., Golden, CO.
PROGRAMS IN RENEWABLE ENERGY
Jan. 1990 48 p
(Contract DE-AC02-83CH-10093)
(DE89-009489; DOE/CH-10093/74) Avail: NTIS HC A03/MF A01

Our nation faces significant challenges as we enter the 1990s: securing a reliable supply of competitively priced energy, improving the quality of our environment, and increasing our share of foreign markets for goods and services. The U.S. Department of Energy's (DOE) Programs in Renewable Energy are working toward meeting these challenges by developing the technologies that make use of our nation's largest energy resource: renewable energy. The sunlight, wind biomass, flowing water, ocean energy, and geothermal energy that make up the renewable energy resource can be found throughout our nation. These resources can provide all the forms of energy our nation needs: liquid fuels, electricity, and heating and cooling. Renewable energy meets about 10 percent of our need for these forms of energy today, yet the potential contribution is many times greater. DOE's Programs in Renewable Energy are working side-by-side with American industry to develop the technologies that convert renewable energy resources into practical, cost-competitive energy. After a decade of progress in research, several of these technologies are poised to make large contributions during the 1990s and beyond. This booklet provides an overview of the renewable energy programs and their plans for FY 1990. Sources of additional information are listed at the back of the booklet. DOE

N90-18810# Midwest Research Inst., Golden, CO. Solar Technical Information Program.
SOLAR BUILDINGS PROGRAM SUMMARY. VOLUME 2: RESEARCH SUMMARIES Report, Fiscal Year 1989
Jan. 1990 47 p
(Contract DE-AC02-83CH-10093)
(DE89-009478; DOE/CH-10093/63-Vol-2) Avail: NTIS HC A03/MF A01

The Solar Buildings Program Summary is a two-volume reference set describing the technological advances and future research and development (R and D) directions of the Solar Buildings Technology Program for FY 1989. Volume II: Research Summaries, consists mainly of detailed descriptions of the various R and D activities performed by the national laboratories and their subcontractors from industry, academia, and nonprofit research institutions. This summary is divided into three main sections. Following the introduction, the first section includes the individual contract descriptions, grouped by directing organization and project area/task. A list of current publications is presented in the second section. The publications are listed alphabetically. The third section contains a list of subcontractors, including the page numbers of the applicable contract descriptions. DOE

N90-18811# Hawaii Natural Energy Inst., Honolulu.
HAWAII INTEGRATED BIOFUELS RESEARCH PROGRAM, PHASE 1 Final Report, 1 Jan. - 31 Dec. 1989
Patrick K. Takahashi Oct. 1989 200 p Prepared for Midwest Research Inst., Golden, CO
(Contracts DE-AC02-83CH-10093; SERI-XK-8-18000-1)
(DE90-006885; HNEI-89-1004-Phase-1) Avail: NTIS HC A08

Hawaii provides a unique environment for production of biomass resources that can be converted into renewable energy products. The purpose of this work is to evaluate the potential of several biomass resources, including sugarcane, eucalyptus, and leucaena, particularly for utilization in thermochemical conversion processes to produce liquid or gaseous transportation fuels. This research

program supports ongoing efforts of the Biofuels and Municipal Solid Waste Technology (BMWT) Program of the Department of Energy (DOE) and has goals that are consistent with BMWT. The Hawaii Natural Energy Institute (HNEI) work completed here consists of research activities that support two of the five renewable fuel cycles being pursued by DOE researchers. The results are directly applicable in the American territories throughout the Pacific Basin and the Caribbean, and also to many parts of the United States and worldwide. The Hawaii Integrated Biofuels Research Program is organized into the following six research tasks, which are presented as appendices in report form: Biomass Resource Assessment and System Modeling (Task 1); Bioenergy Tree Research (Task 2); Breeding, Culture, and Selection of Tropical Grasses for Increased Energy Potential (Task 3); Study of Eucalyptus Plantations for Energy Production in Hawaii (Task 4); Fundamental Solvolysis Research (Task 5); and Effects of Feedstock Composition on Pyrolysis Products (Task 6). DOE

N90-18812# Institute of Gas Technology, Chicago, IL.
SOLID-STATE PROTON CONDUCTORS
Janusz Jewuiski and Terry Osif 1989 5 p Presented at the 1st Annual Fuel Cells Contractors Review Meeting, Morgantown, WV, 2-4 May 1989
(Contract DE-AC21-88MC-24218)
(DE90-007595; CONF-890572-1) Avail: NTIS HC A01/MF A01

Work on this project is divided into three tasks. In the first, a comprehensive literature review was performed for the purpose of collecting data on solid proton conductors. The data was then analyzed with the goal of correlating physical and chemical characteristics with protonic conductivity in order to gain a better understanding of the phenomenon. In the second task, the results of the correlation study were used to choose an electrolyte system in which to work and to aid in the formulation of new candidate proton conductors. Under the third task, a universal test stand was constructed which can measure both electronic and protonic conductivity and which can be converted to use as a solid state fuel cell test stand. Samples of doped SrCeo.95 Yb0.05 O3 have been coated with palladium electrodes. The mechanism responsible for ionic conductivity through this material is currently under study. DOE

45 ENVIRONMENT POLLUTION

Includes atmospheric, noise, thermal, and water pollution.

N90-18813# Corvallis Environmental Research Lab., OR.
EFFECTS OF GLOBAL CLIMATE CHANGE ON AGROECOSYSTEMS: SCOPE OF WORK
Donald L. Phillips Aug. 1989 23 p
(PB90-120023; EPA/600/3-89/076) Avail: NTIS HC A03/MF A01 CSCL 13B

The U.S. Environmental Protection Agency, Office of Research and Development (ORD), is initiating a Global Climate Change Program to evaluate the potential environmental effects of climate change. The document describes one project, Effects of Global Climate Change on Agroecosystems, which will be administered at the EPA Environmental Research Laboratory-Corvallis as part of the ORD program. The document describes the areas in which research will be undertaken in the project over the next five years. It also presents the scientific questions that must be addressed in order to answer important public policy needs concerning the potential environmental effects of global climate change on agroecosystems and it describes the general research approaches that will be used to answer the scientific questions. GRA

N90-18814# Environmental Protection Agency, Las Vegas, NV. Quality Assurance and Methods Development Div.
APPLICATION OF HIGH PERFORMANCE LIQUID CHROMATOGRAPHY/MASS SPECTROMETRY TO ENVIRONMENTAL ANALYSIS Report, 1 Oct. 1988 - 31 May 1989
L. D. Betowski and T. L. Jones Oct. 1989 47 p
(PB90-116963; EPA/600/4-89/033) Avail: NTIS HC A03/MF A01 CSCL 13B

High performance liquid chromatography (HPLC) coupled with mass spectrometry (MS) is described for the analysis of samples for environmental pollutants. During the course of the work different techniques were used to increase both the sensitivity and specificity of HPLC/MS. These included the utilization of two different interfaces for the mass spectrometer, the thermospray and the particle beam systems. Refinements to the thermospray system were made with the use of a wire-repeller to enhance sensitivity and also to increase the structural information obtained from mass spectra. The operation of the instrument in the discharge negative ionization mode further increased the specificity of these techniques as did the use of a triple quadrupole mass spectrometer in the HPLC/MS system. Two different sets of compounds were used in the study. Organic dyes were used to test the improvements in the system. Since work was performed with dyes previously and since dye compounds encompass a variety of structural functionalities, the dyes made good test compounds. Chlorinated herbicides were studied in an effort to analyze for these compounds directly without having to prepare derivatives before separation. GRA

N90-18815# Instituto de Pesquisas Espaciais, Sao Jose dos Campos (Brazil).
REMOTE SENSING OF INTERIOR WATER: PERSPECTIVES [SENSORIAMENTO REMOTO DE AGUAS INTERIORES: PERSPECTIVAS]
Evlyn Marcia LeaodeMoraesNovo and Jose GalisiaTundisi (Sao Paulo Univ., Brazil) Jul. 1989 11 p In PORTUGUESE; ENGLISH summary Presented at the 5th Brazilian Symposium on Remote Sensing, Natal, Brazil, 11-15 Oct. 1988
(INPE-4875-PRE/1486) Avail: NTIS HC A03/MF A01

A short discussion is presented on the information requirements for water quality management as well as on the limitations of limnological methods concerning to the spatial significance of the point samples. Remote sensing techniques are also assessed as additional source of information for water quality management and as motif for new research and application aiming their incorporation to the framework of conventional limnology. Preliminary results from a study carried out in the Barra Bonita Reservoir as part of a technical cooperation between INPE/MCT and CRHEA/USP are also presented. Author

N90-18816# Instituto de Pesquisas Espaciais, Sao Jose dos Campos (Brazil).
PAPER ON GEOGRAPHY IN ENVIRONMENTAL MANAGEMENT: RESEARCH AND NEW TECHNIQUES [O PAPEL DA GEOGRAFIA NO GERENCIAMENTO AMBIENTAL: PESQUISA E NOVAS TECNICAS]
Evlyn Marcia LeaodeMoraesNovo Jun. 1989 9 p In PORTUGUESE; ENGLISH summary Presented at the 3rd Annual Symposium on Applied Geographic Physics, Nova Friburgo, Brazil, 29 May - 3 Jun. 1989 Submitted for publication
(INPE-4840-PRE/1469) Avail: NTIS HC A02/MF A01

Some ideas about the role of geography within the environmental management are presented. The expertise in dealing with new techniques for collecting and processing data is brought as a fundamental step so geographers can participate in the environmental management process. Among the techniques modeling, remote sensing, and information systems were emphasized. Author

N90-18817# Instituto de Pesquisas Espaciais, Sao Jose dos Campos (Brazil).
PHOTOINTERPRETATION WITH INSTRUMENTS FOR EVALUATION OF ENVIRONMENTAL IMPACT: MATA ATLANTICA IN CUBATA
Dalton deMorissonValeriano and Flavio Jorge Ponzoni Aug. 1989 19 p In PORTUGUESE; ENGLISH summary Presented at the National Meeting on Remote Sensing Municipal Planning,

Campo do Jordao-SP, 22-23 Oct. 1987
(INPE-4910-PRE/1511) Avail: NTIS HC A03/MF A01

In order to study the impact of the atmospheric pollution originating from the Cubatao's industrial plant over the Mata Atlantica (a strip of Tropical Rain Forest formation that stretch along the Brazilian eastern coast) on the slopes of the Serra do Mar (a mountain chain that runs parallel to the southeastern coast), color infrared air photographs (1:25,000) were used to map the vegetation cover and the land use of approximately 240 sq km, covering degraded areas (Mogi river valley) and preserved areas (Quilombo river valley). The analysis of the photographs demonstrated that the degradation of the vegetation structure by the air pollution is done by the selective and progressive elimination of the largest elements, which may, in its most intensive level, reduce the forest into shrubbery. Considering that the Mata Atlantica slowly builds its capacity to preserve slope stability, a long period is foreseen in which the risk of a natural diaster by means of landslides will be a great threat to the region in the rainy seasons. Author

N90-18818# Instituto de Pesquisas Espaciais, Sao Jose dos Campos (Brazil).
SOME ASPECTS OF ATMOSPHERIC TURBULENCE IN FORESTS [ALGUNS ASPECTOS DA TURBULENCIA ATMOSFERICA DE FLORESTAS]
Ruberio PradoBritto Oct. 1989 27 p In PORTUGUESE; ENGLISH summary
(INPE-4951-RPE/600) Avail: NTIS HC A03/MF A01

The observations of turbulence phenomena inside and above the canopy are important for the understanding of the atmosphere-forest interactions. There is a scarcity of information concerning the process involved and the instrumentation to be used. In this experiment sonic anemometer was used inside the forest, on fluxotron over the trees, and a tethered balloon in the surface boundary layer. For the characterization of a dynamic interaction forest-atmosphere three layers were considered: from 0 to 25 m inside the canopy; interface vegetation-atmosphere from 25 to 36 m and the boundary layer over the frost greater than 36 m. The experiment showed that a layer (0 to 36 m) existed that is characterized by gravity and relaxation waves with fine structure turbulence. The boundary layer over the canopy showed a developed turbulence, not stationary, influenced by the rugged forest surface. Finally the study showed that the atmosphere-forest interaction is complex due to the conditions of stability inside the canopy, where the forest performed as a semi-confined region. Author

N90-18819# Oak Ridge National Lab., TN. Environmental Sciences Div.
PERSPECTIVES ON AEROSOL DEPOSITION TO NATURAL SURFACES
Bo L. B. Wiman, Michael H. Unsworth, Steven E. Lindberg, Bo Bergkvist, Ruprecht Jaenicke, and Hans-Christen Hansson (Lund Inst. of Tech., Sweden) 1989 40 p Presented at the Workshop on Aerosol Deposition To Natural Surfaces, Lund, Sweden, 2 Sep. 1988
(Contract DE-AC05-84OR-21400)
(DE90-003398; CONF-8809424-1) Avail: NTIS HC A03/MF A01

This paper summarizes the state-of-the art and the research needs in the areas of aerosol residence-time assessments, deposition modelling, and understanding of aerosols in biogeochemistry. Research needs are emphasized from a systems perspective of global environmental change. Although fundamental quantitative knowledge is lacking, some qualitative linkages between source strengths, residence times, removal processes, and the biosphere can be identified. It turns out that not only are the respective areas as such challenged by new problems, superimposed on the fairly well established conventional ones, but these areas also face mutually operating sets of feedbacks between residence times and sink/source characteristics of ecological systems subject to stress. To evaluate the sensitivity of these feedback loops, and to assess whether they are negative (stabilizing interactions) or positive (destabilizing) are important and potentially urgent tasks. Such studies should focus on a common goal, such as developing empirical and theoretical understanding of aerosol resuspension, transport and deposition for application in large-scale circulation models. A basic link in such advancements is that structural change of vegetated surfaces of the biosphere caused by deposition itself, and by changing land-use and climate, be understood and assessed. DOE

N90-18820# Argonne National Lab., IL. Environmental Research Div.
TROPOSPHERIC CHEMISTRY OF NATURAL HYDROCARBONS AND ENERGY-RELATED POLLUTANTS: BIOSPHERE/CLIMATE FEEDBACKS
J. S. Gaffney and N. A. Marley Oct. 1989 18 p Presented at the 198th American Chemical Society National Meeting, Miami Beach, FL, 10-15 Sep. 1989
(Contract W-31-109-eng-38)
(DE90-005643; CONF-890902-23) Avail: NTIS HC A03/MF A01

This paper outlines some of the potential chemical, physical, and biological feedbacks that can occur in the troposphere from energy-related pollutants because of combustion-related activities. A number of examples are presented where biospheric feedbacks are now known or are likely to be important processes affecting the troposphere and stratosphere. Modeling efforts have attempted to simplify or ignore these systems in evaluating a variety of solutions to pollution problems ranging from urban ozone to global climate change. Particular focus is placed upon the potential for short-term solutions to perceived problems on urban or regional scales (e.g., ozone, acid rain) to lead to regional and global scale problems due to unforeseen coupled feedbacks. Modeling studies that do not incorporate the complexity of these systems are likely to yield inaccurate assessments and lead to ineffective pollution abatement strategies. It is strongly suggested that we need to use the models to examine what if scenarios to evaluate possible negative interactions. DOE

N90-18821# Lawrence Livermore National Lab., CA.
VARIATIONS IN VOLATILES IN MAGMA BODIES BASED ON STUDIES OF MELT INCLUSIONS
Thomas A. Vogel (Michigan State Univ., East Lansing.) 15 Jun. 1989 3 p
(Contract W-7405-eng-48)
(DE90-006272; UCRL-21293) Avail: NTIS HC A01/MF A01

Knowledge of volatile concentrations in magmas are important in the prediction of explosive volcanism, and contribute to the understanding of the carbon dioxide budget of the atmosphere. Some important variables that are controlled by volatiles are: crystallization temperature of phases, composition of liquids minimum, and viscosity. Volatiles are also catalysts for reactions. DOE

N90-18822# Atmospheric and Environmental Research, Inc., Cambridge, MA.
NATURAL AND ANTHROPOGENIC CLIMATE CHANGE
Progress Report, 1 Mar. - 1 Nov. 1989
W.-C. Wang and W. J. Gutowski 31 Oct. 1989 3 p
(Contract DE-FG02-86ER-60422)
(DE90-006488; DOE/ER-60422/5) Avail: NTIS HC A01/MF A01

This report discusses a research program which includes three tasks: General Circulation Model (GCM) intercomparison and improvement, climate data-model statistics, and China project science coordination. DOE

N90-18823# Lawrence Livermore National Lab., CA.
EFFECT OF A RANDOM WIND FIELD ON THERMAL BLOOMING INSTABILITIES
J. R. Morris, J. A. Viecelli, and Thomas J. Karr Jan. 1990 14 p Presented at the SPIE Optics, Electro-optics and Laser Applications in Science and Engineering Conference and Exhibition, Los Angeles, CA, 14-19 Jan. 1990

(Contract W-7405-eng-48)
(DE90-007241; UCRL-102653; CONF-900140-7) Avail: NTIS HC A03/MF A01

The effect was numerically investigated of random fluctuations on uncompensated (open-loop) and phase compensated (closed-loop) small scale thermal blooming instabilities of a collimated beam propagating through refractive index turbulence. The ORACLE time dependent, three space dimensional, wave optics code on a Cray X-MP was used. The Monte Carlo random wind fields, v(z), were exponentially correlated along the propagation direction, z. The small scale instabilities are present up to a threshold value of the rms random wind, beyond which beam propagation appears to be stable; the threshold value is nearly independent of the correlation length as long as the latter is much shorter than both the length of the thermal blooming region and the Rayleigh range of dominant perturbations. The open loop calculations use a plane wave beam and a uniform medium. The Strehl ratio at 50 waves of thermal blooming OPD remains approximately constant while S greater than or = 2.3 and then it decreases rapidly as S decreases. The closed loop calculations use a large Fresnel number finite beam, a nonuniform medium of length 2L, absorption (proportional to) exp(-z/L), and a Hufnagel-Valley type C(sub N)(sup 2) profile whose r(sub 0) Fresnel number was 24. For 10 less than or = N(sub p) less than or = 40, no evidence is seem of the closed loop instability at a wind clearing time (20 waves) for S greater than or = (54 + or - 2)/N(sub p), where N(sub p) = (pi) lambda (sub p)(sup 2)/4 lambda L and lambda (sub p) is twice the actuator spacing simulated by a Fourier filter. This result suggests that the ratio of the turbulence scintillation rate to the closed-loop gain for a uniform wind determines the threshold. DOE

46 GEOPHYSICS

Includes aeronomy; upper and lower atmosphere studies; ionospheric and magnetospheric physics; and geomagnetism.

For space radiation see *93 Space Radiation.*

N90-18824*# Massachusetts Inst. of Tech., Cambridge. Earth Resources Lab.

THE INTERPRETATION OF CRUSTAL DYNAMICS DATA IN TERMS OF PLATE INTERACTIONS AND ACTIVE TECTONICS OF THE ANATOLIAN PLATE AND SURROUNDING REGIONS IN THE MIDDLE EAST Semiannual Report, 15 Mar. - 14 Sep. 1989

M. Nafi Toksoz and Robert E. Reilinger 15 Jan. 1990 111 p (Grant NAG5-753)
(NASA-CR-186200; NAS 1.26:186200) Avail: NTIS HC A06/MF A01 CSCL 08G

During the past 6 months, efforts were concentrated on the following areas: (1) Continued development of realistic, finite element modeling of plate interactions and associated deformation in the Eastern Mediterranean; (2) Neotectonic field investigations of seismic faulting along the active fault systems in Turkey with emphasis on identifying seismic gaps along the North Anatolian fault; and (3) Establishment of a GPS regional monitoring network in the zone of ongoing continental collision in eastern Turkey (supported in part by NSF). Author

N90-18825# Instituto de Pesquisas Espaciais, Sao Jose dos Campos (Brazil).

GEOLOGICAL STRUCTURE OF THE STATE OF RIO DE JANEIRO VIEWED THROUGH MSS LANDSAT IMAGERY [A GEOLOGIA ESTRUTURAL DO ESTADO DO RIO DE JANEIRO VISTA ATRAVES DE IMAGENS MSS DO LANDSAT]

Chan Chiang Liu Jun. 1989 14 p In PORTUGUESE; ENGLISH summary Presented at the 5th Brazilian Symposium on Remote Sensing, Natal, Brazil, 11-15 Oct. 1988
(INPE-4826-PRE/1457) Avail: NTIS HC A03/MF A01

Lineaments are the main or sometimes the unique structural feature in the context of regional dimension provided by orbital remote sensing, and the classification of these numerous lineaments becomes a weighty procedure in lineament study. Therefore to develop a sound methodology for classifying the lineaments is necessary and is the main goal. The methodology applied to lineament study in the State of Rio de Janeiro can be summarized into a sequential procedure: identification, extration, comparison, and correlation. From this procedure, lineaments are classified into systems and subsystems from which a sketch of the structural and tectonic evolution of the area can be tentatively inferred and will be used to confront detailed structural data in the future. Author

N90-18826# Instituto de Pesquisas Espaciais, Sao Jose dos Campos (Brazil).

QUANTIFICATION OF STRUCTURAL FIELD DATA IN THE RIO GRANDE DO NORTE BASIN AND NEIGHBORHOOD [QUANTIFICACAO DOS DADOS ESTRUTURAIS DE CAMPO NA BACIA POTIGUAR E ADJACENCIAS]

Jose Eduardo Rodrigues, Chan Chiang Liu, Peter Szatmari, and Osmar Antonio Zanotto Jun. 1989 63 p In PORTUGUESE; ENGLISH summary
(INPE-4821-RPE/591) Avail: NTIS HC A04/MF A01

Structures viewed on outcrops are many, such as joints, folds, fractures, various types of foliations and lineations, various kinds of cleavages and, sometimes, superimposition of multiple generations of folding and faulting. Judgement should be made on what kinds of structure may influence the development of topographic features, because only these ground data may correspond to the morphostructural features interpreted on remote sensed images. From field observations, elongated landforms and straight river courses are frequently concordant with the strike of foliation in mylonite, migmatites, gnaisses, and schists. Huge dip-slopes are often concordant with joint planes. Therefore, these two kinds of structural features were selected to be correlated to the image lineaments. The quantification of these field data, mainly of the joints and fractures are shown. Owing to short of time, detailed lithologic mapping was impossible. Author

N90-18827# Instituto de Pesquisas Espaciais, Sao Jose dos Campos (Brazil).

STUDY OF THE ATMOSPHERIC EMISSIONS OF OI WAVELENGTH 557.7 nm AND O2 (0,0) WAVELENGTH 761.9 nm IN THE EQUATORIAL REGION UTILIZING MEASUREMENT OF PHOTOMETER ON-BOARD A ROCKET M.S. Thesis, 1988 [EDTUDO DAS EMISSOES ATMOSFERICAS OI WAVELENGTH 557.7 NM E O2 (0,0) WAVELENGTH 761.9 NM NA REGIAO EQUATORIAL UTILIZANDO MEDIDAS DE FOTOMETRO A BORDO DE FOGUETE]

Delano Gobbi Jun. 1989 129 p In PORTUGUESE, ENGLISH summary
(INPE-4811-TDL/358) Avail: NTIS HC A07/MF A01

Airglow emissions originate from the atmospheric photochemical processes, whose principal excitation is due to the absorbed solar energy during the daytime. However, at night, the source of photochemical excitation is removed, yet the existence of the nightglow shows that excited species persists. The subject of this work is to show the observed airglow profiles measured by two photometers on-board a sounding rocket, Sonda 3, launched in Natal (5.8 deg S, 35.2 deg W) on December 11, 1985, at 23:30 GMT (20:30 local time). The atomic oxygen OI wavelength 557.7 nm, green line, and O2(b 1 Sigma g+ - X 3 Sigma g-) (0,0) atmospheric band were measured. Both emissions come from 80 to 120 km altitudes. Taking in consideration of recent model calculation and using the present observed profiles numerical density of atomic oxygen are calculated. This is the first simultaneous measurement of the two emissions in the equatorial region. Author

N90-18828# Instituto de Pesquisas Espaciais, Sao Jose dos Campos (Brazil).
CONNECTIONS BETWEEN THE CIRCULATION IN ALTITUDE AND CONVECTION OVER SOUTH AMERICA M.S. Thesis [CONEXOES ENTRE A CIRCULACAO EM ALTITUDE E A CONVECCAO SOBRE A AMERICA DO SUL]
Ana Maria GusmaodeCarvalho Sep. 1989 109 p In PORTUGUESE; ENGLISH summary
(INPE-4923-TDL/383) Avail: NTIS HC A06/MF A01

The connections between the circulation in the upper troposphere of South America and the convection over Amazonia were investigated. The parameters used were monthly grid averages of relative vorticity, longwave radiation, and precipitation for the period 1974 to 1984. The results obtained show that: the intensity of circulation over the Bolivian high and the trough over northeast are well correlated; the Bolivian high and the trough air NE are inversely correlated with the convection over Amazon; there are indications that the South Atlantic Convergence Zone (ZCAS) is important for the mechanism of connection between the Bolivian high and the trough; the beta term in the vorticity equation is very relevant to the dynamic mechanism of the connection between the Bolivian high and the trough in high troposphere of Northeast Brazil. Author

N90-18829# Instituto de Pesquisas Espaciais, Sao Jose dos Campos (Brazil).
THE PATTERNS OF FRACTURE AND THE CONDITIONING TECTONICS IN THE REGION OF THE QUADRILATERO FERRIFERO AND PART OF THE MIGMATITIC-GNANULITIC COMPLEX IN MINAS GERAIS (BRAZIL) [O PADRAO DE FRATURAMENTO E O CONDICIONAMENTO TECTONICO NA REGIAO DO QUADRILATERO FERRIFERO E PARTE DO COMPLEXO MIGMATITO-GRANULITICO DE MINAS GERAIS (BRASIL)]
Athos RibeirodosSantos and Hans D. Schorscher (Sao Paulo Univ., Brazil) Jul. 1989 12 p In PORTUGUESE; ENGLISH summary Presented at the 3rd Brazilian Symposium on Remote Sensing, Rio de Janeiro, Brazil, 28-30 Nov. 1984
(INPE-4895-PRE/1496) Avail: NTIS HC A03/MF A01

The structural evolution of the SE portion of Minas Gerais State, including the Quadrilatero Ferrifero and adjacent parts of the Migmatitic-Granulitic Complex are described. The area of complex policiclic evolution is composed of pre-Cambrian metamorphic rocks, arquean to upper proterozoic in age. In phanerozoic times basaltic magmatism and related tectonism took place principally in the Mesozoic Era, and restricted lacustric sedimentary basins developed in the tertiary and quaternary periods. This study is based on the interpretation of remote sensing products (MSS, RBV, TM and SLAR images) and geological data form literature and field work. An integrated geological map (1:250.000) and a statistical analysis of the patterns of fracturing show the importance of NNE-SSW and E-W directed events of ruptile and ruptile-ductile tectonics in the Archean and in the conditioning of the younger fracture-generations. Further evidences regarding the structural evolution of the Minas Supergroup in the Quadrilaterio Ferrifero revealed different fracture patterns in the Minas - cover in respect to its underlying basement. Author

N90-18830# Air Force Geophysics Lab., Hanscom AFB, MA.
THE 2.7/4.3 MICRON CO2 BRANCHING RATIO MEASUREMENT Interim Scientific Report, Jun. 1984 - Jun. 1987
Steven M. Miller 23 Jan. 1989 30 p
(AF Proj. 2310)
(AD-A215952; AFGL-TR-89-0022; ERP-1019) Avail: NTIS HC A03/MF A01 CSCL 04/1

Two rocket infrared measurement programs during the 1970's (ICE CAP and SPIRE) measured significant amounts of radiation in the upper atmosphere at 2.7 microns. Several papers have been published which attribute this radiation at 2.7 microns to the hot bands of carbon dioxide. To determine the contribution of 2.7 microns radiation from CO2 each of these analyses rely on a simple theoretical calculation of the CO2 branching ratio between 2.7 microns and 4.3 microns. The radiative branching from the CO2(021) combination vibrational energy state to the CO2 (020) and CO2 (000) states is measured using both laser induced fluorescence excitation and spectrally resolved fluorescence experiments. These measurements bound the branching ratio (C02(021) CO2 (020)/CO2(O21) CO2 (000)) between 13 and 16. GRA

N90-18831# Iowa Univ., Iowa City. Dept. of Physics and Astronomy.
PARTICLE SIMULATIONS IN MAGNETOSPHERIC PLASMAS Final Technical Report, 15 Nov. 1988 - 14 Nov. 1989
Ken-Ichi Nishikawa 18 Dec. 1989 12 p Prepared for Defense Technical Information Center, Alexandria, VA
(Contract N00014-89-K-2004)
(AD-A216256) Avail: NTIS HC A02/MF A01 CSCL 04/1

Research is described which was undertaken to understand physical processes involved in plasma waves observed in the magnetospheric plasmas and associated nonlinear phenomena such as heating, diffusion, and acceleration of particles due to excited waves. Some specific areas of study are: Simulation Study of a New Mechanism for Excitation of Kinetic Waves in a Magnetoplasma; Beam Instability in the Foreshock; Whistler Mode Driven by the Spacelab 2 Electron Beam; Simulation of Electron Cyclotron Harmonic Waves by AMPTE Lithium Release. GRA

N90-18832# Nevada Univ., Reno. Desert Research Inst.
STUDIES OF CUBIC ICE CRYSTALS Final Report
William G. Finnegan and Richard L. Pitter 11 Dec. 1989 76 p
(Contract N00014-85-K-0849)
(AD-A216574) Avail: NTIS HC A05/MF A01 CSCL 04/1

This three-year study, conducted for the Innovative Science and Technology Program of the Strategic Defense Initiative Organization through the Office of Naval Research, has produced a number of interesting findings of consequence to the atmospheric sciences. More important, the discovery of one phenomenon--that ionic salts which are present undergo differential ion inclusion into the ice phase of growing ice crystals--results in the explanation of many ice crystal initiation, growth, and interaction processes. These include ice crystal aggregation, morphology and symmetry, secondary ice crystal formation, and coupled oxidation-reduction reactions in growing ice crystal. Implications of these processes involve atmospheric pollution processes, planetary oxygen atmosphere generation, Antarctic ozone depletion processes, and ore bodies of atmospheric origin. Potential roles in thunderstorm electrification can be seen. It is anticipated that these discoveries in ice crystal growth phenomena will apply equally well to crystal growth processes in general. GRA

N90-18833# State Univ. of New York, Stony Brook.
STUDIES OF ATMOSPHERIC MOLECULES BY MULTIPHOTON SPECTROSCOPY Progress Report, 15 Jul. 1989 - 15 Jan. 1990
Philip M. Johnson Jan. 1990 7 p
(Contract DE-FG02-86ER-13590)
(DE90-005829; DOE/ER-13590/7) Avail: NTIS HC A02/MF A01

Building on previous work on the three photon multiphoton ionization spectrum, the MPI-PE spectra was examined for carbon dioxide with a view toward seeing whether the nuclear dynamics of a resonant excited state will influence the multiphoton ionization process. In the case of at least one resonance, the 3p sigma (sup 1) Pi (sub u) Rydberg state, a very dramatic example of ATI is found. The multiphoton ionization spectra was measured of nitrogen molecules which have passed through an electric discharge in a supersonic beam. Higher quality spectra were obtained and several transitions were observed which were not see in the previous study. It is hoped that these new peaks and the higher quality spectra will lead to a breakthrough in the analysis of the many unassigned peaks in the spectra. DOE

N90-18834# Arizona Univ., Tucson. Dept. of Physics.
SOLAR VARIABILITY OBSERVED THROUGH CHANGES IN SOLAR FIGURE AND MEAN DIAMETER Progress Report, 1 Jun. 1989 - 31 May 1990
Henry A. Hill 31 Jan. 1990 9 p
(Contract DE-FG02-87ER-13670)
(DE90-006600; DOE/ER-13670/1) Avail: NTIS HC A02/MF A01

The work performed on solar variability during 1989 at (Santa Clara Lab for Experimental Relativity by Astrometry) SCLERA is reviewed. That portion of the SCLERA research program supported by the Department of Energy has been directed toward the detection and monitoring of climatically significant solar variability by accurate measurement of the variability in solar shape and diameter. Observations were obtained in 1989 and results from analysis of earlier observations obtained. Systematic long term changes in the apparent solar diameter and/or radius were detected and these changes were found to strongly correlate with long term changes in solar total irradiance. Additional evidence for gravity mode coupling was found which may be important to understanding neutrino and fusion energy production rates in the solar core. Each of these findings may be important to anticipating future changes in the solar luminosity. Progress was made in setting up an international network based on SCLERA type instruments to improve the coverage and quality of the observations. A proposal is made for the continuation of support from the DOE for further studies relevant to solar variability forecasting. DOE

N90-18835# International Centre for Theoretical Physics, Trieste (Italy).
STREAMING GRAVITY MODE INSTABILITY
Shui Wang May 1989 11 p Submitted for publication
(DE90-610619; IC-89/103) Avail: NTIS (US Sales Only) HC A03/MF A01

In this paper, we study the stability of a current sheet with a sheared flow in a gravitational field which is perpendicular to the magnetic field and plasma flow. This mixing mode caused by a combined role of the sheared flow and gravity is named the streaming gravity mode instability. The conditions of this mode instability are discussed for an ideal four-layer model in the incompressible limit. DOE

N90-18836# European Space Agency, Paris (France).
AIRBORNE MEASUREMENTS OF THE ELECTRIC FIELD AND THE CHARGE PRECIPITATION PARTICLES IN CONVECTIVE CLOUDS: LOWER POSITIVE CHARGE CENTRES
Pascal Gondot (Office National d'Etudes et de Recherches Aerospatiales, Paris, France) Dec. 1989 150 p Transl. into ONERA of l'Electrisation des Nuages Orangeux: Etude d'un cas de Centre Positif de Basse Altitude par des Moyens Aeriens in Situ (Paris, France, ONERA), 1988 Original language document was announced as N89-27319
(ESA-TT-1157; ONERA-NT-1988-1; ETN-90-96220) Avail: NTIS HC A08/MF A01

A comparative analysis of two meteorological situations studied in south west France in Summer 1984 is presented: 6 June when the cloud tops stopped below the -20 C level and most of the precipitation particles were positively charged, and 28 June, when typical thunderclouds reaching the tropopause occurred, and exploration at nearly the same level showed that the majority of the particles carried negative charges. The sign of the charge on precipitation particles is concluded as relative to the altitude of the cloud top, which implies a given temperature for the level at which precipitation is formed. A detailed case study of three passes made on 6 June through a small isolated cumulus cloud is given. Evidence is presented for the association of positive charge centres at low altitude with the presence of strongly charged graupel. ESA

N90-18837# Lawrence Livermore National Lab., CA.
TEMPORAL RESPONSE OF ATMOSPHERIC TURBULENCE COMPENSATION
Thomas J. Karr 1 Dec. 1989 6 p
(Contract W-7405-eng-48)
(DE90-006354; UCID-21844) Avail: NTIS HC A02/MF A01

The temporal kernel for the phase error variance due to atmospheric turbulence is calculated. This kernel, convolved with the servo transfer function, determines the error of any turbulence compensation scheme. DOE

47 METEOROLOGY AND CLIMATOLOGY

Includes weather forecasting and modification.

N90-18838# National Oceanic and Atmospheric Administration, Boulder, CO. Wave Propagation Lab.
PRELIMINARY COMPARISON OF TEMPERATURE SOUNDINGS OBTAINED FROM SIMULTANEOUS RADIOMETRIC, RADIO-ACOUSTIC, AND RAWINSONDE MEASUREMENTS
Judith A. Schroeder Sep. 1989 27 p
(PB90-119835; NOAA-TM-ERL-WPL-173) Avail: NTIS HC A03/MF A01 CSCL 04B

An experiment was conducted to compare the accuracy of atmospheric temperature soundings obtained simultaneously with a ground-based radio-acoustic sounding system (RASS), a ground-based microwave radiometric system, and a combined RASS/radiometric system at Denver, Colorado, during July and August of 1988. Applying a linear statistical retrieval technique to measurements from all three systems permitted three-way comparisons throughout the troposphere. Accuracy was evaluated by comparison with simultaneous in situ rawinsonde temperature measurements. The root-mean-square (rms) errors for the 22 sets of soundings compared ranged from 0.5 to 2.0 C, depending on altitude. The differences among the three systems were too small to conclude that the combined system performance was significantly better than that of either system alone. GRA

N90-18839# Instituto de Pesquisas Espaciais, Sao Jose dos Campos (Brazil).
INTERTROPICAL CONVERGENCE ZONE (ITCZ) AND ITS RELATIONSHIP WITH THE PRECIPITATION OF THE NORTH-NORTHEAST BRAZILIAN REGION M.S. Thesis [A ZONA DE CONVERGENCIA INTERTROPICAL (ZCIT) E SUA RELACAO COM A PRECIPITACAO DA REGIAO NORTE DO NORDESTE BRASILEIRO]
Cintia Regina BertacchiUvo Aug. 1989 90 p In PORTUGUESE; ENGLISH summary
(INPE-4887-TDL/378) Avail: NTIS HC A05/MF A01

An observational analysis of the relationship between the displacement of the Intertropical Convergence Zone (ITCZ) over the Atlantic Ocean and the precipitation over north-northeast Brazil (Nordeste) is presented. An area between 20 deg S, 30 deg N and 60 deg W and the west coast of Africa was chosen for the analysis. The wind stress, sea surface temperature, and the position of the maximum cloudiness over the ocean were analyzed. The precipitation over northeast was represented by monthly, seasonal, and annual standardized indices of precipitation, calculated from 116 stations over northeast. A similar analysis made for a set of wet and dry years separately indicated that the key factor which determines the quality of the rainy season is the period that the ITCZ stays at its southernmost position. Author

N90-18840# Woods Hole Oceanographic Inst., MA.
SUMMER STUDY PROGRAM IN GEOPHYSICAL FLUID DYNAMICS: THE INFLUENCE OF CONVECTION ON LARGE-SCALE CIRCULATIONS, 1988
Glenn R. Flierl and Pamela J. Goulart, ed. Jul. 1989 370 p Meeting held in Woods Hole, MA, 1988
(Contract N00014-82-G-0079; NSF DMS-85-04166)
(AD-A216024; WHOI-89-26) Avail: NTIS HC A16/MF A02 CSCL 04/2

Areas of study at the summer program are listed: Review of Dry Convection; Other Buoyant Plumes and Thermals; Global

Convection; Moist Thermodynamics; Non Precipitating Cloud; Taxonomy of Precipitating Clouds; The Dynamics of Precipitating Convection; Tropical Cyclones: Observations and Energetics; Dynamics of Tropical Cyclones; Oscillations in Convectively Adjusted Flows; Large Scale Dynamics and Topology Near the Onset of Convection; Entrainment and Detrainment in Cumulus Clouds; Baroclinic Models and Hurricane Motion; Capillary-Gravity Surface Wave Modes in a Closed Vessel With Edge Constraint: Eigen Frequency and Dissipation; Rotating Rayleigh-Benard Convection With Fixed Flux Boundaries; Low Frequencies Oscillations in a Linear Coupled Atmospheric Ocean Model; One Dimensional Model for Microbursts; The 30 to 60 Day Oscillation in the Tropics Wind Evaporation Feedback and Up-Down Asymmetry; 3D Instability of Bounded Elliptical Flow; and A Model of Squall Line Propagation. GRA

N90-18841# Air Force Inst. of Tech., Wright-Patterson AFB, OH. School of Engineering.

SPATIAL REGISTRATION OF TIROS-N WEATHER SATELLITE DATA M.S. Thesis

Charles H. Larcomb Dec. 1989 97 p
(AD-A216041; AFIT/GSO/ENG/89D-10) Avail: NTIS HC A05/MF A01 CSCL 04/2

The purpose of this study was to develop an algorithm to perform spatial registration of TIROS-N weather satellite data using a personal computer. Specific objectives were: (1) to gather currently available information into a unified and understandable form, (2) to develop the background and related theory necessary for the registration of both High Resolution Picture Transmission (HRPT) and Automatic Picture Transmission (APT) data, and (3) to present a specific registration algorithm for TIROS-N weather satellite data. The approach chosen is to use a general elliptical orbit model in conjunction with accurate satellite element sets (orbital parameters) to calculate accurate satellite positions at a given time. Knowing the earth movement and sensor operation as functions of time, the geographic locations of each pixel (picture element) are determined through geometric relations. The algorithm presented converts pixel coordinates to, geographic coordinates (direct referencing) and vice versa (inverse referencing). These algorithms assume an elliptical orbit (with perturbations) and an oblate spheroid earth. The most critical factor is found to be timing. A timing correction method is outlined to visually improve the image registration. GRA

N90-18842# Naval Postgraduate School, Monterey, CA.

SOUNDING AND SURFACE METEOROLOGICAL DATA FROM THE LAND/SEA BREEZE EXPERIMENT (LASBEX) Data Report, Oct. 1988 - Sep. 1989

William J. Shaw and Richard J. Lind 3 Nov. 1989 299 p Prepared for Naval Oceanographic and Atmospheric Research Lab., Monterey, CA
(Contract N6856-87-WR-7635)
(AD-A216269; NPS63-90-001) Avail: NTIS HC A13/MF A02 CSCL 04/2

The Land/Sea Breeze Experiment (LASBEX) was a program designed to investigate the structure and evolution of the coastal marine atmospheric boundary layer with standard and state-of-the-art meteorological systems. Measurements were made in the vicinity of the mouth of the Salinas Valley in central California during the last two weeks of September, 1987. Standard meteorological data from surface and sounding systems during the experiment are documented. GRA

N90-18843# Air Force Academy, CO.

PROCEEDINGS OF THE PROFESSIONAL PILOTS METEOROLOGY TRAINING STANDARDS CONFERENCE Final Report, Mar. - Jul. 1989

Timothy H. Miner Jul. 1989 148 p Conference held in Colorado Springs, CO, 13-14 Apr. 1989
(AD-A216618; USAFA-TR-89-9) Avail: NTIS HC A07/MF A01 CSCL 04/2

This conference accomplished two goals. It developed a complete list of learning objectives for meteorology training for a professional pilot. The conference also allowed these pilots, meteorologists, researchers, and educators to gather together to talk about issues effecting aviation meteorology. Presentations: U.S Air force Military Aircrew Weather Training; The Professional Pilot and Meteorology: A Void in Understanding; Aviation Weather Training; Collegiate Weather Education for Pilots; The Current State of Meteorological Education for Aviation Professionals and Methodologies for Enhanced Learning; A Weather Crisis; Crosschecks, Backdoors, and Outs: Practical Tips from the Pro's; Position Paper on Army Aviation Meteorology Training; and Career Pilot Weather Training Curriculum (A National Weather Service Perspective). GRA

N90-18844# Air Force Geophysics Lab., Hanscom AFB, MA.

COMPARISONS BETWEEN THE RTNEPH (REAL-TIME NEPHANALYSIS) AND AFGL CLOUD LAYER ANALYSIS ALGORITHMS

Robert P. DEntremont, Gary B. Gustafson, James T. Bunting, Michael K. Griffin, and Crystal B. Schaaf 15 Jul. 1989 70 p
(AD-A216637; GL-TR-89-0175; GL-ERP-1033) Avail: NTIS HC A04/MF A01 CSCL 04/2

The Real Time Nephanalysis (RTNEPH) is an automated cloud analysis model in operational use at the Air Force Global Weather Central (AFGWC). In the RTNEPH, polar-orbiting satellite imagery is analyzed in conjunction with conventional meteorological cloud observations to produce a global analysis of cloud attributes such as extent, height, bases, and type. In 1980, an alternative to the RTNEPH layer analysis algorithm was developed at the Air Force Geophysics Laboratory (AFGL). The AFGL algorithm performs a layer analysis using a 16 x 16 array of IR satellite pixels, four times larger than the RTNEPH array size. The AFGL cloud layer algorithm was proposed as an alternative to the current RTNEPH algorithm. The comparison study that was conducted on the AFGL and RTNEPH cloud layer algorithms is described and their differences are characterized in terms of the key meteorological parameters. Recommendations are made for incorporating the AFGL algorithm into the RTNEPH and suggestions for future work in this area. GRA

N90-18845# Naval Postgraduate School, Monterey, CA. Dept. of Meteorology.

FORECASTERS HANDBOOK FOR CENTRAL AMERICA AND ADJACENT WATERS Final Report, Jun. 1986 - Mar. 1989

Forrest R. Williams, Glenn H. Jung, and Robert J. Renard Sep. 1989 508 p Prepared in cooperation with Naval Environmental Prediction Research Facility, Monterey, CA
(AD-A216752; NEPRF-TR-89-08) Avail: NTIS HC A22/MF A03 CSCL 04/2

This handbook describes the analysis and forecasting of both atmospheric and oceanic conditions important to air/sea operations over Central America and adjacent waters. Central America is defined herein to include Guatemala, Belize, El Salvador, Honduras, Nicaragua, Costa Rica and Panama. Case studies using satellite imagery are presented for the rainy season, dry season, and hurricane season. Sections also are included on general climatology and coastal geographic influences. GRA

N90-18846# Naval Postgraduate School, Monterey, CA. Dept. of Meteorology.

DYNAMICS OF AN ERICA (EXPERIMENT ON RAPIDLY INTENSIFYING CYCLONES OVER THE ATLANTIC) CYCLONE M.S. Thesis

Amy E. Chalfant Jun. 1989 56 p
(AD-A216775) Avail: NTIS HC A04/MF A01 CSCL 04/2

Cyclogenesis is studied during Intensive Observation Period (IOP) 2 from the Experiment on Rapidly Intensifying Cyclones over the Atlantic (ERICA) conducted in Winter 1988 to 1989. The detailed synoptic discussion outlines the development of multiple cyclones in the western North Atlantic Ocean. The surface analyses with data included from ships, buoys, and east coast U.S. land stations resolve a dramatic rapid development case with a deepening rate of 30 mb/12h. A comparison of observed events with operational NMC Nested Grid Model and Global Spectral Model forecasts

revealed skillful overall performance. However, there were some deficiencies in handling details of the cyclogenesis event. Diagnostics of the case show destabilization occurring during the pre-cyclogenesis period and strong upper-level forcing for the rapidly developing center. GRA

N90-18847# Massachusetts Inst. of Tech., Lexington. Lincoln Lab.
A CASE STUDY OF THE 24 AUGUST 1986 FLOWS MICROBURST
Mark A. Isaminger, Paul J. Biron, and Robert G. Hallowell 28 Nov. 1989 83 p
(Contract DTFA01-80-Y-10546)
(AD-A216939) Avail: NTIS HC A05/MF A01 CSCL 17/9

From 1984 to 1986, Lincoln Laboratory collected wind shear measurements in the southeastern United States using a pulsed Doppler radar. The major emphasis of the measurement program and subsequent analyses is the development and testing of algorithms that will enable the Terminal Doppler Weather Radar (TDWR) to provide wind shear warnings to the aviation community by detection and tracking gust fronts and microbursts. An important phase of the program involves determining appropriate scan strategies and algorithms to detect other radar measurable features which precede or accompany the surface outflows of microbursts. The detection of features aloft such as convergence, rotation, divergence, storm cells, and descending reflectivity cores may permit advanced recognition of the wind shear while it is less than 10 m/s. A microburst on 24 August 1986 in Huntsville is analyzed with single and dual-Doppler techniques to assess microburst precursors, asymmetry, and forcing mechanisms which could be used for future algorithm development. The microburst producing storm formed within a moist adiabatic, unstable air-mass with weak wind shear at low to mid-levels of the atmosphere. Rotation, convergence, divergent tops, and a descending core were detected prior to the outflow attaining a divergence of 10 m/s. This storm is similar to other Huntsville microburst producing cells in exhibiting upper-level divergence prior to the initial microburst outflow. GRA

N90-18848# European Space Agency, Paris (France).
DOPPLER LIDAR WORKING GROUP REPORT
P. Betout, D. Burridge, Ch. Werner, and T. D. Guyenne, ed. Jun. 1989 51 p
(ESA-SP-1112; ISBN-92-9092-096-3; ETN-90-96226) Copyright Avail: NTIS HC A04/MF A01; ESA Publications Division, ESTEC, Noordwijk, Netherlands, 20 Dutch guilders

The use of a Doppler lidar to measure wind structure, with reference to plans for launching a series of large platforms into polar orbit in the mid nineteen nineties and their possible use in Earth observation, is reported. Lack of wind data from the current observing network is addressed by the use of the Doppler wind lidar in providing full three-dimensional wind fields globally in clean air. Scientific and operational data requirements are described. The Doppler wind lidar is detailed and mission characteristics are outlined. Possible user related and technical studies are proposed. ESA

48 OCEANOGRAPHY

Includes biological, dynamic, and physical oceanography; and marine resources.

For related information see also *43 Earth Resources and Remote Sensing.*

N90-18849# Minerals Management Service, Herndon, VA.
ATLANTIC OUTER CONTINENTAL SHELF: DESCRIPTION OF THE MID-ATLANTIC ENVIRONMENT
S. Allison Abernathy, ed. Jul. 1989 283 p
(PB90-100033; OCS/EIS/EA/MMS-89-0064) Avail: NTIS HC A13/MF A02 CSCL 08C

In compliance with the procedures and goals established by the National Environmental Policy Act, the U.S. Department of the Interior, through the Minerals Management Service (MMS), prepares Environmental Impact Statements (EIS's) and other documentation for proposed Outer Continental Shelf (OCS) Oil and Gas Lease Sales. The potential impacts of OCS oil and gas operations on the marine environment have been subject of much research and public debate. The potential adverse affects from drilling and production discharges and oil spills on marine ecosystems are important environmental issues. A compilation is presented of in-house analyses and studies, conducted as part of the EIS process, that analyzes these impacts. Author

N90-18850# Instituto de Pesquisas Espaciais, Sao Jose dos Campos (Brazil).
COMPARISON OF CIRCULATION OBTAINED THROUGH THE TRAJECTORY OF A DRIFTING BUOY TRACKED BY SATELLITE AND HYDROGRAPHIC DATA IN THE BRANSFIELD STRAIT M.S. Thesis [COMPARACAO DA CIRCULACAO OBTIDA ATRAVES DA TRAJETORIA DE UMA BOIA DE DERIVA RASTREADA POR SATELITE E DE DADOS HIDROGRAFICOS NO ESTREITO DE BRANSFIELD]
Carlos Leandro daSilvaJunior Sep. 1989 169 p In PORTUGUESE; ENGLISH summary
(INPE-4946-TDL/387) Avail: NTIS HC A08/MF A01

An oceanographic drifting buoy developed by INPE and positioned by System ARGOS, using NOAA-6 and NOAA-9 satellites, was launched on 10 March 1986, in Bransfield Strait at 63 deg 7.13 min, 60 deg 22.9 min W. The drifting buoy remained in the area until 14 March 1986, at which time the buoy was recovered by the oceanographic support ship Barao de Teffe. Concurrent with the launching and tracking of this Lagrangian drifter, a set of hydrographic stations was completed. The objective is to describe the oceanic circulation in the surface layer of the Strait of Bransfield, making use of a drifting buoy trajectory and estimates of geostrophic and Ekman currents. The buoy's overall trajectory was divided into 4 parts based on obvious differences within the trajectory. The hydrographic data were used to determine surface and 10 m geostrophic currents, referenced to 500 and 1000 dbar levels. Wind driven currents for the surface and 10 meters depth were also calculated using shipboard wind data. The mean current speed measured by the buoy's displacement was 4 times greater than the geostrophic current speed and 6.7 times greater than the mean wind driven current speed. Closest overall agreement was found between the drifter trajectory and the geostrophic current. The buoy trajectory suggested the presence of a previously unknown surface front, located Southeast of and in proximity to Deception Island. This new front was confirmed from the hydrographic sections. The drifting buoy (System ARGOS) is shown to be a modern remote sensing instrument that makes use of powerful space age technology, whether for the detection and monitoring of regional surface fronts, or for describing the surface layer oceanic circulation in mesoscale, in time and space. Author

N90-18851# Naval Postgraduate School, Monterey, CA.
AN APPLICATION OF OCEAN WAVE-CURRENT REFRACTION TO THE GULF STREAM USING SEASAT SAR DATA
Michael W. Byman Aug. 1989 66 p
(AD-A216769) Avail: NTIS HC A04/MF A01 CSCL 08/3

When ocean waves in deep water interact with a current, the direction of propagation and characteristics of the waves such as height and length are affected. Swell in the open ocean can undergo significant refraction as it passes through major current systems like the Gulf Stream or Antarctic Circumpolar Current. Remote sensing techniques such as synthetic aperture radars (SAR) have the potential to detect wave systems over a wide geographical area. Combining a model for wave refraction in the presence of currents with SAR measurements, the inverse problem of using the measured wave data can be solved to determine the direction and magnitude of the intervening currents. In this study the behavior of swell measured by SAR on a satellite pass over the Gulf Stream is examined. The refraction predicted by a numerical model under conditions of varying current profiles and velocities is compared to SAR generated wave spectra. By

matching the current profile which results in the best correlation of wave refraction to the SAR data, the tomographic problem of measuring the Gulf Stream current is solved. GRA

51 LIFE SCIENCES (GENERAL)

N90-18852*# National Aeronautics and Space Administration. Lyndon B. Johnson Space Center, Houston, TX.
THREE-DIMENSIONAL COCULTURE PROCESS Patent Application
David A. Wolf, inventor (to NASA) and Thomas J. Goodwin, inventor (to NASA) (Krug International, Houston, TX.) 2 Mar. 1989 27 p
(NASA-Case-MSC-21560-1; NAS 1.71:MSC-21560-1; US-Patent-Appl-SN-317931) Avail: NTIS HC A03/MF A01 CSCL 06C

The present invention relates to a 3-dimensional co-culture process, more particularly to methods or co-culturing at least two types of cells in a culture environment, either in space or in unit gravity, with minimum shear stress, freedom for 3-dimensional spatial orientation of the suspended particles and localization of particles with differing or similar sedimentation properties in a similar spatial region to form 3-dimensional tissue-like structures. Several examples of multicellular 3-dimensional experiences are included. The protocol and procedure are also set forth. The process allows simultaneous culture of multiple cell types and supporting substrates in a manner which does not disrupt the 3-dimensional spatial orientation of these components. The co-cultured cells cause a mutual induction effect which mimics the natural hormonal signals and cell interactions found in the intact organism. This causes the tissues to differentiate and form higher 3-dimensional structures such as glands, junctional complexes polypoid geometries, and microvilli which represent the corresponding in-vitro structures to a greater degree than when the cell types are cultured individually or by conventional processes. This process was clearly demonstrated for the case of two epithelial derived colon cancer lines, each co-cultured with normal human fibroblasts and with microcarrier bead substrates. The results clearly demonstrate increased 3-dimensional tissue-like structure and biochemical evidence of an increased differentiation state. With the present invention a variety of cells may be co-cultured to produce tissue which has 3-dimensionality and has some of the characteristics of in-vitro tissue. The process provides enhanced 3-dimensional tissue which create a multicellular organoid differentiation model. NASA

N90-18853*# National Aeronautics and Space Administration. John F. Kennedy Space Center, Cocoa Beach, FL.
CONTINUOUS HYDROPONIC WHEAT PRODUCTION USING A RECIRCULATING SYSTEM
C. L. Mackowiak, L. P. Owens, C. R. Hinkle (Bionetics Corp., Cocoa Beach, FL.), and R. P. Prince Sep. 1989 58 p
(Contract NAS10-10285)
(NASA-TM-102784; NAS 1.15:102784) Avail: NTIS HC A04/MF A01 CSCL 02C

Continuous crop production, where plants of various ages are growing simultaneously in a single recirculating nutrient solution, is a possible alternative to batch production in a Controlled Ecological Life Support System. A study was conducted at John F. Kennedy Space Center where 8 trays (0.24 sq m per tray) of Triticum aestivum L. Yecora Rojo were grown simultaneously in a growth chamber at 23 C, 65 percent relative humidity, 1000 ppm CO2, continuous light, with a continuous flow, thin film nutrient delivery system. The same modified Hoagland nutrient solution was recirculated through the plant trays from an 80 L reservoir throughout the study. It was maintained by periodic addition of water and nutrients based on chemical analyses of the solution. The study was conducted for 216 days, during which 24 trays of wheat were consecutively planted (one every 9 days), 16 of which were grown to maturity and harvested. The remaining 8 trays were harvested on day 216. Grain yields averaged 520 g m(exp -2), and had an average edible biomass of 32 percent. Consecutive yields were unaffected by nutrient solution age. It was concluded that continual wheat production will work in this system over an extended period of time. Certain micronutrient deficiencies and toxicities posed problems and must be addressed in future continuous production systems. Author

52 AEROSPACE MEDICINE

Includes physiological factors; biological effects of radiation; and effects of weightlessness on man and animals.

N90-18854 Kansas State Univ., Manhattan.
THE ROLE OF BLOOD VOLUME IN DETERMINING THE CARDIOVASCULAR ADJUSTMENTS TO EXERCISE Ph.D. Thesis
Mari Karol Hopper 1989 60 p
Avail: Univ. Microfilms Order No. DA8924324

The effect of altering blood volume on mean right atrial pressure (RAP) was determined at rest and during exercise in five horses. Blood volume was increased by intravenously infusing dextran (DI) and decreased by administering a diuretic, furosemide (FUR). DI significantly increased mean pulmonary artery pressure above control during all levels of exercise while FUR reduced it during severe exercise. Thus, increasing blood volume increases central venous filling pressure while decreasing blood volume has the opposite effect. The effects of altering mean right atrial pressure on the cardiovascular adjustments to exercise were determined in six horses. Increasing plasma volume by DI increased RAP at rest and during all levels of exercise while decreasing plasma volume by FUR administration decreased it. Subsequently, cardiac output was increased with DI and reduced with FUR entirely due to change in stroke volume as heart rate was virtually unchanged by either treatment. Mean systemic arterial blood pressure did not change following DI; therefore, calculated total peripheral resistance was reduced. Dissert. Abstr.

N90-18855 Yeshiva Univ., New York, NY.
CORONARY ARTERIAL CAPACITANCE AND SUBENDOCARDIAL VASCULAR PATENCY THROUGHOUT THE CARDIAC CYCLE Ph.D. Thesis
Mengjia Zhao 1988 185 p
Avail: Univ. Microfilms Order No. DA8919248

Coronary blood flow undergoes phasic and transmural changes throughout the cardiac cycle. The mechanisms of these changes have not been completely elucidated. The role of coronary arterial capacitance in temporal and transmural variation of coronary flow was studied. It was hypothesized that coronary arterial capacitance may change the phasic coronary inflow pattern temporally at microcirculatory level and redistributes myocardial blood flow transmurally. The pressure within this capacitive function may act as the distending pressure to maintain vascular patency throughout the cardiac cycle. These hypotheses were tested with two different experimental approaches. In the first series of experiments, the role of coronary arterial capacitance in temporal variation and transmural distribution of the regional blood flow was studied in 15 dogs. In another series of experiments, the exchange vessel patency during normal and subendocardial hypoperfusion was studied by comparing the transmural pattern of exchange vessel surface area with the simultaneous flow pattern in 21 dogs. The results of these two studies suggest that although the apparent coronary inflow ceases during systole, the flow at the exchange level persists throughout the cardiac cycle with the coronary arterial capacitance as the potential driving pressure. Dissert. Abstr.

N90-18856# Oak Ridge National Lab., TN. Health and Safety Research Div.
RISK ANALYSIS: FUNDAMENTAL CONCEPTS, REGULATORY TOXICOLOGY, AND RELATIVE COMPARISONS FROM RADIATION BIOLOGY
Troyce D. Jones 1990 25 p Presented at the Health Physics

Society Midyear Topical Symposium on Risk Analysis, Atlantic City, NJ, 5 Feb. 1990
(Contract DE-AC05-84OR-21400)
(DE90-002466; CONF-900246-1) Avail: NTIS HC A03/MF A01

This talk uses fundamental concepts, and through usage reviews some definitions (which are underlined in the text) in the area of generalized risk analysis, methods currently used in regulatory toxicology to evaluate risk or hazard from carcinogenic and noncarcinogenic chemicals, and basic radiation physics and radiobiology as related to x and gamma photons. After a review of fundamentals, a suggested modification is made to use concepts which have been applied for decades in radiation protection as a template to reduce inaccuracies and uncertainties in hazard evaluations for nonradiological pollutants. A two step process is proposed: first the relative potency of agent A with respect to the reference agent, B, is defined in terms of the treatments, T(sub A), and, T(sub B), which produce equal biological effect. Relative potency is then T(sub B)/T(sub A). This exercise yields a unitless hazard ranking. The second step is to couple the unitless hazard ranking to reference exposures which have been generally regarded as safe. Those reference exposures could be taken as the natural terrestrial radiation background, the toxicological equivalent of a reference meal comprised of common foodstuffs, or the toxicological equivalent of utility processes but otherwise pure drinking water. DOE

N90-18857# Maryland Univ., College Park. Dept. of Electrical Engineering.
EFFECTS OF PULSED AND CW (CONTINUOUS WAVE) 2450 MHz RADIATION ON TRANSFORMATION AND CHROMOSOMES OF HUMAN LYMPHOCYTES IN VITRO Final Report, 1 Oct. 1986 - 15 Dec. 1989
Christopher C. Davis 15 Dec. 1989 52 p
(Contract N00014-86-K-0716)
(AD-A216500) Avail: NTIS HC A04/MF A01 CSCL 06/4

The results of research are described for the following areas: whether spontaneous or phytohemagglutinin-induced transformation of human lymphocytes in vitro is affected by exposure to continuous wave (CW) or pulsed wave (PW) 2450 MHz microwaves; comparison of CW and PW microwave exposure at the same average specific absorption rate (SAR) - PW is markedly different and acts in a non-heating way; comparison of effects obtained by microwave and conventional heating needed to elevate the sample temperature by 0.5, 1.0, 1.5 and 2.0 C; and to determine whether chromosomal aberrations are induced under the conditions of the experiment. GRA

N90-18858# Smith-Kettlewell Inst. of Visual Sciences, San Francisco, CA.
VISUAL PROCESSING OF OBJECT VELOCITY AND ACCELERATION Annual Technical Report No. 1, 15 Oct. 1988 - 14 Oct. 1989
Suzanne P. McKee 14 Dec. 1989 4 p
(Grant AF-AFOSR-0035-89; AF Proj. 2313)
(AD-A216509; AFOSR-89-1884TR) Avail: NTIS HC A01/MF A01 CSCL 06/4

Several models of human motion discrimination have been proposed over the last decade. All are loosely related to the correlator approach originally used by Hassenstein and Reichardt to describe motion discrimination in insect eyes. These correlator models use simple spatial and temporal filtering followed by a non-linear multiplicative operation to account for human direction discrimination of sinusoidal stimuli near contrast threshold. Nevertheless, these models are extremely limited in scope. Research in this laboratory has shown that the correlator models cannot explain human speed discrimination even for sinusoidal targets. Apparently, a higher order network formed by combining local motion energy units is required to encode speed. This laboratory has also studied how different features (object components) are combined so that complicated objects move at a uniform velocity. The combination rules are fairly arbitrary, but are limited by physical constraints. Basically, features with similar contrasts, wavelengths, spatial frequencies and temporal frequencies are combined to form a coherent whole moving at a single perceived velocity. Dissimilar features move independently. GRA

N90-18859# Brigham and Women's Hospital, Boston, MA.
A PROGRAM FOR THE STUDY OF SKELETAL MUSCLE CATABOLISM FOLLOWING PHYSICAL TRAUMA Final Report, 21 Feb. 1986 - 20 Feb. 1989
Douglas W. Wilmore 25 Nov. 1989 16 p
(Contract DAMD17-86-C-6157; DA Proj. 351-62772-A-874)
(AD-A216569) Avail: NTIS HC A03/MF A01 CSCL 06/4

Prostaglandins may play a central role in the protein catabolic response following injury. Following operative injury, blocking prostaglandin generation reduced nitrogen excretion and tended to diminish hind leg amino acid flux. PGE2 infusion increased skeletal muscle amino acid flux. Altering leg blood flow by sympathectomy and nerve stimulation failed to alter skeletal muscle protein breakdown. High dose narcotic anesthesia tended to inhibit catabolic responses, suggesting that the central nervous system is important in these responses. Prostaglandin inhibition should be evaluated as a method of reducing the response to injury in humans. GRA

N90-18860# Harvard Univ., Cambridge, MA. Div. of Applied Sciences.
THE EFFECTS OF LUMINANCE BOUNDARIES ON COLOR PERCEPTION Final Report, 15 Sep. 1986 - 14 Mar. 1989
Richard E. Kronauer, R. T. Eskew, Jr., and Charles F. Stromeyer, III 15 Nov. 1989 47 p
(Grant AF-AFOSR-0338-86; AF Proj. 2313)
(AD-A216741; AFOSR-89-1676TR) Avail: NTIS HC A03/MF A01 CSCL 06/4

When a suprathreshold luminance flash, presented as an increment on a larger background field, accompanies a circular isoluminant chromatic flash at the same spatial location, chromatic threshold is reduced by about two-fold. This facilitation results from the clearly visible edges of the luminance flash (the pedestal) serving to demarcate the test region, segregating it from its surround. Recent signal detection experiments show that this facilitation does not occur as a result of the contour's reducing the spatio-temporal detection uncertainty of the observer; instead of merely directing the observer's attention, the pedestal must alter the properties of chromatic detectors (by changing the extent of spatial integration, for instance). A thin luminance ring can be used to create the facilitating contour. Displacing the ring relative to the test causes the facilitation to decline sharply, as if the visual system integrated uniformly within the demarcated region. However, the contour does not have to enclose the test region: small segments of the ring presented on the test circumference have about half the maximum facilitatory effect, while 180 deg of arcs produces the whole effect. These results can be used as a rigorous means of probing the way in which low level visual attributes (edges, color) interact at higher levels. GRA

N90-18861# Wisconsin Univ., Milwaukee. Dept. of Psychology.
PERCEPTION OF LONG-PERIOD COMPLEX SOUNDS Annual Progress Report, 1 Sep. 1988 - 31 Oct. 1989
Richard M. Warren 27 Nov. 1989 76 p
(Grant AF-AFOSR-0320-88; AF Proj. 2313)
(AD-A216743; AFOSR-89-1677TR) Avail: NTIS HC A05/MF A01 CSCL 06/4

Working with recycled sequences of ten 40 ms items, the discrimination of minimal changes was studied for: sinusoids, vowels, and frozen noise segments. Listeners made ABX judgments for sequences differing only in the ordering of two contiguous items. In contrast with results previously obtained for ten-item sequences presented in transient one-shot bursts, recycled stimuli were readily discriminated by untrained listeners. The relative difficulty of discriminating tonal patterns (measured by response time) was an inverse function of the frequency separation between the permuted tones and the frequency separation between the tones immediately preceding and following the permuted pair. For the vowel sequences, listeners' trial by trial repor indicate that

discrimination of order was mediated by verbal organization involving introduction of illusory consonants and distortion of the vowels. Discrimination of order within sequences of frozen noise was more difficult than found with tone or vowel sequence but all listeners performed at levels well above chance. Additional work with recycled frozen noise is proceeding satisfactorily which deals with the ability to remember and recognize segments up to 1 s in duration, and the relative salience of various spectral regions in this process. GRA

N90-18862# Massachusetts Inst. of Tech., Cambridge. Artificial Intelligence Lab.
RECOGNIZING THREE-DIMENSIONAL OBJECTS WITHOUT THE USE OF MODELS Memorandum Report
Thomas Marill Sep. 1989 27 p
(Contract N00014-85-K-0124)
(AD-A216766; AI-M-1157) Avail: NTIS HC A03/MF A01 CSCL 06/4

We present an approach to the problem of recognizing three-dimensional objects from line-drawings. In this approach there are no models. The system needs only to be given a single picture of an object; it can then recognize the object in arbitrary orientations. GRA

N90-18863# California Univ., Irvine.
ORGANIZATION OF A LARGE-SCALE CORTICAL NETWORK Final Technical Report
Gary Lynch 1989 20 p
(Contract N00014-86-K-0333)
(AD-A216829) Avail: NTIS HC A02/MF A01 CSCL 06/4

This research program has been directed at discovering neurobiological features (cell specializations, activity patterns in collection of neurons, circuit design features) essential to the encoding, organizing, and utilizing recognition memories by networks in mammalian cortex. Three levels of work have been involved: (1) physiological and anatomical analyses of specific, well defined examples of telencephalic networks; (2) translation of the neurobiological results into computer simulations of the networks; and (3) testing of the physiological and behavioral predictions of the computer models. It is anticipated that the results of the research will provide the bases of formal hypotheses regarding the links between cortical properties and computational operations and provide guidelines for the design of novel devices capable of dealing with the difficult computational problems presented by real world environments. GRA

N90-18864# Connecticut Univ., Storrs. Dept. of Communication Sciences.
AUDITORY PERCEPTION Annual Technical Report, 1 Nov. 1988 - 31 Sep. 1989
Marion F. Cohen 27 Nov. 1989 11 p
(Grant AF-AFOSR-0008-89; AF Proj. 2313)
(AD-A217012; AFOSR-89-1674TR) Avail: NTIS HC A03/MF A01 CSCL 06/4

During the past year we have conducted several experiments designed to study those stimulus characteristics which contribute to the ability of the auditory system to separate simultaneous signals. We have studied the effects of synchronous amplitude modulation, specifically the influence of changes in relative level of two stimuli, and have found that by changing relative levels of the two stimuli involved, the ear can detect temporal synchrony over a range of at least four octaves. We have also studied the effects of simultaneous gating, synchronous FM, and harmonicity on the ability of the auditory system to detect a signal in the presence of other stimuli. We have found that each of these characteristics contribute to signal separation. GRA

N90-18865# California Univ., Berkeley. Lawrence Berkeley Lab. Research Medicine and Radiation Biophysics Div.
PERFORMANCE OF A COINCIDENCE BASED BLOOD ACTIVITY MONITOR
William W. Moses Dec. 1989 5 p Presented at the IEEE Nuclear Science Symposium, San Francisco, CA, 22-26 Jan. 1990
(Contracts DE-AC03-76SF-00098; NIH-RR-05918)
(DE90-006105; LBL-27901; CONF-900143-16) Avail: NTIS HC A01/MF A01

A new device was constructed that measures the positron emitting radio tracer concentration in arterial blood by extracting blood with a peristaltic pump, then measuring the activity concentration by detecting coincident pairs of 511 keV photons with a pair of heavy inorganic scintillators attached to photomultiplier tubes. The sensitivity of this device is experimentally determined to be 610 counts/second per micro Ci/ml, and has a paralyzing dead time of 1.2 microsec, so is capable of measuring blood activity concentration as high as 1 mCi/ml. Its performance is compared to two other blood monitoring methods: discrete blood samples counted with a well counter and device that uses a plastic scintillator to directly detect positrons. The positron detection efficiency of this device for (sup 18)F is greater than the plastic scintillation counter, and also eliminates the radioisotope dependent correction factors necessary to convert count rate to absolute concentration. Coincident photon detection also has the potential of reducing the background compared to direct positron detection, thereby increasing the minimum detectable isotope concentration. DOE

N90-18866# Centre d'Etudes et de Recherches de Medecine Aerospatiale, Paris (France). Div. de Chimie-Toxicologie.
STUDY OF RIFAMPICIN FIXATION ON PLASMA PROTEINS BY DERIVATIVE SPECTROPHOTOMETRY
N. Martin, P. Lafargue, P. Levillain, and G. Houin Jun. 1989 23 p In FRENCH; ENGLISH summary
(CERMA-89-25; ETN-90-96256) Avail: NTIS HC A03/MF A01

A new method to study fixation of drug molecules on plasma proteins is developed. The implemented technique is that of the annulation point observed in derivative spectrophotometry. This method is simple, rapid and requires no preliminary separation of the free form from the binded form. The obtained binding parameters of rifampicin on albumin are comparable to those measured by the reference method of dialysis, in equilibrium conditions. ESA

N90-18867# Brookhaven National Lab., Upton, NY. Dept. of Applied Science.
BIOMEDICAL APPLICATIONS OF SYNCHROTRON X RAY MICROSCOPY
K. W. Jones, R. S. Bockman, B. M. Gordon, M. L. Rivers, A. J. Saubermann, G. Schidlovsky, and P. Spanne (Linkoeping Univ., Sweden) Oct. 1989 13 p Presented at the 2nd International Workshop of X Ray Fluorescence (XRF) and PIXE Applications in Life Sciences, Capri, Italy, 29-30 Jun. 1989 Sponsored in part by Swedish Society of Medicine
(Contract DE-AC02-76CH-00016; NIH-P41-RR-01838; NCI-CA-38645; NCI-CA-29502; SMRC-MFR-7557)
(DE90-004957; BNL-42934; CONF-8906283-1) Avail: NTIS HC A03/MF A01

X ray beams produced in synchrotron storage rings are useful for many biomedical experiments since a very high flux of x rays can be delivered to a sample. The beam can be restricted to a diameter of less than 10 micros using appropriate optical systems or collimators. It is then possible to employ these beams to make elemental maps of biological materials using synchrotron radiation induced x ray emission (SRIXE) to identify particular elements or to use differences in the linear attenuation coefficients for computed microtomography (CMT). Biomedical applications of these methods will be illustrated using work done at the Brookhaven X-26 X Ray Microscope. DOE

N90-18868# Brookhaven National Lab., Upton, NY. Dept. of Medicine.
MEASUREMENT OF BODY FAT BY NEUTRON INELASTIC SCATTERING: COMMENTS ON INSTALLATION, OPERATION, AND ERROR ANALYSIS
Joseph J. Kehayias, Steven B. Heymsfield, F. Avraham Dilmanian, Jack Wang, David M. Gunther, and Richard N. Pierson, Jr. (Tufts

Univ., Boston, MA.) 1989 8 p Presented at the 1989 International Symposium on in Vivo Body Composition Studies, Toronto, Ontario, 20-23 Jun. 1989
(Contract DE-AC02-76CH-00016)
(DE90-006765; BNL-43806; CONF-8906269-5) Avail: NTIS HC A02/MF A01

The existing techniques for the in vivo measurement of body fat can be classified into three categories: subtraction of lean body mass from total weight, measurement of a physical property of the body, and neutron inelastic scattering. This paper discusses the technique of neutron inelastic scattering, the analysis of spectral data, and the results. DOE

53 BEHAVIORAL SCIENCES

Includes psychological factors; individual and group behavior; crew training and evaluation; and psychiatric research.

N90-18869# Illinois Univ., Urbana. Dept. of Computer Science.
SYSTEMATICITY AS A SELECTION CONSTRAINT IN ANALOGICAL MAPPING
Catherine A. Clement (University of Eastern Kentucky, Richmond.) and Dedre Gentner 15 Sep. 1989 74 p
(Contracts N00014-89-J-1272; N00014-85-K-0559; HD07205-08)
(AD-A216029; UIUCDCS-R-89-1558; UILU-ENG-89-1777) Avail: NTIS HC A04/MF A01 CSCL 05/8

Analogy is often viewed as a partial similarity match between domains. But since between any two domains there are more partial similarities than good analogies, it follows that analogy is selective. Three experiments examined the selection constraint on which relations are mapped between a base and target in an analogy. In Experiment 1 subjects judged two matches to be included in an analogy: an isolated match, and a match embedded in a larger mapping system. Subjects preferred the embedded match. In Experiments 2 and 3 subjects made analogical predictions about a target domain. Subjects predicted information that followed from a causal system that matched the base domain, rather than the information that was equally plausible, but that created an isolated match with the base. Results support Gentner's (1983, 1989) structure-mapping theory that analogical mapping concerns systems and not individual predicates, and that attention to shared systematic structure constrains the selection of information to include in an analogy. GRA

N90-18870# Illinois Univ., Champaign. Model Based Measurement Lab.
APPROPRIATENESS MEASUREMENT FOR COMPUTERIZED ADAPTIVE TESTS Final Technical Paper, Oct. 1987 - Jun. 1989
Gregory L. Candell and Michael V. Levine Dec. 1989 63 p Submitted for publication
(Contract F41689-87-D-0012)
(AD-A216121; AFHRL-TP-89-15) Avail: NTIS HC A04/MF A01 CSCL 05/8

The effects of an initial sequence of random responses to 15-, 20-, and 25-item adaptive tests were examined in a series of simulation studies. Random responding on as two items had a substantial effect on an examinee's score. Thus it is important to determine whether (as a result of carelessness, test anxiety, computer anxiety, failure to understand instructions, or other reasons) an examinee has answered the first several items haphazardly. It was shown by use of an optimal appropriateness index, the likelihood ratio (LR) index, that a large proportion of faulty test scores can be identified. The performance of LR was evaluated by determining hit rates and false positive rates in a series of studies concerning: (1) comparisons with other indices, (2) the use of a security procedure during item selection for the adaptive test, (3) standardization, and (4) misspecification of the number of items with random answers. The LR index detected initial sequences of random responses with high accuracy with and without a security procedure during item selection. Other appropriateness indices were considerably less accurate. Standardization greatly decreased the power of LR at low false positive rates. Finally, misspecification of the length of the initial segment of random responses systematically reduced the power of the LR index to detect aberrance. GRA

N90-18871# Massachusetts Inst. of Tech., Cambridge. Artificial Intelligence Lab.
A SELF-ORGANIZING MULTIPLE-VIEW REPRESENTATION OF THREE-DIMENSIONAL OBJECTS
Shimon Edelman and Daphna Weinshall Aug. 1989 15 p
(Contracts DACA76-85-C-0010; N00014-85-K-0124)
(AD-A216711; AI-M-1146) Avail: NTIS HC A03/MF A01 CSCL 05/8

We explore representation of 3D objects in which several distinct 2D views are stored for each object. We demonstrate the ability of a two-layer network of threshold summation units to support such representations. Using unsupervised Hebbian relaxation, we trained the network to recognize ten objects from different viewpoints. The training process led to the emergence of compact representations of the specific input views. When tested on novel views of the same objects, the network exhibited a substantial generalization capability. In simulated psychophysical experiments, the network's behavior was qualitatively similar to that of human subjects. GRA

N90-18872# Smith-Kettlewell Inst. of Visual Sciences, San Francisco, CA.
PSYCHOLOGICAL STUDIES OF VISUAL CORTICAL FUNCTION Annual Technical Report, No. 1, 1 Sep. 1988 - 31 Aug. 1989
Ken Nakayama 13 Nov. 1989 4 p
(Grant AF-AFOSR-0326-88; AF Proj. 2313)
(AD-A217029; AFOSR-89-1678TR) Avail: NTIS HC A01/MF A01 CSCL 06/4

We have investigated a number of paradigms where odd targets have to be either detected or discriminated and where set size, prior knowledge of target identity, and other factors were varied. We have set up an eye movement monitoring experiment to use the speed and accuracy of saccades to supplement the psychophysical observations described above. We have been examining the phenomenon of color (or brightness) spreading, developing a paradigm to show that the filling of color could be interrupted by using an after-coming patterned mask. We are also making neutral models to account for the psychophysical observations as they emerge. GRA

54 MAN/SYSTEM TECHNOLOGY AND LIFE SUPPORT

Includes human engineering; biotechnology; and space suits and protective clothing.

For related information see also *16 Space Transportation.*

N90-18873# Anthropology Research Project, Yellow Springs, OH.
ANTHROPOMETRY OF A FIT TEST SAMPLE USED IN EVALUATING THE CURRENT AND IMPROVED MCU-2/P MASKS Summary Report, Aug. 1987 - Mar. 1989
Henry Case, Cav Erving, and Kathleen M. Robinette Mar. 1989 38 p
(Contract F33615-85-C-0531)
(AD-A215173; AAMRL-TR-89-009) Avail: NTIS HC A03/MF A01 CSCL 05/8

Forty-two head and face dimensions were measured on a fit-test sample of 104 subjects employed to evaluate current and improved models of the Air Force MCU-2/P full-face protective mask. The object of the study was to determine whether the sample was anthropometrically representative of the larger Air Force population. Fitting criteria currently in use were also evaluated. Results of the study indicated that head and face dimensions of the male test

sample reflected the distribution among male Air Force personnel. Though selected with similar care, the female sample was, on the whole, somewhat larger than the Air Force females. Quantitative fit testing showed that both masks could be successfully fitted to all but one subject. However, marked differences in measurement results by two teams of measures call into question the choice of sizing categories, mask issue criteria, and tariffing. Further investigation is recommended. GRA

N90-18874# Army Aeromedical Research Lab., Fort Rucker, AL.
EVALUATION OF HELMET RETENTION SYSTEMS USING A PENDULUM DEVICE Final Report
Peter Vyrnwy-Jones, Charles R. Paschal, Jr., and Ronald W. Palmer Sep. 1989 56 p
(AD-A215489; USAARL-89-27) Avail: NTIS HC A04/MF A01 CSCL 05/8

Three methods were evaluated for testing the retention and rotation characteristics of aircrew helmets. Two of these employed static techniques with an anthropometric headform and human subjects. Unfortunately, though simple in execution, these tests were insensitive to the mass and mass distribution of the helmets. However, the third method, the pendulum beam Department of Transportation testing device proved to be a simple and efficient means of differentiating between the various helmets. This method should have a role in the development and testing of future U.S. Army aircrew helmets. GRA

N90-18875# Systems Control Technology, Inc., Arlington, VA.
HUMAN FACTORS ISSUES IN AIRCRAFT MAINTENANCE AND INSPECTION Final Report
William T. Shepherd and James F. Parker, Jr. Oct. 1989 117 p
(Contract DTFA01-87-C-00014)
(AD-A215724; SCT-89-RR-18; DOT/FAA/AM-89/9) Avail: NTIS HC A06/MF A01 CSCL 01/3

The Federal Aviation Administration sponsored a two-day meeting in October 1988 to address issues of human factors and inspection. Presentations were given by some 13 individuals representing the full spectrum of interests in commercial aviation. Presentations also were given by three human factors scientists with backgrounds in vigilance and industrial inspection technology. Each presentation, as well as the following question and answer period, was recorded for transcription and study. The objective of the meeting was to identify human issues of importance, particularly as such issues might contribute to inspection or maintenance error. The desired outcome was to be: (1) an improved understanding of personnel performance in aviation maintenance, and (2) recommendations, as appropriate, to the FAA concerning needed research efforts and/or possible new or revised regulatory actions. Several recommendations were presented to the FAA in the areas of communications, training, management, regulatory review, and research and development. GRA

N90-18876# Oak Ridge National Lab., TN. Telerobotic Systems Section.
TELEOPERATOR SERVOLOOP TUNING USING AN EXPERT SYSTEM
M. W. Noakes 1990 4 p Presented at the 22nd IEEE Southeastern Symposium on System Theory, Cookville, TN, 11-13 Mar. 1990
(Contract DE-AC05-84OR-21400)
(DE90-005674; CONF-900378-3) Avail: NTIS HC A01/MF A01

This paper discusses the development of an expert system for optimizing of the controls tuning of a gear and shaft force-reflecting servomanipulator. Remote maintenance techniques have produced hot-cell manipulators that do not require hands-on repair. However, these manipulators are difficult to tune due to the conflicting priorities of maximizing operator sensation of force reflection and minimizing operator fatigue in combination with the complex nonlinear control algorithms and cross-coupled motions. Due to the heuristic nature of this tuning problem and the emphasis on human perception of performance, an expert system has been developed as an alternative to algorithmic optimization of gains. DOE

55 SPACE BIOLOGY

Includes exobiology; planetary biology; and extraterrestrial life.

No abstracts in this category.

59 MATHEMATICAL AND COMPUTER SCIENCES (GENERAL)

No abstracts in this category.

60 COMPUTER OPERATIONS AND HARDWARE

Includes hardware for computer graphics, firmware, and data processing.

For components see *33 Electronics and Electrical Engineering.*

N90-18877# Penguin Software, Inc., Long Beach, CA.
A MICROCODE COMPILER THAT RUNS ON THE IBM AT AND SUPPORTS CASCADABLE MICROCOMPUTERS, PART 1 Final Report, 23 Sep. 1987 - 22 Sep. 1989
Thomas H. Weight 11 Nov. 1989 36 p
(Contract DAAD07-87-C-0119)
(AD-A215888) Avail: NTIS HC A03/MF A01 CSCL 12/7

A retargetable microcode compiler was developed. The approach does not have a fixed machine independent language, but allows the user to develop a language specific to each particular target machine. The Microcode Compiler starts out with an underlying meta-assembler and builds up a higher level language capability around it. This capability allows the user to incorporate knowledge of target machine design into the language definition, and thus avoid the necessity for resource allocation and code compaction in the application program. This approach results in a microcode development tool which is a very low risk, very fast, and is capable of supporting virtually any digital hardware architecture. GRA

N90-18878# Massachusetts Inst. of Tech., Cambridge. Lab. for Computer Science.
A SCALABLE MULTIPROCESSOR ARCHITECTURE USING CARTESIAN NETWORK: RELATIVE ADDRESSING M.S. Thesis
Joseph Derek Morrison Dec. 1989 140 p Sponsored in part by Apple Computer Corp. and GTE Corp.
(Contracts N00014-84-K-0099; N00014-89-J-1988)
(AD-A216580; MIT/LCS/TR-467) Avail: NTIS HC A07/MF A01 CSCL 12/7

The Computer Architecture Group is developing a new model of computation called L. A highly scalable architecture is described for implementing L called CNRA. In the CNRA architecture, processor/memory pairs are placed at the nodes of a low dimensional Cartesian grid network. Addresses in the system are composed of a routing component which describes a relative path through the interconnection network (the origin of the path is the node on which the address resides), and a memory location component which specifies the memory location to be addressed

on the node at the destination of the routing path. The CNRA addressing system allows sharing of data structures in a style similar to that of global shared memory machines, but does not have the disadvantages normally associated with shared memory machines (i.e., limited address space and memory access latency that increases with system size). How practical CNRA system might be built is discussed. It discusses how the system software might manage the relative pointers in a clean, transparent way, solutions to the problem of testing pointer equivalence, protocols and algorithms for migrating objects to maximize concurrency and communication locality, garbage collection techniques, and other aspects of the CNRA system design. Simulations experiments with a toy program are presented. GRA

N90-18879# Los Alamos National Lab., NM.
PERFORMANCE CHARACTERIZATION OF THE CONVEX C-240 COMPUTER SYSTEM
Rebecca J. Koskela, Margaret L. Simmons, and Harvey J. Wasserman Feb. 1990 11 p
(Contract W-7405-eng-36)
(DE90-006425; LA-11769-MS) Avail: NTIS HC A03/MF A01

This paper considers the sequential, vector, and parallel processing performance of the Convex C-240 computer system. A set of well-characterized FORTRAN benchmarks that have been run on a wide variety of computer systems was used for the study. The data from the C-240 are compared with those obtained on a CRAY X-MP system as well as with the Multiflow Trace-14/300 system. The results suggest that the C-240 system is very nearly capable of providing throughput power equivalent to that of the CRAY X-MP/14 we tested. DOE

N90-18880# Illinois Univ., Chicago.
CEDAR PROJECT: ORIGINAL GOALS AND PROGRESS TO DATE
1990 48 p
(Contract DE-FG02-85ER-25001)
(DE90-006761; DOE/ER-25001/26) Avail: NTIS HC A03/MF A01

The goal of this project, was to demonstrate that supercomputers of the future can exhibit general-purpose behavior and be easy to use. The Cedar Project was based on five key developments which taken together offered a comprehensive solution to achieving high performance computation: the development of VLSI components made large memories and small, fast processors available at low cost; based on many years of work at Illinois and elsewhere, we had designed a shared memory and switch which provide high bandwidth over a wide range of computations and applications areas; the Parafrase project at Illinois had for more than 10 years been aimed at developing software for restructuring ordinary programs to effectively exploit supercomputer architectures; by using a hierarchy of control, we believed that dataflow principles could be used at a high level (macro-dataflow), thus avoiding some of the problems with traditional dataflow methods; and work in numerical algorithms indicated great promise in exploiting multiprocessors without the penalty of high synchronization overhead, which had proved fatal in some earlier studies. In this section we will outline our progress since the beginning of the Cedar Project and briefly describe specific Cedar work that remains to be done. DOE

61 COMPUTER PROGRAMMING AND SOFTWARE

Includes computer programs, routines, alogorithms, and specific applications, e.g., CAD/CAM.

N90-18881# National Inst. of Standards and Technology, Gaithersburg, MD. National Computer Systems Lab.
COMPUTER VIRUSES AND RELATED THREATS: A MANAGEMENT GUIDE Final Report
John P. Wack and Lisa J. Carnahan Aug. 1989 46 p
(PB90-111683; NIST/SP-500/166; LC-89-600750) Avail: NTIS HC A03/MF A01; SOD HC $2.50 as 003-003-02955-6 CSCL 09B

Guidance is provided for managing the threats of computer viruses and related software and unauthorized use. It is emphasized that organizations cannot effectively reduce their vulnerabilities to viruses and related threats unless the organization commits to a virus prevention program, involving the mutual cooperation of all computer managers and users. The guidance is aimed at helping managers prevent and deter virus attacks, detect when they occur or are likely to occur, and then to contain and recover from any damage caused by the attack. An overview is presented of viruses and related software, and several chapters of guidance for managers of multi-user computers, managers and users of personal computer, managers of wide and local area networks including personal computer networks, and managers of end-user groups. Author

N90-18882*# National Aeronautics and Space Administration. Langley Research Center, Hampton, VA.
LOW-ENERGY GAMMA RAY ATTENUATION CHARACTERISTICS OF AVIATION FUELS
Jag J. Singh, Chih-Ping Shen (Old Dominion Univ., Norfolk, VA.), and Danny R. Sprinkle Washington Mar. 1990 40 p
(NASA-TP-2974; L-16719; NAS 1.60:2974) Avail: NTIS HC A03/MF A01 CSCL 09B

Am241 (59.5 keV) gamma ray attenuation characteristics were investigated in 270 aviation fuel (Jet A and Jet A-1) samples from 76 airports around the world as a part of world wide study to measure the variability of aviation fuel properties as a function of season and geographical origin. All measurements were made at room temperature which varied from 20 to 27 C. Fuel densities (rho) were measured concurrently with their linear attenuation coefficients (mu), thus providing a measure of mass attenuation coefficient (mu/rho) for the test samples. In 43 fuel samples, rho and mu values were measured at more than one room temperature, thus providing mu/rho values for them at several temperatures. The results were found to be independent of the temperature at which mu and rho values were measured. It is noted that whereas the individual mu and rho values vary considerably from airport to airport as well as season to season, the mu/rho values for all samples are constant at 0.1843 + or - 0.0013 cu cm/gm. This constancy of mu/rho value for aviation fuels is significant since a nuclear fuel quantity gauging system based on low energy gamma ray attenuation will be viable throughout the world. Author

N90-18883# Instituto de Pesquisas Espaciais, Sao Jose dos Campos (Brazil).
VERTICAL MIGRATION IN OPERATIONAL SYSTEM NUCLEUS [MIGRACAO VERTICAL DE UM NUCLEO DE SISTEMA OPERACIONAL]
Antonio FranciscoJunior Apr. 1989 17 p In PORTUGUESE; ENGLISH summary
(INPE-4879-RPE/593) Avail: NTIS HC A03/MF A01

The application of linear programming to solve the problem of vertical migration is considered in the operational system nucleus developed for the microprogrammed ASTRO computer. Author

N90-18884# Instituto de Pesquisas Espaciais, Sao Jose dos Campos (Brazil).
L: A LANGUAGE FOR SOLUTION OF INCREMENTAL SYSTEMS IN A PARALLEL PROCESSING ENVIRONMENT M.S. Thesis [L - UMA LINGUAGEM PARA SOLUCAO INCREMENTAL DE SISTEMAS EM UM AMBIENTE DE PROCESSAMENTO PARALELO]
Joao Benedito Diehl Jun. 1989 115 p In PORTUGESE
(INPE-4816-TDL/362) Avail: NTIS HC A06/MF A01

A description is presented for a high level language, denominated L, appropriate for programming an incremental computer with parallel processing capability, for the solution of systems which can be represented by mathematical models. The L language is introduced and aspects of its implementation are explained as well. Resources implemented for simulation of

execution of programs written in L in a monoprocessing environment are also presented and an application example is given. Author

N90-18885# Instituto de Pesquisas Espaciais, Sao Jose dos Campos (Brazil).
AN EXACT ALGORITHM FOR THE PROBLEM OF p-MEDIANS M.S. Thesis [UM ALGORITMO EXATO PARA O PROBLEMA DAS P-MEDIANAS]
Hilcea FerreiraMarengoni Sep. 1989 91 p In PORTUGUESE; ENGLISH summary
(INPE-4924-TDL/384) Avail: NTIS HC A05/MF A01

A few heuristic and exact methods for solving the p-median problem are studied. It particularly covers an exact algorithm based on an integer programming formulation of the problem. A branch and bound algorithm is presented and the bounds are obtained by solving the Lagrangean relaxation and using the subgradient optimization method. A data structure that takes into account the matricial character of the problem is developed and the algorithm is implemented to run on a IBM-PC microcomputer. Author

N90-18886# Instituto de Pesquisas Espaciais, Sao Jose dos Campos (Brazil).
AN INTEGRATED VISION ON METHODOLOGIES AND ENVIRONMENTS FOR MODELING AND SIMULATION ASSISTED BY COMPUTER M.S. Thesis [UMA VISAO INTEGRADA SOBRE METODOLOGIAS E AMBIENTES PARA MODELAGEM E SIMULACAO ASSISTIDAS POR COMPUTADOR]
Germano deSouzaKienbaum Jun. 1989 329 p In PORTUGUESE; ENGLISH summary
(INPE-4861-TDL/372) Avail: NTIS HC A15/MF A02

The most recent progresses in the research and development of computer systems for application in discrete-event simulation are described in a comprehensive and comparative way. Two ideal requirements are identified as pursued by all these systems, namely to provide general applicability and high level of assistance in the development of the model complete life cycle. A classification, divided into two categories, traditional and advanced, is suggested to distinguish the way in which these environments are implemented and which relates directly to their capacity in fulfilling these requirements. Among the advanced environments identified, the program generators of the British research line are then studied with special interest. Their potencialities and restrictions are reviewed, to guide an eventual future development of this kind of system for real problems applications. Author

N90-18887# Naval Postgraduate School, Monterey, CA.
DOA (DIRECTION OF ARRIVAL) ESTIMATION BY EIGENDECOMPOSITION USING SINGLE VECTOR LANCZOS' ALGORITHM M.S. Thesis
Daniel E. Gear Jun. 1989 79 p
(AD-A215802) Avail: NTIS HC A05/MF A01 CSCL 17/11

Subspace methods of solving spectral estimation and direction of arrival (DOA) problems involve finding the eigenvalues and eigenvectors of correlation matrices. Using the Lanczos algorithm some of the extreme eigenvalues and eigenvectors can be approximated without requiring the entire matrix decomposition, theoretically saving many computations. A model and a form of the Lanczos algorithm is developed. to solve the DOA problem. The relationship of the number of eigenvectors used to the accuracy of the results in a low signal to noise ratio example is examined. GRA

N90-18888# Carnegie-Mellon Univ., Pittsburgh, PA. Software Engineering Inst.
GUIDELINES FOR THE USE OF THE SAME Final Report
Marc H. Graham May 1989 261 p
(Contract F19628-85-C-0003)
(AD-A215846; CMU/SEI-89-TR-16; ESD-TR-89-24) Avail: NTIS HC A12/MF A02 CSCL 12/5

These guidelines describe the Structured Query Language (SQL) Ada Module Extensions (SAME), a method for the construction of Ada applications that access database management systems whose data manipulation language is SQL. The SAME is not a tool set, but a method of program design and development. There is a set of support software, called the SAME standard packages, which are needed by applications using the SAME. The SAME extends the capabilities of the Module language defined in the ANSI SQL standard to fit the needs of Ada. The defining characteristic of the use of the module language is that the SQL statements appear together, physically separated from the Ada application, in an object called the module. The Ada application accesses the module through procedure calls. The primary audience for this document consists of application developers and technicians creating Ada applications for SQL database management systems. The document contains a complete description of the SAME, including its motivation. It is not intended as a programmer's guide. Organizations using the SAME may wish to create such a guide from this document. Ada programming language. GRA

N90-18889# Washington Univ., Seattle. Applied Physics Lab.
COMPARISON OF TWO NAVY ENVIRONMENTAL DATABASE MODELS: GENERALIZED DIGITAL ENVIRONMENTAL MODEL AND PODESZWA SOUND SPEED PROFILE MODEL
Morris Schulkin Sep. 1989 30 p
(Contract N00039-88-C-0054)
(AD-A215848; APL-UW-TR-8926) Avail: NTIS HC A03/MF A01 CSCL 20/1

The construction of the Generalized Digital Environmental Model (GDEM), the Navy standard for modeling sound speed profiles, and the Podeszwa sound speed profile model which was used by the Naval Underwater Systems Center are reviewed. GDEM, developed by the Naval Oceanographic Office, derives vertical profiles of temperature and salinity in 30' x 30' latitude-longitude grid elements and employs these data to calculate sound speed profiles. The temperature-salinity profiles are derived from quality-screened data from the Master Oceanographic Observation Data Set maintained by the Fleet Numerical Oceanography Center. Podeszwa uses temperature-salinity data from deep Nansen casts and organizes the calculated SSPs into provinces based on temperature-salinity water mass characteristics. In spite of the differences in their construction, the models are found to be essentially equivalent in principle. GRA

N90-18890# Air Force Inst. of Tech., Wright-Patterson AFB, OH. School of Engineering.
DETERMINATION OF THE UNDERLYING TASK SCHEDULING ALGORITHM FOR AND Ada RUNTIME SYSTEM M.S. Thesis
Gary Alen Whitted Dec. 1989 133 p
(AD-A215880; AFIT/GCS/ENG/89D-18) Avail: NTIS HC A07/MF A01 CSCL 12/5

The purpose was to determine whether the task scheduling algorithm of an Ada compiler could be detected using a suite of Ada programs. This was done by identifying the task parameters and algorithm characteristics which differentiate one scheduling algorithm from the others. After these parameters and characteristics were identified, a set of test cases was developed to encompass the various parameter relationships required to detect the execution of individual algorithms. These test cases were modeled using Ada programs. Then, the programs were compiled and executed using several Ada compilers where the task scheduling algorithms of five run-time systems was known. The execution results were analyzed to determine whether the Ada programs were capable of revealing the task scheduling algorithm used by the Ada run-time system. This analysis showed that the detection of five scheduling schemes is possible using a single Ada program. Recommendations are made to improve the current Ada program leading to an automated tool in which the user analysis could be removed. GRA

N90-18891*# Cornell Univ., Ithaca, NY. Dept. of Computer Science.
DECEIT: A FLEXIBLE DISTRIBUTED FILE SYSTEM
Alex Siegel, Kenneth Birman, and Keith Marzullo 7 Dec. 1989

36 p
(Contract NAG2-593; N00014-87-C-8904; ARPA Order 6037)
(NASA-CR-186402; NAS 1.26:186402; AD-A215937; TR89-1042)
Avail: NTIS HC A03/MF A01 CSCL 09/2

Deceit, a distributed file system being developed, focuses on flexible file semantics in relation to efficiency, scalability, and reliability. Deceit servers are interchangeable and collectively provide the illusion of a single, large server machine to any clients of the Deceit service. Non-volatile replicas of each file are stored on a subset of the file servers. The user is able to set parameters on a file to achieve different levels of availability, performance, and one-copy serializability. Deceit also supports a file version control mechanism. In contrast with many recent DFS efforts, Deceit can behave like a plain Sun Network File System server and can be used by any NFS client without modifying any client software. The current Deceit prototype uses the ISIS Distributed Programming Environment for all communication and process group management, an approach that reduces system complexity and increases system robustness. GRA

N90-18892# Scientific Computing Associates, Inc., New Haven, CT.
Ada-LINDA PRELIMINARY REPORT: MOTIVATION, INFORMAL DESCRIPTION, AND EXAMPLES
1989 22 p
(Contract N00014-89-C-0268)
(AD-A216004; SCA-149) Avail: NTIS HC A02/MF A01 CSCL 12/5

SDIO 3405 - Strategic Defense System Software Policy - is typical of many Defense Department policy statements in decreeing that all mission-critical software be implemented in Ada(SDIO 3405). The intentions behind the decree are honorable: A standard programming language and standard notations for specifications and designs are highly desirable to provide a common basis for understanding and to permit the development and wide usage of common tools for maintenance, evaluation and testing. The software developer (duly inspired) wades into the body of the policy statement - only to discover a long section on waiver procedures. Grounds on which the required use of Ada may be waived include: (1) performance, or (2) appropriateness of the Ada programming model (p. 10). Waivers in the second category may be based on the inappropriateness of Ada interprocess communication, initialization or task scheduling, among other things. GRA

N90-18893# Tennessee Univ., Knoxville. Management Science Program.
DISTRIBUTED DECOMPOSITION OF BLOCK-ANGULAR LINEAR PROGRAMS ON A HYPERCUBE COMPUTER
James K. Ho and S. Kingsley Gnanendran Jul. 1989 27 p
(Contract N00014-89-J-1528)
(AD-A216433; MSP-89-3) Avail: NTIS HC A03/MF A01 CSCL 12/5

Algorithms based on the Dantzig-Wolfe decomposition principle for linear programs are implemented on an Intel iPSC-2 Hypercube computer with 64-processors. Computational results with block-angular linear programs from diverse applications are reported. They indicate that the approach of distributed computation on relatively inexpensive multiple processor computers may be very cost effective for large, structured linear programs. It is also shown that by studying certain characteristics of the interaction among the master and subproblems, one can select algorithms that best exploit the parallel processing environment. GRA

N90-18894# Duke Univ., Durham, NC.
PARALLEL ALGORITHMS DERIVATION Quarterly Report, 1 Apr. - 30 Jun. 1989
John H. Reif 1 Jul. 1989 16 p
(Contract N00014-88-K-0548)
(AD-A216452) Avail: NTIS HC A03/MF A01 CSCL 12/4

A system of rules and techniques is developed for derivation of various classes of parallel algorithms including: (1) Systolic algorithms for various fixed connection networks; (2) Randomized parallel algorithms; (3) Parallel algorithms for tree and graph problems; and (4) Parallel algorithms for algebraic problems. The development is emphasized of fundamental derivation techniques that can be utilized in as wide a class of parallel algorithms as possible. The specific algorithms to be derived were themselves carefully chosen to be as fundamental as possible. Algorithms and areas currently under investigation include: parallel list ranking, parallel graph connectivity, automatic parallel compilation from segmented straight-line programs, and derivation of pipelined algorithms for small-diameter networks. GRA

N90-18895# University of Southern California, Marina del Rey. Information Sciences Inst.
APPROACHES TO THE PLANNING OF COHERENT TEXT
Eduard H. Hovy Nov. 1989 24 p Presented at the 4th International Workshop on Text Generation, Catalina Island, CA, Jul. 1988
(Contracts F49620-87-C-0005; N00014-82-K-0149)
(AD-A216463; ISI/RS-89-245) Avail: NTIS HC A03/MF A01 CSCL 05/7

The planning of multisentential text by computer is discussed. In order to construct coherent paragraphs, relations were used from Rhetorical Structure Theory (RST) operationalized as plans. The current method of planning a paragraph using operationalized RST relation/plans is first described in some detail. Then two points are made that illustrate why RST relation/plans are the ideal tool for planning paragraphs. First, these relation/plans can be shown to combine the best features of paragraph-sized schemas and clause-sized planning rules under a top-down planning regime in a way which affords much flexibility to the user. Second, RST relation/plans can support both standard top-down planning and open-ended conversation-like behavior; a small difference in treatment gives rise to either paradigm. GRA

N90-18896# Massachusetts Inst. of Tech., Cambridge. Artificial Intelligence Lab.
A THEORY OF QUANTITATIVE INFERENCE FOR ARTIFACT SETS APPLIED TO A MECHANICAL DESIGN COMPILER Ph.D. Thesis
Allen Corlies Ward Jan. 1989 144 p
(Contract N00014-86-K-0685)
(AD-A216535; AI-TR-1089) Avail: NTIS HC A07/MF A01 CSCL 12/5

This thesis presents the ideas underlying a computer program that takes as input a schematic of a mechanical or hydraulic power transmission system, plus specifications and a utility function, and returns catalog numbers from predefined catalogs for the optimal selection of components implementing the design. Unlike programs for designing single components or systems, the program provides the designer with a high level language in which to compose new designs. It then performs some of the detailed design process. The process of compilation, or transformation from a high to a low level description, is based on a formalization of quantitative inferences about hierarchically organized sets of artifacts and operating conditions. This allows design compilation without the exhaustive enumeration of alternatives. The program has been tested on a wide variety of power transmission and temperature sensing problems. Key elements of the theory have been formally proven. It appears that the theory has applications outside design. GRA

N90-18897# Calspan Corp., Buffalo, NY.
KNOWLEDGE-BASED EXTENSIBLE NATURAL LANGUAGE INTERFACE TECHNOLOGY PROGRAM Final Report, Feb. 1988 - Sep. 1989
Jeannette G. Neal 30 Nov. 1989 69 p
(Contract F49620-88-C-0050)
(AD-A216664; AFOSR-89-1752TR) Avail: NTIS HC A04/MF A01 CSCL 12/9

The problem of developing knowledge-based natural language interface technology that is extensible via natural dialogue between user and computer system is addressed. Natural language understanding systems need to be extensible to accommodate

changes in the target application system to which they interface as well as to accommodate new users. Typically, however, current systems cannot be extended as part of a normal dialogue session. Instead, extensions must be incorporated and compiled into the interface off line before the interface is loaded for use. This can be costly in terms of down-time and frustrating for the new user. The solution that was pursued in this project was to develop a natural language interface system, called Lydia, that is extensible via methods that are modeled after human behavior. Specifically, the following methods were implemented in the Lydia system learning by being told including the ability to understand natural language when it is used as its own meta-language to explain new concepts, relation, and rules and being able to infer the category and attributes of new words from their linguistic context when used in a natural language sentence. GRA

N90-18898# Institute for Defense Analyses, Alexandria, VA.
THE EXECUTIVE WORKSHOP ON COST/PERFORMANCE MEASUREMENT. VOLUME 1: EXECUTIVE SUMMARY Final Report, Apr. - Oct. 1989
Richard T. Cheslow and J. Richard Nelson Oct. 1989 20 p
Workshop held in Alexandria, VA, 31 May - 1 Jun. 1989
(Contract MDA903-89-C-0003)
(AD-A216745; AD-E501181; IDA-P-2321-Vol-1; IDA/HQ-89-34914-Vol-1) Avail: NTIS HC A03/MF A01
CSCL 05/1

On 31 May through 1 June 1989, an executive workshop was held in Alexandria, Virginia, to address problems perceived when applying current cost/performance measurement and management systems to new advanced-technology design and manufacturing methods. The goal was to provide the Department of Defense (DOD) with recommendations for change. This paper is the proceedings of the workshop. Volume 1 contains a summary of findings and recommendations of the attendees. The primary recommendation was that the Under Secretary of Defense (Acquisition) initiate pilot programs to investigate possible changes in cost/performance measurement systems. Continued dialog and cooperation between DOD and industry is also recommended. Volume 2 contains the remarks of the speakers, the panel members, and the discussion team representatives. GRA

N90-18899# Massachusetts Inst. of Tech., Cambridge. Microsystems Technology Labs.
OPTIMUM AND HEURISTIC ALGORITHMS FOR FINITE STATE MACHINE DECOMPOSITION AND PARTITIONING Memorandum Report
Pravnav Ashar, Srinivas Devadas, and A. Richard Newton (California Univ., Berkeley.) Sep. 1989 6 p Presented at the International Conference of Computer Aided Design, Nov. 1989 Sponsored in part by Digital Equipment Corp.; Bell Telephone Labs., Inc.; Semiconductor Research Corp.
(Contracts N00014-87-K-0825; N00014-87-C-0182)
(AD-A216778; VLSI-M-89-558) Avail: NTIS HC A02/MF A01
CSCL 12/9

Techniques have been proposed in the past for various types of finite state machine (FSM) decomposition that use the number of states or edges in the decomposed circuits as the cost function to be optimized. These measures are not reflective of the true logic complexity of the decomposed circuits. These methods have been mainly heuristic in nature and offer limited guarantees as to the quality of the decomposition. In this paper we present optimum and heuristic algorithms for the general decomposition of FSMs such that the sum total of the number of product terms in the one-hot coded and logic minimized submachines is minimum or minimal. This cost function is much more reflective of the area of an optimally state-assigned and minimized submachine than the number of states/edges in the submachine. The problem of optimum two-way FSM decomposition is formulated as one of symbolic-output partitioning and show that this is an easier problem than optimum state assignment. A procedure of constrained prime-implicant generation and covering represents an optimum FSM decomposition algorithm, under the specified cost function. Exact procedures are not viable for large problem instances. A novel iterative optimization strategy of symbolic-implicant expansion and reduction, modified from two-level Boolean minimizers, represents a heuristic algorithm based on our exact procedure. GRA

N90-18900# Massachusetts Inst. of Tech., Cambridge. Dept. of Electrical Engineering.
KAM: AUTOMATIC PLANNING AND INTERPRETATION OF NUMERICAL EXPERIMENTS USING GEOMETRICAL METHODS Ph.D. Thesis
Kenneth Man-Kam Yip Aug. 1989 236 p
(Contracts N00014-86-K-0180; N00014-85-K-0124)
(AD-A216805; AI-TR-1163) Avail: NTIS HC A11/MF A02
CSCL 12/5

KAM is a computer program that can automatically plan, monitor, and interpret numerical experiments with Hamiltonian systems with two degrees of freedom. The program has recently helped solve an open problem in hydrodynamics - the prediction of onset of chaos in a resonantly excited rectangular wave tank of finite depth. Unlike other approaches to qualitative reasoning about physical system dynamics, KAM's ability to control numerical approaches to qualitative reasoning about physical system dynamics, KAM embodies a significant amount of knowledge about nonlinear dynamics. KAM's ability to control numerical experiments arises from the fact that it not only produces pictures for us to see, but also looks at (sic - in its mind's eye) the pictures it draws to guide its own actions. By combining techniques from computer vision with sophisticated dynamical invariants, KAM is able to exploit mathematical knowledge, represented in terms of a grammar that dictates consistency constraints on the structure of the phase space and parameter space. KAM is organized in three semantic levels: orbit recognition, phase space searching, and parameter space searching. Within each level spatial properties and relationships that are not explicitly represented in the initial representation are extracted by applying three operations: (1) aggregation, (2) partition, and (3) classification - iteratively. GRA

N90-18901# Alabama Univ., Huntsville. Dept. of Computer Science.
A PERSPECTIVE OF SOFTWARE REUSE Report, Sep. 1988 - Jan. 1989
James W. Hooper Mar. 1989 66 p
(Contract DAAL03-86-D-0001)
(AD-A216911; ASQBG-I-89-025) Avail: NTIS HC A04/MF A01
CSCL 12/5

In 1980, the U.S. Department of Defense (DOD) spent over $3 billion on software; by 1990, their expenses are expected to grow to $30 billion per year. Even though expenditures are escalating, productivity is falling behind the demand for new software. The same trends are perceivable throughout the software industry--in private companies and government agencies. Jones (1984) estimates that of all the code written in 1983, probably less than 15 percent is unique, novel, and specific to individual applications. Estimates are that on the average only about five percent of code is reused. Thus we see an obvious candidate area for increasing productivity and reducing cost--that is, to reuse existing software products to achieve all or part of the redundant 85 percent of the development. Even a one percent gain, relative to DOD's projected $30 billion, could save $300 million In addition to increases in productivity and reduction in costs, software quality should increase due to the greater use and testing of individual components, with the resulting isolation and correction of any problems discovered. GRA

N90-18902# Army Inst. for Research in Management Information and Computer Sciences, Atlanta, GA.
TECHNOLOGY ASSESSMENT OF SOFTWARE ENGINEERING
Feb. 1989 24 p
(AD-A216943; ASQBG-I-89-011) Avail: NTIS HC A03/MF A01
CSCL 12/5

History shows that engineering evolves from craft and commercial exploitation and that it requires scientific foundations. Science is especially important when natural intuitions about

phenomena are weak. For software engineering, the technical basis is computer science. Characteristics of an engineering practice include iteration between formal analysis and design, heavy use of earlier designs, tradeoffs between alternatives, handbooks and manuals, pragmatic approaches to being cost-effective, and significant economic concerns. The history of software engineering practices precedes the coining of the term Software Engineering in that software was being developed as soon as there were stored program computers. Commercial software development can be described in stages from programming-any-which-way (early 60's) through programming-in-the-small (early 70's) to programming-in-the-large (early 80's). Programming-any-which-way focused on mnemonics, precise use of prose, emphasis on small programs, representing structure - both symbolic information and numeric information - and gaining an elementary understanding of control. GRA

N90-18903# Army Inst. for Research in Management Information and Computer Sciences, Atlanta, GA.
INTEGRATED IMA (INFORMATION MISSION AREAS) IC (INFORMATION CENTER) GUIDE
Jun. 1989 186 p
(AD-A216944; ASQBG-A-89-028) Avail: NTIS HC A09/MF A01 CSCL 05/2

This guide addresses the integration of end-user support for the Army's five Information Mission Areas (IMAs) into the Information Center (IC). Army Regulation 25-1, The Army Information Resources Management Program (18 November 88) defines the IMA disciplines as automation, telecommunications, visual information, records management, and publications and printing. Although library management is also an information service, library management is not generally defined as an IMA discipline. Therefore library management is not addressed in this guide. This guide is based on the current research with respect to ICs for the U.S. Army conducted by the Army Institute for Research in Management Information, Communications, and Computer Sciences (AIRMICS). AIRMICS is the research arm of the U.S. Army Information Systems Engineering Command (ISEC). The guide includes three perspectives on the integration of support for the IMA disciplines in the IC. The first perspective is provided by current Army regulations and pamphlets. GRA

N90-18904# Argonne National Lab., IL.
DERIVATION OF EFFICIENT PARALLEL PROGRAMS: AN EXAMPLE FROM GENETIC SEQUENCE ANALYSIS
Ambuj K. Singh (Texas Univ., Austin.) and Ross Overbeek 1990 27 p Presented at the ACM SIGPLAN Symposium on Principles and Practice of Parallel Programming, Seattle, WA, 15-16 Mar. 1990
(Contract W-31-109-eng-38)
(DE90-005654; CONF-900329-2) Avail: NTIS HC A03/MF A01

Implementation issues such as synchronization of shared data, implementation of abstract data types, and scheduling of processes are usually not addressed in the formal derivation of parallel programs. We seek to redress the situation by considering these issues in the context of developing an efficient implementation of an actual parallel program. The computational problem that we selected is motivated by work in aligning sequences of genetic material. We proceed by developing an algorithm in Unity and investigating the issues that arise in producing an efficient C implementation of the resulting algorithm. Along the way, we develop some theorems about program refinements, and illustrate the usefulness of the theorems in the context of refining the original Unity program. DOE

N90-18905# National Aerospace Lab., Amsterdam (Netherlands). Informatics Div.
USER MANUAL FOR NEXT 1.2: NLR ENGINEERING X-PERT SYSTEM TOOLKIT
P. J. Kat and J. C. Donker 22 Dec. 1987 138 p In DUTCH; ENGLISH summary
(NLR-TR-87178-U; ETN-90-96260) Avail: NTIS HC A07/MF A01

NEXT 1.2 is an expert system shell developed at NLR. NEXT has a knowledge representation mechanism based on a combination of context tree and production rules. The inference mechanism is based on a combination of backward and forward reasoning. NEXT 1.2 is available on a Cyber 180/855 under NOS and on a Vax under VMS. Supply of other implementations can be negotiated. A user manual, written to support the knowledge engineers building knowledge based systems with NEXT, is presented. ESA

N90-18906# Universiteit Twente, Enschede (Netherlands). Dept. of Computer Science.
SIMULATING SIMULTANEOUS PROCESSES WITH APL
E. Molenkamp Sep. 1989 9 p
(Memo-INF-89-47; ISSN-0923-1714; ETN-90-96312) Avail: NTIS HC A02/MF A01

A systematic method to describe and to simulate simultaneous processes with the programming language APL is presented. Simultaneous processes interchange data using an interface such as handshaking, (the description of which interface is possible with APL although simulation is difficult). Two functions are used, WAIT UNTIL, which is always the same, and the supervisor, which depends on the processes to simulate. Examples of description and simulation of a two-way handshake and a multiway handshake are given. ESA

N90-18907# Universiteit Twente, Enschede (Netherlands). Dept. of Computer Science.
A SURVEY OF PERFORMABILITY MODELLING TOOLS
Boudewijn R. Haverkort and Ignas G. Niemegeers Sep. 1989 15 p Submitted for publication
(Memo-INF-89-50; ISSN-0923-1714; ETN-90-96313) Avail: NTIS HC A03/MF A01

The state of the art in computer tools for performability modeling is surveyed. The reasons for doing performability modeling and the mathematical background are discussed. Five tools that incorporate performability aspects, METAPHOR, METASAN, METFAC, SAVE and NUMAS are reviewed. A performability modeling tool, dynamic queueing networks, which is currently being developed, is presented. ESA

62 COMPUTER SYSTEMS

Includes computer networks and special application computer systems.

N90-18908# California Univ., Los Angeles. Dept. of Electrical Engineering.
CONTROL AND STABILIZATION OF LINEAR AND NONLINEAR DISTRIBUTED SYSTEMS Final Technical Report, 1 Apr. 1986 - 31 Dec. 1988
N. Levan and P. K. C. Wang 31 Dec. 1988 20 p Presented at the 1st International Conference in Industrial Applied Mathematics Submitted for publication
(Grant AF-AFOSR-0132-86; AF Proj. 2304)
(AD-A216446; AFOSR-89-1717TR) Avail: NTIS HC A02/MF A01 CSCL 12/2

The results are summarized of a study on the control and stabilization of linear and nonlinear distributed systems. The specific areas of study consists of: (1) stability enhancement of distributed systems describable by abstract linear evolution equations, (2) a translation invariant approach to stability and stabilizability, (3) stabilizability of bilinear systems, (4) application of computer vision in static shape estimation, control, and failure detection in elastic systems, and (5) stabilization and control of distributed systems with application to aeroelastic systems with extendible lifting surfaces. The main objective is to develop applicable mathematical theories and at the same time study specific systems arising from realistic aerospace applications. GRA

N90-18909# Argonne National Lab., IL. Computing and Telecommunications.
PARALLELIZING THE SDI ACCESS ALGORITHM FOR THE CONNECTION MACHINE-2
Thomas F. Ewing, David W. Leibfritz, Janet L. Rutkowski, ed., and Kelly A. Vogel, ed. Dec. 1989 16 p
(Contract W-31-109-eng-38)
(DE90-006382; ANL-89/41) Avail: NTIS HC A03/MF A01

Considerable expertise has been acquired in developing and optimizing algorithms on a collection of multiprocessor computers. One aspect of Argonne research in parallel computing involves the speed and other properties of parallel SDI algorithms. Various algorithms under study have exhibited speedups resulting from parallelization on shared-memory machines. A weapon-target accessibility algorithm called ACCESS exhibited a high degree of inherent parallelism and has been studied on a wide variety of sequential and parallel multiple instruction multiple data machines. To study ACCESS on a massively parallel single instruction multiple data (SIMD) machine architecture, ANL researchers developed a version of ACCESS on a Thinking Machines Corporation 16K processor Connection Machine-2 (CM-2) located at the ACRF. ANL researchers wrote the Connection Machine version of ACCESS in C, a version of C by Thinking Machines Corporation with extensions to accommodate SIMD parallelism. Because of the large number of available physical processors and the ability to create virtual processors on the CM-2, the Connection Machine version of ACCESS was able to process an array of 128 x 1024 tasks in parallel. The CM-2 implementation of ACCESS was faster than both the parallel version run on the Alliant FX/8, the Encore Multimax, and the Sequent Balance and the sequential version run on the ANL Cray X-MP/14. For the benchmark ACCESS problem, the CM-2 at ANL with 16K processors achieved a sustained performance of 400 Mflops. The investigation has demonstrated that achieving optimal performance requires structuring the code carefully to keep all available processors busy and to reduce disruptive communication on the front-end processor. DOE

N90-18910# Argonne National Lab., IL. Mathematics and Computer Science Div.
SUMMER INSTITUTE IN PARALLEL COMPUTING
Jack Dongarra and Ewing Lusk Dec. 1989 7 p Presented at the Summer Institute in Parallel Computing, Argonne, IL, 5-15 Sep. 1989 Sponsored in part by NSF
(Contract W-31-109-eng-38)
(DE90-005532; ANL/MCS-TM-136; CONF-8909296-Summ)
Avail: NTIS HC A02/MF A01

The following features of the summer institute on parallel computing are presented: introduction; background of the summer institute; objective; the attendees; the invited speakers; the Argonne speakers; the schedule; evaluation by the attendees; evaluation by the organizers; and summary. DOE

N90-18911# Stanford Linear Accelerator Center, CA.
COMPUTATION AND CONTROL WITH NEURAL NETS
A. Corneliusen, P. Terdal, T. Knight, and J. Spencer Oct. 1989 17 p Presented at the International Conference on Accelerator and Large Experimental Physics Control Systems, Vancouver, British Columbia, 30 Oct. - 3 Nov. 1989
(Contract DE-AC03-76SF-00515)
(DE90-006460; SU-SLAC-PUB-5035; CONF-891094-14) Avail: NTIS HC A03/MF A01

As energies have increased exponentially with time so have the size and complexity of accelerators and control systems. Neural nets (NN) may offer the kinds of improvements in computation and control that are needed to maintain acceptable functionality. For control their associative characteristics could provide signal conversion or data translation. Because they can do any computation such as least squares, they can close feedback loops autonomously to provide intelligent control at the point of action rather than at a central location that requires transfers, conversions, hand-shaking and other costly repetitions like input protection. Both computation and control can be integrated on a single chip, printed circuit or an optical equivalent that is also inherently faster through full parallel operation. For such reasons one expects lower costs and better results. Such systems could be optimized by integrating sensor and signal processing functions. Distributed nets of such hardware could communicate and provide global monitoring and multiprocessing in various ways e.g., via token, slotted or parallel rings (or Steiner trees) for compatibility with existing systems. Problems and advantages of this approach such as an optimal, real-time Turing machine are discussed. Simple examples are simulated and hardware implemented using discrete elements. DOE

63 CYBERNETICS

Includes feedback and control theory, artificial intelligence, robotics and expert systems.

For related information see also *54 Man/System Technology and Life Support.*

N90-18912# Massachusetts Univ., Amherst. Automation and Robotics Lab.
RALPH: AN AUTOMATIC ROBOT ASSEMBLY LANGUAGE PROGRAMMER: AN OVERVIEW
Bartholomew O. Nnaji May 1989 26 p Presented at the World Conference on Robotics, Gaithersburg, MD, 7-11 May 1989 Sponsored in part by Digital Equipment Corp.
(Grant NSF DMC-86-10417)
(PB90-120973; NSF/ENG-89051) Avail: NTIS HC A03/MF A01 CSCL 09B

Since machine programming requires the understanding of the robot world, there is a need for development of principles which will allow it to happen. An overview of the RALPH project is provided which shows the underlying principles behind such a machine reasoning system and how the principles can be applied to other geometry based tasks. GRA

N90-18913# Instituto de Pesquisas Espaciais, Sao Jose dos Campos (Brazil).
AN INTERACTIVE SYSTEM APPLIED TO THE LINEAR QUADRATIC PROBLEM M.S. Thesis [UM SISTEMA INTERATIVO APLICADO AO PROBLEMA LINEAR QUADRATICO]
Ricardo Acerbi Sep. 1989 209 p In PORTUGUESE; ENGLISH summary
(INPE-4945-TDL/386) Avail: NTIS HC A10/MF A02

A tool for aiding optimal control design, based on the Linear Quadratic approach for multivariables and time invariant systems, is presented. An architecture for a interactive system, based on knowledge extracted from simulations, is proposed. This knowledge aid in orienting the designer in ponderation matrix choice, from design specifications. Simulation results that have aided observation of parameters behavior from ponderation matrix elements are described. Implementation details and test results are realized. Author

N90-18914# Massachusetts Inst. of Tech., Cambridge. Artificial Intelligence Lab.
THE COMPUTATION OF COLOR Ph.D. Thesis
Anya C. Hurlbert Sep. 1989 210 p Sponsored in part by a Whitaker Health Sciences Fund MD/Ph.D. Fellowship
(Contracts DACA76-85-C-0010; N00014-85-K-0124)
(AD-A216531; AI-TR-1154) Avail: NTIS HC A10/MF A02 CSCL 20/6

Color vision has traditionally been the domain of many sciences: physics, physiology, psychology, and philosophy. This thesis maintains that interdisciplinary tradition and looks at color vision from several points of view. It focusses on the phenomenon of color constancy and uses its formulation as a computational problem to link the different viewpoints. The primary contributions of the thesis are: (1) the demonstration of a formal framework for lightness algorithms, which represent one class of solution to the problem of color constancy; (2) the derivation of a new lightness

algorithm based on regularization theory; (3) the synthesis of an adaptive lightness algorithm using learning techniques; (4) the development of a segmentation algorithm that uses color information to mark material boundaries, with guidance from luminance edges; and (5) an experimental investigation into the cues that human observers use to judge the color of the illuminant, demonstrating that under certain conditions, observers ignore correct information from specular reflections in favor of incorrect information from other cues. Other computational approaches to the problem of color constancy are reviewed and some of their links to psychophysics and physiology are explored. GRA

N90-18915# Massachusetts Inst. of Tech., Cambridge. Artificial Intelligence Lab.
GROUPING FOR RECOGNITION
David W. Jacobs Nov. 1989 47 p
(Contracts N00014-86-K-0685; DACA76-85-C-0010; N00014-85-K-0124)
(AD-A216716; AI-M-1177) Avail: NTIS HC A03/MF A01
CSCL 05/8

A new method of grouping edges in order to recognize objects is presented. This grouping method succeeds on images of both 2-D and 3-D objects. So that the recognition system can consider first the collections of edges most likely to lead to the correct recognition of objects, groups are ordered of edges based on the likelihood that a single object produced them. The grouping module estimates this likelihood using the distance that separates edges and their relative orientation. This ordering greatly reduces the amount of computation required to locate objects. Surprisingly, in some circumstances grouping can also improve the accuracy of a recognition system that handles libraries of 2-D, polygonal objects. Second, we show comparable performance of the grouping system on images of 2-D and 3-D objects. This provides evidence that the grouping system could produce significant improvements in the performance of a 3-D recognition system. GRA

N90-18916# Massachusetts Inst. of Tech., Cambridge. Artificial Intelligence Lab.
USING SPECIAL-PURPOSE COMPUTING TO EXAMINE CHAOTIC BEHAVIOR IN NONLINEAR MAPPINGS Thesis
Jason Nieh Sep. 1989 77 p Revised
(Contract N00014-86-K-0180)
(AD-A216800; AI-TR-1139) Avail: NTIS HC A05/MF A01
CSCL 12/6

Most physical phenomena are nonlinear in nature and exhibit the complicated and seemingly random behavior known as chaos. Studying chaotic behavior in nonlinear systems requires numerous computations in order to simulate the behavior of such systems. The Standard Map Machine (SMM) was designed and implemented as a special computer for performing these intensive computations with high speed and high precision. SMM's impressive performance is due to its simple architecture specialized to the numerical computations required to nonlinear systems. The design and implementation of the Standard Map Machine is discussed along with its use in the study of nonlinear mappings, in particular, the study of the standard map. GRA

N90-18917# Massachusetts Inst. of Tech., Cambridge. Dept. of Electrical Engineering and Computer Science.
DERIVATION OF AN EFFICIENT RULE SYSTEM PATTERN MATCHER M.S. Thesis
Jeremy M. Wertheimer Feb. 1989 85 p Sponsored in part by IBM; NYNEX Corp.; and Siemens Corp.
(Contracts N00014-85-K-0487; F49620-88-C-0033; NSF IRI-86-16644)
(AD-A216801; AI-TR-1109) Avail: NTIS HC A05/MF A01
CSCL 12/9

A derivation is presented of an efficient rule system pattern matcher. The matcher efficiently computes all matches between a set of rules and a database. The rules may have multiple patterns. The matcher incrementally updates the set of matches as changes are made to the database. This matcher is modeled on the Rete matcher used in the OPS5 production system. Representation used in the matcher are modeled on the structures used in the model-theoretic semantics of first-order logic. The correspondence is demonstrated between these structures and the data structures used in the Rete matcher. A new structure, the lattice of disjunctive substitutions, is introduced to capture the semantics of the rule system matching computation. An element of this lattice represents the set of all matches between a rule and the terms in a database. The derivation is implemented using program transformations. The derivation has been implemented using a wide spectrum language and an interactive program transformation system. This work is presented as a contribution towards the construction of a library of programming knowledge to facilitate software reuse and automatic programming. GRA

N90-18918# Massachusetts Inst. of Tech., Cambridge. Dept. of Electrical Engineering and Computer Science.
A COLONY ARCHITECTURE FOR AN ARTIFICIAL CREATURE Ph.D. Thesis
Jonathan Connell Aug. 1989 134 p Sponsored in part by Systems Development Foundation and General Motors Corp.
(Contracts N00014-86-K-0685; N00014-85-K-0124)
(AD-A216802; AI-TR-1151) Avail: NTIS HC A07/MF A01
CSCL 12/9

In this report we describe a distributed control system for a mobile robot which operates in an unmodified office environment occupied by moving people. The robot's controller is composed of over 40 separate processes which run on a loosely connected network of 24 processors. Together this ensemble helps the robot locate empty soda cans, collect them with its arm, and bring them back home. A multi-agent system such as this has many advantages over classic monolithic controllers. For instance, it can be developed in stages, each new layer building on the last. It can also be split among several processors or agents, so as new capabilities are required new hardware can be easily added. Furthermore, its performance degrades gracefully - if a single agent fails the robot continues to function, albeit at a lower level of competence. However, in order to achieve these goals the system must be decomposed following certain guidelines. First, the internal workings of each agent should be isolated from all other agents. This improves the modularity of the system and helps prevent implementation dependencies. Second, all decisions should be based on spatially and temporally local information. This keeps the robot from relying on incorrect models of its dynamically changing world and allows it to operate with incomplete sensory input. GRA

N90-18919# Massachusetts Inst. of Tech., Cambridge. Dept. of Electrical Engineering and Computer Science.
THREE-DIMENSIONAL MOTION ESTIMATION USING SHADING INFORMATION IN MULTIPLE FRAMES Ph.D. Thesis
Jean-Pierre Schott Aug. 1989 187 p
(Contract N00014-85-K-0124)
(AD-A216804; AI-TR-1162) Avail: NTIS HC A09/MF A01
CSCL 12/9

Traditionally motion and shading have been treated as two disjoint problems. On the one hand, researchers studying motion or structure from motion often assume uniform lighting conditions over the whole surface and good contrast at high spatial frequencies to minimize the effects of variations of the image irradiance of the patch as the surface moves. On the other hand, researchers primarily concerned with the shape from shading problem only consider static brightness data in order to recover the shape without considering the change of brightness induced by motion. A new formulation for recovering the structure and motion parameters of a moving patch is presented. It is based on using the spatiotemporal derivatives of irradiance that are computed from a time varying irradiance sequence and combined into a differential constraint equation. The new approach determines the rigid body motion and the structure of the patch directly from the irradiance sequence using both motion and shading information. A new constraint equation, the full irradiance constraint equation (FICE), is derived. It links the spatiotemporal gradients of irradiance to the motion and structure parameters and the temporal variations

of the surface shading. This equation separates the contribution to the irradiance spatiotemporal gradients of the gradients due to texture from those due to shading and allows the FICE to be used for textured and textureless surface. GRA

N90-18920# University of Southern California, Los Angeles. Dept. of Electrical Engineering Systems.
PRACTICAL METHODS FOR ROBUST MULTIVARIABLE CONTROL Final Report, 1 Aug. 1988 - 31 Jul. 1989
Michael G. Safonov and Edmond A. Jonckheere 12 Oct. 1989 25 p
(Grant AF-AFOSR-0282-88; AF Proj. 2304)
(AD-A216937; AFOSR-89-1700TR) Avail: NTIS HC A02/MF A01 CSCL 01/2

The design of supermaneuverable fighter aircraft, high precision space-born optical tracking systems and transatmospheric hypervelocity vehicles will pose significant challenges to modern control system design theory. The theme of the research has been making modern control theory work. The product of the research was theory, algorithms and software applicable to multivariable feedback control problems in which there are design constraints requiring robust attainment of stability and control performance objectives in the face of both structured and unstructured uncertainty. GRA

N90-18921# Oak Ridge National Lab., TN.
ARCHITECTURE FOR A HUMAN-ROBOT SYMBIOTIC SYSTEM
Fred W. DePiero, Wayne W. Manges, Reid L. Kress, Mike R. Kedl, and William R. Hamel 1990 6 p Presented at the 22nd IEEE Southeastern Symposium on System Theory, Cookeville, TN, 11-13 Mar. 1990
(Contract DE-AC05-84OR-21400)
(DE90-005670; CONF-900378-2) Avail: NTIS HC A02/MF A01

This paper describes a human-robot symbiont that is under development at Oak Ridge National Laboratory. An overview of the symbiotic system is described that motivates the architecture that has been developed. The architecture is a hierarchical structure that consists of several expert systems which reside above a robot control interface. This interface allows the manipulator to be operated in both a teleoperated and autonomous mode. All these processes coexist with the lowest level of the hierarchy, which is a numerically intensive control algorithm. The architecture is implemented on five processors in a coarsely parallel system. DOE

N90-18922# Universiteit Twente, Enschede (Netherlands). Dept. of Applied Mathematics.
SYSTEM THEORY AND MECHANICS
Arjan vanderSchaft Aug. 1989 29 p Submitted for publication
(MEMO-807; ISSN-0169-2690; ETN-90-96310) Avail: NTIS HC A03/MF A01

A system theoretic approach to mechanics, regarding Hamiltonian systems as conservative mechanical m-ports is discussed. Recent results in the Hamiltonian realization problem are surveyed, and generalizations are shown to be indicated. The potential use for control purposes of the Hamiltonian structure of nonlinear control systems is exemplified. Much work in the system theoretic approach to modeling of physical system and in the control of systems with physical structure remains to be done. ESA

N90-18923# Universiteit Twente, Enschede (Netherlands). Dept. of Computer Science.
FEASIBILITY OF MEALY DESIGN FOR PROCESSOR CONTROLPATHS
A. J. W. M. tenBerg Oct. 1989 35 p
(MEMO-INF-89-53; ISSN-0923-1714; ETN-90-96315) Avail: NTIS HC A03/MF A01

In a comparison of implementations of Mealy and Moore designed processor control paths, the design of an internal control function for instruction set processors is addressed and a model of this control function is developed, which incorporates parameters from the processor's architecture and its datapath. The Moore Mealy comparison is performed independently for some simple hardware configurations. These hardware configurations are selected on their ability to implement both the Moore and Mealy designed finite state machines. The Moore and the Mealy designs are compared for size and delay. A variant of the initial control model is discussed, which is based on relaxation of the timing constraint of the control function. The results show that the Mealy design is not necessarily the optimal design. The comparison provides insight on the architecture parameter ranges for which a Mealy design is preferable above the Moore design for the implementation of the internal control function. ESA

64 NUMERICAL ANALYSIS

Includes iteration, difference equations, and numerical approximation.

N90-18924*# Cornell Univ., Ithaca, NY. Dept. of Computer Science.
LOG-BASED RECOVERY IN ASYNCHRONOUS DISTRIBUTED SYSTEMS Ph.D. Thesis
Kenneth Paul Kane Dec. 1989 145 p Sponsored in part by Siemens Corp.
(Contract NAG2-593; N00140-87-C-8904)
(NASA-CR-186190; NAS 1.26:186190; TR-89-1067) Copyright Avail: NTIS HC A07/MF A01 CSCL 12A

A log-based mechanism is described for restoring consistent states to replicated data objects after failures. Preserving a causal form of consistency based on the notion of virtual time is focused upon in this report. Causal consistency has been shown to apply to a variety of applications, including distributed simulation, task decomposition, and mail delivery systems. Several mechanisms have been proposed for implementing causally consistent recovery, most notably those of Strom and Yemini, and Johnson and Zwaenepoel. The mechanism proposed here differs from these in two major respects. First, a roll-forward style of recovery is implemented. A functioning process is never required to roll-back its state in order to achieve consistency with a recovering process. Second, the mechanism does not require any explicit information about the causal dependencies between updates. Instead, all necessary dependency information is inferred from the orders in which updates are logged by the object servers. This basic recovery technique appears to be applicable to forms of consistency other than causal consistency. In particular, it is shown how the recovery technique can be modified to support an atomic form of consistency (grouping consistency). By combining grouping consistency with casual consistency, it may even be possible to implement serializable consistency within this mechanism. Author

N90-18925# Massachusetts Inst. of Tech., Cambridge. Dept. of Mechanical Engineering.
AN OBJECTIVE TIME-INTEGRATION PROCEDURE FOR ISOTROPIC RATE-INDEPENDENT AND RATE-DEPENDENT ELASTIC-PLASTIC CONSTITUTIVE EQUATIONS
G. G. Weber, A. M. Lush (Cincinnati Univ., OH.), A. Zavaliangos, and L. Anand Jun. 1989 73 p Submitted for publication
(Contract N00014-86-8-0308; NSF MEA-83-15117)
(PB90-121245; NSF/ENG-89048) Avail: NTIS HC A04/MF A01 CSCL 12A

In a large class of rate-independent and rate-dependent elastic-plastic constitutive equations the elasticity is modeled in hypo-elastic form, with the stress rate being taken as the Jaumann derivative, so as to make the constitutive model properly frame-indifferent or objective. A fully-implicit, stable time-integration procedure for implementing such constitutive models in displacement-based finite element procedures is presented. The numerical procedure preserves the very desirable feature of incremental objectivity. The overall procedure is a generalization of the well-known radial-return algorithm of classical rate-independent plasticity and is, therefore, well suited for implementation in large-scale finite element codes. As an example, the time-integration procedure was implemented in the finite

element code ABAQUS. To check the incremental objectivity, accuracy, and stability of the algorithm, some representative problems are solved. GRA

N90-18926# Instituto de Pesquisas Espaciais, Sao Jose dos Campos (Brazil).
MATHEMATICAL METHODS OF PHYSICS 6: INTEGRAL TRANSFORMATION [METODOS MATEMATICOS DA FISICA 6: TRANSFORMADAS INTEGRAIS]
Rene Adalid Medrano-B Apr. 1989 104 p In PORTUGUESE; ENGLISH summary
(Contract FINEP-537/CT)
(INPE-4807-MD/40) Avail: NTIS HC A06/MF A01

Integral transforms that have as a common root the Fourier transform are studied. Among these the Fourier, Fourier-Sine, Fourier-Cosine, and Laplace transforms are globally studied. Using the results that happen to emerge, the delta function and its n-dimensional representation in curvilinear coordinates are also studied. The subject is organized such that individual definitions of the transforms are obtained starting from the Fourier Transform. Next, by defining a generic integral transform, their specific properties are established. The convolution theorem is handled in a similar way. Finite Fourier transforms and an Appendix that gives some special methods of integration are studied briefly. Enlightening examples in the various sections of this monograph are worked out. The present work is based on notes of the Mathematical Methods of Physics course in the graduate program of INPE. Author

N90-18927*# National Aeronautics and Space Administration. Lewis Research Center, Cleveland, OH. Inst. for Computational Mechanics in Propulsion.
ASYMPTOTIC BOUNDARY CONDITIONS FOR DISSIPATIVE WAVES: GENERAL THEORY
Thomas Hagstrom (State Univ. of New York, Stony Brook.) Jan. 1990 21 p
(Grant NASA Order C-99066-G; NSF DMS-89-05314)
(NASA-TM-102497; ICOMP-90-02; E-5291; NAS 1.15:102497)
Avail: NTIS HC A03/MF A01 CSCL 12A

An outstanding issue in the computational analysis of time dependent problems is the imposition of appropriate radiation boundary conditions at artificial boundaries. Accurate conditions are developed which are based on the asymptotic analysis of wave propagation over long ranges. Employing the method of steepest descents, dominant wave groups are identified and simple approximations to the dispersion relation are considered in order to derive local boundary operators. The existence of a small number of dominant wave groups may be expected for systems with dissipation. Estimates of the error as a function of domain size are derived under general hypotheses, leading to convergence results. Some practical aspects of the numerical construction of the asymptotic boundary operators are also discussed. Author

N90-18928# Maryland Univ., College Park. Inst. for Physical Science and Technology.
EFFICIENT PRECONDITIONING FOR THE p-VERSION FINITE ELEMENT METHOD IN TWO DIMENSIONS Final Report
I. Babuska, A. Craig, J. Mandel, and J. Pitkaranta (Helsinki Univ. of Technology, Finland) Oct. 1989 44 p Prepared in cooperation with Colorado Univ., Denver
(Contract N00014-85-K-169; NSF DMS-87-04169)
(AD-A216210; TR-BN-1105; TR-TE-4189) Avail: NTIS HC A03/MF A01 CSCL 12/1

Parallel preconditioners are formulated and analyzed for systems of equations arising from the p-version finite element method. Using new theoretical results for polynomial spaces, it was proven that condition number grows as log squared p, where p is the degree of the polynomial space. Numerical results are presented showing that the condition number indeed grows very slowly with p. GRA

N90-18929# Massachusetts Inst. of Tech., Cambridge. Dept. of Electrical Engineering and Computer Science.
SHOULD A FUNCTION CONTINUE M.S. Thesis
Jon Gary Riecke Sep. 1989 38 p
(Contract N00014-83-K-0125; NSF DCR-85-11190)
(AD-A216406; MIT/LCS/TR-459) Avail: NTIS HC A03/MF A01 CSCL 12/1

It is shown that two lambda-calculus terms can be observationally congruent (i.e., agree in all contexts) but their continuation-passing transforms may not be. It is also shown that two terms may be congruent in all untyped contexts but fail to be congruent in a language with call/cc operators, and that two terms may have the same meaning in a direct semantics but not in a continuation semantics. Hence, familiar reasoning about terms may be unsound in a setting with continuations, demonstrating the need for a theory of continuations. Corrections are made to the original thesis. GRA

N90-18930# Stanford Univ., CA. Dept. of Statistics.
APPROXIMATIONS TO JOINT DISTRIBUTIONS OF DEFINITE QUADRATIC FORMS
D. R. Jensen and Herbert Solomon 21 Nov. 1989 20 p
(Contract N00014-89-J-1627)
(AD-A216434; TR-424) Avail: NTIS HC A02/MF A01 CSCL 12/3

Multidimensional Wilson-Hilferty transformations support Gaussian approximations to certain joint distributions of quadratic forms in Gaussian variables. Central and noncentral distributions are studied and applications are noted. Parameters of the approximating distributions are given up to terms of order omicron(v to the - 3rd power) in the degrees of freedom (nu). Numerical studies validate using these approximations over a range of parameters for an essential subclass of the distributions. GRA

N90-18931# Clarkson Univ., Potsdam, NY. Div. of Research.
DIRECT AND INVERSE SCATTERING PROBLEM ASSOCIATED WITH THE ELLIPTIC SINH-GORDON EQUATION Final Report, 30 Sep. 1986 - 30 Sep. 1989
M. Jaworski (Polish Academy of Sciences, Warsaw.) and D. J. Kaup 14 Nov. 1989 121 p
(Grant AF-AFOSR-0277-86; AF Proj. 2304)
(AD-A216455; AFOSR-89-1720TR) Avail: NTIS HC A06/MF A01 CSCL 12/1

The following is a report on the work achieved during the above period: Linear Stability of Vlasov-Poisson Electron Plasma in Crossed-Fields; Perturbations Propagating Parallel to the Magnetic Field; Two-Dimensional Nonlinear Schrodinger Equation and Self-Focusing in a Two-Fluid Model of Newtonian Cosmological Perturbations; The Third-Order Expansion of the Planar Cold-Fluid Magnetron Equations; and The Time Evolution of the Scattering Data for the Forced Toda Lattice. In addition to the above, there are also the following preprints in various stages of being accepted for publication: Quantization of BiHamiltonian Systems; The Elliptic Sinh-Gordon Equation; Coherent Structures in the Planar Magnetron; A Thermal Instability in the Planar Magnetron; Lattice Equations and Integrable Mappings; and A Model Initial Value Problem in Stimulated Raman Scattering. GRA

N90-18932# Connecticut Univ., Storrs. Dept. of Mathematics.
INVERSE SCATTERING AND TOMOGRAPHY Final Report, 1 Jun. 1986 - 31 May 1989
W. R. Madych 31 May 1989 144 p
(Grant AF-AFOSR-0145-86; AF Proj. 2304)
(AD-A216456; AFOSR-89-1719TR) Avail: NTIS HC A07/MF A01 CSCL 12/2

Topics included are: A Range Theorem for the Radon Transform, Multivariate Interpolation and Conditionally Positive Definite Function, Polyharmonic Cardinal Splines, Solutions of underdetermined systems of linear equations, Multivariate interpolation and conditionally positive definite functions 2. GRA

N90-18933# West Virginia Univ., Morgantown.
LONG PATH CONNECTIVITY OF REGULAR GRAPHS Final Technical Report, Nov. 1988 - Oct. 1989
Cun-Quan Zhang and Yong-Jin Zhu (Academia Sinica, Beijing, China) 15 Oct. 1989 19 p
(Grant AF-AFOSR-0068-89; AF Proj. 2304)
(AD-A216477; AFOSR-89-1862TR) Avail: NTIS HC A02/MF A01 CSCL 12/2

Any pair of vertices in a 4-connected, non-bipartite, k-regular graph are joined by a Hamilton path or a path of length at least 3k-6. GRA

N90-18934# Pittsburgh Univ., PA. Inst. for Computational Mathematics and Applications.
DIFFERENTIAL-GEOMETRIC TECHNIQUES FOR SOLVING DIFFERENTIAL ALGEBRAIC EQUATIONS
Florian A. Potra (Iowa Univ., Iowa City.) and Werner C. Rheinboldt Nov. 1989 39 p
(Contract N00014-90-J-1025; NSF CCR-89-07654)
(AD-A216503; ICMA-89-143) Avail: NTIS HC A03/MF A01 CSCL 12/1

Differential-algebraic systems of equations (DAEs) arise in many areas of science and engineering. In particular, the equations of motion for a constrained mechanical systems considered in this volume are usually modelled as a second order DAE. In recent years the literature on the numerical solution of such systems has grown rapidly. However, up to now, existence theories for nonlinear DAEs are available only for a few selected classes of systems. The differential-geometric approach is based on the observation that, as long as we expect the solution of a DAE to be some smooth path in the space of dependent variables, the system must define a dynamical system in suitable subsets of that space. GRA

N90-18935# Pittsburgh Univ., PA. Inst. for Computational Mathematics and Applications.
NEW ASPECTS IN BIFURCATION WITH SYMMETRY
Patrick J. Rabier Oct. 1989 40 p
(Contract N00014-80-C-9455)
(AD-A216506; ICMA-89-142) Avail: NTIS HC A03/MF A01 CSCL 12/1

It comes as no surprise that the literature devoted to bifurcation problems involving symmetry draws from both analysis and group theory. However, it is more accurate to say that it draws from both analysis and group representation theory, the two being related through the notion of isotropy subgroup. Isotropy subgroups have been crucial to every work having some connection with bifurcation and symmetry. It is shown that there are connections between bifurcation problems and group theory that do not refer to isotropy subgroups and are virtually representation-independent. In particular, it is shown that Lie groups, including finite ones, possess subgroups of a special type, here called intrinsic isotropy subgroups, characterized by a representation-independent property, which play a role in bifurcation problems. GRA

N90-18936# Idaho Univ., Moscow. Dept. of Psychology.
THE FORMATION AND USE OF KNOWLEDGE STRUCTURES IN PROBLEM SOLVING DOMAINS Final Technical Report, 1 Jan. 1988 - 30 Sep. 1989
Sallie E. Gordon and Richard T. Gill 4 Oct. 1989 65 p
(Grant AF-AFOSR-0063-88; AF Proj. 2313)
(AD-A216512; AFOSR-89-1735TR) Avail: NTIS HC A04/MF A01 CSCL 05/8

The goal of this research was to develop and test a method for eliciting knowledge structures used in problem solving. The work was carried out simultaneously in two domains, engineering mechanics and video recording. Two studies resulted in the adaptation of a question probe method for eliciting relevant knowledge structures prior to problem solving. Two additional studies showed that administration of the question probes did not significantly impact subsequent problem solving. Answers from the question probes were therefore translated into a conceptual structure for each subject. A simple associative search model operating upon these structures was able to predict 87 and 93 percent of individual problem solving activities in the engineering and video recording domains, respectively. The predictive capability of the graphs indicate the central role of knowledge structures capability of the graphs indicate the central role of knowledge structures in problem solving processes, at least under circumstances such as those tested. A fifth study evaluated the validity of the conceptual graphs by comparing them with free recall protocols. GRA

N90-18937# Maryland Univ., College Park. Inst. for Physical Science and Technology.
RESEARCH EQUIPMENT Final Report, 1 Sep. 1983 - 31 Jan. 1985
R. Bruce Kellogg 25 Mar. 1989 8 p LIMITED REPRODUCIBILITY: Availability: Document partially illegible
(Grant AF-AFOSR-0286-83; AF Proj. 2304)
(AD-A216515; AFOSR-89-1729TR) Avail: NTIS HC A02/MF A01 CSCL 12/5

The purpose of the report was to provide additional equipment for a computational laboratory dedicated to research in numerical analysis and applied mathematics. The report summarizes the equipment acquired and the research being presently carried out in the laboratory. The research is on topics in boundary integral equations, adaptive finite elements, numerical methods for a scattering problems, continuation methods, and very accurate arithmetic calculations. GRA

N90-18938# West Virginia Univ., Morgantown. Dept. of Mathematics.
FINDING CRITICAL INDEPENDENT SETS AND CRITICAL VERTEX SUBSETS ARE POLYNOMIAL PROBLEMS Final Technical Report, Nov. 1988 - Oct. 1989
Cun-Quan Zhang 15 Oct. 1989 16 p
(Grant AF-AFOSR-0068-89; AF Proj. 2304)
(AD-A216547; AFOSR-89-1864TR) Avail: NTIS HC A03/MF A01 CSCL 12/1

It has been proved by mathematicians that finding a maximum independent set in some certain kinds of graphs is solvable in polynomial time, for example, line graphs, bipartite graphs, circle graphs, circular arc graphs and claw free graphs. But it is well-known that it is an NP-complete problem for general graphs. In this paper, we will investigate another problem -- finding a certain kind of independent set in general graphs. It will be proved in this paper that finding a critical independent set of a graph is solvable in polynomial time. GRA

N90-18939# San Diego State Univ., CA. Center for Research in Mathematics and Science Education.
SCHEMA-BASED THEORIES OF PROBLEM SOLVING Annual Report, 1 Nov. 1988 - 31 Oct. 1989
Stephen K. Reed 1 Nov. 1989 29 p
(Grant AF-AFOSR-0107-89; AF Proj. 2313)
(AD-A216717; AFOSR-89-1673TR) Avail: NTIS HC A03/MF A01 CSCL 05/9

The objective of this research is to construct a schema-based model of problem solving to represent construction of equations for solving algebra word problems. The research summarized is concerned with the selection, use, and description of instructional examples. Experiment 1 shows that mathematical experience was beneficial for improving the selection of good analogies when the analogies are isomorphic to the test problems, but was not beneficial when the analogies are more inclusive than the test problems. In Experiment 2 students were able to effectively combine information from two analogous problems but did significantly worse when combining information from one example and a set of procedures. The last three experiments required that students categorize motion problems according to whether the two distances in a problem should be equated, added, or subtracted. Categorization significantly improved as the number of training examples representing a category increased from one to four (Experiment 3). Categorization was also significantly better when students received both specific and general descriptions of

the examples than when they received only a single description (Experiment 4). However, as shown in Experiment 5, students were unable to form their own general descriptions by comparing similar examples. GRA

N90-18940# Massachusetts Inst. of Tech., Cambridge. Microsystems Technology Labs.
BOOLEAN MINIMIZATION AND ALGEBRAIC FACTORIZATION PROCEDURES FOR FULLY TESTABLE SEQUENTIAL MACHINES Memorandum Report
Srinivas Devadas and Kurt Keutzer (Bell Telephone Labs., Inc., Murray Hill, NJ.) Sep. 1989 6 p Presented at the International Conference of Computer Aided Design, Nov. 1989
(Contract N00014-87-K-0825)
(AD-A216779; VLSI-M-89-557) Avail: NTIS HC A02/MF A01 CSCL 12/7

In this paper we continue to investigate the impact of logic synthesis on the testability of sequential circuits that can be modeled as finite state machines. Complete testability of a sequential circuit is ensured by guaranteeing that each invalid state has an unperturbable distinguishing sequence. To accomplish this we present a novel Boolean minimization procedure of prime implicant generation and constrained covering based on the Quine-McCluskey algorithm that ensures that no single fault can both produce an invalid state and corrupt the distinguishing sequence by which that invalid state can be identified. On completion, it guarantees a prime and irredundant, fully testable Moore or Mealy finite state machine. Given a two-level circuit with these properties we then use constrained algebraic factorization techniques that retain the invariant that no single fault can both produce an invalid state and corrupt the distinguishing sequence by which that invalid state is detected. Besides offering a more detailed understanding of the sources of untestability in sequential circuits than previous approaches, this approach offers significant practical advantages as well. GRA

N90-18941# Massachusetts Inst. of Tech., Cambridge. Artificial Intelligence Lab.
COMPUTATIONAL STRUCTURE OF GPSG (GENERALIZED PHRASE STRUCTURE GRAMMAR) MODELS: REVISED GENERALIZED PHRASE STRUCTURE GRAMMAR M.S. Thesis, 1986
Eric Sven Ristad Sep. 1989 97 p Revised Sponsored in part by Kapor Family Foundation
(Contracts N00014-80-C-0505; N00014-85-K-0124; NSF DCR-85-552543)
(AD-A216803; AI-TR-1170) Avail: NTIS HC A05/MF A01 CSCL 05/7

A central goal of mathematical linguistics is to precisely determine the power of a linguistic theory. Traditionally, formal language theory (the Chomsky hierarchy) and its generative power analyses have translated this question into the narrower question of how unrestricted the rule format of a theory is. Modern computational complexity theory offers another, more useful, translation: how much of what computational resources does a theory consume. Complexity theory also offers a new perspective on descriptive adequacy. In a descriptively adequate linguistic theory, the structural descriptions and computational power of the theory match those of an ideal speaker-hearer. The primary goal is to demonstrate how considerations from computational complexity theory can inform grammatical theorizing. To this end, generalized phrase structure grammar (GPSG) linguistic theory is revised so that its computational power more closely matches the limited computational ability of an ideal speaker-hearer. A second goal is to provide a theoretical framework within which to better understand the wide range of GPSG models that have appeared in the theoretical and computational linguistics literature, embodied in formal definitions as well as in implemented computer programs. GRA

N90-18942# Illinois Univ., Chicago. Dept. of Mathematics, Statistics, and Computer Science.
OPTIMUM SELECTION PROCEDURES IN MULTI-STAGE SCREENING, RELIABILITY, AND TIME Final Technical Status Report, 30 Sep. 1985 - 30 Sep. 1989
Klaus J. Miescke 31 Oct. 1989 11 p
(Grant AF-AFOSR-0347-85; AF Proj. 2304)
(AD-A216811; AFOSR-89-1686TR) Avail: NTIS HC A02/MF A01 CSCL 12/3

Progress is reported in the areas of optimum selection procedures in multistage screening, reliability, and time series analysis problems. Some specific areas of study are: Two-stage Selection Procedures with Screening at the First Stage; Weibull Populations; Normal Populations; Binomial Populations; One-stage Selection Procedures for Nonsymmetric Models; Reliability and Replacement Models; and Trend Analysis in Time Series. GRA

N90-18943# Illinois Univ., Urbana. Dept. of Computer Science.
WAVEFORM METHODS FOR ORDINARY DIFFERENTIAL EQUATIONS Ph.D. Thesis
Fen-Lien Juang Jan. 1990 138 p
(Contract DE-FG02-87ER-25026)
(DE90-006593; DOE/ER-25026/34; UIUCDCS-R-90-1563; UILU-ENG-90-1701) Avail: NTIS HC A07/MF A01

The traditional approach for solving large dynamical systems is time consuming. Waveform method, an iterative technique for solving systems of differential equations, can be used to reduce the processing time. Waveform method was shown to converge superlinearly on finite intervals. A measure of speed of convergence is defined and is used to compare the value of different waveform methods. This measure is the rate of increase of order of accuracy. The speed of the waveform Gauss-Seidel method depends on the numbering of the equations. The numbering of the equations corresponds to a numbering of the directed graph specifying the coupling relations among all equations. It is shown how to compute the rate of order increase from the structure of the numbered graph and hence the optimum numbering, that is, the one which maximizes the speed of convergence. Finally, in a variety of numerical experiments, conducted on a Sun 3/60, it is shown that the different speeds of convergence correspond to different numberings and the effectiveness of the waveform Gauss-Seidel method for large sparse systems. DOE

N90-18944# Technische Univ., Delft (Netherlands).
ANALYSIS OF LINEAR MULTIGRID METHODS FOR ELLIPTIC DIFFERENTIAL EQUATIONS WITH DISCONTINUOUS AND ANISOTROPIC COEFFICIENTS Ph.D. Thesis
Mohammed Khalil 1989 158 p Sponsored in cooperation with Toulouse Univ., France and CROUS, Toulouse, France
(ETN-90-96269) Avail: NTIS HC A08/MF A01

Linear multigrid methods are analyzed and tested for application to the solution of elliptic partial differential equations with discontinous and anisotropic coefficients, discreted with a finite volume method. The vertex-generated and cell-generated multigrid methods are compared by solving a number of two dimensional test problems. A robust and simple smoothing method is found in two dimensions, but for three dimensions only a complex, costly method is found. Satisfactory practical results are obtained with a not completely robust but simple smoothing method, accelerating the multigrid method with a Lanczos-type method. ESA

N90-18945# Oak Ridge Gaseous Diffusion Plant, TN. Data Systems Research and Development Program.
CAN THE SQUARE LAW BE VALIDATED
D. S. Hartley, III Mar. 1989 72 p
(Contract DE-AC05-84OT-21400)
(DE90-007112; K/DSRD-57) Avail: NTIS HC A04/MF A01

This paper addresses the question of validating the homogeneous Lanchestrian square law of attrition by the use of historical data. The available data and some analysis techniques are examined. The result is that the homogeneous Lanchester square law cannot be regarded as a proven attrition algorithm for

warfare; however, the square law cannot be regarded as disproved either. To validate the square law or any other proposed attrition law, data on more battles are required. DOE

N90-18948# Universiteit Twente, Enschede (Netherlands). Dept. of Applied Mathematics.
ON THE DEPTH OF COMBINATORIAL OPTIMIZATION PROBLEMS
W. Kern Aug. 1989 24 p
(MEMO-803; ISSN-0169-2690; ETN-90-96307) Avail: NTIS HC A03/MF A01

A discrete optimization problem, to minimize c(x), where x is a member of X, is considered. Using a hill climbing algorithm the depth of the problem is defined to be the maximum depth of a solution x0 a member of X. This plays an important role in the theory of simulated annealing. The notion of depth is shown to have some interest in its own right. Some upper bounds are proved and the computational complexity of computing the depth function for some selected examples is investigated. ESA

N90-18947# Universiteit Twente, Enschede (Netherlands). Dept. of Applied Mathematics.
APPLICATION OF CHEBYSHEV APPROXIMATION TO CURVE FITTING
W. Wetterling Aug. 1989 10 p
(MEMO-805; ISSN-0169-2690; ETN-90-96309) Avail: NTIS HC A02/MF A01

The problem of curve fitting to a finite set of points in n-dimensional space is considered, using the principle of Chebyshev approximation instead of least squares. An application in railway engineering is described where this type of approximation is essential. For the general problem, optimality conditions are established and a connection to alternation theory is exhibited. ESA

N90-18948# Universiteit Twente, Enschede (Netherlands). Dept. of Applied Mathematics.
NONLINEAR MODEL MATCHING: A LOCAL SOLUTION AND TWO WORKED EXAMPLES
H. J. C. Huijberts Sep. 1989 18 p
(MEMO-809; ISSN-0169-2690; ETN-90-96311) Avail: NTIS HC A03/MF A01

The model matching problem consisting of the designing of a compensator for a given system, called the plant, in such a way that the resulting input-ouput behavior matches that of a prespecified model is addressed. It was shown that in the case that the model is decouplable by static state feedback and generic conditions on the plant are satisfied, the model matching problem is solvable around an equilibrium point if and only if it is solvable for the linearization of plant and model around the equilibrium point. This local solution is presented and the question to what extent the feedback that solves the corresponding linear model matching problem can be used in order to approximately solve the original nonlinear problem, is investigated by means of two examples: the double pendulum and a two-link robot arm with a flexible joint. ESA

N90-18949# Universiteit Twente, Enschede (Netherlands). Dept. of Computer Science.
USING DYNAMIC QUEUEING NETWORKS AS A TOOL FOR SPECIFYING PERFORMABILITY MODELS
Boudewijn R. Haverkort and Ignas G. Niemegeers Sep. 1989 21 p Prepared for presentation at ACM Sigmetrics '90, Boulder, CO, 22-25 May 1990
(Memo-INF-89-51; ISSN-0923-1714; ETN-90-96314) Avail: NTIS HC A03/MF A01

The concept of dynamic queueing networks is introduced and its use in specifying performabiltity models is shown. Queueing networks are used for modeling the performance aspects of a computer system with a dynamic structure, and a Generalized Stochastic Petri Net (GSPN) is used for modeling the fault tolerance aspects of the system. The GSPN is used to construct a Markovian model that describes the dynamic structure, that is, the dependability aspects of the system. The GSPN model world is extended with so called covered transitions which are useful for describing certain phenomena in fault tolerant computer systems. The modeling technique allows assessment of aspects such as recovery, routing and reconfiguration. Examples illustrating suitability and a comparison with other techniques are given ESA

65 STATISTICS AND PROBABILITY

Includes data sampling and smoothing; Monte Carlo method; and stochastic processes.

N90-18950# Instituto de Pesquisas Espaciais, Sao Jose dos Campos (Brazil).
CONTRIBUTION TO THE STUDY OF STABILITY ROBUSTNESS OF NONLINEAR MULTIVARIABLE REGULATORS Ph.D. Thesis [CONTRIBUICAO AO ESTUDO DA ROBUSTEZ DA ESTABILIDADE DE REGULADORES NAO LINEARES MULTIVARIAVEIS]
Jose Jaime daCruz Mar. 1989 209 p In PORTUGUESE; ENGLISH summary
(INPE-4801-TDL/356) Avail: NTIS HC A10/MF A02

A stability robustness analysis of nonlinear time invariant multivariable regulators is performed. Both continuous and discrete-time regulators are considered, the analysis was carried out in the frequency and time domains. The main goal of the frequency domain analysis is the derivation of the absolute stability sectors of linear quadratic and Lyapunov regulators through the Multivariable Popov Criterion. Similar to the case of the evaluation of stability margins, the concept of singular value of matrix transfer functions is shown to be useful also in an absolute stability context. Frequency domain identities are obtained for this purpose. These identities, which are generalized forms of the Kalman Equalities, establish necessary conditions for a given matrix transfer function to represent a closed-loop linear quadratic regulator. In the case of Lyapunov regulators the corresponding identities are necessary conditions for a given matrix transfer function to represent the loop matrix transfer function of such regulators. The analysis accomplished in the time domain is based on a Lyapunov function suggested by the dynamic programming equation associated to the optimal regulator. Both nonlinear and linear quadratic regulators are studied. The stability robustness in the presence of gain and additive perturbations in the control law is considered. The properties of the solution of the Algebraic Riccati Equation are studied as required by the analysis of the linear quadratic regulators, with particular emphasis given to its asymptotical behavior. Indices that quantify the robustness are defined and studied for both kinds of perturbations considered. Author

N90-18951# Instituto de Pesquisas Espaciais, Sao Jose dos Campos (Brazil).
ADAPTIVE STATE ESTIMATION AND SAMPLING RATE ANALYSIS FOR INVARIANT LINEAR DYNAMIC SYSTEMS IN TIME Ph.D. Thesis
Roberto VieiradaFonsecaLopes Nov. 1989 254 p In PORTUGUESE; ENGLISH summary
(INPE-4960-TDL/389) Avail: NTIS HC A12/MF A02

The needs for adaptive techniques to overcome practical difficulties related to the state estimation theory is as old as the applications of the theory itself. An introductory review is presented for adaptive techniques and gives three contributions to this still up-to-date topic. The residue correlation method for noise statistics estimation is extended to cover the continuous signal processing case. A secondary process driven by the residue is defined in such a way that its sample covariance is a finite linear observation of those statistics. It becomes evident that the discrete model with sequential white noise is not consistent with a continuous sampling rate. Then the cross-validation method for fitting the data smoothing degree using the concept of pixel of the output signal which determines its resolution is extended to the continuous case. Results corresponding to different kinds of signals are

analyzed and compared with the state smoothing ones. These theoretical studies give the heuristic motivation for the mesh method - the major contribution of this work. A parametric analysis of the scalar case shows that if the system noise is taken as white the discretization time step must not be greater than the signal resolution. In this case the residue sample covariances that results from processing distinct meshes is a linear observation of both the state and observation noise statistics. On this basis, the meshes method estimates such statistics as well as the ideal sampling rate. Results are presented for a simplified satellite attitude determination problem. Author

N90-18952# Leiden Univ. (Netherlands). Dept. of Mathematics.
RECURRENCE CONDITIONS FOR AVERAGE AND BLACKWELL OPTIMALITY IN DENUMERABLE STATE MARKOV DECISION CHAINS
R. Dekker and A. Hordijk 1989 24 p Sponsored in part by Netherlands Organization for the Advancement of Pure Research
(TW-89-02; ETN-90-96273) Avail: NTIS HC A03/MF A01

An operator theoretical approach for multichain Markov decision processes with a countable state space, compact action sets and unbounded rewards is investigated. Conditions have been presented guaranteeing the existence of a Laurent series expansion for the discounted rewards, the existence of average and Blackwell optimal policies and the existence of solutions for the average and Blackwell optimality equations. These assumptions were operator oriented and formulated as conditions for the deviation matrix. The same approach is shown carried out under recurrence conditions. These new conditions seem easier to check in general and are especially suited for applications in queueing models. ESA

N90-18953# Universiteit Twente, Enschede (Netherlands). Dept. of Applied Mathematics.
KREIM FACTORIZATION OF COVARIANCE OPERATORS OF 2-PARAMETER RANDOM FIELDS AND APPLICATION TO THE LIKELIHOOD RATIO
Rob Luesink and Arunabha Bagchi Aug. 1989 20 p
(MEMO-802; ISSN-0169-2690; ETN-90-96306) Avail: NTIS HC A03/MF A01

The covariance operator of a signal plus noise observation for a 2-parameter random field is factorized, as products of Volterra type operators. As a result of this factorization the determinant of this operator is expressed in terms of the system parameters. This determinant appears in the likelihood functional which plays a significant role in identification and detection problems. ESA

N90-18954# Universiteit Twente, Enschede (Netherlands). Dept. of Applied Mathematics.
STRONG MODERATE DEVIATION THEOREMS
T. Inglot, W. C. M. Kallenberg, and T. Ledwina Aug. 1989 26 p
(Grant CPBP-01.02)
(MEMO-804; ISSN-0169-2690; ETN-90-96308) Avail: NTIS HC A03/MF A01

Strong moderate deviation theorems which are concerned with relative errors in the tails caused by replacing the exact distribution function by its limiting distribution function are studied. A new approach for deriving such theorems is presented using strong approximation inequalities. In this way a strong moderate deviation theorem is obtained for statistics of the form T (alpha n), where T is a seminorm and alpha n is the empirical process. The basic theorem is applied on linear combinations of order statistics, which leads to a substantial improvement of previous results. ESA

66 SYSTEMS ANALYSIS

Includes mathematical modeling; network analysis; and operations research.

N90-18955# Los Alamos National Lab., NM.
SURVIVABILITY AND EFFECTIVENESS OF NEAR-TERM STRATEGIC DEFENSE
Gregory H. Canavan and Edward Teller (Lawrence Livermore National Lab., CA.) Jan. 1990 23 p
(Contract W-7405-eng-36)
(DE90-005805; LA-11345-MS; UC-700) Avail: NTIS HC A03/MF A01

This paper examines the survivability and effectiveness of space-based defensive missiles on a quantified basis. The effectiveness and costs of attack and defense are estimated and cost-exchange ratios are calculated in differing configurations. Various moves and countermoves are compared. Low-weight, self-reliant defensive missiles are found to be most effective. The advantages of the development of decoys for defensive missiles and of a small pilot deployment are discussed. DOE

N90-18956# European Space Agency, Paris (France).
DETERMINISTIC DIFFERENTIAL GAME SOLUTION: THE APPROXIMATE STRATEGY METHOD
C. Marchal (Office National d'Etudes et de Recherches Aerospatiales, Paris, France) Dec. 1989 71 p Transl. into ENGLISH of Resolution des jeux Differentiels Deterministes: La Methode de la Strategie Approchee (Paris, France, ONERA), 1987 Original language document was announced as N89-27450
(ESA-TT-1158; ONERA-NT-1987-6; ETN-90-96221) Avail: NTIS HC A04/MF A01

Deterministic differential games are presented and classified here among other games. They have many singularities, discontinuities and subdivisions. Sufficient conditions of continuity of the value of the game in terms of the initial conditions are given. Most deterministic differential games have a very complex and difficult solution and the approximate strategy method reduces the game to a succession of ordinary problems of optimization and allows a systematic step by step improvement of the strategies. Two good opposing strategies give close upper and lower bounds of the value of the game. Conclusions, including that if the Hamiltonian of the game is either convex or concave with respect to the adjoint vector, the game is equivalent to a problem of optimization, are summarized. ESA

67 THEORETICAL MATHEMATICS

Includes topology and number theory.

No abstracts in this category.

70 PHYSICS (GENERAL)

For precision time and time interval (PTTI) see *35 Instrumentation and Photography;* for geophysics, astrophysics or solar physics see *46 Geophysics, 90 Astrophysics,* or *92 Solar Physics.*

N90-18957*# National Aeronautics and Space Administration. Goddard Space Flight Center, Greenbelt, MD.
ANNIHILATION IN GASES AND GALAXIES
Richard J. Drachman, ed. Washington Jan. 1990 271 p Workshop held in Greenbelt, MD, 19-21 Jul. 1989
(NASA-CP-3058; Rept-90B00019; NAS 1.55:3058) Avail: NTIS HC A12/MF A02 CSCL 20H

This publication contains most of the papers, both invited and

contributed, that were presented at the Workshop of Annihilation in Gases and Galaxies. This was the fifth in a biennial series associated with the International Conference on the Physics of Electronic and Atomic Collisions. Subjects covered included the scattering and annihilation of positrons and positronium atoms in various media, including those of astrophysical interest. In addition, the topics of antimatter and dark matter were covered. For individual titles, see N90-18958 through N90-18996.

N90-18958*# York Univ., Toronto (Ontario). Dept. of Physics.
POSITRON-ALKALI ATOM SCATTERING **c72**
R. P. McEachran, M. Horbatsch, A. D. Stauffer, and S. J. Ward *In* NASA, Goddard Space Flight Center, Annihilation in Gases and Galaxies Jan. 1990 p 1-11 Sponsored by Natural Sciences and Engineering Research Council of Canada (For primary document see N90-18957 11-70)
Avail: NTIS HC A12/MF A02 CSCL 20H

Positron-alkali atom scattering was recently investigated both theoretically and experimentally in the energy range from a few eV up to 100 eV. On the theoretical side calculations of the integrated elastic and excitation cross sections as well as total cross sections for Li, Na and K were based upon either the close-coupling method or the modified Glauber approximation. These theoretical results are in good agreement with experimental measurements of the total cross section for both Na and K. Resonance structures were also found in the L = 0, 1 and 2 partial waves for positron scattering from the alkalis. The structure of these resonances appears to be quite complex and, as expected, they occur in conjunction with the atomic excitation thresholds. Currently both theoretical and experimental work is in progress on positron-Rb scattering in the same energy range. Author

N90-18959*# Wayne State Univ., Detroit, MI. Dept. of Physics and Astronomy.
SCATTERING OF POSITRONS AND ELECTRONS BY ALKALI ATOMS **c72**
T. S. Stein, W. E. Kauppila, C. K. Kwan, R. A. Lukaszew, S. P. Parikh, Y. J. Wan, S. Zhou, and M. S. Dababneh *In* NASA, Goddard Space Flight Center, Annihilation in Gases and Galaxies Jan. 1990 p 13-27 Sponsored by NSF, Washington, DC (For primary document see N90-18957 11-70)
Avail: NTIS HC A12/MF A02 CSCL 20H

Absolute total scattering cross sections (Q sub T's) were measured for positrons and electrons colliding with sodium, potassium, and rubidium in the 1 to 102 eV range, using the same apparatus and experimental approach (a beam transmission technique) for both projectiles. The present results for positron-sodium and -rubidium collisions represent the first Q sub T measurements reported for these collision systems. Features which distinguish the present comparisons between positron- and electron-alkali atom Q sub T's from those for other atoms and molecules (room-temperature gases) which have been used as targets for positrons and electrons are the proximity of the corresponding positron- and electron-alkali atom Q sub T's over the entire energy range of overlap, with an indication of a merging or near-merging of the corresponding positron and electron Q sub T's near (and above) the relatively low energy of about 40 eV, and a general tendency for the positron-alkali atom Q sub T's to be higher than the corresponding electron values as the projectile energy is decreased below about 40 eV. Author

N90-18960*# Government Engineering Coll., Aurangabad (India).
ELASTIC SCATTERING OF e- AND e+ FROM Rb AND Cd **c72**
A. W. Pangantiwar and Rajesh Srivastava (Roorkee Univ., India) *In* NASA, Goddard Space Flight Center, Annihilation in Gases and Galaxies Jan. 1990 p 29-31 (For primary document see N90-18957 11-70)
Avail: NTIS HC A12/MF A02 CSCL 20H

Differential cross section results are calculated for the elastic scattering of electrons and positrons from the ground state of Rb and Cd atoms. An optical model potential approach is used for the calculation. Results are compared with the available electron impact experimental results. Author

N90-18961*# Roorkee Univ. (India). Dept. of Physics.
INELASTIC SCATTERING OF POSITRONS WITH SODIUM **c72**
S. P. Purohit and K. C. Mathur *In* NASA, Goddard Space Flight Center, Annihilation in Gases and Galaxies Jan. 1990 p 33-35 Sponsored by the Council of Scientific and Industrial Research, India (For primary document see N90-18957 11-70)
Avail: NTIS HC A12/MF A02 CSCL 20H

The two potential approach is used to study the resonant 3s-3p excitation of sodium atom by positrons of energy 40 and 54.4eV. The angular variation of coherence and correlation parameters is presented. Comparison with the corresponding parameters in electron scattering is given to see the role of various interaction potentials in electron and positron scattering. Author

N90-18962*# Memorial Univ. of Newfoundland, Saint Johns. Dept. of Physics.
POSITRON COLLISIONS WITH ALKALI-METAL ATOMS **c72**
T. T. Gien *In* NASA, Goddard Space Flight Center, Annihilation in Gases and Galaxies Jan. 1990 p 37-39 (For primary document see N90-18957 11-70)
Avail: NTIS HC A12/MF A02 CSCL 20H

The total cross sections for positron and electron collisions with potassium, sodium, lithium and rubidium are calculated, employing the modified Glauber approximation. The Modified Glauber cross sections for positron collision with potassium and sodium at low intermediate energies are found to agree reasonably well with existing experimental data. Author

N90-18963*# Erlangen-Nuremberg Univ. (Germany, F.R.). Chair for Theoretical Chemistry.
INELASTIC COLLISIONS OF POSITRONS WITH ONE-VALENCE-ELECTRON TARGETS **c72**
Mohamed Assad Abdel-Raouf *In* NASA, Goddard Space Flight Center, Annihilation in Gases and Galaxies Jan. 1990 p 41-43 Sponsored by Deutsche Forschungsgemeinschaft, Fed. Republic of Germany (For primary document see N90-18957 11-70)
Avail: NTIS HC A12/MF A02 CSCL 20H

The total elastic and positronium formation cross sections of the inelastic collisions between positrons and various one-valence-electron atoms, (namely hydrogen, lithium, sodium, potassium and rubidium), and one-valence-electron ions, (namely hydrogen-like, lithium-like and alkaline-earth positive ions) are determined using an elaborate modified coupled-static approximation. Special attention is devoted to the behavior of the Ps cross sections at the energy regions lying above the Ps formation thresholds. Author

N90-18964*# York Univ., Toronto (Ontario). Dept. of Physics.
POSITRON-RUBIDIUM SCATTERING **c72**
R. P. McEachran, M. Horbatsch, and A. D. Stauffer *In* NASA, Goddard Space Flight Center, Annihilation in Gases and Galaxies Jan. 1990 p 45-47 Sponsored by the Natural Sciences and Engineering Research Council of Canada (For primary document see N90-18957 11-70)
Avail: NTIS HC A12/MF A02 CSCL 20H

A 5-state close-coupling calculation (5s-5p-4d-6s-6p) was carried out for positron-Rb scattering in the energy range 3.7 to 28.0 eV. In contrast to the results of similar close-coupling calculations for positron-Na and positron-K scattering the (effective) total integrated cross section has an energy dependence which is contrary to recent experimental measurements. Author

N90-18965*# Indian Association for the Cultivation of Science, Calcutta. Dept. of Theoretical Physics.
THEORETICAL SURVEY ON POSITRONIUM FORMATION AND IONISATION IN POSITRON ATOM SCATTERING **c72**
Madhumita Basu and A. S. Ghosh *In* NASA, Goddard Space Flight Center, Annihilation in Gases and Galaxies Jan. 1990

p 49-62 Sponsored in part by CSIR and INSA (For primary document see N90-18957 11-70)
Avail: NTIS HC A12/MF A02 CSCL 20H

The recent theoretical studies are surveyed and reported on the formation of exotic atoms in positron-hydrogen, positron-helium and positron-lithium scattering specially at intermediate energy region. The ionizations of these targets by positron impact was also considered. Theoretical predictions for both the processes are compared with existing measured values. Author

N90-18966*# Queens Univ., Belfast (Northern Ireland). Dept. of Applied Mathematics.
POSITRON SCATTERING BY ATOMIC HYDROGEN USING OPTICAL POTENTIALS AND WITH POSITRONIUM FORMATION **c72**
H. R. J. Walters *In* NASA, Goddard Space Flight Center, Annihilation in Gases and Galaxies Jan. 1990 p 63-66 (For primary document see N90-18957 11-70)
Avail: NTIS HC A12/MF A02 CSCL 20H

The scattering is considered of positrons by H(ls) in a two-state model which incorporates optical potentials. The model explicitly describes elastic scattering, i.e., positron + H(ls) yields positron + H(ls) and Ps(ls) yields Ps(ls) + p. The inelastic processes positron + H(ls) yields positron + H* Ps(ls) + p yields Ps* + p where * stands for a state other than ls, are implicitly taken into account through the optical potentials, which also allow for polarization of H(ls) and Ps(ls). Author

N90-18967*# Gurudas Coll., Calcutta (India). Dept. of Physics.
POSITRONIUM FORMATION IN Ss STATE IN e+-Li SCATTERING **c72**
K. P. Sarkar, D. Basu, and Madhumita Basu (Indian Association for the Cultivation of Science, Calcutta.) *In* NASA, Goddard Space Flight Center, Annihilation in Gases and Galaxies Jan. 1990 p 67-69 (For primary document see N90-18957 11-70)
Avail: NTIS HC A12/MF A02 CSCL 20H

There are ample theoretical reasons to investigate positron-alkali atom scattering. Moreover, recent measurement on positron-alkali atom system by a Detroit group has renewed much interest in investigating these processes. Positronium (Ps) formation in excited 2s state in positron-Li scattering at intermediate and high energies were studied including second order effects following Basu and Ghosh. Author

N90-18968*# Florida Agricultural and Mechanical Univ., Tallahassee. Dept. of Physics.
NEW PARAMETER-FREE POLARIZATION POTENTIALS IN LOW-ENERGY POSITRON COLLISIONS **c72**
Ashok Jain *In* NASA, Goddard Space Flight Center, Annihilation in Gases and Galaxies Jan. 1990 p 71-86 (For primary document see N90-18957 11-70)
(Contract DE-FC05-85ER-250000)
Avail: NTIS HC A12/MF A02 CSCL 20H

The polarization potential plays a decisive role in shaping up the cross sections in low energy positron collisions with atoms and molecules. However, its inclusion without involving any adjustable parameter, is still a challenge. Various other techniques employed so far for positron collisions are summarized, and a new, nonadjustable and very simple form of the polarization potential for positron-atom (molecule) collisions below the threshold of positronium formation is discussed. This new recently proposed potential is based on the correlation energy of a single positron in a homogeneous electron gas. The correlation energy was calculated by solving the Schrodinger equation of the positron-electron system and fitted to an analytical form in various ranges of the density parameter. In the outside region, the correlation energy is joined smoothly with the correct asymptotic form. This new positron correlation polarization (PCOP) potential was tested on several atomic and molecular targets such as the Ar, CO, and CH4. The results on the total and differential cross sections on these targets are shown along with the experimental data where available. Author

N90-18969*# Nottingham Univ. (England). Dept. of Mathematics.
THE CALCULATION OF THE CONTRIBUTIONS TO LOW ENERGY e+H2 SCATTERING FROM SIGMA u+ AND PION u SYMMETRIES USING THE KOHN VARIATIONAL METHOD **c72**
E. A. G. Armour, D. J. Baker (Science Research Council, Chilton, England), and M. Plummer *In* NASA, Goddard Space Flight Center, Annihilation in Gases and Galaxies Jan. 1990 p 87-89 (For primary document see N90-18957 11-70)
Avail: NTIS HC A12/MF A02 CSCL 20H

Above incident energies of about 2 eV, the contribution to the total cross section in positron+H2 scattering from the sigma g+ symmetry is insufficient to account for the experimental value. Calculations carried out of the lowest partial waves of sigma u+ symmetry and Pion u symmetry using the Kohn variational method are described. The contributions to the total cross section from the two equivalent partial waves of Pion u symmetry significantly reduce the discrepancy with experiment up to incident energies of 4 to 5 eV. Comparisons are made with recent R-matrix calculations performed by Danby and Tennyson. Author

N90-18970*# University Coll., London (England). Dept. of Physics and Astronomy.
AB INITIO R-MATRIX CALCULATIONS OF e+-MOLECULE SCATTERING **c72**
Grahame Danby and Jonathan Tennyson *In* NASA, Goddard Space Flight Center, Annihilation in Gases and Galaxies Jan. 1990 p 91-93 (For primary document see N90-18957 11-70)
Avail: NTIS HC A12/MF A02 CSCL 20H

The adaptation of the molecular R-matrix method, originally developed for electron-molecule collision studies, to positron scattering is discussed. Ab initio R-matrix calculations are presented for collisions of low energy positrons with a number of diatomic systems including H2, HF and N2. Differential elastic cross sections for positron-H2 show a minimum at about 45 deg for collision energies between 0.3 and 0.5 Ryd. The calculations predict a bound state of positronHF. Calculations on inelastic processes in N2 and O2 are also discussed. Author

N90-18971*# Drake Univ., Des Moines, IA. Dept. of Physics and Astronomy.
NUMERICAL GREEN'S FUNCTIONS IN OPTICAL POTENTIAL CALCULATIONS FOR POSITRON SCATTERING FROM ARGON AND NEON **c72**
K. Bartschat, R. P. McEachran, and A. D. Stauffer (York Univ., Toronto, Ontario) *In* NASA, Goddard Space Flight Center, Annihilation in Gases and Galaxies Jan. 1990 p 95-97 Sponsored in part by the Natural Sciences and Engineering Research Council of Canada and Deutsche Forschungsgemeinschaft (For primary document see N90-18957 11-70)
Avail: NTIS HC A12/MF A02 CSCL 20H

An optical potential method was applied to the calculation of positron scattering from the noble gases in order to determine the effect of open excitation channels on the shape of differential scattering cross sections. Author

N90-18972*# East Anglia Univ., Norwich (England). School of Physics.
ANGULAR CORRELATION STUDIES IN NOBLE GASES **c72**
P. G. Coleman *In* NASA, Goddard Space Flight Center, Annihilation in Gases and Galaxies Jan. 1990 p 99-107 (For primary document see N90-18957 11-70)
Avail: NTIS HC A12/MF A02 CSCL 20H

There has been a recent revival of interest in the measurement of angular correlation of annihilation photons from the decay of positrons and positronium in gases. This revival has been stimulated by the possibility offered by the technique to shed new light on the apparently low positronium formation fraction in the heavier noble gases and to provide information on positronium quenching processes in gases such as oxygen. There is also the potential for learning about positronium slowing down in gases. This review

focuses on experimental noble gas work and considers what new information has been, and may be, gained from these studies.
Author

N90-18973*# MacQuarie Univ., Sydney (Australia). School of Mathematics, Physics, Computing and Electronics.
POSITRON EXCITATION OF NEON **c72**
L. A. Parcell, R. P. McEachran, and A. D. Stauffer (York Univ., Toronto, Ontario) *In* NASA, Goddard Space Flight Center, Annihilation in Gases and Galaxies Jan. 1990 p 109-111 Sponsored by Natural Sciences and Engineering Research Council of Canada and Macquarie Univ., Sydney, Australia (For primary document see N90-18957 11-70)
Avail: NTIS HC A12/MF A02 CSCL 20H

The differential and total cross section for the excitation of the 3s1P10 and 3p1P1 states of neon by positron impact were calculated using a distorted-wave approximation. The results agree well with experimental conclusions. Author

N90-18974*# Wayne State Univ., Detroit, MI. Dept. of Physics and Astronomy.
POSITRON-INERT GAS DIFFERENTIAL ELASTIC SCATTERING **c72**
W. E. Kauppila, Steven J. Smith, C. K. Kwan, and T. S. Stein *In* NASA, Goddard Space Flight Center, Annihilation in Gases and Galaxies Jan. 1990 p 113-115 (For primary document see N90-18957 11-70)
(Grant NSF PHY-87-06120)
Avail: NTIS HC A12/MF A02 CSCL 20H

Measurements are being made in a crossed beam experiment of the relative elastic differential cross section (DCS) for 5 to 300 eV positrons scattering from inert gas atoms (He, Ne, Ar, Kr, and Xe) in the angular range from 30 to 134 deg. Results obtained at energies around the positronium (Ps) formation threshold provide evidence that Ps formation and possibly other inelastic channels have an effect on the elastic scattering channel. Author

N90-18975*# Texas Univ., Arlington. Center for Positron Studies.
DIFFERENTIAL ELASTIC SCATTERING CROSS SECTIONS FOR 54.9eV POSITRONS INCIDENT ON HELIUM **c72**
R. L. Chaplin, L. M. Diana, and D. L. Brooks *In* NASA, Goddard Space Flight Center, Annihilation in Gases and Galaxies Jan. 1990 p 117-119 (For primary document see N90-18957 11-70)
(Grant NSF PHY-85-06933)
Avail: NTIS HC A12/MF A02 CSCL 20H

Absolute differential elastic scattering cross sections measured with the 3-m, high resolution, time-of-flight spectrometer are presented for 54.9eV positrons incident on He. Five point moving average differential cross sections are plotted against average scattering angles which range from 14 to 36 deg. Also the averages of five differential cross sections which have adjacent values of scattering angle are plotted versus the corresponding averages of the scattering angles. The curve fitted to these data is shaped like the theoretical curve but has its minimum and its maximum at scattering angles that are about 4 deg higher and 15 deg lower respectively than predicted by theory. Author

N90-18976*# Texas Univ., Arlington. Center for Positron Studies.
TOTAL CROSS SECTIONS FOR POSITRONS SCATTERED ELASTICALLY FROM HELIUM BASED ON NEW MEASUREMENTS OF TOTAL IONIZATION CROSS SECTIONS **c72**
L. M. Diana, R. L. Chaplin, D. L. Brooks, J. T. Adams, and L. K. Reyna *In* NASA, Goddard Space Flight Center, Annihilation in Gases and Galaxies Jan. 1990 p 121-123 (For primary document see N90-18957 11-70)
(Grant NSF PHY-85-06933)
Avail: NTIS HC A12/MF A02 CSCL 20H

An improved technique is presented for employing the 2.3m spectrometer to measure total ionization cross sections, Q sub ion, for positrons incident on He. The new ionization cross section agree with the values reported earlier. Estimates are also presented of total elastic scattering cross section, Q sub el, obtained by subtracting from total scattering cross sections, Q sub tot, reported in the literature, the Q sub ion and Q sub Ps (total positronium formation cross sections) and total excitation cross sections, Q sub ex, published by another researcher. The Q sub ion and Q sub el measured with the 3m high resolution time-of-flight spectrometer for 54.9eV positrons are in accord with the results from the 2.3m spectrometer. The ionization cross sections are in fair agreement with theory tending for the most part to be higher, especially at 76.3 and 88.5eV. The elastic cross section agree quite well with theory to the vicinity of 50eV, but at 60eV and above the experimental elastic cross sections climb to and remain at about 0.30 pi a sub o sq while the theoretical values steadily decrease. Author

N90-18977*# Bielefeld Univ. (Germany, F.R.). Fakultaet fuer Physik.
IONISATION OF ATOMIC HYDROGEN BY POSITRON IMPACT **c72**
Gottfried Spicher, Bjorn Olsson, Wilhelm Raith, Guenther Sinapius, and Wolfgang Sperber *In* NASA, Goddard Space Flight Center, Annihilation in Gases and Galaxies Jan. 1990 p 125-127 Sponsored in part by Deutsche Forschungsgemeinschaft and Bundesministerium fuer Forschung und Technology, Fed. Republic of Germany (For primary document see N90-18957 11-70)
Avail: NTIS HC A12/MF A02 CSCL 20H

With the crossed beam apparatus the relative impact-ionization cross section of atomic hydrogen by positron impact was measured. A layout of the scattering region is given. The first measurements on the ionization of atomic hydrogen by positron impact are also given. Author

N90-18978*# Bielefeld Univ. (Germany, F.R.). Fakultaet fuer Physik.
MULTIPLE-IONIZATION OF XENON ATOMS BY POSITRON IMPACT **c72**
Georg Kruse, Andreas Quermann, Wilhelm Raith, and Guenther Sinapius *In* NASA, Goddard Space Flight Center, Annihilation in Gases and Galaxies Jan. 1990 p 129-130 (For primary document see N90-18957 11-70)
Avail: NTIS HC A12/MF A02 CSCL 20H

Previously the cross sections were measured for positronium formation and single ionization by positron impact for He and H2. With the same apparatus, slightly modified, the single and multiple ionization of xenon is now investigated. The principle of the method is the detection of ion and positron in time correlation which allows the discrimination of positronium formation (whereby the positron vanishes) and the destinction of single, double and triple impact ionization (which lead to different ion flight times from the gas target to the ion detector). By using secondary electrons from the positron moderator, similar measurements were performed on electron impact ionization. By comparing with literature values for electron multiple ionization cross sections, the detection-probability ratios were determined for the differently charged ions. Author

N90-18979*# Aarhus Univ. (Denmark). Inst. of Physics.
DOUBLE IONIZATION OF HELIUM BY PARTICLE IMPACT **c72**
Finn M. Jacobsen *In* NASA, Goddard Space Flight Center, Annihilation in Gases and Galaxies Jan. 1990 p 131-136 (For primary document see N90-18957 11-70)
Avail: NTIS HC A12/MF A02 CSCL 20H

Experimental results are reviewed of the ratio, R sq., of double to single ionization of He by proton, antiproton, electron and positron impact in the energy range from 0.15 to about 10 MeV/amu. At high velocities (greater than 1 to 2 MeV/amu) values of R sq. caused by electron impact merge with those for the proton with the antiproton, electron values being up to a factor of 2 greater than that for the p, positron. At these velocities the single ionization cross sections caused by impact of any of these four particles are indistinguishable. Author

N90-18980*# City Coll. of the City Univ. of New York, NY.
POSITRONIUM REFLECTION AND POSITRONIUM BEAMS **c72**
M. Weber, S. Tang, R. Khatri, S. Berko, K. F. Canter, K. G. Lynn, A. P. Mills, Jr. (Bell Telephone Labs., Inc., Murray Hill, NJ.), L. O. Roellig, and A. J. Viescas *In* NASA, Goddard Space Flight Center, Annihilation in Gases and Galaxies Jan. 1990 p 137-147 (For primary document see N90-18957 11-70)
(Contract DE-AC02-76CH-00016; NSF DMR-86-20168)
Avail: NTIS HC A12/MF A02 CSCL 20H

Specular reflection of positronium, Ps was observed and that there is adequate intensity at higher energies to make further study worthwhile was established. The scattering appears to be restricted to the outermost surface with a mean free path of (0.75 + or - 0.15)A for Ps in LiF(100). With a greater intensity Ps beam one should see higher order diffraction beams as the result of the periodicity of the surface. Ps diffraction thus offers the possibility of being a novel and valuable probe to study the outermost surface and to study adsorbants on it. Two methods for producing Ps beams are described. Author

N90-18981*# Marquette Univ., Milwaukee, WI. Dept. of Chemistry.
LOW-ENERGY SCATTERING OF ELECTRONS AND POSITRONS IN LIQUIDS **c72**
D. M. Schrader *In* NASA, Goddard Space Flight Center, Annihilation in Gases and Galaxies Jan. 1990 p 149-157 Sponsored by the National Science Council, Republic of China (For primary document see N90-18957 11-70)
Avail: NTIS HC A12/MF A02 CSCL 20H

The scattering of low energy electrons and positrons is described for the liquid phase and compared and contrasted with that for the gas phase. Similarities as well as differences are noted. The loci of scattering sites, called spurs in the liquid phase, are considered in detail. In particular, their temporal and spatial evolution is considered from the point of view of scattering. Two emphases are made: one upon the stochastic calculation of the distribution of distances required for slowing down to thermal velocities, and the other upon the calculation of cross sections for energy loss by means of quantum mechanics. Author

N90-18982*# National Aeronautics and Space Administration. Goddard Space Flight Center, Greenbelt, MD.
GRIS OBSERVATIONS OF THE GALACTIC CENTER **c90**
N. Gehreis, S. Barthelmy, B. J. Teegarden, J. Tueller, M. Leventhal, and C. J. MacCallum (Sandia National Labs., Albuquerque, NM.) *In its* Annihilation in Gases and Galaxies Jan. 1990 p 159-168 (For primary document see N90-18957 11-70)
Avail: NTIS HC A12/MF A02 CSCL 03B

The 511 keV positron annihilation line source in the Galactic Center (GC) region has reappeared after being in a quiescent state since the early 1980's. Observations are reported made by the GRIS balloon instrument showing that the 511 keV line has returned to an intensity level similar to that seen in the 1970's. The line width was resolved for the first time and a measurement of the spatial extent of the emission along the galactic plane was made. Gamma ray imaging spectrometer (GRIS) is a high resolution germanium (Ge) spectrometer with a 17 deg field-of-view. Eleven hours of data were obtained from GC pointings on balloon flights over Australia on 1 May 1988 and again on 29 October 1988. An additional seven hours were obtained on 30 October 1988 from a point in the galactic plane (GP) 25 deg west of the center. Preliminary results for the line fluxes from the GC are 9.8 + or - 1.9 in May and 12.3 + or - 1.6 in October, and from the GP are 2.4 + or - 1.6 (1 sigma statistical errors). The flux for the off-center pointing is significantly lower than that for the GC pointings and indicates that the dominant emission is narrowly concentrated at the center. The line width for the GC pointing in October is 3.6 + or - 0.5 keV, which implies a temperature for the annihilation medium of less than or + 10(exp 5)K. A step in the continuum emission at 511 keV is found in both the GC and GP data. The step may be due to orthopositronium three-photon annihilation for the GC, but is too large relative to the 511 keV line for the GP to be simply explained by positronium. Author

N90-18983*# National Aeronautics and Space Administration. Goddard Space Flight Center, Greenbelt, MD.
POSITRON ANNIHILATION IN GAMMA-RAY BURSTS **c93**
Alice K. Harding *In its* Annihilation in Gases and Galaxies Jan. 1990 p 169-183 (For primary document see N90-18957 11-70)
Avail: NTIS HC A12/MF A02 CSCL 03B

Emission features appear at energies of 350 to 450 keV in the spectra of a number of gamma ray burst sources. These features were interpreted as electron-positron annihilation lines, redshifted by the gravitational field near the surface of a neutron star. Evidence that gamma ray bursts originate at neutron stars with magnetic field strengths of approx. 10(exp 12) Gauss came from recent observations of cyclotron scattering harmonics in the spectra of two bursts. Positrons could be produced in gamma ray burst sources either by photon-photon pair production or by one-photon pair production in a strong magnetic field. The annihilation of positrons is affected by the presence of a strong neutron star magnetic field in several ways. The relaxation of transverse momentum conservation causes an intrinsic broadening of the two-photon annihilation line and there is a decrease in the annihilation cross section below the free-space value. An additional channel for one-photon annihilation also becomes possible in high magnetic fields. The physics of pair production and annihilation near strongly magnetized neutron stars will be reviewed. Results from a self-consistent model for non-thermal synchrotron radiation and pair annihilation are beginning to identify the conditions required to produce observable annihilation features from strongly magnetized plasmas. Author

N90-18984*# National Aeronautics and Space Administration. Goddard Space Flight Center, Greenbelt, MD.
ANNIHILATION PHYSICS OF EXOTIC GALACTIC DARK MATTER PARTICLES **c90**
F. W. Stecker *In its* Annihilation in Gases and Galaxies Jan. 1990 p 185-199 (For primary document see N90-18957 11-70)
Avail: NTIS HC A12/MF A02 CSCL 03B

Various theoretical arguments make exotic heavy neutral weakly interacting fermions, particularly those predicted by supersymmetry theory, attractive candidates for making up the large amount of unseen gravitating mass in galactic halos. Such particles can annihilate with each other, producing secondary particles of cosmic-ray energies, among which are antiprotons, positrons, neutrinos, and gamma-rays. Spectra and fluxes of these annihilation products can be calculated, partly by making use of positron electron collider data and quantum chromodynamic models of particle production derived therefrom. These spectra may provide detectable signatures of exotic particle remnants of the big bang. Author

N90-18985*# Lawrence Livermore National Lab., CA. Physics Dept.
OPTICALLY EXCITED STATES IN POSITRONIUM **c72**
R. H. Howell, Klaus P. Ziock, F. Magnotta, Charles D. Dermer, R. A. Failor, and K. M. Jones (Williams Coll., Williamstown, MA.) *In* NASA, Goddard Space Flight Center, Annihilation in Gases and Galaxies Jan. 1990 p 201-207 (For primary document see N90-18957 11-70)
(Contract W-7405-eng-48)
Avail: NTIS HC A12/MF A02 CSCL 20H

Optical excitation are reported of the 1 3S-2 3P transition in positronium, and a second excitation from n=2 to higher n states. The experiment used light from two pulsed dye lasers. Changes in the positronium annihilation rate during and after the laser pulse were used to deduce the excited state populations. The n=2 level was found to be saturable and excitable to a substantial fraction of n=2 positronium to higher levels. Preliminary spectroscopic measurements were performed on n=14 and n=15 positronium. Author

N90-18986*# Lawrence Livermore National Lab., CA. Physics Dept.
STARK AND ZEEMAN EFFECTS ON LASER COOLING OF POSITRONIUM **c72**
Charles D. Dermer *In* NASA, Goddard Space Flight Center, Annihilation in Gases and Galaxies Jan. 1990 p 209-211 (For primary document see N90-18957 11-70)
(Contract W-7405-eng-48)
Avail: NTIS HC A12/MF A02 CSCL 20H

Theoretical work on laser cooling of Positronium, including effects of external magnetic and electric fields, is reviewed and extended. Author

N90-18987*# Bell Telephone Labs., Inc., Murray Hill, NJ.
DECAY RATE AND OTHER PROPERTIES OF THE POSITRONIUM NEGATIVE ION **c72**
A. P. Mills, Jr., P. G. Friedman, and D. M. Zuckerman *In* NASA, Goddard Space Flight Center, Annihilation in Gases and Galaxies Jan. 1990 p 213-221 (For primary document see N90-18957 11-70)
Avail: NTIS HC A12/MF A02 CSCL 20H

A new method for detecting the positronium minus ion is described, and the possibility of a long positronium mean free path in a solid is discussed. Author

N90-18988*# University Coll., London (England). Dept. of Physics and Astronomy.
ANTIHYDROGEN FORMATION IN COLLISIONS OF POSITRONIUM WITH ANTIPROTONS **c72**
J. W. Humberston *In* NASA, Goddard Space Flight Center, Annihilation in Gases and Galaxies Jan. 1990 p 223-228 (For primary document see N90-18957 11-70)
Avail: NTIS HC A12/MF A02 CSCL 20H

Antihydrogen, consisting of a positron orbiting around an antiproton, is the simplest few body system consisting entirely of antimatter and as such is of considerable importance in providing additional tests of the validity of charge conjugation invariance. In addition, the nature of the gravitational interaction between matter and antimatter might more readily be investigated for an electrically neutral system than one which is charged. Before such studies can be undertaken the antihydrogen must, of course, be produced by attachment of a positron to an antipositron. Several production mechanisms have been proposed, the two most favored of which are radiative capture (spontaneous or stimulated) and charge exchange in positronium-antiproton collisions. The cross section for radiative capture is very much less than that for charge exchange, so that it might be thought that the latter process is greatly to be preferred. Various calculations of the cross section for the charge exchange process are briefly reviewed. Author

N90-18989*# Lawrence Livermore National Lab., CA.
ANITPROTON-MATTER INTERACTIONS IN ANTIPROTON APPLICATIONS **c72**
David L. Morgan, Jr. *In* NASA, Goddard Space Flight Center, Annihilation in Gases and Galaxies Jan. 1990 p 229-242 (For primary document see N90-18957 11-70)
(Contracts NAS7-100; W-7405-eng-48)
Avail: NTIS HC A12/MF A02 CSCL 20H

By virtue of the highly energetic particles released when they annihilate in matter, antiprotons have a variety of potentially important applications. Among others, these include remote 3-D density and composition imaging of the human body and also of thick, dense materials, cancer therapy, and spacecraft propulsion. Except for spacecraft propulsion, the required numbers of low energy antiprotons can be produced, stored, and transported through reliance on current or near term technology. Paramount to these applications and to fundamental research involving antiprotons is knowledge of how antiprotons interact with matter. The basic annihilation process is fairly well understood, but the antiproton annihilation and energy loss rates in matter depend in complex ways on a number of atomic processes. The rates, and the corresponding cross sections, were measured or are accurately predictable only for limited combinations of antiproton kinetic energy and material species. Author

N90-18990*# Louisiana State Univ., Baton Rouge. Dept. of Physics and Astronomy.
POSITRONIUM IONS AND MOLECULES **c72**
Y. K. Ho *In* NASA, Goddard Space Flight Center, Annihilation in Gases and Galaxies Jan. 1990 p 243-256 Sponsored by NSF, Washington, DC (For primary document see N90-18957 11-70)
Avail: NTIS HC A12/MF A02 CSCL 20H

Recent theoretical studies on positronium ions and molecules are discussed. A positronium ion is a three particle system consisting of two electrons in singlet spin state, and a positron. Recent studies include calculations of its binding energy, positron annihilation rate, and investigations of its doubly excited resonant states. A positronium molecule is a four body system consisting of two positrons and two electrons in an overall singlet spin state. The recent calculations of its binding energy against the dissociation into two positronium atoms, and studies of auto-detaching states in positronium molecules are discussed. These auto-dissociating states, which are believed to be part of the Rydberg series as a result of a positron attaching to a negatively charged positronium ion, Ps-, would appear as resonances in Ps-Ps scattering. Author

N90-18991*# National Aeronautics and Space Administration. Goddard Space Flight Center, Greenbelt, MD.
SEARCH FOR RESONANCES IN POSITRON-ATOM SYSTEMS **c72**
A. K. Bhatia and Richard J. Drachman *In its* Annihilation in Gases and Galaxies Jan. 1990 p 257-259 (For primary document see N90-18957 11-70)
Avail: NTIS HC A12/MF A02 CSCL 20H

No one likes to see a scattering cross section curve that is too smooth; it is much more interesting to find bumps and wiggles and most interesting if it is possible to understand their cause. Several types of resonances were clearly established in positron-containing systems: those lying just below a degenerate threshold (like 2s-2p in hydrogenic atoms or ions) and those representing Coulomb bound states in a rearranged channel (like Ps + H reversing positron +H(-)). Recently, two new sorts of resonances have been reported for which the resonant mechanism is not clear. The first is a very low lying resonance in the e-Ps system (obtained by an adiabatic expansion method), and the second is a similarly low lying two channel resonance in the positron -H system (obtained by a close-coupling technique.) These developments encouraged the examination of such systems using the standard methods of stabilization and complex rotation. Most of the results are negative; the low lying resonances in either system are verified. Some indication of new resonances in the e(+)-He(+) system is found; this may be caused by the attraction between Ps in the n=2 state and the He(++) nucleus. Author

N90-18992*# York Univ., Toronto (Ontario). Dept. of Physics.
RESONANCES IN LOW-ENERGY POSITRON-ALKALI SCATTERING **c72**
M. Horbatsch, S. J. Ward, R. P. McEachran, and A. D. Stauffer *In* NASA, Goddard Space Flight Center, Annihilation in Gases and Galaxies Jan. 1990 p 261-262 Sponsored by the Natural Sciences and Engineering Research Council of Canada (For primary document see N90-18957 11-70)
Avail: NTIS HC A12/MF A02 CSCL 20H

Close-coupling calculations were performed with up to five target states at energies in the excitation threshold region for positron scattering from Li, Na and K. Resonances were discovered in the L = 0, 1 and 2 channels in the vicinity of the atomic excitation thresholds. The widths of these resonances vary between 0.2 and 130 MeV. Evidence was found for the existence of positron-alkali bound states in all cases. Author

N90-18993*# National Aeronautics and Space Administration. Goddard Space Flight Center, Greenbelt, MD.
POSITRONIUM FORMATION IN e+ PLUS H- COLLISIONS **c72**
Jack C. Straton (Kansas State Univ., Manhattan.) and Richard J. Drachman *In its* Annihilation in Gases and Galaxies Jan. 1990 p 263-271 Sponsored in part by DOE, Washington, DC (For primary document see N90-18957 11-70)
Avail: NTIS HC A12/MF A02 CSCL 20H

Cross sections for positronium formation by capture from the negative hydrogen ion are given. Orthogonalization corrections to the Coulomb (First) Born Approximation (CBA) differential and total cross sections are calculated using approximate H- wave functions of both Lowdin and Chandrasekhar. Various methods of orthogonalizing the unbound projectile to the possible bound states are considered. It is found that treating the atomic nuclei as if they were isotopic spin projections of a single type of nucleon gives cross sections that are an improvement over the CBA. Author

N90-18994*# Bell Telephone Labs., Inc., Murray Hill, NJ.
POSITRON-MOLECULE BOUND STATES AND POSITIVE ION PRODUCTION **c72**
M. Leventhal, A. Passner, and C. M. Surko (California Univ., San Diego.) *In* NASA, Goddard Space Flight Center, Annihilation in Gases and Galaxies Jan. 1990 p 273-283 Sponsored in part by ONR, Washington, DC (For primary document see N90-18957 11-70)
Avail: NTIS HC A12/MF A02 CSCL 20H

The interaction was studied of low energy positrons with large molecules such as alkanes. These data provide evidencce for the existence of long lived resonances and bound states of positrons with neutral molecules. The formation process and the nature of these resonances are discussed. The positive ions produced when a positron annihilates with an electron in one of these resonances were observed and this positive ion formation process is discussed. A review is presented of the current state of the understanding of these positron-molecule resonances and the resulting positive ion formation. A number of outstanding issues in this area is also discussed. Author

N90-18995*# Oak Ridge National Lab., TN. Analytical Chemistry Div.
INITIAL RESULTS OF POSITRON IONIZATION MASS SPECTROMETRY **c72**
D. L. Donohue, L. D. Hulett, Jr., S. A. McLuckey, G. L. Glish, and B. A. Eckenrode *In* NASA, Goddard Space Flight Center, Annihilation in Gases and Galaxies Jan. 1990 p 285-287 (For primary document see N90-18957 11-70)
(Contract DE-AC05-84OR-21400)
Avail: NTIS HC A12/MF A02 CSCL 20H

The use of monoenergetic positrons for the ionization of organic molecules in the gas phase is described. The ionic products are analyzed with a time-of-flight mass spectrometer and detected to produce a mass spectrum. The ionization mechanisms which can be studied in this way include positron impact at energies above the ionization limit of the target molecules, positronium formation in the Ore gap energy range, and positron attachment at energies less than 1eV. The technique of positron ionization mass spectrometry (PIMS) may have analytical utility in that chemical selectivity is observed for one or more of these processes. Author

N90-18996*# Texas Univ., Arlington. Dept. of Physics.
POSITRON ANNIHILATION INDUCED AUGER ELECTRON SPECTROSCOPY **c72**
Alex Weiss, A. R. Koymen, David Mehl, K. O. Jensen, Chun Lei, and K. H. Lee *In* NASA, Goddard Space Flight Center, Annihilation in Gases and Galaxies Jan. 1990 p 289-291 Sponsored in part by the Texas Advanced Research Program and the Robert A. Welch Foundation (For primary document see N90-18957 11-70)
Avail: NTIS HC A12/MF A02 CSCL 20H

Recently, Weiss et al. have demonstrated that it is possible to excite Auger transitions by annihilating core electrons using a low energy (less than 30eV) beam of positrons. This mechanism makes possible a new electron spectroscopy, Positron annihilation induced Auger Electron Spectroscopy (PAES). The probability of exciting an Auger transition is proportional to the overlap of the positron wavefunction with atomic core levels. Since the Auger electron energy provides a signature of the atomic species making the transition, PAES makes it possible to determine the overlap of the positron wavefunction with a particular element. PAES may therefore provide a means of detecting positron-atom complexes. Measurements of PAES intensities from clean and adsorbate covered Cu surfaces are presented which indicate that approx. 5 percent of positrons injected into CU at 25eV produce core annihilations that result in Auger transitions. Author

N90-18997# Instituto de Pesquisas Espaciais, Sao Jose dos Campos (Brazil).
VECTOR FIELDS, LINEAR SPACES AND TENSORS IN PHYSICS. PART 3: TENSOR ANALYSIS AND ITS APPLICATIONS [CAMPOS VETORIAIS, ESPACOS LINEARES E TENSORES NA FISICA. PARTE III - ANALISE TENSORIAL E SUAS APLICACOES]
Rene Adalid Medrano-B Nov. 1989 235 p In PORTUGUESE; ENGLISH summary
(INPE-5000-MD/41) Avail: NTIS HC A11/MF A02

The tensors, their transformation and other properties, from the viewpoint of their interpretation and use in physics are studied. Tensors are first introduced by showing the need of their existence in physics. Then the tensors are formally defined through the transformation properties of their components upon the rotation of orthogonal Cartesian coordinates; other properties of Cartesian tensors including tensor products and derivatives are also studied. A brief treatment of tensors follow which refer to oblique Cartesian coordinates such that the concepts of covariant and contravariant terms emerge in a natural way. Tensors referred to arbitrary curvilinear coordinates are formally treated studing the Jacobian of the transformation, contraction, the fundamental and reciprocal tensors, the quotient theorem, physical components, principal directions, Christoffel symbols, and covariant derivative among several others. An introduction to application of the tensor theory by defining the concept of absolute derivative, deriving the equation of geodesics and the curvature tensor, is offered. The Einstein's gravitational theory, nonetheless part of the applications, is separately treated solving the equations following the Schwarzschild spherically symmetric solution applied to planetary orbits. General relativistic expressions for the Maxwell's equations are also derived. In every chapter, whenever possible, elucidating examples are worked and problems that help better understand the theory are proposed. Author

N90-18998# Oak Ridge National Lab., TN. Solid State Theory Section.
MODERN THEORY OF MAGNETISM Foreign Trip Report
S. H. Liu Feb. 1990 13 p
(Contract DE-AC05-84OR-21400)
(DE90-007374; ORNL/FTR-3527) Avail: NTIS HC A03/MF A01

The author was invited as one of six lecturers to present a series of lectures on the modern theory of magnetism at the Workshop on Modern Theory of Solids. He attended seminars given by South American scientists and interacted with many participants of the workshop. DOE

71 ACOUSTICS

Includes sound generation, transmission and attenuation. For noise pollution see *45 Environmental Pollution.*

N90-18999 National Physical Lab., Teddington (England). Div. of Radiation Science and Acoustics.
NOISE LEVELS FROM A VSTOL AIRCRAFT MEASURED AT GROUND LEVEL AND AT 1.2 m ABOVE THE GROUND
R. C. Payne Oct. 1989 42 p
(NPL-RSA(EXT)-009; ISSN-0955-9655; ETN-90-96287) Copyright Avail: National Physical Lab., Teddington, Middlesex, TW11 OLW, England

During a series of aircraft flight tests using a British Aerospace Sea Harrier (FRS Mk1) noise measurements were obtained using microphones close to the ground plane and at a height of 1.2 m. Substantial differences from ground level to 1.2 m were observed, in measurements of perceived noise level and effective perceived noise level. The differences were found to be dependent on ground cover and flight maneuver and for a microphone located 1.2 m above a grass surface a dependence on precise microphone positioning was observed. The ground-plane microphones produced noise levels which closely approximated pressure-doubled values. A procedure for correcting 1/3 octave band sound pressure levels measured 1.2 m above the ground, to obtain pressure-doubled levels is examined. It is concluded that to avoid significant variations in measured noise levels, measurements should be made using a ground-plane microphone arrangement. ESA

N90-19000# Massachusetts Inst. of Tech., Cambridge. Plasma Fusion Center.
ACOUSTIC EMISSION DIAGNOSTIC TECHNIQUES FOR HIGH-FIELD HIGH CURRENT-DENSITY SUPER INDUCTING POLES
1990 32 p
(Contract DE-AC02-83ER-40121)
(DE90-007400; DOE/ER-40121/T3) Avail: NTIS HC A03/MF A01

Acoustic emission technology was introduced in the late 1970's to monitor superconducting magnets. It has now been firmly established that acoustic signals in superconducting magnets are emitted principally by mechanical events such as conductor strain, conductor motion, frictional motion, and epoxy cracking. Despite earlier suggestions, flux motion, except during flux jumping, does not appear to be an important source of AE signals in superconducting magnets. Of these several potential sources of AE signals in superconducting magnets, mechanical disturbances have been identified to be most important in high-performance, adiabatic magnets such as the dipoles used in accelerators. These mechanical disturbances are transitory, each generating a packet of AE signals that can be located with sensors. Source identification and location has been achieved with a number of superconducting magnets. In this section, the basic principle for the operation of adiabatic magnets is discussed, followed by presentation of some of the important experimental results relevant to the question of premature quench obtained at MIT. DOE

72 ATOMIC AND MOLECULAR PHYSICS

Includes atomic structure, electron properties, and molecular spectra.

N90-19001# Johns Hopkins Univ., Baltimore, MD. Dept. of Physics and Astronomy.
RESEARCH IN THEORETICAL PHYSICS Annual Progress Report, 1 Apr. 1989 - 31 Mar. 1990
G. Domokos and S. Kovesi-Domokos Nov. 1989 23 p
(Contract DE-FG02-85ER-40211)
(DE90-005558; DOE/ER-40211/5) Avail: NTIS HC A03/MF A01

The results are summarized of a research into the nature of the new physical phenomena observed in the interactions of photons and neutrinos of energies less than or = 1 EeV, emitted by various point sources in the sky. Contrary to expectations based on the Standard Model, the extensive air showers generated by these particles contain too many muons by a factor of approx. 100. This phenomenon can be explained by a composite structure of neutrinos, such that at sufficiently high energies they develop strong interactions. This hypothesis can be tested by studying the absorption characteristics of the primaries on the 3 K background. The primaries are found to contain a component which, unlike photons, is not absorbed by the background. It interacts with a cross section of a few mb/nucleon, thus giving further evidence for the existence of a substructure of quarks and leptons. DOE

N90-19002# University of Western Ontario, London. Dept. of Physics.
MERGED BEAM STUDIES INTO THE MECHANISMS OF HYDROGEN MOLECULAR ION RECOMBINATION Final Report, 1 Sep. 1987 - 31 Aug. 1989
J. B. A. Mitchell, F. B. Yousif, Peter VanderDonk, Craig Noren, Harry Chen, Muazzam Orakzai, and Phin Perquin Nov. 1989 31 p
(Grant AF-AFOSR-0365-87; AF Proj. 2301)
(AD-A216469; AFOSR-89-1896TR) Avail: NTIS HC A03/MF A01 CSCL 07/4

Measurements of the dissociative Recombination and Excitation of HeH +, the dissociative excitation of H3(+), the branching ratio for the decay channels for H+(3) (v= O) recombination and the cross section for the recombination of H2(+) (v = O) were performed and are described. A discussion of the relevance of these measurements to the recombination of H3(+) (v = O) is given. GRA

N90-19003# Stevens Inst. of Tech., Hoboken, NJ. Dept. of Physics
SURFACE PRODUCTION OF IONS Final Report, 1 Aug. 1986 - 30 Sep. 1989
Milos Seidl 9 Oct. 1989 145 p
(Grant AF-AFOSR-0299-86; AF Proj. 2301)
(AD-A216470; AFOSR-89-1876TR) Avail: NTIS HC A07/MF A01 CSCL 07/4

It was shown that negative hydrogen ions can be produced with high efficiency by backscattering low energy (order of 1 eV) hydrogen atoms or ions from low work function (less than 1.5 eV) surfaces. This was demonstrated experimentally by backscattering the Maxwellian tail of thermally produced hydrogen atoms from a variety of low work function surfaces. The general nature of the electron transfer process was described by a simple theoretical model. Low incident energy guarantees low energy spread of the negative hydrogen ions. It also makes it possible to consider a variety of adsorbates for reducing the work function of the converter surface. The work function of cesium-oxygen films on silicon can be as low as 0.9 eV but these films are too delicate for use on converter surfaces. Thick cesium oxide films with a work function ranging from 1.2 to 1.4 eV were successfully used on converter surfaces. Surface production of cesium ions from solid electrolyte sources was investigated. Three types of cesium ion guns were developed and used in the experiments. GRA

N90-19004# Oak Ridge National Lab., TN. Health and Safety Research Div.
ATOMIC AND MOLECULAR SPECTRA FROM ELECTRON-EXCITED ALKALI HALIDES
M. Kamada, H. Yamamoto, and T. Arakawa (Osaka Univ., Japan) 1990 8 p Presented at the US-Japan Seminar, Nagoya, Japan, 11-15 Sep. 1989 Submitted for publication
(Contract DE-AC05-84OR-21400)
(DE90-006160; CONF-8909293-1; ISBN-981-02-0102-8) Avail: HC A02/MF A01

When a solid is bombarded with energetic charged particles, constituent atoms eject from the surface to outside of the solid. In recent years, this sputtering phenomenon has extensively been investigated because of its applicability to microfabrication. It has become common understanding that the electronic excitation plays a dominant role in the sputtering process. For example, electronic

excitation of alkali halides leads to the ejection of halogen atoms preferentially along the direction of the crystal. However, there still remains several important problems we have to solve; how alkali atoms are sputtered, what happens in the surface layers after the sputtering of constituent atoms, and so on. The purpose of the present study is to solve these problems. DOE

N90-18958*# York Univ., Toronto (Ontario). Dept. of Physics.
POSITRON-ALKALI ATOM SCATTERING
R. P. McEachran, M. Horbatsch, A. D. Stauffer, and S. J. Ward *In* NASA, Goddard Space Flight Center, Annihilation in Gases and Galaxies Jan. 1990 p 1-11 Sponsored by Natural Sciences and Engineering Research Council of Canada (For primary document see N90-18957 11-70)
Avail: NTIS HC A12/MF A02 CSCL 20H

N90-18959*# Wayne State Univ., Detroit, MI. Dept. of Physics and Astronomy.
SCATTERING OF POSITRONS AND ELECTRONS BY ALKALI ATOMS
T. S. Stein, W. E. Kauppila, C. K. Kwan, R. A. Lukaszew, S. P. Parikh, Y. J. Wan, S. Zhou, and M. S. Dababneh *In* NASA, Goddard Space Flight Center, Annihilation in Gases and Galaxies Jan. 1990 p 13-27 Sponsored by NSF, Washington, DC (For primary document see N90-18957 11-70)
Avail: NTIS HC A12/MF A02 CSCL 20H

N90-18960*# Government Engineering Coll., Aurangabad (India).
ELASTIC SCATTERING OF e- AND e+ FROM Rb AND Cd
A. W. Pangantiwar and Rajesh Srivastava (Roorkee Univ., India) *In* NASA, Goddard Space Flight Center, Annihilation in Gases and Galaxies Jan. 1990 p 29-31 (For primary document see N90-18957 11-70)
Avail: NTIS HC A12/MF A02 CSCL 20H

N90-18961*# Roorkee Univ. (India). Dept. of Physics.
INELASTIC SCATTERING OF POSITRONS WITH SODIUM
S. P. Purohit and K. C. Mathur *In* NASA, Goddard Space Flight Center, Annihilation in Gases and Galaxies Jan. 1990 p 33-35 Sponsored by the Council of Scientific and Industrial Research, India (For primary document see N90-18957 11-70)
Avail: NTIS HC A12/MF A02 CSCL 20H

N90-18962*# Memorial Univ. of Newfoundland, Saint Johns. Dept. of Physics.
POSITRON COLLISIONS WITH ALKALI-METAL ATOMS
T. T. Gien *In* NASA, Goddard Space Flight Center, Annihilation in Gases and Galaxies Jan. 1990 p 37-39 (For primary document see N90-18957 11-70)
Avail: NTIS HC A12/MF A02 CSCL 20H

N90-18963*# Erlangen-Nuremberg Univ. (Germany, F.R.). Chair for Theoretical Chemistry.
INELASTIC COLLISIONS OF POSITRONS WITH ONE-VALENCE-ELECTRON TARGETS
Mohamed Assad Abdel-Raouf *In* NASA, Goddard Space Flight Center, Annihilation in Gases and Galaxies Jan. 1990 p 41-43 Sponsored by Deutsche Forschungsgemeinschaft, Fed. Republic of Germany (For primary document see N90-18957 11-70)
Avail: NTIS HC A12/MF A02 CSCL 20H

N90-18964*# York Univ., Toronto (Ontario). Dept. of Physics.
POSITRON-RUBIDIUM SCATTERING
R. P. McEachran, M. Horbatsch, and A. D. Stauffer *In* NASA, Goddard Space Flight Center, Annihilation in Gases and Galaxies Jan. 1990 p 45-47 Sponsored by the Natural Sciences and Engineering Research Council of Canada (For primary document see N90-18957 11-70)
Avail: NTIS HC A12/MF A02 CSCL 20H

N90-18965*# Indian Association for the Cultivation of Science, Calcutta. Dept. of Theoretical Physics.
THEORETICAL SURVEY ON POSITRONIUM FORMATION AND IONISATION IN POSITRON ATOM SCATTERING
Madhumita Basu and A. S. Ghosh *In* NASA, Goddard Space Flight Center, Annihilation in Gases and Galaxies Jan. 1990 p 49-62 Sponsored in part by CSIR and INSA (For primary document see N90-18957 11-70)
Avail: NTIS HC A12/MF A02 CSCL 20H

N90-18966*# Queens Univ., Belfast (Northern Ireland). Dept. of Applied Mathematics.
POSITRON SCATTERING BY ATOMIC HYDROGEN USING OPTICAL POTENTIALS AND WITH POSITRONIUM FORMATION
H. R. J. Walters *In* NASA, Goddard Space Flight Center, Annihilation in Gases and Galaxies Jan. 1990 p 63-66 (For primary document see N90-18957 11-70)
Avail: NTIS HC A12/MF A02 CSCL 20H

N90-18967*# Gurudas Coll., Calcutta (India). Dept. of Physics.
POSITRONIUM FORMATION IN Ss STATE IN e+-Li SCATTERING
K. P. Sarkar, D. Basu, and Madhumita Basu (Indian Association for the Cultivation of Science, Calcutta.) *In* NASA, Goddard Space Flight Center, Annihilation in Gases and Galaxies Jan. 1990 p 67-69 (For primary document see N90-18957 11-70)
Avail: NTIS HC A12/MF A02 CSCL 20H

N90-18968*# Florida Agricultural and Mechanical Univ., Tallahassee. Dept. of Physics.
NEW PARAMETER-FREE POLARIZATION POTENTIALS IN LOW-ENERGY POSITRON COLLISIONS
Ashok Jain *In* NASA, Goddard Space Flight Center, Annihilation in Gases and Galaxies Jan. 1990 p 71-86 (For primary document see N90-18957 11-70)
(Contract DE-FC05-85ER-250000)
Avail: NTIS HC A12/MF A02 CSCL 20H

N90-18969*# Nottingham Univ. (England). Dept. of Mathematics.
THE CALCULATION OF THE CONTRIBUTIONS TO LOW ENERGY e+H2 SCATTERING FROM SIGMA u+ AND PION u SYMMETRIES USING THE KOHN VARIATIONAL METHOD
E. A. G. Armour, D. J. Baker (Science Research Council, Chilton, England), and M. Plummer *In* NASA, Goddard Space Flight Center, Annihilation in Gases and Galaxies Jan. 1990 p 87-89 (For primary document see N90-18957 11-70)
Avail: NTIS HC A12/MF A02 CSCL 20H

N90-18970*# University Coll., London (England). Dept. of Physics and Astronomy.
AB INITIO R-MATRIX CALCULATIONS OF e+-MOLECULE SCATTERING
Grahame Danby and Jonathan Tennyson *In* NASA, Goddard Space Flight Center, Annihilation in Gases and Galaxies Jan. 1990 p 91-93 (For primary document see N90-18957 11-70)
Avail: NTIS HC A12/MF A02 CSCL 20H

N90-18971*# Drake Univ., Des Moines, IA. Dept. of Physics and Astronomy.
NUMERICAL GREEN'S FUNCTIONS IN OPTICAL POTENTIAL CALCULATIONS FOR POSITRON SCATTERING FROM ARGON AND NEON
K. Bartschat, R. P. McEachran, and A. D. Stauffer (York Univ., Toronto, Ontario) *In* NASA, Goddard Space Flight Center, Annihilation in Gases and Galaxies Jan. 1990 p 95-97 Sponsored in part by the Natural Sciences and Engineering Research Council of Canada and Deutsche Forschungsgemeinschaft (For primary document see N90-18957 11-70)
Avail: NTIS HC A12/MF A02 CSCL 20H

N90-18972*# East Anglia Univ., Norwich (England). School of Physics.
ANGULAR CORRELATION STUDIES IN NOBLE GASES
P. G. Coleman *In* NASA, Goddard Space Flight Center, Annihilation in Gases and Galaxies Jan. 1990 p 99-107 (For primary document see N90-18957 11-70)
Avail: NTIS HC A12/MF A02 CSCL 20H

N90-18973*# MacQuarie Univ., Sydney (Australia). School of Mathematics, Physics, Computing and Electronics.
POSITRON EXCITATION OF NEON
L. A. Parcell, R. P. McEachran, and A. D. Stauffer (York Univ., Toronto, Ontario) *In* NASA, Goddard Space Flight Center, Annihilation in Gases and Galaxies Jan. 1990 p 109-111 Sponsored by Natural Sciences and Engineering Research Council of Canada and Macquarie Univ., Sydney, Australia (For primary document see N90-18957 11-70)
Avail: NTIS HC A12/MF A02 CSCL 20H

N90-18974*# Wayne State Univ., Detroit, MI. Dept. of Physics and Astronomy.
POSITRON-INERT GAS DIFFERENTIAL ELASTIC SCATTERING
W. E. Kauppila, Steven J. Smith, C. K. Kwan, and T. S. Stein *In* NASA, Goddard Space Flight Center, Annihilation in Gases and Galaxies Jan. 1990 p 113-115 (For primary document see N90-18957 11-70)
(Grant NSF PHY-87-06120)
Avail: NTIS HC A12/MF A02 CSCL 20H

N90-18975*# Texas Univ., Arlington. Center for Positron Studies.
DIFFERENTIAL ELASTIC SCATTERING CROSS SECTIONS FOR 54.9eV POSITRONS INCIDENT ON HELIUM
R. L. Chaplin, L. M. Diana, and D. L. Brooks *In* NASA, Goddard Space Flight Center, Annihilation in Gases and Galaxies Jan. 1990 p 117-119 (For primary document see N90-18957 11-70)
(Grant NSF PHY-85-06933)
Avail: NTIS HC A12/MF A02 CSCL 20H

N90-18976*# Texas Univ., Arlington. Center for Positron Studies.
TOTAL CROSS SECTIONS FOR POSITRONS SCATTERED ELASTICALLY FROM HELIUM BASED ON NEW MEASUREMENTS OF TOTAL IONIZATION CROSS SECTIONS
L. M. Diana, R. L. Chaplin, D. L. Brooks, J. T. Adams, and L. K. Reyna *In* NASA, Goddard Space Flight Center, Annihilation in Gases and Galaxies Jan. 1990 p 121-123 (For primary document see N90-18957 11-70)
(Grant NSF PHY-85-06933)
Avail: NTIS HC A12/MF A02 CSCL 20H

N90-18977*# Bielefeld Univ. (Germany, F.R.). Fakultaet fuer Physik.
IONISATION OF ATOMIC HYDROGEN BY POSITRON IMPACT
Gottfried Spicher, Bjorn Olsson, Wilhelm Raith, Guenther Sinapius, and Wolfgang Sperber *In* NASA, Goddard Space Flight Center, Annihilation in Gases and Galaxies Jan. 1990 p 125-127 Sponsored in part by Deutsche Forschungsgemeinschaft and Bundesministerium fuer Forschung und Technology, Fed. Republic of Germany (For primary document see N90-18957 11-70)
Avail: NTIS HC A12/MF A02 CSCL 20H

N90-18978*# Bielefeld Univ. (Germany, F.R.). Fakultaet fuer Physik.
MULTIPLE-IONIZATION OF XENON ATOMS BY POSITRON IMPACT
Georg Kruse, Andreas Quermann, Wilhelm Raith, and Guenther Sinapius *In* NASA, Goddard Space Flight Center, Annihilation in Gases and Galaxies Jan. 1990 p 129-130 (For primary document see N90-18957 11-70)
Avail: NTIS HC A12/MF A02 CSCL 20H

N90-18979*# Aarhus Univ. (Denmark). Inst. of Physics.
DOUBLE IONIZATION OF HELIUM BY PARTICLE IMPACT
Finn M. Jacobsen *In* NASA, Goddard Space Flight Center, Annihilation in Gases and Galaxies Jan. 1990 p 131-136 (For primary document see N90-18957 11-70)
Avail: NTIS HC A12/MF A02 CSCL 20H

N90-18980*# City Coll. of the City Univ. of New York, NY.
POSITRONIUM REFLECTION AND POSITRONIUM BEAMS
M. Weber, S. Tang, R. Khatri, S. Berko, K. F. Canter, K. G. Lynn, A. P. Mills, Jr. (Bell Telephone Labs., Inc., Murray Hill, NJ.), L. O. Roellig, and A. J. Viescas *In* NASA, Goddard Space Flight Center, Annihilation in Gases and Galaxies Jan. 1990 p 137-147 (For primary document see N90-18957 11-70)
(Contract DE-AC02-76CH-00016; NSF DMR-86-20168)
Avail: NTIS HC A12/MF A02 CSCL 20H

N90-18981*# Marquette Univ., Milwaukee, WI. Dept. of Chemistry.
LOW-ENERGY SCATTERING OF ELECTRONS AND POSITRONS IN LIQUIDS
D. M. Schrader *In* NASA, Goddard Space Flight Center, Annihilation in Gases and Galaxies Jan. 1990 p 149-157 Sponsored by the National Science Council, Republic of China (For primary document see N90-18957 11-70)
Avail: NTIS HC A12/MF A02 CSCL 20H

N90-18985*# Lawrence Livermore National Lab., CA. Physics Dept.
OPTICALLY EXCITED STATES IN POSITRONIUM
R. H. Howell, Klaus P. Ziock, F. Magnotta, Charles D. Dermer, R. A. Failor, and K. M. Jones (Williams Coll., Williamstown, MA.) *In* NASA, Goddard Space Flight Center, Annihilation in Gases and Galaxies Jan. 1990 p 201-207 (For primary document see N90-18957 11-70)
(Contract W-7405-eng-48)
Avail: NTIS HC A12/MF A02 CSCL 20H

N90-18986*# Lawrence Livermore National Lab., CA. Physics Dept.
STARK AND ZEEMAN EFFECTS ON LASER COOLING OF POSITRONIUM
Charles D. Dermer *In* NASA, Goddard Space Flight Center, Annihilation in Gases and Galaxies Jan. 1990 p 209-211 (For primary document see N90-18957 11-70)
(Contract W-7405-eng-48)
Avail: NTIS HC A12/MF A02 CSCL 20H

N90-18987*# Bell Telephone Labs., Inc., Murray Hill, NJ.
DECAY RATE AND OTHER PROPERTIES OF THE POSITRONIUM NEGATIVE ION
A. P. Mills, Jr., P. G. Friedman, and D. M. Zuckerman *In* NASA, Goddard Space Flight Center, Annihilation in Gases and Galaxies Jan. 1990 p 213-221 (For primary document see N90-18957 11-70)
Avail: NTIS HC A12/MF A02 CSCL 20H

N90-18988*# University Coll., London (England). Dept. of Physics and Astronomy.
ANTIHYDROGEN FORMATION IN COLLISIONS OF POSITRONIUM WITH ANTIPROTONS
J. W. Humberston *In* NASA, Goddard Space Flight Center, Annihilation in Gases and Galaxies Jan. 1990 p 223-228 (For primary document see N90-18957 11-70)
Avail: NTIS HC A12/MF A02 CSCL 20H

N90-18989*# Lawrence Livermore National Lab., CA.
ANITPROTON-MATTER INTERACTIONS IN ANTIPROTON APPLICATIONS
David L. Morgan, Jr. *In* NASA, Goddard Space Flight Center, Annihilation in Gases and Galaxies Jan. 1990 p 229-242 (For primary document see N90-18957 11-70)
(Contracts NAS7-100; W-7405-eng-48)
Avail: NTIS HC A12/MF A02 CSCL 20H

N90-18990*# Louisiana State Univ., Baton Rouge. Dept. of Physics and Astronomy.
POSITRONIUM IONS AND MOLECULES
Y. K. Ho *In* NASA, Goddard Space Flight Center, Annihilation in Gases and Galaxies Jan. 1990 p 243-256 Sponsored by NSF, Washington, DC (For primary document see N90-18957 11-70)
Avail: NTIS HC A12/MF A02 CSCL 20H

N90-18991*# National Aeronautics and Space Administration. Goddard Space Flight Center, Greenbelt, MD.
SEARCH FOR RESONANCES IN POSITRON-ATOM SYSTEMS
A. K. Bhatia and Richard J. Drachman *In its* Annihilation in Gases and Galaxies Jan. 1990 p 257-259 (For primary document see N90-18957 11-70)
Avail: NTIS HC A12/MF A02 CSCL 20H

N90-18992*# York Univ., Toronto (Ontario). Dept. of Physics.
RESONANCES IN LOW-ENERGY POSITRON-ALKALI SCATTERING
M. Horbatsch, S. J. Ward, R. P. McEachran, and A. D. Stauffer *In* NASA, Goddard Space Flight Center, Annihilation in Gases and Galaxies Jan. 1990 p 261-262 Sponsored by the Natural Sciences and Engineering Research Council of Canada (For primary document see N90-18957 11-70)
Avail: NTIS HC A12/MF A02 CSCL 20H

N90-18993*# National Aeronautics and Space Administration. Goddard Space Flight Center, Greenbelt, MD.
POSITRONIUM FORMATION IN e+ PLUS H- COLLISIONS
Jack C. Straton (Kansas State Univ., Manhattan.) and Richard J. Drachman *In its* Annihilation in Gases and Galaxies Jan. 1990 p 263-271 Sponsored in part by DOE, Washington, DC (For primary document see N90-18957 11-70)
Avail: NTIS HC A12/MF A02 CSCL 20H

N90-18994*# Bell Telephone Labs., Inc., Murray Hill, NJ.
POSITRON-MOLECULE BOUND STATES AND POSITIVE ION PRODUCTION
M. Leventhal, A. Passner, and C. M. Surko (California Univ., San Diego.) *In* NASA, Goddard Space Flight Center, Annihilation in Gases and Galaxies Jan. 1990 p 273-283 Sponsored in part by ONR, Washington, DC (For primary document see N90-18957 11-70)
Avail: NTIS HC A12/MF A02 CSCL 20H

N90-18995*# Oak Ridge National Lab., TN. Analytical Chemistry Div.
INITIAL RESULTS OF POSITRON IONIZATION MASS SPECTROMETRY
D. L. Donohue, L. D. Hulett, Jr., S. A. McLuckey, G. L. Glish, and B. A. Eckenrode *In* NASA, Goddard Space Flight Center, Annihilation in Gases and Galaxies Jan. 1990 p 285-287 (For primary document see N90-18957 11-70)
(Contract DE-AC05-84OR-21400)
Avail: NTIS HC A12/MF A02 CSCL 20H

N90-18996*# Texas Univ., Arlington. Dept. of Physics.
POSITRON ANNIHILATION INDUCED AUGER ELECTRON SPECTROSCOPY
Alex Weiss, A. R. Koymen, David Mehl, K. O. Jensen, Chun Lei, and K. H. Lee *In* NASA, Goddard Space Flight Center, Annihilation in Gases and Galaxies Jan. 1990 p 289-291 Sponsored in part by the Texas Advanced Research Program and the Robert A. Welch Foundation (For primary document see N90-18957 11-70)
Avail: NTIS HC A12/MF A02 CSCL 20H

73 NUCLEAR AND HIGH-ENERGY PHYSICS

Includes elementary and nuclear particles; and reactor theory.

For space radiation see *93 Space Radiation.*

N90-19005# Oregon State Univ., Corvallis. Dept. of Physics.
THEORETICAL STUDIES IN NUCLEAR PHYSICS
Rubin H. Landau and Victor A. Madsen 1990 18 p
(Contract DE-FG06-86ER-40283)
(DE90-005981; DOE/ER-40283/9) Avail: NTIS HC A03/MF A01

Areas of study and discussion are: microscopic imaginary optical potential; isospin effects and charge exchange; multistep inelastic and charge exchange scattering; momentum space proton scattering; pion scattering from nuclei; antiproton studies; antikaons-nucleon interactions; and quantum mechanics. DOE

N90-19006# Minnesota Univ., Minneapolis. School of Physics and Astronomy.
THEORETICAL AND EXPERIMENTAL HIGH ENERGY PHYSICS Progress Report, 1 Jan. - 31 Dec. 1988
S. Gasiorowicz and Keith Ruddick 1988 95 p
(Contract DE-AC02-83ER-40105)
(DE90-006168; DOE/ER-40105/580) Avail: NTIS HC A05/MF A01

Experimental and theoretical work in High Energy Physics is discussed. Some topics discussed are: quantum field theory; supersymmetry; cosmology; superstring model; relic photinos; inflationary universe; dark matter; standard model; supernovae; semileptonic decay; quantum Langevin equation; underground neutrino detection at Soudan; strange quark systems; cosmic ray detection; superconducting super collider detectors; and studies of direct photon production. DOE

N90-19007# Los Alamos National Lab., NM.
SPACE NUCLEAR SAFETY PROGRAM Progress Report, Oct. - Dec. 1987
T. G. George, comp. Feb. 1990 37 p
(Contract W-7405-eng-36)
(DE90-006436; LA-11756-PR) Avail: NTIS HC A03/MF A01

This quarterly report describes studies related to the use of Pu(238)O sub 2 in radioisotope power systems, carried out of the Office of Defense Energy Programs and Special Applications of the U.S. Department of Energy by Los Alamos National Laboratory. The studies are ongoing; the results and conclusions described may change as the work progresses. DOE

N90-19008# EG and G Mound Applied Technologies, Miamisburg, OH.
DESIGN AND OPERATION OF AN INERT GAS FACILITY FOR THERMOELECTRIC GENERATOR STORAGE
C. J. Goebel 1990 6 p Presented at the 7th Symposium on Space Nuclear Power Systems, Albuquerque, NM, 7-11 Jan. 1990
(Contract DE-AC04-88DP-43495)
(DE90-007146; MLM-3623-OP; CONF-900109-20) Avail: NTIS HC A02

While the flight hardware is protected by design from the harsh environments of space, its in-air storage often requires special protection from contaminants such as dust, moisture and other gases. One of these components, the radioisotope thermoelectric generator (RTG) which powers the missions, was deemed particularly vulnerable to pre-launch aging because the generators remain operational at core temperatures in excess of 1000 degrees centigrade throughout the storage period. Any oxygen permitted to enter the devices will react with thermally hot components, preferentially with molybdenum in the insulating foils, and with graphites to form CO/CO2 gases which are corrosive to the thermopile. It was important therefore to minimize the amount of oxygen which could enter, by either limiting the effective in-leakage areas on the generators themselves, or by reducing the relative amount of oxygen within the environment around the

generators, or both. With the generators already assembled and procedures in place to assure minimal in-leakage in handling, the approach of choice was to provide a storage environment which contains significantly less oxygen than normal air. DOE

N90-19009# EG and G Mound Applied Technologies, Miamisburg, OH.
SAFETY ANALYSIS FOR THE GALILEO LIGHT-WEIGHT RADIOISOTOPE HEATER UNIT
Ernest W. Johnson 1990 8 p Presented at the 7th Symposium on Space Nuclear Power Systems, Albuquerque, NM, 7-11 Jan. 1990
(Contract DE-AC04-88DP-43495)
(DE90-007147; MLM-3624-OP; CONF-900109-21) Avail: NTIS HC A02/MF A01

The Light-Weight Radioisotope Heater Unit (LWRHU) will be used on the NASA Galileo Mission to provide thermal energy to the various systems on the orbiter and probe that are adversely affected by the low temperature a spacecraft encounters during a long interplanetary mission. Using these plutonia-fueled sources in 1-W increments permits employment of a single design and provides the spacecraft user the option of how many to use and where to position them to satisfy the proper thermal environment for components requiring such consideration. The use of the radioisotope Pu 238 in these devices necessitates the assessment of postulated radiological risks which might be experienced in case of accidents or malfunctions of the space shuttle or the spacecraft during phases of the mission in the vicinity of the earth. Included are data for the design, mission descriptions, postulated accidents with their consequences, test data, and the derived source terms and personnel exposures for the various events. DOE

N90-19010# EG and G Mound Applied Technologies, Miamisburg, OH.
THERMAL VACUUM LIFE TEST FACILITY FOR RADIOISOTOPE THERMOELECTRIC GENERATORS
R. L. Deaton, C. J. Goebel, and W. R. Amos 1990 9 p Presented at the 7th Symposium on Space Nuclear Power Systems, Albuquerque, NM, 7-11 Jan. 1990
(Contract DE-AC04-88DP-43495)
(DE90-007148; MLM-3622-OP; CONF-900109-22) Avail: NTIS HC A02/MF A01

In the late 1970's, the Department of Energy (DOE) assigned Monsanto Research Corporation, Mound Facility, now operated by EG and G Mound Applied Technologies, the responsibility for assembling and testing General Purpose Heat Source (GPHS) radioisotope thermoelectric generators (RTGs). Assembled and tested were five RTGs, which included four flight units and one non-flight qualification unit. Figure 1 shows the RTG, which was designed by General Electric AstroSpace Division (GE/ASD) to produce 285 W of electrical power. A detailed description of the processes for RTG assembly and testing is presented by Amos and Goebel (1989). The RTG performance data are described by Bennett, et al., (1986). The flight units will provide electrical power for the National Aeronautics and Space Administration's (NASA) Galileo mission to Jupiter (two RTGs) and the joint NASA/European Space Agency (ESA) Ulysses mission to study the polar regions of the sun (one RTG). The remaining flight unit will serve as the spare for both missions, and a non-flight qualification unit was assembled and tested to ensure that performance criteria were adequately met. DOE

74 OPTICS

Includes light phenomena; and optical devices.
For lasers see *36 Lasers and Masers.*

N90-19011# Air Force Inst. of Tech., Wright-Patterson AFB, OH. School of Engineering.
OPTICAL AMPLIFICATION IN 45 DEG - CUT BaTiO3 M.S. Thesis
Kenneth Scott Keppler Dec. 1989 83 p
(AD-A216043; AFIT/GEO/ENG/89D-5) Avail: NTIS HC A05/MF A01 CSCL 20/6

Two-wave coupling in Barium Titanate has been widely investigated because of the high gains predicted theoretically. In this report, optical scattering (or beam fanning) and it's effects on two-wave coupling gain and image amplification are investigated for 45 deg -cut BaTiO3 crystals. Experimental set-ups for beam fanning, two-wave coupling, and image amplification were designed to investigate signal and image outputs versus time. During beam fanning testing, records of transmitted intensity of a single input beam versus time were obtained for various entrance angles, and input intensities. Pump and signal output beam powers versus time were recorded for two-wave coupling tests. Input pump beam powers of 10, 1.0, and 0.1 mW were tested at a wavelength of 514.5 nm. Signal input beam powers ranging from 1.0 to .001 mW were used. In image amplification tests, the Fourier transform and a minified image of a resolution chart were amplified via two-wave coupling. Data from beam fanning and two-wave coupling tests implied that the beam fanning of the pump beam has negligible effect on the two-wave coupling gain of the output signal. GRA

N90-19012# Naval Postgraduate School, Monterey, CA.
DESIGN, IMPLEMENTATION AND TEST OF AN RS-232 COMPATIBLE BI-DIRECTIONAL, FULL DUPLEX, FIBER-OPTIC INTERFACE WITH PROVISION FOR HARDWARE HANDSHAKING ON A MINIMUM OF FIBER-OPTIC LINES M.S. Thesis
Ronald R. Heuler Jun. 1989 129 p
(AD-A216604) Avail: NTIS HC A07/MF A01 CSCL 20/6

The objective was the design and implementation of an RS-232 compatible, bidirectional, full duplex, fiber optic interface with provision for hardware handshaking. Results show that active handshaking lines can be successfully multiplexed, converted to light, transmitted, received, reconverted and demultiplexed pleisiochronously for data communications at 19.2 kilobaud. Use of wavelength division multiplexing and optical duplexing enable the reduction of individual fiber optic lines required from four unidirectional single frequency fibers to two bidirectional fibers at three operating wavelengths. GRA

N90-19013# Naval Postgraduate School, Monterey, CA. Dept. of Physics.
A SIMULATION OF OPTICAL PROPAGATION THROUGH ATMOSPHERIC TURBULENCE USING TWO-DIMENSIONAL FOURIER TRANSFORM TECHNIQUES M.S. Thesis
Jeffrey L. Turner Jun. 1989 79 p
(AD-A216776; NPS61-089-012) Avail: NTIS HC A05/MF A01 CSCL 20/14

Understanding turbulence degradation of electromagnetic wave propagation is essential for efficient operation of laser weapons, target designators, and imaging systems. Random atmospheric refractive index inhomogeneities alter the phase and amplitude of electromagnetic waves. This thesis attempts to model atmospheric turbulence effects by using filtered Gaussian phase screens to represent the random nature of refractive index changes. The simulation uses two-dimensional 512 x 512 fast Fourier transform (FFT) techniques with extended Huygens-Fresnel principles performed on a desk top computer. Simulation verification was accomplished by comparing calculated and theoretical spatial coherence lengths, phi o. Phase only screens produced coherence lengths that were 30 percent larger than theoretical values. By using random phase and amplitude screens, the calculated coherence lengths agreed to within 3 percent of theoretical values. Saturation of the normalized intensity variance, sigma 2/I2, occurred for increasing turbulence using a single phase-amplitude screen. GRA

N90-19014# Rochester Inst. of Tech., NY. Center for Imaging Science.
TECHNIQUES FOR MEASUREMENT OF THE OPTICAL PROPERTIES OF MATERIALS Final Report
John R. Schott, Mark D. Fairchild, Xiaofan Feng, Rolando Raqueno,

Bernard Brower, and Timothy Gallagher Jan. 1990 108 p
(Contract DE-FG01-88DP-20153)
(DE90-006902; DOE/DP-20153/T6; RIT/DIRS-89/90-51-134)
Avail: NTIS HC A06/MF A01

This effort is aimed at the general area of measurement of the optical properties of materials. The type of measurement techniques addressed here are applicable to any studies where optical means are used to study the characteristics of a material. However, the devices developed were designed to accommodate materials as they might be found exposed outdoors, as well as prepared laboratory samples. DOE

N90-19015# Rochester Inst. of Tech., NY. Center for Imaging Science.
VISUAL TARGET DETECTION AND RECOGNITION
Pantazis Mouroulis Jan. 1990 12 p
(Contract DE-FG01-88DP-20153)
(DE90-006903; DOE/DP-20153/T5; RIT/DIRS-89/90-53-136)
Avail: NTIS HC A03/MF A01

One objective of this research was to understand the interaction between visual instrument and observer, in a way that permits meaningful specification of the required optical quality of a visual optical system. Insight is provided into improved quality criteria for automated production, and a better understanding of accommodation effects on instrumental vision. DOE

N90-19016# Rochester Inst. of Tech., NY. Center for Imaging Science.
A MODEL OF INCOMPLETE CHROMATIC ADAPTATION FOR CALCULATING CORRESPONDING COLORS Final Report
Mark D. Fairchild Jan. 1990 25 p
(Contract DE-FG01-88DP-20153)
(DE90-006905; DOE/DP-20153/T3; RIT/DIRS-89/90-64-132)
Avail: NTIS HC A03/MF A01

A new mathematical model of chromatic adaptation for calculating corresponding colors across changes in illumination is formulated and tested. This model consists of a modified von Kries transform that accounts for incomplete levels of adaptation. The model predicts that adaptation will be less complete as the saturation of the adapting stimulus increases and more complete as the luminance of the adapting stimulus increases. The model is tested with experimental results from two different studies and found to be significantly better at predicting corresponding colors than other proposed models. This model represents a first step toward the specification of color appearance across varying conditions. DOE

N90-19017# Lawrence Livermore National Lab., CA. Lab. for Experimental Astrophysics.
A LARGE AREA, LOW COST, GAMMA-RAY, IMAGING SPECTROMETER
Klaus P. Ziock and Charles J. Hailey Jan. 1990 6 p Presented at the Workshop on High Energy Astrophysics in the 21st Century, Taos, NM, 10-14 Dec. 1989
(Contract W-7405-eng-48)
(DE90-006993; UCRL-102762; CONF-891276-1) Avail: NTIS HC A02/MF A01

A low cost per unit-area, imaging, low energy (.1 to 10 MeV) gamma ray spectrometer is being developed. This device has excellent position resolution (approx. 2 mm/511 keV), near unity quantum efficiency and an energy resolution typical of alkali halide-type detectors. The low unit cost is achieved through separation of the energy and position sensing functions in an alkali halide-based gamma ray detector. DOE

75 PLASMA PHYSICS

Includes magnetohydrodynamics and plasma fusion.
For ionospheric plasmas see *46 Geophysics*. For space plasmas see *90 Astrophysics*.

N90-19018# Instituto de Pesquisas Espaciais, Sao Jose dos Campos (Brazil).
HAMILTONIAN ANALYSIS AND SIMULATION OF FREE ELECTRON LASERS Ph.D. Thesis [ANALISE HAMILTONIANA E SIMULACAO DE LASERS DE ELECTRONS LIVRES]
Antonio dePaduaBritoSerbeto Jan. 1989 132 p In PORTUGUESE; ENGLISH summary
(INPE-4785-TDL/351) Avail: NTIS HC A07/MF A01

Using a normalized set of nonlinear equations, which describes a free electron laser (FEL) oscillator, the efficiency of energy extraction from the electron beam to the radiation can be optimized. The optimum values of this efficiency are presented for an untapered and tapered wiggler FEL oscillator. Procedures to determine optimized short-period-wiggler FEL oscillator design are presented. Scaling formula relating the normalized theoretical parameters to dimensional experimental quantities are obtained. Finally, design examples both untapered and tapered 300 GHz, 1.0 MW FEL oscillators to be used as source for Electron Cyclotron Resonance Heating (ECRH) of plasmas in magnetic fusion research and space-borne radar systems are calculated and discussed. Both applications require high power radiation sources at wavelength which is approximately 1 mm. Author

N90-19019# Stanford Univ., CA. High Temperature Gasdynamics Lab.
HIGH GROWTH RATE DIAMOND SYNTHESIS IN A LARGE AREA ATMOSPHERIC PRESSURE INDUCTIVELY COUPLED PLASMA
M. A. Cappelli, T. Owano, M. Gordon, and C. H. Kruger 12 Dec. 1989 14 p Submitted for publication Sponsored in part by DOE and NSF
(Contract N00014-89-J-1197)
(AD-A216090; TR-2) Avail: NTIS HC A02/MF A01 CSCL 13/8

Diamond synthesis is demonstrated in an atmospheric pressure inductively coupled argon-hydrogen-methane plasma. The plasma generated has a free stream active area of 20 sq cm and has an equilibrium electron temperature T sub e of approximately 4000 K. Growth rates are typically in the range of 25 to 50 microns/hour and are found to depend on the processing conditions and position on the substrate. Individual crystallites are analyzed by micro Raman spectroscopy. Large (50 microns) size well faceted crystallites are found to be under a state of compression, displaying shifts in the principal phonon mode as great as 3/cm from that of smaller polycrystalline diamond clusters or secondary nucleation sites. These shifts are shown to be expected within the framework of linear thermal expansion theory and the assumption of negligible stress relief at the crystallite-substrate interface. GRA

N90-19020# Oak Ridge National Lab., TN.
MEASUREMENT OF THE SPACE POTENTIAL OF A HIGH-TEMPERATURE PLASMA BY FAST ATOMIC BEAM SCATTERING ON AN ION PROBE BEAM
A. A. Kabantsev and S. Yu. Tashayev (Academy of Sciences, USSR, Novosibirsk) 1989 12 p Transl. into ENGLISH of Preprint 88-148 Transl. by Language Services, Knoxville, TN
(Contract DE-AC05-84OR-21400)
(DE90-006118; ORNL/tr-89/53; Preprint-88-148) Avail: NTIS HC A03/MF A01

An analysis was made of the possibility of measuring the potential distribution of a high-temperature plasma by scattering fast atoms on an ion probe beam. The proposed method is based on the idea of determining the energy of the ion beam, which depends on the plasma potential, from the energy spectrum of the scattered atoms. Application of this method allows one to avoid a number of fundamental difficulties characteristic of plasma potential measurements which make use of heavy-ion probe beams. DOE

N90-19021# Los Alamos National Lab., NM.
THE LOWER HYBRID DRIFT INSTABILITY AND THE EVOLUTION OF PLASMA GRADIENTS
A. G. Sgro and S. Peter Gary 1989 4 p Presented at the 11th US/Japan Workshop on Field-Reversed Configurations and Compact Toroids, Los Alamos, NV, 7-9 Nov. 1989
(Contract W-7405-eng-36)
(DE90-006521; LA-UR-90-34; CONF-8911130-12) Avail: NTIS HC A01/MF A01

The evolution of plasma gradients is studied with hybrid computer simulations (particle ions, fluid electrons with nonzero mass) carried out in the x-y plane of a plasma with a modest density gradient in the x direction and a magnetic field B = B(sub z)(x)(cflx z). These initial density and magnetic field profiles represent a 1-D equilibrium of the sheath region of a Field Reversed Configuration near the separatrix. DOE

N90-19022# Texas Univ., Austin. Inst. for Fusion Studies.
THE RAPID INWARD DIFFUSION OF COLD IONS IN TOKAMAKS AND THEIR EFFECT ON ION TRANSPORT
A. A. Ware Oct. 1989 22 p
(Contract DE-FG05-80ET-53088)
(DE90-006863; DOE/ET-53088/405; IFSR-405) Avail: NTIS HC A03/MF A01

The observed increase with density of the density asymmetry caused by the centrifugal force of toroidal motion in PDX, which is contrary to conventional theory, is explained by the presence of an excess of low energy ions with 10 to 15 percent concentration. The prime source being recycling, it is shown that low energy ions undergo rapid inward diffusion (too rapid to thermalize with the outward diffusion energetic ions) due to the combined effects of large nu (sub PA), electrostatic diffusion, and negative E(sub r) and partial derivative of T(sub i)/(partial derivative) of r. The presence of the low energy ions alters dramatically the predictions of neoclassical theory and many hydrogen and impurity ion transport phenomena now have simple explanations. DOE

N90-19023# Texas Univ., Austin. Inst. for Fusion Studies.
THE NEOCLASSICAL TRANSPORT OF TOROIDAL MOMENTUM IN TOKAMAKS
A. A. Ware Dec. 1989 9 p
(Contract DE-FG05-80ET-53088)
(DE90-006864; DOE/ET-53088/409; IFSR-409) Avail: NTIS HC A02/MF A01

Allowing for the presence of an expected moderate concentration (approx. 10 percent) of low energy ions in excess of the Maxwellian distribution causes a dramatic change in the neoclassical prediction for momentum transport, leading to agreement in magnitude with experiment. DOE

N90-19024# California Univ., Berkeley. Lawrence Berkeley Lab. Accelerator and Fusion Research Div.
A CONTINUOUS PLASMA FINAL FOCUS
David H. Whittum Nov. 1989 22 p Presented at the Workshop on the Role of Plasmas in Accelerators, Tsukuba, Japan, 28 Aug. - 1 Sep. 1989 Submitted for publication Sponsored in part by National Lab. for High Energy Physics, Tsukuba, Japan
(Contract DE-AC03-76SF-00098)
(DE90-006096; LBL-27965; CONF-8908209-1) Avail: NTIS HC A03/MF A01

Scaling laws are set down for a plasma cell used for transport, focusing and current neutralization of fine, intense, relativistic electron beams. It is found that there exists a minimum beam spot size, sigma (sub min) approx. (var epsilon)(sub n)(l(sub A)/gamma l)(sup 1/2), in such a focusing system. Propagation issues, including channel formation, synchrotron radiation, beam ionization and instabilities, are discussed. Numerical examples are given for a proof-of-principle experiment at KEK, an application for luminosity enhancement at the SLC, and a hypothetical TeV electron-positron collider. For a TeV collider, it is found that the effect of ion-motion on focusing, and the effect of Buneman instability on current neutralization must be considered. DOE

N90-19025# Oak Ridge National Lab., TN.
FOURTH INTERNATIONAL CONFERENCE ON FUSION REACTOR MATERIALS Foreign Trip Report
E. E. Bloom 24 Jan. 1990 19 p
(Contract DE-AC05-84OR-21400)
(DE90-006142; ORNL/FTR-3519) Avail: NTIS HC A03/MF A01

The proceedings from International Conference on Fusion Reactor Materials (ICFRM-4) is presented, along with the results of several workshops, planning meetings, and laboratory visits made by the travelers. The ICFRM-4 is the major forum to present and exchange information on materials research and development in support of the world's fusion development efforts. About 360 papers were presented by the 347 conference attendees. Highlights of the conference are presented. A proposal by the United States to host ICFRM-5 was accepted by the International Advisory Committee. ORNL will be the host laboratory. A meeting of the DOE/JAERI Annex I Steering Committee to review the U.S./Japan Collaborative Testing of First Wall and Blanket Structural Materials with Mixed Spectrum Fission Reactors was held at JAERI Headquarters on December 1. The Japanese emphasized the critical importance of a resumption of HFIR operation. Even though the HFIR outage has lasted three plus years this program has continued to provide new and important data on materials behavior which has particular relevance to ITER. DOE

N90-19026# Texas Univ., Austin. Inst. for Fusion Studies.
THERMONUCLEAR INSTABILITY OF GLOBAL-TYPE SHEAR ALFVEN MODES
J. W. VanDam, G. Y. Fu, and C. Z. Cheng (Princeton Univ., NJ.) Jan. 1990 39 p
(Contracts DE-FG05-80ET-53088; DE-AC02-76CH-03073)
(DE90-007087; DOE/ET-53088/413; IFSR-413) Avail: NTIS HC A03/MF A01

The effects of thermonuclear alpha particles on the stability of global-type shear Alfven waves in toroidal geometry in an ignition tokamak experiment are described. The presence of finite toroidicity can lead to stabilization of the so-called global shear Alfven eigenmode. However, toroidicity induces a new global shear Alfven eigenmode, which can be strongly destabilized via transit resonance with alpha particles. In the proposed International Thermonuclear Experimental Reactor, due to its large size and low density, this latter mode is found to be benign. DOE

N90-19027# JAYCOR, Torrance, CA. Plasma Technology Div.
DEVELOPMENT OF AN rf-DRIVEN PLASMA NEUTRALIZER FOR NEGATIVE IONS Final Technical Report, 1 Sep. 1988 - 31 Aug. 1989
K. G. Moses, J. R. Trow, and J. C. Dooling 30 Nov. 1989 29 p
(Contract DE-FG03-87ER-52144)
(DE90-007298; DOE/ER-52144/T1; J-550-89-505/2513) Avail: NTIS HC A03/MF A01

The assertion that beams of negative ions can be neutralized more efficiently by impacting a plasma, rather than a cold gas target, is confirmed scientifically by the work of K.H. Berkner et al. What remains to be done is the realization of practical means of generating plasmas efficiently with appropriate integrated line densities (target thickness). The work performed by JAYCOR, under this grant, over the past few years has made significant progress towards that goal. In this work, large volumes of plasma are generated using low-frequency pulsed inductive rf discharges within a ring cusp multipole-magnetic field geometry. These plasmas exhibit sufficient line-integrated electron densities and degrees of ionization to neutralize beams of energetic negative ions whose energies exceed 500 keV. The method of plasma generation and the cell configuration used in these studies are directly applicable to higher energy neutral beam injector systems (NBIS). Innate scalability and modularity of the system design facilitates linear stacking to achieve a desired target thickness. Further, the plasma formation process is accomplished with an electrical economy consistent with increased overall electrical efficiency of the NBIS compared to that possible using a cold gas target. DOE

N90-19028# Sandia National Labs., Albuquerque, NM.
MAGNETOHYDRODYNAMIC MODELING OF PLASMA OPENING SWITCHES AND GAS PUFF PLASMAS
Norman F. Roderick, Steven S. Payne, and James Nicholson Nov. 1989 72 p Prepared in cooperation with New Mexico Univ., Albuquerque
(Contract DE-AC04-76DP-00789)
(DE90-005825; SAND-89-7107) Avail: NTIS HC A04/MF A01

This work performed over this twenty-eight month contract period falls into two categories: studies of fluid plasma and transport properties (specifically, microturbulent resistivity) in opening switch plasmas in support of the SNLA PBFA-2 pulsed power program; and calculations of two-dimensional effects in gas puff plasmas in support of the SNLA NARYA program. Results of this work are reported. DOE

N90-19029# British Columbia Univ., Vancouver. TRIUMF Facility.
COMPUTERIZED ANALYSIS OF HYDROGEN PLASMA IN A COMPACT H(SUP -) CUSP SOURCE
D. H. Yuan, K. Jayamanna, and P. W. Schmor Nov. 1989 11 p Presented at the 5th International Symposium on the Production and Neutralization of Negative Ions and Beams, Upton, NY, 30 Oct. - 3 Nov. 1989
(DE90-006881; TRI-PP-89-100; CONF-891055-12) Avail: NTIS (US Sales Only) HC A03/MF A01

A cylindrical Langmuir probe with diam of 0.5 mm, length of 5 mm and the Laframboise theory are used to give an analysis of the plasma parameters in a H(-) cusp source including temperatures and densities of slow, fast electrons and positive ions in a median density plasma. The iteration technique overcomes the problems of conventional Langmuir probe analysis. A VAX based program is used to control the motion and analyze data from the probe. In this paper, we briefly describe the program and present initial results obtained from a compact H(-) volume multicusp source. DOE

76 SOLID-STATE PHYSICS

Includes superconductivity.

For related information, see also *33 Electronics and Electrical Engineering* and *36 Lasers and Masers.*

N90-19030# Los Alamos National Lab., NM.
LUMINESCENCE FROM DEFECTS AND IMPURITY CENTERS IN YTTRIUM OXIDE
M. S. Jahan, D. W. Cooke, B. L. Bennett, W. L. Hults, M. A. Maez, K. C. Ott, and J. L. Smith 1989 5 p Presented at the Materials Research Society Fall Meeting, Boston, MA, 27 Nov. - 2 Dec. 1989
(Contract W-7405-eng-36)
(DE90-004842; LA-UR-89-4150; CONF-8911?19-46) Avail: NTIS HC A01/MF A01

High purity (99.999 percent) Y2O3 powder is used as a starting material for fabricating high temperature superconductors (HTS), and is frequently found as an unreacted second phase in the final product. We have found that as-received Y2O3 contains Tb(3+) paramagnetic impurity ions as determined by Thermally Simulated Luminescence and emission spectra measurements. Deep luminescence traps (presumably Tb(4+) ions) are formed in Y2O3 when it is exposed to gamma rays, x rays, or fluorescent lights. These deep traps can only be removed by annealing the material to near 1600 C. Given the short coherence length of HTS it is possible that order-of-magnitude variations in the Tb impurity concentration of starting materials may affect the ultimate value of surface resistance (R(sub s)). DOE

N90-19031# Air Force Inst. of Tech., Wright-Patterson AFB, OH. School of Engineering.
LUMINESCENCE OF LANTHANIDES AND ACTINIDES IMPLANTED INTO BINARY III-V SEMICONDUCTORS AND AlGaAs Ph.D. Thesis
Gernot S. Pomrenke Dec. 1989 319 p
(AD-A215759; AFIT/DS/ENP/89-4) Avail: NTIS HC A14/MF A02 CSCL 20/5

Through luminescence experiments it was observed that lanthanides, or rare earths, and also actinides, may be successfully introduced into binary and ternary III-V Group semiconductors. The study supports the feasibility of producing infrared light emitting diodes (LEDs) for the 0.9 to 1.7 micron spectral range. Besides systematic spectral characterization through photoluminescence, excitation mechanisms and decay kinetics were also investigated. Ytterbium, erbium, thulium, praseodymium, and uranium were successfully implanted into GaAs, InP, GaP, AlAs, or AlGaAs as observed through photoluminescence and also verified by secondary ion mass spectrometry (SIMS). The impurities were implanted through high (1 MeV), intermediate (380, 390 keV), and low (140 keV) energy standard and nonstandard implantation methods, followed by post-implantation annealing using both rapid thermal and conventional furnace annealing. Details on the implantation techniques are given and implantation statistics were determined. GRA

N90-19032# Arizona State Univ., Tempe.
PROCEEDINGS OF THE 6TH CONFERENCE ON HOT CARRIERS IN SEMICONDUCTORS
Jul. 1989 73 p Conference held in Scottsdale, AZ, 23-28 Jul. 1989
(AD-A215978) Avail: NTIS HC A04/MF A01 CSCL 20/12

The proceedings are presented for the conference. Some areas of study are: Infrared Studies, Low Dimensional Systems and Super lattices; Optical Studies of Fast Processes I; Hot Carriers in Bulk Materials; Quantum Transport and Modeling; Resonant Tunneling, Chaos, Instabilities, and Impact Ionization; Semiconductor Devices I; Fast Processes in Semiconductors II; Semiconductor Devices II, and Closing Remarks. GRA

N90-19033# Rome Air Development Center, Griffiss AFB, NY.
THE INTERACTION OF POLYCRYSTALLINE COPPER FILMS WITH DILUTE AQUEOUS SOLUTIONS OF CUPRIC CHLORIDE Ph.D. Thesis - Syracuse Univ. Report, Sep. 1987 - Mar. 1989
Lois Harper Walsh Oct. 1989 183 p
(AF Proj. 2306)
(AD-A216465; RADC-TR-89-202) Avail: NTIS HC A09/MF A01 CSCL 07/1

In the electronics industry, thin films of copper deposited on substrates are used as electrically conductive paths to interconnect semiconductor devices and other computer components. The dissolution of copper in a dilute aqueous cupric chloride solution was studied to achieve an understanding of the role microstructure plays in the dissolution process. A multi-technique approach was taken using combinations of solution chemistry, computer modeling, and microstructural characterization techniques to analyze as-received samples and to monitor the dissolution process. This latter approach allowed reaction rates and activation energies to be calculated from speciation concentrations derived from computer modeling of known thermochemical reactions. In conjunction with the solution analysis, surface techniques were used to analyze the concentration distribution of the various elements after sample exposure to the etchant. The etching characteristics of the polycrystalline thin copper films are dependent on the film's microstructure. A procedure is suggested that will aid future researchers in the correlation of microstructure and dissolution characteristics of different copper samples prior to mass production of metallization for microelectronic circuits. GRA

N90-19034# Xerox Palo Alto Research Center, CA.
PULSED LASER DEPOSITION OF HIGH T(SUB c) SUPERCONDUCTING THIN FILMS Final Technical Report, 15 Nov. 1988 - 15 Oct. 1989
James B. Boyce and G. A. Neville Connell 20 Dec. 1989 5 p
(Contract F49620-89-C-0017)
(AD-A216507; AFOSR-89-1875TR) Avail: NTIS HC A01/MF A01 CSCL 09/3

Superconducting thin films have been deposited in-situ on

several substrate materials using pulsed excimer laser deposition. On the standard oxide substrates, excellent films were obtained. They had high transition temperatures with narrow transition widths, metallic conductivity in the normal state, low room-temperature resistivity, high critical currents, c-axis orientation, and epitaxial alignment with the substrate. On the more technologically relevant substrates of sapphire and silicon, world record, though less optimal, results were obtained. The transition temperatures were high and metallic conductivity was obtained in the normal state. However, the room-temperature and microwave surface resistivities were higher and the critical currents lower than for the above substrates. These diminished transport properties correlate with the imperfect alignment and epitaxy of the superconductor substrate. For silicon substrates, a buffer layer is required due to high reactivity even at low temperatures. The best results were obtained on clean, hydrogen-terminated surfaces rather than oxidized silicon. Epitaxial alignment was achieved, but there was a substantial spread in orientations, accounting for the diminished transport properties. GRA

N90-19035# Stanford Univ., CA. Dept. of Materials Science and Engineering.
CRYSTAL GROWTH AND MECHANICAL PROPERTIES OF SEMICONDUCTOR ALLOYS Final Report, 15 Apr. 1988 - 15 Apr. 1989
David A. Stevenson 1 Nov. 1989 47 p
(Grant AF-AFOSR-0158-86; AF Proj. 2306)
(AD-A216697; AFOSR-89-1688TR) Avail: NTIS HC A03/MF A01 CSCL 11/6

We describe a study of the mechanical properties and crystal growth of compound semiconductor alloys. We also investigated experimental conditions that may influence the hardness values and, hence, might explain the large variations in hardness values that are described in literature for many semiconductors, specifically the following: (1) differences in the hardness of different grains, across twins, and as the sample is rotated that may rise from crystal orientation affects; (2) differences in hardness arising from the photoplastic effect; and (3) differences in hardness arising from differences in applied loads during hardness testing. We propose to continue this work by: (1) expanding our study a wider range of composition of ZnTe-CdTe superlattices; (2) investigating both strained layer and lattice matched superlattices of InGaAsP; (3) investigating superlattices of Si and Ge; and (4) investigating creep in HgTe and other semiconductors of relatively low melting temperatures. GRA

N90-19036# Arizona State Univ., Tempe. Center for Solid State Electronics Research.
TRANSPORT EFFECTS AND SPECTROSCOPY OF DEFECTS IN MICROSTRUCTURES Final Technical Report, 1 Jul. 1987 - 31 Mar. 1989
Alfred M. Kriman 20 Dec. 1989 15 p
(Contract N00014-87-K-0786)
(AD-A216718) Avail: NTIS HC A03/MF A01 CSCL 20/12

Microstructures were studied in the presence of generalized defects, both point repulsive potentials and slit openings in barriers. A number of transport effects were discovered. For isolated defects a resonance was found to occur at the threshold energies of a quantum well. A scaling relation was found for scatterers near single barriers. A rich spectrum of effects was found for single defects near and within double-barrier structures. The electronic analogue of single slit diffraction was shown to exhibit high fringe visibilities. GRA

N90-19037# George Washington Univ., Washington, DC. Dept. of Chemistry.
UNDERSTANDING ELECTRONEGATIVE EFFECTS IN CORE-LEVEL ELECTRON SPECTROSCOPIES; APPLICATION TO THE HIGH TEMPERATURE SUPERCONDUCTORS Interim Technical Report
David E. Ramaker Dec. 1989 9 p
(Contract N00014-89-J-1103)
(AD-A216728; TR-52) Avail: NTIS HC A02/MF A01 CSCL 20/5

The nature of the core level reflected in x ray photoelectron spectroscopy, Auger electron spectroscopy, and x ray absorption near edge structure is considered. An understanding of the effects of anion and cation electronegativity on spectra for the transition metal halides is obtained. This knowledge is applied to understand similar spectra for the high temperature superconductors. GRA

N90-19038# George Washington Univ., Washington, DC. Dept. of Chemistry.
ABSOLUTE CROSS-SECTIONS FOR DISSOCIATIVE ELECTRON ATTACHMENT IN O2 CONDENSED ON Kr FILMS Interim Technical Report
H. Sambe, David E. Ramaker, M. Deschenes, A. D. Bass, and L. Sanche Dec. 1989 8 p Submitted for publication
(Contract N00014-89-J-1103)
(AD-A216730; TR-50) Avail: NTIS HC A02/MF A01 CSCL 20/5

The absolute dissociative-electron-attachment cross section for O2 condensed on a Kr film is found to be about 20 times larger than that for gaseous O2. This large enhancement is attributed to a downward energy shift (about 0.9 eV) of the O2-(2 Pi sub u) intermediate state due to electronic polarization of the neighboring Kr atoms. Based on the theory developed by O'Malley Phys. Rev. 150, 14 (1966) and 155, 59 (1967), we have shown that this downward shift increases the dissociative attachment by a factor of 21, through a reduction in the autoionization of the intermediate state. GRA

N90-19039# Sandia National Labs., Albuquerque, NM. Optoelectronic Components Development Div.
A GaAs p-n-p-n THYRISTOR MODEL
Weng W. Chow Nov. 1989 19 p
(Contract DE-AC04-76DP-00789)
(DE90-005757; SAND-89-1044) Avail: NTIS HC A03/MF A01

In the radiation-hardened, optically triggered thyristor development being carried out jointly by Organizations 1141 and 2531, a theoretical model was needed to assist in designing the devices. This model had to accurately predict thyristor performance (e.g., breakover voltage and holding current) for different fabrication and experimental parameters such as doping, layer thickness, temperature, and incident optical intensity. This report describes a mode we are currently developing that is based on treating a p-n-p-n thyristor as coupled p-n-p and n-p-n transistors. This approach has the advantages of providing tractability of the physics that govern thyristor behavior without requiring extensive numerical computations. When benchmarked by a more rigorous (and, consequently, computationally more complicated) treatment, our model should provide accurate and fast screening of a wide range of thyristor configurations. Section 2 describes the general thyristor configuration we wish to investigate. The derivation of the basic equations for our thyristor model is presented in Sections 3. These equations depends on the saturation currents and multiplication factors at each p-n junction, and on the current gains of p-n-p and n-p-n transistors. DOE

N90-19040# Massachusetts Inst. of Tech., Cambridge. Plasma Fusion Center.
MECHANICAL DISTURBANCES IN HIGH-PERFORMANCE SUPERCONDUCTING DIPOLES Final Report, 1 May 1983 - 31 May 1989
Y. Iwasa and O. O. Ige 15 Jan. 1990 164 p
(Contract DE-AC02-83ER-40121)
(DE90-006237; DOE/ER-40121/T2) Avail: NTIS HC A08/MF A01

High-performance superconducting dipoles such as those used in accelerators are susceptible to premature quenches or superconducting-to-normal transitions due to mechanical disturbances, chiefly conductor motion and epoxy cracking. The problem generally gets worse as dipole size increases. Two sets of experiments were conducted to investigate this problem. In the first set, performed at 4.2 K, acoustic emission sensors were used

to monitor disturbances in several 16.6-m long prototype dipoles for the Superconducting Supercollider (SSC) during quench tests. The results of these experiments confirmed our earlier experience with smaller magnets that frictional slip of the superconductor is the primary dissipative mechanism in the magnet structure and the major cause of premature quenches. DOE

N90-19041# Oak Ridge National Lab., TN. Metals and Ceramics Div.
ION IMPLANTATION-INDUCED AMORPHIZATION OF CERAMIC OXIDES
D. F. Pedraza 1989 8 p Presented at the Materials Research Society Fall Meeting, Boston, MA, 27 Nov. - 2 Dec. 1989
(Contract DE-AC05-84OR-21400)
(DE90-006564; CONF-891119-90) Avail: NTIS HC A02/MF A01

A mechanism of amorphization by ion implantation in ceramic oxides is studied using a rate theory approach. It is proposed that the production of highly localized lattice distortions causes lattice destabilization and the ensuing transition to the amorphous state. These distortions can be caused by a large point defect buildup. It is argued that point defect retention occurs because of the impossibility of producing antisite defects. It is proposed that point defects on each sublattice can shield or trap point defects on the other sublattice. Similarly, metallic impurities may shield oxygen vacancies or trap oxygen interstitial ions, preventing anion Frenkel pairs from recombining. These effects are modeled in alpha-alumina for low temperature implantations (e.g., around 78 K), where point defects are immobile. It is shown that, at these temperatures, recombination is strongly hindered by the radiation-induced point defects themselves, rather than by the implanted impurities. The high point defect concentration attained by this mechanism is sufficient to raise the free energy of the crystal above the free energy of the amorphous solid. DOE

N90-19042# Oak Ridge National Lab., TN.
DOPANT SITE LOCATION IN DUAL-IMPLANTED GaP USING (111) PLANAR CHANNELING
N. R. Parikh, C. T. Kao, D. R. Lee, J. Muse, M. L. Swanson, T. E. Haynes, R. Venkatasubramanian, and M. Timmons (Research Triangle Inst., Research Triangle Park, NC.) 1989 6 p Presented at the Materials Research Society Fall Meeting, Boston, MA, 27 Nov. - 2 Dec. 1989
(Contract DE-AC05-84OR-21400)
(DE90-006565; CONF-891119-89) Avail: NTIS HC A02/MF A01

Previous studies have indicated that dual implantation can efficiently introduce group IV dopant onto selected sub-lattice sites in III-V compound semiconductors, thus enhancing electrical activation. This phenomenon was studied in GaP using Rutherford Backscattering Spectroscopy (RBS) to determine the lattice location of Sn atoms. Single crystals of GaP (100) were used which had been implanted at 400 C with (120)Sn(+) following previously implanted (69)Ga(+) or (31)P(+). Energies were selected for equivalent projected ranges, and all species were implanted with doses of 1 x 10(exp 15) atoms/sq cm. Asymmetry in the angular scan of the (111) planar channel was then used to determine the sub-lattice location of the implanted Sn. RBS results indicated that for all implants Sn atoms were substituting Ga and P sites equally. However, Hall effect measurements gave p type conduction for GaP implanted with Sn alone, while those with prior implants of Ga or P resulted in n-type conduction. RBS and Hall effect results are explained by a vacancy complex model. DOE

N90-19043# Oak Ridge National Lab., TN. Solid State Div.
IN SITU GROWTH OF EPITAXIAL SUPERCONDUCTING YBa2Cu3O(7-x) FILMS ON INSULATING SEMICONDUCTING AND FERROELECTRIC K(Ta, Nb)O3 BY PULSED LASER ABLATION
J. W. McCamy (Tennessee Univ., Knoxville.), David P. Norton, Douglas H. Lowndes, L. A. Boatner, D. K. Christen, R. Feenstra, and E. Sonder 1989 5 p Presented at the Materials Research Society Fall Meeting, Boston, MA, 27 Nov. - 2 Dec. 1989
(Contract DE-AC05-84OR-21400)
(DE90-006568; CONF-891119-88) Avail: NTIS HC A01/MF A01

K(Ta,Nb)O3 (KTN) is an interesting substrate for use in studies of epitaxial superconducting film substrate interactions because of a moderate lattice parameter mismatch with YBa2Cu3O(7-x) and great versatility in electrical properties. KTN's properties are easily modified by doping to form an n-type semiconductor and/or a ferroelectric with variable ferroelectric (Tc). As an initial step in exploring such studies, the first epitaxial growth experiments of YBa2Cu3O(7-x) films on insulating, semiconducting and ferroelectric KTN single crystals by pulsed laser ablation were performed. It was found that c-axis-normal epitaxial films can be consistently grown with T(sub sc)(R = 0) greater than 90K, Delta T(sub sc) approx. 1.5K, and J(sub c) greater than 1MA/sq cm on semiconducting and/or insulating KTaO3. However, growth on KNbO3 is problematic because of stresses generated by cooling the substrate through first order structural transitions, at even moderate cooling rates. DOE

N90-19044# Pennsylvania Univ., Philadelphia. Dept. of Physics.
STRUCTURE AND VIBRATIONAL EXCITATIONS OF RECONSTRUCTED SEMICONDUCTOR SURFACES Progress Report
Eugene J. Mele Nov. 1989 6 p
(Contract DE-FG02-84ER-45118)
(DE90-006589; DOE/ER-45118/5) Avail: NTIS HC A02/MF A01

Electronic and structural properties were investigated of As thin films lattice matched to crystalline Si along the (111) orientation, and a general study of the influence of surface stress on surfaces elastic waves. These techniques were also applied to study structure at the NiAl surface, and to study stabilization of novel bulk phases of elemental Cu. Several of these works are still underway and are described in more detail. DOE

N90-19045# Oak Ridge National Lab., TN. Solid State Div.
IN SITU GROWTH OF HIGH QUALITY EPITAXIAL YBa2Cu3O(7-x) THIN FILMS AT MODERATE TEMPERATURES BY PULSED LASER ABLATION
Douglas H. Lowndes, David P. Norton, J. W. McCamy, R. Feenstra, J. D. Budai, D. K. Christen, and D. B. Poker Nov. 1989 4 p Presented at the Materials Research Society Fall Meeting, Boston, MA, 27 Nov. - 2 Dec. 1989 Submitted for publication
(Contract DE-AC05-84OR-21400)
(DE90-006629; CONF-891119-85) Avail: NTIS HC A01/MF A01

Pulsed KrF (248 nm) laser ablation was used for in situ growth of smooth, high quality YBa2Cu3O(7-x) epitaxial films of variable thickness on SrTiO3, KTaO3, LaAlO3, cubic ZrO2, and MgO substrates, at temperatures of approx. 600 to 730 C, without higher temperature post-annealing. A rotating target pellet, line focusing by a single cylindrical lens, laser beam scanning over the target, and laser energy densities approx. 2.5 to 3 J/sq cm can be combined to yield films of completely uniform composition and with approx. 25 percent thickness variation over areas approx. 8 sq cm. The best films have (Tc) greater than 92 K and J(sub c)(H = 0, T = 77 K) greater than 2 MA/sq cm. Film growth procedures are described, together with results of superconducting and normal state transport measurements. DOE

N90-19046# Purdue Univ., West Lafayette, IN. Dept. of Physics.
A STUDY OF THE INTERACTION OF LIGHT WITH SURFACES OF SUB-MICRON DIMENSIONS Progress Report
R. Reifenberger Nov. 1989 8 p
(Contract DE-FG02-84ER-45162)
(DE90-006646; DOE/ER-45162/4) Avail: NTIS HC A02/MF A01

The study of the electronic properties of surfaces with sub-micron size is presented. In previous years, the photoexcitation was studied of electrons from field emission tips by a focused Argon ion laser beam tuned to operate at a specific photon energy.

The photoexcited electrons escape into the vacuum by tunneling through a surface potential barrier which is distorted by the application of a strong electric field. The interest in these experiments lies in a better understanding of the photoexcitation process at low photon energies. The techniques that were developed directly measure the excited state energy distribution of electrons emitted through the surface potential barrier. The basic information gained from this research is relevant to opto-electronic devices which rely on photoexcitation of electrons in the presence of strong interfacial electric fields for their operation. DOE

N90-19047# International Centre for Theoretical Physics, Trieste (Italy).
WHAT INFLUENCES ORDER PARAMETERS ACROSS THE SUPERCONDUCTING PHASE BOUNDARY
M. P. Das Aug. 1989 8 p Submitted for publication
(DE90-610663; IC-89/270) Avail: NTIS (US Sales Only) HC A02/MF A01

Phase diagram of high temperature oxide superconductors in the light of most recent experimental data are discussed. Several issues are raised on the nature of superconducting order parameters along the superconducting phase boundary in terms of normal state properties with a view to examining the mechanism of superconductivity in oxides. DOE

N90-19048# International Centre for Theoretical Physics, Trieste (Italy).
PRESSURE INDUCED SUPERCONDUCTIVITY IN ELEMENTAL SOLIDS
R. Asokamani, G. Subramoniam, S. Sankaralingam, S. Pauline, and R. Umamaheswari (Anna Univ., Madras, India) Sep. 1989 16 p Submitted for publication
(DE90-610664; IC-89/271) Avail: NTIS (US Sales Only) HC A03/MF A01

This paper aims at explaining the phenomenon of pressure induced superconductivity that has been experimentally observed in some of the elemental solids such as black phosphorus, tellurium and iodine. As xenon has been shown to become metallic recently at very high pressure, we predict possible superconductivity in Xe. Our calculations are based on the self-consistent electronic band structure calculations performed on the basis of the LMTO method. The band structure outputs are used to calculate the electron phonon coupling constant and the superconducting transition temperature. DOE

N90-19049# Los Alamos National Lab., NM. Center for Nonlinear Studies.
TODA LATTICE WITH TRANSVERSE DEGREE OF FREEDOM
P. L. Christiansen (Rome Univ., Italy), P. S. Lomdahl, and V. Muto 1989 9 p Presented at the 6th Interdisciplinary Workshop on Nonlinear Coherent Structures in Physics, Mechanics, and Biological Systems, Montpellier, France, Jun. 1989 Submitted for publication Sponsored in part by Julie Damms Studiefond; Danish Technical Research Council; and Consiglio Nazionale delle Ricerche, Rome, Italy
(Contract W-7405-eng-36)
(DE90-002414; LA-UR-89-3575; CONF-8906282-1) Avail: NTIS HC A02/MF A01

A transverse degree of freedom is introduced in the Toda lattice. The corresponding continuum approximations are discussed. DOE

N90-19050# Los Alamos National Lab., NM.
SPECTRAL FUNCTIONS FROM QUANTUM MONTE CARLO
R. N. Silver 1989 6 p Presented at the Conference on High T(sub c) Superconductivity, Los Alamos, NM, 6-9 Dec. 1989 Submitted for publication Sponsored in part by Ohio Supercomputing Center
(Contract W-7405-eng-36)
(DE90-004870; LA-UR-89-4259; CONF-891274-1) Avail: NTIS HC A02/MF A01

In his review, D. Scalapino identified two serious limitations on the application of Quantum Monte Carlo (QMC) methods to the models of interest in High (Tc) Superconductivity (HTS). One is the sign problem. The other is the analytic continuation problem, which is how to extract electron spectral functions from QMC calculations of the imaginary time Green's functions. Through-out this Symposium on HTS, the spectral functions have been the focus for the discussion of normal state properties including the applicability of band theory, Fermi liquid theory, marginal Fermi liquids, and novel non-perturbative states. DOE

N90-19051# California Univ., Berkeley. Lawrence Berkeley Lab. Materials and Chemical Sciences Div.
DISLOCATION BEHAVIOUR IN Ge(x)Si(1-x) EPILAYERS ON (001) Si
Eric P. Kvam, D. M. Maher, and C. J. Humphreys (Liverpool Univ., England) Nov. 1989 6 p Presented at the Materials Research Society Fall Meeting, Boston, MA, 27 Nov. - 2 Dec. 1989
(Contract DE-AC03-76SF-00098)
(DE90-007063; LBL-28096; CONF-891119-95) Avail: NTIS HC A02/MF A01

It was observed that the nature of misfit dislocations introduced near the critical thickness in Ge(x)Si(1-x) alloys on (001) Si changes markedly in the region 0.4 less than or = x less than or = 0.5. At or below the lower end of this compositional range, the observed microstructure is comprised almost entirely of 60 deg type dislocations, while at the high end, the dislocation structure is almost entirely Lomer edge type. Concurrent with this change, the dislocation density at the top of the epilayer varies by a factor of about 60X. Similarly, several other observables (e.g., dislocation length and spacing) also change appreciably. Part of the reason for the morphological variation seems to be a change in the source for dislocation introduction, in conjunction with a change in glide behavior of dislocations as a function of film thickness. Evidence will be presented that indicates strain, as well as thickness, has a critical value for some dislocation introduction mechanisms, and that these together determine the resulting microstructure. Furthermore, it appears unlikely that the edge-type Lomer dislocations which appear at about x = 0.5 are either introduced directly, by climb, or grown in, as in the 3-D island growth and coalescence which occurs when x approaches unity. Instead, a two-step mechanism involving glissile dislocations is proposed and discussed. DOE

N90-19052# California Univ., Berkeley. Lawrence Berkeley Lab. Materials and Chemical Sciences Div.
MODIFIED DISLOCATION STRUCTURES IN Ge(x)Si(1-x) DOUBLE EPILAYERS ON (001) Si
Eric P. Kvam Nov. 1989 4 p Presented at the Materials Research Society Fall Meeting, Boston, MA, 27 Nov. - 2 Dec. 1989
(Contract DE-AC03-76SF-00098)
(DE90-007078; LBL-28193; CONF-891119-94) Avail: NTIS HC A01/MF A01

Double epilayers of different compositions of Ge(x)Si(1-x) on (001) Si are observed to have dislocation contents which differ markedly from similar single epilayers. An initial epilayer, grown below its critical thickness, underwent substantial misfit dislocation introduction, while a second epilayer, grown at a composition where edge-type misfit dislocations are normally observed to dominate the morphology, contained mostly 60 deg type dislocations. It is suggested that dislocation entry into the upper, high mismatch epilayer allows many dislocations to enter the buried, low mismatch epilayer, and that this in turn affects the dislocation morphology in the upper layer through strain relief. DOE

N90-19053# Wisconsin Univ., Madison. Dept. of Physics.
FUNDAMENTAL STUDIES OF NEW MAGNETIC HETEROSTRUCTURES: THEIR GROWTH, CRYSTALLOGRAPHIC STRUCTURE, MAGNETIC, AND ELECTRONIC PROPERTIES Progress Report
Marshall Onellion and Peter A. Dowben (Syracuse Univ., NY.) 1990 15 p Sponsored in part by IBM

(Contract DE-FG02-87ER-45319; NSF DMR-86-57109)
(DE90-007381; DOE/ER-45319/T1) Avail: NTIS HC A03/MF A01

As part of our request for renewal of our grant, we include this progress report on the significant results obtained under grant number FG02-89ER-45319, Fundamental Studies of New Magnetic Heterostructures: Their Growth, Crystallographic Structure, Magnetic and Electronic Properties, since the inception of the grant. The results include the scientific accomplishments, the instrumentation developed, and the technological applications of our work. Each area is discussed separately and an initial summary of all areas is provided before the detailed discussion. DOE

N90-19054# Virginia Univ., Charlottesville. Dept. of Physics.
SUPERCONDUCTING MATERIALS Performance Report, 1 Sep. 1989 - 31 Aug. 1990
J. Ruvalds 1990 28 p
(Contract DE-FG05-84ER-45113)
(DE90-007419; DOE/ER-45113/5) Avail: NTIS HC A03/MF A01

Our research on high temperature superconductors has recently produced novel insights for the normal state properties of the copper oxides that have been discovered in the last few years. Advances in materials preparation have produced single crystal samples, and sophisticated surface cleavage techniques have unveiled truly metallic behavior in many respects. Thus, the very recent discovery of a Fermi surface in several cuprate superconductors by photoemission spectroscopy has aroused interest in several experimental features which heretofore were in apparent contrast to the expectations for a conventional Fermi Liquid. Hall coefficient measurements revealed mysterious variations as a function of chemical composition and temperature which are difficult to interpret in terms of a single group of carriers such as a small number of holes. We have shown that the mobility of electrons in a nearly half-filled band is very low in the presence of strong electron-electron coupling, and the associated scattering cross section is very sensitive to the alloy composition. We have shown that Fermi surface nesting in conjunction with on-site Coulomb coupling U of intermediate strength, i.e., U comparable to the electric bandwidth W, yields remarkable modifications of the electronic susceptibility (chi) and the quasiparticle damping (Gamma). DOE

N90-19055# Netherlands Energy Research Foundation, Petten.
CRYSTALLOGRAPHIC AND MAGNETIC PROPERTIES OF (C6 D11 ND3)CuBr3 AND (Zn(1-x)Mn(x))3As2: A NEUTRON SCATTERING STUDY Thesis
G. C. deVries Aug. 1989 157 p
(ECN-219; ETN-90-96259) Avail: NTIS HC A08/MF A01

Both compounds were studied with various neutron scattering techniques. The crystallographic properties were investigated by neutron diffraction. Three dimensional long range order and the one dimensional correlations of the magnetic moments were included and the behavior of the linear spin-wave excitations was studied. The realization of low-dimensional systems gives the opportunity of experimental verification of the theoretical predictions. A description of the neutron scattering, theory and instruments is included. ESA

77 THERMODYNAMICS AND STATISTICAL PHYSICS

Includes quantum mechanics; theoretical physics; and Bose and Fermi statistics.

For related information see also *25 Inorganic and Physical Chemistry* and *34 Fluid Mechanics and Heat Transfer.*

N90-19056# Texas Univ., Austin. Dept. of Physics.
THE FREE ENERGY PRINCIPLE, NEGATIVE ENERGY MODES, AND STABILITY
P. J. Morrison and M. Kotschenreuther Oct. 1989 23 p
Presented at the 4th International Workshop on Nonlinear and Turbulent Processes in Physics, Kiev (USSR), 9-22 Oct. 1989
(Contract DE-FG05-80ET-53088)
(DE90-005368; DOE/ET-53088/280; IFSR-280; CONF-891073-4)
Avail: NTIS HC A03/MF A01

The instability of equilibria of Hamiltonian, fluid and plasma dynamical systems is studied. Usually the dynamical equilibrium of interest is not the state of thermodynamic equilibrium, and does not correspond to a free energy minimum. The relaxation of this type of equilibrium is conventionally considered to be initiated by linear instability. However, there are many cases where linear instability is not present, but the equilibrium is nonlinearly unstable to arbitrarily small perturbations. General free energy expressions for determining the presence of linear or nonlinear instabilities is the subject of study. These expressions are simple and practical, and can be obtained for all equilibria of all ideal fluid and plasma models. By free energy, it is meant that the energy change upon perturbations of the equilibrium that respect dynamical phase space constraints. This quantity is measured by a self-adjoint quadratic form, called delta (sup 2)F. The free energy can result in instability when delta (sup 2)F is indefinite; i.e., there exist accessible perturbations that lower the free energy of the system. DOE

N90-19057# Air Force Inst. of Tech., Wright-Patterson AFB, OH. School of Engineering.
TRANSIENT HEAT TRANSFER MEASUREMENTS ON A FLAT PLATE IN TURBULENT FLOW USING AN ELECTRICAL ANALOG M.S. Thesis
Richard K. Rockwell Dec. 1989 159 p
(AD-A216286; AFIT/GAE/ENY/89D-31) Avail: NTIS HC A08/MF A01 CSCL 20/13

An electrical analog, for heat flux measurement from surface mounted thin film temperature gauges, was built and tested. Typically, the determination of heat transfer from thin film gauges requires the numerical evaluation of an integral. The electrical analog enables the heat transfer to be recorded directly without incorporating numerical error. Once built and tested, the analog is used to measure transient flat plate heat flux with free-stream turbulence. The time varying flow is produced using a low pressure shock tube, with free stream turbulence generated by flow injection upstream of the flat plate. The steady flow portion of the test data is compared to the theoretical flat plate solution for constant free stream and constant plate temperatures. A constant temperature hot wire technique is used to determine free stream turbulence. The hot wire procedure requires performing several experiments with the same flow conditions, but different hot wire operating temperatures. GRA

N90-19058# California Univ., Berkeley. Lawrence Berkeley Lab. Theoretical Physics Group.
GEOMETRIC CONTINUUM REGULARIZATION OF QUANTUM FIELD THEORY
M. B. Halpern (California Univ., Berkeley.) 8 Nov. 1989 27 p
Presented at the Conference on Probabilistic Methods in Quantum Field Theory and Quantum Gravity, Cargese, France, 21-27 Aug. 1989
(Contract DE-AC03-76SF-00098; NSF PHY-85-15857)
(DE90-006099; LBL-27855; UCB-PTH-22/89; CONF-8908189-2)
Avail: NTIS HC A03/MF A01

An overview of the continuum regularization program is given. The program is traced from its roots in stochastic quantization, with emphasis on the examples of regularized gauge theory, the regularized general nonlinear sigma model and regularized quantum gravity. In its coordinate invariant form, the regularization is seen as entirely geometric: only the supermetric on field deformations is regularized, and the prescription provides universal nonperturbative invariant continuum regularization across all quantum field theory. DOE

N90-19059# Pennsylvania Univ., Philadelphia. Dept. of Chemical Engineering.
THERMODYNAMICS OF SYSTEMS WITH VERY MANY COMPONENTS PHASE EQUILIBRIUM Progress Report
Eduardo Giandt, D. Oct. 1989 14 p

(Contract DE-FG02-88ER-13825)
(DE90-007345; DOE/ER-13825/2) Avail: NTIS HC A03/MF A01

This report covers the activities sponsored at the University of Pennsylvania under Contract No. FG02-87ER-13825. The following is a summary of the main points: The semigrand canonical formalism was developed. This is a new and very efficient method for the determination of phase diagrams to any class of mixtures by computer simulation, equally efficient for any number of components, has been demonstrated for binaries. This approach also allows the calculation of phase equilibrium at much higher densities than could be reached before. Density functional theory is a state-of-the-art technique for the study of non-uniform liquids. It relates the properties of fluids in an external field to those of fluids in a different field. All previous work on mixtures, including those of very many components, was tacitly based on the assumption that the components were not too different, or that the cut was narrow. We have for the first time addressed the opposite case, when the components are extremely dissimilar. We have developed the rather novel and very useful concept of infinitely polydisperse' mixtures. Solid liquid equilibrium (SLE) is the single phenomenon most strongly affected by polydispersity, since the presence of even small amounts of an extraneous component can disrupt, and even completely preclude, crystallization. DOE

80 SOCIAL SCIENCES (GENERAL)

Includes educational matters.

No abstracts in this category.

81 ADMINISTRATION AND MANAGEMENT

Includes management planning and research.

N90-19060# Advisory Group for Aerospace Research and Development, Neuilly-Sur-Seine (France).
CALENDAR OF SELECTED AERONAUTICAL AND SPACE MEETINGS
Dec. 1989 117 p In ENGLISH and FRENCH
(AGARD-CAL-90/1; ISBN-92-835-0536-0) Copyright Avail: NTIS HC A06/MF A01; Non-NATO Nationals requests available only from AGARD/Scientific Publications Executive

Three kinds of events are covered by this calendar: technical meetings, conferences, and symposia; exhibitions and technical displays covering the same field of interest; and educational courses given by specialized institutions. For each meeting, exhibition, or course, the following information is given, where known: reference number, data, location, title and sponsor, keywords, and contact code for inquiries. Included are a keyword index, country codes, and a list of organizations. Author

N90-19061# European Space Agency. European Space Research and Technology Center, ESTEC, Noordwijk (Netherlands). Product Assurance and Safety Dept.
CONFIGURATION MANAGEMENT AND CONTROL FOR ESA SPACE SYSTEMS
Mar. 1989 18 p
(ESA-PSS-01-11-Issue-1; ISSN-0379-4059; ETN-90-96300)
Copyright Avail: NTIS HC A03/MF A01

A specification containing the configuration data management and control program requirements that are associated with and complementary to every other ESA discipline is presented. Policies and procedures for the initialization, preparation, review, approval, release, control and status accounting of all design definition and configuration identification data for spacecraft and associated equipment and software are included. ESA

N90-19062# European Space Agency. European Space Research and Technology Center, ESTEC, Noordwijk (Netherlands). Product Assurance and Safety Dept.
COMPONENT SELECTION, PROCUREMENT AND CONTROL FOR ESA SPACE SYSTEMS
Nov. 1988 34 p
(ESA-PSS-01-60-Issue-2; ISSN-0379-4059; ETN-90-96302)
Copyright Avail: NTIS HC A03/MF A01

A specification establishing the requirements for a component selection, procurement and control program, to be applied by contractors and subcontractors to ESA space systems in which the use of components with specific reliability and quality requirements is mandatory is presented. Component program management, engineering and quality assurance are included. Formats of and guidelines for completing part approval documents and declared components lists are given. Contractor deliverables are summarized. ESA

82 DOCUMENTATION AND INFORMATION SCIENCE

Includes information management; information storage and retrieval technology; technical writing; graphic arts; and micrography.

For computer documentation see *61 Computer Programming and Software.*

N90-19063 Temple Univ., Philadelphia, PA.
TEACHING A NEW METHODOLOGY FOR DESIGNING RELATIONAL DATA BASES: AN EXPERIMENT TESTING THE EFFECTIVENESS OF AN INTELLIGENT TUTORING SYSTEM ON COGNITIVE SKILL ACQUISITION (VOLUMES 1 AND 2) Ph.D. Thesis
Judith Dorph Ahrens 1989 615 p
Avail: Univ. Microfilms Order No. DA8920205

The effectiveness of an intelligent tutoring system for teaching the skills needed to use a new data-modelling methodology developed by the research is investigated. The methodology synthesizes normalized relations directly from single- and multi-valued facts about entities. The methodology was translated into a tutorial presentation and a conceptual schema diagramming technique was developed. A CAI-based experiment with 120 undergraduate and 48 graduate students enrolled in Introduction to MIS courses was made. A pretest was given and a mixed-model experimental design was used. Students learned from either an intelligent or a non-intelligent tutor. The experiment tested the proposition that the intelligent tutor would facilitate the acquisition of skills needed to perform data-modelling tasks. Specific hypotheses tested: comprehension of data analysis concepts, terminology, and the conceptual schema; following procedures for converting the conceptual schema into relations; discriminating among design decision rules; applying the methodology to a data-modelling problem; and performance differences between graduate and undergraduate students. The intelligent tutor was effective for teaching rule-based procedural skills to undergraduates. The conclusions were: (1) other cognitive theories and tutorial techniques should be explored for teaching conceptual and analytical material; (2) the significant performance differences between graduates and undergraduates casts doubt on the validity of using undergraduate students as surrogates for practitioners in information sciences research; (3) individual/group characteristics and problem domain characteristics must be used as independent variables in future research models of cognitive skill acquisition.
Dissert. Abstr.

N90-19064 Houston Univ., TX.
A HUMAN FACTORS EXPERIMENTAL COMPARISON OF TWO DATABASE QUERY LANGUAGES Ph.D. Thesis

Minnie Yi-Miin Yen 1989 280 p
Avail: Univ. Microfilms Order No. DA8926459

Modern data base management systems include a variety of different types of languages: data definition languages, data manipulation languages, host languages and query languages. Query language are defined as special purpose languages used in a DBMS environment that are typically interactive, on-line, and able to support ad hoc queries for extraction of and simple computation on data base objects. From prior research in using query languages, critical success factors dictate that such languages be easy to learn, easy to understand, and easy to use. Although a query language may influence the user's behavior by its syntax, it is unrealistic to evaluate a query language without considering the influence of its interactive user interface features. This research was a controlled laboratory experiment where 65 subjects interacted with a relational DBMS called REQUEST in an on-line environment. The experimental design used combined a factorial design and a counter-balanced design in an effort to compare SQL and QBE. The results indicated that query language type did affect user performance on paper and pencil tests with QBE users having higher scores than SQL users especially in the construction of complex queries. In contrast, query language type did not have a significant effect on user performance (correctness of code) on an on-line test but did have an effect on the coding and debugging time of the subjects. In addition, query complexity had a significant effect on user performance and user satisfaction was influenced by query language type. Moreover, order of exposure impacted user performance and user satisfaction on the basis of its interaction with query language type, query complexity, and programming experience. Dissert. Abstr.

N90-19065# Prodata, Inc., Alexandria, VA.
DEFENSE TECHNICAL INFORMATION CENTER EXECUTIVE INFORMATION SYSTEM: DOCUMENTATION AND USER'S MANUAL
John E. Felch and Joseph C. Metzger Nov. 1989 110 p
Prepared for Control Data Corp., Alexandria, VA
(Contract MDA903-88-C-0186)
(AD-A216235) Avail: NTIS HC A06/MF A01 CSCL 05/2

Technical documentation and a user's manual are presented. DTIC's Tactical Plan for Automated Management Information Systems, March 1987, defines the need for statistical decision making information and trend reporting. A DTIC-EIS prototype was developed from the SMDR and Checkbook Systems. The prototype was extended to include active use within specific DTIC-L application areas. Data capture for three applications with data organized in an EIS database, supported by presentation methods was accomplished. Hardware and software constraints are presented in order to complete a fully operational DTIC-EIS. GRA

N90-19066# Department of Defense, Washington, DC. Directorate for Information Operations and Reports.
DoD MANUAL FOR STANDARD DATA ELEMENTS
Jul. 1989 1939 p Supersedes report dated Oct. 1986, AD-A177966
(AD-A216441; DIOR/DoD-5000.12-M) Avail: NTIS HC A99/MF E18 CSCL 05/2

The purpose of this manual is to provide a current reference source for DoD-approved standard data elements and codes. In addition, it contains general guidelines and criteria for the standardization of data elements and data codes. Sections include: Standardization procedures and criteria, which specifies the procedures for standardizing data elements and codes in the Department of Defense and the criteria to be applied in the standardization process; DoD standard data elements and codes, which contains listings of all DoD standard data elements and data codes by standard reference number, name and keyword out of context; and Obsolete data elements and codes, which lists the obsolete DoD Data elements and data codes in standard reference number order, alphabetically by name, and by keyword out of context. GRA

N90-19067# Massachusetts Inst. of Tech., Cambridge. Lab. for Computer Science.
SPECULATIVE COMPUTATION IN MULTILISP Ph.D. Thesis
Randy Brent Osborne Dec. 1989 266 p
(Contracts N00014-83-K-0125; N00014-84-K-0099)
(AD-A216579; MIT/LCS/TR-464) Avail: NTIS HC A12/MF A02 CSCL 12/1

This thesis demonstrates by experiments, that performing computations in parallel before their results are known to be required can yield performance improvements over conventional approaches to parallel computing. We call such eager computation of expressions speculative computation, as opposed to conventional mandatory computation that is used in almost all contemporary parallel programming languages and systems. The major requirements for speculative computation are a means to control computation to favor the most promising computations, and a means to abort computation and reclaim computation resources. We investigate these requirements in the parallel symbolic language Multilisp and conclude that we need the following support for speculative computation: for controlling computation we need ordering (ranking of computations by their promise), demand transitivity, and modularity, and for reclaiming computation we need explicit, reversible reclamation with automatic naming of descendants. The main contribution of this work is a sponsor model which provides this support for speculative computation in Multilisp. A sponsor is an agent which controls the allocation of resources to computation. This sponsor model handles control and reclamation of computation in a single, elegant framework. We also discuss the optimal scheduling of speculative computation and present new results for optimal scheduling in simple cases. GRA

83 ECONOMICS AND COST ANALYSIS

Includes cost effectiveness studies.

No abstracts in this category.

84 LAW, POLITICAL SCIENCE AND SPACE POLICY

Includes NASA appropriation hearings; aviation law; space law and policy; international law; international cooperation; and patent policy.

No abstracts in this category.

85 URBAN TECHNOLOGY AND TRANSPORTATION

Includes applications of space technology to urban problems; technology transfer; technology assessment; and surface and mass transportation.

For related information see also *03 Air Transportation and Safety, 16 Space Transportation,* and *44 Energy Production and Conversion.*

N90-19068# European Space Agency, Paris (France).
PROMOTION OF EUROPEAN SPACE TECHNOLOGY TRANSFER
T. D. Guyenne, ed. and J. J. Hunt, ed. Nov. 1989 60 p In ENGLISH and FRENCH Workshop held in Versailles, France, 10-11 May 1989
(ESA-SP-1122; ISBN-92-9092-060-2; ISSN-0379-6566;

ETN-90-96227) Copyright Avail: NTIS HC A04/MF A01; ESA Publications Div., ESTEC, Noordwijk, Netherlands, 20 Dutch guilders

The improvement of transfer of technology from space to industrial applications was addressed. Specific examples of successful technology are cited. Identification and evaluation of possible technology transfer are discussed. Legal and financial aspects are considered. Conclusions and recommendations are given including the non-active role to be played by ESA in internal technology transfer policy between space firms. A list of participants is included. For individual titles, see N90-19069 through N90-19082.

N90-19069# European Space Agency, Paris (France).
ESA PROJECT TO PROMOTE AND ASSIST TECHNOLOGY TRANSFER BY INDUSTRY
Anne-Marie Hieronimus *In its* Promotion of European Space Technology Transfer Nov. 1989 p 7-9 (For primary document see N90-19068 11-85)
Copyright Avail: NTIS HC A04/MF A01; ESA Publications Div., ESTEC, Noordwijk, Netherlands, 20 Dutch guilders

An ESA promotional policy, aimed at increasing technology transfer from European space firms generating new technologies for European firms engaged in non space activities, is outlined. The establishment of a Technology Transfer Network is proposed and its objectives described, including the establishment of a data base of available transferable technologies and the regular issue of a publicity brochure on successful transfers. Non intervention by ESA in space industry policy is emphasized. ESA

N90-19070# Strasbourg Univ. (France). Bureau d'Economie Theorique et Appliquee.
SPACE TECHNOLOGY TRANSFERS IN EUROPE [LES TRANSFERTS DE TECHNOLOGIES SPATIALES EN EUROPE]
L. Bach, G. Lambert, J. Schachar, P. Cohendet, and M. J. Ledoux *In* ESA, Promotion of European Space Technology Transfer Nov. 1989 p 11-16 In FRENCH (For primary document see N90-19068 11-85)
Copyright Avail: NTIS HC A04/MF A01; ESA Publications Div., ESTEC, Noordwijk, Netherlands, 20 Dutch guilders

Results on two economic analyses of indirect effects of ESA programs and space technology transfers are presented. The transfers constitute an important part of the indirect effects, which in some cases were empirically measured. They relate to a wide diversity of situations, and the variety of factors contributing to their success or failure create a complex process. The intersection in technology terms largely determines the receptive sectors. But the volume and success of transfers is mainly influenced by the adoption by companies of an active promotion of applications of space technology. ESA

N90-19071# Defence Technology Enterprises Ltd., Milton Keynes (England).
DTE AND SPACE TECHNOLOGY TRANSFER
B. L. Herdan *In* ESA, Promotion of European Space Technology Transfer Nov. 1989 p 17-18 (For primary document see N90-19068 11-85)
Copyright Avail: NTIS HC A04/MF A01; ESA Publications Div., ESTEC, Noordwijk, Netherlands, 20 Dutch guilders

The practical experience acquired by DTE (Defence Technology Enterprises) in over three years of technology transfer operations is described. Lessons were learned, and considerable success was achieved. Many firms benefited from access to technology transferred to them under license by DTE. The relevance of this experience is highlighted with reference to new initiatives now contemplated at European level to improve the commercial exploitation of space technology for non-space applications. ESA

N90-19072# Micro Electronics A.S. Space, Horten (Norway).
PURCHASE OF TECHNOLOGY
S. Bisgaard *In* ESA, Promotion of European Space Technology Transfer Nov. 1989 p 19-20 (For primary document see N90-19068 11-85)
Copyright Avail: NTIS HC A04/MF A01; ESA Publications Div., ESTEC, Noordwijk, Netherlands, 20 Dutch guilders

An example of technology transfer and related spin-offs from space activities is described. From a Norwegian research laboratory, the company AME SPACE obtained Surface Acoustic Wave (SAW) technology for application in a space project. This technology transfer, together with other space related activities, resulted in actual and potential spin-off's inside and outside the space market. It is calculated that these spin-off's are 4 to 5 times the value of ESA funded contracts and that they appear 5 to 10 years later. ESA

N90-19073# Vinten Instruments Ltd., Weybridge (England).
THE BRINGING TO MARKET OF THE RF ALERT (A CASE STUDY IN TECHNOLOGY TRANSFER)
R. Curry *In* ESA, Promotion of European Space Technology Transfer Nov. 1989 p 21-22 (For primary document see N90-19068 11-85)
Copyright Avail: NTIS HC A04/MF A01; ESA Publications Div., ESTEC, Noordwijk, Netherlands, 20 Dutch guilders

Events which resulted in the bringing of the RF alert to market from its beginnings as a spinoff from a piece of military research are chronicled. Market surveys and target product specification are discussed. To start the process of technology transfer the need for access to finance for under taking market surveys and proof-of-principle demonstrations is highlighted. To be effective the broker must have a long term view on the returns and a long term involvement. ESA

N90-19074# Centre National d'Etudes Spatiales, Paris (France).
FRENCH APPROACH TO SPACE TECHNOLOGY TRANSFER
F. Bouzitat *In* ESA, Promotion of European Space Technology Transfer Nov. 1989 p 23-26 (For primary document see N90-19068 11-85)
Copyright Avail: NTIS HC A04/MF A01; ESA Publications Div., ESTEC, Noordwijk, Netherlands, 20 Dutch guilders

The creation of Novespace, within the French national space agency, as a company aimed at opening up the space field to non-space industry is described. The creation has led to greater dynamism in technology transfer activities. The reluctance of industrial manufacturers to discuss matters confidential is discussed. About 100 transferable technologies are so far identified, and the benefits for manufacturers seeking a very specific technology, a market study or a feasibility study associated with a technology transfer are highlighted. ESA

N90-19075# Commission of the European Communities (Luxembourg).
INTRODUCTORY REMARKS FOR THE PANEL DISCUSSIONS ON TECHNOLOGY TRANSFER
B. B. Goodman *In* ESA, Promotion of European Space Technology Transfer Nov. 1989 p 27-28 (For primary document see N90-19068 11-85)
Copyright Avail: NTIS HC A04/MF A01; ESA Publications Div., ESTEC, Noordwijk, Netherlands, 20 Dutch guilders

The steps in the technology transfer process are introduced. They include identification; protection; preliminary evaluation; dissemination; and exploitation process which encompasses definition of market needs, identification of partners, technico-economic merit verification, business plan preparation, and implementation. ESA

N90-19076# Defence Technology Enterprises Ltd., Milton Keynes (England).
METHODOLOGY PANEL
R. S. Holdom *In* ESA, Promotion of European Space Technology Transfer Nov. 1989 p 31-33 (For primary document see N90-19068 11-85)
Copyright Avail: NTIS HC A04/MF A01; ESA Publications Div., ESTEC, Noordwijk, Netherlands, 20 Dutch guilders

Methods, techniques and the problems experienced in the following four main steps of the technology transfer process are

presented: finding sources of technology to meet particular needs and finding surplus technology within an organization for wider exploitation outside; evaluating cases and prioritizing before marketing; finding the outlets; and choosing the right licensees and technology transfer route. ESA

N90-19077# Dornier System G.m.b.H., Friedrichshafen (Germany, F.R.).
PROBLEMS ON TRANSFER OF SPACE TECHNOLOGY TO NON-SPACE AREAS AND SOLUTIONS: LEGAL ASPECTS
E. Wolff *In* ESA, Promotion of European Space Technology Transfer Nov. 1989 p 37-39 (For primary document see N90-19068 11-85)
Copyright Avail: NTIS HC A04/MF A01; ESA Publications Div., ESTEC, Noordwijk, Netherlands, 20 Dutch guilders

The transfer of space-derived technology to non-space industries should be increased and this target is shown to be reachable on the basis of the existing procurement regulations of ESA, relating to intellectual property. It is concluded that the transfer of technology would be facilitated, if industry would protect the results from space contracts to the widest possible extent by patents or other similar forms of legal protection. ESA

N90-19078# Battelle Memorial Inst., Geneva (Switzerland).
IDENTIFICATION OF AND RESPONSE TO MARKET DEMAND
A. Sfiligoj *In* ESA, Promotion of European Space Technology Transfer Nov. 1989 p 41-45 (For primary document see N90-19068 11-85)
Copyright Avail: NTIS HC A04/MF A01; ESA Publications Div., ESTEC, Noordwijk, Netherlands, 20 Dutch guilders

Technology transfer can be defined as the process of exchanging know how among companies that consider a given technology as having a commercial potential that can only be tapped completely by adding the different marketing skills. While space related technologies are very close to defense, the diffusion of know how to wider industrial sectors takes place only rarely. The steps that have to be undertaken in the identification process, and some major alternatives that can be adopted in the response phase, are described. ESA

N90-19079# Societe Bertin et Cie, Plaisir (France).
THE IMPROVEMENT OF TECHNOLOGY TRANSFER FROM SPACE TO INDUSTRY
G. Mordchelles-Regnier and J. L. Lafon *In* ESA, Promotion of European Space Technology Transfer Nov. 1989 p 49-52 (For primary document see N90-19068 11-85)
Copyright Avail: NTIS HC A04/MF A01; ESA Publications Div., ESTEC, Noordwijk, Netherlands, 20 Dutch guilders

Three conditions are included to be of utmost importance. Appropriate transfer agents, such as the Contract Research Organization, must be inserted inside research and development. A small but significant part of the budget must be reserved for the necessary adaptation to non space applications. It is essential to think in terms of real time transfer rather than valorization of past results. ESA

N90-19080# Dornier System G.m.b.H., Friedrichshafen (Germany, F.R.).
INTERNAL TECHNOLOGY TRANSFER
E. F. M. Langelueddecke *In* ESA, Promotion of European Space Technology Transfer Nov. 1989 p 53-55 (For primary document see N90-19068 11-85)
Copyright Avail: NTIS HC A04/MF A01; ESA Publications Div., ESTEC, Noordwijk, Netherlands, 20 Dutch guilders

For an aerospace systems house with considerable diversification of activities, internal technology transfer is of vital interest. Although the effects of technology transfers cannot easily be quantified, the fruitful interaction between the space and nonspace sectors was demonstrated by an in-house study. Various examples of internal technology transfers and synergies are cited and demonstrate that people with ingenuity in the right company work structure are the key to multidisciplinary application of basic technologies or know-how. ESA

N90-19081# Messerschmitt-Boelkow-Blohm G.m.b.H., Munich (Germany, F.R.). Space Systems Group.
MAGNETIC SUSPENSION RAILWAY SYSTEMS BASED ON SPACE TECHNOLOGY
E. Gottzein *In* ESA, Promotion of European Space Technology Transfer Nov. 1989 p 57-59 (For primary document see N90-19068 11-85)
Copyright Avail: NTIS HC A04/MF A01; ESA Publications Div., ESTEC, Noordwijk, Netherlands, 20 Dutch guilders

High speed and urban MAGLEV (magnetic levitation) vehicles were developed as alternatives to conventional railway systems. For distances up to 500 km high speed MAGLEV trains promise to be superior to airplanes with regard to energy consumption and traveling time. Mechanical and electrical modularization and decentralized hierarchical control architectures of the levitation and guidance systems are outstanding characteristics of robust operational vehicles. The key technologies developed, based on know how and methods from spacecraft control system development and qualification, are presented. ESA

N90-19082# Aerospatiale, Les Mureaux (France). Sous-Direction des Produits Nouveaux.
AN EXAMPLE OF TECHNOLOGY TRANSFER BY AEROSPATIALE: FIRE PROTECTION MATERIALS
B. Vivier *In* ESA, Promotion of European Space Technology Transfer Nov. 1989 p 69-70 (For primary document see N90-19068 11-85)
Copyright Avail: NTIS HC A04/MF A01; ESA Publications Div., ESTEC, Noordwijk, Netherlands, 20 Dutch guilders

The transfer of a technology developed for aerospace applications to a small company for industrialization and industrial applications is described. The technology involved relates to a high performance fire protection material developed for the thermal protection of specific equipments on board missiles and launchers. The main steps in the transfer are described, including the review of potential industrial application, selection of a license and adaptation of the fabrication process. A first was isssued by the French navy for protection of safety equipment and storage areas on surface vessels and submarines, and a further application is as an aerocoat on transchannel trains. ESA

88 SPACE SCIENCES (GENERAL)

No abstracts in this category.

89 ASTRONOMY

Includes radio, gamma-ray, and infrared astronomy, and astrometry.

N90-19083 Colorado Univ., Boulder.
PERTURBATIONS OF TEST MASS MOTION IN THE SCHWARZSCHILD SPACETIME USING THE METHOD OF HAMILTON AND JACOBI Ph.D. Thesis
Timothy Daniel Allison 1989 141 p
Avail: Univ. Microfilms Order No. DA8923473

A Hamilton-Jacobi perturbation theory was developed and applied to describe relativistic test mass motion in the Schwarzschild spacetime. The form of Hamiltonian used is rigorously derived from the relativistic Lagrangian. A justification for other choices of Hamiltonians is also given. The results of all the intermediate calculations needed to consider arbitrary perturbations of test mass motion in the Schwarzschild geometry are presented. These results are then used to find the perturbed motion of a test mass due to a slowly spinning, spherically symmetric body. The motion is thoroughly examined for a variety

of special orbits. Of particular interest are the results in the presence of a weak gravitational field. Dissert. Abstr.

N90-19084# European Space Agency, Paris (France).
INFRARED SPECTROSCOPY IN ASTRONOMY
B. H. Kaldeich, ed. Sep. 1989 546 p The 22nd Eslab Symposium was held in Salamanca, Spain, 7-9 Dec. 1988
(ESA-SP-290; ISBN-92-9092-002-5; ISSN-0379-6566;
ETN-90-96225) Copyright Avail: NTIS HC A23/MF A04; ESA Publications Div., ESTEC, Noordwijk, Netherlands, 80 Dutch guilders

The proceedings of the 22nd Eslab Symposium, concerning infrared spectroscopy in astronomy are presented. Infrared radiation studies involving Solar System, interstellar medium, stars, and star formation are included. Investigations of the galactic structure and extragalactic astronomy by means of infrared spectra analysis are discussed. The infrared instrumentation developments and equipment are described. Special attention is given to the Infrared Space Observatory (ISO) instrumental advances, capabilities, and planned missions. For individual titles, see N90-19085 through N90-19167.

N90-19085# Observatoire de Paris-Meudon (France).
IR SPECTROSCOPY OF PLANETS AND SATELLITES; VENUS, MARS, GIANT PLANETS, AND TITAN
Th. Encrenaz *In* ESA, Infrared Spectroscopy in Astronomy Sep. 1989 p 3-14 (For primary document see N90-19084 11-89)
Copyright Avail: NTIS HC A23/MF A04; ESA Publications Div., ESTEC, Noordwijk, Netherlands, 80 Dutch guilders

The infrared (IR) observations of Venus, Mars, giant planets, and Titan are summarized. In the case of Venus, infrared spectroscopy observations on the night side can provide information on the layers probed in the 2 to 3 micron region. Mars is going to be the major objective of planetary space exploration and many questions about its aeronomy, the stability of its atmosphere and the interactions atmosphere/surface may be answered by means of infrared spectroscopy. In the case of the giant planets, most of the knowledge of their atmospheric composition comes from IR spectroscopy. From the IRIS experiment, the H/He ratio is determined on Jupiter, Saturn, and Uranus; these results have important implications upon the evolutionary stage of these planets. ESA

N90-19086# Observatoire de Paris-Meudon (France).
INFRARED COMETARY SPECTROSCOPY
J. Crovisier *In* ESA, Infrared Spectroscopy in Astronomy Sep. 1989 p 15-3 (For primary document see N90-19084 11-89)
Copyright Avail: NTIS HC A23/MF A04; ESA Publications Div., ESTEC, Noordwijk, Netherlands, 80 Dutch guilders

The recent observations and theoretical works concerning cometary molecules, relevant to infrared spectroscopy, are reviewed. Infrared spectroscopy, with microwave and submillimeter spectroscopy, is practically the only remote sensing technique able to study stable molecules sublimed from the nucleus or formed by gas phase chemistry in the inner comets. The recent observations of Comet Halley are considered. The observation of a strong and broad emission of CH-bearing molecules around 3.3 microns are discussed. The analysis shows that detailed models must include collisional excitation radiative transfer and chemical pumping. Considerations for the further evolution of infrared spectroscopy are given. ESA

N90-19087# Ecole Normale Superieure, Paris (France). Radioastronomie.
ANALOGIES BETWEEN COMETARY, INTERPLANETARY, AND INTERSTELLAR MATTER **c90**
J.-L. Puget *In* ESA, Infrared Spectroscopy in Astronomy, Sep. 1989 p 37-39 (For primary document see N90-19084 11-89)
Copyright Avail: NTIS HC A23/MF A04; ESA Publications Div., ESTEC, Noordwijk, Netherlands, 80 Dutch guilders

The analogies between interstellar matter and dust in the solar system (both interplanetary and cometary) are discussed. This is possible, not only because some interstellar particles survived the formation of the solar system and are locked in interplanetary dust, but because the physical processes to which cometary and interplanetary dust are subjected are very similar to those at work in interstellar clouds. The difficulties involving the comparison, the isotopic composition and the organic component are presented. ESA

N90-19088*# Observatoire de Paris-Meudon (France).
MEASUREMENTS OF THE D/H RATIO IN PLANETARY ATMOSPHERES BY GROUND BASED INFRARED SPECTROSCOPY **c91**
C. deBergh, B. L. Lutz, T. Owen, and J.-P. Maillard (Institut d'Astrophysique, Paris, France) *In* ESA, Infrared Spectroscopy in Astronomy, Sep. 1989 p 41-47 (For primary document see N90-19084 11-89)
(Grants NsG-7499; NAGw-1505; NGR-33015741)
Copyright Avail: NTIS HC A23/MF A04; ESA Publications Div., ESTEC, Noordwijk, Netherlands, 80 Dutch guilders CSCL 03B

A systematic study of deuterium in the solar system using the molecules CH3D and HDO as tracers is carried out. For the outer solar system, ground-based spectra of Saturn, Uranus, Neptune and Titan in the region of CH3D absorptions near, 1.6 microns are obtained. The analyses of these spectra required extensive high-resolution laboratory studies of both CH4 and CH3D. For the terrestrial planets, the spectrum of Mars in the region of HDO absorption near 3.7 microns, is recorded. A similar study of Venus is underway. The values of D/H derived from these investigations are used to constrain models for the origin and evolution of the various atmospheres. ESA

N90-19089# European Space Agency. European Space Research and Technology Center, ESTEC, Noordwijk (Netherlands). Space Science Dept.
THE UNIDENTIFIED IR BANDS IN LABORATORY, IN INTERSTELLAR MEDIUM, AND IN COMETS **c90**
L. Colangeli, G. Schwehm, E. Bussoletti, S. Fonti, A. Blanco, and V. Orofino (Lecce Univ., Italy) *In its* Infrared Spectroscopy in Astronomy Sep. 1989 p 49-53 Sponsored in part by the Italian Ministry of Public Education (For primary document see N90-19084 11-89)
(Contracts PSN-018-85; CNR-86-157; CNR-87-01079-02)
Copyright Avail: NTIS HC A23/MF A04; ESA Publications Div., ESTEC, Noordwijk, Netherlands, 80 Dutch guilders

A comparative analysis of infrared spectral properties measured in laboratory for various carbonaceous materials is presented. It is shown that hydrogenated amorphous carbon grains, polycyclic aromatic hydrocarbon mixtures and coal tar present features which match in wavelength position some of the unidentified infrared bands. The experimental results are applied to fit both astronomical and cometary observations. Some suggestions about physico-chemical properties of the unidentified infrared band carriers in space and the relationship between interstellar and cometary materials, are derived. ESA

N90-19090# Observatoire de Paris-Meudon (France).
OBSERVATIONS OF CO ON MARS IN THE INFRARED AND MILLIMETRE RANGE **c91**
Th. Encrenaz, F. Billebaud, E. Lellouch, F. Combes, M. Gerin, J.-P. Maillard, and G. Paubert (Institut de Radio Astronomie Millimetrique, Grenoble, France) *In* ESA, Infrared Spectroscopy in Astronomy Sep. 1989 p 55-5 (For primary document see N90-19084 11-89)
Copyright Avail: NTIS HC A23/MF A04; ESA Publications Div., ESTEC, Noordwijk, Netherlands, 80 Dutch guilders

Millimeter observation of Mars in the lines of CO and (C-13)O is reported. Evidence of a significant enhancement of the (C-13)O line with respect to the CO line, is observed. Following this result, high resolution observations of the CO vibrational band at 4.7 microns are performed. Several martian lines of (C-12)O-16, (C-13)O, C(O-17) and C(O-18) are identified and analyzed. From the CO lines, a ratio CO/CO2 = 0.0015 is derived. The other

isotopic lines seem to be significantly enhanced with respect to the terrestrial isotopic ratios of carbon and oxygen. Observations of CO and (C-13)O are recorded in the (1 to 0) and (2 to 1) lines at several positions of the martian disk. ESA

N90-19091# Observatoire de Paris-Meudon (France).
NEAR INFRARED SPECTROSCOPY OF MARS: STUDY OF THE SURFACE MINERALOGY **c91**
Th. Encrenaz and P. Bouchet (European Southern Observatory, La Silla, Chile) *In* ESA, Infrared Spectroscopy in Astronomy Sep. 1989 p 61-6 (For primary document see N90-19084 11-89)
Copyright Avail: NTIS HC A23/MF A04; ESA Publications Div., ESTEC, Noordwijk, Netherlands, 80 Dutch guilders

Spectra of Mars are presented. They were recorded in September and October 1988, at the 1 meter telescope of the European Southern Observatory (Chile), between 2.8 and 5.2 microns with a circular variable filter and a resolving power of 60. Spectra were recorded at the center of the disk, the north region and the south pole with an aperture of 5 arcsec. In all the spectra, a strong absorption around 3 microns due to the OH bond in hydrated silicates, is observed. Weak absorption features seem to be superimposed at 3.4 and 3.8 microns in some spectra. Other absorption features are visible. An absorption feature appears around 5.0 microns, which probably indicates the presence of carbon monoxide chemically bound, on the martian surface. ESA

N90-19092# University Coll., Cardiff (Wales). School of Mathematics.
A UNIFIED MODEL FOR THE 3.28 MICRON AND 3.4 MICRON SPECTRAL FEATURE IN THE INTERSTELLAR MEDIUM AND IN COMETS **c90**
F. Hoyle and N. C. Wickramasinghe *In* ESA, Infrared Spectroscopy in Astronomy Sep. 1989 p 67-7 (For primary document see N90-19084 11-89)
Copyright Avail: NTIS HC A23/MF A04; ESA Publications Div., ESTEC, Noordwijk, Netherlands, 80 Dutch guilders

The 3.4 microns absorption feature seen in the spectra of GCIRS7 is shown to be of interstellar rather than circumstellar origin. The implication is that a large fraction of interstellar grains are organic in character. The 3.28 microns feature seen in emission in planetary nebulae is most likely due to aromatic hydrocarbons which are released as degradation products of organic grains. The same aromatic molecules can also explain the 2200 angstroms interstellar extinction feature. The detailed 2.8 to 3.6 microns profiles of IRS7 can be explained on the basis of grains comprised of material closely resembling biogenic matter in their disposition of CH linkages. Dust particles possessing the same detailed spectral characteristics as the interstellar grains are able to match infrared spectra obtained for Halley's comet. ESA

N90-19093# University Coll., Cardiff (Wales). School of Mathematics.
INTERPRETATION OF THE 10 MICRON AND 20 MICRON ABSORPTION BANDS IN COMETS, THE INTERSTELLAR MEDIUM, AND IN AN EXTERNAL GALAXY **c90**
N. C. Wickramasinghe, F. Hoyle, Q. Majeed, S. Al-Mufti, and M. K. Wallis *In* ESA, Infrared Spectroscopy in Astronomy Sep. 1989 p 73-7 (For primary document see N90-19084 11-89)
Copyright Avail: NTIS HC A23/MF A04; ESA Publications Div., ESTEC, Noordwijk, Netherlands, 80 Dutch guilders

The data for the Trapezium nebula in the wave length range of 8 to 30 microns are presented. They are compared with fluxes computed for models involving Murchison meteorite material, crystalline silicates, organic material and biomaterial. Similar mixtures of these components are shown to be indicated from astronomical data of Comet Halley and the extragalactic source M82. ESA

N90-19094# Royal Observatory, Edinburgh (Scotland).
INFRARED SPECTROSCOPY OF DUST
P. F. Roche *In* ESA, Infrared Spectroscopy in Astronomy Sep. 1989 p 79-9 (For primary document see N90-19084 11-89)
Copyright Avail: NTIS HC A23/MF A04; ESA Publications Div., ESTEC, Noordwijk, Netherlands, 80 Dutch guilders

The observations on the field of infrared astronomy of the interstellar dust are reviewed. The focus is on the observed infrared spectral features detected in astronomical sources mentioning photometric studies, which yield information on the dust temperature. Infrared spectroscopy of dust involving stardust, diffuse interstellar medium and molecular clouds are discussed. Through the identification of spectral features, and comparison with laboratory data of known compounds, infrared spectroscopy can reveal the composition of dust species, but does not readily yield information on particle size. ESA

N90-19095# Princeton Univ. Observatory, NJ.
INTERSTELLAR EXTINCTION IN THE INFRARED **c90**
B. T. Draine *In* ESA, Infrared Spectroscopy in Astronomy Sep. 1989 p 93-9 (For primary document see N90-19084 11-89) (Grant NSF AST-86-12013)
Copyright Avail: NTIS HC A23/MF A04; ESA Publications Div., ESTEC, Noordwijk, Netherlands, 80 Dutch guilders

Extinction by interstellar dust at infrared wavelengths is reviewed. For wavelengths between 0.7 and 7 microns the observed extinction, both in the Galaxy and in the Magellanic clouds, appears to be consistent with a power law (A sub lambda proportional to lambda to the power of minus 1.75). In the 8 to 30 microns region interstellar extinction is dominated by the 9.7 microns and 18 microns silicate features; the absolute strength, the detailed wavelength-dependence of these features, and the possible variation of the profile shape from diffuse clouds to dense clouds, all remain controversial. In the far-infrared, grain emissivity estimates by different authors vary considerably. ESA

N90-19096# Australian Defence Force Academy, Canberra. Dept. of Physics.
SPECTROPOLARIMETRY AS A DIAGNOSTIC OF THE INTERSTELLAR MEDIUM **c90**
D. K. Aitken *In* ESA, Infrared Spectroscopy in Astronomy Sep. 1989 p 99-107 (For primary document see N90-19084 11-89)
Copyright Avail: NTIS HC A23/MF A04; ESA Publications Div., ESTEC, Noordwijk, Netherlands, 80 Dutch guilders

A treatment of the application of infrared spectropolarimetry to the study of the properties of dust grains and their environment, is given. The analysis of the extinction and polarization expected from an arbitrary grain model is outlined. Examples of some of the more recent observational work are presented in terms of their implications for dust grain physics and chemistry and the ambient magnetic field. ESA

N90-19097# Manchester Univ. (England). Dept. of Mathematics.
CHEMISTRY ON INTERSTELLAR GRAINS AND IMPLICATIONS FOR INFRARED SPECTROSCOPY **c90**
T. J. Millar *In* ESA, Infrared Spectroscopy in Astronomy Sep. 1989 p 109-114 (For primary document see N90-19084 11-89)
Copyright Avail: NTIS HC A23/MF A04; ESA Publications Div., ESTEC, Noordwijk, Netherlands, 80 Dutch guilders

The infrared and millimeter wave observations, suggesting that gas-grain interaction is important in dense clouds, are reviewed. This interaction results in the formation of H2O ice in clouds having low extinction. It is shown that the gas extinction molecular cores enables to study grain surface processes. The detection of large saturated molecules indicates that the surface chemistry may be complex. The way in which the unidentified infrared emission bands can be affected by chemical processes is considered. ESA

N90-19098# Max-Planck-Inst. fuer Physik und Astrophysik, Garching (Germany, F.R.). Inst. fuer Extraterrestrische Physik.
PHOTODISSOCIATION REGIONS: OBSERVATIONS AND THEORY **c90**
R. Genzel, A. I. Harris, and J. Stutzki *In* ESA, Infrared Spectroscopy in Astronomy Sep. 1989 p 115-132 (For primary

document see N90-19084 11-89)
Copyright Avail: NTIS HC A23/MF A04; ESA Publications Div., ESTEC, Noordwijk, Netherlands, 80 Dutch guilders

The dissociation of molecules and the ionization of atoms by the far ultraviolet radiation is reviewed. Some basic considerations of early observations and their interpretation are presented. Current observations of photodissociation regions concerning molecular clouds illuminated by nearby hot stars are reported. The results of these observations also illucidate the physical processes in other environments. An overview of present theoretical models is provided. A description of some of the outstanding puzzles is given. ESA

N90-19099*# Arizona State Univ., Tempe. Dept. of Physics.
DUST CONTINUUM SPECTRA FROM MODEL HII REGIONS
P. A. Aannestad and R. J. Emery (Rutherford High Energy Lab., Chilton, England) *In* ESA, Infrared Spectroscopy in Astronomy Sep. 1989 p 133-139 Sponsored in part by NASA, JPL (For primary document see N90-19084 11-89)
Copyright Avail: NTIS HC A23/MF A04; ESA Publications Div., ESTEC, Noordwijk, Netherlands, 80 Dutch guilders CSCL 03A

The infrared spectrum emitted by nebular dust, heated by the ionizing stars in H II blisters and spherical H II regions, is calculated for various model parameters. Absorption of the non-ionizing radiation in a neutral layer is included. Heating by the Lyman alpha photon field is taken into account. The dust is composed of silicate and graphite grains, and evaporation of the grains in the inner region is considered. The models are presented with a view to interpretation of infrared observations of dusty H II regions and can be applied directly to the infrared astronomy satellite survey data. The continuum emission is compared with calculated fine structure line emission. ESA

N90-19100*# National Aeronautics and Space Administration. Ames Research Center, Moffett Field, CA.
IR LINE EMISSION FROM DENSE PHOTODISSOCIATION REGIONS
M. Burton, D. J. Hollenbach, and A. G. G. M. Tielens *In* ESA, Infrared Spectroscopy in Astronomy Sep. 1989 p 141-147 Sponsored by the National Research Council (For primary document see N90-19084 11-89)
Copyright Avail: NTIS HC A23/MF A04; ESA Publications Div., ESTEC, Noordwijk, Netherlands, 80 Dutch guilders CSCL 03A

The results of the study on the molecular and fine structure line emission, from dense photodissociation regions, are discussed. The work is focused on the prediction of the line emission from CO and H2 molecules. It is found that, when the gas density is sufficiently high, self-shielding of the molecules can move the C(+)/CO and H/H2 transitions close to the surfaces of the molecular cloud where they can feel the full effect of heating by the ultraviolet radiation field. Collisional de-excitation of the H2 can move the lower levels towards low temperature emission producing an apparently shocked line ratio for two low-J levels, while the high-J levels retain a fluorescent value. Appreciable emission in high-J CO molecules originates in this warm molecular gas. Comparison with observation suggests that high density clumps are a common phenomena in photodissociation regions. ESA

N90-19101*# National Aeronautics and Space Administration. Ames Research Center, Moffett Field, CA.
AIRBORNE OBSERVATIONS OF THE INFRARED EMISSION BANDS
M. Cohen, J. Bregman, F. C. Witteborn, L. J. Allamandola, D. H. Wooden, A. G. G. M. Tielens, D. M. Rank, and M. Jourdain deMuizon (Leiden Univ., Netherlands) *In* ESA, Infrared Spectroscopy in Astronomy Sep. 1989 p 149-154 (For primary document see N90-19084 11-89)
Copyright Avail: NTIS HC A23/MF A04; ESA Publications Div., ESTEC, Noordwijk, Netherlands, 80 Dutch guilders CSCL 03A

The data concerning low resolution airborne spectra from 5 to 8 microns available for a sample of 40 sources selected from the Infrared Astronomy Satellite low resolution spectral Atlas with polycyclic aromatic hydrocarbon (PAH) emission features, are discussed. A new emission band at 5.2 microns, previously predicted for PAHs, was found in 33 sources; it also correlates with the 7.7 microns band. This extends the spectrum of narrow observed PAH features to 3.3, 5.2, 5.6, 6.2, 6.9, 7.7, 8.7, 11.3, and 12.7 microns. From the data the relative strengths of most of these bands are defined in three separate nebular environments: planetaries, H II regions, and reflection nebulae. The differences in the PAHs spectra in those environments are analyzed. ESA

N90-19102*# Princeton Univ. Observatory, NJ.
IR LINE EMISSION FROM SUPERNOVAE IN MOLECULAR CLOUDS
B. T. Draine and D. Tod Woods *In* ESA, Infrared Spectroscopy in Astronomy Sep. 1989 p 155-159 (For primary document see N90-19084 11-89)
(Grants NGL-31-001-007; NSF AST-86-12013)
Copyright Avail: NTIS HC A23/MF A04; ESA Publications Div., ESTEC, Noordwijk, Netherlands, 80 Dutch guilders CSCL 03A

The absorption of the x rays from a supernova explosion in the surrounding molecular gas is discussed. A supernova explosion in a molecular cloud results in a supernova remnant which radiates a fraction of the approximately 10 to the 51st power erg kinetic energy of the supernova explosion in the form of x rays. The absorption of these x rays in the surrounding molecular gas produces ionization, dissociation, and heating. It is found that a 10(exp 51) erg supernova explosion in a uniform molecular cloud of density equal to 1000 per cubic centimeter results in the emission of photons in the H2 line. This process may contribute appreciably to the strong S(1) line emission seen from some starburst galaxies, such as NGC 6240. ESA

N90-19103# Leiden Univ. (Netherlands). Astrophysics Lab.
INFRARED DIAGNOSTICS FOR INTERSTELLAR SOLID STATE CHEMISTRY
R. Grim *In* ESA, Infrared Spectroscopy in Astronomy Sep. 1989 p 161-167 (For primary document see N90-19084 11-89)
Copyright Avail: NTIS HC A23/MF A04; ESA Publications Div., ESTEC, Noordwijk, Netherlands, 80 Dutch guilders

An overview of the interstellar infrared absorption features is given. The laboratory investigations performed in order to interpret interstellar spectra are considered. The work is focused on the applications of the laboratory work to Infrared Space Observatory (ISO). The infrared spectrum of W33A is presented together with the earlier observations and identifications of grain mantle components. The infrared bands predicted from laboratory research are given. The observations of the diffuse medium in the line of sight towards the Galactic Center is included. ESA

N90-19104# California Inst. of Tech., Pasadena.
INFRARED SPECTROSCOPY AND IMAGING OF SUPERNOVA REMNANTS
J. R. Graham, G. S. Wright, and A. J. Longmore (Royal Norwegian Navy, Haakonsvern.) *In* ESA, Infrared Spectroscopy in Astronomy Sep. 1989 p 169-175 (For primary document see N90-19084 11-89)
Copyright Avail: NTIS HC A23/MF A04; ESA Publications Div., ESTEC, Noordwijk, Netherlands, 80 Dutch guilders

The infrared spectrophotometry and line images of the Crab nebula and Cygnus loop supernova remnants, are presented. In the Crab the filaments have a Fe(II) 1.644 microns/Br gamma ratio value of 10 to 50. H2 emission is found in two filaments, confirming the presence of neutral cores. In the Cygnus loop faint, molecular hydrogen emission is detected in a bright optical filament. An image in the H2 line at 2.122 microns shows that some emission lies beyond the edge of the bright optical emission and is possibly associated with the non-radiative Balmer dominated shocks in this

vicinity. There are also locations where H2 and bright optical line emission are coincident. ESA

N90-19105# Leiden Univ. (Netherlands).
POLYCYCLIC AROMATIC HYDROCARBONS IN THE INFRARED SPECTRA OF IRAS SOURCES
M. JourdaindeMuizon, L. B. dHendencourt, and T. R. Geballe (United Kingdom Infrared Telescope Unit, Hilo, HI.) *In* ESA, Infrared Spectroscopy in Astronomy Sep. 1989 p 177-187 (For primary document see N90-19084 11-89)
Copyright Avail: NTIS HC A23/MF A04; ESA Publications Div., ESTEC, Noordwijk, Netherlands, 80 Dutch guilders

The infrared spectra of the Infrared Astronomy Satellite (IRAS) sources, mainly H II regions and reflection nebulae, are presented. The observations include the IRAS Low Resolution Spectra (LRS) and ground based 3 microns spectra. All sources have strong emission features at 7.7, 8.6 and 11.3 microns in their LRS spectra; in all of them, the strong 3.3 microns emission band, often together with a feature at 3.4 microns and an emission plateau at 3.4 to 3.6 microns are detected. The data are analyzed in the context of the polycyclic aromatic hydrocarbons hypothesis. The size of the molecules and their degree of hydrogenation are investigated. For a few sources, 3 microns spectra at higher resolution reveal the presence of additional emission features in the 3.4 to 3.6 microns region. Possible interpretations for these bands are discussed. New laboratory spectra which show a general fit to the observed spectra are presented. Observational tests are suggested. ESA

N90-19106# Ecole Normale Superieure, Paris (France). Groupe de Physique des Solides.
AN ALMOST TOTAL DISJUNCTION BETWEEN EMISSION AND ABSORPTION DUST FEATURES: WHAT DOES IT TELL US? **c90**
A. Leger, L. B. dHendencourt, L. Verstraete, and P. Ehrenfreund *In* ESA, Infrared Spectroscopy in Astronomy Sep. 1989 p 189-192 (For primary document see N90-19084 11-89)
Copyright Avail: NTIS HC A23/MF A04; ESA Publications Div., ESTEC, Noordwijk, Netherlands, 80 Dutch guilders

The features of absorption and emission spectra of interplanetary dust are analyzed. The absence of overlap between these two spectra is discussed. The comparison between the 3.4 microns band attributed to aliphatic C-H bonds seen in absorption and the 3.3 microns band assigned to aromatic C-H bonds seen only in emission is carried out. An interpretation is proposed. The emission and absorption spectra of the Galaxy M82 central part are shown. The chemical nature of the different populations of the interstellar matter is reviewed. The polycyclic aromatic hydrocarbon and the hydrogenated amorphous carbon models are underlined. ESA

N90-19107*# Aerospace Corp., Los Angeles, CA. Space Sciences Lab.
IRAS LRS SPECTRA OF EXTENDED OBJECTS: THE CRAB NEBULA
D. K. Lynch, J. A. Hackwell, D. J. Edelson, P. Wesselius, R. Olling, and F. P. Israel (Huygens Lab., Leiden, Netherlands) *In* ESA, Infrared Spectroscopy in Astronomy Sep. 1989 p 193-195 Sponsored by the Aerospace Sponsored Research Program (For primary document see N90-19084 11-89)
(Contract JPL-958007)
Copyright Avail: NTIS HC A23/MF A04; ESA Publications Div., ESTEC, Noordwijk, Netherlands, 80 Dutch guilders CSCL 03A

The spectra of extended sources from the raw Infrared Astronomy Satellite (IRAS) Low Resolution Spectrometer (LRS) data, is recovered by means of a nonlinear deconvolution technique built around a maximum entropy algorithm. The results are applied to the Crab Nebula. The deconvolved spectrum of the Crab shows significant departures from a blackbody spectrum, with emission features present at 10.2, 11.3, 12.3 and 12.8 microns. ESA

N90-19108# Stockholm Observatory (Sweden).
WIDE-BEAM BALLOON OBSERVATIONS OF THE 157.7 MICRONS (CII) LINE
H. L. Nordh, S. G. Olofsson, M. Bohlin, U. O. Frisk, and C. V. M. Fridlund (European Space Agency. European Space Research and Technology Center, ESTEC, Noordwijk, Netherlands) *In* ESA, Infrared Spectroscopy in Astronomy Sep. 1989 p 197-201 Sponsored by the Swedish Board for Space Activities and ESTEC (For primary document see N90-19084 11-89)
Copyright Avail: NTIS HC A23/MF A04; ESA Publications Div., ESTEC, Noordwijk, Netherlands, 80 Dutch guilders

The scientific rationale behind the use of a smallsized (30 cm) balloon telescope for wide-beam (11 arc minutes) spectroscopic observations in the far infrared, particularly of the C II line at 157.7 microns is discussed. The technical details of the experiment are summarized. Measurements of W3 performed during a flight in 1987 are reported. The results are shown to be in agreement with published results obtained using the Lear Jet. The prospects of future observations are discussed. ESA

N90-19109# Osservatorio Astrofisico di Arcetri, Florence (Italy).
NEAR INFRARED SPECTROSCOPY OF THE SUPERNOVA REMNANT RCW103
E. Oliva, A. F. M. Moorwood, and I. J. Danziger (European Southern Observatory, Garching, Germany, F.R.) *In* ESA, Infrared Spectroscopy in Astronomy Sep. 1989 p 203-205 (For primary document see N90-19084 11-89)
Copyright Avail: NTIS HC A23/MF A04; ESA Publications Div., ESTEC, Noordwijk, Netherlands, 80 Dutch guilders

The spectroscopic observations of RCW103 supernova remnants, concerning the Fe II, H2, and hydrogen lines, are reported. The RCW103 is the most powerful source of infrared lines emission among the galactic remnants. The flux calibrated spectrum covering the H and K atmospheric windows, the H2 peak and most of the 1.0 to 1.35 microns wavelength region, are given. ESA

N90-19110# Commissariat a l'Energie Atomique, Gif-sur-Yvette (France). Service d'Astrophysique.
A COAL MODEL FOR THE CARRIERS OF THE UNIDENTIFIED IR BANDS **c90**
R. Papoular, J. Conard, M. Guiliano, J. Kister, and G. Mille (Aix-Marseilles Univ., France) *In* ESA, Infrared Spectroscopy in Astronomy Sep. 1989 p 207-211 (For primary document see N90-19084 11-89)
Copyright Avail: NTIS HC A23/MF A04; ESA Publications Div., ESTEC, Noordwijk, Netherlands, 80 Dutch guilders

The unidentified infrared bands are analyzed on the basis of the vitrinite absorbance spectrum. Vitrinite is the organic and major component of coal. Each of the unidentified infrared bands has its counterpart in the vitrinite spectra, which also exhibit a continuum rising toward the blue. The better fit provided by vitrinite over other models is due to the presence of oxygen, as well as hydrogen, in the form of surface functional groups bonded to a bulk, disordered, carbon structure with aliphatic as well as aromatic bonds. The infrared spectrum of vitrinite is analyzed and a comparison with the unidentified bands is carried out. ESA

N90-19111# Centre National de la Recherche Scientifique, Saint Martin d'Heres (France). Lab. de Glaciologie et de Geophysique de l'Environnement.
SPECTROSCOPY AND PHYSICO-CHEMISTRY OF CO:H2O AND CO2:H2O ICES
B. Schmitt, R. Grim, and M. Greenberg (Leiden Univ., Netherlands) *In* ESA, Infrared Spectroscopy in Astronomy Sep. 1989 p 213-219 (For primary document see N90-19084 11-89)
Copyright Avail: NTIS HC A23/MF A04; ESA Publications Div., ESTEC, Noordwijk, Netherlands, 80 Dutch guilders

The results of the laboratory measurements on both the spectral and physical properties of CO:H2O and CO2:H2O ice mixtures are presented. The effects of the composition, the temperature and the thermal history on the H2O (3.1 and 6.0 microns) CO (4.67 microns) and CO2 (4.27 microns) infrared bands are

discussed. It is shown that additional information on the composition and on the history of grain mantles can be obtained from a detailed analysis of these absorption bands. ESA

N90-19112*# Hawaii Univ., Honolulu. Inst. for Astronomy.
MAPPING AND SPECTROSCOPY OF THE 3.3 MICRONS FEATURE IN ORION
K. Sellgren, A. T. Tokunaga, and Y. Nakada (Tokyo Univ., Japan) *In* ESA, Infrared Spectroscopy in Astronomy Sep. 1989 p 221-223 (For primary document see N90-19084 11-89)
(Contract NASw-3159; NSF AST-87-00618; NSF AST-84-20775)
Copyright Avail: NTIS HC A23/MF A04; ESA Publications Div., ESTEC, Noordwijk, Netherlands, 80 Dutch guilders CSCL 03A

The results of spectroscopy of the 3.3 microns feature, H2 emission, and Br alpha, obtained in a spatial cut across the Orion ionization front are presented. The spatial distribution of the 3.3 microns feature peaks between the ionization front and the H2 peak are observed. The shape of the 3.3 microns feature observed at high spectral resolution shows no changes in regions of varying ultraviolet flux and density. The results are discussed in terms of current models for the 3.3 microns emission feature. ESA

N90-19113# Ecole Normale Superieure, Paris (France). Groupe de Physique des Solides.
AN IMPLICATION OF THE IR IDENTIFICATION OF PAHS: THE HEATING OF THE DIFFUSE IS GAS **c90**
L. Verstraete, A. Leger, L. B. dHendencourt, D. Defourneau, and O. Dutuit (Centre National de la Recherche Scientifique, Orsay, France) *In* ESA, Infrared Spectroscopy in Astronomy Sep. 1989 p 225-220 (For primary document see N90-19084 11-89)
Copyright Avail: NTIS HC A23/MF A04; ESA Publications Div., ESTEC, Noordwijk, Netherlands, 80 Dutch guilders

The heating mechanisms of the observed H I diffuse medium warm phase are investigated. The heating due to photoionization of the Polycyclic Aromatic Hydrocarbons (PAHs) is estimated. It is found that PAHs dominate the heating of the cold phase and that it would represent an important fraction of that required for the warm phase. The following topics are discussed: the PAH's photoionization cross sections, the physical quantities for PAH heating and evolution of heating with temperature. ESA

N90-19114# Harvard-Smithsonian Center for Astrophysics, Cambridge, MA.
THE INFRARED SPECTRAL SIGNATURE OF STAR FORMATION **c90**
F. C. Adams *In* ESA, Infrared Spectroscopy in Astronomy Sep. 1989 p 233-243 (For primary document see N90-19084 11-89)
Copyright Avail: NTIS HC A23/MF A04; ESA Publications Div., ESTEC, Noordwijk, Netherlands, 80 Dutch guilders

The current picture of star formation is outlined and the spectral appearance of an evolutionary sequence of young stellar objects is discussed. Protostellar objects, which consist of a central star and disk deeply embedded within an infalling envelope of dust and gas, are considered. It is found that the theoretical spectra are in good agreement with observed infrared spectra of infrared astronomy satellite sources associated with molecular cloud cores. Dust absorption features and the spatial extent of the emitted radiation for these objects are discussed. It is shown that T Tauri stars with excess infrared emission can be understood as young (newly formed) stars with accompanying circumstellar disks. Through theoretical modeling of the spectra, basic disk properties can be derived. ESA

N90-19115*# National Aeronautics and Space Administration. Ames Research Center, Moffett Field, CA.
INFRARED DIAGNOSTICS OF INTERSTELLAR SHOCKS
D. J. Hollenbach, D. F. Chernoff, and C. F. McKee (California Univ., Berkeley.) *In* ESA, Infrared Spectroscopy in Astronomy Sep. 1989 p 245-258 (For primary document see N90-19084 11-89)
(Grant NSF AST-86-15177)
Copyright Avail: NTIS HC A23/MF A04; ESA Publications Div., ESTEC, Noordwijk, Netherlands, 80 Dutch guilders CSCL 03A

The observations and theoretical models concerning interstellar shock waves are discussed. Interstellar shock waves are generated by the supersonic injection of mass into the interstellar medium by young stellar objects, by stellar winds, and by supernovae. Infrared emission lines from the heated, shocked gas provide valuable diagnostics of the density, temperature, velocity field, elemental abundances and extent of the emitting region. It is shown that the comparison of observed spectra from shocked regions with theoretical shock models can provide an estimate of the shock speed and the physical conditions in the preshock gas, including the ionization fraction and the magnetic field strength. ESA

N90-19116# Harvard-Smithsonian Center for Astrophysics, Cambridge, MA.
INFRARED LINE EMISSION FROM HIGH-VELOCITY OUTFLOWS IN STAR-FORMING REGIONS **c90**
G. Melnick *In* ESA, Infrared Spectroscopy in Astronomy Sep. 1989 p 259-268 (For primary document see N90-19084 11-89)
Copyright Avail: NTIS HC A23/MF A04; ESA Publications Div., ESTEC, Noordwijk, Netherlands, 80 Dutch guilders

The ways in which infrared (1 to 200 microns) spectroscopy is used to study high velocity outflows and their interactions with the surrounding molecular gas, are reviewed. It is shown that the near infrared lines of H2, H I, and CO, along with the mid-infrared transition of Si2, and the far infrared lines of OI, CO, OH, and HCN provide direct measurements of the density, temperature, and radiation background at various points in the outflow. In the scope of the work, the following topics are analyzed: the circumstellar environment, the intermediate distance cone, and the interface between the outflow and the parental cloud. ESA

N90-19117# Max-Planck-Inst. fuer Physik und Astrophysik, Garching (Germany, F.R.). Inst. fuer Extraterrestrische Physik.
THE EXCITATION OF MOLECULAR HYDROGEN AND ITS SIGNIFICANCE **c90**
A. Sternberg *In* ESA, Infrared Spectroscopy in Astronomy Sep. 1989 p 269-280 (For primary document see N90-19084 11-89)
Copyright Avail: NTIS HC A23/MF A04; ESA Publications Div., ESTEC, Noordwijk, Netherlands, 80 Dutch guilders

The excitation of molecular hydrogen gas in interstellar environments is reviewed. Observations of infrared H2 emission provide information about gas densities and temperatures, shock velocities, magnetic fields, ultraviolet radiation fields, dust grain properties, interstellar extinction, and molecular formation mechanisms. Some of the recent observational and theoretical developments of interstellar infrared molecular hydrogen emission, are discussed. Emphasis is given to the H2 emission produced in photodissociation regions. Diagnostics of shock versus photo-dissociation region H2 emission are listed. ESA

N90-19118*# National Aeronautics and Space Administration. Ames Research Center, Moffett Field, CA.
HIGH-EXCITATION LINES OF MOLECULAR HYDROGEN: A DISCRIMINANT BETWEEN SHOCK MODELS **c90**
M. Burton, P. Brand, A. Moorhouse, and T. Geballe (Joint Astronomy Centre, Hilo, HI.) *In* ESA, Infrared Spectroscopy in Astronomy Sep. 1989 p 281-285 Sponsored by United Kingdom Science and Engineering Research Council and the National Research Council (For primary document see N90-19084 11-89)
Copyright Avail: NTIS HC A23/MF A04; ESA Publications Div., ESTEC, Noordwijk, Netherlands, 80 Dutch guilders CSCL 03B

The results of column densities of molecular hydrogen, calculated from nineteen infrared line intensities, are discussed. They were measured at peak 1 of the outflow of the Orion molecular

cloud OMC-1. The 1-0 O(7) and 0-0 S(13) lines of H2, at 3.8 microns, are mapped over the source. Their intensity ratio is found to be independent of position in the outflow. These observations are well fitted by a simple cooling-flow model of the line emitting region, but seem to be at variance with predictions of C-shocks current in the literature. ESA

N90-19119# Joint Astronomy Centre, Hilo, HI.
IRCAM OBSERVATIONS OF THE REIPURTH 50 IR SOURCE
M. M. Casali *In* ESA, Infrared Spectroscopy in Astronomy Sep. 1989 p 287-290 (For primary document see N90-19084 11-89)
Copyright Avail: NTIS HC A23/MF A04; ESA Publications Div., ESTEC, Noordwijk, Netherlands, 80 Dutch guilders

The near infrared images of the infrared source associated with the Reipurth 50 variable nebula are discussed. Data is obtained using the infrared camera IRCAM. Images suggest that a single embedded object, visible beyond 2 microns, is the illuminating source of a bent reflection cavity east of the source. An extinction of 20 to 30 visual magnitudes is deduced to the source. The reflection nebula has a blue tip at the furthest point from the source, suggestive of illumination by secondary scattering. ESA

N90-19120# Institut d'Astrophysique, Paris (France).
THE ENVIRONMENT OF YOUNG STELLAR OBJECTS STUDIED BY HIGH-RESOLUTION INFRARED SPECTROSCOPY
J.-P. Maillard and G. F. Michell (Saint Mary's Univ., Halifax, Nova Scotia) *In* ESA, Infrared Spectroscopy in Astronomy Sep. 1989 p 293-297 (For primary document see N90-19084 11-89)
Copyright Avail: NTIS HC A23/MF A04; ESA Publications Div., ESTEC, Noordwijk, Netherlands, 80 Dutch guilders

The observations of luminous embedded young stellar objects at high resolution (8 km/s) in the 4.7 microns region, are reported. The spectra cover most of the M band, showing the lines of the v = 1-0 band of (C-12)O and often of (C-13)O with blueshifted components. The observations of GL 2591, M8-IR, GL 490, W3 IRS5, sources of strong molecular bipolar outflows, and W33A, are reported. This technique is shown to be a very powerful probe of hot gas flows not detected at millimeter wavelengths. In most of the sources the lines are resolved in several distinct velocity components. In W33A, in which the 2140/cm feature of solid CO is detectable, the ratio of solid to gas phase is measured. ESA

N90-19121# European Southern Observatory, Garching (Germany, F.R.).
MOLECULAR HYDROGEN IN THE HII REGION G333.6-0.2 **c90**
A. Monetti and A. F. M. Moorwood · *In* ESA, Infrared Spectroscopy in Astronomy Sep. 1989 p 299-301 (For primary document see N90-19084 11-89)
Copyright Avail: NTIS HC A23/MF A04; ESA Publications Div., ESTEC, Noordwijk, Netherlands, 80 Dutch guilders

The obtained infrared spectral observations and a direct infrared image of the galactic H II region G 333.6-0.2 are discussed. The aim of the analysis is to study the relative distribution of the shocked and the ionized gas components. The K image shows a bright region of approx. 10 arcsec diameter surrounded by extended emission. The H2 and the Br gamma line show nearly the same structure and are concentrated in a (20 by 20 arcsecs) region. The Br gamma emission is approx. 300 times brighter than H2 emission, in the center. The H2 emission outside the central region is measured. The integrated H2 v = 1-0S(1) line intensity from G333.6 is about 10(exp -20 W/sq cm, which is lower than that previously determined from low spectral resolution data. ESA

N90-19122# University Coll., London (England). Dept. of Physics and Astronomy.
PLANETARY NEBULAE **c91**
M. J. Barlow *In* ESA, Infrared Spectroscopy in Astronomy Sep. 1989 p 307-315 (For primary document see N90-19084 11-89)
Copyright Avail: NTIS HC A23/MF A04; ESA Publications Div., ESTEC, Noordwijk, Netherlands, 80 Dutch guilders

The developments that occurred in the field of infrared spectroscopy of planetary nebulae, since 1983, are reviewed. The observations concerning ionic fine structure line emission from planetary nebulae are underlined. The observations and interpretation of molecular hydrogen line emission from planetary nebulae are summarized. The work performed on the identified and unidentified dust emission; features in the infrared spectra and the overall energetics of the continuum dust emission observed from planetary nebulae is discussed. Recent work on the modeling of the dust emission continua and on the derivation of gas-to-dust mass ratios is also reviewed. ESA

N90-19123# Lanchester Polytechnic, Coventry (England). School of Physics and Astronomy.
INFRARED SPECTROSCOPY OF NOVAE AND RELATED OBJECTS
M. Bode *In* ESA, Infrared Spectroscopy in Astronomy Sep. 1989 p 317-327 Sponsored in part by ESA and United Kingdom Science and Engineering Research Council (For primary document see N90-19084 11-89)
Copyright Avail: NTIS HC A23/MF A04; ESA Publications Div., ESTEC, Noordwijk, Netherlands, 80 Dutch guilders

Infrared spectroscopy of classical, dwarf and recurrent novae, is reviewed. The impact of spectroscopy at wavelengths greater than 1 micron on the understanding of objects coming under the blanket title of novae and related stars is analyzed. The work includes the related class of symbiotic stars, some of which also undergo outbursts, and the central systems of which share some common characteristics with their cousins in the above group. Particular attention is paid to classical novae where infrared spectroscopy is invaluable in probing the early chemistry, formation of dust shells, and the origin of coronal line emission seen in many of these objects. ESA

N90-19124# Imperial Coll. of Science and Technology, London (England).
INFRARED SPECTROSCOPY OF SUPERNOVA 1987A
W. P. S. Meikle *In* ESA, Infrared Spectroscopy in Astronomy Sep. 1989 p 329-337 (For primary document see N90-19084 11-89)
Copyright Avail: NTIS HC A23/MF A04; ESA Publications Div., ESTEC, Noordwijk, Netherlands, 80 Dutch guilders

The infrared spectroscopic study of supernova 1987A is carried out. A detailed view of the interior of a supernova explosion is obtained. The supernova 1987A infrared spectrum is analyzed at the early time and by day 200. It is shown that as the supernova aged, forbidden lines became increasingly prominent. About 20 species, including molecules, were identified. Approximate estimates of mass of iron and cobalt in the ejecta were obtained. Comparison of infrared spectral models and observational data is suggested. ESA

N90-19125# Observatoire de Paris-Meudon (France).
HIGH RESOLUTION INFRARED SPECTROSCOPY OF SYMBIOTIC STARS
S. Bensammar *In* ESA, Infrared Spectroscopy in Astronomy Sep. 1989 p 339-341 (For primary document see N90-19084 11-89)
Copyright Avail: NTIS HC A23/MF A04; ESA Publications Div., ESTEC, Noordwijk, Netherlands, 80 Dutch guilders

Early results of high resolution (5,000 to 40,000) infrared spectroscopy (1 to 2.5 microns) of different symbiotic stars are reported. The observation of T GB, RW Hya, Ci Cyg and PU Vul stars is performed with the Fourier transform spectrometer of a 3.6 m telescope. The nature of their cool component is studied and the detected CO absorption lines are discussed. Very different profiles of hydrogen Brackett gamma and helium 10830 angstrom lines are shown for Ci Cyg observed at different phases, while Pu Vul shows very intense emission lines. ESA

N90-19126# Consiglio Nazionale delle Ricerche, Frascati (Italy). Ist. di Fisica dello Spazio Interplanetario.
HERBIG Ae/Be STARS: FINE STRUCTURE FAR-INFRARED LINES
C. Ceccarelli, D. Lorenzetti, P. Saraceno, L. Spinoglio, G. Ingrosso, and F. Strafella (Lecce Univ., Italy) *In* ESA, Infrared Spectroscopy in Astronomy Sep. 1989 p 343-349 (For primary document see N90-19084 11-89)
Copyright Avail: NTIS HC A23/MF A04; ESA Publications Div., ESTEC, Noordwijk, Netherlands, 80 Dutch guilders

The preliminary results on the far infrared fine structure lines in the partially ionized regions around Herbig Ae/Be stars, are presented. An interpretation model is proposed. The main contributions to heating and cooling on a grid of spherical zones, allows an estimate of the line fluxes. The results are compared with the sensitivity of the long wavelength spectrometer on board the future ESA Infrared Space Observatory satellite. ESA

N90-19127# Observatorio Astronomico Nacional, Madrid (Spain).
ICE GRAINS IN THE DUST DISK OF THE BIPOLAR NEBULA M 1-92 **c90**
C. Eiroa and K.-W. Hodapp (Hawaii Univ., Honolulu.) *In* ESA, Infrared Spectroscopy in Astronomy Sep. 1989 p 351-353 (For primary document see N90-19084 11-89)
Copyright Avail: NTIS HC A23/MF A04; ESA Publications Div., ESTEC, Noordwijk, Netherlands, 80 Dutch guilders

The 2.4 to 3.8 microns spectra of the bipolar nebula M 1-92 is investigated. The data is obtained with the cooled grating array spectrometer at the NASA infrared telescope facility. Data is obtained at five positions of the object: one coinciding with the illuminating star, and the rest distributed along the dust torus of the bipolar nebula. No spectral signature is observed at the position of the star. A narrow 3.1 microns absorption is observed in all four positions of the torus. The feature is interpreted as being due to a mixture of pure amorphous and crystalline water ices. ESA

N90-19128# Leiden Univ. (Netherlands).
CO INFRARED BANDS IN ATMOSPHERES OF LONG-PERIOD VARIABLES
A. Heske *In* ESA, Infrared Spectroscopy in Astronomy Sep. 1989 p 355-358 (For primary document see N90-19084 11-89)
Copyright Avail: NTIS HC A23/MF A04; ESA Publications Div., ESTEC, Noordwijk, Netherlands, 80 Dutch guilders

The study of the CO infrared bands in atmospheres of long period variables is presented. The 8 Mira and semiregular variables were observed in the CO fundamental band (4.7 microns) and in the first two overtones (2.3 and 1.55 microns) with low resolution spectroscopy. It is shown that the intensities of the different bands do not follow the Boltzmann distribution for a single temperature. In particular no fundamental band is detected. The width of the second overtone was found to significantly broader than that for the first overtone. The results lead to the conclusion that the different bands are characteristics features for different temperature layers in the atmospheres and circumstellar enevelopes of variables. ESA

N90-19129# Leiden Univ. (Netherlands).
A SURVEY OF PAH EMISSION IN HII REGIONS, PLANETARY AND PROTO-PLANETARY NEBULAE
M. Jourdain deMuizon, P. Cox, and J. Lequeux (Ecole Normale Superieure, Paris, France) *In* ESA, Infrared Spectroscopy in Astronomy Sep. 1989 p 358-362 (For primary document see N90-19084 11-89)
Copyright Avail: NTIS HC A23/MF A04; ESA Publications Div., ESTEC, Noordwijk, Netherlands, 80 Dutch guilders

The results of a systematic investigation of Polycyclic Aromatic Hydrocarbons (PAHs) emission in HII, planetary nebulae and proto-planetary nebulae, are reported. Data is obtained from the low resolution spectra of the Infrared Astronomy Satellite. The results show that: PAHs are formed in carbon rich evolved objects; PAHs emission is ubiquitous in general interstellar medium and requires the presence of ultraviolet photons, in planetary and proto-planetary nebulae, PAHs emission is seen only where an ionizing flux is present and in carbon rich objects. ESA

N90-19130*# Calgary Univ. (Alberta). Dept. of Physics.
UNIDENTIFIED INFRARED FEATURES IN PROTO-PLANETARY NEBULAE
S. Kwok and B. J. Hrivnak (Valparaiso Univ., IN.) *In* ESA, Infrared Spectroscopy in Astronomy Sep. 1989 p 363-366 Sponsored in part by NASA and the Canadian Natural Sciences and Engineering Research Council (For primary document see N90-19084 11-89)
Copyright Avail: NTIS HC A23/MF A04; ESA Publications Div., ESTEC, Noordwijk, Netherlands, 80 Dutch guilders CSCL 03A

The discovery of an unidentified emission feature at 21 microns in the spectra of three protoplanetary nebulae is reported. These objects show large far infrared excess due to a circumstellar dust envelope surrounding a carbon rich central star. Optical, infrared and radio observations of three cool Infrared Astronomy Satellite sources suggest that they are carbon rich objects. Their low resolution spectra show a broad unidentified emission feature at 21 microns which could originate from the bending mode of a hydrocarbon molecule. The similarity of all three objects suggests that this feature is unlikely to be the result of instrumental effects. ESA

N90-19131# Universidad de la Laguna (Spain). Inst. de Astrofisica.
IR SPECTROPHOTOMETRY OF BRIGHT CARBON STARS
C. Lazaro *In* ESA, Infrared Spectroscopy in Astronomy Sep. 1989 p 367-369 (For primary document see N90-19084 11-89)
Copyright Avail: NTIS HC A23/MF A04; ESA Publications Div., ESTEC, Noordwijk, Netherlands, 80 Dutch guilders

The results of medium resolution (R=600) spectrophotometry of 15 bright carbon stars of class N, obtained in the range of lambda:1 to 4.2 microns, are presented. Data is complemented by wide band photometry in JHKLM for a bigger sample. The selected sample of stars does not show evidence of massive circumstellar dust envelopes. The infrared flux is expected to arise from a little disturbed photosphere. The observed flux distributions are compared with those predicted by model atmospheres. The presence, or not, of polyatomic molecules is taken into account. The effective temperatures of the stars is calculated. Important differences arise between the observed spectra and the predictions of models. Their validity, and the possible origins of the disagreement, are discussed. ESA

N90-19132# Catania Astrophysical Observatory (Italy).
DUST IN PLANETARY NEBULAE: IRSPEC OBSERVATIONS IN THE 3.0 MICRON-3.8 MICRON RANGE **c90**
A. Magazzu and G. Strazzulla (Catania Univ., Italy) *In* ESA, Infrared Spectroscopy in Astronomy Sep. 1989 p 371-373 (For primary document see N90-19084 11-89)
Copyright Avail: NTIS HC A23/MF A04; ESA Publications Div., ESTEC, Noordwijk, Netherlands, 80 Dutch guilders

The observations of eight planetary nebulae carried out with the infrared spectrometer, IRSPEC, in the range of 3.0 to 3.8 microns, are reported. They were collected in June 1988 at the European Southern Observatory (Chile) and were performed in a continuous mode with a spectral resolution of about 1100. In the infrared spectra, the unidentified infrared features are observed and discussed in the light of theories concerning dust grain properties. Photometric standard stars are observed in order to data calibrate in flux units. ESA

N90-19133# Osservatorio Astrofisico di Arcetri, Florence (Italy).
NEAR INFRARED (1-4 MICRON) SPECTROSCOPY OF SN1987A
E. Oliva, A. F. M. Moorwood, and I. J. Danziger (European Southern Observatory, Garching, Germany, F.R.) *In* ESA, Infrared

Spectroscopy in Astronomy Sep. 1989 p 375-377 (For primary document see N90-19084 11-89)
Copyright Avail: NTIS HC A23/MF A04; ESA Publications Div., ESTEC, Noordwijk, Netherlands, 80 Dutch guilders

The observations of supernova 1987A between 1.05 and 4.2 microns, at resolving power of 1500, are reported. Data was collected at the European Southern Observatory (Chile), using the grating array infrared spectrometer IRSPEC, during October 1987 and April and October 1988. The main results concerning the red shift of the lines and the forbidden lines are discussed. ESA

N90-19134*# National Aeronautics and Space Administration. Goddard Space Flight Center, Greenbelt, MD.
OBSERVATIONS OF 40-70 MICRON BANDS OF ICE IN IRAS 09371+1212 AND OTHER STARS
A. Omont, S. H. Moseley, T. Forveille, W. Glaccum, P. M. Harvey, and L. Likkel (California Univ., Los Angeles.) *In* ESA, Infrared Spectroscopy in Astronomy Sep. 1989 p 379-380 (For primary document see N90-19084 11-89)
Copyright Avail: NTIS HC A23/MF A04; ESA Publications Div., ESTEC, Noordwijk, Netherlands, 80 Dutch guilders CSCL 03A

The observations of the M giant star, IRAS 09371+1212, in the 40 to 70 microns emission bands, are reported. This star has a circumstellar CO envelope, and a unique infrared color, attributed to ice emission bands. The observations performed in February 1988, using grating spectrometer, showed that the far infrared bands of ice are the strongest known in the sky, and that its dust temperature (50K) is the lowest known for a circumstellar envelope. The 43 microns band of ice is also detected in several very cold circumstellar envelopes. ESA

N90-19135# Imperial Coll. of Science and Technology, London (England).
CARBON MONOXIDE IN SUPERNOVA 1987A **c90**
J. Spyromilio, W. P. S. Meikle, R. C. M. Learner, and D. A. Allen (Anglo-Australian Observatory, Sydney.) *In* ESA, Infrared Spectroscopy in Astronomy Sep. 1989 p 381-384 (For primary document see N90-19084 11-89)
Copyright Avail: NTIS HC A23/MF A04; ESA Publications Div., ESTEC, Noordwijk, Netherlands, 80 Dutch guilders

A model to interpret the supernova 1987A infrared spectra is proposed. Many observations allowed the identification of CO in the supernova spectra. The report considers that the CO forms part of the supernova ejecta and an analysis of the first overtone band using Blotzmann population statistics is presented. The model reproduces well the spectra obtained on days 192 and 255 and implies the presence of about 0.00005 of the solar mass of CO by day 255. By day 284 the fit is less good, due to increasingly prominent emission from other species, possibly in combination with the breakdown of the Blotzmann distribution. ESA

N90-19136# Space Research Organization Netherlands, Utrecht.
PREDICTIONS OF INFRARED RECOMBINATIONS LINES IN STELLAR WINDS OF HOT STARS **c90**
L. H. Strous and H. J. G. L. M. Lamers *In* ESA, Infrared Spectroscopy in Astronomy Sep. 1989 p 385-386 (For primary document see N90-19084 11-89)
Copyright Avail: NTIS HC A23/MF A04; ESA Publications Div., ESTEC, Noordwijk, Netherlands, 80 Dutch guilders

A simple stellar wind model, hydrogenic approximations and scaling laws are used to derive information about recombination lines in the Infrared Space Observatory range (1 to 100 microns). The boundary level from above which recombination lines originate, is estimated for a 40,000 star and the results show that it is in the range n=2 to 10 for the most abundant elements. A simple model to evaluate the population of levels above the boundary level is given. The results are used to produce a table of predictions of fluxes and equivalent widths of recombination lines for H, He, CIII-IV, NIII-V and OIII-V. ESA

N90-19137# Max-Planck-Inst. fuer Kernphysik, Heidelberg (Germany, F.R.).
DETECTION OF SN1986J IN NGC891 AT MILLIMETRE WAVELENGTHS
R. J. Tuffs, R. Chini, and E. Kreysa (Max-Planck-Inst. fuer Radioastronomie, Bonn, Germany, F.R.) *In* ESA, Infrared Spectroscopy in Astronomy Sep. 1989 p 387-390 (For primary document see N90-19084 11-89)
Copyright Avail: NTIS HC A23/MF A04; ESA Publications Div., ESTEC, Noordwijk, Netherlands, 80 Dutch guilders

The observation of supernova 1986j in NGC891 at lambda 1.2 mm and 3 mm at epoch 1986.8, using the 30 m Millimeter Radio Telescope (MRT), is reported. The spectrum observed is flat or rising towards shorter wavelengths. It lies above the extrapolation of the optically thin synchrotron radio spectrum of SN1986j at centimeter wavelengths at a similar epoch. The MRT observations are interpreted as arising from a pulsar powered synchrotron nebula at the center of the expanding layers of supernova ejecta. ESA

N90-19138# London Univ. (England). Dept. of Physics.
JCMT OBSERVATIONS OF THE CIRCUMSTELLAR ENVELOPE IRC+10216
P. G. Williams, G. J. White, and C. A. Sanderson *In* ESA, Infrared Spectroscopy in Astronomy Sep. 1989 p 393-399 (For primary document see N90-19084 11-89)
Copyright Avail: NTIS HC A23/MF A04; ESA Publications Div., ESTEC, Noordwijk, Netherlands, 80 Dutch guilders

The observations of the circumstellar envelope IRC+10216 with the James Clerk Maxwell Telescope (Hawaii) are presented. The radial CO distribution agrees in shape with the Kwan/Linke outflow model, but is lower in intensity by a factor of 0.54. The HCN intensity is nearly double that of CO, but drops off almost twice as rapidly with distance from the source centre. Single spectra at the source centre are also presented for the isotopes (C-13)O, H(C-13)N, C(S-34) and for the lower excitation 3-2 line of HCN and its isotope H(C-13)N. The strength of the HCN lines suggests the dominance of radiative excitation and the existence of additional sources of carbon. The existing data on IRC+10216, is also lacking in reliability, particularly at higher frequencies. A more systematic program of high spatial resolution observations covering a range of excitation energies for several molecules and their isotopes is needed to provide an unambiguous basis for modeling. ESA

N90-19139# Cornell Univ., Ithaca, NY. Dept. of Astronomy.
INFRARED LINES AS PROBES OF GALACTIC STRUCTURE
T. Herter *In* ESA, Infrared Spectroscopy in Astronomy Sep. 1989 p 403-414 (For primary document see N90-19084 11-89)
Copyright Avail: NTIS HC A23/MF A04; ESA Publications Div., ESTEC, Noordwijk, Netherlands, 80 Dutch guilders

The status of infrared, optical and radio observations of H II regions is discussed. These measurements indicate changes in the abundances of O, N, and Ne relative to hydrogen by factors of three or more over the range from 14 kpc to 5 kpc in galactocentric radius. Particular attention is given to the infrared measurements of abundances, which provide a direct means to probe the structure of our galaxy. The implications of the abundance gradient results for galactic nucleosynthesis are discussed. The perspective of infrared measurements in such studies, and the future directions of infrared spectroscopy for exploring galactic structure, are investigated. ESA

N90-19140# Texas Univ., Austin. Dept. of Astronomy.
INFRARED SPECTROSCOPY OF THE CENTRAL FEW PARSECS OF THE GALAXY
J. H. Lacy *In* ESA, Infrared Spectroscopy in Astronomy Sep. 1989 p 415-418 Sponsored by the Texas Advanced Research Program (For primary document see N90-19084 11-89) (Grant NSF AST-85-02401)
Copyright Avail: NTIS HC A23/MF A04; ESA Publications Div., ESTEC, Noordwijk, Netherlands, 80 Dutch guilders

Infrared spectroscopic observations of the Galactic center and their interpretation are discussed. Special attention is given to

attempts to determine whether a massive black hole is present. The mass distribution, through observations of the gas and stellar kinematics, is analyzed. It is pointed out that gas motions indicate the existence of a central object of mass equal to a 3,000,000th of the solar mass. The interpretations of such observations are discussed. The radiation field which excites the gas and the types of stars present is studied. The radiation field may provide evidence to support or deny the dynamical indication of a central black hole, but the evidence is at present ambiguous. It is not yet possible to determine whether a massive black hole exists at the Galactic center. Observations which may resolve the question are discussed. ESA

N90-19141*# Hawaii Univ., Honolulu. Inst. for Astronomy.
STELLAR KINEMATICS IN THE GALACTIC CENTRE c90
M. T. McGinn, K. Sellgren, E. E. Becklin, and D. N. B. Hall *In* ESA, Infrared Spectroscopy in Astronomy Sep. 1989 p 421-424 (For primary document see N90-19084 11-89)
(Contract NASw-3159; NSF AST-87-00618)
Copyright Avail: NTIS HC A23/MF A04; ESA Publications Div., ESTEC, Noordwijk, Netherlands, 80 Dutch guilders CSCL 03B

The observations of the stellar kinematics in the central 8 pc of the Galaxy are presented. It is shown that the spectroscopy of the 2.3 microns CO absorption feature, in late type stars, yields the stellar velocity dispersion and the average stellar radial velocity as a function of galactocentric distance. A sample spectra that illustrates the observed velocity shifts and velocity dispersion is given. The analysis shows that the velocity dispersion of the stars is large, and that it dominates the stellar kinematics. The use of these kinematic data, to probe the mass distribution in the Galactic center, is considered. ESA

N90-19142# Joint Astronomy Centre, Hilo, HI.
AN INFRARED IMAGING FABRY-PEROT STUDY OF THE GALACTIC CENTRE
G. S. Wright, I. S. McLean, and J. Bland (Rice Univ., Houston, TX.) *In* ESA, Infrared Spectroscopy in Astronomy Sep. 1989 p 425-428 (For primary document see N90-19084 11-89)
Copyright Avail: NTIS HC A23/MF A04; ESA Publications Div., ESTEC, Noordwijk, Netherlands, 80 Dutch guilders

The observations of the Galactic center in the Brackett gamma line at 2.166 microns are presented. They were obtained using an imaging Fabry-Perot interferometer and the near infrared camera (IRCAM). The technique allows the obtention of approximately 3,600 spectra in 30 minutes of integration time. The instrumentation and methods used to reconstruct spectra, at each point in the image, are described. Examples of the derived spectra are presented, along with the results of fitting to the line profiles to derive emission line flux images and a relative velocity map. ESA

N90-19143# European Southern Observatory, Garching (Germany, F.R.).
NEAR INFRARED SPECTROSCOPY OF ACTIVE GALAXIES
A. F. M. Moorwood *In* ESA, Infrared Spectroscopy in Astronomy Sep. 1989 p 431-437 (For primary document see N90-19084 11-89)
Copyright Avail: NTIS HC A23/MF A04; ESA Publications Div., ESTEC, Noordwijk, Netherlands, 80 Dutch guilders

Recent progress in applying near infrared spectroscopy to the study of active galactic nuclei is reviewed. This wavelength region contains lines which complement lines in the visible for studies of the reddening and physical conditions. The measurements of hydrogen, helium, O I lines are discussed. The H alpha observations in Seyfert 2 galaxies are presented. The origin of (Fe II) and H2 lines and 3.28 microns feature emission observed in Seyfert type galaxies is considered. Star forming activity and interactions between the active gas and circumstellar gas are discussed. ESA

N90-19144# Imperial Coll. of Science and Technology, London (England). Astrophysics Group.
NEAR-INFRARED SPECTROSCOPY OF STARBURST AND INTERACTING GALAXIES
R. D. Joseph *In* ESA, Infrared Spectroscopy in Astronomy Sep. 1989 p 439-445 (For primary document see N90-19084 11-89)
Copyright Avail: NTIS HC A23/MF A04; ESA Publications Div., ESTEC, Noordwijk, Netherlands, 80 Dutch guilders

An overview of the results concerning near infrared observations, undertaken to date, is presented. The major focus is to illustrate the potential of near infrared spectroscopy to illuminate the physics and astrophysics of starbursts in galaxies. Some of the uncertainties, as well as the conclusion are highlighted. The review leads to the conclusion that the initial exploratory phase of extragalactic near infrared spectroscopy is over. It is shown that with modern infrared instrumentation it is possible to obtain infrared spectra of galaxies throughout a large volume of the local universe. Higher spectral resolution combined with imaging detectors is needed for detailed and quantitative investigation of the astrophysics of individual galaxies. ESA

N90-19145# Royal Observatory, Edinburgh (Scotland).
SPECTROSCOPY OF GALAXIES IN THE MID-INFRARED
P. F. Roche *In* ESA, Infrared Spectroscopy in Astronomy Sep. 1989 p 447-453 (For primary document see N90-19084 11-89)
Copyright Avail: NTIS HC A23/MF A04; ESA Publications Div., ESTEC, Noordwijk, Netherlands, 80 Dutch guilders

The mid-infrared spectral properties of galaxies are described. Because of the sensitivity limitations of existing instruments, observations are limited to those galaxies whose nuclei are bright in the infrared. The emission from active galactic nuclei and from nuclear H II regions is analyzed. The unidentified infrared emission in starburst galaxy nuclei and silicate absorption are discussed. Fine structure emission lines can be used to investigate the excitation of the ionized gas and the temperature. Improved instruments are needed to look at the properties of galaxy disk H II regions and other regions, instead of just the core reachable at present. ESA

N90-19146*# California Univ., Berkeley. Dept. of Physics.
FAR-INFRARED SPECTROSCOPY OF GALAXIES
G. J. Stacey *In* ESA, Infrared Spectroscopy in Astronomy Sep. 1989 p 455-471 (For primary document see N90-19084 11-89)
(Grant NAG2-08)
Copyright Avail: NTIS HC A23/MF A04; ESA Publications Div., ESTEC, Noordwijk, Netherlands, 80 Dutch guilders CSCL 03A

Far infrared (FIR) spectral line emission from galaxies is discussed with respect to past, present and near future observations. A review of the importance of the FIR lines as probes of the interstellar medium is presented. The various fine structure emission lines detected from the archetypal starburst galaxy M82, and the (C II) line radiation which is now observed toward a large variety of external galaxies are discussed. The improvements allowed by the advent of the Stratospheric Observatory For Infrared Astronomy (SOFIA), the Infrared Space Observatory (ISO) and the Space Infrared Telescope Facility (SIRTF) are underlined. ESA

N90-19147# Tel-Aviv Univ. (Israel). Dept. of Astronomy.
INFRARED SPECTROSCOPY OF STAR FORMATION IN GALAXIES: EXTREME CONDITIONS AND VERY SHORT TIME SCALES
S. C. Beck, P. T. P. Ho, and J. L. Turner (California Univ., Los Angeles.) *In* ESA, Infrared Spectroscopy in Astronomy Sep. 1989 p 473-475 (For primary document see N90-19084 11-89)
Copyright Avail: NTIS HC A23/MF A04; ESA Publications Div., ESTEC, Noordwijk, Netherlands, 80 Dutch guilders

The measurements of Brackett alpha and gamma, with a 7.2

arc seconds beam and 350 km/s spectral resolution in 11 infrared bright galaxies, are presented. The fluxes are used as diagnostics of the population of young OB stars. It is observed that: in some galaxies the ratios of Brackett to radio continuum flux are unusual and could indicate the presence of ultra compact HII regions, very low electron temperatures, or widespread departures from Case B recombination; in all galaxies the 10 microns continuum flux exceeds that which can be produced by the Lyman heating of dust. The results lead to the following conclusions: conditions in star formation sources can be quite extreme; Brackett lines are flexible and powerful probes of conditions in external galaxies. ESA

N90-19148# Imperial Coll. of Science and Technology, London (England).
THE STRENGTHS OF THE 2.3 MICRON CO BAND IN LUMINOUS INTERACTING AND MERGING GALAXIES **c90**
R. Doyon, R. D. Joseph, and G. S. Wright (United Kingdom Infrared Telescope Unit, Hilo, HI.) *In* ESA, Infrared Spectroscopy in Astronmy Sep. 1989 p 477-479 (For primary document see N90-19084 11-89)
Copyright Avail: NTIS HC A23/MF A04; ESA Publications Div., ESTEC, Noordwijk, Netherlands, 80 Dutch guilders

Spectra between 2.0 and 2.5 microns are presented for NGC 1614, NGC 2798, NGC 4565, NGC 6240, NGC 253 and ARP 220. It is shown that the strength of the CO band at 2.36 microns in the nucleus of ARP 220 is abnormally strong; it is suggested that this anomaly may be the result of starburst activity. It is also shown that, in the large aperture spectra of ARP 220 and other starburst galaxies, the strength of the CO band is consistent with a normal stellar population typical of a spiral galaxy. This result suggests that the stellar continuum associated with the starburst is very diluted by the normal population, a situation consistent with the starburst being mostly localized in the nucleus. ESA

N90-19149# Cambridge Univ. (England). Inst. of Astronomy.
H-ALPHA EMISSION LINES IN HIGH REDSHIFT QUASARS
B. R. Espey, R. F. Carswell, M. J. Ward, M. G. Smith, and J. A. Bailey (Joint Astronomy Centre, Hilo, HI.) *In* ESA, Infrared Spectroscopy in Astronomy Sep. 1989 p 481-487 Sponsored in part by the United Kingdom Science and Engineering Research Council (For primary document see N90-19084 11-89)
Copyright Avail: NTIS HC A23/MF A04; ESA Publications Div., ESTEC, Noordwijk, Netherlands, 80 Dutch guilders

The infrared spectra of H alpha lines in 18 medium to high redshift quasars, and nearly simultaneous optical spectra, are presented. The infrared spectra is obtained using the Fabry-Perot infrared grating spectrometer. It is observed that H alpha lines redshifted by an average of 1300 km/s with respect to the lines from high ionization species and that the low ionization lines such as O I and Mg II are shifted by similar, or slightly smaller, amounts. The similarity between the velocities of H alpha and Mg II, O I provides some support for models in which the Balmer lines are produced predominantly in a warm HI region, while the Lyman lines arise mainly in a population of optically thin clouds. Data on the change of Ly alpha/H alpha with relative velocity, are also presented. ESA

N90-19150# University Coll., Cardiff (Wales). School of Mathematics.
THE MICROWAVE BACKGROUND IN STEADY-STATE COSMOLOGY **c90**
F. Hoyle and N. C. Wickramasinghe *In* ESA, Infrared Spectroscopy in Astronomy Sep. 1989 p 489-495 (For primary document see N90-19084 11-89)
Copyright Avail: NTIS HC A23/MF A04; ESA Publications Div., ESTEC, Noordwijk, Netherlands, 80 Dutch guilders

The information obtained from the microwave background and the support it brings to the steady state cosmology theory is discussed. The microwave background is explained in terms of an ongoing process. The existence of metallic whiskers in astronomy are analyzed. The implications of the study state condition and the spectrum of the background are explained. Little correspondence with observation and the big bang theory is found, and the possibility of this being the correct interpretation of cosmology is doubted. ESA

N90-19151# European Southern Observatory, Garching (Germany, F.R.). Space Telescope European Coordinating Facility.
A SEARCH FOR THE CO FEATURE IN ACTIVE GALACTIC NUCLEI
L. Hunt and J. Melnick (European Southern Observatory, La Silla, Chile) *In* ESA, Infrared Spectroscopy in Astronomy Sep. 1989 p 497-499 (For primary document see N90-19084 11-89)
Copyright Avail: NTIS HC A23/MF A04; ESA Publications Div., ESTEC, Noordwijk, Netherlands, 80 Dutch guilders

The infrared spectroscopic measurements between 2.1 and 2.5 microns of the NGC 3227, NGC 4151 and NGC 2782, are presented. In the study of active galaxies an alternative approach to answer the question concerning the source of the ionizing continuum is to search for observational evidence of massive star formation. The CO features of the spectra are analyzed. No evidence in the observations is found for a radial increase in the depth of the CO absorption towards the center of the NGC 4151 or NGC 2782. The data suggest the presence of a weak radial gradient in the strength of the CO feature in NGC 3227. ESA

N90-19152# Universidad Autonoma de Madrid, Cantoblanco (Spain). Dept. de Astrofisica.
EVOLUTIONARY SYNTHESIS OF THE FAR-INFRARED EMISSION IN STARBURST GALAXIES **c90**
J. M. M. Mas-Hesse and D. Kunth (Institut d'Astrophysique, Paris, France) *In* ESA, Infrared Spectroscopy in Astronomy Sep. 1989 p 501-506 (For primary document see N90-19084 11-89)
(Contract CAYCIT-PB-85-60)
Copyright Avail: NTIS HC A23/MF A04; ESA Publications Div., ESTEC, Noordwijk, Netherlands, 80 Dutch guilders

The evolutionary population synthesis models are used to study the Far Infrared (FIR) emission in star forming galaxies. The dust particles, heated by the energetic photons (originated in the young massive stars), reradiate the energy thermally in the FIR. The models can explain the tight correlation between the FIR and the radio emission actually observed. Both the thermal and the non-thermal contribution to the radio continuum are considered. The time evolution of the ratio FIR/LH beta is studied. It appears to be a good age indicator. ESA

N90-19153# European Southern Observatory, Garching (Germany, F.R.).
INFRARED (FeII), H AND H2 LINES IN GALAXY NUCLEI
A. F. M. Moorwood and E. Oliva (Osservatorio Astrofisico di Arcetri, Florence, Italy) *In* ESA, Infrared Spectroscopy in Astronomy Sep. 1989 p 507-509 (For primary document see N90-19084 11-89)
Copyright Avail: NTIS HC A23/MF A04; ESA Publications Div., ESTEC, Noordwijk, Netherlands, 80 Dutch guilders

The preliminary results of the spectroscopic of Fe II, H2 and hydrogen recombination line emission are presented. Selected galaxies from a sample of 35, ranging from pure H II region-like to Seyfert 1, are studied. The studies were carried out with the infrared spectrometer IRSPEC at the European Southern Observatory (Chile) 3.6 m telescope. The observations include measurements of additional lines of diagnostic interest: the H2(2 1S(1)) line at 2.247 microns improved linewidth determinations and some limited spatial mapping. ESA

N90-19154# Universidad de la Laguna (Spain). Inst. de Astrofisica.
INFRARED PROPERTIES OF FIVE SPIRAL GALAXIES **c90**
M. Prieto, A. CamposAguilar, and C. Garcia *In* ESA, Infrared Spectroscopy in Astronomy Sep. 1989 p 511-515 (For primary document see N90-19084 11-89)

Copyright Avail: NTIS HC A23/MF A04; ESA Publications Div., ESTEC, Noordwijk, Netherlands, 80 Dutch guilders

The radial profiles of five spiral galaxies (NGC 5194, NGC 3627, NGC 3351, NGC 5055, NGC 4736) in the J and K filters of the near infrared are presented. They were taken with the 1.5 m Carlos Sanchez Telescope of the Observatorio del Teide (Tenerife). The infrared photometric parameters of the disk and bulge of NGC 5194 (M51), are calculated. The infrared spiral arms in this grand-design galaxy are detected. It is found that all these intermediate type spiral galaxies present characteristic bumps of infrared emission near the center. ESA

N90-19155# Edinburgh Univ. (Scotland). Dept. of Astronomy.
FLUORESCENT MOLECULAR HYDROGEN EMISSION FROM STAR-FORMING GALAXIES **c90**

P. Puxley, T. Hawarden, and M. Mountain (Royal Observatory, Edinburgh, Scotland) *In* ESA, Infrared Spectroscopy in Astronomy Sep. 1989 p 517-520 (For primary document see N90-19084 11-89)

Copyright Avail: NTIS HC A23/MF A04; ESA Publications Div., ESTEC, Noordwijk, Netherlands, 80 Dutch guilders

Near infrared molecular hydrogen emission, detected from the central star forming complexes in nearby spiral galaxies, are presented. In all cases, measurement of several transitions demonstrates that the bulk of the line emitting gas is excited by ultraviolet radiation, and not by shocks. For most galaxies, the ratio of the molecular (v=1-0 S(1)) to atomic (Br gamma) hydrogen line strengths can be quantitatively understood, the emitting regions are supposed to consist of individual hot stars (or small clusters) embedded within the parent molecular clouds or forming blisters at their surface. Large central star clusters may account for the handful of galaxies which display relatively weak H2 emission. ESA

N90-19156# Edinburgh Univ. (Scotland). Dept. of Astronomy.
H53-ALPHA EMISSION FROM M82 **c90**

P. Puxley, P. Brand, T. Moore, M. Mountain, N. Nakai, and T. Yamashita (Nobeyema Solar Radio Observatory, Japan) *In* ESA, Infrared Spectroscopy in Astronomy Sep. 1989 p 521-523 (For primary document see N90-19084 11-89)

Copyright Avail: NTIS HC A23/MF A04; ESA Publications Div., ESTEC, Noordwijk, Netherlands, 80 Dutch guilders

The data concerning the first detection of H53 alpha emission from another galaxy is reported. At the frequency of this transition (43 GHz), spontaneous emission dominates and dust extinction can be ignored. The inferred photoionization rate is a factor of 5 larger than estimates based on large aperture Br alpha observations, due to significant dust attenuation at 4 microns. The implication of this high value of the ionization rate, for the allowed mass range of stars, is considered. ESA

N90-19157# Consiglio Nazionale delle Ricerche, Frascati (Italy). Ist. de Fisica dello Spazio Interplanetario.
FAR INFRARED FINE STRUCTURE LINES IN ACTIVE GALAXIES **c90**

L. Spinoglio and M. A. Malkan (California Univ., Los Angeles.) *In* ESA, Infrared Spectroscopy in Astronomy Sep. 1989 p 525-529 (For primary document see N90-19084 11-89)

Copyright Avail: NTIS HC A23/MF A04; ESA Publications Div., ESTEC, Noordwijk, Netherlands, 80 Dutch guilders

The line fluxes of the far infrared fine structure ionic and atomic transitions in the narrow line regions of active galaxies are predicted. A standard photoionization model is used. Data from the observed flux of the Seyfert 2 galaxy NGC 1068 is analyzed. The standard conditions in active galaxies narrow line regions are assumed. The (C II) 158 microns, (O I) 63 microns, (N III) 57 microns, (N II) 122 microns and (O III) 88 microns and 52 microns are detectable at high resolution (R=10,000) with the long wavelength spectrometer, on board the ESA satellite Infrared Space Observatory. ESA

N90-19158# Max-Planck-Inst. fuer Kernphysik, Heidelberg (Germany, F.R.).
THE CORRELATION BETWEEN RADIO AND FAR-INFRARED EMISSION FOR DISK GALAXIES

H. J. Voelk *In* ESA, Infrared Spectroscopy in Astronomy Sep. 1989 p 531-534 (For primary document see N90-19084 11-89)

Copyright Avail: NTIS HC A23/MF A04; ESA Publications Div., ESTEC, Noordwijk, Netherlands, 80 Dutch guilders

A theory for the correlation of the nonthermal radio continuum emission with the Far Infrared (FIR) emission from disk galaxies is proposed. The spatially integrated emission from each galaxy is considered. It is supposed that the energy source for the FIR emission is essentially instantaneously communicating to the radiating dust grains. The radio luminosity is calculated. It is shown that the net dependence of the radio emission on the spatial average of the magnetic field strength B is rather weak. A correlation between the nonthermal radio emission and the thermal X-ray emission from elliptical galaxies is predicted. Its existence prove that supernova remnants are the basic source of cosmic rays for energies lower or equal to 10 to the 15th power eV. ESA

N90-19159# Joint Astronomy Centre, Hilo, HI.
NEAR INFRARED SPECTROSCOPY AND SPECTROSCOPIC IMAGING OF NGC253

G. S. Wright and R. D. Joseph (Imperial Coll. of Science and Technology, London, England) *In* ESA, Infrared Spectroscopy in Astronomy Sep. 1989 p 535-537 (For primary document see N90-19084 11-89)

Copyright Avail: NTIS HC A23/MF A04; ESA Publications Div., ESTEC, Noordwijk, Netherlands, 80 Dutch guilders

The observations of circular variable filter spectroscopy of NGC 253 are analyzed. The measurements show that shock excited H2 is extended over at least 40 seconds along the major axis. The Brackett gamma and the 1.644 microns (Fe II) line are strong on the nucleus with the 1-0S(1) line of H2 less than half the Br gamma flux. The situation is reversed in the non-nuclear positions with the H2 line the strongest in the spectra. Narrow band H2 images of the central regions of NGC 253 are also presented and discussed. The spectra and the images are used to discuss the excitation mechanisms for the line emission in terms of the nuclear starburst and mass motions along the bar. ESA

N90-19160# Consejo Superior de Investigaciones Cientificas, Madrid (Spain). Instituto de Optica.
MEASUREMENT SYSTEM OF SPECTRAL IRRADIANCE IN THE NEAR INFRARED

P. Corredera, A. Pons, J. Campos, and A. Corrons *In* ESA, Infrared Spectroscopy in Astronomy Sep. 1989 p 541-543 (For primary document see N90-19084 11-89)

Copyright Avail: NTIS HC A23/MF A04; ESA Publications Div., ESTEC, Noordwijk, Netherlands, 80 Dutch guilders

An automatic system for the measurement of the absolute spectral irradiance in the 800 to 2500 nanometer region is described. Direct comparison of radiation source is carried out. The automatic system is constructed to provide calibrated sources for instrument and measurement system calibration. The components of the measurement system, as well as evaluation of the different source of the errors contributing to the uncertainty of spectral irradiance measurements, are described. The main characteristics of the built system, besides the accuracy, are the incorporation of low noise and high sensitivity amplifier and the possibility of automatically controlling the measurement by means of a personal computer. The total estimated uncertainty of the measurement system is evaluated to be less than 1%. ESA

N90-19161# Consejo Superior de Investigaciones Cientificas, Madrid (Spain). Instituto de Optica.
PERFORMANCE PARAMETER CHARACTERISATION OF VARIOUS TYPES OF IR SINGLE ELEMENT DETECTORS **c35**

P. Corredera, J. Campos, A. Pons, and A. Corrons *In* ESA, Infrared Spectroscopy in Astronomy Sep. 1989 p 545-548

(For primary document see N90-19084 11-89)
Copyright Avail: NTIS HC A23/MF A04; ESA Publications Div., ESTEC, Noordwijk, Netherlands, 80 Dutch guilders

The optimum value of performance parameters of several types of infrared (IR) semiconductor detectors is determined. The main objective of this work is to select the most suitable detector to be incorporated as detection system in an IR spectroradiometer for the spectral interval from 1 to 3.5 microns. Five semiconductor based detector types, which are sensitive in the spectral range of interest are studied. The measurements performed are presented together with the results obtained in measuring the electrical noise and the response of these detectors against bias voltage, load resistance and modulation frequency. The calculated normalized detectivity and the detector response are used as a figure of merit to select the detector. ESA

N90-19162# Laboratorium voor Ruimteonderzoek, Utrecht (Netherlands).
THE ISO SHORT WAVELENGTH SPECTROMETER **c35**
Th. deGraauw, D. A. Beintema, A. J. Boonstra, W. Luinge, G. Ploeger, J. Spakman, P. R. Wesselius, K. Wildeman, J. Wijnbergen, and S. W. Drapatz (Max-Planck-Inst. fuer Extraterrestrische Physik, Garching, Germany, F.R.) et al *In* ESA, Infrared Spectroscopy in Astronomy Sep. 1989 p 549-551 (For primary document see N90-19084 11-89)
Copyright Avail: NTIS HC A23/MF A04; ESA Publications Div., ESTEC, Noordwijk, Netherlands, 80 Dutch guilders

The design and development status of the Infrared Space Observatory (ISO) Short Wavelength Spectrometer (SWS) and its sub-units are presented, together with an overview of the scientific capabilities. The SWS, one of the two spectrometer of ISO, is a grating instrument that covers the wavelengths between 2.5 microns and 45 microns at a spectral resolution of 1000. A Fabry-Perot interferometer can be used behind the grating section to achieve a spectral resolution of 20,000 in the wavelength range 15 to 35 microns. ESA

N90-19163# European Space Agency. European Space Research and Technology Center, ESTEC, Noordwijk (Netherlands). Astrophysics Div.
THE INFRARED SPACE OBSERVATORY
M. F. Kessler *In its* Infrared Spectroscopy in Astronomy Sep. 1989 p 553-557 (For primary document see N90-19084 11-89)
Copyright Avail: NTIS HC A23/MF A04; ESA Publications Div., ESTEC, Noordwijk, Netherlands, 80 Dutch guilders

The Infrared Space Observatory (ISO), operating at wavelengths from 3 to 200 microns, is described. The satellite essentially consists of a large cryostat containing about 2300 litres of superfluid helium to maintain the telescope (primary mirror diameter of 60 cm) and the scientific instruments at temperatures between 2 K and 8 K. A pointing accuracy of a few arc seconds is provided by a three-axis-stabilization system. ISO's instrument complement consists of four instruments, namely: an imaging photo-polarimeter (3 to 200 microns), a camera (3 to 17 microns), a short wavelength spectrometer (3 to 45 microns) and a long wavelength spectrometer (45 to 180 microns). ISO's scheduled launch date is May 1993 and it is planned to be operational for at least 18 months. ESA

N90-19164# Max-Planck-Inst. fuer Astronomie, Heidelberg (Germany, F.R.).
SPECTROPHOTOMETRY OF DUST WITH ISOPHOT **c35**
D. Lemke, W. Kraetschmer, R. J. Tuffs, E. Kreysa, and A. Leger (Paris VII Univ., France) *In* ESA, Infrared Spectroscopy in Astronomy Sep. 1989 p 559-561 Sponsored by DFVLR, Porz, Fed. Republic of Germany (For primary document see N90-19084 11-89)
Copyright Avail: NTIS HC A23/MF A04; ESA Publications Div., ESTEC, Noordwijk, Netherlands, 80 Dutch guilders

Isophot, a complementary equipment to the instruments of the Infrared Space Observatory, is described. Isophot is optimized to investigate cosmic dust in all its manifestations. The scientific goals of Isophot are underlined. The minimum flux density detectable at 11 microns is calculated, and the system's sensitivity is analyzed. The filters and the reasons for their use are presented. The possibility of detecting Cirrus features is considered. ESA

N90-19165# Royal Observatory, Edinburgh (Scotland).
AN ADVANCED COOLED GRATING SPECTROMETER FOR UKIRT-CGS4 **c35**
C. M. Mountain, R. Wade, D. J. Robertson, and T. J. Lee *In* ESA, Infrared Spectroscopy in Astronomy Sep. 1989 p 563-566 Sponsored by the United Kingdom Science and Engineering Research Council (For primary document see N90-19084 11-89)
Copyright Avail: NTIS HC A23/MF A04; ESA Publications Div., ESTEC, Noordwijk, Netherlands, 80 Dutch guilders

The main features of the Cooled Grating Spectrometer (CGS4), for the United Kingdom Infrared Telescope (UKIRT), are described. The CGS4 for use at 1 to 5 microns is designed to fully utilize foreseeable arrays and to take maximum advantage of the solid imaging detectors. The spectrometer can use low dispersion first order grating in a back-to-back configuration with a high dispersion echelle, giving wavelength resolutions from approximately 1,000 to 24,000. ESA

N90-19166# Royal Observatory, Edinburgh (Scotland).
THE JAMES CLERK MAXWELL TELESCOPE
W. vanderVeen *In* ESA, Infrared Spectroscopy in Astronomy Sep. 1989 p 567-569 (For primary document see N90-19084 11-89)
(Grant ASTRON-782-374-000)
Copyright Avail: NTIS HC A23/MF A04; ESA Publications Div., ESTEC, Noordwijk, Netherlands, 80 Dutch guilders

The James Clerk Maxwell Telescope (JCMT), instrumentation and proposals are summarized. The JCMT is one of the largest telescopes in the world capable of operating in the millimeter and submillimeter regions, with an antenna diameter of 15 m. The JCMT is situated close to the summit of Mauna Kea (Hawaii), and it came into operation in September 1987. The improvements concerning the accuracy of the telescope surface and the absolute pointing accuracy are considered. The JCMT instrumentation in the future are underlined. ESA

N90-19167# Imperial Coll. of Science and Technology, London (England).
ISOPHOT-S, A LOW RESOLUTION 2.5 TO 12 MICRONS SPECTROMETER FOR ISO **c35**
M. Wells, S. Chakaveh, R. D. Joseph, A. V. Pattni, M. J. Selby, D. Lemke, P. Lutzow-Wentzky, P. Vaughn, and F. Garzon (Universidad de la Laguna, Spain) *In* ESA, Infrared Spectroscopy in Astronomy Sep. 1989 p 571-573 (For primary document see N90-19084 11-89)
Copyright Avail: NTIS HC A23/MF A04; ESA Publications Div., ESTEC, Noordwijk, Netherlands, 80 Dutch guilders

The design, spectral coverage and sensitivity of Isophot-S, one of the four sub-experiments of Isophot, are described. Isophot-S is a low resolution near infrared spectrometer, designed to take full advantage of the Infrared Space Observatory (ISO) telescope with its low infrared background, wide field of view, and the complete absence of atmospheric attenuation. It consists of two grating spectrometers which cover the wavelength ranges 2.5 to 5 microns and 6 to 12 microns at resolutions of 0.04 microns and 0.09 microns respectively. The scientific capabilities of the equipment are underlined. ESA

N90-19168# Office National d'Etudes et de Recherches Aerospatiales, Paris (France).
APPLICATION OF WAVEFRONT ANALYSIS TECHNIQUES TO RESTORING OF IMAGES DEGRADED BY ATMOSPHERIC TURBULENCE Ph.D. Thesis - Paris-Sud Univ.
Jerome Primot 1989 210 p In FRENCH; ENGLISH summary (ONERA-PUBL-1989-1; ISSN-0078-379X; ETN-90-96291) Avail: NTIS HC A10/MF A02

A technique for post-processing the images recorded on a telescope output, in order to recover the theoretical resolution, is

proposed. The originality of the method described is that the data from the pupil and focal planes are processed simultaneously. To do so, a second wavefront analysis channel is placed in parallel with the conventional channel on which the degraded images are recorded. This channel is used to continuously evaluate the optical transfer function. The spatial frequencies of the object which are not totally masked by turbulence can be corrected. The complete processing of a set of pairs is described. The limits of the method are characterized and a laboratory experiment was conducted. The signal-to-noise ratio evaluated for this technique allowed it to be situated, with respect to speckle interferometry and interferometry in the pupil plane for various luminance levels of the observed object. ESA

N90-19169*# Lawrence Livermore National Lab., CA.
GAMMA RAY ASTRONOMY AND BLACK HOLE ASTROPHYSICS
Edison P. Liang 3 Jan. 1990 8 p Presented at the Workshop on High Energy Astrophysics in the 21st Century, Taos, NM, 11-12 Dec. 1989 Submitted for publication Prepared in cooperation with Stanford Univ., CA
(Contract NGR-05-020-668; W-7405-eng-48)
(NASA-CR-186496; NAS 1.26:186496; DE90-007253; UCRL-102659; CONF-891276-3) Avail: NTIS HC A02/MF A01 CSCL 03A

One of the most exciting recent developments in black hole astrophysics is the discovery by the HEAO-3 experiment of transient enhanced MeV gamma ray emissions from Cygnus X-1 and the Galactic Center, and the potentially correlated appearance of the 511 keV annihilation line from the Galactic Center (Ling et al., 1987, Riegler et al., 1985). If these soft gamma ray bumps and annihilation lines can be proven to be universal signatures of black hole accretions, then they will provide a new window on the overall black hole phenomenon from stellar mass black holes to AGNs. Hence it is important for future high energy astrophysics space missions to incorporate the study of soft gamma emissions from black hole candidates as a major component of their scientific goals. This paper discusses these goals. DOE

90 ASTROPHYSICS

Includes cosmology; celestial mechanics; space plasmas; and interstellar and interplanetary gases and dust.
For related information see also *75 Plasma Physics*.

N90-19170# Arizona Univ., Tucson.
ZODIACAL DUST BANDS: THEIR RELATION TO ASTEROID FAMILIES Scientific Report No. 3
Mark V. Sykes 25 Sep. 1989 46 p Submitted for publication
(Contract F19628-87-K-0045)
(AD-A216025; GL-TR-89-0269) Avail: NTIS HC A03/MF A01 CSCL 03/1

A mathematical model of the spatial distribution of orbitally evolved collisional debris is developed which reproduces the zodiacal dust band phenomenon. The resultant torus has maxima in particle density at heliocentric latitudes near the mean proper orbital inclinations of its constituent particles, and near the locus of perihelia and aphelia of the particle orbits. These perihelion and aphelion band pairs are fund to have latitudinal and radial separations which are functions of the orbital elements (a, e, i) of the constituent particles, as well as the dispersions in those elements. Models of dust tori associated with seven asteroid families are generated and compared with observations of the principal dust band. Non-equilibrium models of dust band production and evolution offer a framework, it is found that both Themis and Eosasteroid families are much older than the Koronis family. Dust band particles appear not to have experienced any large orbital decay (more than few tenths of an AU) due to Poynting-Robertson drag. GRA

N90-19171# Chicago Univ., IL.
PARTICLE PHYSICS AND COSMOLOGY Progress Report, Jan. 1988 - Jan. 1990
Michael S. Turner Jan. 1990 14 p
(Contract DE-AC02-80ER-10587)
(DE90-006547; DOE/ER-10587/T11) Avail: NTIS HC A03/MF A01

This report contains brief discussions on the following topics: cosmological phase transitions; dark matter; and astrophysical and cosmological constraints to particle properties. DOE

N90-19172# Lawrence Livermore National Lab., CA. Inst. of Geophysics and Planetary Physics.
HYDRODYNAMICAL SIMULATIONS OF COLLISIONS BETWEEN INTERSTELLAR CLOUDS
John C. Lattanzio 21 Nov. 1989 16 p Presented at the 5th Florida Workshop in Nonlinear Astronomy: Nonlinear Astrophysical Fluid Dynamics, Gainesville, FL, 5-7 Oct. 1989
(Contract W-7405-eng-48)
(DE90-006921; UCRL-102500; CONF-8910308-2) Avail: NTIS HC A03/MF A01

A review is made of recent numerical calculations of collisions between interstellar clouds. The numerical method is described, and some of the basic results are highlighted. Emphasis is placed on the conditions necessary to induce gravitational instability, although the wider applications of the results to the structure and appearance of the interstellar medium are also discussed briefly. A recent confrontation between theory and observation is given. DOE

N90-19173# International Centre for Theoretical Physics, Trieste (Italy).
A COMPARISON OF VOID DISTRIBUTIONS IN ABELL CLUSTER CATALOGUE WITH NUMERICAL SIMULATIONS
Yi-peng Jing Aug. 1989 17 p Submitted for publication
(DE90-610640; IC-89/222) Avail: NTIS (US Sales Only) HC A03/MF A01

The void probability functions (VPF) was measured for two virtually redshift complete samples of Abell clusters, and used to test four current theoretical models. The VPF of R greater than or = 1 clusters is lower than that of the explosion model by about one order. The open CDM model (Omega = 0.2) is excluded at greater than or = 3 sigma also due to oversuperclustering. The VPF of the flat neutrinos dominated universe is consistent with the observations, and the flat CDM model could be marginally accepted at 2 sigma in matching the observational VPF. However, all four models are unsuccessful if we combine the two point correlation function and VPF. DOE

N90-19174# International Centre for Theoretical Physics, Trieste (Italy).
A NEW INTERPRETATION OF THE FEATURE OF SiO MASER SPECTRA ASSOCIATED WITH M-TYPE STAR
Hanping Liu and Jin Sun (Beijing Normal Univ., China) Sep. 1989 9 p
(DE90-610641; IC-89/299) Avail: NTIS (US Sales Only) HC A02/MF A01

There exists a systematic redshift of spectra (nu =1,2; J=1-0) of SiO masers associated with a number of late-type M stars. On the contrary, the redshift is rather small for the spectra (nu =1; J=2-1). The latter is approximately symmetrical with respect to the star. For the above, no good interpretation has been given up to now. A new redshift mechanism of SiO spectra, the mechanism of radiation frequency shift, was derived here from the interaction between the radiation field of the star and the energy levels of the maser. Detailed calculations show that, under the influence of the radiation field of the star, the redshift of the SiO spectra (J=1-0) is more substantial than that of the spectra (J=2-1). This is consistent with the result of the observation, and shows that the nonkinematic effect of the spectra is non negligible for the SiO maser of the star. DOE

N90-19175# International Centre for Theoretical Physics, Trieste (Italy).
ON THE MASS TO LIGHT RATIOS OF DWARF SPHEROIDAL GALAXIES
P. Cuddeford and J. C. Miller Jul. 1989 11 p Submitted for publication
(DE90-610645; IC-89/184) Avail: NTIS (US Sales Only) HC A03/MF A01

Previous estimates of the mass to light ratios of local dwarf spheroidal galaxies have indicated they form an inhomogeneous population. A tidal equation is used and it is shown that if it is assumed that all of these dwarf galaxies are on essentially similar orbits around the Milky Way (rather than having perigalactica comparable with their present distances), values can be derived of M/L(sub v) which have a much smaller spread and no longer have correlations with luminosity and distance. It is then possible to maintain the view that either all of these dwarf galaxies contain dark matter or none of them do, with the main determining factor being the currently uncertain mass of the Milky Way. DOE

N90-19176# International Centre for Theoretical Physics, Trieste (Italy).
QUANTUM COSMOLOGICAL ORIGIN OF LARGE SCALE STRUCTURES OF THE UNIVERSE
Yaqub Anini Jul. 1989 16 p Submitted for publication
(DE90-610647; IC-89/219) Avail: NTIS (US Sales Only) HC A03/MF A01

The initial quantum state of matter perturbations about de Sitter minisuperspace model is found. For a large class of boundary conditions (bcs), including those of Hartle-Hawking and Vilenkin, the resulting quantum state is the de Sitter invariant vacuum. This result is found to depend only on the regularity requirement at the euclidean origin of spacetime which is common to all reasonable (bcs). The initial value of the density perturbations implied by these quantum fluctuations are found and evaluated at the initial horizon crossing. The perturbations are found to have an almost scale independent spectrum, and an amplitude which depends on the scale at which inflation took place. The amplitude would have the right value if the scale of inflation is H less than or = 10(exp 15)GeV. DOE

N90-19177# Joint Inst. for Nuclear Research, Dubna (USSR).
ELEMENTARY PARTICLES AND COSMOLOGY
M. I. Dobrolyubov, A. Yu. Ignatev, and M. E. Shaposhnikov 1988 48 p In RUSSIAN
(DE90-610648; JINR-R-2-88-654) Avail: NTIS (US Sales Only) HC A03/MF A01

A series of lectures is devoted to actual problems which arise at the junction of elementary particle physics and cosmology. A brief review is given to the standard theory of hot universe and scenario of inflationary universe, modern state of the problem of baryon universe asymmetry and possible new mechanisms of this asymmetry formation. The possibility of construction of cosmological models on the basis of supersymmetric theories is considered: qualitative evaluation of the modern density of relic particles, cosmological restrictions for the mass of the lightest particle, astrophysical restrictions for the coupling constant of weakly interacting particles and matter are given. A perspective direction of search for light particles in light hadron decays is mentioned. DOE

N90-18982*# National Aeronautics and Space Administration. Goddard Space Flight Center, Greenbelt, MD.
GRIS OBSERVATIONS OF THE GALACTIC CENTER
N. Gehrels, S. Barthelmy, B. J. Teegarden, J. Tueller, M. Leventhal, and C. J. MacCallum (Sandia National Labs., Albuquerque, NM.) *In its* Annihilation in Gases and Galaxies Jan. 1990 p 159-168 (For primary document see N90-18957 11-70)
Avail: NTIS HC A12/MF A02 CSCL 03B

N90-18984*# National Aeronautics and Space Administration. Goddard Space Flight Center, Greenbelt, MD.
ANNIHILATION PHYSICS OF EXOTIC GALACTIC DARK MATTER PARTICLES
F. W. Stecker *In its* Annihilation in Gases and Galaxies Jan. 1990 p 185-199 (For primary document see N90-18957 11-70)
Avail: NTIS HC A12/MF A02 CSCL 03B

N90-19087# Ecole Normale Superieure, Paris (France). Radioastronomie.
ANALOGIES BETWEEN COMETARY, INTERPLANETARY, AND INTERSTELLAR MATTER
J.-L. Puget *In* ESA, Infrared Spectroscopy in Astronomy, Sep. 1989 p 37-39 (For primary document see N90-19084 11-89)
Copyright Avail: NTIS HC A23/MF A04; ESA Publications Div., ESTEC, Noordwijk, Netherlands, 80 Dutch guilders

N90-19089# European Space Agency. European Space Research and Technology Center, ESTEC, Noordwijk (Netherlands). Space Science Dept.
THE UNIDENTIFIED IR BANDS IN LABORATORY, IN INTERSTELLAR MEDIUM, AND IN COMETS
L. Colangeli, G. Schwehm, E. Bussoletti, S. Fonti, A. Blanco, and V. Orofinc (Lecce Univ., Italy) *In its* Infrared Spectroscopy in Astronomy Sep. 1989 p 49-53 Sponsored in part by the Italian Ministry of Public Education (For primary document see N90-19084 11-89)
(Contracts PSN-018-85; CNR-86-157; CNR-87-01079-02)
Copyright Avail: NTIS HC A23/MF A04; ESA Publications Div., ESTEC, Noordwijk, Netherlands, 80 Dutch guilders

N90-19092# University Coll., Cardiff (Wales). School of Mathematics.
A UNIFIED MODEL FOR THE 3.28 MICRON AND 3.4 MICRON SPECTRAL FEATURE IN THE INTERSTELLAR MEDIUM AND IN COMETS
F. Hoyle and N. C. Wickramasinghe *In* ESA, Infrared Spectroscopy in Astronomy Sep. 1989 p 67-7 (For primary document see N90-19084 11-89)
Copyright Avail: NTIS HC A23/MF A04; ESA Publications Div., ESTEC, Noordwijk, Netherlands, 80 Dutch guilders

N90-19093# University Coll., Cardiff (Wales). School of Mathematics.
INTERPRETATION OF THE 10 MICRON AND 20 MICRON ABSORPTION BANDS IN COMETS, THE INTERSTELLAR MEDIUM, AND IN AN EXTERNAL GALAXY
N. C. Wickramasinghe, F. Hoyle, Q. Majeed, S. Al-Mufti, and M. K. Wallis *In* ESA, Infrared Spectroscopy in Astronomy Sep. 1989 p 73-7 (For primary document see N90-19084 11-89)
Copyright Avail: NTIS HC A23/MF A04; ESA Publications Div., ESTEC, Noordwijk, Netherlands, 80 Dutch guilders

N90-19095# Princeton Univ. Observatory, NJ.
INTERSTELLAR EXTINCTION IN THE INFRARED
B. T. Draine *In* ESA, Infrared Spectroscopy in Astronomy Sep. 1989 p 93-9 (For primary document see N90-19084 11-89)
(Grant NSF AST-86-12013)
Copyright Avail: NTIS HC A23/MF A04; ESA Publications Div., ESTEC, Noordwijk, Netherlands, 80 Dutch guilders

N90-19096# Australian Defence Force Academy, Canberra. Dept. of Physics.
SPECTROPOLARIMETRY AS A DIAGNOSTIC OF THE INTERSTELLAR MEDIUM
D. K. Aitken *In* ESA, Infrared Spectroscopy in Astronomy Sep. 1989 p 99-107 (For primary document see N90-19084 11-89)
Copyright Avail: NTIS HC A23/MF A04; ESA Publications Div., ESTEC, Noordwijk, Netherlands, 80 Dutch guilders

N90-19097# Manchester Univ. (England). Dept. of Mathematics.
CHEMISTRY ON INTERSTELLAR GRAINS AND IMPLICATIONS FOR INFRARED SPECTROSCOPY
T. J. Millar *In* ESA, Infrared Spectroscopy in Astronomy Sep. 1989 p 109-114 (For primary document see N90-19084 11-89)
Copyright Avail: NTIS HC A23/MF A04; ESA Publications Div., ESTEC, Noordwijk, Netherlands, 80 Dutch guilders

N90-19098# Max-Planck-Inst. fuer Physik und Astrophysik, Garching (Germany, F.R.). Inst. fuer Extraterrestrische Physik.
PHOTODISSOCIATION REGIONS: OBSERVATIONS AND THEORY
R. Genzel, A. I. Harris, and J. Stutzki *In* ESA, Infrared Spectroscopy in Astronomy Sep. 1989 p 115-132 (For primary document see N90-19084 11-89)
Copyright Avail: NTIS HC A23/MF A04; ESA Publications Div., ESTEC, Noordwijk, Netherlands, 80 Dutch guilders

N90-19106# Ecole Normale Superieure, Paris (France). Groupe de Physique des Solides.
AN ALMOST TOTAL DISJUNCTION BETWEEN EMISSION AND ABSORPTION DUST FEATURES: WHAT DOES IT TELL US?
A. Leger, L. B. dHendencourt, L. Verstraete, and P. Ehrenfreund *In* ESA, Infrared Spectroscopy in Astronomy Sep. 1989 p 189-192 (For primary document see N90-19084 11-89)
Copyright Avail: NTIS HC A23/MF A04; ESA Publications Div., ESTEC, Noordwijk, Netherlands, 80 Dutch guilders

N90-19110# Commissariat a l'Energie Atomique, Gif-sur-Yvette (France). Service d'Astrophysique.
A COAL MODEL FOR THE CARRIERS OF THE UNIDENTIFIED IR BANDS
R. Papoular, J. Conard, M. Guiliano, J. Kister, and G. Mille (Aix-Marseilles Univ., France) *In* ESA, Infrared Spectroscopy in Astronomy Sep. 1989 p 207-211 (For primary document see N90-19084 11-89)
Copyright Avail: NTIS HC A23/MF A04; ESA Publications Div., ESTEC, Noordwijk, Netherlands, 80 Dutch guilders

N90-19113# Ecole Normale Superieure, Paris (France). Groupe de Physique des Solides.
AN IMPLICATION OF THE IR IDENTIFICATION OF PAHS: THE HEATING OF THE DIFFUSE IS GAS
L. Verstraete, A. Leger, L. B. dHendencourt, D. Defourneau, and O. Dutuit (Centre National de la Recherche Scientifique, Orsay, France) *In* ESA, Infrared Spectroscopy in Astronomy Sep. 1989 p 225-220 (For primary document see N90-19084 11-89)
Copyright Avail: NTIS HC A23/MF A04; ESA Publications Div., ESTEC, Noordwijk, Netherlands, 80 Dutch guilders

N90-19114# Harvard-Smithsonian Center for Astrophysics, Cambridge, MA.
THE INFRARED SPECTRAL SIGNATURE OF STAR FORMATION
F. C. Adams *In* ESA, Infrared Spectroscopy in Astronomy Sep. 1989 p 233-243 (For primary document see N90-19084 11-89)
Copyright Avail: NTIS HC A23/MF A04; ESA Publications Div., ESTEC, Noordwijk, Netherlands, 80 Dutch guilders

N90-19116# Harvard-Smithsonian Center for Astrophysics, Cambridge, MA.
INFRARED LINE EMISSION FROM HIGH-VELOCITY OUTFLOWS IN STAR-FORMING REGIONS
G. Melnick *In* ESA, Infrared Spectroscopy in Astronomy Sep. 1989 p 259-268 (For primary document see N90-19084 11-89)
Copyright Avail: NTIS HC A23/MF A04; ESA Publications Div., ESTEC, Noordwijk, Netherlands, 80 Dutch guilders

N90-19117# Max-Planck-Inst. fuer Physik und Astrophysik, Garching (Germany, F.R.). Inst. fuer Extraterrestrische Physik.
THE EXCITATION OF MOLECULAR HYDROGEN AND ITS SIGNIFICANCE
A. Sternberg *In* ESA, Infrared Spectroscopy in Astronomy Sep. 1989 p 269-280 (For primary document see N90-19084 11-89)
Copyright Avail: NTIS HC A23/MF A04; ESA Publications Div., ESTEC, Noordwijk, Netherlands, 80 Dutch guilders

N90-19118*# National Aeronautics and Space Administration. Ames Research Center, Moffett Field, CA.
HIGH-EXCITATION LINES OF MOLECULAR HYDROGEN: A DISCRIMINANT BETWEEN SHOCK MODELS
M. Burton, P. Brand, A. Moorhouse, and T. Geballe (Joint Astronomy Centre, Hilo, HI.) *In* ESA, Infrared Spectroscopy in Astronomy Sep. 1989 p 281-285 Sponsored by United Kingdom Science and Engineering Research Council and the National Research Council (For primary document see N90-19084 11-89)
Copyright Avail: NTIS HC A23/MF A04; ESA Publications Div., ESTEC, Noordwijk, Netherlands, 80 Dutch guilders CSCL 03B

N90-19121# European Southern Observatory, Garching (Germany, F.R.).
MOLECULAR HYDROGEN IN THE HII REGION G333.6-0.2
A. Monetti and A. F. M. Moorwood *In* ESA, Infrared Spectroscopy in Astronomy Sep. 1989 p 299-301 (For primary document see N90-19084 11-89)
Copyright Avail: NTIS HC A23/MF A04; ESA Publications Div., ESTEC, Noordwijk, Netherlands, 80 Dutch guilders

N90-19127# Observatorio Astronomico Nacional, Madrid (Spain).
ICE GRAINS IN THE DUST DISK OF THE BIPOLAR NEBULA M 1-92
C. Eiroa and K.-W. Hodapp (Hawaii Univ., Honolulu.) *In* ESA, Infrared Spectroscopy in Astronomy Sep. 1989 p 351-353 (For primary document see N90-19084 11-89)
Copyright Avail: NTIS HC A23/MF A04; ESA Publications Div., ESTEC, Noordwijk, Netherlands, 80 Dutch guilders

N90-19132# Catania Astrophysical Observatory (Italy).
DUST IN PLANETARY NEBULAE: IRSPEC OBSERVATIONS IN THE 3.0 MICRON-3.8 MICRON RANGE
A. Magazzu and G. Strazzulla (Catania Univ., Italy) *In* ESA, Infrared Spectroscopy in Astronomy Sep. 1989 p 371-373 (For primary document see N90-19084 11-89)
Copyright Avail: NTIS HC A23/MF A04; ESA Publications Div., ESTEC, Noordwijk, Netherlands, 80 Dutch guilders

N90-19135# Imperial Coll. of Science and Technology, London (England).
CARBON MONOXIDE IN SUPERNOVA 1987A
J. Spyromilio, W. P. S. Meikle, R. C. M. Learner, and D. A. Allen (Anglo-Australian Observatory, Sydney.) *In* ESA, Infrared Spectroscopy in Astronomy Sep. 1989 p 381-384 (For primary document see N90-19084 11-89)
Copyright Avail: NTIS HC A23/MF A04; ESA Publications Div., ESTEC, Noordwijk, Netherlands, 80 Dutch guilders

N90-19136# Space Research Organization Netherlands, Utrecht.
PREDICTIONS OF INFRARED RECOMBINATIONS LINES IN STELLAR WINDS OF HOT STARS
L. H. Strous and H. J. G. L. M. Lamers *In* ESA, Infrared Spectroscopy in Astronomy Sep. 1989 p 385-386 (For primary document see N90-19084 11-89)
Copyright Avail: NTIS HC A23/MF A04; ESA Publications Div., ESTEC, Noordwijk, Netherlands, 80 Dutch guilders

N90-19141*# Hawaii Univ., Honolulu. Inst. for Astronomy.
STELLAR KINEMATICS IN THE GALACTIC CENTRE

M. T. McGinn, K. Sellgren, E. E. Becklin, and D. N. B. Hall *In* ESA, Infrared Spectroscopy in Astronomy Sep. 1989 p 421-424 (For primary document see N90-19084 11-89)
(Contract NASw-3159; NSF AST-87-00618)
Copyright Avail: NTIS HC A23/MF A04; ESA Publications Div., ESTEC, Noordwijk, Netherlands, 80 Dutch guilders CSCL 03B

N90-19148# Imperial Coll. of Science and Technology, London (England).
THE STRENGTHS OF THE 2.3 MICRON CO BAND IN LUMINOUS INTERACTING AND MERGING GALAXIES
R. Doyon, R. D. Joseph, and G. S. Wright (United Kingdom Infrared Telescope Unit, Hilo, HI.) *In* ESA, Infrared Spectroscopy in Astronmy Sep. 1989 p 477-479 (For primary document see N90-19084 11-89)
Copyright Avail: NTIS HC A23/MF A04; ESA Publications Div., ESTEC, Noordwijk, Netherlands, 80 Dutch guilders

N90-19150# University Coll., Cardiff (Wales). School of Mathematics.
THE MICROWAVE BACKGROUND IN STEADY-STATE COSMOLOGY
F. Hoyle and N. C. Wickramasinghe *In* ESA, Infrared Spectroscopy in Astronomy Sep. 1989 p 489-495 (For primary document see N90-19084 11-89)
Copyright Avail: NTIS HC A23/MF A04; ESA Publications Div., ESTEC, Noordwijk, Netherlands, 80 Dutch guilders

N90-19152# Universidad Autonoma de Madrid, Cantoblanco (Spain). Dept. de Astrofisica.
EVOLUTIONARY SYNTHESIS OF THE FAR-INFRARED EMISSION IN STARBURST GALAXIES
J. M. M. Mas-Hesse and D. Kunth (Institut d'Astrophysique, Paris, France) *In* ESA, Infrared Spectroscopy in Astronomy Sep. 1989 p 501-506 (For primary document see N90-19084 11-89)
(Contract CAYCIT-PB-85-60)
Copyright Avail: NTIS HC A23/MF A04; ESA Publications Div., ESTEC, Noordwijk, Netherlands, 80 Dutch guilders

N90-19154# Universidad de la Laguna (Spain). Inst. de Astrofisica.
INFRARED PROPERTIES OF FIVE SPIRAL GALAXIES
M. Prieto, A. CamposAguilar, and C. Garcia *In* ESA, Infrared Spectroscopy in Astronomy Sep. 1989 p 511-515 (For primary document see N90-19084 11-89)
Copyright Avail: NTIS HC A23/MF A04; ESA Publications Div., ESTEC, Noordwijk, Netherlands, 80 Dutch guilders

N90-19155# Edinburgh Univ. (Scotland). Dept. of Astronomy.
FLUORESCENT MOLECULAR HYDROGEN EMISSION FROM STAR-FORMING GALAXIES
P. Puxley, T. Hawarden, and M. Mountain (Royal Observatory, Edinburgh, Scotland) *In* ESA, Infrared Spectroscopy in Astronomy Sep. 1989 p 517-520 (For primary document see N90-19084 11-89)
Copyright Avail: NTIS HC A23/MF A04; ESA Publications Div., ESTEC, Noordwijk, Netherlands, 80 Dutch guilders

N90-19156# Edinburgh Univ. (Scotland). Dept. of Astronomy.
H53-ALPHA EMISSION FROM M82
P. Puxley, P. Brand, T. Moore, M. Mountain, N. Nakai, and T. Yamashita (Nobeyema Solar Radio Observatory, Japan) *In* ESA, Infrared Spectroscopy in Astronomy Sep. 1989 p 521-523 (For primary document see N90-19084 11-89)
Copyright Avail: NTIS HC A23/MF A04; ESA Publications Div., ESTEC, Noordwijk, Netherlands, 80 Dutch guilders

N90-19157# Consiglio Nazionale delle Ricerche, Frascati (Italy). Ist. de Fisica dello Spazio Interplanetario.
FAR INFRARED FINE STRUCTURE LINES IN ACTIVE GALAXIES
L. Spinoglio and M. A. Malkan (California Univ., Los Angeles.) *In* ESA, Infrared Spectroscopy in Astronomy Sep. 1989 p 525-529 (For primary document see N90-19084 11-89)
Copyright Avail: NTIS HC A23/MF A04; ESA Publications Div., ESTEC, Noordwijk, Netherlands, 80 Dutch guilders

91 LUNAR AND PLANETARY EXPLORATION

Includes planetology; and manned and unmanned flights. For spacecraft design or space stations see *18 Spacecraft Design, Testing and Performance.*

N90-19178# EG and G Mound Applied Technologies, Miamisburg, OH.
TECHNOLOGY UPDATE-89
Dec. 1989 33 p
(Contract DE-AC04-88DP-43495)
(DE90-005813; MLM-3620) Avail: NTIS HC A03/MF A01
This issue of Technology Update tells about EG and G's role in the Galileo mission to land on Jupiter. Also covered in separate articles is information on tritium imaging, safety analysis of shipping containers, detection of small traces of various elements, and measuring methods. DOE

N90-19179# Oak Ridge National Lab., TN. Computing and Telecommunications Div.
USING THE K-25 C/TD COMMON FILE SYSTEM: A GUIDE TO CFSI
Dec. 1989 211 p
(Contract DE-AC05-84OR-21400)
(DE90-005815; ORNL/M-828) Avail: NTIS HC A10/MF A02
A CFS (Common File System) is a large, centralized file management and storage facility based on software developed at Los Alamos National Laboratory. This manual is a guide to use of the CFS available to users of the Cray UNICOS system at Martin Marietta Energy Systems, Inc., in Oak Ridge, Tennessee. DOE

N90-19088*# Observatoire de Paris-Meudon (France).
MEASUREMENTS OF THE D/H RATIO IN PLANETARY ATMOSPHERES BY GROUND BASED INFRARED SPECTROSCOPY
C. deBergh, B. L. Lutz, T. Owen, and J.-P. Maillard (Institut d'Astrophysique, Paris, France) *In* ESA, Infrared Spectroscopy in Astronomy, Sep. 1989 p 41-47 (For primary document see N90-19084 11-89)
(Grants NsG-7499; NAGw-1505; NGR-33015741)
Copyright Avail: NTIS HC A23/MF A04; ESA Publications Div., ESTEC, Noordwijk, Netherlands, 80 Dutch guilders CSCL 03B

N90-19090# Observatoire de Paris-Meudon (France).
OBSERVATIONS OF CO ON MARS IN THE INFRARED AND MILLIMETRE RANGE
Th. Encrenaz, F. Billebaud, E. Lellouch, F. Combes, M. Gerin, J.-P. Maillard, and G. Paubert (Institut de Radio Astronomie Millimetrique, Grenoble, France) *In* ESA, Infrared Spectroscopy in Astronomy Sep. 1989 p 55-5 (For primary document see N90-19084 11-89)
Copyright Avail: NTIS HC A23/MF A04; ESA Publications Div., ESTEC, Noordwijk, Netherlands, 80 Dutch guilders

N90-19091# Observatoire de Paris-Meudon (France).
NEAR INFRARED SPECTROSCOPY OF MARS: STUDY OF THE SURFACE MINERALOGY
Th. Encrenaz and P. Bouchet (European Southern Observatory, La Silla, Chile) *In* ESA, Infrared Spectroscopy in Astronomy Sep. 1989 p 61-6 (For primary document see N90-19084 11-89)
Copyright Avail: NTIS HC A23/MF A04; ESA Publications Div., ESTEC, Noordwijk, Netherlands, 80 Dutch guilders

N90-19122# University Coll., London (England). Dept. of Physics and Astronomy.
PLANETARY NEBULAE
M. J. Barlow *In* ESA, Infrared Spectroscopy in Astronomy Sep. 1989 p 307-315 (For primary document see N90-19084 11-89)
Copyright Avail: NTIS HC A23/MF A04; ESA Publications Div., ESTEC, Noordwijk, Netherlands, 80 Dutch guilders

92 SOLAR PHYSICS

Includes solar activity, solar flares, solar radiation and sunspots.

For related information see *93 Space Radiation.*

N90-19180# Academy of Sciences (USSR), Novosibirsk. Inst. Yadernoj Fiziki.
MAGNETIC FIELD GENERATION BY ACOUSTIC OSCILLATIONS IN SOLAR ATMOSPHERE
D. D. Ryutov and M. P. Ryutova 1989 9 p In RUSSIAN
(DE90-606054; IYaF-89-23) Avail: NTIS (US Sales Only) HC A02/MF A01

The role of acoustic waves in plasma current excitation and magnetic field generation in the sun atmosphere is considered. Equations describing the force effecting the electron gas due to waves and equations determining the magnetic field evolution are derived. Author

N90-19181*# Catholic Univ. of America, Washington, DC. Dept. of Mechanical Engineering.
INTERACTION OF MINOR IONS WITH FAST AND SLOW SHOCKS Final Report, 1 Oct. - 31 Dec. 1989
Y. C. Whang 9 Mar. 1990 34 p
(Grant NAG5-1291)
(NASA-CR-186372; NAS 1.26:186372) Avail: NTIS HC A03/MF A01 CSCL 03B

The coronal slow shock was predicted to exist embedded in large coronal holes at 4 to 10 solar radii. A three-fluid model was used to study the jumps in minor ions propertes across the coronal slow shock. The jump conditions were formulated in the de Hoffmann-Teller frame of reference. The Rankine-Hugoniot solution determines the MHD flow and the magnetic field across the shocks. For each minor ion species, the fluid equations for the conservation of mass, momentum, and energy can be solved to determine the velocity and the temperature of the ions across the shock. A simularity solution was also obtained for heavy ions. The results show that on the downstream side of the coronal slow shock the ion temperatures are nearly proportional to the ion masses for He, O, Si, and Fe in agreement with observed ion temperatures in the inner solar wind. This indicates that the possibly existing coronal slow shock can be responsible for the observed heating of minor ions in the solar wind. Author

93 SPACE RADIATION

Includes cosmic radiation; and inner and outer earth's radiation belts.

For biological effects of radiation see *52 Aerospace Medicine.* For theory see *73 Nuclear and High-Energy Physics.*

N90-19182# Istituto Nazionale di Fisica Nucleare, Frascati (Italy).
THE TRACK-ETCH DETECTOR FOR THE MACRO EXPERIMENT AT THE GRAN SASSO LABORATORY
1989 4 p Presented at the International Cosmic Ray Conference, Adelaide, Australia, 28 Dec. 1989
(Contract DE-AS05-81ER-40039)
(DE90-003235; DOE/ER-40039/39; CONF-891260-8) Avail: NTIS HC A01/MF A01

The MACRO detector uses three complementary techniques for particle detection: liquid scintillation counters, limited streamer tubes, and track-etch plastics. The track-etch detector is described. Discussed are the track-etch implementation for the first supermodule; tests in progress on CR39 exposed to high energy ions; and the sensitivity of the track-etch system to GUT magnetic monopoles. DOE

N90-19183# Argonne National Lab., IL. High Energy Physics Div.
UNDERGROUND MUON OBSERVATIONS IN THE SOUDAN 2 DETECTOR
W. W. M. Allison, G. J. Alner, I. Ambats, D. S. Ayres, L. Balka, G. D. Barr, W. L. Barrett, D. Benjamin, P. Border, and C. B. Brooks (Oxford Univ., England) et al 11 Sep. 1989 3 p Presented at the 21st International Cosmic Ray Conference, Adelaide, Australia, 6-19 Jan. 1990
(Contract W-31-109-eng-38)
(DE90-005647; ANL-HEP-CP-89-100; CONF-900122-7) Avail: NTIS HC A01/MF A01

The Soudan 2 nucleon decay detector has recorded data since Summer 1988 using a quarter (dimensions 4 m by 8 m by 5 m high) of the eventual detector. This iron-argon time projection chamber records extensive data on each event and has excellent angular and multi-track resolution. The trigger, the event analysis procedure, and the current status of the detector and the underground muon data sample, are described. DOE

N90-19184# Instituto de Pesquisas Espaciais, Sao Jose dos Campos (Brazil).
STUDY OF PECULIAR GALAXIES IN THE SOUTHERN HEMISPHERE M.S. Thesis - Sep. 1988 [ESTUDO DE GALAXIAS PECULIARES DO HEMISFERIO SUL]
Duilia F. M. Rabaca Jun. 1989 73 p In PORTUGUESE; ENGLISH summary
(INPE-4810-TDL/357) Avail: NTIS HC A04/MF A01

The radio continuum emission was investigated at 22 GHz of a sample of southern peculiar galaxies, since the peculiarities are a possible evidence of radio emission. A sample of 24 peculiar galaxies was observed with the antenna of the Radio Observatorio de Itapetinga (ROI-INPE). The observational technique used was to scan through the source in right ascension; the adopted sensibility limit was 3 rms. Three galaxies were detected as radio sources for the first time and the fluxes of 4 well known radio sources in other frequencies were measured at 22 GHz. The obtained flux densities were in the range of 0.5 to 4.5 Jy, showing that the instrument and the observational technique were satisfactory for the observation of weak sources. Author

N90-19185# Minnesota Univ., Minneapolis. Dept. of Astronomy.
PHOTOMETRY OF VARIABLE AFGL SOURCES Final Report, 1 Oct. 1986 - 30 Sep. 1989
Terry Jay Jones, C. O. Bryja, Robert D. Gehrz, Thomas E. Harrison, Joni J. Johnson, Dimitri I. Klebe, and Geoffrey F. Lawrence 15 Sep. 1989 52 p
(Grant AF-AFOSR-0011-87; AF Proj. 2311)
(AD-A216938; AFOSR-89-1699TR) Avail: NTIS HC A04/MF A01 CSCL 03/2

Results of infrared photometric observations of 63 AFGL sources over the past nine years are presented. Using these data together with previous measurements of these stars, pulsation periods and mean photometric characteristics were determined. These stars are found to lie midway between classical Mira variables and the Radio Luminous OH/IR stars in their period distribution and photometric properties. For the sample as a whole, there is no evidence for sudden or transient behavior such as a switch in pulsation mode. Rather, these stars show rapid, but continuous, evolution from shorter period Miras with weak mass loss to longer periods and larger mass loss rates. The carbon rich stars in our sample have the same period distribution as the oxygen rich stars. None of the carbon stars have periods as long as those of the very long period Radio Luminous OH/IR stars. GRA

N90-19186# Louisiana State Univ., Baton Rouge.
CURRENT AND FUTURE USES OF ACCELERATORS IN PARTICLE ASTROPHYSICS
T. Gregory Guzik 1989 9 p Presented at the Particle Astrophysics: NASA Cosmic Ray Program for the 1990's and Beyond, Greenbelt, MD, 6-8 Nov. 1989
(Contract DE-FG05-84ER-40147)
(DE90-006667; CONF-8911161-1) Avail: NTIS HC A02/MF A01

Beams of artificially accelerated heavy ions, protons, antiprotons, electrons, and positrons currently available at (and planned for) numerous facilities around the world are a valuable resource to the Cosmic Ray community. Such beams have been used to test detector concepts, calibrate balloon-borne and space flight experiments and to measure fundamental nuclear physics parameters necessary for the interpretation of Cosmic Ray data. As new experiments are flown the quality and extent of Cosmic Ray measurements will continue to improve. It will be necessary to increase activity at ground based accelerators in order to test/calibrate these new instruments and to maintain (or possibly improve) the ability to interpret these data. In this area, the newly formed Transport Collaboration, supported by NASA, will be providing new nuclear interaction cross section measurements for beams with Z less than or = 58 and supporting new instrument calibrations at the Lawrence Berkeley Laboratory Bevalac accelerator. DOE

N90-19187# Los Alamos National Lab., NM.
SOFT X RAY EMISSION FROM CLASSICAL NOVAE IN OUTBURST
1989 4 p Presented at the Physics of Classical Novae: IAU Colloquium No. 122, Madrid (Spain), 27-30 Jun. 1989
(Contract W-7405-eng-36)
(DE90-006480; LA-UR-90-138; CONF-8906225-2) Avail: NTIS HC A01/MF A01

Theoretical modeling of novae in outburst predicts that they should be active emitters of radiation at soft x ray wavelengths twice during their outburst. The first time occurs very early in the outburst when only a very sensitive all sky survey will be able to detect them. This period lasts only a few hours for the very fastest novae. They again become bright in x rays late in the outburst when the remnant object becomes very hot and is still luminous. Both simulations and observations show that novae can remain very hot for months to years. It is important to observe them at these late times because a measurement both of the flux and temperature can provide information about the mass of the white dwarf, the turn-off time scale, and the energy budget of the outburst. DOE

N90-19188# Lawrence Livermore National Lab., CA. Lab. for Experimental Astrophysics.
IMAGING GERMANIUM TELESCOPE ARRAY FOR GAMMA-RAYS (IGETAGRAY)
Charles J. Hailey, Klaus P. Ziock, Fiona A. Harrison, and Judith Fleishmann (Massachusetts Univ., Amherst.) Jan. 1990 4 p Presented at the Workshop on High Energy Astrophysics in the 21st Century, Taos, NM, 10-14 Dec. 1989
(Contract W-7405-eng-48)
(DE90-006994; UCRL-102763; CONF-891276-2) Avail: NTIS HC A01/MF A01

The Germanium Drift Chamber (GDC) is a gamma ray detector with excellent energy and 1-D spatial resolution. Due to recent developments in coded aperture optics, it is feasible to couple 1-D coded apertures and GDCs in a special array geometry producing a telescope with true 2-D imaging. This Imaging Germanium Telescope Array for Gamma Rays (IGETAGRAY) has made a comparable field of view and sensitivity to true 2-D systems, but simplified engineering requirements. IGETAGRAY will make possible high sensitivity spectroscopy of the gamma ray sky. DOE

N90-18983*# National Aeronautics and Space Administration. Goddard Space Flight Center, Greenbelt, MD.
POSITRON ANNIHILATION IN GAMMA-RAY BURSTS
Alice K. Harding *In its* Annihilation in Gases and Galaxies Jan. 1990 p 169-183 (For primary document see N90-18957 11-70)
Avail: NTIS HC A12/MF A02 CSCL 03B

99 GENERAL

N90-19189# Deutsche Forschungsanstalt fuer Luft- und Raumfahrt, Cologne (Germany, F.R.).
[ACTIVITIES REPORT IN GERMAN AEROSPACE] Annual Report, 1988 - 1989 [JAHRESBERICHT 1988/89]
Sep. 1989 82 p In GERMAN Original contains color illustrations
(ISSN-0070-3966; ETN-90-96280) Avail: NTIS HC A05/MF A01

The atmospheric and space flight research carried out by the DLR over the course of 1988 and 1989 is described. An intensive helicopter design project is described. New quieter helicopter blades are developed. Better aircraft crash resistance is investigated. Earth imaging from low earth orbits is discussed. The synthetic aperture radar carried aboard the Space Shuttle is described. Reduced gravity training of European astronauts is discussed, as are technological spinoffs of DLR space research. ESA

Typical Subject Index Listing

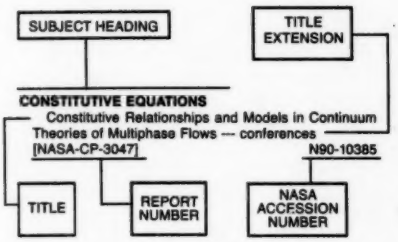

The subject heading is a key to the subject content of the document. Titles, report numbers, and accession numbers of pertinent documents are provided under each subject heading. When the title is insufficiently descriptive of the document content, a title extension has been added, separated from the title by three hyphens. The report number helps to indicate the type of document cited (e.g., NASA report, NASA translation, NASA contractor report). The NASA accession number is the number by which the document abstracts are arranged in this journal and by which the document is sold or requested. The titles, with title extensions if present, are arranged under each subject heading in ascending accession number order. The subject headings have been selected from the latest revision of the *NASA Thesaurus* (NASA SP-7064).

A

ABLATION
In situ growth of epitaxial superconducting YBa2Cu3O(7-x) films on insulating semiconducting and ferroelectric K(Ta, Nb)O3 by pulsed laser ablation
[DE90-006568] N90-19043
In situ growth of high quality epitaxial YBa2Cu3O(7-x) thin films at moderate temperatures by pulsed laser ablation
[DE90-006629] N90-19045

ABLATIVE MATERIALS
Technique for evaluating the erosive properties of ablative internal insulation materials N90-18486

ABLATIVE NOSE CONES
A difference scheme with autocontrol artificial viscosity to predict ablated nosetip shape
[AD-A216625] N90-18452

ABNORMALITIES
Review of component defects, their relationship to manufacturing process, and their effect on materials behaviour (for critical rotating parts) N90-18399

ABSORPTION COOLING
Intermittent Solar Ammonia Absorption Cycle (ISAAC) refrigeration for lesser developed countries
[DE90-006700] N90-18610

ABSORPTION CROSS SECTIONS
Absorption experiments on electron-beam pumped rare gases
[DE90-006504] N90-18722

ABSORPTION SPECTRA
Temperature dependence of photon-gated persistent spectral hole-burning for the meso-tetra-p-tolyl Zn-tetrabenzoporphyrin/chloroform system in poly(methylmethacrylate)
[AD-A216086] N90-18531
Millimeter-wave propagation in the mesosphere
[PB90-119868] N90-18612
Persistant spectral hole-burning: Photon-gating and fundamental statistical limits
[AD-A216084] N90-18640
An almost total disjunction between emission and absorption dust features: What does it tell us?
N90-19106
A coal model for the carriers of the unidentified IR bands N90-19110
Spectroscopy and physico-chemistry of CO:H2O and CO2:H2O ices N90-19111
Infrared line emission from high-velocity outflows in star-forming regions N90-19116

ABSORPTION SPECTROSCOPY
Ultrasensitive laser spectroscopy in solids: Single-molecule detection
[AD-A216085] N90-18716

ABUNDANCE
Infrared lines as probes of galactic structure N90-19139

ACCELERATION (PHYSICS)
Theory for high gain, high power free electron lasers
[DE90-005546] N90-18714
Visual processing of object velocity and acceleration
[AD-A216509] N90-18858

ACCELEROMETERS
Development and polarization of ferroelectric polymer gauges, for dynamical acceleration experiments, as those in ballistics shocks
[ISL-R-119/88] N90-18703

ACCEPTABILITY
Simulation of synthetic aperture radar 3: Evaluation of prototype digital feature analysis data
[AD-A216750] N90-18620

ACCIDENTS
Space nuclear safety program
[DE90-006436] N90-19007
Safety analysis for the Galileo light-weight radioisotope heater unit
[DE90-007147] N90-19009

ACCRETION DISKS
Ice grains in the dust disk of the bipolar nebula M 1-92 N90-19127

ACCUMULATORS
Beam collector and output window for a 35 GHz 100 kW gyrotron
[INPE-4958-RPE/803] N90-18899

ACOUSTIC EMISSION
Damage assessment in composites by acousto-ultrasonic technique
[AD-A216590] N90-18510
Acoustic emission diagnostic techniques for high-field high current-density super inducting poles
[DE90-007400] N90-19000
Mechanical disturbances in high-performance superconducting dipoles
[DE90-006237] N90-19040

ACOUSTIC SOUNDING
Preliminary comparison of temperature soundings obtained from simultaneous radiometric, radio-acoustic, and rawinsonde measurements
[PB90-119835] N90-18838

ACOUSTIC VELOCITY
Comparison of two Navy environmental database models: Generalized Digital Environmental Model and Podeszwa sound speed profile model
[AD-A215848] N90-18889

ACOUSTO-OPTICS
Damage assessment in composites by acousto-ultrasonic technique
[AD-A216590] N90-18510
Applications of acousto-optical correlation devices in radar signal processing
[AD-A216824] N90-18616

ACTINIDE SERIES COMPOUNDS
Luminescence of lanthanides and actinides implanted into binary III-V semiconductors and AlGaAs
[AD-A215759] N90-19031

ACTIVE CONTROL
Active stabilization of aeromechanical systems
[AD-A216629] N90-18672

ACTIVE GALAXIES
Near infrared spectroscopy of active galaxies N90-19143
A search for the CO feature in active galactic nuclei N90-19151
Far infrared fine structure lines in active galaxies N90-19157

ACTUATORS
Flexible heat pipe cold plate
[AD-A216053] N90-18433
Optimization of sensors and actuators positioning aimed at obtaining reduced models for the synthesis of optimal control regulators of flexible structures
[INPE-4760-TDL/348] N90-18450
Development and test of power amplifiers for the driving of low-voltage piezo-actuators in multistable interferometers
[DLR-MITT-89-19] N90-18662

ADA (PROGRAMMING LANGUAGE)
Guidelines for the use of the SAME
[AD-A215846] N90-18888
Determination of the underlying task scheduling algorithm for and Ada runtime system
[AD-A215880] N90-18890
Ada-Linda preliminary report: Motivation, informal description, and examples
[AD-A216004] N90-18892

ADAPTIVE CONTROL
Discrete proportional Plus Integral (PI) multivariable control laws for the Control Reconfigurable Combat Aircraft (CRCA)
[AD-A215664] N90-18431
Appropriateness measurement for computerized adaptive tests
[AD-A216121] N90-18870

ADAPTIVE FILTERS
Orbit determination of artificial Earth satellites through estmation techniques combined with state smoothing techniques
[INPE-4959-TDL/388] N90-18440
A simple algebraic grid adaptation scheme with applications to two- and three-dimensional flow problems
[NASA-TM-102446] N90-18887
Adaptive state estimation and sampling rate analysis for invariant linear dynamic systems in time
[INPE-4960-TDL/389] N90-18951

ADDRESSING
Parallel memory addressing using coincident optical pulses
[AD-A216302] N90-18641
A scalable multiprocessor architecture using Cartesian network: Relative addressing
[AD-A216580] N90-18878

ADHESION
Interfacial chemistry of MoS2 films on Si
[AD-A216527] N90-18532
The improved adhesion of organic polymers to silica and to aluminum metal with zirconium Schiff-base block copolymer coatings
[AD-A216669] N90-18575

ADHESIVE BONDING
Test data of flow field of shuttle SRM nozzle joint with bond defects, using unheated air N90-18484

ADIPOSE TISSUES
Measurement of body fat by neutron inelastic scattering: Comments on installation, operation, and error analysis
[DE90-006765] N90-18868

ADSORPTION
Multicomponent glass surfaces structure and adsorption
[DE90-007179] N90-18596

AERIAL PHOTOGRAPHY
Development of the agricultural information system. Characteristics and results of the Distrito Federal model
[INPE-4940-PRE/1430] N90-18773
Introduction of aerial photography in agricultural research
[BCRS-89-14] N90-18784

AERIAL RECONNAISSANCE
Activities report in DLR research field communication engineering and reconnaissance
[ISSN-0173-0118] N90-18781
AERODYNAMIC BALANCE
Influence of forebody geometry on aerodynamic characteristics and a design guide for defining departure/spin resistant forebody configurations
[AD-A216714] N90-18388
AERODYNAMIC CHARACTERISTICS
Static and rotational aerodynamic data from 0 deg to 90 deg angle of attack for a series of basic and altered forebody shapes
[AD-A216582] N90-18361
Aerodynamic testing of a rotating wind turbine blade
[DE90-000312] N90-18362
Prediction of rotor blade-vortex interaction noise from 2-D aerodynamic calculations and measurements
[ISL-CO-243/88] N90-18365
The effects of wind tunnel data uncertainty on aircraft point performance predictions
[AD-A216091] N90-18387
AERODYNAMIC CONFIGURATIONS
Static and rotational aerodynamic data from 0 deg to 90 deg angle of attack for a series of basic and altered forebody shapes
[AD-A216582] N90-18361
A difference scheme with autocontrol artificial viscosity to predict ablated nosetip shape
[AD-A216625] N90-18452
AERODYNAMIC DRAG
Optimum spanwise camber for minimum induced drag
[BU-403] N90-18369
AERODYNAMIC HEATING
A difference scheme with autocontrol artificial viscosity to predict ablated nosetip shape
[AD-A216625] N90-18452
AERODYNAMIC LOADS
Design guidance to minimize unsteady forces in turbomachines N90-18411
Unsteady blade loads due to wake influence N90-18413
Active stabilization of aeromechanical systems
[AD-A216629] N90-18672
Calculation of flight vibration levels of the AH-1G helicopter and correlation with existing flight vibration measurements
[NASA-CR-181923] N90-18743
AERODYNAMIC STALLING
Measurement of velocity profiles and Reynolds stresses on an oscillating airfoil N90-18427
Stall and recovery in multistage axial flow compressors N90-18429
Active stabilization of aeromechanical systems
[AD-A216629] N90-18672
AERODYNAMICS
Static and rotational aerodynamic data from 0 deg to 90 deg angle of attack for a series of basic and altered forebody shapes
[AD-A216582] N90-18361
Aerodynamic testing of a rotating wind turbine blade
[DE90-000312] N90-18362
Vertical axis wind turbine turbulent response model. Part 2: Response of Sandia National laboratories' 34-meter VAWT with aeroelastic effects
[DE90-005721] N90-18804
Measurements of surface pressures on an operating vertical-axis wind turbine
[DE90-005722] N90-18805
AEROHOMY
Studies of cubic ice crystals
[AD-A216574] N90-18832
AEROSOLS
Perspectives on aerosol deposition to natural surfaces
[DE90-003398] N90-18819
AEROSPACE ENGINEERING
Impact of composites in the aerospace industry
[ETN-90-96231] N90-18527
The manufacturing procedures for composite materials, automation, and robotization
[ETN-90-96232] N90-18528
Materials and structures for 2000 and beyond: An attempted forecast by the Materials and Structures Department of the DLR
[ESA-TT-1154] N90-18609
Comparison of circulation obtained through the trajectory of a drifting buoy tracked by satellite and hydrographic data in the Bransfield Strait
[INPE-4946-TDL/387] N90-18850
Purchase of technology N90-19072
AEROSPACE ENVIRONMENTS
Radiation-hard high-efficiency InP space solar cell development
[AD-A216857] N90-18800
AEROSPACE INDUSTRY
Impact of composites in the aerospace industry
[ETN-90-96231] N90-18527
The manufacturing procedures for composite materials, automation, and robotization
[ETN-90-96232] N90-18528
French approach to space technology transfer N90-19074
AEROSPACE PLANES
Structures and materials technology for hypersonic aerospacecraft
[NASA-TM-102583] N90-18752
AEROSPACE SAFETY
Space nuclear safety program
[DE90-006436] N90-19007
AEROSPACE TECHNOLOGY TRANSFER
Promotion of European Space Technology Transfer
[ESA-SP-1122] N90-19068
ESA project to promote and assist technology transfer by industry N90-19069
Space technology transfers in Europe N90-19070
DTE and space technology transfer N90-19071
Purchase of technology N90-19072
The bringing to market of the RF alert (a case study in technology transfer) N90-19073
French approach to space technology transfer N90-19074
Introductory remarks for the panel discussions on technology transfer N90-19075
Methodology panel N90-19076
Problems on transfer of space technology to non-space areas and solutions: Legal aspects N90-19077
Identification of and response to market demand N90-19078
The improvement of technology transfer from space to industry N90-19079
Internal technology transfer N90-19080
Magnetic suspension railway systems based on space technology N90-19081
An example of technology transfer by Aerospatiale: Fire protection materials N90-19082
AEROSPACE VEHICLES
Analytical formulation for the interaction problem of dynamic reentry, and effects due to flexibility and vibration in an aerospace vehicle
[INPE-4963-TDL/392] N90-18448
Structures and materials technology for hypersonic aerospacecraft
[NASA-TM-102583] N90-18752
AEROTHERMODYNAMICS
Activities report in German aerospace
[ISSN-0070-3966] N90-19189
AGRICULTURE
Evaluation of two methods for acquisition of training statistics for digital analysis of areas prepared for plowing
[INPE-4901-PRE/1502] N90-18763
Radiometric study of wheat and bean crops in three types of latossolo
[INPE-4843-PRE/1472] N90-18767
Relationships between spectral parameters and agronomics of wheat and beam crops
[INPE-4791-RPE/584] N90-18768
Development of the agricultural information system. Characteristics and results of the Distrito Federal model
[INPE-4040-PRE/1430] N90-18773
Spectral response of wheat and its relationship with agronomical prameters
[INPE-4950-RPE/599] N90-18774
Introduction of aerial photography in agricultural research
[BCRS-89-14] N90-18784
Effects of global climate change on agroecosystems: Scope of work
[PB90-120023] N90-18813
AGRISTARS PROJECT
Results of Agrisar-86 for the Flevopolder (Netherlands) test area
[BCRS-89-21] N90-18789
AH-1G HELICOPTER
Calculation of flight vibration levels of the AH-1G helicopter and correlation with existing flight vibration measurements
[NASA-CR-181923] N90-18743
AIR BREATHING ENGINES
Effect of correlation on multi-engine rocket propulsion systems N90-18467
AFOSR/ONR (Air Force Office of Scientific Research/Office of Naval Research) Contractors' Meeting on Combustion Rocket Propulsion Diagnostics of Reacting Flow
[AD-A216094] N90-18491
AIR DATA SYSTEMS
Wind-tunnel investigation of a flush airdata system at Mach numbers from 0.7 to 1.4
[NASA-TM-101697] N90-18395
AIR LAND INTERACTIONS
Sounding and surface meteorological data from the Land/Sea Breeze Experiment (LASBEX)
[AD-A216269] N90-18842
AIR POLLUTION
Photointerpretation with instruments for evaluation of environmental impact: Mata Atlantica in Cubata
[INPE-4910-PRE/1511] N90-18817
Tropospheric chemistry of natural hydrocarbons and energy-related pollutants: Biosphere/climate feedbacks
[DE90-005643] N90-18820
AIR TO AIR REFUELING
Visual servoing for autonomous aircraft refueling
[AD-A216042] N90-18386
AIR TRAFFIC
Dallas/Fort Worth simulation. Volume 2: Appendixes D, E, and F
[AD-A216613] N90-18380
AIR TRAFFIC CONTROL
National airspace system plan: Facilities, equipment, associated development and other capital needs
[AD-A215882] N90-18373
Delivery performance of conventional aircraft by terminal-area, time-based air traffic control: A real-time simulation evaluation
[NASA-TP-2978] N90-18378
Dallas/Fort Worth simulation. Volume 2: Appendixes D, E, and F
[AD-A216613] N90-18380
AIR TRAFFIC CONTROLLERS (PERSONNEL)
Delivery performance of conventional aircraft by terminal-area, time-based air traffic control: A real-time simulation evaluation
[NASA-TP-2978] N90-18378
AIRBORNE LASERS
An evaluation of an airborne laser profiling system for high precision terrain mapping
[AD-A217025] N90-18780
AIRCRAFT COMMUNICATION
Human factors issues in aircraft maintenance and inspection
[AD-A215724] N90-18875
AIRCRAFT CONFIGURATIONS
Fuselage design for a specified Mach-sliced area distribution
[NASA-TP-2975] N90-18385
Influence of forebody geometry on aerodynamic characteristics and a design guide for defining departure/spin resistant forebody configurations
[AD-A216714] N90-18388
A user's manual for the method of moments Aircraft Modeling Code (AMC)
[NASA-CR-186371] N90-18390
AIRCRAFT CONSTRUCTION MATERIALS
The manufacturing procedures for composite materials, automation, and robotization
[ETN-90-96232] N90-18528
Materials and structures for 2000 and beyond: An attempted forecast by the Materials and Structures Department of the DLR
[ESA-TT-1154] N90-18609
AIRCRAFT CONTROL
Possible piloting techniques at hypersonic speeds
[ISL-CO-216/88] N90-18392
Practical methods for robust multivariable control
[AD-A216937] N90-18920
AIRCRAFT DESIGN
Research on a two-dimensional inlet for a supersonic V/STOL propulsion system. Appendix A
[NASA-CR-174945] N90-18364
Fuselage design for a specified Mach-sliced area distribution
[NASA-TP-2975] N90-18385
Influence of forebody geometry on aerodynamic characteristics and a design guide for defining departure/spin resistant forebody configurations
[AD-A216714] N90-18388
AIRCRAFT ENGINES
AGARD/SMP Review: Damage Tolerance for Engine Structures. 2: Defects and Quantitative Materials Behaviour — conference
[AGARD-R-769] N90-18396
AIRCRAFT FUELS
Production of high density aviation fuels via novel zeolite catalyst routes
[AD-A216444] N90-18601
Low-energy gamma ray attenuation characteristics of aviation fuels
[NASA-TP-2974] N90-18882
AIRCRAFT GUIDANCE
The Fourteenth Biennial Guidance Test Symposium, volume 1
[AD-A216925] N90-18383

AIRCRAFT INSTRUMENTS
A simulation evaluation of the engine monitoring and control system display
[NASA-TP-2960] N90-18393
Three input concepts for flight crew interaction with information presented on a large-screen electronic cockpit display
[NASA-TM-4173] N90-18394
AIRCRAFT MAINTENANCE
Human factors issues in aircraft maintenance and inspection
[AD-A215724] N90-18875
AIRCRAFT PERFORMANCE
The effects of wind tunnel data uncertainty on aircraft point performance predictions
[AD-A216091] N90-18367
AIRCRAFT PRODUCTION COSTS
The manufacturing procedures for composite materials, automation, and robotization
[ETN-90-96232] N90-18528
AIRCRAFT RELIABILITY
Preliminary airworthiness evaluation of the Woodward hydromechanical unit installed on T700-GE-700 engines in the UH-60A helicopter
[AD-A216751] N90-18430
AIRCRAFT STRUCTURES
Materials and structures for 2000 and beyond: An attempted forecast by the Materials and Structures Department of the DLR
[ESA-TT-1154] N90-18609
AIRFOILS
Unsteady viscous calculation method for cascades with leading edge induced separation N90-18408
Asymptotic analysis of transonic flow through oscillating cascades N90-18421
Measurement of velocity profiles and Reynolds stresses on an oscillating airfoil N90-18427
AIRFRAMES
Calculation of flight vibration levels of the AH-1G helicopter and correlation with existing flight vibration measurements
[NASA-CR-181923] N90-18743
Fatigue crack initiation and small crack growth in several airframe alloys
[NASA-TM-102596] N90-18746
AIRGLOW
Study of the atmospheric emissions of OI wavelength 557.7 nm and O2 (0,0) wavelength 761.9 nm in the equatorial region utilizing measurement of photometer on-board a rocket
[INPE-4811-TDL/358] N90-18827
AIRPORTS
Synthetic aperture radar imagery of airports and surrounding areas: Archived SAR data
[NASA-CR-4275] N90-18371
Synthetic aperture radar imagery of airports and surrounding areas: Philadelphia Airport
[NASA-CR-4280] N90-18372
Low-energy gamma ray attenuation characteristics of aviation fuels
[NASA-TP-2974] N90-18882
AIRSPACE
National airspace system plan: Facilities, equipment, associated development and other capital needs
[AD-A215882] N90-18373
ALCOHOLS
Optimum catalytic process for alcohol fuels from syngas
[DE90-005290] N90-18600
Optimum catalytic process for alcohol fuels from syngas
[DE90-007188] N90-18604
ALGEBRA
A simple algebraic grid adaptation scheme with applications to two- and three-dimensional flow problems
[NASA-TM-102446] N90-18667
Parallel algorithms derivation
[AD-A216452] N90-18894
Differential-geometric techniques for solving differential algebraic equations
[AD-A216503] N90-18934
Schema-based theories of problem solving
[AD-A216717] N90-18939
ALGORITHMS
Visual servoing for autonomous aircraft refueling
[AD-A216042] N90-18386
Wind-tunnel investigation of a flush airdata system at Mach numbers from 0.7 to 1.4
[NASA-TM-101697] N90-18395
Analysis of whisker-toughened ceramic components: A design engineer's viewpoint
[NASA-TM-102333] N90-18504
Transient responses of coupled systems
[ONERA-RT-13/3596-RY-070-R] N90-18687
A numerical solution to the Boltzmann equation for use in calculating pumping rates in a CO2 discharge laser
[AD-A216376] N90-18718
Fast algorithms for calculating laser wavefront phase compensation given noisy measurements of phase gradient
[DE90-006357] N90-18727
Resource Assessment Project: User needs survey results
[DE89-009502] N90-18802
Spatial registration of TIROS-N weather satellite data
[AD-A216041] N90-18841
Comparisons between the RTNEPH (Real-Time Nephanalysis) and AFGL cloud layer analysis algorithms
[AD-A216637] N90-18844
A case study of the 24 August 1986 FLOWS microburst
[AD-A216939] N90-18847
Teleoperator servoloop tuning using an expert system
[DE90-005674] N90-18876
A scalable multiprocessor architecture using Cartesian network: Relative addressing
[AD-A216580] N90-18878
An exact algorithm for the problem of p-medians
[INPE-4924-TDL/384] N90-18885
DOA (Direction of Arrival) estimation by Eigendecomposition using single vector Lanczos' algorithm
[AD-A215802] N90-18887
Determination of the underlying task scheduling algorithm for and Ada runtime system
[AD-A215880] N90-18890
Distributed decomposition of block-angular linear programs on a hypercube computer
[AD-A216433] N90-18893
Parallel algorithms derivation
[AD-A216452] N90-18894
Optimum and heuristic algorithms for finite state machine decomposition and partitioning
[AD-A216778] N90-18899
Derivation of efficient parallel programs: An example from genetic sequence analysis
[DE90-005654] N90-18904
Parallelizing the SDI ACCESS algorithm for the Connection Machine-2
[DE90-006382] N90-18909
Can the square law be validated
[DE90-007112] N90-18945
On the depth of combinatorial optimization problems
[MEMO-803] N90-18946
ALKALI HALIDES
Atomic and molecular spectra from electron-excited alkali halides
[DE90-006160] N90-19004
ALKALI METALS
Positron-alkali atom scattering N90-18958
Scattering of positrons and electrons by alkali atoms N90-18959
Resonances in low-energy positron-alkali scattering N90-18992
ALLOYING
A fundamental understanding of the effect of alloying elements on the corrosion resistance of rapidly solidified Mg alloys
[AD-A216767] N90-18553
ALLOYS
Crystal growth and mechanical properties of semiconductor alloys
[AD-A216697] N90-19035
ALPHA PARTICLES
Thermonuclear instability of global-type shear Alfven modes
[DE90-007087] N90-19026
ALTERNATIONS
Application of Chebyshev approximation to curve fitting
[MEMO-805] N90-18947
ALUMINUM
Process development and fabrication of space station type aluminum-clad graphite epoxy struts
[NASA-CR-181873] N90-18454
The improved adhesion of organic polymers to silica and to aluminum metal with zirconium Schiff-base block copolymer coatings
[AD-A216669] N90-18575
ALUMINUM ALLOYS
A fundamental understanding of the effect of alloying elements on the corrosion resistance of rapidly solidified Mg alloys
[AD-A216767] N90-18553
Processing and elevated temperature ductility of aluminum alloy 7475
[AD-A216840] N90-18554
Significance of oxide skins on powder for the quality of PM Al materials
[ESA-TT-1178] N90-18580
Cost and energy consumption estimates for the aluminum-air battery anode fuel cycle
[DE90-005810] N90-18656
ALUMINUM COATINGS
The improved adhesion of organic polymers to silica and to aluminum metal with zirconium Schiff-base block copolymer coatings
[AD-A216669] N90-18575
ALUMINUM GALLIUM ARSENIDES
Luminescence of lanthanides and actinides implanted into binary III-V semiconductors and AlGaAs
[AD-A215759] N90-19031
ALUMINUM OXIDES
Significance of oxide skins on powder for the quality of PM Al materials
[ESA-TT-1178] N90-18580
Sintering of a model nickel/alumina catalyst
[ETN-90-96270] N90-18561
Microstructural variations in aluminum oxide coatings deposited using a dual beam ion system
[DE90-006040] N90-18583
Comparison of tension, compression, and flexure creep for alumina and silicon nitride ceramics
[DE90-006154] N90-18586
Ion implantation-induced amorphization of ceramic oxides
[DE90-006564] N90-19041
AMAZON REGION (SOUTH AMERICA)
Connections between the circulation in altitude and convection over South America
[INPE-4923-TDL/383] N90-18828
AMINO ACIDS
Characterization of biopolymer surfaces using scanning microscopies
[AD-A216572] N90-18572
AMMONIA
Intermittent Solar Ammonia Absorption Cycle (ISAAC) refrigeration for lesser developed countries
[DE90-006700] N90-18610
AMMONIUM NITRATES
Investigation of the phase stabilizing effect of 4 percent potassium fluoride on ammonium nitrate
[AD-A215313] N90-18599
AMMUNITION
Measurement of gas leaks between a projectile and the walls of a tube in a ballistic compressor
[ISL-CO-250/88] N90-18694
AMORPHOUS MATERIALS
Improved amorphous metal materials for magnetic pulse compression
[DE90-005723] N90-18555
Ion implantation-induced amorphization of ceramic oxides
[DE90-006564] N90-19041
AMORPHOUS SILICON
Hydrogenated amorphous silicon films prepared by glow discharge of disilane
[DE90-000309] N90-18581
Hydrogenated amorphous and microcrystalline silicon deposited from silane-hydrogen mixtures
[ETN-90-96267] N90-18590
Chemical vapor deposition and photochemical vapor deposition of amorphous silicon photovoltaic devices
[DE89-009510] N90-18803
AMPLIFICATION
Research on free electron lasers
[AD-A215865] N90-18715
Optical amplification in 45 deg - cut BaTiO3
[AD-A216043] N90-19011
AMPLITUDE MODULATION
Auditory perception
[AD-A217012] N90-18664
AMPLITUDES
A simulation of optical propagation through atmospheric turbulence using two-dimensional Fourier transform techniques
[AD-A216776] N90-19013
ANALOGIES
Systematicity as a selection constraint in analogical mapping
[AD-A216029] N90-18869
Analogies between cometary, interplanetary, and interstellar matter N90-19087
ANALYSIS (MATHEMATICS)
Analytic solutions for the decay of turbulent swirling flow in a cylinder
[DE90-005744] N90-18677
ANALYTICAL CHEMISTRY
Fundamental studies of surface processes and trace analysis using solid electrodes
[AD-A216538] N90-18533
ANALYZERS
BEAR electrostatic analyzer: Flight results
[DE90-006511] N90-18625

ANATOMY
Organization of a large-scale cortical network
[AD-A216829] N90-18883
ANGLE OF ATTACK
Static and rotational aerodynamic data from 0 deg to 90 deg angle of attack for a series of basic and altered forebody shapes
[AD-A216582] N90-18361
Influence of forebody geometry on aerodynamic characteristics and a design guide for defining departure/spin resistant forebody configurations
[AD-A216714] N90-18388
Application of variable-gain output feedback for high-alpha control
[NASA-TM-102603] N90-18434
ANGLES (GEOMETRY)
Angle estimation in the presence of mainbeam interference
[AD-A216632] N90-18621
ANGULAR CORRELATION
Angular correlation studies in noble gases N90-18972
ANIONS
Cell performance of ultra-thin polymer cathode systems. Part 1: Anion intercalating polymer cathode
[AD-A216037] N90-18639
ANISOTROPY
Analysis of linear multigrid methods for elliptic differential equations with discontinuous and anisotropic coefficients
[ETN-90-96269] N90-18944
ANNEALING
Structure and reactivity of model thin film catalysts
[DE90-007365] N90-18548
ANNIHILATION REACTIONS
Annihilation in Gases and Galaxies
[NASA-CP-3058] N90-18957
Angular correlation studies in noble gases N90-18972
Total cross sections for positrons scattered elastically from helium based on new measurements of total ionization cross sections N90-18976
Multiple-ionization of xenon atoms by positron impact N90-18978
Positron annihilation in gamma-ray bursts N90-18983
Annihilation physics of exotic galactic dark matter particles N90-18984
Optically excited states in positronium N90-18985
Antiproton-matter interactions in antiproton applications N90-18989
Positron-molecule bound states and positive ion production N90-18994
ANODES
Cost and energy consumption estimates for the aluminum-air battery anode fuel cycle
[DE90-005810] N90-18656
ANOMALIES
Process development and fabrication of space station type aluminum-clad graphite epoxy struts
[NASA-CR-181873] N90-18454
Technique for evaluating the erosive properties of ablative internal insulation materials N90-18466
ANTARCTIC REGIONS
An application of ocean wave-current refraction to the gulf stream using SEASAT SAR data
[AD-A216769] N90-18851
ANTENNA ARRAYS
Reconfigurable antennas, monolithic microwave integrated circuits with feeding networks for microstrip antennas
[AD-A216916] N90-18622
ANTENNA FEEDS
Reconfigurable antennas, monolithic microwave integrated circuits with feeding networks for microstrip antennas
[AD-A216916] N90-18622
ANTENNA RADIATION PATTERNS
ACIRF user's guide: Theory and examples
[AD-A216436] N90-18613
ANTHROPOMETRY
Anthropometry of a fit test sample used in evaluating the current and improved MCU-2/P masks
[AD-A215173] N90-18573
ANTIBIOTICS
Study of rifampicin fixation on plasma proteins by derivative spectrophotometry
[CERMA-89-25] N90-18566
ANTIFRICTION BEARINGS
Life of concentrated contacts in the mixed EHD and boundary film regimes
[AD-A216873] N90-18736
ANTIMATTER
Annihilation in Gases and Galaxies
[NASA-CP-3058] N90-18957
ANTIPROTONS
Antihydrogen formation in collisions of positronium with antiprotons N90-18968
Antiproton-matter interactions in antiproton applications N90-18989
APL (PROGRAMMING LANGUAGE)
Simulating simultaneous processes with APL
[MEMO-INF-89-47] N90-18906
APPROXIMATION
Approximations to joint distributions of definite quadratic forms
[AD-A216434] N90-18930
Strong moderate deviation theorems
[MEMO-804] N90-18954
Deterministic differential game solution: The approximate strategy method
[ESA-TT-1158] N90-18956
APTITUDE
Appropriateness measurement for computerized adaptive tests
[AD-A216121] N90-18870
ARC JET ENGINES
Electric propulsion options for 10 kW class earth-space missions N90-18474
Test facility and preliminary performance of a 100 kW class MPD thruster N90-18476
Arcjet cathode phenomena N90-18477
Arcjet nozzle design impacts N90-18478
Mission options for an electric propulsion demonstration flight test N90-18479
ARCHITECTURE (COMPUTERS)
A microcode compiler that runs on the IBM AT and supports cascadable microcomputers, part 1
[AD-A215888] N90-18877
A scalable multiprocessor architecture using Cartesian network: Relative addressing
[AD-A216580] N90-18878
Performance characterization of the Convex C-240 computer system
[DE90-006425] N90-18879
Ceder project: Original goals and progress to date
[DE90-006761] N90-18880
L: A language for solution of incremental systems in a parallel processing environment
[INPE-4816-TDL/362] N90-18884
Derivation of efficient parallel programs: An example from genetic sequence analysis
[DE90-005654] N90-18904
Parallelizing the SDI ACCESS algorithm for the Connection Machine-2
[DE90-006382] N90-18909
Summer institute in parallel computing
[DE90-005532] N90-18910
Using special-purpose computing to examine chaotic behavior in nonlinear mappings
[AD-A216800] N90-18916
Architecture for a human-robot symbiotic system
[DE90-005670] N90-18921
Using the K-25 C/TD common file system: A guide to CFSI
[DE90-005815] N90-19179
ARGON
The effect of electric field on attachment of electrons to solutes in liquid argon
[DE90-003969] N90-18529
Numerical Green's functions in optical potential calculations for positron scattering from argon and neon N90-18971
ARGON LASERS
A study of the interaction of light with surfaces of sub-micron dimensions
[DE90-005646] N90-19046
ARITHMETIC
Research equipment
[AD-A216515] N90-18937
ARRAYS
Aerodynamic study on forced vibrations on stator rows of axial compressors N90-18412
ARTIFICIAL INTELLIGENCE
SHARP: A multi-mission artificial intelligence system for spacecraft telemetry monitoring and diagnosis
[NASA-CR-186285] N90-18444
An approach centered in production rules for a partition of environment and planning in a visual navigation system (SNV)
[INPE-4813-TDL/360] N90-18737
A self-organizing multiple-view representation of three-dimensional objects
[AD-A216711] N90-18871
KAM: Automatic planning and interpretation of numerical experiments using geometrical methods
[AD-A216805] N90-18900
A colony architecture for an artificial creature
[AD-A216802] N90-18918
Architecture for a human-robot symbiotic system
[DE90-005670] N90-18921
Teaching a new methodology for designing relational data bases: An experiment testing the effectiveness of an intelligent tutoring system on cognitive skill acquisition (volumes 1 and 2) N90-19063
ARTIFICIAL SATELLITES
Orbit determination of artificial Earth satellites through estimation techniques combined with state smoothing techniques
[INPE-4959-TDL/388] N90-18440
Evaluation of influences of errors involved in orbit propagation of artificial satellites
[INPE-4962-TDL/391] N90-18441
ASSEMBLING
RALPH: An automatic Robot Assembly Language Programmer: An overview
[PB90-120973] N90-18912
ASSESSMENTS
Probability of failure and risk assessment of propulsion structural components N90-18470
ASTEROIDS
Zodiacal dust bands: Their relation to asteroid families
[AD-A219025] N90-19170
ASTROMETRY
Solar variability observed through changes in solar figure and mean diameter
[DE90-006600] N90-18834
ASTRONAUT TRAINING
Activities report in German aerospace
[ISSN-0070-3966] N90-19189
ASTRONOMICAL CATALOGS
A comparison of void distributions in Abell cluster catalogue with numerical simulations
[DE90-610640] N90-19173
ASTRONOMICAL MODELS
The microwave background in steady-state cosmology N90-19150
ASTRONOMICAL OBSERVATORIES
The James Clerk Maxwell telescope N90-19166
ASTRONOMICAL PHOTOMETRY
Infrared properties of five spiral galaxies N90-19154
ASTRONOMICAL SPECTROSCOPY
IR spectroscopy of planets and satellites; Venus, Mars, giant planets, and Titan N90-19085
Infrared spectroscopy of dust N90-19094
ASTROPHYSICS
Gamma ray astronomy and black hole astrophysics
[NASA-CR-186496] N90-19169
Particle physics and cosmology
[DE90-006547] N90-19171
Current and future uses of accelerators in particle astrophysics
[DE90-006667] N90-19186
ASYMPTOTIC METHODS
Asymptotic analysis of transonic flow through oscillating cascades N90-18421
Transient responses of coupled systems
[ONERA-RT-13/3596-RY-070-R] N90-18687
Asymptotic boundary conditions for dissipative waves: General theory
[NASA-TM-102497] N90-18927
ASYMPTOTIC SERIES
Using the method of matched asymptotic expansions, analytically investigate the three-dimensional, atmosphere entry problem
[AD-A216287] N90-18451
ATLANTIC OCEAN
Intertropical Convergence Zone (ITCZ) and its relationship with the precipitation of the north-northeast Brazilian region
[INPE-4887-TDL/378] N90-18839
Dynamics of an ERICA (Experiment on Rapidly Intensifying Cyclones over the Atlantic) cyclone
[AD-A216775] N90-18848
ATMOSPHERIC BOUNDARY LAYER
Some aspects of atmospheric turbulence in forests
[INPE-4951-RPE/600] N90-18818
Sounding and surface meteorological data from the Land/Sea Breeze Experiment (LASBEX)
[AD-A216269] N90-18842
ATMOSPHERIC CHEMISTRY
Tropospheric chemistry of natural hydrocarbons and energy-related pollutants: Biosphere/climate feedbacks
[DE90-005643] N90-18820
ATMOSPHERIC CIRCULATION
Perspectives on aerosol deposition to natural surfaces
[DE90-003398] N90-18819
Connections between the circulation in altitude and convection over South America
[INPE-4923-TDL/383] N90-18828
Summer Study Program in Geophysical Fluid Dynamics: The Influence of Convection on Large-Scale Circulations, 1988
[AD-A216024] N90-18840
Dynamics of an ERICA (Experiment on Rapidly Intensifying Cyclones over the Atlantic) cyclone
[AD-A216775] N90-18848

ATMOSPHERIC ELECTRICITY
Airborne measurements of the electric field and the charge precipitation particles in convective clouds: Lower positive charge centres
[ESA-TT-1157] N90-18836
ATMOSPHERIC ENTRY
Using the method of matched asymptotic expansions, analytically investigate the three-dimensional, atmosphere entry problem
[AD-A216287] N90-18451
ATMOSPHERIC MODELS
ACIRF user's guide: Theory and examples
[AD-A216436] N90-18813
Perspectives on aerosol deposition to natural surfaces
[DE90-003398] N90-18819
ATMOSPHERIC PHYSICS
Activities report in DLR research field communication engineering and reconnaissance
[ISSN-0173-0118] N90-18781
Studies of cubic ice crystals
[AD-A216574] N90-18832
ATMOSPHERIC PRESSURE
High growth rate diamond synthesis in a large area atmospheric pressure inductively coupled plasma
[AD-A216090] N90-19019
ATMOSPHERIC REFRACTION
Navigation experiment NAVEX data storage and processing
[ESA-TT-1175] N90-18445
ATMOSPHERIC SOUNDING
Preliminary comparison of temperature soundings obtained from simultaneous radiometric, radio-acoustic, and rawinsonde measurements
[PB90-119835] N90-18838
ATMOSPHERIC TEMPERATURE
Preliminary comparison of temperature soundings obtained from simultaneous radiometric, radio-acoustic, and rawinsonde measurements
[PB90-119835] N90-18838
ATMOSPHERIC TURBULENCE
Some aspects of atmospheric turbulence in forests
[INPE-4951-RPE/600] N90-18818
Temporal response of atmospheric turbulence compensation
[DE90-006354] N90-18837
A simulation of optical propagation through atmospheric turbulence using two-dimensional Fourier transform techniques
[AD-A216776] N90-19013
Application of wavefront analysis techniques to restoring of images degraded by atmospheric turbulence
[ONERA-PUBL-1989-1] N90-19168
ATMOSPHERICS
Temporal response of atmospheric turbulence compensation
[DE90-006354] N90-18837
ATOMIC BEAMS
Measurement of the space potential of a high-temperature plasma by fast atomic beam scattering on an ion probe beam
[DE90-006118] N90-19020
ATOMIC CLOCKS
Determining the effects of microwave power and C-field setting on the frequency of a cesium atomic frequency standard
[AD-A216599] N90-18642
Synchronization of the ground station atomic clocks using three weighted transportable cesium time standards in the Navex navigation experiment
[ESA-TT-1153] N90-18711
ATOMIC COLLISIONS
Scattering of positrons and electrons by alkali atoms N90-18959
Positron collisions with alkali-metal atoms N90-18962
Theoretical survey on positronium formation and ionisation in positron atom scattering N90-18965
New parameter-free polarization potentials in low-energy positron collisions N90-18968
Ionisation of atomic hydrogen by positron impact N90-18977
ATOMIC ENERGY LEVELS
Inelastic collisions of positrons with one-valence-electron targets N90-18963
Positron-rubidium scattering N90-18964
Theoretical survey on positronium formation and ionisation in positron atom scattering N90-18965
The calculation of the contributions to low energy e+H2 scattering from sigma u+ and Pion u symmetries using the Kohn variational method N90-18969
ATOMIC EXCITATIONS
Inelastic collisions of positrons with one-valence-electron targets N90-18963
Positron excitation of neon N90-18973
Optically excited states in positronium N90-18985
Positronium ions and molecules N90-18990
Structure and vibrational excitations of reconstructed semiconductor surfaces
[DE90-006589] N90-19044
ATOMIC PHYSICS
Annihilation physics of exotic galactic dark matter particles N90-18984
ATOMIC SPECTRA
Atomic and molecular spectra from electron-excited alkali halides
[DE90-008160] N90-19004
ATOMIC STRUCTURE
Structure and vibrational excitations of reconstructed semiconductor surfaces
[DE90-006589] N90-19044
ATTITUDE CONTROL
Possible piloting techniques at hypersonic speeds
[ISL-CO-216/88] N90-18392
Data collection and location platforms experimental network: Description of an orbit routine
[INPE-4798-NTE/287] N90-18439
Attitude estimation procedure for spin stabilized satellites
[INPE-4866-TDL/377] N90-18449
AUDIO FREQUENCIES
Perception of long-period complex sounds
[AD-A216743] N90-18861
AUDITORY PERCEPTION
Perception of long-period complex sounds
[AD-A216743] N90-18861
Auditory perception
[AD-A217012] N90-18864
AUDITORY SIGNALS
Auditory perception
[AD-A217012] N90-18864
AUDITORY STIMULI
Auditory perception
[AD-A217012] N90-18864
AUGER SPECTROSCOPY
Spectroscopic evidence for carbon-carbon bonding in carbide layers on metals
[AD-A216726] N90-18512
Extracting chemical information form Auger line shapes
[AD-A216729] N90-18537
Positron annihilation induced Auger electron spectroscopy N90-18996
AUSTENITIC STAINLESS STEELS
Helium permeability through austenitic stainless steel
[DE90-007046] N90-18582
AUTOCORRELATION
Effects of strong scattering on transionospheric propagation
[AD-A216708] N90-18617
AUTOMATIC CONTROL
KAM: Automatic planning and interpretation of numerical experiments using geometrical methods
[AD-A216605] N90-18900
RALPH: An automatic Robot Assembly Language Programmer: An overview
[PB90-120973] N90-18912
AUTONOMY
Autonomous orbit determination using GPS
[INPE-4815-TDL/361] N90-18442
AUXILIARY PROPULSION
Advanced APS impacts on vehicle payloads N90-18472
AVERAGE
Development of a mass averaging temperature probe N90-18418
AVIATION METEOROLOGY
Proceedings of the Professional Pilots Meteorology Training Standards Conference
[AD-A216818] N90-18843
AXIAL LOADS
Compressive strength of carbon/epoxy laminated under multiaxial stress
[DE90-005552] N90-18505
AXIAL STRAIN
Damage in a perforated graphite-epoxy composite plate under monotonic and cyclic biaxial loading
[ESA-TT-1117] N90-18521

B

BACKWARD FACING STEPS
Theoretical investigation of the stabilization of a diffusion flame above a recirculation region
[ESA-TT-1149] N90-18543
BALLOON-BORNE INSTRUMENTS
Wide-beam balloon observations of the 157.7 microns (CII) line N90-19106
BANDWIDTH
A unified model for the 3.28 micron and 3.4 micron spectral feature in the interstellar medium and in comets N90-19092
A coal model for the carriers of the unidentified IR bands N90-19110
BARIUM TITANATES
Optical amplification in 45 deg - cut BaTiO3
[AD-A216043] N90-19011
BEADS
Model filled polymers 3. Rheological behavior of polystyrene containing crosslinked polystyrene beads
[AD-A215867] N90-18567
BEAM INJECTION
Injection parameters and beam oscillations during extraction
[NIKHEF-K/AMPS/89-07] N90-18632
BEAMS (RADIATION)
Determining the effects of microwave power and C-field setting on the frequency of a cesium atomic frequency standard
[AD-A216599] N90-18642
BEARING (DIRECTION)
Grouping for recognition
[AD-A216716] N90-18915
BEND TESTS
Measuring strain in carbon fibre composite laminates using the Raman optomechanical strain gauge N90-18503
Compact reinforced composite basic principles
[CBL-41] N90-18520
BENZENE
Extracting chemical information form Auger line shapes
[AD-A216729] N90-18537
BINARY SYSTEMS (MATERIALS)
The propagation of time harmonic Rayleigh-Lamb waves in a bimaterial plate
[AD-A216834] N90-18749
Luminescence of lanthanides and actinides implanted into binary III-V semiconductors and AlGaAs
[AD-A215759] N90-19031
BIOELECTRICITY
Coronary arterial capacitance and subendocardial vascular patency throughout the cardiac cycle N90-18855
BIOLOGICAL EFFECTS
Risk analysis: Fundamental concepts, regulatory toxicology, and relative comparisons from radiation biology
[DE90-002466] N90-18856
BIOMASS
Relationships between the aerial biomass from ground layers of cerrado and its spectral reflectance
[INPE-4848-PRE/1477] N90-18760
Hawaii integrated biofuels research program, phase 1
[DE90-006885] N90-18811
BIOMASS ENERGY PRODUCTION
Hawaii integrated biofuels research program, phase 1
[DE90-006885] N90-18811
BIOMEDICAL DATA
Biomedical applications of synchrotron x ray microscopy
[DE90-004957] N90-18867
BIOPOLYMERS
Characterization of biopolymer surfaces using scanning microscopies
[AD-A216572] N90-18572
BIOREACTORS
Three-dimensional coculture process
[NASA-CASE-MSC-21560-1] N90-18852
BIRDS
Study of bird ingestions into small inlet area, aircraft turbine engines (May 1987 to April 1988)
[DOT/FAA/CT-89/17] N90-18375
Bird impact tests on a Kevlar 49 structure. Monolithic plates. Oblique-angled impact
[REPT-S3-4273] N90-18376
Remote sensing for the classification and quantification of vegetation in Spring staging areas of Brent geese on the Frisian Islands (Netherlands)
[BCRS-89-27] N90-18790
BISMALEIMIDE
Modified bismaleimides for carbon fibre composites N90-18495
BLACK HOLES (ASTRONOMY)
Infrared spectroscopy of the central few parsecs of the galaxy N90-19140
Gamma ray astronomy and black hole astrophysics
[NASA-CR-186496] N90-19189
BLADE-VORTEX INTERACTION
Prediction of rotor blade-vortex interaction noise from 2-D aerodynamic calculations and measurements
[ISL-CO-243/88] N90-18365
Study of the blade/vortice interaction on a one-blade rotor during forward flight (incompressible, non viscous fluid)
[ISL-R-115/88] N90-18391
Development of a mass averaging temperature probe N90-18418

Methods for making unsteady aerodynamic pressure measurements in a rotating turbine stage N90-18426
BLADES
Calculation of the unsteady two-dimensional, inviscid, compressible flow around a strongly cambered oscillating single blade N90-18409
BLOCK COPOLYMERS
The improved adhesion of organic polymers to silica and to aluminum metal with zirconium Schiff-base block copolymer coatings
[AD-A216669] N90-18575
BLOOD
Performance of a coincidence based blood activity monitor
[DE90-006105] N90-18865
BLOOD FLOW
Coronary arterial capacitance and subendocardial vascular patency throughout the cardiac cycle N90-18855
BLOOD PLASMA
Study of rifampicin fixation on plasma proteins by derivative spectrophotometry
[CERMA-89-25] N90-18866
BLOOD PRESSURE
The role of blood volume in determining the cardiovascular adjustments to exercise N90-18854
BLOOD VOLUME
The role of blood volume in determining the cardiovascular adjustments to exercise N90-18854
BOLTZMANN DISTRIBUTION
The neoclassical transport of toroidal momentum in tokamaks
[DE90-006864] N90-19023
BOLTZMANN TRANSPORT EQUATION
A numerical solution to the Boltzmann equation for use in calculating pumping rates in a CO2 discharge laser
[AD-A216376] N90-18718
BONDING
Enhanced bonding of fiber reinforcements to thermoset resins N90-18496
BOOLEAN ALGEBRA
Boolean minimization and algebraic factorization procedures for fully testable sequential machines
[AD-A216779] N90-18940
BORANES
Metallaboranes as precursors to metallic glasses
[AD-A216946] N90-18577
BORN APPROXIMATION
Positron collisions with alkali-metal atoms N90-18962
The calculation of the contributions to low energy e+H2 scattering from sigma u+ and Pion u symmetries using the Kohn variational method N90-18969
BOUNDARIES
Kinetic relations and the propagation of phase boundaries in solids
[AD-A215861] N90-18747
BOUNDARY LAYER EQUATIONS
Multicellular natural convection in a narrow vertical slot
[AD-A216411] N90-18668
BOUNDARY LAYER SEPARATION
Experimental investigation of the influence of rotor wakes on the development of the profile boundary layer and the performance of an annular compressor cascade N90-18425
Measurement of velocity profiles and Reynolds stresses on an oscillating airfoil N90-18427
Contribution to the study of three-dimensional separation in turbulent incompressible flow
[ESA-TT-1169] N90-18897
BOUNDARY LAYER TRANSITION
Modelling unsteady transition and its effects on profile loss N90-18423
Experimental investigation of the influence of rotor wakes on the development of the profile boundary layer and the performance of an annular compressor cascade N90-18425
BOUNDARY LAYERS
Aerodynamics of unsteady systems. Numerical study of potential flow/boundary layer coupling
[ETN-90-96257] N90-18367
Experimental investigations of the unsteady boundary layer on an oscillating flat plate. Optimization and validation of a code, for calculating the potential flow/boundary layer coupling of a flat plate and of an oscillating profile
[ETN-90-96254] N90-18682
BOUNDARY VALUE PROBLEMS
Asymptotic boundary conditions for dissipative waves: General theory
[NASA-TM-102497] N90-18827
BRANCHING (MATHEMATICS)
New aspects in bifurcation with symmetry
[AD-A216506] N90-18935
BRANCHING (PHYSICS)
The 2.7/4.3 micron CO2 branching ratio measurement
[AD-A215952] N90-18830
BRASSES
Pulsed laser-induced melting of intermediate Cu-Zn phases
[DE90-005404] N90-18713
BRAZIL
TVI: A mathematical model for global estimation of Brazilian cerrado phytomass
[INPE-4836-PRE/1465] N90-18759
Remote sensing applied to the monitoring of mineral extraction in the proximity of urban areas: Pros and cons
[INPE-4867-PRE/1478] N90-18766
Radiometric study of wheat and bean crops in three types of latossolo
[INPE-4843-PRE/1472] N90-18767
Multistage forest volume estimation using a sampling system with probability variables
[INPE-4897-PRE/1498] N90-18769
Development of the agricultural information system. Characteristics and results of the Distrito Federal model
[INPE-4940-PRE/1430] N90-18773
Perspective revision of systematic mapping through orbital imagery
[INPE-4817-PRE/1453] N90-18775
Photointerpretation with instruments for evaluation of environmental impact: Mata Atlantica in Cubata
[INPE-4910-PRE/1511] N90-18817
Geological structure of the State of Rio de Janeiro viewed through MSS LANDSAT imagery
[INPE-4826-PRE/1457] N90-18825
Quantification of structural field data in the Rio Grande do Norte basin and neighborhood
[INPE-4821-RPE/591] N90-18826
The patterns of fracture and the conditioning tectonics in the region of the Quadrilatero Ferrifero and part of the Migmatitic-Gnanulitic Complex in Minas Gerais (Brazil)
[INPE-4895-PRE/1496] N90-18829
Intertropical Convergence Zone (ITCZ) and its relationship with the precipitation of the north-northeast Brazilian region
[INPE-4887-TDL/378] N90-18839
BREADBOARD MODELS
Electronically Variable Pressure Regulator (EVPR) N90-18484
BREATHING APPARATUS
The effects of wearing passenger protective breathing equipment on evacuation times through type 3 and type 4 emergency aircraft exits in clear air and smoke. Phase 1: Evacuations in clear air. Phase 2: Evacuations in smoke
[AD-A216798] N90-18374
BRIGHTNESS
Electron beam and high-speed optical diagnostics for the Los Alamos HIBAF (High Brightness Accelerator FEL) Facility
[DE90-007828] N90-18725
BRITTLE MATERIALS
Spallation and dynamic fracture as an effect of laser induced shock waves in carbon based composite materials
[AD-A216540] N90-18509
BROADBAND
A new broadband pulsed high voltage monitor
[DE90-006264] N90-18651
BROMINE
Feasibility of a super high energy density battery of the Li/BrF3 electrochemical system
[AD-A216575] N90-18799
BROMINE COMPOUNDS
Feasibility of a super high energy density battery of the Li/BrF3 electrochemical system
[AD-A216794] N90-18644
BUNCHING
Instability investigation for storage mode. Microwave instability (single-bunch instability)
[NIKHEF-K/AMPS/89/05] N90-18628
BUOYS
Comparison of circulation obtained through the trajectory of a drifting buoy tracked by satellite and hydrographic data in the Bransfield Strait
[INPE-4946-TDL/387] N90-18850

C

CADMIUM
Elastic scattering of e- and e+ from Rb and Cd N90-18960
CALCIUM OXIDES
High temperature interaction of SO2 with oxide sorbents
[DE90-000435] N90-18545
CALCULUS
Should a function continue
[AD-A216406] N90-18929
CALENDARS
Calendar of selected aeronautical and space meetings
[AGARD-CAL-90/1] N90-19060
CALIBRATING
Feasibility demonstration of a 445N high-performance rocket engine N90-18481
A new broadband pulsed high voltage monitor
[DE90-006264] N90-18651
Measurement of spectral emissivity by Fourier transform infrared spectrometer
[DE89-782319] N90-18698
Construction and calibration of a gas pressure meter with high temporal resolution
[INPE-4953-RPE/602] N90-18700
Electron beam and high-speed optical diagnostics for the Los Alamos HIBAF (High Brightness Accelerator FEL) Facility
[DE90-007828] N90-18725
Measurement system of spectral irradiance in the near infrared N90-19160
CALORIMETERS
Microcalometric studies of gun propellant KKR 8
[FOA-C-20770-2.1] N90-18606
CAMBER
Calculation of the unsteady two-dimensional, inviscid, compressible flow around a strongly cambered oscillating single blade N90-18409
CAMERAS
Visual navigation: Constructing and utilizing simple maps of an indoor environment
[AD-A216761] N90-18382
High speed imaging with a tapped solid state sensor
[DE90-006116] N90-18702
Refurbishment and modification of the Metric Camera (RMK) for reflight on EOM-1 Spacelab mission
[ETN-90-96284] N90-18710
CANOPIES (VEGETATION)
Relationships between the aerial biomass from ground layers of cerrado and its spectral reflectance
[INPE-4848-PRE/1477] N90-18760
Thermal remote sensing in the differentiation of soybean crops (glycine max (L.) merrill) submitted to water deficit
[INPE-4900-PRE/1501] N90-18762
Relationships between spectral parameters and agronomics of wheat and beam crops
[INPE-4791-RPE/584] N90-18768
Evaluation of TM/LANDSAT and HRV/SPOT data in reforested areas
[INPE-4575-RPE/567] N90-18772
Spectral response of wheat and its relationship with agronomical prameters
[INPE-4950-RPE/599] N90-18774
Some aspects of atmospheric turbulence in forests
[INPE-4951-RPE/600] N90-18818
CAPACITANCE
Coronary arterial capacitance and subendocardial vascular patency throughout the cardiac cycle N90-18855
CAPACITORS
Spacecraft thermal control design data, volume 3
[ESA-PSS-03-108-ISSUE-1-VOL-3] N90-18457
Reliability studies of ceramic capacitors
[AD-A216763] N90-18643
CAPILLARY TUBES
Fluorescence and elastic scattering from laser dye-filled capillaries
[AD-A217026] N90-18540
CARBIDES
Continuous preparation of a thin refractory carbide deposit on the surface of carbon fibers: Characterization of the C/SiC fiber N90-18501
Spectroscopic evidence for carbon-carbon bonding in carbide layers on metals
[AD-A216726] N90-18512
CARBON
Effect of propellant flowrate and purity on carbon deposition in LO2/methane gas generators N90-18468
Spectroscopic evidence for carbon-carbon bonding in carbide layers on metals
[AD-A216726] N90-18512
Wide-beam balloon observations of the 157.7 microns (CII) line N90-19108
CARBON DIOXIDE
Oxygen electrode in molten carbonate fuel cells
[DE90-005377] N90-18796
Natural and anthropogenic climate change
[DE90-006488] N90-18822
The 2.7/4.3 micron CO2 branching ratio measurement
[AD-A215952] N90-18830
Studies of atmospheric molecules by multiphoton spectroscopy
[DE90-005829] N90-18833

Spectroscopy and physico-chemistry of CO:H2O and CO2:H2O ices N90-19111
CARBON DIOXIDE CONCENTRATION
Variations in volatiles in magma bodies based on studies of melt inclusions
[DE90-006272] N90-18821
CARBON DIOXIDE LASERS
A numerical solution to the Boltzmann equation for use in calculating pumping rates in a CO2 discharge laser
[AD-A216376] N90-18718
Cloud hole-boring with infrared lasers: Theory and experiment
[DE90-006519] N90-18723
Effects produced by pulsed CO2 lasers
[ISL-R-112/88] N90-18731
Research on sliding spark preionization in a TEA CO2 laser
[ISL-R-113/88] N90-18732
Study of discharge mechanisms and the stability of transverse electric discharges in the gas mixtures
[ISL-R-114/88] N90-18733
CARBON FIBER REINFORCED PLASTICS
Enhanced bonding of fiber reinforcements to thermoset resins N90-18496
Calculation of mechanical properties variations depending on matrix parameters in a composite, as a function of the test temperature
[DT-311/88] N90-18526
Impact of composites in the aerospace industry
[ETN-90-96231] N90-18527
The manufacturing procedures for composite materials, automation, and robotization
[ETN-90-96232] N90-18528
CARBON FIBERS
Modified bismaleimides for carbon fibre composites N90-18495
Interlaminar fracture testing of carbon fibre/PEEK composites validity and applications N90-18497
Continuous preparation of a thin refractory carbide deposit on the surface of carbon fibers: Characterization of the C/SiC fiber N90-18501
Measuring strain in carbon fibre composite laminates using the Raman optomechanical strain gauge N90-18503
CARBON LASERS
Inspection of carbon/epoxy and aluminum honeycomb paraboloidal components by HNDT
[AD-A216796] N90-18514
CARBON MONOXIDE
Observations of CO on Mars in the infrared and millimetre range N90-19090
Spectroscopy and physico-chemistry of CO:H2O and CO2:H2O ices N90-19111
CO infrared bands in atmospheres of long-period variables N90-19128
Carbon monoxide in supernova 1987A N90-19135
The strengths of the 2.3 micron CO band in luminous interacting and merging galaxies N90-19148
A search for the CO feature in active galactic nuclei N90-19151
CARBON STARS
IR spectrophotometry of bright carbon stars N90-19131
CARBON STEELS
The mechanism, measurement, and influence of properties on the galling of metals
[DE90-006533] N90-18558
CARBON-CARBON COMPOSITES
Third European Conference on Composite Materials
[EOARD-LR-89-050] N90-18494
State of the art and future prospects for high temperature composites N90-18498
Spallation and dynamic fracture as an effect of laser induced shock waves in carbon based composite materials
[AD-A216540] N90-18509
CARBONACEOUS MATERIALS
A coal model for the carriers of the unidentified IR bands N90-19110
CARBONATES
Oxygen electrode in molten carbonate fuel cells
[DE90-005377] N90-18796
CARCINOGENS
Risk analysis: Fundamental concepts, regulatory toxicology, and relative comparisons from radiation biology
[DE90-002466] N90-18856
CARDIOVASCULAR SYSTEM
The role of blood volume in determining the cardiovascular adjustments to exercise N90-18854
CARGO
Electric propulsion for manned Mars exploration N90-18480
CARRIER FREQUENCIES
Applications of acousto-optical correlation devices in radar signal processing
[AD-A216624] N90-18616
CARTESIAN COORDINATES
A scalable multiprocessor architecture using Cartesian network: Relative addressing
[AD-A216580] N90-18878
CASCADE FLOW
Unsteady Aerodynamic Phenomena in Turbomachines
[AGARD-CP-468] N90-18405
Numerical investigation of unsteady flow in oscillating turbine and compressor cascades N90-18407
Unsteady viscous calculation method for cascades with leading edge induced separation N90-18408
Aerodynamic superposition principle in vibrating turbine cascades N90-18410
Gust response analysis for cascades operating in nonuniform mean flows N90-18415
High-resolution Euler computations of unsteady transonic flows in cascades N90-18420
Asymptotic analysis of transonic flow through oscillating cascades N90-18421
Experiments on the unsteady flow in a supersonic compressor stage N90-18422
Time-dependent measurements on vibrating annular turbine cascades under various steady state conditions N90-18424
Experimental investigation of the influence of rotor wakes on the development of the profile boundary layer and the performance of an annular compressor cascade N90-18425
CASES (CONTAINERS)
Feasibility of a super high energy density battery of the Li/BrF3 electrochemical system
[AD-A216794] N90-18844
CAST ALLOYS
Identification of a cast iron alloy containing nonstrategic elements
[NASA-CR-185174] N90-18559
CASTINGS
Defects in monoblock cast turbine wheels N90-18400
CASUALTIES
Can the square law be validated
[DE90-007112] N90-18945
CATABOLISM
A program for the study of skeletal muscle catabolism following physical trauma
[AD-A216569] N90-18859
CATALYSTS
Structure and reactivity of model thin film catalysts
[DE90-007365] N90-18546
Sintering of a model nickel/alumina catalyst
[ETN-90-96270] N90-18561
Morphological consequences of catalytic hydrogenation of polymers in the bulk
[DE90-007276] N90-18598
Optimum catalytic process for alcohol fuels from syngas
[DE90-005290] N90-18600
Production of high density aviation fuels via novel zeolite catalyst routes
[AD-A216444] N90-18601
Optimum catalytic process for alcohol fuels from syngas
[DE90-007188] N90-18604
CATHODES
Arcjet cathode phenomena N90-18477
CAVITATION FLOW
Study on the thermodynamical and mechanical conditions for the generation of high operating pressures with liquefied gases for low and very low flow rates
[ESA-TT-1148] N90-18696
CELL CATHODES
Cell performance of ultra-thin polymer cathode systems. Part 1: Anion intercalating polymer cathode
[AD-A216037] N90-18639
CELLS (BIOLOGY)
Three-dimensional coculture process
[NASA-CASE-MSC-21560-1] N90-18852
CELLULOSE NITRATE
Experimental and theoretical research on the injection of ignition gases into a bed of inert powder
[ISL-CO-251/88] N90-18547
CENTRAL AMERICA
Forecasters handbook for Central America and adjacent waters
[AD-A216752] N90-18845
CENTRIFUGAL FORCE
Study of vortex arrays induced artificially and from centrifugal instabilities
[AD-A216499] N90-18669
CERAMIC BONDING
Interfacial chemistry of MoS2 films on Si
[AD-A216527] N90-18532
CERAMIC COATINGS
Laboratory for the processing and evaluation of inorganic matrix composites
[AD-A216881] N90-18516
CERAMIC FIBERS
Sputter deposition of diffusion barrier coatings on SiC monofilaments for use in Ti-based composites N90-18502
CERAMIC MATRIX COMPOSITES
State of the art and future prospects for high temperature composites N90-18498
Silicon carbo-nitride ceramic matrix composites by polymer pyrolysis N90-18499
Ceramic matrix composites, new high performance materials N90-18500
CERAMICS
Analysis of whisker-toughened ceramic components: A design engineer's viewpoint
[NASA-TM-102333] N90-18504
Composite for smoothing the surface of ceramic substrates
[DE90-004005] N90-18585
Colloid and interface chemistry aspects of ceramics
[AD-A216715] N90-18576
Comparison of tension, compression, and flexure creep for alumina and silicon nitride ceramics
[DE90-006154] N90-18586
Microwave radiation absorption by Ho(Y)-Ba-Cu-O superconducting ceramics
[DE90-610665] N90-18588
The design of advanced ceramic composites
[DE90-006613] N90-18592
Microstructural characterization of silicon nitride ceramics processed by pressureless sintering, overpressure sintering, and sinter/HIP
[DE90-007126] N90-18594
Cohesive ceramic fabrication
[DE90-007333] N90-18597
Reliability studies of ceramic capacitors
[AD-A216763] N90-18643
Low cost filter development and control of permeability in high temperature, high pressure ceramic filter elements
[DE90-000403] N90-18676
Biaxial strength and stress rupture of hot-pressed silicon nitride
[AD-A216950] N90-18750
Ion implantation-induced amorphization of ceramic oxides
[DE90-006564] N90-19041
CEREBRAL CORTEX
Organization of a large-scale cortical network
[AD-A216829] N90-18863
Psychological studies of visual cortical function
[AD-A217029] N90-18872
CERTIFICATION
Structures and materials technology for hypersonic aerospacecraft
[NASA-TM-102583] N90-18752
CESIUM
Determining the effects of microwave power and C-field setting on the frequency of a cesium atomic frequency standard
[AD-A216599] N90-18642
CESIUM IONS
Surface production of ions
[AD-A216470] N90-19003
CHANNEL FLOW
Study of vortex arrays induced artificially and from centrifugal instabilities
[AD-A216499] N90-18669
CHANNEL NOISE
Trends in VLF/LF (Very Low Frequency/Low Frequency) modem performance testing
[AD-A216576] N90-18614
CHANNELS (DATA TRANSMISSION)
An adaptive ARQ (Automatic Repeat Request) strategy for packet switching data communication networks
[AD-A216597] N90-18615
Rate compatible punctured codes, their use in military satellite communication systems
[AD-A216723] N90-18619
CHAOS
Concepts and experiments on space-time chaos
[ETN-90-96255] N90-18883
Using special-purpose computing to examine chaotic behavior in nonlinear mappings
[AD-A216800] N90-18916
CHARACTERIZATION
Space station technology summary N90-18482
Characterization and development report for the SA3274-1 and SA3274-2 transient voltage suppressors
[DE90-005712] N90-18649
Performance parameter characterisation of various types of IR single element detectors N90-19161

CHARGE CARRIERS
Proceedings of the 6th Conference on Hot Carriers in Semiconductors
[AD-A215978] N90-19032

CHARGE TRANSFER
Electrochemical investigations of electronically conductive polymers. Part 4: By controlling the supermolecular structure, charge transport rates can be enhanced
[AD-A216603] N90-18573

CHARPY IMPACT TEST
Response of unirradiated and neutron-irradiated vanadium alloys to Charpy-impact loading
[DE90-004878] N90-18551

CHEBYSHEV APPROXIMATION
Spectral multi-domain approximation of the Navier-Stokes equations in curved complex geometries
[ONERA-NT-1987-2] N90-18685
Application of Chebyshev approximation to curve fitting
[MEMO-805] N90-18947

CHELATION
Colloid and interface chemistry aspects of ceramics
[AD-A216715] N90-18576

CHEMICAL ANALYSIS
Extracting chemical information form Auger line shapes
[AD-A216729] N90-18537

CHEMICAL BONDS
Perfluorinated ligands in organometallic chemistry
[AD-A216415] N90-18493
Spectroscopic evidence for carbon-carbon bonding in carbide layers on metals
[AD-A216726] N90-18512
Interfacial chemistry of MoS2 films on Si
[AD-A216527] N90-18532
Ultrafast chemical dynamics of reactions in beams
[AD-A216319] N90-18717

CHEMICAL COMPOSITION
Identification of a cast iron alloy containing nonstrategic elements
[NASA-CR-185174] N90-18559

CHEMICAL MACHINING
Process development and fabrication of space station type aluminum-clad graphite epoxy struts
[NASA-CR-181873] N90-18454

CHEMICAL PROPERTIES
Spectroscopy and physico-chemistry of CO:H2O and CO2:H2O ices N90-19111

CHEMICAL REACTIONS
Chemistry on interstellar grains and implications for infrared spectroscopy N90-19097

CHROMATOGRAPHY
Ion chromatography in the manufacture of multilayer circuit boards
[DE90-005560] N90-18652

CHROMOSOMES
Effects of pulsed and CW (Continuous Wave) 2450 MHz radiation on transformation and chromosomes of human lymphocytes in vitro
[AD-A216500] N90-18857

CIRCUIT BOARDS
Ion chromatography in the manufacture of multilayer circuit boards
[DE90-005560] N90-18652

CIRCUIT DIAGRAMS
A test method for measuring corona inception voltage for transducer autotransformers
[AD-A216818] N90-18646

CIRCUITS
Output performance of idealized microwave power amplifiers
[AD-A216797] N90-18645
Radiation-hard high-efficiency InP space solar cell development
[AD-A216857] N90-18800
Boolean minimization and algebraic factorization procedures for fully testable sequential machines
[AD-A216779] N90-18940

CIRCULAR CONES
Semidiscrete Galerkin modelling of compressible viscous flow past a circular cone at incidence
[NASA-CR-186323] N90-18664

CIRCULAR CYLINDERS
Scattering from an arbitrary cylinder in the presence of a planar media interface using the bymoment method
[DE90-006485] N90-18626

CIRCULATION DISTRIBUTION
Optimum spanwise camber for minimum induced drag
[BU-403] N90-18369

CIVIL AVIATION
Human factors issues in aircraft maintenance and inspection
[AD-A215724] N90-18875

CLASSICAL MECHANICS
Velocity measurement using interferometry
[ISL-CO-221/88] N90-18709

CLASSIFICATIONS
Multiparameter scatterometer for remote sensing (RADSER). Project Scatter: State-of-the-art and future applications
[INPE-4871-PRE/1482] N90-18701
Evaluation of two methods for acquisition of training statistics for digital analysis of areas prepared for plowing
[INPE-4901-PRE/1502] N90-18763
Monitoring of reforested areas through digital analysis of TM data
[INPE-4930-PRE/1420] N90-18764
Multistage forest volume estimation using a sampling system with probability variables
[INPE-4897-PRE/1498] N90-18769
Classification of high resolution imagery using texture attributes
[INPE-4888-TDL/379] N90-18778
Improvement of classification results from satellite imagery to update and differentiate land use classes on topographic maps
[BCRS-89-17] N90-18786
Remote sensing for the classification and quantification of vegetation in Spring staging areas of Brent geese on the Frisian islands (Netherlands)
[BCRS-89-27] N90-18790
Geological structure of the State of Rio de Janeiro viewed through MSS LANDSAT imagery
[INPE-4826-PRE/1457] N90-18825
An integrated vision on methodologies and environments for modeling and simulation assisted by computer
[INPE-4861-TDL/372] N90-18886

CLASSIFIERS
Evaluation of two methods for acquisition of training statistics for digital analysis of areas prepared for plowing
[INPE-4901-PRE/1502] N90-18763
Classification of high resolution imagery using texture attributes
[INPE-4888-TDL/379] N90-18778

CLEAVAGE
Ultrafast chemical dynamics of reactions in beams
[AD-A216319] N90-18717

CLIMATE CHANGE
Effects of global climate change on agroecosystems: Scope of work
[PB90-120023] N90-18813
Perspectives on aerosol deposition to natural surfaces
[DE90-003398] N90-18819
Natural and anthropogenic climate change
[DE90-006488] N90-18822

CLIMATOLOGY
Effects of global climate change on agroecosystems: Scope of work
[PB90-120023] N90-18813
Forecasters handbook for Central America and adjacent waters
[AD-A216752] N90-18845

CLOCKS
Rate compatible punctured codes, their use in military satellite communication systems
[AD-A216723] N90-18619

CLOUD COVER
Comparisons between the RTNEPH (Real-Time Nephanalysis) and AFGL cloud layer analysis algorithms
[AD-A216637] N90-18844

CLOUD PHYSICS
Airborne measurements of the electric field and the charge precipitation particles in convective clouds: Lower positive charge centres
[ESA-TT-1157] N90-18836

CLOUDS (METEOROLOGY)
Cloud hole-boring with infrared lasers: Theory and experiment
[DE90-006519] N90-18723

CLUTTER
Synthetic aperture radar imagery of airports and surrounding areas: Archived SAR data
[NASA-CR-4275] N90-18371
Synthetic aperture radar imagery of airports and surrounding areas: Philadelphia Airport
[NASA-CR-4280] N90-18372

COAL
A coal model for the carriers of the unidentified IR bands N90-19110

COASTAL WATER
Sounding and surface meteorological data from the Land/Sea Breeze Experiment (LASBEX)
[AD-A216269] N90-18842

COATING
Continuous preparation of a thin refractory carbide deposit on the surface of carbon fibers: Characterization of the C/SiC fiber N90-18501
Sputter deposition of diffusion barrier coatings on SiC monofilaments for use in Ti-based composites N90-18502

COATINGS
Calculations of braiding parameters
[AD-A216836] N90-18515
Coating possibilities for magnetic switches
[DE90-006536] N90-18659

COCKPITS
Three input concepts for flight crew interaction with information presented on a large-screen electronic cockpit display
[NASA-TM-4173] N90-18394

CODING
Rate compatible punctured codes, their use in military satellite communication systems
[AD-A216723] N90-18619
A microcode compiler that runs on the IBM AT and supports cascadable microcomputers, part 1
[AD-A215888] N90-18877
DoD manual for standard data elements
[AD-A216441] N90-19066

COGNITION
Teaching a new methodology for designing relational data bases: An experiment testing the effectiveness of an intelligent tutoring system on cognitive skill acquisition (volumes 1 and 2) N90-19063

COHERENCE COEFFICIENT
Cineholography: A relation between the coherence length of the laser and the object velocity
[ISL-CO-234/88] N90-18724

COINCIDENCE CIRCUITS
Parallel memory addressing using coincident optical pulses
[AD-A216302] N90-18641

COLD FLOW TESTS
Cold flow determination of the internal flow environment around the submerged TVC nozzle for the space shuttle SRM N90-18465

COLLECTION
Beam collector and output window for a 35 GHz 100 kW gyrotron
[INPE-4958-RPE/603] N90-18699

COLLISION RATES
A numerical solution to the Boltzmann equation for use in calculating pumping rates in a CO2 discharge laser
[AD-A216376] N90-18718

COLLISIONS
Zodiacal dust bands: Their relation to asteroid families
[AD-A216025] N90-19170
Hydrodynamical simulations of collisions between interstellar clouds
[DE90-006921] N90-19172

COLLOIDS
Colloid and interface chemistry aspects of ceramics
[AD-A216715] N90-18576

COLOR
Relationships between the aerial biomass from ground layers of cerrado and its spectral reflectance
[INPE-4848-PRE/1477] N90-18760
Evaluation of selection techniques for multispectral bands employed in the discrimination of carbonatic rocks
[INPE-4850-TDL/365] N90-18765
Psychological studies of visual cortical function
[AD-A217029] N90-18872
The computation of color
[AD-A216531] N90-18914
A model of incomplete chromatic adaptation for calculating corresponding colors
[DE90-006905] N90-19016

COLOR PHOTOGRAPHY
Photointerpretation with instruments for evaluation of environmental impact: Mata Atlantica in Cubata
[INPE-4910-PRE/1511] N90-18817

COLOR VISION
The effects of luminance boundaries on color perception
[AD-A216741] N90-18860
The computation of color
[AD-A216531] N90-18914

COMBINATIONS (MATHEMATICS)
Strong moderate deviation theorems
[MEMO-804] N90-18954

COMBINATORIAL ANALYSIS
On the depth of combinatorial optimization problems
[MEMO-803] N90-18946

COMBUSTIBLE FLOW
AFOSR/ONR (Air Force Office of Scientific Research/Office of Naval Research) Contractors' Meeting on Combustion Rocket Propulsion Diagnostics of Reacting Flow
[AD-A216094] N90-18491
An investigation of flow structure, mixing and chemical reaction in combusting turbulent flows
[AD-A216739] N90-18538
COMBUSTION
AFOSR/ONR (Air Force Office of Scientific Research/Office of Naval Research) Contractors' Meeting on Combustion Rocket Propulsion Diagnostics of Reacting Flow
[AD-A216094] N90-18491
COMBUSTION CHAMBERS
Combustion instability in solid propellant rockets
[AD-A216740] N90-18492
COMBUSTION PHYSICS
Effect of propellant flowrate and purity on carbon deposition in LO2/methane gas generators N90-18468
Theoretical investigation of the stabilization of a diffusion flame above a recirculation region
[ESA-TT-1149] N90-18543
On the dynamics of the combustion process of hydrogen-air and hydrogen-methane-air mixtures
[DLR-FB-89-39] N90-18548
COMBUSTION STABILITY
Combustion instability in solid propellant rockets
[AD-A216740] N90-18492
On the dynamics of the combustion process of hydrogen-air and hydrogen-methane-air mixtures
[DLR-FB-89-39] N90-18548
COMETS
Infrared cometary spectroscopy N90-19086
Analogies between cometary, interplanetary, and interstellar matter N90-19087
The unidentified IR bands in laboratory, in interstellar medium, and in comets N90-19089
A unified model for the 3.28 micron and 3.4 micron spectral feature in the interstellar medium and in comets N90-19092
Interpretation of the 10 micron and 20 micron absorption bands in comets, the interstellar medium, and in an external galaxy N90-19093
COMMAND LANGUAGES
A user's manual for the method of moments Aircraft Modeling Code (AMC)
[NASA-CR-186371] N90-18390
COMMERCIAL AIRCRAFT
Human factors issues in aircraft maintenance and inspection
[AD-A215724] N90-18875
COMMUNICATION NETWORKS
An adaptive ARQ (Automatic Repeat Request) strategy for packet switching data communication networks
[AD-A216597] N90-18615
Rate compatible punctured codes, their use in military satellite communication systems
[AD-A216723] N90-18619
COMMUNICATIONS TECHNOLOGY SATELLITE
Activities report in DLR research field communication engineering and reconnaissance
[ISSN-0173-0118] N90-18781
COMPETITION
Analysis of competition among the kinds of energy at the era of complexed energy: General review
[DE89-910215] N90-18793
COMPILERS
A microcode compiler that runs on the IBM AT and supports cascadable microcomputers, part 1
[AD-A215888] N90-18877
Determination of the underlying task scheduling algorithm for and Ada runtime system
[AD-A215880] N90-18890
A theory of quantitative inference for artifact sets applied to a mechanical design compiler
[AD-A216535] N90-18896
COMPLEX COMPOUNDS
Perfluorinated ligands in organometallic chemistry
[AD-A216415] N90-18493
COMPONENT RELIABILITY
Transient pressure test article test program N90-18463
Effect of correlation on multi-engine rocket propulsion systems N90-18467
COMPOSITE MATERIALS
Composites design handbook for space structure applications
[ESA-PSS-03-1101-ISSUE-1-REV-1] N90-18459
Third European Conference on Composite Materials
[EOARD-LR-89-050] N90-18494
The processing and mechanical properties of high temperature/high performance composites. Book 2, section 2: Strength and fracture resistance
[AD-A216142] N90-18507
The processing and mechanical properties of high temperature/high performance composites. Book 3, section 2: Strength and fracture resistance, part
[AD-A216143] N90-18508
Calculations of braiding parameters
[AD-A216836] N90-18515
Compact reinforced composite basic principles
[CBL-41] N90-18520
Structural study of thermo-hardenable matrices. Deformation processes of composite matrices as a function of their molecular structure
[ONERA-RT-10/3521-M] N90-18522
Comparison between the damage modes of thermo-hardenable and thermo-plastic composite matrices
[ONERA-RT-47/7086-M] N90-18523
Thermal analysis of polymer composites
[AD-A216947] N90-18578
Electronic and ionic transport in polymers
[AD-A217028] N90-18579
COMPOSITE STRUCTURES
Threaded joint design for composites
[DE90-005553] N90-18506
Preliminary evaluation of the strength of pin-joints in laminated composite materials
[DE90-006353] N90-18524
The design of advanced ceramic composites
[DE90-006613] N90-18592
COMPRESSIBLE BOUNDARY LAYER
Development of a defect stream function, law of the wall/wake method for compressible turbulent boundary layers
[NASA-CR-4286] N90-18675
COMPRESSIBLE FLOW
Calculation of the unsteady two-dimensional, inviscid, compressible flow around a strongly cambered oscillating single blade N90-18409
Semidiscrete Galerkin modelling of compressible viscous flow past a circular cone at incidence
[NASA-CR-186323] N90-18664
Effect of a random wind field on thermal blooming instabilities
[DE90-007241] N90-18823
COMPRESSING
Comparison of tension, compression, and flexure creep for alumina and silicon nitride ceramics
[DE90-006154] N90-18586
COMPRESSION LOADS
Piezoelectric polymer PVDF shock gauge: State of the research art
[ISL-CO-207/89] N90-18705
COMPRESSIVE STRENGTH
Compressive strength of carbon/epoxy laminated under multiaxial stress
[DE90-005552] N90-18505
COMPRESSOR EFFICIENCY
Small displacement, long life on-orbit compressor design and fabrication N90-18489
COMPRESSORS
Numerical investigation of unsteady flow in oscillating turbine and compressor cascades N90-18407
Experiments on the unsteady flow in a supersonic compressor stage N90-18422
Experimental investigation of the influence of rotor wakes on the development of the profile boundary layer and the performance of an annular compressor cascade N90-18425
Compressor performance tests in the compressor research facility N90-18428
Small displacement, long life on-orbit compressor design and fabrication N90-18489
COMPUTATION
Calculations of braiding parameters
[AD-A216836] N90-18515
Computation and control with neural nets
[DE90-006460] N90-18911
Research equipment
[AD-A216515] N90-18937
Speculative computation in multilisp
[AD-A216579] N90-19067
COMPUTATIONAL FLUID DYNAMICS
Prediction of rotor blade-vortex interaction noise from 2-D aerodynamic calculations and measurements
[ISL-CO-243/88] N90-18365
Aerodynamics of unsteady systems. Numerical study of potential flow/boundary layer coupling
[ETN-90-96257] N90-18367
Study of the blade/vortice interaction on a one-blade rotor during forward flight (incompressible, non viscous fluid)
[ISL-R-115/88] N90-18391
Unsteady Aerodynamic Phenomena in Turbomachines
[AGARD-CP-468] N90-18405
Calculation of the unsteady two-dimensional, inviscid, compressible flow around a strongly cambered oscillating single blade N90-18409
Aerodynamic superposition principle in vibrating turbine cascades N90-18410
Unsteady blade loads due to wake influence N90-18413
Unsteady aerodynamic phenomena in a simulated wake and shock wave passing experiment N90-18414
Gust response analysis for cascades operating in nonuniform mean flows N90-18415
Numerical prediction of axial turbine stage aerodynamics N90-18416
Numerical simulation of three-dimensional unsteady flows in turbomachines N90-18417
Blade row interaction effects on compressor measurements N90-18419
High-resolution Euler computations of unsteady transonic flows in cascades N90-18420
Modelling unsteady transition and its effects on profile loss N90-18423
Methods for making unsteady aerodynamic pressure measurements in a rotating turbine stage N90-18426
Measurement of velocity profiles and Reynolds stresses on an oscillating airfoil N90-18427
Stall and recovery in multistage axial flow compressors N90-18429
Cold flow determination of the internal flow environment around the submerged TVC nozzle for the space shuttle SRM N90-18465
Experimental flow models for SSME flowfield characterization N90-18469
Improved computational fluid dynamics for continuum hypersonic flow
[AD-A216981] N90-18674
Direct simulation Monte Carlo of shock reflexion on a wedge with boundary layer
[ISL-CO-245/88] N90-18681
Spectral multi-domain approximation of the Navier-Stokes equations in curved complex geometries
[ONERA-NT-1987-2] N90-18685
Numerical simulation of the incompressible inhomogeneous turbulence in a plane channel flow
[ONERA-NT-1988-5] N90-18686
Interaction between oblique-angled incident shock wave and turbulent boundary layer on a heated wall. Experimental results
[ONERA-RT-84/7078-AY] N90-18688
Numerical simulation of the vortex breakdown
[ONERA-RSF-4/4368-AY-004A] N90-18689
COMPUTATIONAL GRIDS
A simple algebraic grid adaptation scheme with applications to two- and three-dimensional flow problems
[NASA-TM-102446] N90-18667
Analysis of linear multigrid methods for elliptic differential equations with discontinuous and anisotropic coefficients
[ETN-90-96269] N90-18944
COMPUTER AIDED DESIGN
DANCIR (device and circuit simulator): A three dimensional steady-state semiconductor device simulator
[DE90-006370] N90-18658
A theory of quantitative inference for artifact sets applied to a mechanical design compiler
[AD-A216535] N90-18896
RALPH: An automatic Robot Assembly Language Programmer: An overview
[PB90-120973] N90-18912
COMPUTER AIDED MANUFACTURING
The Executive Workshop on Cost/Performance Measurement. Volume 1: Executive summary
[AD-A216745] N90-18898
COMPUTER AIDED TOMOGRAPHY
Computational and visible light experiments for x ray laser holography
[DE90-006774] N90-18707
COMPUTER ASSISTED INSTRUCTION
Teaching a new methodology for designing relational data bases: An experiment testing the effectiveness of an intelligent tutoring system on cognitive skill acquisition (volumes 1 and 2) N90-19063
COMPUTER GRAPHICS
Optimal planning method of underground distribution system, part 2. Application to various types of system configurations
[DE89-782323] N90-18836
A self-organizing multiple-view representation of three-dimensional objects
[AD-A216711] N90-18871
An interactive system applied to the linear quadratic problem
[INPE-4945-TDL/386] N90-18913
COMPUTER INFORMATION SECURITY
Using the K-25 C/TD common file system: A guide to CFSi
[DE90-005815] N90-19179

COMPUTER PROGRAMMING
On the kinematic behavior of robots while executing general robot level commands
[PB90-120965] N90-18735
Guidelines for the use of the SAME
[AD-A215846] N90-18888
Technology assessment of software engineering
[AD-A216943] N90-18902
RALPH: An automatic Robot Assembly Language Programmer: An overview
[PB90-120973] N90-18912
Derivation of an efficient rule system pattern matcher
[AD-A216801] N90-18917
COMPUTER PROGRAMS
A user's manual for the method of moments Aircraft Modeling Code (AMC)
[NASA-CR-186371] N90-18390
Unsteady Aerodynamic Phenomena in Turbomachines
[AGARD-CP-468] N90-18405
Numerical prediction of axial turbine stage aerodynamics N90-18416
Blade row interaction effects on compressor measurements N90-18419
Data collection and location platforms experimental network: Description of an orbit routine
[INPE-4798-NTE/287] N90-18439
Theory and verification of the fiber composite damage model implemented in DYNA3D
[AD-A216600] N90-18511
Development of a progressive failure model for strength of laminated composite structure
[AD-A216966] N90-18517
Numerical simulations of coherent structures in a jet flame with a noncircular cross section
[AD-A216710] N90-18535
Automation and extension of LDV (Laser-Doppler Velocimetry) measurements of off-design flow in a subsonic cascade wind tunnel
[AD-A216627] N90-18670
Computer viruses and related threats: A management guide
[PB90-111683] N90-18881
Guidelines for the use of the SAME
[AD-A215846] N90-18888
Deceit: A flexible distributed file system
[NASA-CR-186402] N90-18891
Approaches to the planning of coherent text
[AD-A216463] N90-18895
Knowledge-based extensible natural language interface technology program
[AD-A216664] N90-18897
KAM: Automatic planning and interpretation of numerical experiments using geometrical methods
[AD-A216805] N90-18900
A perspective of software reuse
[AD-A216911] N90-18901
Technology assessment of software engineering
[AD-A216943] N90-18902
User manual for NEXT 1.2: NLR engineering X-pert system toolkit
[NLR-TR-87178-U] N90-18905
Computational structure of GPSG (Generalized Phrase Structure Grammar) models: Revised generalized phrase structure grammar
[AD-A216803] N90-18941
Configuration management and control for ESA space systems
[ESA-PSS-01-11-ISSUE-1] N90-19061
COMPUTER SYSTEMS PERFORMANCE
Performance characterization of the Convex C-240 computer system
[DE90-006425] N90-18879
Computer viruses and related threats: A management guide
[PB90-111683] N90-18881
A survey of performability modelling tools
[MEMO-INF-89-50] N90-18907
Parallelizing the SDI ACCESS algorithm for the Connection Machine-2
[DE90-006382] N90-18909
Using dynamic queueing networks as a tool for specifying performability models
[MEMO-INF-89-51] N90-18949
COMPUTER TECHNIQUES
Life of concentrated contacts in the mixed EHD and boundary film regimes
[AD-A216673] N90-18738
Spatial registration of TIROS-N weather satellite data
[AD-A216041] N90-18841
Appropriateness measurement for computerized adaptive tests
[AD-A216121] N90-18870
Computerized analysis of hydrogen plasma in a compact H(sup -) cusp source
[DE90-006881] N90-19029
COMPUTER VIRUSES
Computer viruses and related threats: A management guide
[PB90-111683] N90-18881
COMPUTER VISION
Visual navigation: Constructing and utilizing simple maps of an indoor environment
[AD-A216761] N90-18382
An approach centered in production rules for a partition of environment and planning in a visual navigation system (SNV)
[INPE-4813-TDL/360] N90-18737
The computation of color
[AD-A216531] N90-18914
COMPUTERIZED SIMULATION
Delivery performance of conventional aircraft by terminal-area, time-based air traffic control: A real-time simulation evaluation
[NASA-TP-2978] N90-18378
Numerical simulation of three-dimensional unsteady flows in turbomachines N90-18417
Autonomous orbit determination using GPS
[INPE-4815-TDL/361] N90-18442
Cold flow determination of the internal flow environment around the submerged TVC nozzle for the space shuttle SRM N90-18465
Numerical simulations of coherent structures in a jet flame with a noncircular cross section
[AD-A216710] N90-18535
The joint effect of surface microtopography and near-surface structure on microcontact conditions
[DE90-006494] N90-18591
Rate compatible punctured codes, their use in military satellite communication systems
[AD-A216723] N90-18619
Reliability assessment using finite element techniques
[AD-A216907] N90-18647
Performance of a 500 watt Nd:GGG zigzag slab oscillator
[DE90-006263] N90-18657
DANCIR (device and circuit simulator): A three dimensional steady-state semiconductor device simulator
[DE90-006370] N90-18658
Strong source heat transfer simulations based on a GalerKin/gradient least squares method
[DE90-608613] N90-18678
Computational and visible light experiments for x ray laser holography
[DE90-006774] N90-18707
INEX (Integrated Numerical Experiment) simulations of the Boeing FEL system
[DE90-004846] N90-18712
Fast algorithms for calculating laser wavefront phase compensation given noisy measurements of phase gradient
[DE90-006357] N90-18727
Earth model selection for computer simulations
[AD-A216843] N90-18779
Particle simulations in magnetospheric plasmas
[AD-A216256] N90-18831
Organization of a large-scale cortical network
[AD-A216829] N90-18863
A scalable multiprocessor architecture using Cartesian network: Relative addressing
[AD-A216580] N90-18878
L: A language for solution of incremental systems in a parallel processing environment
[INPE-4816-TDL/362] N90-18884
An integrated vision on methodologies and environments for modeling and simulation assisted by computer
[INPE-4861-TDL/372] N90-18886
Comparison of two Navy environmental database models: Generalized Digital Environmental Model and Podeszwa sound speed profile model
[AD-A215848] N90-18889
An interactive system applied to the linear quadratic problem
[INPE-4945-TDL/386] N90-18913
The lower hybrid drift instability and the evolution of plasma gradients
[DE90-006521] N90-19021
The interaction of polycrystalline copper films with dilute aqueous solutions of cupric chloride
[AD-A216465] N90-19033
Hydrodynamical simulations of collisions between interstellar clouds
[DE90-006921] N90-19172
COMPUTERS
Technology assessment of software engineering
[AD-A216943] N90-18902
Integrated IMA (Information Mission Areas) IC (Information Center) guide
[AD-A216944] N90-18903
Research equipment
[AD-A216515] N90-18937
CONCENTRATION (COMPOSITION)
Investigation of multiple scattering in aqueous suspensions of non-absorbing polystrene microspheres using spectrophotometry
[BCRS-89-09] N90-18549
Variations in volatiles in magma bodies based on studies of melt inclusions
[DE90-006272] N90-18821
CONCRETES
High-strength concrete development through 25 years
[CBL-REPRINT-17] N90-18589
CONDENSED MATTER PHYSICS
Modern theory of magnetism
[DE90-007374] N90-18998
CONDENSING
Condensation fluid dynamics and heat transfer on rotating spherical surfaces in a microgravitational field
[DE90-005540] N90-18607
CONDUCTING POLYMERS
Electrochemical investigations of electronically conductive polymers. Part 4: By controlling the supermolecular structure, charge transport rates can be enhanced
[AD-A216603] N90-18573
CONDUCTIVE HEAT TRANSFER
Spacecraft thermal control design data, volume 1
[ESA-PSS-03-108-ISSUE-1-VOL-1] N90-18455
CONDUCTORS
Solid-state proton conductors
[DE90-007595] N90-18812
CONES
The inviscid stability of supersonic flow past a sharp cone
[NASA-CR-181996] N90-18363
CONFERENCES
AGARD/SMP Review: Damage Tolerance for Engine Structures. 2: Defects and Quantitative Materials Behaviour — conference
[AGARD-R-769] N90-18396
Unsteady Aerodynamic Phenomena in Turbomachines
[AGARD-CP-468] N90-18405
The 1989 JANNAF Propulsion Meeting, volume 1
[CPIA-PUBL-515-VOL-1] N90-18462
Third European Conference on Composite Materials
[EOARD-LR-89-050] N90-18494
Proceedings of the 38th International Wire and Cable Symposium
[AD-A216023] N90-18638
Investigation report of the investigation commission for interchange of heat pump technology in Europe
[DE89-782293] N90-18666
The Executive Workshop on Cost/Performance Measurement. Volume 1: Executive summary
[AD-A216745] N90-18898
Calendar of selected aeronautical and space meetings
[AGARD-CAL-90/1] N90-19060
Infrared Spectroscopy in Astronomy
[ESA-SP-290] N90-19084
CONFIGURATION MANAGEMENT
Configuration management and control for ESA space systems
[ESA-PSS-01-11-ISSUE-1] N90-19061
CONICAL NOZZLES
Arcjet nozzle design impacts N90-18478
CONIFERS
Monitoring of reforested areas through digital analysis of TM data
[INPE-4930-PRE/1420] N90-18764
Evaluation of TM/LANDSAT and HRV/SPOT data in reforested areas
[INPE-4575-RPE/567] N90-18772
CONSERVATION LAWS
Interaction of minor ions with fast and slow shocks
[NASA-CR-186372] N90-19181
CONSISTENCY
Log-based recovery in asynchronous distributed systems
[NASA-CR-186190] N90-18924
CONSTITUTIVE EQUATIONS
Kinetic relations and the propagation of phase boundaries in solids
[AD-A215881] N90-18747
An objective time-integration procedure for isotropic rate-independent and rate-dependent elastic-plastic constitutive equations
[PB90-121245] N90-18925
CONSTRUCTION
Optimal planning method of underground distribution system, part 2. Application to various types of system configurations
[DE89-782323] N90-18636
Construction and calibration of a gas pressure meter with high temporal resolution
[INPE-4953-RPE/602] N90-18700

CONTAMINANTS
Application of high performance liquid chromatography/mass spectrometry to environmental analysis
[PB90-116963] N90-18814
Tropospheric chemistry of natural hydrocarbons and energy-related pollutants: Biosphere/climate feedbacks
[DE90-005643] N90-18820
CONTAMINATION
Research project in microelectronic engineering and imaging science
[DE90-006907] N90-18653
CONTINUOUS RADIATION
Effects of pulsed and CW (Continuous Wave) 2450 MHz radiation on transformation and chromosomes of human lymphocytes in vitro
[AD-A216500] N90-18857
CONTINUUM FLOW
Improved computational fluid dynamics for continuum hypersonic flow
[AD-A216981] N90-18674
CONTINUUMS
Geometric continuum regularization of quantum field theory
[DE90-006099] N90-19058
CONTRACTS
The improvement of technology transfer from space to industry N90-19079
CONTROL EQUIPMENT
Design of a new control system for hovercrafts
[ETN-90-96230] N90-18435
CONTROL SURFACES
Discrete proportional Plus Integral (PI) multivariable control laws for the Control Reconfigurable Combat Aircraft (CRCA)
[AD-A215664] N90-18431
CONTROL SYSTEMS DESIGN
The implications of using integrated software support environment for design of guidance and control systems software
[AGARD-AR-229] N90-18432
Application of variable-gain output feedback for high-alpha control
[NASA-TM-102603] N90-18434
Spacecraft thermal control design data, volume 4
[ESA-PSS-03-108-ISSUE-1-VOL-4] N90-18458
Application of artificial intelligence control to the vapor-liquid-solid silicon carbide whisker process
[DE90-007835] N90-18519
Preliminary design of a pointer for movement of a solar simulator
[INPE-4864-TDL/375] N90-18736
Computation and control with neural nets
[DE90-006460] N90-18911
Practical methods for robust multivariable control
[AD-A216937] N90-18920
Feasibility of Mealy design for processor controlpaths
[MEMO-INF-89-53] N90-18923
Nonlinear model matching: A local solution and two worked examples
[MEMO-809] N90-18948
CONTROL THEORY
Application of variable-gain output feedback for high-alpha control
[NASA-TM-102603] N90-18434
Practical methods for robust multivariable control
[AD-A216937] N90-18920
System theory and mechanics
[MEMO-807] N90-18922
CONTROLLERS
Payload vibration isolation in a microgravity environment
[NASA-CR-186191] N90-18744
CONVECTION
Connections between the circulation in altitude and convection over South America
[INPE-4923-TDL/383] N90-18828
CONVECTIVE FLOW
Multicellular natural convection in a narrow vertical slot
[AD-A216411] N90-18668
Modeling convective Marangoni flows with void movement in the presence of solid-liquid phase change
[DE90-006474] N90-18890
Summer Study Program in Geophysical Fluid Dynamics: The Influence of Convection on Large-Scale Circulations, 1988
[AD-A216024] N90-18840
CONVERGENCE
Intertropical Convergence Zone (ITCZ) and its relationship with the precipitation of the north-northeast Brazilian region
[INPE-4887-TDL/378] N90-18839
COOLING
Flexible heat pipe cold plate
[AD-A216053] N90-18435
Dryout stability and inception at low flowrates
[DE90-006955] N90-18892
COOLING SYSTEMS
Beam collector and output window for a 35 GHz 100 kW gyrotron
[INPE-4958-RPE/603] N90-18699
An advanced cooled grating spectrometer for UKIRT-CGS4 N90-19165
COORDINATES
Spatial registration of TIROS-N weather satellite data
[AD-A216041] N90-18841
COORDINATION POLYMERS
Metal coordination polymers as potential high-energy lithographic resists
[AD-A216668] N90-18574
The improved adhesion of organic polymers to silica and to aluminum metal with zirconium Schiff-base block copolymer coatings
[AD-A216669] N90-18575
COPOLYMERIZATION
Modified bismaleimides for carbon fibre composites N90-18495
Control of phase structure in polymer blends
[AD-A217034] N90-18580
COPOLYMERS
Composite for smoothing the surface of ceramic substrates
[DE90-004005] N90-18565
Control of phase structure in polymer blends
[AD-A217034] N90-18580
COPPER
The mechanism, measurement, and influence of properties on the galling of metals
[DE90-006533] N90-18558
Study of the dynamical behavior of copper in a shock wave
[ISL-R-123/88] N90-18679
COPPER ALLOYS
Processing and elevated temperature ductility of aluminum alloy 7475
[AD-A216840] N90-18554
COPPER CHLORIDES
The interaction of polycrystalline copper films with dilute aqueous solutions of cupric chloride
[AD-A216465] N90-19033
COPPER OXIDES
What influences order parameters across the superconducting phase boundary
[DE90-610663] N90-19047
CORES
Understanding electronegative effects in core-level electron spectroscopies; application to the high temperature superconductors
[AD-A216728] N90-19037
CORONAL HOLES
Interaction of minor ions with fast and slow shocks
[NASA-CR-186372] N90-19181
CORONARY CIRCULATION
Coronary arterial capacitance and subendocardial vascular patency throughout the cardiac cycle N90-18855
CORRELATION
The correlation between radio and far-infrared emission for disk galaxies N90-19158
CORRELATORS
Visual processing of object velocity and acceleration
[AD-A216509] N90-18858
CORROSION
A fundamental understanding of the effect of alloying elements on the corrosion resistance of rapidly solidified Mg alloys
[AD-A216767] N90-18553
Corrosion fatigue of iron-chromium-nickel alloys: Fracture mechanics and chemistry
[DE90-006318] N90-18556
Fastener design manual
[NASA-RP-1228] N90-18740
CORROSION RESISTANCE
A fundamental understanding of the effect of alloying elements on the corrosion resistance of rapidly solidified Mg alloys
[AD-A216767] N90-18553
The mechanism, measurement, and influence of properties on the galling of metals
[DE90-006533] N90-18558
COSMIC DUST
Chemistry on interstellar grains and implications for infrared spectroscopy N90-19097
Infrared spectroscopy of novae and related objects N90-19123
Zodiacal dust bands: Their relation to asteroid families
[AD-A216025] N90-19170
COSMIC RAY SHOWERS
Research in theoretical physics
[DE90-005558] N90-19001
COSMIC RAYS
The track-etch detector for the MACRO experiment at the Gran Sasso Laboratory
[DE90-003235] N90-19182
Current and future uses of accelerators in particle astrophysics
[DE90-006667] N90-19186
COSMOLOGY
Theoretical and experimental high energy physics
[DE90-006168] N90-19006
The microwave background in steady-state cosmology N90-19150
Particle physics and cosmology
[DE90-006547] N90-19171
Quantum cosmological origin of large scale structures of the universe
[DE90-610647] N90-19176
Elementary particles and cosmology
[DE90-610648] N90-19177
COST ANALYSIS
The Executive Workshop on Cost/Performance Measurement. Volume 1: Executive summary
[AD-A216745] N90-18898
Survivability and effectiveness of near-term strategic defense
[DE90-005805] N90-18955
COST EFFECTIVENESS
Orbital fluid resupply assessment N90-18487
A perspective of software reuse
[AD-A216911] N90-18901
COST ESTIMATES
Cost and energy consumption estimates for the aluminum-air battery anode fuel cycle
[DE90-005810] N90-18656
COSTS
A perspective of software reuse
[AD-A216911] N90-18901
COUNTING CIRCUITS
Technology development and circuit design for a parallel laser programmable floating point application specific processor
[AD-A215870] N90-18637
COUPLING COEFFICIENTS
Resonances in low-energy positron-alkali scattering N90-18992
COVALENT BONDS
Interfacial chemistry of MoS2 films on Si
[AD-A216527] N90-18532
Extracting chemical information form Auger line shapes
[AD-A216729] N90-18537
COVARIANCE
Adaptive state estimation and sampling rate analysis for invariant linear dynamic systems in time
[INPE-4960-TDL/389] N90-18951
Kreim factorization of covariance operators of 2-parameter random fields and application to the likelihood ratio
[MEMO-802] N90-18953
CRAB NEBULA
Infrared spectroscopy and imaging of supernova remnants N90-19104
IRAS LRS spectra of extended objects: The Crab nebula N90-19107
CRACK INITIATION
Fatigue crack initiation and small crack growth in several airframe alloys
[NASA-TM-102598] N90-18746
CRACK PROPAGATION
The damage tolerance of disc materials: Metallurgical factors; relationship with processing parameters N90-18398
Crack propagation from artificial defects in typical engine disk materials; interpretation of experimental results by means of 3D J integral N90-18401
Corrosion fatigue of iron-chromium-nickel alloys: Fracture mechanics and chemistry
[DE90-006318] N90-18556
Softening mechanisms and microstructural instabilities during high temperature, low cycle fatigue of Ni, Ni3Al, and their metal matrix composites
[DE90-006487] N90-18557
Fatigue crack initiation and small crack growth in several airframe alloys
[NASA-TM-102598] N90-18746
Biaxial strength and stress rupture of hot-pressed silicon nitride
[AD-A216950] N90-18750
CRACKING (FRACTURING)
Defects in monoblock cast turbine wheels N90-18400
Compact reinforced composite basic principles
[CBL-41] N90-18520
CRACKS
Arcjet cathode phenomena N90-18477

CRANES
Robot crane technology program
[PB90-111667] N90-18734
CREEP PROPERTIES
Comparison of tension, compression, and flexure creep for alumina and silicon nitride ceramics
[DE90-006154] N90-18586
CREEP RUPTURE STRENGTH
Identification of a cast iron alloy containing nonstrategic elements
[NASA-CR-185174] N90-18559
Biaxial strength and stress rupture of hot-pressed silicon nitride
[AD-A216950] N90-18750
CREEP STRENGTH
The processing and mechanical properties of high temperature/high performance composites. Book 2, section 2: Strength and fracture resistance
[AD-A216142] N90-18507
CREW WORKSTATIONS
The determination of offgassing products from materials and assembled articles to be used in a manned space vehicle crew compartment
[ESA-PSS-01-729-ISSUE-1] N90-18461
CRITERIA
Optimization of sensors and actuators positioning aimed at obtaining reduced models for the synthesis of optimal control regulators of flexible structures
[INPE-4760-TDL/348] N90-18450
Contribution to the study of stability robustness of nonlinear multivariable regulators
[INPE-4801-TDL/356] N90-18950
CROP GROWTH
Relationships between spectral parameters and agronomics of wheat and beam crops
[INPE-4791-RPE/584] N90-18768
Spectral response of wheat and its relationship with agronomical prameters
[INPE-4950-RPE/599] N90-18774
Results of Agrisar-86 for the Flevopolder (Netherlands) test area
[BCRS-89-21] N90-18789
Continuous hydroponic wheat production using a recirculating system
[NASA-TM-102784] N90-18853
CROP IDENTIFICATION
Multiparameter scatterometer for remote sensing (RADSER). Project Scatter: State-of-the-art and future applications
[INPE-4871-PRE/1482] N90-18701
Results of Agrisar-86 for the Flevopolder (Netherlands) test area
[BCRS-89-21] N90-18789
CROSS FLOW
Low cost filter development and control of permeability in high temperature, high pressure ceramic filter elements
[DE90-000403] N90-18676
CROSSLINKING
Modified bismaleimides for carbon fibre composites N90-18495
Interfacial chemistry of MoS2 films on Si
[AD-A216527] N90-18532
Model filled polymers 3. Rheological behavior of polystyrene containing crosslinked polystyrene beads
[AD-A215867] N90-18567
CRYOGENIC FLUIDS
Zero-gravity vortex vent and PVT gaging system N90-18486
CRYOGENIC ROCKET PROPELLANTS
Advanced APS impacts on vehicle payloads N90-18472
RF modal quantity gaging N90-18483
CRYSTAL DISLOCATIONS
Dislocation behaviour in Ge(x)Si(1-x) epilayers on (001) Si
[DE90-007063] N90-19051
Modified dislocation structures in Ge(x)Si(1-x) double epilayers on (001) Si
[DE90-007078] N90-19052
CRYSTAL GROWTH
Application of artificial intelligence control to the vapor-liquid-solid silicon carbide whisker process
[DE90-007835] N90-18519
Studies of cubic ice crystals
[AD-A216574] N90-18832
Crystal growth and mechanical properties of semiconductor alloys
[AD-A216697] N90-19035
CRYSTAL LATTICES
Ion implantation-induced amorphization of ceramic oxides
[DE90-006564] N90-19041
Dopant site location in dual-implanted GaP using (111) planar channeling
[DE90-006565] N90-19042
Toda lattice with transverse degree of freedom
[DE90-002414] N90-19049
CRYSTAL STRUCTURE
Structure and vibrational excitations of reconstructed semiconductor surfaces
[DE90-006589] N90-19044
Modified dislocation structures in Ge(x)Si(1-x) double epilayers on (001) Si
[DE90-007078] N90-19052
Fundamental studies of new magnetic heterostructures: Their growth, crystallographic structure, magnetic, and electronic properties
[DE90-007381] N90-19053
CRYSTALLOGRAPHY
Fundamental studies of new magnetic heterostructures: Their growth, crystallographic structure, magnetic, and electronic properties
[DE90-007381] N90-19053
Crystallographic and magnetic properties of (C6 D11 ND3)CuBr3 and (Zn(1-x)Mn(x))3As2: A neutron scattering study
[ECN-219] N90-19055
CRYSTALS
Performance of a 500 watt Nd:GGG zigzag slab oscillator
[DE90-006263] N90-18657
Studies of cubic ice crystals
[AD-A216574] N90-18832
Crystal growth and mechanical properties of semiconductor alloys
[AD-A216697] N90-19035
CULTURE TECHNIQUES
Three-dimensional coculture process
[NASA-CASE-MSC-21560-1] N90-18852
CUMULUS CLOUDS
Summer Study Program in Geophysical Fluid Dynamics: The Influence of Convection on Large-Scale Circulations, 1988
[AD-A216024] N90-18840
CURRENT DENSITY
Research on free electron lasers
[AD-A215865] N90-18715
Absorption experiments on electron-beam pumped rare gases
[DE90-006504] N90-18722
CURVE FITTING
Application of Chebyshev approximation to curve fitting
[MEMO-805] N90-18947
CYCLIC HYDROCARBONS
An implication of the IR identification of PAHs: The heating of the diffuse IS gas N90-19113
A survey of PAH emission in HII regions, planetary and proto-planetary nebulae N90-19129
CYCLOHEXANE
Extracting chemical information form Auger line shapes
[AD-A216729] N90-18537
CYCLONES
Dynamics of an ERICA (Experiment on Rapidly Intensifying Cyclones over the Atlantic) cyclone
[AD-A216775] N90-18846
CYCLOTRON RESONANCE DEVICES
Beam collector and output window for a 35 GHz 100 kW gyrotron
[INPE-4958-RPE/603] N90-18699
CYGNUS CONSTELLATION
Infrared spectroscopy and imaging of supernova remnants N90-19104

D

DAMAGE
AGARD/SMP Review: Damage Tolerance for Engine Structures. 2: Defects and Quantitative Materials Behaviour — conference
[AGARD-R-769] N90-18396
The damage tolerance of disc materials: Metallurgical factors; relationship with processing parameters N90-18398
Future technology requirements (related to defects and quantitative material behavior to aid in implementation of damage tolerance for design of engine structures) N90-18403
The need for a common approach within AGARD — engine component defects N90-18404
The processing and mechanical properties of high temperature/high performance composites. Book 2, section 2: Strength and fracture resistance
[AD-A216142] N90-18507
The processing and mechanical properties of high temperature/high performance composites. Book 3, section 2: Strength and fracture resistance, part
[AD-A216143] N90-18508
Theory and verification of the fiber composite damage model implemented in DYNA3D
[AD-A216600] N90-18511
DAMAGE ASSESSMENT
AGARD/SMP Review: Damage Tolerance for Engine Structures. 2: Defects and Quantitative Materials Behaviour — conference
[AGARD-R-769] N90-18396
Damage assessment in composites by acousto-ultrasonic technique
[AD-A216590] N90-18510
Damage in a perforated graphite-epoxy composite plate under monotonic and cyclic biaxial loading
[ESA-TT-1117] N90-18521
DAMPING
Robot crane technology program
[PB90-111667] N90-18734
Control and stabilization of linear and nonlinear distributed systems
[AD-A216446] N90-18908
DARK MATTER
Annihilation physics of exotic galactic dark matter particles N90-18964
Particle physics and cosmology
[DE90-006547] N90-19171
DATA ACQUISITION
Data collection and location platforms experimental network: Description of an orbit routine
[INPE-4798-NTE/287] N90-18439
Electronically Variable Pressure Regulator (EVPR) N90-18484
Experimental investigations of the unsteady boundary layer on an oscillating flat plate. Optimization and validation of a code, for calculating the potential flow/boundary layer coupling of a flat plate and of an oscillating profile
[ETN-90-96254] N90-18682
TVI: A mathematical model for global estimation of Brazilian cerrado phytomass
[INPE-4836-PRE/1465] N90-18759
Paper on geography in environmental management: Research and new techniques
[INPE-4840-PRE/1469] N90-18816
DATA BASE MANAGEMENT SYSTEMS
Guidelines for the use of the SAME
[AD-A215846] N90-18888
A human factors experimental comparison of two database query languages N90-19064
DoD manual for standard data elements
[AD-A216441] N90-19066
DATA BASES
Future technology requirements (related to defects and quantitative material behavior to aid in implementation of damage tolerance for design of engine structures) N90-18403
A battery data base for electric vehicle applications
[DE90-007085] N90-18655
SPOT for landscape: Development of a method for the use of SPOT pictures for the updating of the data base scale of the landscape
[BCRS-89-18] N90-18787
Comparison of two Navy environmental database models: Generalized Digital Environmental Model and Podeszwa sound speed profile model
[AD-A215848] N90-18889
Teaching a new methodology for designing relational data bases: An experiment testing the effectiveness of an intelligent tutoring system on cognitive skill acquisition (volumes 1 and 2) N90-19063
Defense Technical Information Center Executive Information System: Documentation and user's manual
[AD-A216235] N90-19065
DTE and space technology transfer N90-19071
DATA COMPRESSION
Attitude estimation procedure for spin stabilized satellites
[INPE-4866-TDL/377] N90-18449
DATA CORRELATION
Applications of acousto-optical correlation devices in radar signal processing
[AD-A216624] N90-18616
DATA MANAGEMENT
An adaptive ARQ (Automatic Repeat Request) strategy for packet switching data communication networks
[AD-A216597] N90-18615
DATA PROCESSING
Time and frequency-domain identification and verification of BO-105 dynamic models
[AD-A216828] N90-18389
Navigation experiment NAVEX data storage and processing
[ESA-TT-1175] N90-18445
Fast algorithms for calculating laser wavefront phase compensation given noisy measurements of phase gradient
[DE90-006357] N90-18727

A global approach for the identification of structural connection properties
[NASA-TM-102502] N90-18745
Resource Assessment Project: User needs survey results
[DE89-009502] N90-18802
Feasibility of Mealy design for processor controlpaths
[MEMO-INF-89-53] N90-18923
DoD manual for standard data elements
[AD-A216441] N90-19066
Measurement system of spectral irradiance in the near infrared N90-19160

DATA SIMULATION
Simulating simultaneous processes with APL
[MEMO-INF-89-47] N90-18906

DATA SMOOTHING
Adaptive state estimation and sampling rate analysis for invariant linear dynamic systems in time
[INPE-4960-TDL/389] N90-18951

DATA STORAGE
Deceit: A flexible distributed file system
[NASA-CR-186402] N90-18891

DATA TRANSFER (COMPUTERS)
Packet telemetry standard
[ESA-PSS-04-106-ISSUE-1] N90-18447
Simulating simultaneous processes with APL
[MEMO-INF-89-47] N90-18906

DATA TRANSMISSION
An adaptive ARQ (Automatic Repeat Request) strategy for packet switching data communication networks
[AD-A216597] N90-18615

DAYTIME
Study of the atmospheric emissions of OI wavelength 557.7 nm and O2 (0,0) wavelength 761.9 nm in the equatorial region utilizing measurement of photometer on-board a rocket
[INPE-4811-TDL/358] N90-18827

DEBRIS
Zodiacal dust bands: Their relation to asteroid families
[AD-A216025] N90-19170

DECAY RATES
Decay rate and other properties of the positronium negative ion N90-18987

DECISION MAKING
A colony architecture for an artificial creature
[AD-A216802] N90-18918
Optimum selection procedures in multi-stage screening, reliability, and time
[AD-A216811] N90-18942

DECOMPOSITION
Thermal analysis of polymer composites
[AD-A216947] N90-18578
Distributed decomposition of block-angular linear programs on a hypercube computer
[AD-A216433] N90-18893

DEFECTS
Defects: Their behaviour and related design assumptions N90-18397
Review of component defects, their relationship to manufacturing process, and their effect on materials behaviour (for critical rotating parts) N90-18399
Defects in monoblock cast turbine wheels N90-18400
Crack propagation from artificial defects in typical engine disk materials; interpretation of experimental results by means of 3D J integral N90-18401
Review of modelling methods to take account of material structure and defects N90-18402
Future technology requirements (related to defects and quantitative material behavior to aid in implementation of damage tolerance for design of engine structures) N90-18403
The need for a common approach within AGARD — engine component defects N90-18404
Arcjet cathode phenomena N90-18477
Transport effects and spectroscopy of defects in microstructures
[AD-A216718] N90-19036

DEFENSE PROGRAM
The Executive Workshop on Cost/Performance Measurement. Volume 1: Executive summary
[AD-A216745] N90-18898
A perspective of software reuse
[AD-A216911] N90-18901
Survivability and effectiveness of near-term strategic defense
[DE90-005805] N90-18955

DEFLAGRATION
On the dynamics of the combustion process of hydrogen-air and hydrogen-methane-air mixtures
[DLR-FB-89-39] N90-18548

DEFORMATION
Threaded joint design for composites
[DE90-005553] N90-18506
Comparison of tension, compression, and flexure creep for alumina and silicon nitride ceramics
[DE90-006154] N90-18586

DEGASSING
Significance of oxide skins on powder for the quality of PM Al materials
[ESA-TT-1178] N90-18560

DEGRADATION
Feasibility demonstration of a 445N high-performance rocket engine N90-18481
Development of a progressive failure model for strength of laminated composite structure
[AD-A216966] N90-18517
Reliability studies of ceramic capacitors
[AD-A216763] N90-18643
Photointerpretation with instruments for evaluation of environmental impact: Mata Atlantica in Cubata
[INPE-4910-PRE/1511] N90-18817

DEGREES OF FREEDOM
KAM: Automatic planning and interpretation of numerical experiments using geometrical methods
[AD-A216805] N90-18900
Approximations to joint distributions of definite quadratic forms
[AD-A216434] N90-18930
Toda lattice with transverse degree of freedom
[DE90-002414] N90-19049

DELAY
Navigation experiment NAVEX: The self-test delay times in the D1 Spacelab mission
[ESA-TT-1176] N90-18446

DENSITY DISTRIBUTION
The lower hybrid drift instability and the evolution of plasma gradients
[DE90-006521] N90-19021

DENSITY MEASUREMENT
RF modal quantity gaging N90-18483

DEPOSITION
Effect of propellant flowrate and purity on carbon deposition in LO2/methane gas generators N90-18468
Sputter deposition of diffusion barrier coatings on SiC monofilaments for use in Ti-based composites N90-18502
Surface intermediates in thin film deposition on silicon
[AD-A216662] N90-18534
Structure and reactivity of model thin film catalysts
[DE90-007365] N90-18546
Perspectives on aerosol deposition to natural surfaces
[DE90-003398] N90-18819
Pulsed laser deposition of high T(sub c) superconducting thin films
[AD-A216507] N90-19034

DEPTH
On the depth of combinatorial optimization problems
[MEMO-803] N90-18946

DERIVATION
Vector fields, linear spaces and tensors in physics. Part 3: Tensor analysis and its applications
[INPE-5000-MD/41] N90-18897

DESCRIPTIONS
Simulating simultaneous processes with APL
[MEMO-INF-89-47] N90-18906

DESIGN ANALYSIS
Research on a two-dimensional inlet for a supersonic V/STOL propulsion system. Appendix A
[NASA-CR-174945] N90-18364
Defects: Their behaviour and related design assumptions N90-18397
The design of advanced ceramic composites
[DE90-006613] N90-18592
Fastener design manual
[NASA-RP-1228] N90-18740
Development of an experimental space station model for structural dynamics research
[NASA-TM-102601] N90-18751
An interactive system applied to the linear quadratic problem
[INPE-4945-TDL/386] N90-18913
Hamiltonian analysis and simulation of free electron lasers
[INPE-4785-TDL/351] N90-19018
The ISO short wavelength spectrometer N90-19162
The Infrared Space Observatory N90-19163
Spectrophotometry of dust with Isophot N90-19164
An advanced cooled grating spectrometer for UKIRT-CGS4 N90-19165

DESORPTION
Lower limits on the absolute dissociative electron attachment cross section from O2 condensed on rare-gas films
[AD-A216727] N90-18536
Absolute cross-sections for dissociative electron attachment in O2 condensed on Kr films
[AD-A216730] N90-19038

DETECTION
The signals of an ice warning device in dependence on total water content and normalized icing degree
[DLR-FB-89-52] N90-18377
Fluorescence and elastic scattering from laser dye-filled capillaries
[AD-A217026] N90-18540
Visual target detection and recognition
[DE90-006903] N90-19015

DETERMINANTS
Deterministic differential game solution: The approximate strategy method
[ESA-TT-1158] N90-18956

DETONATION
On the dynamics of the combustion process of hydrogen-air and hydrogen-methane-air mixtures
[DLR-FB-89-39] N90-18548
A program of fundamental research on explosives at Los Alamos
[DE90-006509] N90-18602

DETONATORS
Excess transit time as a function of burst current in an exploding bridgewire detonator
[DE90-007168] N90-18708

DEUTERIUM
Measurements of the D/H ratio in planetary atmospheres by ground based infrared spectroscopy N90-19088

DIAMONDS
High growth rate diamond synthesis in a large area atmospheric pressure inductively coupled plasma
[AD-A216090] N90-19019

DIELECTRIC PROPERTIES
Electronic and ionic transport in polymers
[AD-A217026] N90-18579
Reliability studies of ceramic capacitors
[AD-A216763] N90-18643

DIELECTRICS
Reliability studies of ceramic capacitors
[AD-A216763] N90-18643
Coating possibilities for magnetic switches
[DE90-006536] N90-18659

DIFFERENTIAL EQUATIONS
Direct and inverse scattering problem associated with the elliptic Sinh-Gordon equation
[AD-A216455] N90-18931
Differential-geometric techniques for solving differential algebraic equations
[AD-A216503] N90-18934
Waveform methods for ordinary differential equations
[DE90-006593] N90-18943
Deterministic differential game solution: The approximate strategy method
[ESA-TT-1158] N90-18956

DIFFERENTIAL GEOMETRY
Differential-geometric techniques for solving differential algebraic equations
[AD-A216503] N90-18934

DIFFERENTIATION (BIOLOGY)
Three-dimensional coculture process
[NASA-CASE-MSC-21560-1] N90-18852

DIFFUSION ELECTRODES
Fundamental studies of surface processes and trace analysis using solid electrodes
[AD-A216538] N90-18533

DIFFUSION FLAMES
Wick-type liquid-metal combustion
[AD-A216019] N90-18530
Theoretical investigation of the stabilization of a diffusion flame above a recirculation region
[ESA-TT-1149] N90-18543

DIGITAL DATA
Simulation of synthetic aperture radar 3: Evaluation of prototype digital feature analysis data
[AD-A216750] N90-18620
Monitoring of reforested areas through digital analysis of TM data
[INPE-4930-PRE/1420] N90-18764

DIGITAL SIMULATION
Computational aerodynamics of ordered vortex flows
[ETN-90-96272] N90-18368
Orbit determination of artificial Earth satellites through estmation techniques combined with state smoothing techniques
[INPE-4959-TDL/388] N90-18440
Simulation of synthetic aperture radar 3: Evaluation of prototype digital feature analysis data
[AD-A216750] N90-18620
Comparison of two Navy environmental database models: Generalized Digital Environmental Model and Podeszwa sound speed profile model
[AD-A215848] N90-18869

DIMENSIONS
A self-organizing multiple-view representation of three-dimensional objects
[AD-A216711] N90-18871

DIMERIZATION
Strongly coupled one-dimensional system and the polymer
[AD-A216330] N90-18571
DIRECTIONAL CONTROL
Design of a new control system for hovercrafts
[ETN-90-96230] N90-18435
DISCRIMINATION
Visual processing of object velocity and acceleration
[AD-A216509] N90-18858
Perception of long-period complex sounds
[AD-A216743] N90-18861
Auditory perception
[AD-A217012] N90-18864
DISK GALAXIES
The correlation between radio and far-infrared emission for disk galaxies N90-19158
DISPERSING
A study on deformation and break-up of dispersed particles in elongational flow
[ETN-90-96266] N90-18684
DISPLACEMENT
Small displacement, long life on-orbit compressor design and fabrication N90-18489
Intertropical Convergence Zone (ITCZ) and its relationship with the precipitation of the north-northeast Brazilian region
[INPE-4887-TDL/378] N90-18839
DISPLAY DEVICES
A simulation evaluation of the engine monitoring and control system display
[NASA-TP-2960] N90-18393
Three input concepts for flight crew interaction with information presented on a large-screen electronic cockpit display
[NASA-TM-4173] N90-18394
DISSIPATION
Asymptotic boundary conditions for dissipative waves: General theory
[NASA-TM-102497] N90-18927
DISSOCIATION
Lower limits on the absolute dissociative electron attachment cross section from O2 condensed on rare-gas films
[AD-A216727] N90-18536
Absolute cross-sections for dissociative electron attachment in O2 condensed on Kr films
[AD-A216730] N90-19038
DISSOLVING
The interaction of polycrystalline copper films with dilute aqueous solutions of cupric chloride
[AD-A216465] N90-19033
DISTANCE
Evaluation of selection techniques for multispectral bands employed in the discrimination of carbonatic rocks
[INPE-4850-TDL/365] N90-18765
DISTRIBUTED PARAMETER SYSTEMS
Energy decay and boundary control for distributed parameter systems with viscoelastic damping
[AD-A216468] N90-18748
Log-based recovery in asynchronous distributed systems
[NASA-CR-186190] N90-18924
DISTRIBUTED PROCESSING
Deceit: A flexible distributed file system
[NASA-CR-186402] N90-18891
DOPED CRYSTALS
Dopant site location in dual-implanted GaP using (111) planar channeling
[DE90-006565] N90-19042
DOPPLER EFFECT
Efficient detection and signal parameter estimation with application to high dynamic GPS receiver
[NASA-CASE-NPO-17820-1-CU] N90-18379
An error sensitivity model for Doppler positioning using transit satellites
[AD-A216724] N90-18381
Doppler spectra from incoherent backscatter: Principles and examples for application to POLDIRAD
[DLR-FB-89-48] N90-18830
DOPPLER RADAR
Doppler spectra from incoherent backscatter: Principles and examples for application for POLDIRAD
[DLR-FB-89-48] N90-18830
A case study of the 24 August 1986 FLOWS microburst
[AD-A216939] N90-18847
Doppler lidar working group report
[ESA-SP-1112] N90-18848
DRAG REDUCTION
Optimum spanwise camber for minimum induced drag
[BU-403] N90-18369
DRAINAGE
Remote sensing and run-off modelling in the Lake Victoria Basin, Kenya
[BCRS-89-19] N90-18788
DROPS (LIQUIDS)
A study on deformation and break-up of dispersed particles in elongational flow
[ETN-90-96268] N90-18684
Cloud hole-boring with infrared lasers: Theory and experiment
[DE90-006519] N90-18723
DUCTILITY
The processing and mechanical properties of high temperature/high performance composites. Book 2, section 2: Strength and fracture resistance
[AD-A216142] N90-18507
Processing and elevated temperature ductility of aluminum alloy 7475
[AD-A216840] N90-18554
High-strength concrete development through 25 years
[CBL-REPRINT-17] N90-18589
DUPLEXERS
Design, implementation and test of an RS-232 compatible bi-directional, full duplex, fiber-optic interface with provision for hardware handshaking on a minimum of fiber-optic lines
[AD-A216604] N90-19012
DURABILITY
Feasibility demonstration of a 445N high-performance rocket engine N90-18481
DWARF GALAXIES
On the mass to light ratios of dwarf spheroidal galaxies
[DE90-610645] N90-19175
DWARF NOVAE
Infrared spectroscopy of novae and related objects N90-19123
DYE LASERS
Fluorescence and elastic scattering from laser dye-filled capillaries
[AD-A217026] N90-18540
Absorption experiments on electron-beam pumped rare gases
[DE90-006504] N90-18722
DYES
A simple model for amplified spontaneous emission in dyes
[DE90-007249] N90-18730
DYNAMIC CHARACTERISTICS
Model filled polymers 3. Rheological behavior of polystyrene containing crosslinked polystyrene beads
[AD-A215867] N90-18567
Study of the dynamical behavior of copper in a shock wave
[ISL-R-123/88] N90-18679
The dynamics of electrons in very intense lasers
[DE90-007246] N90-18729
Kinetic relations and the propagation of phase boundaries in solids
[AD-A215881] N90-18747
System theory and mechanics
[MEMO-807] N90-18922
DYNAMIC CONTROL
Optimization of sensors and actuators positioning aimed at obtaining reduced models for the synthesis of optimal control regulators of flexible structures
[INPE-4760-TDL/348] N90-18450
Energy decay and boundary control for distributed parameter systems with viscoelastic damping
[AD-A216468] N90-18748
DYNAMIC LOADS
Vertical axis wind turbine turbulent response model. Part 2: Response of Sandia National laboratories' 34-meter VAWT with aeroelastic effects
[DE90-005721] N90-18804
DYNAMIC MODELS
Time and frequency-domain identification and verification of BO-105 dynamic models
[AD-A216828] N90-18389
Autonomous orbit determination using GPS
[INPE-4815-TDL/361] N90-18442
Attitude estimation procedure for spin stabilized satellites
[INPE-4866-TDL/377] N90-18449
Cold flow determination of the internal flow environment around the submerged TVC nozzle for the space shuttle SRM N90-18465
A global approach for the identification of structural connection properties
[NASA-TM-102502] N90-18745
Dynamics of an ERICA (Experiment on Rapidly Intensifying Cyclones over the Atlantic) cyclone
[AD-A216775] N90-18846
DYNAMIC PROGRAMMING
A survey of performability modelling tools
[MEMO-INF-89-50] N90-18907
Using dynamic queueing networks as a tool for specifying performability models
[MEMO-INF-89-51] N90-18949
Contribution to the study of stability robustness of nonlinear multivariable regulators
[INPE-4801-TDL/356] N90-18950
DYNAMIC RESPONSE
Reliability assessment using finite element techniques
[AD-A216907] N90-18647
System properties from frequency response functions, part 1
[ISVR-TR-168-PT-1] N90-18754
DYNAMIC STABILITY
Energy decay and boundary control for distributed parameter systems with viscoelastic damping
[AD-A216468] N90-18748
DYNAMIC STRUCTURAL ANALYSIS
A global approach for the identification of structural connection properties
[NASA-TM-102502] N90-18745
Biaxial strength and stress rupture of hot-pressed silicon nitride
[AD-A216950] N90-18750
Development of an experimental space station model for structural dynamics research
[NASA-TM-102601] N90-18751
DYNAMICAL SYSTEMS
Waveform methods for ordinary differential equations
[DE90-006593] N90-18943
The free energy principle, negative energy modes, and stability
[DE90-005368] N90-19056

E

EAR
Auditory perception
[AD-A217012] N90-18864
EARLY STARS
Infrared diagnostics of interstellar shocks N90-19115
The environment of young stellar objects studied by high-resolution infrared spectroscopy N90-19120
EARTH ATMOSPHERE
Quick, reliable estimates of high-power microwave fluences: The SNEAKY-2 program
[DE90-006347] N90-18624
Fast algorithms for calculating laser wavefront phase compensation given noisy measurements of phase gradient
[DE90-006357] N90-18727
EARTH CRUST
The interpretation of crustal dynamics data in terms of plate interactions and active tectonics of the Anatolian plate and surrounding regions in the Middle East
[NASA-CR-186200] N90-18824
EARTH OBSERVATIONS (FROM SPACE)
Refurbishment and modification of the Metric Camera (RMK) for reflight on EOM-1 Spacelab mission
[ETN-90-96284] N90-18710
Paper on geography in environmental management: Research and new techniques
[INPE-4840-PRE/1469] N90-18516
Activities report in German aerospace
[ISSN-0070-3966] N90-19189
EARTH ORBITAL ENVIRONMENTS
Radio interference in the near-earth environment
[NASA-CR-180479] N90-18823
EARTH ORBITS
Spatial registration of TIROS-N weather satellite data
[AD-A216041] N90-18841
EARTH PLANETARY STRUCTURE
Earth model selection for computer simulations
[AD-A216843] N90-18779
EARTH SURFACE
Orbital remote sensing in the decade of the nineties: New approaches and challenges in geology
[INPE-4838-PRE/1467] N90-18758
ECOLOGY
Perspectives on aerosol deposition to natural surfaces
[DE90-003398] N90-18819
ECONOMIC ANALYSIS
Analysis of inter-energy competition in the age of complex energies
[DE89-910216] N90-18794
Energy markets in the 1990's and beyond: A comparison of energy intensity in the United States and Japan
[DE90-005535] N90-18797
Programs in Renewable Energy
[DE89-009489] N90-18809
Promotion of European Space Technology Transfer
[ESA-SP-1122] N90-19068
Space technology transfers in Europe N90-19070
French approach to space technology transfer N90-19074

ECONOMICS
Remote sensing applied to the monitoring of mineral extraction in the proximity of urban areas: Pros and cons
[INPE-4867-PRE/1478] N90-18766
ECOSYSTEMS
Effects of global climate change on agroecosystems: Scope of work
[PB90-120023] N90-18813
Atlantic outer continental shelf: Description of the Mid-Atlantic environment
[PB90-100033] N90-18849
EDGE DETECTION
The effects of luminance boundaries on color perception
[AD-A216741] N90-18860
EDUCATION
Evaluation of two methods for acquisition of training statistics for digital analysis of areas prepared for plowing
[INPE-4901-PRE/1502] N90-18763
Calendar of selected aeronautical and space meetings
[AGARD-CAL-90/1] N90-19060
EFFECTIVE PERCEIVED NOISE LEVELS
Noise levels from a VSTOL aircraft measured at ground level and at 1.2 m above the ground
[NPL-RSA(EXT)-009] N90-18999
EGYPT
LANDSAT Thematic Mapper for hydrogeological mapping in Egypt
[BCRS-89-28] N90-18791
EIGENVALUES
A comparison of flutter calculations based on eigenvalue and energy method N90-18406
EIGENVECTORS
DOA (Direction of Arrival) estimation by Eigendecomposition using single vector Lanczos' algorithm
[AD-A215802] N90-18887
ELASTIC DEFORMATION
An objective time-integration procedure for isotropic rate-independent and rate-dependent elastic-plastic constitutive equations
[PB90-121245] N90-18925
ELASTIC MEDIA
Defects: Their behaviour and related design assumptions N90-18397
ELASTIC PLATES
The propagation of time harmonic Rayleigh-Lamb waves in a bimaterial plate
[AD-A216834] N90-18749
ELASTIC PROPERTIES
Threaded joint design for composites
[DE90-005553] N90-18506
An objective time-integration procedure for isotropic rate-independent and rate-dependent elastic-plastic constitutive equations
[PB90-121245] N90-18925
ELASTIC SCATTERING
Fluorescence and elastic scattering from laser dye-filled capillaries
[AD-A217026] N90-18540
Positron-alkali atom scattering N90-18958
Elastic scattering of e- and e+ from Rb and Cd N90-18960
Positron-rubidium scattering N90-18964
Positron scattering by atomic hydrogen using optical potentials and with positronium formation N90-18966
Numerical Green's functions in optical potential calculations for positron scattering from argon and neon N90-18971
Positron excitation of neon N90-18973
Positron-inert gas differential elastic scattering N90-18974
Differential elastic scattering cross sections for 54.9eV positrons incident on helium N90-18975
Total cross sections for positrons scattered elastically from helium based on new measurements of total ionization cross sections N90-18976
ELASTIC WAVES
Piezoelectric polymer PVDF shock gauge: State of the research art
[ISL-CO-207/89] N90-18705
ELECTRIC AUTOMOBILES
Advanced battery development
[DE90-006073] N90-18806
ELECTRIC BATTERIES
Cell performance of ultra-thin polymer cathode systems. Part 1: Anion intercalating polymer cathode
[AD-A216037] N90-18639
Lithium ambient-temperature battery reliability
[DE90-005758] N90-18650
A battery data base for electric vehicle applications
[DE90-007085] N90-18655
Feasibility of a super high energy density battery of the Li/BrF3 electrochemical system
[AD-A216575] N90-18799
Advanced battery development
[DE90-006073] N90-18806
ELECTRIC BRIDGES
Microconvective heating of granular explosives by a semiconductor bridge
[DE90-005710] N90-18541
ELECTRIC CHARGE
Airborne measurements of the electric field and the charge precipitation particles in convective clouds: Lower positive charge centres
[ESA-TT-1157] N90-18836
ELECTRIC CONDUCTORS
Flexible heat pipe cold plate
[AD-A216053] N90-18433
Electrochemical investigations of electronically conductive polymers. Part 4: By controlling the supermolecular structure, charge transport rates can be enhanced
[AD-A216603] N90-18573
ELECTRIC CORONA
A test method for measuring corona inception voltage for transducer autotransformers
[AD-A216818] N90-18646
ELECTRIC DISCHARGES
Study of discharge mechanisms and the stability of transverse electric discharges in the gas mixtures
[ISL-R-114/88] N90-18733
ELECTRIC FIELDS
The effect of electric field on attachment of electrons to solutes in liquid argon
[DE90-003969] N90-18529
A study of the interaction of light with surfaces of sub-micron dimensions
[DE90-006645] N90-19046
ELECTRIC FILTERS
High speed imaging with a tapped solid state sensor
[DE90-006116] N90-18702
ELECTRIC GENERATORS
Stirling engine technologies in Japan
[DE89-782296] N90-18795
ELECTRIC MOTOR VEHICLES
A battery data base for electric vehicle applications
[DE90-007085] N90-18655
ELECTRIC POTENTIAL
A test method for measuring corona inception voltage for transducer autotransformers
[AD-A216818] N90-18646
ELECTRIC POWER SUPPLIES
Low weight variable GRV power supply as part of the injector electronics to be developed for the electron accelerator MEA
[DIGEL-1989-6] N90-18661
ELECTRIC PROPULSION
The 1989 JANNAF Propulsion Meeting, volume 1
[CPIA-PUBL-515-VOL-1] N90-18462
Electric propulsion options for 10 kW class earth-space missions N90-18474
Mission options for an electric propulsion demonstration flight test N90-18479
Electric propulsion for manned Mars exploration N90-18480
ELECTRIC ROCKET ENGINES
Arcjet nozzle design impacts N90-18478
ELECTRIC SPARKS
Research on sliding spark preionization in a TEA CO2 laser
[ISL-R-113/88] N90-18732
ELECTRIC WIRE
Proceedings of the 38th International Wire and Cable Symposium
[AD-A216023] N90-18636
ELECTRICAL PROPERTIES
Research relating to crystalline silicon-film on a foreign substrate
[DE90-005720] N90-18582
ELECTRICAL RESISTIVITY
Electrochemical investigations of electronically conductive polymers. Part 4: By controlling the supermolecular structure, charge transport rates can be enhanced
[AD-A216603] N90-18573
Reliability studies of ceramic capacitors
[AD-A216763] N90-18643
ELECTRO-OPTICS
Colloid and interface chemistry aspects of ceramics
[AD-A216715] N90-18576
Optical amplification in 45 deg - cut BaTiO3
[AD-A216043] N90-19011
ELECTROACOUSTIC TRANSDUCERS
A test method for measuring corona inception voltage for transducer autotransformers
[AD-A216818] N90-18646
ELECTROCATALYSTS
Electronic and ionic transport in polymers
[AD-A217028] N90-18579
ELECTROCHEMICAL CORROSION
Feasibility of a super high energy density battery of the Li/BrF3 electrochemical system
[AD-A216794] N90-18644
ELECTROCHEMISTRY
Electronic and ionic transport in polymers
[AD-A217028] N90-18579
Electrochemical investigations of novel solid redox polymerization electrodes
[DE90-006087] N90-18584
Feasibility of a super high energy density battery of the Li/BrF3 electrochemical system
[AD-A216575] N90-18799
Advanced battery development
[DE90-006073] N90-18806
ELECTRODES
Cohesive ceramic fabrication
[DE90-007333] N90-18597
Oxygen electrode in molten carbonate fuel cells
[DE90-005377] N90-18796
Solid-state proton conductors
[DE90-007595] N90-18812
ELECTROLYSIS
Integrated regenerative fuel cell experimental evaluation
[NASA-CR-185183] N90-18808
ELECTROLYTES
Integrated regenerative fuel cell experimental evaluation
[NASA-CR-185183] N90-18808
ELECTROMAGNETIC FIELDS
Scattering from an arbitrary cylinder in the presence of a planar media interface using the bymoment method
[DE90-006465] N90-18626
The dynamics of electrons in very intense lasers
[DE90-007246] N90-18729
ELECTROMAGNETIC INTERFERENCE
Trends in VLF/LF (Very Low Frequency/Low Frequency) modem performance testing
[AD-A216576] N90-18614
ELECTROMAGNETIC PULSES
Parallel memory addressing using coincident optical pulses
[AD-A216302] N90-18641
ELECTROMAGNETIC RADIATION
Effects of pulsed and CW (Continuous Wave) 2450 MHz radiation on transformation and chromosomes of human lymphocytes in vitro
[AD-A216500] N90-18857
ELECTROMAGNETIC SCATTERING
ACIRF user's guide: Theory and examples
[AD-A216436] N90-18613
Effects of strong scattering on transionospheric propagation
[AD-A216708] N90-18617
Scattering from an arbitrary cylinder in the presence of a planar media interface using the bymoment method
[DE90-006465] N90-18626
ELECTROMAGNETIC WAVE TRANSMISSION
A simulation of optical propagation through atmospheric turbulence using two-dimensional Fourier transform techniques
[AD-A216776] N90-19013
ELECTRON ACCELERATORS
Low weight variable GRV power supply as part of the injector electronics to be developed for the electron accelerator MEA
[DIGEL-1989-6] N90-18661
ELECTRON ATTACHMENT
Lower limits on the absolute dissociative electron attachment cross section from O2 condensed on rare-gas films
[AD-A216727] N90-18536
Absolute cross-sections for dissociative electron attachment in O2 condensed on Kr films
[AD-A216730] N90-19038
ELECTRON BEAMS
Research project in microelectronic engineering and imaging science
[DE90-006907] N90-18653
Toroid monitor
[DIGEL-1989-8] N90-18663
Absorption experiments on electron-beam pumped rare gases
[DE90-006504] N90-18722
Electron beam and high-speed optical diagnostics for the Los Alamos HIBAF (High Brightness Accelerator FEL) Facility
[DE90-007828] N90-18725
Positronium reflection and positronium beams N90-18980
A continuous plasma final focus
[DE90-006096] N90-19024

ELECTRON DENSITY (CONCENTRATION)
Effects of strong scattering on transionospheric propagation
[AD-A216708] N90-18617
Quick, reliable estimates of high-power microwave fluences: The SNEAKY-2 program
[DE90-006347] N90-18624
Theory for high gain, high power free electron lasers
[DE90-005546] N90-18714
The rapid inward diffusion of cold ions in tokamaks and their effect on ion transport
[DE90-006863] N90-19022
Computerized analysis of hydrogen plasma in a compact H(sup -) cusp source
[DE90-006881] N90-19029
ELECTRON ENERGY
Positron annihilation induced Auger electron spectroscopy N90-18996
Understanding electronegative effects in core-level electron spectroscopies; application to the high temperature superconductors
[AD-A216726] N90-19037
ELECTRON GAS
Magnetic field generation by acoustic oscillations in solar atmosphere
[DE90-606054] N90-19180
ELECTRON IRRADIATION
Metal coordination polymers as potential high-energy lithographic resists
[AD-A216668] N90-18574
ELECTRON PARAMAGNETIC RESONANCE
Dynamics and stabilization of materials possessing high energy content
[AD-A216320] N90-18570
ELECTRON PLASMA
The dynamics of electrons in very intense lasers
[DE90-007246] N90-18729
ELECTRON SCATTERING
Scattering of positrons and electrons by alkali atoms N90-18959
Elastic scattering of e- and e+ from Rb and Cd N90-18960
Ab initio R-matrix calculations of e+-molecule scattering N90-18970
Positronium reflection and positronium beams N90-18980
Low-energy scattering of electrons and positrons in liquids N90-18981
Resonances in low-energy positron-alkali scattering N90-18992
ELECTRON SPECTROSCOPY
Spectroscopic evidence for carbon-carbon bonding in carbide layers on metals
[AD-A216726] N90-18512
Extracting chemical information form Augar line shapes
[AD-A216729] N90-18537
Dynamics and stabilization of materials possessing high energy content
[AD-A216320] N90-18570
Positron annihilation induced Auger electron spectroscopy N90-18996
ELECTRON TRANSFER
Surface production of ions
[AD-A216470] N90-19003
ELECTRON-POSITRON PAIRS
Search for resonances in positron-atom systems N90-18991
ELECTRONIC CONTROL
Signal processing device to control microwave output
[AD-A216931] N90-18648
ELECTRONIC EQUIPMENT
Reliability assessment using finite element techniques
[AD-A216907] N90-18647
ELECTRONS
The effect of electric field on attachment of electrons to solutes in liquid argon
[DE90-003969] N90-18529
Lower limits on the absolute dissociative electron attachment cross section from O2 condensed on rare-gas films
[AD-A216727] N90-18536
Strongly coupled one-dimensional system and the polymer
[AD-A216330] N90-18571
ELECTROPHORESIS
Fluorescence and elastic scattering from laser dye-filled capillaries
[AD-A217026] N90-18540
ELECTROSTATIC PROBES
BEAR electrostatic analyzer: Flight results
[DE90-006511] N90-18625
Computerized analysis of hydrogen plasma in a compact H(sup -) cusp source
[DE90-006881] N90-19029
ELEMENTARY PARTICLES
Elementary particles and cosmology
[DE90-610648] N90-19177
ELEVATION
Project Floval: Correction of relief effects in eucalyptus reforestration
[INPE-4814-RPE/590] N90-18777
ELLIPSOIDS
Contribution to the study of three-dimensional separation in turbulent incompressible flow
[ESA-TT-1169] N90-18697
ELLIPTIC DIFFERENTIAL EQUATIONS
Analysis of linear multigrid methods for elliptic differential equations with discontinuous and anisotropic coefficients
[ETN-90-96269] N90-18944
EMERGENCIES
The effects of wearing passenger protective breathing equipment on evacuation times through type 3 and type 4 emergency aircraft exits in clear air and smoke. Phase 1: Evacuations in clear air. Phase 2: Evacuations in smoke
[AD-A216798] N90-18374
EMISSION SPECTRA
Solid-state fluorescence above 1000 C: Application to high-temperature laser thermography
[DE90-006422] N90-18721
Properties and performance of the LiCaAlF6:Cr(3+) laser material
[DE90-007242] N90-18728
The 2.7/4.3 micron CO2 branching ratio measurement
[AD-A215952] N90-18830
Studies of atmospheric molecules by multiphoton spectroscopy
[DE90-005829] N90-18833
GRIS observations of the Galactic Center N90-18982
Positron annihilation in gamma-ray bursts N90-18983
Dust continuum spectra from model HII regions N90-19099
IR line emission from dense photodissociation regions N90-19100
Airborne observations of the infrared emission bands N90-19101
IR line emission from supernovae in molecular clouds N90-19102
An almost total disjunction between emission and absorption dust features: What does it tell us? N90-19106
Wide-beam balloon observations of the 157.7 microns (CII) line N90-19108
Mapping and spectroscopy of the 3.3 microns feature in Orion N90-19112
Infrared line emission from high-velocity outflows in star-forming regions N90-19116
High resolution infrared spectroscopy of symbiotic stars N90-19125
A survey of PAH emission in HII regions, planetary and proto-planetary nebulae N90-19129
H53-alpha emission from M82 N90-19156
EMISSIVITY
Interrelationship of spatial and radiometric resolution in the thermal infrared band
[INPE-4860-TDL/371] N90-18771
Techniques for measurement of the optical properties of materials
[DE90-006902] N90-19014
EMITTERS
Radiation-hard high-efficiency InP space solar cell development
[AD-A216857] N90-18800
END-TO-END DATA SYSTEMS
Space station technology summary N90-18482
ENERGY ABSORPTION
Low-energy gamma ray attenuation characteristics of aviation fuels
[NASA-TP-2974] N90-18882
ENERGY CONSERVATION
Energy markets in the 1990's and beyond: A comparison of energy intensity in the United States and Japan
[DE90-005535] N90-18797
ENERGY CONSUMPTION
Cost and energy consumption estimates for the aluminum-air battery anode fuel cycle
[DE90-005810] N90-18656
Thermal remote sensing in the differentiation of soybean crops (glycine max (L.) merrill) submitted to water deficit
[INPE-4900-PRE/1501] N90-18762
Energy markets in the 1990's and beyond: A comparison of energy intensity in the United States and Japan
[DE90-005535] N90-18797
ENERGY CONVERSION
Analysis of competition among the kinds of energy at the era of complexed energy: General review
[DE89-910215] N90-18793
Analysis of inter-energy competition in the age of complex energies
[DE89-910216] N90-18794
ENERGY CONVERSION EFFICIENCY
Research relating to crystalline silicon-film on a foreign substrate
[DE90-005720] N90-18582
ENERGY DISSIPATION
Energy decay and boundary control for distributed parameter systems with viscoelastic damping
[AD-A216468] N90-18748
ENERGY METHODS
A comparison of flutter calculations based on eigenvalue and energy method N90-18406
ENERGY POLICY
Alternative fuels R/D needs: Program directions
[DE90-007053] N90-18603
Analysis of competition among the kinds of energy at the era of complexed energy: General review
[DE89-910215] N90-18793
Analysis of inter-energy competition in the age of complex energies
[DE89-910216] N90-18794
ENERGY SOURCES
The extended equivalent source technique with underdetermined sources
[DE90-006989] N90-18627
Analysis of competition among the kinds of energy at the era of complexed energy: General review
[DE89-910215] N90-18793
ENERGY STORAGE
Lithium ambient-temperature battery reliability
[DE90-005758] N90-18650
ENERGY TECHNOLOGY
Progress in thin film solar photovoltaic technologies
[DE89-009513] N90-18792
Analysis of competition among the kinds of energy at the era of complexed energy: General review
[DE89-910215] N90-18793
Analysis of inter-energy competition in the age of complex energies
[DE89-910216] N90-18794
Advanced battery development
[DE90-006073] N90-18806
Programs in Renewable Energy
[DE89-009489] N90-18809
Hawaii integrated biofuels research program, phase 1
[DE90-006885] N90-18811
ENGINE DESIGN
AGARD/SMP Review: Damage Tolerance for Engine Structures. 2: Defects and Quantitative Materials Behaviour — conference
[AGARD-R-769] N90-18396
Future technology requirements (related to defects and quantitative material behavior to aid in implementation of damage tolerance for design of engine structures) N90-18403
Compressor performance tests in the compressor research facility N90-18428
Stall and recovery in multistage axial flow compressors N90-18429
Stirling engine technologies in Japan
[DE89-782295] N90-18795
ENGINE INLETS
Study of bird ingestions into small inlet area, aircraft turbine engines (May 1987 to April 1988)
[DOT/FAA/CT-89/17] N90-18375
ENGINE MONITORING INSTRUMENTS
A simulation evaluation of the engine monitoring and control system display
[NASA-TP-2960] N90-18393
ENGINE PARTS
AGARD/SMP Review: Damage Tolerance for Engine Structures. 2: Defects and Quantitative Materials Behaviour — conference
[AGARD-R-769] N90-18396
Defects in monoblock cast turbine wheels N90-18400
Crack propagation from artificial defects in typical engine disk materials; interpretation of experimental results by means of 3D J integral N90-18401
Review of modelling methods to take account of material structure and defects N90-18402
Future technology requirements (related to defects and quantitative material behavior to aid in implementation of damage tolerance for design of engine structures) N90-18403
The need for a common approach within AGARD — engine component defects N90-18404
Transient pressure test article test program N90-18463
Probability of failure and risk assessment of propulsion structural components N90-18470
ENGINE TESTING LABORATORIES
Test facility and preliminary performance of a 100 kW class MPD thruster N90-18476

ENGINE TESTS
Test facility and preliminary performance of a 100 kW class MPD thruster N90-18478
ENGINEERING DRAWINGS
Recognizing three-dimensional objects without the use of models
[AD-A216766] N90-18862
ENTRAINMENT
Numerical simulations of coherent structures in a jet flame with a noncircular cross section
[AD-A216710] N90-18535
ENTROPY
Heat capacities of solid polymers (The Advanced THermal Analysis System, ATHAS)
[DE90-007130] N90-18595
The extended equivalent source technique with underdetermined sources
[DE90-006989] N90-18627
ENVIRONMENT EFFECTS
Effects of global climate change on agroecosystems: Scope of work
[PB90-120023] N90-18813
Tropospheric chemistry of natural hydrocarbons and energy-related pollutants: Biosphere/climate feedbacks
[DE90-005643] N90-18820
Natural and anthropogenic climate change
[DE90-006488] N90-18822
Atlantic outer continental shelf: Description of the Mid-Atlantic environment
[PB90-100033] N90-18849
ENVIRONMENT MANAGEMENT
Paper on geography in environmental management: Research and new techniques
[INPE-4840-PRE/1469] N90-18816
Atlantic outer continental shelf: Description of the Mid-Atlantic environment
[PB90-100033] N90-18849
ENVIRONMENT MODELS
Comparison of two Navy environmental database models: Generalized Digital Environmental Model and Podeszwa sound speed profile model
[AD-A215848] N90-18889
ENVIRONMENT POLLUTION
Atlantic outer continental shelf: Description of the Mid-Atlantic environment
[PB90-100033] N90-18849
ENVIRONMENT SIMULATION
Simulation of the dynamic environment for missile component testing: Demonstration
[AD-A216979] N90-18443
ENVIRONMENTAL MONITORING
Remote sensing applied to the monitoring of mineral extraction in the proximity of urban areas: Pros and cons
[INPE-4867-PRE/1478] N90-18766
ERS-1 European remote sensing satellite: A new tool for global environmental monitoring in the 1990's
[ESA-BR-36] N90-18782
Application of high performance liquid chromatography/mass spectrometry to environmental analysis
[PB90-116963] N90-18814
ENVIRONMENTAL QUALITY
Synthetic aperture radar imagery of airports and surrounding areas: Philadelphia Airport
[NASA-CR-4280] N90-18372
ENVIRONMENTAL SURVEYS
Photointerpretation with instruments for evaluation of environmental impact: Mata Atlantica in Cubata
[INPE-4910-PRE/1511] N90-18817
ENVIRONMENTAL TESTS
Simulation of the dynamic environment for missile component testing: Demonstration
[AD-A216979] N90-18443
EPHEMERIDES
Evaluation of influences of errors involved in orbit propagation of artificial satellites
[INPE-4962-TDL/391] N90-18441
EPITAXY
Pulsed laser deposition of high T(sub c) superconducting thin films
[AD-A216507] N90-19034
In situ growth of epitaxial superconducting YBa2Cu3O(7-x) films on insulating semiconducting and ferroelectric K(Ta, Nb)O3 by pulsed laser ablation
[DE90-006568] N90-19043
In situ growth of high quality epitaxial YBa2Cu3O(7-x) thin films at moderate temperatures by pulsed laser ablation
[DE90-006629] N90-19045
EPOXY MATRIX COMPOSITES
Compressive strength of carbon/epoxy laminated under multiaxial stress
[DE90-005552] N90-18505
Calculation of mechanical properties variations depending on matrix parameters in a composite, as a function of the test temperature
[DT-311/88] N90-18526
Impact of composites in the aerospace industry
[ETN-90-96231] N90-18527
EPOXY RESINS
Structural study of thermo-hardenable matrices. Deformation processes of composite matrices as a function of their molecular structure
[ONERA-RT-10/3521-M] N90-18522
EQUATIONS OF MOTION
Analytical formulation for the interaction problem of dynamic reentry, and effects due to flexibility and vibration in an aerospace vehicle
[INPE-4963-TDL/392] N90-18448
Using the method of matched asymptotic expansions, analytically investigate the three-dimensional, atmosphere entry problem
[AD-A216287] N90-18451
Improved computational fluid dynamics for continuum hypersonic flow
[AD-A216981] N90-18674
System properties from frequency response functions, part 1
[ISVR-TR-166-PT-1] N90-18754
EQUATORIAL REGIONS
Study of the atmospheric emissions of OI wavelength 557.7 nm and O2 (0,0) wavelength 761.9 nm in the equatorial region utilizing measurement of photometer on-board a rocket
[INPE-4811-TDL/358] N90-18827
EQUILIBRIUM FLOW
Multicellular natural convection in a narrow vertical slot
[AD-A216411] N90-18668
Development of a defect stream function, law of the wall/wake method for compressible turbulent boundary layers
[NASA-CR-4286] N90-18675
EROSION
Technique for evaluating the erosive properties of ablative internal insulation materials N90-18466
Fundamental aspects of erosion and impact damage
[DE90-006640] N90-18587
Erosion monitoring using remote sensing, part 2
[BCRS-89-15] N90-18785
EROSIVE BURNING
Analysis of propulsive powder combustion products and their corrosive effects
[ISL-CO-248/88] N90-18605
ERROR ANALYSIS
An error sensitivity model for Doppler positioning using transit satellites
[AD-A216724] N90-18381
Evaluation of influences of errors involved in orbit propagation of artificial satellites
[INPE-4962-TDL/391] N90-18441
Autonomous orbit determination using GPS
[INPE-4815-TDL/361] N90-18442
Angle estimation in the presence of mainbeam interference
[AD-A216832] N90-18621
ERROR CORRECTING CODES
An adaptive ARQ (Automatic Repeat Request) strategy for packet switching data communication networks
[AD-A216597] N90-18615
ERROR DETECTION CODES
SHARP: A multi-mission artificial intelligence system for spacecraft telemetry monitoring and diagnosis
[NASA-CR-186285] N90-18444
ERROR FUNCTIONS
Asymptotic boundary conditions for dissipative waves: General theory
[NASA-TM-102497] N90-18927
ERROR SIGNALS
Angle estimation in the presence of mainbeam interference
[AD-A216832] N90-18621
ERRORS
Evaluation of two methods for acquisition of training statistics for digital analysis of areas prepared for plowing
[INPE-4901-PRE/1502] N90-18763
Temporal response of atmospheric turbulence compensation
[DE90-006354] N90-18837
ERS-1 (ESA SATELLITE)
ERS-1 European remote sensing satellite: A new tool for global environmental monitoring in the 1990's
[ESA-BR-36] N90-18782
ESA SPACECRAFT
The determination of offgassing products from materials and assembled articles to be used in a manned space vehicle crew compartment
[ESA-PSS-01-729-ISSUE-1] N90-18461
ESTIMATING
Attitude estimation procedure for spin stabilized satellites
[INPE-4866-TDL/377] N90-18449
ETCHING
Metal coordination polymers as potential high-energy lithographic resists
[AD-A216868] N90-18574
The track-etch detector for the MACRO experiment at the Gran Sasso Laboratory
[DE90-003235] N90-19182
ETHANE
Extracting chemical information form Auger line shapes
[AD-A216729] N90-18537
ETHYL COMPOUNDS
Determination of the minimum energy conformation of alkyl substituted pyrazines
[AD-A216974] N90-18539
ETHYLENE
Extracting chemical information form Auger line shapes
[AD-A216729] N90-18537
EULER EQUATIONS OF MOTION
Numerical investigation of unsteady flow in oscillating turbine and compressor cascades N90-18407
EUROPE
Investigation report of the investigation commission for interchange of heat pump technology in Europe
[DE89-782293] N90-18666
EUROPEAN SPACE AGENCY
ESA project to promote and assist technology transfer by industry N90-19069
EUROPEAN SPACE PROGRAMS
Packet telemetry standard
[ESA-PSS-04-106-ISSUE-1] N90-18447
System safety requirements for ESA space systems and associated equipment
[ESA-PSS-01-40-ISSUE-2] N90-18460
The determination of offgassing products from materials and assembled articles to be used in a manned space vehicle crew compartment
[ESA-PSS-01-729-ISSUE-1] N90-18461
Configuration management and control for ESA space systems
[ESA-PSS-01-11-ISSUE-1] N90-19061
Component selection, procurement and control for ESA space systems
[ESA-PSS-01-60-ISSUE-2] N90-19062
Space technology transfers in Europe N90-19070
The Infrared Space Observatory N90-19163
EVACUATING (TRANSPORTATION)
The effects of wearing passenger protective breathing equipment on evacuation times through type 3 and type 4 emergency aircraft exits in clear air and smoke. Phase 1: Evacuations in clear air. Phase 2: Evacuations in smoke
[AD-A216798] N90-18374
EVAPORATION
Microcomputer enhanced optical investigation of spreading and evaporative processes in ultra thin films
[DE90-006323] N90-18585
Cloud hole-boring with infrared lasers: Theory and experiment
[DE90-006519] N90-18723
Thermal remote sensing in the differentiation of soybean crops (glycine max (L.) merrill) submitted to water deficit
[INPE-4900-PRE/1501] N90-18762
EXCIMER LASERS
Development of KrF lasers for fusion
[DE90-007830] N90-18726
Pulsed laser deposition of high T(sub c) superconducting thin films
[AD-A216507] N90-19034
EXCITATION
A numerical solution to the Boltzmann equation for use in calculating pumping rates in a CO2 discharge laser
[AD-A216376] N90-18718
Study of the atmospheric emissions of OI wavelength 557.7 nm and O2 (0,0) wavelength 761.9 nm in the equatorial region utilizing measurement of photometer on-board a rocket
[INPE-4811-TDL/358] N90-18827
A study of the interaction of light with surfaces of sub-micron dimensions
[DE90-006646] N90-19046
EXPERIMENTATION
Experiments on the unsteady flow in a supersonic compressor stage N90-18422
EXPERT SYSTEMS
Application of artificial intelligence control to the vapor-liquid-solid silicon carbide whisker process
[DE90-007835] N90-18519
Knowledge-based fault detection and analysis for robots: First results for the ROTEX robots
[ESA-TT-1150] N90-18742

Teleoperator servoloop tuning using an expert system [DE90-005674] N90-18876
Knowledge-based extensible natural language interface technology program [AD-A216664] N90-18897
User manual for NEXT 1.2: NLR engineering X-pert system toolkit [NLR-TR-87178-U] N90-18905
Computation and control with neural nets [DE90-006460] N90-18911
Derivation of an efficient rule system pattern matcher [AD-A216801] N90-18917

EXPLODING WIRES
Excess transit time as a function of burst current in an exploding bridgewire detonator [DE90-007168] N90-18708

EXPLOSIVES
Microconvective heating of granular explosives by a semiconductor bridge [DE90-005710] N90-18541
Investigation of the phase stabilizing effect of 4 percent potassium fluoride on ammonium nitrate [AD-A215313] N90-18599
A program of fundamental research on explosives at Los Alamos [DE90-006509] N90-18602

EXTRACTION
Injection parameters and beam oscillations during extraction [NIKHEF-K/AMPS/89-07] N90-18632
Remote sensing applied to the monitoring of mineral extraction in the proximity of urban areas: Pros and cons [INPE-4867-PRE/1478] N90-18766

EYE (ANATOMY)
Visual processing of object velocity and acceleration [AD-A216509] N90-18858

EYE MOVEMENTS
Psychological studies of visual cortical function [AD-A217029] N90-18872

F

FABRICATION
Process development and fabrication of space station type aluminum-clad graphite epoxy struts [NASA-CR-181873] N90-18454
Electronically Variable Pressure Regulator (EVPR) N90-18484
Small displacement, long life on-orbit compressor design and fabrication N90-18489
A statistical evaluation of the variation in laminated composite properties resulting from ply misalignment [DE90-006371] N90-18525
Hydrogenated amorphous silicon films prepared by glow discharge of disilane [DE90-000309] N90-18581
Performance and modeling of superconducting ring resonators at millimeter-wave frequencies [NASA-TM-102526] N90-18634
Cost and energy consumption estimates for the aluminum-air battery anode fuel cycle [DE90-005810] N90-18656

FABRICS
Instrumented impact testing of fabric-reinforced composite materials [AD-A216764] N90-18513

FACTOR ANALYSIS
The effects of wearing passenger protective breathing equipment on evacuation times through type 3 and type 4 emergency aircraft exits in clear air and smoke. Phase 1: Evacuations in clear air. Phase 2: Evacuations in smoke [AD-A216798] N90-18374

FACTORIZATION
Orbit determination of artificial Earth satellites through estmation techniques combined with state smoothing techniques [INPE-4959-TDL/388] N90-18440
Boolean minimization and algebraic factorization procedures for fully testable sequential machines [AD-A216779] N90-18940
Kreim factorization of covariance operators of 2-parameter random fields and application to the likelihood ratio [MEMO-802] N90-18953

FAILURE
Development of a progressive failure model for strength of laminated composite structure [AD-A216966] N90-18517

FAILURE ANALYSIS
Discrete proportional Plus Integral (PI) multivariable control laws for the Control Reconfigurable Combat Aircraft (CRCA) [AD-A215664] N90-18431
SHARP: A multi-mission artificial intelligence system for spacecraft telemetry monitoring and diagnosis [NASA-CR-186285] N90-18444
Effect of correlation on multi-engine rocket propulsion systems N90-18467
Probability of failure and risk assessment of propulsion structural components N90-18470
Electronically Variable Pressure Regulator (EVPR) N90-18484

FAILURE MODES
Review of component defects, their relationship to manufacturing process, and their effect on materials behaviour (for critical rotating parts) N90-18399
A new broadband pulsed high voltage monitor [DE90-006264] N90-18651

FAR INFRARED RADIATION
Wide-beam balloon observations of the 157.7 microns (CII) line N90-19108
Herbig Ae/Be stars: Fine structure far-infrared lines N90-19126
Far-infrared spectroscopy of galaxies N90-19146
Evolutionary synthesis of the far-infrared emission in starburst galaxies N90-19152
Far infrared fine structure lines in active galaxies N90-19157
The correlation between radio and far-infrared emission for disk galaxies N90-19158

FAR ULTRAVIOLET RADIATION
Photodissociation regions: Observations and theory N90-19098

FARM CROPS
Relationships between spectral parameters and agronomics of wheat and beam crops [INPE-4791-RPE/584] N90-18768
Development of the agricultural information system. Characteristics and results of the Distrito Federal model [INPE-4940-PRE/1430] N90-18773

FASTENERS
Fastener design manual [NASA-RP-1228] N90-18745

FATIGUE (MATERIALS)
AGARD/SMP Review: Damage Tolerance for Engine Structures. 2: Defects and Quantitative Materials Behaviour — conference [AGARD-R-769] N90-18396
Identification of a cast iron alloy containing nonstrategic elements [NASA-CR-185174] N90-18559
Life of concentrated contacts in the mixed EHD and boundary film regimes [AD-A216673] N90-18738
Biaxial strength and stress rupture of hot-pressed silicon nitride [AD-A216950] N90-18750

FATIGUE TESTS
The need for a common approach within AGARD — engine component defects N90-18404
Interlaminar fracture testing of carbon fibre/PEEK composites validity and applications N90-18497
Biaxial strength and stress rupture of hot-pressed silicon nitride [AD-A216950] N90-18750

FATS
Measurement of body fat by neutron inelastic scattering: Comments on installation, operation, and error analysis [DE90-006765] N90-18888

FEASIBILITY ANALYSIS
Advanced battery development [DE90-006073] N90-18806
Feasibility of Mealy design for processor controlpaths [MEMO-INF-89-53] N90-18923

FEED SYSTEMS
The 1989 JANNAF Propulsion Meeting, volume 1 [CPIA-PUBL-515-VOL-1] N90-18462

FEEDBACK
Electronically Variable Pressure Regulator (EVPR) N90-18484
Teleoperator servoloop tuning using an expert system [DE90-005674] N90-18876

FEEDBACK CONTROL
Discrete proportional Plus Integral (PI) multivariable control laws for the Control Reconfigurable Combat Aircraft (CRCA) [AD-A215664] N90-18431
Application of variable-gain output feedback for high-alpha control [NASA-TM-102603] N90-18434
Energy decay and boundary control for distributed parameter systems with viscoelastic damping [AD-A216468] N90-18748
Practical methods for robust multivariable control [AD-A216937] N90-18920
Contribution to the study of stability robustness of nonlinear multivariable regulators [INPE-4801-TDL/356] N90-18950

FERROELECTRICITY
Piezoelectric polymer PVDF shock gauge: State of the research art [ISL-CO-207/89] N90-18705
In situ growth of epitaxial superconducting YBa2Cu3O(7-x) films on insulating semiconducting and ferroelectric K(Ta, Nb)O3 by pulsed laser ablation [DE90-006568] N90-19043

FERROMAGNETIC MATERIALS
Improved amorphous metal materials for magnetic pulse compression [DE90-005723] N90-18555
Crystallographic and magnetic properties of (C6 D11 ND3)CuBr3 and (Zn(1-x)Mn(x))3As2: A neutron scattering study [ECN-219] N90-19055

FIBER COMPOSITES
Third European Conference on Composite Materials [EOARD-LR-89-050] N90-18494
Modified bismaleimides for carbon fibre composites N90-18495
Enhanced bonding of fiber reinforcements to thermoset resins N90-18496
Interlaminar fracture testing of carbon fibre/PEEK composites validity and applications N90-18497
State of the art and future prospects for high temperature composites N90-18498
Silicon carbo-nitride ceramic matrix composites by polymer pyrolysis N90-18499
Ceramic matrix composites, new high performance materials N90-18500
Sputter deposition of diffusion barrier coatings on SiC monofilaments for use in Ti-based composites N90-18502
Measuring strain in carbon fibre composite laminates using the Raman optomechanical strain gauge N90-18503
Theory and verification of the fiber composite damage model implemented in DYNA3D [AD-A216600] N90-18511

FIBER OPTICS
Measuring strain in carbon fibre composite laminates using the Raman optomechanical strain gauge N90-18503
Proceedings of the 38th International Wire and Cable Symposium [AD-A216023] N90-18638
Design, implementation and test of an RS-232 compatible bi-directional, full duplex, fiber-optic interface with provision for hardware handshaking on a minimum of fiber-optic lines [AD-A216604] N90-19012

FIBERS
The processing and mechanical properties of high temperature/high performance composites. Book 3, section 2: Strength and fracture resistance, part [AD-A216143] N90-18508
Damage assessment in composites by acousto-ultrasonic technique [AD-A216590] N90-18510
Calculations of braiding parameters [AD-A216836] N90-18515

FIELD THEORY (PHYSICS)
Theoretical and experimental high energy physics [DE90-006168] N90-19006
Geometric continuum regularization of quantum field theory [DE90-006099] N90-19058
Quantum cosmological origin of large scale structures of the universe [DE90-610647] N90-19176

FIGHTER AIRCRAFT
The effects of wind tunnel data uncertainty on aircraft point performance predictions [AD-A216091] N90-18387
Influence of forebody geometry on aerodynamic characteristics and a design guide for defining departure/spin resistant forebody configurations [AD-A216714] N90-18388

FILE MAINTENANCE (COMPUTERS)
Using the K-25 C/TD common file system: A guide to CFSI [DE90-005815] N90-19179

FILLING
Model filled polymers 3. Rheological behavior of polystyrene containing crosslinked polystyrene beads [AD-A215867] N90-18567

FILTRATION
Low cost filter development and control of permeability in high temperature, high pressure ceramic filter elements [DE90-000403] N90-18676

FINANCE
The bringing to market of the RF alert (a case study in technology transfer) N90-19073

FINE STRUCTURE
IR line emission from dense photodissociation regions N90-19100
Herbig Ae/Be stars: Fine structure far-infrared lines N90-19126
Far infrared fine structure lines in active galaxies N90-19157
FINITE DIFFERENCE THEORY
Numerical simulation of the incompressible inhomogeneous turbulence in a plane channel flow [ONERA-NT-1988-5] N90-18686
FINITE ELEMENT METHOD
Theory and verification of the fiber composite damage model implemented in DYNA3D [AD-A216600] N90-18511
Reliability assessment using finite element techniques [AD-A216907] N90-18647
Transient responses of coupled systems [ONERA-RT-13/3596-RY-070-R] N90-18687
Development of an experimental space station model for structural dynamics research [NASA-TM-102601] N90-18751
Optimization of the reference parameters in the accompanying solar panel dynamics [INPE-4795-PRE/1449] N90-18798
The interpretation of crustal dynamics data in terms of plate interactions and active tectonics of the Anatolian plate and surrounding regions in the Middle East [NASA-CR-186200] N90-18824
Efficient preconditioning for the p-version finite element method in two dimensions [AD-A216210] N90-18928
Research equipment [AD-A216515] N90-18937
FINITE VOLUME METHOD
High-resolution Euler computations of unsteady transonic flows in cascades N90-18420
FITTINGS
Space shuttle RCS oxidizer leak repair for STS-26 N90-18485
FIXING
Study of rifampicin fixation on plasma proteins by derivative spectrophotometry [CERMA-89-25] N90-18866
FLAME PROPAGATION
Wick-type liquid-metal combustion [AD-A216019] N90-18530
FLAME STABILITY
Theoretical investigation of the stabilization of a diffusion flame above a recirculation region [ESA-TT-1149] N90-18543
FLAMES
An investigation of flow structure, mixing and chemical reaction in combusting turbulent flows [AD-A216739] N90-18538
Investigation of methods to produce a uniform cloud of fuel particles in a flame tube [NASA-TM-102376] N90-18665
FLANGES
A study of the vibrational transmission through flanged joints [ISVR-TR-181] N90-18755
FLAT PLATES
Experimental investigations of the unsteady boundary layer on an oscillating flat plate. Optimization and validation of a code, for calculating the potential flow/boundary layer coupling of a flat plate and of an oscillating profile [ETN-90-96254] N90-18682
Transient heat transfer measurements on a flat plate in turbulent flow using an electrical analog [AD-A216286] N90-19057
FLEXIBILITY
Analytical formulation for the interaction problem of dynamic reentry, and effects due to flexibility and vibration in an aerospace vehicle [INPE-4963-TDL/392] N90-18448
Orbital fluid resupply assessment N90-18487
FLEXIBLE BODIES
Optimization of sensors and actuators positioning aimed at obtaining reduced models for the synthesis of optimal control regulators of flexible structures [INPE-4760-TDL/348] N90-18450
FLIGHT CLOTHING
Evaluation of helmet retention systems using a pendulum device [AD-A215489] N90-18874
FLIGHT CONTROL
Discrete proportional Plus Integral (PI) multivariable control laws for the Control Reconfigurable Combat Aircraft (CRCA) [AD-A215664] N90-18431
The implications of using integrated software support environment for design of guidance and control systems software [AGARD-AR-229] N90-18432
Flexible heat pipe cold plate [AD-A216053] N90-18433
Application of variable-gain output feedback for high-alpha control [NASA-TM-102603] N90-18434
Practical methods for robust multivariable control [AD-A216937] N90-18920
FLIGHT CREWS
Delivery performance of conventional aircraft by terminal-area, time-based air traffic control: A real-time simulation evaluation [NASA-TP-2978] N90-18378
Three input concepts for flight crew interaction with information presented on a large-screen electronic cockpit display [NASA-TM-4173] N90-18394
Evaluation of helmet retention systems using a pendulum device [AD-A215489] N90-18874
FLIGHT INSTRUMENTS
A simulation evaluation of the engine monitoring and control system display [NASA-TP-2960] N90-18393
Flexible heat pipe cold plate [AD-A216053] N90-18433
FLIGHT PATHS
Dallas/Fort Worth simulation. Volume 2: Appendixes D, E, and F [AD-A216613] N90-18380
FLIGHT SAFETY
Dallas/Fort Worth simulation. Volume 2: Appendixes D, E, and F [AD-A216613] N90-18380
System safety requirements for ESA space systems and associated equipment [ESA-PSS-01-40-ISSUE-2] N90-18460
FLIGHT SIMULATION
Time and frequency-domain identification and verification of BO-105 dynamic models [AD-A216828] N90-18389
FLIGHT TESTS
Time and frequency-domain identification and verification of BO-105 dynamic models [AD-A216828] N90-18389
Wind-tunnel investigation of a flush airdata system at Mach numbers from 0.7 to 1.4 [NASA-TM-101697] N90-18395
Mission options for an electric propulsion demonstration flight test N90-18479
FLIP-FLOPS
Integrated silicon flip-flop sensors [ETN-90-96271] N90-18654
FLOATING POINT ARITHMETIC
Technology development and circuit design for a parallel laser programmable floating point application specific processor [AD-A215870] N90-18637
FLOW CHARACTERISTICS
Study of the blade/vortice interaction on a one-blade rotor during forward flight (incompressible, non viscous fluid) [ISL-R-115/88] N90-18391
Cold flow determination of the internal flow environment around the submerged TVC nozzle for the space shuttle SRM N90-18465
FLOW DISTRIBUTION
Computational aerodynamics of ordered vortex flows [ETN-90-96272] N90-18368
Test data of flow field of shuttle SRM nozzle joint with bond defects, using unheated air N90-18464
Experimental flow models for SSME flowfield characterization N90-18469
Semidiscrete Galerkin modelling of compressible viscous flow past a circular cone at incidence [NASA-CR-186323] N90-18664
Multicellular natural convection in a narrow vertical slot [AD-A216411] N90-18668
Automation and extension of LDV (Laser-Doppler Velocimetry) measurements of off-design flow in a subsonic cascade wind tunnel [AD-A216627] N90-18670
Direct simulation Monte Carlo of shock reflexion on a wedge with boundary layer [ISL-CO-245/88] N90-18681
Coronary arterial capacitance and subendocardial vascular patency throughout the cardiac cycle N90-18855
FLOW GEOMETRY
Experimental flow models for SSME flowfield characterization N90-18469
FLOW MEASUREMENT
Automation and extension of LDV (Laser-Doppler Velocimetry) measurements of off-design flow in a subsonic cascade wind tunnel [AD-A216627] N90-18670
Transient heat transfer measurements on a flat plate in turbulent flow using an electrical analog [AD-A216286] N90-19057
FLOW STABILITY
The inviscid stability of supersonic flow past a sharp cone [NASA-CR-181996] N90-18363
Dryout stability and inception at low flowrates [DE90-006955] N90-18692
FLOW THEORY
Concepts and experiments on space-time chaos [ETN-90-96255] N90-18683
FLOW VELOCITY
Effect of propellant flowrate and purity on carbon deposition in LO2/methane gas generators N90-18468
Numerical investigations of heat transfer and flow rates in rotating cavities. Simulation of the movement generated by wall temperature gradients, by source-sink mass flows or by the differential rotation of the walls, under the influence or coriolis and centrifugal forces [ETN-90-96253] N90-18695
Study on the thermodynamical and mechanical conditions for the generation of high operating pressures with liquefied gases for low and very low flow rates [ESA-TT-1148] N90-18696
FLOW VISUALIZATION
Aerodynamic testing of a rotating wind turbine blade [DE90-000312] N90-18362
Supersonic wind tunnel investigation of a tubular projectile [ISL-CO-306/89] N90-18366
Half model tests on an ONERA calibration model in the transonic wind tunnel Goettingen, Federal Republic of Germany [DLR-MITT-89-20] N90-18370
A study on deformation and break-up of dispersed particles in elongational flow [ETN-90-96268] N90-18684
FLUID DYNAMICS
Summer Study Program in Geophysical Fluid Dynamics: The Influence of Convection on Large-Scale Circulations, 1988 [AD-A216024] N90-18840
FLUID FILMS
Microcomputer enhanced optical investigation of spreading and evaporative processes in ultra thin films [DE90-006323] N90-18585
Life of concentrated contacts in the mixed EHD and boundary film regimes [AD-A216673] N90-18738
FLUID FLOW
Spacecraft thermal control design data, volume 4 [ESA-PSS-03-108-ISSUE-1-VOL-4] N90-18458
Experimental flow models for SSME flowfield characterization N90-18469
Modeling convective Marangoni flows with void movement in the presence of solid-liquid phase change [DE90-006474] N90-18690
Fluidization mechanisms in slurry flow [DE90-006497] N90-18691
FLUID MECHANICS
Experimental and theoretical research on the injection of ignition gases into a bed of inert powder [ISL-CO-251/88] N90-18547
Analytic solutions for the decay of turbulent swirling flow in a cylinder [DE90-005744] N90-18677
Velocity measurement using interferometry [ISL-CO-221/88] N90-18709
FLUID-SOLID INTERACTIONS
Transient responses of coupled systems [ONERA-RT-13/3596-RY-070-R] N90-18687
FLUORESCENCE
Fluorescence and elastic scattering from laser dye-filled capillaries [AD-A217026] N90-18540
Solid-state fluorescence above 1000 C: Application to high-temperature laser thermography [DE90-006422] N90-18721
Fluorescent molecular hydrogen emission from star-forming galaxies N90-19155
FLUORIDES
Feasibility of a super high energy density battery of the Li/BrF3 electrochemical system [AD-A216794] N90-18644
FLUORINATION
Perfluorinated ligands in organometallic chemistry [AD-A216415] N90-18493
FLUOROPOLYMERS
Electronic and ionic transport in polymers [AD-A217028] N90-18579
Development and polarization of ferroelectric polymer gauges, for dynamical acceleration experiments, as those in ballistics shocks [ISL-R-119/88] N90-18703

Feasibility of a super high energy density battery of the Li/BrF3 electrochemical system
[AD-A216575] N90-18799

FLUSHING

Wind-tunnel investigation of a flush airdata system at Mach numbers from 0.7 to 1.4
[NASA-TM-101697] N90-18395

FLUTTER

Unsteady Aerodynamic Phenomena in Turbomachines
[AGARD-CP-468] N90-18405

A comparison of flutter calculations based on eigenvalue and energy method N90-18406

FLUX DENSITY

A numerical solution to the Boltzmann equation for use in calculating pumping rates in a CO2 discharge laser
[AD-A216376] N90-18718

Development of an rf-driven plasma neutralizer for negative ions
[DE90-007298] N90-19027

FOLIAGE

Thermal remote sensing in the differentiation of soybean crops (glycine max (L.) merrill) submitted to water deficit
[INPE-4900-PRE/1501] N90-18762

Relationships between spectral parameters and agronomics of wheat and beam crops
[INPE-4791-RPE/584] N90-18768

FORBIDDEN BANDS

Near infrared (1-4 micron) spectroscopy of SN1987A N90-19133

FORCE DISTRIBUTION

Optimum spanwise camber for minimum induced drag
[BU-403] N90-18369

FORCED VIBRATION

Aerodynamic study on forced vibrations on stator rows of axial compressors N90-18412

Gust response analysis for cascades operating in nonuniform mean flows N90-18415

FOREBODIES

Static and rotational aerodynamic data from 0 deg to 90 deg angle of attack for a series of basic and altered forebody shapes
[AD-A216582] N90-18361

Influence of forebody geometry on aerodynamic characteristics and a design guide for defining departure/spin resistant forebody configurations
[AD-A216714] N90-18388

FORECASTING

Resource Assessment Project: User needs survey results
[DE89-009502] N90-18802

FOREST MANAGEMENT

Monitoring of reforested areas through digital analysis of TM data
[INPE-4930-PRE/1420] N90-18764

Multistage forest volume estimation using a sampling system with probability variables
[INPE-4897-PRE/1498] N90-18769

FORESTS

Monitoring of reforested areas through digital analysis of TM data
[INPE-4930-PRE/1420] N90-18764

Multistage forest volume estimation using a sampling system with probability variables
[INPE-4897-PRE/1498] N90-18769

Photointerpretation with instruments for evaluation of environmental impact: Mata Atlantica in Cubata
[INPE-4910-PRE/1511] N90-18817

Some aspects of atmospheric turbulence in forests
[INPE-4951-RPE/600] N90-18818

FOURIER TRANSFORMATION

High temperature interaction of SO2 with oxide sorbents
[DE90-000435] N90-18545

Measurement of spectral emissivity by Fourier transform infrared spectrometer
[DE89-782319] N90-18698

Mathematical methods of Physics 6: Integral transformation
[INPE-4807-MD/40] N90-18926

A simulation of optical propagation through atmospheric turbulence using two-dimensional Fourier transform techniques
[AD-A216776] N90-19013

FRACTOGRAPHY

Comparison of tension, compression, and flexure creep for alumina and silicon nitride ceramics
[DE90-006154] N90-18586

FRACTURE MECHANICS

AGARD/SMP Review: Damage Tolerance for Engine Structures. 2: Defects and Quantitative Materials Behaviour --- conference
[AGARD-R-769] N90-18396

Defects: Their behaviour and related design assumptions N90-18397

Review of modelling methods to take account of material structure and defects N90-18402

Compact reinforced composite basic principles
[CBL-41] N90-18520

Corrosion fatigue of iron-chromium-nickel alloys: Fracture mechanics and chemistry
[DE90-006318] N90-18556

Identification of a cast iron alloy containing nonstrategic elements
[NASA-CR-185174] N90-18559

Deformation and fracture of ordered intermetallic compounds
[DE90-007422] N90-18563

Fundamental aspects of erosion and impact damage
[DE90-006640] N90-18587

FRACTURE STRENGTH

Modified bismaleimides for carbon fibre composites N90-18495

Analysis of whisker-toughened ceramic components: A design engineer's viewpoint
[NASA-TM-102333] N90-18504

The processing and mechanical properties of high temperature/high performance composites. Book 2, section 2: Strength and fracture resistance
[AD-A216142] N90-18507

Compact reinforced composite basic principles
[CBL-41] N90-18520

Biaxial strength and stress rupture of hot-pressed silicon nitride
[AD-A216950] N90-18750

FRACTURES (MATERIALS)

Spallation and dynamic fracture as an effect of laser induced shock waves in carbon based composite materials
[AD-A216540] N90-18509

The joint effect of surface microtopography and near-surface structure on microcontact conditions
[DE90-006494] N90-18591

FRACTURING

Interlaminar fracture testing of carbon fibre/PEEK composites validity and applications N90-18497

Spallation and dynamic fracture as an effect of laser induced shock waves in carbon based composite materials
[AD-A216540] N90-18509

Deformation and fracture of ordered intermetallic compounds
[DE90-007422] N90-18563

Fracture analysis through photographic imagery of low spatial resolution: A contribution to the study of tectonic evoluation of the Araripe Plateau region
[INPE-4876-PRE/1487] N90-18756

The patterns of fracture and the conditioning tectonics in the region of the Quadrilatero Ferrifero and part of the Migmatitic-Gnanulitic Complex in Minas Gerais (Brazil)
[INPE-4895-PRE/1496] N90-18829

FRANCE

French approach to space technology transfer N90-19074

FREE CONVECTION

Multicellular natural convection in a narrow vertical slot
[AD-A216411] N90-18668

FREE ELECTRON LASERS

INEX (Integrated Numerical Experiment) simulations of the Boeing FEL system
[DE90-004846] N90-18712

Theory for high gain, high power free electron lasers
[DE90-005546] N90-18714

Research on free electron lasers
[AD-A215865] N90-18715

Resonator modes in high gain free electron lasers
[DE90-006098] N90-18720

Electron beam and high-speed optical diagnostics for the Los Alamos HIBAF (High Brightness Accelerator FEL) Facility
[DE90-007826] N90-18725

Hamiltonian analysis and simulation of free electron lasers
[INPE-4785-TDL/351] N90-19018

FREE ENERGY

The free energy principle, negative energy modes, and stability
[DE90-005368] N90-19056

FREEZING

Thermodynamics of systems with very many components phase equilibrium
[DE90-007345] N90-19059

FREQUENCIES

System properties from frequency response functions, part 1
[ISVR-TR-166-PT-1] N90-18754

FREQUENCY MODULATION

On the range resolution of point targets with FMCW radar systems
[DLR-FB-89-47] N90-18629

Auditory perception
[AD-A217012] N90-18864

FREQUENCY STABILITY

Instability investigation for storage mode. Microwave instability (single-bunch instability)
[NIKHEF-K/AMPS/89/05] N90-18628

Determining the effects of microwave power and C-field setting on the frequency of a cesium atomic frequency standard
[AD-A216599] N90-18642

FREQUENCY STANDARDS

Determining the effects of microwave power and C-field setting on the frequency of a cesium atomic frequency standard
[AD-A216599] N90-18642

FRICTION

Life of concentrated contacts in the mixed EHD and boundary film regimes
[AD-A216673] N90-18738

FRONTS (METEOROLOGY)

A case study of the 24 August 1986 FLOWS microburst
[AD-A216939] N90-18847

FUEL CELLS

Cohesive ceramic fabrication
[DE90-007333] N90-18597

Oxygen electrode in molten carbonate fuel cells
[DE90-005377] N90-18796

Solid-state proton conductors
[DE90-007595] N90-18812

FUEL COMBUSTION

Alternative fuels R/D needs: Program directions
[DE90-007053] N90-18803

Investigation of methods to produce a uniform cloud of fuel particles in a flame tube
[NASA-TM-102376] N90-18865

FUEL CONSUMPTION

Federal methanol fleet update
[DE90-006851] N90-18741

FUEL SYSTEMS

Low-energy gamma ray attenuation characteristics of aviation fuels
[NASA-TP-2974] N90-18882

FUEL-AIR RATIO

Numerical simulations of coherent structures in a jet flame with a noncircular cross section
[AD-A216710] N90-18535

FUELS

Hawaii integrated biofuels research program, phase 1
[DE90-006885] N90-18811

FUNCTIONS (MATHEMATICS)

Should a function continue
[AD-A216406] N90-18929

FUSELAGES

Fuselage design for a specified Mach-sliced area distribution
[NASA-TP-2975] N90-18385

FUSES (ORDNANCE)

Simulation of the dynamic environment for missile component testing: Demonstration
[AD-A216979] N90-18443

FUSION REACTORS

Fourth International Conference on Fusion Reactor Materials
[DE90-006142] N90-19025

G

GALACTIC CLUSTERS

A comparison of void distributions in Abell cluster catalogue with numerical simulations
[DE90-610640] N90-19173

GALACTIC EVOLUTION

Evolutionary synthesis of the far-infrared emission in starburst galaxies N90-19152

GALACTIC MASS

Infrared lines as probes of galactic structure N90-19139

GALACTIC NUCLEI

Infrared spectroscopy of the central few parsecs of the galaxy N90-19140

Stellar kinematics in the galactic centre N90-19141

An infrared imaging Fabry-Perot study of the galactic centre N90-19142

Near infrared spectroscopy of active galaxies N90-19143

Spectroscopy of galaxies in the mid-infrared N90-19145

A search for the CO feature in active galactic nuclei N90-19151

Infrared (FeII), H and H2 lines in galaxy nuclei N90-19153

GALACTIC RADIATION

Gamma ray astronomy and black hole astrophysics
[NASA-CR-186496] N90-19169

GALACTIC STRUCTURE
Infrared Spectroscopy in Astronomy [ESA-SP-290] N90-19084
Infrared lines as probes of galactic structure N90-19139

GALAXIES
Spectroscopy of galaxies in the mid-infrared N90-19145
Far-infrared spectroscopy of galaxies N90-19146
Fluorescent molecular hydrogen emission from star-forming galaxies N90-19155
H53-alpha emission from M82 N90-19156

GALERKIN METHOD
Semidiscrete Galerkin modelling of compressible viscous flow past a circular cone at incidence [NASA-CR-186323] N90-18664
Strong source heat transfer simulations based on a GalerKin/gradient least squares method [DE90-608613] N90-18678

GALILEO PROJECT
Technology update-89 [DE90-005813] N90-19178

GALILEO SPACECRAFT
Safety analysis for the Galileo light-weight radioisotope heater unit [DE90-007147] N90-19009

GALLIUM ARSENIDES
A GaAs p-n-p-n thyristor model [DE90-005757] N90-19039

GALLIUM PHOSPHIDES
Dopant site location in dual-implanted GaP using (111) planar channeling [DE90-006565] N90-19042

GAME THEORY
Deterministic differential game solution: The approximate strategy method [ESA-TT-1158] N90-18956

GAMMA RAY ABSORPTION
Low-energy gamma ray attenuation characteristics of aviation fuels [NASA-TP-2974] N90-18882

GAMMA RAY ASTRONOMY
Gamma ray astronomy and black hole astrophysics [NASA-CR-186496] N90-19169
Imaging Germanium Telescope Array for Gamma-Rays (IGETAGRAY) [DE90-006994] N90-19188

GAMMA RAY BURSTS
Positron annihilation in gamma-ray bursts N90-18983

GAMMA RAY SPECTRA
GRIS observations of the Galactic Center N90-18982

GAMMA RAY SPECTROMETERS
A large area, low cost, gamma-ray, imaging spectrometer [DE90-006993] N90-19017

GAMMA RAY TELESCOPES
Imaging Germanium Telescope Array for Gamma-Rays (IGETAGRAY) [DE90-006994] N90-19188

GAMMA RAYS
Low-energy gamma ray attenuation characteristics of aviation fuels [NASA-TP-2974] N90-18882

GAS CHROMATOGRAPHY
Evaluation of a commercial gas chromatography/matrix isolation-infrared spectrometer for quantitative analysis of priority pollutants [DE90-006033] N90-18542

GAS DENSITY
Measurement of gas intensity at high dynamic pressures [ISL-CO-204/89] N90-18680

GAS DISSOCIATION
Lower limits on the absolute dissociative electron attachment cross section from O2 condensed on rare-gas films [AD-A216727] N90-18536
Absolute cross-sections for dissociative electron attachment in O2 condensed on Kr films [AD-A216730] N90-19038

GAS EVOLUTION
Integrated regenerative fuel cell experimental evaluation [NASA-CR-185183] N90-18808

GAS FLOW
Cold flow determination of the internal flow environment around the submerged TVC nozzle for the space shuttle SRM N90-18465

GAS GENERATORS
Effect of propellant flowrate and purity on carbon deposition in LO2/methane gas generators N90-18468
Design and operation of an inert gas facility for thermoelectric generator storage [DE90-007146] N90-19008

GAS INJECTION
Experimental and theoretical research on the injection of ignition gases into a bed of inert powder [ISL-CO-251/88] N90-18547

GAS IONIZATION
Photodissociation regions: Observations and theory N90-19098

GAS MIXTURES
On the dynamics of the combustion process of hydrogen-air and hydrogen-methane-air mixtures [DLR-FB-89-39] N90-18548

GAS PATH ANALYSIS
Measurement of gas leaks between a projectile and the walls of a tube in a ballistic compressor [ISL-CO-250/88] N90-18694

GAS PRESSURE
Helium permeability through austenitic stainless steel [DE90-007046] N90-18562
Construction and calibration of a gas pressure meter with high temporal resolution [INPE-4953-RPE/602] N90-18700

GAS SPECTROSCOPY
Evaluation of a commercial gas chromatography/matrix isolation-infrared spectrometer for quantitative analysis of priority pollutants [DE90-006033] N90-18542

GAS TURBINE ENGINES
Study of bird ingestions into small inlet area, aircraft turbine engines (May 1987 to April 1988) [DOT/FAA/CT-89/17] N90-18375
AGARD/SMP Review: Damage Tolerance for Engine Structures. 2: Defects and Quantitative Materials Behaviour --- conference [AGARD-R-769] N90-18396
Review of modelling methods to take account of material structure and defects N90-18402
The need for a common approach within AGARD --- engine component defects N90-18404

GAS TURBINES
Aerodynamic superposition principle in vibrating turbine cascades N90-18410

GASKETS
A study of the vibrational transmission through flanged joints [ISVR-TR-181] N90-18755

GAUSS EQUATION
Approximations to joint distributions of definite quadratic forms [AD-A216434] N90-18930

GEARS
Life of concentrated contacts in the mixed EHD and boundary film regimes [AD-A216673] N90-18738

GENERATORS
Back swing phenomenon of synchronous generator. Study on ac-dc power system simulator tests [DE89-782321] N90-18635

GEODETIC ACCURACY
Earth model selection for computer simulations [AD-A216843] N90-18779

GEODYNAMICS
The interpretation of crustal dynamics data in terms of plate interactions and active tectonics of the Anatolian plate and surrounding regions in the Middle East [NASA-CR-186200] N90-18824

GEOGRAPHIC INFORMATION SYSTEMS
Land suitability maps and appropriate land use: An approach using SGI and satellite imagery [INPE-4827-PRE/1458] N90-18761
Perspective revision of systematic mapping through orbital imagery [INPE-4817-PRE/1453] N90-18775

GEOGRAPHY
Paper on geography in environmental management: Research and new techniques [INPE-4840-PRE/1469] N90-18816

GEOLOGICAL FAULTS
Fracture analysis through photographic imagery of low spatial resolution: A contribution to the study of tectonic evoluation of the Araripe Plateau region [INPE-4876-PRE/1487] N90-18756
The interpretation of crustal dynamics data in terms of plate interactions and active tectonics of the Anatolian plate and surrounding regions in the Middle East [NASA-CR-186200] N90-18824

GEOLOGY
Orbital remote sensing in the decade of the nineties: New approaches and challenges in geology [INPE-4838-PRE/1467] N90-18758
Geological structure of the State of Rio de Janeiro viewed through MSS LANDSAT imagery [INPE-4826-PRE/1457] N90-18825
The patterns of fracture and the conditioning tectonics in the region of the Quadrilatero Ferrifero and part of the Migmatitic-Gnanulitic Complex in Minas Gerais (Brazil) [INPE-4895-PRE/1496] N90-18829

GEOMETRICAL THEORY OF DIFFRACTION
Telemetry and telecommand omnidirectional antenna in the short wave band [ETN-90-96285] N90-18631

GEOMETRY
A user's manual for the method of moments Aircraft Modeling Code (AMC) [NASA-CR-186371] N90-18390
Probability of failure and risk assessment of propulsion structural components N90-18470

GEOPHYSICS
Summer Study Program in Geophysical Fluid Dynamics: The Influence of Convection on Large-Scale Circulations, 1988 [AD-A216024] N90-18840

GEOTHERMAL ENERGY UTILIZATION
Investigation report of the investigation commission for interchange of heat pump technology in Europe [DE89-782293] N90-18666

GERMANIUM
Imaging Germanium Telescope Array for Gamma-Rays (IGETAGRAY) [DE90-006994] N90-19188

GERMANIUM COMPOUNDS
Dislocation behaviour in Ge(x)Si(1-x) epilayers on (001) Si [DE90-007063] N90-19051
Modified dislocation structures in Ge(x)Si(1-x) double epilayers on (001) Si [DE90-007078] N90-19052

GIANT STARS
Observations of 40-70 micron bands of ice in IRAS 09371+1212 and other stars N90-19134

GLASS
Evaluating a glass surface produced by ductile grinding [DE90-006782] N90-18608

GLASS FIBER REINFORCED PLASTICS
Enhanced bonding of fiber reinforcements to thermoset resins N90-18496

GLASS FIBERS
Thermal analysis of polymer composites [AD-A216947] N90-18578

GLASS LASERS
Spallation and dynamic fracture as an effect of laser induced shock waves in carbon based composite materials [AD-A216540] N90-18509

GLAUBER THEORY
Positron collisions with alkali-metal atoms N90-18962

GLOBAL POSITIONING SYSTEM
The Fourteenth Biennial Guidance Test Symposium, volume 1 [AD-A216925] N90-18383
Autonomous orbit determination using GPS [INPE-4815-TDL/361] N90-18442
The interpretation of crustal dynamics data in terms of plate interactions and active tectonics of the Anatolian plate and surrounding regions in the Middle East [NASA-CR-186200] N90-18824

GLOBAL WARMING
Effects of global climate change on agroecosystems: Scope of work [PB90-120023] N90-18813

GLOBULINS
Characterization of biopolymer surfaces using scanning microscopies [AD-A216572] N90-18572

GLOW DISCHARGES
Hydrogenated amorphous silicon films prepared by glow discharge of disilane [DE90-000309] N90-18581

GOLD
Fundamental studies of surface processes and trace analysis using solid electrodes [AD-A216538] N90-18533

GOVERNMENT/INDUSTRY RELATIONS
Promotion of European Space Technology Transfer [ESA-SP-1122] N90-19068
DTE and space technology transfer N90-19071
Introductory remarks for the panel discussions on technology transfer N90-19075
Problems on transfer of space technology to non-space areas and solutions: Legal aspects N90-19077
The improvement of technology transfer from space to industry N90-19079

GOVERNMENTS
Study on the measures to promote the use of photovoltaic power generating system overseas [DE90-742056] N90-18807

GRAMMARS
Computational structure of GPSG (Generalized Phrase Structure Grammar) models: Revised generalized phrase structure grammar [AD-A216803] N90-18941

GRAND UNIFIED THEORY
The track-etch detector for the MACRO experiment at the Gran Sasso Laboratory
[DE90-003235] N90-19182
GRAPH THEORY
Long path connectivity of regular graphs
[AD-A216477] N90-18933
Finding critical independent sets and critical vertex subsets are polynomial problems
[AD-A216547] N90-18938
GRAPHITE
Extracting chemical information form Auger line shapes
[AD-A216729] N90-18537
GRAPHITE-EPOXY COMPOSITES
Process development and fabrication of space station type aluminum-clad graphite epoxy struts
[NASA-CR-181873] N90-18454
Damage in a perforated graphite-epoxy composite plate under monotonic and cyclic biaxial loading
[ESA-TT-1117] N90-18521
GRATINGS (SPECTRA)
Temperature dependence of photon-gated persistent spectral hole-burning for the meso-tetra-p-tolyl Zn-tetrabenzoporphyrin/chloroform system in poly(methylmethacrylate)
[AD-A216086] N90-18531
An advanced cooled grating spectrometer for UKIRT-CGS4 N90-19165
GRAVITATION
Streaming gravity mode instability
[DE90-610619] N90-18835
GRAVITATIONAL FIELDS
Streaming gravity mode instability
[DE90-610619] N90-18835
GREEN'S FUNCTIONS
Numerical Green's functions in optical potential calculations for positron scattering from argon and neon N90-18971
GREENHOUSE EFFECT
Effects of global climate change on agroecosystems: Scope of work
[PB90-120023] N90-18813
Tropospheric chemistry of natural hydrocarbons and energy-related pollutants: Biosphere/climate feedbacks
[DE90-005643] N90-18820
Natural and anthropogenic climate change
[DE90-006488] N90-18822
GRID GENERATION (MATHEMATICS)
A simple algebraic grid adaptation scheme with applications to two- and three-dimensional flow problems
[NASA-TM-102446] N90-18667
GRINDING (MATERIAL REMOVAL)
Evaluating a glass surface produced by ductile grinding
[DE90-006782] N90-18608
GROUND STATE
VUV (Vacuum Ultraviolet) laser diagnostics of H(-) ion sources
[DE90-006072] N90-18719
Positronium formation in e+ plus H- collisions N90-18993
Positron-molecule bound states and positive ion production N90-18994
GROUND STATIONS
Navigation experiment NAVEX data storage and processing
[ESA-TT-1175] N90-18445
Synchronization of the ground station atomic clocks using three weighted transportable cesium time standards in the Navex navigation experiment
[ESA-TT-1153] N90-18711
Measurements of the D/H ratio in planetary atmospheres by ground based infrared spectroscopy N90-19068
GROUND SUPPORT EQUIPMENT
System safety requirements for ESA space systems and associated equipment
[ESA-PSS-01-40-ISSUE-2] N90-18460
GROUND WATER
LANDSAT Thematic Mapper for hydrogeological mapping in Egypt
[BCRS-89-29] N90-18791
GROUND WAVE PROPAGATION
Practical applications of Loran-C for land mobile use or the possibility to use Loran-C as a vehicle-location or vehicle-navigation system
[ETN-90-96265] N90-18384
GROUND WIND
Multiparameter scatterometer for remote sensing (RADSER). Project Scatter: State-of-the-art and future applications
[INPE-4871-PRE/1482] N90-18701
GROUP DYNAMICS
Grouping for recognition
[AD-A216716] N90-18915
GROUP THEORY
New aspects in bifurcation with symmetry
[AD-A216506] N90-18935
GUIDANCE (MOTION)
The implications of using integrated software support environment for design of guidance and control systems software
[AGARD-AR-229] N90-18432
GUIDE VANES
Unsteady aerodynamic phenomena in a simulated wake and shock wave passing experiment N90-18414
GULF STREAM
An application of ocean wave-current refraction to the gulf stream using SEASAT SAR data
[AD-A216769] N90-18851
GUN PROPELLANTS
Analysis of propulsive powder combustion products and their corrosive effects
[ISL-CO-248/88] N90-18605
Microcalometric studies of gun propellant KKR 8
[FOA-C-20770-2.1] N90-18606
GUST LOADS
Gust response analysis for cascades operating in nonuniform mean flows N90-18415

H

H II REGIONS
Dust continuum spectra from model HII regions N90-19099
Airborne observations of the infrared emission bands N90-19101
Polycyclic aromatic hydrocarbons in the infrared spectra of IRAS sources N90-19105
Mapping and spectroscopy of the 3.3 microns feature in Orion N90-19112
Molecular hydrogen in the HII region G333.6-0.2 N90-19121
A survey of PAH emission in HII regions, planetary and proto-planetary nebulae N90-19129
Infrared lines as probes of galactic structure N90-19139
Spectroscopy of galaxies in the mid-infrared N90-19145
Infrared (FeII), H and H2 lines in galaxy nuclei N90-19153
HALL EFFECT
Magnetohydrodynamic modeling of plasma opening switches and gas puff plasmas
[DE90-005825] N90-19028
Superconducting materials
[DE90-007419] N90-19054
HAMILTON-JACOBI EQUATION
Perturbations of test mass motion in the Schwarzschild spacetime using the method of Hamilton and Jacobi N90-19083
HAMILTONIAN FUNCTIONS
KAM: Automatic planning and interpretation of numerical experiments using geometrical methods
[AD-A216805] N90-18900
System theory and mechanics
[MEMO-807] N90-18922
Long path connectivity of regular graphs
[AD-A216477] N90-18933
Hamiltonian analysis and simulation of free electron lasers
[INPE-4785-TDL/351] N90-19018
Perturbations of test mass motion in the Schwarzschild spacetime using the method of Hamilton and Jacobi N90-19083
HANDBOOKS
Spacecraft thermal control design data, volume 1
[ESA-PSS-03-108-ISSUE-1-VOL-1] N90-18455
Spacecraft thermal control design data, volume 2
[ESA-PSS-03-108-ISSUE-1-VOL-2] N90-18456
Spacecraft thermal control design data, volume 3
[ESA-PSS-03-108-ISSUE-1-VOL-3] N90-18457
Spacecraft thermal control design data, volume 4
[ESA-PSS-03-108-ISSUE-1-VOL-4] N90-18458
Composites design handbook for space structure applications
[ESA-PSS-03-1101-ISSUE-1-REV-1] N90-18459
HARDENING (MATERIALS)
Structural study of thermo-hardenable matrices. Deformation processes of composite matrices as a function of their molecular structure
[ONERA-RT-10/3521-M] N90-18522
Comparison between the damage modes of thermo-hardenable and thermo-plastic composite matrices
[ONERA-RT-47/7086-M] N90-18523
Study of the dynamical behavior of copper in a shock wave
[ISL-R-123/88] N90-18679
HARDNESS
The mechanism, measurement, and influence of properties on the galling of metals
[DE90-006533] N90-18558
HARMONICS
Output performance of idealized microwave power amplifiers
[AD-A216797] N90-18645
HEALTH PHYSICS
Risk analysis: Fundamental concepts, regulatory toxicology, and relative comparisons from radiation biology
[DE90-002466] N90-18856
HEART RATE
The role of blood volume in determining the cardiovascular adjustments to exercise N90-18954
HEAT EXCHANGERS
Spacecraft thermal control design data, volume 4
[ESA-PSS-03-108-ISSUE-1-VOL-4] N90-18458
Condensation fluid dynamics and heat transfer on rotating spherical surfaces in a microgravitational field
[DE90-005540] N90-18607
HEAT FLUX
Improved computational fluid dynamics for continuum hypersonic flow
[AD-A216981] N90-18674
Dryout stability and inception at low flowrates
[DE90-006955] N90-18692
HEAT MEASUREMENT
Heat capacities of solid polymers (The Advanced THermal Analysis System, ATHAS)
[DE90-007130] N90-18595
Microcalometric studies of gun propellant KKR 8
[FOA-C-20770-2.1] N90-18606
HEAT PIPES
Flexible heat pipe cold plate
[AD-A216053] N90-18433
Spacecraft thermal control design data, volume 3
[ESA-PSS-03-108-ISSUE-1-VOL-3] N90-18457
Analytical and experimental investigation of miniature heat pipes, phase 2
[AD-A216945] N90-18673
HEAT PUMPS
Investigation report of the investigation commission for interchange of heat pump technology in Europe
[DE89-782293] N90-18666
Transfer of heat pump technology
[DE90-007373] N90-18693
Stirling engine technologies in Japan
[DE89-782296] N90-18795
HEAT RESISTANT ALLOYS
Crack propagation from artificial defects in typical engine disk materials; interpretation of experimental results by means of 3D J integral N90-18401
HEAT SINKS
Flexible heat pipe cold plate
[AD-A216053] N90-18433
HEAT SOURCES
Investigation report of the investigation commission for interchange of heat pump technology in Europe
[DE89-782293] N90-18666
HEAT STORAGE
Phase-Change Thermal Energy Storage
[DE89-009426] N90-18801
HEAT TRANSFER
Spacecraft thermal control design data, volume 4
[ESA-PSS-03-108-ISSUE-1-VOL-4] N90-18458
Microcomputer enhanced optical investigation of spreading and evaporative processes in ultra thin films
[DE90-006323] N90-18585
Strong source heat transfer simulations based on a GalerKin/gradient least squares method
[DE90-608613] N90-18678
Modeling convective Marangoni flows with void movement in the presence of solid-liquid phase change
[DE90-006474] N90-18690
Transfer of heat pump technology
[DE90-007373] N90-18693
Numerical investigations of heat transfer and flow rates in rotating cavities. Simulation of the movement generated by wall temperature gradients, by source-sink mass flows or by the differential rotation of the walls, under the influence or coriolis and centrifugal forces
[ETN-90-98253] N90-18695
HEAT TRANSFER COEFFICIENTS
Dryout stability and inception at low flowrates
[DE90-006955] N90-18692
HEATERS
Safety analysis for the Galileo light-weight radioisotope heater unit
[DE90-007147] N90-19009

HEATING
Microconvective heating of granular explosives by a semiconductor bridge
[DE90-005710] N90-18541
Measurement of spectral emissivity by Fourier transform infrared spectrometer
[DE89-782319] N90-18698
HEAVY IONS
Interaction of minor ions with fast and slow shocks
[NASA-CR-186372] N90-19181
HELICOPTER DESIGN
Calculation of flight vibration levels of the AH-1G helicopter and correlation with existing flight vibration measurements
[NASA-CR-181923] N90-18743
Activities report in German aerospace
[ISSN-0070-3966] N90-19189
HELICOPTER ENGINES
Preliminary airworthiness evaluation of the Woodward hydromechanical unit installed on T700-GE-700 engines in the UH-60A helicopter
[AD-A216751] N90-18430
HELICOPTERS
Time and frequency-domain identification and verification of BO-105 dynamic models
[AD-A216828] N90-18389
Life of concentrated contacts in the mixed EHD and boundary film regimes
[AD-A216673] N90-18738
HELIOSEISMOLOGY
Optimization of the reference parameters in the accompanying solar panel dynamics
[INPE-4795-PRE/1449] N90-18798
HELIUM
Helium permeability through austenitic stainless steel
[DE90-007046] N90-18562
Differential elastic scattering cross sections for 54.9eV positrons incident on helium N90-18975
Double ionization of helium by particle impact N90-18979
HELIUM ATOMS
Total cross sections for positrons scattered elastically from helium based on new measurements of total ionization cross sections N90-18976
HELMETS
Evaluation of helmet retention systems using a pendulum device
[AD-A215489] N90-18874
HEMODYNAMIC RESPONSES
A program for the study of skeletal muscle catabolism following physical trauma
[AD-A216569] N90-18859
HERBIG-HARO OBJECTS
Herbig Ae/Be stars: Fine structure far-infrared lines N90-19126
HEURISTIC METHODS
An exact algorithm for the problem of p-medians
[INPE-4924-TDL/384] N90-18885
Optimum and heuristic algorithms for finite state machine decomposition and partitioning
[AD-A216778] N90-18899
HIERARCHIES
An approach centered in production rules for a partition of environment and planning in a visual navigation system (SNV)
[INPE-4813-TDL/360] N90-18737
HIGH ALTITUDE
Improved computational fluid dynamics for continuum hypersonic flow
[AD-A216981] N90-18674
HIGH ENERGY INTERACTIONS
Research on free electron lasers
[AD-A215865] N90-18715
Theoretical and experimental high energy physics
[DE90-006168] N90-19006
HIGH FREQUENCIES
Activities report in DLR research field communication engineering and reconnaissance
[ISSN-0173-0118] N90-18781
HIGH GAIN
Resonator modes in high gain free electron lasers
[DE90-006098] N90-18720
HIGH LEVEL LANGUAGES
A microcode compiler that runs on the IBM AT and supports cascadable microcomputers, part 1
[AD-A215888] N90-18877
L: A language for solution of incremental systems in a parallel processing environment
[INPE-4816-TDL/362] N90-18884
HIGH PRESSURE
Study on the thermodynamical and mechanical conditions for the generation of high operating pressures with liquefied gases for low and very low flow rates
[ESA-TT-1148] N90-18696
Piezoelectric polymer PVDF shock gauge: State of the research art
[ISL-CO-207/89] N90-18705
HIGH RESOLUTION
Classification of high resolution imagery using texture attributes
[INPE-4888-TDL/379] N90-18778
The environment of young stellar objects studied by high-resolution infrared spectroscopy N90-19120
JCMT observations of the circumstellar envelope IRC+10216 N90-19138
HIGH SPEED
High speed imaging with a tapped solid state sensor
[DE90-006116] N90-18702
HIGH STRENGTH
The processing and mechanical properties of high temperature/high performance composites. Book 2, section 2: Strength and fracture resistance
[AD-A216142] N90-18507
The processing and mechanical properties of high temperature/high performance composites. Book 3, section 2: Strength and fracture resistance, part
[AD-A216143] N90-18508
HIGH TEMPERATURE
State of the art and future prospects for high temperature composites N90-18498
Processing and elevated temperature ductility of aluminum alloy 7475
[AD-A216840] N90-18554
Solid-state fluorescence above 1000 C: Application to high-temperature laser thermography
[DE90-006422] N90-18721
HIGH TEMPERATURE PLASMAS
Measurement of the space potential of a high-temperature plasma by fast atomic beam scattering on an ion probe beam
[DE90-006118] N90-19020
HIGH TEMPERATURE SUPERCONDUCTORS
Microwave radiation absorption by Ho(Y)-Ba-Cu-O superconducting ceramics
[DE90-610665] N90-18588
Luminescence from defects and impurity centers in yttrium oxide
[DE90-004842] N90-19030
Understanding electronegative effects in core-level electron spectroscopies; application to the high temperature superconductors
[AD-A216726] N90-19037
What influences order parameters across the superconducting phase boundary
[DE90-610663] N90-19047
Spectral functions from Quantum Monte Carlo
[DE90-004870] N90-19050
HIGH TEMPERATURE TESTS
Biaxial strength and stress rupture of hot-pressed silicon nitride
[AD-A216950] N90-18750
HIGH VOLTAGES
A new broadband pulsed high voltage monitor
[DE90-006264] N90-18651
HOLE BURNING
Temperature dependence of photon-gated persistent spectral hole-burning for the meso-tetra-p-tolyl Zn-tetrabenzoporphyrin/chloroform system in poly(methylmethacrylate)
[AD-A216086] N90-18531
Persistant spectral hole-burning: Photon-gating and fundamental statistical limits
[AD-A216084] N90-18640
Cloud hole-boring with infrared lasers: Theory and experiment
[DE90-006519] N90-18723
HOLOGRAPHY
Inspection of carbon/epoxy and aluminum honeycomb paraboloidal components by HNDT
[AD-A216796] N90-18514
Problems of the micro-holographic image analysis
[ISL-CO-201/89] N90-18704
Computational and visible light experiments for x ray laser holography
[DE90-006774] N90-18707
Cineholography: A relation between the coherence length of the laser and the object velocity
[ISL-CO-234/88] N90-18724
HOT CORROSION
Analysis of propulsive powder combustion products and their corrosive effects
[ISL-CO-248/88] N90-18605
HOT PRESSING
Biaxial strength and stress rupture of hot-pressed silicon nitride
[AD-A216950] N90-18750
HOVERCRAFT GROUND EFFECT MACHINES
Design of a new control system for hovercrafts
[ETN-90-96230] N90-18435
HUMAN BEINGS
Visual processing of object velocity and acceleration
[AD-A216509] N90-18858
The computation of color
[AD-A216531] N90-18914
HUMAN BODY
Measurement of body fat by neutron inelastic scattering: Comments on installation, operation, and error analysis
[DE90-006765] N90-18868
HUMAN FACTORS ENGINEERING
The effects of wearing passenger protective breathing equipment on evacuation times through type 3 and type 4 emergency aircraft exits in clear air and smoke. Phase 1: Evacuations in clear air. Phase 2: Evacuations in smoke
[AD-A216798] N90-18374
Space orientation and orbital technology
[ISBN-3-89100-015-4] N90-18437
Anthropometry of a fit test sample used in evaluating the current and improved MCU-2/P masks
[AD-A215173] N90-18873
Evaluation of helmet retention systems using a pendulum device
[AD-A215489] N90-18874
Human factors issues in aircraft maintenance and inspection
[AD-A215724] N90-18875
Architecture for a human-robot symbiotic system
[DE90-005670] N90-18921
A human factors experimental comparison of two database query languages N90-19084
HURRICANES
Forecasters handbook for Central America and adjacent waters
[AD-A216752] N90-18845
HYDRAULIC EQUIPMENT
Flexible heat pipe cold plate
[AD-A216053] N90-18433
HYDRAULIC TEST TUNNELS
Prediction of rotor blade-vortex interaction noise from 2-D aerodynamic calculations and measurements
[ISL-CO-243/88] N90-18365
HYDROCARBON COMBUSTION
Tropospheric chemistry of natural hydrocarbons and energy-related pollutants: Biosphere/climate feedbacks
[DE90-005643] N90-18820
HYDROCARBONS
Production of high density aviation fuels via novel zeolite catalyst routes
[AD-A216444] N90-18601
Tropospheric chemistry of natural hydrocarbons and energy-related pollutants: Biosphere/climate feedbacks
[DE90-005643] N90-18820
Polycyclic aromatic hydrocarbons in the infrared spectra of IRAS sources N90-19105
Unidentified infrared features in proto-planetary nebulae N90-19130
HYDROCRACKING
Production of high density aviation fuels via novel zeolite catalyst routes
[AD-A216444] N90-18601
HYDRODYNAMICS
Concepts and experiments on space-time chaos
[ETN-90-96255] N90-18683
HYDROGEN
The excitation of molecular hydrogen and its significance N90-19117
High-excitation lines of molecular hydrogen: A discriminant between shock models N90-19118
Molecular hydrogen in the HII region G333.6-0.2 N90-19121
Infrared spectroscopy of star formation in galaxies: Extreme conditions and very short time scales N90-19147
H-alpha emission lines in high redshift quasars N90-19149
HYDROGEN ATOMS
VUV (Vacuum Ultraviolet) laser diagnostics of H(-) ion sources
[DE90-006072] N90-18719
Positron scattering by atomic hydrogen using optical potentials and with positronium formation N90-18966
The calculation of the contributions to low energy e+H2 scattering from sigma u+ and Pion u symmetries using the Kohn variational method N90-18969
Ionisation of atomic hydrogen by positron impact N90-18977
HYDROGEN BONDS
Determination of the minimum energy conformation of alkyl substituted pyrazines
[AD-A216974] N90-18539
HYDROGEN CLOUDS
Planetary nebulae N90-19122
Fluorescent molecular hydrogen emission from star-forming galaxies N90-19155

Near infrared spectroscopy and spectroscopic imaging of NGC253 N90-19159

HYDROGEN EMBRITTLEMENT

Response of unirradiated and neutron-irradiated vanadium alloys to Charpy-impact loading [DE90-004878] N90-18551

HYDROGEN IONS

Positronium formation in e+ plus H- collisions N90-18993

Merged beam studies into the mechanisms of hydrogen molecular ion recombination [AD-A216469] N90-19002

Surface production of ions [AD-A216470] N90-19003

HYDROGEN OXYGEN ENGINES

The Pathfinder chemical transfer propulsion program N90-18471

Advanced APS impacts on vehicle payloads N90-18472

HYDROGEN OXYGEN FUEL CELLS

Integrated regenerative fuel cell experimental evaluation [NASA-CR-185183] N90-18808

HYDROGEN PLASMA

Computerized analysis of hydrogen plasma in a compact H(sup -) cusp source [DE90-006881] N90-19029

HYDROGEN PRODUCTION

Antihydrogen formation in collisions of positronium with antiprotons N90-18988

HYDROGEN RECOMBINATIONS

Predictions of infrared recombinations lines in stellar winds of hot stars N90-19136

Infrared (FeII), H and H2 lines in galaxy nuclei N90-19153

H53-alpha emission from M82 N90-19156

HYDROGEN-BASED ENERGY

On the dynamics of the combustion process of hydrogen-air and hydrogen-methane-air mixtures [DLR-FB-89-39] N90-18548

HYDROGENATION

Hydrogenated amorphous silicon films prepared by glow discharge of disilane [DE90-000309] N90-18581

Morphological consequences of catalytic hydrogenation of polymers in the bulk [DE90-007276] N90-18598

HYDROGEOLOGY

LANDSAT Thematic Mapper for hydrogeological mapping in Egypt [BCRS-89-28] N90-18791

HYDROGRAPHY

Comparison of circulation obtained through the trajectory of a drifting buoy tracked by satellite and hydrographic data in the Bransfield Strait [INPE-4946-TDL/387] N90-18850

HYDROLOGY MODELS

Remote sensing and run-off modelling in the Lake Victoria Basin, Kenya [BCRS-89-19] N90-18785

HYDROMECHANICS

Preliminary airworthiness evaluation of the Woodward hydromechanical unit installed on T700-GE-700 engines in the UH-60A helicopter [AD-A216751] N90-18430

HYDROPONICS

Continuous hydroponic wheat production using a recirculating system [NASA-TM-102784] N90-18853

HYDROSTATIC PRESSURE

Piezoelectric polymer PVDF shock gauge: State of the research art [ISL-CO-207/89] N90-18705

HYPERCUBE MULTIPROCESSORS

Distributed decomposition of block-angular linear programs on a hypercube computer [AD-A216433] N90-18893

HYPERSONIC FLIGHT

Possible piloting techniques at hypersonic speeds [ISL-CO-216/88] N90-18392

HYPERSONIC FLOW

Improved computational fluid dynamics for continuum hypersonic flow [AD-A216981] N90-18674

HYPERSONIC FORCES

Possible piloting techniques at hypersonic speeds [ISL-CO-216/88] N90-18392

HYPERSONICS

Structures and materials technology for hypersonic aerospacecraft [NASA-TM-102583] N90-18752

HYPERVELOCITY IMPACT

Spallation and dynamic fracture as an effect of laser induced shock waves in carbon based composite materials [AD-A216540] N90-18509

HYSTERESIS

Stall and recovery in multistage axial flow compressors N90-18429

I

ICE

Intermittent Solar Ammonia Absorption Cycle (ISAAC) refrigeration for lesser developed countries [DE90-006700] N90-18610

Studies of cubic ice crystals [AD-A216574] N90-18832

Spectroscopy and physico-chemistry of CO:H2O and CO2:H2O ices N90-19111

Ice grains in the dust disk of the bipolar nebula M 1-92 N90-19127

Observations of 40-70 micron bands of ice in IRAS 09371+1212 and other stars N90-19134

ICE FORMATION

The signals of an ice warning device in dependence on total water content and normalized icing degree [DLR-FB-89-52] N90-18377

Studies of cubic ice crystals [AD-A216574] N90-18832

ICE MAPPING

ERS-1 European remote sensing satellite: A new tool for global environmental monitoring in the 1990's [ESA-BR-36] N90-18782

ICE REPORTING

The signals of an ice warning device in dependence on total water content and normalized icing degree [DLR-FB-89-52] N90-18377

IGNITERS

Experimental and theoretical research on the injection of ignition gases into a bed of inert powder [ISL-CO-251/88] N90-18547

IGNITION

Microconvective heating of granular explosives by a semiconductor bridge [DE90-005710] N90-18541

ILLUMINANCE

Three-dimensional motion estimation using shading information in multiple frames [AD-A216804] N90-18919

IMAGE ANALYSIS

Problems of the micro-holographic image analysis [ISL-CO-201/89] N90-18704

Evaluation of TM/LANDSAT and HRV/SPOT data in reforested areas [INPE-4575-RPE/567] N90-18772

Classification of high resolution imagery using texture attributes [INPE-4888-TDL/379] N90-18778

Comparisons between the RTNEPH (Real-Time Nephanalysis) and AFGL cloud layer analysis algorithms [AD-A216637] N90-18844

Application of wavefront analysis techniques to restoring of images degraded by atmospheric turbulence [ONERA-PUBL-1989-1] N90-19168

IMAGE INTENSIFIERS

Optical amplification in 45 deg - cut BaTiO3 [AD-A216043] N90-19011

IMAGE PROCESSING

High speed imaging with a tapped solid state sensor [DE90-006116] N90-18702

Problems of the micro-holographic image analysis [ISL-CO-201/89] N90-18704

Geometric correction models for HRV-SPOT images [INPE-5001-TDL/395] N90-18757

Orbital remote sensing in the decade of the nineties: New approaches and challenges in geology [INPE-4838-PRE/1467] N90-18758

Evaluation of selection techniques for multispectral bands employed in the discrimination of carbonatic rocks [INPE-4850-TDL/385] N90-18765

Evaluation of TM/LANDSAT and HRV/SPOT data in reforested areas [INPE-4575-RPE/567] N90-18772

Remote sensing for the classification and quantification of vegetation in Spring staging areas of Brent geese on the Frisian Islands (Netherlands) [BCRS-89-27] N90-18790

Temporal response of atmospheric turbulence compensation [DE90-006354] N90-18837

Visual processing of object velocity and acceleration [AD-A216509] N90-18858

Recognizing three-dimensional objects without the use of models [AD-A216766] N90-18862

Techniques for measurement of the optical properties of materials [DE90-006902] N90-19014

IMAGE RECONSTRUCTION

Problems of the micro-holographic image analysis [ISL-CO-201/89] N90-18704

Application of wavefront analysis techniques to restoring of images degraded by atmospheric turbulence [ONERA-PUBL-1989-1] N90-19168

IMAGE RESOLUTION

Problems of the micro-holographic image analysis [ISL-CO-201/89] N90-18704

Optical amplification in 45 deg - cut BaTiO3 [AD-A216043] N90-19011

IMAGE TUBES

A large area, low cost, gamma-ray, imaging spectrometer [DE90-006993] N90-19017

IMAGERY

Fracture analysis through photographic imagery of low spatial resolution: A contribution to the study of tectonic evoluation of the Araripe Plateau region [INPE-4876-PRE/1487] N90-18756

IMAGING SPECTROMETERS

A large area, low cost, gamma-ray, imaging spectrometer [DE90-006993] N90-19017

IMAGING TECHNIQUES

High speed imaging with a tapped solid state sensor [DE90-006116] N90-18702

Interrelationship of spatial and radiometric resolution in the thermal infrared band [INPE-4860-TDL/371] N90-18771

IMPACT DAMAGE

Instrumented impact testing of fabric-reinforced composite materials [AD-A216764] N90-18513

Fundamental aspects of erosion and impact damage [DE90-006640] N90-18587

Effects of oblique impact on hypervelocity shield performance [DE90-006936] N90-18739

IMPACT RESISTANCE

Bird impact tests on a Kevlar 49 structure. Monolithic plates. Oblique-angled impact [REPT-S3-4273] N90-18376

IMPACT TESTS

Bird impact tests on a Kevlar 49 structure. Monolithic plates. Oblique-angled impact [REPT-S3-4273] N90-18376

Instrumented impact testing of fabric-reinforced composite materials [AD-A216764] N90-18513

IMPLANTATION

Luminescence of lanthanides and actinides implanted into binary III-V semiconductors and AlGaAs [AD-A215759] N90-19031

IMPURITIES

Luminescence from defects and impurity centers in yttrium oxide [DE90-004842] N90-19030

INCIDENCE

Semidiscrete Galerkin modelling of compressible viscous flow past a circular cone at incidence [NASA-CR-186323] N90-18664

INCLUSIONS

Variations in volatiles in magma bodies based on studies of melt inclusions [DE90-006272] N90-18821

INCOHERENT SCATTER RADAR

Doppler spectra from incoherent backscatter: Principles and examples for application for POLDIRAD [DLR-FB-89-48] N90-18630

INCOHERENT SCATTERING

Doppler spectra from incoherent backscatter: Principles and examples for application for POLDIRAD [DLR-FB-89-48] N90-18630

INCOMPRESSIBLE FLOW

Numerical simulation of the incompressible inhomogeneous turbulence in a plane channel flow [ONERA-NT-1988-5] N90-18688

Numerical simulation of the vortex breakdown [ONERA-RSF-4/4368-AY-004A] N90-18689

Modeling convective Marangoni flows with void movement in the presence of solid-liquid phase change [DE90-006474] N90-18690

INDUSTRIAL MANAGEMENT

Internal technology transfer N90-19080

INELASTIC COLLISIONS

Inelastic collisions of positrons with one-valence-electron targets N90-18963

INELASTIC SCATTERING

Measurement of body fat by neutron inelastic scattering: Comments on installation, operation, and error analysis [DE90-006765] N90-18668

Inelastic scattering of positrons with sodium N90-18961

Theoretical survey on positronium formation and ionisation in positron atom scattering N90-18965

Positron scattering by atomic hydrogen using optical potentials and with positronium formation N90-18966

INERTIAL CONFINEMENT FUSION
Development of KrF lasers for fusion [DE90-007830] N90-18726

INERTIAL FUSION (REACTOR)
Development of KrF lasers for fusion [DE90-007830] N90-18726

INFERENCE
A theory of quantitative inference for artifact sets applied to a mechanical design compiler [AD-A216535] N90-18896

INFORMATION MANAGEMENT
Integrated IMA (Information Mission Areas) IC (Information Center) guide [AD-A216944] N90-18903

INFORMATION RETRIEVAL
A human factors experimental comparison of two database query languages N90-19064

INFORMATION SYSTEMS
Development of the agricultural information system. Characteristics and results of the Distrito Federal model [INPE-4940-PRE/1430] N90-18773
Paper on geography in environmental management: Research and new techniques [INPE-4840-PRE/1469] N90-18816
DoD manual for standard data elements [AD-A216441] N90-19066

INFORMATION TRANSFER
An adaptive ARQ (Automatic Repeat Request) strategy for packet switching data communication networks [AD-A216597] N90-18615

INFRARED ABSORPTION
Infrared diagnostics for interstellar solid state chemistry N90-19103

INFRARED ASTRONOMY
Infrared Spectroscopy in Astronomy [ESA-SP-290] N90-19084
Interstellar extinction in the infrared N90-19095
Infrared diagnostics for interstellar solid state chemistry N90-19103
Molecular hydrogen in the HII region G333.6-0.2 N90-19121
Infrared spectroscopy of novae and related objects N90-19123
Infrared spectroscopy of supernova 1987A N90-19124
High resolution infrared spectroscopy of symbiotic stars N90-19125
Ice grains in the dust disk of the bipolar nebula M 1-92 N90-19127
Dust in planetary nebulae: IRSPEC observations in the 3.0 micron-3.8 micron range N90-19132
JCMT observations of the circumstellar envelope IRC+10216 N90-19138

INFRARED ASTRONOMY SATELLITE
Polycyclic aromatic hydrocarbons in the infrared spectra of IRAS sources N90-19105
IRAS LRS spectra of extended objects: The Crab nebula N90-19107

INFRARED DETECTORS
Performance parameter characterisation of various types of IR single element detectors N90-19161

INFRARED IMAGERY
Infrared spectroscopy and imaging of supernova remnants N90-19104
IRCAM observations of the Reipurth 50 IR source N90-19119
An infrared imaging Fabry-Perot study of the galactic centre N90-19142

INFRARED INSTRUMENTS
IRCAM observations of the Reipurth 50 IR source N90-19119

INFRARED INTERFEROMETERS
An infrared imaging Fabry-Perot study of the galactic centre N90-19142

INFRARED LASERS
Cloud hole-boring with infrared lasers: Theory and experiment [DE90-006519] N90-18723

INFRARED PHOTOMETRY
Photometry of variable AFGL sources [AD-A216938] N90-19185

INFRARED RADIATION
Interrelationship of spatial and radiometric resolution in the thermal infrared band [INPE-4860-TDL/371] N90-18771
Proceedings of the 6th Conference on Hot Carriers in Semiconductors [AD-A215978] N90-19032
An advanced cooled grating spectrometer for UKIRT-CGS4 N90-19165
Photometry of variable AFGL sources [AD-A216938] N90-19185

INFRARED SOURCES (ASTRONOMY)
Photometry of variable AFGL sources [AD-A216938] N90-19185

INFRARED SPACE OBSERVATORY (ISO)
Infrared diagnostics for interstellar solid state chemistry N90-19103
The ISO short wavelength spectrometer N90-19162
The Infrared Space Observatory N90-19163
Spectrophotometry of dust with Isophot N90-19164
Isophot-S, a low resolution 2.5 to 12 microns spectrometer for ISO N90-19167

INFRARED SPECTRA
The 2.7/4.3 micron CO2 branching ratio measurement [AD-A215952] N90-18830
Techniques for measurement of the optical properties of materials [DE90-006902] N90-19014
A unified model for the 3.28 micron and 3.4 micron spectral feature in the interstellar medium and in comets N90-19092
Interpretation of the 10 micron and 20 micron absorption bands in comets, the interstellar medium, and in an external galaxy N90-19093
Interstellar extinction in the infrared N90-19095
Spectropolarimetry as a diagnostic of the interstellar medium N90-19096
Airborne observations of the infrared emission bands N90-19101
Polycyclic aromatic hydrocarbons in the infrared spectra of IRAS sources N90-19105
IRAS LRS spectra of extended objects: The Crab nebula N90-19107
Wide-beam balloon observations of the 157.7 microns (CII) line N90-19108
A coal model for the carriers of the unidentified IR bands N90-19110
Spectroscopy and physico-chemistry of CO:H2O and CO2:H2O ices N90-19111
Mapping and spectroscopy of the 3.3 microns feature in Orion N90-19112
An implication of the IR identification of PAHs: The heating of the diffuse IS gas N90-19113
The infrared spectral signature of star formation N90-19114
Infrared diagnostics of interstellar shocks N90-19115
Infrared line emission from high-velocity outflows in star-forming regions N90-19116
The excitation of molecular hydrogen and its significance N90-19117
High-excitation lines of molecular hydrogen: A discriminant between shock models N90-19118
Ice grains in the dust disk of the bipolar nebula M 1-92 N90-19127
IR spectrophotometry of bright carbon stars N90-19131
Carbon monoxide in supernova 1987A N90-19135
Predictions of infrared recombinations lines in stellar winds of hot stars N90-19136
Infrared lines as probes of galactic structure N90-19139
Evolutionary synthesis of the far-infrared emission in starburst galaxies N90-19152
Infrared properties of five spiral galaxies N90-19154
Far infrared fine structure lines in active galaxies N90-19157

INFRARED SPECTROMETERS
Evaluation of a commercial gas chromatography/matrix isolation-infrared spectrometer for quantitative analysis of priority pollutants [DE90-006033] N90-18542
Measurement of spectral emissivity by Fourier transform infrared spectrometer [DE89-782319] N90-18698
The ISO short wavelength spectrometer N90-19162
The Infrared Space Observatory N90-19163
An advanced cooled grating spectrometer for UKIRT-CGS4 N90-19165
Isophot-S, a low resolution 2.5 to 12 microns spectrometer for ISO N90-19167

INFRARED SPECTROSCOPY
Infrared Spectroscopy in Astronomy [ESA-SP-290] N90-19084
IR spectroscopy of planets and satellites; Venus, Mars, giant planets, and Titan N90-19085
Infrared cometary spectroscopy N90-19086
Measurements of the D/H ratio in planetary atmospheres by ground based infrared spectroscopy N90-19088
The unidentified IR bands in laboratory, in interstellar medium, and in comets N90-19089
Observations of CO on Mars in the infrared and millimetre range N90-19090
Near infrared spectroscopy of Mars: Study of the surface mineralogy N90-19091
A unified model for the 3.28 micron and 3.4 micron spectral feature in the interstellar medium and in comets N90-19092
Infrared spectroscopy of dust N90-19094
Chemistry on interstellar grains and implications for infrared spectroscopy N90-19097
Dust continuum spectra from model HII regions N90-19099
IR line emission from dense photodissociation regions N90-19100
IR line emission from supernovae in molecular clouds N90-19102
Infrared spectroscopy and imaging of supernova remnants N90-19104
An almost total disjunction between emission and absorption dust features: What does it tell us? N90-19106
Near infrared spectroscopy of the supernova remnant RCW103 N90-19109
Infrared line emission from high-velocity outflows in star-forming regions N90-19116
The environment of young stellar objects studied by high-resolution infrared spectroscopy N90-19120
Molecular hydrogen in the HII region G333.6-0.2 N90-19121
Planetary nebulae N90-19122
Infrared spectroscopy of novae and related objects N90-19123
Infrared spectroscopy of supernova 1987A N90-19124
High resolution infrared spectroscopy of symbiotic stars N90-19125
CO infrared bands in atmospheres of long-period variables N90-19128
A survey of PAH emission in HII regions, planetary and proto-planetary nebulae N90-19129
Unidentified infrared features in proto-planetary nebulae N90-19130
Dust in planetary nebulae: IRSPEC observations in the 3.0 micron-3.8 micron range N90-19132
Near infrared (1-4 micron) spectroscopy of SN1987A N90-19133
Infrared spectroscopy of the central few parsecs of the galaxy N90-19140
Stellar kinematics in the galactic centre N90-19141
Near infrared spectroscopy of active galaxies N90-19143
Near-infrared spectroscopy of starburst and interacting galaxies N90-19144
Spectroscopy of galaxies in the mid-infrared N90-19145
Far-infrared spectroscopy of galaxies N90-19146
Infrared spectroscopy of star formation in galaxies: Extreme conditions and very short time scales N90-19147
A search for the CO feature in active galactic nuclei N90-19151
Infrared (FeII), H and H2 lines in galaxy nuclei N90-19153
Near infrared spectroscopy and spectroscopic imaging of NGC253 N90-19159

INFRARED TELESCOPES
The Infrared Space Observatory N90-19163
Spectrophotometry of dust with Isophot N90-19164
An advanced cooled grating spectrometer for UKIRT-CGS4 N90-19165

INGESTION (ENGINES)
Study of bird ingestions into small inlet area, aircraft turbine engines (May 1987 to April 1988) [DOT/FAA/CT-89/17] N90-18375

INJECTION
Development of an rf-driven plasma neutralizer for negative ions [DE90-007298] N90-19027

INLET FLOW
Research on a two-dimensional inlet for a supersonic V/STOL propulsion system. Appendix A [NASA-CR-174945] N90-18364

INORGANIC COATINGS
Laboratory for the processing and evaluation of inorganic matrix composites [AD-A216881] N90-18516

INPUT
Three input concepts for flight crew interaction with information presented on a large-screen electronic cockpit display [NASA-TM-4173] N90-18394

INSECTS
Visual processing of object velocity and acceleration [AD-A216509] N90-18858

INSPECTION
Human factors issues in aircraft maintenance and inspection [AD-A215724] N90-18875

INSULATION
The 1989 JANNAF Propulsion Meeting, volume 1
[CPIA-PUBL-515-VOL-1] N90-18462
Technique for evaluating the erosive properties of ablative internal insulation materials N90-18466
INTEGERS
An exact algorithm for the problem of p-medians
[INPE-4924-TDL/384] N90-18885
INTEGRAL TRANSFORMATIONS
Mathematical methods of Physics 6: Integral transformation
[INPE-4807-MD/40] N90-18926
INTEGRATED CIRCUITS
Reconfigurable antennas, monolithic microwave integrated circuits with feeding networks for microstrip antennas
[AD-A216916] N90-18622
DANCIR (device and circuit simulator): A three dimensional steady-state semiconductor device simulator
[DE90-006370] N90-18658
INTERACTING GALAXIES
Near-infrared spectroscopy of starburst and interacting galaxies N90-19144
The strengths of the 2.3 micron CO band in luminous interacting and merging galaxies N90-19148
INTERCALATION
Cell performance of ultra-thin polymer cathode systems. Part 1: Anion intercalating polymer cathode
[AD-A216037] N90-18639
INTERFACES
Design, implementation and test of an RS-232 compatible bi-directional, full duplex, fiber-optic interface with provision for hardware handshaking on a minimum of fiber-optic lines
[AD-A216604] N90-19012
INTERFERENCE IMMUNITY
Radio interference in the near-earth environment
[NASA-CR-180479] N90-18623
INTERFEROMETERS
Development and test of power amplifiers for the driving of low-voltage piezo-actuators in multistable interferometers
[DLR-MITT-89-19] N90-18662
INTERGALACTIC MEDIA
Interpretation of the 10 micron and 20 micron absorption bands in comets, the interstellar medium, and in an external galaxy N90-19093
INTERIOR BALLISTICS
Measurement of gas leaks between a projectile and the walls of a tube in a ballistic compressor
[ISL-CO-250/88] N90-18694
INTERMETALLICS
The processing and mechanical properties of high temperature/high performance composites. Book 3, section 2: Strength and fracture resistance, part
[AD-A216143] N90-18508
Deformation and fracture of ordered intermetallic compounds
[DE90-007422] N90-18563
INTERNAL COMBUSTION ENGINES
Federal methanol fleet update
[DE90-006851] N90-18741
INTERNATIONAL COOPERATION
Long term planning for space flight activities within the DFVLR
[DFVLR-IB-303-88/2] N90-18438
ESA project to promote and assist technology transfer by industry N90-19069
INTERPLANETARY DUST
Analogies between cometary, interplanetary, and interstellar matter N90-19087
Infrared spectroscopy of dust N90-19094
Interstellar extinction in the infrared N90-19095
Spectropolarimetry as a diagnostic of the interstellar medium N90-19096
Dust continuum spectra from model HII regions N90-19099
Infrared diagnostics for interstellar solid state chemistry N90-19103
An almost total disjunction between emission and absorption dust features: What does it tell us? N90-19106
Planetary nebulae N90-19122
Ice grains in the dust disk of the bipolar nebula M 1-92 N90-19127
Dust in planetary nebulae: IRSPEC observations in the 3.0 micron-3.8 micron range N90-19132
INTERPLANETARY SPACE
Zodiacal dust bands: Their relation to asteroid families
[AD-A216025] N90-19170
INTERPOLATION
Inverse scattering and tomography
[AD-A216456] N90-18932
INTERSTELLAR EXTINCTION
Interstellar extinction in the infrared N90-19095
INTERSTELLAR GAS
Infrared diagnostics of interstellar shocks N90-19115
The excitation of molecular hydrogen and its significance N90-19117
INTERSTELLAR MATTER
Analogies between cometary, interplanetary, and interstellar matter N90-19087
The unidentified IR bands in laboratory, in interstellar medium, and in comets N90-19089
A unified model for the 3.28 micron and 3.4 micron spectral feature in the interstellar medium and in comets N90-19092
Interpretation of the 10 micron and 20 micron absorption bands in comets, the interstellar medium, and in an external galaxy N90-19093
Spectropolarimetry as a diagnostic of the interstellar medium N90-19096
Chemistry on interstellar grains and implications for infrared spectroscopy N90-19097
A coal model for the carriers of the unidentified IR bands N90-19110
An implication of the IR identification of PAHs: The heating of the diffuse IS gas N90-19113
Hydrodynamical simulations of collisions between interstellar clouds
[DE90-006921] N90-19172
INVERSE SCATTERING
Direct and inverse scattering problem associated with the elliptic Sinh-Gordon equation
[AD-A216455] N90-18931
Inverse scattering and tomography
[AD-A216456] N90-18932
INVERSIONS
An application of ocean wave-current refraction to the gulf stream using SEASAT SAR data
[AD-A216769] N90-18851
INVISCID FLOW
The inviscid stability of supersonic flow past a sharp cone
[NASA-CR-181996] N90-18363
Calculation of the unsteady two-dimensional, inviscid, compressible flow around a strongly cambered oscillating single blade N90-18409
ION BEAMS
Microstructural variations in aluminum oxide coatings deposited using a dual beam ion system
[DE90-006040] N90-18583
Merged beam studies into the mechanisms of hydrogen molecular ion recombination
[AD-A216469] N90-19002
Development of an rf-driven plasma neutralizer for negative ions
[DE90-007298] N90-19027
ION EMISSION
Surface production of ions
[AD-A216470] N90-19003
ION EXCHANGING
Electronic and ionic transport in polymers
[AD-A217028] N90-18579
ION IMPACT
Multiple-ionization of xenon atoms by positron impact N90-18978
Surface production of ions
[AD-A216470] N90-19003
ION IMPLANTATION
Ion implantation-induced amorphization of ceramic oxides
[DE90-006564] N90-19041
Dopant site location in dual-implanted GaP using (111) planar channeling
[DE90-006565] N90-19042
ION PROBES
Measurement of the space potential of a high-temperature plasma by fast atomic beam scattering on an ion probe beam
[DE90-006118] N90-19020
ION PRODUCTION RATES
Positron-molecule bound states and positive ion production N90-18994
Initial results of positron ionization mass spectrometry N90-18995
ION PROPULSION
Performance of large area xenon ion thrusters for orbit transfer missions N90-18475
Mission options for an electric propulsion demonstration flight test N90-18479
Viability study of ionic microthruster tests on MECB satellite
[INPE-4973-RPE/605] N90-18490
ION RECOMBINATION
Merged beam studies into the mechanisms of hydrogen molecular ion recombination
[AD-A216469] N90-19002
ION SOURCES
VUV (Vacuum Ultraviolet) laser diagnostics of H(-) ion sources
[DE90-006072] N90-18719
Surface production of ions
[AD-A216470] N90-19003
Computerized analysis of hydrogen plasma in a compact H(sup -) cusp source
[DE90-006881] N90-19029
ION TEMPERATURE
Interaction of minor ions with fast and slow shocks
[NASA-CR-186372] N90-19181
IONIC DIFFUSION
The rapid inward diffusion of cold ions in tokamaks and their effect on ion transport
[DE90-006863] N90-19022
IONIZATION
Research on sliding spark preionization in a TEA CO2 laser
[ISL-R-113/88] N90-18732
Proceedings of the 6th Conference on Hot Carriers in Semiconductors
[AD-A215978] N90-19032
IONIZATION CROSS SECTIONS
Lower limits on the absolute dissociative electron attachment cross section from O2 condensed on rare-gas films
[AD-A216727] N90-18536
Theoretical survey on positronium formation and ionisation in positron atom scattering N90-18965
Total cross sections for positrons scattered elastically from helium based on new measurements of total ionization cross sections N90-18976
Ionisation of atomic hydrogen by positron impact N90-18977
Multiple-ionization of xenon atoms by positron impact N90-18978
Double ionization of helium by particle impact N90-18979
Absolute cross-sections for dissociative electron attachment in O2 condensed on Kr films
[AD-A216730] N90-19038
An implication of the IR identification of PAHs: The heating of the diffuse IS gas N90-19113
Current and future uses of accelerators in particle astrophysics
[DE90-006667] N90-19186
IONIZATION GAGES
Construction and calibration of a gas pressure meter with high temporal resolution
[INPE-4953-RPE/602] N90-18700
IONIZATION POTENTIALS
Positron scattering by atomic hydrogen using optical potentials and with positronium formation N90-18966
New parameter-free polarization potentials in low-energy positron collisions N90-18968
IONOSPHERIC DISTURBANCES
ACIRF user's guide: Theory and examples
[AD-A216436] N90-18613
IONOSPHERIC PROPAGATION
Effects of strong scattering on transionospheric propagation
[AD-A216706] N90-18617
IONS
Electronic and ionic transport in polymers
[AD-A217028] N90-18579
Interaction of minor ions with fast and slow shocks
[NASA-CR-186372] N90-19181
IRON
Infrared (FeII), H and H2 lines in galaxy nuclei N90-19153
Near infrared spectroscopy and spectroscopic imaging of NGC253 N90-19159
IRON ALLOYS
Corrosion fatigue of iron-chromium-nickel alloys: Fracture mechanics and chemistry
[DE90-006318] N90-18556
Identification of a cast iron alloy containing nonstrategic elements
[NASA-CR-185174] N90-18559
IRON COMPOUNDS
Metallaboranes as precursors to metallic glasses
[AD-A216946] N90-18577
IRRADIANCE
Measurement system of spectral irradiance in the near infrared N90-19160
IRRADIATION
Nonlinear optical processes in one-dimensional polymers
[AD-A216103] N90-18568
Polymerization of nitro compounds on silver surfaces during surface-enhanced Raman scattering
[AD-A216116] N90-18569
ISOTOPE SEPARATION
Helium permeability through austenitic stainless steel
[DE90-007046] N90-18582

ISOTOPES
Safety analysis for the Galileo light-weight radioisotope heater unit
[DE90-007147] N90-19009
ISOTOPIC SPIN
Theoretical studies in nuclear physics
[DE90-005981] N90-19005
ISOTROPIC MEDIA
Defects: Their behaviour and related design assumptions N90-18397
ISOTROPY
An objective time-integration procedure for isotropic rate-independent and rate-dependent elastic-plastic constitutive equations
[PB90-121245] N90-18925
ITERATION
Optimum and heuristic algorithms for finite state machine decomposition and partitioning
[AD-A216778] N90-18899
ITERATIVE SOLUTION
KAM: Automatic planning and interpretation of numerical experiments using geometrical methods
[AD-A216805] N90-18900
Waveform methods for ordinary differential equations
[DE90-006593] N90-18943

J

JAPAN
Optimal planning method of underground distribution system, part 2. Application to various types of system configurations
[DE89-782323] N90-18636
Energy markets in the 1990's and beyond: A comparison of energy intensity in the United States and Japan
[DE90-005535] N90-18797
JET AIRCRAFT NOISE
Noise levels from a VSTOL aircraft measured at ground level and at 1.2 m above the ground
[NPL-RSA(EXT)-009] N90-18999
JET FLOW
Numerical simulations of coherent structures in a jet flame with a noncircular cross section
[AD-A216710] N90-18535
JET MIXING FLOW
An investigation of flow structure, mixing and chemical reaction in combusting turbulent flows
[AD-A216739] N90-18538
JOINTS (JUNCTIONS)
Test data of flow field of shuttle SRM nozzle joint with bond defects, using unheated air N90-18464
Threaded joint design for composites
[DE90-005553] N90-18506
Preliminary evaluation of the strength of pin-joints in laminated composite materials
[DE90-006353] N90-18524
A global approach for the identification of structural connection properties
[NASA-TM-102502] N90-18745
A study of the vibrational transmission through flanged joints
[ISVR-TR-181] N90-18755
JUDGMENTS
Systematicity as a selection constraint in analogical mapping
[AD-A216029] N90-18869
JUPITER (PLANET)
Technology update-89
[DE90-005813] N90-19178

K

KALMAN FILTERS
An error sensitivity model for Doppler positioning using transit satellites
[AD-A216724] N90-18381
Orbit determination of artificial Earth satellites through estmation techniques combined with state smoothing techniques
[INPE-4959-TDL/388] N90-18440
KENYA
Remote sensing and run-off modelling in the Lake Victoria Basin, Kenya
[BCRS-89-19] N90-18788
KERNEL FUNCTIONS
Temporal response of atmospheric turbulence compensation
[DE90-006354] N90-18837
KEVLAR (TRADEMARK)
Bird impact tests on a Kevlar 49 structure. Monolithic plates. Oblique-angled impact
[REPT-S3-4273] N90-18376
KINEMATICS
On the kinematic behavior of robots while executing general robot level commands
[PB90-120965] N90-18735
Preliminary design of a pointer for movement of a solar simulator
[INPE-4864-TDL/375] N90-18736
KINETIC ENERGY
Anitproton-matter interactions in antiproton applications N90-18989
KINETIC THEORY
Kinetic relations and the propagation of phase boundaries in solids
[AD-A215881] N90-18747
KINETICS
Electrochemical investigations of novel solid redox polymerization electrodes
[DE90-006087] N90-18584
A numerical solution to the Boltzmann equation for use in calculating pumping rates in a CO2 discharge laser
[AD-A216376] N90-18718
KNOWLEDGE
The formation and use of knowledge structures in problem solving domains
[AD-A216512] N90-18936
KNOWLEDGE BASES (ARTIFICIAL INTELLIGENCE)
Knowledge-based fault detection and analysis for robots: First results for the ROTEX robots
[ESA-TT-1150] N90-18742
User manual for NEXT 1.2: NLR engineering X-pert system toolkit
[NLR-TR-87178-U] N90-18905
KRYPTON
Lower limits on the absolute dissociative electron attachment cross section from O2 condensed on rare-gas films
[AD-A216727] N90-18536
Absolute cross-sections for dissociative electron attachment in O2 condensed on Kr films
[AD-A216730] N90-19038
KRYPTON FLUORIDE LASERS
Development of KrF lasers for fusion
[DE90-007830] N90-18726

L

LABORATORIES
Space-based radar simulation laboratory
[AD-A216722] N90-18618
LAKES
Remote sensing and run-off modelling in the Lake Victoria Basin, Kenya
[BCRS-89-19] N90-18788
LAMB WAVES
The propagation of time harmonic Rayleigh-Lamb waves in a bimaterial plate
[AD-A216834] N90-18749
LAMINAR FLOW
Numerical investigations of heat transfer and flow rates in rotating cavities. Simulation of the movement generated by wall temperature gradients, by source-sink mass flows or by the differential rotation of the walls, under the influence or coriolis and centrifugal forces
[ETN-90-96253] N90-18695
LAMINAR HEAT TRANSFER
Study of vortex arrays induced artificially and from centrifugal instabilities
[AD-A216499] N90-18669
Dryout stability and inception at low flowrates
[DE90-006955] N90-18692
LAMINATES
Measuring strain in carbon fibre composite laminates using the Raman optomechanical strain gauge N90-18503
Compressive strength of carbon/epoxy laminated under multiaxial stress
[DE90-005552] N90-18505
Threaded joint design for composites
[DE90-005553] N90-18506
Damage assessment in composites by acousto-ultrasonic technique
[AD-A216590] N90-18510
Theory and verification of the fiber composite damage model implemented in DYNA3D
[AD-A216800] N90-18511
Instrumented impact testing of fabric-reinforced composite materials
[AD-A216764] N90-18513
Development of a progressive failure model for strength of laminated composite structure
[AD-A216966] N90-18517
A statistical evaluation of the variation in laminated composite properties resulting from ply misalignment
[DE90-006371] N90-18525
LAND USE
Land suitability maps and appropriate land use: An approach using SGI and satellite imagery
[INPE-4827-PRE/1458] N90-18781
Development of the agricultural information system. Characteristics and results of the Distrito Federal model
[INPE-4940-PRE/1430] N90-18773
Improvement of classification results from satellite imagery to update and differentiate land use classes on topographic maps
[BCRS-89-17] N90-18786
Photointerpretation with instruments for evaluation of environmental impact: Mata Atlantica in Cubata
[INPE-4910-PRE/1511] N90-18817
LANDFORMS
Quantification of structural field data in the Rio Grande do Norte basin and neighborhood
[INPE-4821-RPE/591] N90-18826
LARGE DEPLOYABLE REFLECTOR
Support trusses for large precision segmented reflectors: Preliminary design and analysis
[NASA-TM-101560] N90-18453
LASER ANEMOMETERS
Experimental investigations of the unsteady boundary layer on an oscillating flat plate. Optimization and validation of a code, for calculating the potential flow/boundary layer coupling of a flat plate and of an oscillating profile
[ETN-90-96254] N90-18682
LASER APPLICATIONS
Technology development and circuit design for a parallel laser programmable floating point application specific processor
[AD-A215870] N90-18637
Performance of a 500 watt Nd:GGG zigzag slab oscillator
[DE90-006263] N90-18657
Solid-state fluorescence above 1000 C: Application to high-temperature laser thermography
[DE90-006422] N90-18721
Fast algorithms for calculating laser wavefront phase compensation given noisy measurements of phase gradient
[DE90-006357] N90-18727
Stark and Zeeman effects on laser cooling of positronium N90-18986
LASER BEAMS
Temperature dependence of photon-gated persistent spectral hole-burning for the meso-tetra-p-tolyl Zn-tetrabenzoporphyrin/chloroform system in poly(methylmethacrylate)
[AD-A216086] N90-18531
Nonlinear optical processes in one-dimensional polymers
[AD-A216103] N90-18568
Theory for high gain, high power free electron lasers
[DE90-005546] N90-18714
Ultrafast chemical dynamics of reactions in beams
[AD-A216319] N90-18717
A study of the interaction of light with surfaces of sub-micron dimensions
[DE90-006646] N90-19046
LASER DAMAGE
Spallation and dynamic fracture as an effect of laser induced shock waves in carbon based composite materials
[AD-A216540] N90-18509
LASER DOPPLER VELOCIMETERS
Automation and extension of LDV (Laser-Doppler Velocimetry) measurements of off-design flow in a subsonic cascade wind tunnel
[AD-A216627] N90-18670
Measurement of gas intensity at high dynamic pressures
[ISL-CO-204/89] N90-18680
LASER FUSION
Development of KrF lasers for fusion
[DE90-007830] N90-18726
LASER INDUCED FLUORESCENCE
An investigation of flow structure, mixing and chemical reaction in combusting turbulent flows
[AD-A216739] N90-18538
Fluorescence and elastic scattering from laser dye-filled capillaries
[AD-A217026] N90-18540
LASER MATERIALS
Spallation and dynamic fracture as an effect of laser induced shock waves in carbon based composite materials
[AD-A216540] N90-18509
Properties and performance of the LiCaAlF6:Cr(3+) laser material
[DE90-007242] N90-18728
LASER OUTPUTS
A numerical solution to the Boltzmann equation for use in calculating pumping rates in a CO2 discharge laser
[AD-A216376] N90-18718

Study of discharge mechanisms and the stability of transverse electric discharges in the gas mixtures
[ISL-R-114/88] N90-18733
LASER SPECTROMETERS
Fluorescence and elastic scattering from laser dye-filled capillaries
[AD-A217026] N90-18540
LASER SPECTROSCOPY
Determination of the minimum energy conformation of alkyl substituted pyrazines
[AD-A216974] N90-18539
Persistant spectral hole-burning: Photon-gating and fundamental statistical limits
[AD-A216084] N90-18640
Ultrasensitive laser spectroscopy in solids: Single-molecule detection
[AD-A216085] N90-18716
VUV (Vacuum Ultraviolot) laser diagnostics of H(-) ion sources
[DE90-006072] N90-18719
LASER STABILITY
Effect of a random wind field on thermal blooming instabilities
[DE90-007241] N90-18823
LASER TARGET INTERACTIONS
Effects produced by pulsed CO2 lasers
[ISL-R-112/88] N90-18731
LASERS
Performance and modeling of superconducting ring resonators at millimeter-wave frequencies
[NASA-TM-102526] N90-18634
LATE STARS
CO infrared bands in atmospheres of long-period variables N90-19128
Stellar kinematics in the galactic centre N90-19141
LATTICE VIBRATIONS
Strongly coupled one-dimensional system and the polymer
[AD-A216330] N90-18571
Structure and vibrational excitations of reconstructed semiconductor surfaces
[DE90-006589] N90-19044
LAW (JURISPRUDENCE)
Introductory remarks for the panel discussions on technology transfer N90-19075
Problems on transfer of space technology to non-space areas and solutions: Legal aspects N90-19077
LEAD (METAL)
Fundamental studies of surface processes and trace analysis using solid electrodes
[AD-A216538] N90-18533
LEADING EDGES
Unsteady viscous calculation method for cascades with leading edge induced separation N90-18406
LEAKAGE
Space shuttle RCS oxidizer leak repair for STS-26 N90-18485
Superfluid helium orbital resupply coupling N90-18488
LEARNING
Teaching a new methodology for designing relational data bases: An experiment testing the effectiveness of an intelligent tutoring system on cognitive skill acquisition (volumes 1 and 2) N90-19063
LEAST SQUARES METHOD
Strong source heat transfer simulations based on a GalerKin/gradient least squares method
[DE90-008613] N90-18678
LEGUMINOUS PLANTS
Radiometric study of wheat and bean crops in three types of latossolo
[INPE-4843-PRE/1472] N90-18767
LIAPUNOV FUNCTIONS
Contribution to the study of stability robustness of nonlinear multivariable regulators
[INPE-4801-TDL/356] N90-18950
LICENSING
Methodology panel N90-19076
LIE GROUPS
New aspects in bifurcation with symmetry
[AD-A216506] N90-18935
LIFE (DURABILITY)
AGARD/SMP Review: Damage Tolerance for Engine Structures. 2: Defects and Quantitative Materials Behaviour — conference
[AGARD-R-769] N90-18396
Review of modelling methods to take account of material structure and defects N90-18402
Life of concentrated contacts in the mixed EHD and boundary film regimes
[AD-A216673] N90-18738
LIFT
Using the method of matched asymptotic expansions, analytically investigate the three-dimensional, atmosphere entry problem
[AD-A216287] N90-18451
LIGANDS
Perfluorinated ligands in organometallic chemistry
[AD-A216415] N90-18493
LIGHT (VISIBLE RADIATION)
Investigation of multiple scattering in aqueous suspensions of non-absorbing polystrene microspheres using spectrophotometry
[BCRS-89-09] N90-18549
LIGHT SCATTERING
Fluorescence and elastic scattering from laser dye-filled capillaries
[AD-A217026] N90-18540
Optical amplification in 45 deg - cut BaTiO3
[AD-A216043] N90-19011
LIKELIHOOD RATIO
Kreim factorization of covariance operators of 2-parameter random fields and application to the likelihood ratio
[MEMO-802] N90-18953
LIMNOLOGY
Remote sensing of interior water: Perspectives
[INPE-4875-PRE/1486] N90-18815
LINE SHAPE
Extracting chemical information form Auger line shapes
[AD-A216729] N90-18537
LINE SPECTRA
Temperature dependence of photon-gated persistent spectral hole-burning for the meso-tetra-p-tolyl Zn-tetrabenzoporphyrin/chloroform system in poly(methylmethacrylate)
[AD-A216086] N90-18531
Millimeter-wave propagation in the mesosphere
[PB90-119668] N90-18612
Ultrasensitive laser spectroscopy in solids: Single-molecule detection
[AD-A216085] N90-18716
GRIS observations of the Galactic Center N90-18982
Positron annihilation in gamma-ray bursts N90-18983
IR line emission from dense photodissociation regions N90-19100
Near infrared spectroscopy of the supernova remnant RCW103 N90-19109
High-excitation lines of molecular hydrogen: A discriminant between shock models N90-19118
Planetary nebulae N90-19122
Observations of 40-70 micron bands of ice in IRAS 09371+1212 and other stars N90-19134
Predictions of infrared recombinations lines in stellar winds of hot stars N90-19136
JCMT observations of the circumstellar envelope IRC+10216 N90-19138
Infrared lines as probes of galactic structure N90-19139
An infrared imaging Fabry-Perot study of the galactic centre N90-19142
The strengths of the 2.3 micron CO band in luminous interacting and merging galaxies N90-19148
H-alpha emission lines in high redshift quasars N90-19149
Infrared (FeII), H and H2 lines in galaxy nuclei N90-19153
LINEAR ACCELERATORS
Electron beam and high-speed optical diagnostics for the Los Alamos HIBAF (High Brightness Accelerator FEL) Facility
[DE90-007828] N90-18725
LINEAR EVOLUTION EQUATIONS
Control and stabilization of linear and nonlinear distributed systems
[AD-A216446] N90-18908
LINEAR PROGRAMMING
Optimum spanwise camber for minimum induced drag
[BU-403] N90-18369
Vertical migration in operational system nucleus
[INPE-4879-RPE/593] N90-18883
Distributed decomposition of block-angular linear programs on a hypercube computer
[AD-A216433] N90-18893
Recurrence conditions for average and Blackwell optimality in denumerable state Markov decision chains
[TW-89-02] N90-18952
LINEAR QUADRATIC REGULATOR
An interactive system applied to the linear quadratic problem
[INPE-4945-TDL/386] N90-18913
Contribution to the study of stability robustness of nonlinear multivariable regulators
[INPE-4801-TDL/356] N90-18950
LINEAR SYSTEMS
Control and stabilization of linear and nonlinear distributed systems
[AD-A216446] N90-18908
Adaptive state estimation and sampling rate analysis for invariant linear dynamic systems in time
[INPE-4960-TDL/389] N90-18951
LINEARIZATION
Computational aerodynamics of ordered vortex flows
[ETN-90-96272] N90-18368
Nonlinear model matching: A local solution and two worked examples
[MEMO-809] N90-18948
LINGUISTICS
Approaches to the planning of coherent text
[AD-A216463] N90-18895
Knowledge-based extensible natural language interface technology program
[AD-A216664] N90-18897
Computational structure of GPSG (Generalized Phrase Structure Grammar) models: Revised generalized phrase structure grammar
[AD-A216803] N90-18941
LIQUEFIED GASES
Study on the thermodynamical and mechanical conditions for the generation of high operating pressures with liquefied gases for low and very low flow rates
[ESA-TT-1148] N90-18696
LIQUID CHROMATOGRAPHY
Application of high performance liquid chromatography/mass spectrometry to environmental analysis
[PB90-116963] N90-18814
LIQUID FUELS
Optimum catalytic process for alcohol fuels from syngas
[DE90-005290] N90-18600
LIQUID HELIUM 2
Superfluid helium orbital resupply coupling N90-18488
LIQUID LITHIUM
Wick-type liquid-metal combustion
[AD-A216019] N90-18530
LIQUID PHASES
Low-energy scattering of electrons and positrons in liquids N90-18981
LIQUID ROCKET PROPELLANTS
Orbital fluid resupply assessment N90-18487
LIQUID-VAPOR INTERFACES
Analytical and experimental investigation of miniature heat pipes, phase 2
[AD-A216945] N90-18673
LITHIUM
Lithium ambient-temperature battery reliability
[DE90-005758] N90-18650
Feasibility of a super high energy density battery of the Li/BrF3 electrochemical system
[AD-A216575] N90-18799
Positronium formation in Ss state in e+-Li scattering N90-18967
LITHIUM COMPOUNDS
Properties and performance of the LiCaAlF6:Cr(3+) laser material
[DE90-007242] N90-18728
LITHOGRAPHY
Inspection of carbon/epoxy and aluminum honeycomb paraboloidal components by HNDT
[AD-A216796] N90-18514
Metal coordination polymers as potential high-energy lithographic resists
[AD-A216668] N90-18574
Research project in microelectronic engineering and imaging science
[DE90-006907] N90-18653
LOAD TESTS
Compressive strength of carbon/epoxy laminated under multiaxial stress
[DE90-005552] N90-18505
LOADS (FORCES)
A comparison of flutter calculations based on eigenvalue and energy method N90-18406
Blade row interaction effects on compressor measurements N90-18419
Fastener design manual
[NASA-RP-1228] N90-18740
LOCAL AREA NETWORKS
Computer viruses and related threats: A management guide
[PB90-111683] N90-18881
LOGISTICS
Orbital fluid resupply assessment N90-18487
LORAN C
Practical applications of Loran-C for land mobile use or the possibility to use Loran-C as a vehicle-location or vehicle-navigation system
[ETN-90-98265] N90-18384
LOUVERS
Spacecraft thermal control design data, volume 3
[ESA-PSS-03-108-ISSUE-1-VOL-3] N90-18457

LOW COST
A large area, low cost, gamma-ray, imaging spectrometer
[DE90-006993] N90-19017
LOW FREQUENCIES
Trends in VLF/LF (Very Low Frequency/Low Frequency) modem performance testing
[AD-A216578] N90-18614
LOW SPEED
Study on the thermodynamical and mechanical conditions for the generation of high operating pressures with liquefied gases for low and very low flow rates
[ESA-TT-1148] N90-18696
LOW SPEED WIND TUNNELS
The DFVLR 3-m x 3-m low speed wind tunnel (NWG) in Goettingen
[ESA-TT-1156] N90-18436
LOW TEMPERATURE
Low temperature specific heat and magnetic susceptibility of NbTi and NbTiMn alloys
[DE90-005390] N90-18552
LOW VOLTAGE
Development and test of power amplifiers for the driving of low-voltage piezo-actuators in multistable interferometers
[DLR-MITT-89-19] N90-18662
LOW WEIGHT
Low weight variable GRV power supply as part of the injector electronics to be developed for the electron accelerator MEA
[DIGEL-1989-6] N90-18661
LUBRICANTS
Life of concentrated contacts in the mixed EHD and boundary film regimes
[AD-A216673] N90-18738
LUBRICATION SYSTEMS
Life of concentrated contacts in the mixed EHD and boundary film regimes
[AD-A216673] N90-18738
LUMINANCE
The effects of luminance boundaries on color perception
[AD-A216741] N90-18860
The computation of color
[AD-A216531] N90-18914
LUMINESCENCE
Luminescence from defects and impurity centers in yttrium oxide
[DE90-004842] N90-19030
LUMINOSITY
Soft x ray emission from classical novae in outburst
[DE90-006480] N90-19187
LYMAN ALPHA RADIATION
H-alpha emission lines in high redshift quasars
N90-19149

M

M STARS
Observations of 40-70 micron bands of ice in IRAS 09371+1212 and other stars N90-19134
A new interpretation of the feature of SiO maser spectra associated with M-type star
[DE90-610641] N90-19174
MACH NUMBER
Fuselage design for a specified Mach-sliced area distribution
[NASA-TP-2975] N90-18385
MAGMA
Variations in volatiles in magma bodies based on studies of melt inclusions
[DE90-006272] N90-18821
MAGNESIUM ALLOYS
A fundamental understanding of the effect of alloying elements on the corrosion resistance of rapidly solidified Mg alloys
[AD-A216767] N90-18553
Processing and elevated temperature ductility of aluminum alloy 7475
[AD-A216840] N90-18554
MAGNESIUM OXIDES
Biaxial strength and stress rupture of hot-pressed silicon nitride
[AD-A216950] N90-18750
MAGNETIC COMPRESSION
Improved amorphous metal materials for magnetic pulse compression
[DE90-005723] N90-18555
MAGNETIC DIPOLES
Acoustic emission diagnostic techniques for high-field high current-density super inducting poles
[DE90-007400] N90-19000
Mechanical disturbances in high-performance superconducting dipoles
[DE90-006237] N90-19040
MAGNETIC FIELDS
Microwave radiation absorption by Ho(Y)-Ba-Cu-O superconducting ceramics
[DE90-610665] N90-18588
Streaming gravity mode instability
[DE90-610619] N90-18835
Development of an rf-driven plasma neutralizer for negative ions
[DE90-007298] N90-19027
MAGNETIC LEVITATION VEHICLES
Magnetic suspension railway systems based on space technology N90-19081
MAGNETIC MATERIALS
Fundamental studies of new magnetic heterostructures: Their growth, crystallographic structure, magnetic, and electronic properties
[DE90-007381] N90-19053
MAGNETIC PERMEABILITY
Low temperature specific heat and magnetic susceptibility of NbTi and NbTiMn alloys
[DE90-005390] N90-18552
MAGNETIC PROPERTIES
Improved amorphous metal materials for magnetic pulse compression
[DE90-005723] N90-18555
Modern theory of magnetism
[DE90-007374] N90-18998
Fundamental studies of new magnetic heterostructures: Their growth, crystallographic structure, magnetic, and electronic properties
[DE90-007381] N90-19053
Crystallographic and magnetic properties of (C6 D11 ND3)CuBr3 and (Zn(1-x)Mn(x))3As2: A neutron scattering study
[ECN-219] N90-19055
MAGNETOHYDRODYNAMIC FLOW
Interaction of minor ions with fast and slow shocks
[NASA-CR-186372] N90-19181
MAGNETOHYDRODYNAMIC STABILITY
Particle simulations in magnetospheric plasmas
[AD-A216256] N90-18831
Streaming gravity mode instability
[DE90-610619] N90-18835
Direct and inverse scattering problem associated with the elliptic Sinh-Gordon equation
[AD-A216455] N90-18931
The lower hybrid drift instability and the evolution of plasma gradients
[DE90-006521] N90-19021
The free energy principle, negative energy modes, and stability
[DE90-005368] N90-19056
MAGNETOHYDRODYNAMIC WAVES
Thermonuclear instability of global-type shear Alfven modes
[DE90-007087] N90-19026
MAGNETOHYDRODYNAMICS
Cohesive ceramic fabrication
[DE90-007333] N90-18597
Magnetohydrodynamic modeling of plasma opening switches and gas puff plasmas
[DE90-005825] N90-19028
MAGNETOPLASMADYNAMICS
Test facility and preliminary performance of a 100 kW class MPD thruster N90-18476
MAGNETOSPHERIC INSTABILITY
Particle simulations in magnetospheric plasmas
[AD-A216256] N90-18831
MAINTENANCE
Space shuttle RCS oxidizer leak repair for STS-26
N90-18485
MAN ENVIRONMENT INTERACTIONS
Natural and anthropogenic climate change
[DE90-006488] N90-18822
MAN MACHINE SYSTEMS
Three input concepts for flight crew interaction with information presented on a large-screen electronic cockpit display
[NASA-TM-4173] N90-18394
MAN-COMPUTER INTERFACE
Knowledge-based extensible natural language interface technology program
[AD-A216664] N90-18897
A human factors experimental comparison of two database query languages N90-19064
MANAGEMENT INFORMATION SYSTEMS
Integrated IMA (Information Mission Areas) IC (Information Center) guide
[AD-A216944] N90-18903
Defense Technical Information Center Executive Information System: Documentation and user's manual
[AD-A216235] N90-19065
MANAGEMENT METHODS
Integrated IMA (Information Mission Areas) IC (Information Center) guide
[AD-A216944] N90-18903
MANAGEMENT PLANNING
National airspace system plan: Facilities, equipment, associated development and other capital needs
[AD-A215882] N90-18373
The Pathfinder chemical transfer propulsion program
N90-18471
MANAGEMENT SYSTEMS
Superfluid helium orbital resupply coupling
N90-18488
MANDRELS
Calculations of braiding parameters
[AD-A216836] N90-18515
MANEUVERABILITY
Possible piloting techniques at hypersonic speeds
[ISL-CO-216/88] N90-18392
Discrete proportional Plus Integral (PI) multivariable control laws for the Control Reconfigurable Combat Aircraft (CRCA)
[AD-A215664] N90-18431
Design of a new control system for hovercrafts
[ETN-90-96230] N90-18435
MANGANESE ALLOYS
Low temperature specific heat and magnetic susceptibility of NbTi and NbTiMn alloys
[DE90-005390] N90-18552
MANIPULATORS
On the kinematic behavior of robots while executing general robot level commands
[PB90-120965] N90-18735
Preliminary design of a pointer for movement of a solar simulator
[INPE-4864-TDL/375] N90-18736
Teleoperator servoloop tuning using an expert system
[DE90-005674] N90-18876
Architecture for a human-robot symbiotic system
[DE90-005670] N90-18921
MANUALS
Fastener design manual
[NASA-RP-1228] N90-18740
DoD manual for standard data elements
[AD-A216441] N90-19066
MANUFACTURING
Defects: Their behaviour and related design assumptions N90-18397
Review of component defects, their relationship to manufacturing process, and their effect on materials behaviour (for critical rotating parts) N90-18399
Process development and fabrication of space station type aluminum-clad graphite epoxy struts
[NASA-CR-181873] N90-18454
Ion chromatography in the manufacture of multilayer circuit boards
[DE90-005560] N90-18652
Cost and energy consumption estimates for the aluminum-air battery anode fuel cycle
[DE90-005810] N90-18656
MAPPING
An evaluation of an airborne laser profiling system for high precision terrain mapping
[AD-A217025] N90-18780
Systematicity as a selection constraint in analogical mapping
[AD-A216029] N90-18869
Using special-purpose computing to examine chaotic behavior in nonlinear mappings
[AD-A216800] N90-18916
MARANGONI CONVECTION
Modeling convective Marangoni flows with void movement in the presence of solid-liquid phase change
[DE90-008474] N90-18690
MARINE CHEMISTRY
On the applicability of CAESAR for the remote sensing of bottom depth and bottom composition of shallow waters: A model study
[BCRS-89-13] N90-18783
MARINE ENVIRONMENTS
Sounding and surface meteorological data from the Land/Sea Breeze Experiment (LASBEX)
[AD-A216269] N90-18842
MARKET RESEARCH
The bringing to market of the RF alert (a case study in technology transfer) N90-19073
Introductory remarks for the panel discussions on technology transfer N90-19075
MARKETING
Methodology panel N90-19076
Identification of and response to market demand
N90-19078
MARKOV CHAINS
Recurrence conditions for average and Blackwell optimality in denumerable state Markov decision chains
[TW-89-02] N90-18952
MARS (PLANET)
Observations of CO on Mars in the infrared and millimetre range N90-19090

Near infrared spectroscopy of Mars: Study of the surface mineralogy N90-19091

MASERS

A new interpretation of the feature of SiO maser spectra associated with M-type star
[DE90-610841] N90-19174

MASKS

Anthropometry of a fit test sample used in evaluating the current and improved MCU-2/P masks
[AD-A215173] N90-18873

MASS

Development of a mass averaging temperature probe N90-18418

MASS DISTRIBUTION

Evaluation of helmet retention systems using a pendulum device
[AD-A215489] N90-18874

Mapping and spectroscopy of the 3.3 microns feature in Orion N90-19112

MASS SPECTRA

Initial results of positron ionization mass spectrometry N90-18995

MASS SPECTROSCOPY

Evaluation of a commercial gas chromatography/matrix isolation-infrared spectrometer for quantitative analysis of priority pollutants
[DE90-006033] N90-18542

Application of high performance liquid chromatography/mass spectrometry to environmental analysis
[PB90-116963] N90-18814

MASS TO LIGHT RATIOS

On the mass to light ratios of dwarf spheroidal galaxies
[DE90-610645] N90-19175

MASS TRANSFER

Oxygen electrode in molten carbonate fuel cells
[DE90-005377] N90-18796

Perspectives on aerosol deposition to natural surfaces
[DE90-003398] N90-18819

MASSIVELY PARALLEL PROCESSORS

Parallelizing the SDI ACCESS algorithm for the Connection Machine-2
[DE90-006362] N90-18909

MATCHING

Derivation of an efficient rule system pattern matcher
[AD-A216801] N90-18917

MATERIALS HANDLING

RF modal quantity gaging N90-18483

MATHEMATICAL MODELS

The inviscid stability of supersonic flow past a sharp cone
[NASA-CR-181996] N90-18363

Computational aerodynamics of ordered vortex flows
[ETN-90-96272] N90-18368

Review of modelling methods to take account of material structure and defects N90-18402

Unsteady viscous calculation method for cascades with leading edge induced separation N90-18408

Aerodynamic study on forced vibrations on stator rows of axial compressors N90-18412

Unsteady blade loads due to wake influence N90-18413

Asymptotic analysis of transonic flow through oscillating cascades N90-18421

Modelling unsteady transition and its effects on profile loss N90-18423

Stall and recovery in multistage axial flow compressors N90-18429

Autonomous orbit determination using GPS
[INPE-4815-TDL/361] N90-18442

Experimental flow models for SSME flowfield characterization N90-18469

The processing and mechanical properties of high temperature/high performance composites. Book 2, section 2: Strength and fracture resistance
[AD-A216142] N90-18507

The processing and mechanical properties of high temperature/high performance composites. Book 3, section 2: Strength and fracture resistance, part
[AD-A216143] N90-18508

Development of a progressive failure model for strength of laminated composite structure
[AD-A216066] N90-18517

Experimental and theoretical research on the injection of ignition gases into a bed of inert powder
[ISL-CO-251/88] N90-18547

Analytical and experimental investigation of miniature heat pipes, phase 2
[AD-A216945] N90-18673

Dryout stability and inception at low flowrates
[DE90-006955] N90-18692

INEX (Integrated Numerical Experiment) simulations of the Boeing FEL system
[DE90-004846] N90-18712

Theory for high gain, high power free electron lasers
[DE90-005548] N90-18714

Research on free electron lasers
[AD-A215865] N90-18715

Development of an experimental space station model for structural dynamics research
[NASA-TM-102601] N90-18751

Geometric correction models for HRV-SPOT images
[INPE-5001-TDL/395] N90-18757

TVI: A mathematical model for global estimation of Brazilian cerrado phytomass
[INPE-4836-PRE/1465] N90-18759

Earth model selection for computer simulations
[AD-A216843] N90-18779

Variations in volatiles in magma bodies based on studies of melt inclusions
[DE90-006272] N90-18821

Effect of a random wind field on thermal blooming instabilities
[DE90-007241] N90-18823

L: A language for solution of incremental systems in a parallel processing environment
[INPE-4816-TDL/362] N90-18884

An integrated vision on methodologies and environments for modeling and simulation assisted by computer
[INPE-4861-TDL/372] N90-18886

An objective time-integration procedure for isotropic rate-independent and rate-dependent elastic-plastic constitutive equations
[PB90-121245] N90-18925

Computational structure of GPSG (Generalized Phrase Structure Grammar) models: Revised generalized phrase structure grammar
[AD-A216803] N90-18941

Analysis of linear multigrid methods for elliptic differential equations with discontinuous and anisotropic coefficients
[ETN-90-96269] N90-18944

Can the square law be validated
[DE90-007112] N90-18945

Using dynamic queueing networks as a tool for specifying performability models
[MEMO-INF-89-51] N90-18949

Adaptive state estimation and sampling rate analysis for invariant linear dynamic systems in time
[INPE-4960-TDL/389] N90-18951

A model of incomplete chromatic adaptation for calculating corresponding colors
[DE90-006905] N90-19016

Magnetohydrodynamic modeling of plasma opening switches and gas puff plasmas
[DE90-005825] N90-19028

Mechanical disturbances in high-performance superconducting dipoles
[DE90-006237] N90-19040

MATHEMATICAL PROGRAMMING

Deterministic differential game solution: The approximate strategy method
[ESA-TT-1158] N90-18956

MATRICES (MATHEMATICS)

Ab initio R-matrix calculations of e+-molecule scattering N90-18970

MATRIX MATERIALS

The processing and mechanical properties of high temperature/high performance composites. Book 2, section 2: Strength and fracture resistance
[AD-A216142] N90-18507

The processing and mechanical properties of high temperature/high performance composites. Book 3, section 2: Strength and fracture resistance, part
[AD-A216143] N90-18508

Mechanical properties and microstructure of Si3N4-whisker-reinforced Si3N4 matrix composite
[DE90-005651] N90-18518

Comparison between the damage modes of thermo-hardenable and thermo-plastic composite matrices
[ONERA-RT-47/7086-M] N90-18523

MATTER (PHYSICS)

Antiproton-matter interactions in antiproton applications N90-18989

MAXIMUM LIKELIHOOD ESTIMATES

Evaluation of two methods for acquisition of training statistics for digital analysis of areas prepared for plowing
[INPE-4901-PRE/1502] N90-18763

MAXWELL EQUATION

Vector fields, linear spaces and tensors in physics. Part 3: Tensor analysis and its applications
[INPE-5000-MD/41] N90-18997

MEAN FREE PATH

Decay rate and other properties of the positronium negative ion N90-18967

MEASURE AND INTEGRATION

An objective time-integration procedure for isotropic rate-independent and rate-dependent elastic-plastic constitutive equations
[PB90-121245] N90-18925

MEASURING INSTRUMENTS

Piezoelectric polymer PVDF shock gauge: State of the research art
[ISL-CO-207/89] N90-18705

Techniques for measurement of the optical properties of materials
[DE90-006902] N90-19014

MECHANICAL DEVICES

A theory of quantitative inference for artifact sets applied to a mechanical design compiler
[AD-A216535] N90-18896

MECHANICAL ENGINEERING

A theory of quantitative inference for artifact sets applied to a mechanical design compiler
[AD-A216535] N90-18896

MECHANICAL PROPERTIES

Ceramic matrix composites, new high performance materials N90-18500

The processing and mechanical properties of high temperature/high performance composites. Book 2, section 2: Strength and fracture resistance
[AD-A216142] N90-18507

The processing and mechanical properties of high temperature/high performance composites. Book 3, section 2: Strength and fracture resistance, part
[AD-A216143] N90-18508

Preliminary evaluation of the strength of pin-joints in laminated composite materials
[DE90-006353] N90-18524

A statistical evaluation of the variation in laminated composite properties resulting from ply misalignment
[DE90-006371] N90-18525

Calculation of mechanical properties variations depending on matrix parameters in a composite, as a function of the test temperature
[DT-311/88] N90-18526

Impact of composites in the aerospace industry
[ETN-90-96231] N90-18527

Identification of a cast iron alloy containing nonstrategic elements
[NASA-CR-185174] N90-18559

Model filled polymers 3. Rheological behavior of polystyrene containing crosslinked polystyrene beads
[AD-A215867] N90-18567

Characterization and development report for the SA3274-1 and SA3274-2 transient voltage suppressors
[DE90-005712] N90-18649

Crystal growth and mechanical properties of semiconductor alloys
[AD-A216697] N90-19035

MELT SPINNING

The processing and mechanical properties of high temperature/high performance composites. Book 2, section 2: Strength and fracture resistance
[AD-A216142] N90-18507

The processing and mechanical properties of high temperature/high performance composites. Book 3, section 2: Strength and fracture resistance, part
[AD-A216143] N90-18508

MELTING

Pulsed laser-induced melting of intermediate Cu-Zn phases
[DE90-005404] N90-18713

MEMBRANES

Perforated monolayers
[DE90-005469] N90-18566

MEMORY

Organization of a large-scale cortical network
[AD-A216829] N90-18863

MEMORY (COMPUTERS)

Cedar project: Original goals and progress to date
[DE90-006761] N90-18880

MERCURY (METAL)

Fundamental studies of surface processes and trace analysis using solid electrodes
[AD-A216538] N90-18533

MESOSCALE PHENOMENA

Comparison of circulation obtained through the trajectory of a drifting buoy tracked by satellite and hydrographic data in the Bransfield Strait
[INPE-4946-TDL/387] N90-18850

MESOSPHERE

Millimeter-wave propagation in the mesosphere
[PB90-119868] N90-18612

MESOZOIC ERA

The patterns of fracture and the conditioning tectonics in the region of the Quadrilatero Ferrifero and part of the Migmatitic-Gnanulitic Complex in Minas Gerais (Brazil)
[INPE-4895-PRE/1496] N90-18829

METABOLISM
Thermal remote sensing in the differentiation of soybean crops (glycine max (L.) merrill) submitted to water deficit
[INPE-4900-PRE/1501] N90-18762
METAL AIR BATTERIES
Cost and energy consumption estimates for the aluminum-air battery anode fuel cycle
[DE90-005810] N90-18656
METAL BONDING
Spectroscopic evidence for carbon-carbon bonding in carbide layers on metals
[AD-A216726] N90-18512
METAL COATINGS
The improved adhesion of organic polymers to silica and to aluminum metal with zirconium Schiff-base block copolymer coatings
[AD-A216669] N90-18575
Microstructural variations in aluminum oxide coatings deposited using a dual beam ion system
[DE90-006040] N90-18583
METAL COMBUSTION
Wick-type liquid-metal combustion
[AD-A216019] N90-18530
METAL FATIGUE
Corrosion fatigue of iron-chromium-nickel alloys: Fracture mechanics and chemistry
[DE90-006318] N90-18556
Softening mechanisms and microstructural instabilities during high temperature, low cycle fatigue of Ni, Ni3Al, and their metal matrix composites
[DE90-006487] N90-18557
METAL FILMS
Time-resolved measurements of solidification and undercooling in metals and alloys
[DE90-007074] N90-18564
Polymerization of nitro compounds on silver surfaces during surface-enhanced Raman scattering
[AD-A216116] N90-18569
The interaction of polycrystalline copper films with dilute aqueous solutions of cupric chloride
[AD-A216465] N90-19033
METAL FLUORIDES
Investigation of the phase stabilizing effect of 4 percent potassium fluoride on ammonium nitrate
[AD-A215313] N90-18599
Feasibility of a super high energy density battery of the Li/BrF3 electrochemical system
[AD-A216575] N90-18799
METAL MATRIX COMPOSITES
Sputter deposition of diffusion barrier coatings on SiC monofilaments for use in Ti-based composites
N90-18502
Laboratory for the processing and evaluation of inorganic matrix composites
[AD-A216881] N90-18516
Softening mechanisms and microstructural instabilities during high temperature, low cycle fatigue of Ni, Ni3Al, and their metal matrix composites
[DE90-006487] N90-18557
METAL OXIDES
Pulsed laser deposition of high T(sub c) superconducting thin films
[AD-A216507] N90-19034
METAL PLATES
Effects of oblique impact on hypervelocity shield performance
[DE90-006936] N90-18739
METAL POWDER
Laboratory for the processing and evaluation of inorganic matrix composites
[AD-A216881] N90-18516
METALLIC GLASSES
Metallaboranes as precursors to metallic glasses
[AD-A216946] N90-18577
METALLURGY
The damage tolerance of disc materials: Metallurgical factors; relationship with processing parameters
N90-18398
METAMORPHISM (GEOLOGY)
Quantification of structural field data in the Rio Grande do Norte basin and neighborhood
[INPE-4821-RPE/591] N90-18826
The patterns of fracture and the conditioning tectonics in the region of the Quadrilatero Ferrifero and part of the Migmatitic-Gnanulitic Complex in Minas Gerais (Brazil)
[INPE-4895-PRE/1496] N90-18829
METEOROLOGICAL PARAMETERS
Sounding and surface meteorological data from the Land/Sea Breeze Experiment (LASBEX)
[AD-A216269] N90-18842
Proceedings of the Professional Pilots Meteorology Training Standards Conference
[AD-A216618] N90-18843
METEOROLOGICAL RADAR
A case study of the 24 August 1986 FLOWS microburst
[AD-A216939] N90-18847
METHANE
Effect of propellant flowrate and purity on carbon deposition in LO2/methane gas generators N90-18488
Extracting chemical information form Auger line shapes
[AD-A216729] N90-18537
METHOD OF MOMENTS
A user's manual for the method of moments Aircraft Modeling Code (AMC)
[NASA-CR-186371] N90-18390
METHYL ALCOHOL
Federal methanol fleet update
[DE90-006851] N90-18741
Hawaii integrated biofuels research program, phase 1
[DE90-006885] N90-18811
METHYL COMPOUNDS
Determination of the minimum energy conformation of alkyl substituted pyrazines
[AD-A216974] N90-18539
MICHELSON INTERFEROMETERS
Measurement of gas intensity at high dynamic pressures
[ISL-CO-204/89] N90-18680
Velocity measurement using interferometry
[ISL-CO-221/88] N90-18709
MICROBURSTS (METEOROLOGY)
Synthetic aperture radar imagery of airports and surrounding areas: Archived SAR data
[NASA-CR-4275] N90-18371
Synthetic aperture radar imagery of airports and surrounding areas: Philadelphia Airport
[NASA-CR-4280] N90-18372
A case study of the 24 August 1986 FLOWS microburst
[AD-A216939] N90-18847
MICROCOMPUTERS
Microcomputer enhanced optical investigation of spreading and evaporative processes in ultra thin films
[DE90-006323] N90-18585
A microcode compiler that runs on the IBM AT and supports cascadable microcomputers, part 1
[AD-A215888] N90-18877
MICROELECTRONICS
Research project in microelectronic engineering and imaging science
[DE90-006907] N90-18653
MICROPROGRAMMING
A microcode compiler that runs on the IBM AT and supports cascadable microcomputers, part 1
[AD-A215888] N90-18877
MICROROCKET ENGINES
Viability study of ionic microthruster tests on MECB satellite
[INPE-4973-RPE/605] N90-18490
MICROSCOPY
Biomedical applications of synchrotron x ray microscopy
[DE90-004957] N90-18867
MICROSTRIP ANTENNAS
Reconfigurable antennas, monolithic microwave integrated circuits with feeding networks for microstrip antennas
[AD-A216916] N90-18622
MICROSTRUCTURE
Defects: Their behaviour and related design assumptions N90-18397
Review of component defects, their relationship to manufacturing process, and their effect on materials behaviour (for critical rotating parts) N90-18399
Future technology requirements (related to defects and quantitative material behavior to aid in implementation of damage tolerance for design of engine structures)
N90-18403
State of the art and future prospects for high temperature composites N90-18498
Laboratory for the processing and evaluation of inorganic matrix composites
[AD-A216881] N90-18516
Mechanical properties and microstructure of Si3N4-whisker-reinforced Si3N4 matrix composite
[DE90-005651] N90-18518
Corrosion fatigue of iron-chromium-nickel alloys: Fracture mechanics and chemistry
[DE90-006318] N90-18556
Softening mechanisms and microstructural instabilities during high temperature, low cycle fatigue of Ni, Ni3Al, and their metal matrix composites
[DE90-006487] N90-18557
The mechanism, measurement, and influence of properties on the galling of metals
[DE90-006533] N90-18558
Colloid and interface chemistry aspects of ceramics
[AD-A216715] N90-18576
Microstructural variations in aluminum oxide coatings deposited using a dual beam ion system
[DE90-006040] N90-18583
The design of advanced ceramic composites
[DE90-006613] N90-18592
Microstructural characterization of silicon nitride ceramics processed by pressureless sintering, overpressure sintering, and sinter/HIP
[DE90-007126] N90-18594
Creep in shear of experimental solder joints
[DE90-007062] N90-18753
The interaction of polycrystalline copper films with dilute aqueous solutions of cupric chloride
[AD-A216465] N90-19033
Transport effects and spectroscopy of defects in microstructures
[AD-A216718] N90-19036
Dislocation behaviour in Ge(x)Si(1-x) epilayers on (001) Si
[DE90-007063] N90-19051
MICROWAVE AMPLIFIERS
Output performance of idealized microwave power amplifiers
[AD-A216797] N90-18645
MICROWAVE CIRCUITS
Reconfigurable antennas, monolithic microwave integrated circuits with feeding networks for microstrip antennas
[AD-A216916] N90-18622
MICROWAVE IMAGERY
Multiparameter scatterometer for remote sensing (RADSER). Project Scatter: State-of-the-art and future applications
[INPE-4871-PRE/1482] N90-18701
MICROWAVE OSCILLATORS
Hamiltonian analysis and simulation of free electron lasers
[INPE-4785-TDL/351] N90-19018
MICROWAVE SPECTRA
Observations of CO on Mars in the infrared and millimetre range N90-19090
The microwave background in steady-state cosmology
N90-19150
MICROWAVES
Microwave radiation absorption by Ho(Y)-Ba-Cu-O superconducting ceramics
[DE90-610665] N90-18588
Quick, reliable estimates of high-power microwave fluences: The SNEAKY-2 program
[DE90-006347] N90-18624
Instability investigation for storage mode. Microwave instability (single-bunch instability)
[NIKHEF-K/AMPS/89/05] N90-18628
Determining the effects of microwave power and C-field setting on the frequency of a cesium atomic frequency standard
[AD-A216599] N90-18642
Output performance of idealized microwave power amplifiers
[AD-A216797] N90-18645
Signal processing device to control microwave output
[AD-A216931] N90-18648
Effects of pulsed and CW (Continuous Wave) 2450 MHz radiation on transformation and chromosomes of human lymphocytes in vitro
[AD-A216500] N90-18857
MIE SCATTERING
An investigation of flow structure, mixing and chemical reaction in combusting turbulent flows
[AD-A216739] N90-18538
MIGRATION
Vertical migration in operational system nucleus
[INPE-4879-RPE/593] N90-18883
MILITARY SPACECRAFT
Rate compatible punctured codes, their use in military satellite communication systems
[AD-A216723] N90-18619
MILKY WAY GALAXY
Infrared spectroscopy of the central few parsecs of the galaxy N90-19140
On the mass to light ratios of dwarf spheroidal galaxies
[DE90-610645] N90-19175
MILLIMETER WAVES
Millimeter-wave propagation in the mesosphere
[PB90-119868] N90-18612
Performance and modeling of superconducting ring resonators at millimeter-wave frequencies
[NASA-TM-102526] N90-18634
Chemistry on interstellar grains and implications for infrared spectroscopy N90-19097
Detection of SN1986j in NGC891 at millimetre wavelengths N90-19137
The James Clerk Maxwell telescope N90-19166

MINERALOGY
Near infrared spectroscopy of Mars: Study of the surface mineralogy N90-19091
MINERALS
Remote sensing applied to the monitoring of mineral extraction in the proximity of urban areas: Pros and cons [INPE-4867-PRE/1478] N90-18766
MINIATURIZATION
Experiments on the unsteady flow in a supersonic compressor stage N90-18422
Small displacement, long life on-orbit compressor design and fabrication N90-18489
Analytical and experimental investigation of miniature heat pipes, phase 2 [AD-A216945] N90-18673
MINING
Remote sensing applied to the monitoring of mineral extraction in the proximity of urban areas: Pros and cons [INPE-4867-PRE/1478] N90-18766
MISSILE COMPONENTS
Simulation of the dynamic environment for missile component testing: Demonstration [AD-A216979] N90-18443
MISSILE CONTROL
The implications of using integrated software support environment for design of guidance and control systems software [AGARD-AR-229] N90-18432
MISSILES
Combustion instability in solid propellant rockets [AD-A216740] N90-18492
MISSION PLANNING
A perspective on the use of storable propellants for future space vehicle propulsion N90-18473
Mission options for an electric propulsion demonstration flight test N90-18479
MIXING
Numerical simulations of coherent structures in a jet flame with a noncircular cross section [AD-A216710] N90-18535
Control of phase structure in polymer blends [AD-A217034] N90-18580
Investigation of methods to produce a uniform cloud of fuel particles in a flame tube [NASA-TM-102376] N90-18665
MIXTURES
Control of phase structure in polymer blends [AD-A217034] N90-18580
MOBILE COMMUNICATION SYSTEMS
Practical applications of Loran-C for land mobile use or the possibility to use Loran-C as a vehicle-location or vehicle-navigation system [ETN-90-95265] N90-18384
MODEMS
Trends in VLF/LF (Very Low Frequency/Low Frequency) modem performance testing [AD-A216576] N90-18614
MOLECULAR CLOUDS
Photodissociation regions: Observations and theory N90-19096
IR line emission from dense photodissociation regions N90-19100
IR line emission from supernovae in molecular clouds N90-19102
The excitation of molecular hydrogen and its significance N90-19117
Molecular hydrogen in the HII region G333.6-0.2 N90-19121
Hydrodynamical simulations of collisions between interstellar clouds [DE90-006921] N90-19172
MOLECULAR COLLISIONS
Ab initio R-matrix calculations of e+-molecule scattering N90-18970
MOLECULAR EXCITATION
Determination of the minimum energy conformation of alkyl substituted pyrazines [AD-A216974] N90-18539
Studies of atmospheric molecules by multiphoton spectroscopy [DE90-005829] N90-18833
Merged beam studies into the mechanisms of hydrogen molecular ion recombination [AD-A216469] N90-19002
The excitation of molecular hydrogen and its significance N90-19117
High-excitation lines of molecular hydrogen: A discriminant between shock models N90-19118
MOLECULAR IONS
Merged beam studies into the mechanisms of hydrogen molecular ion recombination [AD-A216469] N90-19002
MOLECULAR SPECTRA
A simple model for amplified spontaneous emission in dyes [DE90-007249] N90-18730
Atomic and molecular spectra from electron-excited alkali halides [DE90-006160] N90-19004
A coal model for the carriers of the unidentified IR bands N90-19110
The environment of young stellar objects studied by high-resolution infrared spectroscopy N90-19120
JCMT observations of the circumstellar envelope IRC+10216 N90-19138
MOLECULAR STRUCTURE
Structural study of thermo-hardenable matrices. Deformation processes of composite matrices as a function of their molecular structure [ONERA-RT-10/3521-M] N90-18522
Perforated monolayers [DE90-005469] N90-18566
Electrochemical investigations of electronically conductive polymers. Part 4: By controlling the supermolecular structure, charge transport rates can be enhanced [AD-A216603] N90-18573
Infrared cometary spectroscopy N90-19086
MOLECULES
Ultrasensitive laser spectroscopy in solids: Single-molecule detection [AD-A216085] N90-18716
MOLTEN SALT ELECTROLYTES
Oxygen electrode in molten carbonate fuel cells [DE90-005377] N90-18796
MOLYBDENUM OXIDES
Interfacial chemistry of MoS2 films on Si [AD-A216527] N90-18532
MOMENTUM TRANSFER
The neoclassical transport of toroidal momentum in tokamaks [DE90-006864] N90-19023
MONITORS
A new broadband pulsed high voltage monitor [DE90-006264] N90-18651
Toroid monitor [DIGEL-1989-8] N90-18663
Acoustic emission diagnostic techniques for high-field high current-density super inducting poles [DE90-007400] N90-19000
MONOPROPELLANTS
Orbital fluid resupply assessment N90-18487
MONTE CARLO METHOD
Angle estimation in the presence of mainbeam interference [AD-A216832] N90-18621
Spectral functions from Quantum Monte Carlo [DE90-004870] N90-19050
MORPHOLOGY
Morphological consequences of catalytic hydrogenation of polymers in the bulk [DE90-007276] N90-18598
Fatigue crack initiation and small crack growth in several airframe alloys [NASA-TM-102598] N90-18746
Modified dislocation structures in Ge(x)Si(1-x) double epilayers on (001) Si [DE90-007078] N90-19052
MOSAICS
Fracture analysis through photographic imagery of low spatial resolution: A contribution to the study of tectonic evoluation of the Araripe Plateau region [INPE-4876-PRE/1487] N90-18756
MOUNTAINS
Photointerpretation with instruments for evaluation of environmental impact: Mata Atlantica in Cubata [INPE-4910-PRE/1511] N90-18817
MULTIPROCESSING (COMPUTERS)
Parallel memory addressing using coincident optical pulses [AD-A216302] N90-18641
A scalable multiprocessor architecture using Cartesian network: Relative addressing [AD-A216580] N90-18678
Cedar project: Original goals and progress to date [DE90-006761] N90-18880
Distributed decomposition of block-angular linear programs on a hypercube computer [AD-A216433] N90-18893
Summer institute in parallel computing [DE90-005532] N90-18910
MULTISPECTRAL PHOTOGRAPHY
Introduction of aerial photography in agricultural research [BCRS-89-14] N90-18784
MULTIVARIATE STATISTICAL ANALYSIS
Discrete proportional Plus Integral (PI) multivariable control laws for the Control Reconfigurable Combat Aircraft (CRCA) [AD-A215664] N90-18431
Practical methods for robust multivariable control [AD-A216937] N90-18920
Inverse scattering and tomography [AD-A216456] N90-18932
MUONS
Underground muon observations in the Soudan 2 detector [DE90-005647] N90-19183
MUSCULOSKELETAL SYSTEM
A program for the study of skeletal muscle catabolism following physical trauma [AD-A216569] N90-18859
MYOCARDIUM
Coronary arterial capacitance and subendocardial vascular patency throughout the cardiac cycle N90-18855

N

N-P-N JUNCTIONS
A GaAs p-n-p-n thyristor model [DE90-005757] N90-19039
N-TYPE SEMICONDUCTORS
Dopant site location in dual-implanted GaP using (111) planar channeling [DE90-006565] N90-19042
In situ growth of epitaxial superconducting YBa2Cu3O(7-x) films on insulating semiconducting and ferroelectric K(Ta, Nb)O3 by pulsed laser ablation [DE90-006568] N90-19043
NASA PROGRAMS
Space station technology summary N90-18482
NASA SPACE PROGRAMS
The Pathfinder chemical transfer propulsion program N90-18471
NATIONAL AIRSPACE SYSTEM
National airspace system plan: Facilities, equipment, associated development and other capital needs [AD-A215882] N90-18373
NATIONAL PARKS
Physiognomy of vegetation cover in the PNPM identified through the TM/LANDSAT sensor: A multitemporal analysis [INPE-4834-PRE/1464] N90-18776
NATURAL LANGUAGE (COMPUTERS)
Knowledge-based extensible natural language interface technology program [AD-A216664] N90-18697
NAVIER-STOKES EQUATION
Numerical simulation of three-dimensional unsteady flows in turbomachines N90-18417
Measurement of velocity profiles and Reynolds stresses on an oscillating airfoil N90-18427
Numerical simulations of coherent structures in a jet flame with a noncircular cross section [AD-A216710] N90-18535
Improved computational fluid dynamics for continuum hypersonic flow [AD-A216981] N90-18674
Spectral multi-domain approximation of the Navier-Stokes equations in curved complex geometries [ONERA-NT-1987-2] N90-18685
Numerical simulation of the vortex breakdown [ONERA-RSF-4/4368-AY-004A] N90-18689
NAVIGATION
Visual navigation: Constructing and utilizing simple maps of an indoor environment [AD-A216761] N90-18382
An approach centered in production rules for a partition of environment and planning in a visual navigation system (SNV) [INPE-4813-TDL/360] N90-18737
NAVIGATION AIDS
An error sensitivity model for Doppler positioning using transit satellites [AD-A216724] N90-18381
The Fourteenth Biennial Guidance Test Symposium, volume 1 [AD-A216925] N90-18383
NAVIGATION SATELLITES
Navigation experiment NAVEX data storage and processing [ESA-TT-1175] N90-18445
Navigation experiment NAVEX: The self-test delay times in the D1 Spacelab mission [ESA-TT-1176] N90-18446
NEAR INFRARED RADIATION
Near infrared spectroscopy of Mars: Study of the surface mineralogy N90-19091
Near infrared spectroscopy of the supernova remnant RCW103 N90-19109
IRCAM observations of the Reipurth 50 IR source N90-19119
Near infrared (1-4 micron) spectroscopy of SN1987A N90-19133
Near-infrared spectroscopy of starburst and interacting galaxies N90-19144

Infrared properties of five spiral galaxies N90-19154
Fluorescent molecular hydrogen emission from star-forming galaxies N90-19155
Near infrared spectroscopy and spectroscopic imaging of NGC253 N90-19159
Measurement system of spectral irradiance in the near infrared N90-19160
Isophot-S, a low resolution 2.5 to 12 microns spectrometer for ISO N90-19167

NEBULAE
Ice grains in the dust disk of the bipolar nebula M 1-92 N90-19127
Detection of SN1986j in NGC891 at millimetre wavelengths N90-19137

NEGATIVE IONS
Decay rate and other properties of the positronium negative ion N90-18987
Positronium ions and molecules N90-18990
Development of an rf-driven plasma neutralizer for negative ions
[DE90-007298] N90-19027

NEODYMIUM LASERS
Spallation and dynamic fracture as an effect of laser induced shock waves in carbon based composite materials
[AD-A216540] N90-18509

NEON
Numerical Green's functions in optical potential calculations for positron scattering from argon and neon N90-18971
Positron excitation of neon N90-18973

NEPHANALYSIS
Comparisons between the RTNEPH (Real-Time Nephanalysis) and AFGL cloud layer analysis algorithms
[AD-A216637] N90-18844

NEPHELOMETERS
Fluorescence and elastic scattering from laser dye-filled capillaries
[AD-A217026] N90-18540

NETHERLANDS
Results of Agrisar-86 for the Flevopolder (Netherlands) test area
[BCRS-89-21] N90-18789
Remote sensing for the classification and quantification of vegetation in Spring staging areas of Brent geese on the Frisian Islands (Netherlands)
[BCRS-89-27] N90-18790

NETWORK ANALYSIS
Feasibility of Mealy design for processor controlpaths
[MEMO-INF-89-53] N90-18923

NEURAL NETS
Computation and control with neural nets
[DE90-006460] N90-18911

NEUROLOGY
Organization of a large-scale cortical network
[AD-A216829] N90-18863

NEURONS
Organization of a large-scale cortical network
[AD-A216829] N90-18863

NEUTRAL BEAMS
Development of an rf-driven plasma neutralizer for negative ions
[DE90-007298] N90-19027

NEUTRALIZERS
Development of an rf-driven plasma neutralizer for negative ions
[DE90-007298] N90-19027

NEUTRINOS
Research in theoretical physics
[DE90-005558] N90-19001

NEUTRON DIFFRACTION
Crystallographic and magnetic properties of (C6 D11 ND3)CuBr3 and (Zn(1-x)Mn(x))3As2: A neutron scattering study
[ECN-219] N90-19055

NEUTRON IRRADIATION
Response of unirradiated and neutron-irradiated vanadium alloys to Charpy-impact loading
[DE90-004878] N90-18551

NEUTRON SCATTERING
Measurement of body fat by neutron inelastic scattering: Comments on installation, operation, and error analysis
[DE90-006765] N90-18868

NEUTRON STARS
Positron annihilation in gamma-ray bursts N90-18983

NICKEL
Spectroscopic evidence for carbon-carbon bonding in carbide layers on metals
[AD-A216726] N90-18512
Time-resolved measurements of solidification and undercooling in metals and alloys
[DE90-007074] N90-18564

NICKEL ALLOYS
Defects in monoblock cast turbine wheels N90-18400
Sintering of a model nickel/alumina catalyst
[ETN-90-96270] N90-18561

NIGHTGLOW
Study of the atmospheric emissions of OI wavelength 557.7 nm and O2 (0,0) wavelength 761.9 nm in the equatorial region utilizing measurement of photometer on-board a rocket
[INPE-4811-TDL/358] N90-18827

NIOBIUM ALLOYS
Low temperature specific heat and magnetic susceptibility of NbTi and NbTiMn alloys
[DE90-005390] N90-18552

NITRIC OXIDE
A program of fundamental research on explosives at Los Alamos
[DE90-006509] N90-18602

NITROBENZENES
Polymerization of nitro compounds on silver surfaces during surface-enhanced Raman scattering
[AD-A216116] N90-18569

NITROGEN TETROXIDE
Space shuttle RCS oxidizer leak repair for STS-26 N90-18485

NOISE INTENSITY
Noise levels from a VSTOL aircraft measured at ground level and at 1.2 m above the ground
[NPL-RSA(EXT)-009] N90-18999

NOISE MEASUREMENT
Noise levels from a VSTOL aircraft measured at ground level and at 1.2 m above the ground
[NPL-RSA(EXT)-009] N90-18999

NOISE REDUCTION
Fuselage design for a specified Mach-sliced area distribution
[NASA-TP-2975] N90-18385

NOISE TEMPERATURE
Interrelationship of spatial and radiometric resolution in the thermal infrared band
[INPE-4860-TDL/371] N90-18771

NONDESTRUCTIVE TESTS
Inspection of carbon/epoxy and aluminum honeycomb paraboloidal components by HNDT
[AD-A216796] N90-18514

NONEQUILIBRIUM IONIZATION
Improved computational fluid dynamics for continuum hypersonic flow
[AD-A216981] N90-18674

NONLINEAR EQUATIONS
Hamiltonian analysis and simulation of free electron lasers
[INPE-4785-TDL/351] N90-19018

NONLINEAR PROGRAMMING
An exact algorithm for the problem of p-medians
[INPE-4924-TDL/384] N90-18885

NONLINEAR SYSTEMS
Control and stabilization of linear and nonlinear distributed systems
[AD-A216446] N90-18908
Using special-purpose computing to examine chaotic behavior in nonlinear mappings
[AD-A216800] N90-18916
Nonlinear model matching: A local solution and two worked examples
[MEMO-809] N90-18948

NONLINEARITY
Contribution to the study of stability robustness of nonlinear multivariable regulators
[INPE-4801-TDL/356] N90-18950

NOVAE
Soft x ray emission from classical novae in outburst
[DE90-006480] N90-19187

NOZZLE DESIGN
Arcjet nozzle design impacts N90-18478

NUCLEAR BINDING ENERGY
Positronium ions and molecules N90-18990

NUCLEAR ELECTRIC PROPULSION
Electric propulsion for manned Mars exploration N90-18480

NUCLEAR EXPLOSIONS
ACIRF user's guide: Theory and examples
[AD-A216436] N90-18613

NUCLEAR PHYSICS
Theoretical studies in nuclear physics
[DE90-005981] N90-19005

NUCLEAR WEAPONS
Survivability and effectiveness of near-term strategic defense
[DE90-005805] N90-18955

NUCLEATION
Investigation of the phase stabilizing effect of 4 percent potassium fluoride on ammonium nitrate
[AD-A215313] N90-18599

NUCLEONS
Underground muon observations in the Soudan 2 detector
[DE90-005647] N90-19183

NUMERICAL ANALYSIS
Damage in a perforated graphite-epoxy composite plate under monotonic and cyclic biaxial loading
[ESA-TT-1117] N90-18521
KAM: Automatic planning and interpretation of numerical experiments using geometrical methods
[AD-A216805] N90-18900

NUMERICAL CONTROL
Mechanical disturbances in high-performance superconducting dipoles
[DE90-006237] N90-19040

NUMERICAL FLOW VISUALIZATION
Numerical simulation of the vortex breakdown
[ONERA-RSF-4/4368-AY-004A] N90-18689
Numerical investigations of heat transfer and flow rates in rotating cavities. Simulation of the movement generated by wall temperature gradients, by source-sink mass flows or by the differential rotation of the walls, under the influence or coriolis and centrifugal forces
[ETN-90-96253] N90-18695

NUMERICAL INTEGRATION
Autonomous orbit determination using GPS
[INPE-4815-TDL/361] N90-18442

NUTATION
Nonlinear optical processes in one-dimensional polymers
[AD-A216103] N90-18568

NUTRIENTS
Continuous hydroponic wheat production using a recirculating system
[NASA-TM-102784] N90-18853

O

O RING SEALS
Test data of flow field of shuttle SRM nozzle joint with bond defects, using unheated air N90-18484

O STARS
Predictions of infrared recombinations lines in stellar winds of hot stars N90-19136

OCEAN BOTTOM
On the applicability of CAESAR for the remote sensing of bottom depth and bottom composition of shallow waters: A model study
[BCRS-89-13] N90-18783

OCEAN CURRENTS
An application of ocean wave-current refraction to the gulf stream using SEASAT SAR data
[AD-A216769] N90-18851

OCEAN SURFACE
Multiparameter scatterometer for remote sensing (RADSER). Project Scatter: State-of-the-art and future applications
[INPE-4871-PRE/1482] N90-18701
Intertropical Convergence Zone (ITCZ) and its relationship with the precipitation of the north-northeast Brazilian region
[INPE-4887-TDL/378] N90-18839

OCEANOGRAPHY
ERS-1 European remote sensing satellite: A new tool for global environmental monitoring in the 1990's
[ESA-BR-36] N90-18782
Forecasters handbook for Central America and adjacent waters
[AD-A216752] N90-18845
Comparison of circulation obtained through the trajectory of a drifting buoy tracked by satellite and hydrographic data in the Bransfield Strait
[INPE-4946-TDL/387] N90-18850

OCEANS
An application of ocean wave-current refraction to the gulf stream using SEASAT SAR data
[AD-A216769] N90-18851

OFFSHORE ENERGY SOURCES
Atlantic outer continental shelf: Description of the Mid-Atlantic environment
[PB90-100033] N90-18849

OIL EXPLORATION
Atlantic outer continental shelf: Description of the Mid-Atlantic environment
[PB90-100033] N90-18849

OMNIDIRECTIONAL ANTENNAS
Telemetry and telecommand omnidirectional antenna in the short wave band
[ETN-90-96285] N90-18631

ONBOARD DATA PROCESSING
Experimental investigations of the unsteady boundary layer on an oscillating flat plate. Optimization and validation of a code, for calculating the potential flow/boundary layer coupling of a flat plate and of an oscillating profile
[ETN-90-96254] N90-18682

OPERATING SYSTEMS (COMPUTERS)
The implications of using integrated software support environment for design of guidance and control systems software
[AGARD-AR-229] N90-18432
Vertical migration in operational system nucleus
[INPE-4879-RPE/593] N90-18883
L: A language for solution of incremental systems in a parallel processing environment
[INPE-4816-TDL/362] N90-18884
OPERATIONS RESEARCH
Integrated silicon flip-flop sensors
[ETN-90-96271] N90-18854
Parallel algorithms derivation
[AD-A216452] N90-18894
OPERATORS (MATHEMATICS)
Recurrence conditions for average and Blackwell optimality in denumerable state Markov decision chains
[TW-89-02] N90-18952
Kreim factorization of covariance operators of 2-parameter random fields and application to the likelihood ratio
[MEMO-802] N90-18953
OPTICAL CORRECTION PROCEDURE
Geometric correction models for HRV-SPOT images
[INPE-5001-TDL/395] N90-18757
OPTICAL COUPLING
Optical amplification in 45 deg - cut BaTiO3
[AD-A216043] N90-19011
OPTICAL DATA PROCESSING
Application of wavefront analysis techniques to restoring of images degraded by atmospheric turbulence
[ONERA-PUBL-1989-1] N90-19168
OPTICAL MEASUREMENT
Techniques for measurement of the optical properties of materials
[DE90-006902] N90-19014
OPTICAL MEMORY (DATA STORAGE)
Parallel memory addressing using coincident optical pulses
[AD-A216302] N90-18641
OPTICAL POLARIZATION
Properties and performance of the LiCaAlF6:Cr(3+) laser material
[DE90-007242] N90-18728
OPTICAL PROPERTIES
Nonlinear optical processes in one-dimensional polymers
[AD-A216103] N90-18568
Evaluating a glass surface produced by ductile grinding
[DE90-006782] N90-18608
Performance of a 500 watt Nd:GGG zigzag slab oscillator
[DE90-006263] N90-18657
Techniques for measurement of the optical properties of materials
[DE90-006902] N90-19014
OPTICAL PUMPING
Properties and performance of the LiCaAlF6:Cr(3+) laser material
[DE90-007242] N90-18728
A simple model for amplified spontaneous emission in dyes
[DE90-007249] N90-18730
OPTICAL RADAR
Doppler lidar working group report
[ESA-SP-1112] N90-18848
OPTICAL TRACKING
An evaluation of an airborne laser profiling system for high precision terrain mapping
[AD-A217025] N90-18780
OPTIMAL CONTROL
Optimization of sensors and actuators positioning aimed at obtaining reduced models for the synthesis of optimal control regulators of flexible structures
[INPE-4760-TDL/348] N90-18450
An interactive system applied to the linear quadratic problem
[INPE-4945-TDL/386] N90-18913
OPTIMIZATION
Practical applications of Loran-C for land mobile use or the possibility to use Loran-C as a vehicle-location or vehicle-navigation system
[ETN-90-96265] N90-18384
Optimization of sensors and actuators positioning aimed at obtaining reduced models for the synthesis of optimal control regulators of flexible structures
[INPE-4760-TDL/348] N90-18450
Interlaminar fracture testing of carbon fibre/PEEK composites validity and applications N90-18497
Optimum catalytic process for alcohol fuels from syngas
[DE90-007188] N90-18604
On the range resolution of point targets with FMCW radar systems
[DLR-FB-89-47] N90-18629
Optimal planning method of underground distribution system, part 2. Application to various types of system configurations
[DE89-782323] N90-18636
Resonator modes in high gain free electron lasers
[DE90-006096] N90-18720
Study of discharge mechanisms and the stability of transverse electric discharges in the gas mixtures
[ISL-R-114/88] N90-18733
Optimization of the reference parameters in the accompanying solar panel dynamics
[INPE-4795-PRE/1449] N90-18798
Optimum and heuristic algorithms for finite state machine decomposition and partitioning
[AD-A216778] N90-18899
Optimum selection procedures in multi-stage screening, reliability, and time
[AD-A216811] N90-18942
On the depth of combinatorial optimization problems
[MEMO-803] N90-18946
OPTOELECTRONIC DEVICES
Activities report in DLR research field communication engineering and reconnaissance
[ISSN-0173-0118] N90-18781
ORBIT CALCULATION
Orbit determination of artificial Earth satellites through estmation techniques combined with state smoothing techniques
[INPE-4959-TDL/388] N90-18440
Autonomous orbit determination using GPS
[INPE-4815-TDL/361] N90-18442
Using the method of matched asymptotic expansions, analytically investigate the three-dimensional, atmosphere entry problem
[AD-A216287] N90-18451
ORBITAL ELEMENTS
Evaluation of influences of errors involved in orbit propagation of artificial satellites
[INPE-4962-TDL/391] N90-18441
ORBITAL MANEUVERS
Performance of large area xenon ion thrusters for orbit transfer missions N90-18475
ORBITAL MECHANICS
Data collection and location platforms experimental network: Description of an orbit routine
[INPE-4798-NTE/287] N90-18439
Using the method of matched asymptotic expansions, analytically investigate the three-dimensional, atmosphere entry problem
[AD-A216287] N90-18451
ORBITS
An error sensitivity model for Doppler positioning using transit satellites
[AD-A216724] N90-18381
ORGANIZATIONS
Calendar of selected aeronautical and space meetings
[AGARD-CAL-90/1] N90-19060
ORGANOMETALLIC COMPOUNDS
Perfluorinated ligands in organometallic chemistry
[AD-A216415] N90-18493
Enhanced bonding of fiber reinforcements to thermoset resins N90-18496
Reliability studies of ceramic capacitors
[AD-A216763] N90-18643
ORGANOMETALLIC POLYMERS
Electronic and ionic transport in polymers
[AD-A217028] N90-18579
ORION NEBULA
Mapping and spectroscopy of the 3.3 microns feature in Orion N90-19112
OSCILLATIONS
Unsteady Aerodynamic Phenomena in Turbomachines
[AGARD-CP-468] N90-18405
Numerical investigation of unsteady flow in oscillating turbine and compressor cascades N90-18407
Calculation of the unsteady two-dimensional, inviscid, compressible flow around a strongly cambered oscillating single blade N90-18409
Asymptotic analysis of transonic flow through oscillating cascades N90-18421
Measurement of velocity profiles and Reynolds stresses on an oscillating airfoil N90-18427
Injection parameters and beam oscillations during extraction
[NIKHEF-K/AMPS/89-07] N90-18632
Back swing phenomenon of synchronous generator. Study on ac-dc power system simulator tests
[DE89-782321] N90-18635
Experimental investigations of the unsteady boundary layer on an oscillating flat plate. Optimization and validation of a code, for calculating the potential flow/boundary layer coupling of a flat plate and of an oscillating profile
[ETN-90-96254] N90-18682
OSCILLATORS
Performance of a 500 watt Nd:GGG zigzag slab oscillator
[DE90-006263] N90-18657
OUTCROPS
Quantification of structural field data in the Rio Grande do Norte basin and neighborhood
[INPE-4821-RPE/591] N90-18826
OVENS
Signal processing device to control microwave output
[AD-A216931] N90-18648
OVERPRESSURE
Microstructural characterization of silicon nitride ceramics processed by pressureless sintering, overpressure sintering, and sinter/HIP
[DE90-007126] N90-18594
OXIDE FILMS
Interfacial chemistry of MoS2 films on Si
[AD-A216527] N90-18532
Significance of oxide skins on powder for the quality of PM Al materials
[ESA-TT-1178] N90-18560
OXIDIZERS
Space shuttle RCS oxidizer leak repair for STS-26 N90-18485
OXYGEN
Lower limits on the absolute dissociative electron attachment cross section from O2 condensed on rare-gas films
[AD-A216727] N90-18536
Millimeter-wave propagation in the mesosphere
[PB90-119868] N90-18612
Oxygen electrode in molten carbonate fuel cells
[DE90-005377] N90-18796
Design and operation of an inert gas facility for thermoelectric generator storage
[DE90-007146] N90-19008
OXYGEN ATOMS
Absolute cross-sections for dissociative electron attachment in O2 condensed on Kr films
[AD-A216730] N90-19038

P

P-N-P-N JUNCTIONS
A GaAs p-n-p-n thyristor model
[DE90-005757] N90-19039
P-TYPE SEMICONDUCTORS
Dopant site location in dual-implanted GaP using (111) planar channeling
[DE90-006565] N90-19042
PACIFIC OCEAN
Forecasters handbook for Central America and adjacent waters
[AD-A216752] N90-18845
PACKET SWITCHING
Packet telemetry standard
[ESA-PSS-04-106-ISSUE-1] N90-18447
An adaptive ARQ (Automatic Repeat Request) strategy for packet switching data communication networks
[AD-A216597] N90-18615
PAIR PRODUCTION
Antihydrogen formation in collisions of positronium with antiprotons N90-18988
Positronium formation in e+ plus H- collisions N90-18993
PARALLEL PROCESSING (COMPUTERS)
Visual servoing for autonomous aircraft refueling
[AD-A216042] N90-18388
Technology development and circuit design for a parallel laser programmable floating point application specific processor
[AD-A215870] N90-18637
Parallel memory addressing using coincident optical pulses
[AD-A216302] N90-18641
Performance characterization of the Convex C-240 computer system
[DE90-006425] N90-18879
L: A language for solution of incremental systems in a parallel processing environment
[INPE-4816-TDL/362] N90-18884
Parallel algorithms derivation
[AD-A216452] N90-18894
Derivation of efficient parallel programs: An example from genetic sequence analysis
[DE90-005654] N90-18904
Summer institute in parallel computing
[DE90-005532] N90-18910
Computation and control with neural nets
[DE90-006460] N90-18911
Speculative computation in multilisp
[AD-A216579] N90-19067

PARALLEL PROGRAMMING
Technology development and circuit design for a parallel laser programmable floating point application specific processor
[AD-A215870] N90-18637
Derivation of efficient parallel programs: An example from genetic sequence analysis
[DE90-005654] N90-18904
Speculative computation in multilisp
[AD-A216579] N90-19067

PARAMETER IDENTIFICATION
Efficient detection and signal parameter estimation with application to high dynamic GPS receiver
[NASA-CASE-NPO-17820-1-CU] N90-18379
The damage tolerance of disc materials: Metallurgical factors; relationship with processing parameters
N90-18398
Injection parameters and beam oscillations during extraction
[NIKHEF-K/AMPS/89-07] N90-18632
A global approach for the identification of structural connection properties
[NASA-TM-102502] N90-18745
Optimization of the reference parameters in the accompanying solar panel dynamics
[INPE-4795-PRE/1449] N90-18798
Connections between the circulation in altitude and convection over South America
[INPE-4923-TDL/383] N90-18828
An interactive system applied to the linear quadratic problem
[INPE-4945-TDL/386] N90-18913

PARTICLE ACCELERATORS
Computation and control with neural nets
[DE90-006460] N90-18911
Current and future uses of accelerators in particle astrophysics
[DE90-006667] N90-19186

PARTICLE BEAMS
Optically excited states in positronium N90-18985

PARTICLE COLLISIONS
Annihilation physics of exotic galactic dark matter particles N90-18984
Antihydrogen formation in collisions of positronium with antiprotons N90-18988
Positronium formation in e+ plus H- collisions
N90-18993

PARTICLE INTERACTIONS
Strongly coupled one-dimensional system and the polymer
[AD-A216330] N90-18571
Low-energy scattering of electrons and positrons in liquids N90-18981

PARTICLE MASS
Elementary particles and cosmology
[DE90-610648] N90-19177

PARTICLE MOTION
Beam collector and output window for a 35 GHz 100 kW gyrotron
[INPE-4958-RPE/603] N90-18699

PARTICLE PRECIPITATION
Airborne measurements of the electric field and the charge precipitation particles in convective clouds: Lower positive charge centres
[ESA-TT-1157] N90-18836

PARTICLE PRODUCTION
Theoretical survey on positronium formation and ionisation in positron atom scattering N90-18965
Positron scattering by atomic hydrogen using optical potentials and with positronium formation N90-18966
Positronium formation in Ss state in e+-Li scattering
N90-18967
Angular correlation studies in noble gases
N90-18972
Annihilation physics of exotic galactic dark matter particles N90-18984
Optically excited states in positronium N90-18985
Elementary particles and cosmology
[DE90-610648] N90-19177

PARTICLE SIZE DISTRIBUTION
Fluidization mechanisms in slurry flow
[DE90-006497] N90-18691

PARTICLE TRACKS
The track-etch detector for the MACRO experiment at the Gran Sasso Laboratory
[DE90-003235] N90-19182

PARTICLES
Chemistry on interstellar grains and implications for infrared spectroscopy N90-19097
Infrared diagnostics for interstellar solid state chemistry N90-19103

PASSENGER AIRCRAFT
The effects of wearing passenger protective breathing equipment on evacuation times through type 3 and type 4 emergency aircraft exits in clear air and smoke. Phase 1: Evacuations in clear air. Phase 2: Evacuations in smoke
[AD-A216798] N90-18374

PASSENGERS
The effects of wearing passenger protective breathing equipment on evacuation times through type 3 and type 4 emergency aircraft exits in clear air and smoke. Phase 1: Evacuations in clear air. Phase 2: Evacuations in smoke
[AD-A216798] N90-18374

PATTERN RECOGNITION
Recognizing three-dimensional objects without the use of models
[AD-A216766] N90-18862
Derivation of an efficient rule system pattern matcher
[AD-A216801] N90-18917
Visual target detection and recognition
[DE90-006903] N90-19015

PATTERN REGISTRATION
Spatial registration of TIROS-N weather satellite data
[AD-A216041] N90-18841
Derivation of an efficient rule system pattern matcher
[AD-A216801] N90-18917

PAYLOAD CONTROL
Payload vibration isolation in a microgravity environment
[NASA-CR-186191] N90-18744

PAYLOAD DELIVERY (STS)
Advanced APS impacts on vehicle payloads
N90-18472

PAYLOADS
Electric propulsion for manned Mars exploration
N90-18480
BEAR electrostatic analyzer: Flight results
[DE90-006511] N90-18625
Payload vibration isolation in a microgravity environment
[NASA-CR-186191] N90-18744

PECULIAR GALAXIES
Study of peculiar galaxies in the Southern Hemisphere
[INPE-4810-TDL/357] N90-19184

PEEK
Interlaminar fracture testing of carbon fibre/PEEK composites validity and applications N90-18497

PENDULUMS
Evaluation of helmet retention systems using a pendulum device
[AD-A215489] N90-18874

PERFLUORO COMPOUNDS
Perfluorinated ligands in organometallic chemistry
[AD-A216415] N90-18493

PERFORMANCE PREDICTION
The effects of wind tunnel data uncertainty on aircraft point performance predictions
[AD-A216091] N90-18387
Numerical prediction of axial turbine stage aerodynamics N90-18416
Development of a mass averaging temperature probe
N90-18418
Application of variable-gain output feedback for high-alpha control
[NASA-TM-102603] N90-18434
Performance parameter characterisation of various types of IR single element detectors N90-19161

PERFORMANCE TESTS
Research on a two-dimensional inlet for a supersonic V/STOL propulsion system. Appendix A
[NASA-CR-174945] N90-18364
The signals of an ice warning device in dependence on total water content and normalized icing degree
[DLR-FB-89-52] N90-18377
Compressor performance tests in the compressor research facility N90-18428
Transient pressure test article test program
N90-18463
Trends in VLF/LF (Very Low Frequency/Low Frequency) modem performance testing
[AD-A216576] N90-18614
A new broadband pulsed high voltage monitor
[DE90-006264] N90-18651
Performance of a 500 watt Nd:GGG zigzag slab oscillator
[DE90-006263] N90-18657
Integrated regenerative fuel cell experimental evaluation
[NASA-CR-185183] N90-18808
Anthropometry of a fit test sample used in evaluating the current and improved MCU-2/P masks
[AD-A215173] N90-18873
Evaluation of helmet retention systems using a pendulum device
[AD-A215489] N90-18874
Mechanical disturbances in high-performance superconducting dipoles
[DE90-006237] N90-19040

PERMEABILITY
Helium permeability through austenitic stainless steel
[DE90-007046] N90-18562

PERSONNEL
Airborne radar systems specialist, AFSC 118X2
[AD-A215450] N90-18611

PERSONNEL DEVELOPMENT
Airborne radar systems specialist, AFSC 118X2
[AD-A215450] N90-18611

PERTURBATION
Evaluation of influences of errors involved in orbit propagation of artificial satellites
[INPE-4962-TDL/391] N90-18441

PERTURBATION THEORY
Thermodynamics of systems with very many components phase equilibrium
[DE90-007345] N90-19059
Perturbations of test mass motion in the Schwarzschild spacetime using the method of Hamilton and Jacobi
N90-19083

PHASE CHANGE MATERIALS
Spacecraft thermal control design data, volume 3
[ESA-PSS-03-108-ISSUE-1-VOL-3] N90-18457

PHASE DIAGRAMS
Pulsed laser-induced melting of intermediate Cu-Zn phases
[DE90-005404] N90-18713
What influences order parameters across the superconducting phase boundary
[DE90-610663] N90-19047
Thermodynamics of systems with very many components phase equilibrium
[DE90-007345] N90-19059

PHASE TRANSFORMATIONS
Investigation of the phase stabilizing effect of 4 percent potassium fluoride on ammonium nitrate
[AD-A215313] N90-18599
Modeling convective Marangoni flows with void movement in the presence of solid-liquid phase change
[DE90-006474] N90-18690
Kinetic relations and the propagation of phase boundaries in solids
[AD-A215881] N90-18747
Particle physics and cosmology
[DE90-006547] N90-19171

PHENOMENOLOGY
Performance and modeling of superconducting ring resonators at millimeter-wave frequencies
[NASA-TM-102528] N90-18634

PHOSPHORS
Solid-state fluorescence above 1000 C: Application to high-temperature laser thermography
[DE90-006422] N90-18721

PHOTOCHEMICAL REACTIONS
Temperature dependence of photon-gated persistent spectral hole-burning for the meso-tetra-p-tolyl Zn-tetrabenzoporphyrin/chloroform system in poly(methylmethacrylate)
[AD-A216086] N90-18531
Ultrafast chemical dynamics of reactions in beams
[AD-A216319] N90-18717
Chemical vapor deposition and photochemical vapor deposition of amorphous silicon photovoltaic devices
[DE89-009510] N90-18803
Study of the atmospheric emissions of OI wavelength 557.7 nm and O2 (0,0) wavelength 761.9 nm in the equatorial region utilizing measurement of photometer on-board a rocket
[INPE-4811-TDL/358] N90-18827

PHOTODIODES
State of the art in semiconductor detectors
[DE90-005567] N90-18706

PHOTODISSOCIATION
Photodissociation regions: Observations and theory
N90-19098
IR line emission from dense photodissociation regions
N90-19100

PHOTOELECTRIC EFFECT
Metal coordination polymers as potential high-energy lithographic resists
[AD-A216668] N90-18574

PHOTOELECTROCHEMISTRY
Perfluorinated ligands in organometallic chemistry
[AD-A216415] N90-18493

PHOTOELECTRON SPECTROSCOPY
Understanding electronegative effects in core-level electron spectroscopies; application to the high temperature superconductors
[AD-A216728] N90-19037

PHOTOGRAPHS
Fracture analysis through photographic imagery of low spatial resolution: A contribution to the study of tectonic evolution of the Araripe Plateau region
[INPE-4876-PRE/1487] N90-18756
Recognizing three-dimensional objects without the use of models
[AD-A216766] N90-18862
PHOTOGRAPHY
Orbital remote sensing in the decade of the nineties: New approaches and challenges in geology
[INPE-4838-PRE/1467] N90-18758
PHOTOINTERPRETATION
Photointerpretation with instruments for evaluation of environmental impact: Mata Atlantica in Cubata
[INPE-4910-PRE/1511] N90-18817
PHOTOIONIZATION
Studies of atmospheric molecules by multiphoton spectroscopy
[DE90-005829] N90-18833
An implication of the IR identification of PAHs: The heating of the diffuse IS gas N90-19113
PHOTOLUMINESCENCE
Luminescence of lanthanides and actinides implanted into binary III-V semiconductors and AlGaAs
[AD-A215759] N90-19031
PHOTOMAPPING
Introduction of aerial photography in agricultural research
[BCRS-89-14] N90-18784
PHOTOMICROGRAPHY
Research project in microelectronic engineering and imaging science
[DE90-006907] N90-18653
PHOTON BEAMS
A study of the interaction of light with surfaces of sub-micron dimensions
[DE90-006646] N90-19046
PHOTONS
Persistant spectral hole-burning: Photon-gating and fundamental statistical limits
[AD-A216084] N90-18640
Angular correlation studies in noble gases N90-18972
Research in theoretical physics
[DE90-005558] N90-19001
PHOTOVOLTAIC CONVERSION
Study on the measures to promote the use of photovoltaic power generating system overseas
[DE90-742056] N90-18607
PHYSICAL EXERCISE
The role of blood volume in determining the cardiovascular adjustments to exercise N90-18654
PHYSIOLOGICAL EFFECTS
The role of blood volume in determining the cardiovascular adjustments to exercise N90-18654
Effects of pulsed and CW (Continuous Wave) 2450 MHz radiation on transformation and chromosomes of human lymphocytes in vitro
[AD-A216500] N90-18857
Fourth International Conference on Fusion Reactor Materials
[DE90-006142] N90-19025
PIEZOELECTRICITY
Development and test of power amplifiers for the driving of low-voltage piezo-actuators in multistable interferometers
[DLR-MITT-89-19] N90-18662
Piezoelectric polymer PVDF shock gauge: State of the research art
[ISL-CO-207/89] N90-18705
PILOT PERFORMANCE
Delivery performance of conventional aircraft by terminal-area, time-based air traffic control: A real-time simulation evaluation
[NASA-TP-2978] N90-18378
Three input concepts for flight crew interaction with information presented on a large-screen electronic cockpit display
[NASA-TM-4173] N90-18394
PILOT TRAINING
Proceedings of the Professional Pilots Meteorology Training Standards Conference
[AD-A216618] N90-18843
PINS
Preliminary evaluation of the strength of pin-joints in laminated composite materials
[DE90-006353] N90-18524
PIPES (TUBES)
Space shuttle RCS oxidizer leak repair for STS-26 N90-18485
Failure probability estimate of Type 304 stainless steel piping
[DE90-003696] N90-18550
PIXELS
Project Floval: Correction of relief effects in eucalyptus reforestration
[INPE-4814-RPE/590] N90-18777
PLANETARY ATMOSPHERES
IR spectroscopy of planets and satellites; Venus, Mars, giant planets, and Titan N90-19085
Measurements of the D/H ratio in planetary atmospheres by ground based infrared spectroscopy N90-19088
PLANETARY GEOLOGY
Near infrared spectroscopy of Mars: Study of the surface mineralogy N90-19091
PLANETARY NEBULAE
Airborne observations of the infrared emission bands N90-19101
Planetary nebulae N90-19122
A survey of PAH emission in HII regions, planetary and proto-planetary nebulae N90-19129
Unidentified infrared features in proto-planetary nebulae N90-19130
Dust in planetary nebulae: IRSPEC observations in the 3.0 micron-3.8 micron range N90-19132
PLANETARY ORBITS
Vector fields, linear spaces and tensors in physics. Part 3: Tensor analysis and its applications
[INPE-5000-MD/41] N90-18997
PLANNING
Optimal planning method of underground distribution system, part 2. Application to various types of system configurations
[DE89-782323] N90-18636
Approaches to the planning of coherent text
[AD-A216463] N90-18895
PLASMA COMPRESSION
High growth rate diamond synthesis in a large area atmospheric pressure inductively coupled plasma
[AD-A216090] N90-19019
PLASMA DENSITY
The lower hybrid drift instability and the evolution of plasma gradients
[DE90-006521] N90-19021
PLASMA DIAGNOSTICS
Measurement of the space potential of a high-temperature plasma by fast atomic beam scattering on an ion probe beam
[DE90-006118] N90-19020
Computerized analysis of hydrogen plasma in a compact H(sup -) cusp source
[DE90-006881] N90-19029
PLASMA EQUILIBRIUM
The free energy principle, negative energy modes, and stability
[DE90-005368] N90-19056
PLASMA FOCUS
A continuous plasma final focus
[DE90-006096] N90-19024
PLASMA PROPULSION
Test facility and preliminary performance of a 100 kW class MPD thruster N90-18476
PLASMA WAVES
Particle simulations in magnetospheric plasmas
[AD-A216256] N90-18831
Magnetic field generation by acoustic oscillations in solar atmosphere
[DE90-606054] N90-19180
PLASMAS (PHYSICS)
Streaming gravity mode instability
[DE90-610619] N90-18835
Hamiltonian analysis and simulation of free electron lasers
[INPE-4785-TDL/351] N90-19018
Development of an rf-driven plasma neutralizer for negative ions
[DE90-007298] N90-19027
Magnetohydrodynamic modeling of plasma opening switches and gas puff plasmas
[DE90-005825] N90-19028
PLASTIC DEFORMATION
Deformation and fracture of ordered intermetallic compounds
[DE90-007422] N90-18563
An objective time-integration procedure for isotropic rate-independent and rate-dependent elastic-plastic constitutive equations
[PB90-121245] N90-18925
PLASTIC PROPERTIES
An objective time-integration procedure for isotropic rate-independent and rate-dependent elastic-plastic constitutive equations
[PB90-121245] N90-18925
PLATES (STRUCTURAL MEMBERS)
Damage in a perforated graphite-epoxy composite plate under monotonic and cyclic biaxial loading
[ESA-TT-1117] N90-18521
A study of the vibrational transmission through flanged joints
[ISVR-TR-181] N90-18755
PLATES (TECTONICS)
The interpretation of crustal dynamics data in terms of plate interactions and active tectonics of the Anatolian plate and surrounding regions in the Middle East
[NASA-CR-186200] N90-18824
PLATINUM
Fundamental studies of surface processes and trace analysis using solid electrodes
[AD-A216538] N90-18533
Structure and reactivity of model thin film catalysts
[DE90-007365] N90-18546
Multicomponent glass surfaces structure and adsorption
[DE90-007179] N90-18596
PLOTTING
Model filled polymers 3. Rheological behavior of polystyrene containing crosslinked polystyrene beads
[AD-A215867] N90-18567
A numerical solution to the Boltzmann equation for use in calculating pumping rates in a CO2 discharge laser
[AD-A216376] N90-18718
PLOWING
Evaluation of two methods for acquisition of training statistics for digital analysis of areas prepared for plowing
[INPE-4901-PRE/1502] N90-18763
PLY ORIENTATION
A statistical evaluation of the variation in laminated composite properties resulting from ply misalignment
[DE90-006371] N90-18525
POINT DEFECTS
Ion implantation-induced amorphization of ceramic oxides
[DE90-006564] N90-19041
POINT SOURCES
Research in theoretical physics
[DE90-005558] N90-19001
IRCAM observations of the Reipurth 50 IR source N90-19119
POINTING CONTROL SYSTEMS
Preliminary design of a pointer for movement of a solar simulator
[INPE-4864-TDL/375] N90-18736
POLARIMETERS
Spectropolarimetry as a diagnostic of the interstellar medium N90-19096
POLARIZATION (WAVES)
Millimeter-wave propagation in the mesosphere
[PB90-119868] N90-18612
New parameter-free polarization potentials in low-energy positron collisions N90-18968
POLARIZATION CHARACTERISTICS
Development and polarization of ferroelectric polymer gauges, for dynamical acceleration experiments, as those in ballistics shocks
[ISL-R-119/88] N90-18703
POLARIZED ELECTROMAGNETIC RADIATION
The extended equivalent source technique with underdetermined sources
[DE90-006989] N90-18627
POLITICS
Remote sensing applied to vegetation as subsidized in municipal planning
[INPE-4908-PRE/1509] N90-18770
POLLUTION
Application of high performance liquid chromatography/mass spectrometry to environmental analysis
[PB90-116963] N90-18814
POLLUTION MONITORING
Application of high performance liquid chromatography/mass spectrometry to environmental analysis
[PB90-116963] N90-18814
POLYATOMIC MOLECULES
IR spectrophotometry of bright carbon stars N90-19131
POLYBUTADIENE
Morphological consequences of catalytic hydrogenation of polymers in the bulk
[DE90-007276] N90-18598
POLYCRYSTALS
Fundamental studies of surface processes and trace analysis using solid electrodes
[AD-A216538] N90-18533
Research relating to crystalline silicon-film on a foreign substrate
[DE90-005720] N90-18582
High growth rate diamond synthesis in a large area atmospheric pressure inductively coupled plasma
[AD-A216090] N90-19019

The interaction of polycrystalline copper films with dilute aqueous solutions of cupric chloride
[AD-A216465] N90-19033

POLYESTER RESINS
Instrumented impact testing of fabric-reinforced composite materials
[AD-A216764] N90-18513

POLYETHYLENES
Extracting chemical information form Auger line shapes
[AD-A216729] N90-18537

POLYGONS
Grouping for recognition
[AD-A216716] N90-18915

POLYMER BLENDS
Control of phase structure in polymer blends
[AD-A217034] N90-18580

POLYMER CHEMISTRY
Laboratory for the processing and evaluation of inorganic matrix composites
[AD-A216681] N90-18516
Dynamics and stabilization of materials possessing high energy content
[AD-A216320] N90-18570

POLYMERIC FILMS
Electronic and ionic transport in polymers
[AD-A217028] N90-18579
Cell performance of ultra-thin polymer cathode systems. Part 1: Anion intercalating polymer cathode
[AD-A216037] N90-18639

POLYMERIZATION
Perforated monolayers
[DE90-005469] N90-18566
Polymerization of nitro compounds on silver surfaces during surface-enhanced Raman scattering
[AD-A216116] N90-18569
Electrochemical investigations of novel solid redox polymerization electrodes
[DE90-006087] N90-18584
Morphological consequences of catalytic hydrogenation of polymers in the bulk
[DE90-007276] N90-18598

POLYMERS
Heat capacities of solid polymers (The Advanced THermal Analysis System, ATHAS)
[DE90-007130] N90-18595
A study on deformation and break-up of dispersed particles in elongational flow
[ETN-90-96268] N90-18684

POLYMORPHISM
Investigation of the phase stabilizing effect of 4 percent potassium fluoride on ammonium nitrate
[AD-A215313] N90-18599

POLYNOMIALS
Efficient preconditioning for the p-version finite element method in two dimensions
[AD-A216210] N90-18928
Finding critical independent sets and critical vertex subsets are polynomial problems
[AD-A216547] N90-18936

POLYSTYRENE
Investigation of multiple scattering in aqueous suspensions of non-absorbing polystrene microspheres using spectrophotometry
[BCRS-89-09] N90-18549
Model filled polymers 3. Rheological behavior of polystyrene containing crosslinked polystyrene beads
[AD-A215867] N90-18567

POLYVINYL FLUORIDE
Piezoelectric polymer PVDF shock gauge: State of the research art
[ISL-CO-207/89] N90-18705

POROSITY
Perforated monolayers
[DE90-005469] N90-18566

POSITION (LOCATION)
Practical applications of Loran-C for land mobile use or the possibility to use Loran-C as a vehicle-location or vehicle-navigation system
[ETN-90-96265] N90-18384
Data collection and location platforms experimental network: Description of an orbit routine
[INPE-4798-NTE/287] N90-18439

POSITION ERRORS
An error sensitivity model for Doppler positioning using transit satellites
[AD-A216724] N90-18381

POSITIONING
Optimization of sensors and actuators positioning aimed at obtaining reduced models for the synthesis of optimal control regulators of flexible structures
[INPE-4760-TDL/348] N90-18450
Robot crane technology program
[PB90-111667] N90-18734

POSITRON ANNIHILATION
Inelastic scattering of positrons with sodium
N90-18961
GRIS observations of the Galactic Center
N90-18982
Positron annihilation in gamma-ray bursts N90-18983
Positronium ions and molecules N90-18990
Positron annihilation induced Auger electron spectroscopy N90-18996

POSITRONIUM
Annihilation in Gases and Galaxies
[NASA-CP-3058] N90-18957
Inelastic collisions of positrons with one-valence-electron targets N90-18963
Theoretical survey on positronium formation and ionisation in positron atom scattering N90-18965
Positronium formation in Ss state in e+-Li scattering
N90-18967
Positronium reflection and positronium beams
N90-18980
Optically excited states in positronium N90-18985
Stark and Zeeman effects on laser cooling of positronium N90-18986
Decay rate and other properties of the positronium negative ion N90-18987
Antihydrogen formation in collisions of positronium with antiprotons N90-18988
Positronium ions and molecules N90-18990
Positronium formation in e+ plus H- collisions
N90-18993

POSITRONS
Annihilation in Gases and Galaxies
[NASA-CP-3058] N90-18957
Positron-alkali atom scattering N90-18958
Scattering of positrons and electrons by alkali atoms
N90-18959
Elastic scattering of e- and e+ from Rb and Cd
N90-18960
Positron collisions with alkali-metal atoms
N90-18962
Inelastic collisions of positrons with one-valence-electron targets N90-18963
Positron-rubidium scattering N90-18964
Positron scattering by atomic hydrogen using optical potentials and with positronium formation N90-18966
New parameter-free polarization potentials in low-energy positron collisions N90-18968
The calculation of the contributions to low energy e+H2 scattering from sigma u+ and Pion u symmetries using the Kohn variational method N90-18969
Ab initio R-matrix calculations of e+-molecule scattering N90-18970
Numerical Green's functions in optical potential calculations for positron scattering from argon and neon
N90-18971
Positron excitation of neon N90-18973
Positron-inert gas differential elastic scattering
N90-18974
Differential elastic scattering cross sections for 54.9eV positrons incident on helium N90-18975
Total cross sections for positrons scattered elastically from helium based on new measurements of total ionization cross sections N90-18976
Ionisation of atomic hydrogen by positron impact
N90-18977
Multiple-ionization of xenon atoms by positron impact
N90-18978
Double ionization of helium by particle impact
N90-18979
Low-energy scattering of electrons and positrons in liquids N90-18981
Search for resonances in positron-atom systems
N90-18991
Resonances in low-energy positron-alkali scattering
N90-18992
Positron-molecule bound states and positive ion production N90-18994
Initial results of positron ionization mass spectrometry
N90-18995

POTASSIUM COMPOUNDS
Investigation of the phase stabilizing effect of 4 percent potassium fluoride on ammonium nitrate
[AD-A215313] N90-18599

POTASSIUM OXIDES
In situ growth of epitaxial superconducting YBa2Cu3O(7-x) films on insulating semiconducting and ferroelectric K(Ta, Nb)O3 by pulsed laser ablation
[DE90-006568] N90-19043

POTENTIAL ENERGY
Numerical Green's functions in optical potential calculations for positron scattering from argon and neon
N90-18971

POTENTIAL FLOW
Aerodynamics of unsteady systems. Numerical study of potential flow/boundary layer coupling
[ETN-90-96257] N90-18367
Experimental investigations of the unsteady boundary layer on an oscillating flat plate. Optimization and validation of a code, for calculating the potential flow/boundary layer coupling of a flat plate and of an oscillating profile
[ETN-90-96254] N90-18682

POWDER (PARTICLES)
Synthesis of high-purity sinterable silicon nitride powder
[DE90-007050] N90-18593
Analysis of propulsive powder combustion products and their corrosive effects
[ISL-CO-248/88] N90-18605

POWDER METALLURGY
Significance of oxide skins on powder for the quality of PM Al materials
[ESA-TT-1178] N90-18560

POWDERED ALUMINUM
Significance of oxide skins on powder for the quality of PM Al materials
[ESA-TT-1178] N90-18560

POWER AMPLIFIERS
Output performance of idealized microwave power amplifiers
[AD-A216797] N90-18645
Development and test of power amplifiers for the driving of low-voltage piezo-actuators in multistable interferometers
[DLR-MITT-89-19] N90-18662

PRANDTL NUMBER
Multicellular natural convection in a narrow vertical slot
[AD-A216411] N90-18668

PRECAMBRIAN PERIOD
The patterns of fracture and the conditioning tectonics in the region of the Quadrilatero Ferrifero and part of the Migmatitic-Gnanulitic Complex in Minas Gerais (Brazil)
[INPE-4895-PRE/1496] N90-18829

PRECIPITATION (METEOROLOGY)
Intertropical Convergence Zone (ITCZ) and its relationship with the precipitation of the north-northeast Brazilian region
[INPE-4887-TDL/378] N90-18839

PRECIPITATION PARTICLE MEASUREMENT
Airborne measurements of the electric field and the charge precipitation particles in convective clouds: Lower positive charge centres
[ESA-TT-1157] N90-18836

PRECONDITIONING
Efficient preconditioning for the p-version finite element method in two dimensions
[AD-A216210] N90-18928

PREDICTION ANALYSIS TECHNIQUES
The effects of wind tunnel data uncertainty on aircraft point performance predictions
[AD-A216091] N90-18387
Numerical investigation of unsteady flow in oscillating turbine and compressor cascades N90-18407
Development of an experimental space station model for structural dynamics research
[NASA-TM-102601] N90-18751

PREPROCESSING
Geometric correction models for HRV-SPOT images
[INPE-5001-TDL/395] N90-18757

PRESSURE
Measurements of surface pressures on an operating vertical-axis wind turbine
[DE90-005722] N90-18805

PRESSURE DISTRIBUTION
Supersonic wind tunnel investigation of a tubular projectile
[ISL-CO-306/89] N90-18366

PRESSURE EFFECTS
Transient pressure test article test program
N90-18463
Study of the dynamical behavior of copper in a shock wave
[ISL-R-123/88] N90-18679

PRESSURE GRADIENTS
Numerical simulation of the incompressible inhomogeneous turbulence in a plane channel flow
[ONERA-NT-1988-5] N90-18686

PRESSURE MEASUREMENT
Aerodynamic testing of a rotating wind turbine blade
[DE90-000312] N90-18362
Methods for making unsteady aerodynamic pressure measurements in a rotating turbine stage N90-18426
Piezoelectric polymer PVDF shock gauge: State of the research art
[ISL-CO-207/89] N90-18705
Measurements of surface pressures on an operating vertical-axis wind turbine
[DE90-005722] N90-18805

PRESSURE OSCILLATIONS
Wick-type liquid-metal combustion
[AD-A216019] N90-18530

PRESSURE RATIO
Experiments on the unsteady flow in a supersonic compressor stage N90-18422
PRESSURE REGULATORS
Electronically Variable Pressure Regulator (EVPR) N90-18484
PRESSURE SENSORS
Zero-gravity vortex vent and PVT gaging system N90-18486
PRINTED CIRCUITS
Ion chromatography in the manufacture of multilayer circuit boards
[DE90-005560] N90-18652
PROBABILITY DISTRIBUTION FUNCTIONS
Strong moderate deviation theorems
[MEMO-804] N90-18954
PROBABILITY THEORY
Probability of failure and risk assessment of propulsion structural components N90-18470
Failure probability estimate of Type 304 stainless steel piping
[DE90-003896] N90-18550
Multistage forest volume estimation using a sampling system with probability variables
[INPE-4897-PRE/1498] N90-18769
A comparison of void distributions in Abell cluster catalogue with numerical simulations
[DE90-610640] N90-19173
PROBLEM SOLVING
An approach centered in production rules for a partition of environment and planning in a visual navigation system (SNV)
[INPE-4813-TDL/360] N90-18737
An integrated vision on methodologies and environments for modeling and simulation assisted by computer
[INPE-4861-TDL/372] N90-18886
Differential-geometric techniques for solving differential algebraic equations
[AD-A216503] N90-18934
The formation and use of knowledge structures in problem solving domains
[AD-A216512] N90-18936
Finding critical independent sets and critical vertex subsets are polynomial problems
[AD-A216547] N90-18938
Schema-based theories of problem solving
[AD-A216717] N90-18939
PROCESS CONTROL (INDUSTRY)
Application of artificial intelligence control to the vapor-liquid-solid silicon carbide whisker process
[DE90-007835] N90-18519
Control of phase structure in polymer blends
[AD-A217034] N90-18580
Optimum catalytic process for alcohol fuels from syngas
[DE90-007188] N90-18604
Ion chromatography in the manufacture of multilayer circuit boards
[DE90-005560] N90-18652
PROCUREMENT POLICY
Component selection, procurement and control for ESA space systems
[ESA-PSS-01-60-ISSUE-2] N90-19062
PRODUCT DEVELOPMENT
French approach to space technology transfer N90-19074
Identification of and response to market demand N90-19078
An example of technology transfer by Aerospatiale: Fire protection materials N90-19082
PRODUCTION ENGINEERING
The Executive Workshop on Cost/Performance Measurement. Volume 1: Executive summary
[AD-A216745] N90-18898
PRODUCTIVITY
National airspace system plan: Facilities, equipment, associated development and other capital needs
[AD-A215882] N90-18373
A perspective of software reuse
[AD-A216911] N90-18901
PROGRAMMING (SCHEDULING)
Ada-Linda preliminary report: Motivation, informal description, and examples
[AD-A216004] N90-18892
PROGRAMMING LANGUAGES
Derivation of efficient parallel programs: An example from genetic sequence analysis
[DE90-005654] N90-18904
RALPH: An automatic Robot Assembly Language Programmer: An overview
[PB90-120973] N90-18912
Speculative computation in multilisp
[AD-A216579] N90-19067
PROJECT MANAGEMENT
Long term planning for space flight activities within the DFVLR
[DFVLR-IB-303-88/2] N90-18438
Refurbishment and modification of the Metric Camera (RMK) for reflight on EOM-1 Spacelab mission
[ETN-90-96284] N90-18710
Activities report in German aerospace
[ISSN-0070-3966] N90-19189
PROJECTILES
Supersonic wind tunnel investigation of a tubular projectile
[ISL-CO-306/89] N90-18366
Measurement of gas leaks between a projectile and the walls of a tube in a ballistic compressor
[ISL-CO-250/88] N90-18694
Effects of oblique impact on hypervelocity shield performance
[DE90-006936] N90-18739
PROPELLANT ADDITIVES
Investigation of the phase stabilizing effect of 4 percent potassium fluoride on ammonium nitrate
[AD-A215313] N90-18599
PROPELLANT COMBUSTION
Test data of flow field of shuttle SRM nozzle joint with bond defects, using unheated air N90-18464
PROPELLANT STORAGE
Investigation of the phase stabilizing effect of 4 percent potassium fluoride on ammonium nitrate
[AD-A215313] N90-18599
PROPELLANT TRANSFER
Orbital fluid resupply assessment N90-18487
PROPELLANTS
Effect of propellant flowrate and purity on carbon deposition in LO2/methane gas generators N90-18468
PROPORTIONAL CONTROL
Discrete proportional Plus Integral (PI) multivariable control laws for the Control Reconfigurable Combat Aircraft (CRCA)
[AD-A215664] N90-18431
PROPULSION
AFOSR/ONR (Air Force Office of Scientific Research/Office of Naval Research) Contractors' Meeting on Combustion Rocket Propulsion Diagnostics of Reacting Flow
[AD-A216094] N90-18491
PROPULSION SYSTEM CONFIGURATIONS
The 1989 JANNAF Propulsion Meeting, volume 1
[CPIA-PUBL-515-VOL-1] N90-18462
A perspective on the use of storable propellants for future space vehicle propulsion N90-18473
Electric propulsion options for 10 kW class earth-space missions N90-18474
Performance of large area xenon ion thrusters for orbit transfer missions N90-18475
Mission options for an electric propulsion demonstration flight test N90-18479
Electric propulsion for manned Mars exploration N90-18480
PROPULSION SYSTEM PERFORMANCE
Advanced APS impacts on vehicle payloads N90-18472
Electric propulsion options for 10 kW class earth-space missions N90-18474
Performance of large area xenon ion thrusters for orbit transfer missions N90-18475
Test facility and preliminary performance of a 100 kW class MPD thruster N90-18476
Mission options for an electric propulsion demonstration flight test N90-18479
Electric propulsion for manned Mars exploration N90-18480
PROPULSIVE EFFICIENCY
Advanced APS impacts on vehicle payloads N90-18472
PROPYL COMPOUNDS
Determination of the minimum energy conformation of alkyl substituted pyrazines
[AD-A216974] N90-18539
PROSTAGLANDINS
A program for the study of skeletal muscle catabolism following physical trauma
[AD-A216589] N90-18859
PROTECTIVE CLOTHING
Anthropometry of a fit test sample used in evaluating the current and improved MCU-2/P masks
[AD-A215173] N90-18873
PROTECTIVE COATINGS
Sputter deposition of diffusion barrier coatings on SiC monofilaments for use in Ti-based composites N90-18502
PROTEINS
Characterization of biopolymer surfaces using scanning microscopies
[AD-A216572] N90-18572
A program for the study of skeletal muscle catabolism following physical trauma
[AD-A216589] N90-18859
Study of rifampicin fixation on plasma proteins by derivative spectrophotometry
[CERMA-89-25] N90-18866
PROTON IMPACT
Double ionization of helium by particle impact N90-18979
PROTONS
Solid-state proton conductors
[DE90-007595] N90-18812
PROTOPLANETS
A survey of PAH emission in HII regions, planetary and proto-planetary nebulae N90-19129
Unidentified infrared features in proto-planetary nebulae N90-19130
PROTOSTARS
The infrared spectral signature of star formation N90-19114
PROTOTYPES
Space station technology summary N90-18482
Electronically Variable Pressure Regulator (EVPR) N90-18484
Zero-gravity vortex vent and PVT gaging system N90-18486
Small displacement, long life on-orbit compressor design and fabrication N90-18489
PSYCHOLOGICAL FACTORS
Systematicity as a selection constraint in analogical mapping
[AD-A216029] N90-18869
PSYCHOLOGICAL TESTS
Systematicity as a selection constraint in analogical mapping
[AD-A216029] N90-18869
Appropriateness measurement for computerized adaptive tests
[AD-A216121] N90-18870
PSYCHOPHYSICS
A self-organizing multiple-view representation of three-dimensional objects
[AD-A216711] N90-18871
Psychological studies of visual cortical function
[AD-A217029] N90-18872
PULSE COMPRESSION
Improved amorphous metal materials for magnetic pulse compression
[DE90-005723] N90-18555
Coating possibilities for magnetic switches
[DE90-006536] N90-18659
PULSE DURATION MODULATION
Instability investigation for storage mode. Microwave instability (single-bunch instability)
[NIKHEF-K/AMPS/89/05] N90-18628
PULSED LASERS
Cineholography: A relation between the coherence length of the laser and the object velocity
[ISL-CO-234/88] N90-18724
Effects produced by pulsed CO2 lasers
[ISL-R-112/88] N90-18731
Pulsed laser deposition of high T(sub c) superconducting thin films
[AD-A216507] N90-19034
In situ growth of epitaxial superconducting YBa2Cu3O(7-x) films on insulating semiconducting and ferroelectric K(Ta, Nb)O3 by pulsed laser ablation
[DE90-006568] N90-19043
In situ growth of high quality epitaxial YBa2Cu3O(7-x) thin films at moderate temperatures by pulsed laser ablation
[DE90-006629] N90-19045
PULSED RADIATION
Effects of pulsed and CW (Continuous Wave) 2450 MHz radiation on transformation and chromosomes of human lymphocytes in vitro
[AD-A216500] N90-18857
PUMPS
Study on the thermodynamical and mechanical conditions for the generation of high operating pressures with liquefied gases for low and very low flow rates
[ESA-TT-1148] N90-18696
PURITY
Effect of propellant flowrate and purity on carbon deposition in LO2/methane gas generators N90-18468
PYRAZINES
Determination of the minimum energy conformation of alkyl substituted pyrazines
[AD-A216974] N90-18539
PYROLYSIS
Silicon carbo-nitride ceramic matrix composites by polymer pyrolysis N90-18499
Hawaii integrated biofuels research program, phase 1
[DE90-006885] N90-18811

PYROTECHNICS
Analysis of propulsive powder combustion products and their corrosive effects
[ISL-CO-248/88] N90-18605
PYRROLES
Electronic and ionic transport in polymers
[AD-A217028] N90-18579

Q

QUADRATIC EQUATIONS
Approximations to joint distributions of definite quadratic forms
[AD-A216434] N90-18930
QUANTITATIVE ANALYSIS
Extracting chemical information form Auger line shapes
[AD-A216729] N90-18537
Evaluation of a commercial gas chromatography/matrix isolation-infrared spectrometer for quantitative analysis of priority pollutants
[DE90-006033] N90-18542
Erosion monitoring using remote sensing, part 2
[BCRS-89-15] N90-18785
Variations in volatiles in magma bodies based on studies of melt inclusions
[DE90-006272] N90-18821
QUANTUM EFFICIENCY
Radiation-hard high-efficiency InP space solar cell development
[AD-A216857] N90-18800
QUANTUM THEORY
Theoretical and experimental high energy physics
[DE90-006168] N90-19006
Transport effects and spectroscopy of defects in microstructures
[AD-A216718] N90-19036
Spectral functions from Quantum Monte Carlo
[DE90-004870] N90-19050
Geometric continuum regularization of quantum field theory
[DE90-006099] N90-19058
Quantum cosmological origin of large scale structures of the universe
[DE90-610647] N90-19176
QUASARS
H-alpha emission lines in high redshift quasars N90-19149
QUENCHING (ATOMIC PHYSICS)
Stark and Zeeman effects on laser cooling of positronium N90-18986
QUERY LANGUAGES
Guidelines for the use of the SAME
[AD-A215846] N90-18888
A human factors experimental comparison of two database query languages N90-19064
QUEUEING THEORY
A survey of performability modelling tools
[MEMO-INF-89-50] N90-18907
Using dynamic queueing networks as a tool for specifying performability models
[MEMO-INF-89-51] N90-18949
Recurrence conditions for average and Blackwell optimality in denumerable state Markov decision chains
[TW-89-02] N90-18952

R

RADAR
Navigation experiment NAVEX data storage and processing
[ESA-TT-1175] N90-18445
RADAR DATA
Applications of acousto-optical correlation devices in radar signal processing
[AD-A216624] N90-18616
Simulation of synthetic aperture radar 3: Evaluation of prototype digital feature analysis data
[AD-A216750] N90-18620
RADAR IMAGERY
Synthetic aperture radar imagery of airports and surrounding areas: Archived SAR data
[NASA-CR-4275] N90-18371
Synthetic aperture radar imagery of airports and surrounding areas: Philadelphia Airport
[NASA-CR-4280] N90-18372
Simulation of synthetic aperture radar 3: Evaluation of prototype digital feature analysis data
[AD-A216750] N90-18620
Orbital remote sensing in the decade of the nineties: New approaches and challenges in geology
[INPE-4838-PRE/1467] N90-18758
RADAR MAPS
Simulation of synthetic aperture radar 3: Evaluation of prototype digital feature analysis data
[AD-A216750] N90-18620
RADAR NETWORKS
Multitarget tracking by single sensor: Analysis of the main approaches developed in this area
[ESA-TT-1171] N90-18633
RADAR RESOLUTION
On the range resolution of point targets with FMCW radar systems
[DLR-FB-89-47] N90-18629
RADAR SCATTERING
Synthetic aperture radar imagery of airports and surrounding areas: Archived SAR data
[NASA-CR-4275] N90-18371
RADIANCE
Project Floval: Correction of relief effects in eucalyptus reforestration
[INPE-4814-RPE/590] N90-18777
RADIATION ABSORPTION
Microwave radiation absorption by Ho(Y)-Ba-Cu-O superconducting ceramics
[DE90-610665] N90-18588
Research in theoretical physics
[DE90-005558] N90-19001
RADIATION COUNTERS
The track-etch detector for the MACRO experiment at the Gran Sasso Laboratory
[DE90-003235] N90-19182
RADIATION DETECTORS
Underground muon observations in the Soudan 2 detector
[DE90-005647] N90-19183
RADIATION DOSAGE
Effects of pulsed and CW (Continuous Wave) 2450 MHz radiation on transformation and chromosomes of human lymphocytes in vitro
[AD-A216500] N90-18857
Performance of a coincidence based blood activity monitor
[DE90-006105] N90-18865
RADIATION EFFECTS
Response of unirradiated and neutron-irradiated vanadium alloys to Charpy-impact loading
[DE90-004878] N90-18551
Effects of pulsed and CW (Continuous Wave) 2450 MHz radiation on transformation and chromosomes of human lymphocytes in vitro
[AD-A216500] N90-18857
Fourth International Conference on Fusion Reactor Materials
[DE90-006142] N90-19025
RADIATION HARDENING
Radiation-hard high-efficiency InP space solar cell development
[AD-A216857] N90-18800
A GaAs p-n-p-n thyristor model
[DE90-005757] N90-19039
RADIATION HAZARDS
Safety analysis for the Galileo light-weight radioisotope heater unit
[DE90-007147] N90-19009
RADIATION PROTECTION
Space nuclear safety program
[DE90-006436] N90-19007
RADIATIVE HEAT TRANSFER
Spacecraft thermal control design data, volume 1
[ESA-PSS-03-108-ISSUE-1-VOL-1] N90-18455
Condensation fluid dynamics and heat transfer on rotating spherical surfaces in a microgravitational field
[DE90-005540] N90-18607
RADIO ALTIMETERS
An evaluation of an airborne laser profiling system for high precision terrain mapping
[AD-A217025] N90-18780
RADIO ASTRONOMY
Study of peculiar galaxies in the Southern Hemisphere
[INPE-4810-TDL/357] N90-19184
RADIO EMISSION
Study of peculiar galaxies in the Southern Hemisphere
[INPE-4810-TDL/357] N90-19184
RADIO FREQUENCIES
RF modal quantity gaging N90-18483
ACIRF user's guide: Theory and examples
[AD-A216436] N90-18613
RADIO FREQUENCY DISCHARGE
Hydrogenated amorphous and microcrystalline silicon deposited from silane-hydrogen mixtures
[ETN-90-96267] N90-18590
RADIO FREQUENCY INTERFERENCE
Radio interference in the near-earth environment
[NASA-CR-180479] N90-18623
RADIO PROBING
Preliminary comparison of temperature soundings obtained from simultaneous radiometric, radio-acoustic, and rawinsonde measurements
[PB90-119835] N90-18838
RADIO SIGNALS
Navigation experiment NAVEX: The self-test delay times in the D1 Spacelab mission
[ESA-TT-1176] N90-18448
RADIO SOURCES (ASTRONOMY)
The correlation between radio and far-infrared emission for disk galaxies N90-19158
RADIOACTIVE DECAY
Helium permeability through austenitic stainless steel
[DE90-007046] N90-18562
Underground muon observations in the Soudan 2 detector
[DE90-005647] N90-19183
RADIOACTIVE ISOTOPES
Performance of a coincidence based blood activity monitor
[DE90-006105] N90-18865
RADIOACTIVITY
Performance of a coincidence based blood activity monitor
[DE90-006105] N90-18865
RADIOGRAPHY
Damage in a perforated graphite-epoxy composite plate under monotonic and cyclic biaxial loading
[ESA-TT-1117] N90-18521
RADIOMETERS
Radiometric study of wheat and bean crops in three types of latossolo
[INPE-4843-PRE/1472] N90-18767
Spectral response of wheat and its relationship with agronomical prameters
[INPE-4950-RPE/599] N90-18774
RADIOMETRIC RESOLUTION
Interrelationship of spatial and radiometric resolution in the thermal infrared band
[INPE-4860-TDL/371] N90-18771
RAIN
Remote sensing and run-off modelling in the Lake Victoria Basin, Kenya
[BCRS-89-19] N90-18788
RAMAN SPECTRA
Polymerization of nitro compounds on silver surfaces during surface-enhanced Raman scattering
[AD-A216116] N90-18569
RANDOM NOISE
Adaptive state estimation and sampling rate analysis for invariant linear dynamic systems in time
[INPE-4960-TDL/389] N90-18951
RANDOM SIGNALS
Kreim factorization of covariance operators of 2-parameter random fields and application to the likelihood ratio
[MEMO-802] N90-18953
RANGEFINDING
On the range resolution of point targets with FMCW radar systems
[DLR-FB-89-47] N90-18629
RANKINE-HUGONIOT RELATION
Interaction of minor ions with fast and slow shocks
[NASA-CR-186372] N90-19181
RARE EARTH ALLOYS
Fundamental studies of new magnetic heterostructures: Their growth, crystallographic structure, magnetic, and electronic properties
[DE90-007381] N90-19053
RARE EARTH COMPOUNDS
Luminescence of lanthanides and actinides implanted into binary III-V semiconductors and AlGaAs
[AD-A215759] N90-19031
RARE GASES
Absorption experiments on electron-beam pumped rare gases
[DE90-006504] N90-18722
Angular correlation studies in noble gases N90-18972
Positron-inert gas differential elastic scattering N90-18974
Absolute cross-sections for dissociative electron attachment in O2 condensed on Kr films
[AD-A216730] N90-19038
RATES (PER TIME)
Rate compatible punctured codes, their use in military satellite communication systems
[AD-A216723] N90-18619
RAWINSONDES
Preliminary comparison of temperature soundings obtained from simultaneous radiometric, radio-acoustic, and rawinsonde measurements
[PB90-119835] N90-18838

RAYLEIGH WAVES
The propagation of time harmonic Rayleigh-Lamb waves in a bimaterial plate
[AD-A216834] N90-18749
REACTION KINETICS
High temperature interaction of SO2 with oxide sorbents
[DE90-000435] N90-18545
Pulsed laser-induced melting of intermediate Cu-Zn phases
[DE90-005404] N90-18713
Ultrafast chemical dynamics of reactions in beams
[AD-A216319] N90-18717
Kinetic relations and the propagation of phase boundaries in solids
[AD-A215881] N90-18747
The interaction of polycrystalline copper films with dilute aqueous solutions of cupric chloride
[AD-A216465] N90-19033
REACTIVITY
Structure and reactivity of model thin film catalysts
[DE90-007365] N90-18546
REACTOR MATERIALS
Fourth International Conference on Fusion Reactor Materials
[DE90-006142] N90-19025
REACTOR SAFETY
Space nuclear safety program
[DE90-006436] N90-19007
REACTOR TECHNOLOGY
Failure probability estimate of Type 304 stainless steel piping
[DE90-003896] N90-18550
READ-ONLY MEMORY DEVICES
Technology development and circuit design for a parallel laser programmable floating point application specific processor
[AD-A215870] N90-18637
REAL TIME OPERATION
Delivery performance of conventional aircraft by terminal-area, time-based air traffic control: A real-time simulation evaluation
[NASA-TP-2978] N90-18378
SHARP: A multi-mission artificial intelligence system for spacecraft telemetry monitoring and diagnosis
[NASA-CR-186285] N90-18444
Ultrafast chemical dynamics of reactions in beams
[AD-A216319] N90-18717
Comparisons between the RTNEPH (Real-Time Nephanalysis) and AFGL cloud layer analysis algorithms
[AD-A216637] N90-18844
RECEIVERS
Efficient detection and signal parameter estimation with application to high dynamic GPS receiver
[NASA-CASE-NPO-17820-1-CU] N90-18379
RECIPROCAL THEOREMS
Vector fields, linear spaces and tensors in physics. Part 3: Tensor analysis and its applications
[INPE-5000-MD/41] N90-18997
RECIRCULATIVE FLUID FLOW
Theoretical investigation of the stabilization of a diffusion flame above a recirculation region
[ESA-TT-1149] N90-18543
Continuous hydroponic wheat production using a recirculating system
[NASA-TM-102784] N90-18853
RECONNAISSANCE
Development of the agricultural information system. Characteristics and results of the Distrito Federal model
[INPE-4940-PRE/1430] N90-18773
RECOVERY
Stall and recovery in multistage axial flow compressors N90-18429
RECRYSTALLIZATION
Softening mechanisms and microstructural instabilities during high temperature, low cycle fatigue of Ni, Ni3Al, and their metal matrix composites
[DE90-006487] N90-18557
RED SHIFT
Near infrared (1-4 micron) spectroscopy of SN1987A N90-19133
Near infrared spectroscopy of active galaxies N90-19143
H-alpha emission lines in high redshift quasars N90-19149
A comparison of void distributions in Abell cluster catalogue with numerical simulations
[DE90-610640] N90-19173
A new interpretation of the feature of SiO maser spectra associated with M-type star
[DE90-610641] N90-19174
REDUCED GRAVITY
Zero-gravity vortex vent and PVT gaging system N90-18486
Investigation of methods to produce a uniform cloud of fuel particles in a flame tube
[NASA-TM-102376] N90-18665
Payload vibration isolation in a microgravity environment
[NASA-CR-186191] N90-18744
REDUCTION (CHEMISTRY)
Perfluorinated ligands in organometallic chemistry
[AD-A216415] N90-18493
REDUNDANCY
A perspective of software reuse
[AD-A216911] N90-18901
REENTRY EFFECTS
Analytical formulation for the interaction problem of dynamic reentry, and effects due to flexibility and vibration in an aerospace vehicle
[INPE-4963-TDL/392] N90-18448
REENTRY TRAJECTORIES
Using the method of matched asymptotic expansions, analytically investigate the three-dimensional, atmosphere entry problem
[AD-A216287] N90-18451
REFLECTION
The propagation of time harmonic Rayleigh-Lamb waves in a bimaterial plate
[AD-A216834] N90-18749
REFLECTION NEBULAE
Polycyclic aromatic hydrocarbons in the infrared spectra of IRAS sources N90-19105
IRCAM observations of the Reipurth 50 IR source N90-19119
REFORESTATION
Monitoring of reforested areas through digital analysis of TM data
[INPE-4930-PRE/1420] N90-18764
Project Floval: Correction of relief effects in eucalyptus reforestration
[INPE-4814-RPE/590] N90-18777
REFRACTIVITY
Measurement of gas intensity at high dynamic pressures
[ISL-CO-204/89] N90-18680
A simulation of optical propagation through atmospheric turbulence using two-dimensional Fourier transform techniques
[AD-A216776] N90-19013
REFRACTORIES
Ceramic matrix composites, new high performance materials N90-18500
REFRACTORY COATINGS
Continuous preparation of a thin refractory carbide deposit on the surface of carbon fibers: Characterization of the C/SiC fiber N90-18501
Metallaboranes as precursors to metallic glasses
[AD-A216946] N90-18577
REFRACTORY MATERIALS
The processing and mechanical properties of high temperature/high performance composites. Book 3, section 2: Strength and fracture resistance, part
[AD-A216143] N90-18508
REFRIGERATING
Intermittent Solar Ammonia Absorption Cycle (ISAAC) refrigeration for lesser developed countries
[DE90-006700] N90-18610
REGENERATIVE COOLING
Spacecraft thermal control design data, volume 4
[ESA-PSS-03-108-ISSUE-1-VOL-4] N90-18458
REGENERATIVE FUEL CELLS
Integrated regenerative fuel cell experimental evaluation
[NASA-CR-185183] N90-18808
REGRESSION ANALYSIS
TVI: A mathematical model for global estimation of Brazilian cerrado phytomass
[INPE-4835-PRE/1485] N90-18759
Can the square law be validated
[DE90-007112] N90-18945
REGULATORS
Optimization of sensors and actuators positioning aimed at obtaining reduced models for the synthesis of optimal control regulators of flexible structures
[INPE-4760-TDL/348] N90-18450
REINFORCEMENT (STRUCTURES)
Compact reinforced composite basic principles
[CBL-41] N90-18520
High-strength concrete development through 25 years
[CBL-REPRINT-17] N90-18589
REINFORCING MATERIALS
Instrumented impact testing of fabric-reinforced composite materials
[AD-A216764] N90-18513
Thermal analysis of polymer composites
[AD-A216947] N90-18578
RELATIVISTIC PLASMAS
The dynamics of electrons in very intense lasers
[DE90-007248] N90-18729
A continuous plasma final focus
[DE90-006096] N90-19024
RELAXATION METHOD (MATHEMATICS)
An exact algorithm for the problem of p-medians
[INPE-4924-TDL/384] N90-18885
RELIABILITY
Multitarget tracking by single sensor: Analysis of the main approaches developed in this area
[ESA-TT-1171] N90-18633
Reliability studies of ceramic capacitors
[AD-A216763] N90-18643
A test method for measuring corona inception voltage for transducer autotransformers
[AD-A216818] N90-18646
Reliability assessment using finite element techniques
[AD-A216907] N90-18647
Lithium ambient-temperature battery reliability
[DE90-005758] N90-18650
Deceit: A flexible distributed file system
[NASA-CR-186402] N90-18891
Optimum selection procedures in multi-stage screening, reliability, and time
[AD-A216811] N90-18942
RELIABILITY ENGINEERING
Knowledge-based fault detection and analysis for robots: First results for the ROTEX robots
[ESA-TT-1150] N90-18742
Component selection, procurement and control for ESA space systems
[ESA-PSS-01-60-ISSUE-2] N90-19062
RELIEF MAPS
Land suitability maps and appropriate land use: An approach using SGI and satellite imagery
[INPE-4827-PRE/1458] N90-18761
Development of the agricultural information system. Characteristics and results of the Distrito Federal model
[INPE-4940-PRE/1430] N90-18773
Perspective revision of systematic mapping through orbital imagery
[INPE-4817-PRE/1453] N90-18775
REMOTE CONTROL
Electronically Variable Pressure Regulator (EVPR) N90-18484
REMOTE SENSING
Multiparameter scatterometer for remote sensing (RADSER). Project Scatter: State-of-the-art and future applications
[INPE-4871-PRE/1482] N90-18701
Orbital remote sensing in the decade of the nineties: New approaches and challenges in geology
[INPE-4838-PRE/1467] N90-18758
Remote sensing applied to the monitoring of mineral extraction in the proximity of urban areas: Pros and cons
[INPE-4867-PRE/1478] N90-18766
Remote sensing applied to vegetation as subsidized in municipal planning
[INPE-4908-PRE/1509] N90-18770
ERS-1 European remote sensing satellite: A new tool for global environmental monitoring in the 1990's
[ESA-BR-36] N90-18782
On the applicability of CAESAR for the remote sensing of bottom depth and bottom composition of shallow waters: A model study
[BCRS-89-13] N90-18783
Erosion monitoring using remote sensing, part 2
[BCRS-89-15] N90-18785
Remote sensing and run-off modelling in the Lake Victoria Basin, Kenya
[BCRS-89-19] N90-18788
Remote sensing for the classification and quantification of vegetation in Spring staging areas of Brent geese on the Frisian Islands (Netherlands)
[BCRS-89-27] N90-18790
Remote sensing of interior water: Perspectives
[INPE-4875-PRE/1486] N90-18815
REMOTE SENSORS
An application of ocean wave-current refraction to the gulf stream using SEASAT SAR data
[AD-A216769] N90-18851
REQUIREMENTS
Development of a mass averaging temperature probe N90-18418
RESEARCH AND DEVELOPMENT
Development of a mass averaging temperature probe N90-18418
The DFVLR 3-m x 3-m low speed wind tunnel (NWG) in Goettingen
[ESA-TT-1156] N90-18436
Study on the measures to promote the use of photovoltaic power generating system overseas
[DE90-742056] N90-18807
Calendar of selected aeronautical and space meetings
[AGARD-CAL-90/1] N90-19060
RESEARCH FACILITIES
Compressor performance tests in the compressor research facility N90-18428

Research equipment
[AD-A216515] N90-18937
RESEARCH MANAGEMENT
The Pathfinder chemical transfer propulsion program N90-18471
RESERVOIRS
Erosion monitoring using remote sensing, part 2
[BCRS-89-15] N90-18785
Remote sensing of interior water: Perspectives
[INPE-4875-PRE/1486] N90-18815
RESIN MATRIX COMPOSITES
Enhanced bonding of fiber reinforcements to thermoset resins N90-18496
RESINS
Rheological tests of Rigidite 5245 using the cone-plate and parallel plates method
[DT-310/88] N90-18544
RESONANCE
Resonances in low-energy positron-alkali scattering N90-18992
Positron-molecule bound states and positive ion production N90-18994
RESONANCE FLUORESCENCE
The 2.7/4.3 micron CO2 branching ratio measurement
[AD-A215952] N90-18830
RESONANCE SCATTERING
Positron-alkali atom scattering N90-18958
Inelastic scattering of positrons with sodium N90-18961
RESONANT FREQUENCIES
Radio interference in the near-earth environment
[NASA-CR-180479] N90-18623
Performance and modeling of superconducting ring resonators at millimeter-wave frequencies
[NASA-TM-102526] N90-18634
RESONANT VIBRATION
Performance of a 500 watt Nd:GGG zigzag slab oscillator
[DE90-006263] N90-18657
RESONATORS
Performance and modeling of superconducting ring resonators at millimeter-wave frequencies
[NASA-TM-102526] N90-18634
Resonator modes in high gain free electron lasers
[DE90-006098] N90-18720
RESOURCES MANAGEMENT
LANDSAT Thematic Mapper for hydrogeological mapping in Egypt
[BCRS-89-28] N90-18791
Remote sensing of interior water: Perspectives
[INPE-4875-PRE/1486] N90-18815
REUSABLE ROCKET ENGINES
The Pathfinder chemical transfer propulsion program N90-18471
REVERSE FIELD PINCH
The lower hybrid drift instability and the evolution of plasma gradients
[DE90-006521] N90-19021
REYNOLDS STRESS
Measurement of velocity profiles and Reynolds stresses on an oscillating airfoil N90-18427
RHEOLOGY
Model filled polymers 3. Rheological behavior of polystyrene containing crosslinked polystyrene beads
[AD-A215867] N90-18567
A study on deformation and break-up of dispersed particles in elongational flow
[ETN-90-96268] N90-18684
RIGID STRUCTURES
Time and frequency-domain identification and verification of BO-105 dynamic models
[AD-A216828] N90-18389
RISK
Probability of failure and risk assessment of propulsion structural components N90-18470
Risk analysis: Fundamental concepts, regulatory toxicology, and relative comparisons from radiation biology
[DE90-002466] N90-18856
RIVER BASINS
Erosion monitoring using remote sensing, part 2
[BCRS-89-15] N90-18785
RIVERS
Quantification of structural field data in the Rio Grande do Norte basin and neighborhood
[INPE-4821-RPE/591] N90-18826
RIVETS
Fastener design manual
[NASA-RP-1228] N90-18740
ROBOT DYNAMICS
On the kinematic behavior of robots while executing general robot level commands
[PB90-120965] N90-18735
An approach centered in production rules for a partition of environment and planning in a visual navigation system (SNV)
[INPE-4813-TDL/360] N90-18737
ROBOTICS
Visual servoing for autonomous aircraft refueling
[AD-A216042] N90-18386
Space orientation and orbital technology
[ISBN-3-89100-015-4] N90-18437
Superfluid helium orbital resupply coupling N90-18488
The manufacturing procedures for composite materials, automation, and robotization
[ETN-90-96232] N90-18528
ROBOTS
Visual navigation: Constructing and utilizing simple maps of an indoor environment
[AD-A216761] N90-18382
Robot crane technology program
[PB90-111667] N90-18734
On the kinematic behavior of robots while executing general robot level commands
[PB90-120965] N90-18735
Knowledge-based fault detection and analysis for robots: First results for the ROTEX robots
[ESA-TT-1150] N90-18742
Teleoperator servoloop tuning using an expert system
[DE90-005674] N90-18876
RALPH: An automatic Robot Assembly Language Programmer: An overview
[PB90-120973] N90-18912
A colony architecture for an artificial creature
[AD-A216802] N90-18918
Architecture for a human-robot symbiotic system
[DE90-005670] N90-18921
ROBUSTNESS (MATHEMATICS)
Contribution to the study of stability robustness of nonlinear multivariable regulators
[INPE-4801-TDL/356] N90-18950
ROCKET ENGINE DESIGN
Transient pressure test article test program N90-18463
Effect of correlation on multi-engine rocket propulsion systems N90-18467
The Pathfinder chemical transfer propulsion program N90-18471
Feasibility demonstration of a 445N high-performance rocket engine N90-18481
ROCKET ENGINES
The 1989 JANNAF Propulsion Meeting, volume 1
[CPIA-PUBL-515-VOL-1] N90-18462
Effect of correlation on multi-engine rocket propulsion systems N90-18467
AFOSR/ONR (Air Force Office of Scientific Research/Office of Naval Research) Contractors' Meeting on Combustion Rocket Propulsion Diagnostics of Reacting Flow
[AD-A216094] N90-18491
ROCKET FLIGHT
BEAR electrostatic analyzer: Flight results
[DE90-006511] N90-18625
ROCKET NOZZLES
Cold flow determination of the internal flow environment around the submerged TVC nozzle for the space shuttle SRM N90-18465
ROCKET OXIDIZERS
Investigation of the phase stabilizing effect of 4 percent potassium fluoride on ammonium nitrate
[AD-A215313] N90-18599
ROCKS
Evaluation of selection techniques for multispectral bands employed in the discrimination of carbonatic rocks
[INPE-4850-TDL/365] N90-18765
ROTARY STABILITY
Active stabilization of aeromechanical systems
[AD-A216629] N90-18672
ROTARY WINGS
Prediction of rotor blade-vortex interaction noise from 2-D aerodynamic calculations and measurements
[ISL-CO-243/88] N90-18365
ROTATING BODIES
Condensation fluid dynamics and heat transfer on rotating spherical surfaces in a microgravitational field
[DE90-005540] N90-18607
ROTATING DISKS
Numerical investigations of heat transfer and flow rates in rotating cavities. Simulation of the movement generated by wall temperature gradients, by source-sink mass flows or by the differential rotation of the walls, under the influence or coriolis and centrifugal forces
[ETN-90-96253] N90-18695
ROTATION
Static and rotational aerodynamic data from 0 deg to 90 deg angle of attack for a series of basic and altered forebody shapes
[AD-A216582] N90-18361
Review of component defects, their relationship to manufacturing process, and their effect on materials behaviour (for critical rotating parts) N90-18399
ROTOR BLADES (TURBOMACHINERY)
Study of the blade/vortice interaction on a one-blade rotor during forward flight (incompressible, non viscous fluid)
[ISL-R-115/88] N90-18391
Design guidance to minimize unsteady forces in turbomachines N90-18411
Unsteady blade loads due to wake influence N90-18413
Gust response analysis for cascades operating in nonuniform mean flows N90-18415
Blade row interaction effects on compressor measurements N90-18419
Modelling unsteady transition and its effects on profile loss N90-18423
Experimental investigation of the influence of rotor wakes on the development of the profile boundary layer and the performance of an annular compressor cascade N90-18425
ROUGHNESS
The joint effect of surface microtopography and near-surface structure on microcontact conditions
[DE90-006494] N90-18591
RUBIDIUM
Elastic scattering of e- and e+ from Rb and Cd N90-18960
Positron-rubidium scattering N90-18964
RUNWAYS
Dallas/Fort Worth simulation. Volume 2: Appendixes D, E, and F
[AD-A216613] N90-18380
RUTHENIUM
Spectroscopic evidence for carbon-carbon bonding in carbide layers on metals
[AD-A216726] N90-18512

S

SAFETY
RF modal quantity gaging N90-18483
Superfluid helium orbital resupply coupling N90-18488
Safety analysis for the Galileo light-weight radioisotope heater unit
[DE90-007147] N90-19009
SAMPLING
Multistage forest volume estimation using a sampling system with probability variables
[INPE-4897-PRE/1498] N90-18769
Adaptive state estimation and sampling rate analysis for invariant linear dynamic systems in time
[INPE-4960-TDL/389] N90-18951
SATELLITE ATMOSPHERES
IR spectroscopy of planets and satellites; Venus, Mars, giant planets, and Titan N90-19085
SATELLITE COMMUNICATION
Rate compatible punctured codes, their use in military satellite communication systems
[AD-A216723] N90-18619
SATELLITE DESIGN
Space orientation and orbital technology
[ISBN-3-89100-015-4] N90-18437
SATELLITE IMAGERY
TVI: A mathematical model for global estimation of Brazilian cerrado phytomass
[INPE-4836-PRE/1485] N90-18759
Land suitability maps and appropriate land use: An approach using SGI and satellite imagery
[INPE-4827-PRE/1458] N90-18761
Evaluation of two methods for acquisition of training statistics for digital analysis of areas prepared for plowing
[INPE-4901-PRE/1502] N90-18763
Multistage forest volume estimation using a sampling system with probability variables
[INPE-4897-PRE/1498] N90-18769
Development of the agricultural information system. Characteristics and results of the Distrito Federal model
[INPE-4940-PRE/1430] N90-18773
Perspective revision of systematic mapping through orbital imagery
[INPE-4817-PRE/1453] N90-18775
Physiognomy of vegetation cover in the PNPM identified through the TM/LANDSAT sensor: A multitemporal analysis
[INPE-4834-PRE/1464] N90-18776

Project Floval: Correction of relief effects in eucalyptus reforestration
[INPE-4814-RPE/590] N90-18777
Classification of high resolution imagery using texture attributes
[INPE-4888-TDL/379] N90-18778
Improvement of classification results from satellite imagery to update and differentiate land use classes on topographic maps
[BCRS-89-17] N90-18786
SPOT for landscape: Development of a method for the use of SPOT pictures for the updating of the data base scale of the landscape
[BCRS-89-18] N90-18787
Remote sensing and run-off modelling in the Lake Victoria Basin, Kenya
[BCRS-89-19] N90-18788
Geological structure of the State of Rio de Janeiro viewed through MSS LANDSAT imagery
[INPE-4826-PRE/1457] N90-18825

SATELLITE LIFETIME
Arcjet nozzle design impacts N90-18478

SATELLITE OBSERVATION
Airborne observations of the infrared emission bands N90-19101
Polycyclic aromatic hydrocarbons in the infrared spectra of IRAS sources N90-19105

SATELLITE PERTURBATION
Spatial registration of TIROS-N weather satellite data
[AD-A216041] N90-18841

SATELLITE-BORNE PHOTOGRAPHY
Forecasters handbook for Central America and adjacent waters
[AD-A216752] N90-18845

SCALING LAWS
A continuous plasma final focus
[DE90-006096] N90-19024

SCANNING TUNNELING MICROSCOPY
Characterization of biopolymer surfaces using scanning microscopies
[AD-A216572] N90-18572

SCATTERING
Investigation of multiple scattering in aqueous suspensions of non-absorbing polystrene microspheres using spectrophotometry
[BCRS-89-09] N90-18549
The extended equivalent source technique with underdetermined sources
[DE90-006989] N90-18627
Transport effects and spectroscopy of defects in microstructures
[AD-A216718] N90-19036

SCATTERING CROSS SECTIONS
Annihilation in Gases and Galaxies
[NASA-CP-3058] N90-18957
Positron-alkali atom scattering N90-18958
Scattering of positrons and electrons by alkali atoms N90-18959
Positron collisions with alkali-metal atoms N90-18962
Inelastic collisions of positrons with one-valence-electron targets N90-18963
Positron-rubidium scattering N90-18964
Positronium formation in Ss state in e+-Li scattering N90-18967
New parameter-free polarization potentials in low-energy positron collisions N90-18968
The calculation of the contributions to low energy e+H2 scattering from sigma u+ and Pion u symmetries using the Kohn variational method N90-18969
Ab initio R-matrix calculations of e+-molecule scattering N90-18970
Positron excitation of neon N90-18973
Positron-inert gas differential elastic scattering N90-18974
Differential elastic scattering cross sections for 54.9eV positrons incident on helium N90-18975
Total cross sections for positrons scattered elastically from helium based on new measurements of total ionization cross sections N90-18976
Low-energy scattering of electrons and positrons in liquids N90-18981
Antiproton-matter interactions in antiproton applications N90-18989
Search for resonances in positron-atom systems N90-18991
Positronium formation in e+ plus H- collisions N90-18993
Theoretical studies in nuclear physics
[DE90-005981] N90-19005
Measurement of the space potential of a high-temperature plasma by fast atomic beam scattering on an ion probe beam
[DE90-006118] N90-19020

SCATTEROMETERS
Multiparameter scatterometer for remote sensing (RADSER). Project Scatter: State-of-the-art and future applications
[INPE-4871-PRE/1582] N90-18701

SCHEDULES
Calendar of selected aeronautical and space meetings
[AGARD-CAL-90/1] N90-19060

SCHEDULING
Determination of the underlying task scheduling algorithm for and Ada runtime system
[AD-A215880] N90-18690
Speculative computation in multilisp
[AD-A216579] N90-19057

SCHLIEREN PHOTOGRAPHY
An investigation of flow structure, mixing and chemical reaction in combusting turbulent flows
[AD-A216739] N90-18538

SCHROEDINGER EQUATION
Direct and inverse scattering problem associated with the elliptic Sinh-Gordon equation
[AD-A216455] N90-18931

SCHWARZSCHILD METRIC
Vector fields, linear spaces and tensors in physics. Part 3: Tensor analysis and its applications
[INPE-5000-MD/41] N90-18997
Perturbations of test mass motion in the Schwarzschild spacetime using the method of Hamilton and Jacobi N90-19083

SCINTILLATION COUNTERS
Performance of a coincidence based blood activity monitor
[DE90-006105] N90-18865

SEA STATES
ERS-1 European remote sensing satellite: A new tool for global environmental monitoring in the 1990's
[ESA-BR-36] N90-18782

SEA SURFACE TEMPERATURE
Intertropical Convergence Zone (ITCZ) and its relationship with the precipitation of the north-northeast Brazilian region
[INPE-4887-TDL/378] N90-18839

SEARCHING
The formation and use of knowledge structures in problem solving domains
[AD-A216512] N90-18936

SEASAT SATELLITES
An application of ocean wave-current refraction to the gulf stream using SEASAT SAR data
[AD-A216769] N90-18851

SEDIMENTS
Erosion monitoring using remote sensing, part 2
[BCRS-89-15] N90-18785

SEISMOLOGY
The interpretation of crustal dynamics data in terms of plate interactions and active tectonics of the Anatolian plate and surrounding regions in the Middle East
[NASA-CR-186200] N90-18824

SELECTION
Evaluation of selection techniques for multispectral bands employed in the discrimination of carbonatic rocks
[INPE-4850-TDL/365] N90-18765
Optimum selection procedures in multi-stage screening, reliability, and time
[AD-A216811] N90-18942

SELF TESTS
Navigation experiment NAVEX: The self-test delay times in the D1 Spacelab mission
[ESA-TT-1176] N90-18446
Knowledge-based fault detection and analysis for robots: First results for the ROTEX robots
[ESA-TT-1150] N90-18742

SEMANTICS
Should a function continue
[AD-A216406] N90-18929

SEMICONDUCTING FILMS
Hydrogenated amorphous and microcrystalline silicon deposited from silane-hydrogen mixtures
[ETN-90-96267] N90-18590

SEMICONDUCTOR DEVICES
DANCIR (device and circuit simulator): A three dimensional steady-state semiconductor device simulator
[DE90-006370] N90-18658

SEMICONDUCTOR DIODES
High speed imaging with a tapped solid state sensor
[DE90-006116] N90-18702

SEMICONDUCTORS (MATERIALS)
Microconvective heating of granular explosives by a semiconductor bridge
[DE90-005710] N90-18541
State of the art in semiconductor detectors
[DE90-005567] N90-18706
Luminescence of lanthanides and actinides implanted into binary III-V semiconductors and AlGaAs
[AD-A215759] N90-19031
Proceedings of the 6th Conference on Hot Carriers in Semiconductors
[AD-A215978] N90-19032
Crystal growth and mechanical properties of semiconductor alloys
[AD-A216697] N90-19035
Structure and vibrational excitations of reconstructed semiconductor surfaces
[DE90-006589] N90-19044
Crystallographic and magnetic properties of (C6 D11 ND3)CuBr3 and (Zn(1-x)Mn(x))3As2: A neutron scattering study
[ECN-219] N90-19055

SENSORY PERCEPTION
Visual navigation: Constructing and utilizing simple maps of an indoor environment
[AD-A216761] N90-18382
A colony architecture for an artificial creature
[AD-A216802] N90-18918

SEPARATED FLOW
Unsteady viscous calculation method for cascades with leading edge induced separation N90-18408

SEPARATORS
Low cost filter development and control of permeability in high temperature, high pressure ceramic filter elements
[DE90-000403] N90-18676

SEQUENCING
Boolean minimization and algebraic factorization procedures for fully testable sequential machines
[AD-A216779] N90-18940

SERIES EXPANSION
Using the method of matched asymptotic expansions, analytically investigate the three-dimensional, atmosphere entry problem
[AD-A216287] N90-18451

SERVOMECHANISMS
Teleoperator servoloop tuning using an expert system
[DE90-005674] N90-18876
Architecture for a human-robot symbiotic system
[DE90-005670] N90-18921

SEWAGE
Investigation report of the investigation commission for interchange of heat pump technology in Europe
[DE89-782293] N90-18686

SHADOWS
Three-dimensional motion estimation using shading information in multiple frames
[AD-A216804] N90-18919

SHALLOW WATER
On the applicability of CAESAR for the remote sensing of bottom depth and bottom composition of shallow waters: A model study
[BCRS-89-13] N90-18783

SHAPE CONTROL
A difference scheme with autocontrol artificial viscosity to predict ablated nosetip shape
[AD-A216625] N90-18452

SHAPES
A user's manual for the method of moments Aircraft Modeling Code (AMC)
[NASA-CR-186371] N90-18390

SHEAR CREEP
Creep in shear of experimental solder joints
[DE90-007062] N90-18753

SHEAR LAYERS
Computational aerodynamics of ordered vortex flows
[ETN-90-96272] N90-18368

SHEAR PROPERTIES
Model filled polymers 3. Rheological behavior of polystyrene containing crosslinked polystyrene beads
[AD-A215867] N90-18567

SHEAR STRAIN
Creep in shear of experimental solder joints
[DE90-007062] N90-18753

SHEAR STRESS
Turbulence structure of mixing swirling flows
[AD-A216628] N90-18671

SHIELDING
Effects of oblique impact on hypervelocity shield performance
[DE90-006936] N90-18739

SHOCK SIMULATORS
Direct simulation Monte Carlo of shock reflexion on a wedge with boundary layer
[ISL-CO-245/88] N90-18681

SHOCK WAVE ATTENUATION
Spallation and dynamic fracture as an effect of laser induced shock waves in carbon based composite materials
[AD-A216540] N90-18509

SHOCK WAVE INTERACTION
Spallation and dynamic fracture as an effect of laser induced shock waves in carbon based composite materials
[AD-A216540] N90-18509
Infrared line emission from high-velocity outflows in star-forming regions N90-19116
SHOCK WAVES
Unsteady aerodynamic phenomena in a simulated wake and shock wave passing experiment N90-18414
Time-dependent measurements on vibrating annular turbine cascades under various steady state conditions N90-18424
Spallation and dynamic fracture as an effect of laser induced shock waves in carbon based composite materials
[AD-A216540] N90-18509
Study of the dynamical behavior of copper in a shock wave
[ISL-R-123/88] N90-18679
Direct simulation Monte Carlo of shock reflexion on a wedge with boundary layer
[ISL-CO-245/88] N90-18681
Transient responses of coupled systems
[ONERA-RT-13/3596-RY-070-R] N90-18687
Interaction between oblique-angled incident shock wave and turbulent boundary layer on a heated wall. Experimental results
[ONERA-RT-84/7078-AY] N90-18688
Piezoelectric polymer PVDF shock gauge: State of the research art
[ISL-CO-207/89] N90-18705
Infrared diagnostics of interstellar shocks N90-19115
High-excitation lines of molecular hydrogen: A discriminant between shock models N90-19118
Interaction of minor ions with fast and slow shocks
[NASA-CR-186372] N90-19181
SHORT WAVE RADIATION
The ISO short wavelength spectrometer N90-19162
SHORT WAVE RADIO TRANSMISSION
Telemetry and telecommand omnidirectional antenna in the short wave band
[ETN-90-96285] N90-18631
SIGNAL DETECTION
The effects of luminance boundaries on color perception
[AD-A216741] N90-18860
SIGNAL DISTORTION
Angle estimation in the presence of mainbeam interference
[AD-A216832] N90-18621
SIGNAL PROCESSING
Efficient detection and signal parameter estimation with application to high dynamic GPS receiver
[NASA-CASE-NPO-17820-1-CU] N90-18379
Applications of acousto-optical correlation devices in radar signal processing
[AD-A216624] N90-18616
Multitarget tracking by single sensor: Analysis of the main approaches developed in this area
[ESA-TT-1171] N90-18633
Signal processing device to control microwave output
[AD-A216931] N90-18648
Adaptive state estimation and sampling rate analysis for invariant linear dynamic systems in time
[INPE-4960-TDL/389] N90-18951
SIGNAL RECEPTION
DOA (Direction of Arrival) estimation by Eigendecomposition using single vector Lanczos' algorithm
[AD-A215802] N90-18887
SIGNAL TO NOISE RATIOS
Applications of acousto-optical correlation devices in radar signal processing
[AD-A216624] N90-18616
Angle estimation in the presence of mainbeam interference
[AD-A216832] N90-18621
DOA (Direction of Arrival) estimation by Eigendecomposition using single vector Lanczos' algorithm
[AD-A215802] N90-18887
SILANES
Composite for smoothing the surface of ceramic substrates
[DE90-004005] N90-18565
SILICA GLASS
Multicomponent glass surfaces structure and adsorption
[DE90-007179] N90-18596
SILICIDES
Dislocation behaviour in Ge(x)Si(1-x) epilayers on (001) Si
[DE90-007063] N90-19051
Modified dislocation structures in Ge(x)Si(1-x) double epilayers on (001) Si
[DE90-007078] N90-19052
SILICON
Interfacial chemistry of MoS2 films on Si
[AD-A216527] N90-18532
Surface intermediates in thin film deposition on silicon
[AD-A216662] N90-18534
Time-resolved measurements of solidification and undercooling in metals and alloys
[DE90-007074] N90-18564
Research relating to crystalline silicon-film on a foreign substrate
[DE90-005720] N90-18582
Integrated silicon flip-flop sensors
[ETN-90-96271] N90-18654
SILICON CARBIDES
Third European Conference on Composite Materials
[EOARD-LR-89-050] N90-18494
Silicon carbo-nitride ceramic matrix composites by polymer pyrolysis N90-18499
Ceramic matrix composites, new high performance materials N90-18500
Continuous preparation of a thin refractory carbide deposit on the surface of carbon fibers: Characterization of the C/SiC fiber N90-18501
Sputter deposition of diffusion barrier coatings on SiC monofilaments for use in Ti-based composites N90-18502
Laboratory for the processing and evaluation of inorganic matrix composites
[AD-A216881] N90-18516
Application of artificial intelligence control to the vapor-liquid-solid silicon carbide whisker process
[DE90-007835] N90-18519
Fundamental aspects of erosion and impact damage
[DE90-006640] N90-18587
SILICON DIOXIDE
The improved adhesion of organic polymers to silica and to aluminum metal with zirconium Schiff-base block copolymer coatings
[AD-A216669] N90-18575
SILICON FILMS
Hydrogenated amorphous silicon films prepared by glow discharge of disilane
[DE90-000309] N90-18581
SILICON NITRIDES
Silicon carbo-nitride ceramic matrix composites by polymer pyrolysis N90-18499
Mechanical properties and microstructure of Si3N4-whisker-reinforced Si3N4 matrix composite
[DE90-005651] N90-18518
Comparison of tension, compression, and flexure creep for alumina and silicon nitride ceramics
[DE90-006154] N90-18586
Synthesis of high-purity sinterable silicon nitride powder
[DE90-007050] N90-18593
Microstructural characterization of silicon nitride ceramics processed by pressureless sintering, overpressure sintering, and sinter/HIP
[DE90-007126] N90-18594
Biaxial strength and stress rupture of hot-pressed silicon nitride
[AD-A216950] N90-18750
SILICON OXIDES
A new interpretation of the feature of SiO maser spectra associated with M-type star
[DE90-610641] N90-19174
SILVER
Polymerization of nitro compounds on silver surfaces during surface-enhanced Raman scattering
[AD-A216116] N90-18569
SILVER COMPOUNDS
Fundamental studies of surface processes and trace analysis using solid electrodes
[AD-A216538] N90-18533
SIMD (COMPUTERS)
Parallelizing the SDI ACCESS algorithm for the Connection Machine-2
[DE90-006382] N90-18909
SIMULATION
Dallas/Fort Worth simulation. Volume 2: Appendixes D, E, and F
[AD-A216613] N90-18380
Space-based radar simulation laboratory
[AD-A216722] N90-18618
A self-organizing multiple-view representation of three-dimensional objects
[AD-A216711] N90-18871
Log-based recovery in asynchronous distributed systems
[NASA-CR-186190] N90-18924
Hamiltonian analysis and simulation of free electron lasers
[INPE-4785-TDL/351] N90-19018
SIMULATORS
Space-based radar simulation laboratory
[AD-A216722] N90-18618
Back swing phenomenon of synchronous generator. Study on ac-dc power system simulator tests
[DE89-782321] N90-18635
SINGLE CRYSTALS
Surface intermediates in thin film deposition on silicon
[AD-A216662] N90-18534
SINTERING
Sintering of a model nickel/alumina catalyst
[ETN-90-96270] N90-18561
Microstructural characterization of silicon nitride ceramics processed by pressureless sintering, overpressure sintering, and sinter/HIP
[DE90-007126] N90-18594
SIZE (DIMENSIONS)
Psychological studies of visual cortical function
[AD-A217029] N90-18872
SIZE DISTRIBUTION
Colloid and interface chemistry aspects of ceramics
[AD-A216715] N90-18576
SLIDING FRICTION
The mechanism, measurement, and influence of properties on the galling of metals
[DE90-006533] N90-18558
The joint effect of surface microtopography and near-surface structure on microcontact conditions
[DE90-006494] N90-18591
SLIP CASTING
Low cost filter development and control of permeability in high temperature, high pressure ceramic filter elements
[DE90-000403] N90-18678
SLURRIES
Optimum catalytic process for alcohol fuels from syngas
[DE90-007188] N90-18604
Fluidization mechanisms in slurry flow
[DE90-006497] N90-18691
SMOOTHING
Orbit determination of artificial Earth satellites through estmation techniques combined with state smoothing techniques
[INPE-4959-TDL/388] N90-18440
SODIUM
Inelastic scattering of positrons with sodium N90-18961
SOFTENING
Softening mechanisms and microstructural instabilities during high temperature, low cycle fatigue of Ni, Ni3Al, and their metal matrix composites
[DE90-006487] N90-18557
SOFTWARE ENGINEERING
The implications of using integrated software support environment for design of guidance and control systems software
[AGARD-AR-229] N90-18432
Vertical migration in operational system nucleus
[INPE-4879-RPE/593] N90-18883
Technology assessment of software engineering
[AD-A216943] N90-18902
SOFTWARE TOOLS
Aerodynamics of unsteady systems. Numerical study of potential flow/boundary layer coupling
[ETN-90-96257] N90-18367
Ada-Linda preliminary report: Motivation, informal description, and examples
[AD-A216004] N90-18892
User manual for NEXT 1.2: NLR engineering X-pert system toolkit
[NLR-TR-87178-U] N90-18905
A survey of performability modelling tools
[MEMO-INF-89-50] N90-18907
SOIL MAPPING
Land suitability maps and appropriate land use: An approach using SGI and satellite imagery
[INPE-4827-PRE/1458] N90-18761
SOIL MOISTURE
Multiparameter scatterometer for remote sensing (RADSER). Project Scatter: State-of-the-art and future applications
[INPE-4871-PRE/1482] N90-18701
SOIL SCIENCE
Radiometric study of wheat and bean crops in three types of latossolo
[INPE-4843-PRE/1472] N90-18767
Relationships between spectral parameters and agronomics of wheat and beam crops
[INPE-4791-RPE/584] N90-18768
Spectral response of wheat and its relationship with agronomical prameters
[INPE-4950-RPE/599] N90-18774

SOLAR ACTIVITY
Solar variability observed through changes in solar figure and mean diameter
[DE90-006600] N90-18834
SOLAR CELLS
Hydrogenated amorphous silicon films prepared by glow discharge of disilane
[DE90-000309] N90-18581
Progress in thin film solar photovoltaic technologies
[DE89-009513] N90-18792
Optimization of the reference parameters in the accompanying solar panel dynamics
[INPE-4795-PRE/1449] N90-18798
Radiation-hard high-efficiency InP space solar cell development
[AD-A216857] N90-18800
Chemical vapor deposition and photochemical vapor deposition of amorphous silicon photovoltaic devices
[DE89-009510] N90-18803
Study on the measures to promote the use of photovoltaic power generating system overseas
[DE90-742056] N90-18807
SOLAR COLLECTORS
Phase-Change Thermal Energy Storage
[DE89-009426] N90-18801
SOLAR CONSTANT
Solar variability observed through changes in solar figure and mean diameter
[DE90-006600] N90-18834
SOLAR COOLING
Solar buildings program summary. Volume 2: Research summaries
[DE89-009478] N90-18810
SOLAR CORONA
Magnetic field generation by acoustic oscillations in solar atmosphere
[DE90-606054] N90-19180
SOLAR CYCLES
Intermittent Solar Ammonia Absorption Cycle (ISAAC) refrigeration for lesser developed countries
[DE90-006700] N90-18610
SOLAR DIAMETER
Solar variability observed through changes in solar figure and mean diameter
[DE90-006600] N90-18834
SOLAR ENERGY
Study of the atmospheric emissions of OI wavelength 557.7 nm and O2 (0,0) wavelength 761.9 nm in the equatorial region utilizing measurement of photometer on-board a rocket
[INPE-4811-TDL/358] N90-18827
SOLAR ENERGY CONVERSION
Progress in thin film solar photovoltaic technologies
[DE89-009513] N90-18792
Resource Assessment Project: User needs survey results
[DE89-009502] N90-18802
SOLAR GRAVITATION
Solar variability observed through changes in solar figure and mean diameter
[DE90-006600] N90-18834
SOLAR HEATING
Solar buildings program summary. Volume 2: Research summaries
[DE89-009478] N90-18810
SOLAR HOUSES
Solar buildings program summary. Volume 2: Research summaries
[DE89-009478] N90-18810
SOLAR MAGNETIC FIELD
Magnetic field generation by acoustic oscillations in solar atmosphere
[DE90-606054] N90-19180
SOLAR NEUTRINOS
Solar variability observed through changes in solar figure and mean diameter
[DE90-006600] N90-18834
SOLAR RADIATION
Resource Assessment Project: User needs survey results
[DE89-009502] N90-18802
SOLAR SIMULATORS
Preliminary design of a pointer for movement of a solar simulator
[INPE-4864-TDL/375] N90-18736
SOLAR SYSTEM
Infrared cometary spectroscopy N90-19086
SOLAR THERMAL ELECTRIC POWER PLANTS
Phase-Change Thermal Energy Storage
[DE89-009426] N90-18801
SOLAR WIND
Interaction of minor ions with fast and slow shocks
[NASA-CR-186372] N90-19181
SOLDERED JOINTS
Creep in shear of experimental solder joints
[DE90-007062] N90-18753
SOLID ELECTRODES
Fundamental studies of surface processes and trace analysis using solid electrodes
[AD-A216538] N90-18533
Electrochemical investigations of novel solid redox polymerization electrodes
[DE90-006087] N90-18584
SOLID PROPELLANT ROCKET ENGINES
Combustion instability in solid propellant rockets
[AD-A216740] N90-18492
SOLID PROPELLANTS
Combustion instability in solid propellant rockets
[AD-A216740] N90-18492
SOLID STATE
High speed imaging with a tapped solid state sensor
[DE90-006116] N90-18702
Solid-state fluorescence above 1000 C: Application to high-temperature laser thermography
[DE90-006422] N90-18721
Solid-state proton conductors
[DE90-007595] N90-18812
SOLID STATE LASERS
Properties and performance of the LiCaAlF6:Cr(3+) laser material
[DE90-007242] N90-18728
SOLID-SOLID INTERFACES
Interfacial chemistry of MoS2 films on Si
[AD-A216527] N90-18532
Colloid and interface chemistry aspects of ceramics
[AD-A216715] N90-18576
SOLIDIFICATION
A fundamental understanding of the effect of alloying elements on the corrosion resistance of rapidly solidified Mg alloys
[AD-A216767] N90-18553
Time-resolved measurements of solidification and undercooling in metals and alloys
[DE90-007074] N90-18564
Pulsed laser-induced melting of intermediate Cu-Zn phases
[DE90-005404] N90-18713
SOLIDS
Kinetic relations and the propagation of phase boundaries in solids
[AD-A215881] N90-18747
Modern theory of magnetism
[DE90-007374] N90-18998
Pressure induced superconductivity in elemental solids
[DE90-610664] N90-19048
SOLUTES
The effect of electric field on attachment of electrons to solutes in liquid argon
[DE90-003969] N90-18529
SONAR
Visual navigation: Constructing and utilizing simple maps of an indoor environment
[AD-A216761] N90-18382
SORBENTS
High temperature interaction of SO2 with oxide sorbents
[DE90-000435] N90-18545
SOUND LOCALIZATION
Perception of long-period complex sounds
[AD-A216743] N90-18861
SOUND PRESSURE
Noise levels from a VSTOL aircraft measured at ground level and at 1.2 m above the ground
[NPL-RSA(EXT)-009] N90-18999
SOUND WAVES
Magnetic field generation by acoustic oscillations in solar atmosphere
[DE90-606054] N90-19180
SOUTH AMERICA
Connections between the circulation in altitude and convection over South America
[INPE-4923-TDL/383] N90-18828
SOUTHERN HEMISPHERE
Study of peculiar galaxies in the Southern Hemisphere
[INPE-4810-TDL/357] N90-19184
SOYBEANS
Thermal remote sensing in the differentiation of soybean crops (glycine max (L.) merrill) submitted to water deficit
[INPE-4900-PRE/1501] N90-18762
SPACE BASED RADAR
Space-based radar simulation laboratory
[AD-A216722] N90-18618
SPACE CHARGE
BEAR electrostatic analyzer: Flight results
[DE90-006511] N90-18625
The dynamics of electrons in very intense lasers
[DE90-007246] N90-18729
SPACE COOLING (BUILDINGS)
Solar buildings program summary. Volume 2: Research summaries
[DE89-009478] N90-18810
SPACE ERECTABLE STRUCTURES
Support trusses for large precision segmented reflectors: Preliminary design and analysis
[NASA-TM-101560] N90-18453
SPACE HEATING (BUILDINGS)
Solar buildings program summary. Volume 2: Research summaries
[DE89-009478] N90-18810
SPACE MISSIONS
A perspective on the use of storable propellants for future space vehicle propulsion N90-18473
SPACE PERCEPTION
Visual processing of object velocity and acceleration
[AD-A216509] N90-18858
SPACE PLASMAS
Particle simulations in magnetospheric plasmas
[AD-A216256] N90-18831
SPACE PLATFORMS
Orbital fluid resupply assessment N90-18487
SPACE POWER REACTORS
Space nuclear safety program
[DE90-006436] N90-19007
SPACE PROGRAMS
Purchase of technology N90-19072
The bringing to market of the RF alert (a case study in technology transfer) N90-19073
SPACE SHUTTLE BOOSTERS
The 1989 JANNAF Propulsion Meeting, volume 1
[CPIA-PUBL-515-VOL-1] N90-18462
Transient pressure test article test program N90-18463
Test data of flow field of shuttle SRM nozzle joint with bond defects, using unheated air N90-18464
Cold flow determination of the internal flow environment around the submerged TVC nozzle for the space shuttle SRM N90-18465
Technique for evaluating the erosive properties of ablative internal insulation materials N90-18466
SPACE SHUTTLE MAIN ENGINE
Experimental flow models for SSME flowfield characterization N90-18469
SPACE SHUTTLE ORBITERS
Orbital fluid resupply assessment N90-18487
SPACE SHUTTLES
Space shuttle RCS oxidizer leak repair for STS-26 N90-18485
Superfluid helium orbital resupply coupling N90-18488
Technology update-89
[DE90-005813] N90-19178
SPACE STATIONS
Process development and fabrication of space station type aluminum-clad graphite epoxy struts
[NASA-CR-181873] N90-18454
Space station technology summary N90-18482
Zero-gravity vortex vent and PVT gaging system N90-18486
Orbital fluid resupply assessment N90-18487
Payload vibration isolation in a microgravity environment
[NASA-CR-186191] N90-18744
Development of an experimental space station model for structural dynamics research
[NASA-TM-102601] N90-18751
SPACE SURVEILLANCE (SPACEBORNE)
Space-based radar simulation laboratory
[AD-A216722] N90-18618
SPACE TRANSPORTATION
A perspective on the use of storable propellants for future space vehicle propulsion N90-18473
SPACE WEAPONS
Survivability and effectiveness of near-term strategic defense
[DE90-005805] N90-18955
SPACE-TIME FUNCTIONS
Concepts and experiments on space-time chaos
[ETN-90-96255] N90-18683
Perturbations of test mass motion in the Schwarzschild spacetime using the method of Hamilton and Jacobi N90-19083
SPACEBORNE ASTRONOMY
Herbig Ae/Be stars: Fine structure far-infrared lines N90-19126
SPACEBORNE EXPERIMENTS
Navigation experiment NAVEX data storage and processing
[ESA-TT-1175] N90-18445
Navigation experiment NAVEX: The self-test delay times in the D1 Spacelab mission
[ESA-TT-1176] N90-18446
Investigation of methods to produce a uniform cloud of fuel particles in a flame tube
[NASA-TM-102376] N90-18665

Synchronization of the ground station atomic clocks using three weighted transportable cesium time standards in the Navex navigation experiment
[ESA-TT-1153] N90-18711
SPACECRAFT COMMUNICATION
Packet telemetry standard
[ESA-PSS-04-106-ISSUE-1] N90-18447
SPACECRAFT COMPONENTS
Component selection, procurement and control for ESA space systems
[ESA-PSS-01-60-ISSUE-2] N90-19062
SPACECRAFT CONSTRUCTION MATERIALS
Composites design handbook for space structure applications
[ESA-PSS-03-1101-ISSUE-1-REV-1] N90-18459
The determination of offgassing products from materials and assembled articles to be used in a manned space vehicle crew compartment
[ESA-PSS-01-729-ISSUE-1] N90-18461
State of the art and future prospects for high temperature composites N90-18498
Materials and structures for 2000 and beyond: An attempted forecast by the Materials and Structures Department of the DLR
[ESA-TT-1154] N90-18609
SPACECRAFT CONTROL
Configuration management and control for ESA space systems
[ESA-PSS-01-11-ISSUE-1] N90-19061
Magnetic suspension railway systems based on space technology N90-19081
SPACECRAFT DESIGN
Spacecraft thermal control design data, volume 1
[ESA-PSS-03-108-ISSUE-1-VOL-1] N90-18455
Spacecraft thermal control design data, volume 2
[ESA-PSS-03-108-ISSUE-1-VOL-2] N90-18456
Spacecraft thermal control design data, volume 3
[ESA-PSS-03-108-ISSUE-1-VOL-3] N90-18457
Spacecraft thermal control design data, volume 4
[ESA-PSS-03-108-ISSUE-1-VOL-4] N90-18458
Composites design handbook for space structure applications
[ESA-PSS-03-1101-ISSUE-1-REV-1] N90-18459
SPACECRAFT ENVIRONMENTS
The determination of offgassing products from materials and assembled articles to be used in a manned space vehicle crew compartment
[ESA-PSS-01-729-ISSUE-1] N90-18461
Design and operation of an inert gas facility for thermoelectric generator storage
[DE90-007146] N90-19008
SPACECRAFT EQUIPMENT
System safety requirements for ESA space systems and associated equipment
[ESA-PSS-01-40-ISSUE-2] N90-18460
SPACECRAFT LAUNCHING
Space shuttle RCS oxidizer leak repair for STS-26 N90-18485
Superfluid helium orbital resupply coupling N90-18488
SPACECRAFT POWER SUPPLIES
Design and operation of an inert gas facility for thermoelectric generator storage
[DE90-007146] N90-19008
SPACECRAFT PROPULSION
The Pathfinder chemical transfer propulsion program N90-18471
Advanced APS impacts on vehicle payloads N90-18472
Electric propulsion options for 10 kW class earth-space missions N90-18474
Test facility and preliminary performance of a 100 kW class MPD thruster N90-18476
Feasibility demonstration of a 445N high-performance rocket engine N90-18481
Space station technology summary N90-18482
Viability study of ionic microthruster tests on MECB satellite
[INPE-4973-RPE/605] N90-18490
SPACECRAFT RADIATORS
Spacecraft thermal control design data, volume 3
[ESA-PSS-03-108-ISSUE-1-VOL-3] N90-18457
Condensation fluid dynamics and heat transfer on rotating spherical surfaces in a microgravitational field
[DE90-005540] N90-18607
SPACECRAFT SHIELDING
Spacecraft thermal control design data, volume 2
[ESA-PSS-03-108-ISSUE-1-VOL-2] N90-18456
SPACECRAFT STRUCTURES
Materials and structures for 2000 and beyond: An attempted forecast by the Materials and Structures Department of the DLR
[ESA-TT-1154] N90-18609
SPACECRAFT TEMPERATURE
Spacecraft thermal control design data, volume 1
[ESA-PSS-03-108-ISSUE-1-VOL-1] N90-18455
Spacecraft thermal control design data, volume 2
[ESA-PSS-03-108-ISSUE-1-VOL-2] N90-18456
Spacecraft thermal control design data, volume 3
[ESA-PSS-03-108-ISSUE-1-VOL-3] N90-18457
Spacecraft thermal control design data, volume 4
[ESA-PSS-03-108-ISSUE-1-VOL-4] N90-18458
SPACECRAFT TRACKING
Efficient detection and signal parameter estimation with application to high dynamic GPS receiver
[NASA-CASE-NPO-17820-1-CU] N90-18379
SPACECRAFT TRAJECTORIES
Orbit determination of artificial Earth satellites through estmation techniques combined with state smoothing techniques
[INPE-4959-TDL/388] N90-18440
SPACELAB PAYLOADS
Refurbishment and modification of the Metric Camera (RMK) for reflight on EOM-1 Spacelab mission
[ETN-90-96284] N90-18710
Knowledge-based fault detection and analysis for robots: First results for the ROTEX robots
[ESA-TT-1150] N90-18742
SPACING
Blade row interaction effects on compressor measurements N90-18419
SPALLATION
Spallation and dynamic fracture as an effect of laser induced shock waves in carbon based composite materials
[AD-A216540] N90-18509
SPATIAL DISTRIBUTION
An investigation of flow structure, mixing and chemical reaction in combusting turbulent flows
[AD-A216739] N90-18538
A colony architecture for an artificial creature
[AD-A216802] N90-18918
Zodiacal dust bands: Their relation to asteroid families
[AD-A216025] N90-19170
SPATIAL RESOLUTION
Fracture analysis through photographic imagery of low spatial resolution: A contribution to the study of tectonic evoluation of the Araripe Plateau region
[INPE-4876-PRE/1487] N90-18756
Perspective revision of systematic mapping through orbital imagery
[INPE-4817-PRE/1453] N90-18775
The effects of luminance boundaries on color perception
[AD-A216741] N90-18860
Three-dimensional motion estimation using shading information in multiple frames
[AD-A216804] N90-18919
SPECIFIC HEAT
Low temperature specific heat and magnetic susceptibility of NbTi and NbTiMn alloys
[DE90-005390] N90-18552
Heat capacities of solid polymers (The Advanced THermal Analysis System, ATHAS)
[DE90-007130] N90-18595
SPECIFICATIONS
The determination of offgassing products from materials and assembled articles to be used in a manned space vehicle crew compartment
[ESA-PSS-01-729-ISSUE-1] N90-18461
A battery data base for electric vehicle applications
[DE90-007085] N90-18655
An interactive system applied to the linear quadratic problem
[INPE-4945-TDL/386] N90-18913
SPECTRA
Numerical simulations of coherent structures in a jet flame with a noncircular cross section
[AD-A216710] N90-18535
Reliability studies of ceramic capacitors
[AD-A216763] N90-18643
SPECTRAL EMISSION
Measurement of spectral emissivity by Fourier transform infrared spectrometer
[DE89-782319] N90-18698
SPECTRAL LINE WIDTH
GRIS observations of the Galactic Center N90-18982
Dust in planetary nebulae: IRSPEC observations in the 3.0 micron-3.8 micron range N90-19132
SPECTRAL METHODS
Spectral multi-domain approximation of the Navier-Stokes equations in curved complex geometries
[ONERA-NT-1987-2] N90-18685
DOA (Direction of Arrival) estimation by Eigendecomposition using single vector Lanczos' algorithm
[AD-A215802] N90-18887
SPECTRAL REFLECTANCE
Relationships between the aerial biomass from ground layers of cerrado and its spectral reflectance
[INPE-4848-PRE/1477] N90-18760
SPECTRAL RESOLUTION
On the range resolution of point targets with FMCW radar systems
[DLR-FB-89-47] N90-18629
IRAS LRS spectra of extended objects: The Crab nebula N90-19107
High resolution infrared spectroscopy of symbiotic stars N90-19125
Isophot-S, a low resolution 2.5 to 12 microns spectrometer for ISO N90-19167
SPECTRAL SIGNATURES
Evaluation of two methods for acquisition of training statistics for digital analysis of areas prepared for plowing
[INPE-4901-PRE/1502] N90-18763
The infrared spectral signature of star formation N90-19114
SPECTROMETERS
Linear Variable Differential Transformer (LVDT) with conditioner for the control of stepping motor drivers (part of the sliding-foil follower system of the Emin spectrometers)
[DIGEL-1989-9] N90-18660
SPECTROPHOTOMETRY
Investigation of multiple scattering in aqueous suspensions of non-absorbing polystrene microspheres using spectrophotometry
[BCRS-89-09] N90-18549
Study of rifampicin fixation on plasma proteins by derivative spectrophotometry
[CERMA-89-25] N90-18866
Spectrophotometry of dust with Isophot N90-19164
SPECTRORADIOMETERS
Performance parameter characterisation of various types of IR single element detectors N90-19161
SPECTROSCOPIC ANALYSIS
Application of high performance liquid chromatography/mass spectrometry to environmental analysis
[PB90-116963] N90-18814
SPECTROSCOPY
Fluorescence and elastic scattering from laser dye-filled capillaries
[AD-A217026] N90-18540
Transport effects and spectroscopy of defects in microstructures
[AD-A216718] N90-19036
SPECTRUM ANALYSIS
Doppler spectra from incoherent backscatter: Principles and examples for application for POLDIRAD
[DLR-FB-89-48] N90-18630
Relationships between spectral parameters and agronomics of wheat and beam crops
[INPE-4791-RPE/584] N90-18768
Spectral response of wheat and its relationship with agronomical prameters
[INPE-4950-RPE/599] N90-18774
IR spectroscopy of planets and satellites; Venus, Mars, giant planets, and Titan N90-19085
Interpretation of the 10 micron and 20 micron absorption bands in comets, the interstellar medium, and in an external galaxy N90-19093
Spectropolarimetry as a diagnostic of the interstellar medium N90-19096
The infrared spectral signature of star formation N90-19114
Infrared spectroscopy of supernova 1987A N90-19124
Herbig Ae/Be stars: Fine structure far-infrared lines N90-19126
CO infrared bands in atmospheres of long-period variables N90-19128
Measurement system of spectral irradiance in the near infrared N90-19160
SPECULAR REFLECTION
Positronium reflection and positronium beams N90-18980
SPEECH RECOGNITION
Perception of long-period complex sounds
[AD-A216743] N90-18861
Knowledge-based extensible natural language interface technology program
[AD-A216664] N90-18897
SPIN RESONANCE
Search for resonances in positron-atom systems N90-18991
SPIN-SPIN COUPLING
Positron-rubidium scattering N90-18964
SPIRAL GALAXIES
Infrared properties of five spiral galaxies N90-19154
SPONTANEOUS EMISSION
A simple model for amplified spontaneous emission in dyes
[DE90-007249] N90-18730

SPOT (FRENCH SATELLITE)
SPOT for landscape: Development of a method for the use of SPOT pictures for the updating of the data base scale of the landscape
[BCRS-89-18] N90-18787

SPREADING
Microcomputer enhanced optical investigation of spreading and evaporative processes in ultra thin films
[DE90-006323] N90-18585

SPUTTERING
Sputter deposition of diffusion barrier coatings on SiC monofilaments for use in Ti-based composites N90-18502

STABILITY
Nonlinear optical processes in one-dimensional polymers
[AD-A216103] N90-18568
Strongly coupled one-dimensional system and the polymer
[AD-A216330] N90-18571
Contribution to the study of stability robustness of nonlinear multivariable regulators
[INPE-4801-TDL/356] N90-18950

STABILITY TESTS
Microcalometric studies of gun propellant KKR 8
[FOA-C-20770-2.1] N90-18606

STABILIZATION
Dynamics and stabilization of materials possessing high energy content
[AD-A216320] N90-18570
Control and stabilization of linear and nonlinear distributed systems
[AD-A216446] N90-18908

STAINLESS STEELS
Failure probability estimate of Type 304 stainless steel piping
[DE90-003696] N90-18550

STANDARDIZATION
DoD manual for standard data elements
[AD-A216441] N90-19066

STANDARDS
Packet telemetry standard
[ESA-PSS-04-106-ISSUE-1] N90-18447

STAR DISTRIBUTION
Infrared spectroscopy of star formation in galaxies: Extreme conditions and very short time scales N90-19147

STAR FORMATION
Infrared Spectroscopy in Astronomy
[ESA-SP-290] N90-19084
The infrared spectral signature of star formation N90-19114
Infrared line emission from high-velocity outflows in star-forming regions N90-19116
Far-infrared spectroscopy of galaxies N90-19146
Infrared spectroscopy of star formation in galaxies: Extreme conditions and very short time scales N90-19147
A search for the CO feature in active galactic nuclei N90-19151
Fluorescent molecular hydrogen emission from star-forming galaxies N90-19155
H53-alpha emission from M82 N90-19156

STARBURST GALAXIES
Near-infrared spectroscopy of starburst and interacting galaxies N90-19144
Infrared spectroscopy of star formation in galaxies: Extreme conditions and very short time scales N90-19147
The strengths of the 2.3 micron CO band in luminous interacting and merging galaxies N90-19148
Evolutionary synthesis of the far-infrared emission in starburst galaxies N90-19152
Near infrared spectroscopy and spectroscopic imaging of NGC253 N90-19159

STARK EFFECT
Stark and Zeeman effects on laser cooling of positronium N90-18986

STARS
Infrared Spectroscopy in Astronomy
[ESA-SP-290] N90-19084

STATE ESTIMATION
Autonomous orbit determination using GPS
[INPE-4815-TDL/361] N90-18442
Adaptive state estimation and sampling rate analysis for invariant linear dynamic systems in time
[INPE-4960-TDL/389] N90-18951

STATIC MODELS
Experimental flow models for SSME flowfield characterization N90-18469

STATIC PRESSURE
Turbulence structure of mixing swirling flows
[AD-A216628] N90-18671

STATISTICAL ANALYSIS
Multistage forest volume estimation using a sampling system with probability variables
[INPE-4897-PRE/1498] N90-18769
The patterns of fracture and the conditioning tectonics in the region of the Quadrilatero Ferrifero and part of the Migmatitic-Gnanulitic Complex in Minas Gerais (Brazil)
[INPE-4895-PRE/1496] N90-18829
An integrated vision on methodologies and environments for modeling and simulation assisted by computer
[INPE-4861-TDL/372] N90-18886
A comparison of void distributions in Abell cluster catalogue with numerical simulations
[DE90-610640] N90-19173

STATORS
Aerodynamic study on forced vibrations on stator rows of axial compressors N90-18412
Blade row interaction effects on compressor measurements N90-18419

STEADY STATE
Compressor performance tests in the compressor research facility N90-18428
Investigation of methods to produce a uniform cloud of fuel particles in a flame tube
[NASA-TM-102376] N90-18665
The microwave background in steady-state cosmology N90-19150

STEAM TURBINES
Aerodynamic superposition principle in vibrating turbine cascades N90-18410
Phase-Change Thermal Energy Storage
[DE89-009426] N90-18801

STELLAR ATMOSPHERES
CO infrared bands in atmospheres of long-period variables N90-19128
IR spectrophotometry of bright carbon stars N90-19131

STELLAR ENVELOPES
Unidentified infrared features in proto-planetary nebulae N90-19130
IR spectrophotometry of bright carbon stars N90-19131
Observations of 40-70 micron bands of ice in IRAS 09371+1212 and other stars N90-19134
JCMT observations of the circumstellar envelope IRC+10216 N90-19138

STELLAR EVOLUTION
Infrared spectroscopy of supernova 1987A N90-19124
Unidentified infrared features in proto-planetary nebulae N90-19130
Carbon monoxide in supernova 1987A N90-19135
Detection of SN1986j in NGC891 at millimetre wavelengths N90-19137
Photometry of variable AFGL sources
[AD-A216938] N90-19165

STELLAR LUMINOSITY
On the mass to light ratios of dwarf spheroidal galaxies
[DE90-610645] N90-19175

STELLAR MASS
Annihilation physics of exotic galactic dark matter particles N90-18984

STELLAR MASS EJECTION
Infrared diagnostics of interstellar shocks N90-19115

STELLAR MODELS
Carbon monoxide in supernova 1987A N90-19135

STELLAR MOTIONS
Stellar kinematics in the galactic centre N90-19141

STELLAR RADIATION
Herbig Ae/Be stars: Fine structure far-infrared lines N90-19126
Soft x ray emission from classical novae in outburst
[DE90-006480] N90-19187

STELLAR SPECTRA
The environment of young stellar objects studied by high-resolution infrared spectroscopy N90-19120
High resolution infrared spectroscopy of symbiotic stars N90-19125
Detection of SN1986j in NGC891 at millimetre wavelengths N90-19137
A new interpretation of the feature of SiO maser spectra associated with M-type star
[DE90-610641] N90-19174

STELLAR SPECTROPHOTOMETRY
Infrared spectroscopy and imaging of supernova remnants N90-19104
IR spectrophotometry of bright carbon stars N90-19131

STELLAR WINDS
Predictions of infrared recombinations lines in stellar winds of hot stars N90-19136

STEPPING MOTORS
Linear Variable Differential Transformer (LVDT) with conditioner for the control of stepping motor drivers (part of the sliding-foil follower system of the Emin spectrometers)
[DIGEL-1989-9] N90-18660

STIFFNESS
A global approach for the identification of structural connection properties
[NASA-TM-102502] N90-18745

STIMULATED EMISSION
Research on sliding spark preionization in a TEA CO2 laser
[ISL-R-113/88] N90-18732

STIRLING ENGINES
Identification of a cast iron alloy containing nonstrategic elements
[NASA-CR-185174] N90-18559
Stirling engine technologies in Japan
[DE89-782296] N90-18795

STOCHASTIC PROCESSES
Evaluation of influences of errors involved in orbit propagation of artificial satellites
[INPE-4962-TDL/391] N90-18441

STORABLE PROPELLANTS
A perspective on the use of storable propellants for future space vehicle propulsion N90-18473

STORAGE BATTERIES
Feasibility of a super high energy density battery of the Li/BrF3 electrochemical system
[AD-A216794] N90-18644

STORAGE RINGS (PARTICLE ACCELERATORS)
Instability investigation for storage mode. Microwave instability (single-bunch instability)
[NIKHEF-K/AMPS/89/05] N90-18628
Biomedical applications of synchrotron x ray microscopy
[DE90-004957] N90-18867

STORAGE STABILITY
Investigation of the phase stabilizing effect of 4 percent potassium fluoride on ammonium nitrate
[AD-A215313] N90-18599
Instability investigation for storage mode. Microwave instability (single-bunch instability)
[NIKHEF-K/AMPS/89/05] N90-18628

STORAGE TANKS
Zero-gravity vortex vent and PVT gaging system N90-18486

STRAIN GAGES
Aerodynamic testing of a rotating wind turbine blade
[DE90-000312] N90-18962

STRAIN MEASUREMENT
Measuring strain in carbon fibre composite laminates using the Raman optomechanical strain gauge N90-18503

STRAIN RATE
An objective time-integration procedure for isotropic rate-independent and rate-dependent elastic-plastic constitutive equations
[PB90-121245] N90-18925

STRAITS
Comparison of circulation obtained through the trajectory of a drifting buoy tracked by satellite and hydrographic data in the Bransfield Strait
[INPE-4946-TDL/387] N90-18850

STRAPDOWN INERTIAL GUIDANCE
The Fourteenth Biennial Guidance Test Symposium, volume 1
[AD-A216925] N90-18383

STRATEGIC MATERIALS
Identification of a cast iron alloy containing nonstrategic elements
[NASA-CR-185174] N90-18559

STRATEGY
Remote sensing applied to vegetation as subsidized in municipal planning
[INPE-4908-PRE/1509] N90-18770
Survivability and effectiveness of near-term strategic defense
[DE90-005805] N90-18955

STREAM FUNCTIONS (FLUIDS)
Development of a defect stream function, law of the wall/wake method for compressible turbulent boundary layers
[NASA-CR-4286] N90-18675

STRESS ANALYSIS
Theory and verification of the fiber composite damage model implemented in DYNA3D
[AD-A216600] N90-18511
Development of a progressive failure model for strength of laminated composite structure
[AD-A216966] N90-18517

STRESS CORROSION
Biaxial strength and stress rupture of hot-pressed silicon nitride
[AD-A216950] N90-18750

STRESS CORROSION CRACKING
Failure probability estimate of Type 304 stainless steel piping
[DE90-003896] N90-18550
STRESS INTENSITY FACTORS
Crack propagation from artificial defects in typical engine disk materials; interpretation of experimental results by means of 3D J integral N90-18401
Fatigue crack initiation and small crack growth in several airframe alloys
[NASA-TM-102598] N90-18746
STRESS-STRAIN RELATIONSHIPS
Improved computational fluid dynamics for continuum hypersonic flow
[AD-A216981] N90-18674
STRONGLY COUPLED PLASMAS
High growth rate diamond synthesis in a large area atmospheric pressure inductively coupled plasma
[AD-A216090] N90-19019
STRUCTURAL ANALYSIS
Support trusses for large precision segmented reflectors: Preliminary design and analysis
[NASA-TM-101560] N90-18453
Probability of failure and risk assessment of propulsion structural components N90-18470
Hydrogenated amorphous and microcrystalline silicon deposited from silane-hydrogen mixtures
[ETN-90-96267] N90-18590
STRUCTURAL DESIGN
Design guidance to minimize unsteady forces in turbomachines N90-18411
Composites design handbook for space structure applications
[ESA-PSS-03-1101-ISSUE-1-REV-1] N90-18459
Probability of failure and risk assessment of propulsion structural components N90-18470
Small displacement, long life on-orbit compressor design and fabrication N90-18489
Structures and materials technology for hypersonic aerospacecraft
[NASA-TM-102583] N90-18752
STRUCTURAL DESIGN CRITERIA
Structures and materials technology for hypersonic aerospacecraft
[NASA-TM-102583] N90-18752
STRUCTURAL ENGINEERING
Structures and materials technology for hypersonic aerospacecraft
[NASA-TM-102583] N90-18752
STRUCTURAL FAILURE
Biaxial strength and stress rupture of hot-pressed silicon nitride
[AD-A216950] N90-18750
STRUCTURAL MEMBERS
Life of concentrated contacts in the mixed EHD and boundary film regimes
[AD-A216673] N90-18738
STRUCTURAL PROPERTIES (GEOLOGY)
Fracture analysis through photographic imagery of low spatial resolution: A contribution to the study of tectonic evoluation of the Araripe Plateau region
[INPE-4876-PRE/1487] N90-18756
Evaluation of selection techniques for multispectral bands employed in the discrimination of carbonatic rocks
[INPE-4850-TDL/365] N90-18765
Geological structure of the State of Rio de Janeiro viewed through MSS LANDSAT imagery
[INPE-4826-PRE/1457] N90-18825
Quantification of structural field data in the Rio Grande do Norte basin and neighborhood
[INPE-4821-RPE/591] N90-18826
STRUCTURAL RELIABILITY
Analysis of whisker-toughened ceramic components: A design engineer's viewpoint
[NASA-TM-102333] N90-18504
STRUCTURAL STABILITY
Study of vortex arrays induced artificially and from centrifugal instabilities
[AD-A216499] N90-18669
Active stabilization of aeromechanical systems
[AD-A216629] N90-18672
STRUCTURAL VIBRATION
Analytical formulation for the interaction problem of dynamic reentry, and effects due to flexibility and vibration in an aerospace vehicle
[INPE-4963-TDL/392] N90-18448
A study of the vibrational transmission through flanged joints
[ISVR-TR-181] N90-18755
STRUTS
Process development and fabrication of space station type aluminum-clad graphite epoxy struts
[NASA-CR-181873] N90-18454
SUBMILLIMETER WAVES
The James Clerk Maxwell telescope N90-19166
SUBSTRATES
Research relating to crystalline silicon-film on a foreign substrate
[DE90-005720] N90-18582
Pulsed laser deposition of high T(sub c) superconducting thin films
[AD-A216507] N90-19034
SUCTION
Time-dependent measurements on vibrating annular turbine cascades under various steady state conditions N90-18424
SULFATION
High temperature interaction of SO2 with oxide sorbents
[DE90-000435] N90-18545
SULFONATES
Nonlinear optical processes in one-dimensional polymers
[AD-A216103] N90-18568
SULFUR DIOXIDES
High temperature interaction of SO2 with oxide sorbents
[DE90-000435] N90-18545
SULFUR FLUORIDES
Wick-type liquid-metal combustion
[AD-A216019] N90-18530
SUPERCOMPUTERS
Performance characterization of the Convex C-240 computer system
[DE90-006425] N90-18879
Cedar project: Original goals and progress to date
[DE90-006761] N90-18880
SUPERCONDUCTING FILMS
Pulsed laser deposition of high T(sub c) superconducting thin films
[AD-A216507] N90-19034
In situ growth of epitaxial superconducting YBa2Cu3O(7-x) films on insulating semiconducting and ferroelectric K(Ta, Nb)O3 by pulsed laser ablation
[DE90-006568] N90-19043
In situ growth of high quality epitaxial YBa2Cu3O(7-x) thin films at moderate temperatures by pulsed laser ablation
[DE90-006629] N90-19045
SUPERCONDUCTING MAGNETS
Acoustic emission diagnostic techniques for high-field high current-density super inducting poles
[DE90-007400] N90-19000
SUPERCONDUCTING SUPER COLLIDER
Acoustic emission diagnostic techniques for high-field high current-density super inducting poles
[DE90-007400] N90-19000
SUPERCONDUCTIVITY
Microwave radiation absorption by Ho(Y)-Ba-Cu-O superconducting ceramics
[DE90-610665] N90-18588
Performance and modeling of superconducting ring resonators at millimeter-wave frequencies
[NASA-TM-102526] N90-18634
Mechanical disturbances in high-performance superconducting dipoles
[DE90-006237] N90-19040
Pressure induced superconductivity in elemental solids
[DE90-610664] N90-19048
Spectral functions from Quantum Monte Carlo
[DE90-004870] N90-19050
Superconducting materials
[DE90-007419] N90-19054
SUPERCONDUCTORS
Pulsed laser deposition of high T(sub c) superconducting thin films
[AD-A216507] N90-19034
Understanding electronegative effects in core-level electron spectroscopies; application to the high temperature superconductors
[AD-A216728] N90-19037
Superconducting materials
[DE90-007419] N90-19054
SUPERCOOLING
Time-resolved measurements of solidification and undercooling in metals and alloys
[DE90-007074] N90-18564
SUPERFLUIDITY
Superfluid helium orbital resupply coupling N90-18488
SUPERLATTICES
Crystal growth and mechanical properties of semiconductor alloys
[AD-A216697] N90-19035
SUPERNOVA REMNANTS
Infrared spectroscopy and imaging of supernova remnants N90-19104
Near infrared spectroscopy of the supernova remnant RCW103 N90-19109
SUPERNOVA 1987A
Infrared spectroscopy of supernova 1987A N90-19124
Near infrared (1-4 micron) spectroscopy of SN1987A N90-19133
Carbon monoxide in supernova 1987A N90-19135
SUPERNOVAE
Theoretical and experimental high energy physics
[DE90-006168] N90-19006
IR line emission from supernovae in molecular clouds N90-19102
Detection of SN1986j in NGC891 at millimetre wavelengths N90-19137
SUPERPLASTICITY
Processing and elevated temperature ductility of aluminum alloy 7475
[AD-A216840] N90-18554
SUPERPOSITION (MATHEMATICS)
Aerodynamic superposition principle in vibrating turbine cascades N90-18410
SUPERSONIC AIRCRAFT
Determination of the minimum energy conformation of alkyl substituted pyrazines
[AD-A216974] N90-18539
SUPERSONIC FLOW
The inviscid stability of supersonic flow past a sharp cone
[NASA-CR-181996] N90-18383
Experiments on the unsteady flow in a supersonic compressor stage N90-18422
Interaction between oblique-angled incident shock wave and turbulent boundary layer on a heated wall. Experimental results
[ONERA-RT-84/7078-AY] N90-18688
SUPPRESSORS
Characterization and development report for the SA3274-1 and SA3274-2 transient voltage suppressors
[DE90-005712] N90-18649
SURFACE FINISHING
Composite for smoothing the surface of ceramic substrates
[DE90-004005] N90-18565
SURFACE LAYERS
Pulsed laser deposition of high T(sub c) superconducting thin films
[AD-A216507] N90-19034
SURFACE PROPERTIES
Arcjet cathode phenomena N90-18477
Structure and reactivity of model thin film catalysts
[DE90-007365] N90-18546
Characterization of biopolymer surfaces using scanning microscopies
[AD-A216572] N90-18572
The joint effect of surface microtopography and near-surface structure on microcontact conditions
[DE90-006494] N90-18591
Multicomponent glass surfaces structure and adsorption
[DE90-007179] N90-18596
Evaluating a glass surface produced by ductile grinding
[DE90-006782] N90-18608
SURFACE REACTIONS
Surface intermediates in thin film deposition on silicon
[AD-A216662] N90-18534
Polymerization of nitro compounds on silver surfaces during surface-enhanced Raman scattering
[AD-A216116] N90-18569
SURFACE TEMPERATURE
Spacecraft thermal control design data, volume 1
[ESA-PSS-03-108-ISSUE-1-VOL-1] N90-18455
SURVEILLANCE RADAR
Multitarget tracking by single sensor: Analysis of the main approaches developed in this area
[ESA-TT-1171] N90-18633
SURVEYS
Resource Assessment Project: User needs survey results
[DE89-009502] N90-18802
SWIRLING
Turbulence structure of mixing swirling flows
[AD-A216828] N90-18671
Analytic solutions for the decay of turbulent swirling flow in a cylinder
[DE90-005744] N90-18677
SWITCHES
Coating possibilities for magnetic switches
[DE90-006536] N90-18659
Magnetohydrodynamic modeling of plasma opening switches and gas puff plasmas
[DE90-005825] N90-19026
SYMBIOTIC STARS
Infrared spectroscopy of novae and related objects N90-19123
High resolution infrared spectroscopy of symbiotic stars N90-19125

SYMMETRY
New aspects in bifurcation with symmetry
[AD-A216506] N90-18935
SYMPATHETIC NERVOUS SYSTEM
A program for the study of skeletal muscle catabolism following physical trauma
[AD-A216569] N90-18859
SYNCHRONISM
Synchronization of the ground station atomic clocks using three weighted transportable cesium time standards in the Navex navigation experiment
[ESA-TT-1153] N90-18711
Log-based recovery in asynchronous distributed systems
[NASA-CR-186190] N90-18924
SYNCHROTRON RADIATION
Biomedical applications of synchrotron x ray microscopy
[DE90-004957] N90-18867
A continuous plasma final focus
[DE90-006096] N90-19024
SYNTHESIS (CHEMISTRY)
Synthesis of high-purity sinterable silicon nitride powder
[DE90-007050] N90-18593
Optimum catalytic process for alcohol fuels from syngas
[DE90-005290] N90-18600
High growth rate diamond synthesis in a large area atmospheric pressure inductively coupled plasma
[AD-A216090] N90-19019
SYNTHETIC APERTURE RADAR
Synthetic aperture radar imagery of airports and surrounding areas: Archived SAR data
[NASA-CR-4275] N90-18371
Synthetic aperture radar imagery of airports and surrounding areas: Philadelphia Airport
[NASA-CR-4280] N90-18372
Simulation of synthetic aperture radar 3: Evaluation of prototype digital feature analysis data
[AD-A216750] N90-18620
An application of ocean wave-current refraction to the gulf stream using SEASAT SAR data
[AD-A216769] N90-18851
Activities report in German aerospace
[ISSN-0070-3966] N90-19189
SYNTHETIC FUELS
Optimum catalytic process for alcohol fuels from syngas
[DE90-005290] N90-18600
Alternative fuels R/D needs: Program directions
[DE90-007053] N90-18603
Optimum catalytic process for alcohol fuels from syngas
[DE90-007188] N90-18604
SYSTEM IDENTIFICATION
System properties from frequency response functions, part 1
[ISVR-TR-166-PT-1] N90-18754
SYSTEMS ANALYSIS
Airborne radar systems specialist, AFSC 118X2
[AD-A215450] N90-18611
SYSTEMS ENGINEERING
National airspace system plan: Facilities, equipment, associated development and other capital needs
[AD-A215882] N90-18373
Design of a new control system for hovercrafts
[ETN-90-96230] N90-18435
System safety requirements for ESA space systems and associated equipment
[ESA-PSS-01-40-ISSUE-2] N90-18460
Back swing phenomenon of synchronous generator. Study on ac-dc power system simulator tests
[DE89-782321] N90-18635
Optimal planning method of underground distribution system, part 2. Application to various types of system configurations
[DE89-782323] N90-18636
Integrated silicon flip-flop sensors
[ETN-90-96271] N90-18654
User manual for NEXT 1.2: NLR engineering X-pert system toolkit
[NLR-TR-87178-U] N90-18905
SYSTEMS INTEGRATION
The implications of using integrated software support environment for design of guidance and control systems software
[AGARD-AR-229] N90-18432
Integrated regenerative fuel cell experimental evaluation
[NASA-CR-185183] N90-18808
An integrated vision on methodologies and environments for modeling and simulation assisted by computer
[INPE-4861-TDL/372] N90-18886
SYSTEMS STABILITY
System properties from frequency response functions, part 1
[ISVR-TR-166-PT-1] N90-18754

T

TARGET ACQUISITION
Visual target detection and recognition
[DE90-006903] N90-19015
TARGET RECOGNITION
Psychological studies of visual cortical function
[AD-A217029] N90-18872
A simulation of optical propagation through atmospheric turbulence using two-dimensional Fourier transform techniques
[AD-A216776] N90-19013
TARGETS
Spallation and dynamic fracture as an effect of laser induced shock waves in carbon based composite materials
[AD-A216540] N90-18509
TEA LASERS
Research on sliding spark preionization in a TEA CO2 laser
[ISL-R-113/88] N90-18732
TECHNOLOGICAL FORECASTING
Space orientation and orbital technology
[ISBN-3-89100-015-4] N90-18437
Long term planning for space flight activities within the DFVLR
[DFVLR-IB-303-88/2] N90-18438
Materials and structures for 2000 and beyond: An attempted forecast by the Materials and Structures Department of the DLR
[ESA-TT-1154] N90-18609
Methodology panel N90-19076
TECHNOLOGY ASSESSMENT
Rheological tests of Rigidite 5245 using the cone-plate and parallel plates method
[DT-310/88] N90-18544
Technology assessment of software engineering
[AD-A216943] N90-18902
Mechanical disturbances in high-performance superconducting dipoles
[DE90-006237] N90-19040
TECHNOLOGY TRANSFER
Long term planning for space flight activities within the DFVLR
[DFVLR-IB-303-88/2] N90-18438
Transfer of heat pump technology
[DE90-007373] N90-18693
Programs in Renewable Energy
[DE89-009489] N90-18809
TECHNOLOGY UTILIZATION
The DFVLR 3-m x 3-m low speed wind tunnel (NWG) in Goettingen
[ESA-TT-1156] N90-18436
Materials and structures for 2000 and beyond: An attempted forecast by the Materials and Structures Department of the DLR
[ESA-TT-1154] N90-18609
Technology development and circuit design for a parallel laser programmable floating point application specific processor
[AD-A215870] N90-18637
Promotion of European Space Technology Transfer
[ESA-SP-1122] N90-19068
ESA project to promote and assist technology transfer by industry N90-19069
Space technology transfers in Europe N90-19070
DTE and space technology transfer N90-19071
Purchase of technology N90-19072
The bringing to market of the RF alert (a case study in technology transfer) N90-19073
French approach to space technology transfer N90-19074
Introductory remarks for the panel discussions on technology transfer N90-19075
Methodology panel N90-19076
Problems on transfer of space technology to non-space areas and solutions: Legal aspects N90-19077
Identification of and response to market demand N90-19078
The improvement of technology transfer from space to industry N90-19079
Internal technology transfer N90-19080
Magnetic suspension railway systems based on space technology N90-19081
An example of technology transfer by Aerospatiale: Fire protection materials N90-19082
TECTONICS
Fracture analysis through photographic imagery of low spatial resolution: A contribution to the study of tectonic evoluation of the Araripe Plateau region
[INPE-4876-PRE/1487] N90-18756
The interpretation of crustal dynamics data in terms of plate interactions and active tectonics of the Anatolian plate and surrounding regions in the Middle East
[NASA-CR-186200] N90-18824
Geological structure of the State of Rio de Janeiro viewed through MSS LANDSAT imagery
[INPE-4826-PRE/1457] N90-18825
The patterns of fracture and the conditioning tectonics in the region of the Quadrilatero Ferrifero and part of the Migmatitic-Gnanulitic Complex in Minas Gerais (Brazil)
[INPE-4895-PRE/1496] N90-18829
TELECOMMUNICATION
Integrated IMA (Information Mission Areas) IC (Information Center) guide
[AD-A216944] N90-18903
TELEMETRY
SHARP: A multi-mission artificial intelligence system for spacecraft telemetry monitoring and diagnosis
[NASA-CR-186285] N90-18444
Packet telemetry standard
[ESA-PSS-04-106-ISSUE-1] N90-18447
Telemetry and telecommand omnidirectional antenna in the short wave band
[ETN-90-96285] N90-18631
TELEOPERATORS
Teleoperator servoloop tuning using an expert system
[DE90-005674] N90-18876
TELEPHONY
Proceedings of the 38th International Wire and Cable Symposium
[AD-A216023] N90-18638
TELESCOPES
JCMT observations of the circumstellar envelope IRC+10216 N90-19138
The James Clerk Maxwell telescope N90-19166
Imaging Germanium Telescope Array for Gamma-Rays (IGETAGRAY)
[DE90-006994] N90-19188
TEMPERATURE CONTROL
Spacecraft thermal control design data, volume 1
[ESA-PSS-03-108-ISSUE-1-VOL-1] N90-18455
Spacecraft thermal control design data, volume 2
[ESA-PSS-03-108-ISSUE-1-VOL-2] N90-18456
Spacecraft thermal control design data, volume 3
[ESA-PSS-03-108-ISSUE-1-VOL-3] N90-18457
Spacecraft thermal control design data, volume 4
[ESA-PSS-03-108-ISSUE-1-VOL-4] N90-18458
Condensation fluid dynamics and heat transfer on rotating spherical surfaces in a microgravitational field
[DE90-005540] N90-18607
TEMPERATURE DEPENDENCE
Navigation experiment NAVEX: The self-test delay times in the D1 Spacelab mission
[ESA-TT-1176] N90-18446
Temperature dependence of photon-gated persistent spectral hole-burning for the meso-tetra-p-tolyl Zn-tetrabenzoporphyrin/chloroform system in poly(methylmethacrylate)
[AD-A216086] N90-18531
Microwave radiation absorption by Ho(Y)-Ba-Cu-O superconducting ceramics
[DE90-610665] N90-18588
Strong source heat transfer simulations based on a GalerKin/gradient least squares method
[DE90-608613] N90-18678
TEMPERATURE EFFECTS
Structural study of thermo-hardenable matrices. Deformation processes of composite matrices as a function of their molecular structure
[ONERA-RT-10/3521-M] N90-18522
Comparison between the damage modes of thermo-hardenable and thermo-plastic composite matrices
[ONERA-RT-47/7086-M] N90-18523
Calculation of mechanical properties variations depending on matrix parameters in a composite, as a function of the test temperature
[DT-311/88] N90-18526
High temperature interaction of SO2 with oxide sorbents
[DE90-000435] N90-18545
Thermal remote sensing in the differentiation of soybean crops (glycine max (L.) merrill) submitted to water deficit
[INPE-4900-PRE/1501] N90-18762
In situ growth of high quality epitaxial YBa2Cu3O(7-x) thin films at moderate temperatures by pulsed laser ablation
[DE90-006629] N90-19045
TEMPERATURE MEASUREMENT
Thermal analysis of polymer composites
[AD-A216947] N90-18578

Solid-state fluorescence above 1000 C: Application to high-temperature laser thermography
[DE90-006422] N90-18721
Preliminary comparison of temperature soundings obtained from simultaneous radiometric, radio-acoustic, and rawinsonde measurements
[PB90-119835] N90-18838
Transient heat transfer measurements on a flat plate in turbulent flow using an electrical analog
[AD-A216286] N90-19057

TEMPERATURE MEASURING INSTRUMENTS
Development of a mass averaging temperature probe N90-18418

TEMPORAL RESOLUTION
Physiognomy of vegetation cover in the PNPM identified through the TM/LANDSAT sensor: A multitemporal analysis
[INPE-4834-PRE/1464] N90-18776
Three-dimensional motion estimation using shading information in multiple frames
[AD-A216804] N90-18919

TENSILE PROPERTIES
Preliminary evaluation of the strength of pin-joints in laminated composite materials
[DE90-006353] N90-18524

TENSILE STRENGTH
Development of a progressive failure model for strength of laminated composite structure
[AD-A216966] N90-18517

TENSOR ANALYSIS
Vector fields, linear spaces and tensors in physics. Part 3: Tensor analysis and its applications
[INPE-5000-MD/41] N90-18997

TENSORS
Vector fields, linear spaces and tensors in physics. Part 3: Tensor analysis and its applications
[INPE-5000-MD/41] N90-18997

TERMINAL BALLISTICS
Effects of oblique impact on hypervelocity shield performance
[DE90-006936] N90-18739

TERRACES (LANDFORMS)
Fracture analysis through photographic imagery of low spatial resolution: A contribution to the study of tectonic evoluation of the Araripe Plateau region
[INPE-4876-PRE/1487] N90-18756

TERRAIN
Project Floval: Correction of relief effects in eucalyptus reforestration
[INPE-4814-RPE/590] N90-18777
An evaluation of an airborne laser profiling system for high precision terrain mapping
[AD-A217025] N90-18780
SPOT for landscape: Development of a method for the use of SPOT pictures for the updating of the data base scale of the landscape
[BCRS-89-18] N90-18787

TERRAIN ANALYSIS
An evaluation of an airborne laser profiling system for high precision terrain mapping
[AD-A217025] N90-18780

TEST FACILITIES
Simulation of the dynamic environment for missile component testing: Demonstration
[AD-A216979] N90-18443
Preliminary design of a pointer for movement of a solar simulator
[INPE-4864-TDL/375] N90-18736
Resource Assessment Project: User needs survey results
[DE89-009502] N90-18802
Thermal vacuum life test facility for radioisotope thermoelectric generators
[DE90-007148] N90-19010

TEST FIRING
Technique for evaluating the erosive properties of ablative internal insulation materials N90-18466

TEST STANDS
Feasibility demonstration of a 445N high-performance rocket engine N90-18481

TEXTS
Approaches to the planning of coherent text
[AD-A216463] N90-18895

TEXTURES
Classification of high resolution imagery using texture attributes
[INPE-4888-TDL/379] N90-18778

THEMATIC MAPPERS (LANDSAT)
Improvement of classification results from satellite imagery to update and differentiate land use classes on topographic maps
[BCRS-89-17] N90-18786
LANDSAT Thematic Mapper for hydrogeological mapping in Egypt
[BCRS-89-28] N90-18791

THEMATIC MAPPING
Monitoring of reforested areas through digital analysis of TM data
[INPE-4930-PRE/1420] N90-18764
Evaluation of selection techniques for multispectral bands employed in the discrimination of carbonatic rocks
[INPE-4850-TDL/365] N90-18765
Radiometric study of wheat and bean crops in three types of latossolo
[INPE-4843-PRE/1472] N90-18767
Relationships between spectral parameters and agronomics of wheat and beam crops
[INPE-4791-RPE/584] N90-18768
Remote sensing applied to vegetation as subsidized in municipal planning
[INPE-4908-PRE/1509] N90-18770
Evaluation of TM/LANDSAT and HRV/SPOT data in reforested areas
[INPE-4575-RPE/567] N90-18772
Perspective revision of systematic mapping through orbital imagery
[INPE-4817-PRE/1453] N90-18775
Physiognomy of vegetation cover in the PNPM identified through the TM/LANDSAT sensor: A multitemporal analysis
[INPE-4834-PRE/1464] N90-18776
Project Floval: Correction of relief effects in eucalyptus reforestration
[INPE-4814-RPE/590] N90-18777
On the applicability of CAESAR for the remote sensing of bottom depth and bottom composition of shallow waters: A model study
[BCRS-89-13] N90-18783
LANDSAT Thematic Mapper for hydrogeological mapping in Egypt
[BCRS-89-28] N90-18791
Quantification of structural field data in the Rio Grande do Norte basin and neighborhood
[INPE-4821-RPE/591] N90-18826

THEOREMS
Mathematical methods of Physics 6: Integral transformation
[INPE-4807-MD/40] N90-18926
Strong moderate deviation theorems
[MEMO-804] N90-18954

THEORETICAL PHYSICS
Mathematical methods of Physics 6: Integral transformation
[INPE-4807-MD/40] N90-18926
Theoretical studies in nuclear physics
[DE90-005981] N90-19005
Theoretical and experimental high energy physics
[DE90-006168] N90-19006

THERMAL ANALYSIS
Spacecraft thermal control design data, volume 4
[ESA-PSS-03-108-ISSUE-1-VOL-4] N90-18458
Thermal analysis of polymer composites
[AD-A216947] N90-18578
Heat capacities of solid polymers (The Advanced THermal Analysis System, ATHAS)
[DE90-007130] N90-18595

THERMAL BLOOMING
Effect of a random wind field on thermal blooming instabilities
[DE90-007241] N90-18823

THERMAL CONTROL COATINGS
Spacecraft thermal control design data, volume 2
[ESA-PSS-03-108-ISSUE-1-VOL-2] N90-18456

THERMAL DEGRADATION
Arcjet cathode phenomena N90-18477
Design and operation of an inert gas facility for thermoelectric generator storage
[DE90-007146] N90-19008
Thermal vacuum life test facility for radioisotope thermoelectric generators
[DE90-007148] N90-19010

THERMAL ENERGY
Phase-Change Thermal Energy Storage
[DE89-009426] N90-18801

THERMAL FATIGUE
Softening mechanisms and microstructural instabilities during high temperature, low cycle fatigue of Ni, Ni3Al, and their metal matrix composites
[DE90-006487] N90-18557
Creep in shear of experimental solder joints
[DE90-007062] N90-18753

THERMAL INSTABILITY
Direct and inverse scattering problem associated with the elliptic Sinh-Gordon equation
[AD-A216455] N90-18931

THERMAL INSULATION
Spacecraft thermal control design data, volume 2
[ESA-PSS-03-108-ISSUE-1-VOL-2] N90-18456

THERMAL MAPPING
Thermal remote sensing in the differentiation of soybean crops (glycine max (L.) merrill) submitted to water deficit
[INPE-4900-PRE/1501] N90-18762
Interrelationship of spatial and radiometric resolution in the thermal infrared band
[INPE-4860-TDL/371] N90-18771
Infrared spectroscopy of dust N90-19094

THERMAL PLASMAS
High growth rate diamond synthesis in a large area atmospheric pressure inductively coupled plasma
[AD-A216090] N90-19019

THERMAL PROTECTION
Spacecraft thermal control design data, volume 1
[ESA-PSS-03-108-ISSUE-1-VOL-1] N90-18455
An example of technology transfer by Aerospatiale: Fire protection materials N90-19082

THERMAL STABILITY
Thermal analysis of polymer composites
[AD-A216947] N90-18578

THERMAL VACUUM TESTS
Thermal vacuum life test facility for radioisotope thermoelectric generators
[DE90-007148] N90-19010

THERMODYNAMIC EQUILIBRIUM
Measurement of spectral emissivity by Fourier transform infrared spectrometer
[DE89-782319] N90-18898
The free energy principle, negative energy modes, and stability
[DE90-005368] N90-19056

THERMODYNAMIC PROPERTIES
Reliability assessment using finite element techniques
[AD-A216907] N90-18647
Spectroscopy and physico-chemistry of CO:H2O and CO2:H2O ices N90-19111

THERMODYNAMICS
Processing and elevated temperature ductility of aluminum alloy 7475
[AD-A216840] N90-18554
Control of phase structure in polymer blends
[AD-A217034] N90-18580
Summer Study Program in Geophysical Fluid Dynamics: The Influence of Convection on Large-Scale Circulations, 1988
[AD-A216024] N90-18840
Thermodynamics of systems with very many components phase equilibrium
[DE90-007345] N90-19059

THERMOELECTRIC GENERATORS
Design and operation of an inert gas facility for thermoelectric generator storage
[DE90-007146] N90-19008
Thermal vacuum life test facility for radioisotope thermoelectric generators
[DE90-007148] N90-19010

THERMOPHYSICAL PROPERTIES
Beam collector and output window for a 35 GHz 100 kW gyrotron
[INPE-4958-RPE/603] N90-18699

THERMOPLASTIC RESINS
Comparison between the damage modes of thermo-hardenable and thermo-plastic composite matrices
[ONERA-RT-47/7086-M] N90-18523

THERMOSETTING RESINS
Enhanced bonding of fiber reinforcements to thermoset resins N90-18496

THIN FILMS
Interfacial chemistry of MoS2 films on Si
[AD-A216527] N90-18532
Surface intermediates in thin film deposition on silicon
[AD-A216662] N90-18534
Structure and reactivity of model thin film catalysts
[DE90-007365] N90-18546
Perforated monolayers
[DE90-005469] N90-18566
Metallaboranes as precursors to metallic glasses
[AD-A216946] N90-18577
Hydrogenated amorphous silicon films prepared by glow discharge of disilane
[DE90-000309] N90-18581
Research relating to crystalline silicon-film on a foreign substrate
[DE90-005720] N90-18582
Microcomputer enhanced optical investigation of spreading and evaporative processes in ultra thin films
[DE90-006323] N90-18585
Cell performance of ultra-thin polymer cathode systems. Part 1: Anion intercalating polymer cathode
[AD-A216037] N90-18639
Progress in thin film solar photovoltaic technologies
[DE89-009513] N90-18792
Chemical vapor deposition and photochemical vapor deposition of amorphous silicon photovoltaic devices
[DE89-009510] N90-18803

Pulsed laser deposition of high T(sub c) superconducting thin films
[AD-A216507] N90-19034
Structure and vibrational excitations of reconstructed semiconductor surfaces
[DE90-006589] N90-19044
In situ growth of high quality epitaxial YBa2Cu3O(7-x) thin films at moderate temperatures by pulsed laser ablation
[DE90-006629] N90-19045

THREADS
Threaded joint design for composites
[DE90-005553] N90-18506
Fastener design manual
[NASA-RP-1228] N90-18740

THREE DIMENSIONAL COMPOSITES
Theory and verification of the fiber composite damage model implemented in DYNA3D
[AD-A216600] N90-18511

THREE DIMENSIONAL FLOW
Numerical simulation of three-dimensional unsteady flows in turbomachines N90-18417
A simple algebraic grid adaptation scheme with applications to two- and three-dimensional flow problems
[NASA-TM-102446] N90-18667
Contribution to the study of three-dimensional separation in turbulent incompressible flow
[ESA-TT-1169] N90-18697
Doppler lidar working group report
[ESA-SP-1112] N90-18848

THREE DIMENSIONAL MODELS
Three-dimensional coculture process
[NASA-CASE-MSC-21560-1] N90-18852
Recognizing three-dimensional objects without the use of models
[AD-A216766] N90-18862

THREE DIMENSIONAL MOTION
Three-dimensional motion estimation using shading information in multiple frames
[AD-A216804] N90-18919

THRUST CHAMBERS
Feasibility demonstration of a 445N high-performance rocket engine N90-18481

THRUST MEASUREMENT
Arcjet nozzle design impacts N90-18478

THYRISTORS
A GaAs p-n-p-n thyristor model
[DE90-005757] N90-19039

TIME DEPENDENCE
Time-dependent measurements on vibrating annular turbine cascades under various steady state conditions N90-18424

TIME FUNCTIONS
Excess transit time as a function of burst current in an exploding bridgewire detonator
[DE90-007168] N90-18708

TIME MEASUREMENT
Navigation experiment NAVEX data storage and processing
[ESA-TT-1175] N90-18445
Synchronization of the ground station atomic clocks using three weighted transportable cesium time standards in the Navex navigation experiment
[ESA-TT-1153] N90-18711

TIME OPTIMAL CONTROL
Control and stabilization of linear and nonlinear distributed systems
[AD-A216446] N90-18908

TIME SERIES ANALYSIS
Optimum selection procedures in multi-stage screening, reliability, and time
[AD-A216811] N90-18942

TIME SIGNALS
Navigation experiment NAVEX: The self-test delay times in the D1 Spacelab mission
[ESA-TT-1176] N90-18446
Synchronization of the ground station atomic clocks using three weighted transportable cesium time standards in the Navex navigation experiment
[ESA-TT-1153] N90-18711

TIROS N SERIES SATELLITES
Spatial registration of TIROS-N weather satellite data
[AD-A216041] N90-18841

TISSUES (BIOLOGY)
Three-dimensional coculture process
[NASA-CASE-MSC-21560-1] N90-18852

TITANIUM ALLOYS
Low temperature specific heat and magnetic susceptibility of NbTi and NbTiMn alloys
[DE90-005390] N90-18552

TOKAMAK DEVICES
The rapid inward diffusion of cold ions in tokamaks and their effect on ion transport
[DE90-006863] N90-19022
Thermonuclear instability of global-type shear Alfven modes
[DE90-007087] N90-19026

TOLERANCES (MECHANICS)
AGARD/SMP Review: Damage Tolerance for Engine Structures. 2: Defects and Quantitative Materials Behaviour — conference
[AGARD-R-769] N90-18396
The damage tolerance of disc materials: Metallurgical factors; relationship with processing parameters N90-18398
Future technology requirements (related to defects and quantitative material behavior to aid in implementation of damage tolerance for design of engine structures) N90-18403

TOLUENE
Nonlinear optical processes in one-dimensional polymers
[AD-A216103] N90-18568

TOMOGRAPHY
An application of ocean wave-current refraction to the gulf stream using SEASAT SAR data
[AD-A216769] N90-18851
Inverse scattering and tomography
[AD-A216456] N90-18932

TOPOGRAPHY
Land suitability maps and appropriate land use: An approach using SGI and satellite imagery
[INPE-4827-PRE/1458] N90-18761
Perspective revision of systematic mapping through orbital imagery
[INPE-4817-PRE/1453] N90-18775
Improvement of classification results from satellite imagery to update and differentiate land use classes on topographic maps
[BCRS-89-17] N90-18786
SPOT for landscape: Development of a method for the use of SPOT pictures for the updating of the data base scale of the landscape
[BCRS-89-18] N90-18787
Quantification of structural field data in the Rio Grande do Norte basin and neighborhood
[INPE-4821-RPE/591] N90-18826

TOROIDS
Toroid monitor
[DIGEL-1989-8] N90-18663

TORQUE
Electronically Variable Pressure Regulator (EVPR) N90-18484
Back swing phenomenon of synchronous generator. Study on ac-dc power system simulator tests
[DE89-782321] N90-18635

TOXICITY
Risk analysis: Fundamental concepts, regulatory toxicology, and relative comparisons from radiation biology
[DE90-002466] N90-18856

TRACE ELEMENTS
Technology update-89
[DE90-005813] N90-19178

TRACKING (POSITION)
An evaluation of an airborne laser profiling system for high precision terrain mapping
[AD-A217025] N90-18780

TRACKING FILTERS
Multitarget tracking by single sensor: Analysis of the main approaches developed in this area
[ESA-TT-1171] N90-18633

TRACKING RADAR
Multitarget tracking by single sensor: Analysis of the main approaches developed in this area
[ESA-TT-1171] N90-18633

TRACKING STATIONS
Navigation experiment NAVEX data storage and processing
[ESA-TT-1175] N90-18445

TRAINING ANALYSIS
Evaluation of two methods for acquisition of training statistics for digital analysis of areas prepared for plowing
[INPE-4901-PRE/1502] N90-18763

TRAINING EVALUATION
Airborne radar systems specialist, AFSC 118X2
[AD-A215450] N90-18611
Schema-based theories of problem solving
[AD-A216717] N90-18939

TRAINING SIMULATORS
Simulation of synthetic aperture radar 3: Evaluation of prototype digital feature analysis data
[AD-A216750] N90-18620

TRAJECTORIES
Spatial registration of TIROS-N weather satellite data
[AD-A216041] N90-18841

TRAJECTORY MEASUREMENT
Comparison of circulation obtained through the trajectory of a drifting buoy tracked by satellite and hydrographic data in the Bransfield Strait
[INPE-4946-TDL/387] N90-18850

TRANSCONDUCTANCE
Output performance of idealized microwave power amplifiers
[AD-A216797] N90-18845

TRANSDUCERS
Integrated silicon flip-flop sensors
[ETN-90-96271] N90-18654

TRANSFORMERS
A test method for measuring corona inception voltage for transducer autotransformers
[AD-A216818] N90-18648
Linear Variable Differential Transformer (LVDT) with conditioner for the control of stepping motor drivers (part of the sliding-foil follower system of the Emin spectrometers)
[DIGEL-1989-9] N90-18660
Toroid monitor
[DIGEL-1989-8] N90-18663

TRANSIENT PRESSURES
Transient pressure test article test program N90-18463

TRANSIENT RESPONSE
Transient pressure test article test program N90-18463
Transient responses of coupled systems
[ONERA-RT-13/3596-RY-070-R] N90-18687

TRANSISTORS
A GaAs p-n-p-n thyristor model
[DE90-005757] N90-19039

TRANSIT SATELLITES
An error sensitivity model for Doppler positioning using transit satellites
[AD-A216724] N90-18381

TRANSIT TIME
Excess transit time as a function of burst current in an exploding bridgewire detonator
[DE90-007168] N90-18708

TRANSITION TEMPERATURE
Calculation of mechanical properties variations depending on matrix parameters in a composite, as a function of the test temperature
[DT-311/88] N90-18526
Pressure induced superconductivity in elemental solids
[DE90-610664] N90-19048

TRANSMISSION LINES
Proceedings of the 38th International Wire and Cable Symposium
[AD-A216023] N90-18638
Design, implementation and test of an RS-232 compatible bi-directional, full duplex, fiber-optic interface with provision for hardware handshaking on a minimum of fiber-optic lines
[AD-A216604] N90-19012

TRANSMISSIONS (MACHINE ELEMENTS)
Life of concentrated contacts in the mixed EHD and boundary film regimes
[AD-A216673] N90-18738
A theory of quantitative inference for artifact sets applied to a mechanical design compiler
[AD-A216535] N90-18896

TRANSONIC FLOW
High-resolution Euler computations of unsteady transonic flows in cascades N90-18420
Asymptotic analysis of transonic flow through oscillating cascades N90-18421

TRANSONIC WIND TUNNELS
Half model tests on an ONERA calibration model in the transonic wind tunnel Goettingen, Federal Republic of Germany
[DLR-MITT-89-20] N90-18370

TRANSPONDERS
An error sensitivity model for Doppler positioning using transit satellites
[AD-A216724] N90-18381

TRANSPORT PROPERTIES
A numerical solution to the Boltzmann equation for use in calculating pumping rates in a CO2 discharge laser
[AD-A216376] N90-18718
Magnetohydrodynamic modeling of plasma opening switches and gas puff plasmas
[DE90-005825] N90-19028
Transport effects and spectroscopy of defects in microstructures
[AD-A216718] N90-19036

TRANSPORT THEORY
The neoclassical transport of toroidal momentum in tokamaks
[DE90-006864] N90-19023

TRAVELING WAVES
Active stabilization of aeromechanical systems
[AD-A216629] N90-18672

TRENDS
Remote sensing applied to vegetation as subsidized in municipal planning
[INPE-4908-PRE/1509] N90-18770

TRIBOLOGY
The joint effect of surface microtopography and near-surface structure on microcontact conditions
[DE90-006494] N90-18591

TRITIUM
Technology update-89
[DE90-005813] N90-19178

TROPICAL REGIONS
Spectral response of wheat and its relationship with agronomical prameters
[INPE-4950-RPE/599] N90-18774
Photointerpretation with instruments for evaluation of environmental impact: Mata Atlantica in Cubata
[INPE-4910-PRE/1511] N90-18817

TROPOSPHERE
Tropospheric chemistry of natural hydrocarbons and energy-related pollutants: Biosphere/climate feedbacks
[DE90-005643] N90-18820
Connections between the circulation in altitude and convection over South America
[INPE-4923-TDL/383] N90-18828

TRUNCATION ERRORS
Evaluation of influences of errors involved in orbit propagation of artiificial satellites
[INPE-4962-TDL/391] N90-18441

TRUSSES
Support trusses for large precision segmented reflectors: Preliminary design and analysis
[NASA-TM-101560] N90-18453
Process development and fabrication of space station type aluminum-clad graphite epoxy struts
[NASA-CR-181873] N90-18454

TUNABLE LASERS
Absorption experiments on electron-beam pumped rare gases
[DE90-006504] N90-18722

TUNGSTEN
Structure and reactivity of model thin film catalysts
[DE90-007365] N90-18546

TURBINE BLADES
Aerodynamic testing of a rotating wind turbine blade
[DE90-000312] N90-18362
A comparison of flutter calculations based on eigenvalue and energy method N90-18406
Unsteady aerodynamic phenomena in a simulated wake and shock wave passing experiment N90-18414
Time-dependent measurements on vibrating annular turbine cascades under various steady state conditions N90-18424
Measurements of surface pressures on an operating vertical-axis wind turbine
[DE90-005722] N90-18805

TURBINE WHEELS
Defects in monoblock cast turbine wheels N90-18400

TURBOCOMPRESSORS
Aerodynamic study on forced vibrations on stator rows of axial compressors N90-18412
Numerical prediction of axial turbine stage aerodynamics N90-18416
Stall and recovery in multistage axial flow compressors N90-18429

TURBOMACHINE BLADES
Automation and extension of LDV (Laser-Doppler Velocimetry) measurements of off-design flow in a subsonic cascade wind tunnel
[AD-A216627] N90-18670

TURBOMACHINERY
Unsteady Aerodynamic Phenomena in Turbomachines
[AGARD-CP-468] N90-18405
Numerical investigation of unsteady flow in oscillating turbine and compressor cascades N90-18407
Numerical simulation of three-dimensional unsteady flows in turbomachines N90-18417
Numerical investigations of heat transfer and flow rates in rotating cavities. Simulation of the movement generated by wall temperature gradients, by source-sink mass flows or by the differential rotation of the walls, under the influence or coriolis and centrifugal forces
[ETN-90-96253] N90-16a95

TURBULENCE
Fluidization mechanisms in slurry flow
[DE90-006497] N90-18691
Vertical axis wind turbine turbulent response model. Part 2: Response of Sandia National laboratories' 34-meter VAWT with aeroelastic effects
[DE90-005721] N90-18804

TURBULENCE MODELS
Turbulence structure of mixing swirling flows
[AD-A216628] N90-18671

TURBULENT BOUNDARY LAYER
Study of vortex arrays induced artificially and from centrifugal instabilities
[AD-A216499] N90-18669
Development of a defect stream function, law of the wall/wake method for compressible turbulent boundary layers
[NASA-CR-4286] N90-18675
Interaction between oblique-angled incident shock wave and turbulent boundary layer on a heated wall. Experimental results
[ONERA-RT-84/7078-AY] N90-18888

TURBULENT DIFFUSION
An investigation of flow structure, mixing and chemical reaction in combusting turbulent flows
[AD-A216739] N90-18538

TURBULENT FLOW
An investigation of flow structure, mixing and chemical reaction in combusting turbulent flows
[AD-A216739] N90-18538
Turbulence structure of mixing swirling flows
[AD-A216628] N90-18671
Analytic solutions for the decay of turbulent swirling flow in a cylinder
[DE90-005744] N90-18677
Concepts and experiments on space-time chaos
[ETN-90-96255] N90-18683
Numerical simulation of the incompressible inhomogeneous turbulence in a plane channel flow
[ONERA-NT-1988-5] N90-18686
Contribution to the study of three-dimensional separation in turbulent incompressible flow
[ESA-TT-1169] N90-18697
Vertical axis wind turbine turbulent response model. Part 2: Response of Sandia National laboratories' 34-meter VAWT with aeroelastic effects
[DE90-005721] N90-18804
Transient heat transfer measurements on a flat plate in turbulent flow using an electrical analog
[AD-A216286] N90-19057

TURBULENT HEAT TRANSFER
Transient heat transfer measurements on a flat plate in turbulent flow using an electrical analog
[AD-A216286] N90-19057

TURBULENT JETS
Numerical simulations of coherent structures in a jet flame with a noncircular cross section
[AD-A216710] N90-18535

TURING MACHINES
Optimum and heuristic algorithms for finite state machine decomposition and partitioning
[AD-A216778] N90-18899
Boolean minimization and algebraic factorization procedures for fully testable sequential machines
[AD-A216779] N90-18940

TVD SCHEMES
High-resolution Euler computations of unsteady transonic flows in cascades N90-18420

TWINNING
Deformation and fracture of ordered intermetallic compounds
[DE90-007422] N90-18563

TWO DIMENSIONAL FLOW
Calculation of the unsteady two-dimensional, inviscid, compressible flow around a strongly cambered oscillating single blade N90-18409
A simple algebraic grid adaptation scheme with applications to two- and three-dimensional flow problems
[NASA-TM-102446] N90-18667

TWO DIMENSIONAL MODELS
Test data of flow field of shuttle SRM nozzle joint with bond defects, using unheated air N90-18464

TWO PHASE FLOW
Direct and inverse scattering problem associated with the elliptic Sinh-Gordon equation
[AD-A216455] N90-18931

U

UH-60A HELICOPTER
Preliminary airworthiness evaluation of the Woodward hydromechanical unit installed on T700-GE-700 engines in the UH-60A helicopter
[AD-A216751] N90-18430

ULTRASHORT PULSED LASERS
The dynamics of electrons in very intense lasers
[DE90-007246] N90-18729

ULTRASONIC SPECTROSCOPY
Ultrasensitive laser spectroscopy in solids: Single-molecule detection
[AD-A216085] N90-18716

UNDERGROUND TRANSMISSION LINES
Optimal planning method of underground distribution system, part 2. Application to various types of system configurations
[DE89-782323] N90-18636

UNDERWATER COMMUNICATION
Trends in VLF/LF (Very Low Frequency/Low Frequency) modem performance testing
[AD-A216576] N90-18614

UNITED STATES
Energy markets in the 1990's and beyond: A comparison of energy intensity in the United States and Japan
[DE90-005535] N90-18797

UNSTEADY AERODYNAMICS
Aerodynamics of unsteady systems. Numerical study of potential flow/boundary layer coupling
[ETN-90-96257] N90-18367
Unsteady Aerodynamic Phenomena in Turbomachines
[AGARD-CP-468] N90-18405
A comparison of flutter calculations based on eigenvalue and energy method N90-18406
Aerodynamic superposition principle in vibrating turbine cascades N90-18410
Design guidance to minimize unsteady forces in turbomachines N90-18411
Unsteady blade loads due to wake influence N90-18413
Unsteady aerodynamic phenomena in a simulated wake and shock wave passing experiment N90-18414
Gust response analysis for cascades operating in nonuniform mean flows N90-18415
Numerical prediction of axial turbine stage aerodynamics N90-18416
Time-dependent measurements on vibrating annular turbine cascades under various steady state conditions N90-18424
Methods for making unsteady aerodynamic pressure measurements in a rotating turbine stage N90-18426

UNSTEADY FLOW
Numerical investigation of unsteady flow in oscillating turbine and compressor cascades N90-18407
Unsteady viscous calculation method for cascades with leading edge induced separation N90-18408
Calculation of the unsteady two-dimensional, inviscid, compressible flow around a strongly cambered oscillating single blade N90-18409
Aerodynamic study on forced vibrations on stator rows of axial compressors N90-18412
Numerical simulation of three-dimensional unsteady flows in turbomachines N90-18417
High-resolution Euler computations of unsteady transonic flows in cascades N90-18420
Experiments on the unsteady flow in a supersonic compressor stage N90-18422
Modelling unsteady transition and its effects on profile loss N90-18423
Experimental investigation of the influence of rotor wakes on the development of the profile boundary layer and the performance of an annular compressor cascade N90-18425
Small displacement, long life on-orbit compressor design and fabrication N90-18489
An investigation of flow structure, mixing and chemical reaction in combusting turbulent flows
[AD-A216739] N90-18538
Active stabilization of aeromechanical systems
[AD-A216629] N90-18672

URBAN PLANNING
Remote sensing applied to vegetation as subsidized in municipal planning
[INPE-4908-PRE/1509] N90-18770

USER MANUALS (COMPUTER PROGRAMS)
A user's manual for the method of moments Aircraft Modeling Code (AMC)
[NASA-CR-186371] N90-18390
ACIRF user's guide: Theory and examples
[AD-A216436] N90-18613
User manual for NEXT 1.2: NLR engineering X-pert system toolkit
[NLR-TR-87178-U] N90-18905
Defense Technical Information Center Executive Information System: Documentation and user's manual
[AD-A216235] N90-19065
Using the K-25 C/TD common file system: A guide to CFSI
[DE90-005815] N90-19179

USER REQUIREMENTS
Determination of the underlying task scheduling algorithm for and Ada runtime system
[AD-A215880] N90-18890

V

V/STOL AIRCRAFT
Research on a two-dimensional inlet for a supersonic V/STOL propulsion system. Appendix A
[NASA-CR-174945] N90-18364
VACUUM DEPOSITION
Microstructural variations in aluminum oxide coatings deposited using a dual beam ion system
[DE90-006040] N90-18583
VANADIUM ALLOYS
Response of unirradiated and neutron-irradiated vanadium alloys to Charpy-impact loading
[DE90-004878] N90-18551
VAPOR DEPOSITION
Continuous preparation of a thin refractory carbide deposit on the surface of carbon fibers: Characterization of the C/SiC fiber N90-18501
Metallaboranes as precursors to metallic glasses
[AD-A216946] N90-18577
Chemical vapor deposition and photochemical vapor deposition of amorphous silicon photovoltaic devices
[DE89-009510] N90-18803
VAPOR PHASES
Determination of the minimum energy conformation of alkyl substituted pyrazines
[AD-A216974] N90-18539
Low-energy scattering of electrons and positrons in liquids N90-18981
Initial results of positron ionization mass spectrometry N90-18995
VARIABLE STARS
The infrared spectral signature of star formation N90-19114
CO infrared bands in atmospheres of long-period variables N90-19128
Photometry of variable AFGL sources
[AD-A216938] N90-19185
VEGETATION
Orbital remote sensing in the decade of the nineties: New approaches and challenges in geology
[INPE-4838-PRE/1467] N90-18758
Remote sensing applied to vegetation as subsidized in municipal planning
[INPE-4908-PRE/1509] N90-18770
Physiognomy of vegetation cover in the PNPM identified through the TM/LANDSAT sensor: A multitemporal analysis
[INPE-4834-PRE/1464] N90-18776
Remote sensing for the classification and quantification of vegetation in Spring staging areas of Brent geese on the Frisian Islands (Netherlands)
[BCRS-89-27] N90-18790
VEGETATIVE INDEX
TVI: A mathematical model for global estimation of Brazilian cerrado phytomass
[INPE-4836-PRE/1465] N90-18759
Relationships between the aerial biomass from ground layers of cerrado and its spectral reflectance
[INPE-4848-PRE/1477] N90-18760
VEHICLES
Practical applications of Loran-C for land mobile use or the possibility to use Loran-C as a vehicle-location or vehicle-navigation system
[ETN-90-96265] N90-18384
VELOCITY
Cineholography: A relation between the coherence length of the laser and the object velocity
[ISL-CO-234/88] N90-18724
Visual processing of object velocity and acceleration
[AD-A216509] N90-18858
VELOCITY DISTRIBUTION
Gust response analysis for cascades operating in nonuniform mean flows N90-18415
Measurement of velocity profiles and Reynolds stresses on an oscillating airfoil N90-18427
Turbulence structure of mixing swirling flows
[AD-A216628] N90-18671
Effect of a random wind field on thermal blooming instabilities
[DE90-007241] N90-18823
VELOCITY MEASUREMENT
Automation and extension of LDV (Laser-Doppler Velocimetry) measurements of off-design flow in a subsonic cascade wind tunnel
[AD-A216627] N90-18670
Velocity measurement using interferometry
[ISL-CO-221/88] N90-18709
VENTING
Zero-gravity vortex vent and PVT gaging system N90-18486
VENTS
Zero-gravity vortex vent and PVT gaging system N90-18486
VERY LOW FREQUENCIES
Trends in VLF/LF (Very Low Frequency/Low Frequency) modem performance testing
[AD-A216576] N90-18614
VIABILITY
Viability study of ionic microthruster tests on MECB satellite
[INPE-4973-RPE/605] N90-18490
VIBRATION
Aerodynamic superposition principle in vibrating turbine cascades N90-18410
Time-dependent measurements on vibrating annular turbine cascades under various steady state conditions N90-18424
Calculation of flight vibration levels of the AH-1G helicopter and correlation with existing flight vibration measurements
[NASA-CR-181923] N90-18743
Payload vibration isolation in a microgravity environment
[NASA-CR-186191] N90-18744
Optimization of the reference parameters in the accompanying solar panel dynamics
[INPE-4795-PRE/1449] N90-18798
VIBRATION EFFECTS
A study of the vibrational transmission through flanged joints
[ISVR-TR-181] N90-18755
VIBRATION ISOLATORS
Payload vibration isolation in a microgravity environment
[NASA-CR-186191] N90-18744
VIBRATION MEASUREMENT
Calculation of flight vibration levels of the AH-1G helicopter and correlation with existing flight vibration measurements
[NASA-CR-181923] N90-18743
VIBRATION TESTS
Simulation of the dynamic environment for missile component testing: Demonstration
[AD-A216979] N90-18443
VIBRATIONAL SPECTRA
VUV (Vacuum Ultraviolet) laser diagnostics of H(-) ion sources
[DE90-006072] N90-18719
The 2.7/4.3 micron CO2 branching ratio measurement
[AD-A215952] N90-18830
Toda lattice with transverse degree of freedom
[DE90-002414] N90-19049
VIBRATORY LOADS
Calculation of flight vibration levels of the AH-1G helicopter and correlation with existing flight vibration measurements
[NASA-CR-181923] N90-18743
VINYLIDENE
Development and polarization of ferroelectric polymer gauges, for dynamical acceleration experiments, as those in ballistics shocks
[ISL-R-119/88] N90-18703
VISCOELASTIC DAMPING
Energy decay and boundary control for distributed parameter systems with viscoelastic damping
[AD-A216468] N90-18748
VISCOMETERS
Rheological tests of Rigidite 5245 using the cone-plate and parallel plates method
[DT-310/88] N90-18544
VISCOSITY
A difference scheme with autocontrol artificial viscosity to predict ablated nosetip shape
[AD-A216625] N90-18452
VISCOUS FLOW
Unsteady viscous calculation method for cascades with leading edge induced separation N90-18408
Semidiscrete Galerkin modelling of compressible viscous flow past a circular cone at incidence
[NASA-CR-186323] N90-18684
Improved computational fluid dynamics for continuum hypersonic flow
[AD-A216981] N90-18674
VISCOUS FLUIDS
Spectral multi-domain approximation of the Navier-Stokes equations in curved complex geometries
[ONERA-NT-1987-2] N90-18685
VISIBLE SPECTRUM
Computational and visible light experiments for x ray laser holography
[DE90-006774] N90-18707
VISUAL ACCOMMODATION
A model of incomplete chromatic adaptation for calculating corresponding colors
[DE90-006905] N9C-19016
VISUAL PERCEPTION
Visual servoing for autonomous aircraft refueling
[AD-A216042] N90-18386
Visual processing of object velocity and acceleration
[AD-A216509] N90-18858
The effects of luminance boundaries on color perception
[AD-A216741] N90-18860
Recognizing three-dimensional objects without the use of models
[AD-A216766] N90-18862
Visual target detection and recognition
[DE90-006903] N90-19015
VOIDS
Arcjet cathode phenomena N90-18477
Investigation of methods to produce a uniform cloud of fuel particles in a flame tube
[NASA-TM-102376] N90-18665
Modeling convective Marangoni flows with void movement in the presence of solid-liquid phase change
[DE90-006474] N90-18690
VOLATILITY
Variations in volatiles in magma bodies based on studies of melt inclusions
[DE90-006272] N90-18821
VOLTAGE REGULATORS
Characterization and development report for the SA3274-1 and SA3274-2 transient voltage suppressors
[DE90-005712] N90-18649
VOLUMETRIC EFFICIENCY
Study of discharge mechanisms and the stability of transverse electric discharges in the gas mixtures
[ISL-R-114/88] N90-18733
VORTEX BREAKDOWN
Numerical simulation of the vortex breakdown
[ONERA-RSF-4/4368-AY-004A] N90-18689
VORTEX GENERATORS
Study of vortex arrays induced artificially and from centrifugal instabilities
[AD-A216499] N90-18669
VORTICES
Computational aerodynamics of ordered vortex flows
[ETN-90-96272] N90-18368
Study of the blade/vortice interaction on a one-blade rotor during forward flight (incompressible, non viscous fluid)
[ISL-R-115/88] N90-18391
Unsteady Aerodynamic Phenomena in Turbomachines
[AGARD-CP-468] N90-18405
Gust response analysis for cascades operating in nonuniform mean flows N90-18415
Zero-gravity vortex vent and PVT gaging system N90-18486
Numerical simulations of coherent structures in a jet flame with a noncircular cross section
[AD-A216710] N90-18535
VORTICITY EQUATIONS
Connections between the circulation in altitude and convection over South America
[INPE-4923-TDL/383] N90-18828
VOYAGER 2 SPACECRAFT
SHARP: A multi-mission artificial intelligence system for spacecraft telemetry monitoring and diagnosis
[NASA-CR-186285] N90-18444

W

WAKES
Design guidance to minimize unsteady forces in turbomachines N90-18411
Aerodynamic study on forced vibrations on stator rows of axial compressors N90-18412
Unsteady blade loads due to wake influence N90-18413
Unsteady aerodynamic phenomena in a simulated wake and shock wave passing experiment N90-18414
Modelling unsteady transition and its effects on profile loss N90-18423
Experimental investigation of the influence of rotor wakes on the development of the profile boundary layer and the performance of an annular compressor cascade N90-18425
WALL FLOW
Development of a defect stream function, law of the wall/wake method for compressible turbulent boundary layers
[NASA-CR-4286] N90-18675
WARFARE
Can the square law be validated
[DE90-007112] N90-18945
WARNING SYSTEMS
The signals of an ice warning device in dependence on total water content and normalized icing degree
[DLR-FB-89-52] N90-18377
WATER
Remote sensing of interior water: Perspectives
[INPE-4875-PRE/1486] N90-18815

Spectroscopy and physico-chemistry of CO:H2O and CO2:H2O ices N90-19111

WATER DEPTH
On the applicability of CAESAR for the remote sensing of bottom depth and bottom composition of shallow waters: A model study
[BCRS-89-13] N90-18783

WATER LOSS
Thermal remote sensing in the differentiation of soybean crops (glycine max (L.) merrill) submitted to water deficit
[INPE-4900-PRE/1501] N90-18762

WATER QUALITY
Remote sensing of interior water: Perspectives
[INPE-4875-PRE/1486] N90-18815

WATER VAPOR
Cloud hole-boring with infrared lasers: Theory and experiment
[DE90-006519] N90-18723

WAVE DISPERSION
Asymptotic boundary conditions for dissipative waves: General theory
[NASA-TM-102497] N90-18927

WAVE EQUATIONS
Theoretical and experimental high energy physics
[DE90-006168] N90-19006

WAVE FRONTS
Fast algorithms for calculating laser wavefront phase compensation given noisy measurements of phase gradient
[DE90-006357] N90-18727
Application of wavefront analysis techniques to restoring of images degraded by atmospheric turbulence
[ONERA-PUBL-1989-1] N90-19168

WAVE INTERACTION
Interaction between oblique-angled incident shock wave and turbulent boundary layer on a heated wall. Experimental results
[ONERA-RT-84/7078-AY] N90-18688

WAVE PROPAGATION
Damage assessment in composites by acousto-ultrasonic technique
[AD-A216590] N90-18510
Millimeter-wave propagation in the mesosphere
[PB90-119868] N90-18612
Quick, reliable estimates of high-power microwave fluences: The SNEAKY-2 program
[DE90-006347] N90-18624
Piezoelectric polymer PVDF shock gauge: State of the research art
[ISL-CO-207/89] N90-18705
The propagation of time harmonic Rayleigh-Lamb waves in a bimaterial plate
[AD-A216834] N90-18749
Asymptotic boundary conditions for dissipative waves: General theory
[NASA-TM-102497] N90-18927

WAVEFORMS
Waveform methods for ordinary differential equations
[DE90-006593] N90-18943

WEAPONS DEVELOPMENT
Measurement of gas leaks between a projectile and the walls of a tube in a ballistic compressor
[ISL-CO-250/88] N90-18694
Effects produced by pulsed CO2 lasers
[ISL-R-112/88] N90-18731

WEAR
The mechanism, measurement, and influence of properties on the galling of metals
[DE90-006533] N90-18558
The joint effect of surface microtopography and near-surface structure on microcontact conditions
[DE90-006494] N90-18591

WEATHER
Federal methanol fleet update
[DE90-006851] N90-18741

WEATHER FORECASTING
ERS-1 European remote sensing satellite: A new tool for global environmental monitoring in the 1990's
[ESA-BR-36] N90-18782
Forecasters handbook for Central America and adjacent waters
[AD-A216752] N90-18845
Dynamics of an ERICA (Experiment on Rapidly Intensifying Cyclones over the Atlantic) cyclone
[AD-A216775] N90-18846

WEIBULL DENSITY FUNCTIONS
Optimum selection procedures in multi-stage screening, reliability, and time
[AD-A216811] N90-18942

WHEAT
Radiometric study of wheat and bean crops in three types of latossoio
[INPE-4843-PRE/1472] N90-18767
Relationships between spectral parameters and agronomics of wheat and beam crops
[INPE-4791-RPE/584] N90-18768
Spectral response of wheat and its relationship with agronomical prameters
[INPE-4950-RPE/599] N90-18774
Continuous hydroponic wheat production using a recirculating system
[NASA-TM-102784] N90-18853

WHISKER COMPOSITES
Analysis of whisker-toughened ceramic components: A design engineer's viewpoint
[NASA-TM-102333] N90-18504
Mechanical properties and microstructure of Si3N4-whisker-reinforced Si3N4 matrix composite
[DE90-005651] N90-18518

WHISKERS (CRYSTALS)
Application of artificial intelligence control to the vapor-liquid-solid silicon carbide whisker process
[DE90-007835] N90-18519

WHITE DWARF STARS
Soft x ray emission from classical novae in outburst
[DE90-006480] N90-19187

WICKS
Wick-type liquid-metal combustion
[AD-A216019] N90-18530

WIGGLER MAGNETS
INEX (Integrated Numerical Experiment) simulations of the Boeing FEL system
[DE90-004846] N90-18712

WIND (METEOROLOGY)
Doppler lidar working group report
[ESA-SP-1112] N90-18848

WIND EFFECTS
The effects of wind tunnel data uncertainty on aircraft point performance predictions
[AD-A216091] N90-18387

WIND SHEAR
A case study of the 24 August 1986 FLOWS microburst
[AD-A216939] N90-18847

WIND TUNNEL CALIBRATION
Half model tests on an ONERA calibration model in the transonic wind tunnel Goettingen, Federal Republic of Germany
[DLR-MITT-89-20] N90-18370

WIND TUNNEL MODELS
Supersonic wind tunnel investigation of a tubular projectile
[ISL-CO-306/89] N90-18366
The DFVLR 3-m x 3-m low speed wind tunnel (NWG) in Goettingen
[ESA-TT-1156] N90-18436
Contribution to the study of three-dimensional separation in turbulent incompressible flow
[ESA-TT-1169] N90-18697

WIND TUNNEL TESTS
Aerodynamic testing of a rotating wind turbine blade
[DE90-000312] N90-18362
Half model tests on an ONERA calibration model in the transonic wind tunnel Goettingen, Federal Republic of Germany
[DLR-MITT-89-20] N90-18370
The effects of wind tunnel data uncertainty on aircraft point performance predictions
[AD-A216091] N90-18387
Wind-tunnel investigation of a flush airdata system at Mach numbers from 0.7 to 1.4
[NASA-TM-101697] N90-18395
The DFVLR 3-m x 3-m low speed wind tunnel (NWG) in Goettingen
[ESA-TT-1156] N90-18436
Automation and extension of LDV (Laser-Doppler Velocimetry) measurements of off-design flow in a subsonic cascade wind tunnel
[AD-A216627] N90-18670
Measurements of surface pressures on an operating vertical-axis wind turbine
[DE90-005722] N90-18805

WIND TUNNELS
Wind-tunnel investigation of a flush airdata system at Mach numbers from 0.7 to 1.4
[NASA-TM-101697] N90-18395

WIND TURBINES
Aerodynamic testing of a rotating wind turbine blade
[DE90-000312] N90-18362
Vertical axis wind turbine turbulent response model. Part 2: Response of Sandia National laboratories' 34-meter VAWT with aeroelastic effects
[DE90-005721] N90-18804
Measurements of surface pressures on an operating vertical-axis wind turbine
[DE90-005722] N90-18805

WIND VELOCITY
Multiparameter scatterometer for remote sensing (RADSER). Project Scatter: State-of-the-art and future applications
[INPE-4871-PRE/1482] N90-18701
Effect of a random wind field on thermal blooming instabilities
[DE90-007241] N90-18823

WING CAMBER
Optimum spanwise camber for minimum induced drag
[BU-403] N90-18389

WING FLOW METHOD TESTS
Aerodynamics of unsteady systems. Numerical study of potential flow/boundary layer coupling
[ETN-90-96257] N90-18367

WINGS
Half model tests on an ONERA calibration model in the transonic wind tunnel Goettingen, Federal Republic of Germany
[DLR-MITT-89-20] N90-18370

WIRE
Proceedings of the 38th International Wire and Cable Symposium
[AD-A216023] N90-18638

WORDS (LANGUAGE)
Schema-based theories of problem solving
[AD-A216717] N90-18939

WORK FUNCTIONS
Surface production of ions
[AD-A216470] N90-19003

WORKING FLUIDS
Spacecraft thermal control design data, volume 4
[ESA-PSS-03-108-ISSUE-1-VOL-4] N90-18458

X

X RAY ANALYSIS
Damage in a perforated graphite-epoxy composite plate under monotonic and cyclic biaxial loading
[ESA-TT-1117] N90-18521
Biomedical applications of synchrotron x ray microscopy
[DE90-004957] N90-18867

X RAY ASTRONOMY
State of the art in semiconductor detectors
[DE90-005567] N90-18706

X RAY INSPECTION
Inspection of carbon/epoxy and aluminum honeycomb paraboloidal components by HNDT
[AD-A216796] N90-18514

X RAY LASERS
Inspection of carbon/epoxy and aluminum honeycomb paraboloidal components by HNDT
[AD-A216796] N90-18514
Computational and visible light experiments for x ray laser holography
[DE90-006774] N90-18707

X RAY SPECTROSCOPY
Understanding electronegative effects in core-level electron spectroscopies; application to the high temperature superconductors
[AD-A216728] N90-19037

X RAYS
Soft x ray emission from classical novae in outburst
[DE90-006480] N90-19187

XENON
Performance of large area xenon ion thrusters for orbit transfer missions N90-18475
Multiple-ionization of xenon atoms by positron impact N90-18978

Y

YTTRIUM OXIDES
Luminescence from defects and impurity centers in yttrium oxide
[DE90-004842] N90-19030

Z

ZEEMAN EFFECT
Millimeter-wave propagation in the mesosphere
[PB90-119868] N90-18612
Stark and Zeeman effects on laser cooling of positronium N90-18986

ZEOLITES
Production of high density aviation fuels via novel zeolite catalyst routes
[AD-A216444] N90-18601

ZINC ALLOYS
Processing and elevated temperature ductility of aluminum alloy 7475
[AD-A216840] N90-18554

ZIRCONIUM
The improved adhesion of organic polymers to silica and to aluminum metal with zirconium Schiff-base block copolymer coatings
[AD-A216669] N90-18575

ZIRCONIUM OXIDES
Fundamental aspects of erosion and impact damage
[DE90-006640] N90-18587

Typical Personal Author Index Listing

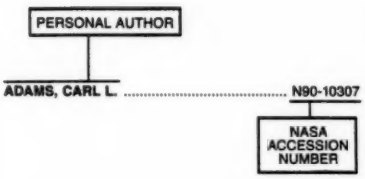

Listings in this index are arranged alphabetically by personal author. The NASA accession number denotes the number by which the citation is identified.

A

AANNESTAD, P. A. N90-19099
ABBOTT, TERENCE S. N90-18393
ABDEL-RAOUF, MOHAMED ASSAD N90-18963
ABEL, L. C. N90-18469
ABERNATHY, S. ALLISON N90-18849
ABEYARATNE, ROHAN N90-18747
ABRISHAMIAN, HOOSH N90-18734
ACERBI, RICARDO N90-18913
ADAMS, F. C. N90-19114
ADAMS, J. T. N90-18976
ADAMS, MARY S. N90-18385
AGNES, A. N90-18682
AHRENS, JUDITH DORPH N90-19063
AINSWORTH, R. W. N90-18426
AITKEN, D. K. N90-19096
AKINS, ROBERT E. N90-18605
AKLONIS, J. J. N90-18567
AL-MUFTI, S. N90-19093
ALBE, F. N90-18724
ALBUS, JAMES S. N90-18734
ALEXANDER, RICHARD M. N90-18744
ALGEO, RICHARD D. N90-18380
ALIEV, M. K. N90-18588
ALIPACHA, M. N90-18682
ALLAMANDOLA, L. J. N90-19101
ALLEN, D. A. N90-19135
ALLEN, J. L. N90-18426
ALLISON, S. W. N90-18721
ALLISON, TIMOTHY DANIEL N90-19083
ALLISON, W. W. M. N90-19183
ALMEIDAFILHO, RAIMUNDO N90-18758
ALNER, G. J. N90-19183
ALVESMOREIRA, MAURICIO N90-18773
ALVIMDEOLIVEIRA, ENI N90-18777
AMBATS, I. N90-19183
AMBROSE, W. P. N90-18531
N90-18716
AMOS, W. R. N90-19010
ANAND, L. N90-18925
ANDERL, R. A. N90-18562
ANDERSON, H. U. N90-18643
ANDERSON, HUGH R. N90-18625
ANDERSON, R. A. N90-18651
ANDRADE, J. D. N90-18572
ANINI, YAQUB N90-19176
ANTON, D. L. N90-18559
AOYAGI, P. N90-18622
APPEL, MARSHALL A. N90-18481
APPLEBY, A. JOHN N90-18796
ARAKAWA, T. N90-19004
ARCHER, RONALD D. N90-18574
N90-18575
ARMOUR, E. A. G. N90-18969
ASADA, MINORU N90-18635
ASHAR, PRAVNAV N90-18899
ASOKAMANI, R. N90-19048
ATHERTON, L. J. N90-18728
ATTEMA, EVERT N90-18782
ATWATER, HARRY A. N90-18564
AWADALLA, N. G. N90-18550
AYRES, D. S. N90-19183
AZIZ, M. J. N90-18564

B

BABIN, B. R. N90-18673
BABUSKA, I. N90-18928
BACCHUS, D. L. N90-18465
BACH, L. N90-19070
BACHE, HANS HENRIK N90-18520
N90-18589
BACHELET, E. J. N90-18398
BAER, M. R. N90-18541
BAGCHI, ARUNABHA N90-18953
BAILEY, J. A. N90-19149
BAILEY, R. S. N90-18559
BAKER, D. J. N90-18969
BAKER, J. R. N90-18467
BALKA, L. N90-19183
BARBI, C. N90-18682
BARDSLEY, J. N. N90-18729
BARGER, RAYMOND L. N90-18385
BARLOW, M. J. N90-19122
BARNETT, ALLEN M. N90-18582
BARNHART, B. N90-18361
N90-18388
BARON, B. N. N90-18803
BARR, G. D. N90-19183
BARRETT, RICHARD T. N90-18740
BARRETT, W. L. N90-19183
BARROSDEANDRADE, VALERIA MARIA N90-18778
BARROSO, J. J. N90-18699
BARTHELMY, S. N90-18982
BARTSCHAT, K. N90-18971
BASCOM, W. N90-18572
BASS, A. D. N90-19038
BASSI, F. N90-18420
BASTOS, ANTONIO FREDERICO N90-18771
BASU, D. N90-18967
BASU, MADHUMITA N90-18965
N90-18967
BATCHELDER, D. N90-18503
BAUER, F. N90-18703
N90-18705
BAUMERT, WERNER N90-18436
BECHER, PAUL F. N90-18592
BECK, S. C. N90-19147
BECKLIN, E. E. N90-19141
BEGUIER, C. N90-18367
BEINTEMA, D. A. N90-19162
BELL, HERBERT H. N90-18620
BELLEUDY, J. N90-18682
BENDER, STEVEN C. N90-18712
BENJAMIN, D. N90-19183
BENNETT, B. L. N90-19030
BENSAMMAR, S. N90-19125
BENZIGER, JAY B. N90-18534
BERGER, H. N90-18687
BERGKVIST, BO N90-18819
BERGMANN, HEINRICH N90-18609
BERKO, S. N90-18980
BERKOPEC, FRANK D. N90-18471
BERNER, C. N90-18366
BERNSTEIN, E. R. N90-18539
BERTACCHIUVO, CINTIA REGINA N90-18839
BERTRAND, P. A. N90-18532
BETOUT, P. N90-18848
BETOWSKI, L. D. N90-18814
BEVENSEE, R. M. N90-18627
BHASIN, K. B. N90-18834
BHATIA, A. K. N90-18991
BIHRLE, W., JR. N90-18381
N90-18388
BIJLSMA, R. J. N90-18790
BILLEBAUD, F. N90-19090
BILLONNET, GILLES N90-18417
BIRKAN, M. A. N90-18491
BIRMAN, KENNETH N90-18891
BIRON, PAUL J. N90-18847
BISGAARD, S. N90-19072
BITENCOURTPEREIRA, MARISA DANTAS .. N90-18760
BIVENS, GRETCHEN A. N90-18647
BLAEDEL, K. L. N90-18608
BLANCO, A. N90-19089
BLAND, J. N90-19142
BLINK, J. N90-18657
BLOCH, B. N90-18522
BLOOM, E. E. N90-19025
BOATNER, L. A. N90-19043
BOCKMAN, R. S. N90-18867
BODE, M. N90-19123
BOELCS, A. N90-18410
N90-18424
BOERIO, F. J. N90-18569
BOES, J. C. N90-18663
BOHLIN, M. N90-19108
BONTOUX, P. N90-18695
BOONSTRA, A. J. N90-19162
BORDER, P. N90-19183
BOSCOPEREIRADOSREIS, JOAO N90-18701
BOSSARD, J. A. N90-18468
BOSTELMAN, ROGER N90-18734
BOTT, W. N90-18732
BOUCHET, P. N90-19091
BOUIX, J. N90-18501
BOUZITAT, F. N90-19074
BOWMAN, CRAIG T. N90-18538
BOYCE, JAMES B. N90-19034
BOYD, WILLIAM C. N90-18473
BOYER, KEITH M. N90-18429
BRAAM, F. N90-18468
BRAND, P. N90-19118
N90-19156
BRASE, JAMES M. N90-18707
BRASHER, WARREN L. N90-18473
BRAUN, QUENTER N90-18631
BRAUNSCHEIDEL, E. N90-18482
BREGMAN, J. N90-19101
BRENEMAN, J. E. N90-18467
BREWER, E. D. N90-18739
BRILEY, G. N90-18482
BRODERS, MARTIN A. N90-18693
BROICHHAUSEN, K. D. N90-18422
BROOKS, C. B. N90-19183
BROOKS, D. L. N90-18975
N90-18976
BROWER, BERNARD N90-19014
BRUCKENSTEIN, STANLEY N90-18533
BRYJA, C. O. N90-19185
BUDAI, J. D. N90-19045
BUGOS, A. R. N90-18721
BUNK, WOLFGANG N90-18609
BUNTING, JAMES T. N90-18844
BURKE, A. F. N90-18655
BURKHARDT, W. M. N90-18468
BURNS, ROBERT J. N90-18685
BURRIDGE, D. N90-18848
BURTON, M. N90-19100
N90-19118
BUSSOLETTI, E. N90-19089
BUTTERFIELD, C. P. N90-18362
BYMAN, MICHAEL W. N90-18851

C

CAIRD, J. A. N90-18728
CALABRESI, GIANNA N90-18782
CAMPBELL, CHARLES S. N90-18691
CAMPOS, J. N90-19160
N90-19161
CAMPOSAGUILAR, A. N90-19154
CANAVAN, GREGORY H. N90-18955
CANDELL, GREGORY L. N90-18870
CANGELLARIS, ANDREAS C. N90-18626
CANTER, K. F. N90-18980
CANTWELL, BRIAN J. N90-18538
CANTWELL, W. N90-18497
CAPLOT, M. N90-18365
CAPPELLI, M. A. N90-19019
CAPRON, WILLIAM R. N90-18378
CARAMANA, E. J. N90-18723
CARD, MICHAEL F. N90-18752
CARNAHAN, LISA J. N90-18881
CARSWELL, R. F. N90-19149

CASALI, M. M. N90-19119
CASE, HENRY N90-18873
CATES, M. R. N90-18721
CAVALIER, J. C. N90-18500
CECCARELLI, C. N90-19126
CELSODECARVALHO, VITOR N90-18770
CHAKAVEH, S. N90-19167
CHALFANT, AMY E. N90-18846
CHAMIS, CHRISTOS C. N90-18470
CHAN, C. D. N90-18712
CHANETZ, BRUNO N90-18697
CHANG, KURNG Y. N90-18443
CHANG, WULU N90-18631
CHAOUCHE, A. N90-18695
CHAPLIN, R. L. N90-18975
N90-18976
CHAPMAN, DEAN R. N90-18674
CHASE, L. L. N90-18728
CHEN, HARRY N90-19002
CHEN, L. D. N90-18530
CHENG, C. Z. N90-19026
CHERNOFF, D. F. N90-19115
CHESLOW, RICHARD T. N90-18898
CHIARULLI, DONALD M. N90-18641
CHIFFAUDEL, ARNAUD N90-18683
CHINI, R. N90-19137
CHITWOOD, W. E. N90-18496
CHOREY, C. M. N90-18634
CHOW, WENG W. N90-19039
CHOY, L. W. N90-18780
CHRISTEN, D. K. N90-19043
N90-19045
CHRISTIANSEN, P. L. N90-19049
CHRISTIE, D. N90-18657
CHU, C.-Y. N90-18518
CHUANG, S. L. N90-18622
CLARSON, S. J. N90-18569
CLEMENT, CATHERINE A. N90-18869
CLEVERS, J. G. P. W. N90-18784
CLOUTMAN, LAWRENCE D. N90-18677
CLOYD, J. D. N90-18387
CLYNE, T. W. N90-18502
COHEN, M. N90-19101
COHEN, MARION F. N90-18864
COHENDET, P. N90-19070
COLANGELI, L. N90-19089
COLEMAN, P. G. N90-18972
COLLINGS, E. W. N90-18552
COLLINS, TIMOTHY J. N90-18453
COLSON, WILLIAM B. N90-18714
N90-18715
COLVIN, G. E., JR. N90-18505
COMBES, F. N90-19090
CONARD, J. N90-19110
CONNELL, G. A. NEVILLE N90-19034
CONNELL, JONATHAN N90-18916
COOK, S. C. N90-18418
COOKE, D. W. N90-19030
COOPER, C. V. N90-18559
COOPER, PAUL W. N90-18708
COPENHAVER, W. W. N90-18428
CORNELIUS, W. D. N90-18725
CORNELIUSEN, A. N90-18911
CORNIE, JAMES A. N90-18516
CORREDERA, P. N90-19160
N90-19161
CORREIA, LUCRETIA AGNES N90-18561
CORRONS, A. N90-19160
N90-19161
COTTENOT, C. N90-18523
COX, P. N90-19129
CRAIG, A. N90-18928
CRANE, PETER M. N90-18620
CRANE, R. M. N90-18513
CRAVEY, W. R. N90-18651
CREDEUR, LEONARD N90-18378
CREPANI, EDISON N90-18756
CROSBIE, G. M. N90-18593
CROVISIER, J. N90-19086
CUDDEFORD, P. N90-19175
CUMMING, WILLIAM N90-18574
CURRAN, FRANCIS M. N90-18474
N90-18477
N90-18478
CURRY, R. N90-19073
CZUCHLEWSKI, S. J. N90-18722

D

DABABNEH, M. S. N90-18959
DACRUZ, JOSE JAIME N90-18950
DAGALAKIS, NICHOLAS G. N90-18734
DALLUM, G. N90-18657
DANA, ROGER A. N90-18613
DANBY, GRAHAME N90-18970
DANZIGER, I. J. N90-19109
N90-19133
DAS, M. P. N90-19047
DASILVAJUNIOR, CARLOS LEANDRO N90-18850
DAUGHERTY, W. L. N90-18550
DAVE, BHASKER B. N90-18796
DAVIES, P. N90-18497
DAVIN, J. N90-18657
DAVIS, CHRISTOPHER C. N90-18857
DAVIS, P. J. N90-18608
DEACON, DAVID A. G. N90-18720
DEASSISFLEURY, CASSIA N90-18798
DEATON, R. L. N90-19010
DEBERGH, C. N90-19088
DEFFENBAUGH, D. D. N90-18489
DEFOURNEAU, D. N90-19113
DEGRAAUW, TH. N90-19162
DEJONGHE, LUTGARD C. N90-18584
DEKKER, R. N90-18952
DELERY, J. N90-18688
DELVENTHAL, R. A. N90-18482
N90-18485
DEMARET, R. N90-18857
DEMELLOLOURENCAO, PAULO TADEU N90-18450
DEMMEL, JOHANN N90-18377
DEMORISSONVALERIANO, DALTON N90-18760
N90-18766
N90-18770
N90-18817
DEMUIZON, M. JOURDAIN N90-19101
N90-19129
DENTREMONT, ROBERT P. N90-18844
DEOLIVEFERREIRA, LEONARDO N90-18448
DEOLIVEIRAALMEIDA, SERGIO ALBERTO N90-18772
DEPADUABRITOSERBETO, ANTONIO N90-19018
DEPIERO, FRED W. N90-18921
DERMER, CHARLES D. N90-18985
N90-18986
DERUYCK, J. N90-18427
DESCHAMPS, VERONIQUE N90-18886
DESCHENES, M. N90-18536
N90-19038
DESOUZABIFFI, ANTONIO JOSE N90-18773
DESOUZAKIENBAUM, GERMANO N90-18886
DEVADAS, SRINIVAS N90-18899
N90-18940
DEVEER, A. A. N90-18787
DEVRIES, G. C. N90-19055
DEZERT, JEAN N90-18633
DHENDENCOURT, L. B. N90-19105
N90-19106
N90-19113
DIANA, L. M. N90-18975
N90-18976
DICKES, E. N90-18361
N90-18388
DIEBEL, DEAN L. N90-18646
DIEHL, JOAO BENEDITO N90-18884
DIETZ, A. J. N90-18426
DILMANIAN, F. AVRAHAM N90-18868
DIRKX, G. H. P. N90-18787
DITARANTO, R. A. N90-18743
DOBROLYUBOV, M. I. N90-19177
DOBSON, B. J. N90-18754
DOMBEK, B. DUANE N90-18600
DOMIAN, FRANCES A. N90-18582
DOMOKOS, G. N90-19001
DONGARRA, JACK N90-18910
DONKER, J. C. N90-18905
DONOHUE, D. L. N90-18995
DONZE, M. N90-18549
DOOLING, J. C. N90-19027
DOSSANTOS, JOAO ROBERTO N90-18759
N90-18770
DOSSANTOSCARRARA, ALCY RODOLFO N90-18738
DOWBEN, PETER A. N90-19053
DOWELL, D. H. N90-18712
DOWNEY, M. G. N90-18486
DOYON, R. N90-19148
DRACHMAN, RICHARD J. N90-18957
N90-18991
N90-18993
DRAINE, B. T. N90-19095
N90-19102
DRAKE, JOHN B. N90-18690
DRAPATZ, S. W. N90-19162
DUBELAAR, G. B. J. N90-18549
DUCK, PETER W. N90-18363
DUFFEY, R. B. N90-18692
DUFFY, STEPHEN F. N90-18504
DUGUNDJI, J. N90-18672
DUJARDIN, SOPHIE N90-18679
DUTRADOCARMO, EDUARDO G. N90-18678
DUTUIT, O. N90-19113
DYMEK, CHESTER J., JR. N90-18494

E

EBEL, STEVEN J. N90-18644
N90-18799
EBERHARDT, RALPH N. N90-18487
ECKENRODE, B. A. N90-18995
EDELMAN, SHIMON N90-18871
EDELSON, D. J. N90-19107
EDIGHOFFER, HAROLD E. N90-18751
EGGLESTON, DEBRA S. N90-18462
EHRENFREUND, P. N90-19106
EICHERT, HELMUT N90-18548
EIROA, C. N90-19127
ELDER, R. L. N90-18418
ELIEZER, S. N90-18509
ELMENDORF, W. N90-18422
EMERY, R. J. N90-19099
ENCRENAZ, TH. N90-19085
N90-19090
N90-19091
ENGEL, WALTER N90-18599
ENSHENG, WEI N90-18514
EPIPHANIO, JOSE CARLOS NEVES N90-18762
EPSTEIN, A. H. N90-18419
N90-18672
ERICKSON, DONALD C. N90-18610
ERICKSON, W. C. N90-18623
ERVING, CAV N90-18873
ESKEW, R. T., JR. N90-18860
ESPEY, B. R. N90-19149
EVANS, A. G. N90-18507
N90-18508
EVANS, S. N90-18482
EVERETT, R. A., JR. N90-18746
EWING, THOMAS F. N90-18909
EXTREMET, G. P. N90-18695

F

FADILLAH, S. N90-18785
FAGET, H. M. N90-18485
FAGOT, H. N90-18724
FAILOR, R. A. N90-18985
FAIRCHILD, MARK D. N90-19014
N90-19016
FARDO, MAURO N90-18702
FAVIER, D. N90-18682
FAVRE, J. P. N90-18523
FAVROW, L. H. N90-18559
FEA, MAURIZIO N90-18782
FEENSTRA, R. N90-19043
N90-19045
FEHLNER, THOMAS P. N90-18577
FELCH, JOHN E. N90-19065
FELDMAN, R. B. N90-18725
FENG, L. N90-18572
FENG, XIAOFAN N90-19014
FERBER, M. K. N90-18586
FERREIRA, JOSE LEONARDO N90-18490
FERREIRA, JULIO GUIMARAES N90-18490
FERREIRAMACHADOESILVA, ANTONIO JOSE
N90-18757
FERREIRAMARENGONI, HILCEA N90-18885
FERRI, J. L. N90-18676
FEUERBACHER, BERNDT N90-18609
FEYOCK, BRYAN W. N90-18582
FICHTER, W. B. N90-18453
FIGUEIRA, JOSEPH F. N90-18726
FILHO, ANTONIO MONTES N90-18490
FILHO, PEDRO HERNANDEZ N90-18764
N90-18772
FINNEGAN, WILLIAM G. N90-18832
FLANDRO, GARY A. N90-18492
FLEISHMANN, JUDITH N90-19188
FLETCHER, JAY W. N90-18389
FLIERL, GLENN R. N90-18840
FLORIO, JOHN, JR. N90-18578
FOELKER, JAMIE L. N90-18431
FOERSCHING, HANS N90-18609
FOERSTER, K. M. N90-18409
FOLLSTAEDT, DAVID M. N90-18713
FONTAINE, J. P. N90-18695
FONTI, S. N90-19089
FORD, DAVID H. N90-18582
FORMAGGIO, ANTONIO ROBERTO N90-18761
N90-18763
N90-18767
N90-18768
FORVEILLE, T. N90-19134
FOURMAUX, ANTOINE N90-18417
FOURNIER, D. N90-18400
FOUSSEKIS, D. N90-18367
FRANCA, LEOPOLDO P. N90-18678
FRANCIS, RICHARD N90-18782

FRANCISCOJUNIOR, ANTONIO N90-18883
FRANKLIN, JERROLD E. N90-18481
FRANSSON, T. H. N90-18410
N90-18424
FRAUNIE, P. N90-18367
FREDIANI, ALDO N90-18401
FRIDLUND, C. V. M. N90-19108
FRIEDMAN, P. G. N90-18987
FRISK, U. O. N90-19108
FRYSZ, CHRISTINE A. N90-18644
N90-18799
FU, G. Y. N90-19026
FU, ROULI N90-18571
FUKUTOME, ATSUSHI N90-18636
FULLER, LYNN N90-18653

G

GABAYSON, S. M. N90-18496
GADELHADESOUZA, LUIZ CARLOS N90-18439
GAFFNEY, J. S. N90-18820
GAGLIANO, S. N90-18682
GALATOLO, ROBERTO N90-18401
GALISIATUNDISI, JOSE N90-18815
GALLAGHER, TIMOTHY N90-19014
GALLUS, H. E. N90-18407
N90-18413
N90-18425
GANDHI, K. N90-18567
GARCIA, C. N90-19154
GARNER, CHARLES N90-18479
GAROFALINI, STEPHEN H. N90-18596
GARRISON, JOHN C. N90-18730
GARY, S. PETER N90-19021
GARZON, F. N90-19167
GASIOROWICZ, S. N90-19006
GATTI, E. N90-18706
GAVEL, DON N90-18727
GAZAIX, M. N90-18408
GEAR, DANIEL E. N90-18887
GEBALLE, T. N90-19118
GEBALLE, T. R. N90-19105
GEHRELS, N. N90-18982
GEHRZ, ROBERT D. N90-19185
GENTNER, DEDRE N90-18869
GENZEL, R. N90-19098
GEORGE, A. N90-18680
GEORGE, T. G. N90-19007
GEORGE, THOMAS F. N90-18568
N90-18571
GERIN, M. N90-19090
GERLACH, C. R. N90-18489
GERNERT, NELSON J. N90-18433
GESSNER, FREDRICK B. N90-18671
GHOSH, A. N90-18465
GHOSH, A. S. N90-18965
GIANDT, EDUARDO, D. N90-19059
GIEN, T. T. N90-18962
GILATH, I. N90-18509
GILES, M. B. N90-18419
GILL, RICHARD T. N90-18936
GILLIOM, LAURA R. N90-18598
GINERIS, DENISE J. N90-18371
N90-18372
GIRAUD, M. N90-18366
GIRODROUX-LAVIGNE, P. N90-18408
GLACCUM, W. N90-19134
GLISH, G. L. N90-18995
GNANENDRAN, S. KINGSLEY N90-18893
GOBBI, DELANO N90-18827
GOEBEL, C. J. N90-19008
N90-19010
GONDOT, PASCAL N90-18836
GONZALEZVILLALOBOS, ALVARO N90-18773
GOODMAN, B. B. N90-19075
GOODWIN, KENNETH R. N90-18734
GOODWIN, THOMAS J. N90-18852
GORDON, B. M. N90-18867
GORDON, M. N90-19019
GORDON, SALLIE E. N90-18936
GOTTSTEIN, G. N90-18557
GOTTZEIN, E. N90-19081
GOULART, PAMELA J. N90-18840
GOURSAT, P. N90-18499
GRAHAM, J. R. N90-19104
GRAHAM, MARC H. N90-18888
GRAHAM, R. A. N90-18705
GRAVES, R. L. N90-18603
GREAR, J. F. N90-18658
GREENBERG, M. N90-19111
GREITZER, E. M. N90-18672
GRIFFIN, L. W. N90-18416
GRIFFIN, MICHAEL K. N90-18844
GRIM, R. N90-19103
N90-19111
GROOT, J. S. N90-18789
GROVES, SCOTT E. N90-18524
GRUENHAGEN, WOLFGANG V. N90-18389
GRUENINGER, GERHARD N90-18609
GRUMMON, D. S. N90-18557
GUANHUA, HUANG N90-18514
GUENETTE, G. R. N90-18672
GUILIANO, M. N90-19110
GUNTHER, DAVID M. N90-18868
GURULE, A. M. N90-18649
GUSMAODECARVALHO, ANA MARIA N90-18828
GUSTAFSON, GARY B. N90-18844
GUTH, KURTIS J. N90-18615
GUTOWSKI, W. J. N90-18822
GUYENNE, DUC N90-18782
GUYENNE, T. D. N90-18848
N90-19068
GUZIK, T. GREGORY N90-19186

H

HAAG, THOMAS W. N90-18476
N90-18477
N90-18478
HACKWELL, J. A. N90-19107
HAERTIG, J. N90-18365
N90-18391
HAGSTROM, THOMAS N90-18927
HAHN, H. T. N90-18506
N90-18510
HAILEY, CHARLES J. N90-19017
N90-19188
HAIR, LEROY M. N90-18464
HALL, D. N. B. N90-19141
HALL, KENNETH C. N90-18415
HALL, ROBERT B. N90-18582
HALLOWELL, ROBERT G. N90-18847
HALPERN, M. B. N90-19058
HAMEL, WILLIAM R. N90-18921
HAMMEL, REINHARD N90-18629
HAMMESFAHR, JENS N90-18445
N90-18446
HANNSGEN, KENNETH B. N90-18748
HANNUM, NED P. N90-18471
HANSEN, JAMES G. R. N90-18494
HANSON, D. E. N90-18722
HANSON, FRANCIS V. N90-18601
HANSSON, HANS-CHRISTEN N90-18819
HANSSON, JAN N90-18606
HARDIN, J. E. N90-18655
HARDING, ALICE K. N90-18983
HARJES, H. C. N90-18659
HARNISCHMACHER, K. N90-18703
HARRIS, A. I. N90-19098
HARRISON, FIONA A. N90-19188
HARRISON, THOMAS E. N90-19185
HARTLEY, D. S., III N90-18945
HARVEY, P. M. N90-19134
HAVERKORT, BOUDEWIJN R. N90-18907
N90-18949
HAWARDEN, T. N90-19155
HAYNES, T. E. N90-19042
HAZARIKA, B. N90-18427
HEGEDUS, S. S. N90-18803
HEINEN, V. O. N90-18634
HEINIG, K. N90-18406
HEINRICHKUX, HERMANN JOHANN N90-18701
HENDERSON, JACK B. N90-18578
HENDERSON, R. E. N90-18411
HENDRICH, W. R. N90-18739
HENGEL, JOHN E. N90-18464
HERDAN, B. L. N90-19071
HERNANDEZFILHO, PEDRO N90-18769
N90-18770
N90-18776
HERTER, T. N90-19139
HERZOG, M. N90-18495
HESKE, A. N90-19128
HEULER, RONALD R. N90-19012
HEYMSFIELD, STEVEN B. N90-18868
HIERONIMUS, ANNE-MARIE N90-19069
HIGGINS, E. ARNOLD N90-18374
HILL, HENRY A. N90-18834
HILLS, C. R. N90-18583
HINCKLEY, C. MARTIN N90-18525
HINKLE, C. R. N90-18853
HIRATA, YUICHI N90-18635
HIRNISCHMACHER, K. N90-18705
HIRSCH, C. N90-18427
HITCHCOCK, LLOYD N90-18380
HITNER, J. M. N90-18466
HO, J. C. N90-18552
HO, JAMES K. N90-18893
HO, P. T. P. N90-19147
HO, Y. K. N90-18990
HODAPP, K.-W. N90-19127
HODSON, H. P. N90-18429
HOEIJMAKERS, H. W. M. N90-18368
HOEPPNER, DAVID W. N90-18403
HOFFMANN, HANS-EBERHARD N90-18377
HOLCK, D. K. N90-18649
HOLDOM, R. S. N90-19076
HOLLENBACH, D. J. N90-19100
N90-19115
HOLROYD, RICHARD A. N90-18529
HOLTZ, JOACHIM N90-18781
HONEY, DAVID ALAN N90-18718
HONG, CHUNG K. N90-18730
HOOGEBOOM, P. N90-18789
HOOPER, JAMES W. N90-18901
HOPPER, MARI KAROL N90-18854
HORBATSCH, M. N90-18958
N90-18964
N90-18992
HORDIJK, A. N90-18952
HORLOCK, J. H. N90-18411
HOTOP, HANS-JUERGEN N90-18742
HOUCK, JACOB A. N90-18378
HOUIN, G. N90-18866
HOVY, EDUARD H. N90-18895
HOWELL, R. H. N90-18985
HOYLE, F. N90-19092
N90-19093
N90-19150
HRIVNAK, B. J. N90-19130
HSU, ANDREW T. N90-18667
HSU, K. Y. N90-18530
HUCKELBRIDGE, ARTHUR A. N90-18745
HUFFORD, GEORGE A. N90-18612
HUGENSCHMIDT, M. N90-18731
HUGHES, E. D. N90-18692
HUGHES, R. S. N90-18728
HUGHES, RUSSELL P. N90-18493
HUIJBERTS, H. J. C. N90-18948
HULETT, L. D., JR. N90-18995
HULSTROM, R. L. N90-18802
HULTS, W. L. N90-19030
HUMBERSTON, J. W. N90-18988
HUMPHREYS, C. J. N90-19051
HUNT, J. J. N90-19068
HUNT, L. N90-19151
HURLBERT, ANYA C. N90-18914
HURLBERT, E. N90-18484
HUTSON, F. L. N90-18512

I

IACABUCCI, R. N90-18482
IGE, O. O. N90-19040
IGNATEV, A. YU. N90-19177
IM, HOONG-SUN N90-18539
INGLOT, T. N90-18954
INGROSSO, G. N90-19126
INIZAN, G. N90-18521
ISAMINGER, MARK A. N90-18847
ISRAEL, F. P. N90-19107
ITOH, T. N90-18634
IVES, L. K. N90-18558
IWASA, Y. N90-19040

J

JACOBS, DAVID W. N90-18915
JACOBSEN, FINN M. N90-18979
JAEGER, CALVIN D. N90-18650
JAENICKE, RUPRECHT N90-18819
JAHAN, M. S. N90-19030
JAIN, ASHOK N90-18968
JAMES, MARK L. N90-18444
JAMET, J. F. N90-18498
JANK, THOMAS N90-18630
JARMAN, DAVID C. N90-18668
JAWORSKI, M. N90-18931
JAYAMANNA, K. N90-19029
JEAL, R. H. N90-18397
JENKINS, S. L. N90-18465
JENSEN, D. R. N90-18930
JENSEN, K. O. N90-18996
JEWUISKI, JANUSZ N90-18812
JING, YI-PENG N90-19173
JOHNSON, A. B. N90-18414
JOHNSON, ERNEST W. N90-19009
JOHNSON, J. LORRAINE N90-18625
JOHNSON, JEROME A. N90-18665
JOHNSON, JONI J. N90-19185
JOHNSON, PHILIP M. N90-18833
JOHNSON, WALTER A. N90-18642
JONCKHEERE, EDMOND A. N90-18920
JONES, DENISE R. N90-18394

JONES, K. M. N90-18985
JONES, K. W. N90-18867
JONES, T. L. N90-18814
JONES, TERRY JAY N90-19185
JONES, TROYCE D. N90-18856
JOSEPH, R. D. N90-19144
N90-19148
N90-19159
N90-19167
JOU, W. H. N90-18535
JOUBERT, H. N90-18412
JOURDAINDEMUIZON, M. N90-19105
JUANG, FEN-LIEN N90-18943
JUNG, GLENN H. N90-18845
JUSKA, T. D. N90-18513

K

KABANTSEV, A. A. N90-19020
KADOR, L. N90-18716
KALDEICH, B. H. N90-19084
KALETKA, JUERGEN N90-18389
KALLAS, M. N. N90-18506
KALLENBERG, W. C. M. N90-18954
KAMADA, M. N90-19004
KAMRAN, MEHRAN N90-18735
KANE, KENNETH PAUL N90-18924
KAO, C. T. N90-19042
KARR, THOMAS J. N90-18823
N90-18837
KARUZA, SARUNAS K. N90-18642
KAT, P. J. N90-18905
KAU, H. P. N90-18407
KAUKE, G. K. N90-18422
KAUP, D. J. N90-18931
KAUPPILA, W. E. N90-18959
N90-18974
KAUSCH, H. H. N90-18497
KAWASAKI, NARITAKE N90-18666
KEDL, MIKE R. N90-18921
KEHAYIAS, JOSEPH J. N90-18868
KELLOGG, R. BRUCE N90-18937
KENDALL, CHRISTOPHER L. N90-18582
KEPPLER, KENNETH SCOTT N90-19011
KERN, W. N90-18946
KESSLER, M. F. N90-19163
KEUTZER, KURT N90-18940
KHALIL, MOHAMMED N90-18944
KHATRI, R. N90-18980
KHOLBEV, I. N90-18588
KIESCHKE, R. N90-18502
KISER, D. M. N90-18655
KISTER, J. N90-19110
KLEBE, DIMITRI I. N90-19185
KLEIN, ANDREW C. N90-18607
KLOSE, A. N90-18406
KLUWICK, ALFRED N90-18421
KNIGHT, T. N90-18911
KNOWLES, JAMES K. N90-18747
KOEL, B. E. N90-18512
KOITIKUGA, HELIO N90-18440
KOLLER, FRANZ N90-18421
KONCZALLA, MATTHIAS N90-18543
KONG, K. S. N90-18634
KONIG, P. N90-18495
KOSASA, YOSHITAKE N90-18635
KOSKELA, REBECCA J. N90-18879
KOTSCHENREUTHER, M. N90-19056
KOVESI-DOMOKOS, S. N90-19001
KOYMEN, A. R. N90-18996
KRAETSCHMER, W. N90-19164
KRAYBILL, D. N90-18651
KRESS, REID L. N90-18921
KRETSCHMER, FRANK F., JR. N90-18621
KREYSA, E. N90-19137
N90-19164
KRIJGSMAN, J. N90-18549
KRIMAN, ALFRED M. N90-19036
KROHN, B. J. N90-18722
KRONAUER, RICHARD E. N90-18860
KRUGER, C. H. N90-19019
KRUGER, J. N90-18553
KRUSE, GEORG N90-18978
KUMANO, TERUHISA N90-18635
KUMAR, RAJENDRA N90-18379
KUNKEL, W. B. N90-18719
KUNTH, D. N90-19152
KUSHNER, LAWRENCE J. N90-18645
KVAM, ERIC P. N90-19051
N90-19052
KWAN, C. K. N90-18959
N90-18974
KWAY, W. L. N90-18728
KWOK, S. N90-19130

L

LACOMBE, A. N90-18500
LACY, J. H. N90-19140
LAFARGUE, P. N90-18866
LAFON, J. L. N90-19079
LALOR, N. N90-18755
LAMBERT, G. N90-19070
LAMERS, H. J. G. L. M. N90-19136
LANDAU, RUBIN H. N90-19005
LANGELUEDDECKE, E. F. M. N90-19080
LANSAW, P. TINA N90-18481
LARCOMB, CHARLES H. N90-18841
LARSON, TERRY J. N90-18395
LATTANZIO, JOHN C. N90-19172
LAVIA, A. N90-18526
LAWRENCE, CHARLES N90-18745
LAWRENCE, GEOFFREY F. N90-19185
LAWSON, DENISE L. N90-18444
LAZARO, C. N90-19131
LE, T. H. N90-18689
LEAODEMORAESNOVO, EVLYN MARCIA N90-18815
N90-18816
LEARNER, R. C. M. N90-19135
LEBALLEUR, J. C. N90-18408
LEDOUX, M. J. N90-19070
LEDWINA, T. N90-18954
LEE, D. R. N90-19042
LEE, DAVID N90-18777
LEE, DAVID CHUNG LIANG N90-18764
N90-18769
N90-18772
LEE, H. G. N90-18754
LEE, H. Y. N90-18634
LEE, J. N90-18510
LEE, JAMES D. N90-18734
LEE, K. H. N90-18996
LEE, L. M. N90-18705
LEE, ROBERT N90-18626
LEE, T. J. N90-19165
LEGER, A. N90-19106
N90-19113
N90-19164
LEI, CHUN N90-18996
LEIBFRITZ, DAVID W. N90-18909
LEISTNER, DETLEF N90-18631
LEKOUDIS, S. G. N90-18491
LELLOUCH, E. N90-19090
LEMEUR, ALAIN N90-18417
LEMKE, D. N90-19164
N90-19167
LEMKEY, F. D. N90-18559
LEQUEUX, J. N90-19129
LEROY, S. S. N90-18779
LESAIN, ALAIN N90-18417
LEUNG, K. N. N90-18719
LEVAN, N. N90-18908
LEVENTHAL, M. N90-18982
N90-18994
LEVILLAIN, P. N90-18866
LEVINE, MICHAEL V. N90-18870
LEVITAN, STEVEN P. N90-18641
LI, XIAO-SHEN N90-18568
LIAN, WEIJIAN N90-18654
LIANG, EDISON P. N90-19169
LICHT, H. H. N90-18605
LIEBE, HANS J. N90-18612
LIKKEL, L. N90-19134
LIMADALGE, JULIO CESAR N90-18775
LIN, DUO L. N90-18568
N90-18571
LIN, FENG-LING C. N90-18621
LIN, J. N. N90-18572
LIND, RICHARD J. N90-18842
LINDBERG, STEVEN E. N90-18819
LIU, A. H. N90-18585
LIU, CHAN CHIANG N90-18825
N90-18826
LIU, HANPING N90-19174
LIU, MEILIN N90-18584
LIU, S. H. N90-18998
LO, Y. T. N90-18622
LOHR, GARY W. N90-18378
LOMDAHL, P. S. N90-19049
LONG, C. N90-18695
LONG, R. A. N90-18676
LONGMORE, A. J. N90-19104
LOOMIS, B. A. N90-18551
LORENZ-MEYER, WOLFGANG N90-18370
LORENZETTI, D. N90-19126
LOWNDES, DOUGLAS H. N90-19043
N90-19045
LOWREY, A. R. N90-18712
LOWSON, MARTIN V. N90-18369
LUDWIG, GERSON OTTO N90-18490
LUESINK, ROB N90-18953
LUINGE, W. N90-19162
LUKASZEW, R. A. N90-18959
LUMPKIN, A. H. N90-18725
LUMPKIN, ALEXANDER H. N90-18712
LUNDBERG, R. N90-18499
LUSH, A. M. N90-18925
LUSK, EWING N90-18910
LUTZ, B. L. N90-19088
LUTZOW-WENTZKY, P. N90-19167
LYNCH, D. K. N90-19107
LYNCH, GARY N90-18863
LYNE, PEGGY J. N90-18374
LYNN, K. G. N90-18980
LYTLE, JOHN K. N90-18667
LYU, H. Y. N90-18530

M

MAAS, R. N90-18632
MAATOUCH, A. N90-18367
MACCALLUM, C. J. N90-18982
MACCORMACK, ROBERT W. N90-18674
MACH, H. N90-18547
N90-18694
MACKOWIAK, C. L. N90-18853
MADEY, JOHN M. J. N90-18720
MADEY, THEODORE E. N90-18546
MADSEN, VICTOR A. N90-19005
MADYCH, W. R. N90-18932
MAEDA, MICHI N90-18565
MAEZ, M. A. N90-19030
MAGAZZU, A. N90-19132
MAGINA, FLAVIO N90-18701
MAGNOTTA, F. N90-18985
MAHER, D. M. N90-19051
MAILAENDER, MARTIN N90-18609
MAILLARD, J.-P. N90-19088
N90-19090
N90-19120
MAJEED, Q. N90-19093
MAKAR, G. L. N90-18553
MALKAN, M. A. N90-19157
MANDEL, J. N90-18928
MANDERSCHEID, JANE M. N90-18504
MANES, K. N90-18657
MANGES, WAYNE W. N90-18921
MANN, G. A. N90-18659
MANTENIEKS, M. A. N90-18476
MARCHAL, C. N90-18956
MAREES, G. N90-18783
MARESCA, C. N90-18682
MARILL, THOMAS N90-18862
MARK, J. L. N90-18364
MARK, JAMES E. N90-18598
MARLEY, N. A. N90-18820
MARQUESFERNANDES, MAURICIO N90-18777
MARQUESNOGUEIRA, CARLOS ANTONIO N90-18737
MARTAWATI, LANNY N90-18785
MARTIN-CARRILLO, A. N90-18435
N90-18527
MARTIN, CHARLES R. N90-18573
MARTIN, N. N90-18866
MARTIN, RONALD E. N90-18808
MARTINEZ, M. J. N90-18541
MARTINO, JOSEPH P. N90-18375
MARYNICK, DENNIS S. N90-18579
MARZULLO, KEITH N90-18891
MAS-HESSE, J. M. M. N90-19152
MASETTA, J. P. N90-18489
MASKELL, S. Y. N90-18618
MASTERNAK, TADEUSZ J. N90-18451
MATHIEU, G. N90-18680
MATHUR, K. C. N90-18961
MATIJEVIC, EGON N90-18576
MCANALLY, JAMES V. N90-18464
MCCAMY, J. W. N90-19043
N90-19045
MCCOMB, HARVEY G., JR. N90-18752
MCCOMB, J. C. N90-18466
MCCONNAUGHEY, H. V. N90-18416
MCCOOL, JOHN I. N90-18591
N90-18738
MCCOWN, A. W. N90-18722
MCCOY, B. W. N90-18780
MCDONALD, S. C. N90-18797
MCEACHRAN, R. P. N90-18958
N90-18964
N90-18971
N90-18973
N90-18992
MCGARRY, M. A. N90-18364
MCGILL, R. N. N90-18741
MCGINN, M. T. N90-19141
MCGOWAN, PAUL E. N90-18751

MCKEE, C. F. N90-19115
MCKEE, SUZANNE P. N90-18858
MCLEAN, GARNET A. N90-18374
MCLEAN, I. S. N90-19142
MCLUCKEY, S. A. N90-18995
MCMILLAN, J. CHRISTOPHER N90-18381
MCMURTRY, C. H. N90-18594
MCMURTRY, P. A. N90-18535
MCVEY, BRIAN D. N90-18712
MEADE, ANDREW JAMES, JR. N90-18664
MEDRANO-B, RENE ADALID N90-18926
N90-18997
MEGE, P. N90-18689
MEHL, DAVID N90-18996
MEHRABIAN, R. N90-18507
N90-18508
MEHTA, H. S. N90-18550
MEIER, K. L. N90-18725
MEIKLE, W. P. S. N90-19124
N90-19135
MELE, EUGENE J. N90-19044
MELHEM, RAMI G. N90-18641
MELNICK, G. N90-19116
MELNICK, J. N90-19151
MENON, S. N90-18535
MESSENGERPARADA, LEOPOLDO N90-18701
METIVET, BRIGITTE N90-18685
METZGER, JOSEPH C. N90-19065
MEYER, WERNER N90-18630
MEZA, J. C. N90-18658
MICHELL, G. F. N90-19120
MIESCKE, KLAUS J. N90-18942
MILLAR, T. J. N90-19097
MILLE, G. N90-19110
MILLER, J. C. N90-19175
MILLER, STEVEN M. N90-18830
MILLS, A. P., JR. N90-18980
N90-18987
MINER, TIMOTHY H. N90-18843
MING, R. S. N90-18755
MISKI, TUNCER N90-18710
MITCHELL, J. B. A. N90-19002
MIXON, T. N90-18513
MIYAKAWA, MINORU N90-18698
MOERNER, W. E. N90-18531
N90-18640
N90-18716
MOES, TIMOTHY R. N90-18395
MOLAU, N. E. N90-18651
MOLENKAMP, E. N90-18906
MOLINARD, G. N90-18682
MOLL, J. R. N90-18785
MONETTI, A. N90-19121
MONTAUDO, GIORGIO N90-18569
MONTE, S. J. N90-18496
MOORE, T. N90-19156
MOORHOUSE, A. N90-19118
MOORWOOD, A. F. M. N90-19109
N90-19121
N90-19133
N90-19143
N90-19153
MORASH, D. H. N90-18488
MORDCHELLES-REGNIER, G. N90-19079
MORE, K. L. N90-18594
MOREIRA, MAURICIO ALVES N90-18763
MORGAN, DAVID L., JR. N90-18989
MORGAN, F. A. N90-18659
MORRIS, J. R. N90-18823
MORRIS, J. W., JR. N90-18753
MORRISON, JOSEPH DEREK N90-18878
MORRISON, P. J. N90-19056
MORSE, DAVID L. N90-18625
MORSE, R. L. N90-18723
MOSELEY, S. H. N90-19134
MOSES, K. G. N90-19027
MOSES, WILLIAM W. N90-18865
MOULIN, C. N90-18497
MOUNTAIN, C. M. N90-19165
MOUNTAIN, M. N90-19155
N90-19156
MOURICHOUX, H. N90-18501
MOUROULIS, PANTAZIS N90-19015
MUMINOV, T. M. N90-18588
MUNOZ-ESQUER, P. N90-18528
MURRAY, KENNETH D. N90-18670
MURRAY, YVONNE D. N90-18511
MURROW, HAROLD N. N90-18752
MUSE, J. N90-19042
MUTO, V. N90-19049

N

NAGATA, P. K. N90-18562
NAKADA, Y. N90-19112
NAKAI, N. N90-19156
NAKANO, YUKIO N90-18898
NAKAYAMA, KEN N90-18872
NAOI, KATSUHIKO N90-18639
NATHEL, HOWARD N90-18730
NAUMANN, HANS N90-18662
NAUMANN, K. W. N90-18392
NEAL, JEANNETTE G. N90-18897
NEGREIROSDEPAIVA, RICARDO N90-18442
NELSEN, E. N. N90-18362
NELSON, J. RICHARD N90-18898
NELSON, R. O. N90-18484
NEVESEPIPHANIO, JOSE CARLOS N90-18767
N90-18768
NEWMAN, E. H. N90-18390
NEWMAN, J. C., JR. N90-18746
NEWTON, A. RICHARD N90-18899
NICHOLSON, J. M. N90-18593
NICHOLSON, JAMES N90-19028
NIEH, JASON N90-18916
NIEMEGEERS, IGNAS G. N90-18907
N90-18949
NIERATSCHKER, WILLI N90-18696
NIEUWKAMER, R. L. M. N90-18785
NIEZGODA, THOMAS F. N90-18665
NIIYA, K. Y. N90-18468
NISHIDA, EIJI N90-18585
NISHIKAWA, KEN-ICHI N90-18831
NNAJI, BARTHOLOMEW O. N90-18735
N90-18912
NOAKES, M. W. N90-18876
NORDH, H. L. N90-19108
NOREN, CRAIG N90-19002
NORTON, DAVID P. N90-19043
N90-19045
NOWOTNY, H. N90-18559

O

OBRIEN, WALTER F. N90-18429
OCHAYA, VEN O. N90-18574
OERTEL, H. N90-18681
OHAYON, R. N90-18687
OLDFIELD, M. L. G. N90-18414
OLIMOV, B. A. N90-18588
OLIVA, E. N90-19109
N90-19133
N90-19153
OLLING, R. N90-19107
OLOFSSON, S. G. N90-19108
OLSON, JOSEPH R. N90-18625
OLSSON, BJORN N90-18977
OMONT, A. N90-19134
ONELLION, MARSHALL N90-19053
ONSTOTT, ROBERT G. N90-18371
N90-18372
ORAKZAI, MUAZZAM N90-19002
OROFINO, V. N90-19089
OSBORNE, RANDY BRENT N90-19067
OSIF, TERRY N90-18812
OSNAGHI, C. N90-18420
OSTDIEK, F. R. N90-18428
OSTROFF, AARON J. N90-18434
OTT, K. C. N90-19030
OUTTERS, L. N90-18695
OVERBEEK, ROSS N90-18904
OWANO, T. N90-19019
OWEN, T. N90-19088
OWENBY, RODNEY N. N90-18708
OWENS, BOONE B. N90-18639
OWENS, L. P. N90-18853

P

PALASZEWSKI, BRYAN N90-18480
PALKO, JOSEPH L. N90-18504
PALMER, RONALD W. N90-18874
PANGANTIWAR, A. W. N90-18960
PANITZ, J. K. G. N90-18583
PAPOULAR, R. N90-19110
PARCELL, L. A. N90-18973
PARDESSUS, TH. N90-18404
PARIKH, N. R. N90-19042
PARIKH, S. P. N90-18959
PARK, M. N90-18567
PARKER, JAMES F., JR. N90-18875
PARKES, J. E. N90-18476
PARKINSON, W. J. N90-18519
PASCHAL, CHARLES R., JR. N90-18874
PASSNER, A. N90-18994
PATTERSON, M. J. N90-18474
PATTNI, A. V. N90-19167
PAUBERT, G. N90-19090
PAUL, DONALD R. N90-18580
PAUL, LEE E. N90-18380
PAULEY, KEITH A. N90-18607
PAULINE, S. N90-19048
PAYNE, J. N90-18539
PAYNE, R. C. N90-18999
PAYNE, STEPHEN A. N90-18728
PAYNE, STEVEN S. N90-19028
PEDRAZA, D. F. N90-19041
PEERCY, PAUL S. N90-18564
N90-18713
PENETRANTE, B. M. N90-18729
PENLAND, J. N90-18657
PENTEADOARANHA, JOSE AUGUSTO N90-18798
PEREIRA, NILSON ALVES N90-18775
PEREPEZKO, JOHN H. N90-18713
PERQUIN, PHIN N90-19002
PETERS, DONALD C. N90-18707
PETERS, M. E. N90-18390
PETERSON, G. P. N90-18673
PETERSON, M. B. N90-18558
PHILLIPS, DONALD L. N90-18813
PHILLIPS, E. P. N90-18746
PICH, J. J. N90-18779
PICKARD, A. C. N90-18399
PIERSON, RICHARD N., JR. N90-18868
PINTO, J. G. N90-18648
PIOTROWSKI, JOSEPH L. N90-18430
PITKARANTA, J. N90-18928
PITTER, RICHARD L. N90-18832
PLA, FREDERIC G. N90-18685
PLOEGER, G. N90-19162
PLUMMER, M. N90-18969
POGATSHNIK, G. J. N90-18721
POKER, D. B. N90-19045
POMERANTZ, MARTIN N90-18579
POMRENKE, GERNOT S. N90-19031
PONGRATZ, MORRIS N90-18625
PONS, A. N90-19160
N90-19161
PONTHENIER, J. L. N90-18501
PONZONI, FLAVIO JORGE N90-18776
N90-18777
N90-18817
POTRA, FLORIAN A. N90-18934
POTTER, DOUGLAS W. N90-18625
POUPINET, D. N90-18682
PRADOBRITTO, RUBERIO N90-18818
PREDMESKY, R. L. N90-18593
PRICE, EDWARD W. N90-18492
PRIETO, M. N90-19154
PRIMOT, JEROME N90-19168
PRINCE, R. P. N90-18853
PUGET, J.-L. N90-19087
PUROHIT, S. P. N90-18961
PUXLEY, P. N90-19155
N90-19156
PYSZCZEK, MICHAEL F. N90-18844
N90-18799

Q

QUERMANN, ANDREAS N90-18978
QUIGLEY, G. P. N90-18723
QUIK, P. G. N90-18384
QUINN, GEORGE D. N90-18750

R

RABACA, DUILIA F. M. N90-19184
RABE, D. C. N90-18428
RABIER, PATRICK J. N90-18935
RAITANO, P. N90-18476
RAITH, WILHELM N90-18977
N90-18978
RAJESHWAR, KRISHNAN N90-18579
RAMAKER, DAVID E. N90-18512
N90-18536
N90-18537
N90-19037
N90-19038
RAMARAO, KONDAPALLI N90-18441
RAMSEY, P. E. N90-18469
RAND, JAMES A. N90-18582
RANDRIAMAMPIANINA, A. N90-18695
RANGANATH, S. N90-18550
RANK, D. M. N90-19101
RAQUENO, ROLANDO N90-19014
RAQUET, JOHN F. N90-18477
RATKOVICH, JOHN N90-18554
RAWLIN, VINCENT K. N90-18475
REAGAN, P. V. N90-18364
RECALDERAMOS, FACUNDO SALOMON N90-18772
REED, BRIAN D. N90-18472
REED, STEPHEN K. N90-18939

REGEN, S. L. N90-18566
REHAK, P. N90-18706
REIF, JOHN H. N90-18894
REIFENBERGER, R. N90-19046
REILINGER, ROBERT E. N90-18824
REINICKE, R. H. N90-18484
RENARD, ROBERT J. N90-18845
RENGGANIS, HENI N90-18785
REYNA, L. K. N90-18976
REYNOLDS, JOHN R. N90-18579
REZAI, K. N90-18402
RHEINBOLDT, WERNER C. N90-18934
RIBEIRODOSSANTOS, ATHOS N90-18829
RICHARD, H. N90-18497
RIECKE, JON GARY N90-18929
RIGBY, M. J. N90-18414
RIHA, J. N90-18703
N90-18705
RING, L. R. N90-18454
RIOSNETO, ATAIR N90-18798
RISTAD, ERIC SVEN N90-18941
RIVERA, THOMAS N90-18602
RIVERS, M. L. N90-18867
ROBERTSON, D. J. N90-19165
ROBINETTE, KATHLEEN M. N90-18873
ROCHE, P. F. N90-19094
N90-19145
ROCHELEAU, R. E. N90-18803
ROCK, MARY LOU N90-18582
ROCKWELL, RICHARD K. N90-19057
RODERICK, NORMAN F. N90-19028
RODRIGUES, JOSE EDUARDO N90-18826
RODRIGUES, LUIZ FLAVIO N90-18701
ROELLIG, L. O. N90-18980
ROMANOFSKY, R. R. N90-18634
ROMER, W. N90-18495
RONCHETTI, V. N90-18412
ROQUEDEASSIS, OSWALDO N90-18769
ROSE, E. A. N90-18722
ROSS, TH. N90-18732
ROSSI, J. O. N90-18700
ROUGES, J. M. N90-18500
ROUSSEL-DUPRE, R. N90-18624
ROUX, B. N90-18695
ROY, G. S. N90-18491
ROYER, H. N90-18704
RUBINSTEIN, ROBERT N90-18665
RUDDICK, KEITH N90-19006
RUDORFF, BERNARDO F. T. N90-18774
RUFFINS, TODD R. N90-18582
RUTKOWSKI, JANET L. N90-18909
RUVALDS, J. N90-19054
RYDER, M. O. N90-18488
RYUTOV, D. D. N90-19180
RYUTOVA, M. P. N90-19180

S

SACILOTTI, LUCIANO N90-18701
SAFONOV, MICHAEL G. N90-18920
SALASALVES, DIOGENES N90-18761
SALOVEY, R. N90-18567
SAMARA, G. N90-18705
SAMBE, H. N90-18536
N90-19038
SANCHE, L. N90-18536
N90-19038
SANCHEZ, J. N90-18526
N90-18544
SANDERSON, C. A. N90-19138
SANDMAN, JULIE N90-18430
SANDONATO, GILBERTO MARREGA N90-18490
SANKARALINGAM, S. N90-19048
SANKEWITSCH, V. N90-18743
SANTOS, C. N90-18700
SARACENO, P. N90-19126
SARACHIK, KAREN BETH N90-18382
SARKAR, K. P. N90-18967
SARMENTO, JOSE LUIZ N90-18701
SAUBERMANN, A. J. N90-18867
SAVINI, M. N90-18420
SAX, HARTMUT N90-18436
SCANDRETT, CLYDE N90-18749
SCHAAF, CRYSTAL B. N90-18844
SCHACHAR, J. N90-19070
SCHAEFER, DALE W. N90-18598
SCHAFFAR, M. N90-18391
SCHIDLOVSKY, G. N90-18867
SCHILD, HERBERT N90-18711
SCHITTKE, H. J. N90-18547
SCHLAEFLI, D. N90-18410
N90-18424
SCHLICH, HUGO N90-18560
SCHMIDT, B. N90-18581
SCHMIDT, WALTER N90-18662
SCHMITT, B. N90-19111
SCHMITT, R. N90-18733
SCHMOR, P. W. N90-19029
SCHNEIDER, JOHN F. N90-18542
SCHNEIDER, KEN R. N90-18542
SCHNEIDER, STEVEN J. N90-18472
SCHOENBERG, R. J. N90-18488
SCHOENMAN, LEONARD N90-18481
SCHORSCHER, HANS D. N90-18829
SCHOTT, JEAN-PIERRE N90-18919
SCHOTT, JOHN R. N90-19014
SCHRADER, D. M. N90-18981
SCHROEDER, E. C. N90-18489
SCHROEDER, JUDITH A. N90-18838
SCHULKIN, MORRIS N90-18889
SCHULZ, H. D. N90-18425
SCHUSTER, JOACHIM N90-18377
SCHWEHM, G. N90-19089
SCRIBER, MICHAEL W. N90-18637
SECOR, H. V. N90-18539
SEEHRA, M. S. N90-18545
SEEMAN, J. I. N90-18539
SEGURA, E. N90-18695
SEHRA, A. K. N90-18419
SEIDL, MILOS N90-19003
SEILER, F. N90-18680
N90-18681
SEKERAK, EDWARD M. N90-18540
SELBY, M. J. N90-19167
SELKREGG, K. R. N90-18594
SELLGREN, K. N90-19112
N90-19141
SERVATY, S. N90-18413
SESHADRI, S. G. N90-18594
SFILIGOJ, A. N90-19078
SGRO, A. G. N90-19021
SHAFFER, TIMOTHY D. N90-18579
SHALEK, PETER D. N90-18519
SHANG, T. N90-18419
SHAPOSHNIKOV, M. E. N90-19177
SHARP, D. J. N90-18659
SHARPE, D. N90-18503
SHAW, STEPHEN J. N90-18363
SHAW, WILLIAM J. N90-18842
SHEN, CHIH-PING N90-18882
SHEPHERD, JOHN T. N90-18432
SHEPHERD, WILLIAM T. N90-18875
SHIAO, MICHAEL C. N90-18470
SHIMABUKURO, YOSIO EDEMIR N90-18764
N90-18769
SHINN, M. D. N90-18728
SHIPMAN, RICHARD P. N90-18386
SHOCKET, EPHRAIM N90-18380
SHUHY, J. L. N90-18780
SIEGEL, ALEX N90-18891
SIEGERT, CLIFFORD E. N90-18665
SIEMERS, PAUL M., III N90-18395
SIERADZKI, K. N90-18553
SIGETY, P. N90-18522
N90-18523
SILVA, GIL N90-18773
SILVER, R. N. N90-19050
SIMEAODEMEDEIROS, JOSE N90-18769
SIMMONS, MARGARET L. N90-18879
SINAPIUS, GUENTHER N90-18977
N90-18978
SINDELAR, R. L. N90-18550
SINGER, PAUL A. N90-18614
SINGH, AMBUJ K. N90-18904
SINGH, J. P. N90-18518
SINGH, JAG J. N90-18882
SKINN, DONALD A. N90-18375
SMEETS, G. N90-18709
SMEGGIL, J. G. N90-18559
SMITH, D. L. N90-18551
SMITH, J. E. N90-18739
SMITH, J. L. N90-19030
SMITH, L. K. N90-18728
SMITH, M. G. N90-19149
SMITH, PATRICK M. N90-18564
SMITH, R. D. N90-18552
SMITH, ROBERT E. N90-18652
SMITH, STEVEN J. N90-18974
SMYRL, WILLIAM H. N90-18639
SNOW, D. B. N90-18559
SOARESGALVAO, WOUGRAN N90-18765
SOLOMON, HERBERT N90-18930
SOMEKH, R. N90-18502
SONDER, E. N90-19043
SOVEY, J. S. N90-18478
SOVIE, AMY J. N90-18478
SPAKMAN, J. N90-19162
SPANNE, P. N90-18857
SPENCER, J. N90-18911
SPERBER, WOLFGANG N90-18977
SPICHER, GOTTFRIED N90-18977
SPINOGLIO, L. N90-19126
N90-19157
SPIRO, STEPHANIE E. N90-18542
SPITZER, D. N90-18783
SPRAGUE, RICHARD A. N90-18617
SPRINKLE, DANNY R. N90-18882
SPYROMILIO, J. N90-19135
SRINIVASAN, SUPRAMANIAM N90-18796
SRIVASTAVA, RAJESH N90-18960
STACEY, G. J. N90-19146
STALTER, M. N90-18688
STAUFFER, A. D. N90-18958
N90-18964
N90-18971
N90-18973
N90-18992
STEAR, EDWIN B. N90-18432
STECKER, F. W. N90-18984
STEIN, T. S. N90-18959
N90-18974
STEIN, W. E. N90-18725
STENZENBERGER, H. N90-18495
STEPHENS, J. R. N90-18723
STERNBERG, A. N90-19117
STEVENSON, DAVID A. N90-19035
STIMPSON, G. J. N90-18755
STOFLETH, JEROME H. N90-18708
STRAFELLA, F. N90-19126
STRANGE, KAREN L. N90-18462
STRATON, JACK C. N90-18993
STRAZZULLA, G. N90-19132
STROMEYER, CHARLES F., III N90-18860
STROUS, L. H. N90-19136
STRUBE, CLAUS-DIETER N90-18742
STUTZIN, G. C. N90-18719
STUTZKI, J. N90-19098
SUBRAMONIAM, G. N90-19048
SUGERMAN, G. N90-18496
SUJANANI, M. N90-18585
SUN, JIN N90-19174
SUN, L. N90-18567
SUN, XIN N90-18571
SURKO, C. M. N90-18994
SUZUKI, KENICHI N90-18635
SWAIN, M. H. N90-18746
SWANSON, M. L. N90-19042
SWANSON, S. R. N90-18505
SYKES, MARK V. N90-19170
SZATMARI, PETER N90-18826

T

TADROS, R. N. N90-18402
TAKAHASHI, PATRICK K. N90-18811
TAKASO, SEIICHI N90-18635
TALLANT, D. R. N90-18583
TANG, P. Y. N90-18517
TANG, S. N90-18980
TANIGUCHI, HIROTO N90-18635
TASHAYEV, S. YU. N90-19020
TEEGARDEN, B. J. N90-18982
TEIXEIRABATISTA, GETULIO N90-18774
TELLER, EDWARD N90-18955
TENBERG, A. J. W. M. N90-18923
TENNYSON, JONATHAN N90-18970
TERDAL, P. N90-18911
TEST, FREDERICK L. N90-18578
THEVAR, G. R. N90-18545
THODE, LESTER E. N90-18712
THOMAS, D. G. N90-18739
THOMAS, EDWARD V. N90-18650
THOMPSON, MICHAEL O. N90-18564
THUNNISSEN, H. A. M. N90-18787
TIELENS, A. G. G. M. N90-19100
N90-19101
TIMMONS, M. N90-19042
TIMS, A. C. N90-18646
TISCHLER, MARK B. N90-18389
TISHKOFF, J. M. N90-18491
TOKAR, ROBERT L. N90-18712
TOKSOZ, M. NAFI N90-18824
TOKUNAGA, A. T. N90-19112
TRAMONTANO, VALENTINO J. N90-18574
TREVATHAN, J. T. N90-18486
TRIBULA, D. N90-18753
TROW, J. R. N90-19027
TSAI, TSUNG-MING N90-18734
TSAI, W. H. N90-18569
TSAO, J. Y. N90-18564
TUELLER, J. N90-18982
TUFFS, R. J. N90-19137
N90-19164
TUNNELL, T. W. N90-18624
TURKO, BOJAN T. N90-18702
TURNER, J. L. N90-19147

TURNER, JEFFREY L. N90-19013
TURNER, MICHAEL S. N90-19171
TURRO, NICHOLAS J. N90-18570
TUZZOLO, MICHAEL F. N90-18669

U

UEDA, M. N90-18700
ULIANA, E. A. N90-18780
ULLAL, H. S. N90-18792
UMAMAHESWARI, R. N90-19048
UNDERWOOD, F. N90-18503
UNSWORTH, MICHAEL H. N90-18819

V

VALAVANI, L. N90-18672
VALERIOFILHO, MARIO N90-18762
VANDAM, J. W. N90-19026
VANDERDONK, PETER N90-19002
VANDERLAAN, F. B. N90-18787
VANDERLINDEN, J. P. N90-18788
VANDERPUTTEN, RONALD N90-18661
VANDERREIJDEN-STOLK, CHRISTINE N90-18684
VANDERSCHAFT, ARJAN N90-18922
VANDERVEEN, W. N90-19166
VANDYKE, LEON S. N90-18573
VANES, J. T. N90-18660
N90-18663
VANLEUVEN, K. N90-18483
VANOORT, RONALD CORNELIS N90-18590
VANT, JAMES H. B. N90-18374
VANTRIGT, J. N90-18660
VARGASDEASSUNCAO, GETULIO N90-18761
N90-18763
VASUDEVAN, NARESH N90-18749
VAUGHAN, C. N90-18695
VAUGHN, P. N90-19167
VAVRYSHCHUK, YA. N90-18588
VENKATASUBRAMANIAN, R. N90-19042
VERDON, JOSEPH M. N90-18415
VERSTRAETE, L. N90-19106
N90-19113
VIANEISOARES, JOAO N90-18701
VIBBART, CHARLES M. N90-18463
VIECELLI, J. A. N90-18823
VIEIRADAFONSECALOPES, ROBERTO N90-18951
VIEIRAGUEDES, ULISSES THADEU N90-18449
VIERIRADIAS, LUIZ ALBERTO N90-18777
VIESCAS, A. J. N90-18980
VINCENT, C. N90-18501
VINCENT, H. N90-18501
VINSON, J. B. N90-18649
VISCO, STEVEN J. N90-18584
VITORELLO, ICARO N90-18762
VIVIER, B. N90-19082
VOELK, H. J. N90-19158
VOGEL, KELLY A. N90-18909
VOGEL, THOMAS A. N90-18821
VOIT, FRANK J. N90-18642
VOLOSYANYJ, S. P. N90-18588
VYRNWY-JONES, PETER N90-18874

W

WACK, JOHN P. N90-18881
WADE, R. N90-19165
WAGNER, LYLE C. N90-18619
WAHLS, RICHARD A. N90-18675
WALLACE, JOHN W. N90-18751
WALLIS, M. K. N90-19093
WALSH, LOIS HARPER N90-19033
WALSH, THOMAS P. N90-18430
WALTERS, H. R. J. N90-18966
WAN, Y. J. N90-18959
WANG, BING N90-18575
WANG, JACK N90-18868
WANG, P. K. C. N90-18908
WANG, SHUI N90-18835
WANG, W.-C. N90-18822
WARD, ALLEN CORLIES N90-18896
WARD, M. J. N90-19149
WARD, S. J. N90-18958
N90-18992
WARE, A. A. N90-19022
N90-19023
WARNER, J. D. N90-18634
WARREN, RICHARD M. N90-18861
WASSERMAN, HARVEY J. N90-18879
WAYNER, P. C., JR. N90-18585
WEBB, BRENT J. N90-18607
WEBER, G. G. N90-18925
WEBER, M. N90-18980
WEBSTER, R. B. N90-18723
WEI, ROBERT P. N90-18556
WEIGHT, THOMAS H. N90-18877
WEINSHALL, DAPHNA N90-18871
WEISMANN, H. J. N90-18581
WEISS, ALEX N90-18996
WELLS, M. N90-19167
WERNER, CH. N90-18848
WERTHEIMER, JEREMY M. N90-18917
WESSELING, J. W. N90-18788
WESSELIUS, P. N90-19107
WESSELIUS, P. R. N90-19162
WEST, JEFFREY A. N90-18564
WEST, PAUL V. N90-18574
WETTERLING, W. N90-18947
WHANG, Y. C. N90-19181
WHEELER, P. N90-18651
WHEELER, PHILIP C. N90-18515
WHEELER, ROBERT L. N90-18748
WHITE, G. J. N90-19138
WHITE, RALPH E. N90-18796
WHITENTON, E. P. N90-18558
WHITESIDES, R. H. N90-18465
WHITTED, GARY ALEN N90-18890
WHITTUM, DAVID H. N90-19024
WICKRAMASINGHE, N. C. N90-19092
N90-19093
N90-19150
WIDJAYA, JOYCE MARTHA N90-18785
WIJNBERGEN, J. N90-19162
WILDEMAN, K. N90-19162
WILLIAMS, FORREST R. N90-18845
WILLIAMS, P. G. N90-19138
WILMORE, DOUGLAS W. N90-18859
WIMAN, BO L. B. N90-18819
WINTER, CARL-JOCHEN N90-18609
WIRTH, GUNTER N90-18750
WIT, P. N90-18788
WITTEBORN, F. C. N90-19101
WOJTOWICZ, D. N90-18651
WOLF, DAVID A. N90-18852
WOLFF, E. N90-19077
WOODEN, D. H. N90-19101
WOODS, D. TOD N90-19102
WRIGHT, G. S. N90-19104
N90-19142
N90-19148
N90-19159
WU, C. Y. N90-18552
WU, CHANG-QIN N90-18571
WU, D. N90-18673
WU, Y. Y. N90-18828
WUNDERLICH, BERNHARD N90-18595

X

XIE, MING N90-18720
XU, JIEPING N90-18616

Y

YAMAMOTO, H. N90-19004
YAMASHITA, T. N90-19156
YANCEY, CHARLES N90-18734
YANG, MAOZHAG N90-18452
YEN, MINNIE YI-MIIN N90-19064
YEREMIAN, A. D. N90-18712
YIP, KENNETH MAN-KAM N90-18900
YOO, M. H. N90-18563
YORK, G. W. N90-18723
YORKEY, THOMAS J. N90-18707
YOSHIMITSU, TSUKASA N90-18636
YOUNG, A. T. N90-18719
YOUNG, CHRISTOPHER J. N90-18430
YOUNG, LLOYD M. N90-18712
N90-18725
YOUSIF, F. B. N90-19002
YU, KUANXIN N90-18616
YUAN, D. H. N90-19029

Z

ZANOTTO, OSMAR ANTONIO N90-18826
ZAPATA, L. N90-18657
ZAVALIANGOS, A. N90-18925
ZEWAIL, AHMED H. N90-18717
ZHANG, CUN-QUAN N90-18933
N90-18938
ZHAO, MENGJIA N90-18855
ZHOU, S. N90-18959
ZHU, YONG-JIN N90-18933
ZIMMERMANN, ANITA N90-18446
ZIOCK, KLAUS P. N90-18985
N90-19017
N90-19188
ZUCKERMAN, D. M. N90-18987
ZURAWSKI, ROBERT L. N90-18471
ZWEIBEL, K. N90-18792

Typical Corporate Source Index Listing

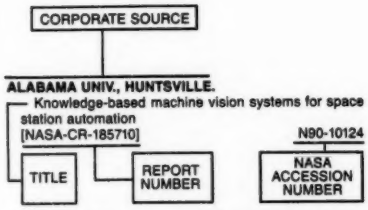

Listings in this index are arranged alphabetically by corporate source. The title of the document provides the user with a brief description of the subject matter. The report number helps to indicate the type of document cited (e.g., NASA report, translation, NASA contractor report). The NASA accession number denotes the number by which the citation is identified. The titles are arranged under each corporate source in ascending accession number order.

A

AALBORG PORTLAND (DENMARK).
Compact reinforced composite basic principles
[CBL-41] N90-18520
High-strength concrete development through 25 years
[CBL-REPRINT-17] N90-18589

AARHUS UNIV. (DENMARK).
Double ionization of helium by particle impact
N90-18979

ACADEMY OF SCIENCES (USSR), NOVOSIBIRSK.
Magnetic field generation by acoustic oscillations in solar atmosphere
[DE90-606054] N90-19180

ADVISORY GROUP FOR AEROSPACE RESEARCH AND DEVELOPMENT, NEUILLY-SUR-SEINE (FRANCE).
AGARD/SMP Review: Damage Tolerance for Engine Structures. 2: Defects and Quantitative Materials Behaviour
[AGARD-R-789] N90-18396
Unsteady Aerodynamic Phenomena in Turbomachines
[AGARD-CP-468] N90-18405
The implications of using integrated software support environment for design of guidance and control systems software
[AGARD-AR-229] N90-18432
Calendar of selected aeronautical and space meetings
[AGARD-CAL-90/1] N90-19060

AEROSPACE CORP., EL SEGUNDO, CA.
Interfacial chemistry of MoS2 films on Si
[AD-A216527] N90-18532
Determining the effects of microwave power and C-field setting on the frequency of a cesium atomic frequency standard
[AD-A216599] N90-18642

AEROSPACE CORP., LOS ANGELES, CA.
IRAS LRS spectra of extended objects: The Crab nebula N90-19107

AEROSPATIALE, LES MUREAUX (FRANCE).
An example of technology transfer by Aerospatiale: Fire protection materials N90-19082

AEROSPATIALE AQUITAINE, SAINT-MEDARD EN JALLES (FRANCE).
State of the art and future prospects for high temperature composites N90-18498

AGENCY OF INDUSTRIAL SCIENCE AND TECHNOLOGY, TOKYO (JAPAN).
Stirling engine technologies in Japan
[DE89-782296] N90-18795

AIR FORCE ACADEMY, CO.
Proceedings of the Professional Pilots Meteorology Training Standards Conference
[AD-A216618] N90-18843

AIR FORCE GEOPHYSICS LAB., HANSCOM AFB, MA.
The 2.7/4.3 micron CO2 branching ratio measurement
[AD-A215952] N90-18830
Comparisons between the RTNEPH (Real-Time Nephanalysis) and AFGL cloud layer analysis algorithms
[AD-A216637] N90-18844

AIR FORCE HUMAN RESOURCES LAB., BROOKS AFB, TX.
Simulation of synthetic aperture radar 3: Evaluation of prototype digital feature analysis data
[AD-A216750] N90-18620

AIR FORCE INST. OF TECH., WRIGHT-PATTERSON AFB, OH.
Visual servoing for autonomous aircraft refueling
[AD-A216042] N90-18386
Discrete proportional Plus Integral (PI) multivariable control laws for the Control Reconfigurable Combat Aircraft (CRCA)
[AD-A215664] N90-18431
Using the method of matched asymptotic expansions, analytically investigate the three-dimensional, atmosphere entry problem
[AD-A216287] N90-18451
Technology development and circuit design for a parallel laser programmable floating point application specific processor
[AD-A215870] N90-18637
Multicellular natural convection in a narrow vertical slot
[AD-A216411] N90-18668
A numerical solution to the Boltzmann equation for use in calculating pumping rates in a CO2 discharge laser
[AD-A216378] N90-18718
Spatial registration of TIROS-N weather satellite data
[AD-A216041] N90-18841
Determination of the underlying task scheduling algorithm for and Ada runtime system
[AD-A215880] N90-18890
Optical amplification in 45 deg - cut BaTiO3
[AD-A216043] N90-19011
Luminescence of lanthanides and actinides implanted into binary III-V semiconductors and AlGaAs
[AD-A215759] N90-19031
Transient heat transfer measurements on a flat plate in turbulent flow using an electrical analog
[AD-A216286] N90-19057

AIR FORCE OCCUPATIONAL MEASUREMENT CENTER, RANDOLPH AFB, TX.
Airborne radar systems specialist, AFSC 118X2
[AD-A215450] N90-18611

AIR FORCE OFFICE OF SCIENTIFIC RESEARCH, BOLLING AFB, WASHINGTON, DC.
AFOSR/ONR (Air Force Office of Scientific Research/Office of Naval Research) Contractors' Meeting on Combustion Rocket Propulsion Diagnostics of Reacting Flow
[AD-A216094] N90-18491

AIR FORCE SYSTEMS COMMAND, WRIGHT-PATTERSON AFB, OH.
A difference scheme with autocontrol artificial viscosity to predict ablated nosetip shape
[AD-A216625] N90-18452
Inspection of carbon/epoxy and aluminum honeycomb paraboloidal components by HNDT
[AD-A216796] N90-18514
* Applications of acousto-optical correlation devices in radar signal processing
[AD-A216624] N90-18616

AIR FORCE WEAPONS LAB., KIRTLAND AFB, NM.
Effects of oblique impact on hypervelocity shield performance
[DE90-006936] N90-18739

AIX-MARSEILLES UNIV. (FRANCE).
Aerodynamics of unsteady systems. Numerical study of potential flow/boundary layer coupling
[ETN-90-96257] N90-18367

ALABAMA UNIV., HUNTSVILLE.
A perspective of software reuse
[AD-A216911] N90-18901

ALLIED-SIGNAL AEROSPACE CO., KANSAS CITY, MO.
Ion chromatography in the manufacture of multilayer circuit boards
[DE90-005560] N90-18652

ALLIED-SIGNAL CORP., MORRISTOWN, NJ.
Improved amorphous metal materials for magnetic pulse compression
[DE90-005723] N90-18555

ANTHROPOLOGY RESEARCH PROJECT, YELLOW SPRINGS, OH.
Anthropometry of a fit test sample used in evaluating the current and improved MCU-2/P masks
[AD-A215173] N90-18873

APTEK, INC., SAN JOSE, CA.
Theory and verification of the fiber composite damage model implemented in DYNA3D
[AD-A216600] N90-18511

ARGONNE NATIONAL LAB., IL.
Mechanical properties and microstructure of Si3N4-whisker-reinforced Si3N4 matrix composite
[DE90-005051] N90-18518
Evaluation of a commercial gas chromatography/matrix isolation-infrared spectrometer for quantitative analysis of priority pollutants
[DE90-006033] N90-18542
Response of unirradiated and neutron-irradiated vanadium alloys to Charpy-impact loading
[DE90-004878] N90-18551
Tropospheric chemistry of natural hydrocarbons and energy-related pollutants: Biosphere/climate feedbacks
[DE90-005643] N90-18820
Derivation of efficient parallel programs: An example from genetic sequence analysis
[DE90-005654] N90-18904
Parallelizing the SDI ACCESS algorithm for the Connection Machine-2
[DE90-006382] N90-18909
Summer institute in parallel computing
[DE90-005532] N90-18910
Underground muon observations in the Soudan 2 detector
[DE90-005647] N90-19183

ARIZONA STATE UNIV., TEMPE.
Proceedings of the 6th Conference on Hot Carriers in Semiconductors
[AD-A215978] N90-19032
Transport effects and spectroscopy of defects in microstructures
[AD-A216718] N90-19036
Dust continuum spectra from model HII regions
N90-19099

ARIZONA UNIV., TUCSON.
Fluorescence and elastic scattering from laser dye-filled capillaries
[AD-A217026] N90-18540
Scattering from an arbitrary cylinder in the presence of a planar media interface using the bymoment method
[DE90-006465] N90-18626
Solar variability observed through changes in solar figure and mean diameter
[DE90-006600] N90-18634
Zodiacal dust bands: Their relation to asteroid families
[AD-A216025] N90-19170

ARMY AEROMEDICAL RESEARCH LAB., FORT RUCKER, AL.
Evaluation of helmet retention systems using a pendulum device
[AD-A215489] N90-18874

ARMY ARMAMENT RESEARCH, DEVELOPMENT AND ENGINEERING CENTER, WATERVLIET, NY.
Calculations of braiding parameters
[AD-A216836] N90-18515

ARMY AVIATION ENGINEERING FLIGHT ACTIVITY, EDWARDS AFB, CA.
Preliminary airworthiness evaluation of the Woodward hydromechanical unit installed on T700-GE-700 engines in the UH-60A helicopter
[AD-A216751] N90-18430

ARMY AVIATION RESEARCH AND DEVELOPMENT COMMAND, MOFFETT FIELD, CA.
Time and frequency-domain identification and verification of BO-105 dynamic models
[AD-A216628] N90-18389
ARMY COMMUNICATIONS-ELECTRONICS COMMAND, FORT MONMOUTH, NJ.
Proceedings of the 38th International Wire and Cable Symposium
[AD-A216023] N90-18638
ARMY INST. FOR RESEARCH IN MANAGEMENT INFORMATION AND COMPUTER SCIENCES, ATLANTA, GA.
Technology assessment of software engineering
[AD-A216943] N90-18902
Integrated IMA (Information Mission Areas) IC (Information Center) guide
[AD-A216944] N90-18903
ARMY MATERIALS TECHNOLOGY LAB., WATERTOWN, MA.
Biaxial strength and stress rupture of hot-pressed silicon nitride
[AD-A216950] N90-18750
ARNOLD ENGINEERING DEVELOPMENT CENTER, ARNOLD AIR FORCE STATION, TN.
The effects of wind tunnel data uncertainty on aircraft point performance predictions
[AD-A216091] N90-18387
ASTROSYSTEMS INTERNATIONAL, INC., NEWARK, DE.
Research relating to crystalline silicon-film on a foreign substrate
[DE90-005720] N90-18582
ATMOSPHERIC AND ENVIRONMENTAL RESEARCH, INC., CAMBRIDGE, MA.
Natural and anthropogenic climate change
[DE90-006486] N90-18822
AUSTRALIAN DEFENCE FORCE ACADEMY, CANBERRA.
Spectropolarimetry as a diagnostic of the interstellar medium N90-19096

B

BALL AEROSPACE SYSTEMS DIV., BOULDER, CO.
RF modal quantity gaging N90-18483
BATTELLE COLUMBUS LABS., OH.
Low temperature specific heat and magnetic susceptibility of NbTi and NbTiMn alloys
[DE90-005390] N90-18552
BATTELLE MEMORIAL INST., GENEVA (SWITZERLAND).
Identification of and response to market demand N90-19078
BELEIDSCOMMIE REMOTE SENSING, DELFT (NETHERLANDS).
Investigation of multiple scattering in aqueous suspensions of non-absorbing polystrene microspheres using spectrophotometry
[BCRS-89-09] N90-18549
On the applicability of CAESAR for the remote sensing of bottom depth and bottom composition of shallow waters: A model study
[BCRS-89-13] N90-18783
Introduction of aerial photography in agricultural research
[BCRS-89-14] N90-18784
Erosion monitoring using remote sensing, part 2
[BCRS-89-15] N90-18785
Improvement of classification results from satellite imagery to update and differentiate land use classes on topographic maps
[BCRS-89-17] N90-18786
SPOT for landscape: Development of a method for the use of SPOT pictures for the updating of the data base scale of the landscape
[BCRS-89-18] N90-18787
Remote sensing and run-off modelling in the Lake Victoria Basin, Kenya
[BCRS-89-19] N90-18788
Results of Agrisar-86 for the Flevopolder (Netherlands) test area
[BCRS-89-21] N90-18789
Remote sensing for the classification and quantification of vegetation in Spring staging areas of Brent geese on the Frisian Islands (Netherlands)
[BCRS-89-27] N90-18790
LANDSAT Thematic Mapper for hydrogeological mapping in Egypt
[BCRS-89-28] N90-18791
BELL TELEPHONE LABS., INC., MURRAY HILL, NJ.
Decay rate and other properties of the positronium negative ion N90-18987
Positron-molecule bound states and positive ion production N90-18994
BERKELEY RESEARCH ASSOCIATES, INC., CA.
Theory for high gain, high power free electron lasers
[DE90-005546] N90-18714
Research on free electron lasers
[AD-A215865] N90-18715
BIELEFELD UNIV. (GERMANY, F.R.).
Ionisation of atomic hydrogen by positron impact N90-18977
Multiple-ionization of xenon atoms by positron impact N90-18978
BIHRLE APPLIED RESEARCH, INC., JERICHO, NY.
Static and rotational aerodynamic data from 0 deg to 90 deg angle of attack for a series of basic and altered forebody shapes
[AD-A216582] N90-18361
Influence of forebody geometry on aerodynamic characteristics and a design guide for defining departure/spin resistant forebody configurations
[AD-A216714] N90-18368
BOEING HELICOPTER CO., PHILADELPHIA, PA.
Calculation of flight vibration levels of the AH-1G helicopter and correlation with existing flight vibration measurements
[NASA-CR-181923] N90-18743
BRIGHAM AND WOMEN'S HOSPITAL, BOSTON, MA.
A program for the study of skeletal muscle catabolism following physical trauma
[AD-A216569] N90-18859
BRISTOL UNIV. (ENGLAND).
Optimum spanwise camber for minimum induced drag
[BU-403] N90-18369
BRITISH AEROSPACE PUBLIC LTD. CO., KINGSTON-UPON-THAMES (ENGLAND).
Measuring strain in carbon fibre composite laminates using the Raman optomechanical strain gauge N90-18503
BRITISH COLUMBIA UNIV., VANCOUVER.
Computerized analysis of hydrogen plasma in a compact H(sup -) cusp source
[DE90-006881] N90-19029
BROOKHAVEN NATIONAL LAB., UPTON, NY.
The effect of electric field on attachment of electrons to solutes in liquid argon
[DE90-003968] N90-18529
State of the art in semiconductor detectors
[DE90-005567] N90-18706
Biomedical applications of synchrotron x ray microscopy
[DE90-004957] N90-18867
Measurement of body fat by neutron inelastic scattering: Comments on installation, operation, and error analysis
[DE90-006785] N90-18868

C

CALGARY UNIV. (ALBERTA).
Unidentified infrared features in proto-planetary nebulae N90-19130
CALIFORNIA INST. OF TECH., PASADENA.
Ultrafast chemical dynamics of reactions in beams
[AD-A216319] N90-18717
Kinetic relations and the propagation of phase boundaries in solids
[AD-A215881] N90-18747
Infrared spectroscopy and imaging of supernova remnants N90-19104
CALIFORNIA UNIV., BERKELEY.
Semidiscrete Galerkin modelling of compressible viscous flow past a circular cone at incidence
[NASA-CR-186323] N90-18664
Creep in shear of experimental solder joints
[DE90-007062] N90-18753
Far-infrared spectroscopy of galaxies N90-19148
CALIFORNIA UNIV., BERKELEY. LAWRENCE BERKELEY LAB.
Electrochemical investigations of novel solid redox polymerization electrodes
[DE90-006087] N90-18584
High speed imaging with a tapped solid state sensor
[DE90-006116] N90-18702
VUV (Vacuum Ultraviolet) laser diagnostics of H(-) ion sources
[DE90-006072] N90-18719
Resonator modes in high gain free electron lasers
[DE90-006098] N90-18720
Creep in shear of experimental solder joints
[DE90-007062] N90-18753
Performance of a coincidence based blood activity monitor
[DE90-006105] N90-18885
A continuous plasma final focus
[DE90-006096] N90-19024
Dislocation behaviour in Ge(x)Si(1-x) epilayers on (001) Si
[DE90-007063] N90-19051
Modified dislocation structures in Ge(x)Si(1-x) double epilayers on (001) Si
[DE90-007078] N90-19052
Geometric continuum regularization of quantum field theory
[DE90-006099] N90-19058
CALIFORNIA UNIV., IRVINE.
Organization of a large-scale cortical network
[AD-A216829] N90-18883
CALIFORNIA UNIV., LOS ANGELES.
Control and stabilization of linear and nonlinear distributed systems
[AD-A216446] N90-18908
CALIFORNIA UNIV., SANTA BARBARA.
The processing and mechanical properties of high temperature/high performance composites. Book 2, section 2: Strength and fracture resistance
[AD-A216142] N90-18507
The processing and mechanical properties of high temperature/high performance composites. Book 3, section 2: Strength and fracture resistance, part
[AD-A216143] N90-18508
CALSPAN CORP., BUFFALO, NY.
Knowledge-based extensible natural language interface technology program
[AD-A216664] N90-18897
CAMBRIDGE UNIV. (ENGLAND).
Modelling unsteady transition and its effects on profile loss N90-18423
Sputter deposition of diffusion barrier coatings on SiC monofilaments for use in Ti-based composites N90-18502
H-alpha emission lines in high redshift quasars N90-19149
CARBORUNDUM CO., NIAGARA FALLS, NY.
Microstructural characterization of silicon nitride ceramics processed by pressureless sintering, overpressure sintering, and sinter/HIP
[DE90-007126] N90-18594
CARNEGIE-MELLON UNIV., PITTSBURGH, PA.
Guidelines for the use of the SAME
[AD-A215846] N90-18888
CATANIA ASTROPHYSICAL OBSERVATORY (ITALY).
Dust in planetary nebulae: IRSPEC observations in the 3.0 micron-3.8 micron range N90-19132
CATANIA UNIV. (ITALY).
High-resolution Euler computations of unsteady transonic flows in cascades N90-18420
CATHOLIC UNIV. OF AMERICA, WASHINGTON, DC.
Interaction of minor ions with fast and slow shocks
[NASA-CR-186372] N90-19181
CBY ASSOCIATES, INC., WASHINGTON, DC.
Phase-Change Thermal Energy Storage
[DE89-009426] N90-18801
CENTRAL RESEARCH INST. OF ELECTRIC POWER INDUSTRY, TOKYO (JAPAN).
Back swing phenomenon of synchronous generator. Study on ac-dc power system simulator tests
[DE89-782321] N90-18635
Optimal planning method of underground distribution system, part 2. Application to various types of system configurations
[DE89-782323] N90-18636
Measurement of spectral emissivity by Fourier transform infrared spectrometer
[DE89-782319] N90-18898
CENTRE D'ESSAIS AERONAUTIQUE TOULOUSE (FRANCE).
Bird impact tests on a Kevlar 49 structure. Monolithic plates. Oblique-angled impact
[REPT-S3-4273] N90-18378
The need for a common approach within AGARD N90-18404
CENTRE D'ETUDES ET DE RECHERCHES DE MEDECINE AEROSPATIALE, PARIS (FRANCE).
Study of rifampicin fixation on plasma proteins by derivative spectrophotometry
[CERMA-89-25] N90-18866
CENTRE NATIONAL D'ETUDES SPATIALES, PARIS (FRANCE).
French approach to space technology transfer N90-19074
CENTRE NATIONAL DE LA RECHERCHE SCIENTIFIQUE, SAINT MARTIN D'HERES (FRANCE).
Spectroscopy and physico-chemistry of CO:H2O and CO2:H2O ices N90-19111
CENTRO DE PESQUISAS AGROPECUARIA DOS CERRADOS, PLANALTINA (BRAZIL).
Thermal remote sensing in the differentiation of soybean crops (glycine max (L.) merrill) submitted to water deficit
[INPE-4900-PRE/1501] N90-18762
CHICAGO UNIV., IL.
Particle physics and cosmology
[DE90-006547] N90-19171

CINCINNATI UNIV., OH.
Polymerization of nitro compounds on silver surfaces during surface-enhanced Raman scattering
[AD-A216116] N90-18569
CITY COLL. OF THE CITY UNIV. OF NEW YORK, NY.
Positronium reflection and positronium beams N90-18980
CLARKSON UNIV., POTSDAM, NY.
Colloid and interface chemistry aspects of ceramics
[AD-A216715] N90-18578
Direct and inverse scattering problem associated with the elliptic Sinh-Gordon equation
[AD-A216455] N90-18931
COLORADO STATE UNIV., FORT COLLINS.
Determination of the minimum energy conformation of alkyl substituted pyrazines
[AD-A216974] N90-18539
COLORADO UNIV., BOULDER.
Perturbations of test mass motion in the Schwarzschild spacetime using the method of Hamilton and Jacobi N90-19083
COLUMBIA UNIV., NEW YORK, NY.
Dynamics and stabilization of materials possessing high energy content
[AD-A216320] N90-18570
COMMISSARIAT A L'ENERGIE ATOMIQUE, GIF-SUR-YVETTE (FRANCE).
A coal model for the carriers of the unidentified IR bands N90-19110
COMMISSION OF THE EUROPEAN COMMUNITIES (LUXEMBOURG).
Introductory remarks for the panel discussions on technology transfer N90-19075
CONNECTICUT UNIV., STORRS.
Auditory perception
[AD-A217012] N90-18864
Inverse scattering and tomography
[AD-A216456] N90-18932
CONSEJO SUPERIOR DE INVESTIGACIONES CIENTIFICAS, MADRID (SPAIN).
Measurement system of spectral irradiance in the near infrared N90-19160
Performance parameter characterisation of various types of IR single element detectors N90-19161
CONSIGLIO NAZIONALE DELLE RICERCHE, FRASCATI (ITALY).
Herbig Ae/Be stars: Fine structure far-infrared lines N90-19126
Far infrared fine structure lines in active galaxies N90-19157
CONSTRUCCIONES AERONAUTICAS S.A., MADRID (SPAIN).
Design of a new control system for hovercrafts
[ETN-90-96230] N90-18435
Calculation of mechanical properties variations depending on matrix parameters in a composite, as a function of the test temperature
[DT-311/88] N90-18526
Impact of composites in the aerospace industry
[ETN-90-96231] N90-18527
The manufacturing procedures for composite materials, automation, and robotization
[ETN-90-96232] N90-18528
Rheological tests of Rigidite 5245 using the cone-plate and parallel plates method
[DT-310/88] N90-18544
CONTROL DATA CORP., ALEXANDRIA, VA.
Defense Technical Information Center Executive Information System: Documentation and user's manual
[AD-A216235] N90-19065
CORNELL UNIV., ITHACA, NY.
Deceit: A flexible distributed file system
[NASA-CR-186402] N90-18891
Log-based recovery in asynchronous distributed systems
[NASA-CR-186190] N90-18924
Infrared lines as probes of galactic structure N90-19139
CORVALLIS ENVIRONMENTAL RESEARCH LAB., OR.
Effects of global climate change on agroecosystems: Scope of work
[PB90-120023] N90-18813

D

DARTMOUTH COLL., HANOVER, NH.
Perfluorinated ligands in organometallic chemistry
[AD-A216415] N90-18493
DAVID TAYLOR RESEARCH CENTER, BETHESDA, MD.
Instrumented impact testing of fabric-reinforced composite materials
[AD-A216764] N90-18513
DAYTON UNIV., OH.
Study of bird ingestions into small inlet area, aircraft turbine engines (May 1987 to April 1988)
[DOT/FAA/CT-89/17] N90-18375
DEFENCE RESEARCH ESTABLISHMENT, OTTAWA (ONTARIO).
An error sensitivity model for Doppler positioning using transit satellites
[AD-A216724] N90-18381
Space-based radar simulation laboratory
[AD-A216722] N90-18618
Rate compatible punctured codes, their use in military satellite communication systems
[AD-A216723] N90-18619
DEFENCE TECHNOLOGY ENTERPRISES LTD., MILTON KEYNES (ENGLAND).
DTE and space technology transfer N90-19071
Methodology panel N90-19076
DEFENSE TECHNICAL INFORMATION CENTER, ALEXANDRIA, VA.
Particle simulations in magnetospheric plasmas
[AD-A216256] N90-18831
DELAWARE UNIV., NEWARK.
Chemical vapor deposition and photochemical vapor deposition of amorphous silicon photovoltaic devices
[DE89-009510] N90-18803
DEPARTMENT OF DEFENSE, WASHINGTON, DC.
DoD manual for standard data elements
[AD-A216441] N90-19066
DEUTSCHE FORSCHUNGSANSTALT FUER LUFT- UND RAUMFAHRT, BRUNSWICK (GERMANY, F.R.).
Development and test of power amplifiers for the driving of low-voltage piezo-actuators in multistable interferometers
[DLR-MITT-89-19] N90-18662
DEUTSCHE FORSCHUNGSANSTALT FUER LUFT- UND RAUMFAHRT, COLOGNE (GERMANY, F.R.).
Space orientation and orbital technology
[ISBN-3-89100-015-4] N90-18437
Long term planning for space flight activities within the DFVLR
[DFVLR-IB-303-88/2] N90-18438
Activities report in DLR research field communication engineering and reconnaissance
[ISSN-0173-0118] N90-18781
Activities report in German aerospace
[ISSN-0070-3966] N90-19189
DEUTSCHE FORSCHUNGSANSTALT FUER LUFT- UND RAUMFAHRT, GOETTINGEN (GERMANY, F.R.).
Half model tests on an ONERA calibration model in the transonic wind tunnel Goettingen, Federal Republic of Germany
[DLR-MITT-89-20] N90-18370
DEUTSCHE FORSCHUNGSANSTALT FUER LUFT- UND RAUMFAHRT, OBERPFAFFENHOFEN (GERMANY, F.R.).
The signals of an ice warning device in dependence on total water content and normalized icing degree
[DLR-FB-89-52] N90-18377
On the range resolution of point targets with FMCW radar systems
[DLR-FB-89-47] N90-18629
Doppler spectra from incoherent backscatter: Principles and examples for application for POLDIRAD
[DLR-FB-89-48] N90-18630
DEUTSCHE FORSCHUNGSANSTALT FUER LUFT- UND RAUMFAHRT, STUTTGART (GERMANY, F.R.).
On the dynamics of the combustion process of hydrogen-air and hydrogen-methane-air mixtures
[DLR-FB-89-39] N90-18548
DHV RAADGEVEND INGENIEURSBUREAU B.V., AMERSFOORT (NETHERLANDS).
Improvement of classification results from satellite imagery to update and differentiate land use classes on topographic maps
[BCRS-89-17] N90-18786
Remote sensing and run-off modelling in the Lake Victoria Basin, Kenya
[BCRS-89-19] N90-18788
DORNIER SYSTEM G.M.B.H., FRIEDRICHSHAFEN (GERMANY, F.R.).
Problems on transfer of space technology to non-space areas and solutions: Legal aspects N90-19077
Internal technology transfer N90-19080
DRAKE UNIV., DES MOINES, IA.
Numerical Green's functions in optical potential calculations for positron scattering from argon and neon N90-18971
DUKE UNIV., DURHAM, NC.
Parallel algorithms derivation
[AD-A216452] N90-18894

E

EAST ANGLIA UNIV., NORWICH (ENGLAND).
Angular correlation studies in noble gases N90-18972
ECOLE NORMALE SUPERIEURE, PARIS (FRANCE).
Concepts and experiments on space-time chaos
[ETN-90-96255] N90-18883
Analogies between cometary, interplanetary, and interstellar matter N90-19087
An almost total disjunction between emission and absorption dust features: What does it tell us? N90-19106
An implication of the IR identification of PAHs: The heating of the diffuse IS gas N90-19113
ECOLE POLYTECHNIQUE FEDERALE DE LAUSANNE (SWITZERLAND).
Aerodynamic superposition principle in vibrating turbine cascades N90-18410
Time-dependent measurements on vibrating annular turbine cascades under various steady state conditions N90-18424
Interlaminar fracture testing of carbon fibre/PEEK composites validity and applications N90-18497
EDGERTON, GERMESHAUSEN AND GRIER, INC., IDAHO FALLS, ID.
Dryout stability and inception at low flowrates
[DE90-006955] N90-18892
EDINBURGH UNIV. (SCOTLAND).
Fluorescent molecular hydrogen emission from star-forming galaxies N90-19155
H53-alpha emission from M82 N90-19156
EG AND G MOUND APPLIED TECHNOLOGIES, MIAMISBURG, OH.
Design and operation of an inert gas facility for thermoelectric generator storage
[DE90-007146] N90-19008
Safety analysis for the Galileo light-weight radioisotope heater unit
[DE90-007147] N90-19009
Thermal vacuum life test facility for radioisotope thermoelectric generators
[DE90-007148] N90-19010
Technology update-89
[DE90-005813] N90-19178
ENERGY CONCEPTS CO., ANNAPOLIS, MD.
Intermittent Solar Ammonia Absorption Cycle (ISAAC) refrigeration for lesser developed countries
[DE90-006700] N90-18610
ENVIRONMENTAL PROTECTION AGENCY, LAS VEGAS, NV.
Application of high performance liquid chromatography/mass spectrometry to environmental analysis
[PB90-116963] N90-18814
ENVIRONMENTAL RESEARCH INST. OF MICHIGAN, ANN ARBOR.
Synthetic aperture radar imagery of airports and surrounding areas: Archived SAR data
[NASA-CR-4275] N90-18371
Synthetic aperture radar imagery of airports and surrounding areas: Philadelphia Airport
[NASA-CR-4280] N90-18372
ERLANGEN-NUREMBERG UNIV. (GERMANY, F.R.).
Inelastic collisions of positrons with one-valence-electron targets N90-18963
ERNO RAUMFAHRTTECHNIK G.M.B.H. BREMEN (GERMANY, F.R.).
Refurbishment and modification of the Metric Camera (RMK) for reflight on EOM-1 Spacelab mission
[ETN-90-96284] N90-18710
EUROPEAN OFFICE OF AEROSPACE RESEARCH AND DEVELOPMENT, FPO NEW YORK, NY.
Third European Conference on Composite Materials
[EOARD-LR-89-050] N90-18494
EUROPEAN SOUTHERN OBSERVATORY, GARCHING (GERMANY, F.R.).
Molecular hydrogen in the HII region G333.6-0.2 N90-19121
Near infrared spectroscopy of active galaxies N90-19143
A search for the CO feature in active galactic nuclei N90-19151
Infrared (FeII), H and H2 lines in galaxy nuclei N90-19153
EUROPEAN SPACE AGENCY, PARIS (FRANCE).
The DFVLR 3-m x 3-m low speed wind tunnel (NWG) in Goettingen
[ESA-TT-1156] N90-18436
Navigation experiment NAVEX data storage and processing
[ESA-TT-1175] N90-18445
Navigation experiment NAVEX: The self-test delay times in the D1 Spacelab mission
[ESA-TT-1176] N90-18446

Packet telemetry standard
[ESA-PSS-04-106-ISSUE-1] N90-18447
Spacecraft thermal control design data, volume 1
[ESA-PSS-03-108-ISSUE-1-VOL-1] N90-18455
Spacecraft thermal control design data, volume 2
[ESA-PSS-03-108-ISSUE-1-VOL-2] N90-18456
Spacecraft thermal control design data, volume 3
[ESA-PSS-03-108-ISSUE-1-VOL-3] N90-18457
Spacecraft thermal control design data, volume 4
[ESA-PSS-03-108-ISSUE-1-VOL-4] N90-18458
Damage in a perforated graphite-epoxy composite plate under monotonic and cyclic biaxial loading
[ESA-TT-1117] N90-18521
Theoretical investigation of the stabilization of a diffusion flame above a recirculation region
[ESA-TT-1149] N90-18543
Significance of oxide skins on powder for the quality of PM Al materials
[ESA-TT-1178] N90-18560
Materials and structures for 2000 and beyond: An attempted forecast by the Materials and Structures Department of the DLR
[ESA-TT-1154] N90-18609
Multitarget tracking by single sensor: Analysis of the main approaches developed in this area
[ESA-TT-1171] N90-18833
Study on the thermodynamical and mechanical conditions for the generation of high operating pressures with liquefied gases for low and very low flow rates
[ESA-TT-1148] N90-18696
Contribution to the study of three-dimensional separation in turbulent incompressible flow
[ESA-TT-1169] N90-18697
Synchronization of the ground station atomic clocks using three weighted transportable cesium time standards in the Navex navigation experiment
[ESA-TT-1153] N90-18711
Knowledge-based fault detection and analysis for robots: First results for the ROTEX robots
[ESA-TT-1150] N90-18742
ERS-1 European remote sensing satellite: A new tool for global environmental monitoring in the 1990's
[ESA-BR-36] N90-18782
Airborne measurements of the electric field and the charge precipitation particles in convective clouds: Lower positive charge centres
[ESA-TT-1157] N90-18836
Doppler lidar working group report
[ESA-SP-1112] N90-18848
Deterministic differential game solution: The approximate strategy method
[ESA-TT-1158] N90-18956
Promotion of European Space Technology Transfer
[ESA-SP-1122] N90-19068
ESA project to promote and assist technology transfer by industry N90-19069
Infrared Spectroscopy in Astronomy
[ESA-SP-290] N90-19084

EUROPEAN SPACE AGENCY. EUROPEAN SPACE RESEARCH AND TECHNOLOGY CENTER, ESTEC, NOORDWIJK (NETHERLANDS).
Spacecraft thermal control design data, volume 1
[ESA-PSS-03-108-ISSUE-1-VOL-1] N90-18455
Spacecraft thermal control design data, volume 2
[ESA-PSS-03-108-ISSUE-1-VOL-2] N90-18456
Spacecraft thermal control design data, volume 3
[ESA-PSS-03-108-ISSUE-1-VOL-3] N90-18457
Spacecraft thermal control design data, volume 4
[ESA-PSS-03-108-ISSUE-1-VOL-4] N90-18458
Composites design handbook for space structure applications
[ESA-PSS-03-1101-ISSUE-1-REV-1] N90-18459
System safety requirements for ESA space systems and associated equipment
[ESA-PSS-01-40-ISSUE-2] N90-18460
The determination of offgassing products from materials and assembled articles to be used in a manned space vehicle crew compartment
[ESA-PSS-01-729-ISSUE-1] N90-18461
Configuration management and control for ESA space systems
[ESA-PSS-01-11-ISSUE-1] N90-19061
Component selection, procurement and control for ESA space systems
[ESA-PSS-01-60-ISSUE-2] N90-19062
The unidentified IR bands in laboratory, in interstellar medium, and in comets N90-19089
The Infrared Space Observatory N90-19163

F

FEDERAL AVIATION ADMINISTRATION, ATLANTIC CITY, NJ.
Dallas/Fort Worth simulation. Volume 2: Appendixes D, E, and F
[AD-A216613] N90-18380

FEDERAL AVIATION ADMINISTRATION, WASHINGTON, DC.
National airspace system plan: Facilities, equipment, associated development and other capital needs
[AD-A215682] N90-18373
The effects of wearing passenger protective breathing equipment on evacuation times through type 3 and type 4 emergency aircraft exits in clear air and smoke. Phase 1: Evacuations in clear air. Phase 2: Evacuations in smoke
[AD-A216798] N90-18374

FLORIDA AGRICULTURAL AND MECHANICAL UNIV., TALLAHASSEE.
New parameter-free polarization potentials in low-energy positron collisions N90-18968

FLOW RESEARCH, INC., KENT, WA.
Numerical simulations of coherent structures in a jet flame with a noncircular cross section
[AD-A216710] N90-18535

FRAUNHOFER-INST. FUER CHEMISCHE TECHNOLOGIE, BERGHAUSEN (GERMANY, F.R.).
Investigation of the phase stabilizing effect of 4 percent potassium fluoride on ammonium nitrate
[AD-A215313] N90-18599

G

GEORGE WASHINGTON UNIV., WASHINGTON, DC.
Spectroscopic evidence for carbon-carbon bonding in carbide layers on metals
[AD-A216726] N90-18512
Lower limits on the absolute dissociative electron attachment cross section from O2 condensed on rare-gas films
[AD-A216727] N90-18536
Extracting chemical information form Auger line shapes
[AD-A216729] N90-18537
Understanding electronegative effects in core-level electron spectroscopies; application to the high temperature superconductors
[AD-A216728] N90-19037
Absolute cross-sections for dissociative electron attachment in O2 condensed on Kr films
[AD-A216730] N90-19038

GEORGIA INST. OF TECH., ATLANTA.
Combustion instability in solid propellant rockets
[AD-A216740] N90-18492

GOVERNMENT ENGINEERING COLL., AURANGABAD (INDIA).
Elastic scattering of e- and e+ from Rb and Cd N90-18960

GTE SYLVANIA, INC., TOWANDA, PA.
Low cost filter development and control of permeability in high temperature, high pressure ceramic filter elements
[DE90-000403] N90-18676

GURUDAS COLL., CALCUTTA (INDIA).
Positronium formation in Se state in e+-Li scattering N90-18967

H

HARVARD-SMITHSONIAN CENTER FOR ASTROPHYSICS, CAMBRIDGE, MA.
The infrared spectral signature of star formation N90-19114
Infrared line emission from high-velocity outflows in star-forming regions N90-19116

HARVARD UNIV., CAMBRIDGE, MA.
The effects of luminance boundaries on color perception
[AD-A216741] N90-18860

HAWAII NATURAL ENERGY INST., HONOLULU.
Hawaii integrated biofuels research program, phase 1
[DE90-006685] N90-18811

HAWAII UNIV., HONOLULU.
Mapping and spectroscopy of the 3.3 microns feature in Orion N90-19112
Stellar kinematics in the galactic centre N90-19141

HEAT PUMP TECHNOLOGY CENTER OF JAPAN, TOKYO.
Investigation report of the investigation commission for interchange of heat pump technology in Europe
[DE89-782293] N90-18666
Stirling engine technologies in Japan
[DE89-782296] N90-18795

HOUSTON UNIV., TX.
A human factors experimental comparison of two database query languages N90-19064

I

IDAHO NATIONAL ENGINEERING LAB., IDAHO FALLS.
Helium permeability through austenitic stainless steel
[DE90-007048] N90-18562
A battery data base for electric vehicle applications
[DE90-007065] N90-18655

IDAHO UNIV., MOSCOW.
The formation and use of knowledge structures in problem solving domains
[AD-A216512] N90-18936

ILLINOIS UNIV., CHAMPAIGN.
Appropriateness measurement for computerized adaptive tests
[AD-A216121] N90-18870

ILLINOIS UNIV., CHICAGO.
Cedar project: Original goals and progress to date
[DE90-006761] N90-18880
Optimum selection procedures in multi-stage screening, reliability, and time
[AD-A216811] N90-18942

ILLINOIS UNIV., URBANA.
Reconfigurable antennas, monolithic microwave integrated circuits with feeding networks for microstrip antennas
[AD-A216916] N90-18622
Systematicity as a selection constraint in analogical mapping
[AD-A216029] N90-18869
Waveform methods for ordinary differential equations
[DE90-006593] N90-18943

IMPERIAL COLL. OF SCIENCE AND TECHNOLOGY, LONDON (ENGLAND).
Infrared spectroscopy of supernova 1987A N90-19124
Carbon monoxide in supernova 1987A N90-19135
Near-infrared spectroscopy of starburst and interacting galaxies N90-19144
The strengths of the 2.3 micron CO band in luminous interacting and merging galaxies N90-19148
Isophot-S, a low resolution 2.5 to 12 microns spectrometer for ISO N90-19167

INDAL TECHNOLOGIES, INC., MISSISSAUGA (ONTARIO).
Vertical axis wind turbine turbulent response model. Part 2: Response of Sandia National laboratories' 34-meter VAWT with aeroelastic effects
[DE90-005721] N90-18804

INDIAN ASSOCIATION FOR THE CULTIVATION OF SCIENCE, CALCUTTA.
Theoretical survey on positronium formation and ionisation in positron atom scattering N90-18965

INSTITUT D'ASTROPHYSIQUE, PARIS (FRANCE).
The environment of young stellar objects studied by high-resolution infrared spectroscopy N90-19120

INSTITUT DE MECANIQUE DES FLUIDES DE MARSEILLE (FRANCE).
Experimental investigations of the unsteady boundary layer on an oscillating flat plate. Optimization and validation of a code, for calculating the potential flow/boundary layer coupling of a flat plate and of an oscillating profile
[ETN-90-96254] N90-18682
Numerical investigations of heat transfer and flow rates in rotating cavities. Simulation of the movement generated by wall temperature gradients, by source-sink mass flows or by the differential rotation of the walls, under the influence or coriolis and centrifugal forces
[ETN-90-96253] N90-18695

INSTITUT FRANCO-ALLEMAND DE RECHERCHES, SAINT-LOUIS (FRANCE).
Prediction of rotor blade-vortex interaction noise from 2-D aerodynamic calculations and measurements
[ISL-CO-243/88] N90-18385
Supersonic wind tunnel investigation of a tubular projectile
[ISL-CO-306/89] N90-18386
Study of the blade/vortice interaction on a one-blade rotor during forward flight (incompressible, non viscous fluid)
[ISL-R-115/88] N90-18391
Possible piloting techniques at hypersonic speeds
[ISL-CO-216/88] N90-18392
Experimental and theoretical research on the injection of ignition gases into a bed of inert powder
[ISL-CO-251/88] N90-18547
Analysis of propulsive powder combustion products and their corrosive effects
[ISL-CO-248/88] N90-18605

Study of the dynamical behavior of copper in a shock wave
[ISL-R-123/88] N90-18679
Measurement of gas intensity at high dynamic pressures
[ISL-CO-204/89] N90-18680
Direct simulation Monte Carlo of shock reflexion on a wedge with boundary layer
[ISL-CO-245/88] N90-18681
Measurement of gas leaks between a projectile and the walls of a tube in a ballistic compressor
[ISL-CO-250/88] N90-18694
Development and polarization of ferroelectric polymer gauges, for dynamical acceleration experiments, as those in ballistics shocks
[ISL-R-119/88] N90-18703
Problems of the micro-holographic image analysis
[ISL-CO-201/89] N90-18704
Piezoelectric polymer PVDF shock gauge: State of the research art
[ISL-CO-207/89] N90-18705
Velocity measurement using interferometry
[ISL-CO-221/88] N90-18709
Cineholography: A relation between the coherence length of the laser and the object velocity
[ISL-CO-234/88] N90-18724
Effects produced by pulsed CO2 lasers
[ISL-R-112/88] N90-18731
Research on sliding spark preionization in a TEA CO2 laser
[ISL-R-113/88] N90-18732
Study of discharge mechanisms and the stability of transverse electric discharges in the gas mixtures
[ISL-R-114/88] N90-18733

INSTITUTE FOR COMPUTER APPLICATIONS IN SCIENCE AND ENGINEERING, HAMPTON, VA.
The inviscid stability of supersonic flow past a sharp cone
[NASA-CR-181996] N90-18363

INSTITUTE FOR DEFENSE ANALYSES, ALEXANDRIA, VA.
The Executive Workshop on Cost/Performance Measurement. Volume 1: Executive summary
[AD-A216745] N90-18898

INSTITUTE FOR TELECOMMUNICATION SCIENCES, BOULDER, CO.
Millimeter-wave propagation in the mesosphere
[PB90-119868] N90-18612

INSTITUTE OF ENERGY ECONOMICS OF JAPAN.
Analysis of competition among the kinds of energy at the era of complexed energy: General review
[DE89-910215] N90-18793
Analysis of inter-energy competition in the age of complex energies
[DE89-910216] N90-18794

INSTITUTE OF GAS TECHNOLOGY, CHICAGO, IL.
Solid-state proton conductors
[DE90-007595] N90-18812

INSTITUTO DE PESQUISAS ESPACIAIS, SAO JOSE DOS CAMPOS (BRAZIL).
Data collection and location platforms experimental network: Description of an orbit routine
[INPE-4798-NTE/287] N90-18439
Orbit determination of artificial Earth satellites through estmation techniques combined with state smoothing techniques
[INPE-4959-TDL/388] N90-18440
Evaluation of influences of errors involved in orbit propagation of artificial satellites
[INPE-4962-TDL/391] N90-18441
Autonomous orbit determination using GPS
[INPE-4815-TDL/361] N90-18442
Analytical formulation for the interaction problem of dynamic reentry, and effects due to flexibility and vibration in an aerospace vehicle
[INPE-4963-TDL/392] N90-18448
Attitude estimation procedure for spin stabilized satellites
[INPE-4866-TDL/377] N90-18449
Optimization of sensors and actuators positioning aimed at obtaining reduced models for the synthesis of optimal control regulators of flexible structures
[INPE-4760-TDL/348] N90-18450
Viability study of ionic microthruster tests on MECB satellite
[INPE-4973-RPE/605] N90-18490
Beam collector and output window for a 35 GHz 100 kW gyrotron
[INPE-4958-RPE/603] N90-18699
Construction and calibration of a gas pressure meter with high temporal resolution
[INPE-4953-RPE/602] N90-18700
Multiparameter scatterometer for remote sensing (RADSER). Project Scatter: State-of-the-art and future applications
[INPE-4871-PRE/1482] N90-18701
Preliminary design of a pointer for movement of a solar simulator
[INPE-4864-TDL/375] N90-18736
An approach centered in production rules for a partition of environment and planning in a visual navigation system (SNV)
[INPE-4813-TDL/360] N90-18737
Fracture analysis through photographic imagery of low spatial resolution: A contribution to the study of tectonic evoluation of the Araripe Plateau region
[INPE-4876-PRE/1487] N90-18756
Geometric correction models for HRV-SPOT images
[INPE-5001-TDL/395] N90-18757
Orbital remote sensing in the decade of the nineties: New approaches and challenges in geology
[INPE-4838-PRE/1467] N90-18758
TVI: A mathematical model for global estimation of Brazilian cerrado phytomass
[INPE-4836-PRE/1465] N90-18759
Relationships between the aerial biomass from ground layers of cerrado and its spectral reflectance
[INPE-4848-PRE/1477] N90-18760
Land suitability maps and appropriate land use: An approach using SGI and satellite imagery
[INPE-4827-PRE/1458] N90-18761
Thermal remote sensing in the differentiation of soybean crops (glycine max (L.) merrill) submitted to water deficit
[INPE-4900-PRE/1501] N90-18762
Evaluation of two methods for acquisition of training statistics for digital analysis of areas prepared for plowing
[INPE-4901-PRE/1502] N90-18763
Monitoring of reforested areas through digital analysis of TM data
[INPE-4930-PRE/1420] N90-18764
Evaluation of selection techniques for multispectral bands employed in the discrimination of carbonatic rocks
[INPE-4850-TDL/385] N90-18765
Remote sensing applied to the monitoring of mineral extraction in the proximity of urban areas: Pros and cons
[INPE-4867-PRE/1478] N90-18766
Radiometric study of wheat and bean crops in three types of latossolo
[INPE-4843-PRE/1472] N90-18767
Relationships between spectral parameters and agronomics of wheat and beam crops
[INPE-4791-RPE/584] N90-18768
Multistage forest volume estimation using a sampling system with probability variables
[INPE-4897-PRE/1498] N90-18769
Remote sensing applied to vegetation as subsidized in municipal planning
[INPE-4908-PRE/1509] N90-18770
Interrelationship of spatial and radiometric resolution in the thermal infrared band
[INPE-4860-TDL/371] N90-18771
Evaluation of TM/LANDSAT and HRV/SPOT data in reforested areas
[INPE-4575-RPE/567] N90-18772
Development of the agricultural information system. Characteristics and results of the Distrito Federal model
[INPE-4940-PRE/1430] N90-18773
Spectral response of wheat and its relationship with agronomical prameters
[INPE-4950-RPE/599] N90-18774
Perspective revision of systematic mapping through orbital imagery
[INPE-4817-PRE/1453] N90-18775
Physiognomy of vegetation cover in the PNPM identified through the TM/LANDSAT sensor: A multitemporal analysis
[INPE-4834-PRE/1464] N90-18776
Project Floval: Correction of relief effects in eucalyptus reforestration
[INPE-4814-RPE/590] N90-18777
Classification of high resolution imagery using texture attributes
[INPE-4888-TDL/379] N90-18778
Optimization of the reference parameters in the accompanying solar panel dynamics
[INPE-4795-PRE/1449] N90-18798
Remote sensing of interior water: Perspectives
[INPE-4875-PRE/1486] N90-18815
Paper on geography in environmental management: Research and new techniques
[INPE-4840-PRE/1469] N90-18816
Photointerpretation with instruments for evaluation of environmental impact: Mata Atlantica in Cubata
[INPE-4910-PRE/1511] N90-18817
Some aspects of atmospheric turbulence in forests
[INPE-4951-RPE/600] N90-18818
Geological structure of the State of Rio de Janeiro viewed through MSS LANDSAT imagery
[INPE-4826-PRE/1457] N90-18825
Quantification of structural field data in the Rio Grande do Norte basin and neighborhood
[INPE-4821-RPE/591] N90-18826
Study of the atmospheric emissions of OI wavelength 557.7 nm and O2 (0,0) wavelength 761.9 nm in the equatorial region utilizing measurement of photometer on-board a rocket
[INPE-4811-TDL/358] N90-18827
Connections between the circulation in altitude and convection over South America
[INPE-4923-TDL/383] N90-18828
The patterns of fracture and the conditioning tectonics in the region of the Quadrilatero Ferrifero and part of the Migmatitic-Gnanulitic Complex in Minas Gerais (Brazil)
[INPE-4895-PRE/1496] N90-18829
Intertropical Convergence Zone (ITCZ) and its relationship with the precipitation of the north-northeast Brazilian region
[INPE-4887-TDL/378] N90-18839
Comparison of circulation obtained through the trajectory of a drifting buoy tracked by satellite and hydrographic data in the Bransfield Strait
[INPE-4946-TDL/387] N90-18850
Vertical migration in operational system nucleus
[INPE-4879-RPE/593] N90-18883
L: A language for solution of incremental systems in a parallel processing environment
[INPE-4816-TDL/362] N90-18884
An exact algorithm for the problem of p-medians
[INPE-4924-TDL/384] N90-18885
An integrated vision on methodologies and environments for modeling and simulation assisted by computer
[INPE-4861-TDL/372] N90-18886
An interactive system applied to the linear quadratic problem
[INPE-4945-TDL/386] N90-18913
Mathematical methods of Physics 6: Integral transformation
[INPE-4807-MD/40] N90-18926
Contribution to the study of stability robustness of nonlinear multivariable regulators
[INPE-4801-TDL/356] N90-18950
Adaptive state estimation and sampling rate analysis for invariant linear dynamic systems in time
[INPE-4960-TDL/389] N90-18951
Vector fields, linear spaces and tensors in physics. Part 3: Tensor analysis and its applications
[INPE-5000-MD/41] N90-18997
Hamiltonian analysis and simulation of free electron lasers
[INPE-4785-TDL/351] N90-19018
Study of peculiar galaxies in the Southern Hemisphere
[INPE-4810-TDL/357] N90-19184

INTERNATIONAL BUSINESS MACHINES CORP., SAN JOSE, CA.
Temperature dependence of photon-gated persistent spectral hole-burning for the meso-tetra-p-tolyl Zn-tetrabenzoporphyrin/chloroform system in poly(methylmethacrylate)
[AD-A216086] N90-18531
Persistant spectral hole-burning: Photon-gating and fundamental statistical limits
[AD-A216084] N90-18640
Ultrasensitive laser spectroscopy in solids: Single-molecule detection
[AD-A216085] N90-18716

INTERNATIONAL CENTRE FOR THEORETICAL PHYSICS, TRIESTE (ITALY).
Streaming gravity mode instability
[DE90-610619] N90-18835
What influences order parameters across the superconducting phase boundary
[DE90-610663] N90-19047
Pressure induced superconductivity in elemental solids
[DE90-610664] N90-19048
A comparison of void distributions in Abell cluster catalogue with numerical simulations
[DE90-610640] N90-19173
A new interpretation of the feature of SiO maser spectra associated with M-type star
[DE90-610641] N90-19174
On the mass to light ratios of dwarf spheroidal galaxies
[DE90-610645] N90-19175
Quantum cosmological origin of large scale structures of the universe
[DE90-610647] N90-19176

INTERNATIONAL FUEL CELLS CORP., SOUTH WINDSOR, CT.
Integrated regenerative fuel cell experimental evaluation
[NASA-CR-185183] N90-18808

IOWA UNIV., IOWA CITY.
Wick-type liquid-metal combustion
[AD-A216019] N90-18530

Particle simulations in magnetospheric plasmas
[AD-A216256] N90-18831

ISTITUTO NAZIONALE DI FISICA NUCLEARE, FRASCATI (ITALY).
The track-etch detector for the MACRO experiment at the Gran Sasso Laboratory
[DE90-003235] N90-19182

J

JAYCOR, TORRANCE, CA.
Development of an rf-driven plasma neutralizer for negative ions
[DE90-007298] N90-19027

JET PROPULSION LAB., CALIFORNIA INST. OF TECH., PASADENA.
Simulation of the dynamic environment for missile component testing: Demonstration
[AD-A216979] N90-18443
SHARP: A multi-mission artificial intelligence system for spacecraft telemetry monitoring and diagnosis
[NASA-CR-186285] N90-18444
Technique for evaluating the erosive properties of ablative internal insulation materials N90-18466
Mission options for an electric propulsion demonstration flight test N90-18479
Electric propulsion for manned Mars exploration N90-18480
Feasibility demonstration of a 445N high-performance rocket engine N90-18481
Radio interference in the near-earth environment
[NASA-CR-180479] N90-18623

JOHNS HOPKINS UNIV., BALTIMORE, MD.
A fundamental understanding of the effect of alloying elements on the corrosion resistance of rapidly solidified Mg alloys
[AD-A216767] N90-18553
Research in theoretical physics
[DE90-005558] N90-19001

JOHNS HOPKINS UNIV., LAUREL, MD.
The 1989 JANNAF Propulsion Meeting, volume 1
[CPIA-PUBL-515-VOL-1] N90-18462

JOINT ASTRONOMY CENTRE, HILO, HI.
IRCAM observations of the Reipurth 50 IR source N90-19119
An infrared imaging Fabry-Perot study of the galactic centre N90-19142
Near infrared spectroscopy and spectroscopic imaging of NGC253 N90-19159

JOINT INST. FOR NUCLEAR RESEARCH, DUBNA (USSR).
Microwave radiation absorption by Ho(Y)-Ba-Cu-O superconducting ceramics
[DE90-610665] N90-18588
Elementary particles and cosmology
[DE90-610648] N90-19177

K

KANSAS STATE UNIV., MANHATTAN.
The role of blood volume in determining the cardiovascular adjustments to exercise N90-18654

KENRICH PETROCHEMICALS, INC., BAYONNE, NJ.
Enhanced bonding of fiber reinforcements to thermoset resins N90-18496

KEURING VAN ELECTROTECHNISCHE MATERIALEN N.V., ARNHEM (NETHERLANDS).
Investigation of multiple scattering in aqueous suspensions of non-absorbing polystrene microspheres using spectrophotometry
[BCRS-89-09] N90-18549

L

LA SAPIENZA UNIV., ROME (ITALY).
Crack propagation from artificial defects in typical engine disk materials; interpretation of experimental results by means of 3D J integral N90-18401

LABORATORIO DE COMPUTACAO CIENTIFICA, RIO DE JANEIRO (BRAZIL).
Strong source heat transfer simulations based on a GalerKin/gradient least squares method
[DE90-608613] N90-18678

LABORATORIUM VOOR RUIMTEONDERZOEK, UTRECHT (NETHERLANDS).
The ISO short wavelength spectrometer N90-19182

LANCHESTER POLYTECHNIC, COVENTRY (ENGLAND).
Infrared spectroscopy of novae and related objects N90-19123

LAWRENCE LIVERMORE NATIONAL LAB., CA.
Compressive strength of carbon/epoxy laminated under multiaxial stress
[DE90-005552] N90-18505
Threaded joint design for composites
[DE90-005553] N90-18506
Preliminary evaluation of the strength of pin-joints in laminated composite materials
[DE90-006353] N90-18524
Evaluating a glass surface produced by ductile grinding
[DE90-006782] N90-18608
The extended equivalent source technique with underdetermined sources
[DE90-006989] N90-18627
A new broadband pulsed high voltage monitor
[DE90-006264] N90-18651
Performance of a 500 watt Nd:GGG zigzag slab oscillator
[DE90-006263] N90-18657
Analytic solutions for the decay of turbulent swirling flow in a cylinder
[DE90-005744] N90-18677
Computational and visible light experiments for x ray laser holography
[DE90-006774] N90-18707
Theory for high gain, high power free electron lasers
[DE90-005546] N90-18714
Fast algorithms for calculating laser wavefront phase compensation given noisy measurements of phase gradient
[DE90-006357] N90-18727
Properties and performance of the LiCaAlF6:Cr(3+) laser material
[DE90-007242] N90-18728
The dynamics of electrons in very intense lasers
[DE90-007246] N90-18729
A simple model for amplified spontaneous emission in dyes
[DE90-007249] N90-18730
Variations in volatiles in magma bodies based on studies of melt inclusions
[DE90-006272] N90-18821
Effect of a random wind field on thermal blooming instabilities
[DE90-007241] N90-18823
Temporal response of atmospheric turbulence compensation
[DE90-006354] N90-18837
Optically excited states in positronium N90-18985
Stark and Zeeman effects on laser cooling of positronium N90-18986
Anitproton-matter interactions in antiproton applications N90-18989
A large area, low cost, gamma-ray, imaging spectrometer
[DE90-006993] N90-19017
Gamma ray astronomy and black hole astrophysics
[NASA-CR-186496] N90-19169
Hydrodynamical simulations of collisions between interstellar clouds
[DE90-006921] N90-19172
Imaging Germanium Telescope Array for Gamma-Rays (IGETAGRAY)
[DE90-006994] N90-19188

LEHIGH UNIV., BETHLEHEM, PA.
Corrosion fatigue of iron-chromium-nickel alloys: Fracture mechanics and chemistry
[DE90-006318] N90-18556
Perforated monolayers
[DE90-005469] N90-18566

LEIDEN UNIV. (NETHERLANDS).
Recurrence conditions for average and Blackwell optimality in denumerable state Markov decision chains
[TW-89-02] N90-18952
Infrared diagnostics for interstellar solid state chemistry N90-19103
Polycyclic aromatic hydrocarbons in the infrared spectra of IRAS sources N90-19105
CO infrared bands in atmospheres of long-period variables N90-19128
A survey of PAH emission in HII regions, planetary and proto-planetary nebulae N90-19129

LOCKHEED MISSILES AND SPACE CO., SUNNYVALE, CA.
Process development and fabrication of space station type aluminum-clad graphite epoxy struts
[NASA-CR-181873] N90-18454

LONDON UNIV. (ENGLAND).
JCMT observations of the circumstellar envelope IRC+10216 N90-19138

LOS ALAMOS NATIONAL LAB., NM.
Application of artificial intelligence control to the vapor-liquid-solid silicon carbide whisker process
[DE90-007835] N90-18519
A program of fundamental research on explosives at Los Alamos
[DE90-006509] N90-18602
Quick, reliable estimates of high-power microwave fluences: The SNEAKY-2 program
[DE90-006347] N90-18624
BEAR electrostatic analyzer: Flight results
[DE90-006511] N90-18625
INEX (Integrated Numerical Experiment) simulations of the Boeing FEL system
[DE90-004846] N90-18712
Solid-state fluorescence above 1000 C: Application to high-temperature laser thermography
[DE90-006422] N90-18721
Absorption experiments on electron-beam pumped rare gases
[DE90-006504] N90-18722
Cloud hole-boring with infrared lasers: Theory and experiment
[DE90-006519] N90-18723
Electron beam and high-speed optical diagnostics for the Los Alamos HIBAF (High Brightness Accelerator FEL) Facility
[DE90-007828] N90-18725
Development of KrF lasers for fusion
[DE90-007830] N90-18726
Performance characterization of the Convex C-240 computer system
[DE90-006425] N90-18879
Survivability and effectiveness of near-term strategic defense
[DE90-005805] N90-18955
Space nuclear safety program
[DE90-006436] N90-19007
The lower hybrid drift instability and the evolution of plasma gradients
[DE90-006521] N90-19021
Luminescence from defects and impurity centers in yttrium oxide
[DE90-004842] N90-19030
Toda lattice with transverse degree of freedom
[DE90-002414] N90-19049
Spectral functions from Quantum Monte Carlo
[DE90-004870] N90-19050
Soft x ray emission from classical novae in outburst
[DE90-006480] N90-19187

LOUISIANA STATE UNIV., BATON ROUGE.
Positronium ions and molecules N90-18990
Current and future uses of accelerators in particle astrophysics
[DE90-006657] N90-19186

LUZ INTERNATIONAL LTD., LOS ANGELES, CA.
Phase-Change Thermal Energy Storage
[DE89-009426] N90-18801

LYON-1 UNIV., VILLEURBANNE (FRANCE).
Continuous preparation of a thin refractory carbide deposit on the surface of carbon fibers: Characterization of the C/SiC fiber N90-18501

M

MACQUARIE UNIV., SYDNEY (AUSTRALIA).
Positron excitation of neon N90-18973

MANCHESTER UNIV. (ENGLAND).
Chemistry on interstellar grains and implications for infrared spectroscopy N90-19097

MARQUETTE UNIV., MILWAUKEE, WI.
Low-energy scattering of electrons and positrons in liquids N90-18981

MARTIN MARIETTA SPACE SYSTEMS, INC., DENVER, CO.
Orbital fluid resupply assessment N90-18487

MARYLAND UNIV., COLLEGE PARK.
Effects of pulsed and CW (Continuous Wave) 2450 MHz radiation on transformation and chromosomes of human lymphocytes in vitro
[AD-A216500] N90-18857
Efficient preconditioning for the p-version finite element method in two dimensions
[AD-A216210] N90-18928
Research equipment
[AD-A216515] N90-18937

MASSACHUSETTS INST. OF TECH., CAMBRIDGE.
Visual navigation: Constructing and utilizing simple maps of an indoor environment
[AD-A216761] N90-18382
Blade row interaction effects on compressor measurements N90-18419
Laboratory for the processing and evaluation of inorganic matrix composites
[AD-A216881] N90-18516
Active stabilization of aeromechanical systems
[AD-A216629] N90-18672
Kinetic relations and the propagation of phase boundaries in solids
[AD-A215881] N90-18747

The interpretation of crustal dynamics data in terms of plate interactions and active tectonics of the Anatolian plate and surrounding regions in the Middle East
[NASA-CR-186200] N90-18824
Recognizing three-dimensional objects without the use of models
[AD-A216766] N90-18862
A self-organizing multiple-view representation of three-dimensional objects
[AD-A216711] N90-18871
A scalable multiprocessor architecture using Cartesian network: Relative addressing
[AD-A216580] N90-18878
A theory of quantitative inference for artifact sets applied to a mechanical design compiler
[AD-A216535] N90-18896
Optimum and heuristic algorithms for finite state machine decomposition and partitioning
[AD-A216778] N90-18899
KAM: Automatic planning and interpretation of numerical experiments using geometrical methods
[AD-A216805] N90-18900
The computation of color
[AD-A216531] N90-18914
Grouping for recognition
[AD-A216716] N90-18915
Using special-purpose computing to examine chaotic behavior in nonlinear mappings
[AD-A216800] N90-18916
Derivation of an efficient rule system pattern matcher
[AD-A216801] N90-18917
A colony architecture for an artificial creature
[AD-A216802] N90-18918
Three-dimensional motion estimation using shading information in multiple frames
[AD-A216804] N90-18919
An objective time-integration procedure for isotropic rate-independent and rate-dependent elastic-plastic constitutive equations
[PB90-121245] N90-18925
Should a function continue
[AD-A216406] N90-18929
Boolean minimization and algebraic factorization procedures for fully testable sequential machines
[AD-A216779] N90-18940
Computational structure of GPSG (Generalized Phrase Structure Grammar) models: Revised generalized phrase structure grammar
[AD-A216803] N90-18941
Acoustic emission diagnostic techniques for high-field high current-density super inducting poles
[DE90-007400] N90-19000
Mechanical disturbances in high-performance superconducting dipoles
[DE90-006237] N90-19040
Speculative computation in multilisp
[AD-A216579] N90-19067

MASSACHUSETTS INST. OF TECH., LEXINGTON.
Output performance of idealized microwave power amplifiers
[AD-A216797] N90-18845
A case study of the 24 August 1986 FLOWS microburst
[AD-A216939] N90-18847

MASSACHUSETTS UNIV., AMHERST.
Metal coordination polymers as potential high-energy lithographic resists
[AD-A216668] N90-18574
The improved adhesion of organic polymers to silica and to aluminum metal with zirconium Schiff-base block copolymer coatings
[AD-A216669] N90-18575
On the kinematic behavior of robots while executing general robot level commands
[PB90-120965] N90-18735
RALPH: An automatic Robot Assembly Language Programmer: An overview
[PB90-120973] N90-18912

MAX-PLANCK-INST. FUER ASTRONOMIE, HEIDELBERG (GERMANY, F.R.).
Spectrophotometry of dust with Isophot N90-19164

MAX-PLANCK-INST. FUER KERNPHYSIK, HEIDELBERG (GERMANY, F.R.).
Detection of SN1986j in NGC891 at millimetre wavelengths N90-19137
The correlation between radio and far-infrared emission for disk galaxies N90-19158

MAX-PLANCK-INST. FUER PHYSIK UND ASTROPHYSIK, GARCHING (GERMANY, F.R.).
Photodissociation regions: Observations and theory N90-19098
The excitation of molecular hydrogen and its significance N90-19117

MCDONNELL AIRCRAFT CO., HOUSTON, TX.
Research on a two-dimensional inlet for a supersonic V/STOL propulsion system. Appendix A
[NASA-CR-174945] N90-18364

MEMORIAL UNIV. OF NEWFOUNDLAND, SAINT JOHNS.
Positron collisions with alkali-metal atoms N90-18962

MESSERSCHMITT-BOELKOW-BLOHM G.M.B.H., BREMEN (GERMANY, F.R.).
Refurbishment and modification of the Metric Camera (RMK) for reflight on EOM-1 Spacelab mission
[ETN-90-96284] N90-18710

MESSERSCHMITT-BOELKOW-BLOHM G.M.B.H., MUNICH (GERMANY, F.R.).
Magnetic suspension railway systems based on space technology N90-19081

MESSERSCHMITT-BOELKOW-BLOHM G.M.B.H., OTTOBRUNN (GERMANY, F.R.).
Telemetry and telecommand omnidirectional antenna in the short wave band
[ETN-90-96285] N90-18631

MICHIGAN STATE UNIV., EAST LANSING.
Softening mechanisms and microstructural instabilities during high temperature, low cycle fatigue of Ni, Ni3Al, and their metal matrix composites
[DE90-006487] N90-18557

MICRO ELECTRONICS A.S. SPACE, HORTEN (NORWAY).
Purchase of technology N90-19072

MIDWEST RESEARCH INST., GOLDEN, CO.
Aerodynamic testing of a rotating wind turbine blade
[DE90-000312] N90-18362
Hydrogenated amorphous silicon films prepared by glow discharge of disilane
[DE90-000309] N90-18581
Progress in thin film solar photovoltaic technologies
[DE89-009513] N90-18792
Phase-Change Thermal Energy Storage
[DE89-009426] N90-18801
Resource Assessment Project: User needs survey results
[DE89-009502] N90-18802
Chemical vapor deposition and photochemical vapor deposition of amorphous silicon photovoltaic devices
[DE89-009510] N90-18803
Programs in Renewable Energy
[DE89-009489] N90-18809
Solar buildings program summary. Volume 2: Research summaries
[DE89-009478] N90-18810
Hawaii integrated biofuels research program, phase 1
[DE90-006885] N90-18811

MINERALS MANAGEMENT SERVICE, HERNDON, VA.
Atlantic outer continental shelf: Description of the Mid-Atlantic environment
[PB90-100033] N90-18849

MINNESOTA UNIV., MINNEAPOLIS.
Cell performance of ultra-thin polymer cathode systems. Part 1: Anion intercalating polymer cathode
[AD-A216037] N90-18639
Theoretical and experimental high energy physics
[DE90-006168] N90-19006
Photometry of variable AFGL sources
[AD-A216938] N90-19185

MISSION RESEARCH CORP., SANTA BARBARA, CA.
ACIRF user's guide: Theory and examples
[AD-A216436] N90-18613

MISSOURI UNIV., ROLLA.
Reliability studies of ceramic capacitors
[AD-A216763] N90-18643

MOTOREN- UND TURBINEN-UNION MUENCHEN G.M.B.H. (GERMANY, F.R.).
A comparison of flutter calculations based on eigenvalue and energy method N90-18406
Unsteady blade loads due to wake influence N90-18413

MRC BEARINGS-SKF AEROSPACE, JAMESTOWN, NY.
The joint effect of surface microtopography and near-surface structure on microcontact conditions
[DE90-006494] N90-18591
Life of concentrated contacts in the mixed EHD and boundary film regimes
[AD-A216673] N90-18738

MSE, INC., BUTTE, MT.
Cohesive ceramic fabrication
[DE90-007333] N90-18597

N

NATIONAAL INST. VOOR KERNFYSICA EN HOGE ENERGIEFYSICA, AMSTERDAM (NETHERLANDS).
Instability investigation for storage mode. Microwave instability (single-bunch instability)
[NIKHEF-K/AMPS/89/05] N90-18628
Injection parameters and beam oscillations during extraction
[NIKHEF-K/AMPS/89-07] N90-18632
Linear Variable Differential Transformer (LVDT) with conditioner for the control of stepping motor drivers (part of the sliding-foil follower system of the Emin spectrometers)
[DIGEL-1989-9] N90-18660
Low weight variable GRV power supply as part of the injector electronics to be developed for the electron accelerator MEA
[DIGEL-1989-6] N90-18661
Toroid monitor
[DIGEL-1989-8] N90-18663

NATIONAL AERONAUTICS AND SPACE ADMINISTRATION. AMES RESEARCH CENTER, MOFFETT FIELD, CA.
IR line emission from dense photodissociation regions N90-19100
Airborne observations of the infrared emission bands N90-19101
Infrared diagnostics of interstellar shocks N90-19115
High-excitation lines of molecular hydrogen: A discriminant between shock models N90-19118

NATIONAL AERONAUTICS AND SPACE ADMINISTRATION. GODDARD SPACE FLIGHT CENTER, GREENBELT, MD.
Annihilation in Gases and Galaxies
[NASA-CP-3058] N90-18957
GRIS observations of the Galactic Center N90-18982
Positron annihilation in gamma-ray bursts N90-18983
Annihilation physics of exotic galactic dark matter particles N90-18984
Search for resonances in positron-atom systems N90-18991
Positronium formation in e+ plus H- collisions N90-18993
Observations of 40-70 micron bands of ice in IRAS 09371+1212 and other stars N90-19134

NATIONAL AERONAUTICS AND SPACE ADMINISTRATION. HUGH L. DRYDEN FLIGHT RESEARCH FACILITY, EDWARDS, CA.
Wind-tunnel investigation of a flush airdata system at Mach numbers from 0.7 to 1.4
[NASA-TM-101697] N90-18395

NATIONAL AERONAUTICS AND SPACE ADMINISTRATION. JOHN F. KENNEDY SPACE CENTER, COCOA BEACH, FL.
Continuous hydroponic wheat production using a recirculating system
[NASA-TM-102784] N90-18853

NATIONAL AERONAUTICS AND SPACE ADMINISTRATION. LYNDON B. JOHNSON SPACE CENTER, HOUSTON, TX.
A perspective on the use of storable propellants for future space vehicle propulsion N90-18473
Space station technology summary N90-18482
Electronically Variable Pressure Regulator (EVPR) N90-18484
Space shuttle RCS oxidizer leak repair for STS-26 N90-18485
Zero-gravity vortex vent and PVT gaging system N90-18486
Superfluid helium orbital resupply coupling N90-18488
Small displacement, long life on-orbit compressor design and fabrication N90-18489
Three-dimensional coculture process
[NASA-CASE-MSC-21560-1] N90-18852

NATIONAL AERONAUTICS AND SPACE ADMINISTRATION. LANGLEY RESEARCH CENTER, HAMPTON, VA.
Delivery performance of conventional aircraft by terminal-area, time-based air traffic control: A real-time simulation evaluation
[NASA-TP-2978] N90-18378
Fuselage design for a specified Mach-sliced area distribution
[NASA-TP-2975] N90-18385
A simulation evaluation of the engine monitoring and control system display
[NASA-TP-2960] N90-18393
Three input concepts for flight crew interaction with information presented on a large-screen electronic cockpit display
[NASA-TM-4173] N90-18394
Application of variable-gain output feedback for high-alpha control
[NASA-TM-102603] N90-18434
Support trusses for large precision segmented reflectors: Preliminary design and analysis
[NASA-TM-101560] N90-18453
Fatigue crack initiation and small crack growth in several airframe alloys
[NASA-TM-102598] N90-18746

Development of an experimental space station model for structural dynamics research
[NASA-TM-102601] N90-18751
Structures and materials technology for hypersonic aerospacecraft
[NASA-TM-102583] N90-18752
Low-energy gamma ray attenuation characteristics of aviation fuels
[NASA-TP-2974] N90-18882

NATIONAL AERONAUTICS AND SPACE ADMINISTRATION. LEWIS RESEARCH CENTER, CLEVELAND, OH.
Probability of failure and risk assessment of propulsion structural components N90-18470
The Pathfinder chemical transfer propulsion program N90-18471
Advanced APS impacts on vehicle payloads N90-18472
Electric propulsion options for 10 kW class earth-space missions N90-18474
Performance of large area xenon ion thrusters for orbit transfer missions N90-18475
Test facility and preliminary performance of a 100 kW class MPD thruster N90-18476
Arcjet cathode phenomena N90-18477
Arcjet nozzle design impacts N90-18478
Analysis of whisker-toughened ceramic components: A design engineer's viewpoint
[NASA-TM-102333] N90-18504
Performance and modeling of superconducting ring resonators at millimeter-wave frequencies
[NASA-TM-102526] N90-18634
Investigation of methods to produce a uniform cloud of fuel particles in a flame tube
[NASA-TM-102376] N90-18665
A simple algebraic grid adaptation scheme with applications to two- and three-dimensional flow problems
[NASA-TM-102446] N90-18667
Fastener design manual
[NASA-RP-1228] N90-18740
A global approach for the identification of structural connection properties
[NASA-TM-102502] N90-18745
Asymptotic boundary conditions for dissipative waves: General theory
[NASA-TM-102497] N90-18927

NATIONAL AERONAUTICS AND SPACE ADMINISTRATION. MARSHALL SPACE FLIGHT CENTER, HUNTSVILLE, AL.
Numerical prediction of axial turbine stage aerodynamics N90-18416
Transient pressure test article test program N90-18463
Test data of flow field of shuttle SRM nozzle joint with bond defects, using unheated air N90-18464
Cold flow determination of the internal flow environment around the submerged TVC nozzle for the space shuttle SRM N90-18465
Effect of propellant flowrate and purity on carbon deposition in LO2/methane gas generators N90-18468
Experimental flow models for SSME flowfield characterization N90-18469

NATIONAL AERONAUTICS AND SPACE ADMINISTRATION. PASADENA OFFICE, CA.
Efficient detection and signal parameter estimation with application to high dynamic GPS receiver
[NASA-CASE-NPO-17820-1-CU] N90-18379

NATIONAL AEROSPACE LAB., AMSTERDAM (NETHERLANDS).
User manual for NEXT 1.2: NLR engineering X-pert system toolkit
[NLR-TR-87178-U] N90-18905

NATIONAL AEROSPACE LAB., EMMELOORD (NETHERLANDS).
Improvement of classification results from satellite imagery to update and differentiate land use classes on topographic maps
[BCRS-89-17] N90-18786

NATIONAL INST. OF STANDARDS AND TECHNOLOGY, GAITHERSBURG, MD.
The mechanism, measurement, and influence of properties on the galling of metals
[DE90-006533] N90-18558
Robot crane technology program
[PB90-111667] N90-18734
Computer viruses and related threats: A management guide
[PB90-111683] N90-18881

NATIONAL OCEANIC AND ATMOSPHERIC ADMINISTRATION, BOULDER, CO.
Preliminary comparison of temperature soundings obtained from simultaneous radiometric, radio-acoustic, and rawinsonde measurements
[PB90-119835] N90-18838

NATIONAL PHYSICAL LAB., TEDDINGTON (ENGLAND).
Noise levels from a VSTOL aircraft measured at ground level and at 1.2 m above the ground
[NPL-RSA(EXT)-009] N90-18999

NAVAL ENVIRONMENTAL PREDICTION RESEARCH FACILITY, MONTEREY, CA.
Forecasters handbook for Central America and adjacent waters
[AD-A216752] N90-18845

NAVAL OCEAN SYSTEMS CENTER, SAN DIEGO, CA.
Development of a progressive failure model for strength of laminated composite structure
[AD-A216966] N90-18517
Trends in VLF/LF (Very Low Frequency/Low Frequency) modem performance testing
[AD-A216578] N90-18614
Effects of strong scattering on transionospheric propagation
[AD-A216708] N90-18617

NAVAL OCEANOGRAPHIC AND ATMOSPHERIC RESEARCH LAB., MONTEREY, CA.
Sounding and surface meteorological data from the Land/Sea Breeze Experiment (LASBEX)
[AD-A216269] N90-18842

NAVAL POSTGRADUATE SCHOOL, MONTEREY, CA.
Processing and elevated temperature ductility of aluminum alloy 7475
[AD-A216840] N90-18554
An adaptive ARQ (Automatic Repeat Request) strategy for packet switching data communication networks
[AD-A216597] N90-18615
Study of vortex arrays induced artificially and from centrifugal instabilities
[AD-A216499] N90-18669
Automation and extension of LDV (Laser-Doppler Velocimetry) measurements of off-design flow in a subsonic cascade wind tunnel
[AD-A216627] N90-18670
The propagation of time harmonic Rayleigh-Lamb waves in a bimaterial plate
[AD-A216834] N90-18749
Sounding and surface meteorological data from the Land/Sea Breeze Experiment (LASBEX)
[AD-A216269] N90-18842
Forecasters handbook for Central America and adjacent waters
[AD-A216752] N90-18845
Dynamics of an ERICA (Experiment on Rapidly Intensifying Cyclones over the Atlantic) cyclone
[AD-A216775] N90-18846
An application of ocean wave-current refraction to the gulf stream using SEASAT SAR data
[AD-A216769] N90-18851
DOA (Direction of Arrival) estimation by Eigendecomposition using single vector Lanczos' algorithm
[AD-A215802] N90-18887
Design, implementation and test of an RS-232 compatible bi-directional, full duplex, fiber-optic interface with provision for hardware handshaking on a minimum of fiber-optic lines
[AD-A216804] N90-19012
A simulation of optical propagation through atmospheric turbulence using two-dimensional Fourier transform techniques
[AD-A216776] N90-19013

NAVAL RESEARCH LAB., WASHINGTON, DC.
Angle estimation in the presence of mainbeam interference
[AD-A216832] N90-18621
A test method for measuring corona inception voltage for transducer autotransformers
[AD-A216818] N90-18646
Earth model selection for computer simulations
[AD-A216843] N90-18779
An evaluation of an airborne laser profiling system for high precision terrain mapping
[AD-A217025] N90-18780

NETHERLANDS ENERGY RESEARCH FOUNDATION, PETTEN.
Crystallographic and magnetic properties of (C6 D11 ND3)CuBr3 and (Zn(1-x)Mn(x))3As2: A neutron scattering study
[ECN-219] N90-19055

NEVADA UNIV., RENO.
Studies of cubic ice crystals
[AD-A216574] N90-18832

NEW ENERGY DEVELOPMENT ORGANIZATION, TOKYO (JAPAN).
Study on the measures to promote the use of photovoltaic power generating system overseas
[DE90-742056] N90-18807

NEW MEXICO UNIV., ALBUQUERQUE.
Magnetohydrodynamic modeling of plasma opening switches and gas puff plasmas
[DE90-005825] N90-19028

NIHON UNIV., TOKYO (JAPAN).
Composite for smoothing the surface of ceramic substrates
[DE90-004005] N90-18565

NORTH CAROLINA STATE UNIV., RALEIGH.
Fundamental aspects of erosion and impact damage
[DE90-006640] N90-18587
Development of a defect stream function, law of the wall/wake method for compressible turbulent boundary layers
[NASA-CR-4286] N90-18675

NOTRE DAME UNIV., IN.
Metallaboranes as precursors to metallic glasses
[AD-A216946] N90-18577

NOTTINGHAM UNIV. (ENGLAND).
The calculation of the contributions to low energy e+H2 scattering from sigma u+ and Pion u symmetries using the Kohn variational method N90-18969

O

OAK RIDGE GASEOUS DIFFUSION PLANT, TN.
Can the square law be validated
[DE90-007112] N90-18945

OAK RIDGE NATIONAL LAB., TN.
The mechanism, measurement, and influence of properties on the galling of metals
[DE90-006533] N90-18558
Deformation and fracture of ordered intermetallic compounds
[DE90-007422] N90-18563
Comparison of tension, compression, and flexure creep for alumina and silicon nitride ceramics
[DE90-006154] N90-18586
The design of advanced ceramic composites
[DE90-006613] N90-18592
Synthesis of high-purity sinterable silicon nitride powder
[DE90-007050] N90-18593
Heat capacities of solid polymers (The Advanced THermal Analysis System, ATHAS)
[DE90-007130] N90-18595
Alternative fuels R/D needs: Program directions
[DE90-007053] N90-18603
Modeling convective Marangoni flows with void movement in the presence of solid-liquid phase change
[DE90-006474] N90-18690
Transfer of heat pump technology
[DE90-007373] N90-18693
Solid-state fluorescence above 1000 C: Application to high-temperature laser thermography
[DE90-006422] N90-18721
Effects of oblique impact on hypervelocity shield performance
[DE90-006936] N90-18739
Federal methanol fleet update
[DE90-006851] N90-18741
Perspectives on aerosol deposition to natural surfaces
[DE90-003398] N90-18819
Risk analysis: Fundamental concepts, regulatory toxicology, and relative comparisons from radiation biology
[DE90-002466] N90-18856
Teleoperator servoloop tuning using an expert system
[DE90-005674] N90-18876
Architecture for a human-robot symbiotic system
[DE90-005670] N90-18921
Initial results of positron ionization mass spectrometry N90-18995
Modern theory of magnetism
[DE90-007374] N90-18998
Atomic and molecular spectra from electron-excited alkali halides
[DE90-006160] N90-19004
Measurement of the space potential of a high-temperature plasma by fast atomic beam scattering on an ion probe beam
[DE90-006118] N90-19020
Fourth International Conference on Fusion Reactor Materials
[DE90-006142] N90-19025
Ion implantation-induced amorphization of ceramic oxides
[DE90-006564] N90-19041
Dopant site location in dual-implanted GaP using (111) planar channeling
[DE90-006565] N90-19042
In situ growth of epitaxial superconducting YBa2Cu3O(7-x) films on insulating semiconducting and ferroelectric K(Ta, Nb)O3 by pulsed laser ablation
[DE90-006568] N90-19043
In situ growth of high quality epitaxial YBa2Cu3O(7-x) thin films at moderate temperatures by pulsed laser ablation
[DE90-006629] N90-19045

Using the K-25 C/TD common file system: A guide to CFSI
[DE90-005815] N90-19179

OBSERVATOIRE DE PARIS-MEUDON (FRANCE).
IR spectroscopy of planets and satellites; Venus, Mars, giant planets, and Titan N90-19085
Infrared cometary spectroscopy N90-19086
Measurements of the D/H ratio in planetary atmospheres by ground based infrared spectroscopy N90-19088
Observations of CO on Mars in the infrared and millimetre range N90-19090
Near infrared spectroscopy of Mars: Study of the surface mineralogy N90-19091
High resolution infrared spectroscopy of symbiotic stars N90-19125

OBSERVATORIO ASTRONOMICO NACIONAL, MADRID (SPAIN).
Ice grains in the dust disk of the bipolar nebula M 1-92 N90-19127

OFFICE NATIONAL D'ETUDES ET DE RECHERCHES AEROSPATIALES, PARIS (FRANCE).
Unsteady viscous calculation method for cascades with leading edge induced separation N90-18408
Numerical simulation of three-dimensional unsteady flows in turbomachines N90-18417
Structural study of thermo-hardenable matrices. Deformation processes of composite matrices as a function of their molecular structure
[ONERA-RT-10/3521-M] N90-18522
Comparison between the damage modes of thermo-hardenable and thermo-plastic composite matrices
[ONERA-RT-47/7086-M] N90-18523
Spectral multi-domain approximation of the Navier-Stokes equations in curved complex geometries
[ONERA-NT-1987-2] N90-18685
Numerical simulation of the incompressible inhomogeneous turbulence in a plane channel flow
[ONERA-NT-1988-5] N90-18686
Transient responses of coupled systems
[ONERA-RT-13/3596-RY-070-R] N90-18687
Interaction between oblique-angled incident shock wave and turbulent boundary layer on a heated wall. Experimental results
[ONERA-RT-84/7078-AY] N90-18688
Numerical simulation of the vortex breakdown
[ONERA-RSF-4/4368-AY-004A] N90-18689
Application of wavefront analysis techniques to restoring of images degraded by atmospheric turbulence
[ONERA-PUBL-1989-1] N90-19168

OHIO STATE UNIV., COLUMBUS.
A user's manual for the method of moments Aircraft Modeling Code (AMC)
[NASA-CR-186371] N90-18390

OREGON STATE UNIV., CORVALLIS.
Theoretical studies in nuclear physics
[DE90-005981] N90-19005

ORGANISATIE VOOR TOEGEPAST NATUURWETENSCHAPPELIJK ONDERZOEK, RIJSWIJK (NETHERLANDS).
Investigation of multiple scattering in aqueous suspensions of non-absorbing polystrene microspheres using spectrophotometry
[BCRS-89-09] N90-18549

OSSERVATORIO ASTROFISICO DI ARCETRI, FLORENCE (ITALY).
Near infrared spectroscopy of the supernova remnant RCW103 N90-19109
Near infrared (1-4 micron) spectroscopy of SN1987A N90-19133

OXFORD UNIV. (ENGLAND).
Methods for making unsteady aerodynamic pressure measurements in a rotating turbine stage N90-18426

P

PACIFIC NORTHWEST LAB., RICHLAND, WA.
Condensation fluid dynamics and heat transfer on rotating spherical surfaces in a microgravitational field
[DE90-005540] N90-18607
Cost and energy consumption estimates for the aluminum-air battery anode fuel cycle
[DE90-005810] N90-18656
Energy markets in the 1990's and beyond: A comparison of energy intensity in the United States and Japan
[DE90-005535] N90-18797

PENGUIN SOFTWARE, INC., LONG BEACH, CA.
A microcode compiler that runs on the IBM AT and supports cascadable microcomputers, part 1
[AD-A215888] N90-18877

PENNSYLVANIA STATE UNIV., UNIVERSITY PARK.
Design guidance to minimize unsteady forces in turbomachines N90-18411
Threaded joint design for composites
[DE90-005553] N90-18506
Damage assessment in composites by acousto-ultrasonic technique
[AD-A216590] N90-18510

PENNSYLVANIA UNIV., PHILADELPHIA.
Structure and vibrational excitations of reconstructed semiconductor surfaces
[DE90-006589] N90-19044
Thermodynamics of systems with very many components phase equilibrium
[DE90-007345] N90-19059

PITTSBURGH ENERGY TECHNOLOGY CENTER, PA.
Fluidization mechanisms in slurry flow
[DE90-006497] N90-18691

PITTSBURGH UNIV., PA.
Parallel memory addressing using coincident optical pulses
[AD-A216302] N90-18641
Differential-geometric techniques for solving differential algebraic equations
[AD-A216503] N90-18934
New aspects in bifurcation with symmetry
[AD-A216506] N90-18935

PRATT AND WHITNEY AIRCRAFT, WEST PALM BEACH, FL.
Effect of correlation on multi-engine rocket propulsion systems N90-18467

PRATT AND WHITNEY AIRCRAFT OF CANADA LTD., LONGUEUIL (QUEBEC).
Review of modelling methods to take account of material structure and defects N90-18402

PRINCETON UNIV., NJ.
Surface intermediates in thin film deposition on silicon
[AD-A216662] N90-18534

PRINCETON UNIV. OBSERVATORY, NJ.
Interstellar extinction in the infrared N90-19095
IR line emission from supernovae in molecular clouds N90-19102

PRODATA, INC., ALEXANDRIA, VA.
Defense Technical Information Center Executive Information System: Documentation and user's manual
[AD-A216235] N90-19065

PURDUE UNIV., WEST LAFAYETTE, IN.
A study of the interaction of light with surfaces of sub-micron dimensions
[DE90-006646] N90-19046

PUSAT LITBANG PENGAIRAN, BANDUNG (INDONESIA).
Erosion monitoring using remote sensing, part 2
[BCRS-89-15] N90-18785

Q

QUEENS UNIV., BELFAST (NORTHERN IRELAND).
Positron scattering by atomic hydrogen using optical potentials and with positronium formation N90-18966

R

RENSSELAER POLYTECHNIC INST., TROY, NY.
Microcomputer enhanced optical investigation of spreading and evaporative processes in ultra thin films
[DE90-006323] N90-18585

RHODE ISLAND UNIV., KINGSTON.
Thermal analysis of polymer composites
[AD-A216947] N90-18578

ROCHESTER INST. OF TECH., NY.
Research project in microelectronic engineering and imaging science
[DE90-006907] N90-18653
Techniques for measurement of the optical properties of materials
[DE90-006902] N90-19014
Visual target detection and recognition
[DE90-006903] N90-19015
A model of incomplete chromatic adaptation for calculating corresponding colors
[DE90-006905] N90-19016

ROLLS-ROYCE LTD., DERBY (ENGLAND).
Defects: Their behaviour and related design assumptions N90-18397
Review of component defects, their relationship to manufacturing process, and their effect on materials behaviour (for critical rotating parts) N90-18399
Development of a mass averaging temperature probe N90-18418

ROME AIR DEVELOPMENT CENTER, GRIFFISS AFB, NY.
Reliability assessment using finite element techniques
[AD-A216907] N90-18647
The interaction of polycrystalline copper films with dilute aqueous solutions of cupric chloride
[AD-A216465] N90-19033

ROORKEE UNIV. (INDIA).
Inelastic scattering of positrons with sodium N90-18861

ROYAL OBSERVATORY, EDINBURGH (SCOTLAND).
Infrared spectroscopy of dust N90-19094
Spectroscopy of galaxies in the mid-infrared N90-19145
An advanced cooled grating spectrometer for UKIRT-CGS4 N90-19165
The James Clerk Maxwell telescope N90-19166

RUTGERS - THE STATE UNIV., NEW BRUNSWICK, NJ.
Multicomponent glass surfaces structure and adsorption
[DE90-007179] N90-18596

RUTGERS - THE STATE UNIV., PISCATAWAY, NJ.
Structure and reactivity of model thin film catalysts
[DE90-007365] N90-18548

S

SAN DIEGO STATE UNIV., CA.
Signal processing device to control microwave output
[AD-A216931] N90-18648
Schema-based theories of problem solving
[AD-A216717] N90-18939

SANDIA NATIONAL LABS., ALBUQUERQUE, NM.
A statistical evaluation of the variation in laminated composite properties resulting from ply misalignment
[DE90-006371] N90-18525
Microconvective heating of granular explosives by a semiconductor bridge
[DE90-005710] N90-18541
Improved amorphous metal materials for magnetic pulse compression
[DE90-005723] N90-18555
Time-resolved measurements of solidification and undercooling in metals and alloys
[DE90-007074] N90-18564
Composite for smoothing the surface of ceramic substrates
[DE90-004005] N90-18565
Research relating to crystalline silicon-film on a foreign substrate
[DE90-005720] N90-18582
Microstructural variations in aluminum oxide coatings deposited using a dual beam ion system
[DE90-006040] N90-18583
Morphological consequences of catalytic hydrogenation of polymers in the bulk
[DE90-007276] N90-18598
Scattering from an arbitrary cylinder in the presence of a planar media interface using the bymoment method
[DE90-006485] N90-18626
Characterization and development report for the SA3274-1 and SA3274-2 transient voltage suppressors
[DE90-005712] N90-18649
Lithium ambient-temperature battery reliability
[DE90-005758] N90-18650
DANCIR (device and circuit simulator): A three dimensional steady-state semiconductor device simulator
[DE90-006370] N90-18658
Coating possibilities for magnetic switches
[DE90-006536] N90-18659
Excess transit time as a function of burst current in an exploding bridgewire detonator
[DE90-007168] N90-18708
Pulsed laser-induced melting of intermediate Cu-Zn phases
[DE90-005404] N90-18713
Vertical axis wind turbine turbulent response model. Part 2: Response of Sandia National laboratories' 34-meter VAWT with aeroelastic effects
[DE90-005721] N90-18804
Measurements of surface pressures on an operating vertical-axis wind turbine
[DE90-005722] N90-18805
Advanced battery development
[DE90-006073] N90-18806
Magnetohydrodynamic modeling of plasma opening switches and gas puff plasmas
[DE90-005825] N90-19028
A GaAs p-n-p-n thyristor model
[DE90-005757] N90-19039

SCHLUMBERGER CAMBRIDGE RESEARCH (ENGLAND).
Unsteady aerodynamic phenomena in a simulated wake and shock wave passing experiment N90-18414

SCIENTIFIC COMPUTING ASSOCIATES, INC., NEW HAVEN, CT.
Ada-Linda preliminary report: Motivation, informal description, and examples
[AD-A216004] N90-18892

SMITH-KETTLEWELL INST. OF VISUAL SCIENCES, SAN FRANCISCO, CA.
Visual processing of object velocity and acceleration [AD-A216509] N90-18858
Psychological studies of visual cortical function [AD-A217029] N90-18872
SOCIETE BERTIN ET CIE, PLAISIR (FRANCE).
The improvement of technology transfer from space to industry N90-19079
SOCIETE EUROPEENNE DE PROPULSION, SAINT-MEDARD-EN-JALLES (FRANCE).
Ceramic matrix composites, new high performance materials N90-18500
SOCIETE NATIONALE D'ETUDE ET DE CONSTRUCTION DE MOTEURS D'AVIATION, EVRY CEDEX (FRANCE).
The damage tolerance of disc materials: Metallurgical factors; relationship with processing parameters N90-18398
SOCIETE NATIONALE D'ETUDE ET DE CONSTRUCTION DE MOTEURS D'AVIATION, MOISSY-CRAMAYEL (FRANCE).
Aerodynamic study on forced vibrations on stator rows of axial compressors N90-18412
SOREQ RESEARCH ESTABLISHMENT, ISRAEL ATOMIC ENERGY COMMISSION, YAVNEH.
Spallation and dynamic fracture as an effect of laser induced shock waves in carbon based composite materials
[AD-A216540] N90-18509
SOUTHAMPTON UNIV. (ENGLAND).
System properties from frequency response functions, part 1
[ISVR-TR-166-PT-1] N90-18754
A study of the vibrational transmission through flanged joints
[ISVR-TR-181] N90-18755
SPACE RESEARCH ORGANIZATION NETHERLANDS, UTRECHT.
Predictions of infrared recombinations lines in stellar winds of hot stars N90-19136
SPIRE CORP., BEDFORD, MA.
Radiation-hard high-efficiency InP space solar cell development
[AD-A216857] N90-18800
STANFORD LINEAR ACCELERATOR CENTER, CA.
Computation and control with neural nets
[DE90-006460] N90-18911
STANFORD UNIV., CA.
An investigation of flow structure, mixing and chemical reaction in combusting turbulent flows
[AD-A216739] N90-18538
Improved computational fluid dynamics for continuum hypersonic flow
[AD-A216981] N90-18674
Approximations to joint distributions of definite quadratic forms
[AD-A216434] N90-18930
High growth rate diamond synthesis in a large area atmospheric pressure inductively coupled plasma
[AD-A216090] N90-19019
Crystal growth and mechanical properties of semiconductor alloys
[AD-A216697] N90-19035
Gamma ray astronomy and black hole astrophysics
[NASA-CR-186496] N90-19169
STATE UNIV. OF NEW YORK, BUFFALO.
Fundamental studies of surface processes and trace analysis using solid electrodes
[AD-A216538] N90-18533
Nonlinear optical processes in one-dimensional polymers
[AD-A216103] N90-18568
Strongly coupled one-dimensional system and the polymer
[AD-A216330] N90-18571
STATE UNIV. OF NEW YORK, STONY BROOK.
Studies of atmospheric molecules by multiphoton spectroscopy
[DE90-005829] N90-18833
STEVENS INST. OF TECH., HOBOKEN, NJ.
Surface production of ions
[AD-A216470] N90-19003
STOCKHOLM OBSERVATORY (SWEDEN).
Wide-beam balloon observations of the 157.7 microns (CII) line N90-19108
STRASBOURG UNIV. (FRANCE).
Space technology transfers in Europe N90-19070
STUTTGART UNIV. (GERMANY, F.R.).
Calculation of the unsteady two-dimensional, inviscid, compressible flow around a strongly cambered oscillating single blade N90-18409
SWEDISH DEFENCE RESEARCH ESTABLISHMENT, STOCKHOLM.
Microcalometric studies of gun propellant KKR 8
[FOA-C-20770-2.1] N90-18606
SWEDISH INST. FOR SILICATE RESEARCH, GOTHEBORG.
Silicon carbo-nitride ceramic matrix composites by polymer pyrolysis N90-18499
SYSTEMS CONTROL TECHNOLOGY, INC., ARLINGTON, VA.
Human factors issues in aircraft maintenance and inspection
[AD-A215724] N90-18875

T

TECHNISCHE HOCHSCHULE, AACHEN (GERMANY, F.R.).
Numerical investigation of unsteady flow in oscillating turbine and compressor cascades N90-18407
Experiments on the unsteady flow in a supersonic compressor stage N90-18422
Experimental investigation of the influence of rotor wakes on the development of the profile boundary layer and the performance of an annular compressor cascade N90-18425
TECHNISCHE UNIV., DELFT (NETHERLANDS).
Computational aerodynamics of ordered vortex flows
[ETN-90-06272] N90-18368
Practical applications of Loran-C for land mobile use or the possibility to use Loran-C as a vehicle-location or vehicle-navigation system
[ETN-90-06265] N90-18384
Sintering of a model nickel/alumina catalyst
[ETN-90-06270] N90-18561
Hydrogenated amorphous and microcrystalline silicon deposited from silane-hydrogen mixtures
[ETN-90-06267] N90-18590
Integrated silicon flip-flop sensors
[ETN-90-06271] N90-18654
A study on deformation and break-up of dispersed particles in elongational flow
[ETN-90-06268] N90-18684
Analysis of linear multigrid methods for elliptic differential equations with discontinuous and anisotropic coefficients
[ETN-90-06269] N90-18944
TECHNOCHEMIE G.M.B.H., DOSSENHEIM (GERMANY, F.R.).
Modified bismaleimides for carbon fibre composites N90-18495
TEL-AVIV UNIV. (ISRAEL).
Infrared spectroscopy of star formation in galaxies: Extreme conditions and very short time scales N90-19147
TEMPLE UNIV., PHILADELPHIA, PA.
Teaching a new methodology for designing relational data bases: An experiment testing the effectiveness of an intelligent tutoring system on cognitive skill acquisition (volumes 1 and 2) N90-19063
TENNESSEE UNIV., KNOXVILLE.
Heat capacities of solid polymers (The Advanced THermal Analysis System, ATHAS)
[DE90-007130] N90-18595
Distributed decomposition of block-angular linear programs on a hypercube computer
[AD-A216433] N90-18693
TEST GROUP (6585TH), HOLLOMAN AFB, NM.
The Fourteenth Biennial Guidance Test Symposium, volume 1
[AD-A216925] N90-18383
TEXAS A&M UNIV., COLLEGE STATION.
Electrochemical investigations of electronically conductive polymers. Part 4: By controlling the supermolecular structure, charge transport rates can be enhanced
[AD-A216603] N90-18573
Analytical and experimental investigation of miniature heat pipes, phase 2
[AD-A216945] N90-18673
Payload vibration isolation in a microgravity environment
[NASA-CR-186191] N90-18744
Oxygen electrode in molten carbonate fuel cells
[DE90-005377] N90-18796
TEXAS UNIV., ARLINGTON.
Electronic and ionic transport in polymers
[AD-A217028] N90-18579
Differential elastic scattering cross sections for 54.9eV positrons incident on helium N90-18975
Total cross sections for positrons scattered elastically from helium based on new measurements of total ionization cross sections N90-18976
Positron annihilation induced Auger electron spectroscopy N90-18998
TEXAS UNIV., AUSTIN.
Control of phase structure in polymer blends
[AD-A217034] N90-18580
The rapid inward diffusion of cold ions in tokamaks and their effect on ion transport
[DE90-006863] N90-19022
The neoclassical transport of toroidal momentum in tokamaks
[DE90-006864] N90-19023
Thermonuclear instability of global-type shear Alfven modes
[DE90-007087] N90-19026
The free energy principle, negative energy modes, and stability
[DE90-005368] N90-19056
Infrared spectroscopy of the central few parsecs of the galaxy N90-19140
THERMACORE, INC., LANCASTER, PA.
Flexible heat pipe cold plate
[AD-A216053] N90-18433
TURBONECA S.A. - BREVETS SZYDLOWSKI, BIZANOS (FRANCE).
Defects in monoblock cast turbine wheels N90-18400

U

UHT CORP., DOBBS FERRY, NY.
Hydrogenated amorphous silicon films prepared by glow discharge of disilane
[DE90-000309] N90-18581
UNION CARBIDE CORP., SOUTH CHARLESTON, WV.
Optimum catalytic process for alcohol fuels from syngas
[DE90-005290] N90-18600
Optimum catalytic process for alcohol fuels from syngas
[DE90-007188] N90-18604
UNITED TECHNOLOGIES RESEARCH CENTER, EAST HARTFORD, CT.
Gust response analysis for cascades operating in nonuniform mean flows N90-18415
Identification of a cast iron alloy containing nonstrategic elements
[NASA-CR-185174] N90-18559
UNIVERSIDAD AUTONOMA DE MADRID, CANTOBLANCO (SPAIN).
Evolutionary synthesis of the far-infrared emission in starburst galaxies N90-19152
UNIVERSIDAD DE LA LAGUNA (SPAIN).
IR spectrophotometry of bright carbon stars N90-19131
Infrared properties of five spiral galaxies N90-19154
UNIVERSIDAD POLITECNICA DE MADRID (SPAIN).
Spacecraft thermal control design data, volume 1
[ESA-PSS-03-108-ISSUE-1-VOL-1] N90-18455
Spacecraft thermal control design data, volume 2
[ESA-PSS-03-108-ISSUE-1-VOL-2] N90-18456
Spacecraft thermal control design data, volume 3
[ESA-PSS-03-108-ISSUE-1-VOL-3] N90-18457
Spacecraft thermal control design data, volume 4
[ESA-PSS-03-108-ISSUE-1-VOL-4] N90-18458
UNIVERSITEIT TWENTE, ENSCHEDE (NETHERLANDS).
Simulating simultaneous processes with APL
[MEMO-INF-89-47] N90-18906
A survey of performability modelling tools
[MEMO-INF-89-50] N90-18907
System theory and mechanics
[MEMO-807] N90-18922
Feasibility of Mealy design for processor controlpaths
[MEMO-INF-89-53] N90-18923
On the depth of combinatorial optimization problems
[MEMO-803] N90-18946
Application of Chebyshev approximation to curve fitting
[MEMO-805] N90-18947
Nonlinear model matching: A local solution and two worked examples
[MEMO-809] N90-18948
Using dynamic queueing networks as a tool for specifying performability models
[MEMO-INF-89-51] N90-18949
Kreim factorization of covariance operators of 2-parameter random fields and application to the likelihood ratio
[MEMO-802] N90-18953
Strong moderate deviation theorems
[MEMO-804] N90-18954
UNIVERSITY COLL., CARDIFF (WALES).
A unified model for the 3.28 micron and 3.4 micron spectral feature in the interstellar medium and in comets N90-19092
Interpretation of the 10 micron and 20 micron absorption bands in comets, the interstellar medium, and in an external galaxy N90-19093
The microwave background in steady-state cosmology N90-19150

UNIVERSITY COLL., LONDON (ENGLAND).
Ab initio R-matrix calculations of e+-molecule scattering N90-18970
Antihydrogen formation in collisions of positronium with antiprotons N90-18988
Planetary nebulae N90-19122

UNIVERSITY OF SOUTHERN CALIFORNIA, LOS ANGELES.
Model filled polymers 3. Rheological behavior of polystyrene containing crosslinked polystyrene beads [AD-A215867] N90-18567
Fluidization mechanisms in slurry flow [DE90-006497] N90-18691
Practical methods for robust multivariable control [AD-A216937] N90-18920

UNIVERSITY OF SOUTHERN CALIFORNIA, MARINA DEL REY.
Approaches to the planning of coherent text [AD-A216463] N90-18895

UNIVERSITY OF WESTERN ONTARIO, LONDON.
Merged beam studies into the mechanisms of hydrogen molecular ion recombination [AD-A216469] N90-19002

UTAH UNIV., SALT LAKE CITY.
Future technology requirements (related to defects and quantitative material behavior to aid in implementation of damage tolerance for design of engine structures) N90-18403
Compressive strength of carbon/epoxy laminated under multiaxial stress [DE90-005552] N90-18505
Characterization of biopolymer surfaces using scanning microscopies [AD-A216572] N90-18572
Production of high density aviation fuels via novel zeolite catalyst routes [AD-A216444] N90-18601

V

VINTEN INSTRUMENTS LTD., WEYBRIDGE (ENGLAND).
The bringing to market of the RF alert (a case study in technology transfer) N90-19073

VIRGINIA POLYTECHNIC INST. AND STATE UNIV., BLACKSBURG.
Stall and recovery in multistage axial flow compressors N90-18429
Energy decay and boundary control for distributed parameter systems with viscoelastic damping [AD-A216468] N90-18748

VIRGINIA UNIV., CHARLOTTESVILLE.
Superconducting materials [DE90-007419] N90-19054

VRIJE UNIV., BRUSSELS (BELGIUM).
Measurement of velocity profiles and Reynolds stresses on an oscillating airfoil N90-18427

W

WASHINGTON AND LEE UNIV., LEXINGTON, VA.
Measurements of surface pressures on an operating vertical-axis wind turbine [DE90-005722] N90-18805

WASHINGTON UNIV., SEATTLE.
Turbulence structure of mixing swirling flows [AD-A216628] N90-18671
Comparison of two Navy environmental database models: Generalized Digital Environmental Model and Podeszwa sound speed profile model [AD-A215848] N90-18889

WAYNE STATE UNIV., DETROIT, MI.
Scattering of positrons and electrons by alkali atoms N90-18959
Positron-inert gas differential elastic scattering N90-18974

WEST VIRGINIA UNIV., MORGANTOWN.
High temperature interaction of SO2 with oxide sorbents [DE90-000435] N90-18545
Long path connectivity of regular graphs [AD-A216477] N90-18933
Finding critical independent sets and critical vertex subsets are polynomial problems [AD-A216547] N90-18938

WESTINGHOUSE SAVANNAH RIVER CO., AIKEN, SC.
Failure probability estimate of Type 304 stainless steel piping [DE90-003896] N90-18550

WIEN UNIV. (AUSTRIA).
Asymptotic analysis of transonic flow through oscillating cascades N90-18421

WILSON GREATBATCH LTD., CLARENCE, NY.
Feasibility of a super high energy density battery of the Li/BrF3 electrochemical system [AD-A216794] N90-18644
Feasibility of a super high energy density battery of the Li/BrF3 electrochemical system [AD-A216575] N90-18799

WISCONSIN UNIV., MADISON.
Fundamental studies of new magnetic heterostructures: Their growth, crystallographic structure, magnetic, and electronic properties [DE90-007381] N90-19053

WISCONSIN UNIV., MILWAUKEE.
Perception of long-period complex sounds [AD-A216743] N90-18861

WOODS HOLE OCEANOGRAPHIC INST., MA.
Summer Study Program in Geophysical Fluid Dynamics: The Influence of Convection on Large-Scale Circulations, 1988 [AD-A216024] N90-18840

WRIGHT RESEARCH DEVELOPMENT CENTER, WRIGHT-PATTERSON AFB, OH.
Compressor performance tests in the compressor research facility N90-18428

X

XEROX PALO ALTO RESEARCH CENTER, CA.
Pulsed laser deposition of high T(sub c) superconducting thin films [AD-A216507] N90-19034

Y

YESHIVA UNIV., NEW YORK, NY.
Coronary arterial capacitance and subendocardial vascular patency throughout the cardiac cycle N90-18855

YORK UNIV., TORONTO (ONTARIO).
Positron-alkali atom scattering N90-18958
Positron-rubidium scattering N90-18964
Resonances in low-energy positron-alkali scattering N90-18992

Typical Contract Number Index Listing

Listings in this index are arranged alphanumerically by contract number. Under each contract number the NASA accession numbers denoting documents that have been produced as a result of research done under that contract are arranged in ascending order. The NASA accession number denotes the number by which the citation is identified.

AF PROJ. 2301 ..... N90-19002
N90-19003
AF PROJ. 2303 ..... N90-18493
N90-18533
N90-18534
N90-18570
N90-18717
AF PROJ. 2304 ..... N90-18748
N90-18908
N90-18920
N90-18931
N90-18932
N90-18933
N90-18937
N90-18938
N90-18942
AF PROJ. 2305 ..... N90-18622
AF PROJ. 2306 ..... N90-18553
N90-19033
N90-19035
AF PROJ. 2307 ..... N90-18671
N90-18672
AF PROJ. 2308 ..... N90-18538
AF PROJ. 2310 ..... N90-18830
AF PROJ. 2311 ..... N90-19185
AF PROJ. 2313 ..... N90-18858
N90-18860
N90-18861
N90-18864
N90-18872
N90-18936
N90-18939
AF PROJ. 2338 ..... N90-18647
AF PROJ. 3048 ..... N90-18601
AF-AFOSR-0008-89 ..... N90-18864
AF-AFOSR-0011-87 ..... N90-19185
AF-AFOSR-0035-89 ..... N90-18858
AF-AFOSR-0037-87 ..... N90-18533
AF-AFOSR-0043-88 ..... N90-18570
AF-AFOSR-0050-86 ..... N90-18534
AF-AFOSR-0063-86 ..... N90-18936
AF-AFOSR-0068-89 ..... N90-18933
N90-18938
AF-AFOSR-0071-87 ..... N90-18717
AF-AFOSR-0075-86 ..... N90-18493
AF-AFOSR-0085-86 ..... N90-18748
AF-AFOSR-0107-89 ..... N90-18939
AF-AFOSR-0132-86 ..... N90-18908
AF-AFOSR-0145-86 ..... N90-18932
AF-AFOSR-0158-86 ..... N90-19035
AF-AFOSR-0198-88 ..... N90-18641
AF-AFOSR-0273-85 ..... N90-18671
AF-AFOSR-0277-86 ..... N90-18931
AF-AFOSR-0282-88 ..... N90-18920
AF-AFOSR-0286-83 ..... N90-18937
AF-AFOSR-0299-86 ..... N90-19003
AF-AFOSR-0320-88 ..... N90-18861
AF-AFOSR-0326-88 ..... N90-18872
AF-AFOSR-0338-86 ..... N90-18860
AF-AFOSR-0339-88 ..... N90-18553
AF-AFOSR-0347-85 ..... N90-18942
AF-AFOSR-0365-87 ..... N90-19002
AF-AFOSR-0373-84 ..... N90-18538
AF-AFOSR-0398-87 ..... N90-18672
ARO-MIPR-118-86 ..... N90-18443
ARO-MIPR-125-85 ..... N90-18443
ARO-MIPR-141-87 ..... N90-18443
ARPA ORDER 6037 ..... N90-18891
ARPA ORDER 6380 ..... N90-18734
ASTRON-782-374-000 ..... N90-19166
BMFT-FZ-01-YH-88-112 ..... N90-18631
BMFT-01-QS-104 ..... N90-18710
CAYCIT-PB-85-60 ..... N90-19152
CNR-86-157 ..... N90-19089
CNR-87-01079-02 ..... N90-19089
CPBP-01.02 ..... N90-18954
DA PROJ. 1L1-61102-BH-57 ..... N90-18599
DA PROJ. 1L1-61205-AH-84 ..... N90-18750
DA PROJ. 351-62772-A-874 ..... N90-18859
DAAD07-87-C-0119 ..... N90-18877
DAAL03-86-D-0001 ..... N90-18901
DAAL03-86-G-0072 ..... N90-18578
DAAL03-86-K-0136 ..... N90-18577
DAAL03-86-K-0139 ..... N90-18674
DAAL03-88-K-0004 ..... N90-18580
DACA76-85-C-0010 ..... N90-18871
N90-18914
N90-18915
DAJA45-85-C-0039 ..... N90-18427
DAJA45-87-C-0032 ..... N90-18509
DAJA45-89-M-0078 ..... N90-18599
DALL03-86-0122 ..... N90-18720
DAMD17-86-C-6157 ..... N90-18859
DE-AC02-76CH-00016 ..... N90-18529
N90-18706
N90-18867
N90-18868
N90-18980
DE-AC02-76CH-03073 ..... N90-19026
DE-AC02-80ER-10587 ..... N90-19171
DE-AC02-83CH-10093 ..... N90-18362
N90-18581
N90-18792
N90-18801
N90-18802
N90-18803
N90-18809
N90-18810
N90-18811
DE-AC02-83ER-40105 ..... N90-19006
DE-AC02-83ER-40121 ..... N90-19000
N90-19040
DE-AC02-86ER-40296 ..... N90-18552
DE-AC02-87CE-90001 ..... N90-18591
DE-AC03-76SF-00098 ..... N90-18584
N90-18702
N90-18719
N90-18720
N90-18753
N90-18865
N90-19024
N90-19051
N90-19052
N90-19058
DE-AC03-76SF-00515 ..... N90-18911
DE-AC04-76DP-00613 ..... N90-18652
DE-AC04-76DP-00789 ..... N90-18541
N90-18555
N90-18564
N90-18565
N90-18582
N90-18583
N90-18598
N90-18626
N90-18649
N90-18650
N90-18658
N90-18659
N90-18708
N90-18713
N90-18804
N90-18805
N90-18808
N90-19028
N90-19039
DE-AC04-76DR-00789 ..... N90-18525
DE-AC04-88DP-43495 ..... N90-19008
N90-19009
N90-19010
N90-19178
DE-AC05-84OR-21400 ..... N90-18558
N90-18563
N90-18586
N90-18592
N90-18593
N90-18594
N90-18595
N90-18603
N90-18690
N90-18693
N90-18721
N90-18739
N90-18741
N90-18819
N90-18856
N90-18876
N90-18921
N90-18995
N90-18998
N90-19004
N90-19020
N90-19025
N90-19041
N90-19042
N90-19043
N90-19045
N90-19179
DE-AC05-84OT-21400 ..... N90-18945
DE-AC06-76RL-01830 ..... N90-18607
N90-18656
N90-18797
DE-AC07-76ID-01570 ..... N90-18562
N90-18655
N90-18692
DE-AC07-88ID-12735 ..... N90-18597
DE-AC09-76SR-00001 ..... N90-18550
DE-AC09-89SR-18035 ..... N90-18550
DE-AC21-86MC-23250 ..... N90-18676
DE-AC21-86MC-23259 ..... N90-18545
DE-AC21-88MC-24218 ..... N90-18812
DE-AC22-88PC-90013 ..... N90-18600
N90-18604
DE-AI01-77CS-51040 ..... N90-18559
DE-AI05-83OR-21322 ..... N90-18558
DE-AS05-81ER-40039 ..... N90-19182
DE-FC05-85ER-250000 ..... N90-18968
DE-FG01-87CE-15325 ..... N90-18610
DE-FG01-88DP-20153 ..... N90-18653
N90-19014
N90-19015
N90-19016
DE-FG02-84ER-45118 ..... N90-19044
DE-FG02-84ER-45162 ..... N90-19046
DE-FG02-85ER-13403 ..... N90-18566
DE-FG02-85ER-25001 ..... N90-18880
DE-FG02-85ER-40211 ..... N90-19001
DE-FG02-85ER-45205 ..... N90-18557
DE-FG02-86ER-13590 ..... N90-18833
DE-FG02-86ER-60422 ..... N90-18822
DE-FG02-87ER-13670 ..... N90-18834
DE-FG02-87ER-25026 ..... N90-18943
DE-FG02-87ER-45319 ..... N90-19053
DE-FG02-88ER-13825 ..... N90-19059
DE-FG02-88ER-45354 ..... N90-18556
DE-FG02-89ER-14045 ..... N90-18585
DE-FG03-87ER-52144 ..... N90-19027
DE-FG05-80ET-53088 ..... N90-19022
N90-19023
N90-19026
N90-19056
DE-FG05-84ER-40147 ..... N90-19186
DE-FG05-84ER-45113 ..... N90-19054
DE-FG05-84ER-45118 ..... N90-18587
DE-FG05-88ER-45368 ..... N90-18596
DE-FG05-89ER-13985 ..... N90-18546
DE-FG06-86ER-40283 ..... N90-19005
DE-FG22-88PC-90957 ..... N90-18691

DE-FG22-87PC-79931 ..... N90-18706
DEN3-262 ..... N90-18559
DNA001-87-C-0169 ..... N90-18613
DNA001-88-C-0040 ..... N90-18511
DRET-82-272 ..... N90-18367
DRET-87-34-001 ..... N90-18522
N90-18667
N90-18668
DRET-87-34-083-00-470-75-01 ..... N90-18695
DRET-87-070 ..... N90-18679
DRET-87-272 ..... N90-18662
DRET-88-34-001 ..... N90-18523
N90-18669
DTFA01-80-Y-10546 ..... N90-18847
DTFA01-87-C-00014 ..... N90-18875
DTFA03-88-C-00024 ..... N90-18375
ETCA/CTME/RM-20221/85 ..... N90-18703
FINEP-537/CT N90-18926
F04701-88-C-0089 ..... N90-18532
N90-18642
F19628-85-C-0003 ..... N90-18886
F19628-85-K-0052 ..... N90-18622
F19628-87-K-0045 ..... N90-19170
F19628-90-C-0002 ..... N90-18645
F33615-84-C-2475 ..... N90-18414
F33615-85-C-0531 ..... N90-18873
F33615-85-C-2567 ..... N90-18601
F33615-88-C-2723 ..... N90-18673
F33615-88-C-3624 ..... N90-18361
N90-18388
F41689-87-D-0012 ..... N90-18870
F49620-84-C-0012 ..... N90-18720
F49620-85-C-0142 ..... N90-18576
F49620-86-C-0005 ..... N90-18492
F49620-86-C-0009 ..... N90-18571
F49620-86-K-0022 ..... N90-18491
F49620-87-C-0005 ..... N90-18895
F49620-88-C-0033 ..... N90-18917
F49620-88-C-0050 ..... N90-18897
F49620-89-C-0017 ..... N90-19034
HD07205-08 ..... N90-18869
IEP-87/22 ..... N90-18683
JPL-958007 ..... N90-19107
LANL-9-X58-7568P-1 ..... N90-18825
MDA903-88-C-0186 ..... N90-19065
MDA903-89-C-0003 ..... N90-18898
MIPR-W31-RPD-7-D4041 ..... N90-18727
MIPR-W31-RPD-83-A072 ..... N90-18857
NAGW-1505 ..... N90-19088
NAG2-08 ..... N90-19146
NAG2-483 ..... N90-18664
NAG2-593 ..... N90-18691
N90-18924
NAG5-753 ..... N90-18824
NAG5-1291 ..... N90-19181
NASA ORDER C-99066-G N90-18927
NASW-3159 ..... N90-19112
N90-19141
NAS1-17497 ..... N90-18743
NAS1-18229 ..... N90-18454
NAS1-18465 ..... N90-18371
N90-18372
NAS1-18605 ..... N90-18363
NAS2-12037 ..... N90-18469
NAS3-22156 ..... N90-18364
NAS3-22234 ..... N90-18808
NAS3-25266 ..... N90-18667
NAS3-25425 ..... N90-18415
NAS7-100 ..... N90-18989
NAS7-918 ..... N90-18379
N90-18444
NAS8-36300 ..... N90-18464
N90-18465
NAS8-36668 ..... N90-18467
NAS8-37505 ..... N90-18464
N90-18469
NAS9-17378 ..... N90-18483
NAS9-17585 ..... N90-18487
NAS9-17854 ..... N90-18487
NAS9-17872 ..... N90-18488
NAS9-17907 ..... N90-18484
NAS9-17972 ..... N90-18744
NAS9-18051 ..... N90-18489
NAS10-10285 ..... N90-18853
NCC1-117 ..... N90-18675
NCI-CA-29502 ..... N90-18867
NCI-CA-38645 ..... N90-18867
NGL-31-001-007 ..... N90-19102
NGR-05-020-668 ..... N90-19169
NGR-33015741 ..... N90-19088
NIH-P41-RR-01838 ..... N90-18867
NIH-RR-05918 ..... N90-18865
NSF AST-84-20775 ..... N90-19112
NSF AST-85-02401 ..... N90-19140
NSF AST-86-12013 ..... N90-19095
N90-19102
NSF AST-86-15177 ..... N90-19115
NSF AST-87-00618 ..... N90-19112
N90-19141
NSF CCR-89-07654 ..... N90-18934
NSF CHE-86-20274 ..... N90-18571
NSF DCR-85-11190 ..... N90-18929
NSF DCR-85-552543 ..... N90-18941
NSF DMC-86-10417 ..... N90-18735
N90-18912
NSF DMR-86-03131 ..... N90-18580
NSF DMR-86-20168 ..... N90-18980
NSF DMR-86-57109 ..... N90-19053
NSF DMR-88-18412 ..... N90-18595
NSF DMS-85-04166 ..... N90-18840
NSF DMS-87-04169 ..... N90-18928
NSF DMS-89-05314 ..... N90-18927
NSF IRI-86-16644 ..... N90-18917
NSF MEA-83-15117 ..... N90-18925
NSF PHY-85-06933 ..... N90-18975
N90-18976
NSF PHY-85-15857 ..... N90-19058
NSF PHY-87-06120 ..... N90-18974
NSFC-863-715-22 ..... N90-18571
NSG-1498 ..... N90-18390
NSG-7499 ..... N90-19088
N6856-87-WR-7635 ..... N90-18842
N00014-79-C-0647 ..... N90-18539
N00014-80-C-0505 ..... N90-18941
N00014-80-C-9455 ..... N90-18935
N00014-82-G-0079 ..... N90-18840
N00014-82-K-0149 ..... N90-18895
N00014-82-K-0294 ..... N90-18643
N00014-82-K-0612 ..... N90-18573
N00014-83-K-0125 ..... N90-18929
N90-19067
N00014-84-C-0708 ..... N90-18531
N90-18640
N90-18716
N00014-84-K-0099 ..... N90-18878
N90-19067
N00014-85-K-169 ..... N90-18928
N00014-85-K-0124 ..... N90-18382
N90-18862
N90-18871
N90-18900
N90-18914
N90-18915
N90-18918
N90-18919
N90-18941
N00014-85-K-0487 ..... N90-18917
N00014-85-K-0535 ..... N90-18720
N00014-85-K-0559 ..... N90-18869
N00014-85-K-0645 ..... N90-18516
N00014-85-K-0849 ..... N90-18832
N00014-86-K-0043 ..... N90-18571
N00014-86-K-0180 ..... N90-18900
N90-18916
N00014-86-K-0333 ..... N90-18863
N00014-86-K-0345 ..... N90-18574
N90-18575
N00014-86-K-0685 ..... N90-18382
N90-18896
N90-18915
N90-18918
N00014-86-K-0716 ..... N90-18857
N00014-86-K-0753 ..... N90-18507
N90-18508
N90-18713
N00014-86-K-0769 ..... N90-18579
N00014-86-8-0306 ..... N90-18925
N00014-87-C-0182 ..... N90-18899
N00014-87-C-0490 ..... N90-18715
N00014-87-C-8904 ..... N90-18891
N00014-87-K-0117 ..... N90-18747
N00014-87-K-0786 ..... N90-19036
N00014-87-K-0825 ..... N90-18899
N90-18940
N00014-87-0143 ..... N90-18510
N00014-88-C-0588 ..... N90-18535
N00014-88-K-0302 ..... N90-18567
N00014-88-K-0360 ..... N90-18639
N00014-88-K-0415 ..... N90-18572
N00014-88-K-0548 ..... N90-18894
N00014-89-C-0232 ..... N90-18799
N00014-89-C-0268 ..... N90-18892
N00014-89-C-2148 ..... N90-18800
N00014-89-J-1103 ..... N90-18512
N90-18536
N90-18537
N90-19037
N90-19038
N00014-89-J-1186 ..... N90-18530
N00014-89-J-1197 ..... N90-19019
N00014-89-J-1272 ..... N90-18869
N00014-89-J-1528 ..... N90-18893
N00014-89-J-1590 ..... N90-18569
N00014-89-J-1627 ..... N90-18930
N00014-89-J-1988 ..... N90-18878
N00014-89-K-2004 ..... N90-18831
N00014-90-J-1025 ..... N90-18934
N00014-90-J-1193 ..... N90-18568
N00039-88-C-0054 ..... N90-18889
N00039-89-C-5301 ..... N90-18462
N00140-83-C-7149 ..... N90-18738
N00140-87-C-8904 ..... N90-18924
N62269-88-C-0210 ..... N90-18433
N68001-85-D-0203 ..... N90-18648
PSN-018-85 ..... N90-19089
SERI-XK-8-18000-1 ..... N90-18811
SMRC-MFR-7557 ..... N90-18867
W-31-109-ENG-38 ..... N90-18518
N90-18542
N90-18551
N90-18820
N90-18904
N90-18909
N90-18910
N90-19183
W-7405-ENG-36 ..... N90-18519
N90-18602
N90-18624
N90-18625
N90-18712
N90-18719
N90-18722
N90-18723
N90-18725
N90-18726
N90-18879
N90-18955
N90-19007
N90-19021
N90-19030
N90-19049
N90-19050
N90-19187
W-7405-ENG-48 ..... N90-18505
N90-18506
N90-18524
N90-18608
N90-18627
N90-18651
N90-18657
N90-18677
N90-18707
N90-18714
N90-18727
N90-18728
N90-18729
N90-18730
N90-18821
N90-18823
N90-18837
N90-18985
N90-18986
N90-18989
N90-19017
N90-19169
N90-19172
N90-19188
141-20-10-10 ..... N90-18882
170-10-01-08 ..... N90-18957
188-44-53 ..... N90-19100
307-51-00 ..... N90-18634
505-60-01-02 ..... N90-18385
N90-18675
505-60-21 ..... N90-18395
505-62-21 ..... N90-18667
N90-18927
505-63-1B N90-18745
505-63-01-05 ..... N90-18746
505-63-51-01 ..... N90-18743
505-66-01-02 ..... N90-18434
505-66-41-01 ..... N90-18378
505-67-01-02 ..... N90-18393
N90-18394
505-67-41-57 ..... N90-18371
N90-18372
505-90-21-01 ..... N90-18363
506-43-41-02 ..... N90-18454
506-43-71-04 ..... N90-18752
585-02-31-01 ..... N90-18453
590-14-31-01 ..... N90-18751
894-24-00 ..... N90-18865
778-32-11 ..... N90-18504

Typical Report Number Index Listing

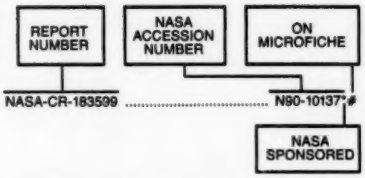

Listings in this index are arranged alphanumerically by report number. The NASA accession number denotes the number by which the citation is identified. An asterisk (*) indicates that the item is a NASA report. A pound sign (#) indicates that the item is available on microfiche.

A-89-4R ..... N90-18511 #

AAMRL-TR-89-009 ..... N90-18873 #

AD-A215173 ..... N90-18873 #
AD-A215313 ..... N90-18599 #
AD-A215450 ..... N90-18611 #
AD-A215489 ..... N90-18874 #
AD-A215664 ..... N90-18431 #
AD-A215724 ..... N90-18875 #
AD-A215759 ..... N90-19031 #
AD-A215802 ..... N90-18887 #
AD-A215846 ..... N90-18888 #
AD-A215848 ..... N90-18889 #
AD-A215865 ..... N90-18715 #
AD-A215867 ..... N90-18567 #
AD-A215870 ..... N90-18637 #
AD-A215880 ..... N90-18890 #
AD-A215881 ..... N90-18747 #
AD-A215882 ..... N90-18373 #
AD-A215888 ..... N90-18877 #
AD-A215937 ..... N90-18891* #
AD-A215952 ..... N90-18830 #
AD-A215978 ..... N90-19032 #
AD-A216004 ..... N90-18892 #
AD-A216019 ..... N90-18530 #
AD-A216023 ..... N90-18638 #
AD-A216024 ..... N90-18840 #
AD-A216025 ..... N90-19170 #
AD-A216029 ..... N90-18869 #
AD-A216037 ..... N90-18639 #
AD-A216041 ..... N90-18841 #
AD-A216042 ..... N90-18386 #
AD-A216043 ..... N90-19011 #
AD-A216053 ..... N90-18433 #
AD-A216084 ..... N90-18640 #
AD-A216085 ..... N90-18716 #
AD-A216086 ..... N90-18531 #
AD-A216090 ..... N90-19019 #
AD-A216091 ..... N90-18387 #
AD-A216094 ..... N90-18491 #
AD-A216103 ..... N90-18568 #
AD-A216116 ..... N90-18569 #
AD-A216121 ..... N90-18870 #
AD-A216142 ..... N90-18507 #
AD-A216143 ..... N90-18508 #
AD-A216210 ..... N90-18928 #
AD-A216235 ..... N90-19065 #
AD-A216256 ..... N90-18831 #
AD-A216269 ..... N90-18842 #
AD-A216286 ..... N90-19057 #
AD-A216287 ..... N90-18451 #
AD-A216302 ..... N90-18641 #
AD-A216319 ..... N90-18717 #
AD-A216320 ..... N90-18570 #
AD-A216330 ..... N90-18571 #
AD-A216376 ..... N90-18718 #
AD-A216406 ..... N90-18929 #
AD-A216411 ..... N90-18668 #
AD-A216415 ..... N90-18493 #
AD-A216433 ..... N90-18893 #
AD-A216434 ..... N90-18930 #
AD-A216436 ..... N90-18613 #
AD-A216441 ..... N90-19066 #
AD-A216444 ..... N90-18601 #
AD-A216446 ..... N90-18908 #
AD-A216452 ..... N90-18894 #
AD-A216455 ..... N90-18931 #
AD-A216458 ..... N90-18932 #
AD-A216463 ..... N90-18895 #
AD-A216465 ..... N90-19033 #
AD-A216468 ..... N90-18748 #
AD-A216469 ..... N90-19002 #
AD-A216470 ..... N90-19003 #
AD-A216477 ..... N90-18933 #
AD-A216499 ..... N90-18669 #
AD-A216500 ..... N90-18857 #
AD-A216503 ..... N90-18934 #
AD-A216506 ..... N90-18935 #
AD-A216507 ..... N90-19034 #
AD-A216509 ..... N90-18858 #
AD-A216512 ..... N90-18936 #
AD-A216515 ..... N90-18937 #
AD-A216527 ..... N90-18532 #
AD-A216531 ..... N90-18914 #
AD-A216535 ..... N90-18896 #
AD-A216538 ..... N90-18533 #
AD-A216540 ..... N90-18509 #
AD-A216547 ..... N90-18938 #
AD-A216569 ..... N90-18859 #
AD-A216572 ..... N90-18572 #
AD-A216574 ..... N90-18832 #
AD-A216575 ..... N90-18799 #
AD-A216576 ..... N90-18614 #
AD-A216579 ..... N90-19067 #
AD-A216580 ..... N90-18878 #
AD-A216582 ..... N90-18361 #
AD-A216590 ..... N90-18510 #
AD-A216597 ..... N90-18815 #
AD-A216599 ..... N90-18642 #
AD-A216600 ..... N90-18511 #
AD-A216603 ..... N90-18573 #
AD-A216604 ..... N90-19012 #
AD-A216613 ..... N90-18380 #
AD-A216618 ..... N90-18843 #
AD-A216624 ..... N90-18616 #
AD-A216625 ..... N90-18452 #
AD-A216627 ..... N90-18670 #
AD-A216628 ..... N90-18671 #
AD-A216629 ..... N90-18672 #
AD-A216637 ..... N90-18844 #
AD-A216662 ..... N90-18534 #
AD-A216664 ..... N90-18897 #
AD-A216668 ..... N90-18574 #
AD-A216669 ..... N90-18575 #
AD-A216673 ..... N90-18738 #
AD-A216697 ..... N90-19035 #
AD-A216708 ..... N90-18617 #
AD-A216710 ..... N90-18535 #
AD-A216711 ..... N90-18871 #
AD-A216714 ..... N90-18388 #
AD-A216715 ..... N90-18576 #
AD-A216716 ..... N90-18915 #
AD-A216717 ..... N90-18939 #
AD-A216718 ..... N90-19036 #
AD-A216722 ..... N90-18618 #
AD-A216723 ..... N90-18619 #
AD-A216724 ..... N90-18381 #
AD-A216726 ..... N90-18512 #
AD-A216727 ..... N90-18536 #
AD-A216728 ..... N90-19037 #
AD-A216729 ..... N90-18537 #
AD-A216730 ..... N90-19038 #
AD-A216739 ..... N90-18538 #
AD-A216740 ..... N90-18492 #
AD-A216741 ..... N90-18860 #
AD-A216743 ..... N90-18861 #
AD-A216745 ..... N90-18898 #
AD-A216750 ..... N90-18620 #
AD-A216751 ..... N90-18430 #
AD-A216752 ..... N90-18845 #
AD-A216761 ..... N90-18382 #
AD-A216763 ..... N90-18643 #
AD-A216764 ..... N90-18513 #
AD-A216766 ..... N90-18862 #
AD-A216767 ..... N90-18553 #
AD-A216769 ..... N90-18851 #
AD-A216775 ..... N90-18846 #
AD-A216776 ..... N90-19013 #
AD-A216778 ..... N90-18899 #
AD-A216779 ..... N90-18940 #
AD-A216794 ..... N90-18644 #
AD-A216796 ..... N90-18514 #
AD-A216797 ..... N90-18645 #
AD-A216798 ..... N90-18374 #
AD-A216800 ..... N90-18916 #
AD-A216801 ..... N90-18917 #
AD-A216802 ..... N90-18918 #
AD-A216803 ..... N90-18941 #
AD-A216804 ..... N90-18919 #
AD-A216805 ..... N90-18900 #
AD-A216811 ..... N90-18942 #
AD-A216818 ..... N90-18646 #
AD-A216828 ..... N90-18389 #
AD-A216829 ..... N90-18863 #
AD-A216832 ..... N90-18621 #
AD-A216834 ..... N90-18749 #
AD-A216836 ..... N90-18515 #
AD-A216840 ..... N90-18554 #
AD-A216843 ..... N90-18779 #
AD-A216857 ..... N90-18800 #
AD-A216881 ..... N90-18516 #
AD-A216907 ..... N90-18647 #
AD-A216911 ..... N90-18901 #
AD-A216916 ..... N90-18622 #
AD-A216925 ..... N90-18383 #
AD-A216931 ..... N90-18648 #
AD-A216937 ..... N90-18920 #
AD-A216938 ..... N90-19185 #
AD-A216939 ..... N90-18847 #
AD-A216943 ..... N90-18902 #
AD-A216944 ..... N90-18903 #
AD-A216945 ..... N90-18673 #
AD-A216946 ..... N90-18577 #
AD-A216947 ..... N90-18578 #
AD-A216950 ..... N90-18750 #
AD-A216968 ..... N90-18517 #
AD-A216974 ..... N90-18539 #
AD-A216979 ..... N90-18443 #
AD-A216981 ..... N90-18674 #
AD-A217012 ..... N90-18864 #
AD-A217025 ..... N90-18780 #
AD-A217026 ..... N90-18540 #
AD-A217028 ..... N90-18579 #
AD-A217029 ..... N90-18872 #
AD-A217034 ..... N90-18580 #

AD-E501181 ..... N90-18898 #

AEDC-TR-89-14 ..... N90-18387 #

AEFA-89-14 ..... N90-18430 #

AFGL-TR-89-0022 ..... N90-18830 #

AFHRL-TP-89-15 ..... N90-18870 #

AFHRL-TR-89-4 ..... N90-18620 #

AFIT/DS/ENP/89-4 ..... N90-19031 #

AFIT/GA/ENY/89D-4 ..... N90-18451 #

AFIT/GAE/ENY/89D-16 ..... N90-18668 #
AFIT/GAE/ENY/89D-31 ..... N90-19057 #

AFIT/GCE/ENG/89D-6 ..... N90-18637 #

AFIT/GCS/ENG/89D-18 ..... N90-18890 #

AFIT/GE/ENG/89-12 ..... N90-18431 #
AFIT/GE/ENG/89D-48 ..... N90-18388 #

AFIT/GEO/ENG/89D-5 ..... N90-19011 #

AFIT/GEP/ENP/89D-5 ..... N90-18718 #

AFIT/GSO/ENG/89D-10 ..... N90-18841 #

AFOSR-89-0460TR ..... N90-18492 #
AFOSR-89-1671TR ..... N90-18553 #
AFOSR-89-1672TR ..... N90-18576 #
AFOSR-89-1673TR ..... N90-18939 #
AFOSR-89-1674TR ..... N90-18864 #
AFOSR-89-1676TR ..... N90-18860 #
AFOSR-89-1677TR ..... N90-18861 #
AFOSR-89-1678TR ..... N90-18872 #
AFOSR-89-1679TR ..... N90-18538 #
AFOSR-89-1686TR ..... N90-18942 #
AFOSR-89-1688TR ..... N90-19035 #
AFOSR-89-1699TR ..... N90-19185 #
AFOSR-89-1700TR ..... N90-18920 #
AFOSR-89-1702TR ..... N90-18841 #
AFOSR-89-1711TR ..... N90-18491 #
AFOSR-89-1717TR ..... N90-18908 #
AFOSR-89-1719TR ..... N90-18932 #
AFOSR-89-1720TR ..... N90-18931 #
AFOSR-89-1729TR ..... N90-18937 #
AFOSR-89-1735TR ..... N90-18936 #
AFOSR-89-1752TR ..... N90-18897 #
AFOSR-89-1754TR ..... N90-18534 #
AFOSR-89-1779TR ..... N90-18533 #
AFOSR-89-1817TR ..... N90-18717 #
AFOSR-89-1818TR ..... N90-18570 #
AFOSR-89-1819TR ..... N90-18493 #
AFOSR-89-1862TR ..... N90-18933 #
AFOSR-89-1864TR ..... N90-18938 #
AFOSR-89-1875TR ..... N90-19034 #
AFOSR-89-1876TR ..... N90-19003 #
AFOSR-89-1877TR ..... N90-18671 #
AFOSR-89-1878TR ..... N90-18672 #
AFOSR-89-1884TR ..... N90-18858 #
AFOSR-89-1895TR ..... N90-18748 #
AFOSR-89-1896TR ..... N90-19002 #

AGARD-AR-229 ..... N90-18432 #

AGARD-CAL-90/1 ..... N90-19080 #

AGARD-CP-468 ..... N90-18405 #

AGARD-R-789 ..... N90-18396 #

AI-M-1146 ..... N90-18871 #
AI-M-1157 ..... N90-18862 #
AI-M-1177 ..... N90-18915 #

AI-TR-1089 ..... N90-18896 #
AI-TR-1109 ..... N90-18917 #
AI-TR-1113 ..... N90-18382 #
AI-TR-1139 ..... N90-18916 #
AI-TR-1151 ..... N90-18918 #
AI-TR-1154 ..... N90-18914 #
AI-TR-1162 ..... N90-18919 #
AI-TR-1163 ..... N90-18900 #
AI-TR-1170 ..... N90-18941 #

ALS/TR-89-02 ..... N90-18565 #

ANL-HEP-CP-89-100 ..... N90-19183 #

ANL-89/41 ..... N90-18909 #

ANL/ACL-89/2 ..... N90-18542 #

ANL/MCS-TM-136 ..... N90-18910 #

APL-UW-TR-8926 ..... N90-18889 #

ARCCB-TR-89032 ..... N90-18515 #

ARO-21113.2-EG ..... N90-18443 #
ARO-23547.2-CH ..... N90-18577 #
ARO-23801.5-MS-F ..... N90-18578 #
ARO-24461.12-EG ..... N90-18674 #
ARO-25229.7-CH ..... N90-18580 #

ASQBG-A-89-026 ..... N90-18903 #

ASQBG-I-89-011 ..... N90-18902 #
ASQBG-I-89-025 ..... N90-18901 #

ATR-89(4752)-3 ..... N90-18532 #

AVSCOM-TM-90-B-001 ..... N90-18746* #

BAR-89-2 ..... N90-18361 #
BAR-89-3 ..... N90-18388 #

BCRS-89-09 ..... N90-18549 #
BCRS-89-13 ..... N90-18783 #
BCRS-89-14 ..... N90-18784 #
BCRS-89-15 ..... N90-18785 #
BCRS-89-17 ..... N90-18786 #
BCRS-89-18 ..... N90-18787 #
BCRS-89-19 ..... N90-18788 #
BCRS-89-21 ..... N90-18789 #
BCRS-89-27 ..... N90-18790 #
BCRS-89-28 ..... N90-18791 #

BNL-42934 ..... N90-18867 #
BNL-43129 ..... N90-18529 #
BNL-43538 ..... N90-18706 #
BNL-43806 ..... N90-18866 #

BRA-89-347R ..... N90-18714 #
BRA-89-349R ..... N90-18715 #

BU-403 ..... N90-18369 #

CBL-REPRINT-17 ..... N90-18589 #

CBL-41 ..... N90-18520 #

CEAT-NT-10/S/83 ..... N90-18376 #

CERMA-89-25 ..... N90-18866 #

CMU/SEI-89-TR-16 ..... N90-18888 #

CONF-890160-2 ..... N90-18655 #
CONF-890572-1 ..... N90-18812 #
CONF-890610-7 ..... N90-18382 #
CONF-890660-10 ..... N90-18627 #
CONF-890665-54 ..... N90-18651 #
CONF-890701-25 ..... N90-18552 #
CONF-890902-23 ..... N90-18820 #
CONF-891055-6 ..... N90-18719 #
CONF-891055-12 ..... N90-19029 #
CONF-891073-4 ..... N90-19056 #
CONF-891093-23 ..... N90-18583 #
CONF-891094-14 ..... N90-18911 #
CONF-891119-46 ..... N90-19030 #
CONF-891119-80 ..... N90-18713 #
CONF-891119-85 ..... N90-19045 #
CONF-891119-88 ..... N90-19043 #
CONF-891119-89 ..... N90-19042 #
CONF-891119-90 ..... N90-19041 #
CONF-891119-93 ..... N90-18519 #
CONF-891119-94 ..... N90-19052 #
CONF-891119-95 ..... N90-19051 #
CONF-891119-97 ..... N90-18598 #
CONF-891119-98 ..... N90-18564 #
CONF-891204-14 ..... N90-18551 #
CONF-891208-29 ..... N90-18753 #
CONF-891210-1 ..... N90-18792 #
CONF-891260-8 ..... N90-19182 #
CONF-891261-4 ..... N90-18723 #
CONF-891261-6 ..... N90-18722 #
CONF-891261-7 ..... N90-18726 #
CONF-891274-1 ..... N90-19050 #
CONF-891276-1 ..... N90-19017 #
CONF-891276-2 ..... N90-19188 #
CONF-891276-3 ..... N90-19189* #
CONF-900109-18 ..... N90-18607 #
CONF-900109-20 ..... N90-19008 #
CONF-900109-21 ..... N90-19009 #
CONF-900109-22 ..... N90-19010 #
CONF-900122-7 ..... N90-19183 #
CONF-900140-4 ..... N90-18657 #
CONF-900140-7 ..... N90-18823 #
CONF-900140-8 ..... N90-18726 #
CONF-900143-16 ..... N90-18665 #
CONF-900143-17 ..... N90-18702 #
CONF-900159-1 ..... N90-18652 #
CONF-900160-1 ..... N90-18518 #
CONF-900160-2 ..... N90-18586 #
CONF-900160-3 ..... N90-18594 #
CONF-900246-1 ..... N90-18856 #
CONF-900254-1 ..... N90-18708 #
CONF-900266-1 ..... N90-18595 #
CONF-900280-1 ..... N90-18659 #
CONF-900329-2 ..... N90-18904 #
CONF-900378-2 ..... N90-18921 #
CONF-900378-3 ..... N90-18878 #
CONF-900393-1 ..... N90-18592 #
CONF-900394-1 ..... N90-18602 #
CONF-8612178 ..... N90-18795 #
CONF-8809424-1 ..... N90-18819 #
CONF-8810464-SUMM ..... N90-18801 #
CONF-8904259-2 ..... N90-18608 #
CONF-8905192-3 ..... N90-18707 #
CONF-8905194-7 ..... N90-18706 #
CONF-8906225-2 ..... N90-19187 #
CONF-8906269-5 ..... N90-18868 #
CONF-8906282-1 ..... N90-19049 #
CONF-8906283-1 ..... N90-18867 #
CONF-8907183-1 ..... N90-18729 #
CONF-8908134-20 ..... N90-18712 #
CONF-8908134-24 ..... N90-18720 #
CONF-8908134-27 ..... N90-18725 #
CONF-8908189-2 ..... N90-19058 #
CONF-8908209-1 ..... N90-19024 #
CONF-8909293-1 ..... N90-19004 #
CONF-8909296-SUMM ..... N90-18910 #
CONF-8910107-9 ..... N90-18584 #
CONF-8910162-6 ..... N90-18797 #
CONF-8910192-8-REV-1 ..... N90-18550 #
CONF-8910248-4 ..... N90-18741 #
CONF-8910248-5 ..... N90-18603 #
CONF-8910248-6 ..... N90-18593 #
CONF-8910308-2 ..... N90-19172 #
CONF-8910358-1 ..... N90-19625 #
CONF-8911130-12 ..... N90-19021 #
CONF-8911161-1 ..... N90-19186 #

CPIA-PUBL-515-VOL-1 ..... N90-18462 #

CRIE-T-87080 ..... N90-18635 #
CRIE-T-87090 ..... N90-18636 #
CRIE-T-87109 ..... N90-18698 #

DE89-009426 ..... N90-18801 #
DE89-009478 ..... N90-18810 #
DE89-009489 ..... N90-18809 #
DE89-009502 ..... N90-18802 #
DE89-009510 ..... N90-18803 #
DE89-009513 ..... N90-18792 #
DE89-782293 ..... N90-18666 #
DE89-782296 ..... N90-18795 #
DE89-782319 ..... N90-18698 #
DE89-782321 ..... N90-18635 #
DE89-782323 ..... N90-18636 #
DE89-910215 ..... N90-18793 #
DE89-910216 ..... N90-18794 #
DE90-000309 ..... N90-18581 #
DE90-000312 ..... N90-18362 #
DE90-000403 ..... N90-18676 #
DE90-000435 ..... N90-18545 #
DE90-002414 ..... N90-19049 #
DE90-002466 ..... N90-18856 #
DE90-003235 ..... N90-19182 #
DE90-003396 ..... N90-18819 #
DE90-003896 ..... N90-18550 #
DE90-003969 ..... N90-18529 #
DE90-004005 ..... N90-18585 #
DE90-004842 ..... N90-19030 #
DE90-004846 ..... N90-18712 #
DE90-004870 ..... N90-19050 #
DE90-004878 ..... N90-18551 #
DE90-004957 ..... N90-18867 #
DE90-005290 ..... N90-18600 #
DE90-005368 ..... N90-19056 #
DE90-005377 ..... N90-18796 #
DE90-005390 ..... N90-18552 #
DE90-005404 ..... N90-18713 #
DE90-005469 ..... N90-18566 #
DE90-005532 ..... N90-18910 #
DE90-005535 ..... N90-18797 #
DE90-005540 ..... N90-18607 #
DE90-005546 ..... N90-18714 #
DE90-005552 ..... N90-18505 #
DE90-005553 ..... N90-18506 #
DE90-005558 ..... N90-19001 #
DE90-005560 ..... N90-18652 #
DE90-005567 ..... N90-18706 #
DE90-005643 ..... N90-18820 #
DE90-005647 ..... N90-19183 #
DE90-005651 ..... N90-18518 #
DE90-005654 ..... N90-18904 #
DE90-005670 ..... N90-18921 #
DE90-005674 ..... N90-18876 #
DE90-005710 ..... N90-18541 #
DE90-005712 ..... N90-18649 #
DE90-005720 ..... N90-18582 #
DE90-005721 ..... N90-18804 #
DE90-005722 ..... N90-18805 #
DE90-005723 ..... N90-18555 #
DE90-005744 ..... N90-18677 #
DE90-005757 ..... N90-19039 #
DE90-005758 ..... N90-18650 #
DE90-005805 ..... N90-18955 #
DE90-005810 ..... N90-18656 #
DE90-005813 ..... N90-19178 #
DE90-005815 ..... N90-19179 #
DE90-005825 ..... N90-19028 #
DE90-005829 ..... N90-18833 #
DE90-005981 ..... N90-19005 #
DE90-006033 ..... N90-18542 #
DE90-006040 ..... N90-18583 #
DE90-006072 ..... N90-18719 #
DE90-006073 ..... N90-18806 #
DE90-006087 ..... N90-18584 #
DE90-006096 ..... N90-19024 #
DE90-006098 ..... N90-18720 #

DE90-006099 ..... N90-19058 #
DE90-006105 ..... N90-18865 #
DE90-006116 ..... N90-18702 #
DE90-006118 ..... N90-19020 #
DE90-006142 ..... N90-19025 #
DE90-006154 ..... N90-18586 #
DE90-006160 ..... N90-19004 #
DE90-006168 ..... N90-19006 #
DE90-006237 ..... N90-19040 #
DE90-006263 ..... N90-18857 #
DE90-006264 ..... N90-18651 #
DE90-006272 ..... N90-18821 #
DE90-006318 ..... N90-18556 #
DE90-006323 ..... N90-18585 #
DE90-006347 ..... N90-18624 #
DE90-006353 ..... N90-18524 #
DE90-006354 ..... N90-18837 #
DE90-006357 ..... N90-18727 #
DE90-006370 ..... N90-18658 #
DE90-006371 ..... N90-18525 #
DE90-006382 ..... N90-18909 #
DE90-006422 ..... N90-18721 #
DE90-006425 ..... N90-18879 #
DE90-006436 ..... N90-19007 #
DE90-006460 ..... N90-18911 #
DE90-006465 ..... N90-18626 #
DE90-006474 ..... N90-18690 #
DE90-006480 ..... N90-19187 #
DE90-006487 ..... N90-18557 #
DE90-006488 ..... N90-18822 #
DE90-006494 ..... N90-18591 #
DE90-006497 ..... N90-18691 #
DE90-006504 ..... N90-18722 #
DE90-006509 ..... N90-18602 #
DE90-006511 ..... N90-18625 #
DE90-006519 ..... N90-18723 #
DE90-006521 ..... N90-19021 #
DE90-006533 ..... N90-18558 #
DE90-006536 ..... N90-18659 #
DE90-006547 ..... N90-19171 #
DE90-006564 ..... N90-19041 #
DE90-006565 ..... N90-19042 #
DE90-006568 ..... N90-19043 #
DE90-006589 ..... N90-19044 #
DE90-006593 ..... N90-18943 #
DE90-006600 ..... N90-18834 #
DE90-006613 ..... N90-18592 #
DE90-006629 ..... N90-19045 #
DE90-006640 ..... N90-18587 #
DE90-006648 ..... N90-19046 #
DE90-006667 ..... N90-19186 #
DE90-006700 ..... N90-18610 #
DE90-006761 ..... N90-18860 #
DE90-006765 ..... N90-18868 #
DE90-006774 ..... N90-18707 #
DE90-006782 ..... N90-18608 #
DE90-006851 ..... N90-18741 #
DE90-006863 ..... N90-19022 #
DE90-006864 ..... N90-19023 #
DE90-006881 ..... N90-19029 #
DE90-006885 ..... N90-18811 #
DE90-006902 ..... N90-19014 #
DE90-006903 ..... N90-19015 #
DE90-006905 ..... N90-19016 #
DE90-006907 ..... N90-18653 #
DE90-006921 ..... N90-19172 #
DE90-006936 ..... N90-18739 #
DE90-006955 ..... N90-18692 #
DE90-006989 ..... N90-18627 #
DE90-006993 ..... N90-19017 #
DE90-006994 ..... N90-19188 #
DE90-007046 ..... N90-18562 #
DE90-007050 ..... N90-18593 #
DE90-007053 ..... N90-18603 #
DE90-007062 ..... N90-18753 #
DE90-007063 ..... N90-19051 #
DE90-007074 ..... N90-18564 #
DE90-007078 ..... N90-19052 #
DE90-007085 ..... N90-18655 #
DE90-007087 ..... N90-19026 #
DE90-007112 ..... N90-18945 #
DE90-007126 ..... N90-18594 #
DE90-007130 ..... N90-18595 #
DE90-007146 ..... N90-19008 #
DE90-007147 ..... N90-19009 #
DE90-007148 ..... N90-19010 #
DE90-007168 ..... N90-18708 #
DE90-007179 ..... N90-18596 #
DE90-007188 ..... N90-18604 #
DE90-007241 ..... N90-18823 #
DE90-007242 ..... N90-18728 #
DE90-007246 ..... N90-18729 #
DE90-007249 ..... N90-18730 #
DE90-007253 ..... N90-19169* #
DE90-007276 ..... N90-18598 #
DE90-007298 ..... N90-19027 #
DE90-007333 ..... N90-18597 #
DE90-007345 ..... N90-19059 #
DE90-007365 ..... N90-18546 #
DE90-007373 ..... N90-18693 #
DE90-007374 ..... N90-18998 #
DE90-007381 ..... N90-19053 #
DE90-007400 ..... N90-19000 #
DE90-007419 ..... N90-19054 #
DE90-007422 ..... N90-18563 #
DE90-007595 ..... N90-18812 #
DE90-007828 ..... N90-18725 #
DE90-007830 ..... N90-18726 #
DE90-007835 ..... N90-18519 #
DE90-606054 ..... N90-19180 #
DE90-606613 ..... N90-18678 #
DE90-610619 ..... N90-18835 #
DE90-610640 ..... N90-19173 #
DE90-610641 ..... N90-19174 #
DE90-610645 ..... N90-19175 #
DE90-610647 ..... N90-19176 #
DE90-610648 ..... N90-19177 #
DE90-610663 ..... N90-19047 #
DE90-610664 ..... N90-19048 #
DE90-610665 ..... N90-18588 #
DE90-742056 ..... N90-18807 #

DFVLR-FB-88-54 ..... N90-18696 #
DFVLR-FB-89-02 ..... N90-18543 #
DFVLR-FB-89-03 ..... N90-18742 #
DFVLR-FB-89-11 ..... N90-18580 #

DFVLR-IB-303-88/2 ..... N90-18438 #

DFVLR-MITT-89-01 ..... N90-18711 #
DFVLR-MITT-89-02 ..... N90-18609 #
DFVLR-MITT-89-05 ..... N90-18436 #
DFVLR-MITT-89-09 ..... N90-18445 #
DFVLR-MITT-89-10 ..... N90-18446 #

DHV-JWVDB-8902 ..... N90-18786 #

DIGEL-1989-6 ..... N90-18661 #
DIGEL-1989-8 ..... N90-18663 #
DIGEL-1989-9 ..... N90-18660 #

DIOR/DOD-5000.12-M ..... N90-19046 #

DLR-FB-89-39 ..... N90-18548 #
DLR-FB-89-47 ..... N90-18629 #
DLR-FB-89-48 ..... N90-18630 #
DLR-FB-89-52 ..... N90-18377 #

DLR-MITT-89-19 ..... N90-18662 #
DLR-MITT-89-20 ..... N90-18370 #

DNA-TR-88-175 ..... N90-18613 #
DNA-TR-89-132 ..... N90-18511 #

DOE/CE-15325/T4 ..... N90-18610 #
DOE/CE-90001/7 ..... N90-18591 #

DOE/CH-10093/83-VOL-2 ..... N90-18810 #
DOE/CH-10093/74 ..... N90-18809 #

DOE/DP-20153/T1 ..... N90-18653 #
DOE/DP-20153/T3 ..... N90-19016 #
DOE/DP-20153/T5 ..... N90-19015 #
DOE/DP-20153/T6 ..... N90-19014 #

DOE/ER-10587/T11 ..... N90-19171 #
DOE/ER-13403/2 ..... N90-18566 #
DOE/ER-13590/7 ..... N90-18633 #
DOE/ER-13670/1 ..... N90-18634 #
DOE/ER-13825/2 ..... N90-19059 #
DOE/ER-13985/1 ..... N90-18548 #
DOE/ER-14045/1 ..... N90-18585 #
DOE/ER-25001/26 ..... N90-18680 #
DOE/ER-25026/34 ..... N90-18943 #
DOE/ER-40039/39 ..... N90-19182 #
DOE/ER-40105/580 ..... N90-19006 #
DOE/ER-40121/T2 ..... N90-19040 #
DOE/ER-40121/T3 ..... N90-19000 #
DOE/ER-40211/5 ..... N90-19001 #
DOE/ER-40283/9 ..... N90-19005 #
DOE/ER-45113/5 ..... N90-19054 #
DOE/ER-45115/6 ..... N90-18587 #
DOE/ER-45118/5 ..... N90-19044 #
DOE/ER-45162/4 ..... N90-19046 #
DOE/ER-45205/5 ..... N90-18557 #
DOE/ER-45319/T1 ..... N90-19053 #
DOE/ER-45354/T2 ..... N90-18556 #
DOE/ER-45368/2 ..... N90-18596 #
DOE/ER-52144/T1 ..... N90-19027 #
DOE/ER-60422/5 ..... N90-18822 #

DOE/ET-53088/280 ..... N90-19056 #
DOE/ET-53088/405 ..... N90-19022 #
DOE/ET-53088/409 ..... N90-19023 #
DOE/ET-53088/413 ..... N90-19026 #

DOE/ID-12735/T5 ..... N90-18597 #

DOE/MC-23250/2750 ..... N90-18676 #
DOE/MC-23259/2781 ..... N90-18545 #

DOE/NASA/0282-1 ..... N90-18559* #

DOE/PC-79931/T5 ..... N90-18796 #
DOE/PC-90013/T10 ..... N90-18600 #
DOE/PC-90013/T11 ..... N90-18604 #
DOE/PC-90957/T8 ..... N90-18691 #

DOT/FAA/AM-89/9 ..... N90-18675 #
DOT/FAA/AM-89/12-PHASE-1/2 ..... N90-18374 #

DOT/FAA/CT-TN89/28-VOL-2 ..... N90-18360 #

DOT/FAA/CT-89/17 ..... N90-18375 #

DOT/FAA/DS-89/14 ..... N90-18371* #
DOT/FAA/DS-89/15 ..... N90-18372* #

DP-MS-89-83-REV-1 ..... N90-18550 #

DREO-TN-89-19 ..... N90-18619 #
DREO-TN-89-24 ..... N90-18618 #

DREO-1015 ..... N90-18381 #

DT-310/88 ..... N90-18544 #
DT-311/88 ..... N90-18526 #

DTRC/SME-89-20 ..... N90-18513 #

E-4911 ..... N90-18740* #
E-5042 ..... N90-18504* #
E-5110 ..... N90-18665* #
E-5229 ..... N90-18667* #
E-5291 ..... N90-18927* #
E-5303 ..... N90-18745* #
E-5334 ..... N90-18634* #

ECN-219 ..... N90-19055 #

EGG-EAST-8491 ..... N90-18692 #

EGG-M-89410 ..... N90-18655 #

EGG-MS-8714 ..... N90-18562 #

EOARD-LR-89-050 ..... N90-18494 #

EPA/600/3-89/076 ..... N90-18813 #
EPA/600/4-89/033 ..... N90-18814 #

ERP-1019 ..... N90-18830 #

ESA-BR-36 ..... N90-18782 #

ESA-PSS-01-11-ISSUE-1 ..... N90-19061 #
ESA-PSS-01-40-ISSUE-2 ..... N90-18460 #
ESA-PSS-01-60-ISSUE-2 ..... N90-19062 #
ESA-PSS-01-729-ISSUE-1 ..... N90-18461 #
ESA-PSS-03-108-ISSUE-1-VOL-1 ..... N90-18455 #
ESA-PSS-03-108-ISSUE-1-VOL-2 ..... N90-18456 #
ESA-PSS-03-108-ISSUE-1-VOL-3 ..... N90-18457 #
ESA-PSS-03-108-ISSUE-1-VOL-4 ..... N90-18458 #
ESA-PSS-03-1101-ISSUE-1-REV-1 ..... N90-18459 #
ESA-PSS-04-106-ISSUE-1 ..... N90-18447 #

ESA-SP-290 ..... N90-19064 #
ESA-SP-1112 ..... N90-18848 #
ESA-SP-1122 ..... N90-19066 #

ESA-TT-1117 ..... N90-18521 #
ESA-TT-1148 ..... N90-18696 #
ESA-TT-1149 ..... N90-18543 #
ESA-TT-1150 ..... N90-18742 #
ESA-TT-1153 ..... N90-18711 #
ESA-TT-1154 ..... N90-18609 #
ESA-TT-1156 ..... N90-18436 #
ESA-TT-1157 ..... N90-18836 #
ESA-TT-1158 ..... N90-18956 #
ESA-TT-1169 ..... N90-18697 #
ESA-TT-1171 ..... N90-18633 #
ESA-TT-1175 ..... N90-18445 #
ESA-TT-1176 ..... N90-18446 #
ESA-TT-1178 ..... N90-18580 #
ESA-TT-1195 ..... N90-18370 #
ESA-TT-1196 ..... N90-18662 #
ESA-TT-1197 ..... N90-18630 #
ESA-TT-1198 ..... N90-18548 #

ESD-TR-89-24 ..... N90-18888 #
ESD-TR-89-291 ..... N90-18845 #

ESG-80 ..... N90-18720 #

ETDE/JP-MF-9782296 ..... N90-18795 #

ETN-90-96207 ..... N90-18589 #
ETN-90-96208 ..... N90-18520 #
ETN-90-96211 ..... N90-18455 #
ETN-90-96212 ..... N90-18456 #
ETN-90-96213 ..... N90-18457 #
ETN-90-96214 ..... N90-18458 #
ETN-90-96215 ..... N90-18521 #
ETN-90-96216 ..... N90-18543 #
ETN-90-96217 ..... N90-18742 #
ETN-90-96218 ..... N90-18609 #
ETN-90-96219 ..... N90-18436 #
ETN-90-96220 ..... N90-18836 #
ETN-90-96221 ..... N90-18956 #
ETN-90-96222 ..... N90-18445 #
ETN-90-96223 ..... N90-18446 #
ETN-90-96224 ..... N90-18560 #
ETN-90-96225 ..... N90-19084 #
ETN-90-96226 ..... N90-18848 #
ETN-90-96227 ..... N90-19068 #
ETN-90-96228 ..... N90-18544 #
ETN-90-96229 ..... N90-18526 #
ETN-90-96230 ..... N90-18435 #
ETN-90-96231 ..... N90-18527 #
ETN-90-96232 ..... N90-18528 #
ETN-90-96234 ..... N90-18731 #
ETN-90-96235 ..... N90-18732 #
ETN-90-96236 ..... N90-18733 #
ETN-90-96237 ..... N90-18391 #
ETN-90-96239 ..... N90-18703 #
ETN-90-96240 ..... N90-18679 #
ETN-90-96241 ..... N90-18704 #
ETN-90-96242 ..... N90-18680 #
ETN-90-96243 ..... N90-18705 #
ETN-90-96244 ..... N90-18392 #
ETN-90-96245 ..... N90-18709 #
ETN-90-96246 ..... N90-18724 #
ETN-90-96247 ..... N90-18365 #
ETN-90-96248 ..... N90-18681 #
ETN-90-96249 ..... N90-18605 #
ETN-90-96250 ..... N90-18694 #
ETN-90-96251 ..... N90-18547 #
ETN-90-96252 ..... N90-18366 #
ETN-90-96253 ..... N90-18695 #
ETN-90-96254 ..... N90-18682 #
ETN-90-96255 ..... N90-18683 #
ETN-90-96256 ..... N90-18686 #
ETN-90-96257 ..... N90-18367 #
ETN-90-96258 ..... N90-18376 #
ETN-90-96259 ..... N90-19055 #
ETN-90-96260 ..... N90-18905 #
ETN-90-96261 ..... N90-18628 #
ETN-90-96262 ..... N90-18754 #
ETN-90-96263 ..... N90-18660 #
ETN-90-96264 ..... N90-18755 #
ETN-90-96265 ..... N90-18384 #
ETN-90-96266 ..... N90-18661 #
ETN-90-96267 ..... N90-18590 #
ETN-90-96268 ..... N90-18684 #
ETN-90-96269 ..... N90-18944 #
ETN-90-96270 ..... N90-18561 #
ETN-90-96271 ..... N90-18654 #
ETN-90-96272 ..... N90-18368 #
ETN-90-96273 ..... N90-18952 #
ETN-90-96274 ..... N90-18662 #
ETN-90-96275 ..... N90-18370 #
ETN-90-96276 ..... N90-18548 #
ETN-90-96277 ..... N90-18629 #
ETN-90-96278 ..... N90-18630 #
ETN-90-96279 ..... N90-18377 #
ETN-90-96280 ..... N90-19189 #
ETN-90-96281 ..... N90-18781 #
ETN-90-96282 ..... N90-18437 #
ETN-90-96283 ..... N90-18438 #
ETN-90-96284 ..... N90-18710 #
ETN-90-96285 ..... N90-18631 #
ETN-90-96286 ..... N90-18369 #
ETN-90-96287 ..... N90-18999
ETN-90-96288 ..... N90-18685 #
ETN-90-96289 ..... N90-18686 #
ETN-90-96291 ..... N90-19168 #
ETN-90-96292 ..... N90-18522 #
ETN-90-96293 ..... N90-18687 #
ETN-90-96294 ..... N90-18523 #
ETN-90-96295 ..... N90-18688 #
ETN-90-96296 ..... N90-18689 #
ETN-90-96297 ..... N90-18459 #
ETN-90-96298 ..... N90-18782 #
ETN-90-96300 ..... N90-19061 #
ETN-90-96301 ..... N90-18460 #
ETN-90-96302 ..... N90-19062 #
ETN-90-96303 ..... N90-18461 #
ETN-90-96304 ..... N90-18447 #
ETN-90-96305 ..... N90-18606 #
ETN-90-96306 ..... N90-18953 #
ETN-90-96307 ..... N90-18946 #
ETN-90-96308 ..... N90-18954 #
ETN-90-96309 ..... N90-18947 #
ETN-90-96310 ..... N90-18922 #
ETN-90-96311 ..... N90-18948 #
ETN-90-96312 ..... N90-18906 #
ETN-90-96313 ..... N90-18907 #
ETN-90-96314 ..... N90-18949 #
ETN-90-96315 ..... N90-18923 #
ETN-90-96316 ..... N90-18549 #
ETN-90-96317 ..... N90-18783 #
ETN-90-96318 ..... N90-18784 #
ETN-90-96319 ..... N90-18785 #
ETN-90-96320 ..... N90-18786 #
ETN-90-96321 ..... N90-18787 #
ETN-90-96322 ..... N90-18788 #
ETN-90-96323 ..... N90-18789 #
ETN-90-96324 ..... N90-18790 #
ETN-90-96325 ..... N90-18791 #
ETN-90-96326 ..... N90-18632 #
ETN-90-96327 ..... N90-18663 #
ETN-90-96329 ..... N90-18696 #
ETN-90-96330 ..... N90-18711 #
ETN-90-96331 ..... N90-18697 #
ETN-90-96332 ..... N90-18633 #

FCR-10555A ..... N90-18808* #

FLOW-RR-494 ..... N90-18535 #

FOA-C-20770-2.1 ..... N90-18606 #

FR-716199-14 ..... N90-18390* #

FTD-ID(RS)T-0712-89 ..... N90-18616 #
FTD-ID(RS)T-0718-89 ..... N90-18514 #

GL-ERP-1033 ..... N90-18844 #

GL-TR-89-0175 ..... N90-18844 #
GL-TR-89-0269 ..... N90-19170 #

H-1544 ..... N90-18395* #

HNEI-89-1004-PHASE-1 ..... N90-18811 #

HPTC-07 ..... N90-18666 #

IC-89/103 ..... N90-18835 #
IC-89/184 ..... N90-19175 #
IC-89/219 ..... N90-19176 #
IC-89/222 ..... N90-19173 #
IC-89/270 ..... N90-19047 #
IC-89/271 ..... N90-19048 #
IC-89/299 ..... N90-19174 #

ICASE-90-14 ..... N90-18363* #

ICMA-89-142 ..... N90-18935 #
ICMA-89-143 ..... N90-18934 #

ICOMP-90-02 ..... N90-18927* #

IDA-P-2321-VOL-1 ..... N90-18398 #

IDA/HQ-89-34914-VOL-1 ..... N90-18898 #

IEE-SR-205 ..... N90-18793 #
IEE-SR-206 ..... N90-18794 #

IFSR-280 ..... N90-19056 #
IFSR-405 ..... N90-19022 #
IFSR-409 ..... N90-19023 #
IFSR-413 ..... N90-19026 #

INPE-4575-RPE/567 ..... N90-18772 #
INPE-4760-TDL/348 ..... N90-18450 #
INPE-4785-TDL/351 ..... N90-19018 #
INPE-4791-RPE/584 ..... N90-18768 #
INPE-4795-PRE/1449 ..... N90-18796 #
INPE-4798-NTE/287 ..... N90-18439 #
INPE-4801-TDL/356 ..... N90-18950 #
INPE-4807-MD/40 ..... N90-18926 #
INPE-4810-TDL/357 ..... N90-19184 #
INPE-4811-TDL/358 ..... N90-18827 #
INPE-4813-TDL/360 ..... N90-18737 #
INPE-4814-RPE/590 ..... N90-18777 #
INPE-4815-TDL/361 ..... N90-18442 #
INPE-4816-TDL/362 ..... N90-18884 #
INPE-4817-PRE/1453 ..... N90-18775 #
INPE-4821-RPE/591 ..... N90-18826 #
INPE-4826-PRE/1457 ..... N90-18825 #
INPE-4827-PRE/1458 ..... N90-18781 #
INPE-4834-PRE/1464 ..... N90-18776 #
INPE-4836-PRE/1465 ..... N90-18759 #
INPE-4838-PRE/1467 ..... N90-18758 #
INPE-4840-PRE/1469 ..... N90-18816 #
INPE-4843-PRE/1472 ..... N90-18767 #
INPE-4848-PRE/1477 ..... N90-18760 #
INPE-4850-TDL/365 ..... N90-18765 #
INPE-4860-TDL/371 ..... N90-18771 #
INPE-4861-TDL/372 ..... N90-18886 #
INPE-4864-TDL/375 ..... N90-18736 #
INPE-4866-TDL/377 ..... N90-18449 #
INPE-4867-PRE/1478 ..... N90-18766 #
INPE-4871-PRE/1482 ..... N90-18701 #
INPE-4875-PRE/1486 ..... N90-18815 #
INPE-4876-PRE/1487 ..... N90-18756 #
INPE-4879-RPE/593 ..... N90-18883 #
INPE-4887-TDL/378 ..... N90-18839 #
INPE-4888-TDL/379 ..... N90-18778 #
INPE-4895-PRE/1496 ..... N90-18829 #
INPE-4897-PRE/1498 ..... N90-18769 #
INPE-4900-PRE/1501 ..... N90-18762 #
INPE-4901-PRE/1502 ..... N90-18763 #
INPE-4908-PRE/1509 ..... N90-18770 #
INPE-4910-PRE/1511 ..... N90-18817 #
INPE-4923-TDL/383 ..... N90-18828 #
INPE-4924-TDL/384 ..... N90-18885 #
INPE-4930-PRE/1420 ..... N90-18764 #
INPE-4940-PRE/1430 ..... N90-18773 #
INPE-4945-TDL/386 ..... N90-18913 #
INPE-4946-TDL/387 ..... N90-18850 #
INPE-4950-RPE/599 ..... N90-18774 #
INPE-4951-RPE/600 ..... N90-18818 #
INPE-4953-RPE/602 ..... N90-18700 #
INPE-4958-RPE/603 ..... N90-18899 #
INPE-4959-TDL/388 ..... N90-18440 #
INPE-4960-TDL/389 ..... N90-18951 #
INPE-4962-TDL/391 ..... N90-18441 #
INPE-4963-TDL/392 ..... N90-18448 #
INPE-4973-RPE/605 ..... N90-18490 #
INPE-5000-MD/41 ..... N90-18897 #
INPE-5001-TDL/395 ..... N90-18757 #

ISBN-3-89100-015-4 ..... N90-18437 #
ISBN-87-89132-02-5 ..... N90-18520 #
ISBN-92-835-0518-2 ..... N90-18396 #
ISBN-92-835-0536-0 ..... N90-19060 #
ISBN-92-835-0536-7 ..... N90-18432 #
ISBN-92-835-0543-3 ..... N90-18405 #
ISBN-92-9092-002-5 ..... N90-19084 #
ISBN-92-9092-019-X ..... N90-18782 #
ISBN-92-9092-060-2 ..... N90-19068 #
ISBN-92-9092-096-3 ..... N90-18848 #
ISBN-981-02-0102-8 ..... N90-19004 #

ISI/RS-89-245 ..... N90-18895 #

ISL-CO-201/89 ..... N90-18704 #
ISL-CO-204/89 ..... N90-18680 #
ISL-CO-207/89 ..... N90-18705 #
ISL-CO-216/88 ..... N90-18392 #
ISL-CO-221/88 ..... N90-18709 #
ISL-CO-234/88 ..... N90-18724 #
ISL-CO-243/88 ..... N90-18365 #
ISL-CO-245/88 ..... N90-18681 #
ISL-CO-248/88 ..... N90-18605 #
ISL-CO-250/88 ..... N90-18694 #
ISL-CO-251/88 ..... N90-18547 #
ISL-CO-306/89 ..... N90-18366 #

ISL-R-112/88 ..... N90-18731 #
ISL-R-113/88 ..... N90-18732 #
ISL-R-114/88 ..... N90-18733 #
ISL-R-115/88 ..... N90-18391 #
ISL-R-119/88 ..... N90-18703 #
ISL-R-123/88 ..... N90-18679 #

ISSN-0070-3966 ..... N90-19189 #
ISSN-0078-378X ..... N90-19168 #
ISSN-0078-3781 ..... N90-18685 #
ISSN-0078-3781 ..... N90-18686 #
ISSN-0169-2690 ..... N90-18922 #
ISSN-0169-2690 ..... N90-18946 #
ISSN-0169-2690 ..... N90-18947 #
ISSN-0169-2690 ..... N90-18948 #
ISSN-0169-2690 ..... N90-18953 #
ISSN-0169-2690 ..... N90-18954 #
ISSN-0171-1342 ..... N90-18377 #
ISSN-0171-1342 ..... N90-18548 #
ISSN-0171-1342 ..... N90-18629 #
ISSN-0171-1342 ..... N90-18630 #
ISSN-0173-0118 ..... N90-18781 #
ISSN-0176-7739 ..... N90-18370 #
ISSN-0176-7739 ..... N90-18662 #
ISSN-0347-3694 ..... N90-18606 #

ISSN-0379-4059 ..... N90-18447 #
ISSN-0379-4059 ..... N90-18455 #
ISSN-0379-4059 ..... N90-18456 #
ISSN-0379-4059 ..... N90-18457 #
ISSN-0379-4059 ..... N90-18458 #
ISSN-0379-4059 ..... N90-18460 #
ISSN-0379-4059 ..... N90-18461 #
ISSN-0379-4059 ..... N90-19061 #
ISSN-0379-4059 ..... N90-19062 #
ISSN-0379-6566 ..... N90-19065 #
ISSN-0379-6566 ..... N90-19084 #
ISSN-0902-8277 ..... N90-18520 #
ISSN-0923-1714 ..... N90-18906 #
ISSN-0923-1714 ..... N90-18907 #
ISSN-0923-1714 ..... N90-18923 #
ISSN-0923-1714 ..... N90-18949 #
ISSN-0955-9655 ..... N90-18999

ISVR-TR-166-PT-1 ..... N90-18754 #
ISVR-TR-181 ..... N90-18755 #

IYAF-89-23 ..... N90-19180 #

J-550-89-505/2513 ..... N90-19027 #

JA-8281 ..... N90-18645 #

JINR-R-2-88-654 ..... N90-19177 #
JINR-R-14-88-477 ..... N90-18588 #

JPL-D-8041 ..... N90-18443 #

JPL-PUBL-88-30 ..... N90-18623* #
JPL-PUBL-89-23 ..... N90-18444* #

K/DSRD-57 ..... N90-18945 #

KCP-613-4247 ..... N90-18652 #

L-16615 ..... N90-18378* #
L-16637 ..... N90-18393* #
L-16642 ..... N90-18394* #
L-16651 ..... N90-18385* #
L-16719 ..... N90-18882* #

LA-UR-89-3575 ..... N90-19049 #
LA-UR-89-4150 ..... N90-19030 #
LA-UR-89-4165 ..... N90-18712 #
LA-UR-89-4259 ..... N90-19050 #
LA-UR-90-33 ..... N90-18519 #
LA-UR-90-34 ..... N90-19021 #
LA-UR-90-72 ..... N90-18726 #
LA-UR-90-98 ..... N90-18725 #
LA-UR-90-138 ..... N90-19187 #
LA-UR-90-166 ..... N90-18723 #
LA-UR-90-200 ..... N90-18722 #
LA-UR-90-255 ..... N90-18602 #
LA-UR-90-298 ..... N90-18625 #

LA-11345-MS ..... N90-18955 #
LA-11680-MS ..... N90-18624 #
LA-11756-PR ..... N90-19007 #
LA-11769-MS ..... N90-18879 #

LBL-27048 ..... N90-18702 #
LBL-27775 ..... N90-18753 #
LBL-27855 ..... N90-19058 #
LBL-27893 ..... N90-18720 #
LBL-27901 ..... N90-18885 #
LBL-27963 ..... N90-18584 #
LBL-27985 ..... N90-19024 #
LBL-28096 ..... N90-19051 #
LBL-28111 ..... N90-18719 #
LBL-28193 ..... N90-19052 #

LC-89-600750 ..... N90-18881 #

LMSC/F186352 ..... N90-18454* #

LNCC-011/89 ..... N90-18678 #

MEMO-INF-89-47 ..... N90-18906 #
MEMO-INF-89-50 ..... N90-18907 #
MEMO-INF-89-51 ..... N90-18949 #
MEMO-INF-89-53 ..... N90-18923 #

MEMO-802 ..... N90-18953 #
MEMO-803 ..... N90-18946 #
MEMO-804 ..... N90-18954 #
MEMO-805 ..... N90-18947 #
MEMO-807 ..... N90-18922 #
MEMO-809 ..... N90-18948 #

MIT/LCS/TR-459 ..... N90-18929 #
MIT/LCS/TR-464 ..... N90-19067 #
MIT/LCS/TR-467 ..... N90-18878 #

MLM-3620 ..... N90-19178 #
MLM-3622-OP ..... N90-19010 #
MLM-3623-OP ..... N90-19008 #
MLM-3624-OP ..... N90-19009 #

MRC-R-1198 ..... N90-18613 #

MSD-TR-89-21-VOL-1 ..... N90-18383 #

MSP-89-3 ..... N90-18893 #

MTL-TR-89-101 ..... N90-18750 #

NADC-89067-60 ..... N90-18433 #

NAPC-PE-204C ..... N90-18738 #

NAS 1.15:4173 ..... N90-18394* #
NAS 1.15:101560 ..... N90-18453* #
NAS 1.15:101697 ..... N90-18395* #
NAS 1.15:102333 ..... N90-18504* #
NAS 1.15:102376 ..... N90-18665* #
NAS 1.15:102446 ..... N90-18667* #
NAS 1.15:102497 ..... N90-18927* #
NAS 1.15:102502 ..... N90-18745* #
NAS 1.15:102526 ..... N90-18634* #
NAS 1.15:102583 ..... N90-18752* #
NAS 1.15:102598 ..... N90-18746* #
NAS 1.15:102601 ..... N90-18751* #
NAS 1.15:102603 ..... N90-18434* #
NAS 1.15:102784 ..... N90-18853* #
NAS 1.26:4275 ..... N90-18371* #
NAS 1.26:4280 ..... N90-18372* #
NAS 1.26:4286 ..... N90-18675* #
NAS 1.26:174945 ..... N90-18364*
NAS 1.26:180479 ..... N90-18623* #
NAS 1.26:181873 ..... N90-18454* #
NAS 1.26:181923 ..... N90-18743* #
NAS 1.26:181996 ..... N90-18363* #
NAS 1.26:185174 ..... N90-18559* #
NAS 1.26:185183 ..... N90-18808* #
NAS 1.26:186190 ..... N90-18924* #
NAS 1.26:186191 ..... N90-18744* #
NAS 1.26:186200 ..... N90-18824* #
NAS 1.26:186285 ..... N90-18444* #
NAS 1.26:186323 ..... N90-18664* #
NAS 1.26:186371 ..... N90-18390* #
NAS 1.26:186372 ..... N90-19181* #
NAS 1.26:186402 ..... N90-18891* #
NAS 1.26:186496 ..... N90-19169* #
NAS 1.55:3058 ..... N90-18957* #
NAS 1.60:2960 ..... N90-18393* #
NAS 1.60:2974 ..... N90-18882* #
NAS 1.60:2975 ..... N90-18385* #
NAS 1.60:2978 ..... N90-18378* #
NAS 1.61:1228 ..... N90-18740* #
NAS 1.71:MSC-21560-1 ..... N90-18852* #
NAS 1.71:NPO-17820-1-CU ..... N90-18379* #

NASA-CASE-MSC-21560-1 ..... N90-18852* #

NASA-CASE-NPO-17820-1-CU ..... N90-18379* #

NASA-CP-3058 ..... N90-18957* #

NASA-CR-4275 ..... N90-18371* #
NASA-CR-4280 ..... N90-18372* #
NASA-CR-4286 ..... N90-18675* #
NASA-CR-174945 ..... N90-18364*
NASA-CR-180479 ..... N90-18623* #
NASA-CR-181873 ..... N90-18454* #
NASA-CR-181923 ..... N90-18743* #
NASA-CR-181996 ..... N90-18363* #
NASA-CR-185174 ..... N90-18559* #
NASA-CR-185183 ..... N90-18808* #
NASA-CR-186190 ..... N90-18924* #
NASA-CR-186191 ..... N90-18744* #
NASA-CR-186200 ..... N90-18824* #
NASA-CR-186285 ..... N90-18444* #
NASA-CR-186323 ..... N90-18664* #
NASA-CR-186371 ..... N90-18390* #
NASA-CR-186372 ..... N90-19181* #
NASA-CR-186402 ..... N90-18891* #
NASA-CR-186496 ..... N90-19169* #

NASA-RP-1228 ..... N90-18740* #

NASA-TM-4173 ..... N90-18394* #
NASA-TM-101560 ..... N90-18453* #
NASA-TM-101697 ..... N90-18395* #
NASA-TM-102333 ..... N90-18504* #
NASA-TM-102376 ..... N90-18665* #
NASA-TM-102446 ..... N90-18667* #
NASA-TM-102497 ..... N90-18927* #
NASA-TM-102502 ..... N90-18745* #
NASA-TM-102526 ..... N90-18634* #

NASA-TM-102583 ..... N90-18752* #
NASA-TM-102598 ..... N90-18746* #
NASA-TM-102601 ..... N90-18751* #
NASA-TM-102603 ..... N90-18434* #
NASA-TM-102784 ..... N90-18853* #

NASA-TP-2960 ..... N90-18393* #
NASA-TP-2974 ..... N90-18882* #
NASA-TP-2975 ..... N90-18385* #
NASA-TP-2978 ..... N90-18378* #

NEDOJ-P-8821 ..... N90-18807 #

NEPRF-TR-89-08 ..... N90-18845 #

NIKHEF-K/AMPS/89-07 ..... N90-18632 #
NIKHEF-K/AMPS/89/05 ..... N90-18628 #

NIOZ-1988-10 ..... N90-18783 #

NIST/SP-500/166 ..... N90-18881 #

NIST/TN-1267 ..... N90-18734 #

NISTIR-89-4064 ..... N90-18558 #

NLR-TR-87178-U ..... N90-18905 #
NLR-TR-88155-U ..... N90-18786 #

NOAA-TM-ERL-WPL-173 ..... N90-18838 #

NOSC/TD-1687 ..... N90-18517 #

NOSC/TR-1312 ..... N90-18617 #
NOSC/TR-1633 ..... N90-18648 #

NPL-RSA(EXT)-009 ..... N90-18999

NPS53-90-001 ..... N90-18749 #
NPS61-089-012 ..... N90-19013 #
NPS63-90-001 ..... N90-18842 #

NRL-MR-6559 ..... N90-18646 #
NRL-MR-6581 ..... N90-18760 #

NRL-9227 ..... N90-18779 #
NRL-9234 ..... N90-18621 #

NSF/ENG-89048 ..... N90-18925 #
NSF/ENG-89050 ..... N90-18735 #
NSF/ENG-89051 ..... N90-18912 #

NTIA-89-249 ..... N90-18612 #

OCS/EIS/EA/MMS-89-0064 ..... N90-18849 #

ONERA-NT-1987-2 ..... N90-18685 #
ONERA-NT-1987-5 ..... N90-18521 #
ONERA-NT-1987-6 ..... N90-18956 #
ONERA-NT-1988-1 ..... N90-18836 #
ONERA-NT-1988-5 ..... N90-18686 #
ONERA-NT-1988-6 ..... N90-18697 #
ONERA-NT-1988-10 ..... N90-18833 #

ONERA-PUBL-1989-1 ..... N90-19168 #

ONERA-RSF-4/4368-AY-004A ..... N90-18689 #

ONERA-RT-10/3521-M ..... N90-18522 #
ONERA-RT-13/3596-RY-070-R ..... N90-18687 #
ONERA-RT-47/7086-M ..... N90-18523 #
ONERA-RT-84/7078-AY ..... N90-18688 #

ORNL-6516 ..... N90-18690 #

ORNL/ATD-21 ..... N90-18721 #

ORNL/FTR-3519 ..... N90-19025 #
ORNL/FTR-3524 ..... N90-18693 #
ORNL/FTR-3527 ..... N90-18998 #
ORNL/FTR-3529 ..... N90-18563 #

ORNL/M-828 ..... N90-19179 #

ORNL/SUB-83-21322/01 ..... N90-18558 #

ORNL/TM-11390 ..... N90-18739 #

ORNL/TR-89/53 ..... N90-19020 #

PB90-100033 ..... N90-18849 #
PB90-111667 ..... N90-18734 #
PB90-111683 ..... N90-18881 #
PB90-116963 ..... N90-18814 #
PB90-119835 ..... N90-18838 #
PB90-119868 ..... N90-18612 #

PB90-120023 ..... N90-18813 #
PB90-120965 ..... N90-18735 #
PB90-120973 ..... N90-18912 #
PB90-121245 ..... N90-18925 #

PNL-SA-17325 ..... N90-18797 #
PNL-SA-17331 ..... N90-18607 #

PNL-7230 ..... N90-18656 #

PREPRINT-88-148 ..... N90-19020 #

Q-784 ..... N90-18785 #

R/D-5528-MS-01 ..... N90-18509 #

RADC-TR-89-123 ..... N90-18622 #
RADC-TR-89-202 ..... N90-19033 #
RADC-TR-89-281 ..... N90-18647 #

REPT-S3-4273 ..... N90-18376 #

REPT-90B00019 ..... N90-18957* #

RIN-89/5 ..... N90-18790 #

RIT/DIRS-89/90-51-134 ..... N90-19014 #
RIT/DIRS-89/90-53-136 ..... N90-19015 #
RIT/DIRS-89/90-54-132 ..... N90-19016 #

R89-917447-32 ..... N90-18559* #

SAND-87-2119 ..... N90-18650 #
SAND-89-1044 ..... N90-19039 #
SAND-89-1489 ..... N90-18606 #
SAND-89-1558C ..... N90-18713 #
SAND-89-1712C ..... N90-18598 #
SAND-89-2033 ..... N90-18541 #
SAND-89-2267 ..... N90-18649 #
SAND-89-2327C ..... N90-18708 #
SAND-89-2569C ..... N90-18583 #
SAND-89-7033 ..... N90-18582 #
SAND-89-7042-PT-2 ..... N90-18804 #
SAND-89-7051 ..... N90-18805 #
SAND-89-7095 ..... N90-18555 #
SAND-89-7107 ..... N90-19028 #
SAND-89-7153 ..... N90-18626 #
SAND-89-8266 ..... N90-18658 #
SAND-90-0152C ..... N90-18564 #
SAND-90-0277C ..... N90-18659 #
SAND-90-8205 ..... N90-18525 #

SCA-149 ..... N90-18892 #

SCT-89-RR-18 ..... N90-18875 #

SERI/PR-215-2961 ..... N90-18802 #

SERI/STR-211-3601 ..... N90-18803 #
SERI/STR-211-3620 ..... N90-18581 #
SERI/STR-250-3516 ..... N90-18801 #

SERI/TP-211-3604 ..... N90-18792 #
SERI/TP-257-3490 ..... N90-18362 #

SPIRE-QR-10120-02 ..... N90-18800 #

SSD-TR-89-91 ..... N90-18842 #

SU-SLAC-PUB-5035 ..... N90-18811 #

S3912A ..... N90-18433 #

TR-BN-1105 ..... N90-18928 #

TR-TE-4189 ..... N90-18926 #

TR-2 ..... N90-19019 #
TR-3 ..... N90-18569 #
TR-10 ..... N90-18747 #
TR-16 ..... N90-18574 #
TR-17 ..... N90-18575 #
TR-20-ONR-PT-1 ..... N90-18639 #
TR-21 ..... N90-18716 #
TR-22 ..... N90-18640 #
TR-23 ..... N90-18531 #
TR-43 ..... N90-18573 #
TR-49 ..... N90-18512 #
TR-50 ..... N90-19038 #
TR-51 ..... N90-18537 #
TR-52 ..... N90-19037 #
TR-53 ..... N90-18536 #
TR-67 ..... N90-18539 #
TR-89-1067 ..... N90-18924* #
TR-424 ..... N90-18930 #
TR-0089(4470-03)-1 ..... N90-18642 #

TRI-PP-89-100 ..... N90-19029 #

TR89-1042 ..... N90-18891* #

TW-89-02 ..... N90-18952 #

UBUFFALO/DC/89/TR-3 ..... N90-18568 #
UBUFFALO/DC/89/TR-118 ..... N90-18571 #

UC-700 ..... N90-18955 #

UCB-PTH-22/89 ..... N90-19058 #

UCID-21814 ..... N90-18727 #
UCID-21844 ..... N90-18837 #
UCID-21862 ..... N90-18677 #
UCID-21947 ..... N90-18524 #
UCID-21950 ..... N90-18730 #

UCRL-21235 ..... N90-18505 #
UCRL-21236 ..... N90-18506 #
UCRL-21280 ..... N90-18714 #
UCRL-21293 ..... N90-18821 #
UCRL-100232 ..... N90-18627 #
UCRL-100364 ..... N90-18651 #
UCRL-100755 ..... N90-18606 #
UCRL-101572 ..... N90-18707 #
UCRL-101720 ..... N90-18728 #
UCRL-102275 ..... N90-18657 #
UCRL-102500 ..... N90-19172 #
UCRL-102651 ..... N90-18729 #
UCRL-102653 ..... N90-18823 #
UCRL-102659 ..... N90-19169* #
UCRL-102762 ..... N90-19017 #
UCRL-102763 ..... N90-19188 #

UDR-TR-89-03 ..... N90-18375 #

UILU-ENG-89-1777 ..... N90-18869 #
UILU-ENG-90-1701 ..... N90-18943 #

UIUCDCS-R-89-1558 ..... N90-18869 #
UIUCDCS-R-90-1563 ..... N90-18943 #

US-PATENT-APPL-SN-317931 ..... N90-18852* #
US-PATENT-APPL-SN-429734 ..... N90-18379* #

USAARL-89-27 ..... N90-18874 #

USAFA-TR-89-9 ..... N90-18843 #

VLSI-M-89-557 ..... N90-18940 #
VLSI-M-89-558 ..... N90-18899 #

WGL-MLR-89-30 ..... N90-18644 #
WGL-MLR-89-41 ..... N90-18799 #

WHOI-89-26 ..... N90-18840 #

WRDC-TR-89-2067 ..... N90-18673 #
WRDC-TR-89-2097 ..... N90-18601 #
WRDC-TR-89-3079 ..... N90-18388 #
WRDC-TR-89-3090 ..... N90-18361 #

Appendix—About STAR

Scientific and Technical Aerospace Reports (STAR) is a major component of a comprehensive National Aeronautics and Space Administration information system covering aeronautics, space, and supporting disciplines. *STAR* is issued on the 8th and 23rd of each month and announces current publications of the following types:

- NASA, NASA contractor, and NASA grantee reports
- Reports issued by other U.S. Government agencies, domestic and foreign institutions, universities, and private firms
- Translations in report form
- NASA-owned patents and patent applications
- Other U.S. Government agency and foreign patents and patent applications
- Domestic and foreign dissertations and theses

Journal, book, and conference literature, cover-to-cover journal translations, and certain foreign dissertations are announced in a companion journal, *International Aerospace Abstracts (IAA),* available on subscription from the American Institute of Aeronautics and Astronautics, Technical Information Service, 555 West 57th Street, 12th Floor, New York, NY 10019.

SUBJECT SCOPE

The subject scope of *STAR* and *IAA* includes all aspects of aeronautics and space research and development, supporting basic and applied research, and applications. Aerospace aspects of earth resources, energy development, conservation, oceanography, environmental protection, urban transportation, and other topics of high national priority are also covered.

OTHER NASA PUBLICATIONS

Other NASA publications and information services are described in the publication, *The NASA Scientific and Technical Information System ... and How to Use It,* available without charge from the NASA Scientific and Technical Information Facility, P.O. Box 8757, BWI Airport, MD 21240.

HOW TO USE *STAR* SUBJECT CATEGORIES

STAR is categorized by 10 major subject divisions broken down further into 76 specific subject categories and one general division/category. The major subject divisions are listed on page ii in the Table of Contents, together with a note for each that defines its scope and provides any cross-references. For example:

AERONAUTICS

Includes aeronautics (general); aerodynamics; air transportation and safety; aircraft communications and navigation; aircraft design, testing and performance; aircraft instrumentation; aircraft propulsion and power; aircraft stability and control; and research and support facilities (air).

For related information see also *Astronautics.*

Each major division is further divided into as many as nine specific categories, which are identified by category numbers.

Abstracts in *STAR* are grouped by subject category, the categories appearing in sequential order. Category breaks in the abstract section are identified by the category number and title, and a scope note. Cross-references to other categories are provided as appropriate. For example:

02 AERODYNAMICS

Includes aerodynamics of bodies, combinations, wings, rotors, and control surfaces; and internal flow in ducts and turbomachinery.

For related information see also *34 Fluid Mechanics and Heat Transfer.*

CROSS-REFERENCES

Individual *STAR* abstracts are not ordinarily cross-referenced, except for certain conference reports or book translations that have had separate abstracts written for their component papers or chapters. Citations and abstracts of the components follow immediately after those of the parent document. When the subject content of a component differs sufficiently from the general content of the parent, a cross-reference citation also is printed at the end of the category to which it normally would have been assigned if it were independent.

DOCUMENTS ON MICROFICHE

Documents on microfiche(1) are designated by a pound sign (#) following the accession number. The pound sign is used without regard to the source or quality of the microfiche.

LIMITED REPRODUCIBILITY

A Note of Limited Reproducibility appears in the citation, if one or a combination of the following factors affect the reproducibility of more than 20% of the document. These factors include: faint or broken type, color photographs, black and white photographs, foldouts, dot matrix print, charts/graphs with script notation, non-Roman alphabet, or some other factor that limits the reproducibility of that document. This notation also appears on the microfiche header, with the specific causing factor checked off on a list visible in the second frame.

COLOR COPIES

An increasing number of NASA scientific and technical reports are being produced with color graphs, charts, illustrations, and photographs. A message indicating that a document has color pages follows the Sales and Pricing (SAP) information in the *STAR* citation.

Registered users of the NASA Scientific and Technical Information System will receive ordered documents with color at no *additional* cost, as long as stock copies of that document are available. Otherwise, an additional fee of $2.00 per color page, over and above the standard document price will be charged. The NASA STI Facility staff will work with registered users over the telephone to inform and meet each individual's ordering needs.

AVAILABILITIES

One or more sources from which a document announced in *STAR* is available to the public is given in each citation. The most commonly indicated sources and their acronyms or abbreviations are listed below. If the publication is available from a source other than those listed, the publisher and his address will be displayed on the availability line or in combination with the corporate source line.

Avail: NTIS. Sold by the National Technical Information Service. Prices for hard copy (HC) and microfiche (MF) are indicated by a price code following the letters HC or MF in the *STAR* citation. Current values for the price codes are given in the tables on page A-7.

(1) A microfiche is a transparent sheet of film, 105 by 148 mm in size, containing as many as 60 to 98 pages of information reduced to micro images (not to exceed 26:1 reduction).

Initially distributed microfiche under the NTIS SRIM (Selected Research in Microfiche) is available at greatly reduced unit prices. For this service and for information concerning subscription to NASA printed reports, consult the NTIS Subscription Section, Springfield, VA 22161.

NOTE ON ORDERING DOCUMENTS: When ordering NASA publications (those followed by the * symbol), use the N accession number. NASA patent applications (only the specifications are offered) should be ordered by the US-Patent-Appl-SN number. Non-NASA publications (no asterisk) should be ordered by the AD, PB, or other *report number* shown on the last line of the citation, not by the N accession number. It is also advisable to cite the title and other bibliographic identification.

Avail: SOD (or GPO). Sold by the Superintendent of Documents, U.S. Government Printing Office, in hard copy. The current price and order number are given following the availability line. (NTIS will fill microfiche requests, as indicated above, for those documents identified by a # symbol.)

Avail: BLL (formerly NLL): British Library Lending Division, Boston Spa, Wetherby, Yorkshire, England. Photocopies available from this organization at the price shown. (If none is given, address inquiry to the BLL.)

Avail: DOE Depository Libraries. Organizations in U.S. cities and abroad that maintain collections of Department of Energy reports, usually in microfiche form, are listed in *Energy Research Abstracts.* Services available from the DOE and its depositories are described in a booklet, *DOE Technical Information Center - Its Functions and Services* (TID-4660), which may be obtained without charge from the DOE Technical Information Center.

Avail: ESDU. Pricing information on specific data, computer programs, and details on Engineering Sciences Data Unit (ESDU) topic categories can be obtained from ESDU International Ltd. Requesters in North America should use the Virginia address while all other requesters should use the London address, both of which are on page A-6.

Avail: Fachinformationszentrum, Karlsruhe. Sold by the Fachinformationszentrum Energie, Physik, Mathematik GMBH, Eggenstein Leopoldshafen, Federal Republic of Germany, at the price shown in deutschmarks (DM).

Avail: HMSO. Publications of Her Majesty's Stationery Office are sold in the U.S. by Pendragon House, Inc. (PHI), Redwood City, CA. The U.S. price (including a service and mailing charge) is given, or a conversion table may be obtained from PHI.

Avail: NASA Public Document Rooms. Documents so indicated may be examined at or purchased from the National Aeronautics and Space Administration, Public Documents Room (Room 126), 600 Independence Ave., S.W., Washington, DC 20546, or public document rooms located at NASA installations, and the NASA Pasadena Office at the Jet Propulsion Laboratory.

Avail: Univ. Microfilms. Documents so indicated are dissertations selected from *Dissertation Abstracts* and are sold by University Microfilms as xerographic copy (HC) and microfilm. All requests should cite the author and the Order Number as they appear in the citation.

Avail: US Patent and Trademark Office. Sold by Commissioner of Patents and Trademarks, U.S. Patent and Trademark Office, at the standard price of

$1.50 each, postage free. (See discussion of NASA patents and patent applications below.)

Avail: (US Sales Only). These foreign documents are available to users within the United States from the National Technical Information Service (NTIS). They are available to users outside the United States through the International Nuclear Information Service (INIS) representative in their country, or by applying directly to the issuing organization.

Avail: USGS. Originals of many reports from the U.S. Geological Survey, which may contain color illustrations, or otherwise may not have the quality of illustrations preserved in the microfiche or facsimile reproduction, may be examined by the public at the libraries of the USGS field offices whose addresses are listed in this Introduction. The libraries may be queried concerning the availability of specific documents and the possible utilization of local copying services, such as color reproduction.

Avail: Issuing Activity, or Corporate Author, or no indication of availability. Inquiries as to the availability of these documents should be addressed to the organization shown in the citation as the corporate author of the document.

NASA PATENTS AND PATENT APPLICATIONS

Patents and patent applications owned by NASA are announced in *STAR* under appropriate subject categories and are referenced in the *STAR* indexes. In the Report/Accession Number Index, patents are indexed by the NASA Case Number (which appears in lieu of the report number in other indexes), the U.S. Patent Number, the U.S. Patent Application Serial Number, and the U.S. Patent Class. Patent applications for which patents have not yet been issued are indexed by the NASA Case Number and the U.S. Patent Application Serial Number.

NASA *patent application specifications* are sold in paper copy and microfiche by the National Technical Information Service (NTIS). The US-Patent-Appl-SN- number should be used in ordering either paper copy or microfiche from NTIS. Printed copies of *patents* (which are not microfiched) are available for purchase from:

Commissioner of Patents and Trademarks
U.S. Patent and Trademark Office
Washington, DC 20231

When ordering patents, the U.S. Patent Number should be used, and payment must be remitted in advance, by money order or check payable to the Commissioner of Patents and Trademarks. Prepaid purchase coupons for ordering are also available from the Patent and Trademark Office. The patents and patent applications announced in *STAR* are owned by NASA and are available for royalty-free licensing. Requests for licensing terms and further information should be addressed to:

Associate General Counsel for Intellectual Property/Code GP
National Aeronautics and Space Administration
Washington, DC 20546

ELIGIBILITY AND REGISTRATION FOR NASA INFORMATION PRODUCTS AND SERVICES

A variety of services is available to organizations of the following types that have registered with NASA to receive specific services or products:

1. NASA offices and installations, contractors, subcontractors, grantees, and consultants;
2. Other U.S. Government agencies and their contractors;
3. Libraries in the United States that have arrangements with NASA to maintain collections of NASA documents for public reference;
4. Other organizations in the United States having a need for NASA documents in work related to aeronautics and space research;
5. Organizations abroad that have established reciprocal document exchange arrangements with NASA.

Only the central service points or central points of document acquisition and control within qualified organizations are eligible to register for NASA products and services. Domestic organizations that may be eligible to receive various classes of NASA publications and services should address their requests for registration or for further information to:

NASA Scientific and Technical Information Facility
ATTN: Registration Services
P.O. Box 8757
BWI Airport, MD 21240
301-621-0153

Organizations abroad should direct requests to Manager, International STI Activities, NTT, NASA Headquarters, Washington, DC 20546.

AVAILABILITY OF *STAR* ABSTRACTS ON MICROFICHE

Microfiche of the abstract sections of this issue and other issues of *STAR* are available on annual subscription from NTIS as PB90-911300, Attn: Subscriptions, 5285 Port Royal Road, Springfield, VA 22161. Annual subscription rates are $75.50 North America; $151.00 foreign. Abstract sections for previous years retroactive to 1964 are available at the current rates. Microfiche for individual *STAR* issue abstract sections are not available.

PUBLIC COLLECTIONS OF NASA DOCUMENTS

DOMESTIC: NASA and NASA-sponsored documents and a large number of aerospace publications are available to the public for reference purposes at the library maintained by the American Institute of Aeronautics and Astronautics, Technical Information Service, 555 West 57th Street, 12th Floor, New York, NY 10019

EUROPEAN: An extensive collection of NASA and NASA-sponsored publications is maintained by the British Library Lending Division, Boston Spa, Wetherby, Yorkshire, England, for public access. The British Library Lending Division also has available many of the non-NASA publications cited in *STAR*. European requesters may purchase facsimile copy or microfiche of NASA and NASA-sponsored documents, those identified by both the symbols # and * from ESA - Information Retrieval Service, European Space Agency, 8-10 rue Mario-Nikis, 75738 Paris CEDEX 15, France.

FEDERAL DEPOSITORY LIBRARY PROGRAM

In order to provide the general public with greater access to U.S. Government publications, Congress established the Federal Depository Library Program under the Government Printing Office (GPO), with 51 regional depositories responsible for permanent retention of material, inter-library loan, and reference services. At least one copy of nearly every NASA and NASA-sponsored publication, either in printed or microfiche format, is received and retained by the 51 regional depositories. A list of the regional GPO libraries, arranged alphabetically by state, appears on the inside back cover. These libraries are *not* sales outlets. A local library can contact a Regional Depository to help locate specific reports, or direct contact may be made by an individual.

ADDRESSES OF ORGANIZATIONS

American Institute of Aeronautics and Astronautics
Technical Information Service
555 West 57th Street, 12th Floor
New York, New York 10019

British Library Lending Division,
Boston Spa, Wetherby, Yorkshire,
England

Commissioner of Patents and Trademarks
U.S. Patent and Trademark Office
Washington, DC 20231

Department of Energy
Technical Information Center
P.O. Box 62
Oak Ridge, Tennessee 37830

European Space Agency-Information Retrieval Service
ESRIN
Via Galileo Galilei
00044 Frascati (Rome) Italy

Engineering Sciences Data Unit International
P.O. Box 1633
Manassas, Virginia 22110

Engineering Sciences Data Unit International, Ltd.
251-259 Regent Street
London, W1R 7AD, England

Fachinformationszentrum Energie, Physik, Mathematik
GMBH
7514 Eggenstein Leopoldshafen
Federal Republic of Germany

Her Majesty's Stationery Office
P.O. Box 569, S.E. 1
London, England

NASA Scientific and Technical Information Facility
P.O. Box 8757
BWI Airport, Maryland 21240

National Aeronautics and Space Administration
Scientific and Technical Information Division (NTT)
Washington, DC 20546

National Technical Information Service
5285 Port Royal Road
Springfield, Virginia 22161

Pendragon House, Inc.
899 Broadway Avenue
Redwood City, California 94063

Superintendent of Documents
U.S. Government Printing Office
Washington, DC 20402

University Microfilms
A Xerox Company
300 North Zeeb Road
Ann Arbor, Michigan 48106

University Microfilms, Ltd.
Tylers Green
London, England

U.S. Geological Survey Library National Center
MS 950
12201 Sunrise Valley Drive
Reston, Virginia 22092

U.S. Geological Survey Library
2255 North Gemini Drive
Flagstaff, Arizona 86001

U.S. Geological Survey
345 Middlefield Road
Menlo Park, California 94025

U.S. Geological Survey Library
Box 25046
Denver Federal Center, MS914
Denver, Colorado 80225

NTIS PRICE SCHEDULES

(Effective January 1, 1990)

Schedule A
STANDARD PRICE DOCUMENTS AND MICROFICHE

PRICE CODE	NORTH AMERICAN PRICE	FOREIGN PRICE
A01	$ 8.00	$ 16.00
A02	11.00	22.00
A03	15.00	30.00
A04-A05	17.00	34.00
A06-A09	23.00	46.00
A10-A13	31.00	62.00
A14-A17	39.00	78.00
A18-A21	45.00	90.00
A22-A25	53.00	106.00
A99	*	*
N01	60.00	120.00
N02	59.00	118.00
N03	20.00	40.00

Schedule E
EXCEPTION PRICE DOCUMENTS AND MICROFICHE

PRICE CODE	NORTH AMERICAN PRICE	FOREIGN PRICE
E01	$10.00	$ 20.00
E02	12.00	24.00
E03	14.00	28.00
E04	16.50	33.00
E05	18.50	37.00
E06	21.50	43.00
E07	24.00	48.00
E08	27.00	54.00
E09	29.50	59.00
E10	32.50	65.00
E11	35.00	70.00
E12	38.50	77.00
E13	41.00	82.00
E14	45.00	90.00
E15	48.50	97.00
E16	53.00	106.00
E17	57.50	115.00
E18	62.00	124.00
E19	69.00	138.00
E20	80.00	160.00
E99	*	*

* Contact NTIS for price quote.

IMPORTANT NOTICE

NTIS Shipping and Handling Charges
U.S., Canada, Mexico — ADD $3.00 per TOTAL ORDER
All Other Countries — ADD $4.00 per TOTAL ORDER

Exceptions — Does NOT apply to:
ORDERS REQUESTING NTIS RUSH HANDLING
ORDERS FOR SUBSCRIPTION OR STANDING ORDER PRODUCTS *ONLY*

NOTE: Each additional delivery address on an order requires a separate shipping and handling charge.

FEDERAL REGIONAL DEPOSITORY LIBRARIES

ALABAMA

AUBURN UNIV. AT MONTGOMERY LIBRARY
Documents Department
Montgomery, AL 36193
(205) 279-9110 ext.253

UNIV. OF ALABAMA LIBRARY
Reference Department/Documents
Box S
Tuscaloosa, AL 35486
(205) 348-6046

ARIZONA

DEPT. OF LIBRARY, ARCHIVES, AND PUBLIC RECORDS
Third Floor State Capitol
1700 West Washington
Phoenix, AZ 85007
(602) 255-4121

ARKANSAS

ARKANSAS STATE LIBRARY
Documents Service Section
One Capitol Mall
Little Rock, AR 72201
(501) 371-2090

CALIFORNIA

CALIFORNIA STATE LIBRARY
Govt. Publications Section
914 Capitol Mall
Sacramento, CA 95814
(916) 322-4572

COLORADO

UNIV. OF COLORADO
Norlin Library
Government Publications Division
Campus Box 184
Boulder, CO 80309
(303) 492-8834

DENVER PUBLIC LIBRARY
Govt. Pub. Department
1357 Broadway
Denver, CO 80203
(303) 571-2346

CONNECTICUT

CONNECTICUT STATE LIBRARY
231 Capitol Avenue
Hartford, CT 06106
(203) 566-4971

FLORIDA

UNIV. OF FLORIDA LIBRARIES
Documents Department
Library West
Gainesville, FL 32611
(904) 392-0367

GEORGIA

UNIV. OF GEORGIA LIBRARIES
Government Documents Dept.
Athens, GA 30602
(404) 542-8949

HAWAII

UNIV. OF HAWAII
Hamilton Library
Government Documents Collection
2550 The Mall
Honolulu, HI 96822
(808) 948-8230

IDAHO

UNIV. OF IDAHO LIBRARY
Documents Section
Moscow, ID 83843
(208) 885-6344

ILLINOIS

ILLINOIS STATE LIBRARY
Federal Documents
Centennial Building
Springfield, IL 62756
(217) 782-5012

INDIANA

INDIANA STATE LIBRARY
Serials Section
140 North Senate Avenue
Indianapolis, IN 46204
(317) 232-3686

IOWA

UNIV. OF IOWA LIBRARIES
Government Publications Dept.
Iowa City, IA 52242
(319) 335-5926

KANSAS

UNIVERSITY OF KANSAS
Spencer Research Library
Government Documents
Lawrence, KS 66045
(913) 864-4662

KENTUCKY

UNIV. OF KENTUCKY LIBRARIES
Government Publications/Maps Dept.
Lexington, KY 40506
(606) 257-8400

LOUISIANA

LOUISIANA STATE UNIVERSITY
Middleton Library
Government Documents Dept.
Baton Rouge, LA 70803
(504) 388-2570

LOUISIANA TECHNICAL UNIV.
Prescott Memorial Library
Government Documents Dept.
Ruston, LA 71272
(318) 257-4962

MAINE

UNIVERSITY OF MAINE
Raymond H. Fogler Library
Govt. Documents & Microforms Dept.
Orono, ME 04469
(207) 581-1680

MARYLAND

UNIVERSITY OF MARYLAND
McKeldin Library
Documents/Maps Room
College Park, MD 20742
(301) 454-3034

MASSACHUSETTS

BOSTON PUBLIC LIBRARY
Government Documents Dept.
666 Boylston Street
Boston, MA 02117
(617) 536-5400 ext.226

MICHIGAN

DETROIT PUBLIC LIBRARY
5201 Woodward Avenue
Detroit, MI 48202
(313) 833-1409

LIBRARY OF MICHIGAN
Government Documents
P.O. Box 30007
735 E. Michigan Avenue
Lansing, MI 48909
(517) 373-1593

MINNESOTA

UNIVERSITY OF MINNESOTA
Wilson Library
Government Publications
309 Nineteenth Avenue South
Minneapolis, MN 55455
(612) 373-7813

MISSISSIPPI

UNIV. OF MISSISSIPPI LIB.
Government Documents Dept.
106 Old Gym Bldg.
University, MS 38677
(601) 232-5857

MISSOURI

University of Missouri at Columbia Library
Government Documents
Columbia, MO 65201
(314) 882-6733

MONTANA

UNIV. OF MONTANA
Mansfield Library
Documents Division
Missoula, MT 59812
(406) 243-6700

NEBRASKA

UNIVERSITY OF NEBRASKA - LINCOLN
Love Memorial Library
Documents Department
Lincoln, NE 68588
(402) 472-2562

NEVADA

UNIV. OF NEVADA-RENO LIB.
Govt. Pub. Department
Reno, NV 89557
(702) 784-6579

NEW JERSEY

NEWARK PUBLIC LIBRARY
U.S. Documents Division
5 Washington Street
P.O. Box 630
Newark, NJ 07101
(201) 733-7812

NEW MEXICO

UNIVERSITY OF NEW MEXICO
General Library
Government Publications/Maps Dept.
Albuquerque, NM 87131
(505) 277-5441

NEW MEXICO STATE LIBRARY
325 Don Gaspar Avenue
Santa Fe, NM 87501
(505) 827-3826

NEW YORK

NEW YORK STATE LIBRARY
Documents Sect. Cultural Educ. Ctr.
Empire State Plaza
Albany, NY 12230
(518) 474-5563

NORTH CAROLINA

UNIVERSITY OF NORTH CAROLINA AT CHAPEL HILL
Davis Library 080A
BA/SS Department Documents
Chapel Hill, NC 27514
(919) 962-1151

NORTH DAKOTA

NORTH DAKOTA STATE UNIVERSITY LIBRARY
Government Documents Dept.
Fargo, ND 58105
(701) 237-8352
In cooperation with Univ. of North Dakota, Chester Fritz Library
Grand Forks

OHIO

STATE LIBRARY OF OHIO
Documents Section
65 South Front Street
Columbus, OH 43266
(614) 644-7051

OKLAHOMA

OKLAHOMA DEPT. OF LIBRARIES
Government Documents
200 NE 18th Street
Oklahoma City, OK 73105
(405) 521-2502, ext. 252

OKLAHOMA STATE UNIV. LIB.
Documents Department
Stillwater, OK 74078
(405) 624-0489

OREGON

PORTLAND STATE UNIV.
Millar Library
934 SW Harrison - P.O. Box 1151
Portland, OR 97207
(503) 229-3673

PENNSYLVANIA

STATE LIBRARY OF PENN.
Government Publications Section
Box 1601
Walnut St. & Commonwealth Ave.
Harrisburg, PA 17105
(717) 787-3752

SOUTH CAROLINA

CLEMSON UNIV. COOPER LIB.
Documents Department
Clemson, SC 29634
(803) 656-5174
In cooperation with Univ. of South Carolina, Thomas Cooper Library, Columbia

TEXAS

TEXAS STATE LIBRARY
Public Services Department
P.O. Box 12927 - 1201 Brazos
Austin, TX 78711
(512) 463-5455

TEXAS TECH. UNIV. LIBRARY
Documents Department
Lubbock, TX 79409
(806) 742-2268

UTAH

UTAH STATE UNIVERSITY
Merrill Library & Learning Resources Center, UMC-30
Documents Department
Logan, UT 84322
(801) 750-2682

VIRGINIA

UNIVERSITY OF VIRGINIA
Alderman Library
Government Documents
Charlottesville, VA 22903
(804) 924-3133

WASHINGTON

WASHINGTON STATE LIBRARY
Document Section
Olympia, WA 98504
(206) 753-4027

WEST VIRGINIA

WEST VIRGINIA UNIV. LIB.
Government Documents Section
P.O. Box 6069
Morgantown, WV 26506
(304) 293-3640

WISCONSIN

ST. HIST SOC. OF WISCONSIN LIB.
Government Pub. Section
816 State Street
Madison, WI 53706
(608) 262-2781
In cooperation with Univ. of Wisconsin-Madison, Memorial Library

MILWAUKEE PUBLIC LIBRARY
Documents Division
814 West Wisconsin Avenue
Milwaukee, WI 53233
(414) 278-3065

WYOMING

WYOMING STATE LIBRARY
Supreme Court & Library Bldg.
Cheyenne, WY 82002
(307) 777-5919

National Aeronautics and
Space Administration
Code NTT
Washington, D.C.
20546
Official Business
Penalty for Private Use, $300

SPECIAL FOURTH-CLASS RATE
POSTAGE & FEES PAID
NASA
PERMIT No. G27

POSTMASTER: If Undeliverable (Section 158
Postal Manual) Do Not Return